

BEFORE THE ILLINOIS POLLUTION CONTROL BOARD

In the Matter of:)

STANDARD FOR THE DISPOSAL OF)
COAL COMBUSTION RESIDUALS)
IN SURFACE IMPOUNDMENTS:)
PROPOSED NEW 35 ILL. ADMIN.)
CODE 845)

PCB 2020-019
(Rulemaking - Water)

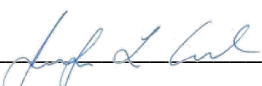
NOTICE OF ELECTRONIC FILING

To: Attached Service List

PLEASE TAKE NOTICE that on August 27, 2020, I electronically filed with the Clerk of the Illinois Pollution Control Board (“Board”) the **JOINT TESTIMONY OF SCOTT M. PAYNE, PhD, PG and IAN MAGRUDER, M.S.** and **Attachments**, copies of which are served on you along with this notice. Attachments are being filed separately due to size restrictions.

Dated: August 27, 2020

Respectfully Submitted,



Jennifer Cassel (IL Bar No. 6296047)
Earthjustice
311 S. Wacker Dr., Suite 1400
Chicago, IL 60606
(312) 500-2198 (phone)
jcassel@earthjustice.org

/s/Thomas Cmar
Thomas Cmar (IL Bar No. 6298307)
Earthjustice
311 S. Wacker Dr., Suite 1400
Chicago, IL 60606
T: (312) 500-2191
tcmar@earthjustice.org

/s/ Mychal Ozaeta
Mychal Ozaeta (ARDC No. #6331185)
Earthjustice
707 Wilshire Blvd., Suite 4300
Los Angeles, CA 90017
T: 213-766-1069
mozaeta@earthjustice.org

/s/ Melissa Legge
Melissa Legge (ARDC No. #6334808)
Earthjustice
48 Wall Street, 15th Floor
New York, NY 10005
T: 212 823-4978
mlegge@earthjustice.org

Attorneys for Prairie Rivers Network

/s/ Kiana Courtney
Kiana Courtney (IL Bar No. #6334333)
Environmental Law & Policy Center
35 E. Wacker Drive, Suite 1600
Chicago, Illinois 60601
KCourtney@elpc.org

/s/Jeffrey T. Hammons
Jeffrey T. Hammons, (IL Bar No. #6324007)
Environmental Law & Policy Center
1440 G Street NW
Washington DC, 20005
T: (785) 217-5722
JHammons@elpc.org

Attorneys for Environmental Law & Policy Center

/s/ Faith E. Bugel
Faith E. Bugel
1004 Mohawk

Wilmette, IL 60091
(312) 282-9119
fbugel@gmail.com

Attorney for Sierra Club

BEFORE THE ILLINOIS POLLUTION CONTROL BOARD

In the Matter of:)
)
)
STANDARD FOR THE DISPOSAL OF)
COAL COMBUSTION RESIDUALS) PCB 2020-019
IN SURFACE IMPOUNDMENTS:) (Rulemaking - Water)
PROPOSED NEW 35 ILL. ADMIN.)
CODE 845)
)
)
)
)

JOINT TESTIMONY OF SCOTT M. PAYNE, PhD, PG and IAN MAGRUDER, M.S.

August 24, 2020

1. Introduction

The Illinois Environmental Protection Agency (IEPA) is proposing comprehensive rules regarding the design, construction, operation, corrective action, closure and post-closure care of surface impoundments containing coal combustion residuals (CCR). In this testimony we present recommended rule language based on our professional experience preparing and reviewing groundwater flow and transport models and our experience reviewing past groundwater modeling practices prepared for IEPA in support of Closure Plans for CCR facilities in Illinois.

Section 2 presents our qualifications. Section 3 provides a problem statement describing deficiencies in past groundwater modeling practices prepared for IEPA in support of Closure Plans for CCR facilities in Illinois. Section 4 provides recommended rule language aimed at ensuring that groundwater models prepared in support of corrective action and closure plans for Illinois CCR facilities are properly developed and documented and to address the deficiencies in the models we have reviewed which were used to support past closure planning. The goal of our recommendations is to ensure that future groundwater modeling follows acceptable practices and will result in models that accurately represent current conditions and are capable of making reliable predictions of the long-term effects of closure and corrective actions.



Scott M. Payne, PhD, PG
Principal Scientist
KirK Engineering & Natural Resources, Inc.

A handwritten signature in black ink, appearing to read 'I. Magruder', is positioned in the upper left corner of the page.

Ian Magruder, M.S.
Senior Hydrogeologist
KirK Engineering & Natural Resources, Inc.

Table of Contents

1. Introduction.....	1
2. Qualifications.....	4
3. Problem Statement.....	5
Comment a. Groundwater models do not agree with the conceptual site model.....	5
Comment b. Groundwater site characterization and modeling omits relevant groundwater elevation data.....	9
Comment c. Model boundary conditions are not based on supportable data.....	10
Comment d. Modeled hydraulic conductivity is not based on testing performed at the site.....	12
Comment e. Modeled contaminant source concentrations and leachate percolation rates are not based on accurate data.....	13
Comment f. Groundwater models do not consider attenuation of contaminants in the aquifer.....	16
Comment g. Model calibration is poor and calibration is not quantitatively assessed.....	17
Comment h. Modeling does not evaluate the effects of groundwater contact with CCR.....	19
Comment i. Variations in groundwater flow direction are not adequately accounted for in site characterization, water quality monitoring, or modeling.....	26
Comment j. Forecast uncertainty.....	30
Comment k. Modeling documentation does not include all of the information necessary to understand and review the model.....	31
Comment l. Plans which leave CCR in contact with groundwater are likely to result in long-term exceedance of water quality standards and require perpetual plume monitoring and institutional controls.....	32
Comment m. The State of Illinois would benefit from a specific guidance document for groundwater flow and contaminant transport model development and review.....	33
4. Recommend rule language.....	34
845.220 Construction Permits.....	34
845.620 Hydrogeologic Site Characterization.....	38
845.660 Assessment of Corrective Measures.....	42
845.670 Corrective Action Plan.....	43
845.710 Closure Alternatives.....	45
5. References.....	46

Appendices:

Appendix 1. Mann-Kendall trend analysis of water levels at the Hennepin East Ash Pond No. 2

Appendix 2. Hennepin cross-section D-D' with model layers and hydraulic conductivity

Appendix 3. Hennepin East Ash Pond Modeled Boron Concentration and Load

Appendix 4. Meredosia Power Station Illinois River Flooding 4/29/2013

Appendix 5. Linear regression analysis of Hennepin modeled hydraulic conductivity and measured values

Appendix 6. CVs

2. Qualifications

We express the opinions and recommendations in this letter based on our qualifications as consultants working on RCRA facilities and coal ash sites. Our qualifications are summarized here; full curricula vitae are attached.

Scott M. Payne, Ph.D., P.G.

Dr. Payne has over thirty-four years of experience as a professional hydrogeologist and environmental consultant. He has extensive experience in planning, project management, environmental assessment, surface and groundwater protection, and environmental analysis and permitting. He has extensive experience in toxic waste site studies and cleanup, lined impoundment design, landfill assessment, Superfund and RCRA regulatory support. He has worked on dozens of other CERCLA and RCRA facilities across the U.S. Dr. Payne is the author of *Strategies for Accelerating Cleanup at Toxic Waste Sites*, published internationally by Lewis Publishers of New York. In his book, he outlines streamlining regulatory processes, effectively negotiating decisions and actions, environmental leadership, and applying practical solutions to remedy environmental problems. Dr. Payne served as an adjunct professor at Montana State University and taught surface and groundwater modeling for graduate and undergraduate students in the Environmental Science and Land Resource Department.

Ian Magruder, M.S.

Mr. Magruder has twenty years' professional experience working on toxic and hazardous waste site characterization, remediation, and water quality protection. He has worked extensively in recent years reviewing cleanup plans for coal ash sites written under state and federal regulatory authority and working with State of Montana Department of Environmental Quality to better understand coal ash groundwater contaminant remediation plans. Mr. Magruder writes and reviews sampling and analysis plans and work plans for contaminated site remediation and waste characterization studies. He has taken hundreds of soil and groundwater samples for inorganic and organic contaminants including metals, inorganics, petroleum contaminants, solvents, PCBs, pesticides, and radionuclides. He has provided construction and health and safety oversight of remediation construction projects. Mr. Magruder has served for seventeen years as a technical advisor for a Superfund committee in Butte, Montana, and has evaluated the risks inherent in mine waste and wood treatment chemicals to humans and the environment. That experience includes review of EPA risk assessment, feasibility, remedial investigation, and remedial action plans. Mr. Magruder has a Master of Science degree in in Geology with a hydrogeologic

emphasis. He has an extensive background in modeling and formerly studied under one of the industry's leading authors of applied groundwater modeling.

3. Problem Statement

We have reviewed hydrogeologic characterization reports, CCR impoundment leachate percolation models, and groundwater model reports prepared for closure plans submitted between 2016 and 2018 for three Illinois coal powered electric plants: Vistra's Hennepin Power Station in Putnam County, the Ameren's Meredosia Power Station in Morgan County, and Vistra's Wood River Power Station (closed by Dynegy) in Madison County. Each of these three groundwater modeling efforts was intended to prepare a model capable of both simulating existing contaminant plumes and predicting the efficacy of proposed closure measures for remediating and protecting groundwater long-term. All three models reviewed contain fatal flaws which render them inaccurate for predicting either the efficacy of proposed closure measures or the groundwater remediation timeframe. Our review of these closure plan documents makes it clear that the process of evaluating corrective action needs and appropriate closure plan methods used by at least two of the three major coal plant owner/operators in Illinois is severely deficient from lack of regulatory constraint. Our professional opinion is that an adequate regulatory framework, an official technical guidance document which details required modeling practices, and close oversight by IEPA are necessary to prevent Illinois from having severe and perpetual groundwater pollution problems near these retired coal powered electric plants in the long-term.

In this section, we describe common deficiencies we find in these past modeling efforts. In section 4, we propose rule language intended to help to ensure that future modeling conducted in support of closure plans follows generally acceptable modeling practices and avoids the flaws evident in these past modeling efforts. The example model deficiencies below are labeled alphabetically as "Comment a.", "Comment b.", etc., so that we can cross reference the deficiencies in existing modeling with proposed rule language which we recommend be adopted to provide regulatory clarity, described in section 4 below.

Comment a. Groundwater models do not agree with the conceptual site model

A conceptual site model (CSM) is a descriptive presentation of the site, included in either the hydrogeologic assessment or modeling report, which discusses the groundwater flow, aquifer properties, and contaminant release and transport pathways. The CSM informs the groundwater modeling team, regulators, and public what is known about the site so that the site can be accurately understood and modeled. One purpose of the CSM is to provide the framework that needs to be included in the modeling; implicit in this is that models developed for the site should be based upon and agree with the CSM. If modeling results provide evidence that the CSM should be revised, any revision of the CSM needs to be documented and supported with evidence. Despite this, models have been developed at the three sites we have reviewed which do not agree with the CSMs for those sites or the actual site conditions.

a.1. Examples of vertical percolation models that do not agree with the conceptual site model

Common to all three of the sites reviewed are vertical leachate percolation models that do not agree with the CSM or field data. EPA's Hydrologic Evaluation of Landfill Performance (HELP)

Model is commonly used to model vertical percolation and leachate production for CCR units. The HELP model is also commonly used to predict the time for hydrostatic equilibrium to be achieved in the moisture flux through capped CCR units. The HELP model is also commonly misapplied.

HELP assumes free drainage occurs from the landfill bottom. The HELP model Engineering Documentation (EPA 1994, p. 108) states in Section 5.1 Methods of Solution: “Percolation through soil liners is modeled by Darcy’s law, assuming free drainage from the bottom of the liner.” A free drainage boundary condition exists where the pressure head has a unit gradient, which means the only contribution to the gradient in hydraulic head is gravitational. This means the model is not meant to be applied to situations where the lower layers are in contact with groundwater, because groundwater flow is not solely gravitational. HELP is not intended to model leachate flux from the bottom of a waste unit which is in contact with groundwater (Tolaymat 2020).

When the HELP model is misapplied to CCR units which are in contact with groundwater, it will provide inaccurate predictions of hydrostatic equilibrium and leachate percolation rates because the hydrologic setting violates the model assumptions.

In the Hennepin Closure Plan, NRT (2017c) used HELP for the proposed design of the cap system to predict the time for a capped CCR unit to reach hydrostatic equilibrium conditions. The HELP results were also used as input data for recharge rates in the MODFLOW groundwater flow model used to predict pond hydraulics and leachate transport when the cap is in-place. Conceptually, NRT uses HELP to model a free-draining waste unit which extends 55’ below the base of the CCR. However, in reality, the water table separation is typically less than 4’ below the base of the CCR unit, the long-term trend in the water table is rising (Appendix 1), and the CCR is periodically inundated by rising groundwater. Not surprisingly, the HELP model erroneously predicts that hydrostatic equilibrium is quickly reached following the site closure plan. In reality, the periodic inundation of the CCR by groundwater will both increase the time it takes for water to percolate through the capped CCR unit and create a perpetual pattern of rewetting and draining of the CCR at the base of the unit.

In the Meredosia Closure Plan, Geotechnology (2016) uses HELP to model a free-draining waste unit that extends 40’ below the base of the CCR. Again, the groundwater is typically less than 5’ below the base of the CCR unit and the CCR is inundated on close to an annual basis by rising groundwater during elevated stage of the Illinois River.

In the Wood River Closure Plan, NRT (2016b) uses a HELP model with the lowest layer (referred to in the Hydrostatic Modeling Report as the foundation soil) in Ponds 1 and 2W that is 9’ below the mean groundwater elevation and 16-21’ below the maximum measured groundwater elevation reported in the Hydrogeologic Site Characterization Report (NRT 2016). The modeled lowest layer in Pond 2E is 0.2’ below the average groundwater elevation and 8’ below the maximum measured groundwater elevation reported in NRT (2016).

In all three of these examples, the CSM and site characterization data depict unlined CCR units which are commonly inundated by rising groundwater levels. When groundwater is in contact

with the CCR, the downward percolation of CCR leachate will cease and the CCR will be rewetted, providing a source for additional leachate. Despite this being clearly portrayed in the site data, the modeling in all three of these cases fails to account for the actual site conditions and, as a result provides inaccurate predictions of hydrostatic equilibrium, leachate percolation rates, and closure performance.

a.2. Example of groundwater model which does not match site geology and hydrogeologic properties described in the conceptual site model

Standard modeling practices include a CSM which outlines the geologic and hydrogeologic conditions of a site which affect groundwater flow (Anderson et al. 2015). The CSM typically provides cross-sections which show geologic units and their physical orientation such as thickness, depth, and the slope of dipping layers. The CSM will also describe the hydrogeologic properties of the aquifer, including hydraulic conductivity, storativity, etc. Grids and layers in a groundwater model should reasonably match the CSM.

At the Hennepin site, the modeled grid and hydraulic conductivity does not agree with the geologic cross-sections. Appendix 2 is a copy of Figure 8 of the Hennepin Hydrogeologic Site Characterization Report (NRT 2017), which we have drawn the model layers on, showing that the model layers do not remotely match the actual site geology. There is no discussion in the Groundwater Modeling Report (NRT 2017b) as to why the model does not agree with the geologic cross sections or use the site characterization data for hydraulic conductivity.

The modeled hydraulic conductivity in the Hennepin model also does not agree with hydraulic conductivity tested at the site. Table 1 compares the tested hydraulic conductivity presented in the Hennepin Hydrogeologic Site Characterization Report (NRT 2017) with the modeled values. The Hennepin site groundwater model places the highest hydraulic conductivity in the lower Henry Formation geologic unit which the geologic cross sections show to be finer grained: “sand and gravel with fines” and “silt/clay”. Finer grained deposits typically have lower hydraulic conductivity. The use of the two modeled high conductivity (1000 ft/d) layers in the model will cause contaminants to be simulated to travel lower in the aquifer than the geologic cross sections suggest is the real case, negatively affecting model calibration. Model calibration involves adjusting model parameters so that they match field measured groundwater elevations, concentrations, and measured or calculated flow rates. If the model is based on an inaccurate depiction of the actual site conditions, calibration will be negatively affected, and model parameters may need to be further adjusted to compensate for the inaccuracy. There is no discussion in the Groundwater Modeling Report (NRT 2017b) as to why the modeled hydraulic conductivity does not reflect the cross-sections or field tested hydraulic conductivity values.

The Hennepin Groundwater Modeling Report states, the “model had moderately high to high sensitivity to the horizontal hydraulic conductivity used over most of the domain.” In this case, the hydraulic conductivity array does not match the site geology and field measured hydraulic conductivity. The high sensitivity reported tells us that the prediction results are likely to be inaccurate. This illustrates the importance of having the groundwater model agree with the site data and conceptual model.

Table 1. Comparison of field measured hydraulic conductivity (K) and modeled values at the Hennepin Site (data adapted from NRT 2017 and 2017b).

Well	Site characterization field data (from NRT 2017, Table 4)	Modeled values (NRT 2017b)	Location
	K (ft/d)	K (ft/d)	
02	9,072	500	East of Pond No. 4
03	125	500-1000	Pond No. 2 river berm
04	62	500	Leachate Pond river berm
05	12	500	Landfill river berm
06	167	500-1000	Pond No. 2 river berm
07	105	35	Upgradient background
08	27	500	Primary Pond upgradient berm
08D	454	100-1000	Primary Pond upgradient berm
10	1,049	500	Pond No. 2 upgradient berm
11	624	1000	Pond No. 2 upgradient berm
12	340	500	Landfill upgradient berm
13	822	1000	Landfill upgradient berm
14	no data		
15	1,049	500	Leachate pond upgradient berm
16	2,155	500	Primary Pond upgradient berm
17	68	500	Polishing Pond upgradient berm
018S	215	500	Pond No. 2 river berm
018D	0.3	100	Pond No. 2 river berm
019S	170	500	Leachate pond river berm
019D	108	100-1000	Leachate pond river berm

a.3. Example where the conceptual site model is based on the computer model, not actual site conditions

Standard groundwater modeling practices are for the computer model to be based upon the CSM. However, the Hennepin Groundwater Model Report (NRT 2017b, p. 3) in describing the CSM states, “Since the ash fill is modeled as unsaturated throughout the simulated timeframe, the conceptual model for transport assumes the only source of boron to the system originates from boron that leaches to recharge water during percolation through ash above the water table.” In this instance, the CSM is stated to be based on a simplifying assumption in the computer model. Despite the simplifying assumption in the modeling that groundwater inundation does not release boron, the Hennepin Hydrogeologic Site Characterization Report describes that boron concentrations at downgradient wells are correlated with river stage and inundation of the CCR unit by groundwater (NRT 2017, page 19); selenium concentrations follow the same pattern (NRT 2017, pp. 21-22, 27). The Groundwater Modeling Report itself states, “occasional increases in boron concentrations were observed to coincide with the precipitation/flood events and localized saturation of the ash.” (NRT 2017b, p. 3). In this situation, the CSM is based on an assumption in the modeling exercise. This puts the cart before the horse. The CSM should inform the model.

These examples show the need for regulatory requirements that ensure appropriate data is collected and an adequate CSM is developed for the site. The examples also show that a regulatory requirement is needed to ensure that groundwater flow and transport models accurately represent and agree with the CSM.

Comment b. Groundwater site characterization and modeling omits relevant groundwater elevation data

Groundwater monitoring at CCR facilities includes measurements of groundwater elevation. The elevation data is required to prepare groundwater flow maps, determine relationships between surface water stage such as river flooding and groundwater flow, and to evaluate the separation of CCR from groundwater and potential for leaching. All available groundwater elevation data should be included in hydrogeologic characterization reports, considered in site conceptual model development, and used as calibration targets in groundwater flow models. Despite the importance of considering long-term records of groundwater elevations when evaluating contaminant release and transport at CCR facilities, hydrogeologic characterization reports and groundwater modeling efforts have omitted relevant data, instead focusing on a few recent years’ data.

The Hennepin Groundwater Modeling report (NRT 2017b) indicates that groundwater level data has been collected since 1995. However, only 2012 through 2016 data are included in the Site Characterization Report.

The Wood River Hydrogeologic Site Characterization Report (NRT 2016, p. 2-5) provides measured groundwater levels in Table 4 for 2010-2015. However, the same report indicates that monitoring wells were installed in 1982. (*Id.*) Despite the long-term data set apparently available,

the Wood River groundwater model (NRT 2016c, p. 2-2)) only uses water levels from a single measurement event from November 2014 for model calibration.

At each of these sites, the entirety of the groundwater elevation dataset is needed to evaluate transient flow conditions, separation between CCR and groundwater, variability of the groundwater flow and elevation to climate, and for use in model calibration. By focusing on a small subset of recent years' data, or by only calibrating the model to a single month's data the modeling efforts suffer from only considering a small range of conditions. Model calibration is also missing important data which could be used as a calibration target, resulting in a model capable of making accurate predictions regarding closure efficacy. These examples show the need for regulations that require that the entirety of the available groundwater monitoring data be included in the hydrogeologic site characterization and model calibration.

Comment c. Model boundary conditions are not based on supportable data

Models commonly use features which simulate rivers leaking or groundwater flowing into the modeled area from up-gradient sources as boundaries. It is critical that these "boundary conditions" (rivers, ponds, percolation of precipitation, groundwater inflows, CCR unit leakage, etc.) be modeled appropriately because they provide flow to the groundwater system which affects flow direction, contaminant transport, and the timeframe for groundwater remediation to meet water quality standards. Accurate model predictive capability relies on boundary conditions being accurately simulated. Inaccurate model boundaries may also lead to cascading errors during model calibration. For instance, if specified flow boundaries are estimated to be higher than actual conditions, then hydraulic conductivity is likely to be increased during model calibration to accommodate for the erroneous boundary condition in order to meet head calibration targets. A model having both boundary condition flux and hydraulic conductivity modeled unrealistically high will result in much higher dilution capacity for contaminants than reality, despite the model being calibrated.

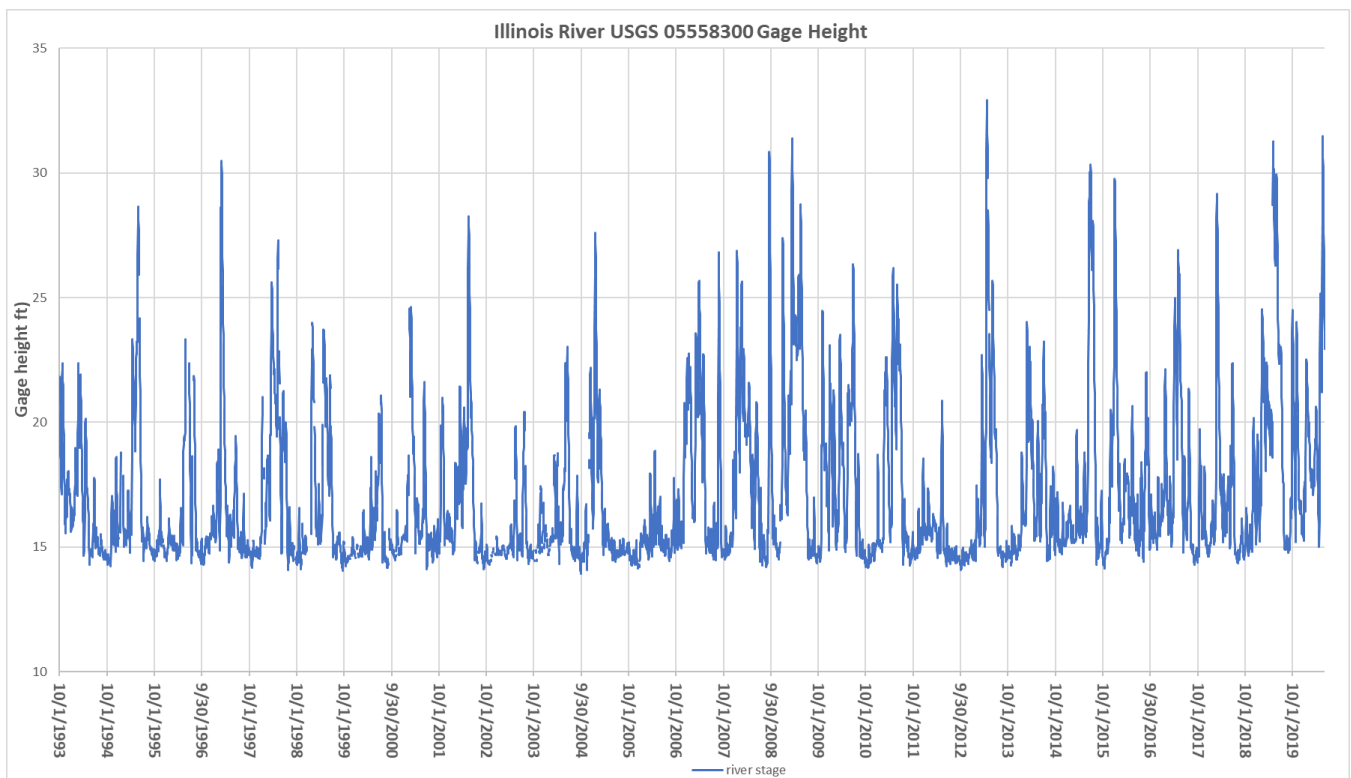
Boundary conditions should be constrained by supportable data for the groundwater system to the extent possible. The source of the data should be clearly specified in the modeling report. Boundary conditions should not be arbitrarily defined with a lack of any real data. If distant boundary conditions do not have any supportable data they may be estimated based on extrapolation of site data and off site topographic or geologic data if the methods are clearly defined. The flux rates across boundary conditions should also be tested to evaluate if the boundary response is realistic (Reilly and Harbaugh 2004, pp. 16-17). Boundary flux rates should be compared to a groundwater budget prepared for the modeled area to evaluate if they are within expected range of flow (Anderson et al. 2015). A water budget is a tabulation of field-based estimates of inflows and outflows from the modeled area. By checking the boundary flux against an independent estimate of flow into and out of the model, the modeler can evaluate if boundary flux is reasonable given site data. We recommend this groundwater budget be prepared as part of the conceptual site model.

In the Hennepin Groundwater Model Report (NRT 2017b, p. 6), the only description of the upgradient model boundary is "The head value for the upgradient constant head boundary was modified from the 2010 model during calibration." We do not know if the boundary was

originally assigned based on actual water level measurements upgradient, which would be the appropriate way to assign a constant head boundary. The fact that it was adjusted during calibration suggests it was not assigned based on supportable data; instead the boundary was adjusted until the model fit the site calibration data. This is inappropriate because there are likely adjustments to the model that need to be made nearer to the CCR unit (such as using the field measured hydraulic parameters) that would also create a calibrated model.

The Hennepin model also uses a river boundary with a constant river stage of 444.0 feet in a transient model. The actual river stage of the Illinois River is highly variable, with flooding common (Figure 1). The Hennepin Hydrogeologic Characterization Report (NRT 2017) clearly shows that elevated river stage causes near equal increases in groundwater levels, with higher stage leading to a complete reversal of groundwater flow direction and inundation of CCR at the facility by groundwater. Despite this clear evidence of the importance of the river stage on groundwater and contaminant transport, the modeling report simply states that the fixed river boundary is acceptable because it is “within observed surface water elevations at the site.” (NRT 2017b, p. 7).

Figure 1. Illinois River stage at Henry, Illinois near the Hennepin Power Station reported by USGS.



The Wood River groundwater model (NRT 2016b) uses a general head boundary to simulate the inflow of groundwater from areas upgradient of the power plant. The modeling report provides no groundwater data to support the elevation assigned to this general head boundary; instead the

elevation values were determined during calibration. The problem with this is the elevation values were not assigned based on supportable data; instead the elevation values were adjusted until the model fit the calibration data. The elevation values should be constrained by actual measurements to improve model calibration. The modeling effort failed to quantify the amount of water entering or leaving the model from this boundary and evaluate whether it is reasonable given known hydrogeologic parameters. The approach leads to further uncertainty and inaccuracy in the model. The water table elevation at this model boundary should be measured or interpolated from field data and that elevation should help to constrain other model attributes during calibration. This will lead to a more accurate model, capable of making reliable prediction accuracy. The Wood River modeling report clearly identifies the model as highly sensitive to that general head boundary elevation, meaning the elevation has great implications on the model result and prediction.

These examples show that regulations are needed to ensure that model boundary conditions accurately reflect site characterization data and that boundary flux should be audited with an independent water budget.

Comment d. Modeled hydraulic conductivity is not based on testing performed at the site

Hydraulic conductivity, which is the ease with which a particular geology or soil allows groundwater to flow through it, is one of the most important model parameters to have quality data measured at the site. All three of the models reviewed report high sensitivity to hydraulic conductivity, meaning the modeled hydraulic conductivity values have great implications on the model result and prediction accuracy. Hydraulic conductivity values described in a conceptual site model and used in flow modeling need to be determined from testing performed at the site.

At the Meredosia CCR facility, the monitoring wells were not tested for hydraulic conductivity; a single value is identified as appropriate for the site which the Meredosia Hydrogeologic Assessment Report indicates comes from “values for wells along the Illinois waterway” (Geotechnology 2016, p. 12). However, the report does not provide any information on how or where hydraulic conductivity was tested, or a reference for finding that information. Further, it is not clear if the value was considered in the modeling because they do not report what hydraulic conductivity values are even used in the model. The site characterization and modeling are severely deficient owing to the lack of site-specific measurements of hydraulic conductivity, despite there being at least nine monitoring wells at the site which could be tested.

The Hennepin CCR facility groundwater model (NRT 2017b) suffers from a different problem. At Hennepin, site measured hydraulic conductivity data is available and reported in the Hydrogeologic Site Characterization Report Hennepin. But that data is not used in the modeling effort. This issue at Hennepin is introduced under example a.2. above because the groundwater model grid layers and hydraulic conductivity do not agree with the site conceptual model. This example also illustrates the deficiencies in considering site-specific information in modeling CCR contamination and the effects of impoundment closure. The only limits on hydraulic conductivity mentioned in the Hennepin Groundwater Model Report are that “Measured hydraulic conductivities of the Henry Formation sands and gravels range from 0.3 to 8,503 feet/day;” and, “[t]he assigned hydraulic conductivity values in the model are within observed

ranges.” (NRT 2017b, Page 6). These observed values range over four orders of magnitude (the highest value is 28,000 times the lowest value). This is not a reasonable or adequate characterization of site hydrogeology or constraint on modeled parameters. In fact, we find that the model was not developed using the field tested hydraulic conductivity at all. The field measured hydraulic conductivity presented in the Hennepin Site Characterization Report (NRT 2017) are compared to the modeled values described in the Groundwater Model Report (NRT 2017b) in Table 1 above showing that the model was not parameterized using the specific site data, instead hydraulic conductivity values of 35, 100, 500, and 1000 were apparently arbitrarily chosen. There is a complete lack of correlation in the field data versus the model values as shown in Appendix 5. If the model and its predictions are to resemble reality, the model must be based on actual site conditions. The hydraulic conductivity data for the Hennepin model suggests this is not the case.

These examples show that regulations are needed to ensure that appropriate tests are performed to provide site-specific hydraulic conductivity values. By virtue of the need for water quality data, monitoring wells are available for aquifer testing, and wells are likely to be ideally located for providing the data needed. Regulations are also needed to ensure that this data is used when developing groundwater models.

Comment e. Modeled contaminant source concentrations and leachate percolation rates are not based on accurate data

The accuracy of contaminant transport models is highly dependent on having accurate information on the contaminant source concentration and percolation rates from CCR impoundments. Despite this, the groundwater models for the three sites we reviewed had either no or extremely limited data on contaminant concentration in the impoundment leachate. Additionally, all three models relied upon a faulty application of EPA’s Hydrologic Evaluation of Landfill Performance (HELP) Model, which violated the basic HELP assumption that the waste unit is free draining. The HELP model results which were used to provide the critical contaminant percolation flux rate in the groundwater models are completely inaccurate because they do not represent the real-world situation. The deficiencies with the HELP modeling are further described in Comment a.1. above.

We found in our review of the three closure plan groundwater models that owner/operators are typically using the model calibration process to determine contaminant source concentration. There are two issues with this: one is that CCR leachate concentration should be relatively easily sampled at most sites; the second issue is that using model calibration to arrive at source concentration allows inaccuracies in other model parameters to perpetuate through the calibration process, compounding in the calibrated source concentration. CCR porewater leachate concentration should be measured in each CCR unit, such that a statistically supportable estimate of the concentration is known, and those concentrations should be used as constraint during calibration of other parameters in the model.

The CCR should be sampled by installing piezometers in saturated impoundments or lysimeters in unsaturated impoundments and sampling porewater which has had sufficient residence time for leaching to occur and which is representative of the leachate leaving the CCR unit. Samples

collected from surface water in a CCR unit are less accurate because they lack residence time within the CCR matrix and may be representative of other water management practices or more dilute than the CCR leachate.

Alternatively, leachate testing of CCR could be used to determine source concentrations. Leachability testing should use the Leaching Environmental Assessment Framework (LEAF), which is the U.S. EPA recommended leaching test method for CCR (Kosson et al. 2009, 2014). LEAF better captures the pH-dependent leaching of oxyanion contaminants arsenate As(V) and selenite Se(IV); arsenic and selenium are of particular concern because of their propensity to leach and potential for bio-magnification in aquatic life in receiving waters (Schwartz et al. 2018). Single-point leachability tests such as TCLP or the SPLP are not recommended. Kosson et al. (2009, pp. ii-iii) are clear that the (single-point pH) SPLP test will give inaccurate predictions of actual CCR leaching to groundwater, “for CCRs, the rate of constituent release to the environment is affected by leaching conditions (in some cases dramatically so), and that leaching evaluation under a single set of conditions will, in many cases, lead to inaccurate conclusions about expected leaching in the field.” This tells us the SPLP test should not be used to make predictions about groundwater cleanup or leachability of the CCR, which is proposed to be left in place in fill at the site.

The Hennepin model shows the type of questionable estimates of leachate concentration that result when calibration is used to arrive at the concentrations. In the Hennepin model (NRT 2017b) contaminant source concentrations are assigned arbitrary values without any sampling data to support the concentrations. As shown in Table 2, the source concentrations in the calibrated Hennepin model vary from 5 to 20 mg/L within a single pond. This is described in the modeling report as being due to a higher concentration of fly ash in the eastern portion of the pond. However, no actual water quality data are provided to support this.

Table 2. Boron source flux, concentration, and calculated load in the Hennepin site Closure Plan model (from model input values NRT (2017b) during stress period 2).

Zone	Description	Area ft ²	Contaminant source flux (recharge) rate (ft/d)	Concentration (mg/L)	Boron load (kg/day)
9	Primary and Polishing Pond	1,158,555	0.004	4	525
10	Ash Pond No. 2 "high recharge area" (NE corner)	68,492	0.045	20	1,746
13	Ash Pond No. 2 "high recharge area"	77,742	0.045	10	991
3	Ash Pond No. 2 (east side)	721,336	0.0036	16	1,177
5	Ash Pond No. 2 (west side)	675,285	0.0036	9	620

7	Ash Pond No. 2 (embankment)	53,725	0.0045	5	34
---	--------------------------------	--------	--------	---	----

Contaminant loading (concentration x leachate flux rate) in the Hennepin model is even more questionable. Table 2 shows how the contaminant load was modeled entering the groundwater system. These contaminant source boundaries, concentrations, and loading rates are shown visually in Appendix 3. The model simulates almost nine times as much contamination originating in the closed and dewatered Ash Pond No. 2 compared to the active Primary Pond and the Polishing Pond (Table 3). The Primary and Polishing Ponds are reported to contain water within the CCR to a depth of as much as 30 feet. Although the Primary and Polishing Ponds are clay lined, clay liners are typically leaky, especially at greater ponded water depth. The fact that the model simulates nine times more boron loading from the closed and dewatered Ash Pond No. 2 is extremely questionable. This is typical however of the type of result when source concentration is based on model calibration and not actual site sampling data.

Table 3. Summary of modeled boron load by pond for the Hennepin site (Summarized from calculated loads in Table 2).

Modeled contaminant source	Boron load (kg/day)
Closed and dewatered Pond No. 2	4,566
Active Primary and Polishing Pond	525

The Meredosia model has a similar deficiency in modeled leachate concentration. The source concentration of boron and arsenic in the Fly Ash and Bottom Ash Ponds was based on calibration results at the end of twenty-five years (Geotechnology 2016, p. 177). What this means is the boron leachate concentration is the result of calibrating the source concentration to a model with inadequately supported estimates of hydraulic conductivity and flux values determined from a faulty application of the HELP model, which violated the model free-draining assumption. The result is the Meredosia modeled boron leachate concentration of 25 mg/L is less than the concentration routinely measured in the aquifer at downgradient well APW-3, a conclusion which does not make sense.

The Meredosia model also uses an arsenic source concentration for both fly ash and bottom ash which is based on a paper by Wang et al., 2005, which itself is only based on three fly ash samples from unidentified location. The authors of that paper clearly explain the great variability in CCR arsenic concentration, stating that bituminous coal fly ash can range from 1 to 1000 ppm, depending on coal source and combustion technology. Further, the concentration they measured for fly ash was applied to the Meredosia model for bottom ash, simply because there was no site data available.

These examples show the need for regulations that require owner/operators to sample CCR leachate to provide accurate site-specific data, and this data should be used when modeling contaminant source concentration groundwater.

Comment f. Groundwater models do not consider attenuation of contaminants in the aquifer

Many of the inorganic contaminants typical of coal ash (boron, cadmium, cobalt, selenium, etc.) do not behave conservatively in groundwater and are subject to attenuation (e.g. Masahiro 1987). Attenuation, as we refer to it for CCR contaminants, means chemical processes such as sorption that cause contaminants to exhibit slowed transport or to be immobilized. This attenuation can increase the cleanup timeframe of the contaminant plume because dissipation of contaminants takes longer. Contaminant transport of attenuated chemicals is typically modeled using a retardation factor to approximate attenuation between the contaminant and aquifer matrix. Groundwater models which do not account for attenuation may underestimate the groundwater remediation timeframe because contaminants are modeled to travel faster than reality and are diluted or otherwise dissipated in the model because of the lack of consideration for attenuation. Models that do not account for attenuation may also suffer from additional inaccuracies because during model calibration, other parameters such as hydraulic conductivity, dispersion, and contaminant flux rates are adjusted to bring the model into calibration, when in fact it is the attenuation that needs to be calibrated.

The model developed for the Hennepin Site (NRT 2017b) does not simulate boron attenuation. This is one reason why the model predicts boron, which is currently about 2.5 times higher than the Class I Standard downgradient of the CCR unit, cleans up within two years of capping the CCR unit. If attenuation were accurately modeled, the cleanup timeframe may be longer. Additionally, having site-specific data for source concentration would allow other model parameters, such as hydraulic properties, to be adjusted to more realistic values when calibrating the model to measured contaminant concentrations in groundwater.

Similarly, the Meredosia modeling effort (Geotechnology 2016) did not consider or evaluate contaminant attenuation. A retardation factor is used when simulating attenuation in the MT3D modeling program. The model report states, “Retardation and decay were not used to be conservative.” The fact is this is not conservative. The contaminant plume will likely take longer to clean up than simulated by the model if the contaminants are attenuated.

All models developed for CCR facilities should evaluate contaminant attenuation at the site and derive site-specific values for attenuation/retardation if contaminants are attenuating. Retardation factors used in the model should be specific to the geologic units modeled, because different lithology commonly have different attenuation characteristics. Retardation factors should also be subject to a model sensitivity analysis to evaluate how uncertainty in attenuation affects model predictions.

Retardation factors can be calculated based on difference in plume front distance at a given time, as shown in Domenico and Schwartz (1990) and Anderson et al. (2015). Using site data, retardation factors should be calculated using multiple sets of upgradient and downgradient wells

whenever possible. Retardation factors can also be estimated based on analysis of the contaminant partition coefficient as described by EPA (1999).

Dispersion also needs to be accounted for in groundwater transport models. Dispersion includes both the processes of chemical diffusion and advective dispersion that effectively spread contaminant concentrations during groundwater transport. The result of dispersion is the contaminant plume advancing faster than calculated using groundwater travel times and contaminant retardation factors alone. Although one effect of dispersion is to lessen peak concentrations with travel distance, dispersion can also cause contaminant concentrations to remain above water quality standards for longer periods of time at a location because the plume is spread out longitudinally. Dispersion should be evaluated and modeled in all groundwater transport models. Dispersivity is the parameter used to model dispersion; there are a number of methods available to estimate dispersivity (e.g. Freeze and Cherry 1979; Gelhar et al. 1992).

Dispersion is reported to be modeled at the Hennepin (NRT 2017b) and Wood River (NRT 2016c) sites; but as described in Comment k., those model reports do not provide details on how the dispersion values were derived. The Meredosia model report (Geotechnology 2016) does not mention whether dispersion was modeled.

These examples show the need for regulations that require contaminant attenuation and dispersion to be evaluated and modeled if appropriate for the site.

Comment g. Model calibration is poor and calibration is not quantitatively assessed

Accurate model calibration is critical to ensure that model predictions of closure and corrective action performance are accurate. Groundwater models are typically calibrated, by adjusting model parameters, so that they match field measured groundwater elevations and measured or calculated flow rates. These measurements are referred to as calibration targets. Standard modeling practices include having pre-defined calibration targets, goals for model calibration accuracy, and the model calibration and accuracy is quantitatively assessed (Anderson et al. 2015). It is important that calibration targets include as much of the available site data as possible to produce an accurate model. The closure plan models we reviewed fail to set calibration criteria or quantitatively assess the accuracy of the calibration. Furthermore, it is obvious from the results reported that the models are very poorly calibrated giving little faith that these models are capable of simulating actual site conditions.

The Hennepin Groundwater Model Report (NRT 2017b, p. 9) includes the simple statement, “modeled heads at all monitoring wells fall within the range of observed values.” The problem with this approach is there a large range of observed groundwater elevations at each well and the fact that the modeled value falls within that range has little bearing on the model accuracy. The Hennepin report also includes figures of modeled and measured head and concentration showing the model poorly simulates the existing data. There is no assessment in the report of how the poor calibration affects model predictions.

The Meredosia groundwater model report (Geotechnology 2016) provides no data or discussion on the model calibration residuals or accuracy of the calibration.

In the Wood River model (NRT 2016c), the calibration apparently only used a single month's water level measurements for head calibration, from November 2014, despite the Hydrogeologic Site Characterization Report (NRT 2016) tabulating quarterly water level monitoring for 2010-2015 and indicating that monitoring wells were installed in 1982. The Wood River model is reported to be calibrated to measured boron concentration time-series from numerous wells for 1995-2015; however the graphs showing measured and modeled concentration show a very poor calibration; in many of the wells, the trend in measured concentration is opposite of that produced by the model.

Standard practices for model calibration should include the following:

1. The modeling effort should identify predetermined quantitative calibration targets that model calibration seeks to meet (Anderson et al. 2015).
2. A summary statistical target for head calibration target for each modeled time period (Anderson et al. 2015).
3. Model calibration should seek a normal distribution of model error for each time period (Anderson et al. 2015).
4. The model calibration process should seek to remove any negative or positive bias in modeled head and any departures from normal distribution of head or concentration residuals should be explained (Anderson et al. 2015).
5. Flow/flux calibration targets should be included in each calibration effort because different combinations of the ratio of groundwater recharge to hydraulic conductivity will lead to the same modeled head (i.e. head calibration targets cannot identify unique solutions). Flow/flux calibration targets can use measured groundwater discharge to a river or spring, calculated flow and velocity from tracer tests or analysis of contaminant plume breakthrough time, calculated groundwater flow based on field measured gradients and hydraulic conductivity, or other supportable methods for determining groundwater flow, discharge, or recharge (Anderson et al. 2015).
6. The groundwater budget developed for the modeled area (described in Comment c.) should be compared to the modeled water budget (Anderson et al. 2015).
7. Model boundary condition response to modeled stresses should be checked to ensure that it is reasonable and conforms to assumptions that were made when choosing boundary type and value (Reilly and Harbaugh 2004).
8. Modeled concentration should simulate measured contaminant impacts within calibration criteria. Specifically, the model must simulate concentrations accurately in areas where contaminants have been measured above water quality standards.
9. Model results which fall outside of the calibration targets should be evaluated in the model documentation as to potential reasons why the model cannot be calibrated for the specific observation location and the potential effects that lack of calibration has on model predictions.

These examples show that regulations should require calibration targets to be developed prior to modeling, and the performance of model calibration should be quantitatively described in the modeling report.

Comment h. Modeling does not evaluate the effects of groundwater contact with CCR

All three of the CCR facilities we reviewed have a high water table, and the CCR is frequently inundated with groundwater. This is a common situation where coal fired power plants are sited next to a major river and the impoundments are constructed on the floodplain. The regular inundation of CCR in unlined or poorly lined impoundments creates a perpetual source of contamination to groundwater because the high groundwater will rewet the CCR even after the CCR impoundment is capped and closed. This contaminant pathway should be evaluated in all closure plans and accounted for in models used to predict the performance of the closure plan. However, all three of the modeling efforts reviewed either ignore or dismiss the contaminant pathway.

Both field data collected during the site characterization effort and modeling need to be specifically directed at measuring groundwater inundation and evaluating the resulting contaminant release. Continuous groundwater level data are needed to evaluate the frequency and magnitude of groundwater inundation. Water level measurements should be recorded at least daily in one monitoring well upgradient and one downgradient of the CCR unit. Wells installed to comply with the Federal CCR Rule (40 CFR Subpart D) located at the waste boundary and in the uppermost aquifer should be used for monitoring separation from groundwater. Water level data loggers are widely available and economical for recording continuous water levels; despite this, not one of the three sites we reviewed reported using digital technology to monitor continuous water levels in monitoring wells.

The Hennepin site experiences inundation of CCR by groundwater during regular flood events on the Illinois River. The Hennepin Groundwater Model Report Section 1.2.4 (NRT 2017b, p. 3) acknowledges that these flood inundation events impact contaminant release from CCR: “occasional increases in boron concentrations were observed to coincide with the precipitation/flood events and localized saturation of the ash.” However, the groundwater modeling performed to predict the performance of the proposed closure plan (NRT 2017b) disregards this impact. The modeled leachate is inclusive of only precipitation percolating through the CCR and ignores the effects of groundwater rise rewetting CCR. No evidence is provided in the Hennepin model report that contaminant release from flood inundation of the CCR is not a cause of groundwater standard exceedances.

We compared the river stage to the quarterly groundwater level monitoring data presented in the Hennepin Hydrogeologic Site Characterization Report (NRT 2017) to evaluate if quarterly monitoring was capturing the magnitude and frequency of groundwater inundation. Figure 3 shows the Illinois River stage near the Hennepin site. For reference, the orange boxes in Figure 3 are the dates of quarterly water level measurements (see Table 4 below). On 6/22/2015, the highest quarterly ground water level is reported in the Hennepin Hydrogeologic Site Characterization Report (NRT 2017); the level was greater than 4 ft above the lowest CCR in Pond No. 2. The second highest quarterly measurement was taken on 6/6/2013 when the river stage was slightly over 25 ft and the groundwater was 0.5 ft above the lowest CCR.

Figure 3. Illinois River stage at USGS 05558300 at Henry, Illinois near the Hennepin site. Orange boxes denote the dates of quarterly groundwater monitoring.

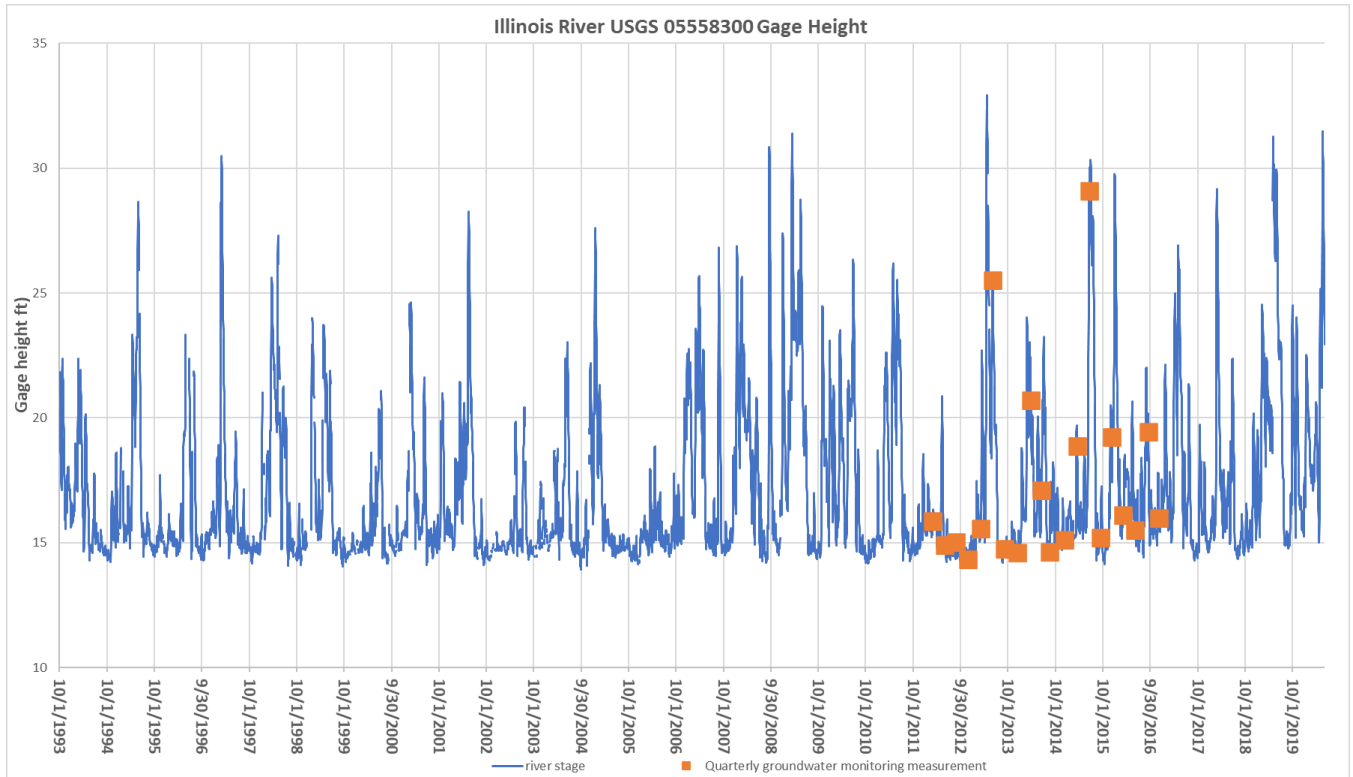


Figure 3 shows the river stage is commonly as high as it was during 6/22/2015 and reaches the 25 ft level at which the CCR begins to inundate approximately annually. The orange boxes illustrate that quarterly groundwater level data miss the frequency and magnitude of periodic inundation events presented in the continuous hydrograph for the Illinois River because quarterly measurements miss the highest groundwater levels in all years, and missed the flood event in years when the annual hydrograph peak occurs between quarterly measurements. Daily data is needed to measure the frequency and magnitude of groundwater inundation and to assess whether CCR impoundments will continue to produce leachate and contaminate groundwater in perpetuity.

Table 4. Reported CCR separation in quarterly groundwater monitoring from the Hennepin Site. Negative values highlighted indicate the CCR is inundated with groundwater. (Data adapted from NRT 2017)

Date	MW-10 water level	MW-03/03R water level	Bottom of CCR in Pond No. 2	Separation at south side (MW-10)	Separation at north side (MW-03/03R)
3/1/2012	446.31	446.27	451	4.69	4.73
5/30/2012	446.49	446.39		4.51	4.61
8/28/2012	444.72	444.68		6.28	6.32
11/27/2012	446.35	446.22		4.65	4.78
3/7/2013	445.73	445.61		5.27	5.39
6/6/2013	451.56	451.62		-0.56	-0.62
9/3/2013	445.72	445.63		5.28	5.37
12/11/2013	447.13	446.08		3.87	4.92
3/26/2014	449.01	448.9		1.99	2.1
6/18/2014	447.83	447.75		3.17	3.25
8/20/2014	448.04	447.76		2.96	3.24
12/9/2014	447.01	NR		3.99	
3/18/2015	447.01	446.98		3.99	4.02
6/22/2015	455.52	455.64		-4.52	-4.64
9/16/2015	448.32	447.92		2.68	3.08
12/8/2015	449	448.75		2	2.25
3/8/2016	447.63	447.33		3.37	3.67
6/7/2016	448.63	448.25		2.37	2.75
9/15/2016	450.27	450.05		0.73	0.95
12/9/2016	448.2	447.87	2.8	3.13	

The lack of consideration for CCR groundwater inundation in the Hennepin model may explain why the model calibration required adding a leachate source not explained by the site conceptual model. NRT reports that model calibration required including a small strip of greatly enhanced contaminant release, “Ash Pond No. 2 - High Recharge Area,” along the bottom of Pond No. 2 with a leachate percolation rate equal to 197.1 in/yr (16.4 feet per year). These contaminant source boundaries, concentrations, and loading rates are shown visually in Appendix 3; contaminant loading rates are summarized in Table 5. In fact, this area of enhanced leachate is the greatest source of contamination in the model, despite this being a closed and reportedly “dewatered” CCR pond.

Table 5. Summary of modeled boron load in the Ash Pond No. 2 “high recharge area” (Summarized from calculated loads in Table 2).

Modeled contaminant source	Boron load (kg/day)
Closed Ash Pond No. 2 "high recharge areas"	2,736
All other simulated contaminant sources including the active Primary Pond, Polishing Pond, and higher elevation areas of closed Ash Pond No. 2.	2,355

The fact that model calibration required adding this area of extremely high input of CCR leachate from the closed and reportedly “dewatered” Ash Pond No. 2 likely indicates that in reality contaminants are being released by periodic inundation of the lowest CCR in the pond when the Illinois River floods. This exemplifies the need for groundwater models to include realistic assessment and simulation of the daily groundwater hydrograph and any contact or inundation between groundwater and CCR.

We developed similar tables of CCR inundation at the Meredosia and Wood River sites. Table 6 shows the quarterly measured separation between groundwater and CCR at the Meredosia site. Similar to Hennepin, the Wood River site experiences regular inundation by groundwater which is not accounted for in the modeling. Figure 4 shows orange boxes on the dates of the quarterly groundwater monitoring. The orange boxes show that quarterly groundwater level monitoring does not occur during the peak hydrograph shown in blue, and most years the quarterly monitoring fails to capture groundwater elevation during the flood event at all. This again indicates that the frequency and magnitude of the inundation is not accounted for in the quarterly monitoring. The 6/24/2011 water level measurement was not completed at the downgradient wells APW-2 and APW-3 apparently because the river was flooding and the monitoring wells were submerged. Appendix 4 shows an air photo of the Meredosia site with the Illinois River at flood stage on 4/29/2013, indicating that during regular flood events the river encroaches on the CCR impoundment and the downgradient wells are submerged.

Table 6. Reported CCR separation in quarterly groundwater monitoring from the Meredosia Site. Negative values highlighted indicate the CCR is inundated with groundwater. (Data adapted from Geotechnology 2016)

Date	APW-2 water level	APW-3 water level	APW-5 water level	Bottom of CCR in Fly Ash Pond	Separation at APW-2	Separation at APW-3	Separation at APW-5
11/17/2010	423.87	422.76	427.6	426	2.13	3.24	-1.6
12/13/2010	423.73	422.93	427.8		2.27	3.07	-1.8
3/14/2011	428.57	430.58	430.6		-2.57	-4.58	-4.6
6/24/2011	no data	no data	438.5				-12.5
9/15/2011	424.22	422.38	429.8		1.78	3.62	-3.8
10/28/2011	423.27	421.68	428.7		2.73	4.32	-2.7
3/26/2012	423.6	423.48	426		2.4	2.52	0
6/18/2012	422.41	422.33	425.9		3.59	3.67	0.1
9/17/2012	421.28	420.36	424.02		4.72	5.64	1.98
8/25/2015	427.2	425.18	434.65		-1.2	0.82	-8.65
12/21/2015	427.82	431.49	429.53		-1.82	-5.49	-3.53
2/18/2016	428.66	427.54	433.78		-2.66	-1.54	-7.78

Note: Elevation of the bottom of fly ash is assumed from the berm top surface elevation contours in Geotechnology Hydrogeologic Characterization Report plate 2 and the reported Fly Ash Pond height of 24'. Plate 2 shows the current lowest upper surface elevation of CCR in the Fly Ash Pond is 431'.

Figure 4. Illinois River stage at USGS 05585500 at Meredosia, Illinois. Orange boxes denote the dates of quarterly groundwater monitoring.

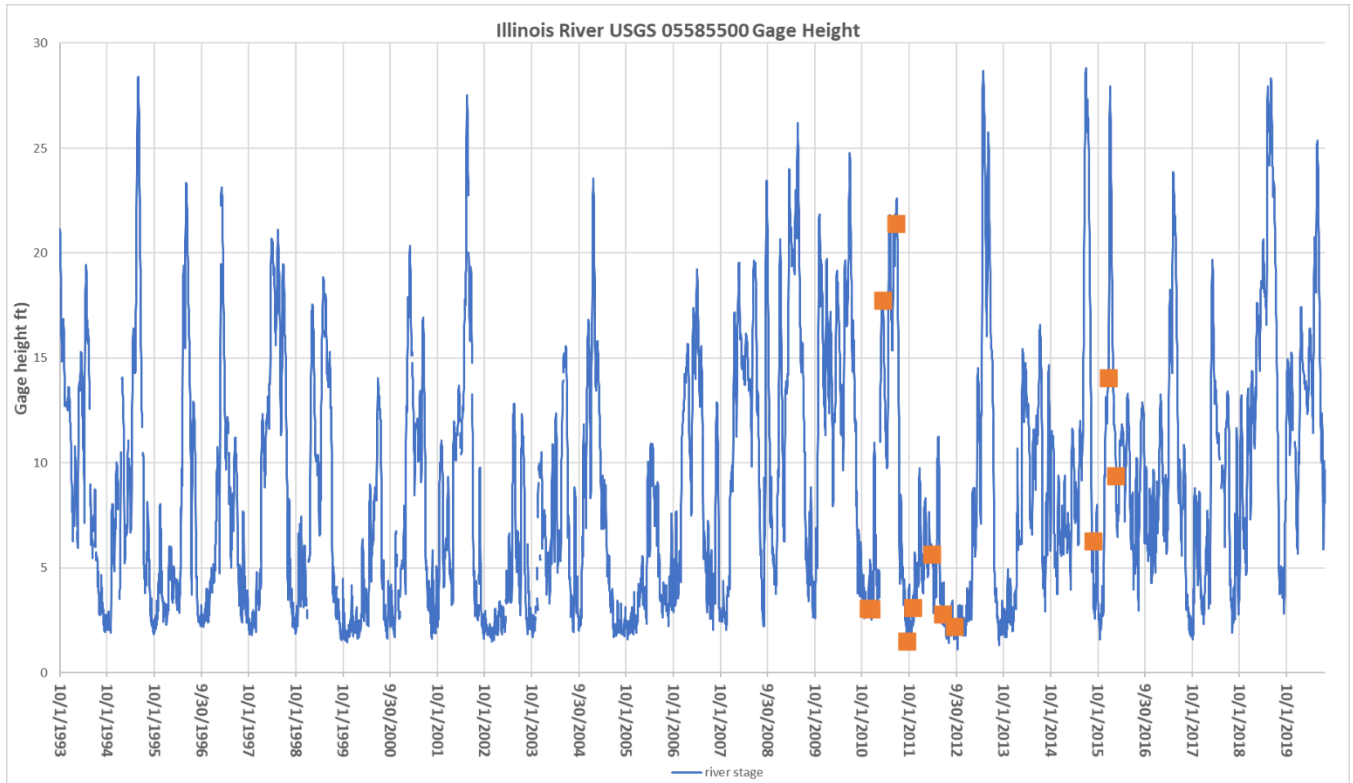


Table 7 shows the separation between groundwater and CCR at the Wood River Site. The West Ash Pond Complex at Wood River Power Station was constructed on the floodplain of the Mississippi River, partially on what was a backwater area prior to power plant construction (shown in Figure 5 below). The area was a wetland prior to construction of the ponds and wetlands are currently present just outside of the pond berm. The wetlands indicate that high groundwater levels are a natural and continuing occurrence in the area. Groundwater levels further increase when river stage increases. Highlighted values in Table 7 indicate that the CCR has been inundated by groundwater up to approximately 12 feet deep during the available quarterly measurements. The CCR in the ponds is rewetted when it is inundated by groundwater, regardless of what efforts are made to cap the pond. The modeling performed for the Wood River Closure Plan ignores this contaminant pathway and is incapable of accurately predicting the long-term performance of the closure.

Table 7. Reported CCR separation in quarterly groundwater monitoring from the Wood River Site. Negative values highlighted indicate the CCR is inundated with groundwater. (Data adapted from NRT 2016)

Date	well 04 water level	well 32R water level	well 02 water level	Bottom of CCR in Pond 1 and 2W	Liner in Pond 2E	Separation at Pond 1 south side (well 02)	Separation at Pond 2W west side (well 04)	Separation at Pond 2W north side (well 32R)	Separation at Pond 2E (well 32R)
Mar-10	407.1	407.98	406.4	407	415	0.6	-0.1	-0.98	7.02
Jun-10	411.93	412.82	414.36			-7.36	-4.93	-5.82	2.18
Sep-10	411.74	411.89	413.47			-6.47	-4.74	-4.89	3.11
Nov-10	407.26	408.42	406.7			0.3	-0.26	-1.42	6.58
Mar-11	411.24	409.16	412.76			-5.76	-4.24	-2.16	5.84
Jun-11	414.38	415.27	418.78			-11.78	-7.38	-8.27	-0.27
Sep-11	405.68	407.7	405.73			1.27	1.32	-0.7	7.3
Nov-11	403.23	405.36	403.01			3.99	3.77	1.64	9.64
Mar-12	408.92	407.52	408.16			-1.16	-1.92	-0.52	7.48
Jun-12	405.38	406.32	404.6			2.4	1.62	0.68	8.68
Aug-12		403.72	400.55			6.45		3.28	11.28
Nov-12	404.06	403.27					2.94	3.73	11.73
Feb-13	404.41	403.53	401.8			5.2	2.59	3.47	11.47
May-13	415.13	413.78	417.9			-10.9	-8.13	-6.78	1.22
Aug-13	407.36	407.74	404.19			2.81	-0.36	-0.74	7.26
Nov-13	404.27	404.44	401.95			5.05	2.73	2.56	10.56
Feb-14	406.46	404.63	403.71			3.29	0.54	2.37	10.37
May-14	410.8	408.84	409.78			-2.78	-3.8	-1.84	6.16
Sep-14	409.2	407.85	406.62			0.38	-2.2	-0.85	7.15
Nov-14	405.7	406.78	403.98			3.02	1.3	0.22	8.22
Mar-15	405.24	405.25	402.75			4.25	1.76	1.75	9.75
May-15	410.13	408.33	408.91			-1.91	-3.13	-1.33	6.67
Sep-15	406.95	408.74	405.71			1.29	0.05	-1.74	6.26
Nov-15	403.21	404.98	402.18			4.82	3.79	2.025	10.025

Notes: Elevation of the bottom of CCR in Ponds 1 and 2W and liner elevation in Pond 2E is reported in NRT (2016).
 Indicates CCR is inundated with groundwater in Ponds 1 and 2W or above the liner in Pond 2E.

Figure 5. Location of the Wood River Power Station West Ash Pond Complex shown on a 1941 aerial photo.



These examples show that regulations are needed to ensure that contact between CCR and groundwater is adequately described in the hydrogeologic site characterization. Regulations are also needed to ensure that contaminant leaching to groundwater is adequately characterized and accurately portrayed in groundwater models.

Comment i. Variations in groundwater flow direction are not adequately accounted for in site characterization, water quality monitoring, or modeling

All three sites we reviewed experience periodic reversal of groundwater flow when rivers adjacent to the site have elevated stage. These flow reversals should be accounted for in groundwater modeling because they have the capability of transporting contaminant plumes in what would otherwise be upgradient directions. Variations in groundwater flow have important implications for, and should be accounted for, in developing conceptual site models, choosing background monitoring wells, alternative source demonstrations, and groundwater modeling. Ignoring significant variability in groundwater flow direction may cause corrective actions and

closure plans to miss critical contaminant pathways to groundwater and to human or environmental receptors.

The Hennepin groundwater model and background monitoring wells all assume that groundwater flows in a single direction, typical of non-flooding conditions on the Illinois River. The Hennepin Hydrogeologic Site Characterization Report (NRT 2017) states that groundwater flow was reversed, away from the Illinois River, during three quarterly groundwater monitoring events, indicating the flow reversal is a common occurrence. However, as discussed in Comment b. above the Hydrogeologic Site Characterization Report does not provide data for every monitoring event and instead focuses on relatively small window of recent data. As discussed in Comment h. and shown in figure 3, the Hennepin quarterly groundwater level measurements commonly miss peak stage in the Illinois River, and likely miss periods of groundwater flow reversal. The available data indicate that it is likely that groundwater flow reversals are a common occurrence at the site. Despite this, the Hennepin model treats the Illinois River as a static boundary with a stage equal to typical low flow conditions. Figure 3 shows that there is no typical stage for this river; stage is inherently variable, which results in variable flow direction and contaminant release as described in other comments in this document. This underscores the importance of both considering the variability in groundwater flow direction in the site conceptual model and modeling surface water features that affect groundwater flow with transient (variable) stage.

The Hennepin Hydrogeologic Site Characterization Report and groundwater modeling discussion seeks to minimize these groundwater flow reversals, suggesting they are short term and without consequence; but the data provided to support this is inadequate. In fact, they present an analysis of water quality during the flood event for wells which are actually upgradient during the flow reversal to attempt to show that the flooding does not release contaminants.

We used data provided in the Hennepin Hydrogeologic Site Characterization Report to evaluate how far groundwater flows during a flow reversal in what is normally the upgradient direction in order to assess potential impacts to background monitoring wells or receptors off the site.

Table 8 shows groundwater flow velocity provided in the Hennepin Site Characterization Report under typical (non-flooding) conditions. This is the flow direction and velocity considered in the groundwater model (NRT 2017b) and groundwater monitoring plan.

Table 8. Groundwater flow velocities September and December of 2015 (excerpt from NRT 2017, Tbl. 3)

Hydrogeologic Site Characterization Report
East Ash Pond No. 2, Hennepin Power Station

September 16, 2015				
	Average Hydraulic Conductivity (cm/s)	Horizontal Hydraulic Gradient	Effective Porosity	Velocity (ft/day)
Well 10 to Well 03R	2E-01	0.0006	0.22	1.5
Well 12 to Well 05R	8E-03	0.0003	0.22	0.03
Well 17 to Well 12	2E-02	0.003	0.22	0.7
December 8, 2015				
	Average Hydraulic Conductivity (cm/s)	Horizontal Hydraulic Gradient	Effective Porosity	Velocity (ft/day)
Well 10 to Well 03R	2E-01	0.0004	0.22	0.9
Well 12 to Well 05R	8E-03	0.0002	0.22	0.02
Well 17 to Well 12	2E-02	0.002	0.22	0.5

Note:

1) cm/sec x 2,835 = feet/day

2) Source of hydraulic conductivity values was the Initial Facility Report for the New Coal Combustion Landfill (Kelron/NRT, December 10, 2010)

In Table 9, we recalculate the groundwater flow velocity from table 8, using the reported groundwater flow gradient of 0.01 (section 3.3.2.2 of NRT 2017, p. 11) when flooding of the Illinois River causes groundwater flow to reverse direction.

Table 9. Groundwater velocity at the Hennepin site during a flood caused groundwater reversal.

	Average Hydraulic Conductivity (cm/s)	Horizontal Hydraulic Gradient	Effective Porosity	Velocity (ft/day)	Distance water would travel in 30 days (ft)
Well 10 to Well 03R	2.00E-01	0.01	0.22	25.77	773
Well 12 to Well 05R	8.00E-03	0.01	0.22	1.03	31
Well 17 to Well 12	2.00E-02	0.01	0.22	2.58	77

The groundwater flow gradient is relatively much steeper during the flood reversal, approximately seventeen to fifty times steeper underneath Pond No. 2 compared to the dates presented in the Closure Plan (Table 8). Groundwater flow is therefore be seventeen to fifty times faster. This high velocity of groundwater moving in what is typically the upgradient direction has the potential to transport significant contamination a long distance in a short period of time. It also has the potential to leach CCR at an accelerated rate.

The last column in Table 9 shows that groundwater could travel up to 773 ft during a 30-day long flooding reversal. Our analysis of groundwater velocity does not consider dispersion and attenuation, because these are in-depth analyses that need to be performed in the site characterization. Our analysis does however exemplify how far into the typically upgradient

direction that conservative contaminants may be transported. In Dynegy's monitoring plan, "upgradient" monitoring well (08/08D) is only 200' south of a leaky, unlined CCR impoundment. This "background" well is likely impacted by periodic reversal of groundwater flow direction. Background wells are supposed to be unimpacted by site contaminants; but this example shows this may not be the case. Site characterization and monitoring plans should account for flow reversals when selecting background wells and models should accurately portray contaminant transport during a flow reversal.

The Wood River site also frequently experiences groundwater flow reversal. The potential for impacts to offsite wells is higher at Wood River because there are community public water supply wells in the direction that flow reverses. The Wood River Hydrogeologic Site Characterization Report (NRT 2016, p. 2-6) reports there are 42 off site water wells within a 2,500 feet radius of the Wood River Power Station property and five of these are community water supply wells.

The Wood River Hydrogeologic Site Characterization Report (NRT 2016) and Groundwater Model Report (NRT 2016c) lack adequate analysis of potential impact to these wells. The Hydrogeologic Site Characterization Report for Wood River (WRPS) states, "The results of the water well survey, combined with the information contained within the annual groundwater monitoring reports, indicate that there are no water wells, potable or non-potable, that are likely to be impacted by groundwater from the West Ash Pond Complex with the exception of wells located directly south of the WRPS. All other water wells, located to the northwest, north, northeast, east, and southeast, are either upgradient during most the year (i.e. are not downgradient of the prevailing southerly direction of groundwater flow), and/or are located beyond a groundwater to surface water discharge zone (i.e., Wood River). The potential for groundwater emanating from the West Ash Pond Complex to affect wells located anywhere but directly south of the WRPS is very low." (NRT 2016, p. 2-7).

The Wood River Hydrogeologic Site Characterization Report includes insufficient data and supporting evidence for the conclusion that the potential for groundwater from the ponds to affect these off-site wells is "very low." According to the Hydrogeologic Site Characterization Report, the groundwater flow is reversed for approximately 1/3 of each year. This suggests that there is no consistent upgradient direction that is safe from contaminants owing solely to its location. No evidence is provided that the Wood River is a "groundwater to surface water discharge zone" during a flow reversal and Figure 9 shows groundwater flowing from the ponds in the direction of the City of East Alton public water supply well field, the location of which is shown in Appendix D of NRT (2016).

Additionally, there is no indication that the Wood River model (NRT 2016c) simulates these flow reversals. The model simplifies the hydrograph of the Mississippi River into two generalized river stage time periods, using the average river stage measured by US Army Corp of Engineers adjacent to the site for March through July (flood stage) and August through February (base stage) NRT 2016c, tbl. 3-3). The problem with this approach is flood stage is effectively averaged out using a 5-month mean and the model does not simulate the conditions of the flow reversal. The flow model is only calibrated to groundwater elevation measurement from a single

month during base stage and the model calibration is generally poor as discussed in Comment g. above. Model inaccuracy owing to the averaging of river stage is compounded because the model also fails to account for groundwater inundation of the CCR located in the unlined impoundments occurring approximately two thirds of the year, which we describe in Comment h.

These examples illuminate the need for regulations to require that hydrogeologic site characterizations analyze the effects of transient variations in groundwater flow and account for that variability in groundwater models and water quality monitoring plans.

Comment j. Forecast uncertainty

None of the groundwater modeling efforts we reviewed evaluate the uncertainty in the modeling predictions and how the level of accuracy achieved by the model should be interpreted when reviewing the model predictions regarding closure plan performance and contaminant plume dissipation over time. Modeling practices commonly include a sensitivity analysis which evaluates how adjustments to model parameter values (e.g. +/- 25%) affect calibration. The result of the sensitivity analysis is a quantitative understanding of how much the various model parameters influence model calibration. More highly sensitive parameters should ideally be subject to better accuracy because inaccuracies in their modeled values have correspondingly more influence on model results. The three model reports we reviewed all evaluate the sensitivity of various model parameters and find that the model is highly sensitive to a number of the modeled parameters, such as hydraulic conductivity, source concentrations, river boundaries, etc. But the modeling reports do nothing with the revelation that the model is highly sensitive to parameters, many of which are poorly defined or simulated in the model.

The sensitivity analyses typically provided with groundwater modeling reports can identify which model parameters the solution and forecast predictions are most sensitive to, but it is not capable of identifying the range of possible solutions given uncertainties in site data. To evaluate the effects of sensitive parameters on model accuracy, forecast uncertainty analysis is now a standard modeling procedure for models which are used to make regulatory decisions based on quantitative modeling predictions such as the ability of a closure plan to meet water quality standards. The components of a forecast uncertainty analysis are described in detail by Anderson et al. (2015). A forecast uncertainty analysis will allow the electric power utility to adequately describe model uncertainty and to explain the range of potential performance outcomes of closure plans and corrective actions.

We recommend that a forecast uncertainty analysis be performed at a minimum for modeled sites where water quality sampling or the site conceptual model indicates potential risk to human health and drinking water supplies, not just sites with existing data showing offsite migration of contaminants exceeding human health standards. The forecast uncertainty analysis should assess the minimum to maximum range of values in the calculated water balance and hydraulic parameters. At a minimum, the forecast uncertainty analysis should test the highly sensitive model parameters.

Comment k. Modeling documentation does not include all of the information necessary to understand and review the model

IEPA and the public need to have a complete understanding of the source of data and rationale for model set up to review groundwater models used to predict closure performance. The source of model parameter values and boundary condition choices must be clearly laid out in the modeling documentation provided with the Closure Plan. Additionally, the model report should describe how the model was developed to agree with the conceptual site model (described in detail in Comment a), and the modeling methods used and their appropriateness to the problem being solved (Reilly and Harbaugh 2004). All documentation of model development should be included in the modeling report; it is not sufficient for an owner/operator to reference previous modeling documentation they have prepared that is not included as an attachment to the modeling report or easily available to the public. Publicly available documents such as hydrogeologic studies or scientific literature may be concisely referenced and not attached; however the appropriateness of the data sourced from such reports should be described in the modeling report.

The modeling documents we reviewed in some cases do not adequately document model development. For instance, in the Hennepin site Groundwater Modeling Report (NRT 2017b, p. 6), the description of the development of the hydraulic conductivity array is not provided: “The hydraulic conductivity values were based on the 2010 model.” The referenced document is not available on Dynegey’s public document page (<https://www.luminant.com/ccr/>) and the modeling report does not indicate where the document can be obtained.

The Meredosia groundwater model documentation (Geotechnology 2016) provides very little information on model development. It does not report hydraulic conductivity values, boundary condition flux rates, modeled river stage, or any quantitative information on model calibration.

The Wood River model does not describe the source of the leachate concentration value used and does not provide any quantitative information on model calibration as described in Comment g. above. The Wood River Groundwater Model Report states that flow and transport percolation rates for the East Ash Pond Complex were taken from the Transport Model Investigation for the New East Ash Pond (NRT 2006), but that report is not attached to the modeling documentation. The report also assigns stage elevation to the Mississippi River, a highly sensitive model boundary, based on the previous report (NRT 2000); that report is not attached to the modeling report and the data is twenty years old. (NRT 2016, p. 1-2). Contemporary data should be included, and the entirety of the data record presented in the modeling report.

Adequate modeling documentation is necessary for IEPA to be able to thoroughly review models prepared by CCR facility owner/operators. Our review of the model reports generated for the three sites in Illinois indicate that owner/operators may not adequately document model development either because the importance of model documentation is not understood, it is costly to do so, or proper documentation will reveal severe deficiencies in the modeling process.

Model documentation should be adequate such that the public can provide third party review of the model. Members of the public often have irreplaceable knowledge of local hydrogeology,

soil, geology/seismic, and climatic conditions which are relevant to site characterization and modeling. It is our professional experience that state natural resource agencies and geologic surveys and researchers at nearby colleges and universities often have the most accurate and in-depth knowledge of these site-specific conditions. Consultants who work for coal plant owner/operators may be from out-of-state and lack this site-specific knowledge. Public review and comment is needed for IEPA to have all available relevant information to ensure local site-specific knowledge is included in model development, sensitive receptors are identified, and models are thoroughly reviewed. Our review supports the need for a regulatory requirement that model documentation provide a complete description of the model development, parameter arrays, boundary attributes, and quantitative calibration assessment. All of this information should be included in the model report. We also recommend that IPCB require IEPA to develop model review guidance such as Reilly and Harbaugh (2004), or at a minimum, a model review checklist specific to modeling Illinois CCR facilities to ensure that models are appropriately developed and include the required elements in the proposed rule language in section 4.

Comment l. Plans which leave CCR in contact with groundwater are likely to result in long-term exceedance of water quality standards and require perpetual plume monitoring and institutional controls

The closure plans for the Hennepin (CEC 2018), Meredosia (Geotechnology 2016b), and Wood River (AECOM, 2016) all propose to leave CCR in place with cover systems designed to limit the infiltration of precipitation into the CCR impoundment. In each case, CCR in unlined impoundments at the facility is inundated by groundwater during some portion of a typical year (see Comment h for further discussion). In each case, the owner/operator of the facility has prepared a closure plan with supporting models that ignore, and descriptive analysis which seeks to discount, the fact that the CCR is periodically inundated with groundwater. In none of these instances have the owner/operators quantitatively evaluated the contribution to the contaminant plume from reoccurring inundation of the CCR by groundwater, nor have they predicted the effects of this into the future. It is our opinion that periodic inundation of the CCR will rewet the CCR leading to perpetual water quality impacts.

The water quality impacts will likely include long-term exceedance of water quality standards in groundwater. Long-term water quality exceedances will require institutional controls such as regular water quality monitoring, groundwater control zones, or other water use restrictions to avoid human consumption of the impacted water. The potential need for long-term institutional controls is not accounted for in the closure plans because they fail to adequately model and predict the periodic inundation of the CCR by groundwater. It is our opinion that the water quality monitoring and institutional control needs will likely long surpass the 30-year post closure timeframe which is planned for. The safest method available to avoid long-term water quality exceedances, risks to human health, and institutional control requirements for CCR impoundments which are regularly in contact with groundwater is to excavate and remove the CCR to a landfill compliant with current federal regulations (40 CFR Subpart D). Other states such as Montana (Montana DEQ 2019, Montana DEQ 2020) have required owner/operators to remove CCR that is in contact with groundwater where it is causing exceedances of water quality

standards and the owner/operator has not provided an alternative remedy capable of eliminating long-term leaching of the CCR.

In the absence of adequate analysis and modeling demonstrating that inundation of CCR by groundwater will not cause water quality exceedances and that no alternative remedy exists to protect CCR left in place from groundwater contact, we recommend that CCR impoundments which have the potential to be regularly in contact with groundwater be excavated and removed to a federal compliant CCR landfill.

Comment m. The State of Illinois would benefit from a specific guidance document for groundwater flow and contaminant transport model development and review.

Illinois is developing new comprehensive rules for design, construction, operation, corrective action, closure and post-closure care of surface impoundments with CCR which include requirements for groundwater modeling. State and Federal agencies generally provide guidance or policy documentation to support work on complex technical requirements, such as groundwater flow and contaminant transport modeling. Rules alone may be insufficient to clearly define acceptable modeling practices. Currently, multiple states, USGS, U.S. EPA, and professional trade groups provide guidance or policy documentation on some or all aspects of groundwater flow and contaminant transport modeling, depending on their technical needs, regulatory requirements, and data quality objectives. There are also other textbooks and guidance useful to support meeting the requirements of the proposed rules which detail best practices. We found that most states and federal agencies opt for developing specific guidance or policy documentation that focuses on the specific technical needs or regulatory frameworks to which the guidance or policy applies versus requiring the use of textbook guidance that is germane to all modeling. Example modeling and policy guidance includes that offered by Georgia's Environmental Protection Division (GEPD 2016). Example model review guidance includes that offered by USGS (Reilly and Harbaugh 2004).

The State of Illinois would benefit from adopting an official groundwater and transport modeling guidance document under the proposed rule. The goal of the guidance would be to more clearly define best practices as they relate to the proposed rule and clarify the Agency's requirements for modelers attempting to meet requirements set by the Agency. The document should also include the procedures by which the Agency will review models developed under the proposed rule. States typically form a committee or authorize the state environmental regulatory agency to develop modeling guidance. IPCB should include in this rulemaking a requirement that a groundwater flow and transport modeling guidance document and model review document be developed that addresses the specific modeling needs relevant to CCR contaminated sites.

4. Recommend rule language

The following provides a roadmap between recommended changes to the R 2020-019 rulemaking proposal with references to the statement of need in Section 3, above. Proposed changes to rule language are organized by rule section. The box references and summarizes the statement of need for the proposed change and references the problem statement in Section 3.

Rule language that remains the same as the Agency's proposed language in the proposed rule are shown in black font; additions are shown in underline; deletions are shown in strikethrough.

845.220 Construction Permits

In Section 3 we present numerous examples of modeling deficiencies that occur with a lack of regulatory constraints on the site characterization, modeling, and model documentation. Changes proposed in this section seek to address the most critical elements required to prepare accurate groundwater flow and transport models of CCR facilities. We recommend the corrective action and closure performance modeling sections (845.220(c)(2) and (d)(3) respectively) specify minimum modeling requirements. The proposed changes outlined under this section as well as the proposed changes outlined to 845.620 Hydrogeologic Site Characterization discussed below address the following modeling needs.

Comment a. indicates the need for groundwater models to be based upon site characterization and conceptual site model. Parts B and H of (c)(2) and (d)(3) respectively address this need.

Comment b. indicates the need for groundwater models to be developed and calibrated using the entirety of site characterization data available. Parts B and H of (c)(2) and (d)(3) respectively address this need.

Comment c. indicates the need for model boundaries to be based on site data or actual field measurement. Part B and H of (c)(2) and (d)(3) respectively address this need.

Comment d. indicates the need for model hydraulic properties to be based on site-specific testing. Parts B and H of (c)(2) and (d)(3) respectively address this need.

Comment e. indicates the need for contaminant source concentration and CCR leachate flux to be accurately modeled. Parts B and F of (c)(2) and (d)(3) respectively address this need.

Comment f. indicates the need for models to consider transport attenuation for each contaminant and each geologic unit at the site. Parts B and H of (c)(2) and (d)(3) respectively address this need

Comment g. indicates the need for robust model calibration targets, better model calibration, and adequate reporting of model calibration performance. Parts C, D, E, and H of (c)(2) and (d)(3) respectively address this need.

Comment h. indicates the need to consider groundwater contact with CCR in alternative analyses and modeling. Parts B, F, and H of (c)(2) and (d)(3) respectively address this need.

Comment i. indicates the need to account for variability in groundwater flow direction in contaminant transport modeling and in evaluating the potential impacts to human and

environmental receptors, including drinking water supplies. Parts B, D, and H of (c)(2) and (d)(3) respectively address this need.

Comment j. indicates the need for analysis of uncertainty in model predictions to evaluate the range of simulated outcomes in contaminant transport and groundwater remediation. Parts G and H of (c)(2) and (d)(3) respectively address this need.

Comment k. indicates that model documentation needs to include all information for the Agency or public to review and understand model development, calibration, and predictive application. This comment also demonstrates that model documentation should describe the appropriateness of the chosen modeling methods to the problem being solved and conceptual site model. Part H of (c)(2) and (d)(3) respectively addresses this need.

Comment m. indicates the need for State of Illinois to develop an official groundwater flow and transport modeling guidance and policy document to more clearly define best practices as they relate to the proposed rule and remove any misunderstanding by modelers attempting to meet requirements set by the Agency. The document should also include procedures for model review by the Agency. Part L of (c)(2) and (d)(3) respectively addresses this need, but is reserved so that the Agency has sufficient time to develop and publish the guidance and policy document.

845.220 c) Corrective Action Construction

2) Groundwater modeling, including:

A) the results of groundwater contaminant transport modeling and calculations showing how the corrective action will achieve compliance with the applicable groundwater standards;

~~B) all modeling inputs and assumptions;~~

B) Model properties and boundaries based on the Hydrogeologic Site Characterization data and conceptual site model required in 845.620. Model boundary conditions shall be based on site characterization data or calculations or estimates informed by site characterization data and not be defined based on assumptions or determined during model calibration.

C) Pre-defined calibration targets which consider the entirety of available Hydrogeologic Site Characterization data required in 845.620. Calibration targets shall include head and flux targets.

D) Adequate model calibration. Calibration shall seek to achieve a normal distribution of model error for each time period and remove any negative or positive bias in modeled head.

E) Summary statistics for head and flux calibration for each modeled time period.

F) Calculated or modeled CCR leachate flux which accurately accounts for variable groundwater elevations and any contact between CCR and groundwater.

G) At sites where either existing water quality sampling, the site conceptual model, or Agency discretion indicates potential risk to human health and drinking water supplies, a model forecast uncertainty analysis. At a minimum, the forecast uncertainty analysis shall assess the estimated minimum to maximum range of possible values in boundary attributes and hydraulic parameters in which sensitivity testing of the calibrated model result in a change greater than 20% in Sum of Squared Residuals (SSR).

H) Modeling documentation including description of how the model is developed to represent the conceptual site model and data required in 845.620, a statement on the appropriateness of the chosen modeling methods for the purposes of simulating the flow and transport mechanisms described in the site conceptual model, complete description of modeling inputs and assumptions, assessment of calibration performance, evaluation of model results which fall outside of the calibration targets as to potential reasons why the model cannot be calibrated and the potential effects that lack of calibration has on model predictions, results of parameter sensitivity analysis, results of the model forecast uncertainty analysis if required under G. Model documentation shall include all information on model development and avoid the use of data sources or references which are not readily available to the public;

€I) description of the fate and transport of contaminants with the selected corrective action over time;

ĐJ) capture zone modeling, if applicable; and

€K) provide the Agency any necessary licenses and software needed to review and access both the model and the data contained within the model.

L) Reserved. Model development and review shall follow the Agency's official modeling guidance and policy document.

845.220 d) Closure Construction.

3) Groundwater modeling, including

A) the results of groundwater contaminant transport modeling and calculations showing how the closure will achieve compliance with the applicable groundwater standards;

~~B) all modeling inputs and assumptions;~~

B) Model properties and boundaries based on the Hydrogeologic Site Characterization data and conceptual site model required in 845.620. Model boundary conditions shall be based on site characterization data or calculations or estimates informed by site characterization data and not be defined based on assumptions or determined during model calibration.

C) Pre-defined calibration targets which consider the entirety of available Hydrogeologic Site Characterization data required in 845.620. Calibration targets shall include head and flux targets.

D) Adequate model calibration. Calibration shall seek to achieve a normal distribution of model error for each time period and remove any negative or positive bias in modeled head.

E) Summary statistics for head and flux calibration for each modeled time period.

F) Calculated or modeled CCR leachate flux which accurately accounts for variable groundwater elevations and any contact between CCR and groundwater.

G) At sites where either existing water quality sampling, the site conceptual model, or Agency discretion indicates potential risk to human health and drinking water supplies, a model forecast uncertainty analysis. At a minimum, the forecast uncertainty analysis shall assess the estimated minimum to maximum range of possible values in boundary attributes and hydraulic parameters in which sensitivity testing of the calibrated model result in a change greater than 20% in Sum of Squared Residuals (SSR).

H) Modeling documentation including description of how the model is developed to represent the conceptual site model and data required in 845.620, a statement on the appropriateness of the chosen modeling platforms for the purposes of simulating the flow and transport mechanisms described in the site conceptual model, complete description of modeling inputs and assumptions, assessment of calibration performance, evaluation of model results which fall outside of the calibration targets as to potential reasons why the model cannot be calibrated and the potential effects that lack of calibration has on model predictions, results of parameter sensitivity analysis, results of the model forecast uncertainty analysis if required under G. Model documentation shall include all information on model development and avoid the use of data sources or references which are not readily available to the public;

€I) description of the fate and transport of contaminants with the selected closure over time;

ĐJ) capture zone modeling, if applicable; and

€K) provide the Agency any necessary licenses and software needed to review and access both the model and the data contained within the model.

L) *Reserved.* Model development and review shall follow the Agency's official modeling guidance and policy document.

845.620 Hydrogeologic Site Characterization

In Section 3 we present numerous examples of modeling deficiencies that occur with a lack of regulatory constraints on the site characterization, modeling, and model documentation. Changes proposed in this section seek to ensure that adequate site characterization is specified in the rule, collected by the electric power industry, and that data is reported and available for groundwater modeling efforts.

Comment a. indicates a need for closure plans to provide a clearly defined Conceptual Site Model (CSM) and for the groundwater model to be based upon and agree with the CSM. Part (b)(20) addresses this need.

Comment a.1., c., and e. indicate the need for accurate leachate percolation rates based on accurate description of CCR contact with groundwater and describes how leachate percolation is being erroneously modeled using EPA's HELP model. Parts (b)(17)(A), (18), (19), and (20)(G) address this need.

Comment b. above indicates the need for the entire record of groundwater level elevation/water table depth to be evaluated in the site characterization and conceptual site model development. Parts (b)(17)(A) and (19) address this need.

Comment d. indicates the need for groundwater modeling to use site-specific values of hydraulic conductivity which is derived from testing of wells at the site for each hydrostratigraphic unit which has potential to transport contaminants. Part (b)(17)(B) and (20)(C) address this need.

Comment e. indicates that leachate concentration should be measured in each CCR unit, such that a statistically supportable estimate of the concentration is known. Part (b)(13) addresses this need.

Comment f. indicates that a site-specific analysis of contaminant attenuation and dispersion properties should be performed for each geologic unit which has the potential to transport contaminants to evaluate the transport characteristics of each parameter. Attenuation and dispersion data should be provided in the site characterization because it is relevant to the physical and chemical properties of the geologic layers present and should be considered in development of the conceptual site model. Parts (b)(16) and (20) address this need.

Comment g. indicates that accurate estimates of groundwater flux rates are needed to provide quantitative calibration targets that can constrain unique model solutions. Parts (b)(17)(F), (18), and (20)(F) address this need.

Comment h. indicates the need for Assessment of Corrective Measures and Closure Alternatives analysis to evaluate the frequency and magnitude of groundwater contact with CCR including a need to monitor groundwater level elevation/water table depth of the shallowest aquifer using continuous or daily records. Parts (b)(17)(A), (18), (19) and (20)(G) address this need.

Comment i. shows the need to evaluate the effects of variations in groundwater flow direction on contaminant transport and present the variable flow direction in potentiometric maps. Parts (b)(11), (17)(A), (17)(E), (20)(D), and (20)(E) address this need.

We recommend deletion of “seasonal and temporal fluctuations in groundwater flow” from (b)(2) because this is addressed in (b)(17)(A), (D), and (E), (b)(19), and (b)(20)(D).

We recommend deletion of “identified as migration pathways and geologic layers that limit migration” from (b)(17) because model calibration and predictive accuracy is a function of the accuracy of the entire model, not just those geologic layers which are contaminant migration pathways and aquitards that limit migration. Accurate hydraulic characteristics are needed for all groundwater pathways which significantly affect groundwater flow, not just those which affect contaminant migration.

845.620 a) The owner or operator of the CCR surface impoundment must design and implement a hydrogeologic site characterization.

b) The hydrogeologic site characterization shall include but not be limited to the following:

- 1) Geologic well logs/boring logs;
- 2) Climatic aspects of the site, ~~including seasonal and temporal fluctuations in groundwater flow;~~
- 3) Identification of nearby surface water bodies and drinking water intakes;
- 4) Identification of nearby pumping wells and associated uses of the groundwater;
- 5) Identification of nearby dedicated nature preserves;
- 6) Geologic setting;
- 7) Structural characteristics;
- 8) Geologic cross-sections;
- 9) Soil characteristics;
- 10) Identification of confining layers;
- 11) Identification of potential migration pathways;
- 12) Groundwater quality data;
- 13) Statistically supportable data for CCR leachate concentration measured from porewater in each CCR impoundment.
- ~~14~~14) Vertical and horizontal extent of the geologic layers to a minimum depth of 100 feet below land surface, including lithology and stratigraphy;
- ~~15~~15) A map displaying any known underground mines beneath a CCR surface impoundment;
- ~~15~~16) Chemical and physical properties of the geologic layers to a minimum depth of 100 feet below land surface. Properties reported shall include but not be limited to site-

specific contaminant attenuation and dispersion properties for each geologic unit which has the potential to transport contaminants associated with CCR at the site;

1617) Hydraulic characteristics of the each geologic layers, soil, or fill which significantly affect groundwater flow or contaminant transport identified as migration pathways and geologic layers that limit migration, including:

A) Groundwater elevation and water table depth. The entirety of the available groundwater elevation dataset for the site shall be included. Water table depth recorded at least daily in one monitoring well upgradient and one downgradient of the CCR impoundment.

B) hydraulic conductivities derived from tests performed at the site using standard practices for evaluating hydraulic conductivity. Each hydrostratigraphic/geologic unit containing shallow groundwater or which has potential to transport contaminants shall be tested;

C) effective and total porosities;

D) direction and velocity of groundwater flow; and

E) map(s) of the potentiometric surface. potentiometric maps representative of prevalent groundwater flow conditions, including maps demonstrating variability in the direction of groundwater flow that has the potential to affect contaminant transport;

F) measurements or estimates of groundwater flux rates, including recharge and discharge;

18) Modeled or measured CCR impoundment percolation rates which account for site specific groundwater elevations in part 17) A;

19) Measurements of CCR separation from groundwater, including daily groundwater elevation measurements where available, and evaluation of separation during seasonal high groundwater elevation for all CCR impoundments;

20) A conceptual site model description which includes at a minimum the following:

A) groundwater system boundaries;

B) geologic/hydrostratigraphic units that affect flow;

C) hydrogeologic properties for each hydrostratigraphic unit;

D) description of groundwater flow, any variability in flow direction, and effects on contaminant transport;

E) sources and sinks (recharge and discharge boundaries) such as precipitation, evapotranspiration, groundwater and surface water exchange, pumping, and seepage from power plant operations and CCR impoundments and landfills;

F) a groundwater budget based on the available information, which can be compared with the modeled water budget and boundary condition flux during model calibration;

G) contaminant sources and mechanisms of contaminant release to groundwater;

H) contaminant transport properties including attenuation and dispersion mechanisms;

~~1721~~) groundwater classification pursuant to 35 Ill. Adm. Code 620; and

~~1822~~) Any other information requested by the Agency.

845.660 Assessment of Corrective Measures

This section requires the Assessment of Corrective Measures to evaluate the performance of the potential corrective measures, but it does not reference the modeling requirements specified in Section 845.220. The groundwater flow and transport model is the appropriate tool to use to assess the performance of corrective measure alternatives. Specification of modeling requirements is needed for the modeling to be performed properly and to address the needs we outline in Section 845.220. Part (c)(1) addresses this need.

845.660 c) The assessment under subsection (a) of this Section must include an analysis of the effectiveness of potential corrective measures in meeting all of the requirements and objectives of the corrective action plan as described under Section 845.670 addressing at least the following:

- 1) The performance, reliability, ease of implementation, and potential impacts of appropriate potential remedies, including safety impacts, cross-media impacts, and control of exposure to any residual contamination. A description of the performance of corrective measures assessed using a model developed pursuant to Section 845.220 (c)(2);
- 2) The time required to begin and complete the corrective action plan; and
- 3) The institutional requirements, such as state or local permit requirements or other environmental or public health requirements, that may substantially affect implementation of the corrective action plan.

845.670 Corrective Action Plan

This section requires the Corrective Action Plan to attain groundwater protection standards and the Corrective Action Alternatives Analysis to predict the time required to achieve those standards, but it does not reference the modeling requirements specified in Section 845.220. The groundwater flow and transport model is the appropriate tool to use to predict the timeframe for attainment of groundwater protection standards. Specification of modeling requirements is needed for the modeling to be performed properly and to address the needs we outline in Section 845.220. Parts (d)(2) and (e)(1)(E) address this need.

845.670 d) The selected remedy in the corrective action plan must:

- 1) Be protective of human health and the environment;
- 2) Attain the groundwater protection standards as specified in Section 845.600. Prediction of corrective action attainment of groundwater protection standards shall be demonstrated using a model developed pursuant to Section 845.220 (c)(2);
- 3) Control the source(s) of releases so as to reduce or eliminate, to the maximum extent feasible, further releases of constituents in Section 845.600 of this Part into the environment;
- 4) Remove from the environment as much of the contaminated material that was released from the CCR surface impoundment as is feasible, taking into account factors such as avoiding inappropriate disturbance of sensitive ecosystems; and
- 5) Comply with standards for management of wastes as specified in Section 845.680(d).

e) Corrective Action Alternatives Analysis. In selecting a remedy that meets the standards of subsection (d) of this Section, the owner or operator of the CCR surface impoundment shall consider the following evaluation factors:

- 1) The long- and short-term effectiveness and protectiveness of the potential remedy(s), along with the degree of certainty that the remedy will prove successful based on consideration of the following:
 - A) Magnitude of reduction of existing risks;
 - B) Magnitude of residual risks in terms of likelihood of further releases due to CCR remaining following implementation of a remedy;
 - C) The type and degree of long-term management required, including monitoring, operation, and maintenance;
 - D) Short-term risks that might be posed to the community or the environment during implementation of such a remedy, including potential threats to human health and the environment associated with excavation, transportation, and re-disposal of contaminants;

E) Time until groundwater protection standards in Section 845.600 are achieved.
Prediction of the time to achieve groundwater protection standards shall be demonstrated using a model developed pursuant to Section 845.220 (c)(2);

F) The potential for exposure of humans and environmental receptors to remaining wastes, considering the potential threat to human health and the environment associated with excavation, transportation, re-disposal, containment or changes in groundwater flow;

845.710 Closure Alternatives

This section requires groundwater contaminant transport modeling but does not reference the modeling requirements specified in Section 845.220. Specification of modeling requirements is needed for the modeling to be performed properly and address the needs we outline in Section 845.220. Part (d)(2) addresses this need.

845.710 d) The analysis for each alternative completed pursuant to this Section must:

- 1) meet or exceed a class 4 estimate under the AACE Classification Standard, incorporated by reference in Section 845.150, or a comparable classification practice as provided in the AACE Classification Standard;
- 2) contain the results of groundwater contaminant transport modeling prepared pursuant with Section 845.220 (d)(3) and calculations showing how the closure alternative will achieve compliance with the applicable groundwater protection standards;
- 3) include a description of the fate and transport of contaminants with the closure alternative over time including consideration of seasonal variations
- 4) assess impacts to waters in the state.

5. References

- Anderson, M.P., Woessner, W.W., and Hunt, R.J., 2015. Applied Groundwater Modeling. 2nd ed. Elsevier Press (textbook, not provided as attachment).
- AECOM, 2016. Closure and Post-Closure Care Plan for the Wood River West Ash Complex. Prepared for Dynegy Midwest Generation LLC. October 2016.
- CEC, 2018. Closure and Post-Closure Care Plan for the Hennepin East Ash Pond No. 2 Hennepin Power Station Putnam County, Illinois. Prepared by Civil & Environmental Consultants, Inc. for Dynegy Midwest Generation, LLC. February 2018.
- Domenico, P.A. and Schwartz, F.W., 1990. Physical and chemical Hydrogeology. John Wiley and sons. New York. pp. 410-420 (textbook, not provided as attachment).
- EPA, 1994. The Hydrologic Evaluation of Landfill Performance (HELP) Model Engineering Documentation for Version 3. EPA/600/R-94/168b. September 1994.
- EPA, 1999. Understanding Variation in Partition Coefficient, K_d , Values. Volume I: The K_d Model, Methods of Measurement, and Application to Chemical Reaction Codes. 402-R-99-004A, August 1999.
- EPA, 2007. Monitored Natural Attenuation of Inorganic Contaminants in Ground Water EPA/600/R-07/139 October 2007 (<https://archive.epa.gov/ada/web/html/mna.html>).
- Freeze, R. A. and J. A. Cherry. 1979. Groundwater. Prentice-Hall, Englewood Cliffs, NJ. 604 pp (textbook, not provided as attachment).
- Gelhar, L.W., Welty, C., Rehfeldt, K.R. 1992. A critical review of data on field-scale dispersion in aquifers. Water Resources Research, Volume28, Issue7, July 1992, Pages 1955-1974.
- Geotechnology, 2016. Hydrogeologic Assessment Report Fly Ash Pond and Bottom Ash Pond, Meredosia Power Station. Geotechnology, Inc. December 13, 2016. Prepared for AmerenEnergy Medina Valley Cogen, LLC. (This includes the Appendix D HELP and Appendix E Model description).
- Geotechnology, 2016b. Closure Plan Fly Ash Pond and Bottom Ash Pond, Meredosia Power Station. Geotechnology, Inc. December 9, 2016. Prepared for AmerenEnergy Medina Valley Cogen, LLC.
- GEPD. 2016. Guidance: Groundwater Contaminant Fate and Transport Modeling. Georgia Environmental Protection Division Land Protection Branch. October 2016.
- Kosson, D., F. Sanchez, P. Kariher, L.H. Turner, R. Delapp, P. Seignette. 2009. Characterization of Coal Combustion Residues from Electric Utilities – Leaching and Characterization Data. EPA-600/R-09/151 December 2009.
- Kosson, D.S., H.A. van der Sloot, A.C. Garrabrants and P.F.A.B. Seignette. 2014. Leaching Test Relationships, Laboratory-to-Field Comparisons and Recommendations for Leaching Evaluation

using Leaching Environmental Assessment Framework (LEAF). EPA-600/R-14/061 October 2014.

Masahiro, S. 1987. Relationship between adsorption of arsenic (III) and boron by soil and soil properties. *Environmental Science & Technology* 21 (11), 1126-1130, available for purchase at <https://pubs.acs.org/doi/10.1021/es00164a016>.

Montana DEQ. 2019. Letter to Mr. Gordon Criswell, Talen Montana RE: DEQ Comments on Units 1&2 Revised Remedy Evaluation Report, January 2019. April 22, 2019.

Montana DEQ. 2020. Letter to Mr. Gordon Criswell, Talen Montana, LLC. May 21, 2020.

NRT, 2016. Hydrogeologic Site Characterization Report West Ash Pond Complex Wood River Power Station Alton, Illinois. Prepared by Natural Resource Technology, Inc. for Dynegy Operating Company. October 19, 2016.

NRT, 2016b. Hydrostatic Modeling Report West Ash Pond Complex Wood River Power Station Alton, Illinois. Prepared by Natural Resource Technology, Inc. for Dynegy Operating Company. October 19, 2016.

NRT, 2016c. Groundwater Model Report West Ash Pond Complex Wood River Power Station Alton, Illinois. Prepared by Natural Resource Technology, Inc. for Dynegy Operating Company. October 19, 2016.

NRT, 2017. Appendix A of CEC (2018): Hydrogeologic Site Characterization Report Hennepin East Ash Pond No. 2 Hennepin, Illinois. Prepared by Natural Resource Technology for Dynegy Midwest Generation, LLC. December 20, 2017.

NRT, 2017b. Appendix D of CEC (2018): Groundwater Model Report Hennepin East Ash Pond No. 2 Hennepin, Illinois. Prepared by Natural Resource Technology for Dynegy Midwest Generation, LLC. December 20, 2017.

NRT, 2017c. Appendix C of CEC (2018): Hydrostatic Modeling Report Hennepin East Ash Pond No. 2 Hennepin, Illinois. Prepared by Natural Resource Technology for Dynegy Midwest Generation, LLC. December 20, 2017.

Reilly, T.E. and Harbaugh, A.W. 2004. Guidelines for Evaluating Ground-Water Flow Models. USGS Scientific Investigations Report 2004-5038. <https://doi.org/10.3133/sir20045038>.

Schwartz, Grace E., James C. Hower, Allison L. Phillips, Nelson Rivera, Avner Vengosh, and Heileen Hsu-Kim. 2018. Ranking Coal Ash Materials for Their Potential to Leach Arsenic and Selenium. *Environmental Engineering Science*, Vol. 35, No. 7.

Tolaymat, Thabet, Ph.D., P.E. 2020. Personal communication via email. USEPA Office of Research and Development Center for Environmental Solutions and Emergency Response, Cincinnati, Ohio 45232.

Wang, T., Wang, J., Burken, J., and Ban, H. 2005. The Leaching Behavior of Arsenic from Fly Ash. 2005 World of Coal Ash, Lexington, Kentucky, USA (April, 2005).

ATTACHMENTS

1. Appendix 1. Mann-Kendall trend analysis of water levels at the Hennepin East Ash Pond No. 2.
2. Appendix 2. Hennepin cross-section D-D' with model layers and hydraulic conductivity.
3. Appendix 3. Hennepin East Ash Pond Modeled Boron Concentration and Load.
4. Appendix 4. Meredosia Power Station Illinois River Flooding 4/29/2013.
5. Appendix 5. Linear regression analysis of Hennepin modeled hydraulic conductivity and measured values.
6. Appendix 6. CVs.
7. AECOM, 2016. Closure and Post-Closure Care Plan for the Wood River West Ash Complex. Prepared for Dynegy Midwest Generation LLC. October 2016.
8. CEC, 2018. Closure and Post-Closure Care Plan for the Hennepin East Ash Pond No. 2 Hennepin Power Station Putnam County, Illinois. Prepared by Civil & Environmental Consultants, Inc. for Dynegy Midwest Generation, LLC. February 2018.
9. EPA, 1994. HELP User Guide for Version 3. EPA/600/R-94/168b. September 1994.
10. EPA, 1999. Understanding Variation in Partition Coefficient, K_d , Values. Volume I: The K_d Model, Methods of Measurement, and Application to Chemical Reaction Codes. 402-R-99-004A, August 1999.
11. EPA, 2007. Monitored Natural Attenuation of Inorganic Contaminants in Ground Water EPA/600/R-07/139 October 2007 (<https://archive.epa.gov/ada/web/html/mna.html>).
12. Gelhar, L.W., Welty, C., Rehfeldt, K.R. 1992. A critical review of data on field-scale dispersion in aquifers. Water Resources Research, Volume 28, Issue 7, July 1992, Pages 1955-1974.
13. Geotechnology, 2016. Hydrogeologic Assessment Report Fly Ash Pond and Bottom Ash Pond, Meredosia Power Station. Geotechnology, Inc. December 13, 2016. Prepared for AmerenEnergy Medina Valley Cogen, LLC. (This includes the Appendix D HELP and Appendix E Model description).
14. Geotechnology, 2016b. Closure Plan Fly Ash Pond and Bottom Ash Pond, Meredosia Power Station. Geotechnology, Inc. December 9, 2016. Prepared for AmerenEnergy Medina Valley Cogen, LLC.
15. GEPD. 2016. Guidance: Groundwater Contaminant Fate and Transport Modeling. Georgia Environmental Protection Division Land Protection Branch. October 2016.
16. Kosson, D., F. Sanchez, P. Kariher, L.H. Turner, R. Delapp, P. Seignette. 2009. Characterization of Coal Combustion Residues from Electric Utilities – Leaching and Characterization Data. EPA-600/R-09/151 December 2009.
17. Kosson, D.S., H.A. van der Sloot, A.C. Garrabrants and P.F.A.B. Seignette. 2014. Leaching Test Relationships, Laboratory-to-Field Comparisons and Recommendations for Leaching Evaluation using Leaching Environmental Assessment Framework (LEAF). EPA-600/R-14/061 October 2014.
18. Montana DEQ. 2019. Letter to Mr. Gordon Criswell, Talen Montana RE: DEQ Comments on Units 1&2 Revised Remedy Evaluation Report, January 2019. April 22, 2019.

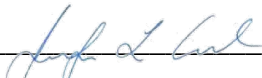
19. Montana DEQ. 2020. Letter to Mr. Gordon Criswell, Talen Montana, LLC. May 21, 2020.
20. NRT, 2016. Hydrogeologic Site Characterization Report West Ash Pond Complex Wood River Power Station Alton, Illinois. Prepared by Natural Resource Technology, Inc. for Dynegy Operating Company. October 19, 2016.
21. NRT, 2016b. Hydrostatic Modeling Report West Ash Pond Complex Wood River Power Station Alton, Illinois. Prepared by Natural Resource Technology, Inc. for Dynegy Operating Company. October 19, 2016.
22. NRT, 2016c. Groundwater Model Report West Ash Pond Complex Wood River Power Station Alton, Illinois. Prepared by Natural Resource Technology, Inc. for Dynegy Operating Company. October 19, 2016.
23. NRT, 2017. Appendix A of CEC (2018): Hydrogeologic Site Characterization Report Hennepin East Ash Pond No. 2 Hennepin, Illinois. Prepared by Natural Resource Technology for Dynegy Midwest Generation, LLC. December 20, 2017.
24. NRT, 2017b. Appendix D of CEC (2018): Groundwater Model Report Hennepin East Ash Pond No. 2 Hennepin, Illinois. Prepared by Natural Resource Technology for Dynegy Midwest Generation, LLC. December 20, 2017.
25. NRT, 2017c. Appendix C of CEC (2018): Hydrostatic Modeling Report Hennepin East Ash Pond No. 2 Hennepin, Illinois. Prepared by Natural Resource Technology for Dynegy Midwest Generation, LLC. December 20, 2017.
26. Reilly, T.E. and Harbaugh, A.W. 2004. Guidelines for Evaluating Ground-Water Flow Models. USGS Scientific Investigations Report 2004-5038.
<https://doi.org/10.3133/sir20045038>.
27. Schwartz, Grace E., James C. Hower, Allison L. Phillips, Nelson Rivera, Avner Vengosh, and Heileen Hsu-Kim. 2018. Ranking Coal Ash Materials for Their Potential to Leach Arsenic and Selenium. Environmental Engineering Science, Vol. 35, No. 7.
28. Tolaymat, Thabet, Ph.D., P.E. 2020. Personal communication via email. USEPA Office of Research and Development Center for Environmental Solutions and Emergency Response, Cincinnati, Ohio 45232.
29. Wang, T., Wang, J., Burken, J., and Ban, H. 2005. The Leaching Behavior of Arsenic from Fly Ash. 2005 World of Coal Ash, Lexington, Kentucky, USA (April, 2005).

[ATTACHMENTS WILL BE UPLOADED SEPARATELY]

CERTIFICATE OF SERVICE

The undersigned, Jennifer L. Cassel, an attorney, certifies that I have served by email the Clerk and by email the individuals with email addresses named on the Service List provided on the Board's website, available at <https://pcb.illinois.gov/Cases/GetCaseDetailsById?caseId=16858>, a true and correct copies of the **JOINT TESTIMONY OF SCOTT M. PAYNE, PhD, PG and IAN MAGRUDER, M.S.** and **ATTACHMENTS** before 5 p.m. Central Time on August 27, 2020. The number of pages in the email transmission is 3,408 pages.

Respectfully Submitted,



Jennifer Cassel (IL Bar No. 6296047)
Earthjustice
311 S. Wacker Dr., Suite 1400
Chicago, IL 60606
(312) 500-2198 (phone)
jcassel@earthjustice.org

SERVICE LIST

<p>Don Brown Clerk of the Board Don.brown@illinois.gov Illinois Pollution Control Board James R. Thompson Center Suite 11-500 100 West Randolph Chicago, Illinois 60601</p>	<p>Christine M. Zeivel Christine.Zeivel@illinois.gov Stefanie Diers Stefanie.Diers@illinois.gov Illinois Environmental Protection Agency 1021 North Grand Avenue East P.O. Box 19276 Springfield, IL 62794-9276</p>
<p>Virginia I. Yang - Deputy Counsel virginia.yang@illinois.gov Nick San Diego - Staff Attorney nick.sandiego@illinois.gov Robert G. Mool bob.mool@illinois.gov Paul Mauer - Senior Dam Safety Eng. Paul.Mauer@illinois.gov Renee Snow - General Counsel renee.snow@illinois.gov Illinois Department of Natural Resources One Natural Resources Way Springfield, IL 62702-1271</p>	<p>Matthew J. Dunn, Chief mdunn@atg.state.il.us Stephen Sylvester Sr. Asst. Attorney General ssylvester@atg.state.il.us Andrew Armstrong, Chief aarmstrong@atg.state.il.us Kathryn A. Pamentner KPamentner@atg.state.il.us 69 West Washington Street, Suite 1800 Chicago, IL 60602</p>
<p>Deborah Williams Regulatory Affairs Director Deborah.Williams@cwlp.com City of Springfield Office of Utilities 800 E. Monroe, 4th Floor Municipal Building East</p>	<p>Kim Knowles Kknowles@prairierivers.org Andrew Rehn Arehn@prairierivers.org 1902 Fox Dr., Ste. 6 Champaign, IL 61820</p>
<p>Faith Bugel fbugel@gmail.com 1004 Mohawk Wilmette, IL 60091</p>	<p>Jeffrey Hammons Jhammons@elpc.org Kiana Courtney KCourtney@elpc.org Environmental Law & Policy Center 35 E. Wacker Dr., Ste. 1600 Chicago, IL 60601</p>

<p>Keith Harley kharley@kentlaw.edu Daryl Grable dgrable@clclaw.org Chicago Legal Clinic, Inc. 211 W. Wacker, Suite 750 Chicago, IL 60606</p>	<p>Michael Smallwood Msmallwood@ameren.com 1901 Choteau Ave. St. Louis, MO 63103</p>
<p>Mark A. Bilut Mbilit@mwe.com McDermott, Will & Emery 227 W. Monroe Street Chicago, IL 60606-5096</p>	<p>Abel Russ, Attorney aruss@environmentalintegrity.org Environmental Integrity Project 1000 Vermont, Ave NW, Ste. 1100 Washington, DC 20005</p>
<p>Susan M. Franzetti Sf@nijmanfranzetti.com Kristen Laughridge Gale kg@nijmanfranzetti.com Vincent R. Angermeier va@nijmanfranzetti.com Nijman Franzetti LLP 10 S. Lasalle St., Ste. 3600 Chicago, IL 60603</p>	<p>Alec M Davis, Executive Director adavis@ierg.org Kelly Thompson kthompson@ierg.org IERG 215 E. Adams St. Springfield, IL 62701</p>
<p>Walter Stone, Vice President Walter.stone@nrg.com NRG Energy, Inc. 8301 Professional Place, Suite 230 Landover, MD 20785</p>	<p>Cynthia Skrukrud Cynthia.Skrukrud@sierraclub.org Jack Darin Jack.Darin@sierraclub.org Christine Nannicelli christine.nannicelli@sierraclub.org Sierra Club 70 E. Lake Street, Ste. 1500 Chicago, IL 60601-7447</p>
<p>Stephen J. Bonebrake sbonebrake@schiffhardin.com Joshua R. More jmore@schiffhardin.com Ryan C. Granholm rgranholm@schiffhardin.com Schiff Hardin, LLP 233 S. Wacker Dr., Ste. 7100 Chicago, IL 60606-6473</p>	<p>Jennifer M. Martin Jennifer.Martin@heplerbroom.com Melissa Brown Melissa.Brown@heplerbroom.com HeplerBroom LLC 4340 Acer Grove Drive Springfield, IL 62711</p>

<p>Alisha Anker, Vice President, Regulatory & Market Affairs aanker@ppi.coop Prairie Power Inc. 3130 Pleasant Runn Springfield, IL 62711</p>	<p>Chris Newman newman.christopherm@epa.gov Jessica Schumaker Schumacher.Jessica@epa.gov U.S. EPA, Region 5 77 West Jackson Blvd. Chicago, IL 60604-3590</p>
<p>Gibson, Dunn, & Crutcher, LLP Michael L. Raiff mraiff@gibsondunn.com 2001 Ross Avenue Suite 2100 Dallas, TX 75201</p>	<p>Earthjustice Jennifer Cassel jcassel@earthjustice.org Thomas Cmar tcmar@earthjustice.org Melissa Legge mlegge@earthjustice.org Mychal Ozaeta mozaeta@earthjustice.org 311 S. Wacker Drive Suite 1400 Chicago, IL 60606</p>
<p>BROWN, HAY, & STEPHENS, LLP Claire A. Manning cmanning@bhslaw.com Anthony D. Schuering aschuering@bhslaw.com 205 S. Fifth Street, Suite 700 Springfield, IL 62705</p>	

**The following are attachments to the testimony of Scott M. Payne,
PhD, PG and Ian Magruder, M.S..**

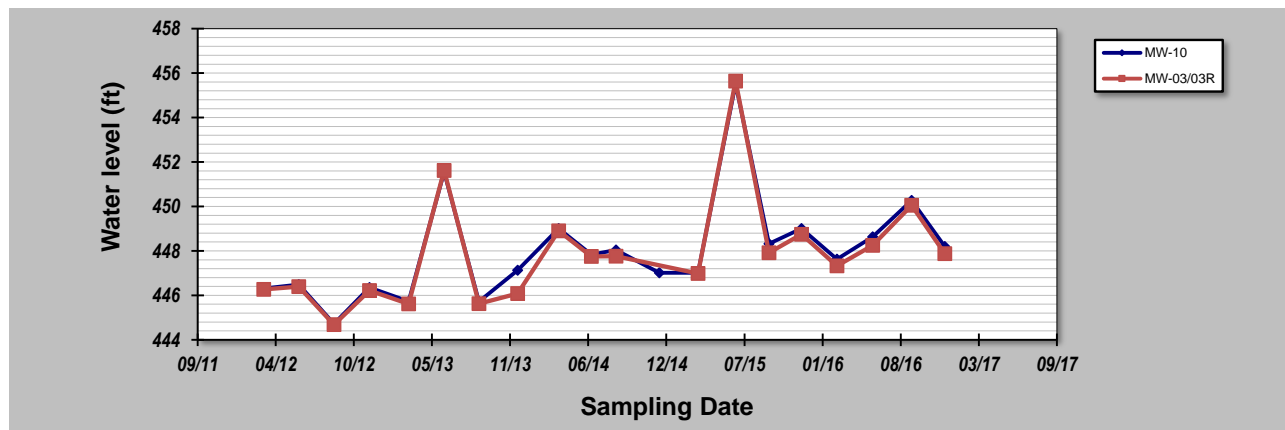
ATTACHMENT 1

GSI MANN-KENDALL TOOLKIT for Constituent Trend Analysis

Evaluation Date: **7-Jun-20** Job ID: **NA**
 Facility Name: **Hennepin East Ash Pond No. 2** Constituent: **Water level**
 Conducted By: **Ian Magruder** Concentration Units: **ft**

Sampling Point ID: **MW-10** **MW-03/03R**

Sampling Event	Sampling Date	WATER LEVEL CONCENTRATION (ft)					
1	3/1/2012	446.31	446.27				
2	5/30/2012	446.49	446.39				
3	8/28/2012	444.72	444.68				
4	11/27/2012	446.35	446.22				
5	3/7/2013	445.73	445.61				
6	6/6/2013	451.56	451.62				
7	9/3/2013	445.72	445.63				
8	12/11/2013	447.13	446.08				
9	3/26/2014	449.01	448.9				
10	6/18/2014	447.83	447.75				
11	8/20/2014	448.04	447.76				
12	12/9/2014	447.01					
13	3/18/2015	447.01	446.98				
14	6/22/2015	455.52	455.64				
15	9/16/2015	448.32	447.92				
16	12/8/2015	449	448.75				
17	3/8/2016	447.63	447.33				
18	6/7/2016	448.63	448.25				
19	9/15/2016	450.27	450.05				
20	12/9/2016	448.2	447.87				
21							
22							
23							
24							
25							
Coefficient of Variation:		0.01	0.01				
Mann-Kendall Statistic (S):		83	71				
Confidence Factor:		99.7%	99.4%				
Concentration Trend:		Increasing	Increasing				

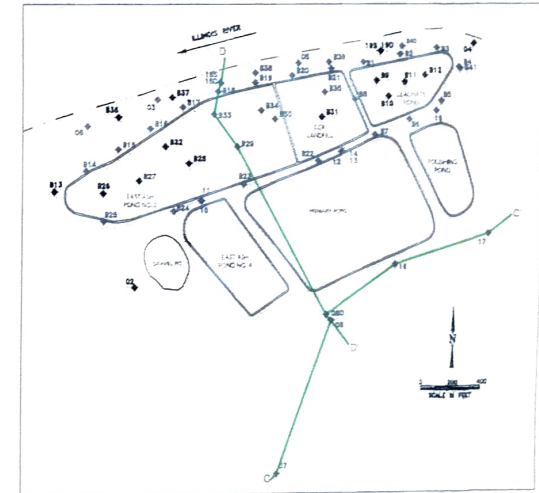
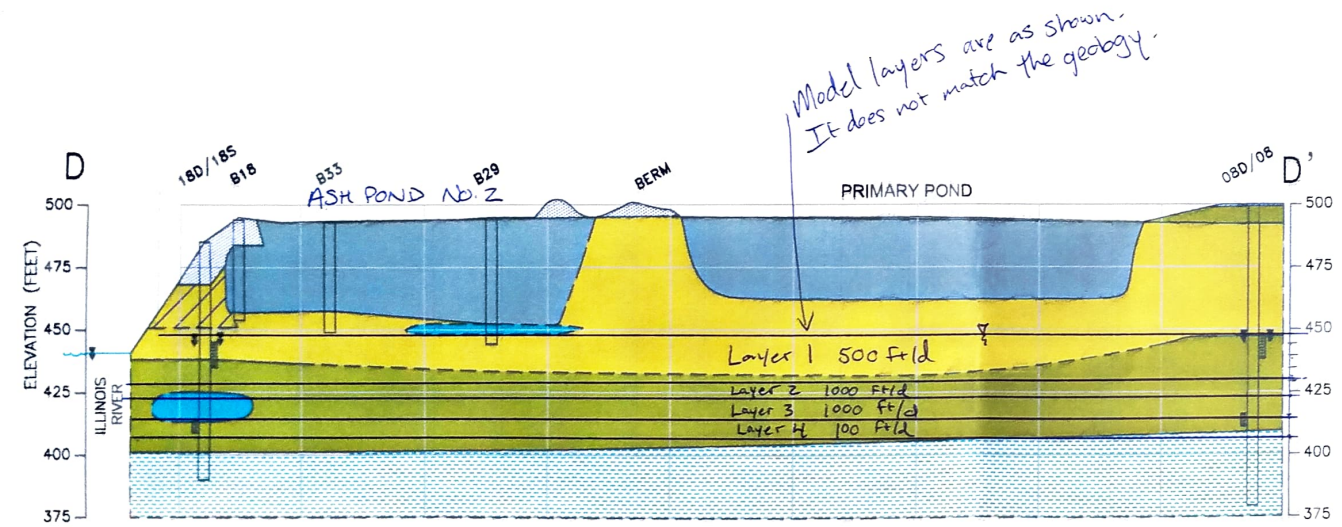
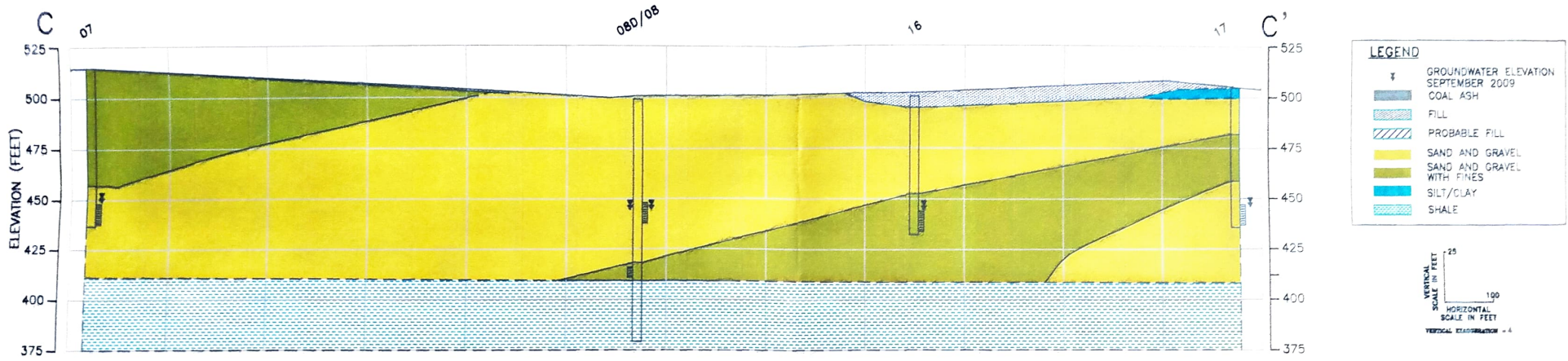


Notes:

- At least four independent sampling events per well are required for calculating the trend. *Methodology is valid for 4 to 40 samples.*
- Confidence in Trend = Confidence (in percent) that constituent concentration is increasing (S>0) or decreasing (S<0): >95% = Increasing or Decreasing; ≥ 90% = Probably Increasing or Probably Decreasing; < 90% and S>0 = No Trend; < 90%, S≤0, and COV ≥ 1 = No Trend; < 90% and COV < 1 = Stable.
- Methodology based on "MAROS: A Decision Support System for Optimizing Monitoring Plans", J.J. Aziz, M. Ling, H.S. Rifai, C.J. Newell, and J.R. Gonzales, *Ground Water*, 41(3):355-367, 2003.

DISCLAIMER: The GSI Mann-Kendall Toolkit is available "as is". Considerable care has been exercised in preparing this software product; however, no party, including without limitation GSI Environmental Inc., makes any representation or warranty regarding the accuracy, correctness, or completeness of the information contained herein, and no such party shall be liable for any direct, indirect, consequential, incidental or other damages resulting from the use of this product or the information contained herein. Information in this publication is subject to change without notice. GSI Environmental Inc., disclaims any responsibility or obligation to update the information contained herein.

ATTACHMENT 2



Note: Cross-sections are based on data collected through 2009 and do not represent or include any subsequent changes due to grading, landfill construction, or other site activities. Cross-sections are modified from the following report: Natural Resource Technology and Kelron Environmental; December 19, 2010. New Coal Combustion Waste (CCW) Landfill, Initial Facility Report, Hydrogeologic Studies and Evaluations, Section 25 Hydrogeological Investigation, Hennepin Power Station, Hennepin, Illinois.



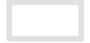






FIGURE NO. 8

PROJECT NO. 1940/3.0
DRAWN BY: KXW 09/27/10
CHECKED BY: BOH 12/08/10
APPROVED BY: BRH 12/08/10

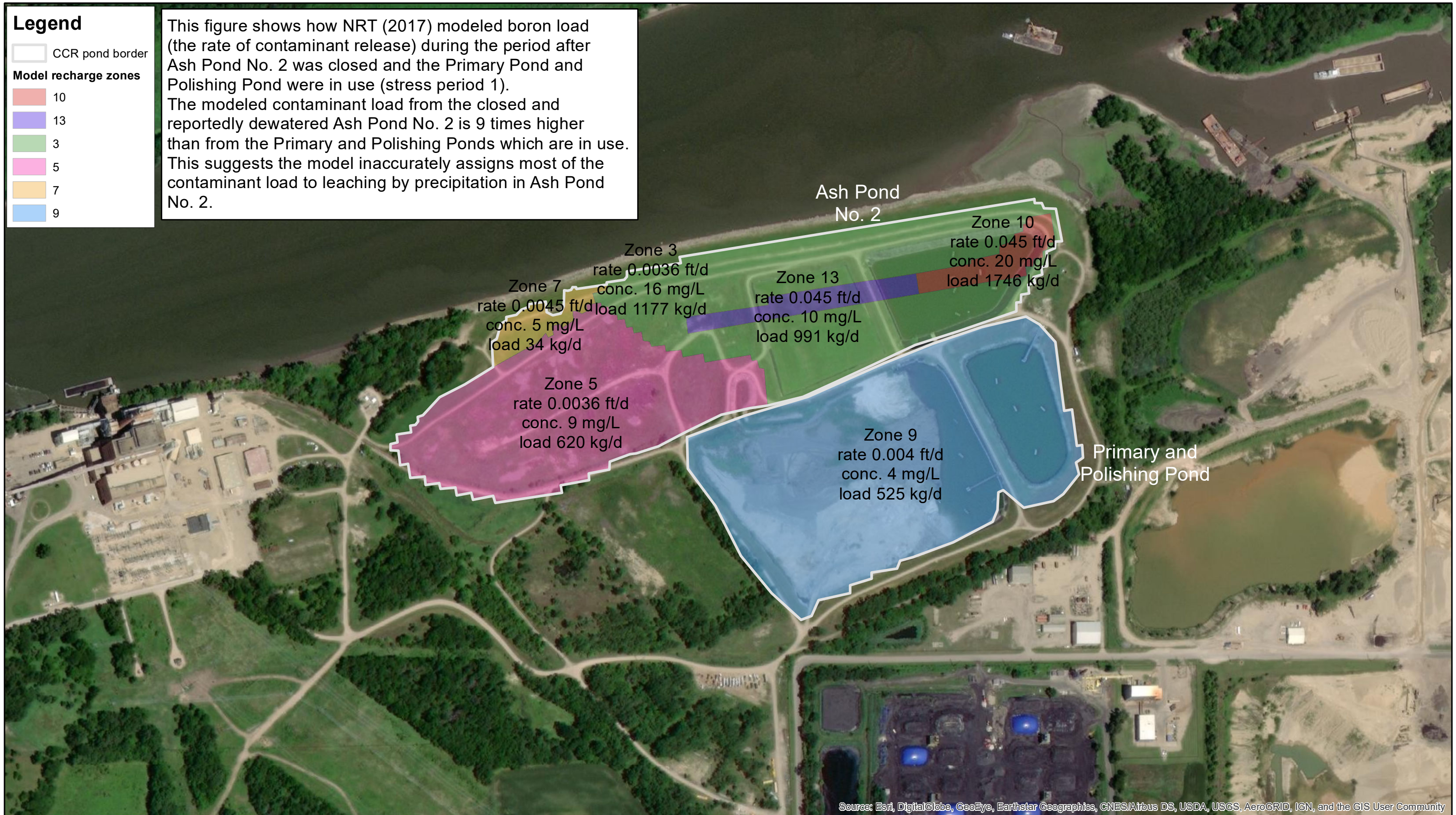
GEOLOGIC CROSS SECTIONS C-C' AND D-D'
HYDROGEOLOGIC SITE CHARACTERIZATION REPORT
EAST ASH POND NO. 2
DYNEGY MIDWEST GENERATION, LLC
HENNEPIN POWER STATION, HENNEPIN, ILLINOIS

ATTACHMENT 3

Legend

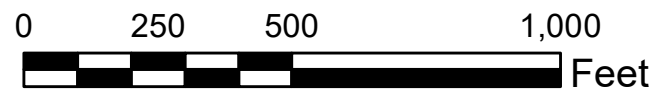
-  CCR pond border
- Model recharge zones**
-  10
-  13
-  3
-  5
-  7
-  9

This figure shows how NRT (2017) modeled boron load (the rate of contaminant release) during the period after Ash Pond No. 2 was closed and the Primary Pond and Polishing Pond were in use (stress period 1). The modeled contaminant load from the closed and reportedly dewatered Ash Pond No. 2 is 9 times higher than from the Primary and Polishing Ponds which are in use. This suggests the model inaccurately assigns most of the contaminant load to leaching by precipitation in Ash Pond No. 2.



Source: Esri, DigitalGlobe, GeoEye, Earthstar Geographics, CNES/Airbus DS, USDA, USGS, AeroGRID, IGN, and the GIS User Community

**Hennepin East Ash Pond
Modeled Boron Concentration and
Load (stress period 1)**



Sheet No.
1

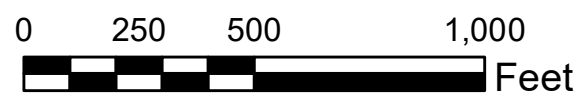
KirK Engineering & Natural Resources, Inc.	
Designed By:	Ian Magruder
Checked by:	Scott Payne, PhD
Date:	7/8/2020

ATTACHMENT 4



Source: Esri, DigitalGlobe, GeoEye, Earthstar Geographics, CNES/Airbus DS, USDA, USGS, AeroGRID, IGN, and the GIS User Community

**Meredosia Power Station
Illinois River Flooding 4/29/2013**



Sheet No.
1

Kirk Engineering & Natural Resources, Inc.

Designed By: Ian Magruder

Checked by: Scott Payne, PhD

Date: 7/28/2020

ATTACHMENT 5

Attachment 5. Linear regression analysis of Hennepin modeled hydraulic conductivity and measured values.

The figure shows a linear regression analysis between field and modeled hydraulic conductivity (K). Values are presented in Table 1.

We would expect the regression analysis to show a linear relationship, with a slope of 1 and an R² approaching 1, if the field measured data matched the modeled values reasonably well. Instead, the R² value of 0.0044 shows there is no correlation between measured and modeled hydraulic conductivity.

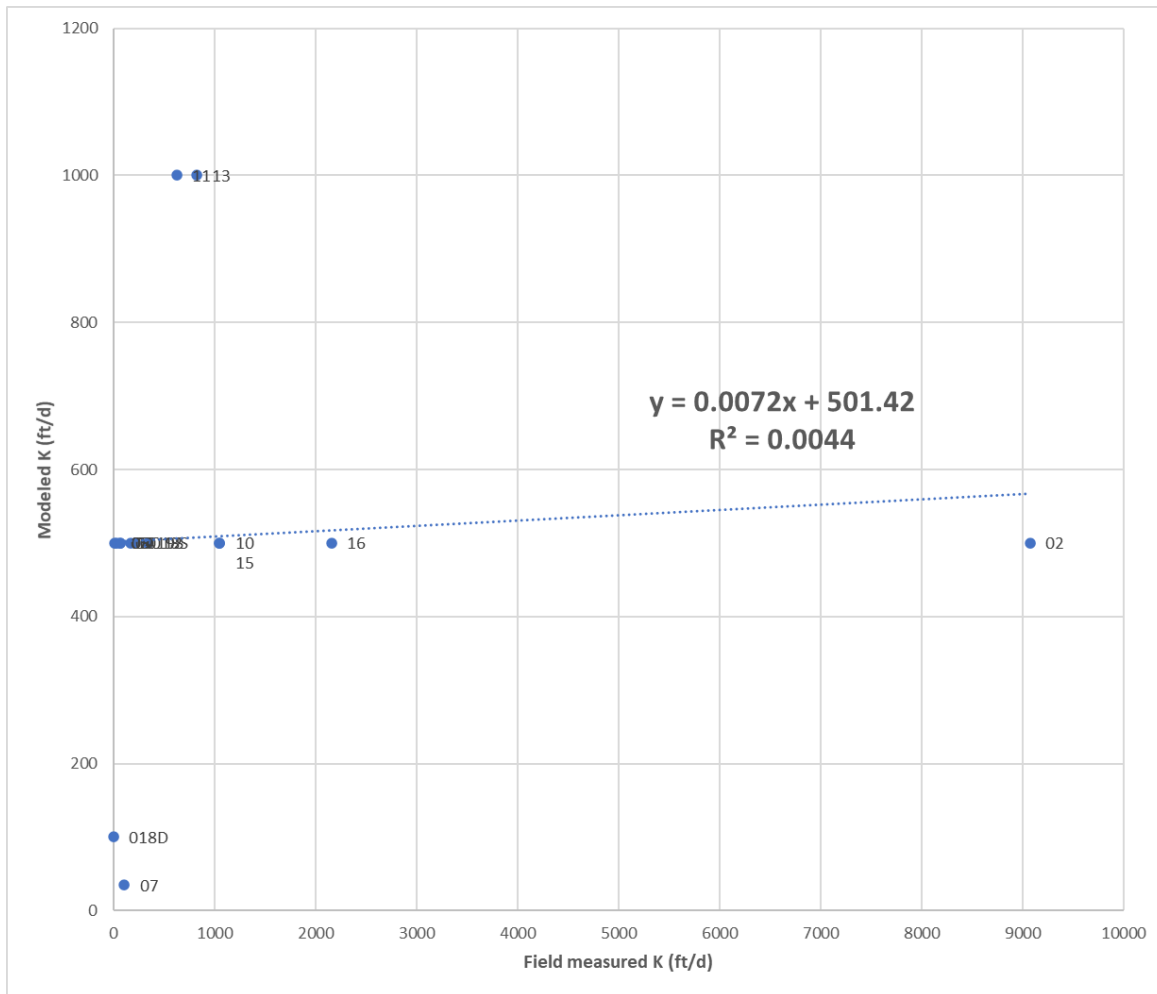


Table 1. Comparison of field measured hydraulic conductivity (K) and modeled values at the Hennepin Site (data adapted from NRT 2017 and 2017b).

Well	Site characterization field data (from NRT 2017, Table 4)	Modeled values (NRT 2017b)	Location
	K (ft/d)	K (ft/d)	
02	9,072	500	East of Pond No. 4

03	125	500-1000	Pond No. 2 river berm
04	62	500	Leachate Pond river berm
05	12	500	Landfill river berm
06	167	500-1000	Pond No. 2 river berm
07	105	35	Upgradient background
08	27	500	Primary Pond upgradient berm
08D	454	100-1000	Primary Pond upgradient berm
10	1,049	500	Pond No. 2 upgradient berm
11	624	1000	Pond No. 2 upgradient berm
12	340	500	Landfill upgradient berm
13	822	1000	Landfill upgradient berm
14	no data		
15	1,049	500	Leachate pond upgradient berm
16	2,155	500	Primary Pond upgradient berm
17	68	500	Polishing Pond upgradient berm
018S	215	500	Pond No. 2 river berm
018D	0.3	100	Pond No. 2 river berm
019S	170	500	Leachate pond river berm
019D	108	100-1000	Leachate pond river berm

ATTACHMENT 6

Kirk Engineering & Natural Resources, Inc.

SCOTT M. PAYNE, Ph.D., P.G.

Principal and Business Owner
(406) 842-7224, cell (406) 431-1345
scott_payne@kirkenr.com

EDUCATION

- Ph.D., Geosciences with a Hydrogeology Emphasis, University of Montana 2009
- M.S., Geology with a Hydrogeology Emphasis, University of Montana, 1989
- B.S., Earth Science, Northland College, 1985

EMPLOYMENT HISTORY

- Kirk Engineering & Natural Resources, Inc., Principal and Business Owner, 1998 – Present
- Montana State University, Professor Department of Land Resources and Environmental Sciences, 2013–2015
- Tetra Tech EM Inc., Program Manager, 1991 – 1998
- Hydrometrics, Sr. Hydrogeologist, 1988 – 1991
- University of Montana, Research Assistant/Teaching Assistant, 1987 – 1988
- Environmental Solutions, Inc. (now TRC), Hydrogeologist, 1985 – 1986

EXPERIENCE

Dr. Payne has over 34 years of experience as a professional hydrogeologist. He has extensive experience in toxic waste site studies and cleanup, Superfund and RCRA regulatory support; conducting analytical and numerical surface water and groundwater flow / solute transport models, monitoring and assessment of physical and chemical conditions of surface water and groundwater, and environmental and water policy development. Dr. Payne served as an adjunct professor at Montana State University and taught surface and groundwater modeling for graduate and undergraduate students in the Environmental Science and Land Resource Department.

Dr. Payne gained his hazardous waste management experience through work conducted for the U.S. Navy in California. He previously served as the program manager for environmental activities at the Fleet Industrial Supply Center, Oakland, California, under the Comprehensive Long-term Environmental Action Navy (CLEAN) Contract. He has worked on dozens of other CERCLA and RCRA facilities across the Western U.S. He is author of *Strategies for Accelerating Cleanup at Toxic Waste Sites* published internationally by Lewis Publishers. In his book he outlines streamlining regulatory processes, effectively negotiating decisions and actions, environmental leadership, and applying practical solutions to remedy environmental problems.

Dr. Payne's litigation support experience for hazardous waste site legal proceedings includes providing expert witness support in cases involving a proposed Controlled Groundwater Area associated with a RCRA corrective action site and a State of Montana CECRA Superfund site where the public was exposed to groundwater and vapor intrusion from leaked solvent organic contaminants. As an expert witness, he provided professional opinions on monitoring well construction, water use from wells, and groundwater flow and solute transport modeling.

SELECTED MODELING PROJECTS

East Helena Smelter Arsenic Transport Model – Dr. Payne developed a groundwater flow and solute transport model for a lead smelter Superfund site, located in East Helena, Montana. Dr. Payne was responsible for simulating groundwater flow conditions and surface water interaction over a 6-square mile area, predicting arsenic concentration and transport over a 500-year period. As part of remedial design, Dr. Payne conducted

SCOTT M. PAYNE, Ph.D., P.G

additional computer modeling that included simulating drawdown from proposed recovery wells installed at the plant site and resultant arsenic recovery.

Burlington Northern Paradise RCRA site model review – For a private client, Dr. Payne reviewed a MODFLOW groundwater flow and a BIO1D solute transport model for the BN Paradise site. A groundwater control zone was proposed for the site, and Dr. Payne reviewed the proposal for completeness and technical merit on how it would affect adjacent properties.

Superfund Technical Assistance model review – Dr. Payne provides technical oversight of cleanup plans for the Butte, MT area Superfund sites under an EPA grant for the Citizens Technical Environmental Committee (CTEC). He reviews groundwater and solute transport models, groundwater contamination, and Superfund remediation plans, and meets with EPA and responsible parties to encourage improved ways to cleanup groundwater.

U.S. EPA Technical Oversight Support – Dr. Payne provided the U.S. Environmental Protection Agency (EPA) oversight support on numerous cleanup projects with his duties including reviewing sampling and analysis reports, RI/FS documents, RD/RA documents, and large modeling reports prepared by consultants. As part of his oversight work, he prepared numerical groundwater flow models to validate work being reviewed and proposed ways to accelerate action at sites to streamline protection of human health and the environment. Dr. Payne's work also provided cost estimates for the Superfund Innovative Technologies Evaluation (SITE) program.

Lower Ruby Valley Groundwater Management Plan – This project for the Ruby Valley Conservation District, Montana modeled water use within the Ruby River Basin and recommended conservation measures to protect water quality and stream flow. The project resulted in a basin-scale groundwater-surface water model, constructed using the MODFLOW platform, which includes simulation of stream flow, irrigated fields, and all ditches and canals in the valley. Predictive modeling was used to evaluate the effects of irrigation and canal management changes and new groundwater use from residential development on streamflow.

U.S. Army Independent Technical Review Team – Dr. Payne served as an expert Hydrogeologist for the U.S. Army in a prestigious capacity as a team member of the ITRT. The team's focus was reviewing the current technical status of several west coast Army installations undergoing environmental cleanup and also to meet with installation project teams to make recommendations that fast-track the environmental cleanup process. Each ITRT member was from a different part of the nation and had specific expertise need for the project. Dr. Payne focused his review efforts on installation hydrogeology, reviewing technical documents that included groundwater modeling, and identify streamlining and cost saving opportunities that are described in his book *Strategies for Accelerating Cleanup at Toxic Waste Sites* published by Lewis Publishers.

Navy Point Molate Fuel Depot – Dr. Payne prepared a numerical groundwater flow model to estimate groundwater pumping rates for a pump and treat groundwater remediation system constructed within a slurry wall. Dr. Payne efforts were used to help select the proper pump size and well placement at the site to recover floating and dissolved petroleum contamination at this former fueling depot in Richman, California.

Bozeman Solvent Site – This State Superfund site in Bozeman, Montana was under Interim Order by the State of Montana to evaluate the potential source of tetrachloroethylene groundwater contamination. The contaminants were present in residential wells in the area and people's health had been severely affected. Dr. Payne was involved with developing removal actions; helping install a soil vapor extraction system; preparing numerical and analytical models for groundwater flow and contaminant fate and transport; modeling to predict plume movement and capture of contaminants in domestic wells located in nearby residential areas; and conducting various field operations. Dr. Payne served as factual and expert witness, providing expert disclosure and rebuttal statements for the project.

Oilfield brine solute transport modeling – Using PLASM 2-D and Random Walk, Dr. Payne modeled steady state and transient groundwater flow and solute transport of brines from an oil well reserve pit in eastern Montana. His investigation included site characterization using electromagnetic induction (EM) and surface resistivity;

SCOTT M. PAYNE, Ph.D., P.G

installation of lysimeters and monitoring wells; water quality sampling; aquifer testing; and development of a water quality database.

Water right modeling – New water appropriations in Montana require predicting impacts to senior water right holders. Working for an agricultural producer in Montana, Scott oversaw a MODFLOW model to predict the drawdown from a new irrigation well. Model results were used to show the extent of significant drawdown and to investigate those boundary conditions which would limit the size of the pumping cone of depression.

Subdivision review of impacts to groundwater – Dr. Payne oversaw the development of a water supply system for Aspen Springs development near Bozeman, MT, which required evaluating that the quantity of groundwater available for existing and new water uses. A MODFLOW model was prepared to predict the drawdown on surrounding existing wells.

Technical review of mine expansion EIS and drawdown modeling – Working on behalf of an agricultural producer, Dr. Payne reviewed an EIS and supporting groundwater modeling report. The producer was experiencing reduced water flow from springs on their property used for stock water. Dr. Payne reviewed the hydrogeologic data in the EIS and groundwater modeling results used to predict groundwater flow impacts from increased mine dewatering pumping rates. In his review he found that the model was inappropriate for evaluating impacts to the producer's springs due to issues with model set up and assumptions made by the EIS team.

FIELD EXPERIENCE

- Designed, installed and logged over 200 monitoring wells, boreholes, water wells
- Designed, installed and logged over 50 water supply and production wells
- Performed over 75 aquifer tests and numerous slug / packer tests, and interpreted results
- Mapped geology and groundwater systems throughout the western US
- Numerous field applications of electromagnetic, resistivity, and magnetic geophysics
- Collected over one thousand groundwater and surface water quality samples
- Collected over three thousand soil samples
- Interpreted thousands of organic, metals, & common ion water and soil chemistry reports
- Measured hundreds of stream flows on streams and rivers
- Completed over 100 miles of riparian assessments in western Montana
- Completed dozens of CERCLA, RCRA, UST, TSCA, CWA studies at various scales
- Completed dozens of water supply, water conservation, & water rights studies
- Completed dozens of watershed chemical, physical, and biologic assessments
- Completed multiple groundwater and surface water hydrology & solute transport models

PROFESSIONAL CREDENTIALS, AFFILIATIONS, AND COMMUNITY SERVICE

- Professional Geologist, Wyoming, PG-1676, 1992 – present
- Professional Geologist, California, PG-6199, 1995 – present
- National AWRA member
- US Navy 1996 Outstanding Performance Military Base Remediation San Francisco, CA

PUBLICATIONS AND PRESENTATIONS

Donohue, D.A., Huffsmith, R.L., Payne, S.M., 1994, Identification of a High Yield Aquifer Deep in the Helena Valley, West-Central Montana. October 13 and 14 AWRA Conference, Missoula, Montana.

Payne, S.M., 1988, Modeling of Hydrogeologic Conditions and Groundwater Quality Near an Oil Well Reserve Pit in Richland County, Montana. Montana Bureau of Mines and Geology Open File Report.

Payne, S.M., 1993, Implementing Preremedial Investigation Cleanup on Large Multiple-Site Projects. Proceedings from the 74th Annual American Association for the Advancement of Science, Pacific Division, June 20 – 24, 1993.

Payne, S.M., 1994, Implementing Accelerated Cleanup on Large Multiple-Site Projects. The Proceedings of the NWWA Eighth Annual National Outdoor Action Conference, May 23 – 25, 1994. S. Payne presentation speaker at conference.

Payne, S.M., 1997, Integrating Technical Decision-making and Environmental Leadership. HazWaste World Superfund XVIII December 2 – 5, 1997 Conference Proceedings, Washington DC.

Payne, S.M., 1997, Strategies for Accelerating Cleanup at Toxic Waste Sites. Lewis Publishers/CRC Press, NY, December.

Payne, S.M. 2001, Nutrient Reduction in the Flathead Basin. October, AWRA Conference, Missoula, MT

Payne, S.M., 2003, A Groundwater Classification System for Watershed Planning and Conservation of Ecotones in Basin Fill Sediments of the Rocky Mountain West, Poster Presentation, Montana Chapter AWA Annual Conference, Butte, MT, October.

Payne, S.M., 2010. Classification of Aquifers. Ph.D. Dissertation, University of Montana.

Payne, S.M., I. Magruder and W. Woessner, 2013. "Application of a Groundwater Classification System and GIS Mapping System for the Lower Ruby Valley Watershed, Southwest Montana," Journal of Water Resource and Protection, Vol. 5 No. 8, pp. 775–791. doi: 10.4236/jwarp.2013.58079.

Payne, S.M. and Holston, M. 2000, Overview of the Flathead Lake Voluntary Nutrient Reduction Strategy (VNRS). Clark Fork Symposium 2000 Posters, Missoula, MT.

Payne, S.M. and Woessner, W.W. 2010. An Aquifer Classification System and GIS-based Analysis Tool for Watershed Managers in the Western US, Journal of American Water Resources, v46, no.5, pp1003–1023.

Reiten, J.C. and Payne, S.M. 1991. Impacts of Oil Field Wastes on Soil and Groundwater in Richland County, Montana. Part III. Montana Bureau of Mines and Geology, Open File Rept. 237-C.

Woessner, W.W., Lazuk R., Payne S.M., 1989, Characterization of Aquifer Heterogeneities using EM and Surface Electrical Resistivity Surveys at the Lubrecht Experimental Forest, Western Montana. The Proceedings of the NWWA Third Annual National Outdoor Action Conference, May 22 – 25, 1989. S. Payne presentation speaker at conference.

Kirk Engineering & Natural Resources, Inc.

IAN MAGRUDER, M.S.

Senior Hydrogeologist

(406) 439-0049

ian_magruder@kirkenr.com

EDUCATION

- M.S., Geology (hydrogeology emphasis). University of Montana, Missoula, Montana, 2006
- B.A., Geology with High Honors (environmental geology emphasis). University of Montana, Missoula, Montana, 1998

EMPLOYMENT HISTORY

- KirK Engineering & Natural Resources, Inc., Senior Hydrogeologist, 2002 – present
- Montana Bureau of Mines and Geology Research Hydrology Division, Research Specialist II, 2001
- Contract Hydrogeologist for the Ruby Valley Conservation District, 2000

EXPERIENCE

Mr. Magruder has 20 years' experience as a professional hydrogeologist with extensive experience working on toxic and hazardous waste characterization, contaminated site remediation, and groundwater contaminant cleanup. He has an extensive background in modeling and formerly studied under one of the industry's leading authors of applied groundwater modeling. His modeling has included numerical and analytical groundwater flow models, geochemical fate and transport, discharge and mixing zones, groundwater-surface water interaction, and plant/soil/ecosystem water use.

Mr. Magruder's coal ash remediation experience includes authoring a cleanup and disposal plan for ash impoundments at the second largest coal fired power plant in the Western U.S and providing technical review of coal ash groundwater contaminant modeling. He has also served for seventeen years as a technical advisor for mine waste and wood treatment Superfund sites where he has evaluated contaminant risks and recognized contaminant pathways and human and environmental risks not identified in studies performed by EPA and responsible parties. Mr. Magruder has extensive waste characterization and remediation sampling experience. He has taken hundreds of soil and groundwater samples for inorganic and organic contaminants such as heavy metals, petroleum contaminants, solvents, PCBs, pesticides, herbicides, and radionuclides.

SELECTED MODELING PROJECTS

Colstrip Steam Electric Station groundwater modeling review – Working on behalf of a grassroots environmental organization, Mr. Magruder provides ongoing technical review of groundwater flow and contaminant transport modeling prepared by the power company's consultants for three large coal ash disposal areas. Mr. Magruder's cleanup plan and modeling review includes written technical comments to Montana DEQ, as well as face to face meetings with the agency director and the lieutenant governor. His work has been instrumental in affecting DEQ's decision to require removal of coal ash disposed in contact with groundwater.

Superfund Technical Assistance contaminant transport modeling - Mr. Magruder provides the Citizens Environmental Technical Committee with broad-based scientific expertise to better understand the Superfund cleanup in Butte, MT. He reviews mine waste and wood treatment chemical remedial investigation and cleanup plans. To inform review of official EPA proposed plans, he has prepared groundwater solute transport models of buried mine waste to evaluate remedial alternatives and to better understand the timeframe for cleanup of heavy metal contaminants under a waste removal scenario.

IAN MAGRUDER, M.S.

Public water supply vulnerability to pipeline rupture – Mr. Magruder was lead hydrogeologist for a major petroleum company conducting a pipeline risk analysis in Washington state. His aquifer risk evaluation considered geologic, hydrogeologic, and human factors affecting pipeline rupture vulnerability. He developed numerous petroleum spill contaminant transport models, prepared aquifer vulnerability maps, ranked risk to public water supply wells, and was lead author of an aquifer vulnerability report recommending risk mitigation options.

Hardrock mine drawdown modeling – Metal mining often involves pumping and treating large quantities of groundwater to allow mining below ground. Working for several mining companies, Mr. Magruder provided transient MODFLOW simulations to evaluate mine dewatering requirements and to predict water table decline. The results were used to plan for replacement of private well water supplies. He managed field data collection for these projects to provide high quality data for the models, including water level measurement in wells, aquifer testing, geologic mapping, and streamflow measurement of groundwater interaction.

Mine discharge modeling – Mr. Magruder has provided groundwater modeling services for several mining clients to evaluate discharge disposal alternatives for treated mine water. He used MODFLOW models to assess the aquifer capacity to accept discharge water and to transport and dilute elevated nitrates in the water resulting from blasting activities. He prepared soil and plant water balance models to evaluate land application evapotranspiration capacity of discharge water.

Groundwater recharge and ecosystem water use modeling – Mr. Magruder developed a transient MODFLOW model coupled with an ecosystem process model to evaluate plant, soil, and climate effects on groundwater recharge. Mr. Magruder was lead author presenting this research in the journal *Groundwater* (Vol. 47, issue 6).

Ruby Basin groundwater-surface water model – Mr. Magruder developed a transient MODFLOW model for the Ruby Valley Conservation District and Montana DEQ which includes simulation of groundwater flow, river flow, irrigated fields, and all ditches and canals in the watershed. His predictive modeling evaluated the potential impacts to the Ruby River caused by irrigation and canal management changes and new residential subdivision groundwater use. Mr. Magruder presented the findings to numerous water user groups, watershed councils, the annual meeting of the Montana Section of the American Water Resource Association, and the Water Policy Interim Committee of the Montana Legislature.

Water Rights Permitting – Working for several agricultural producers in Montana, Mr. Magruder developed transient MODFLOW models to predict the drawdown from new irrigation well use and impacts to hydraulically connected surface waters to assist with water right permitting.

Subdivision Review – Mr. Magruder developed site specific MODFLOW models for several residential developments to predict the drawdown impacts to existing wells and springs and show the quantity of groundwater available is sufficient for both existing and new water uses.

FIELD EXPERIENCE

- Designed, installation oversight, logging, and testing dozens of public water supply wells
- Designed, installation oversight, and logging of dozens of monitoring wells and test holes
- Performed over 25 aquifer tests and interpreted results
- Conducted groundwater tracer testing
- Conducted ground-penetrating radar (GPR) investigations of aquifer stratigraphy and flowpaths
- Collected hundreds of groundwater and surface water quality samples
- Collected hundreds of soil samples for contaminated site characterization
- Interpreted thousands of organic, metals, & common ion water and soil analytical reports
- Measured hundreds of stream flows
- Collected dozens of algae and benthic macroinvertebrate samples to characterize stream health

IAN MAGRUDER, M.S.

PROFESSIONAL CREDENTIALS, AFFILIATIONS, AND COMMUNITY SERVICE

- Missoula County Board of Health, Water Quality Advisory Council – Council Chair, member 2006-present.
- Technical advisor, DNRC Montana Water Supply Initiative, Clark Fork/Kootenai Basin Advisory Council.
- Manuscript reviewer for the journal Ground Water, National Ground Water Association.
- Clark Fork River Task Force technical advisor 2013-2015

PUBLICATIONS AND PRESENTATIONS

Magruder, I., Woessner, W. Payne, S., Radil, A. 2004. A Biogeochemical (BGC) Process Model Approach for Estimating Mountain Recharge to Intermontane Basin Groundwater Systems. Poster presentation, The Geological Society of America Annual Meeting: Geoscience in a Changing World, November 7-10, Denver, CO.

Magruder, Ian. 2008. The Ruby Groundwater/Surface Water Interaction Modeling Project: Evaluating Connections between Water Management and River Flows. Technical presentation at Montana AWRA 25th Annual Meeting: Water Sustainability: Challenges for Montana. October 2-3, Big Sky, MT.

Magruder, I.A., Woessner, W.W., Running, S.W. 2009. Ecohydrologic Process Modeling of Mountain Block Groundwater Recharge. Ground Water, National Ground Water Association, Vol. 47:6.

Magruder, Ian. 2012. Climate Cycles, Dewatering a Gold Mine, and Human Perception of Normal Streamflow. Oral presentation at Montana AWRA Annual Meeting, Montana's Water Resources: Water Management in the Face of Uncertainty. October 11-12, Fairmont, Montana.

Magruder, Ian. 2015. Mitigation and aquifer recharge opportunities in the Clark Fork Basin. Oral presentation at the 2015 Clark Fork Symposium, University of Montana, Missoula, April 23-24, 2015.

Magruder, Ian. 2015. I have to do what to get a new water right?? – Mitigation and aquifer recharge options elaborated. Oral presentation at Montana AWRA Annual Meeting, Linking Water Research to Policy and Water Management, Missoula, October 7-9, 2015.

KirK Engineering & Natural Resources, Inc. 2015. Clark Fork Water Supply Report Series I - Water Availability and Mitigation Options in the Clark Fork Basin and attached Modeling Report. Prepared for Clark Fork River Basin Task Force and Montana DNRC. <http://dnrc.mt.gov/divisions/water/management/regional-river-basin-information/clark-fork-kootenai-river-basins>

KirK Engineering & Natural Resources, Inc. 2015. Clark Fork Water Supply Report Series III - Enhanced Conservation and Management in the Montana Clark Fork River Basin. Prepared for Clark Fork River Basin Task Force and Montana DNRC. <http://dnrc.mt.gov/divisions/water/management/regional-river-basin-information/clark-fork-kootenai-river-basins>

ATTACHMENT 7

W1190700004
06L



DYNEGY MIDWEST GENERATION, LLC
Wood River Station Site
#1 Chessen Lane
Alton, IL 60436
618.343.7761

By UPS

IEPA - DIVISION OF RECORDS MANAGEMENT
RELEASABLE

November 28, 2016

AUG 25 2017

William E. Buscher, P.G.
Manager, Hydrogeology and Compliance Unit
Groundwater Section, Division of Public Water Supplies, Bureau of Water
Illinois Environmental Protection Agency
1021 North Grand Avenue East
Springfield, IL 62794

REVIEWER: RDH

Re: Wood River Site
Inactive West Ash Pond System Cells 1, 2W, and 2E
Submittal of Closure and Post-Closure Care Plans and an Application for a GMZ

Mr. Buscher:

As requested at our meeting with former IEPA Director Mrs. Lisa Bonnett in March 2015, a telephone call with Mr. Sonjay Sofat in September 2015, and my meeting with you and members of your staff on October 14, 2015, Dynegy Midwest Generation, LLC (DMG) is submitting herein for the Agency's review and approval the enclosed two-volume Closure and Post Closure Care Plans for three inactive CCR surface impoundments (Cells 1, 2W, and 2E) that are part of the former west ash pond system of the now retired Wood River Power Station. The structure of the enclosed plans is based specifically upon the outline reviewed and revised by your office on February 24, 2016. They also reflect comments received from your office on similar plans submitted earlier this year for the Baldwin and Duck Creek stations. The plans were prepared by AECOM (St. Louis, MO) and by Natural Resources Technology (Bloomington, IL).

An application for a Groundwater Management Zone (GMZ) is enclosed as Appendix F in Volume 2. Actually a GMZ has existed around the west ash pond system since the mid-1990s, but a formal application consistent with Appendix D of 35 Ill. Adm. Code Part 620 is nevertheless being submitted herein. The extent of the GMZ applied for herein is the same as the GMZ previously approved by the IEPA.

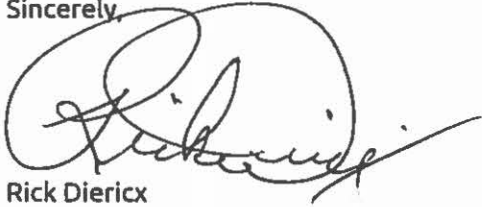
Please note in Section 1.1 that fly ash "mined" from ash pond no.1 and raw coal remaining on the coal pile may both be used as crown fill material in west ash pond cells 2W and 2E. In addition, bottom ash from the east ash pond system may also be "mined" and beneficially reused for this same purpose.

Your expedited review of the enclosed plans would be very much appreciated, as closure of these surface impoundments is subject to deadlines in USEPA's April 17, 2015 CCR rule. Delays in receiving approval of the plans will jeopardize compliance with those deadlines.

Please contact me (tel. no. 618-343-7761) or Thomas L. Davis (tel. no. 618-343-7757) of my staff if you have any questions regarding the submitted information.

RECEIVED
NOV 29 2016
Div. of Public Water Supplies
Illinois EPA

Sincerely,

A handwritten signature in black ink, appearing to read "Rick Dierix". The signature is written in a cursive style with a large, circular initial "R" and a long, sweeping tail that extends to the right.

Rick Dierix
Managing Director – Environmental



Submitted to
Dynergy Midwest Generation,
LLC
Wood River Power Station
#1 Chessen Lane
Alton, IL 62002

Submitted by
AECOM
1001 Highlands Plaza Drive West,
Suite 300
St. Louis, MO 63110
October 2016

RECEIVED

NOV 29 2015

Div. of Public Water Supplies
Illinois EPA

IEPA - DIVISION OF RECORDS MANAGEMENT
RELEASABLE

AUG 25 2017

REVIEWER: RDH

Closure and Post-Closure Care Plan for the Wood River West Ash Complex at

Dynergy Midwest Generation, LLC
Wood River Power Station
#1 Chessen Lane
Alton, IL 62002

Table of Contents

Executive Summary of Closure Plan and Post-Closure Care Plan.....	1
1 Closure Plan.....	1-1
1.1 Description of Proposed Closure Activities.....	1-1
1.2 Engineering Plans and Specifications for the Proposed Closure Activities.....	1-1
1.2.1 Final Cover System.....	1-1
1.2.2 Final Slope Design.....	1-2
1.2.3 Summary of Slope Stability Evaluations.....	1-2
1.3 Proposed Timeline for Implementation and Completion of Proposed Closure Activities.....	1-2
1.4 Description of the Construction Quality Assurance Program for Proposed Closure Activities.....	1-3
1.5 Summary of Groundwater Monitoring Plan.....	1-3
1.6 Professional Certification and Seal.....	1-5
2 Environmental Impacts of Proposed Closure Activities.....	2-1
2.1 Summary of Pre-Closure Groundwater Conditions.....	2-1
2.2 Summary of Modeled Post-Closure Groundwater Conditions.....	2-1
2.3 Anticipated Effects of the Closed Impoundment on Nearby Surface Waters.....	2-2
3 Post-Closure Care Plan.....	3-1
3.1 Description of Post-Closure Care Activities.....	3-1
3.2 Description of the Planned Use of the Property during the Post-Closure Care Period.....	3-1
3.3 Stormwater Management.....	3-1
3.4 Professional Certification and Seal.....	3-3
3.5 Professional Certifications and Seals.....	3-3

List of Figures

Figure G-100	Cover Sheet and Location Map
Figure G-101	Existing Conditions
Figure C-100	Overall Grading Plan and Sheet Layout
Figure C-101	Grading Plan 1
Figure C-102	Grading Plan 2
Figure C-103	Grading Plan 3
Figure C-104	Grading Plan 4
Figure C-105	Grading Plan 5
Figure C-106	Sections A-B-C
Figure C-107	Sections D-E
Figure C-108	Details

List of Appendices

Appendix A	Hydrogeologic Site Characterization Report
Appendix B	Groundwater Monitoring Plan
Appendix C	Hydrostatic Modeling Report
Appendix D	Groundwater Model Report
Appendix E	Slope and Stability Calculations
Appendix F	Groundwater Management Zone (GMZ) Application
Appendix G	Construction Quality Assurance Plan

Executive Summary of Closure Plan and Post-Closure Care Plan

The Wood River West Ash Complex is comprised of West Ash Pond 1, West Ash Pond 2E and West Ash Pond 2W at the Wood River Power Station, located in Alton in Madison County, Illinois. In November 2015, in accordance with 40 CFR Part 257, Subpart D, Dynegy Midwest Generation, LLC submitted to the Illinois Environmental Protection Agency (IEPA) a notice of intent to close the inactive West Ash Pond 2W. A notice of intent to close the West Ash Pond 1 was submitted by August 2016 and a notice of intent to close the West Ash Pond 2E was submitted October 2016.

West Ash Pond 1, West Ash Pond 2E, and West Ash Pond 2W are inactive Coal Combustion Residuals (CCR) surface impoundments separated by splitter dikes. West Ash Pond 2E contains a geomembrane liner system and West Ash Ponds 1 and 2W are unlined. The Wood River West Ash Complex will be closed by leaving CCR in place and using an alternative geomembrane cover system. This design will control the potential for water infiltration into the closed CCR unit and will allow drainage of surface water off of the cover system.

After closure activities are complete, post-closure activities, which include groundwater monitoring and maintenance of the final cover system, will occur. The closure and post-closure care activities will be in accordance with 40 CFR §257.102 and §257.104, respectively.

This document contains a closure plan and a post-closure care plan prepared in accordance with the outline approved by the IEPA on February 23, 2016. Closure construction activities may begin upon approval of this closure and post-closure care plan by the IEPA. The closure activities are estimated to be completed by November 18, 2020.

1 Closure Plan

Following approval by the IEPA and acquisition of required permits, closure activities for the Wood River West Ash Complex will be performed according to this plan. The location of the Wood River West Ash Complex and the individual impoundments are shown on Figure G-100 and Figure G-101.

1.1 Description of Proposed Closure Activities

Closure of the Wood River West Ash Complex will occur over a multi-year construction period and is estimated to be completed no later than November 18, 2020. Closure construction activities will include, but are not limited to, relocating and/or reshaping the existing CCR within the West Ash Complex to achieve acceptable grades for closure and constructing a cover system that complies with 40 CFR Part 257, Subpart D (CCR Rule). Removal of free water may be required prior to the relocation and grading of CCR and fill materials. As part of the reshaping of the CCR, fly ash mined from West Ash Pond 1 may be placed as crown fill material in West Ash Ponds 2W and 2E. The remaining coal in the coal pile will also be used to supplement the fill volume. In addition, CCR (primarily bottom ash) from the Primary East Ash Pond may be beneficially used as crown fill, and soil from a borrow source will be used to supplement the fill volume if necessary in order to reach final grades in preparation for the cap system for the West Ash Complex. Portions of the dike around West Ash Pond 1 will be cut down and the excess soils will be used as capping material in the West Ash Complex. The final cover system will comply with the applicable design requirements of the CCR Rule, including establishment of a vegetative cover to minimize long-term erosion.

Stormwater runoff from the final cover system will be collected and managed. A stormwater management system will be constructed to convey stormwater runoff from the cover system to interior drainage channels and will be routed through culvert pipes to the existing Pond 3. See Figures C-101 and C-102.

An existing transmission tower is located on the dike between the West Ash Ponds 1 and 2W. The transmission tower will remain in place and the area surrounding this transmission tower will be closed in place with a final cover system in compliance with the CCR Rule. See Figures C-101 and C-102.

1.2 Engineering Plans and Specifications for the Proposed Closure Activities

The engineering plans and design specifications for the final cover system and closure activities will meet the requirements of the CCR Rule for closure by leaving CCR in place.

1.2.1 Final Cover System

The final cover system will be constructed in direct contact with the graded CCR material. The final cover system design will meet the requirements of the CCR Rule such that the permeability shall be less than or equal to the permeability of the existing bottom liner or subsoils present below the CCR material, or a permeability no greater than 1×10^{-5} cm/sec, whichever is less. This will be achieved for the West Ash Complex through construction of an alternate geomembrane cover system. The requirement for the final cover system to be less permeable than the bottom layer allows water in the pore space of the CCR to drain into the foundation soils and not accumulate in the closed CCR impoundments. The bottom liner system for Pond 2E consists of a geomembrane. Ponds 1 and 2W are unlined. The closure design achieves the requirements of the low permeability layer and a protective layer to limit accumulation of water in the CCR impoundments. The geomembrane cover system will be installed over Ponds 1, 2W, and 2E and consist of, from bottom to top, a 40-mil LLDPE geomembrane membrane, a geocomposite drainage layer, and a minimum 18-inch protective cover soil layer. An erosion layer consisting of no less than 6-inches of earthen material capable of sustaining native plant growth will be placed on top of the protective cover soil layer. Details of the final cover system can be found on Figure C-106. Final cover system sections can be found on Figures C-103 through C-105.

1.2.2 Final Slope Design

The geometry of the final cover will provide a series of mounded surfaces for stormwater runoff control. The final cover will have a minimum planar slope of 2%, generally ranging from 2% to 2.75%, and will be graded to convey stormwater runoff to drainage channels. The drainage channels have slopes between 0.5% and 1.0% and will be lined with turf reinforced mats (TRM) where required to reduce the potential for erosion.

The crest elevation of West Ash Pond 1 will be lowered; however, the exterior slope grades will remain unchanged. The interior slopes will be 3H:1V and the top of the berm will be lowered as shown on Figure C-103. The exterior slopes and crest elevation of West Ash Ponds 2E and 2W will remain unchanged. Some limited areas of the West Ash Pond 2W cover system will have a 3H:1V slope near the western edge of the West Ash Complex as shown on Figure C-104.

Grading plans for the Wood River West Ash Complex can be found on Figures C-100 through C-102. The key design elements, including cover permeability, final cover slope and drainage channel slopes, will control the post-closure infiltration into the CCR material left in-place and preclude the probability of future impoundment of water at the units.

1.2.3 Summary of Slope Stability Evaluations

Based on the preliminary geotechnical analysis attached in Appendix C, the final slope of the perimeter berms and cover will meet the stability requirements of the CCR Rule to prevent sloughing or movement of the final cover system. The design allows for settlement as well as incidental, localized settling and subsidence.

1.3 Proposed Timeline for Implementation and Completion of Proposed Closure Activities

Closure of the Wood River West Ash Complex is estimated to be completed no later than November 18, 2020. Closure may commence following IEPA approval of this closure plan and in receipt of applicable permits for closure construction activities. Closure activities are scheduled to begin in 2016. The construction schedule includes time for construction activities such as; mobilization of contractors and setup of construction support facilities, installation of stormwater management system, site maintenance during construction activities, and seasonal shutdowns and demobilization of contractors and construction support personnel.

Estimated timing for major activity phases during each year are as follows:

– Years 1 – 2

- Acquire applicable permits for construction activities
- Begin construction activities; possibly including pumping to remove surface water, dewatering of the CCR, relocating and/or reshaping the existing CCR and construction of drainage structures

– Years 2 – 5

- Continue construction activities; possibly including pumping to remove surface water, dewatering of the CCR, relocating and/or reshaping the existing CCR, construction of drainage structures and construction of the final cover system

– Years 3 – 5

- Complete construction activities; possibly including pumping to remove surface water, dewatering of the CCR, relocating and/or reshaping the existing CCR, construction of drainage structures and construction of the final cover system
- Complete construction of final cover system
- Establish final cover vegetation
- Perform final grading and contouring of the storm water management system
- Perform regulatory compliance follow-up with state agency

1.4 Description of the Construction Quality Assurance Program for Proposed Closure Activities

The Construction Quality Assurance (CQA) Plan describes the CQA program for the closure of the Wood River West Ash Complex. The CQA Plan contains procedures for inspecting, monitoring, testing, and sampling to confirm compliance with the project plans and specifications. The site-specific CQA Plan is attached in Appendix E.

Key elements of the CQA Plan include:

- Establishment of several key project personnel roles and responsibilities, including a CQA consultant to serve as an on-site representative, to perform field tests and provide written documentation that the final cover system is constructed in accordance with the applicable plans and specifications. The CQA consultant team will include a CQA Officer who is an Illinois-licensed Professional Engineer and who will supervise inspections and testing, certify on-site activities, and review and approve weekly construction reports.
- Regularly scheduled safety and construction progress meetings.
- Standards and inspection and testing procedures for the following materials: earth cover and CCR materials, aggregates, geosynthetics, piping, concrete and grout.
- Specifications for surveying to verify that thickness and grade tolerances of construction components are in accordance with plans and specifications.
- Compilation of project documentation including plans, specifications, schedules, and inspection and testing logs in weekly summary reports certified by the CQA Officer. Additional progress reports at regular intervals are detailed in the CQA Plan.

1.5 Summary of Groundwater Monitoring Plan

The proposed groundwater monitoring plan, which has been developed based on the data presented in the Natural Resource Technology (NRT) Hydrogeologic Characterization Report (Appendix A), is provided in Appendix B. Groundwater will be monitored to evaluate post-closure groundwater quality and trends and demonstrate compliance with groundwater quality standards for Class I: Potable Resource Groundwater throughout the post-closure care period. The proposed groundwater monitoring system is designed to enable detection and measurement of CCR constituents if they should enter the groundwater from the Wood River West Ash Complex.

The proposed groundwater monitoring well network consists of a sufficient number of wells, installed at appropriate locations and depths, to monitor post-closure compliance with groundwater quality standards. The well network consists of 11 existing monitoring wells, seven of which will be used for groundwater quality monitoring and an additional four for monitoring of groundwater elevations. In addition to field parameters, seven of these monitoring wells (two upgradient, one background, and four downgradient) will be used for compliance sampling and analytical testing for the following parameters: inorganic totals for chloride, fluoride, sulfate, Total Dissolved Solids (TDS), and Radium 226/228; and metal totals for antimony, arsenic, barium, beryllium, boron, cadmium, calcium, chromium, cobalt, lead, lithium, mercury, molybdenum, selenium, and thallium. The locations of the proposed groundwater monitoring wells can be found on Figure 5 of the Natural Resource Technology (NRT) report in Appendix B.

Specifications for each monitoring well will meet IEPA design and construction requirements. Monitoring wells will be inspected during each groundwater sampling event. Maintenance will be performed as needed to assure that the monitoring wells provide representative groundwater samples.

Statistical analysis of the laboratory analytical data will be reported to IEPA with the annual report for the facility. Compliance with applicable groundwater quality standards will be achieved when there are no statistically significant increasing trends detected at the downgradient boundaries that are attributed to the Wood River West Ash Ponds 1, 2E, and 2W. Details of the proposed groundwater monitoring plan can be found in the attached NRT report in Appendix B.

The monitoring well network as proposed also meets USEPA CFR Part 257 requirements for monitoring the Uppermost Aquifer, which is the Primary Sand Unit that underlies the entire Wood River Power Station. The proposed USEPA CCR network consists of the same three upgradient/background wells and four downgradient wells as the proposed IEPA monitoring well network. Groundwater samples will be collected and analyzed for all Appendix III and IV parameters as listed in the CCR Rule. Reporting requirements will be in accordance with the CCR Rule.

1.6 Professional Certification and Seal

CCR Unit: Dynegy Midwest Generation, LLC; Wood River Power Station; Wood River West Ash Complex

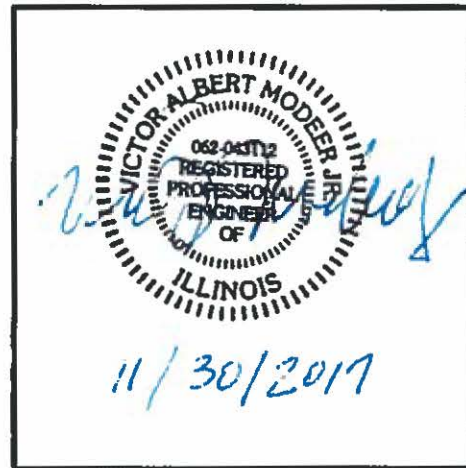
I, Victor Modeer, PE, D.G.E., being a Registered Professional Engineer in good standing in the State of Illinois, do hereby certify, to the best of my knowledge, information, and belief, that the information contained in this Closure Plan dated October 2016 has been prepared in accordance with the accepted practice of engineering.

Victor A. Modeer Jr

Printed Name

10/27/16

Date



2 Environmental Impacts of Proposed Closure Activities

The information referenced in this section was derived from various reports prepared by NRT, including the Hydrogeologic Site Characterization Report, Groundwater Monitoring Plan, Hydrostatic Modeling Report, and the Groundwater Management Zone Application. An Illinois licensed Professional Geologist signed the attached documents prepared by NRT (Appendix A – D and F).

2.1 Summary of Pre-Closure Groundwater Conditions

Sampling and analysis of groundwater from monitoring wells at the Wood River West Ash Ponds 1, 2E, and 2W has been conducted quarterly or semi-annually since 1995. Parameters that have been detected in groundwater in downgradient monitoring wells at concentrations exceeding the Class I groundwater quality standards include boron, manganese, TDS, and pH, with exceedances of manganese, TDS, and pH attributable to anthropogenic sources or naturally occurring geochemical variability. Boron is the only primary indicator of the presence of CCR leachate constituents in groundwater for this site. Hydrogeological site characterization and groundwater quality data are discussed in detail in the NRT Hydrogeologic Site Characterization Report attached as Appendix A.

2.2 Summary of Modeled Post-Closure Groundwater Conditions

The Hydrologic Evaluation of Landfill Performance (HELP) model was used to calculate the time for groundwater beneath each of the three CCR units to reach hydrostatic equilibrium. Hydrostatic model results, discussed in detail in the NRT Hydrostatic Modeling Report attached as Appendix C, indicate equilibrium for the geomembrane cover system at West Ash Pond 1 and West Ash Pond 2W will be reached approximately ten years after installation of the final cover design meeting CCR Rule requirements. The NRT report indicates equilibrium for the West Ash Pond 2E is not reached within the 100-year simulation. However, hydraulic head for the geomembrane cover system meeting CCR Rule requirements at West Ash Pond 2E is expected to keep decreasing beyond the 100-year simulation duration following cap completion, with heads decreasing from current 120 inches average head to less than 60 inches, as a result of the basal composite/synthetic liner system already in place.

A groundwater flow and transport model, Groundwater Model Report, included in Appendix D, was prepared for the entire West Ash Complex. The Groundwater Model Report indicates the following:

- Under baseline conditions with no cover on any of the three West Ash Complex impoundments, the primary CCR indicator, boron, is predicted to reach peak concentrations in approximately 300 years before starting to decrease.
- The CCR plume extent with a geomembrane cover system at West Ash Complex is predicted to begin contracting after one year.
- Based on the maximum modeled plume extents, under both baseline conditions and the planned cover closure scenario, no potable or non-potable water supply wells are predicted to show exceedances of groundwater quality standards related to CCR leachate. The only known wells (excluding monitoring wells and piezometers) that exist in the vicinity of the West Ash Complex, or within the area of actual or modeled Class I groundwater exceedances, are pressure relief wells along the adjacent levee.

Closure in place of the Wood River Ash Complex, as proposed, will result in a reduction of leachate production, decreasing boron concentrations along with other CCR leachate parameters, and contraction of the groundwater contaminant plume. The current horizontal extent of the parameters of concern related to CCR leachate (boron) that exceed Class I groundwater standards is within the Wood River Power Station's property with the possible exception of a narrow strip along the Great River Road (i.e., Route 143) that is not owned by Dynegy Midwest Generation, LLC (DMG). DMG owns the property both north and south of the Great River Road extending to the banks of the Mississippi River. The modeled boron plume exceeding the Class I standard extends southward and southeastward towards the Mississippi River, but within the Wood River Power Station's property.

2.3 Anticipated Effects of the Closed Impoundment on Nearby Surface Waters

Groundwater flow in the Primary Sand Unit that underlies the Wood River Ash Complex is predominantly south and southeast towards the Mississippi River. Groundwater in the Primary Sand Unit discharges via base flow to the Mississippi River during base stage and low river levels. During spring flooding and high Mississippi River stages groundwater flow is northerly. After flood levels subside, the flow direction reverts to more normal conditions and groundwater again discharges to the river.

Impacts of groundwater with elevated concentrations of CCR constituents, principally boron, from beneath the closed Wood River Ash Complex on the Mississippi River will be negligible.

3 Post-Closure Care Plan

Following closure of West Ash Complex, post-closure care will be performed according to this plan. The closed impoundments will be monitored and maintained for a post-closure period that is anticipated to continue for 30 years. The post-closure period may extend beyond 30 years if additional groundwater monitoring is required to assess groundwater constituents as compared to background levels.

3.1 Description of Post-Closure Care Activities

Throughout the post-closure care period, periodic, typically annual, visual inspections of the final cover system for evidence of settlement, subsidence, erosion, or other damage that may affect the integrity of the final cover system will be performed. Noted damage will be repaired in order to maintain the effectiveness of the final cover system. Repair activities may include, but are not limited to replacing cover soil and repairing drainage channels that have been eroded, filling in depressions with soil, and reseeding areas of failed vegetation.

Groundwater samples will be collected and analyzed for inorganic chemical parameters that are indicator constituents for CCR leachate. In addition, each groundwater sampling event will measure field parameters and groundwater levels. The proposed groundwater monitoring plan will monitor and evaluate groundwater quality to demonstrate compliance with the groundwater quality standards for Class II: General Resource Groundwater.

The end of the post-closure period will be documented in accordance with the CCR Rule. Post-closure documentation will be maintained for at least five years in accordance with the CCR Rule.

3.2 Description of the Planned Use of the Property during the Post-Closure Care Period

Following closure, a notation will be recorded on the deed to the property or on some instrument that is normally examined during a title search to identify that the land has been used as a CCR impoundment. The notation will provide notice that use of the land is restricted to activities that will not disturb the integrity of the final cover system or groundwater monitoring system.

The Wood River Power Station will not continue to be used as a power generating facility after closure of the Wood River West Ash Complex. Activity on and around the final cover and stormwater systems for the closed impoundments will include ongoing post-closure inspection, maintenance and monitoring activities. Planned post-closure use of the property will not disturb or damage the integrity of the final cover system or groundwater monitoring system.

3.3 Stormwater Management

The key design elements of the stormwater management system, including cover permeability, final cover slope and drainage channel slopes will minimize post-closure infiltration of liquids into the CCR left in-place and will preclude the probability of future impoundment of water at the impoundments. The stormwater management system is designed for a 25-year, 24-hour storm event and will be constructed during closure and grading of the final cover system. Stormwater management features and erosion controls will be integrated with reshaping of the CCR surface and placement of the cover system to promote positive surface drainage and minimize erosion.

Stormwater from the finished cover system on the Wood River West Ash Complex will drain through a series of drainage channels on the cover system, through culverts and eventually draining into the existing Pond 3. The drainage channels on the cover system will be earthen channels lined with grass and TRM where required. The culverts are sized to be 24-inch diameter pipes to pass the 25-year storm without ponding of water on the cover system, and to pass the 100-year storm with minimum ponding while attenuating the discharge into Pond 3. There

will be no permanent storage of storm or surface water upstream of Pond 3. The external embankments of Pond 3 will be raised to increase freeboard for preventing overtopping of stormwater during the design storm. See Figure C-100. Details of drainage channels are provided on Figure C-106.

3.4 Professional Certification and Seal

CCR Unit: Dynegy Midwest Generation, LLC; Wood River Power Station; Wood River West Ash Complex

I, Victor Modeer, PE, D.GE., being a Registered Professional Engineer in good standing in the State of Illinois, do hereby certify, to the best of my knowledge, information, and belief, that the information contained in this Post-Closure Care Plan dated October 2016 has been prepared in accordance with the accepted practice of engineering.

Victor A Modeer Jr

Printed Name

10/27/16

Date



Figures

DYNEGY MIDWEST GENERATION, LLC

WOOD RIVER POWER STATION

ALTON, ILLINOIS

PERMIT DRAWINGS

FOR CLOSURE OF THE WOOD RIVER WEST ASH COMPLEX



1001 Highlands Plaza
Drive West, Suite 300
St. Louis, Mo. 63110-1337
314 429-0100 (phone)
314 429-0462 (fax)

DYNEGY MIDWEST
GENERATION, LLC
1500 East Port Plaza Drive
Collinsville, IL 62234

WOOD RIVER
POWER STATION
ALTON, IL

PERMIT DRAWINGS
FOR CLOSURE OF THE
WOOD RIVER WEST
ASH COMPLEX

ISSUED FOR BIDDING

ISSUED FOR CONSTRUCTION

REVISIONS

NO	DESCRIPTION	DATE

AECOM PROJECT NO 60501530

DRAWN BY LEH

DESIGNED BY LEH

CHECKED BY RHM

DATE CREATED 10/13/2015

PLOT DATE 10/27/2016

SCALE AS SHOWN

ACAD VER 2015

SHEET TITLE

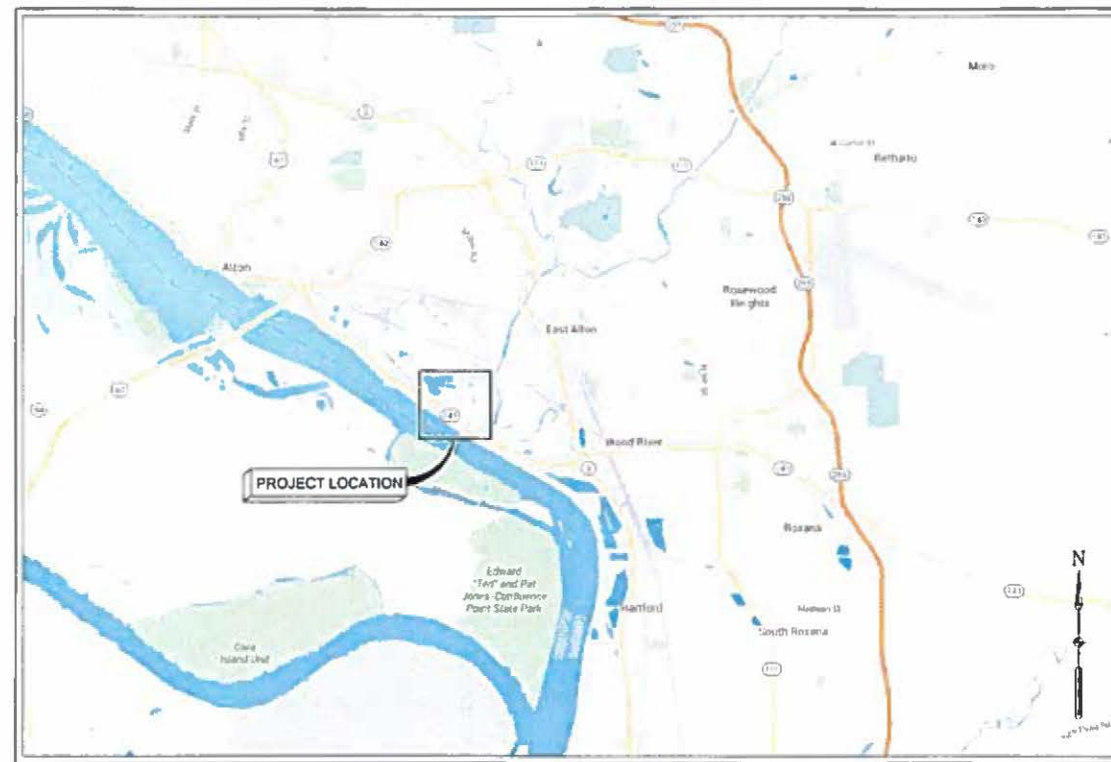
COVER SHEET AND
LOCATION MAP

G-100

SHEET 1 OF 9



STATE MAP
NOT TO SCALE



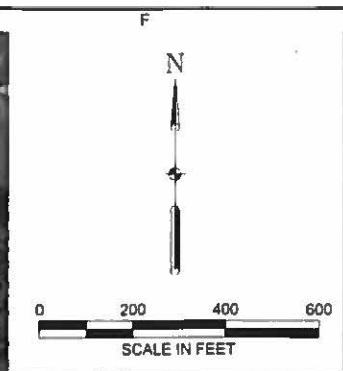
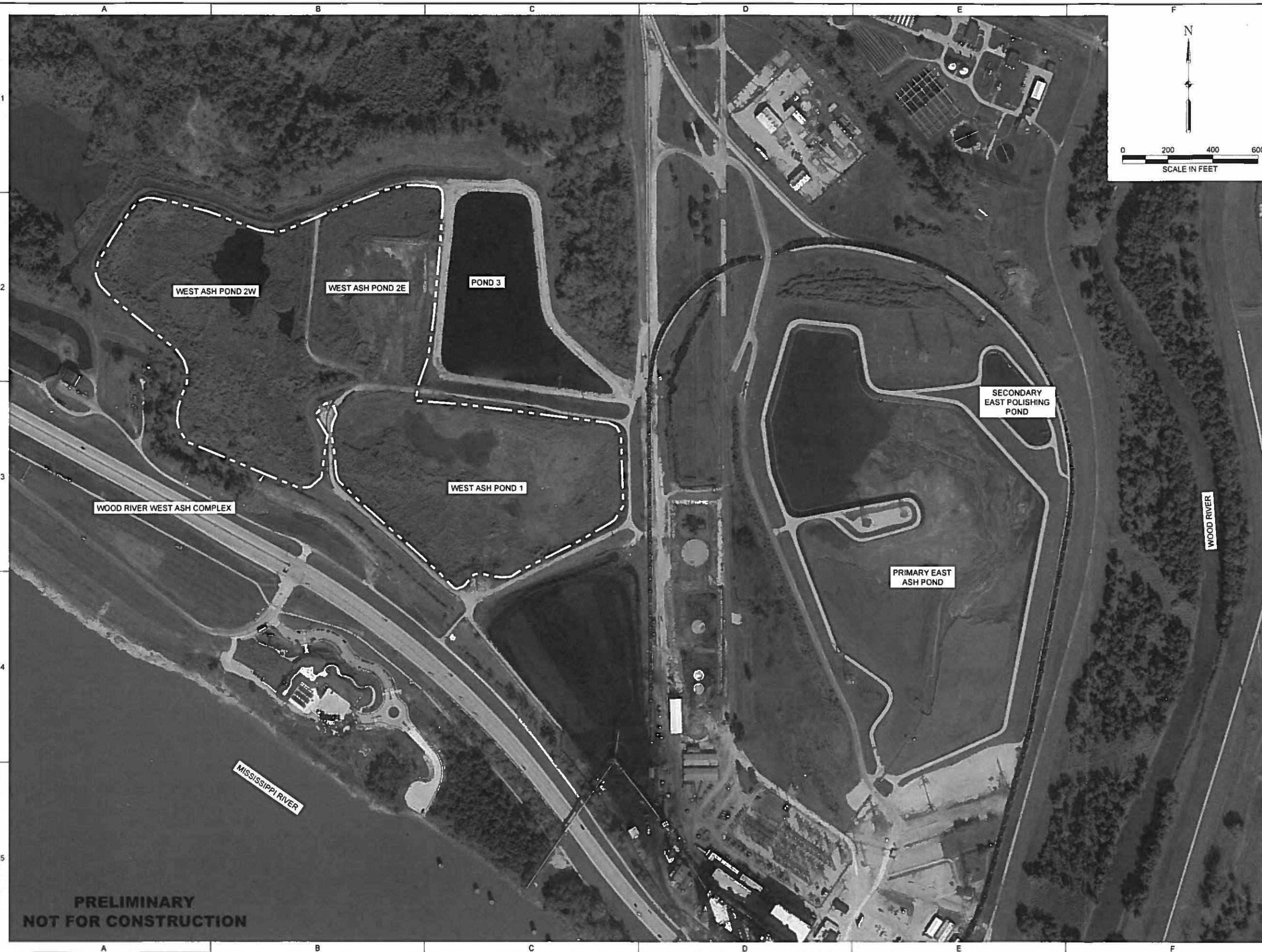
LOCATION MAP
NOT TO SCALE

DRAWINGS LIST		
SHEET NO.	DRAWING NO.	DRAWING TITLE
1	G-100	COVER SHEET AND LOCATION MAP
2	G-101	EXISTING CONDITIONS
3	C-100	OVERALL GRADING PLAN
4	C-101	GRADING PLAN
5	C-102	GRADING PLAN
6	C-103	SECTION A
7	C-104	SECTIONS B AND C
8	C-105	SECTIONS D AND E
9	C-106	DETAILS

**PRELIMINARY
NOT FOR CONSTRUCTION**

AECOM DRAWING PATH: P:\Projects\Geotech\60428794_DynergyCCR\15_Wood River West Closure Plan\Drawings\COVER SHEET.dwg

I:\Projects\Geotech\60428794_Dynegy\CR\15_Wood River West Closure Plan\Drawings\WOR-EXISTING CONDITIONS.dwg
 10/27/2016 12:21 PM
 AECOM DRAWING



AECOM
 1001 Highlands Plaza
 Drive West, Suite 300
 St. Louis, Mo. 63110-1337
 314 429-0100 (phone)
 314 429-0462 (fax)

DYNEGY MIDWEST GENERATION, LLC
 1500 East Port Plaza Drive
 Collinsville, IL 62234

**WOOD RIVER POWER STATION
 ALTON, IL**
 PERMIT DRAWINGS
 FOR CLOSURE OF THE
 WOOD RIVER WEST
 ASH COMPLEX

ISSUED FOR BIDDING _____ DATE BY _____

ISSUED FOR CONSTRUCTION _____ DATE BY _____

REVISIONS		
NO	DESCRIPTION	DATE

AECOM PROJECT NO	60501530
DRAWN BY	MJC
DESIGNED BY	MJC
CHECKED BY	LF
DATE CREATED	4/25/2016
PLOT DATE	10/27/2016
SCALE	1" = 200'
ACAD VER	2015

SHEET TITLE

EXISTING CONDITIONS

G-101

SHEET 2 OF 9

**PRELIMINARY
NOT FOR CONSTRUCTION**

AECOM DRAWING PATH: P:\Projects\Geotech\60128794_DynegyCOR\15_Wood River West Closure Plan\Drawings\WDR-SITE PLAN.dwg
 DWG, TWA, 10/27/2016 12:21 PM

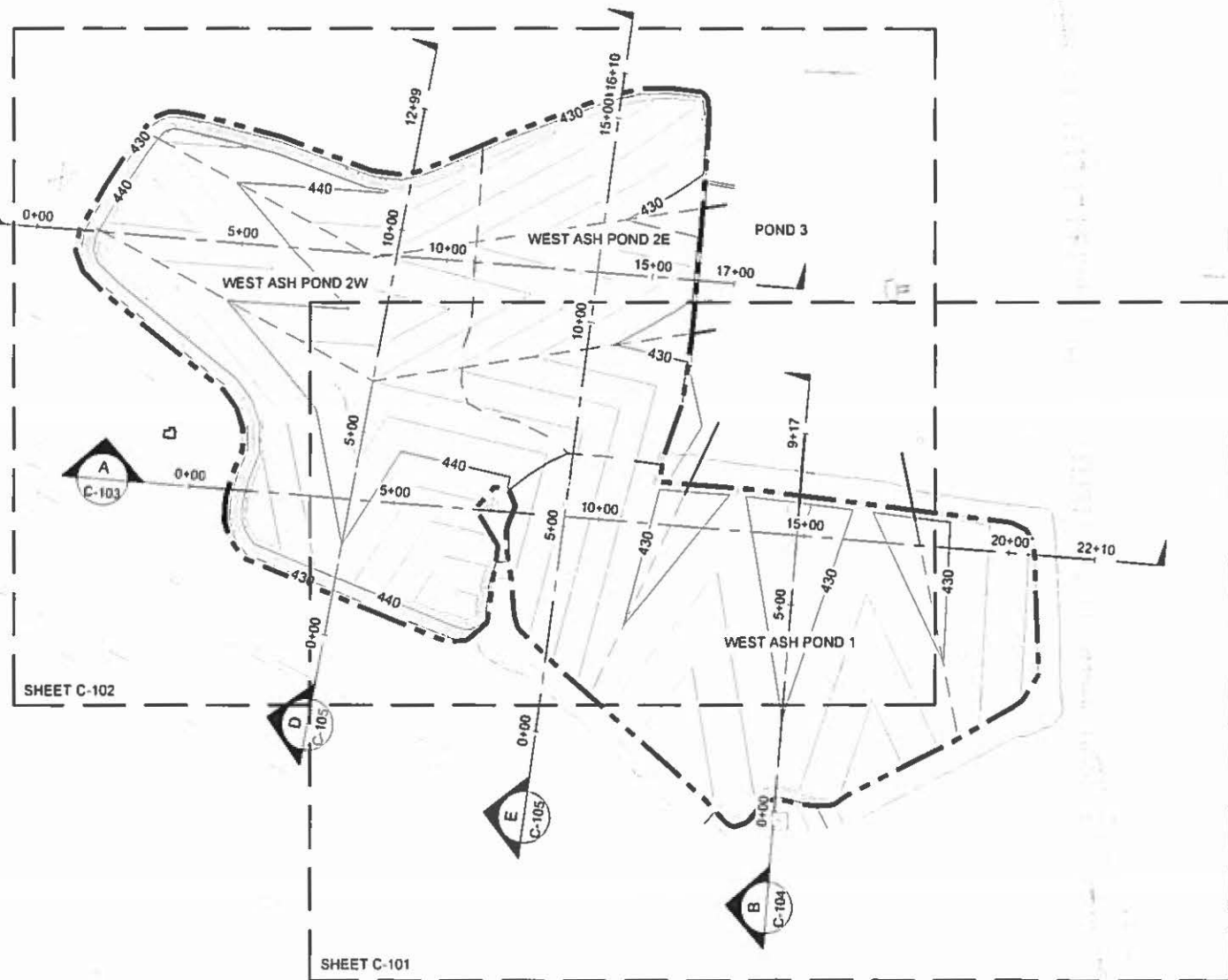
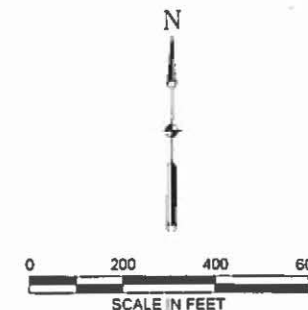
AECOM

1001 Highlands Plaza
 Drive West, Suite 300
 St. Louis, Mo 63110-1337
 314 429-0100 (phone)
 314 429-0482 (fax)

**DYNEGY MIDWEST
 GENERATION, LLC**
 1500 East Port Plaza Drive
 Collinsville, IL 62234

**WOOD RIVER
 POWER STATION
 ALTON, IL**

**PERMIT DRAWINGS
 FOR CLOSURE OF THE
 WOOD RIVER WEST
 ASH COMPLEX**



SECONDARY
 EAST POLISHING
 POND

PRIMARY EAST
 ASH POND

WOOD RIVER

MISSISSIPPI RIVER

**PRELIMINARY
 NOT FOR CONSTRUCTION**

NOTES:

- 1 THE EXISTING GROUND CONTOURS WERE CREATED FROM AERIAL SURVEY PERFORMED BY SURDEX ON AUGUST 17, 2015 AND BATHYMETRIC SURVEY COMPLETED BY WEAVER CONSULTANTS GROUP ON SEPTEMBER 22, 2015. AREAS SURROUNDING THE EAST ASH COMPLEX WERE SUPPLEMENTED WITH PUBLICLY AVAILABLE INFORMATION BY MADISON COUNTY LIDAR DIRECTORY
- 2 EXISTING AND PROPOSED GRADE CONTOURS ARE SHOWN AT 2 FOOT ELEVATION INTERVALS
- 3 PROPOSED CONTOURS REPRESENT TOP OF COVER SYSTEM
- 4 SEE GRADING PLANS FOR CONTOUR AND SLOPE LABELS
- 5 TYPICAL COVER SYSTEM HAS A MINIMUM OF 18" OF SOIL COVER, 6" OF EROSION LAYER, A GEOCOMPOSITE, AND A GEOMEMBRANE SEE DETAIL 1 ON SHEET C-106

LEGEND

- EXISTING MAJOR CONTOURS
- EXISTING MINOR CONTOURS
- PROPOSED MAJOR CONTOURS
- PROPOSED MINOR CONTOURS
- EXISTING PROCESS WATER PIPES
- EXISTING STORM WATER PIPES
- EXISTING FORCEMAIN
- EXISTING RAILROAD
- EXISTING TRANSMISSION TOWER
- EXISTING OVERHEAD WIRE
- POND LIMITS
- PROPOSED LIMITS OF COVER SYSTEM
- PROPOSED COVER SYSTEM VALLEY
- PROPOSED CULVERTS

ISSUED FOR BIDDING _____ DATE BY _____

ISSUED FOR CONSTRUCTION _____ DATE BY _____

REVISIONS		
NO	DESCRIPTION	DATE

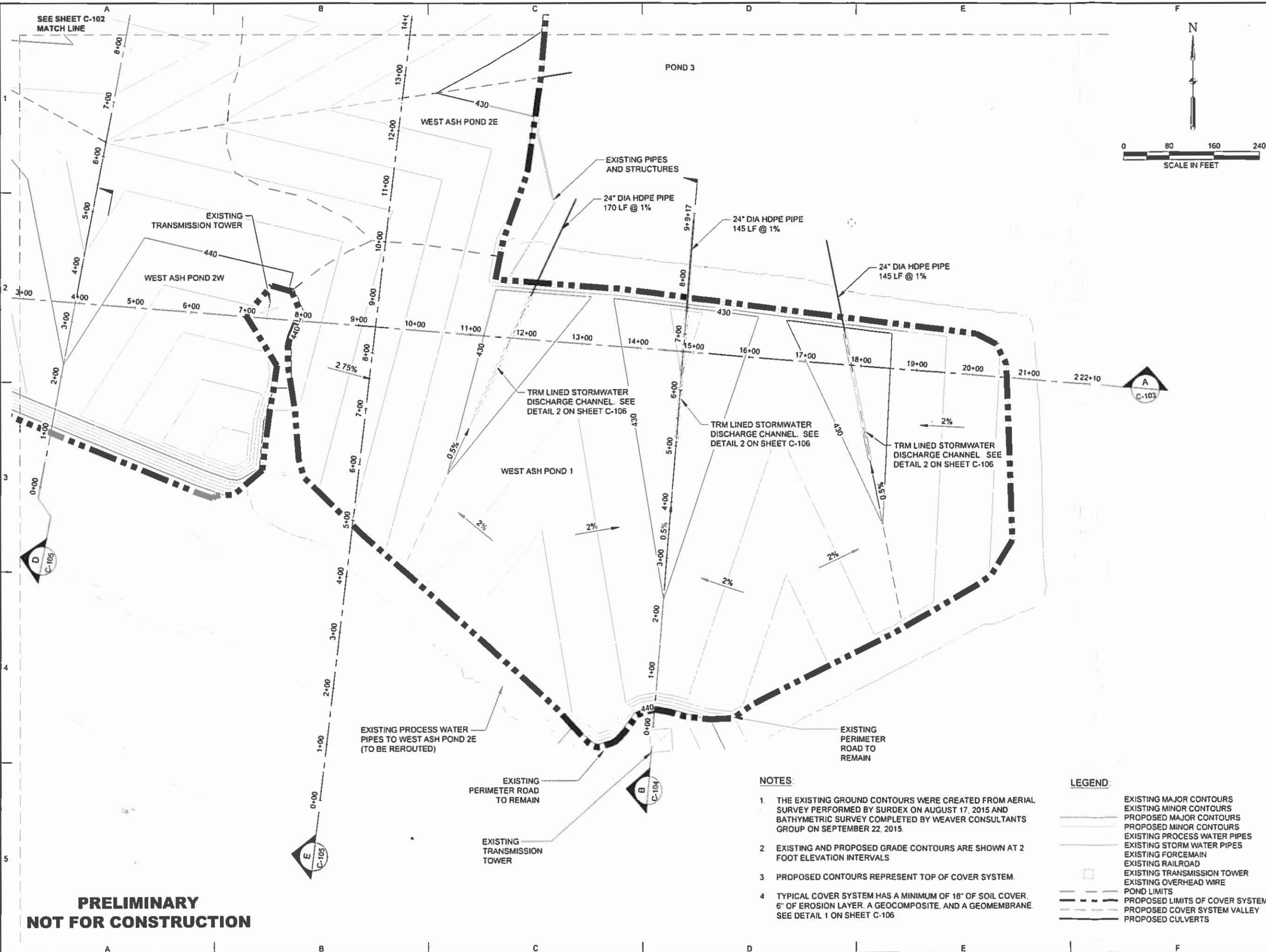
AECOM PROJECT NO	60501530
DRAWN BY	LEH
DESIGNED BY	LEH
CHECKED BY	RHH
DATE CREATED	10/13/2015
PLOT DATE	10/27/2016
SCALE	1" = 200'
ACAD VER	2015

SHEET TITLE
OVERALL GRADING PLAN

C-100

SHEET 2 OF 9

AECOM DRAWING PATH: P:\Projects\Geotech\50426794_Dynergy\Drawings\WDR-GRADING PLAN 1.dwg
 CARUSO, MICHAEL, 11/10/2016 4:01 PM



1001 Highlands Plaza
 Drive West, Suite 300
 St. Louis, Mo. 63110-1337
 314 429-0100 (phone)
 314 429-0462 (fax)

DYNEGY MIDWEST GENERATION, LLC
 1500 East Port Plaza Drive
 Collinsville, IL 62234

**WOOD RIVER POWER STATION
 ALTON, IL**
**PERMIT DRAWINGS
 FOR CLOSURE OF THE
 WOOD RIVER WEST
 ASH COMPLEX**

ISSUED FOR BIDDING _____ DATE BY _____

ISSUED FOR CONSTRUCTION _____ DATE BY _____

REVISIONS		
NO	DESCRIPTION	DATE

AECOM PROJECT NO	60501530
DRAWN BY	LEH
DESIGNED BY	LEH
CHECKED BY	RHH
DATE CREATED	10/13/2015
PLOT DATE	11/10/2016
SCALE	1" = 80'
ACAD VER.	2015

SHEET TITLE

GRADING PLAN

C-101

SHEET 3 OF 9

**PRELIMINARY
NOT FOR CONSTRUCTION**

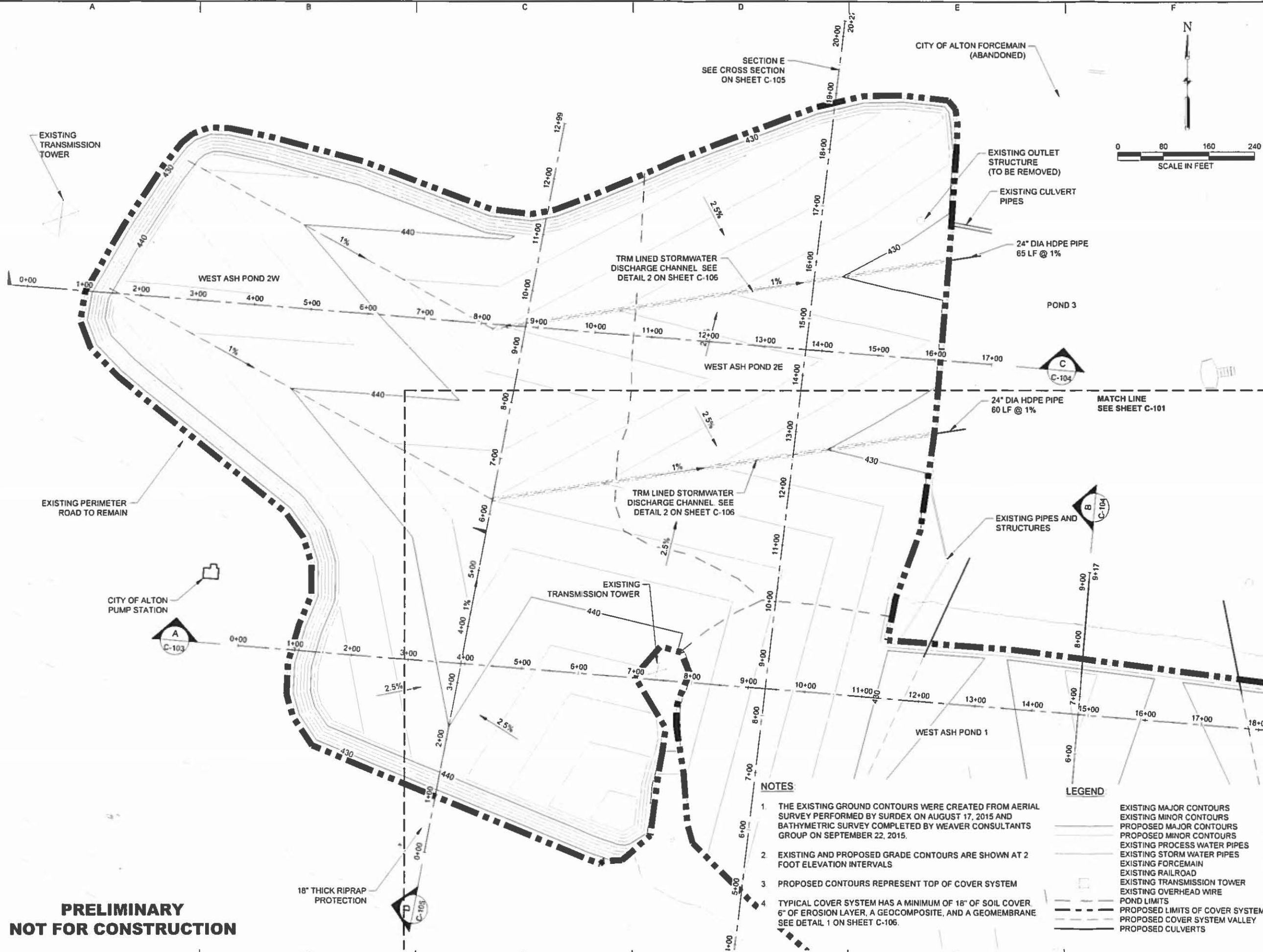
- NOTES**
- THE EXISTING GROUND CONTOURS WERE CREATED FROM AERIAL SURVEY PERFORMED BY SURDEX ON AUGUST 17, 2015 AND BATHYMETRIC SURVEY COMPLETED BY WEAVER CONSULTANTS GROUP ON SEPTEMBER 22, 2015.
 - EXISTING AND PROPOSED GRADE CONTOURS ARE SHOWN AT 2 FOOT ELEVATION INTERVALS
 - PROPOSED CONTOURS REPRESENT TOP OF COVER SYSTEM.
 - TYPICAL COVER SYSTEM HAS A MINIMUM OF 18" OF SOIL COVER, 6" OF EROSION LAYER, A GEOCOMPOSITE, AND A GEOMEMBRANE. SEE DETAIL 1 ON SHEET C-106

AECOM DRAWING PATH: P:\Projects\Geotech\60428794_DynegyCER\15_Wood River West Closure Plan\Drawings\WDR-GRADING PLAN 2.dwg

AECOM
 1001 Highlands Plaza
 Drive West, Suite 300
 St. Louis, Mo. 63110-1337
 314 429-0100 (phone)
 314 429-0462 (fax)

DYNEGY MIDWEST GENERATION, LLC
 1500 East Port Plaza Drive
 Collinsville, IL 62234

**WOOD RIVER POWER STATION
 ALTON, IL**
 PERMIT DRAWINGS
 FOR CLOSURE OF THE
 WOOD RIVER WEST
 ASH COMPLEX



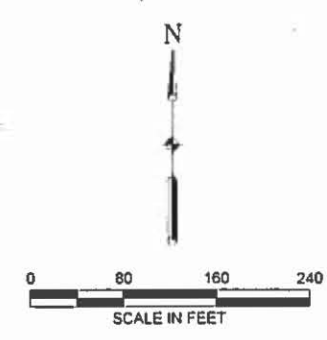
**PRELIMINARY
 NOT FOR CONSTRUCTION**

NOTES

1. THE EXISTING GROUND CONTOURS WERE CREATED FROM AERIAL SURVEY PERFORMED BY SURDEX ON AUGUST 17, 2015 AND BATHYMETRIC SURVEY COMPLETED BY WEAVER CONSULTANTS GROUP ON SEPTEMBER 22, 2015.
2. EXISTING AND PROPOSED GRADE CONTOURS ARE SHOWN AT 2 FOOT ELEVATION INTERVALS
3. PROPOSED CONTOURS REPRESENT TOP OF COVER SYSTEM
4. TYPICAL COVER SYSTEM HAS A MINIMUM OF 18" OF SOIL COVER, 6" OF EROSION LAYER, A GEOCOMPOSITE, AND A GEOMEMBRANE. SEE DETAIL 1 ON SHEET C-106.

LEGEND

- EXISTING MAJOR CONTOURS
- EXISTING MINOR CONTOURS
- PROPOSED MAJOR CONTOURS
- PROPOSED MINOR CONTOURS
- EXISTING PROCESS WATER PIPES
- EXISTING STORM WATER PIPES
- EXISTING FORCEMAIN
- EXISTING RAILROAD
- EXISTING TRANSMISSION TOWER
- EXISTING OVERHEAD WIRE
- POND LIMITS
- PROPOSED LIMITS OF COVER SYSTEM
- PROPOSED COVER SYSTEM VALLEY
- PROPOSED CULVERTS



ISSUED FOR BIDDING _____ DATE _____

ISSUED FOR CONSTRUCTION _____ DATE _____

REVISIONS		
NO	DESCRIPTION	DATE

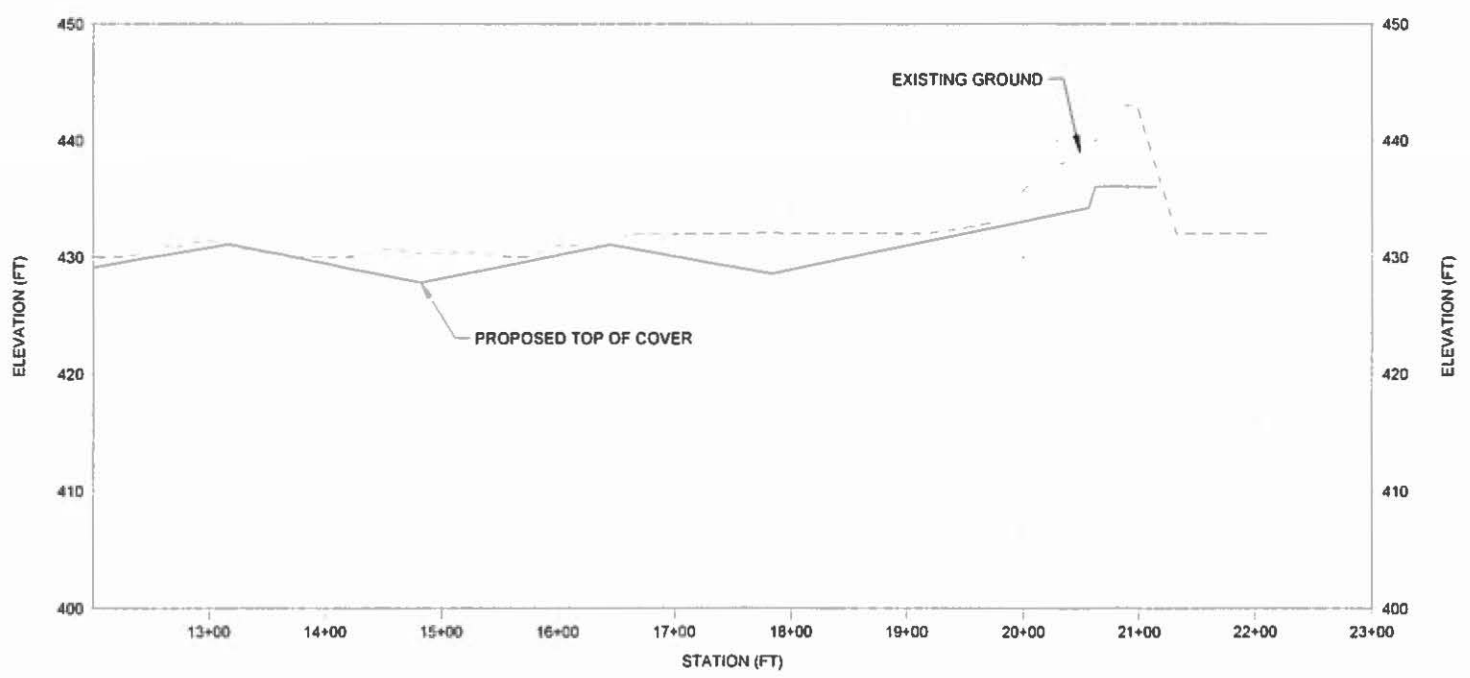
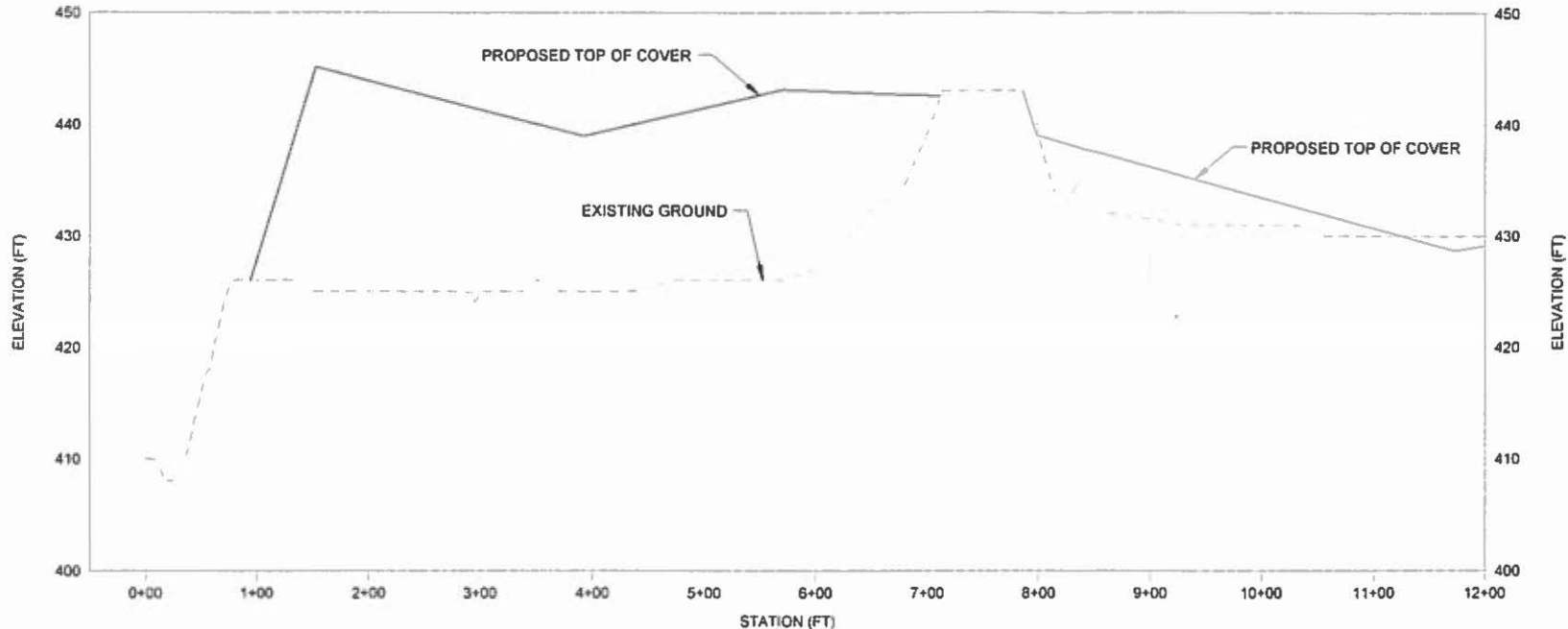
AECOM PROJECT NO	60501530
DRAWN BY	LEH
DESIGNED BY	LEH
CHECKED BY	RHM
DATE CREATED	10/15/2015
PLOT DATE	10/27/2015
SCALE	1" = 80'
ACAD VER	2015

SHEET TITLE

GRADING PLAN

C-102
 SHEET 4 OF 9

AECOM DRAWING PATH: P:\Projects\Geotech\60428794_DynegyCCR\15_Wood River West Closure Plan\Drawings\WDR-CROSS SECTIONS.dwg
 LHM, TMA, 10/27/2016 12:23 PM



A SECTION A
 C-100 HORIZONTAL SCALE 1" = 80'
 VERTICAL SCALE 1" = 8'

**PRELIMINARY
NOT FOR CONSTRUCTION**

NOTES

1. THE EXISTING GROUND ELEVATIONS SHOWN ARE FROM AERIAL SURVEY PERFORMED BY SURDEX ON AUGUST 17, 2015 AND BATHYMETRIC SURVEY COMPLETED BY WEAVER CONSULTANTS GROUP ON SEPTEMBER 22, 2015
2. EXISTING GRADE ELEVATIONS REFLECT TOP OF ASH WITHIN THE WOOD RIVER WEST ASH COMPLEX AND EXISTING GROUND SURFACE ELEVATIONS OUTSIDE WOOD RIVER WEST ASH COMPLEX.
3. PROPOSED GRADE ELEVATIONS REFLECT TOP OF COVER SYSTEM WITHIN WOOD RIVER WEST ASH COMPLEX AND PROPOSED GROUND SURFACE ELEVATIONS OUTSIDE WOOD RIVER WEST ASH COMPLEX.



1001 Highlands Plaza
 Drive West, Suite 300
 St. Louis, Mo. 63110-1337
 314 429-0100 (phone)
 314 429-0462 (fax)

**DYNEGY MIDWEST
GENERATION, LLC**
 1500 East Port Plaza Drive
 Collinsville, IL 62234

**WOOD RIVER
POWER STATION
ALTON, IL**

**PERMIT DRAWINGS
FOR CLOSURE OF THE
WOOD RIVER WEST
ASH COMPLEX**

ISSUED FOR BIDDING _____ DATE BY _____

ISSUED FOR CONSTRUCTION _____ DATE BY _____

REVISIONS		
NO	DESCRIPTION	DATE

AECOM PROJECT NO	60501530
DRAWN BY	LEH
DESIGNED BY	LEH
CHECKED BY	RHH
DATE CREATED	10/13/2015
PLOT DATE	10/27/2016
SCALE	AS SHOWN
ACAD VER	2015

SHEET TITLE

SECTION A

C-103

SHEET 5 OF 9

AECOM DRAWING PATH: P:\Projects\Geotech\0428794_Dynegy\CDR\15_Wood River West Closure Plan\Drawings\WOR-CROSS SECTIONS.dwg
 UBL 14A_10/27/2016 12:23 PM

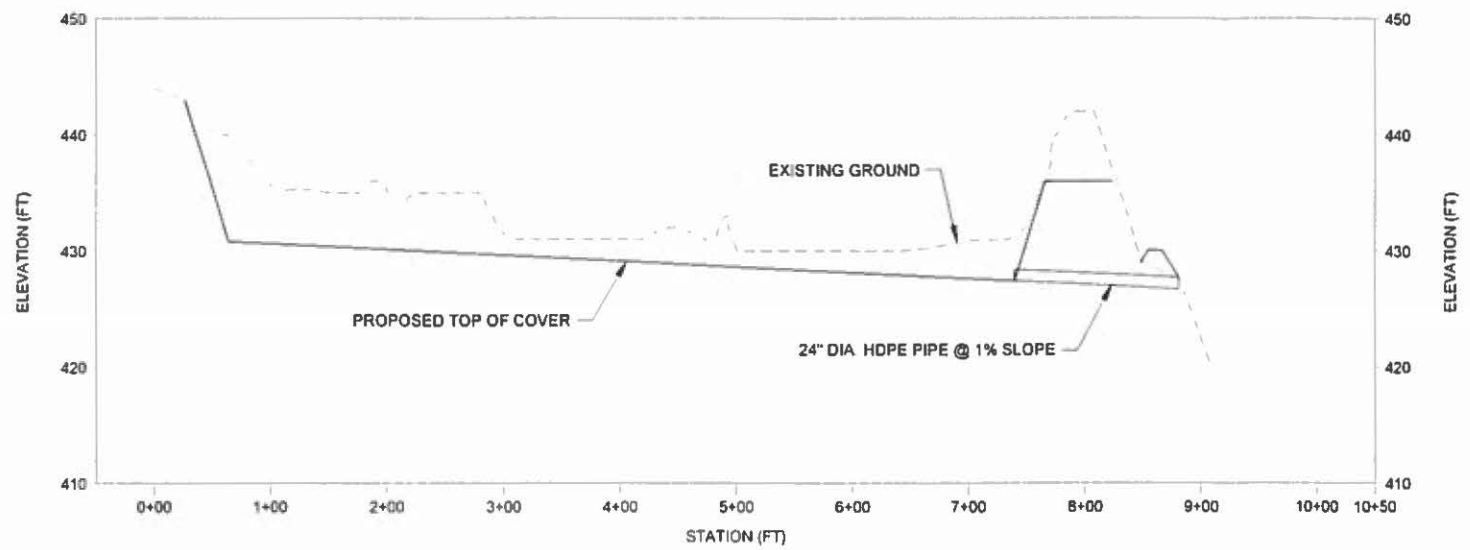


1001 Highlands Plaza
 Drive West, Suite 300
 St. Louis, Mo. 63110-1337
 314 429-0100 (phone)
 314 429-0462 (fax)

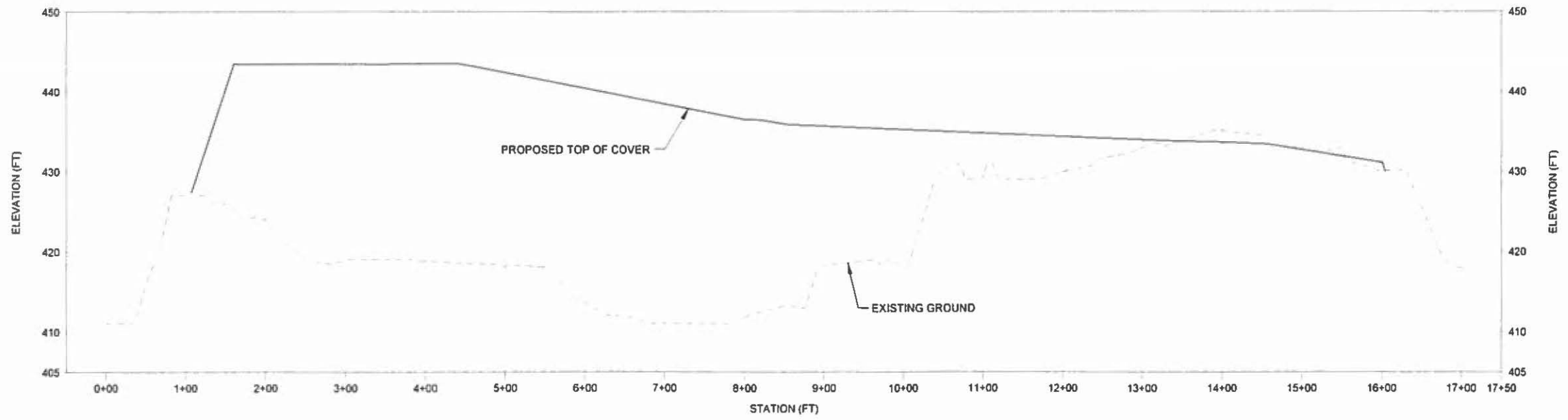
**DYNEGY MIDWEST
 GENERATION, LLC**
 1500 East Port Plaza Drive
 Collinsville, IL 62234

**WOOD RIVER
 POWER STATION
 ALTON, IL**

**PERMIT DRAWINGS
 FOR CLOSURE OF THE
 WOOD RIVER WEST
 ASH COMPLEX**



B SECTION B
 C-100 HORIZONTAL SCALE 1" = 80'
 VERTICAL SCALE 1" = 8'



C SECTION C
 C-100 HORIZONTAL SCALE 1" = 80'
 VERTICAL SCALE 1" = 8'

NOTES:

- THE EXISTING GROUND ELEVATIONS SHOWN ARE FROM AERIAL SURVEY PERFORMED BY SURDEX ON AUGUST 17, 2015 AND BATHYMETRIC SURVEY COMPLETED BY WEAVER CONSULTANTS GROUP ON SEPTEMBER 22, 2015.
- EXISTING GRADE ELEVATIONS REFLECT TOP OF ASH WITHIN THE WOOD RIVER WEST ASH COMPLEX AND EXISTING GROUND SURFACE ELEVATIONS OUTSIDE WOOD RIVER WEST ASH COMPLEX.
- PROPOSED GRADE ELEVATIONS REFLECT TOP OF COVER SYSTEM WITHIN WOOD RIVER WEST ASH COMPLEX AND PROPOSED GROUND SURFACE ELEVATIONS OUTSIDE WOOD RIVER WEST ASH COMPLEX.

**PRELIMINARY
NOT FOR CONSTRUCTION**

ISSUED FOR BIDDING _____ DATE BY _____

ISSUED FOR CONSTRUCTION _____ DATE BY _____

REVISIONS		
NO	DESCRIPTION	DATE

AECOM PROJECT NO	60501530
DRAWN BY	LEH
DESIGNED BY	LEH
CHECKED BY	RHH
DATE CREATED	10/13/2015
PLOT DATE	10/27/2016
SCALE	AS SHOWN
ACAD VER	2015

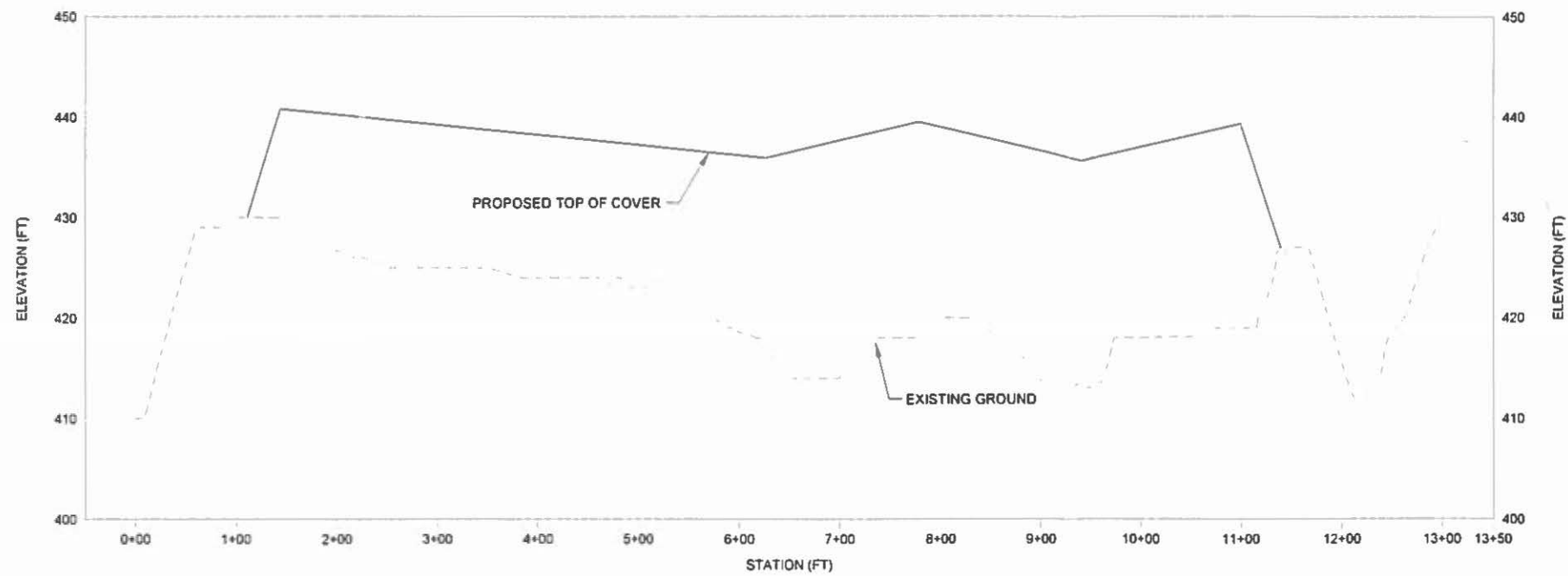
SHEET TITLE

SECTIONS B AND C

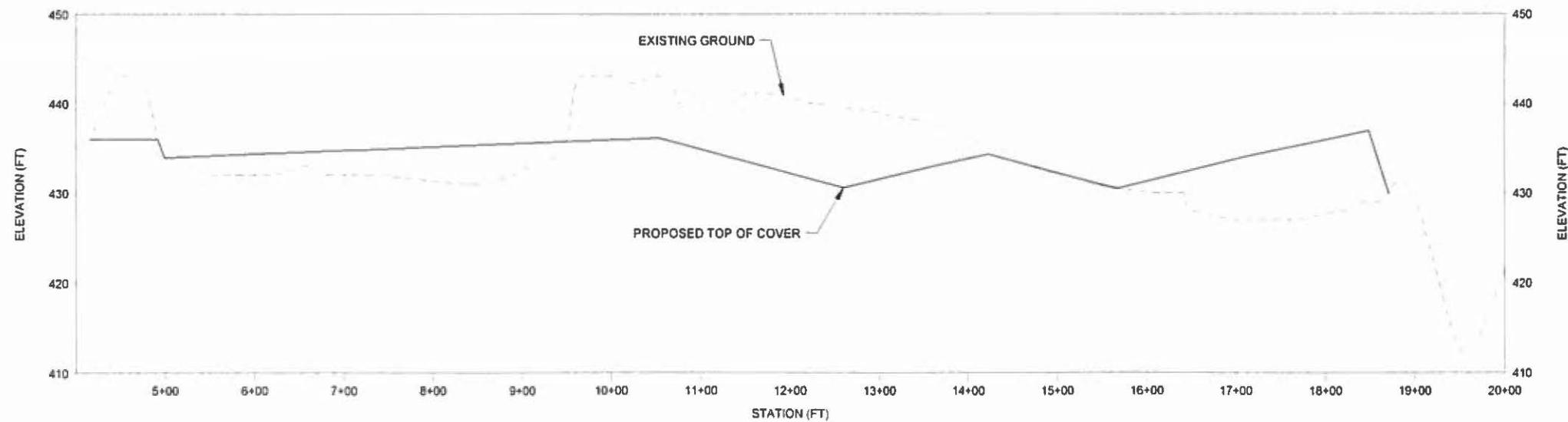
C-104

SHEET 6 OF 9

AECOM 05:44:36 PAH: P:\Projects\Gotech\60426794_DynergyCER\15_Wood River West Closure Plan\Drawings\WDR-CROSS SECTIONS.dwg 10/27/2016 12:23 PM



D SECTION D
 C-100 HORIZONTAL SCALE 1" = 80'
 VERTICAL SCALE 1" = 8'



E SECTION E
 C-100 HORIZONTAL SCALE 1" = 80'
 VERTICAL SCALE 1" = 8'

- NOTES**
- 1 THE EXISTING GROUND ELEVATIONS SHOWN ARE FROM AERIAL SURVEY PERFORMED BY SURDEX ON AUGUST 17, 2015 AND BATHYMETRIC SURVEY COMPLETED BY WEAVER CONSULTANTS GROUP ON SEPTEMBER 22, 2015.
 - 2 EXISTING GRADE ELEVATIONS REFLECT TOP OF ASH WITHIN THE WOOD RIVER WEST ASH COMPLEX AND EXISTING GROUND SURFACE ELEVATIONS OUTSIDE WOOD RIVER WEST ASH COMPLEX.
 - 3 PROPOSED GRADE ELEVATIONS REFLECT TOP OF COVER SYSTEM WITHIN WOOD RIVER WEST ASH COMPLEX AND PROPOSED GROUND SURFACE ELEVATIONS OUTSIDE WOOD RIVER WEST ASH COMPLEX.

**PRELIMINARY
 NOT FOR CONSTRUCTION**



1001 Highlands Plaza
 Drive West, Suite 300
 St. Louis, Mo. 63110-1337
 314 429-0100 (phone)
 314 429-0462 (fax)

**DYNEGY MIDWEST
 GENERATION, LLC**
 1500 East Port Plaza Drive
 Collinsville, IL 62234

**WOOD RIVER
 POWER STATION
 ALTON, IL**

**PERMIT DRAWINGS
 FOR CLOSURE OF THE
 WOOD RIVER WEST
 ASH COMPLEX**

ISSUED FOR BIDDING DATE BY

ISSUED FOR CONSTRUCTION DATE BY

REVISIONS		
NO	DESCRIPTION	DATE

AECOM PROJECT NO	60501530
DRAWN BY	LEH
DESIGNED BY	LEH
CHECKED BY	RHH
DATE CREATED	10/13/2015
PLOT DATE	10/27/2016
SCALE	AS SHOWN
ACAD VER	2015

SHEET TITLE

SECTIONS D AND E

C-105

SHEET 7 OF 9

AECOM DRAWING PATH: P:\Projects\Geotech\60428734_DynegyCCR\15_Wood River West Closure Plan\Drawings\WDR-DTANS.dwg
 10/27/2016 12:23 PM



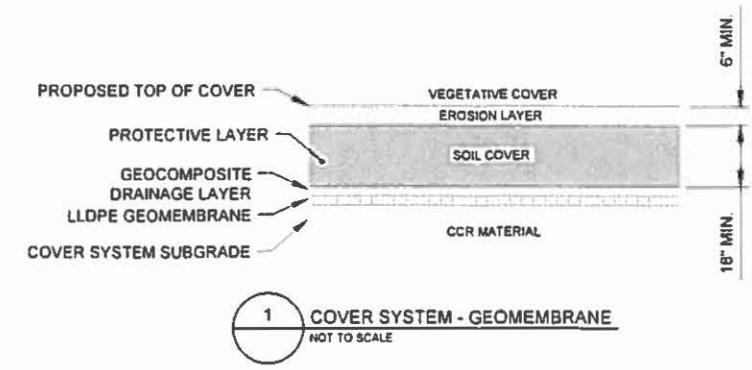
1001 Highlands Plaza
 Drive West, Suite 300
 St. Louis, Mo. 63110-1337
 314 429-0100 (phone)
 314 429-0462 (fax)

DYNEGY MIDWEST GENERATION, LLC

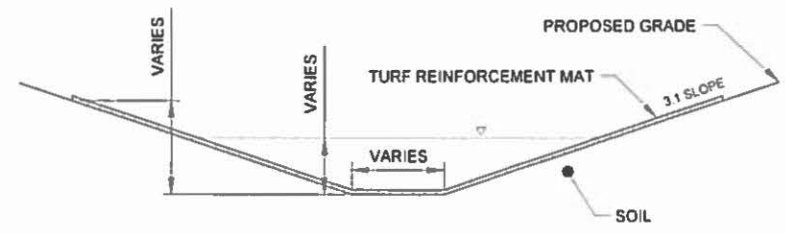
1500 East Port Plaza Drive
 Collinsville, IL 62234

WOOD RIVER POWER STATION ALTON, IL

PERMIT DRAWINGS FOR CLOSURE OF THE WOOD RIVER WEST ASH COMPLEX



1 COVER SYSTEM - GEOMEMBRANE
 NOT TO SCALE



2 TRM LINED STORMWATER DISCHARGE CHANNEL
 NOT TO SCALE

ISSUED FOR BIDDING _____ DATE BY _____

ISSUED FOR CONSTRUCTION _____ DATE BY _____

REVISIONS		
NO	DESCRIPTION	DATE

AECOM PROJECT NO	60501530
DRAWN BY	LEH
DESIGNED BY	LEH
CHECKED BY	RHH
DATE CREATED	10/13/2015
PLOT DATE	10/27/2016
SCALE	AS SHOWN
ACAD VER	2015

SHEET TITLE

DETAILS

C-106

**PRELIMINARY
NOT FOR CONSTRUCTION**

ATTACHMENT 8

**CLOSURE AND POST-CLOSURE CARE PLAN
FOR THE HENNEPIN EAST ASH POND NO. 2
HENNEPIN POWER STATION
PUTNAM COUNTY, ILLINOIS**

Submitted to:



**Dynergy Midwest Generation, LLC
Hennepin Power Station
13498 East 800th Street
Hennepin, Illinois 61327**

Submitted by:

**Civil & Environmental Consultants, Inc.
555 Butterfield Road, Suite 300
Lombard, Illinois 60148**

February 2018

CEC Project 171-101

**CLOSURE AND
POST-CLOSURE
CARE PLAN
HENNEPIN EAST
ASH POND NO. 2**

**HENNEPIN POWER
STATION
PUTNAM COUNTY,
ILLINOIS**

Submitted to:

**Dynegy Midwest
Generation, LLC
Hennepin Power Station
13498 East 800th Street
Hennepin, Illinois 61327**

Submitted by:

**Civil & Environmental
Consultants, Inc.
555 Butterfield Road,
Suite 300
Lombard, Illinois 60148**

February 2018

**CEC Project No.
171-101**

**CLOSURE AND POST-CLOSURE CARE PLAN
FOR THE HENNEPIN EAST ASH POND NO. 2
AT**

**Dynegy Midwest Generation, LLC
Hennepin Power Station
13498 East 800th Street
Hennepin, Illinois 61327**

**Submitted to:
Dynegy Midwest Generation, LLC
Hennepin Power Station
13498 East 800th Street
Hennepin, Illinois 61327**

**Submitted by:
Civil & Environmental Consultants, Inc.
555 Butterfield Road, Suite 300
Lombard, Illinois 60148**

CEC Project 171-101.0410

February 2018



Civil & Environmental Consultants, Inc.

**The following are attachments to the testimony of Scott M. Payne,
PhD, PG and Ian Magruder, M.S..**

ATTACHMENT 9

EPA/600/R-94/168a
September 1994

**THE HYDROLOGIC EVALUATION OF LANDFILL
PERFORMANCE (HELP) MODEL**

USER'S GUIDE FOR VERSION 3

by

Paul R. Schroeder, Cheryl M. Lloyd, and Paul A. Zappi
Environmental Laboratory
U.S. Army Corps of Engineers
Waterways Experiment Station
Vicksburg, Mississippi 39180-6199

and

Nadim M. Aziz
Department of Civil Engineering
Clemson University
Clemson, South Carolina 29634-0911

Interagency Agreement No. DW21931425

Project Officer

Robert E. Landreth
Waste Minimization, Destruction and Disposal Research Division
Risk Reduction Engineering Laboratory
Cincinnati, Ohio 45268

**RISK REDUCTION ENGINEERING LABORATORY
OFFICE OF RESEARCH AND DEVELOPMENT
U.S. ENVIRONMENTAL PROTECTION AGENCY
CINCINNATI, OHIO 45268**

 Printed on Recycled Paper

DISCLAIMER

The information in this document has been funded wholly or in part by the United States Environmental Protection Agency under Interagency Agreement No. DW21931425 to the U.S. Army Engineer Waterways Experiment Station. It has been subjected to the Agency's peer and administrative review, and it has been approved for publication as an EPA document. Mention of trade names or commercial products does not constitute endorsement or recommendation for use.

FOREWORD

Today's rapidly developing and changing technologies and industrial products and practices frequently carry with them the increased generation of materials that, if improperly dealt with, can threaten both public health and the environment. Abandoned waste sites and accidental releases of toxic and hazardous substances to the environment also have important environmental and public health implications. The Risk Reduction Engineering Laboratory assists in providing an authoritative and defensible engineering basis for assessing and solving these problems. Its products support the policies, programs and regulations of the Environmental Protection Agency, the permitting and other responsibilities of State and local governments, and the needs of both large and small businesses in handling their wastes responsibly and economically.

This report presents guidance on the use of the Hydrologic Evaluation of Landfill Performance (HELP) computer program. The HELP program is a quasi-two-dimensional hydrologic model for conducting water balance analysis of landfills, cover systems, and other solid waste containment facilities. The model accepts weather, soil and design data, and uses solution techniques that account for the effects of surface storage, snowmelt, runoff, infiltration, evapotranspiration, vegetative growth, soil moisture storage, lateral subsurface drainage, leachate recirculation, unsaturated vertical drainage, and leakage through soil, geomembrane or composite liners. Landfill systems including various combinations of vegetation, cover soils, waste cells, lateral drain layers, low permeability barrier soils, and synthetic geomembrane liners may be modeled. The model facilitates rapid estimation of the amounts of runoff, evapotranspiration, drainage, leachate collection and liner leakage that may be expected to result from the operation of a wide variety of landfill designs. The primary purpose of the model is to assist in the comparison of design alternatives. The model is a tool for both designers and permit writers.

E. Timothy Oppelt, Director
Risk Reduction Engineering Laboratory

ABSTRACT

The Hydrologic Evaluation of Landfill Performance (HELP) computer program is a quasi-two-dimensional hydrologic model of water movement across, into, through and out of landfills. The model accepts weather, soil and design data and uses solution techniques that account for the effects of surface storage, snowmelt, runoff, infiltration, evapotranspiration, vegetative growth, soil moisture storage, lateral subsurface drainage, leachate recirculation, unsaturated vertical drainage, and leakage through soil, geomembrane or composite liners. Landfill systems including various combinations of vegetation, cover soils, waste cells, lateral drain layers, low permeability barrier soils, and synthetic geomembrane liners may be modeled. The program was developed to conduct water balance analyses of landfills, cover systems, and solid waste disposal and containment facilities. As such, the model facilitates rapid estimation of the amounts of runoff, evapotranspiration, drainage, leachate collection, and liner leakage that may be expected to result from the operation of a wide variety of landfill designs. The primary purpose of the model is to assist in the comparison of design alternatives as judged by their water balances. The model, applicable to open, partially closed, and fully closed sites, is a tool for both designers and permit writers.

This report documents the solution methods and process descriptions used in Version 3 of the HELP model. Program documentation including program options, system and operating requirements, file structures, program structure and variable descriptions are provided in a separate report. Section 1 provides basic program identification. Section 2 provides a narrative description of the simulation model. Section 3 presents data generation algorithms and default values used in Version 3. Section 4 describes the method of solution and hydrologic process algorithms. Section 5 lists the assumptions and limitations of the HELP model.

The user interface or input facility is written in the Quick Basic environment of Microsoft Basic Professional Development System Version 7.1 and runs under DOS 2.1 or higher on IBM-PC and compatible computers. The HELP program uses an interactive and a user-friendly input facility designed to provide the user with as much assistance as possible in preparing data to run the model. The program provides weather and soil data file management, default data sources, interactive layer editing, on-line help, and data verification and accepts weather data from the most commonly used sources with several different formats.

HELP Version 3 represents a significant advancement over the input techniques of Version 2. Users of the HELP model should find HELP Version 3 easy to use and should be able to use it for many purposes, such as preparing and editing landfill profiles and weather data. Version 3 facilitates use of metric units, international applications, and designs with geosynthetic materials.

This report should be cited as follows:

Schroeder, P. R., Dozier, T.S., Zappi, P. A., McEnroe, B. M., Sjostrom, J. W., and Peyton, R. L. (1994). "The Hydrologic Evaluation of Landfill Performance (HELP) Model: Engineering Documentation for Version 3," EPA/600/9-94/xxx, U.S. Environmental Protection Agency Risk Reduction Engineering Laboratory, Cincinnati, OH.

This report was submitted in partial fulfillment of Interagency Agreement Number DW21931425 between the U.S. Environmental Protection Agency and the U.S. Army Engineer Waterways Experiment Station, Vicksburg, MS. This report covers a period from November 1988 to August 1994 and work was completed as of August 1994.

CONTENTS

	<u>Page</u>
DISCLAIMER	ii
FOREWORD	iii
ABSTRACT	iv
FIGURES	viii
TABLES	ix
ACKNOWLEDGMENTS	x
1. INTRODUCTION	1
1.1 Background	1
1.2 Overview	3
1.3 System and Operating Documentation	3
1.3.1 Computer Equipment	3
1.3.2 Required Hardware	3
1.3.3 Software Requirements	4
2. BASIC LANDFILL DESIGN CONCEPTS	5
2.1 Background	5
2.2 Leachate Production	5
2.3 Design for Leachate Control	6
3. PROGRAM DEFINITIONS, OPTIONS AND LIMITATIONS	9
3.1 Introduction	9
3.2 Weather Data Requirements	9
3.2.1 Evapotranspiration Data	9
3.2.2 Precipitation Data	14
3.2.3 Temperature Data	19
3.2.4 Solar Radiation Data	22
3.3 Soil and Design Data Requirements	24
3.3.1 Landfill General Information	24
3.3.2 Layer Data	25
3.3.3 Lateral Drainage Layer Design Data	25
3.3.4 Geomembrane Liner Data	26
3.3.5 Runoff Curve Number Information	26

CONTENTS (continued)

	<u>Page</u>
3.4 Landfill Profile and Layer Descriptions	26
3.5 Soil Characteristics	29
3.6 Geomembrane Characteristics	33
3.7 Site Characteristics	35
3.8 Overview of Modeling Procedure	36
3.9 Assumptions and Limitations	37
3.9.1 Solution Methods	37
3.9.2 Limits of Application	39
4. PROGRAM INPUT	42
4.1 Introduction	42
4.2 Definitions and Rules	42
4.3 Program Structure	45
4.4 Main Menu	45
4.5 Weather Data	47
4.5.1 Weather Data File Selection	47
4.5.2 Evapotranspiration (ET) Data	49
4.5.3 Precipitation, Temperature and Solar Radiation Data	51
4.5.4 Saving Weather Data	60
4.6 Soil and Design Data	62
4.6.1 Soil and Design Data File Selection	62
4.6.2 Landfill General Information	64
4.6.3 Landfill Layer Design	65
4.6.4 Runoff Curve Number	73
4.6.5 Verifying and Saving Soil and Design Data	75
4.7 Executing the Simulation	77
4.8 Viewing Results	79
4.9 Printing Results	79
4.10 Displaying Guidance	81
4.11 Quitting HELP	81
REFERENCES	82
BIBLIOGRAPHY	84
APPENDIX A: Calculating Soil, Waste and Material Properties	A1

FIGURES

<u>No.</u>		<u>Page</u>
1	Schematic of Landfill Profile Illustrating Typical Landfill Features	7
2	Relation between SCS Curve Number and Default Soil Texture Number for Various Levels of Vegetation	36
3	HELP3 Main Menu	46
4	Schematic of Weather Data Module	47
5	Schematic of "Weather Data - File Editing" Screen	48
6	Schematic of "Evapotranspiration Data" Screen	50
7	Schematic of "Precipitation, Temperature and Solar Radiation" Screen	52
8	Precipitation Options	52
9	Temperature Options	53
10	Solar Radiation Options	54
11	"Weather Data - File Saving" Screen Options	61
12	Schematic of Soil and Design Data Module	62
13	"Soil and Design Data - File Editing" Screen Options	63
14	Schematic of "Landfill General Information" Screen	64
15	Schematic of Landfill Layer Data	66
16	Schematic of "Runoff Curve Number Information" Screen Options	73
17	Verify and Save Soil and Design Data Options	75
18	Schematic of "Execute Simulation" Option	78
19	Schematic of "View Results" Option	80
20	Schematic of "Print Results" Option	80

TABLES

<u>No.</u>		<u>Page</u>
1	Cities For Evapotranspiration Data and Synthetic Temperature and Solar Radiation Data	11
2	Cities For Default Historical Precipitation Data	15
3	Cities For Synthetic Precipitation Data	17
4	Default Soil, Waste, and Geosynthetic Characteristics	30

ACKNOWLEDGMENTS

The support of the project by the Waste Minimization, Destruction and Disposal Research Division, Risk Reduction Engineering Laboratory, U.S. Environmental Protection Agency, Cincinnati, OH and the Headquarters, U.S. Army Corps of Engineers, Washington, DC, through Interagency Agreement No. DW21931425 is appreciated. In particular, the authors wish to thank the U.S. EPA Project Officer, Mr. Robert Landreth, for his long standing support.

The draft version of this document was prepared at Clemson University by Dr. Nadim M. Aziz, the author of the HELP Version 3 user interface, under contract with the USEPA Risk Reduction Engineering Laboratory and the USAE Waterways Experiment Station. The final version of this document was prepared at the USAE Waterways Experiment Station by Dr. Paul R. Schroeder and Ms. Cheryl M. Lloyd. Appendix A was written by Mr. Paul A. Zappi. The figures used in the report were prepared by Messrs. Jimmy Farrell and Christopher Chao.

The report and user interface were reviewed by Messrs. Elba A. Dardeau, Jr., and Daniel E. Averett. This report has not been subjected to the EPA review and, therefore, the contents do not necessarily reflect the views of the Agency, and no official endorsement should be inferred.

SECTION 1

INTRODUCTION

The Hydrologic Evaluation of Landfill Performance (HELP) computer program is a quasi-two-dimensional hydrologic model of water movement across, into, through and out of landfills. The model accepts weather, soil and design data, and uses solution techniques that account for the effects of surface storage, snowmelt, runoff, infiltration, evapotranspiration, vegetative growth, soil moisture storage, lateral subsurface drainage, leachate recirculation, unsaturated vertical drainage, and leakage through soil, geomembrane or composite liners. Landfill systems including various combinations of vegetation, cover soils, waste cells, lateral drain layers, low permeability barrier soils, and synthetic geomembrane liners may be modeled. The program was developed to conduct water balance analysis of landfills, cover systems and solid waste disposal and containment facilities. As such, the model facilitates rapid estimation of the amounts of runoff, evapotranspiration, drainage, leachate collection and liner leakage that may be expected to result from the operation of a wide variety of landfill designs. The primary purpose of the model is to assist in the comparison of design alternatives as judged by their water balances. The model, applicable to open, partially closed, and fully closed sites, is a tool for both designers and permit writers.

1.1 BACKGROUND

The HELP program, Versions 1, 2 and 3, was developed by the U.S. Army Engineer Waterways Experiment Station (WES), Vicksburg, MS, for the U.S. Environmental Protection Agency (EPA), Risk Reduction Engineering Laboratory, Cincinnati, OH, in response to needs in the Resource Conservation and Recovery Act (RCRA) and the Comprehensive Environmental Response, Compensation and Liability Act (CERCLA, better known as Superfund) as identified by the EPA Office of Solid Waste, Washington, DC.

HELP Version 1 (Schroeder et al., 1984) represented a major advance beyond the Hydrologic Simulation on Solid Waste Disposal Sites (HSSWDS) program (Perrier and Gibson, 1980; Schroeder and Gibson, 1982), which was also developed at WES. The HSSWDS model simulated only the cover system, did not model lateral flow through drainage layers, and handled vertical drainage only in a rudimentary manner. The infiltration, percolation and evapotranspiration routines were almost identical to those used in the Chemicals, Runoff, and Erosion from Agricultural Management Systems (CREAMS) model, which was developed by Knisel (1980) for the U.S. Department of Agriculture (USDA). The runoff and infiltration routines relied heavily on the Hydrology Section of the National Engineering Handbook (USDA, Soil Conservation Service, 1985). Version 1 of the HELP model incorporated a lateral subsurface drainage model and improved unsaturated drainage and liner leakage models into the HSSWDS

model. In addition, the HELP model provided simulation of the entire landfill including leachate collection and liner systems.

Version 2 (Schroeder et al., 1988) represented a great enhancement of the capabilities of the HELP model. The WGEN synthetic weather generator developed by the USDA Agricultural Research Service (ARS) (Richardson and Wright, 1984) was added to the model to yield daily values of precipitation, temperature and solar radiation. This replaced the use of normal mean monthly temperature and solar radiation values and improved the modeling of snow and evapotranspiration. Also, a vegetative growth model from the Simulator for Water Resources in Rural Basins (SWRRB) model developed by the ARS (Arnold et al., 1989) was merged into the HELP model to calculate daily leaf area indices. Modeling of unsaturated hydraulic conductivity and flow and lateral drainage computations were improved. Accuracy was increased with the use of double precision. Default soil data were improved, and the model permitted use of more layers and initialization of soil moisture content. Input and editing were simplified. Output was clarified, and standard deviations were reported.

In Version 3, the HELP model has been greatly enhanced beyond Version 2. The number of layers that can be modeled has been increased. The default soil/material texture list has been expanded to contain additional waste materials, geomembranes, geosynthetic drainage nets and compacted soils. The model also permits the use of a user-built library of soil textures. Computation of leachate recirculation between soil layers and groundwater drainage into the landfill have been added. Moreover, HELP Version 3 accounts for leakage through geomembranes due to manufacturing defects (pinholes) and installation defects (punctures, tears and seaming flaws) and by vapor diffusion through the liner. The estimation of runoff from the surface of the landfill has been improved to account for large landfill surface slopes and slope lengths. The snowmelt model has been replaced with an energy-based model; the Priestly-Taylor potential evapotranspiration model has been replaced with a Penman method, incorporating wind and humidity effects as well as long wave radiation losses (heat loss at night). A frozen soil model has been added to improve infiltration and runoff predictions in cold regions. The unsaturated vertical drainage model has also been improved to aid in storage computations. Input and editing have been further simplified with interactive, full-screen, menu-driven input techniques.

In addition, the HELP Version 3 model provides a variety of methods for specifying precipitation, temperature and solar radiation data. Now, data from the most commonly available government and commercial sources can be imported easily. Moreover, data used in HELP Version 2 can still be used with minimum user effort. Specifying weather data manually and editing previously entered weather data can be easily done by using built-in spreadsheet facilities.

The use of data files in Version 3 is much simpler and more convenient than HELP Version 2 because data are saved permanently in user defined file names at a user-specified location. Similarly, the user has more flexibility to define units for every type

of data needed to run the HELP model. Finally, Version 3 of the HELP model provides on-line help at every step of the data preparation process.

Although applicable to most landfill applications, the HELP model was developed specifically to perform hazardous and municipal waste disposal landfill evaluations as required by RCRA. Hazardous waste disposal landfills generally should have a liner to prevent migration of waste from the landfill, a final cover to minimize the production of leachate following closure, careful controls of runoff and runoff, and limits on the buildup of leachate head over the liner to no more than 1 ft. The HELP model is useful for predicting the amounts of runoff, drainage, and leachate expected for reasonable designs as well as the buildup of leachate above the liner. However, the model should not be expected to produce credible results from input unrepresentative of landfills.

1.2 OVERVIEW

The principal purpose of this User's Guide is to provide the basic information needed to use the computer program. Thus, while some attention must be given to definitions, descriptions of variables and interpretation of results, only a minimal amount of such information is provided. Detailed documentation providing in-depth coverage of the theory and assumptions on which the model is based and the internal logic of the program is also available (Schroeder et al., 1994). Potential HELP users are strongly encouraged to study the documentation and this User's Guide before attempting to use the program to evaluate a landfill design. Additional documentation concerning the sensitivity of program inputs, application of the model and verification of model predictions are under development.

1.3 SYSTEM AND OPERATING DOCUMENTATION

1.3.1 Computer Equipment

The model entitled "The Hydrologic Evaluation of Landfill Performance" (HELP) was written to run on IBM-compatible personal computers (PC) under the DOS environment.

1.3.2 Required Hardware

The following IBM-compatible CPU (8088, 80286, 80386 or 80486) hardware is required:

1. Monitor, preferably color EGA or better

2. Floppy disk drive (5.25-inch double-sided, double- or high-density; or 3.5-inch double-sided, double- or high-density)
3. Hard disk drive or a second floppy disk drive
4. 400k bytes or more of available RAM memory
5. 8087, 80287, 80387 or 80486 math co-processor
6. Printer, if a hard copy is desired

1.3.3 Software Requirements

The user must use Microsoft or compatible Disk Operating Systems (MS-DOS) Version 2.10 or a higher version. The user interface executable module was compiled and linked with Microsoft Basic Professional Development System 7.1. Other executable components were compiled with the Ryan-McFarland FORTRAN Version 2.42. The Microsoft Basic Professional Development System and Ryan-McFarland FORTRAN compiler are not needed to run the HELP Model.

SECTION 2

BASIC LANDFILL DESIGN CONCEPTS

2.1 BACKGROUND

Over the past 20 to 30 years, the sanitary landfill has come to be widely recognized as an economic and effective means for disposal of municipal and industrial solid wastes. Today, modern methods of landfill construction and management are sufficiently developed to ensure that even large volumes of such materials can be handled and disposed of in such a way as to protect public health and minimize adverse effects on the environment.

Recently, public attention has been focused on a special class of materials commonly referred to as hazardous wastes. The chemical and physical diversity, environmental persistence, and acute and chronic detrimental effects on human, plant and animal health of many of these substances are such that great care must be exercised in their disposal. Hazardous wastes are produced in such large quantities and are so diverse that universally acceptable disposal methods have yet to be devised. However, for the present, disposal or storage in secure landfills is usually a prudent approach. The current state of the art is an extension of sanitary landfill technology using very conservative design criteria. Some important basic principles and concepts of landfill design are summarized below. Specific emphasis is given to disposal of hazardous materials, but the discussion is also applicable to ordinary sanitary landfills.

2.2 LEACHATE PRODUCTION

Storage of any waste material in a landfill poses several potential problems. One problem is the possible contamination of soil, groundwater and surface water that may occur as leachate produced by water or liquid wastes moving into, through and out of the landfill migrates into adjacent areas. This problem is especially important when hazardous wastes are involved because many of these substances are quite resistant to biological or chemical degradation and, thus, are expected to persist in their original form for many years, perhaps even for centuries. Given this possibility hazardous waste landfills should be designed to prevent any waste or leachate from ever moving into adjacent areas. This objective is beyond the capability of current technology but does represent a goal in the design and operation of today's landfills. The HELP model has been developed specifically as a tool to be used by designers and regulatory reviewers for selecting practical designs that minimize potential contamination problems.

In the context of a landfill, leachate is described as liquid that has percolated through the layers of waste material. Thus, leachate may be composed of liquids that originate from a number of sources, including precipitation, groundwater, consolidation, initial

moisture storage, and reactions associated with decomposition of waste materials. The chemical quality of leachate varies as a function of a number of factors, including the quantity produced, the original nature of the buried waste materials, and the various chemical and biochemical reactions that may occur as the waste materials decompose. In the absence of evidence to the contrary, most regulatory agencies prefer to assume that any leachate produced will contaminate either ground or surface waters; in the light of the potential water quality impact of leachate contamination, this assumption appears reasonable.

The quantity of leachate produced is affected to some extent by decomposition reactions and initial moisture content; however, it is largely governed by the amount of external water entering the landfill. Thus, a key first step in controlling leachate migration is to limit production by preventing, to the extent feasible, the entry of external water into the waste layers. A second step is to collect any leachate that is produced for subsequent treatment and disposal. Techniques are currently available to limit the amount of leachate that migrates into adjoining areas to a virtually immeasurable volume, as long as the integrity of the landfill structure and leachate control system is maintained.

2.3 DESIGN FOR LEACHATE CONTROL

A schematic profile view of a somewhat typical hazardous waste landfill is shown in Figure 1. The bottom layer of soil may be naturally existing material or it may be hauled in, placed and compacted to specifications following excavation to a suitable subgrade. In either case, the base of the landfill should act as a liner with some minimum thickness and a very low hydraulic conductivity (or permeability). Treatments may be used on the barrier soil to reduce its permeability to an acceptable level. As an added factor of safety, an impermeable synthetic membrane may be placed on the top of the barrier soil layer to form a composite liner.

Immediately above the bottom composite liner is a leakage detection drainage layer to collect leakage from the primary liner, in this case, a geomembrane. Above the primary liner are a geosynthetic drainage net and a sand layer that serve as drainage layers for leachate collection. The drain layers composed of sand are typically at least 1-ft thick and have suitably spaced perforated or open joint drain pipe embedded below the surface of the liner. The leachate collection drainage layer serves to collect any leachate that may percolate through the waste layers. In this case where the liner is solely a geomembrane, a drainage net may be used to rapidly drain leachate from the liner, avoiding a significant buildup of head and limiting leakage. The liners are sloped to prevent ponding by encouraging leachate to flow toward the drains. The net effect is that very little leachate should percolate through the primary liner and virtually no migration of leachate through the bottom composite liner to the natural formations below. Taken as a whole, the drainage layers, geomembrane liners, and barrier soil liners may be referred to as the leachate collection and removal system (drain/liner system) and more specifically a double liner system.

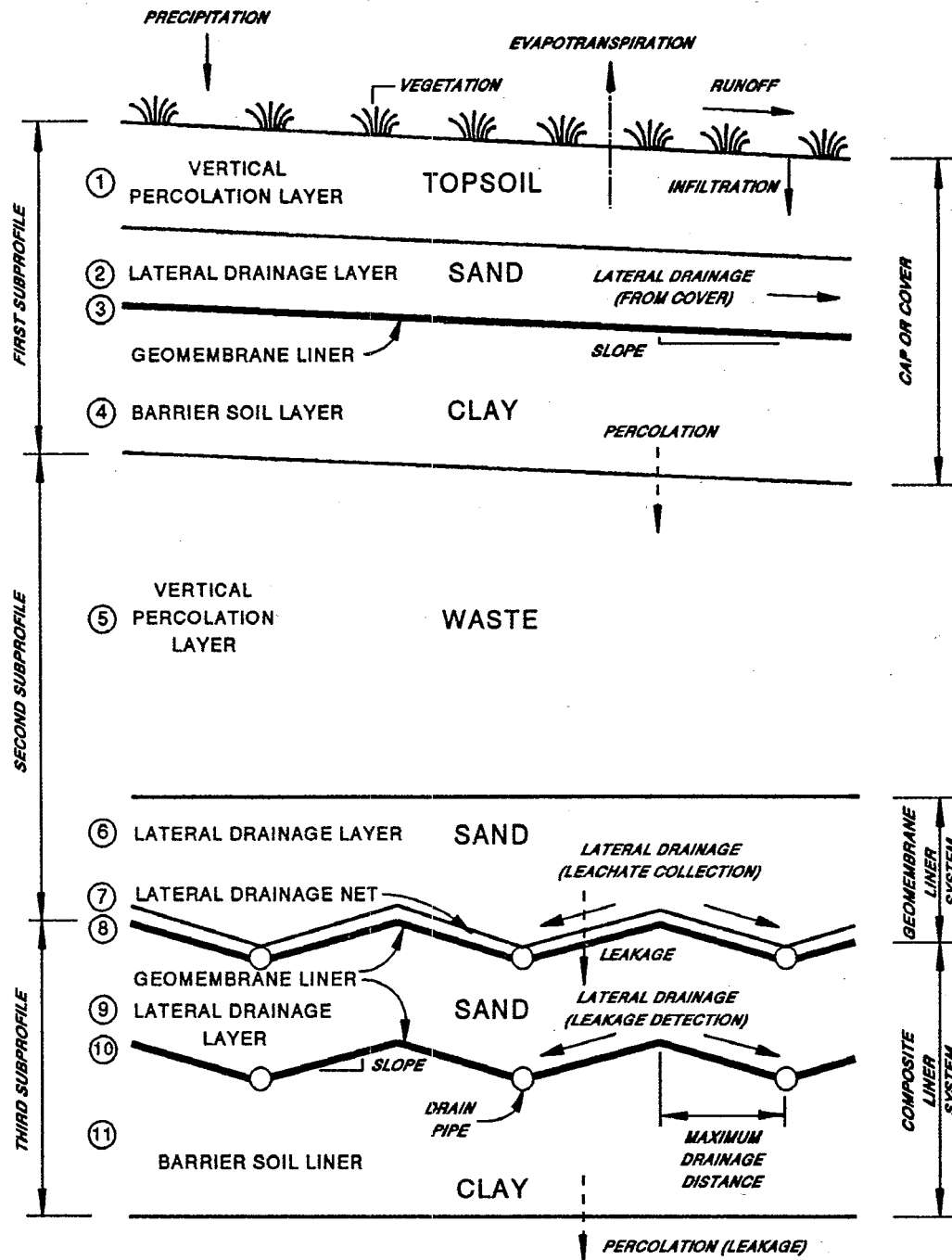


Figure 1. Schematic of Landfill Profile Illustrating Typical Landfill Features

After the landfill is closed, the leachate collection and removal system serves basically in a back-up capacity. However, while the landfill is open and waste is being added, these components constitute the principal defense against contamination of adjacent areas. Thus, care must be given to their design and construction.

Day-to-day operation of a modern sanitary landfill calls for wastes to be placed in relatively thin lifts, compacted, and covered with soil each day. Thus, wastes should not remain exposed for more than a few hours. Although the daily soil cover serves effectively to hide the wastes and limit the access of nuisance insects and potential disease vectors, it is of limited value for preventing the formation of leachate. Thus, even though a similar procedure can be used for hazardous wastes, the drainage/liner system must function well throughout and after the active life of the landfill.

When the capacity of the landfill is reached, the waste cells may be covered with a cap or final cover, typically composed of four distinct layers as shown in Figure 1. At the base of the cap is a drainage layer and a liner system layer similar to that used at the base of the landfill. Again, a geomembrane liner would normally be used in conjunction with the barrier soil liner for hazardous waste landfill but has been used less frequently in municipal waste landfills. The top of the barrier soil layer is graded so that water percolating into the drainage layer will tend to move horizontally toward some removal system (drain) located at the edge of the landfill or subunit thereof.

A layer of soil suitable for vegetative growth is placed at the top of final cover system to complete the landfill. A 2-ft-thick layer of soil having a loamy, silty nature serves this purpose well. The upper surface is graded so that runoff is restricted and infiltration is controlled to provide moisture for vegetation while limiting percolation through the topsoil. Runoff is promoted but controlled to prevent excessive erosion of the cap. The vegetation used should be selected for ease of establishment in a given area, promotion of evapotranspiration and year-round protection from erosion. The root system should not penetrate, disrupt or desiccate the upper liner system (Layers # 3 and # 4). Grasses are usually best for this purpose; however, local experts should be consulted to aid in selection of appropriate species.

The combination of site selection, surface grading, transpiration from vegetation, soil evaporation, drainage through the sand, and the low hydraulic conductivity of the barrier soil liner serves effectively to minimize leachate production from external water. Added effectiveness is gained by the use of geomembrane liners in the cap in conjunction with the barrier soil liner. The cap should be no more permeable than the leachate collection and removal system so that the landfill will not gradually fill and overflow into adjacent areas following abandonment of the landfill. This phenomenon is sometimes referred to as the "bathtub" effect.

SECTION 3

PROGRAM DEFINITIONS, OPTIONS AND LIMITATIONS

3.1 INTRODUCTION

The HELP program was developed to provide landfill designers and regulators with a tool for rapid, economical screening of alternative designs. The program may be used to estimate the magnitudes of various components of the water budget, including the volume of leachate produced and the thickness of water-saturated soil (head) above liners. The results may be used to compare the leachate production potential of alternative designs, to select and size appropriate drainage and collection systems, and to size leachate treatment facilities.

The program uses weather (climatic), soil and design data to generate daily estimates of water movement across, into, through and out of landfills. To accomplish this objective and compute a water balance, daily precipitation is partitioned into surface storage (snow), snowmelt, interception, runoff, infiltration, surface evaporation, evapotranspiration from soil, subsurface moisture storage, liner leakage (percolation), and subsurface lateral drainage to collection, removal and recirculation systems.

This section discusses data requirements, nomenclature, important assumptions and limitations, and other fundamental information needed to run the program. The program documentation report (Schroeder et al., 1994) contains detailed explanations of the solution techniques employed and the computer programs.

The HELP program requires three general types of input data: weather data, soil data and design data. A summary of input options and data requirements is presented in this section. Section 4 provides step-by-step input instructions.

3.2 WEATHER DATA REQUIREMENTS

The weather data required in the HELP model are classified into four groups: evapotranspiration, precipitation, temperature, and solar radiation data. The HELP user may enter weather data using several options depending on the type of weather data being considered. The requirements for each weather data type are listed below. The units used are also listed next to each data type and/or variable. Customary units are based on the US Customary units, and Metric implies SI units.

3.2.1 Evapotranspiration Data

The evapotranspiration data can be entered in one of two ways:

1. Default Evapotranspiration Option with Location Specific Guidance (Customary and Metric Units). This option uses the data provided by the HELP model for selected U.S. cities. The cities are listed in Table 1. The data needed for this option are:

- **Location**
- **Evaporative zone depth** (Guidance is available for the selected location based on a thick layer of loamy soil with a grassy form of vegetation. Clayey soils would generally have larger evaporative zone depths since it exerts greater capillary suction; analogously, sandy soils would have smaller evaporative depths. Shrubs and trees with tap roots would have larger evaporative zone depths than the values given in the guidance.) The user must specify an evaporative zone depth and can use the guidance along with specific design information to select a value. The program does not permit the evaporative depth to exceed the depth to the top of the topmost liner. Similarly, the evaporative zone depth would not be expected to extend very far into a sand drainage layer. The evaporative zone depth must be greater than zero. The evaporative zone depth is the maximum depth from which water may be removed by evapotranspiration. The value specified influences the storage of water near the surface and therefore directly affects the computations for evapotranspiration and runoff. Where surface vegetation is present, the evaporative depth should at least equal the expected average depth of root penetration. The influence of plant roots usually extends somewhat below the depth of root penetration because of capillary suction to the roots. The depth specified should be characteristic of the maximum depth to which the moisture changes near the surface due to drying over the course of a year, typically occurring during peak evaporative demand or when peak quantity of vegetation is present. Setting the evaporative depth equal to the expected average root depth would tend to yield a low estimate of evapotranspiration and a high estimate of drainage through the evaporative zone. An evaporative depth should be specified for bare ground to account for direct evaporation from the soil; this depth would be a function of the soil type and vapor and heat flux at the surface. The depth of capillary draw to the surface without vegetation or to the root zone may be only several inches in gravels; in sands the depth may be about 4 to 8 inches, in silts about 8 to 18 inches, and in clays about 12 to 60 inches.
- **Maximum leaf area index** (Guidance is available for the selected location). The user must enter a maximum value of leaf area index for the vegetative cover. Leaf area index (LAI) is defined as the dimensionless ratio of the leaf area of actively transpiring vegetation to the nominal surface area of the land on which the vegetation is growing. The program provides the user with a maximum LAI value typical of the location selected if the value entered by the user cannot be supported without irrigation because of low rainfall or a short growing season. This statement should be considered only as a warning. The maximum LAI for bare ground is zero. For a poor stand of grass the LAI could approach 1.0; for a fair stand of grass, 2.0; for a good stand of grass, 3.5; and for an excellent

**TABLE 1. CITIES FOR EVAPOTRANSPIRATION DATA AND
SYNTHETIC TEMPERATURE AND SOLAR RADIATION DATA**

ALABAMA	GEORGIA	MICHIGAN	NEW YORK
Birmingham	Atlanta	Detroit	Albany
Mobile	Augusta	East Lansing	Buffalo
Montgomery	Macon	Grand Rapids	Central Park
ALASKA	Savannah	Sault Sainte Marie	Ithaca
Annette	Watkinsville	MINNESOTA	New York
Bethel	HAWAII	Duluth	Syracuse
Fairbanks	Honolulu	Minneapolis	NORTH CAROLINA
ARIZONA	IDAHO	St. Cloud	Asheville
Flagstaff	Boise	MISSISSIPPI	Charlotte
Phoenix	Pocatello	Jackson	Greensboro
Tucson	ILLINOIS	Meridian	Raleigh
Yuma	Chicago	MISSOURI	NORTH DAKOTA
ARKANSAS	East St. Louis	Columbia	Bismarck
Fort Smith	INDIANA	Kansas City	Williston
Little Rock	Evansville	St. Louis	OHIO
CALIFORNIA	Fort Wayne	MONTANA	Cincinnati
Bakersfield	Indianapolis	Billings	Cleveland
Blue Canyon	IOWA	Glasgow	Columbus
Eureka	Des Moines	Great Falls	Put-in-Bay
Fresno	Dubuque	Havre	Toledo
Los Angeles	KANSAS	Helena	OKLAHOMA
Mt. Shasta	Dodge City	Kalispell	Oklahoma City
Sacramento	Topeka	Miles City	Tulsa
San Diego	Wichita	NEBRASKA	OREGON
San Francisco	KENTUCKY	Grand Island	Astoria
Santa Maria	Covington	North Platte	Burns
COLORADO	Lexington	Omaha	Meacham
Colorado Springs	Louisville	Scottsbluff	Medford
Denver	LOUISIANA	NEVADA	Pendleton
Grand Junction	Baton Rouge	Elko	Portland
Pueblo	Lake Charles	Ely	Salem
CONNECTICUT	New Orleans	Las Vegas	Sexton Summit
Bridgeport	Shreveport	Reno	PENNSYLVANIA
Hartford	MAINE	Winnemucca	Philadelphia
New Haven	Augusta	NEW HAMPSHIRE	Pittsburgh
Windsor Locks	Bangor	Concord	RHODE ISLAND
DELAWARE	Caribou	Mt. Washington	Providence
Wilmington	Portland	Nashua	SOUTH CAROLINA
DISTRICT OF COLUMBIA	MARYLAND	NEW JERSEY	Charleston
Washington	Baltimore	Edison	Columbia
FLORIDA	MASSACHUSETTS	Newark	SOUTH DAKOTA
Jacksonville	Boston	Seabrook	Huron
Miami	Nantucket	NEW MEXICO	Rapid City
Orlando	Plainfield	Albuquerque	TENNESSEE
Tallahassee	Worcester	Roswell	Chattanooga
Tampa			Knoxville
West Palm Beach			Memphis
			Nashville

(Continued)

TABLE 1 (continued). CITIES FOR EVAPOTRANSPIRATION DATA AND SYNTHETIC TEMPERATURE AND SOLAR RADIATION DATA

TEXAS	UTAH	WASHINGTON	WISCONSIN
Abilene	Cedar City	Olympia	Green Bay
Amarillo	Milford	Pullman	Lacrosse
Austin	Salt Lake City	Seattle	Madison
Brownsville	VERMONT	Spokane	Milwaukee
Corpus Christi	Burlington	Stampede Pass	WYOMING
Dallas	Montpelier	Walla Walla	Cheyenne
El Paso	Rutland	Yakima	Lander
Galveston	VIRGINIA	WEST VIRGINIA	PUERTO RICO
Houston	Lynchburg	Charleston	San Juan
Midland	Norfolk		
San Antonio	Richmond		
Temple			
Waco			

(Concluded)

stand of grass, 5.0. The LAI for dense stands of trees and shrubbery would also approach 5. The program is largely insensitive to values above 5. If the vegetative species limit plant transpiration (such as succulent plants), the maximum LAI value should be reduced to a value equivalent of the LAI for a stand of grass that would yield a similar quantity of plant transpiration. Most landfills would tend to have at best a fair stand of grass and often only a poor stand of grass because landfills are not designed as ideal support systems for vegetative growth. Surface soils are commonly shallow and provide little moisture storage for dry periods. Many covers may have drains to remove infiltrated water quickly, reducing moisture storage. Some covers have liners near the surface restricting root penetration and causing frequent saturation of the surface soil which limits oxygen availability to the roots. Some landfills produce large quantities of gas which, if uncontrolled, reduces the oxygen availability in the rooting zone and therefore limits plant growth.

The program produces values for the Julian dates starting and ending the growing season, the annual average wind speed, and the quarterly average relative humidity for the location. The values for the growing season should be checked carefully to agree with the germination and harvesting (end of seasonal growth) dates for your type of vegetation. For example, grasses in southern California would germinate in the fall when the rains occur and die off in late spring when the soil moisture is depleted. This contrasts with a typical growing season, which would start in the spring and end in the fall.

2. Manual Option (Customary and Metric Units). The data needed for this option are:

- **Location**
- **Evaporative zone depth.** The user must specify an evaporative zone depth and can use the guidance given under the default option along with specific design information to select a value. The program does not permit the evaporative depth to exceed the depth to the top of the topmost barrier soil layer. Similarly, the evaporative zone depth would not be expected to extend very far into a sand drainage layer. The evaporative zone depth must be greater than zero. The evaporative zone depth is the maximum depth from which water may be removed by evapotranspiration. The value specified influences the storage of water near the surface and, therefore, directly affects the computations for evapotranspiration and runoff. Where surface vegetation is present, the evaporative depth should at least equal the expected average depth of root penetration. The influence of plant roots usually extends somewhat below the depth of root penetration because of capillary suction to the roots. The depth specified should be characteristic of the maximum depth to which the moisture changes near the surface due to drying over the course of a year, typically occurring during peak evaporative demand or when peak quantity of vegetation is present. Setting the evaporative depth equal to the expected average root depth would tend to yield a low estimate of evapotranspiration and a high estimate of drainage through the evaporative zone. An evaporative depth should be specified for bare ground to account for direct evaporation from the soil; this depth would be a function of the soil type and vapor and heat flux at the surface. The depth of capillary draw to the surface without vegetation or to the root zone may be only several inches in gravels; in sands the depth may be about 4 to 8 inches, in silts about 8 to 18 inches, and in clays about 12 to 60 inches. Rooting depth is dependent on many factors -- species, moisture availability, maturation, soil type and plant density. In humid areas where moisture is readily available near the surface, grasses may have rooting depth of 6 to 24 inches. In drier areas, the rooting depth is very sensitive to plant species and to the depth to which moisture is stored and may range from 6 to 48 inches. The evaporative zone depth would be somewhat greater than the rooting depth. The local Agricultural Extension Service office can provide information on characteristic rooting depths for vegetation in specific areas.
- **Maximum leaf area index.** The user must enter a maximum value of leaf area index (LAI) for the vegetative cover. LAI is defined as the dimensionless ratio of the leaf area of actively transpiring vegetation to the nominal surface area of the land on which the vegetation is growing. The program provides the user with a maximum LAI value typical of the location selected if the value entered by the user cannot be supported without irrigation because of low rainfall or a short growing season. This statement should be considered only as a warning. The maximum LAI for bare ground is zero. For a poor stand of grass the LAI could approach 1.0; for a fair stand of grass, 2.0; for a good stand of grass, 3.5; and for an excellent stand of grass, 5.0. The LAI for dense stands of trees and shrubbery would also approach 5. The program is largely insensitive to values

above 5. If the vegetative species limit plant transpiration (such as succulent plants), the maximum LAI value should be reduced to a value equivalent of the LAI for a stand of grass that would yield a similar quantity of plant transpiration. Most landfills would tend to have, at best, a fair stand of grass and often only a poor stand of grass because landfills are not designed as ideal support systems for vegetative growth. Surface soils are commonly shallow and provide little moisture storage for dry periods. Many covers may have drains to remove infiltrated water quickly, reducing moisture storage. Some covers have liners near the surface restricting root penetration and causing frequent saturation of the surface soil which limits oxygen availability to the roots. Some landfills produce large quantities of gas which, if uncontrolled, reduces the oxygen availability in the rooting zone and therefore limits plant growth.

- **Dates starting and ending the growing season.** The start of the growing season is based on mean daily temperature and plant species. Typically, the start of the growing season for grasses is the Julian date (day of the year) when the normal mean daily temperature rises above 50 to 55 degrees Fahrenheit. The growing season ends when the normal mean daily temperatures falls below 50 to 55 degrees Fahrenheit. In cooler climates the start and end would be at lower temperatures and in warmer climates at higher temperatures. Data on normal mean daily temperature is available from "Climates of the States" (Ruffner, 1985) and the "Climatic Atlas of the United States" (NOAA, 1974). In locations where the growing season extends year-round, the start of the growing season should be reported as day 0 and the end as day 367. The values for the growing season should be checked carefully to agree with the germination and harvesting (end of seasonal growth) dates for your type of vegetation. For example, grasses in southern California would germinate in the fall when the rains occur and die in late spring when the soil moisture is depleted. This contrasts with a typical growing season which would start in the spring and end in the fall.
- **Normal average annual wind speed.** This data is available from NOAA annual climatological data summary, "Climates of the States" (Ruffner, 1985) and the "Climatic Atlas of the United States" (NOAA, 1974).
- **Normal average quarterly relative humidity.** This data is available from NOAA annual climatological data summary, "Climates of the States" (Ruffner, 1985) and the "Climatic Atlas of the United States" (NOAA, 1974).

3.2.2 Precipitation Data

1. **Default Precipitation Option (Customary Units).** The user may select 5 years of historical precipitation data for any of the 102 U.S. cities listed in Table 2. The input needed for this option is:

TABLE 2. CITIES FOR DEFAULT HISTORICAL PRECIPITATION DATA

ALASKA	IDAHO	NEBRASKA	PENNSYLVANIA
Annette	Boise	Grand Island	Philadelphia
Bethel	Pocatello	North Omaha	Pittsburgh
Fairbanks	ILLINOIS	NEVADA	RHODE ISLAND
ARIZONA	Chicago	Ely	Providence
Flagstaff	East St. Louis	Las Vegas	SOUTH CAROLINA
Phoenix	INDIANA	NEW HAMPSHIRE	Charleston
Tucson	Indianapolis	Concord	SOUTH DAKOTA
ARKANSAS	IOWA	Nashua	Rapid City
Little Rock	Des Moines	NEW JERSEY	TENNESSEE
CALIFORNIA	KANSAS	Edison	Knoxville
Fresno	Dodge City	Seabrook	Nashville
Los Angeles	Topeka	NEW MEXICO	TEXAS
Sacramento	KENTUCKY	Albuquerque	Brownsville
San Diego	Lexington	NEW YORK	Dallas
Santa Maria	LOUISIANA	Albany	El Paso
COLORADO	Lake Charles	Central Park	Midland
Denver	New Orleans	Ithaca	San Antonio
Grand Junction	Shreveport	New York	UTAH
CONNECTICUT	MAINE	Syracuse	Cedar City
Bridgeport	Augusta	NORTH CAROLINA	Salt Lake City
Hartford	Bangor	Greensboro	VERMONT
New Haven	Caribou	NORTH DAKOTA	Burlington
FLORIDA	Portland	Bismarck	Montpelier
Jacksonville	MASSACHUSETTS	OHIO	Rutland
Miami	Boston	Cincinnati	VIRGINIA
Orlando	Plainfield	Cleveland	Lynchburg
Tallahassee	Worcester	Columbus	Norfolk
Tampa	MICHIGAN	Put-in-Bay	WASHINGTON
West Palm Beach	East Lansing	OKLAHOMA	Pullman
GEORGIA	Sault Sainte Marie	Oklahoma City	Seattle
Atlanta	MINNESOTA	Tulsa	Yakima
Watkinsville	St. Cloud	OREGON	WISCONSIN
HAWAII	MISSOURI	Astoria	Madison
Honolulu	Columbia	Medford	WYOMING
	MONTANA	Portland	Cheyenne
	Glasgow		Lander
	Great Falls		PUERTO RICO
			San Juan

- Location

NOTE: The user should be aware of the limitations of using the default historical precipitation data. None of the 102 locations for which data are available may be representative of the study site because rainfall is spatially very variable. In addition, the 5 years for which default data are available (1974-1978 in most cases) may not be typical, but were unusually wet or dry. The user should examine the rainfall and determine how representative it is of normal, wet and dry years at the study site. In addition, simulations should be run for more than five years to determine long-term performance of the landfill using, if necessary, another precipitation input option to examine the design under the range of possible weather conditions.

2. ***Synthetic Precipitation Option (Customary or Metric Units)***. The program will generate from 1 to 100 years of daily precipitation data stochastically for the selected location using a synthetic weather generator. The precipitation data will have approximately the same statistical characteristics as the historic data at the selected location. If desired, the user can enter normal mean monthly precipitation values for the specific location to improve the statistical characteristics of the resulting daily values. The user is advised to enter normal mean monthly precipitation values if the project site is located more than a few miles from the city selected from Table 3 or if the land use or topography varies between the site and city. The daily values will vary from month to month and from year to year and will not equal the normal values entered. The same data is produced every time the option is used for a given location. The data required by the synthetic weather generator are:

- Location (select from a list of 139 U.S. cities in Table 3)
- Number of years of data to be generated
- Normal mean monthly precipitation (Optional, default values are available.)

3. ***Create/Edit Precipitation Option (Customary or Metric Units)***. Under the Create option, the user may enter from 1 to 100 years of daily precipitation data manually. The years, which need not be consecutive, can be entered in any order. The user may add or delete years of data or rearrange the order of the years of data. This same option can be used to edit the daily values of any year of data; commonly, this is used to add severe storm events, such as the 25-year, 24-hour precipitation event. The data required are:

- Location
- One or more years of daily precipitation data

TABLE 3. CITIES FOR SYNTHETIC PRECIPITATION DATA

ALABAMA	INDIANA	NEBRASKA	RHODE ISLAND
Birmingham	Evansville	Grand Island	Providence
Mobile	Fort Wayne	North Platte	SOUTH CAROLINA
Montgomery	Indianapolis	Scottsbluff	Charleston
ARIZONA	IOWA	NEVADA	Columbia
Flagstaff	Des Moines	Elko	SOUTH DAKOTA
Phoenix	Dubuque	Las Vegas	Huron
Yuma	KANSAS	Reno	Rapid City
ARKANSAS	Dodge City	Winnemucca	TENNESSEE
Fort Smith	Topeka	NEW HAMPSHIRE	Chattanooga
Little Rock	Wichita	Concord	Knoxville
CALIFORNIA	KENTUCKY	Mt. Washington	Memphis
Bakersfield	Covington	NEW JERSEY	Nashville
Blue Canyon	Lexington	Newark	TEXAS
Eureka	Louisville	NEW MEXICO	Abilene
Fresno	LOUISIANA	Albuquerque	Amarillo
Mt. Shasta	Baton Rouge	Roswell	Austin
San Diego	New Orleans	NEW YORK	Brownsville
San Francisco	Shreveport	Albany	Corpus Christi
COLORADO	MAINE	Buffalo	Dallas
Colorado Springs	Caribou	New York	El Paso
Denver	Portland	Syracuse	Galveston
Grand Junction	MARYLAND	NORTH CAROLINA	Houston
Pueblo	Baltimore	Asheville	San Antonio
CONNECTICUT	MASSACHUSETTS	Charlotte	Temple
Windsor Locks	Boston	Greensboro	Waco
DELAWARE	Nantucket	Raleigh	UTAH
Wilmington	MICHIGAN	NORTH DAKOTA	Milford
DISTRICT OF COLUMBIA	Detroit	Bismarck	Salt Lake City
Washington	Grand Rapids	Williston	VIRGINIA
FLORIDA	MINNESOTA	OHIO	Norfolk
Jacksonville	Duluth	Cleveland	Richmond
Miami	Minneapolis	Columbus	WASHINGTON
Tallahassee	MISSISSIPPI	Toledo	Olympia
Tampa	Jackson	OKLAHOMA	Spokane
GEORGIA	Meridian	Oklahoma City	Stampede Pass
Atlanta	MISSOURI	Tulsa	Walla Walla
Augusta	Columbia	OREGON	Yakima
Macon	Kansas City	Burns	WEST VIRGINIA
Savannah	St. Louis	Meachem	Charleston
IDAHO	MONTANA	Medford	WISCONSIN
Boise	Billings	Pendleton	Green Bay
Pocatello	Great Falls	Portland	Lacrosse
ILLINOIS	Havre	Salem	Madison
Chicago	Helena	Sexton Summit	Milwaukee
	Kalispell	PENNSYLVANIA	WYOMING
	Miles City	Philadelphia	Cheyenne
		Pittsburgh	

4. ***NOAA Tape Precipitation Option (Customary Units)***. The option will convert the NOAA Summary of Day daily precipitation data written to diskette in ASCII print as-on-tape format into the format used by Version 3 of the HELP model. The following data are required for this option:

- Location
- NOAA ASCII print file of Summary of Day daily precipitation data in as-on-tape format

NOTE: Daily precipitation data and normal mean monthly precipitation values for most locations are readily available in publications or on diskette from NOAA. Information on climatological data sources can be obtained from the National Climatic Data Center (NCDC), NOAA, Federal Building, Asheville, NC 28801, (704) 259-0682.

5. ***Climatedata™ Precipitation Option (Customary Units)***. The program will convert daily precipitation data from an ASCII print file prepared by the Climatedata™ CD-ROM data base program into the format used by Version 3 of the HELP model. The Climatedata™ format is used by other CD-ROM, state and regional data bases and, therefore, those files can also be converted by this option. For example, the State of California and the Midwest Climatic Data Consortium used this same format. The following data are required for this option:

- Location
- Climatedata™ prepared file containing daily precipitation data

NOTE: Hydrosphere Data Products, Inc. sells NOAA Summary of the Day precipitation data in a 4-disc CD-ROM data base called Climatedata™, one disc for each of four U.S. regions. Information on Climatedata™ is available from Hydrosphere, 1002 Walnut, Suite 200, Boulder, CO 80302, (800) 949-4937.

6. ***ASCII Precipitation Option (Customary or Metric Units)***. The HELP model converts daily precipitation data in an ASCII file to the HELP format. Each year of ASCII precipitation data should be stored in a separate file. The first 365 or 366 values will be converted; excess data will be ignored. Inadequate data will yield an error. This option should also be used to convert data from spreadsheet format by first printing each year of precipitation to individual print files. The following data are required for this option:

- Location
- Files containing ASCII data

- Years
7. **HELP Version 2 Data Option (Customary Units).** Version 3 of the HELP model converts precipitation data prepared for use in Version 2 of the HELP model (Schroeder et al., 1988b) into the HELP Version 3 format. This option requires the following data:
- Location
 - File containing HELP Version 2 data
8. **Canadian Climatological Data Option (Metric Units).** The HELP model converts Canadian Climatological Data (Surface) in compressed or uncompressed diskette formats into the HELP Version 3 format. The following data are required by this option:
- Location
 - Canadian Climatological Data file containing years of daily precipitation values

NOTE: Canadian Climatological Data for most locations are readily available in publications of the Environment Canada, Atmospheric Environment Service, Canadian Climate Centre, Data Management Division, 4905 Dufferin Street, Downsview, Ontario, Canada M3H 5T4.

3.2.3 Temperature Data

1. **Synthetic Temperature Option (Customary or Metric Units).** The program will generate from 1 to 100 years of temperature data stochastically for the selected location. The synthetic generation of daily temperature values is a weak function of precipitation and as such the user must first specify the precipitation. Generation of temperature data is limited to the number of years of precipitation data available. The synthetic temperature data will have approximately the same statistical characteristics as the historic data at the selected location. If desired, the user can enter normal mean monthly temperature values for the specific location to improve the statistical characteristics of the resulting daily values. The user is advised to enter normal mean monthly temperature values if the project site is located more than 100 miles from the city selected from Table 1 or if the difference in elevation between the site and the city is more than 500 feet. The data required by the synthetic weather generator are:
- Location (select from a list of 183 U.S. cities in Table 1)
 - Number of years of data to be generated

- Years of daily precipitation values
 - Normal mean monthly temperature (Optional, default values are available.)
2. **Create/Edit Temperature Option (Customary or Metric Units).** Under the create option, the user may enter up to 100 years of daily temperature data manually. The years, which need not be consecutive, can be entered in any order. The user may add or delete years of data or rearrange the order of the years of data. This same option can be used to edit the daily values of any year of data. The data required are:
- Location
 - One or more years of daily temperature data
3. **NOAA Tape Temperature Option (Customary Units).** This option will convert the NOAA Summary of Day daily temperature data written to diskette in ASCII print as-on-tape format into the format used by Version 3 of the HELP model. The program will accept either mean daily temperature or daily maximum and minimum temperature values. If maximum and minimum temperatures are used, the program averages the two to compute the daily mean temperature value. If mean temperature values are used, the same file is specified as the maximum and minimum temperature files. The following data are required for this option:
- Location
 - NOAA ASCII print file of Summary of Day data file containing years of daily maximum temperature values or daily mean temperature values in as-on-tape format
 - NOAA ASCII print file of Summary of Day data file containing years of daily minimum temperature values or daily mean temperature values in as-on-tape format
- NOTE: Daily temperature (mean or maximum and minimum) data and normal mean monthly temperature values for most locations are readily available in publications or on diskette from NOAA. Information on climatological data sources can be obtained from the National Climatic Data Center, NOAA, Federal Building, Asheville, NC 28801, (704) 259-0682.
4. **Climatedata™ Temperature Option (Customary Units).** The program will convert daily maximum and minimum temperature data from ASCII print files prepared by the Climatedata™ CD-ROM data base program into the daily mean temperature data file format used by Version 3 of the HELP model. The Climatedata™ format is also used by other CD-ROM, state and regional data bases and therefore those

files can also be converted by this option. For example, the State of California and the Midwest Climatic Data Consortium used this same format. The following data are required for this option:

- Location
- Climatedata™ prepared file containing daily maximum temperature data
- Climatedata™ prepared file containing daily minimum temperature data

NOTE: Hydrosphere Data Products, Inc. sells NOAA Summary of the Day daily temperature data in a 4-disc CD-ROM data base called Climatedata™, one disc for each of four U.S. regions. Information on Climatedata™ is available from Hydrosphere, 1002 Walnut, Suite 200, Boulder, CO 80302, (800) 949-4937.

5. *ASCII Temperature Option (Customary or Metric Units)*. The HELP model converts daily mean temperature data in an ASCII file to the HELP format. Each year of ASCII temperature data should be stored in a separate file. The program will convert the first 365 or 366 values; excess data will be ignored. Inadequate data will yield an error. This option should also be used to convert data from spreadsheet format by first printing each year of temperature to individual print files. The following data are required for this option:

- Location
- Files containing ASCII data
- Years

6. *HELP Version 2 Data Option (Customary Units)*. Version 3 of the HELP model converts temperature data prepared for use in Version 2 of the HELP model (Schroeder et al., 1988b) into the HELP Version 3 format. This option requires the following data:

- Location
- File containing HELP Version 2 data

7. *Canadian Climatological Data Option (Metric Units)*. The HELP model converts Canadian Climatological Data (Surface) in compressed or uncompressed diskette formats into the HELP Version 3 format. Conversion is available only for daily mean temperature values. The following data are required by this option:

- Location
- Canadian Climatological Data file containing years of daily mean temperature values

NOTE: Canadian Climatological Data for most locations are readily available in publications of the Environment Canada, Atmospheric Environment Service, Canadian Climate Centre, Data Management Division, 4905 Dufferin Street, Downsview, Ontario, Canada M3H 5T4.

3.2.4 Solar Radiation Data

1. *Synthetic Solar Radiation Option (Customary or Metric Units)*. The program will generate from 1 to 100 years of daily solar radiation data stochastically for the selected location. The synthetic generation of daily solar radiation values is a strong function of precipitation and as such the user must first specify the precipitation. Generation of solar radiation data is limited to the number of years of precipitation data available. The synthetic solar radiation data will have approximately the same statistical characteristics as the historic data at the selected location. If desired, the user can enter the latitude for the specific location to improve the computation of potential solar radiation and the resulting daily values. The user is advised to enter the latitude if the project site is more than 50 miles north or south of the city selected from Table 1. The data required by the synthetic weather generator are:

- Location (select from a list of 183 U.S. cities in Table 1)
- Number of years of data to be generated
- Years of daily precipitation values
- Latitude (optional, default value is available.)

2. *Create/Edit Solar Radiation Option (Customary or Metric Units)*. Under the create option, the user may enter up to 100 years of daily solar radiation data manually. The years, which need not be consecutive, can be entered in any order. The user may add or delete years of data or rearrange the order of the years of data. This same option can be used to edit the daily values of any year of data. The input requirements are:

- Location
- One or more years of daily solar radiation data

3. ***NOAA Tape Solar Radiation Option (Customary Units)***. This option will convert the NOAA Surface Airways Hourly solar radiation data written to diskette in ASCII print as-on-tape format into the format used by Version 3 of the HELP model. The following data are required for this option:

- Location
- NOAA ASCII print file of Surface Airways Hourly solar radiation data in as-on-tape format

NOTE: Daily temperature (mean or maximum and minimum) data and normal mean monthly temperature values for most locations are readily available in publications or on diskette from the NOAA. Information on climatological data sources can be obtained from the National Climatic Data Center, NOAA, Federal Building, Asheville, NC 28801, (704) 259-0682.

4. ***Climatedata™ Solar Radiation Option (Customary Units)***. The program will convert the Surface Airways ASCII print files of daily average solar radiation data into a daily solar radiation data file of the format used by HELP Version 3. It is anticipated that this option may also work with some other data sources as they become available. The following data are required for this option:

- Location
- Surface Airways prepared file containing years of daily solar radiation data

NOTE: EarthInfo Inc. sells NOAA Surface Airways daily global solar radiation data in a 12-disc CD-ROM data base called Surface Airways as part of their NOAA data base, three discs for each of four U.S. regions. Information on Surface Airways is available from EarthInfo Inc., 5541 Central Avenue, Boulder, CO 80301-2846, (303) 938-1788. Hydrosphere Inc. is also developing a CD-ROM data base of NOAA Surface Airways data as part of their Climatedata™. Information on Climatedata™ is available from Hydrosphere, 1002 Walnut, Suite 200, Boulder, CO 80302, (800) 949-4937.

5. ***ASCII Solar Radiation Option (Customary or Metric Units)***. The HELP model converts daily solar radiation data in an ASCII file to the HELP format. Each year of ASCII daily solar radiation data should be stored in a separate file. The program will convert the first 365 or 366 values; excess data will be ignored. Inadequate data will yield an error. This option should also be used to convert data from spreadsheet format by first printing each year of solar radiation to individual print files. The following data are required for this option:

- Location

- Files containing ASCII data
 - Years
6. *HELP Version 2 Data Option (Customary Units)*. Version 3 of the HELP model converts solar radiation data prepared for use in Version 2 of the HELP model (Schroeder et al., 1988b) into the HELP Version 3 format. This option requires the following data:
- Location
 - File containing HELP Version 2 data
7. *Canadian Climatological Data Option (Metric Units)*. The HELP model converts Canadian Climatological Data (Surface) in compressed or uncompressed diskette formats into the HELP Version 3 format. Conversion is available only for hourly global solar radiation values. The input requirements are:
- Location
 - Canadian Climatological Data file containing years of hourly global solar radiation values

NOTE: Canadian Climatological Data for most locations are readily available in publications of the Environment Canada, Atmospheric Environment Service, Canadian Climate Centre, Data Management Division, 4905 Dufferin Street, Downsview, Ontario, Canada M3H 5T4.

3.3 SOIL AND DESIGN DATA REQUIREMENTS

The user may enter soil data by using the default soil/material textures option, the user-defined soil texture option, or a manual option. If the user selects a default soil texture, the program will display porosity, field capacity, wilting point, and hydraulic conductivity values of the soil that is stored as default. There are 42 default soil/material textures. If user-defined soil textures are selected, the program will display the porosity, field capacity, wilting point, and hydraulic conductivity of the selected soil from the user-defined soil texture data file. In the manual soil texture option, the user must specify values for the soil parameters. General data requirements for all options are listed below. Detailed explanations are given in Sections 3.4 through 3.9.

3.3.1 Landfill General Information

1. Project title

2. Landfill area (*Customary or Metric*)
3. Percentage of landfill area where runoff is possible
4. Method of initialization of moisture storage (user-specified or program initialized to near steady-state)
5. Initial snow water storage (optional, needed when moisture storage is user-specified)

3.3.2 Layer Data

1. Layer type (Four types of layers are permitted -- 1) vertical percolation, 2) lateral drainage, 3) barrier soil liner and 4) geomembrane liner.)
2. Layer thickness (*Customary or Metric*)
3. Soil texture
 - Select from 42 default soil/material textures to get the following data.
 - Porosity, in vol/vol
 - Field capacity, in vol/vol
 - Wilting point, in vol/vol
 - Saturated hydraulic conductivity (cm/sec)
 - Select from user-built soil texture library to get the following data.
 - Porosity, in vol/vol
 - Field capacity, in vol/vol
 - Wilting point, in vol/vol
 - Saturated hydraulic conductivity (cm/sec)
 - Enter the following data for manual soil texture descriptions.
 - Porosity, in vol/vol
 - Field capacity, in vol/vol
 - Wilting point, in vol/vol
 - Saturated hydraulic conductivity (cm/sec)
4. Initial volumetric soil water content (storage), in vol/vol (optional, needed when initial moisture storage is user-specified)
5. Rate of subsurface inflow to layer (*Customary or Metric*)

3.3.3 Lateral Drainage Layer Design Data

1. Maximum drainage length (*Customary or Metric*)
2. Drain slope, percent
3. Percentage of leachate collected from drainage layer that is recirculated
4. Layer to receive recirculated leachate from drainage layer

3.3.4 Geomembrane Liner Data

1. Pinhole density in geomembrane liner (*Customary or Metric*)
2. Geomembrane liner installation defects (*Customary or Metric*)
3. Geomembrane liner placement quality (six available options)
4. Geomembrane liner saturated hydraulic conductivity (vapor diffusivity), cm/sec
5. Geotextile transmissivity, cm²/sec (optional, when placed with geomembrane)

3.3.5 Runoff Curve Number Information

Three methods are available to define a SCS AMC II runoff curve number.

1. User-specified curve number used without modification
2. User-specified curve number modified for surface slope and slope length
3. Curve number computed by HELP program based on surface slope, slope length, default soil texture, and quantity of vegetative cover

3.4 LANDFILL PROFILE AND LAYER DESCRIPTIONS

The HELP program may be used to model landfills with up to twenty layers of materials -- soils, geosynthetics, wastes or other materials. Figure 1 shows a typical landfill profile with eleven layers. The program recognizes four general types of layers.

1. Vertical percolation layers
2. Lateral drainage layers
3. Barrier soil liners

4. Geomembrane liners

It must be noted that correct classification of layers is very important because the program models the flow of water through the four types of layers in different ways.

Flow in a vertical percolation layer (e.g., Layers 1 and 5 in Figure 1) is by unsaturated vertical drainage downward due to gravity drainage; upward flux due to evapotranspiration is modeled as an extraction. The rate of gravity drainage (percolation) in a vertical percolation layer is a function of soil moisture and soil parameters. The saturated hydraulic conductivity specified for a vertical percolation layer should be in the vertical direction for anisotropic materials. The main role of a vertical percolation layer is to provide moisture storage. Waste layers and layers designed to support vegetation and provide evaporative storage are normally designated as vertical percolation layers.

Lateral drainage layers (e.g., Layers 2, 6, 7 and 9 in Figure 1) are layers directly above liners that are designed to promote drainage laterally to a collection and removal system. Vertical flow in a lateral drainage layer is modeled in the same manner as a vertical percolation layer, but saturated lateral drainage is allowed. The saturated hydraulic conductivity specified for a lateral drainage layer should be in the lateral direction (downslope) for anisotropic materials. A lateral drainage layer may be underlain by only another lateral drainage layer or a liner. The drainage slope specified for a lateral drainage should be the slope of the surface of the liner underlying the drainage layer in the direction of flow (the maximum gradient for a section of liner in a single plane) and may range from 0 to 50 percent. The drainage length specified for a lateral drainage layer is the length of the horizontal projection of a representative flow path from the crest to the collector rather than the distance along the slope. For slopes of less than 10 percent, the difference is negligible. The drainage length must be greater than zero but does not have a practical upper limit. Recirculation is permitted from lateral drainage layers directly above a liner where 0 to 100 percent of the drainage collected can be recirculated and redistributed in a user-specified vertical percolation or lateral drainage layer.

Barrier soil liners (e.g., Layers 4, and 11 in Figure 1) are intended to restrict vertical drainage (percolation/leakage). These layers should have saturated hydraulic conductivities substantially lower than those of the other types of layers. Liners are assumed to be saturated at all times but leak only when there is a positive head on the top surface of the liner. The percolation rate depends upon the depth of water-saturated soil (head) above the base of the liner, the thickness of the liner and the saturated hydraulic conductivity. The saturated hydraulic conductivity specified for a barrier soil liner should be its value for passing the expected permeant in the vertical direction for anisotropic materials. The program allows only downward saturated flow in barrier soil liners. Evapotranspiration and lateral drainage are not permitted from a liner. Thus, any water moving into a liner will eventually percolate through the liner. In Version 3 composite liners are modeled as two layers -- a geomembrane liner and a barrier soil liner as shown in Figure 1.

Geomembrane liners (e.g., Layers 3, 8 and 10 in Figure 1) are virtually impermeable synthetic membranes that reduce the area of vertical drainage/percolation/leakage to a very small fraction of the area located near manufacturing flaws and installation defects (punctures, tears and faulty seaming). A small quantity of vapor transport across the membrane also occurs and can be modeled by specifying the vapor diffusivity as the saturated hydraulic conductivity of the geomembrane. Geomembranes leak only when there is a positive head on the top surface of the liner. The leakage rate depends on the depth of saturated soil (head) above the liner, the saturated hydraulic conductivity of the drainage limiting soil layer adjacent to the membrane, the contact between the membrane and the adjacent drainage limiting soil layer, geomembrane properties and the size and number of holes in the geomembrane liner. Aging of geomembranes is not considered.

While the HELP program is quite flexible, there are some basic rules that must be followed regarding the arrangement of layers in the profile.

1. A vertical percolation layer may not be underlying a lateral drainage layer.
2. A barrier soil liner may not be underlying another barrier soil liner.
3. A geomembrane liner may not be placed directly between two barrier soil liners.
4. A geomembrane liner may not be underlying another geomembrane liner.
5. A barrier soil liner may not be placed directly between two geomembrane liners.
6. When a barrier soil liner or a geomembrane liner is not placed directly below the lowest drainage layer, all drainage layers below the lowest liner are treated as vertical percolation layers. Thus, no lateral drainage is computed for the bottom section of the landfill.
7. The top layer may not be a barrier soil liner.
8. The top layer may not be a geomembrane liner.
9. The profile can contain no more than a total of five barrier soil liners and geomembrane liners.

The HELP model does not permit two barrier soil liners to be adjacent to each other. If a design has two soil layers adjacent to each other that would be expected to act as a single liner and both soils will remain nearly saturated and contribute significantly to the head loss and restriction of vertical drainage, then the thickness of the two layers should be summed and an effective saturated hydraulic conductivity should be computed for the combined liner. The effective saturated hydraulic conductivity should be computed as follows:

$$K_e = \frac{T_e}{\sum_{i=1}^n \frac{T_i}{K_i}} = \frac{T_1 + T_2}{\frac{T_1}{K_1} + \frac{T_2}{K_2}} \quad (1)$$

where

- K_e = effective saturated hydraulic conductivity of combined liner
- T_e = effective thickness of combined liner
- T_i = thickness of liner soil i
- K_i = saturated hydraulic conductivity of liner soil i
- n = number of liner soils in the combined liner

For computational purposes, the soil profile is partitioned into subprofiles. Subprofiles are defined in relation to the location of the liners. The first (top) subprofile shown on Figure 1 extends from the landfill surface to the bottom of the highest liner system (bottom of the composite liner, Layer 4) upper barrier soil layer. The second subprofile extends from the top of the layer (Layer 5) below the bottom of the first liner system to the base of the second liner system (Layer 8). The third (bottom) subprofile extends from the top of the layer below the second liner system (the leakage detection drainage layer, Layer 9) to the base of the lowest liner (Layer 11). The program allows up to five liner systems and, therefore, five subprofiles plus an additional subprofile of vertical percolation layers below the bottom liner system. The program models the flow of water through one subprofile at a time from top to bottom, with the percolation or leakage from one subprofile serving as the inflow to the underlying subprofile.

3.5 SOIL CHARACTERISTICS

The user can assign soil characteristics to a layer using the default option, the user defined soil option, or the manual option. Table 4 shows the default characteristics for 42 soil/material types. The soil texture types are classified according to two standard systems, the U.S. Department of Agriculture textural classification system and the Unified Soil Classification System. The default characteristics of types 1 through 15 are typical of surficial and disturbed agricultural soils, which may be less consolidated and more aerated than soils typically placed in landfills (Breazeale and McGeorge, 1949; England, 1970; Lutton et al., 1979; Rawls et al., 1982). Clays and silts in landfills would generally be compacted except within the vegetative layer, which might be tilled to promote vegetative growth. Untilled vegetative layers may be more compacted than the loams listed in Table 4. Soil texture types 22 through 29 are compacted soils. Type 18 is representative of typical municipal solid waste that has been compacted; type 19 is the same waste but it accounts for 65 percent of the waste being in dead zones not contributing to drainage and storage. Soil types 16 and 17 denote very well compacted clay soils that might be used for barrier soil liners. The user assigns default soil characteristics to a layer by specifying the appropriate number for the material type. The

TABLE 4. DEFAULT SOIL, WASTE, AND GEOSYNTHETIC CHARACTERISTICS

Classification			Total Porosity	Field Capacity	Wilting Point	Saturated Hydraulic Conductivity
HELP	USDA	USCS	vol/vol	vol/vol	vol/vol	cm/sec
1	CoS	SP	0.417	0.045	0.018	1.0x10 ⁻²
2	S	SW	0.437	0.062	0.024	5.8x10 ⁻³
3	FS	SW	0.457	0.083	0.033	3.1x10 ⁻³
4	LS	SM	0.437	0.105	0.047	1.7x10 ⁻³
5	LFS	SM	0.457	0.131	0.058	1.0x10 ⁻³
6	SL	SM	0.453	0.190	0.085	7.2x10 ⁻⁴
7	FSL	SM	0.473	0.222	0.104	5.2x10 ⁻⁴
8	L	ML	0.463	0.232	0.116	3.7x10 ⁻⁴
9	SiL	ML	0.501	0.284	0.135	1.9x10 ⁻⁴
10	SCL	SC	0.398	0.244	0.136	1.2x10 ⁻⁴
11	CL	CL	0.464	0.310	0.187	6.4x10 ⁻⁵
12	SiCL	CL	0.471	0.342	0.210	4.2x10 ⁻⁵
13	SC	SC	0.430	0.321	0.221	3.3x10 ⁻⁵
14	SiC	CH	0.479	0.371	0.251	2.5x10 ⁻⁵
15	C	CH	0.475	0.378	0.265	1.7x10 ⁻⁵
16	Barrier Soil		0.427	0.418	0.367	1.0x10 ⁻⁷
17	Bentonite Mat (0.6 cm)		0.750	0.747	0.400	3.0x10 ⁻⁹
18	Municipal Waste (900 lb/yd ³ or 312 kg/m ³)		0.671	0.292	0.077	1.0x10 ⁻³
19	Municipal Waste (channeling and dead zones)		0.168	0.073	0.019	1.0x10 ⁻³
20	Drainage Net (0.5 cm)		0.850	0.010	0.005	1.0x10 ⁻¹
21	Gravel		0.397	0.032	0.013	3.0x10 ⁻¹
22	L*	ML	0.419	0.307	0.180	1.9x10 ⁻⁵
23	SiL*	ML	0.461	0.360	0.203	9.0x10 ⁻⁶
24	SCL*	SC	0.365	0.305	0.202	2.7x10 ⁻⁶
25	CL*	CL	0.437	0.373	0.266	3.6x10 ⁻⁶
26	SiCL*	CL	0.445	0.393	0.277	1.9x10 ⁻⁶
27	SC*	SC	0.400	0.366	0.288	7.8x10 ⁻⁷
28	SiC*	CH	0.452	0.411	0.311	1.2x10 ⁻⁶
29	C*	CH	0.451	0.419	0.332	6.8x10 ⁻⁷
30	Coal-Burning Electric Plant Fly Ash*		0.541	0.187	0.047	5.0x10 ⁻⁵
31	Coal-Burning Electric Plant Bottom Ash*		0.578	0.076	0.025	4.1x10 ⁻³
32	Municipal Incinerator Fly Ash*		0.450	0.116	0.049	1.0x10 ⁻²
33	Fine Copper Slag*		0.375	0.055	0.020	4.1x10 ⁻²
34	Drainage Net (0.6 cm)		0.850	0.010	0.005	3.3x10 ⁻¹

* Moderately Compacted

(Continued)

TABLE 4 (continued). DEFAULT SOIL, WASTE, AND GEOSYNTHETIC CHARACTERISTICS

Classification		Total Porosity	Field Capacity	Wilting Point	Saturated Hydraulic Conductivity
HELP	Geomembrane Material	vol/vol	vol/vol	vol/vol	cm/sec
35	High Density Polyethylene (HDPE)				2.0×10^{-13}
36	Low Density Polyethylene (LDPE)				4.0×10^{-13}
37	Polyvinyl Chloride (PVC)				2.0×10^{-11}
38	Butyl Rubber				1.0×10^{-12}
39	Chlorinated Polyethylene (CPE)				4.0×10^{-12}
40	Hypalon or Chlorosulfonated Polyethylene (CSPE)				3.0×10^{-12}
41	Ethylene-Propylene Diene Monomer (EPDM)				2.0×10^{-12}
42	Neoprene				3.0×10^{-12}

(concluded)

user-defined soil option accepts non-default soil characteristics for layers assigned soil type numbers greater than 42. This is especially convenient for specifying characteristics of waste layers. User-specified soil characteristics can be assigned any soil type number greater than 42.

When a default soil type is used to describe the top soil layer, the program adjusts the saturated hydraulic conductivities of the soils in the top half of the evaporative zone for the effects of root channels. The saturated hydraulic conductivity value is multiplied by an empirical factor that is computed as a function of the user-specified maximum leaf area index. Example values of this factor are 1.0 for a maximum LAI of 0 (bare ground), 1.8 for a maximum LAI of 1 (poor stand of grass), 3.0 for a maximum LAI of 2 (fair stand of grass), 4.2 for a maximum LAI of 3.3 (good stand of grass) and 5.0 for a maximum LAI of 5 (excellent stand of grass).

The manual option requires values for porosity, field capacity, wilting point, and saturated hydraulic conductivity. These and related soil properties are defined below.

Soil Water Storage (Volumetric Content): the ratio of the volume of water in a soil to the total volume occupied by the soil, water and voids.

Total Porosity: the soil water storage/volumetric content at saturation (fraction of total volume).

Field Capacity: the soil water storage/volumetric content after a prolonged period of gravity drainage from saturation corresponding to the soil water storage when a soil exerts a soil suction of 1/3 bar.

Wilting Point: the lowest soil water storage/volumetric content that can be achieved by plant transpiration or air-drying, that is the moisture content where a plant will be permanently wilted corresponding to the soil water storage when a soil exerts a soil suction of 15 bars.

Saturated Hydraulic Conductivity: the rate at which water drains through a saturated soil under a unit pressure gradient.

Porosity, field capacity and wilting point are all dimensionless numbers between 0 and 1. Porosity must be greater than field capacity, which in turn must be greater than the wilting point. The wilting point must be greater than zero. The values for porosity, field capacity and wilting point are not used for liners, except for initializing the soil water storage of liners to the porosity value.

The soil moisture retention properties of a layer should be adjusted downward if some volume of the layer does not participate in the drainage and storage of infiltrated water. This condition commonly exists in shallow layers of municipal solid waste because municipal solid waste is very heterogeneous and poorly compacted. The plastics in the waste also channels the drainage, limits the spreading of infiltration, and restricts the wetting of the waste and, therefore, the storage. Default soil texture number 19 provides adjusted retention values for a municipal solid waste with significant channeling; it assumes that only 25 percent of the volume is actively involved in drainage and storage of infiltration. As the values were computed by multiplying the values for municipal solid waste (default texture number 18) by 0.25; the initial soil water content would also be multiply by 0.25.

The HELP user has the option of specifying the initial volumetric water storage (content) of all layers except liners. Liners are assumed to remain saturated at all times. If the user chooses not to specify initial water contents, the program estimates values near steady-state and then runs one year of initialization to refine the estimates before starting the simulation. The soil water contents at the end of this year of initialization are taken as the initial values for the simulation period. The program then runs the complete simulation, starting again from the beginning of the first year of data. The results for the initialization period are not reported. To improve initialization to steady-state moisture storage, the user should replace thick vertical percolation and lateral drainage layers, that are below the evaporative zone and above the saturated zone above liners, with thin layers. Then, run the simulation for a number of years until steady-state is approximated. The final dimensionless water storage values after nearing steady-state should then be specified as the initial water contents in your actual simulation using the true dimensions of the layers.

The initial moisture content of municipal solid waste is a function of the composition of the waste; reported values for fresh wastes range from about 0.08 to 0.20 vol/vol. The average value is about 0.12 vol/vol for compacted municipal solid waste. If using default waste texture 19, where 75% of the volume is inactive, the initial moisture content should be that of only the active portion, 25% of the values reported above.

The soil water storage or content used in the HELP model is on a per volume basis (θ), volume of water (V_w) per total (bulk--soil, water and air) soil volume ($V_t = V_s + V_w + V_a$), which is characteristic of practice in agronomy and soil physics. Engineers more commonly express moisture content on a per mass basis (w), mass of water (M_w) per mass of soil (M_s). The two can be related to each other by knowing the dry bulk density (ρ_{db}), dry bulk specific gravity (Γ_{db}) of the soil (ratio of dry bulk density to water density (ρ_w)), wet bulk density (ρ_{wb}), wet bulk specific gravity (Γ_{wb}) of the soil (ratio of wet bulk density to water density).

$$\theta = w \frac{\rho_{db}}{\rho_w} = w \Gamma_{db} \quad (2)$$

$$\theta = \frac{w}{1 + w} \frac{\rho_{wb}}{\rho_w} = \frac{w}{1 + w} \Gamma_{wb} \quad (3)$$

3.6 GEOMEMBRANE CHARACTERISTICS

The user can assign geomembrane liner characteristics (vapor diffusivity/saturated hydraulic conductivity) to a layer using the default option, the user-defined soil option, or the manual option. Saturated hydraulic conductivity for geomembranes is defined in terms of its equivalence to the vapor diffusivity. The porosity, field capacity, wilting point and initial moisture content are not needed for geomembranes. Table 4 shows the default characteristics for 12 geomembrane liners. The user assigns default soil characteristics to a layer simply by specifying the appropriate geomembrane liner texture number. The user-defined option accepts user specified geomembrane liner characteristics for layers assigned textures greater than 42. Manual geomembrane liner characteristics can be assigned any texture greater than 42.

Regardless of the method of specifying the geomembrane "soil" characteristics, the program also requires values for geomembrane liner thickness, pinhole density, installation defect density, geomembrane placement quality, and the transmissivity of geotextiles separating geomembranes and drainage limiting soils. These parameters are defined below.

Pinhole Density: the number of defects (diameter of hole equal to or smaller than the geomembrane thickness; hole estimated as 1 mm in diameter) in a given area generally resulting from manufacturing flaws such as polymerization deficiencies.

Installation Defect Density: the number of defects (diameter of hole larger than the geomembrane thickness; hole estimated as 1 cm² in area) per acre resulting primarily from seaming faults and punctures during installation.

Geotextile Transmissivity: the product of the in-plane saturated hydraulic conductivity and thickness of the geotextile.

The density of pinholes and installation defects is a subject of speculation. Ideally, geomembranes would not have any defects. If any were known to exist during construction, the defects would be repaired. However, geomembranes are known to leak and therefore reasonably conservative estimates of the defect densities should be specified to determine the maximum probable leakage quantities.

The density of defects has been measured at a number of landfills and other facilities and reported in the literature. These findings provide guidance for estimating the defect densities. Typical geomembranes may have about 0.5 to 1 pinholes per acre (1 to 2 pinholes per hectare) from manufacturing defects. The density of installation defects is a function of the quality of installation, testing, materials, surface preparation, equipment, and QA/QC program. Representative installation defect densities as a function of the quality of installation are given below for landfills being built today with the state-of-the-art in materials, equipment and QA/QC. In the last column the frequency of achieving a particular installation quality is given. The estimates are based on limited data but are characteristic of the recommendations provided in the literature.

<u>Installation Quality</u>	<u>Defect Density (number per acre)</u>	<u>Frequency (percent)</u>
Excellent	Up to 1	10
Good	1 to 4	40
Fair	4 to 10	40
Poor	10 to 20*	10

- * Higher defect densities have been reported for older landfills with poor installation operations and materials; however, these high densities are not characteristic of modern practice.

The user must also enter the placement quality of the geomembrane liner if pinholes or installation defects are reported. There are six different possible entries for the geomembrane liner placement quality. The program selects which equation will be used to compute the geomembrane based on the placement quality specified and the saturated hydraulic conductivity of the lower permeability soil (drainage limiting soil) adjacent to

the geomembrane. The program has different equations for three ranges of saturated hydraulic conductivity: greater than or equal to 0.1 cm/sec; less than 0.1 and greater than or equal to 0.0001 cm/sec; and less than 0.0001 cm/sec.

1. *Perfect*: Assumes perfect contact between geomembrane and adjacent soil that limits drainage rate (no gap, "sprayed-on" seal between membrane and soil formed in place).
2. *Excellent*: Assumes exceptional contact between geomembrane and adjacent soil that limits drainage rate (typically achievable only in the lab or small field lysimeters).
3. *Good*: Assumes good field installation with well-prepared, smooth soil surface and geomembrane wrinkle control to insure good contact between geomembrane and adjacent soil that limits drainage rate.
4. *Poor*: Assumes poor field installation with a less well-prepared soil surface and/or geomembrane wrinkling providing poor contact between geomembrane and adjacent soil that limits drainage rate, resulting in a larger gap for spreading and greater leakage.
5. *Worst Case*: Assumes that contact between geomembrane and adjacent soil does not limit drainage rate, resulting in a leakage rate controlled only by the hole.
6. *Geotextile separating geomembrane liner and drainage limiting soil*: Assumes leakage spreading and rate is controlled by the in-plane transmissivity of the geotextile separating the geomembrane and the adjacent soil layer that would have otherwise limited the drainage. This quality would not normally be used with a geosynthetic clay liner (GCL) as the controlling soil layer. Upon wetting, the bentonite swells and extrudes into the geotextile, filling its voids and reducing its transmissivity below the point where it can contribute significantly to spreading of leakage. GCL's, when properly placed, tend to have intimate contact with the geomembrane (Harpur et al., 1993).

3.7 SITE CHARACTERISTICS

The user must also supply a value of the Soil Conservation Service (SCS) runoff curve number for Antecedent Moisture Condition II (AMC-II) or provide information so that a curve number can be computed. Unlike Version 2 of the HELP model, Version 3 accounts for surface slope effects on curve number and runoff. In Version 3 of the HELP model, there are three different options by which a curve number can be obtained.

1. A curve number defined by the user

2. A curve number defined by the user and modified according to the surface slope and slope length of the landfill
3. A curve number is computed by the HELP model based on landfill surface slope, slope length, soil texture of the top layer, and the vegetative cover. Some general guidance for selection of runoff curve numbers is provided in Figure 2 (USDA, Soil Conservation Service, 1985).

Two of the options account for surface slope. The correlation between surface slope conditions and curve number were developed for slopes ranging from 1 percent to as high as 50 percent and for slope lengths ranging from 50 feet to 2000 feet.

3.8 OVERVIEW OF MODELING PROCEDURE

The hydrologic processes modeled by the program can be divided into two categories: surface processes and subsurface processes. The surface processes modeled are snowmelt, interception of rainfall by vegetation, surface runoff, and surface evaporation. The subsurface processes modeled are evaporation from soil profile, plant transpiration, unsaturated vertical drainage, barrier soil liner percolation, geomembrane leakage and saturated lateral drainage.

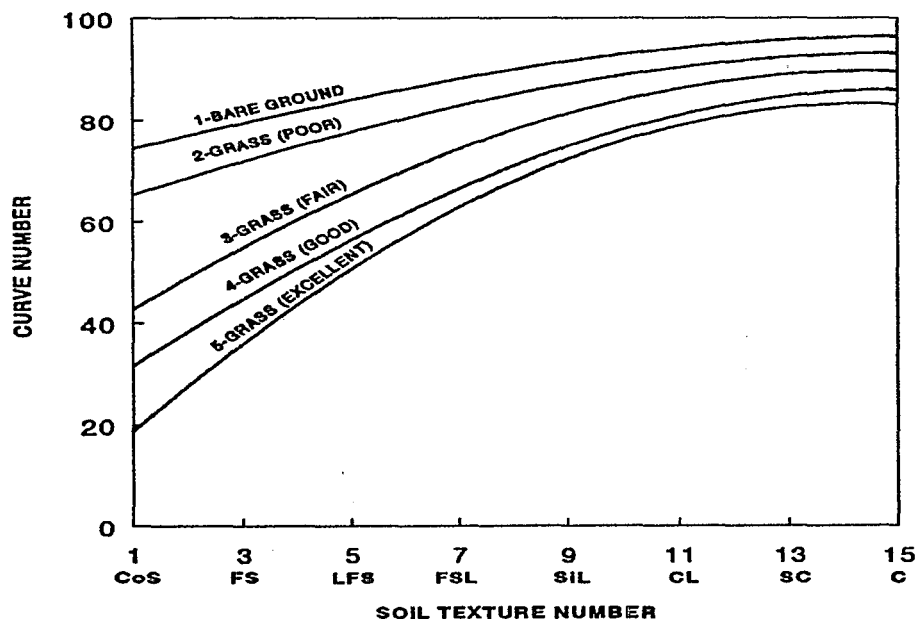


Figure 2. Relation between SCS Curve Number and Default Soil Texture Number for Various Levels of Vegetation

Daily infiltration into the landfill is determined indirectly from a surface water balance. Infiltration is assumed to equal the sum of rainfall, surface storage and snowmelt, minus the sum of runoff, additional storage in snowpack and evaporation of surface water. No liquid water is assumed to be held in surface storage from one day to the next except in the snowpack or when the top soil is saturated and runoff is not permitted. Each day, the free available water for infiltration, runoff, or evaporation from water on the surface is determined from the surface storage, discharge from the snowpack, and rainfall. Snowfall is added to the surface snow storage, which is depleted by either evaporation or melting. Snowmelt is added to the free available water and is treated as rainfall except that it is not intercepted by vegetation. The free available water is used to compute the runoff by the SCS rainfall-runoff relationship. The interception is the measure of water available to evaporate from the surface. Interception in excess of the potential evaporation is added to infiltration. Surface evaporation is then computed. Potential evaporation from the surface is first applied to the interception; any excess is applied to the snowmelt, then to the snowpack and finally to the groundmelt. Potential evaporation in excess of the evaporation from the surface is applied to the soil column and plant transpiration. The snowmelt and rainfall that does not run off or evaporate is assumed to infiltrate into the landfill along with any groundmelt that does not evaporate.

The first subsurface processes considered are soil evaporation and plant transpiration from the evaporative zone of the upper subprofile. A vegetative growth model accounts for the daily growth and decay of the surface vegetation. The other subsurface processes are modeled one subprofile at a time, from top to bottom, using a design-dependent time step ranging from 30 minutes to 6 hours. A storage-routing procedure is used to redistribute the soil water among the modeling segments that comprise the subprofile. This procedure accounts for infiltration or percolation into the subprofile and evapotranspiration from the evaporative zone. Then, if the subprofile contains a liner, the program computes the head on the liner. The head on the liner is then used to compute the leakage/percolation through the liner and, if lateral drainage is permitted above the top of the liner, the lateral drainage to the collection and removal system.

3.9 ASSUMPTIONS AND LIMITATIONS

3.9.1 Solution Methods

The modeling procedures documented in the previous section are necessarily based on many simplifying assumptions. Generally, these assumptions are reasonable and consistent with the objectives of the program when applied to standard landfill designs. However, some of these assumptions may not be reasonable for unusual designs. The major assumptions and limitations of the program are summarized below.

Runoff is computed using the SCS method based on daily amounts of rainfall and

snowmelt. The program assumes that areas adjacent to the landfill do not drain onto the landfill. The time distribution of rainfall intensity is not considered. The program cannot be expected to give accurate estimates of runoff volumes for individual storm events on the basis of daily rainfall data. However, because the SCS rainfall-runoff relation is based on considerable daily field data, long-term estimates of runoff should be reasonable. The SCS method does not explicitly consider the length and slope of the surface over which overland flow occurs. This limitation has been removed by developing and implementing into the HELP input routine a procedure for computing curve numbers that take into consideration the effect of slope and slope length. The limitation, however, remains on the user specified curve number (the first method). This limitation is not a concern provided that the slope and slope length of the landfill do not differ dramatically from those of the test plots upon which the SCS method is based. Use of the SCS method probably underestimates runoff somewhat where the overland flow distance is very short or the slope is very steep or when the rainfall duration is very short and the intensity is very high.

The HELP model assumes Darcian flow by gravity influences through homogeneous soil and waste layers. It does not consider explicitly preferential flow through channels such as cracks, root holes, or animal burrows but allows for vertical drainage through the evaporative zone at moisture contents below field capacity. Similarly, the program allows vertical drainage from a layer at moisture contents below field capacity when the inflow would occupy a significant fraction of the available storage capacity below field capacity. The drainage rate out of a segment is assumed to equal the unsaturated hydraulic conductivity of the segment corresponding to its moisture content, provided that the underlying segment is not a liner and is not saturated. In addition to these special cases, the drainage rate out of a segment can be limited by the saturated hydraulic conductivity of the segment below it. When limited, the program computes an effective gradient for saturated flow through the lower segment. This permits vertical percolation or lateral drainage layers to be arranged without restrictions on their properties as long as they perform as their layer description implies and not as liners.

The model assumes that a. the soil moisture retention properties and unsaturated hydraulic conductivity can be calculated from the saturated hydraulic conductivity and limited soil moisture retention parameters (porosity, field capacity and wilting point) and b. the soil moisture retention properties fit a Brooks-Corey relation (Brooks et al., 1964) defined by the three soil moisture retention parameters. Upon obtaining the Brooks-Corey parameters, the model assumes that the unsaturated hydraulic conductivity relation with soil moisture is well described by the Campbell equation.

The model does not explicitly compute flow by differences in soil suction (soil suction gradient) and, as such, does not model the draw of water upward by capillary drying. This draw of water upward is modeled as an extraction rather than transport of water upward. Therefore, it is important that the evaporative zone depth be specified as the depth of capillary drying. Drainage downward by soil suction exerted by dry soils lower in the landfill profile is modeled as Darcian flow for any soil having a relative

moisture content greater than the lower soils. The drainage rate is equal to the unsaturated hydraulic conductivity computed as a function of the soil moisture content. As such, the rate is assumed to be independent of the pressure gradient.

Leakage through barrier soil liners is modeled as saturated Darcian flow. Leakage is assumed to occur only as long as there is head on the surface of the liner. The model assumes that the head driving the percolation can be represented by the average head across the entire liner and can be estimated from the soil moisture storage. It is also assumed that the liner underlies the entire area of the landfill and, conservatively, that when leakage occurs, the entire area of the landfill leaks. The model does not consider aging or drying of the liner and, therefore, the saturated hydraulic conductivity of the liner does not vary as a function of time.

Geomembranes are assumed to leak primarily through holes. The leakage passes through the holes and spreads between the geomembrane and soil until the head is dissipated. The leakage then percolates through the soil at the rate dependent on the saturated hydraulic conductivity and the pressure gradient. Therefore, the net effect of a geomembrane is to reduce the area of percolation through the liner system. The program assumes the holes to be uniformly distributed and the head is distributed across the entire liner. The model does not consider aging of the liner and therefore the number and size of the holes do not vary as a function of time. In addition, it is conservatively assumed that the head on the holes can be represented by the average head across the entire liner and can be estimated from the soil moisture storage and that the liner underlies the entire area of the landfill.

The lateral drainage model is based on the assumption that the saturated depth profile is characteristic of the steady-state profile for the given average depth of saturation. As such, the model assumes that the lateral drainage rate for steady-state drainage at a given average depth of saturation is representative of unsteady lateral drainage rate for the same average saturated depth. In actuality the rate would be somewhat larger for periods when the depth is building and somewhat smaller for periods when the depth is falling. Steady drainage implies that saturated conditions exist above the entire surface of the liner, agreeing with the assumptions for leakage through liner systems.

The model assumes the vegetative growth and decay can be characterized by a vegetative growth model developed for crops and perennial grasses. In addition, it is assumed that the vegetation transpires water, shades the surface, intercepts rainfall and reduces runoff in similar quantities as grasses or as an adjusted equivalence of LAI.

3.9.2 Limits of Application

The model can handle water routing through or storage in up to twenty soil or waste layers; as many as five liner systems may be employed. The simulation period can range from 1 to 100 years. The model cannot simulate a capillary break or unsaturated lateral drainage.

The model has limits on the arrangement of layers in the landfill profile. Each layer must be described as being one of four types: vertical percolation layer, lateral drainage layer, barrier soil liner, or geomembrane liner. The model does not permit a vertical percolation layer to be placed directly below a lateral drainage layer. A barrier soil liner may not underlie another barrier soil liner. Geomembranes cannot envelop a barrier soil liner and barrier soil liners cannot envelop a geomembrane. The top layer may not be a liner. If a liner is not placed directly below the lowest lateral drainage layer, the lateral drainage layers in the lowest subprofile are treated by the model as vertical percolation layers. No other restrictions are placed on the order of the layers.

The lateral drainage equation was developed for the expected range of hazardous waste landfill design specifications. Permissible ranges for slope of the drainage layer are 0 to 50 percent. Due to dimensionless structure of the lateral drainage equation, there are no practical limits in the maximum drainage length.

Several interrelations must exist between the soil characteristics of a layer and of the soil subprofile. The porosity, field capacity and wilting point can theoretically range from 0 to 1 units of volume per volume; however, the porosity must be greater than the field capacity, and the field capacity must be greater than the wilting point. Initial soil moisture storage must be greater than or equal to the wilting point and less than or equal to the porosity. The initial moisture content of liners must be equal to the porosity and the liners remain saturated. The field capacity and wilting point values are not used for barrier soil liners. Values for porosity, field capacity and wilting point are not needed for geomembranes.

Values for the leaf area index may range from 0 for bare ground to 5 for an excellent stand of grass. Detailed recommendations for leaf area indices and evaporative depths are given in the program.

The default values for the evaporation coefficient are based on experimental results. The basis for the calculation of these default values is described by Schroeder et al. (1994). The model imposes upper and lower limits of 5.1 and 3.3 so as not to exceed the range of experimental data.

Surface runoff from adjacent areas does not run onto the landfill, and the physical characteristics of the landfill specified by the user remain constant over the modeling period. No adjustments are made for the changes that occur in these characteristics as the landfill ages. Additionally, the program cannot model the filling process within a single simulation. Aging of materials and staging of the landfill operation must be modeled by successive simulations.

Default Soil Characteristics

The HELP model contains default values of soil characteristics based on soil texture class. The documentation for Version 3 describes the origin of these default values

(Schroeder et al., 1994). Recommended default values for LAI and evaporative depth based on thick loamy top soils are given in the program.

Manual Soil Characteristics

The HELP model computes values for the three Brooks-Corey parameters as described in the documentation for Version 3 (Schroeder et al., 1994) based on the values for porosity, field capacity and wilting point.

Soil Moisture Initialization

The soil moisture of the layers may be initialized by the user or the program. When initialized by the program, the process consists of three steps. The first step sets the soil moisture of all layers except barrier soil liners equal to field capacity and all barrier soil liners to porosity (saturation). In the second step, the program computes a soil moisture for each layer below the top barrier soil liner. These soil moisture contents are computed to yield an unsaturated hydraulic conductivity equal to 85 percent of the lowest effective saturated hydraulic conductivity of the all liner systems above the layer, including consideration for the presence of a synthetic geomembrane liner. If the unsaturated hydraulic conductivity is less than 1×10^{-6} cm/sec and if the computed soil moisture is greater than field capacity, the soil moisture is set to equal computed soil moisture instead of the field capacity. The third step in the initialization consists of running the model for one year of simulation using the first year of climate data and the initial soil moisture values selected in the second step. At the end of this year of initialization, the soil moisture values existing at that point are reported as the initial soil moisture values. The simulation is then restarted using the first year of climate data.

Synthetic Temperature and Solar Radiation Values

The synthetically generated temperature and solar radiation values are assumed to be representative of the climate at the site. Synthetic daily temperature is a function of normal mean monthly temperature and the occurrence of rainfall. Synthetic daily solar radiation is a function of latitude, occurrence of rainfall, average daily dry-day solar radiation and average daily wet-day solar radiation.

SECTION 4

PROGRAM INPUT

4.1 INTRODUCTION

This section describes the procedures and options available to input data, execute the model, and obtain results. The discussion includes general input information, some definitions and rules, the program structure, and detailed explanations of the options reached from the Main Menu. Guidance is given throughout the section for selecting the most appropriate values in certain situations, but the main purpose of this section is to describe the mechanics of using the user interface. Detailed guidance on the definitions of input parameters and selection of their values is presented in Section 3.

Version 3 of the HELP program is started by typing "HELP3" from the DOS prompt in the directory where the program resides. The program starts by displaying a title screen, a preface, a disclaimer and then the main menu. The user moves from the title screen to the main menu by striking any key such as the space bar. Upon reaching the main menu, the user can select any of seven options. The program automatically solicits input from the user based on the option selected. In general the HELP model requires the following data, some of which may be selected from the default values.

1. Units
2. Location
3. Weather data file names
4. Evapotranspiration information
5. Precipitation data
6. Temperature data
7. Solar radiation data
8. Soil and design data file name
9. General landfill and site information
10. Landfill profile and soil/waste/geomembrane data
11. SCS runoff curve number information

4.2 DEFINITIONS AND RULES

There are a few fundamental rules regarding the input facility that a user must keep in mind when using the model. These rules should be followed to move around the screens and to move within the same screen. Below are some definitions and rules.

1. *Screens.* A screen in the HELP user interface as used in this report is a single screen of information. These screens are divided into three categories:

- **Input Screen:** a screen on which the user can input data
- **Selection Screen:** a screen from which the user selects an entry from a list
- **On-line Help Screen:** a screen where assistance is provided. General assistance on the interface is displayed by pressing the *F1* key, technical assistance by pressing the *F2* key, and key operations by pressing the *F3* key.

This terminology is used throughout this section. Each module consists of two types of screens: "primary" and "secondary." Primary screens are main screens that form a loop for each option of HELP. Secondary screens are displayed from the primary screens as part of the input process. These screens can be input screens or selection screens.

2. **Input Cells.** When the program highlights a number of spaces (called an "input cell" throughout this section), an input from the user is expected. At any input cell, the user has one of several options: enter the data requested, accept existing value, seek on-line help, or select one of the menu items listed at the bottom of the screen. Each cell is associated with a variable that is used directly or indirectly in the HELP model. Therefore, every effort must be made to assign a value to each cell when applicable. The user may input the value the first time around, or return to the cell at a later time during the program session. If an input cell is left blank, a value of zero will be assigned to the corresponding variable. If zero is not an appropriate answer to the question, it will produce erroneous results. The program will warn the user when a blank or zero is an inappropriate value.

Trailing decimal points are not required on input because the program automatically knows whether to treat a value as an integer or a floating point variable. For example, if a user wishes to enter the number nine, either 9, 9. or 9.00 is acceptable, provided the input cell is wide enough.

3. **Selection Cells.** These are cells that are used to select from a list of options. Selection cells highlight one item at a time. An item/option must be highlighted before it can be selected. Selection is made by pressing the *Enter* key.
4. **Moving Between Cells.** The user can move from one input screen to another, by pressing the *Page Down* key for the next screen or *Page Up* key for the previous screen in the loop of primary or secondary screens. Input screens are arranged in a loop format such that if the *Page Down* key is pressed from the last input screen the control will return to the first screen, and vice versa. The *up and down arrows* are used to move up and down through the cells of a screen. If the *up arrow* is pressed from the first cell on the screen, control will transfer to the last cell on the same screen, and vice versa. The *Tab and Shift-Tab* keys can be used to move to the right and to the left, respectively, among input and selection cells that are located on the same line. In addition, the *left and right arrows* may be used to move between

selection cells that are located on the same line.

5. **Moving Within an Input Cell.** Each input cell is set to a given width depending on the type of information expected to be entered in that cell. The cursor will be initially located on the first character space of the cell. The *left and right arrow* keys may be used to move the cursor to different spaces within the cell. If a value is typed in the first space of the cell, the cell contents will be deleted. To delete a character, move the cursor to the character location and then press the *Delete* key, or move the cursor to the space that is to the right of the character and then press the *Backspace* key. A character can be inserted between characters in an input cell by moving the cursor to the desired position and then pressing the *Insert* key. The *Insert* key will shift all characters that are at and to the right of the cursor one position to the right.
6. **Terminating.** At any time during the session, the user may press the *F9* key to quit without saving changes, return to the main menu or exit the program. The *Esc* key and the *Ctrl-Break* keys will end some options and allow you to continue with other operations. The *F10* key is used to save the data or proceed. If necessary, the user can terminate input or execution by rebooting (*Ctrl-Alt-Del* keys), resetting, or turning off the computer; however, the user is discouraged from terminating a run in these manners because some of the data may be lost.
7. **On-Line Help.** On-line help is available to the user from any cell location on the screen. By pressing *F1*, information about the operations and purpose of the screen is displayed, and by pressing *F2*, specific technical assistance for the highlighted cell is displayed. Note that the on-line help screens contain sections from this User's Guide and that the figures and tables mentioned on the screens are located in this document. The *F3* key displays various functions of keystrokes. Other specific information of the input screen is listed in menu line(s) at the bottom of screen.
8. **System of Units.** Throughout the HELP program the user is required to select a system of units. The HELP model allows the user to use either the customary system of units (a mixture of U.S. Customary and metric units traditionally used in landfill design and in Version 2 of the HELP model) or the Metric (SI) system of units. The user is not restricted to the same system for all data types; for example, the soil and design data can be in one system of units and the weather data can be in the other system. Moreover, it is not necessary for all types of weather data to have the same system of units (i.e., evapotranspiration data can be in the Metric system of units, while precipitation data is in customary units; the solar radiation data can be in customary units, while temperature data is in Metric units, and so on). Appropriate units are displayed in proper locations to keep the user aware of which units should be used for each data entry. Consistency in units is only required within each data type.

4.3 PROGRAM STRUCTURE

The flow or logic of the input facility of the HELP program may be viewed as a tree structure. The tree structure consists of nodes where new branches of the tree are started. The first node is called the trunk, root or parent node, and the terminal nodes of the tree are called leaves. All components (nodes) of the tree structure in the HELP model are screens that have different functions as defined previously, with the trunk node being the Main Menu. During an input session, the user should reach the leaf node if all the data for a given branch (module) are entered. Some of the nodes (screens) are common to more than one branch. The user must return to the node where the branch started in order to go to another branch. These movements can be accomplished with the special keys discussed above, such as *Page Up*, *Page Down*, *F9*, *F10*, etc.

4.4 MAIN MENU

At the beginning of each run, the Main Menu is displayed. A schematic of the main menu in Figure 3 shows the seven available modules (branches). Selection from the main menu is made by either moving the cursor to the desired module or by pressing the number of that option. Once a selection is made, program control transfers into an environment specific to that option and cannot transfer to another main menu option without exiting that environment to the main menu and then selecting another option. A brief description of each main menu option is presented below. More details are given in the following sections about specific data requirements for each option.

Option 1 on the main menu is "*Enter/Edit Weather Data.*" This module permits the user to read evapotranspiration, precipitation, temperature, and solar radiation data files and then review, edit, and save the data or create new files. There are four primary screens in this module; they are a file selection screen, evapotranspiration data screen, a screen that controls the method used for specifying precipitation, temperature and solar radiation data, and a screen for saving weather data files. Several options are available for specifying precipitation, temperature and solar radiations data. These vary from using default data (for precipitation only) to synthetic and other user-defined data sources, such as NOAA Tape, Climatedata™, ASCII data, HELP Version 2 data, and Canadian Climatological data. Data may also be entered manually. Default and synthetic weather data generation is performed by selecting the city of interest from a list of cities and specifying (optional) additional data.

Option 2 on the main menu is "*Enter/Edit Soil and Design Data.*" This module allows the user to read an already existing soil and design data file and then review, edit, and save the data or create a new data file. There are eight primary screens in the soil and design data module; they are a file selection screen, a landfill general information screen, three screens for entering design, soil and geomembrane liner data by layers, a screen for entering a runoff curve number, a data verification screen, and a screen for saving the soil and design data file. Input screens associated with this module provide

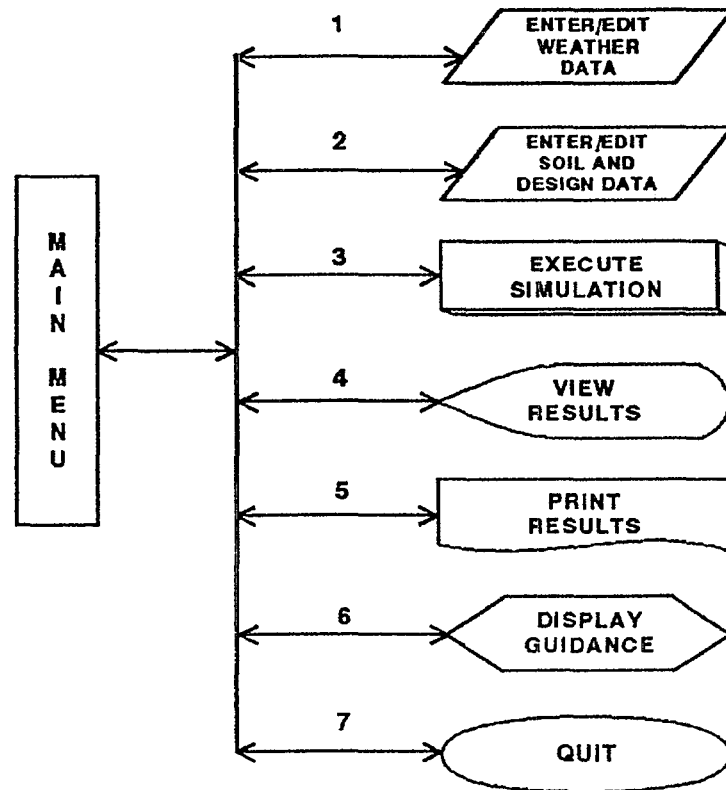


Figure 3. HELP3 Main Menu

cells for entering project title; system of units; initial soil conditions; landfill area; layer design information, such as layer type, thickness, soil texture, drainage characteristics; geomembrane liner information; and runoff curve number information including the ability to adjust the curve number a function of surface slope and length. At the end of this module, the user may request that the data be checked for possible violation of the design rules explained in Section 3. Under this module, the HELP model verifies the design data, soil and geomembrane liner properties and layer arrangement.

Option 3 on the main menu is "*Execute Simulation.*" In this option the user defines the data files to be used in running the simulation component of the HELP model and selects the output frequency and simulation duration desired from execution. In this option the user can also view the list of files available and can make file selections from these lists.

Option 4 on the main menu is "*View Results.*" This option allows the user to browse through the output file and examine the results of the run after executing the program. Option 5 is "*Print Results,*" and Option 6 is "*Display Guidance*" on general landfill design procedures and on the HELP model itself, containing much of the text of

this user's guide. Finally, Option 7 is used to "Quit" running the model and return to DOS.

In the following sections, detailed explanations of the main menu options are presented, and methods of data entry to the program and various options are discussed.

4.5 WEATHER DATA

As mentioned above, this module is selected from the main menu by pressing 1, "Enter/Edit Weather Data." A schematic of this module is shown in Figure 4. In this module, the user can specify all of the weather data (evapotranspiration, precipitation, temperature and solar radiation) required to run the model. The four primary screens in this module are "Weather Data - File Editing", "Evapotranspiration Data", "Precipitation, Temperature, and Solar Radiation Data", and "Weather Data - File Saving". Several secondary screens may appear during the session depending upon the action taken by the user. On-line help screens are always available for display by pressing *F1* or *F2*. The individual primary screens and their secondary screens of this module are discussed below.

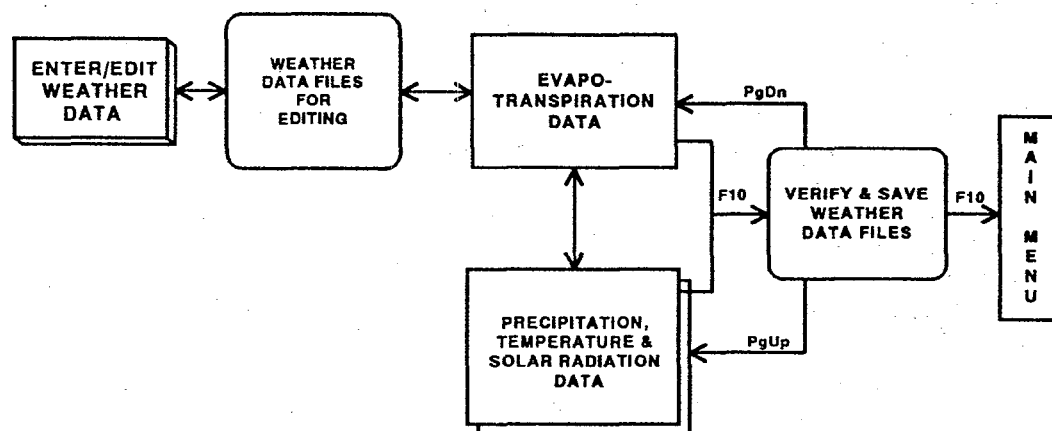


Figure 4. Schematic of Weather Data Module

4.5.1 Weather Data File Selection

The first screen in the weather data module is the "Weather Data - File Editing" screen. A schematic of this screen is shown in Figure 5. On this screen, the user may enter file names of existing files to select previously generated HELP Version 3 files for editing or leave the file names blank to create new data. One file name for each of the four types of weather data to be edited is needed. The DOS path may be specified if

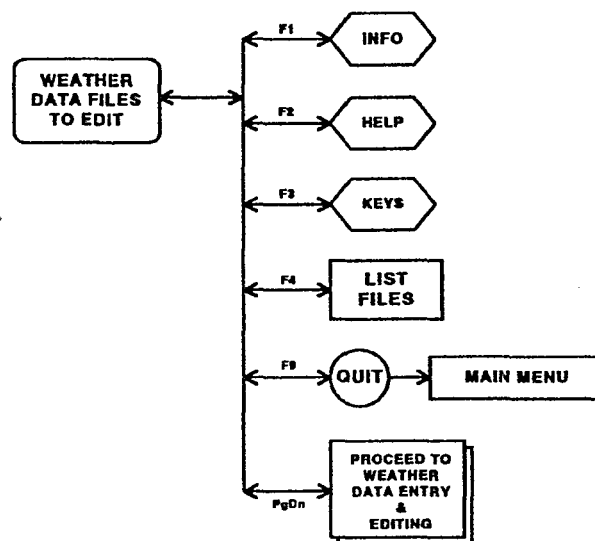


Figure 5. Schematic of "Weather Data - File Editing" Screen

different from the active or default drive and subdirectory, such as C:\HELP3\DATA. The following gives file naming and extension information as displayed on the screen.

<u>Data Type</u>	<u>DOS Path (Drive and/or Subdirectory)</u>	<u>User Specified File Name</u>
Precipitation		*.D4
Temperature		*.D7
Solar radiation		*.D13
Evapotranspiration		*.D11

* Any valid DOS name that the user desires (up to eight characters) is acceptable. The HELP program supplies the extension.

This convention must be always remembered when selecting file names for editing, saving, or converting data from other sources. However, when typing a file name on this screen, the user should not enter the extension because the program automatically assigns the proper extension to the file according to the weather types.

The current directory is displayed on the screen. The user may obtain a listing of all data files that reside on the current directory by pressing *F4*. By pressing *F4*, the program obtains a directory of all files that pertain to the weather data cell from which *F4* was pressed. For example, if *F4* was pressed from the temperature file cell, the program will display the list of files with an extension of D7 that reside on the currently specified directory. Up to 120 data files for any weather data type can be displayed on

the screen. The name of the current directory where these files are located is also displayed. To obtain the data files pertaining to the weather information needed that reside in another directory, the user should type in the name of a valid drive and subdirectory in the Directory column and then press *F4* for the list of files in that subdirectory. To display a directory for another type of data, move the cursor to the row for that data type and repeat the process listed above.

To select a file from the list of displayed files, move the cursor to the desired file name and press *Enter*. This action transfers control back to the previous screen, and the name of the file just selected will be displayed in the proper cell. The user can exit the "Data Files" screen without selecting a file by pressing the *Esc* key.

If the user wants to enter the file name in the file cell, the user must first enter the correct directory name. If an invalid directory is entered, the program will display the message, "Invalid Directory," and replace the entered directory name with the default directory name (where the program was started). The user then has another opportunity to enter the correct directory name. If the program cannot find the file name as entered, the message, "File Not Found," will be displayed. The previously entered file name is erased and the user has another opportunity to enter a correct file name. Pressing *Page Down* causes the program to read the valid data files selected and then proceeds to the first weather data entry screen.

4.5.2 Evapotranspiration (ET) Data

The evapotranspiration data requirements are listed in Section 3 and are entered to the program from the "Evapotranspiration Data" screen. This screen contains all information required by the HELP model to construct the evapotranspiration data file (*.D11). If the user specified an edit file name for the evapotranspiration data, the contents of the file will be displayed in the appropriate cells on this screen. The user can move the cursor to any cell to edit its contents. However, if no file was selected as an edit file, then data must be specified by the user. First, the user must select the system of units to be used for the evapotranspiration data, which may be entered in customary or metric units as explained in a previous section. A schematic of this screen is shown in Figure 6. The two methods for entering this data are the manual option and the default option.

Manual Option

This option requires the user to enter all evapotranspiration data manually. The user should first specify a location in the form of a city, state and latitude, followed by the evaporative zone depth, the maximum leaf area index, the Julian dates of the start (planting) and end (harvest) of the growing season, the annual average wind speed, and quarterly average relative humidities (in percentages) for the entered location.

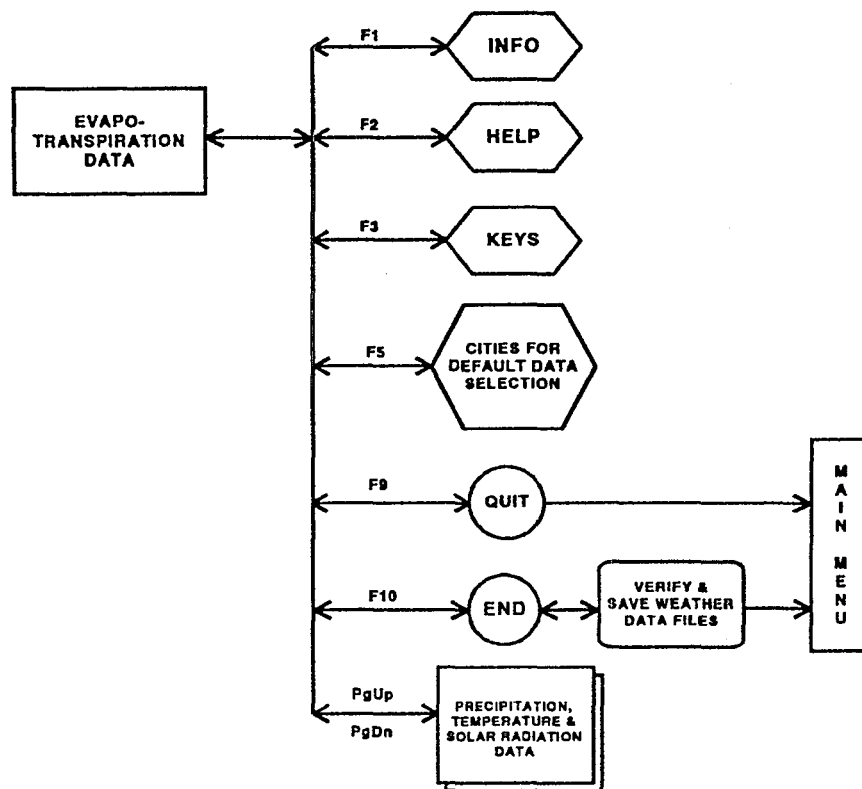


Figure 6. Schematic of "Evapotranspiration Data" Screen

Default Option

This option takes advantage of an available list of cities for which default values are provided for most of the evapotranspiration data; guidance information is available for the rest of the data. This option is triggered from any input cell on the "Evapotranspiration Data" screen by pressing *F5* and selecting a location (state and city) from a displayed list of locations. This list of cities is the same as that in Table 3.

Once a city is selected, the program automatically displays values in the appropriate input cells for the city, state, latitude, growing season dates, wind speed, and the four quarterly humidity values for that location. The program, however, displays guidance information on the evaporative zone depth for that location depending on the vegetative cover. The user must enter a value of the evaporative zone depth that is appropriate for the landfill design, location, top soil, and vegetation. (See Section 3 for detailed guidance.)

The user must also enter a value for the maximum leaf area index for the site. If the value entered is greater than the default maximum allowable value based on the climate for the selected city, the program will display that value only as a guidance to the user.

The user is not forced to change the entered value.

If the user decides to edit the name of the city or state, the program will erase the guidance information. Guidance is provided only for cities that are selected from the list obtained by pressing *F5*.

The location of the landfill being evaluated is likely to be some distance from all of the listed cities. In this case, the user has the option to select a city that has an similar climate and edit the values to improve the data or to simply enter the information manually.

The bottom line of the "Evapotranspiration Data" screen provides additional help information. Once all data are entered, the user can move on to another screen by pressing *Page Up* or *Page Down*, return to the main menu by pressing *F9*, or proceed to save the evapotranspiration data by pressing *F10*.

4.5.3 Precipitation, Temperature and Solar Radiation Data

The second screen in the weather data module is entitled "Precipitation, Temperature and Solar Radiation." From this screen, the user can select methods for creating the precipitation data file (*.D4), the temperature data file (*.D7), and the solar radiation data file (*.D13). A schematic of the main options available on this screen are shown in Figure 7. In Version 3 of the HELP model, all of the weather data need not be generated by the same method. For example, the user can enter the precipitation data using the synthetic weather generator, the temperature data using data from a NOAA data file, and solar radiation from an ASCII file. Seven options are available for entering temperature and solar radiation data. Under the precipitation data there are the same seven plus a default option. Figures 8, 9, and 10 show the possible options.

Default Precipitation

If the *default precipitation option (Customary Units Only)* is selected, the program will prompt the user with the list of states having default data. The HELP model provides default precipitation values for the list of cities in Table 1. To select a state, move the cursor to the desired state name and press *Enter*. At this time the program prompts the user with the list of cities in the selected state for which default precipitation data is available. Similarly, the city can be selected by moving the cursor to the desired city and pressing *Enter*. The user can return to the "Precipitation, Temperature and Solar Radiation" screen from either list by pressing *Esc*. By doing so, neither a city nor a state is considered selected. However, once a city is selected, the program reads the five years of default precipitation data for the selected city. The usefulness of the default precipitation option is limited since it contains only five years of precipitation data. It is additionally limiting since these five years may be dry or wet years and may not be representative of the site in question.

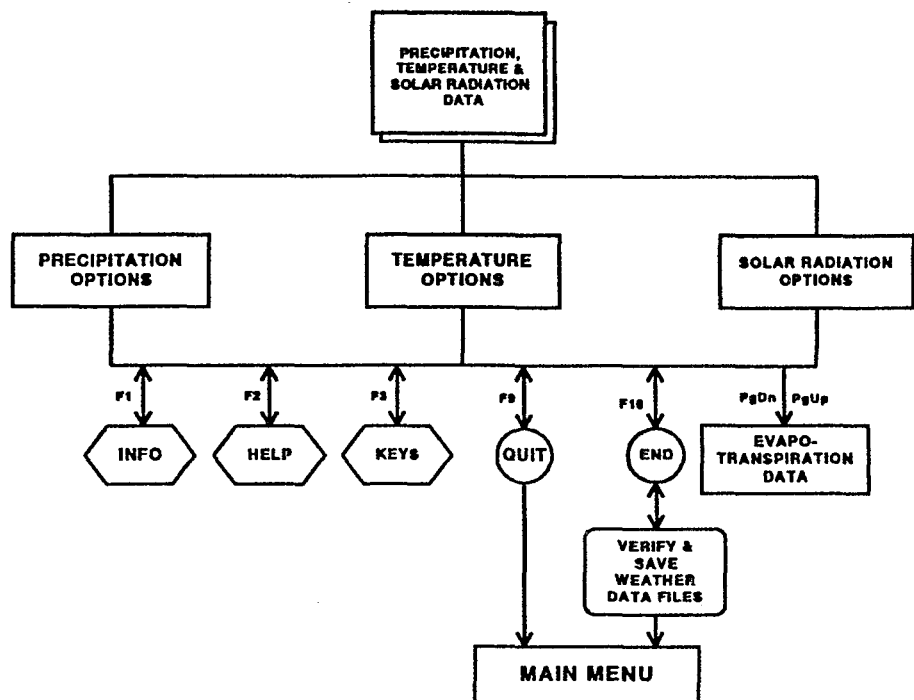


Figure 7. Schematic of "Precipitation, Temperature and Solar Radiation" Screen

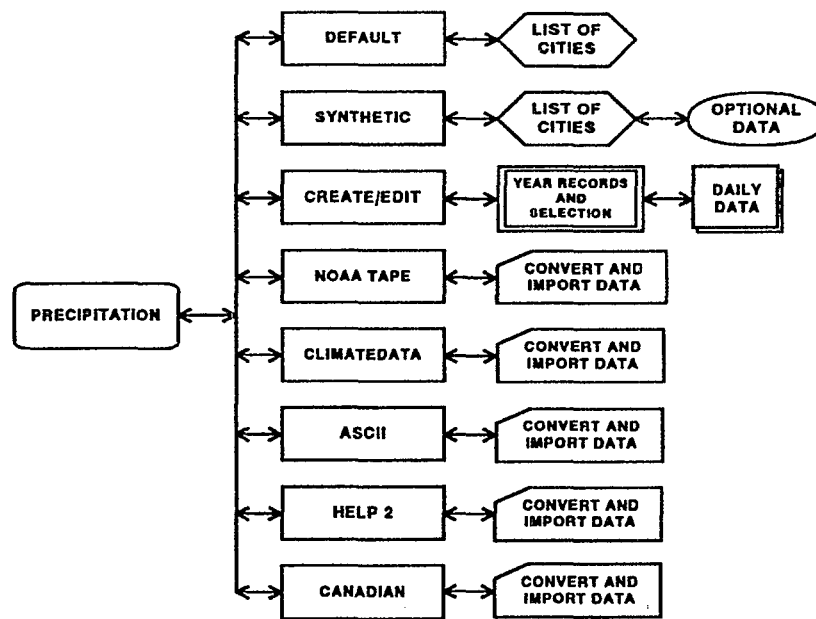


Figure 8. Precipitation Options

The following options are available for entering "Precipitation, Temperature, and Solar Radiation" data.

Synthetic

The second available method for entering precipitation data is to use the *synthetic weather generator (Customary or Metric Units)*. (This is the first method on the screen for entering temperature and solar radiation data.) This option can be selected for temperature and solar radiation only if the user has previously entered precipitation data since the synthetic weather generator requires precipitation values for generating both temperature and solar radiation. By selecting the synthetic data option, the program prompts the user with a list of states for which it has synthetic weather data coefficients. Again the user can move the cursor to the appropriate state and press *Enter* to obtain the list of cities in that state for which synthetic data can be generated. From this list, the user can select the city where the project is located or a city with a climate similar to the project location. Selection is accomplished by moving the cursor to the selection cell highlighting the desired city and pressing *Enter*. At any time, the user may abandon the input for the synthetic weather generator by pressing *Esc*; the program will return to the "Precipitation, Temperature and Solar Radiation" screen without loss of previously entered data.

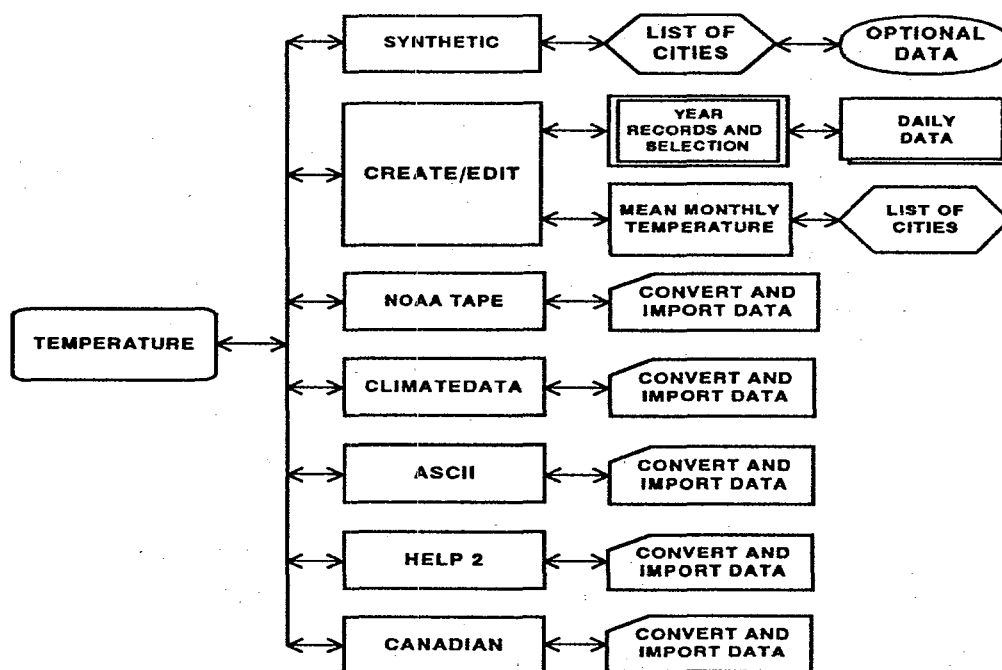


Figure 9. Temperature Options

Once a city is selected, the program displays another screen called "Synthetic Precipitation Data", "Synthetic Temperature Data" or "Synthetic Solar Radiation Data." On this screen, the city and state are displayed, and the user is asked to provide additional information. The first value that must be entered is the number of years of synthetic data to be generated. The rest of the information on the screen is optional. For precipitation, the user can elect to use the default normal mean monthly precipitation values provided by the HELP program or to enter normal mean monthly precipitation values to be used in generating the synthetic precipitation for that location. For temperature, the user has the option to use the default normal mean monthly temperature values provided by the HELP program or to enter normal mean monthly temperature values to be used in generating the synthetic temperature for that location. Users are encouraged to enter their own normal mean monthly values especially if the landfill is not located at the selected city. The program uses the normal mean monthly data to adjust the data generated by the synthetic weather generator. If the user decides not to use the default values, the program will transfer control to the normal mean monthly data option under the "User" heading. At this time the user must input values for January through December. A blank cell for a given month will be recorded as zero, and the user must be careful not to leave a cell without an entry. A zero entry, however, is a valid entry. For solar radiation the optional value is the latitude for the location. The default latitude of the selected city will be displayed, but the user is encouraged to enter the latitude of the actual landfill location to obtain better solar radiation values.

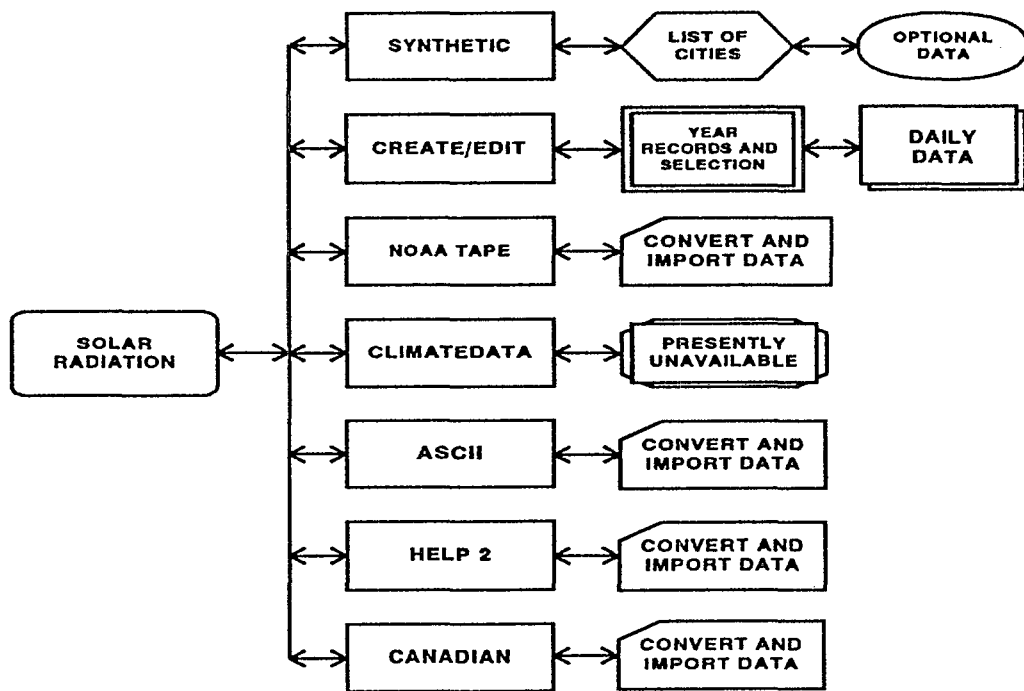


Figure 10. Solar Radiation Options

Create/Edit

If the user selects the *create/edit* option (*Customary or Metric Units*) for manually entering or editing precipitation, temperature and/or solar radiation data, the program prompts the user with a request to enter the city and state of the location and the units that will be used for entering the data manually. These requests appear on the same screen as "Precipitation, Temperature and Solar Radiation" screen and will be filled in with information when editing an existing data file. The user may press the *Esc* key to abandon the entry of this information and return to the selection of another weather data option. Once the location and units are specified, the program displays the yearly data screen.

Yearly Data Screen

This screen is like a spreadsheet that has four columns. Two of these columns are for the precipitation data, and one column each is for temperature and solar radiation. The first column is for the year for which the precipitation data is to be entered, and the second column is for total annual precipitation. The user cannot access the yearly total precipitation column since this total is computed by the program after the daily data for the year is entered. If the user reaches this screen from the precipitation option on the "Precipitation, Temperature, and Solar Radiation" screen, the user will only be able to move within the column under precipitation. Similarly, if the user reaches this screen from the temperature data option, then only movement in the temperature column is permitted, and analogously, for the solar radiation option.

To enter a new year of daily values, the user should move the cursor to a empty cell, type in the year and press *Enter*. The program will display the daily data screen on which the daily values are entered. The user can return to the yearly data screen by pressing *F10* to retain the data (to a temporary file) or by pressing *Esc* to abandon the created data.

The user can enter up to 100 years of daily data. The yearly data screen can only display 20 rows at a time. The user, however, can move the cursor to the bottom of the screen and then cursor down to move to the next row until the hundredth row is displayed. Similarly, the user can move the cursor upward to display the rows in the spreadsheet that are not shown on the screen, if any. To move down 20 rows, press *Page Down*, and to move up 20 rows, press *Page Up*. To reach the last row, press *End*, and to go to the first row press *Home*.

To edit an existing year of daily values, the user must first create and/or read weather data. If the data were previously saved, the user should specify the existing data file "Weather Data - File Editing" screen immediately after selecting the "Enter/Edit Weather Data" option from the main menu. The HELP model reads the data from the edit file and stores it in a temporary file. Upon entering the *create/edit* option, the

program displays the list of years for precipitation, the total annual precipitation for each year, and a list of years for the temperature and solar radiation data. To edit, move the cursor to the year that is to be edited and press *Enter*. The program will display the daily data screen and the user may type over any values that need to be edited. The operation of the yearly data spreadsheet and the daily data spreadsheet is the same when editing existing data or when creating new data.

After entering or editing years of daily weather data, the user can return to the "Precipitation, Temperature and Solar Radiation" screen to exercise other weather data options. To retain the newly created or edited years of daily weather data, the user should press *F10* from the yearly data screen; the program will then replace the existing temporary data file containing all of the years of data for that type of weather data. To lose the newly entered or edited daily data, the user should press *F9* or *Esc*; the program will retain the previously existing temporary data file containing the values of that type of weather data prior to entering the *create/edit* option.

Daily Data Screen

Upon selecting or specifying a year from the yearly data screen, the program displays the daily data screen, a spreadsheet for entering daily data. This spreadsheet consists of 10 columns and 37 rows. The spreadsheet contains information on the file name, the year, month, and day. This information is displayed at the top of the spreadsheet. The day and month are continuously updated as the user moves from one cell to another. The first day is considered January 1, and the last day is December 31. The spreadsheet is divided into two parts, the first part being rows 1 through 19, and the second part, rows 20 through 37. The user can move the cursor to the bottom of the screen and cursor down to move to the next row until the 37th row is displayed. Similarly, the user can move the cursor upward to display any rows in the spreadsheet that are not shown. To move from the upper to the lower portions of the spreadsheet and vice versa, press *Page Down* and *Page Up*, respectively. To reach the last cell in the spreadsheet, press *End*, and to return to the first cell, press *Home*.

The user should input values one day at a time without leaving empty cells between months. For example, the first month (January) will extend to the first cell (or column) in the fourth row. The values for the first day in February should start in column 2 of row 4; no empty cells are left between months. An empty cell is considered by the program to indicate a value of zero for that day. A zero is a valid entry. The program keeps track of leap years and adjusts the month and day at the top of the spreadsheet accordingly. Since there are 37 lines with each line containing 10 days of data, there will be empty cells at the end of line 37 in the spreadsheet. These cells are ignored by the program.

If the user decides to quit entering data in the daily spreadsheet and return to the yearly spreadsheet, the user should press the *Esc* key. By doing so, whatever data were

entered on the daily data sheet will be lost; the previously existing data will be retained. To exit the daily spreadsheet and retain the data entered on that sheet, the user should press **F10**. Note that the **F10** key will retain the data in a temporary file only and not in any previously selected file. A separate temporary file is maintained for each year of daily data.

Once the user returns to the yearly weather sheet, more years can be entered or edited, and the daily values for these years can be input on the daily sheet in the same manner described above. After exiting the precipitation spreadsheet by pressing **F10**, and upon returning to the yearly sheet, the annual total precipitation for that year is computed and displayed next to the year.

Editing Data on Yearly Data Screen

Besides selecting years for creating or editing daily data, the user has the options on the yearly data screen to select only a portion of a weather file for future use, to rearrange the years of data, to repeat the same year(s) of data for a longer simulation period or to insert years of data into an existing file. These options are performed using the functions to add (insert) a year above or below an existing year in the list of years, delete a year, move a year to a position above or below an existing year in the list of years, or copy a year to a position above or below an existing year in the list of years. The options are performed only on the type of data (precipitation, temperature or solar radiation) highlighted when the *create/edit* option was selected. This is done by using the following key combinations of functions:

- Alt A** adds/inserts a year (either new, being moved or being copied) above the highlighted year (where the cursor is positioned)
- Alt B** adds/inserts a year (either new, being moved or being copied) below the highlighted year (where the cursor is positioned)
- Alt D** deletes the highlighted year (where the cursor is positioned)
- Alt M** tags the highlighted year (where the cursor is positioned) to be moved to another location to be designated using the cursor and **Alt A** or **Alt B**
- Alt C** tags the highlighted year (where the cursor is positioned) to be copied to another location to be designated using the cursor and **Alt A** or **Alt B**

To add a new year directly above a certain year, for example above the year on line 29 (Line numbering is shown on the left edge of the screen.), the user should move the cursor to line 29, hold the **Alt** key down, and press **A**. The result of this action is

that a blank cell is inserted above line 29, and the program shifts the year on line 29 and all the years below it one line downward (i.e. year on line 29 moves to line 30, year on line 30 moves to line 31, etc.), and line 29 will be a blank line for the user to enter the value for the new year.

To add a year directly below a certain year, for example below the year on line 5, the user should move the cursor to line 5, hold the *Alt* key down, and press *B*. The result of this action is that a blank cell is inserted below line 5, and the program shifts the year on line 6 and all the years below it one line downward (i.e. year on line 6 moves to line 7, year on line 7 moves to line 8, etc.), and line 6 will be a blank cell for the user to enter the value of the new year.

The *Alt D* combination causes the program to delete a year from the list of years. For example, to delete the year on line 15, the user should move the cursor to line 15, hold the *Alt* key down, and press *D*. The program will delete information on line 15 and will shift the years on lines 16 to 100 upward one line (i.e., year on line 16 moves to line 15, year on line 17 moves to line 16, etc.), and cell on line 100 becomes an empty cell. The user is cautioned that the deleted year cannot be recovered without quitting and losing all changes (*F9* or *Esc*). The original temporary file is replaced only when the changes are finally retained by pressing *F10* from the yearly data screen.

The copy command allows the user to place a year that is identical to another year on another line. For example, to copy the year on line 70 to line 5, move the cursor to line 70 and press the *Alt C* combination, then move the cursor to line 5 and press the *Alt A* combination. At this point, the user must specify a value for the new year; the value must be different from the value of any other year in the data set for that type of weather data. This action will cause the new value for the year to appear on line 5 but the daily values will be the same as those found for the year copied and previously found in line 70. (The user may obtain the same result after the *Alt C* combination by moving to line 4 and pressing the combination *Alt B*).

The move command allows the user to move one year from one location on the yearly data screen to another. For example, to move the year on line 32 above the year on line 56, move the cursor to line 32, press the *Alt M* combination, and move the cursor to line 56 and press the *Alt A* combination. This action will cause the year on line 32 to be deleted and be placed directly above the year on line 56. (The user may obtain the same result after the *Alt M* combination by moving to line 55 and pressing the combination *Alt B*).

The *Esc* key can be used to quit the move and copy functions (after pressing *Alt M* or *Alt C* and before pressing *Alt A* or *Alt B*). By editing the data as discussed above, the user is actually arranging the order of the precipitation data of the years. Actual rearranging of data in the data file, however, takes place only after the user presses *F10*.

NOAA Tape Data

This option allows the user to enter data to the HELP model from a NOAA data set (*Customary Units Only*). If this option is selected, the user must enter the city and state for the site and the NOAA file name. For the precipitation and temperature options, the NOAA data file should contain daily Summary of Day data written in as-on-tape format. Note that for temperature data two file names are requested, one for the maximum temperature and the other for the minimum temperature. If the user has only a mean temperature data file, the mean temperature data file name should be entered for both maximum and minimum temperature data file names. For the solar radiation option the NOAA data file should contain hourly Surface Airways data written in as-on-tape format. Example NOAA data files are included with the HELP program -- PC49215A.PRN for precipitation, MX49215A.PRN for maximum temperature and MN49215A.PRN for minimum temperature. When entering the NOAA file name, the user should include the DOS path (if the file location is different than the default directory), file name and extension. The user can abandon the entry of this data by pressing *Esc*. Once valid information is entered, the program reads the data from the specified file and converts it to the HELP Version 3 format.

Climatedata™

This option allows the user to enter daily precipitation or temperature data to the HELP model from Climatedata™ (*Customary Units Only*). If this option is selected, the user must enter the city and state for the site and the Climatedata™ file name. Note that for temperature data, two file names are requested, one for the maximum temperature file and the other for the minimum temperature file. The Climatedata™ file should have been created by exporting or printing the CD-ROM data to an ASCII print file. This same format is used by data bases other than Climatedata™ and therefore these data bases can be converted using this same option. Example Climatedata™ files are included with the HELP program -- BIRM.PRC for precipitation, BIRM.MAX for maximum temperature and BIRM.MIN for minimum temperature. When entering the Climatedata™ file name, the user should include the DOS path (if the file location is different than the default directory), file name and extension. The user can abandon the entry of this data by pressing *Esc*. Once valid information is entered, the program reads the data from the specified file and converts it to the HELP Version 3 format.

ASCII Data

This option allows the user to enter daily weather data to the HELP model from ASCII data files (*Customary or Metric Units*). The ASCII data set is composed of lines of data whose values are separated by a blank(s), a comma or other non-numeric symbol. If this option is selected, the user must enter the city and state for the site, the units of the data in the ASCII files. The user can abandon the entry of this data by pressing *Esc*. Once valid information is entered, the program then asks for the file name and year of the ASCII data set, one year at a time. Each file should contain only one year of daily

values for a particular type of data, either precipitation, mean temperature or solar radiation. Example ASCII data files are included with the HELP program -- RAIN.1 and RAIN.2 for precipitation, TEMP.1 and TEMP.2 for temperature and SOLAR.1 and SOLAR.2 for solar radiation. When entering the ASCII data file name, the user should include the DOS path (if the file location is different than the default directory), file name and extension. In order to return from this option to the "Precipitation, Temperature, and Solar Radiation" screen, press *Esc*.

HELP 2

This option allows the user to enter weather data to the HELP model Version 3 from a data file used in the HELP model Version 2 (*Customary Units Only*). If this option is selected, the user must enter the city and state for the site and the HELP Version 2 data file name. Example HELP 2 data files are included with the HELP program -- ALA4 for precipitation, ALA7 for temperature and ALA13 for solar radiation. When entering the HELP 2 data file name, the user should include the DOS path (if the file location is different than the default directory), file name and extension. The user can abandon the entry of this data by pressing *Esc*. Once valid information is entered, the program reads the data from the specified file and converts it to the HELP Version 3 format.

Canadian

This option allows the user to enter weather data to the HELP model from a Canadian Climatological Data (Surface) file (*Metric Units Only*). If this option is selected, the user must enter the city and state for the site and the Canadian Climatological Data file name. The precipitation and mean temperature data files should contain daily values written in either compressed or uncompressed diskette format. The solar radiation data file should contain hourly global solar radiation values also written in either compressed or uncompressed diskette format. Example Canadian data files are included with the HELP program -- CAN4.DAT and CCAN4.DAT for precipitation, CAN7.DAT and CCAN7.DAT for temperature and CAN13.DAT and CCAN13.DAT for solar radiation. When entering the Canadian data file name, the user should include the DOS path (if the file location is different than the default directory), file name and extension. The user can abandon the entry of this data by pressing *Esc*. Once valid information is entered, the program reads the data from the specified file and converts it to the HELP Version 3 format.

4.5.4 Saving Weather Data

During the creation of the weather data explained above, the data are saved in temporary files. To save the data to permanent files, the user must press *F10* from the primary screens. Once the *F10* key is pressed, the program verifies that all the data have been entered. If any of the data is incomplete, the program displays a list of the problem areas. The user can return to the primary screens to complete the data or continue to

save the incomplete data. After displaying the deficiencies, the program displays the "Weather Data - File Saving" screen. Here the user may save all or only some of the four weather types, or completely abandon the save option. The user should tag each type of data to be saved by entering a "Y" in the "SAVE" column and those not to be saved by entering a "N" in the "SAVE" column. Default file names are displayed in appropriate locations on this screen; these are the same names as used in Version 2. At this time, the user may enter new file names for any or all of the four types of weather data. (See Section 4.5.1 for file naming convention used in HELP.) If the file already exists, the program will display "File Already Exists" after entering the name. After replacing all file names of interest, the user should press *F10* or *Page Down* to complete the saving to the requested file names. If files already exists for any of the file names as they would for the default names, the program will ask the user about overwriting each existing file. If the user answers "Y" for all of the files, the program will overwrite the files, complete the saving process and return to the main menu. If the user answers "N" for any file, the program will interrupt the saving, return to the "SAVE" column and change the tag to "N". The user can then change the tag back to "Y", rename the file, and restart the saving by pressing *F10* or *Page Down*. The program provides other options listed on the "File Saving" screen to enable the user to return the weather data entry screens (*Page Up*) or to return to the main menu without saving the data (*F9*). The user must be cautioned that the *F9* option will cause all the data created (if any) to be lost. Figure 11 shows the available options.

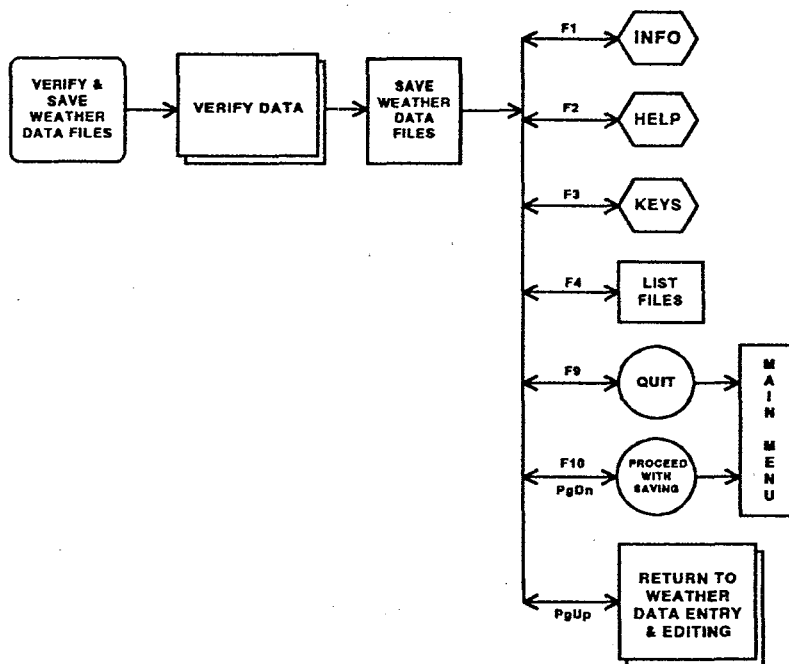


Figure 11. "Weather Data - File Saving" Screen Options

4.6 SOIL AND DESIGN DATA

This module is selected from the main menu by pressing 2, "*Enter/Edit Soil and Design.*" While in this module, the user will be able to enter site information, a landfill profile, layer design data, characteristics of soils, geomembranes and other materials, and SCS runoff curve number information. The primary screens in this module are the "Soil and Design Data - File Editing" screen, "Landfill General Information" screen, three Landfill Profile Design and Layer Data screens, "Runoff Curve Number Information" screen, "Verification and Saving" screen and "Soil and Design Data - File Saving" screen. Several secondary screens may appear during the session depending on the action taken by the user. On-line help screens are always available for display by pressing *F1* or *F2*. The individual primary screens and their secondary screens of this module are discussed below. Figure 12 shows a schematic of the soil and design data module.

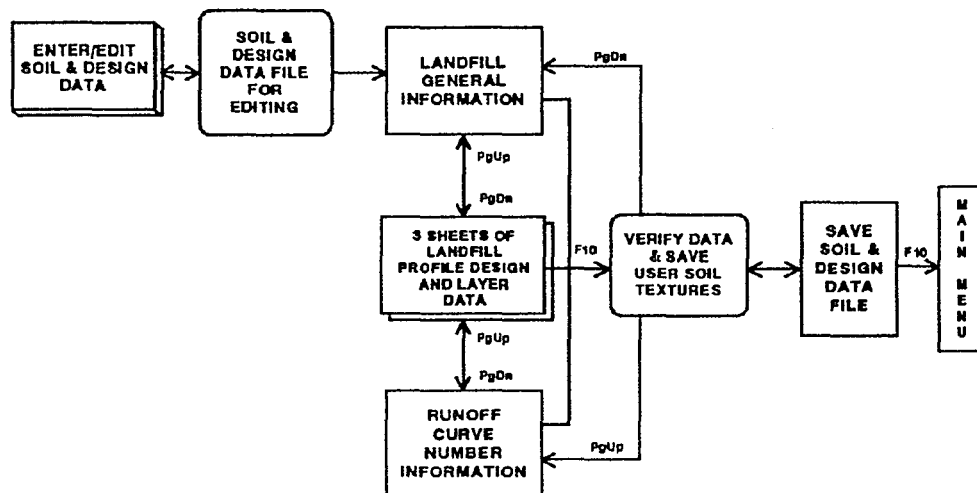


Figure 12. Schematic of Soil and Design Data Module

4.6.1 Soil and Design Data File Selection

The first screen in the soil and design module is the "Soil and Design Data - File Editing" screen. A schematic of this screen is shown in Figure 13. On this screen the user may enter the file name of an existing file to select a previously generated HELP Version 3 file for editing or leave the file name blank to create new data. When selecting a file to be edited, the user may specify the DOS path if different from the default drive and subdirectory, such as C:\HELP3\DATA. The default directory is initially displayed in the directory cell on the screen. If the user specifies a drive or a directory that does not exist, the program will display respectively "Invalid Drive" or

"Invalid Directory" and replaces the content with the default directory. The soil and design data file may have any valid DOS name of up to 8 characters. If the user enters an illegal file name, the program displays "Bad File Name" and clears the file name. If the user specifies a file name that does not exist, the program displays "File Not Found" and clears the file name. The program adds an extension of .D10 to the file name. As such, the user should not specify the extension in HELP Version 3 whenever entering a file name for editing or saving.

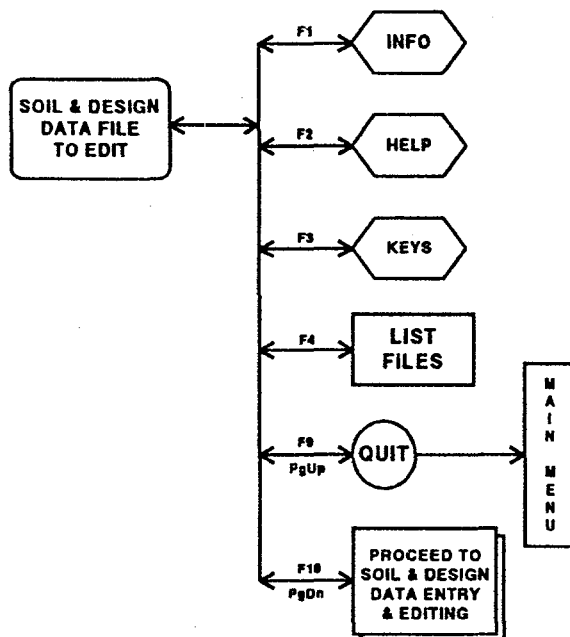


Figure 13. "Soil and Design Data - File Editing" Screen Options

As shown in Figure 13, the user may obtain a listing of all soil and design data files that reside on the directory currently specified in the directory cell by pressing **F4**. Up to 120 data files can be displayed on the screen. The name of the current directory where these files are located is also displayed. To change to another directory, the user should enter the name of that directory in the column labeled DIRECTORY. To select a file from the list of displayed files, move the cursor to the file and select it by pressing **Enter**. This transfers control back to the previous screen and the name of the file just selected will be displayed in the proper cell. The user can exit the list-of-files screen without selecting a file by pressing **F4** again or **Esc**.

When ready to proceed to enter new data or edit existing data, the user should press **Page Down** or **F10**. The program then reads the data file to be edited, if a file is specified, and proceeds to the "Landfill General Information" screen. If a new data set is to be created (file name left blank), the program initializes the soil and design data and

then asks for the system of units to be used throughout the module (*Customary or Metric*). Proper units are displayed throughout the module for entries that require units.

4.6.2 Landfill General Information

The second input screen in the soil and design data module is the "Landfill General Information" screen. Figure 14 shows the screen and its branches as a schematic. By moving the cursor to the appropriate cell, the user can enter new information or edit the information that was read from the edit file. The first entry is the *project title* which is only used for identification of the simulation.

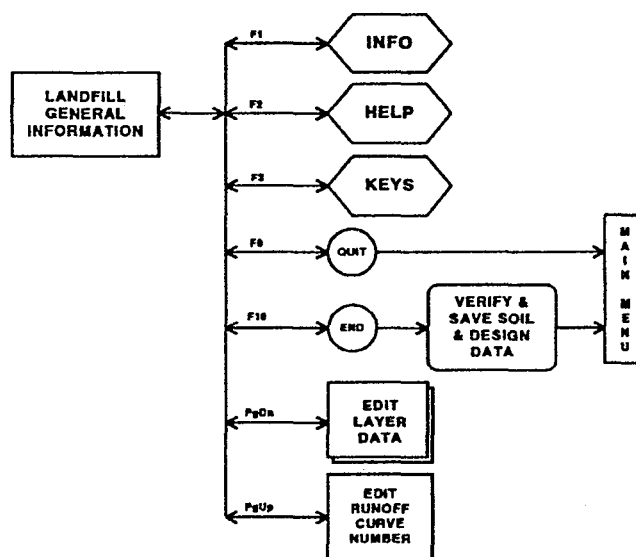


Figure 14. Schematic of "Landfill General Information" Screen

The second entry on this screen is the *landfill area*. The units of the area are displayed next to the input cell according to the system of units selected. The user should enter the area in acres for Customary units or in hectares for Metric units. The third entry is for the *percent of area where runoff is possible*. This variable specifies the portion of the area that is sloped in a manner that would permit drainage off the surface. The runoff estimates predicted by the model are equal to the computed runoff by the curve number method times this percent. The difference between the computed runoff and the actual runoff is added to the infiltration.

Next, the user must select the method of *moisture content initialization*; that is whether or not the user wishes to specify the initial moisture storage. If the user answers "N" (no) to this question, the program assumes near steady-state values and then runs

the first year of the simulation to improve the initialization to steady-state. The soil water contents at the end of this year of initialization are taken as the initial values for the simulation period. The program then runs the complete simulation, starting again at the beginning of the first year of weather data. The results for the initialization period are not reported. However, if the user answers "Y" (yes), the user is requested to enter the *amount of water or snow water on the surface* in the units selected. Later, the user should enter the initial moisture content of each layer as explained in the next section.

4.6.3 Landfill Layer Data

The next step in the soil and design data module is to input the design specifications of the landfill profile, one layer at a time. Layer data are entered in three screens. These screens have a spreadsheet layout where each row represents a layer. Figure 15 shows the three spreadsheets and their associated screens. The first row of cells on the screens is the uppermost layer in the landfill. Each column of cells on the screens represents a variable or a property of the layer or its material. Variable names are listed in the first two rows of the screen, and the third row contains the units of that variable, if any. Every highlighted cell is associated with a highlighted property (heading of a column) and a highlighted layer number (row label). The user should enter the value of the specified property for the corresponding layer. All entries must obey certain rules which are discussed below.

Layer Type

The user should input *layer type* in the first column of the spreadsheet. The four layer types and their associated code numbers that the program recognizes are vertical percolation (1), lateral drainage (2), barrier soil liner (3), and geomembrane liner (4). These are defined as follows:

1. A layer of moderate to high permeability material that drains vertically primarily as unsaturated flow is classified as a *vertical percolation layer* as long as it is not underlain by a liner with a lateral drainage collection and removal system. The primary purpose of a vertical percolation layer is to provide moisture storage; as such, top soil layers and waste layers are often vertical percolation layers.
2. A layer of moderate to high permeability material that is underlain by a liner with a lateral drainage collection and removal system is classified as a *lateral drainage layer*. The layer drains vertically primarily as unsaturated flow and laterally as a saturated flow.
3. A layer of low permeability soil designed to limit percolation/leakage is classified as a *barrier soil liner*. The layer drains only vertically as a saturated flow.

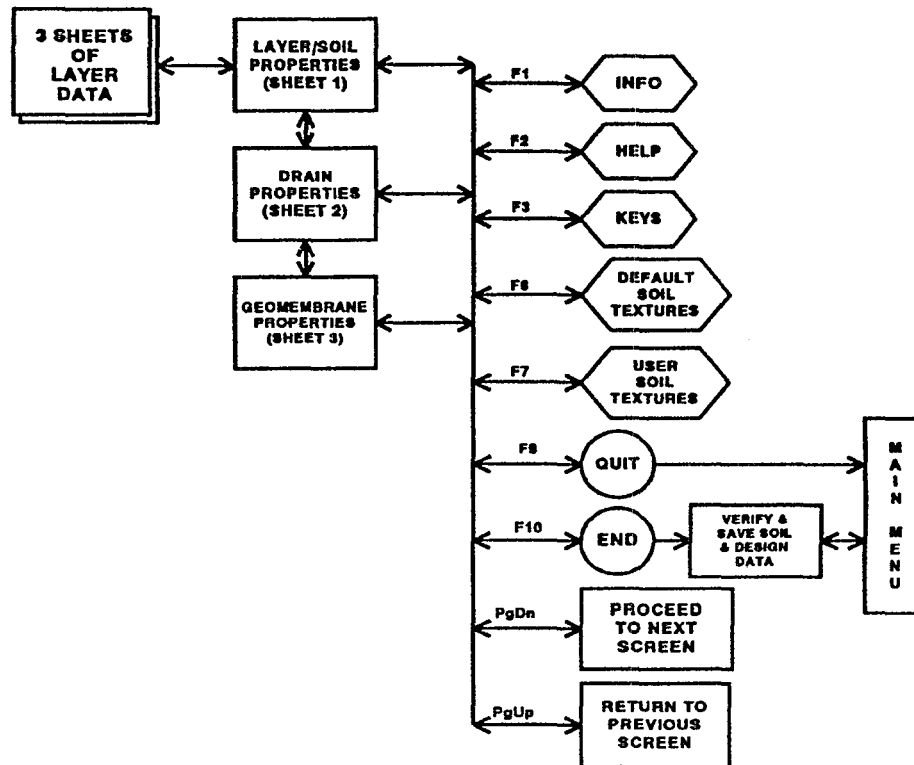


Figure 15. Schematic of Landfill Layer Data

4. A geomembrane (synthetic flexible membrane liner) designed to restrict vertical drainage and limit leakage is classified as a *geomembrane liner*. Leakage is modeled as vapor diffusion and leakage through small manufacturing defects and installation flaws.

While the HELP program is quite flexible, there are some basic rules regarding the arrangement of layers in the profile that must be followed.

1. A vertical percolation layer may not be underlying a lateral drainage layer.
2. A barrier soil liner may not be underlying another barrier soil liner.
3. A geomembrane liner may not be placed directly between two barrier soil liners.
4. A geomembrane liner may not be underlying another geomembrane liner.
5. A barrier soil liner may not be placed directly between two geomembrane liners.
6. When a barrier soil liner or a geomembrane liner is not placed directly below the lowest drainage layer, all drainage layers below the lowest liner are treated as

vertical percolation layers. Thus, no lateral drainage is computed for the bottom section of the landfill.

7. The top layer may not be a barrier soil liner.
8. The top layer may not be a geomembrane liner.
9. The profile can contain no more than a total of five barrier soil liners and geomembrane liners.

The program checks for rule violations only at the time the user saves the data. Therefore, to reduce the time involved in evaluating a landfill, the user is encouraged to design a proper layer sequence before saving the data.

In the second column, which has the heading "*Layer Thickness*," the user should enter the thickness of each layer in the landfill profile even for the geomembrane liner, in inches or cm. The values must be greater than zero; a blank cell is taken as a value of zero. Again, during data verification the program checks for layer thickness of zero and issues a violation statement when the user tries to save the data.

In the third column, the user should enter the *soil texture number* of the soil that forms the layer. The 4 possible options for the user to enter soil texture numbers are:

1. Select from a list of default textures for 42 soils, wastes, geomembranes, geosynthetics and other materials.
2. Select from a library of user-defined textures that were previously saved and numbered by the user (up to 100 such textures are allowed).
3. Enter a new soil texture number that can be used again in this design and that can later be saved in the library of user defined textures (material properties must also be entered manually for this texture).
4. Leave the texture number blank and enter the material properties manually.

Default Soil/Material Textures

Default soil/material textures have numbers from 1 to 42 and are listed in Table 4. The user can either type the soil texture number or press *F6* to select a texture from the list of default textures. If the user enters a default soil/material texture number manually, the program automatically assigns the default values for *porosity*, *field capacity*, *wilting point*, and *hydraulic conductivity* to the layer. On the other hand, the user may press *F6* to obtain the list of soil textures on a separate screen. On the soil texture screen, the user can move the cursor to the desired texture or press *Page Down* to display the rest of the default soil textures. After cursoring to the desired texture,

press *Enter* to select it. At this time, program control returns to layer spreadsheet screen and displays the selected soil texture number, along with the porosity, field capacity, wilting point, and hydraulic conductivity in appropriate cells. Notice that the only information available for the default geomembrane liners is the hydraulic conductivity (liner vapor diffusivity). If the user changes any of the four soil properties obtained for a default soil/material texture, the program automatically resets the soil texture number to 0. The user can then assign the values a new soil texture number that is not used in either the list of default or previously saved user defined textures if the user wishes to save the material characteristics for future use.

As mentioned above, default soil/material textures are obtained by pressing *F6* and are available on all three screens. To move from one screen of default soil/material textures to another the user should press *Page Up* or *Page Down*. To return to the layer spreadsheet without making a selection, press *Esc*. A selection is made only by moving the cursor to the desired soil texture and pressing *Enter*.

User-Defined Soil Texture

In Version 3 of the HELP model, the user has three options to specify material characteristics, in addition to selecting soil textures from the default list. One method is to enter all of the material characteristics manually without specifying a soil texture number. This method is used when the user does not wish to save these characteristics for use again in this simulation or future simulations. The second method, which allows the user to assign a new soil texture number to the manually entered values for the soil properties, is used when the same characteristics are to be used in future simulations and the characteristics are to be permanently saved in a library of user-defined textures. A library of up to 100 soil textures may be saved in a "user-defined soil texture" data file. The creation and addition of textures to this file are explained in Section 4.6.5 of this User's Guide. The third method is to select a user-defined texture that was previously saved in the library. If this library of user-defined soil textures exists, the user can display the list of available textures for selection by pressing *F7*. Selecting a user-defined soil texture for a given layer is identical to that of selecting a default soil/material textures; the user should move the cursor to the desired soil texture and press *Enter*. At this point, program control returns to the layer spreadsheet and displays soil texture values, porosity, field capacity, wilting point, and hydraulic conductivity of the selected soil in the layer (row) where *F7* was pressed. Also, in the same manner as in default soil/material textures, the user can simply type the number of the user-defined soil texture in "Soil Texture No." column of the first screen of the layer spreadsheets, and the program will automatically obtain the soil characteristics for that soil texture and place them in the proper location on the layer spreadsheet.

Whenever *F7* is pressed, control transfers to the user-defined soil textures. To move among pages of soil textures press *Page Up* and *Page Down*. To make a selection, press *Enter*, and to return to the layer spreadsheet without making a selection, press *Esc*.

The values entered for the moisture storage parameters in columns 4 through 7 of the first screen of layer spreadsheets are interrelated. In column 4 the *porosity* must be greater than zero but less than 1. In column 5 the *field capacity* must be between zero and 1 but must be smaller than the porosity. In column 6 the *wilting point* must be greater than zero but less than the field capacity. In column 7 the *initial moisture content* must be greater than or equal to the wilting point and less than or equal to the porosity. If the user had indicated on the "Landfill General Information" screen that the program should specify initial moisture content for the soil layers, the program will ignore all input in column 7. As such, the user does not need to enter data in this column. On the other hand, if the user had indicated that the user wishes to specify the initial moisture content, these values must be entered manually. An empty cell is interpreted as zero for initial moisture, violating the rules. If the layer is a liner, the program during execution automatically sets the initial water content equal to the porosity of the layer. The program will detect violations of these values and will report them to the user during verifications when the data is to be saved to a file.

The second screen of layer spreadsheets can be obtained by pressing *Page Down*. On this sheet the user will notice that the layer type is already appearing. In the first column of cells the *saturated hydraulic conductivity* must be specified in the appropriate units (cm/sec). If the soil texture selected was a default soil/material texture or a user-defined soil texture, the saturated hydraulic conductivity will be displayed in this column. Remember that changing the saturated hydraulic conductivity causes the soil texture number on the previous screen to revert to zero in the same manner as changing any of the other material characteristics (porosity, field capacity or wilting point).

Drainage Layer Design

Information on lateral drainage layer design must be entered manually for each lateral drainage layer directly above the liner regardless of the method used to enter soil textures. The required information is the drainage length, drainage layer slope, recirculation percentage and recirculation destination. These parameters are found in the second through fifth column of cells on the second spreadsheet screen of layer data. These columns are used only for the lateral drainage layers directly above the liner; data placed in rows for other layers will be ignored during execution. The second column of cells on this second screen of layer data is for entering the *maximum drainage length* of lateral drainage layers, which is the length of the horizontal projection of the flow path down the slope of a liner to the water/leachate collection system. This length must be greater than zero. In third column of cells the user should enter the *drain slope* in percent. This slope is the maximum gradient of the surface of the liner at the base of the lateral drainage layer; this is the slope along the flow path.

In Version 3, the HELP program allows *leachate/drainage recirculation* to be simulated. The amount of leachate/lateral drainage to be recirculated from a given layer should be entered as a percent of the layer's drainage in the fourth column of cells. The layer to which this leachate drainage should be recirculated should be entered on the

same row in the fifth column of cells. The value entered is the number of the layer receiving recirculation. Layer numbers are those numbers displayed on the left side of the screen. These numbers are 1 through 20 and refer to the order of the layers in the profile. The HELP model does not allow leachate recirculation to a liner.

Version 3 of the HELP model also allows the user to specify *subsurface inflow* into the landfill from a groundwater source. The amount of subsurface inflow into each layer should be entered in the last column of the second spreadsheet of layer data and is considered to be a steady flow rate into the landfill at the layer where the inflow value is entered. If subsurface inflow is specified for the bottom layer, the program will assume no leakage through the bottom of the landfill. For most landfills, the inflows will be zero and this column can be left blank.

After entering the necessary values in the second spreadsheet screen of layer data, the user should press *Page Down* to go to the third and last screen of layer data. Pressing *Page Up* will return to the first spreadsheet of layer data, allowing the user to edit the previously entered values. Again, on the third spreadsheet screen, the layer type of all layers in the profile are displayed to aid in positioning data on the screen.

Geomembrane Liner Design

All of the entries on third screen of layer data pertain to geomembrane liner properties such as *geomembrane liner pinhole density*, *geomembrane liner installation defect density*, *geomembrane liner placement quality*, and associated *geotextile transmissivity* (if present). Values must be entered for each geomembrane liner (layer type 4) in the profile. Guidance on estimating the pinhole and installation defect density as well as definitions for these parameters is provided in Section 3. The placement quality options are also described in Section 3 and are presented below. The geotextile transmissivity should be specified only when a placement quality of 6 is used.

In the third column of cells the user should input the geomembrane liner placement quality. The HELP program recognizes the following six types of placement quality.

1. Perfect contact
2. Excellent contact
3. Good field placement
4. Poor field placement
5. Bad contact -- worst case
6. Geotextile separating geomembrane liner and controlling soil layer

Typically, placement quality 6 would not be used with a geosynthetic clay liner (GCL) despite the presence of a geotextile since, upon wetting, the clay extrudes through the geotextile and provides intimate contact with the geomembrane.

After completing input for one layer, the user can go back to the first spreadsheet and enter information for other layers. *Page Up* and *Page Down* are used to move backward and forward between spreadsheets. The user may also input values on one spreadsheet completely filling it, and move on to the next spreadsheet filling in the information for the layers entered in the first spreadsheet and so on. No blank rows be left in the spreadsheet between layers; however, if the user does leave some blank lines, the program will not save these as layers.

Layer Editing

While entering or editing the properties of the layers in the landfill defined in the three spreadsheets of layer data, the user has the option to add a layer to the profile, delete a layer, move a layer to another location in the profile, or copy a layer to another location. When using these layer editing functions, the program operates simultaneously on all three screens of layer data. This is done by using the following key combinations:

Alt A adds/inserts a layer (either new, being moved or being copied) above the highlighted layer (where the cursor is positioned)

Alt B adds/inserts a layer (either new, being moved or being copied) below the highlighted layer (where the cursor is positioned)

Alt D deletes the highlighted layer (where the cursor is positioned)

Alt M tags the highlighted layer (where the cursor is positioned) to be moved to another location to be designated using the cursor and *Alt A* or *Alt B*

Alt C tags the highlighted layer (where the cursor is positioned) to be copied to another location to be designated using the cursor and *Alt A* or *Alt B*

To add a new layer directly above a certain layer, for example above the layer on line 6 (shown on the left edge of the screen), the user should move the cursor to line 6, hold the *Alt* key down, and press *A*. The result of this action is that a blank line is inserted above the layer that was at line 6, and the program shifts the layer on line 6 and all the layers below it one line downward (i.e. layer on line 6 moves to line 7, layer on line 7 moves to line 8, etc.), and line 6 will be a blank line for the user to enter the values for the new layer.

To add a layer right below a certain layer, for example below the layer on line 5, the user should move the cursor to line 5, hold the *Alt* key down, and press *B*. The

result of this action is that a blank line is inserted below line 5, and the program shifts the layer on line 6 and all the layers below it one line downward (i.e. layer on line 6 moves to line 7, layer on line 7 moves to line 8, etc.), and line 6 will be a blank cell for the user to enter the value of the new layer.

The *Alt D* combination causes the program to delete a layer from the list of layers. For example, to delete the layer on line 3, the user should move the cursor to line 3, hold the *Alt* key down and press *D*. The program will delete all information on line 3 and will shift the layers on lines 4 to 20 upward one line (i.e., layer on line 4 moves to line 3, layer on line 5 moves to line 4, etc.), and line 20 becomes a blank line. The user is cautioned that the deleted layer cannot be recovered without quitting and losing all changes (*F9* or *Esc*).

The copy command allows the user to place a layer that is identical to another layer on another line. For example, to copy the layer on line 7 to line 2, move the cursor to line 7 and press the *Alt C* combination, then move the cursor to line 2 and press the *Alt A* combination. This action will cause the program to insert a layer with values the same as those formerly found at line 7 above the layer formerly found at line 2. The layers formerly at and below line 2 will be moved downward one line. (The user may obtain the same result after the *Alt C* combination by moving to line 1 and pressing the combination *Alt B*).

The move command allows the user to move a layer from one row on the screens of layer data to another row. For example, to move the layer on line 3 above the layer on line 6, move the cursor to line 3, press the *Alt M* combination, and move the cursor to line 6 and press the *Alt A* combination. This action will cause the layer on line 3 to be deleted and be placed directly above the layer on line 6. This will cause line 4 to move up one line to line 3, line 5 to move to line 4 and line 3 to move to line 5; the other lines will be unchanged. (The user may obtain the same result after the *Alt M* combination by moving to line 5 and pressing the combination *Alt B*).

The *Esc* key can be used to quit the move and copy functions (after pressing *Alt M* or *Alt C* and before pressing *Alt A* or *Alt B*). By editing the data as discussed above, the user may arrange the order of the layers and run the model to test several possible configurations.

If the user has 20 lines completely filled with layers and then decides to add or copy a layer, the layer that is already in line 20 will disappear and cannot be recovered. Therefore, care must be taken not to add layers that will cause the loss of the layers at the bottom of the spreadsheet.

When all the layers of the profile are entered, press *Page Down* from the third layer spreadsheet to proceed with the rest of the soil and design data entry. Pressing *Page Up* from the first layer spreadsheet passes control to the "Landfill General Information" screen.

4.6.4 Runoff Curve Number

The "Runoff Curve Number Information" screen may be reached from the third layer spreadsheet by pressing *Page Down*, or from the "Landfill General Information" Screen by pressing *Page Up*. A schematic of the options associated with the "Runoff Curve Number Information" screen is shown in Figure 16. This screen is composed of three options that can be used to specify the runoff curve number. The first option is to use an *user-specified curve number* that the HELP model will use without modification. The second option is to request the HELP model to *modify a user-specified curve number* according to the surface slope and surface slope length. In the third option the user requests a *HELP model computed runoff curve number* based on surface slope, slope length, soil texture of the top layer in the landfill profile, and vegetation. To select one of these three options, the user should move the cursor to the desired option and press *Enter*. This action will cause the program to transfer control down to the box for the option selected. For each option, the user must input all required information. Although the user can move from one box to the other (use *Tab* and *Shift Tab* keys), care should be taken to insure that the desired method is the one that will be used by HELP. The HELP model uses that option in which data was last entered; this option is marked by a small arrow in front of the option.

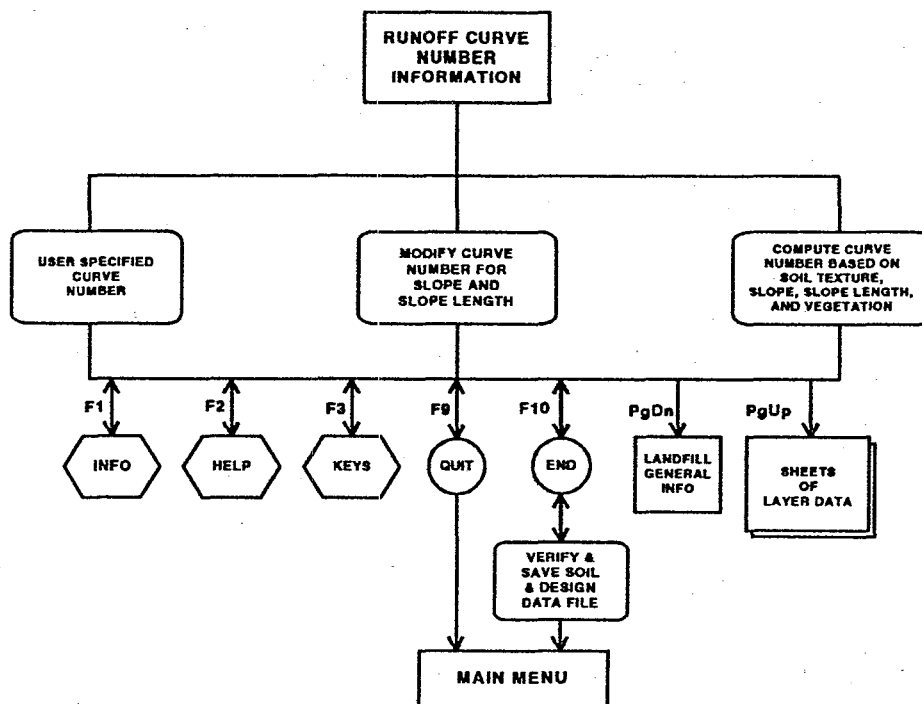


Figure 16. Schematic of "Runoff Curve Number Information" Screen Options

The user should refer to the HELP model documentation for Version 3 for the techniques used in the computation of the curve number based on slope and slope length. The value of the slope must be input in percent, and slope length must be input in the units indicated. If the top layer in the landfill is obtained from the default soil/material textures, the soil texture number for that layer will be displayed in the appropriate cell on the screen. The user can solicit help on the *vegetation cover* by pressing the *F2* key. The only valid entries for the vegetation are 1 through 5, according to the following:

1. Bare ground
2. Poor stand of grass
3. Fair stand of grass
4. Good stand of grass
5. Excellent stand of grass

If the user selects the option that requires the HELP model to compute the curve number, the program first calculates the SCS runoff curve number for landfills with mild surface slopes (2 to 5 percent) based on the vegetation type and the soil texture on the top layer if one of the default soil/material textures is selected (soil texture types 1 through 18, 20 and 22 through 29) in the same manner as Version 2 (Schroeder et al., 1988b). HELP Version 3 then adjusts the SCS runoff curve number based on the surface slope and the length of the slope.

4.6.5 Verifying and Saving Soil and Design Data

Pressing *F10* anywhere in the soil and design option transfers control to the "Verification and Saving" screen. This screen provides the user with several options: verify landfill general design data, verify soil layer/geomembrane properties, verify layer arrangement, review/save user-defined soil textures, and save soil and design data. The user can select any of these options by moving the cursor to the option and pressing *Enter*. Figure 17 shows the verify and save soil and design data options.

The user can verify the data before attempting to save the data by exercising the first three options on the "Verification and Saving" screen. These options are available mainly for the convenience of the new user since experienced users will be familiar with data requirements and the data will always be verified before saving. To check the data entered on the general landfill and runoff information screens, the user should select the first option, "Verify Landfill General Information Design Data." If there are no violations or warnings, the program will write "OK" to the right of the option; otherwise the program will list the problems and then write "BAD" to the right of the option.

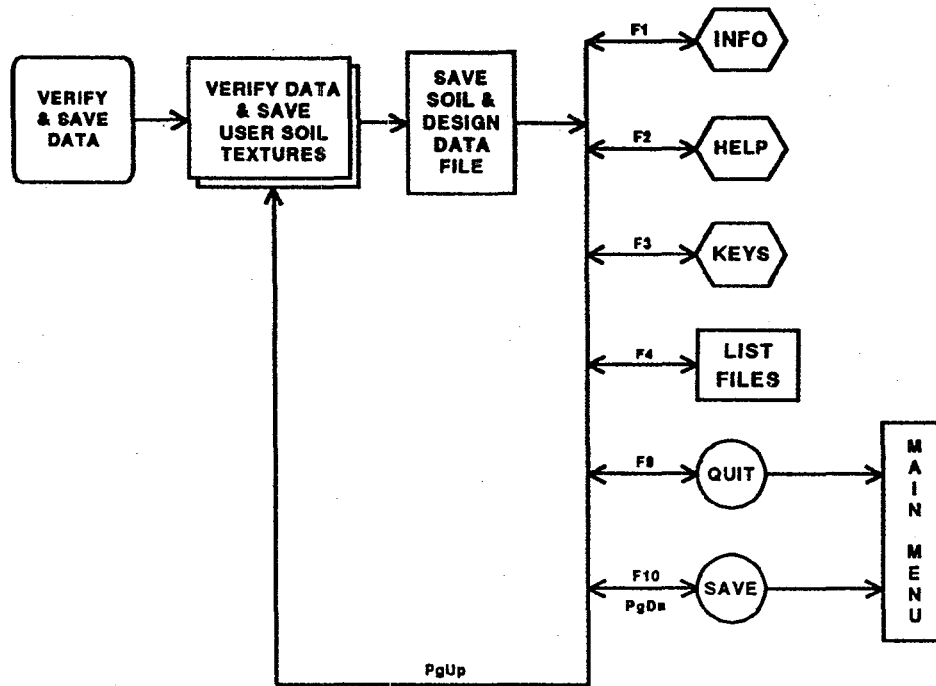


Figure 17. Verify and Save Soil and Design Data Options

The user can check the layer descriptions (the values on a row of the third screens of layer data) by selecting the "Verify Soil Layer/Geomembrane Properties" option. The program will examine each row for completeness for the type of layer described; for example, the program will insure that a placement quality was entered for all geomembrane liners (layer type 4). It will also check for the appropriateness of the values; for example, it will insure that the porosity is greater than the field capacity. If there are no violations or warnings, the program will write "OK" to the right of the option; otherwise the program will list the problems and then write "BAD" to the right of the option. Similarly, the user can check for violations in the ordering of the layers from top to bottom based on the layer types specified by selecting the "Verify Layer Arrangement" option. This option will check the nine rules for ordering of layers; for example, the program will insure that the top layer is not a liner. This option operates in the same manner as the verification options.

Another available option on this screen is to review the user defined soil textures that were used in the landfill profile for inclusion in or deletion from the library of user defined soil textures. Upon selecting this option, the program lists all of the non-zero user-defined soil textures used in the profile and allows the user to enter or edit a name to describe the material in the user soil library. Then after entering the names or labels, the user should tag all of the soil textures to be included in the library with a "Y" in the column of cells under the "SAVE" heading. Similarly, the user should tag all of the soil

textures to be deleted from or not included in the library with a "N" in the column of cells under the "SAVE" heading. To complete the additions and deletions to the library, the user should press *F10*; to cancel the additions and deletions and return to the "Verification and Saving" screen, the user should press *Esc* or *F9*.

If the user selects the "Save Soil and Design Data" option, the program automatically checks for possible violation of rules or errors in the soil and design data. This checking encompasses verification of presence, arrangement and values entered for the general landfill information, the landfill profile and layer data, and the runoff curve number information. The program scans through the three landfill profile spreadsheets of layer data one layer at a time and reports the errors as they are encountered. If any violations or inconsistencies are found, the program displays them on multiple screens. The user should press *Enter* or *Page Down* to proceed through the screens and reach the "File Saving" screen where the data can be saved in a file. If the user wishes to return to "Verification and Saving" screen, press *Esc*.

Upon reaching the "File Saving" screen, the user can return to the verification and input screens to correct violations by editing the data. To return, press *Page Up* successively until the desired screen is reached. On the other hand, the user can still save the data now and make corrections at a later time if there were violations. However, it should not be expected that the HELP model will provide meaningful answers for such data.

Soil and design data are saved in a file specified on the "Soil and Design Data - File Saving" screen. The program displays the default file name, DATA10, for saving in the default directory. DATA10 is the same name for the soil and design data as used in Version 2 except that Version 3 adds an extension of .D10 to the specified soil and design data file name. To save the data, the user should enter "Y" in the "Save" column. Then, the user should specify the directory in which to save the file. If the directory cannot be found, the program responds "Invalid Directory" and replaces it with the default directory. After the directory, the user should enter the file name (no extension or period). If the file already exists, the program will display "File Already Exists." After entering the file name, the user should press *F10* or *Page Down* to complete the saving to the requested file name. If the file already exists as the default file would, the program will ask whether the user wishes to have the existing file overwritten. If the user answers "Y", the program will overwrite the file, complete the saving process and return to the main menu. If the user answers "N", the program will interrupt the saving, return to the "SAVE" column and change the tag to "N". The user can then change the tag back to "Y", rename the file, and restart the saving by pressing *F10* or *Page Down*. The program provides other options listed on the "File Saving" screen to provide the means for the user to display a directory of existing soil and design data files (*F4*), to return to the data entry screens (*Page Up*) or to return to the main menu without saving the data (*F9*). The user must be cautioned that the *F9* option will cause all the data created (if any) to be lost. Figure 17 shows the available options.

4.7 EXECUTING THE SIMULATION

Option 3 on the main menu is "Execute Simulation". This option is composed of two primary screens: "Execution Files - File Management" screen and "Output Selection" screen and is shown schematically in Figure 18.

Execution Files

This screen is used to define the weather and soil and design data files that contain the data to be used in the HELP model simulation. Six files must be specified to run HELP model. The input data files required are a precipitation data file, a temperature data file, a solar radiation data file, an evapotranspiration data file, and a soil and design data file; and for output, the HELP model requires one file on which the results are to be written.

The user must enter the file names without extension since the HELP model recognizes the following extensions for the various types of files:

- .D4 for precipitation data
- .D7 for temperature data
- .D11 for evapotranspiration data
- .D13 for solar radiation data
- .D10 for soil and design data
- .OUT for the output

When the program initially displays the "Execution Files - File Management" screen, the program lists the default directory name in each cell in the directory column and the file names of each type of data that were used in the last simulation. The user should enter the directory, if different than the default directory, for each type of file. If an invalid directory is entered, the program displays the message "Invalid Directory" and replaces the directory with the default directory. If user enters a file name that could not be found on the specified directory, then the program displays the message "File Not Found" and erases the file name.

As shown in Figure 18, the user may obtain a list of all files that reside on the current directory by pressing *F4*. When the user presses *F4*, the program obtains a directory of all files that pertain to the type of file at the cell where *F4* was pressed. For example, if *F4* was pressed from the temperature file cell, the program will display the list of files with extension D7 that reside on the current directory displayed in temperature file row. Up to 120 data files for any file type can be displayed on a

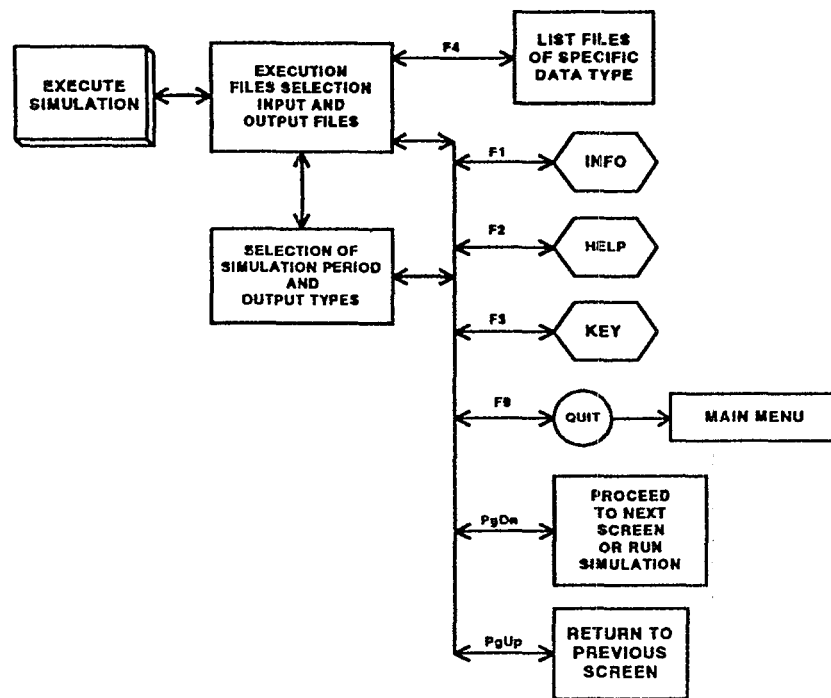


Figure 18. Schematic of "Execute Simulation" Option

separate screen. The name of the current directory where these files are located is also displayed. The user can obtain the list of data files with the same extension that are available in another valid directory by entering the name of that directory in the column labeled DIRECTORY and on the same row as the file type of interest.

To select a file from the list of displayed files, move the cursor to the file and select it by pressing *Enter*. This transfers control back to the previous screen and the name of the file just selected will be displayed in the proper cell. The user can exit the list-of-files screen without selecting a file by pressing the *Esc* key.

Once file names have been selected, the user can proceed to the next screen of the execution module by pressing *Page Down* or *F10*. If the output file already exists, the user is prompted with a warning indicating that this file already exists. The program then asks whether the file should be overwritten. If the user answers "N", the program moves the cursor to the output file name cell so that the user can enter a new file name. If the user answers "Y", the program proceeds to the "Output Selection" screen. Before displaying the next screen, the program reads the weather data files to determine the maximum allowable simulation period.

Output Selection

On this screen, the user selects the units of the HELP model output, the number of

years to simulate, and the output frequency. The user may use a maximum of 100 years of simulation provided that weather data are available for that many years. If the weather data in the selected files have a different number of years, the HELP model allows the simulation period to be no larger than the minimum number of years available in any of the daily weather data files. If the simulation period selected is smaller than the maximum allowable period, the program will use the years of weather data starting at the top of the files.

The rest of the information available on this screen is for selecting the type of optional output desired (daily, monthly or annual). The user may select any, all or none of the available options. The program will always write the summary output to the output file as well as a description of the input data. In order to select additional or different output frequencies, move the cursor to the desired output frequency and type "Y". Once all execution files and output frequency data are selected, the user should press *Page Down* or *F10* to start the simulation. To move back to the "Execution Files" screen, press *Page Up*.

4.8 VIEWING RESULTS

Option 4 on the main menu is to view the results of execution. This option is used to browse through the output file before printing. Figure 19 is a schematic of this option. The program displays the "View Results" screen. The user should enter the desired directory and file name. The file name can be selected from a list of files by pressing *F4*. After selecting the file, press *Page Down* or *F10* to display the selected file. The viewing function uses the LIST program written by Vernon D. Büerg and instructions on its use are available on screen by typing ? or *F1*. To display other types of files, first enter the extension of the file of interest, then the directory and the file name. To return to the main menu, press *Page Down* or *F10*.

4.9 PRINTING RESULTS

Option 5 on the main menu is used to print the output file. Figure 20 is a schematic of this option. The program displays the "Print Results" screen. The user should enter the desired directory and file name. The file name can be selected from a list of files by pressing *F4*. After selecting the file, press *Page Down* or *F10* to print the selected file. The print function uses the DOS PRINT command and instructions on its use are available in a DOS manual. The output file is 80 characters wide for all output options except daily output, which can be up to 132 characters wide. When printing output with daily results, it may be necessary to select a compressed font on your printer before printing to avoid wrapping or loss of output.

To print other types of files, first enter the extension of the file of interest, then the directory and the file name. To return to the main menu, press *Page Down* or *F10*.

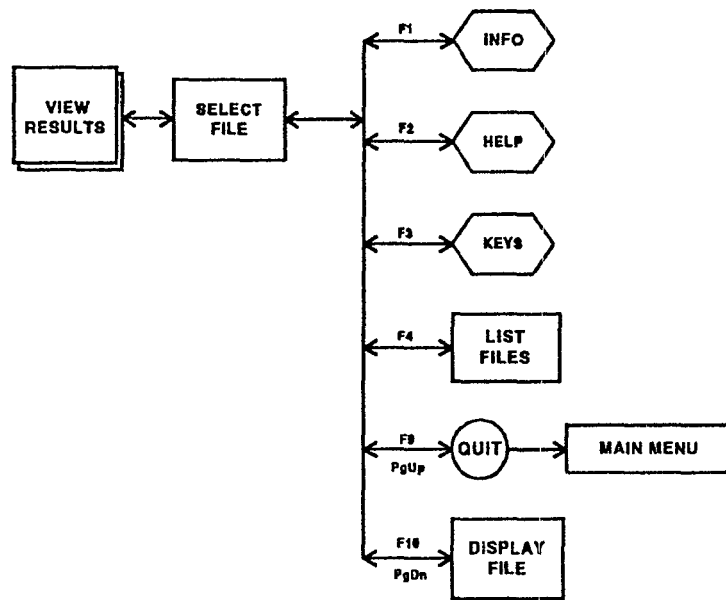


Figure 19. Schematic of "View Results" Option

Alternatively, the output file or any data file, which are ASCII text files, could be imported into other software such as word processors and printed in the format desired. Similarly, the output, in total or part, can be printed within the Viewing Option using the LIST program and blocking sections to be printed.

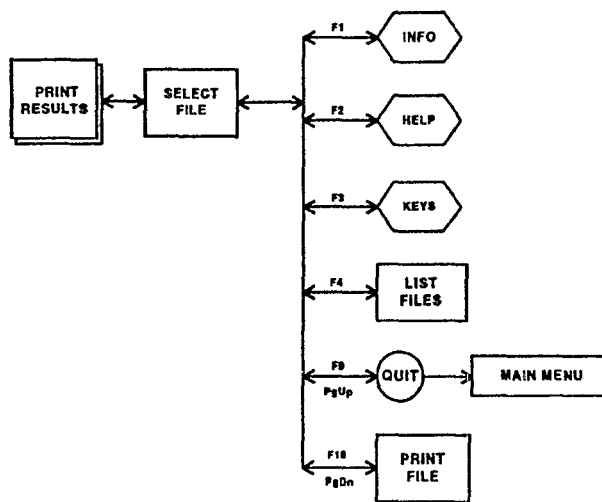


Figure 20. Schematic of "Print Results" Option

4.10 DISPLAYING GUIDANCE

On-line help is provided throughout the program. However, option 6 on the main menu gives an overview of the HELP program, as well as, general criteria for landfill design and guidance on using the model. Most of this user guide is displayed in this option and the guidance refers to figures and tables in this guide. In addition, the on-line guidance uses the same section numbering as this guide.

4.11 QUITTING HELP

Option 7 on the main menu is to quit the HELP program and return to DOS.

REFERENCES

- Arnold, J. G., Williams, J. R., Nicks, A. D., and Sammons, N. B. (1989). "SWRRB, A basin scale simulation model for soil and water resources management," Texas A&M University Press, College Station, TX. 142 pp.
- Breazeale, E., and McGeorge, W. T. (1949). "A new technic for determining wilting percentage of soil," *Soil Science* 68, 371-374.
- Brooks, R. H., and Corey, A. T. (1964). "Hydraulic properties of porous media," *Hydrology Papers* (3), Colorado State University, Fort Collins, CO. 27 pp.
- England, C. B. (1970). "Land capability: A hydrologic response unit in agricultural watersheds," ARS 41-172, USDA Agricultural Research Service. 12 pp.
- Harpur, W. A., Wilson-Fahmy, R. F., and Koerner, R. M. (1993). "Evaluation of the contact between geosynthetic clay liners and geomembranes in terms of transmissivity," *Proceedings of GRI Seminar on Geosynthetic Liner Systems*, Geosynthetic Research Institute, Drexel University, Philadelphia, PA. 143-154.
- Knisel, W. J., Jr., Editor. (1980). "CREAMS, A field scale model for chemicals, runoff, and erosion from agricultural management systems, volumes I, II and III." USDA-SEA, Conservation Research Report 26. 643 pp.
- Lutton, R. J., Regan, G. L., and Jones, L. W. (1979). "Design and construction of covers for soil waste landfills," EPA-600/2-79-165, US Environmental Protection Agency, Cincinnati, OH. 249 pp.
- National Oceanic and Atmospheric Administration. (1974). *Climatic atlas of the United States*. US Department of Commerce, Environmental Science Services Administration, National Climatic Center, Asheville, NC. 80 pp.
- Perrier, E. R., and Gibson, A. C. (1980). "Hydrologic simulation on solid waste disposal sites," EPA-SW-868, US Environmental Protection Agency, Cincinnati, OH. 111 pp.
- Rawls, W. J., Brakensiek, D. L., and Saxton, K. E. (1982). "Estimation of soil water properties," *Transactions of the American Society of Agricultural Engineers* 25(5), 1316-1320.
- Richardson, C. W., and Wright, D. A. (1984). "WGEN: A model for generating daily weather variables," ARS-8, USDA Agricultural Research Service. 83 pp.

Ruffner, J. A. (1985). *Climates of the states, National Oceanic and Atmospheric Administration narrative summaries, tables, and maps for each state, volume 1 Alabama - New Mexico and volume 2 New York - Wyoming and territories.* Gale Research Company, Detroit, MI. 758 pp. and 1572 pp.

Schroeder, P. R., and Gibson, A. C. (1982). "Supporting documentation for the hydrologic simulation model for estimating percolation at solid waste disposal sites (HSSWDS)," Draft Report, US Environmental Protection Agency, Cincinnati, OH. 153 pp.

Schroeder, P. R., Gibson, A. C., and Smolen, M. D. (1984). "The hydrologic evaluation of landfill performance (HELP) model, volume II, documentation for version 1," EPA/530-SW-84-010, US Environmental Protection Agency, Cincinnati, OH. 256 pp.

Schroeder, P. R., Peyton, R. L., McEnroe, B. M., and Sjostrom, J. W. (1988). "The hydrologic evaluation of landfill performance (HELP) model: Volume III. User's guide for version 2," Internal Working Document EL-92-1, Report 1, US Army Engineer Waterways Experiment Station, Vicksburg, MS. 87 pp.

Schroeder, P. R., McEnroe, B. M., Peyton, R. L., and Sjostrom, J. W. (1988). "The hydrologic evaluation of landfill performance (HELP) model: Volume IV. Documentation for version 2," Internal Working Document EL-92-1, Report 2, US Army Engineer Waterways Experiment Station, Vicksburg, MS. 72 pp.

Schroeder, P. R., Dozier, T. S., Zappi, P. A., McEnroe, B. M., Sjostrom, J.W., and Peyton, R.L. (1994). "The hydrologic evaluation of landfill performance (HELP) model: Engineering documentation for version 3," EPA/600/8-94/xxx, US Environmental Protection Agency, Cincinnati, OH. 105 pp.

USDA, Soil Conservation Service. (1985). "Chapter 9, hydrologic soil-cover complexes." *National engineering handbook, section 4, hydrology.* US Government Printing Office, Washington, D.C. 11 pp.

BIBLIOGRAPHY

- Darilek, G. T., Laine, D. L., and Parra, J. O. (1989). "The electrical leak location method geomembrane liners: Development and applications." *Geosynthetics '89 Conference Proceedings*. San Diego, CA, 456-466.
- Giroud, J. P., and Bonaparte, R. (1989). "Leakage through liners constructed with geomembranes -- part I. Geomembrane liners," *Geotextiles and Geomembranes* 8(1), 27-67.
- Giroud, J. P., and Bonaparte, R. (1989). "Leakage through liners constructed with geomembranes -- part II. Composite liners," *Geotextiles and Geomembranes* 8(2), 71-111.
- Giroud, J. P., Khatami, A., and Badu-Tweneboah, K. (1989). "Evaluation of the rate of leakage through composite liners," *Geotextiles and Geomembranes* 8(4), 337-340.
- McEnroe, B. M., and Schroeder, P. R. (1988). "Leachate collection in landfills: Steady case," *Journal of the Environmental Engineering Division* 114(5), 1052-1062.
- Oweis, I. S., Smith, D. A., Ellwood, R. B., and Greene, D. S. (1990). "Hydraulic characteristics of municipal refuse," *Journal of Geotechnical Engineering* 116(4), 539-553.
- US Environmental Protection Agency. (1985). "Covers for uncontrolled hazardous waste sites," EPA/540/2-85/002, Hazardous Waste Engineering Research Laboratory, Cincinnati, OH. 529 pp.
- US Environmental Protection Agency. (1988). "Guide to technical resources for the design of land disposal facilities," EPA/625/6-88/018, Risk Reduction Engineering Laboratory, Cincinnati, OH. 63 pp.
- US Environmental Protection Agency. (1989). "Technical guidance document: Final covers for hazardous waste landfills and surface impoundments," EPA/530-SW-89-047, Office of Solid Waste and Emergency Response, Washington, D.C. 39 pp.

APPENDIX A

CALCULATING SOIL, WASTE AND MATERIAL PROPERTIES

A.1 BACKGROUND

The HELP program requires values for the total porosity, field capacity, wilting point, and saturated hydraulic conductivity of each layer of soil, waste, or other material in a landfill profile. These values can be selected from a list of default materials provided by the HELP program (Table 4) or specified by the user. User-specified values can be measured, estimated, or calculated using empirical or semi-empirical methods presented in this appendix. Selecting the HELP values from default materials or calculating them based on empirical or semi-empirical techniques are not intended to replace laboratory or field generated data. Default and calculated values are suitable for planning purposes, parametric studies, and design comparisons, but are not recommended for accurate water balance predictions. The default and calculated values are for water retention and flow; therefore, leachate is assumed to behave the same as water. The effects of macropores resulting from poor construction practices, burrowing animals, desiccation cracks, etc. are not taken into account in the calculation of the properties or in the default values, but the saturated hydraulic conductivity of the surface soil described by the default values is modified for grassy vegetation.

A.2 EMPIRICAL METHOD

The empirical method for calculating HELP program user-defined values employs empirical equations reported by Brakensiek et al. (1984) and Springer and Lane (1987) to determine soil water retention parameters (field capacity and wilting point) and an empirical equation developed by Kozeny-Carman to determine saturated hydraulic conductivity. The total porosity and percent sand, silt, and clay of each layer is the minimum data required to calculate user-defined values using this method.

A.2.1 Total Porosity

Total porosity is a measure of the volume of void (water and air) space in the bulk volume of porous media. At 100 percent saturation, total porosity is equivalent to the volumetric water content of the media (volume of water per total volume of media) or

$$\text{Total Porosity} = \frac{\text{Water Volume}}{\text{Total Volume}} \quad (\text{A-1})$$

Total porosity can be calculated by developing a solid, liquid, and air phase relationship of each layer. This relationship can be calculated using the water content (on a weight basis) and density (wet or dry) of a sample. Introductory geotechnical engineering textbooks such as Holtz and Kovacs (1981) and Perloff and Baron (1976) provide detail guidance for determining phase relationships. Total porosity is also related to void ratio (ratio of void volume to solid volume) by the following equation:

$$\text{Total Porosity} = \frac{\text{Void Ratio}}{1 + \text{Void Ratio}} \quad (\text{A-2})$$

A.2.2 Soil-Water Retention

Field capacity is the volumetric water content of a soil or waste layer at a capillary pressure of 0.33 bars. Field capacity is also referred to as the volumetric water content of a soil remaining following a prolonged period of gravity drainage. Wilting point is the volumetric water content of a soil or waste layer at a capillary pressure of 15 bars. Wilting point is also referred to as the lowest volumetric water content that can be achieved by plant transpiration. The general relation among soil moisture retention parameters and soil texture class is shown below.

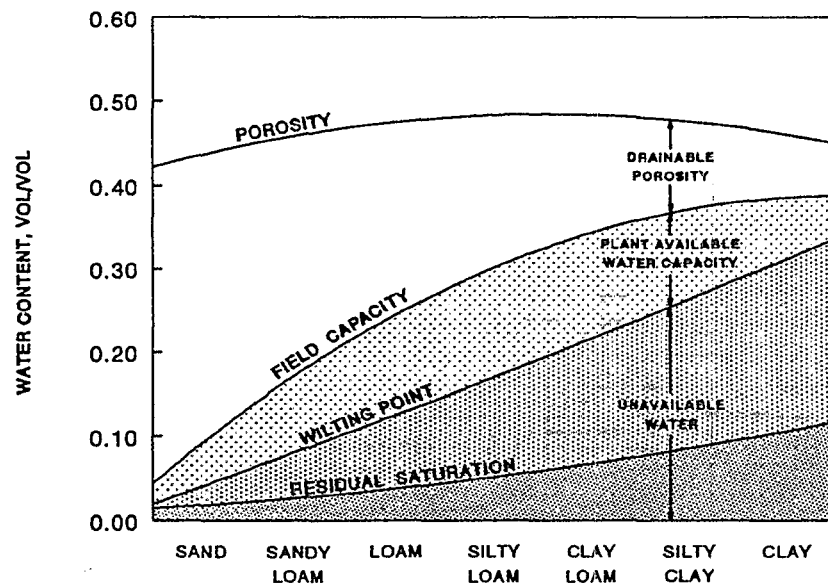


Figure A-21. General Relation Among Soil Moisture Retention Properties and Soil Texture Class

Brakensiek et al. (1984) and Springer and Lane (1987) reported the following empirical equations, which were developed using data from natural soils with a wide range of sand (5-70 percent) and clay (5-60 percent) content:

$$\text{Field Capacity} = 0.1535 - (0.0018)(\% \text{ Sand}) + (0.0039)(\% \text{ Clay}) + (0.1943)(\text{Total Porosity}) \quad (\text{A-3})$$

$$\text{Wilting Point} = 0.0370 - (0.0004)(\% \text{ Sand}) + (0.0044)(\% \text{ Clay}) + (0.0482)(\text{Total Porosity}) \quad (\text{A-4})$$

Sand and clay percentages should be determined using a grain size distribution chart and particle sizes defined by the U.S. Department of Agriculture textural soil classification system. According to this system, sand particles range in size from 0.05 mm to 2.0 mm, silt particles from 0.002 mm to 0.05 mm, and clay particles are less than 0.002 mm.

Numerous other equations relating field capacity and wilting point to soil textural properties have been developed. Most of these equations were developed using site-specific data. However, Gupta and Larson (1979) developed empirical equations for field capacity and wilting point using data from separate and mixed samples of dredged sediment and soil from 10 geographic locations in eastern and central United States. Rawls and Brakensiek (1982) and Rawls et al. (1982) also developed empirical equations by fitting the Brooks and Corey's (1964) soil water retention equation to soil water retention and matrix potential data from 500 natural soils in 18 states. Rawls' (1982) equations are not applicable to soils subjected to compactive efforts.

Williams et al. (1992) concluded that equations used to predict water contents based on texture and bulk density alone provided poorer estimates of water content, with large errors at some capillary pressures, in comparison with models that incorporate even one known value of water content. HELP users generally do not have adequate information to use models that require unsaturated water content information; therefore, Equations A-3 and A-4 are used to calculate the water retention of soil and waste layers.

A.2.3 Saturated Hydraulic Conductivity

Saturated hydraulic conductivity (sometimes referred to as the coefficient of permeability) is used as a constant in Darcy's law governing flow through porous media. Hydraulic conductivity is a function of media properties, such as the particle size, void ratio, composition, fabric and degree of saturation, and the kinematic viscosity of the fluid moving through the media. Saturated hydraulic conductivity is used to describe flow through porous media where the void spaces are filled with a wetting fluid (e.g. water). Permeability, unlike saturated hydraulic conductivity, is solely a function of

media properties. Henri Darcy's experiments resulted in the following equation for hydraulic conductivity (Freeze and Cherry, 1979):

$$K = \left(\frac{g}{\nu} \right) C d^2 \quad (\text{A-5})$$

where

K = hydraulic conductivity, cm/sec

g = acceleration due to gravity, 981 cm/sec²

ν = kinematic viscosity of water, 1.14 x 10⁻² cm²/sec at 15°C

C = proportionality constant, replaced in Equation A-6 by a function of the porosity

d = particle diameter, cm, approximated for nonuniform particles by Equation A-7

Darcy's proportionality constant is dependent on the shape and packing of the soil grains (Freeze and Cherry, 1979). Since porosity represents an integrated measure of the packing arrangement in a porous media, the following semi-empirical, uniform pore-size equation relating Darcy's proportionality constant and porosity was developed by Kozeny-Carman (Freeze and Cherry, 1979):

$$K_s = \left(\frac{g}{\nu} \right) \left[\frac{n^3}{(1-n)^2} \right] \left(\frac{d_g^2}{1.80 \times 10^4} \right) \quad (\text{A-6})$$

where

K_s = saturated hydraulic conductivity, cm/sec

g = acceleration due to gravity = 981 cm/sec²

ν = kinematic viscosity of water, 1.14 x 10⁻² cm²/sec at 15°C

n = total porosity

d_g = geometric mean soil particle diameter, mm, computed by Equation A-7

The original Kozeny equation was obtained from a theoretical derivation of Darcy's Law where the porous media was treated as a bundle of capillary tubes (Bear 1972). Carman introduced an empirical coefficient to Kozeny's equation to produce the semi-empirical Kozeny-Carman equation (Brutsaert 1967). The Kozeny-Carman's equation reported in Freeze and Cherry (1979) was altered to allow the mean particle size to be entered in millimeters.

Freeze and Cherry (1979) indicated that the particle diameter of a non-uniform soil can be described using a mean particle size diameter. Shirazi and Boersma (1984)

indicated that geometric rather than arithmetic statistical properties are advocated for describing soil samples. The reason, in part, is that there is a wide range of particle sizes in a natural soil sample making the geometric scale much more suitable than the arithmetic scale. Therefore, the mean particle diameter in Kozeny-Carman's equation reported in Freeze and Cherry (1979) was identified as the geometric mean soil particle diameter.

Shirazi et al. (1988) and Shiozawa and Campbell (1991) indicated that bimodal models describe particle grain size curves more accurately than unimodal models. However, analysis performed by Shiozawa and Campbell (1991) on six Washington state soils exhibiting varying sand, silt, and clay fractions indicated that the unimodal model accurately predicted the geometric mean soil particle diameter in all soils tested. Therefore, Shiozawa and Campbell (1991) developed an equation for geometric mean soil particle diameter by using the unimodal model developed by Shirazi and Boersma (1984); using geometric mean particles sizes based on the USDA classification system, as recommended by Shirazi, et al. (1988); and assuming that the soil was composed entirely of clay, silt, and sand. Shiozawa and Campbell's (1991) equation was altered to relate percent silt and clay to the particle diameter; resulting in the following equation:

$$d_g = \exp [-1.151 - 0.07713 (\% \text{ Clay}) - 0.03454 (\% \text{ Silt})] \quad (\text{A-7})$$

where

$$d_g = \text{geometric mean soil particle diameter, mm}$$

Percent silt and clay should be determined using a grain size distribution chart and grain sizes defined by the U.S. Department of Agriculture (USDA) textural soil classification system (see para A.2.2).

Kozeny-Carman's equation coupled with Shiozuwa and Campbell's equation for mean diameter was applied to soils data provided by Lane and Washburn (1946). These data included void ratio and grain size distribution curves for three soils composed of differing degrees of silt and sand. The saturated hydraulic conductivity predicted by Kozeny-Carman's equation was compared with laboratory data provided by Lane and Washburn (1946). This comparison indicated that Kozeny-Carman's saturated hydraulic conductivity equation coupled with Shiozuwa and Campbell's mean diameter equation can overpredict measured values by one to two orders of magnitude. Although conservative, these results reemphasize the fact that semi-empirical equations are not meant to replace laboratory or field measured data.

Numerous other empirical equations, with limited application, have been developed to estimate saturated hydraulic conductivity from the physical properties of soils. For example, Freeze and Cherry (1979), Holtz and Kovacs (1981), and Lambe and Whitman (1969) presented various forms of Allen Hazen's equation for determining the saturated hydraulic conductivity of silt, sand, and gravel soils. Rawls and Brakensiek (1985) also

presented an equation for determining the saturated hydraulic conductivity of soils with varying degrees of sand (5-70 percent) and clay (5-60 percent).

A.3 SEMI-EMPIRICAL METHOD

The semi-empirical method for determining the HELP program user-defined values employs a theoretical equation developed by Brooks and Corey (1964) to determine soil-water retention parameters (field capacity and wilting point) and a semi-empirical equation developed by Brutsaert (1967) and Rawls et al. (1982) to calculate saturated hydraulic conductivity. The total porosity, residual volumetric water content, pore-size distribution index, and bubbling pressure of each layer are the minimum data required to calculate the user-defined values for this method. As previously mentioned, total porosity can be calculated using Equation A-1 or A-2.

A.3.1 Soil-Water Retention

The HELP program does not allow the user to define the Brooks-Corey parameters (residual volumetric water content, pore-size distribution index, and bubbling pressure) of the soil, waste, or barrier layers; therefore, if these data are available, the user must first calculate field capacity and wilting point using Brooks and Corey's (1964) water retention equation:

$$\frac{\theta - \theta_r}{\phi - \theta_r} = \left(\frac{\psi_b}{\psi} \right)^\lambda \quad (\text{A-8})$$

where

θ = volumetric water content (field capacity or wilting point), unitless

θ_r = residual saturation volumetric water content, unitless

ϕ = total porosity, unitless

λ = pore-size distribution index, unitless

ψ = capillary pressure, bars (at field capacity, 0.33, or wilting point, 15.0)

ψ_b = bubbling pressure, bars

The volumetric water content in Equation A-8 is, by definition, equivalent to field capacity at a capillary pressure of 0.33 bar and is equivalent to wilting point at a capillary pressure of 15 bars. The HELP program will use the calculated field capacity and wilting point values to recalculate the Brooks-Corey parameters; however, because the program estimates the residual saturation water content from the wilting point before using Equation A-8 to calculate the other Brooks-Corey parameters, the program values will differ slightly from the laboratory data.

A.3.2 Saturated Hydraulic Conductivity

Brutsaert (1967) derived a saturated hydraulic conductivity relation by substituting Brooks-Corey's water retention equation into the Childs and Collis-George (1950) series-parallel coefficient of permeability integral. Rawls et al. (1982 and 1983) presented the following form of Brutsaert's (1967) equation:

$$K_s = a \frac{(\phi - \theta_r)^2}{(\psi_b)^2} \frac{\lambda^2}{(\lambda + 1)(\lambda + 2)} \quad (\text{A-9})$$

where

- K_s = saturated hydraulic conductivity, cm/sec
- a = constant representing the effects of various fluid constants and gravity, 21 cm³/sec
- ϕ = total porosity, unitless
- θ_r = residual volumetric water content, unitless
- ψ_b = bubbling pressure, cm
- λ = pore-size distribution index, unitless

Childs and Collis-George's (1950) series-parallel coefficient of permeability model assumes that the porous media is equivalent to a number of parallel portions each with a different hydraulic conductivity and each with uniform pore size. The hydraulic conductivity of each portion is obtained from the assumption of a bundle of capillary tubes parallel to the direction of flow. The media is fractured at a normal plane with two resulting faces, which are then rejoined after some random displacement (Brutsaert, 1967).

Rawls et al. (1982) fit Equation A-9 (using geometric mean values for Brooks-Corey parameters) to saturated hydraulic conductivity values from their data base and obtained a good correlation between these and predicted values. Rawls et al. (1982) and Rawls et al. (1983) subsequently recommended using an "a" constant of 21 cm/sec. However, Rawls et al. (1982) fit Equation A-9 to data presented by other researchers and obtained saturated hydraulic conductivities that overpredicted the data by three to four times. Although conservative, these results re-emphasize the fact that empirical equations are not meant to replace laboratory or field measured data.

A.4 VEGETATED, SATURATED HYDRAULIC CONDUCTIVITY

If the saturated hydraulic conductivity of a soil or waste layer is not selected from the HELP default data base, the program will not adjust the saturated hydraulic conductivity to account for root penetration by surface vegetation. Therefore, the user

must adjust the saturated hydraulic conductivity in the top half of the evaporative zone. The program adjusts the default values using the following equation developed by regressing changes in infiltration resulting from vegetation.

$$(K_s)_v = [1.0 + 0.5966 (LAI) + 0.132659 (LAI)^2 + 0.1123454 (LAI)^3 - 0.04777627 (LAI)^4 + 0.004325035 (LAI)^5] (K_s) \quad (A-10)$$

where

$(K_s)_v$ = vegetated saturated hydraulic conductivity in top half of evaporative zone, cm/sec

LAI = leaf area index, unitless

K_s = unvegetated saturated hydraulic conductivity in top half of evaporative zone, cm/sec

A.5 CONCLUSIONS

The HELP program user-defined values for total porosity, field capacity, wilting point, and saturated hydraulic conductivity can be conservatively calculated using empirical or semi-empirical methods presented in this appendix. Total porosity, percent sand, silt and clay, and particle diameter are the minimum data required to calculate user-defined values using the empirical method. Total porosity and Brooks-Corey parameters are the minimum data required for the semi-empirical method. Where available, comparisons with measured values re-emphasized the fact that neither of these methods is intended to replace laboratory or field generated data.

A.6 REFERENCES

- Bear, J. (1972). *Dynamics of fluids in porous media*. American Elsevier Publishing Company, New York. 764 pp.
- Brakensiek, D. L., Rawls, W. J., and Stephenson, G. R. (1984). "Modifying SCS hydrologic soil groups and curve numbers for rangeland soils." *Annual meeting of the American society of agricultural engineers, Pacific northwest region*. Kennewick, WA, USDA-ARS, Paper Number PNR-84-203. 13 pp.
- Brooks, R. H., and Corey, A. T. (1964). "Hydraulic properties of porous media," *Hydrology Papers* (3), Colorado State University, Fort Collins, CO. 27 pp.
- Brutsaert, W. (1967). "Some methods of calculating unsaturated permeability," *Transactions of the American Society of Agricultural Engineers* 10(3), 400-404.

Childs, E. C., and Collis-George, N. (1950). "The permeability of porous material," *Proceeding of the Royal Society* 201, Section A.

Freeze, R. A., and Cherry, J. A. (1979). *Groundwater*. Prentice-Hall, Englewood Cliffs, NJ. 604 pp.

Gupta, S. C., and Larson, W. E. (1979). "Estimating soil water retention characteristics from particle size distribution, organic matter percent, and bulk density," *Water Resources Research* 15(6), 1633-1635.

Holtz, R. D., and Kovacs, W. D. (1981). *An introduction to geotechnical engineering*. Prentice-Hall, Englewood Cliffs, NJ. 733 pp.

Lambe, T. W., and Whitman, R. V. (1969). *Soil mechanics*. John Wiley and Sons, New York. 553 pp.

Lane, K. S., and Washburn, D. E. (1946). "Capillary tests by capillarimeter and by soil filled tubes." *Proceedings of the twenty-sixth annual meeting of the Highway Research Board*, Washington, D.C., 460-473.

Perloff, W. H., and Baron, W. (1976). *Soil mechanics - principles and applications*. John Wiley and Sons, New York. 745 pp.

Rawls, W. J., and Brakensiek, D. L. (1982). "Estimating soil water retention from soil properties," *Journal of the Irrigation and Drainage Division* 108(IR2), 166-171.

Rawls, W. J., and Brakensiek, D. L. (1985). "Prediction of soil water properties for hydrologic modelling." *Proceedings of watershed management in the eighties*. B. Jones and T. J. Ward, ed., American Society of Civil Engineers, New York, 293-299.

Rawls, W. J., Brakensiek, D. L., and Saxton, K. E. (1982). "Estimation of soil water properties," *Transactions of the American Society of Agricultural Engineers* 25(5), 1316-1320.

Rawls, W. J., Brakensiek, D. L., and Soni, B. (1983). "Agricultural management effects on soil water processes - part I: Soil water retention and green and ampt infiltration parameters," *Transactions of the American Society of Agricultural Engineers* 26(6), 1747-1757.

Shiozawa, S., and Campbell, G. S. (1991). "On the calculation of mean particle diameter and standard deviation from sand, silt, and clay fractions," *Soil Science* 152(6), 427-431.

Shirazi, M. A., and Boersma, L. (1984). "A unifying quantitative analysis of soil texture," *Soil Science Society of America Journal* 48(1), 142-147.

Shirazi, M. A., Boersma, L., and Hart, J. W. (1988). "A unifying quantitative analysis of soil texture: Improvement of precision and extension of scale," *Soil Science Society of America Journal* 52(1), 181-190.

Springer, E. P., and Lane, L. J. (1987). "Hydrology-component parameter estimation." *Chapter 6, simulation of production and utilization of rangelands (SPUR) - documentation and user guide*. J. R. Wight and J. W. Skiles, eds, ARS-63, US Department of Agriculture, Agricultural Research Service. 372 pp.

Williams, R. D., Ahujam, L. R., and Naney, J. W. (1992). "Comparison of methods to estimate soil water characteristics from soil texture, bulk density, and limited data," *Soil Science* 153(3), 172-184.

ATTACHMENT 10



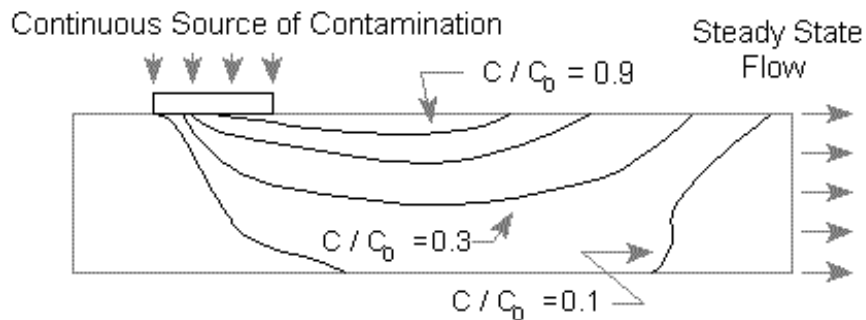
UNDERSTANDING VARIATION IN PARTITION COEFFICIENT, K_d , VALUES



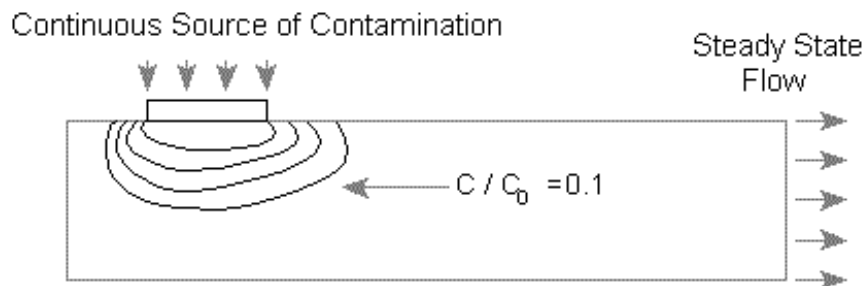
Volume I:

The K_d Model, Methods of Measurement, and Application of Chemical Reaction Codes

Case I: $K_d = 1$ ml/g



Case II: $K_d = 10$ ml/g



**UNDERSTANDING VARIATION IN
PARTITION COEFFICIENT, K_d , VALUES**

Volume I:

**The K_d Model, Methods of Measurement, and
Application of Chemical Reaction Codes**

August 1999

A Cooperative Effort By:

**Office of Radiation and Indoor Air
Office of Solid Waste and Emergency Response
U.S. Environmental Protection Agency
Washington, DC 20460**

**Office of Environmental Restoration
U.S. Department of Energy
Washington, DC 20585**

NOTICE

The following two-volume report is intended solely as guidance to EPA and other environmental professionals. This document does not constitute rulemaking by the Agency, and cannot be relied on to create a substantive or procedural right enforceable by any party in litigation with the United States. EPA may take action that is at variance with the information, policies, and procedures in this document and may change them at any time without public notice.

Reference herein to any specific commercial products, process, or service by trade name, trademark, manufacturer, or otherwise, does not necessarily constitute or imply its endorsement, recommendation, or favoring by the United States Government.

FOREWORD

Understanding the long-term behavior of contaminants in the subsurface is becoming increasingly more important as the nation addresses groundwater contamination. Groundwater contamination is a national concern as about 50 percent of the United States population receives its drinking water from groundwater. It is the goal of the Environmental Protection Agency (EPA) to prevent adverse effects to human health and the environment and to protect the environmental integrity of the nation's groundwater.

Once groundwater is contaminated, it is important to understand how the contaminant moves in the subsurface environment. Proper understanding of the contaminant fate and transport is necessary in order to characterize the risks associated with the contamination and to develop, when necessary, emergency or remedial action plans. The parameter known as the partition (or distribution) coefficient (K_d) is one of the most important parameters used in estimating the migration potential of contaminants present in aqueous solutions in contact with surface, subsurface and suspended solids.

This two-volume report describes: (1) the conceptualization, measurement, and use of the partition coefficient parameter; and (2) the geochemical aqueous solution and sorbent properties that are most important in controlling adsorption/retardation behavior of selected contaminants. Volume I of this document focuses on providing EPA and other environmental remediation professionals with a reasoned and documented discussion of the major issues related to the selection and measurement of the partition coefficient for a select group of contaminants. The selected contaminants investigated in this two-volume document include: chromium, cadmium, cesium, lead, plutonium, radon, strontium, thorium, tritium (^3H), and uranium. This two-volume report also addresses a void that has existed on this subject in both this Agency and in the user community.

It is important to note that soil scientists and geochemists knowledgeable of sorption processes in natural environments have long known that generic or default partition coefficient values found in the literature can result in significant errors when used to predict the absolute impacts of contaminant migration or site-remediation options. Accordingly, one of the major recommendations of this report is that for site-specific calculations, partition coefficient values measured at site-specific conditions are absolutely essential.

For those cases when the partition coefficient parameter is not or cannot be measured, Volume II of this document: (1) provides a "thumb-nail sketch" of the key geochemical processes affecting the sorption of the selected contaminants; (2) provides references to related key experimental and review articles for further reading; (3) identifies the important aqueous- and solid-phase parameters controlling the sorption of these contaminants in the subsurface environment under oxidizing conditions; and (4) identifies, when possible, minimum and maximum conservative partition coefficient values for each contaminant as a function of the key geochemical processes affecting their sorption.

This publication is the result of a cooperative effort between the EPA Office of Radiation and Indoor Air, Office of Solid Waste and Emergency Response, and the Department of Energy Office of Environmental Restoration (EM-40). In addition, this publication is produced as part of ORIA's long-term strategic plan to assist in the remediation of contaminated sites. It is published and made available to assist all environmental remediation professionals in the cleanup of groundwater sources all over the United States.

Stephen D. Page, Director
Office of Radiation and Indoor Air

ACKNOWLEDGMENTS

Ronald G. Wilhelm from ORIA's Center for Remediation Technology and Tools was the project lead and EPA Project Officer for this two-volume report. Paul Beam, Environmental Restoration Program (EM-40), was the project lead and sponsor for the Department of Energy (DOE). Project support was provided by both DOE/EM-40 and EPA's Office of Remedial and Emergency Response (OERR).

EPA/ORIA wishes to thank the following people for their assistance and technical review comments on various drafts of this report:

Patrick V. Brady, U.S. DOE, Sandia National Laboratories
David S. Brown, U.S. EPA, National Exposure Research Laboratory
Joe Eidelberg, U.S. EPA, Region 9
Amy Gamerdinger, Washington State University
Richard Graham, U.S. EPA, Region 8
John Griggs, U.S. EPA, National Air and Radiation Environmental Laboratory
David M. Kargbo, U.S. EPA, Region 3
Ralph Ludwig, U.S. EPA, National Risk Management Research Laboratory
Irma McKnight, U.S. EPA, Office of Radiation and Indoor Air
William N. O'Steen, U.S. EPA, Region 4
David J. Reisman, U.S. EPA, National Risk Management Research Laboratory
Kyle Rogers, U.S. EPA, Region 5
Joe R. Williams, U.S. EPA, National Risk Management Research Laboratory
OSWER Regional Groundwater Forum Members

In addition, special acknowledgment goes to Carey A. Johnston from ORIA's Center for Remediation Technology and Tools for his contributions in the development, production, and review of this document.

Principal authorship in production of this guide was provided by the Department of Energy's Pacific Northwest National Laboratory (PNNL) under the Interagency Agreement Number DW89937220-01-03. Lynnette Downing served as the Department of Energy's Project Officer for this Interagency Agreement. PNNL authors involved in this project include:

Kenneth M. Krupka
Daniel I. Kaplan
Gene Whelan
R. Jeffrey Serne
Shas V. Mattigod

**TO COMMENT ON THIS GUIDE OR PROVIDE INFORMATION FOR FUTURE
UPDATES:**

Send all comments/updates to:

U.S. Environmental Protection Agency
Office of Radiation and Indoor Air
Attention: Understanding Variation in Partition (K_d) Values
401 M Street, SW (6602J)
Washington, DC 20460

or

webmaster.oria@epa.gov

ABSTRACT

This two-volume report describes the conceptualization, measurement, and use of the partition (or distribution) coefficient, K_d , parameter, and the geochemical aqueous solution and sorbent properties that are most important in controlling adsorption/retardation behavior of selected contaminants. The report is provided for technical staff from EPA and other organizations who are responsible for prioritizing site remediation and waste management decisions. Volume I discusses the technical issues associated with the measurement of K_d values and its use in formulating the retardation factor, R_f . The K_d concept and methods for measurement of K_d values are discussed in detail in Volume I. Particular attention is directed at providing an understanding of: (1) the use of K_d values in formulating R_f , (2) the difference between the original thermodynamic K_d parameter derived from ion-exchange literature and its “empiricized” use in contaminant transport codes, and (3) the explicit and implicit assumptions underlying the use of the K_d parameter in contaminant transport codes. A conceptual overview of chemical reaction models and their use in addressing technical defensibility issues associated with data from K_d studies is presented. The capabilities of EPA’s geochemical reaction model MINTEQA2 and its different conceptual adsorption models are also reviewed. Volume II provides a “thumb-nail sketch” of the key geochemical processes affecting the sorption of selected inorganic contaminants, and a summary of K_d values given in the literature for these contaminants under oxidizing conditions. The contaminants chosen for the first phase of this project include chromium, cadmium, cesium, lead, plutonium, radon, strontium, thorium, tritium (^3H), and uranium. Important aqueous speciation, (co)precipitation/dissolution, and adsorption reactions are discussed for each contaminant. References to related key experimental and review articles for further reading are also listed.

CONTENTS

	<u>Page</u>
NOTICE	ii
FOREWORD	iii
ACKNOWLEDGMENTS	v
FUTURE UPDATES	vi
ABSTRACT	vii
LIST OF FIGURES	xii
LIST OF TABLES	xiv
1.0 Introduction	1.1
2.0 The K_d Model And Its Use In Contaminant Transport Modeling	2.1
2.1 Introduction	2.1
2.2 Aqueous Geochemical Processes	2.3
2.2.1 Aqueous Complexation	2.3
2.2.2 Oxidation-Reduction (Redox) Chemistry	2.5
2.2.3 Sorption	2.8
2.2.3.1 Adsorption	2.10
2.2.3.1.1 Ion Exchange	2.13
2.2.3.2 Precipitation	2.13
2.3 Sorption Models	2.16
2.3.1 Constant Partition Coefficient (K_d) Model	2.16
2.3.2 Parametric K_d Model	2.19
2.3.3 Isotherm Adsorption Models	2.20
2.3.4 Mechanistic Adsorption Models	2.26
2.4 Effects of Unsaturated Conditions on Transport	2.27
2.5 Effects of Chemical Heterogeneity on Transport	2.33
2.5.1 Coupled Hydraulic and Chemical Heterogeneity	2.34
2.6 Diffusion	2.35
2.7 Subsurface Mobile Colloids	2.37
2.7.1 Concept of 3-Phase Solute Transport	2.37
2.7.2 Sources of Groundwater Mobile Colloids	2.38
2.7.3 Case Studies of Mobile-Colloid Enhanced Transport of	

Metals and Radionuclides	2.39
2.8 Anion Exclusion	2.39
2.9 Summary	2.40
3.0 Methods, Issues, and Criteria for Measuring K_d Values	3.1
3.1 Introduction	3.1
3.2 Methods for Determining K_d Values	3.2
3.2.1 Laboratory Batch Method	3.3
3.2.2 In-situ Batch Method	3.8
3.2.3 Laboratory Flow-Through Method	3.9
3.2.4 Field Modeling Method	3.14
3.2.5 K_{oc} Method	3.14
3.3 Issues Regarding Measuring and Selecting K_d Values	3.16
3.3.1 Using Simple Versus Complex Systems to Measure K_d Values	3.16
3.3.2 Field Variability	3.18
3.3.3 The “Gravel Issue”	3.19
3.3.4 The “Colloid Issue”	3.21
3.3.5 Particle Concentration Effect	3.22
3.4 Methods of Acquiring K_d Values from the Literature for Screening Calculations ...	3.23
3.4.1 K_d Look-Up Table Approach: Issues Regarding Selection of K_d Values from the Literature	3.23
3.4.2 Parametric K_d Approach	3.26
3.4.3 Mechanistic Adsorption Models	3.28
3.5 Summary	3.28
4.0 Groundwater Calibration Assessment Based on Partition Coefficients: Derivation and Examples	4.1
4.1 Introduction	4.1
4.2 Calibration: Location, Arrival Time, and Concentration	4.1
4.3 Illustrative Calculations to Help Quantify K_d Using Analytical Models	4.4
4.3.1 Governing Equations	4.4
4.3.2 Travel Time and the Partition Coefficient	4.7
4.3.3 Mass and the Partition Coefficient	4.8

4.3.4	Dispersion and the Partition Coefficient	4.10
4.4	Modeling Sensitivities to Variations in the Partition Coefficient	4.11
4.4.1	Relationship Between Partition Coefficients and Risk	4.11
4.4.2	Partition Coefficient as a Calibration Parameter in Transport Modeling	4.12
4.5	Summary	4.14
5.0	Application of Chemical Reaction Codes	5.1
5.1	Background	5.1
5.1.1	Definition of Chemical Reaction Modeling	5.2
5.1.2	Reviews of Chemical Reaction Models	5.3
5.1.3	Aqueous Speciation-Solubility Versus Reaction Path Codes	5.4
5.1.4	Adsorption Models in Chemical Reaction Codes	5.5
5.1.5	Output from Chemical Reaction Modeling	5.7
5.1.6	Assumptions and Data Needs	5.9
5.1.7	Symposiums on Chemical Reaction Modeling	5.10
5.2	MINTEQA2 Chemical Reaction Code	5.11
5.2.1	Background	5.11
5.2.2	Code Availability	5.11
5.2.3	Aqueous Speciation Submodel	5.12
5.2.3.1	Example of Modeling Study	5.13
5.2.3.2	Application to Evaluation of K_d Values	5.15
5.2.4	Solubility Submodel	5.16
5.2.4.1	Example of Modeling Study	5.17
5.2.4.2	Application to Evaluation of K_d Values	5.18
5.2.5	Precipitation/Dissolution Submodel	5.18
5.2.5.1	Example of Modeling Study	5.19
5.2.5.2	Application to Evaluation of K_d Values	5.20
5.2.6	Adsorption Submodel	5.21
5.2.6.1	Examples of Modeling Studies	5.22
5.2.6.2	Application to Evaluation of K_d Values	5.23
5.2.7	MINTEQA2 Databases	5.24
5.2.7.1	Thermodynamic Database	5.24
5.2.7.1.1	Basic Equations	5.25
5.2.7.1.2	Structure of Thermodynamic Database Files	5.26
5.2.7.1.3	Database Components	5.26
5.2.7.1.4	Status Relative to Project Scope	5.27
5.2.7.1.5	Issues Related to Database Modifications	5.32
5.2.7.2	Sorption Database	5.33

5.2.7.2.1 Status Relative to Project Scope	5.33
5.2.7.2.2 Published Database Sources	5.33
5.3 Adsorption Model Options in MINTEQA2	5.35
5.3.1 Electrostatic Versus Non-Electrostatic Models	5.36
5.3.2 Activity Partition Coefficient (K_d) Model	5.40
5.3.3 Activity Langmuir Model	5.42
5.3.4 Activity Freundlich Model	5.44
5.3.5 Ion Exchange Model	5.45
5.3.6 Diffuse Layer Model	5.45
5.3.7 Constant Capacitance Model	5.47
5.3.8 Triple Layer Model	5.48
5.4 Summary	5.50
6.0 References	6.1
Appendix A - Acronyms, Abbreviations, Symbols, and Notation	A.1
Appendix B - Definitions	B.1
Appendix C - Standard Method Used at Pacific Northwest National Laboratory for Measuring Laboratory Batch K_d Values	C.1

LIST OF FIGURES

	<u>Page</u>
Figure 2.1. Diffuse double layer and surface charge of a mineral surface	2.11
Figure 2.2. Four types of adsorption isotherm curves shown schematically in parlance of Giles <i>et al.</i> (1973)	2.22
Figure 2.3. Schematic diagram for conceptual model of water distribution in saturated (top two figures) and unsaturated soils (bottom two figures) suggesting differences in the unsaturated flow regime (indicated by arrows) for soils with varying texture	2.30
Figure 2.4. Development of hydraulic heterogeneity (decreasing ϕ_m) in unsaturated, non-aggregated soils with decreasing moisture saturation.	2.32
Figure 3.1. Procedure for measuring a batch K_d value (EPA 1991)	3.4
Figure 3.2. Demonstration calculation showing affect on overall K_d by multiple species that have different individual K_d values and are kinetically slow at interconverting between each composition state.	3.7
Figure 3.3. Procedure for measuring a column K_d value	3.9
Figure 3.4. Schematic diagram showing the relative concentrations of a constituent at the input source (figures on left) and in the effluent (figures on right) as a function of time for a pulse versus step input	3.11
Figure 4.1. Relative relationships between input-data quality, output uncertainty, and types of problems addressed by each level of assessment	4.2
Figure 4.2. Example illustrating a MEPAS ^{90}Sr calibration with K_d equaling 0.8 ml/g and 1 monitored-data point	4.13
Figure 4.3. Example illustrating MEPAS ^{90}Sr calibrations with K_d equaling 0.4 and 0.8 ml/g and several monitored-data points	4.14
Figure 5.1. Distribution of dominant U(VI) aqueous species for leachates buffered at pH 7.0 by local ground water (Figure 5.1a) and at pH 12.5 by cement pore fluids (Figure 5.1b)	5.14
Figure 5.2. Saturation Indices calculated for rutherfordine (UO_2CO_3) as a function of	

pH for solution analyses from Sergeyeva et al. (1972)	5.17
Figure 5.3. Maximum concentration limits calculated for total dissolved uranium as a function of pH based on the equilibrium solubilities of schoepite and uranophane	5.20
Figure 5.4. Schematic representation of the triple layer model showing surface species and surface charge-potential relationships	5.37
Figure 5.5. Schematic representation of the constant capacitance layer model showing surface species and surface charge-potential relationships	5.38

LIST OF TABLES

	<u>Page</u>
Table 2.1. List of several redox-sensitive metals and their possible valence states in soil/groundwater systems	2.6
Table 2.2. Sequence of Principal Electron Acceptors in neutral pH aquatic systems (Sposito 1989)	2.7
Table 2.3. Zero-point-of-charge, pH_{zpc}	2.9
Table 2.4. Cation exchange capacities (CEC) for several clay minerals (Grim 1968)	2.14
Table 2.5. Summary of chemical processes affecting attenuation and mobility of contaminants	2.41
Table 3.1. Representative chemical species in acidic and basic soil solutions (after Sposito 1989).	3.17
Table 3.2. Example of a K_d look-up table for uranium, uranium(VI), and uranium(IV)	3.25
Table 3.3. Advantages, disadvantages, and assumptions of K_d determination methods and the assumptions in applying these K_d values to contaminant transport models	3.30
Table 5.1. Chemical reaction models described in the literature	5.4
Table 5.2. Examples of technical symposiums held on development, applications, and data needs for chemical reaction modeling	5.10
Table 5.3. Component species in MINTEQA2 thermodynamic database	5.29
Table 5.4. Organic ligands in MINTEQA2 thermodynamic database	5.31

1.0 Introduction

The objective of this two volume report is to provide a reasoned and documented discussion on the technical issues associated with the measurement of partition (or distribution) coefficient, K_d ,^{1,2} values and their use in formulating the contaminant retardation factor, R_f . Specifically, it describes the rate of contaminant transport relative to that of groundwater. The retardation factor is the empirical parameter commonly used in transport models to describe the chemical interaction between the contaminant and geological materials (*i.e.*, soils, sediments, and rocks). *Throughout this report, the term “soil” will be used as general term to refer to all unconsolidated geologic materials.*³ The contaminant retardation factor includes processes such as surface adsorption, absorption into the soil structure, precipitation, and physical filtration of colloids. This report is provided for technical staff from EPA and other organizations who are responsible for prioritizing site remediation and waste management decisions.

Volume I contains a detailed discussion of the K_d concept, its use in fate and transport computer codes, and the methods for the measurement of K_d values. The focus of Chapter 2 is on providing an understanding of (1) the use of K_d values in formulating R_f , (2) the difference between the original thermodynamic K_d parameter derived from the ion-exchange literature and its “empiricized” use in contaminant transport codes, and (3) the explicit and implicit assumptions underlying the use of the K_d parameter in contaminant transport codes.

The K_d parameter is very important in estimating the potential for the adsorption of dissolved contaminants in contact with soil. As typically used in fate and contaminant transport calculations, the K_d is defined as the ratio of the contaminant concentration associated with the solid to the contaminant concentration in the surrounding aqueous solution when the system is at equilibrium. Soil and geochemists knowledgeable of sorption processes in natural environments have long known that generic or default K_d values can result in significant error when used to predict the absolute impacts of contaminant migration or site-remediation options. Therefore, for site-specific calculations, K_d values measured at site-specific conditions are absolutely essential.

¹ Throughout this report, the term “partition coefficient” will be used to refer to the K_d “linear isotherm” sorption model. It should be noted, however, that the terms “partition coefficient” and “distribution coefficient” are used interchangeably in the literature for the K_d model.

² A list of acronyms, abbreviations, symbols, and notation is given in Appendix A. A list of definitions is given in Appendix B

³ The terms “sediment” and “soil” have particular meanings depending on one’s technical discipline. For example, the term “sediment” is often reserved for transported and deposited particles derived from soil, rocks, or biological material. “Soil” is sometimes limited to referring to the top layer of the earth’s surface, suitable for plant life. In this report, the term “soil” was selected as a general term to refer to all unconsolidated geologic materials.

To address some of this concern when using generic or default K_d values for screening calculations, modelers often incorporate a degree of conservatism into their calculations by selecting limiting or bounding conservative K_d values. For example, the most conservative estimate from an off-site risk perspective of contaminant migration through the subsurface natural soil is to assume that the soil has little or no ability to slow (retard) contaminant movement (*i.e.*, a minimum bounding K_d value). Consequently, the contaminant would migrate in the direction and, for a K_d value of ≈ 0 , travel at the rate of water. Such an assumption may in fact be appropriate for certain contaminants such as tritium, but may be too conservative for other contaminants, such as thorium or plutonium, which react strongly with soils and may migrate 10^2 to 10^6 times more slowly than the water. On the other hand, to estimate the maximum risks (and costs) associated with on-site remediation options, the bounding K_d value for a contaminant will be a maximum value (*i.e.*, maximize retardation).

The K_d value is usually a measured parameter that is obtained from laboratory experiments. The general methods used to measure K_d values (Chapters 3 and 4) include the laboratory batch method, *in-situ* batch method, laboratory flow-through (or column) method, field modeling method, and K_{oc} method. The ancillary information needed regarding the adsorbent (soil), solution (contaminated ground-water or process waste water), contaminant (concentration, valence state, speciation distribution), and laboratory details (spike addition methodology, phase separation techniques, contact times) are summarized. The advantages, disadvantages, and, perhaps more importantly, the underlying assumptions of each method are also presented.

A conceptual overview of geochemical modeling calculations and computer codes as they pertain to evaluating K_d values and modeling of adsorption processes is discussed in detail in Chapter 5. The use of geochemical codes in evaluating aqueous speciation, solubility, and adsorption processes associated with contaminant fate studies is reviewed. This approach is compared to the traditional calculations that rely on the constant K_d construct. The use of geochemical modeling to address quality assurance and technical defensibility issues concerning available K_d data and the measurement of K_d values is also discussed. The geochemical modeling review includes a brief description of the EPA's MINTEQA2 geochemical code and a summary of the types of conceptual models it contains to quantify adsorption reactions. The status of radionuclide thermodynamic and contaminant adsorption model databases for the MINTEQA2 code is also reviewed.

The main focus of Volume II is to: (1) provide a "thumb-nail sketch" of the key geochemical processes affecting the sorption of a selected set of contaminants; (2) provide references to related key experimental and review articles for further reading; (3) identify the important aqueous- and solid-phase parameters controlling the sorption of these contaminants in the subsurface environment under oxidizing conditions; and (4) identify, when possible, minimum and maximum conservative K_d values for each contaminant as a function key geochemical processes affecting their sorption. The contaminants chosen for the first phase of this project include chromium, cadmium, cesium, lead, plutonium, radon, strontium, thorium, tritium (^3H), and uranium. The selection of these contaminants by EPA and PNNL project staff was based on two

criteria. First, the contaminant had to be of high priority to the site remediation or risk assessment activities of EPA. Second, due to budgetary constraints, a subset of the large number of contaminants that met the first criteria were selected to represent categories of contaminants based on their chemical behavior. The six nonexclusive categories are:

- Cations - cadmium, cesium, lead, plutonium, strontium, thorium, and uranium
- Anions - chromium(VI) (as chromate)
- Radionuclides - cesium, plutonium, radon, strontium, thorium, tritium (^3H), and uranium
- Conservatively transported contaminants - tritium (^3H) and radon
- Nonconservatively transported contaminants - other than tritium (^3H) and radon
- Redox sensitive elements - chromium, lead, plutonium, and uranium

The general principles of geochemistry discussed in both volumes of this report can be used to estimate the geochemical interactions of similar elements for which data are not available. For example, contaminants present primarily in anionic form, such as Cr(VI), tend to adsorb to a limited extent to soils. Thus, one might generalize that other anions, such as nitrate, chloride, and U(VI)-anionic complexes, would also adsorb to a limited extent. Literature on the adsorption of these 3 solutes show no or very little adsorption.

The concentration of contaminants in groundwater is controlled primarily by the amount of contaminant present at the source; rate of release from the source; hydrologic factors such as dispersion, advection, and dilution; and a number of geochemical processes including aqueous geochemical processes, adsorption/desorption, precipitation, and diffusion. To accurately predict contaminant transport through the subsurface, it is essential that the important geochemical processes affecting contaminant transport be identified and, perhaps more importantly, accurately described in a mathematically defensible manner. Dissolution/precipitation and adsorption/desorption are usually the most important processes affecting contaminant interaction with soils. Dissolution/precipitation is more likely to be the key process where chemical nonequilibrium exists, such as at a point source, an area where high contaminant concentrations exist, or where steep pH or oxidation-reduction (redox) gradients exist. Adsorption/desorption will likely be the key process controlling inorganic contaminant migration in areas where the naturally-present constituents are already in equilibrium and only the anthropogenic constituents (contaminants) are out of equilibrium, such as in areas far from the point source. Diffusion flux spreads solute via a concentration gradient (*i.e.*, Fick's law). Diffusion is a dominant transport mechanism when advection is insignificant, and is usually a negligible transport mechanism when water is being advected in response to various forces.

2.0 The K_d Model And Its Use In Contaminant Transport Modeling

2.1 Introduction

The concentration of contaminants in groundwater¹ is determined by the amount, concentration, and nature of contaminant present at the source, rate of release from the source, and a number of geochemical processes including aqueous and sorption geochemical processes (Section 2.2) and -diffusion (Section 2.6). Recently, attention has been directed at additional geochemical processes that can enhance the transport of certain contaminants: colloid-facilitated transport of contaminants (Section 2.7) and anion exclusion (Section 2.8). These latter processes are difficult to quantify, and the extent to which they occur has not been determined. To predict contaminant transport through the subsurface accurately, it is essential that the important geochemical processes affecting the contaminant transport be identified and, perhaps more importantly, accurately described in a mathematically defensible manner. Dissolution/precipitation and adsorption/desorption are considered the most important processes affecting contaminant interaction with soils. Dissolution/precipitation is more likely to be the key process where chemical nonequilibrium exists, such as at a waste disposal facility (*i.e.*, point source), an area where high contaminant concentrations exist, or where steep pH or oxidation-reduction (redox) gradients exist. Adsorption/desorption will likely be the key process controlling contaminant migration in areas where chemical equilibrium exists, such as in areas far from the disposal facilities or spill sites.

The simplest and most common method of estimating contaminant retardation (*i.e.*, the inverse of the relative transport rate of a contaminant compared to that of water) is based on partition (or distribution) coefficient, K_d ,² values (Section 2.3.1). In turn, the K_d value is a direct measure of the partitioning of a contaminant between the solid and aqueous phases. It is an empirical metric that attempts to account for various chemical and physical retardation mechanisms that are influenced by a myriad of variables. Ideally, site-specific K_d values would be available for the range of aqueous and geological conditions in the system to be modeled.

Values for K_d not only vary greatly between contaminants, but also vary as a function of aqueous and solid phase chemistry (Delegard and Barney, 1983; Kaplan and Serne, 1995; Kaplan *et al.*, 1994c). For example, uranium K_d values can vary over 6 orders of magnitude depending on the composition of the aqueous and solid phase chemistry (see Volume II, Appendix J). A more

¹ For information regarding the background concentration levels of macro and trace constituents, including elements of regulatory-interest such as arsenic, cadmium, chromium, lead, and mercury, in soils and groundwater systems, the reader is referred to Lindsay (1979), Hem (1985), Sposito (1989, 1994), Langmuir (1997), and other similar sources and the references cited therein.

² A list of acronyms, abbreviations, symbols, and notation is given in Appendix A. A list of definitions is given in Appendix B.

robust approach to describing the partitioning of contaminants between the aqueous and solid phases is the parametric K_d model, which varies the K_d value according to the chemistry and mineralogy of the system at the node¹ being modeled (Section 2.3.2). Though this approach is more accurate, it has not been used frequently. The added complexity in solving the transport equation with the parametric K_d adsorption model and its empirical nature may be why this technique has been used sparingly.

Inherent in the K_d “linear isotherm” adsorption model is the assumption that adsorption of the contaminant of interest is independent of its concentration in the aqueous phase. Partitioning of a contaminant on soil can often be described using the K_d model, but typically only for low contaminant concentrations as would exist some distance away (far field) from the source of contamination. It is common knowledge that contaminant adsorption on soils can deviate from the linear relationship required by the K_d construct. This is possible for conditions as might exist in leachates or groundwaters near waste sources where contaminant concentrations are large enough to affect the saturation of surface adsorption sites. Non-linear isotherm models (Section 2.3.3) are used to describe the case where sorption relationships deviate from linearity.

Mechanistic models explicitly accommodate the dependency of K_d values on contaminant concentration, competing ion concentration, variable surface charge on the absorbent, and solution species distribution. Incorporating mechanistic or semi-mechanistic adsorption concepts into transport models is desirable because the models become more robust and, perhaps more importantly from the standpoint of regulators and the public, scientifically defensible. However, less attention will be directed to mechanistic adsorption models because the focus of this project is on the K_d model which is currently the most common method for quantifying chemical interactions of dissolved contaminants with soils for performance assessment, risk assessment, and remedial investigation calculations. The complexity of installing these mechanistic adsorption models into existing computer codes used to model contaminant transport is difficult to accomplish. Additionally, these models also require a more intense and costly data collection effort than will likely be available to many contaminant transport modelers, license requestors, or responsible parties. A brief description of the state of the science and references to excellent review articles are presented (Section 2.3.4).

The purpose of this chapter is to provide a primer to modelers and site managers on the key geochemical processes affecting contaminant transport through soils. Attention is directed at describing how geochemical processes are accounted for in transport models by using the partition coefficient (K_d) to describe the partitioning of aqueous phase constituents to a solid phase. Particular attention is directed at: (1) defining the application of the K_d parameter, (2) the explicit and implicit assumptions underlying its use in transport codes, and (3) the difference between the original thermodynamic K_d parameter derived from ion-exchange literature and its “empiricized” use in formulating the retardation factors used in contaminant transport

¹ A “node” is the center of a computation cell within a grid used to define the area or volume being modeled.

codes. In addition to geochemical processes, related issues pertaining to the effects of unsaturated conditions, chemical heterogeneity, diffusion, and subsurface mobile colloids on contaminant transport are also briefly discussed. These processes and their effects on contaminant mobility are summarized in a table at the end of this chapter.

2.2 *Aqueous Geochemical Processes*

Groundwater modelers are commonly provided with the total concentration of a number of dissolved substances in and around a contaminant plume. While total concentrations of these constituents indicate the extent of contamination, they give little insight into the forms in which the metals are present in the plume or their mobility and bioavailability. Contaminants can occur in a plume as soluble-free, soluble-complexed, adsorbed, organically complexed, precipitated, or coprecipitated species (Sposito, 1989). The geochemical processes that contribute to the formation of these species and their potential effect on contaminant transport are discussed in this chapter.

2.2.1 *Aqueous Complexation*

Sposito (1989) calculated that a typical soil solution will easily contain 100 to 200 different soluble species, many of them involving metal cations and organic ligands. A complex is said to form whenever a molecular unit, such as an ion, acts as a central group to attract and form a close association with other atoms or molecules. The aqueous species $\text{Th}(\text{OH})_4^{4+}$ (aq), $(\text{UO}_2)_3(\text{OH})_5^+$, and HCO_3^- are complexes with Th^{4+} (thorium), UO_2^{2+} (hexavalent uranium), and CO_3^{2-} (carbonate), respectively, acting as the central group. The associated ions, OH^- or H^+ , in these complexes are termed ligands. If 2 or more bonds are formed between a single ligand and a metal cation, the complex is termed a chelate. The complex formed between Al^{3+} and citric acid $[\text{Al}(\text{COO})_2\text{COH}(\text{CH}_2\text{COOH})]^+$, in which 2 COO^- groups and 1 COH group of the citric acid molecule are coordinated to Al^{3+} , is an example of a chelate. If the central group and ligands in a complex are in direct contact, the complex is called inner-sphere. If one or more water molecules is interposed between the central group and a ligand, the complex is outer-sphere. If the ligands in a complex are water molecules [*e.g.*, as in $\text{Ca}(\text{H}_2\text{O})_6^{2+}$], the unit is called a solvation complex or, more frequently, a free species. Inner-sphere complexes usually are much more stable than outer-sphere complexes, because the latter cannot easily involve ionic or covalent bonding between the central group.

Most of the complexes likely to form in groundwater are metal-ligand complexes, which may be either inner-sphere or outer-sphere. As an example, consider the formation of a neutral sulfate complex with a bivalent metal cation (M^{2+}) as the central group:¹

¹ Unless otherwise noted, all species listed in equations in this appendix refer to aqueous species.



where the metal M can be cadmium, chromium, lead, mercury, strontium, *etc.* The equilibrium (or stability) constant, $K_{r,T}$, corresponding to Equation 2.1 is:

$$K_{r,T} = \frac{\{MSO_4^{\prime\prime}(\text{aq})\}}{\{M^{2+}\}\{SO_4^{2-}\}} \quad (2.2)$$

where quantities indicated by { } represent species activities. The equilibrium constant can describe the distribution of a given constituent among its possible chemical forms if complex formation and dissociation reactions are at equilibrium. The equilibrium constant is affected by a number of factors, including the ionic strength of the aqueous phase, presence of competing reactions, and temperature.

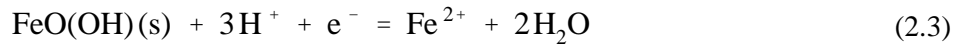
The most common complexing anions present in groundwater are HCO_3^-/CO_3^{2-} , Cl^- , SO_4^{2-} , and humic substances (*i.e.*, organic materials). Some synthetic organic ligands may also be present in groundwater at contaminated sites. Dissolved PO_4^{3-} can also be a strong inorganic complexant, but is generally not very soluble in natural groundwaters. The relative propensity of the inorganic ligands to form complexes with many metals is: $CO_3^{2-} > SO_4^{2-} > PO_4^{3-} > Cl^-$ (Stumm and Morgan, 1981). Carbonate complexation may be equally important in carbonate systems, especially for tetravalent metals (Kim, 1986; Rai *et al.*, 1990). There can be a large number of dissolved, small-chain humic substances present in groundwater and their complexation properties with metals and radionuclides are not well understood. Complexes with humic substances are likely to be very important in systems containing appreciable amounts of humic substances (>1 mg/l). In shallow aquifers, organic ligands from humic materials can be present in significant concentration and dominate the metal chemistry (Freeze and Cherry, 1979). The chelate anion, EDTA,¹ which is a common industrial reagent, forms strong complexes with many cations, much stronger than carbonate and humic substances (Kim, 1986). Some metal-organic ligand complexes can be fairly stable and require low pH conditions (or high pH for some metal-organic complexes) to dissociate the complex.

Complexation usually results in lowering the solution concentration (*i.e.*, activity) of the central molecule (*i.e.*, uncomplexed free species). Possible outcomes of lowering the activity of the free species of the metal include lowering the potential for adsorption and increasing its solubility, both of which can enhance migration potential. On the other hand, some complexants (*e.g.*, certain humic acids) readily bond to soils and thus retard the migration of the complexed metals.

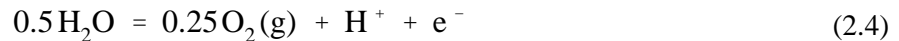
¹ EDTA is ethylene diamine triacetic acid.

2.2.2 Oxidation-Reduction (Redox) Chemistry

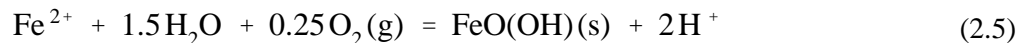
An oxidation-reduction (redox) reaction is a chemical reaction in which electrons are transferred completely from one species to another. The chemical species that loses electrons in this charge transfer process is described as oxidized, and the species receiving electrons is described as reduced. For example, in the reaction involving iron species:



the solid phase, goethite [FeO(OH) (s)], is the oxidized species, and Fe²⁺ is the reduced species. Equation 2.3 is a reduction half-reaction in which an electron in aqueous solution, denoted e⁻, serves as one of the reactants. This species, like the proton in aqueous solution, is understood in a formal sense to participate in charge transfer processes. The overall redox reaction in a system must always be the combination of 2 half-reactions, an oxidation half-reaction and reduction half-reaction, such that the species e⁻ does not exist explicitly. For example, to represent the oxidation of Fe²⁺, Equation 2.3 could be combined (or coupled) with the half-reaction involving the oxidation of H₂O:



Combining Equation 2.3 with Equation 2.4 results in the cancellation of the aqueous electron and the oxidation of Fe²⁺ via the reduction of O₂ (g) and subsequent precipitation of hydrous iron oxide. This is a possible reaction describing Fe²⁺ leaching from a reduced environment in the near field to the oxidizing environment of the far field:



Equation 2.5 could represent a scenario in which Fe²⁺ is leached from a reducing environment, where it is mobile, into an oxidized environment, where Fe³⁺ precipitates as the mineral goethite.

The electron activity is a useful conceptual device for describing the redox status of aqueous systems, just as the aqueous proton activity is so useful for describing the acid-base status of soils. Similar to pH, the propensity of a system to be oxidized can be expressed by the negative common logarithm of the free-electron activity, pE:

$$\text{pE} = -\log \{ \text{e}^- \} . \quad (2.6)$$

The range of pE in the natural environment varies between approximately 7 and 17 in the vadose zone (Sposito, 1989). If anoxic conditions exist, say in a bog area, than the pE may get as low as -3. The most important chemical elements affected by redox reactions in ambient groundwater are carbon, nitrogen, oxygen, sulfur, manganese, and iron. In contaminated groundwater, this list

increases to include arsenic, cobalt, chromium, iodine, molybdenum, neptunium, plutonium, selenium, technetium, uranium, and others. Table 2.1 lists several redox-sensitive metals and the

Table 2.1. List of several redox-sensitive metals and their possible valence states in soil/groundwater systems.

Element	Valence States	Element	Valence States
Americium	+3, +4, +5, and +6	Neptunium	+3, +4, +5, and +6
Antimony	+3 and +5	Plutonium	+2, +3, +4, +5, and +6
Arsenic	+3 and +5	Ruthenium	+2, +3, +4, +6, and +7
Chromium	+2, +3, and +6	Selenium	-2, +4, and +6
Copper	+1 and +2	Technetium	+2, +3, +4, +5, +6, and +7
Iron	+2 and +3	Thallium	+1 and +3
Manganese	+2 and +3	Uranium	+3, +4, +5, and +6
Mercury	+1 and +2	Vanadium	+2, +3, +4, and +5

different valence states that they may be present as in soil/groundwater systems. The speciation of a metal in solution between its different valence states will depend on the site geochemistry, especially with respect to pH and redox conditions. Moreover, not all of the valence states for each metal are equally important from the standpoint of dominance in solution, adsorption behavior, solubility, and toxicity. For those redox-sensitive elements that are part of this project's scope (*i.e.*, chromium, plutonium, and uranium), these issues are discussed in detail in Volume II of this report.

There is a well defined sequence of reduction of inorganic elements (Table 2.2). When an oxidized system is reduced, the order that oxidized species disappear are O_2 , NO_3^- , Mn^{2+} , Fe^{2+} , HS^- , and H_2 . As the pE of the system drops below +11.0, enough electrons become available to reduce O_2 (g) to H_2O . Below a pE of 5, O_2 (g) is not stable in pH neutral systems. Above pE = 5, O_2 (g) is consumed in the respiration processes of aerobic microorganisms. As the pE decreases below 8, electrons become available to reduce NO_3^- to NO_2^- . As the system pE value drops into the range of 7 to 5, electrons become plentiful enough to support the reduction of iron and manganese in solid phases. Iron reduction does not occur until O_2 and NO_3^- are depleted, but manganese reduction can be initiated in the presence of NO_3^- . In the case of iron and manganese,

decreasing pE results in solid-phase dissolution, because the stable forms of Mn(IV) and Fe(III) are solid phases. Besides the increase in solution concentrations of iron and manganese expected from this effect of lowered pE, a marked increase is usually observed in the aqueous phase concentrations of metals such as cadmium, chromium, or lead, and of ligands such as H_2PO_4^- or

Table 2.2. Sequence of Principal Electron Acceptors in neutral pH aquatic systems (Sposito, 1989).

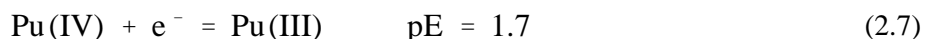
Reduction Half-Reactions	Range of Initial pE Values
$0.5 \text{ O}_2 (\text{g}) + 2 \text{ e}^- + 2 \text{ H}^+ = \text{H}_2\text{O}$	5.0 to 11.0
$\text{NO}_3^- + 2 \text{ e}^- + 2 \text{ H}^+ = \text{NO}_2^- + \text{H}_2\text{O}$	3.4 to 8.5
$\text{MnO}_2 (\text{s}) + 2 \text{ e}^- + 4 \text{ H}^+ = \text{Mn}^{2+} + 2 \text{ H}_2\text{O}$	3.4 to 6.8
$\text{FeOOH} (\text{s}) + \text{ e}^- + 3 \text{ H}^+ = \text{Fe}^{2+} + 2 \text{ H}_2\text{O}$	1.7 to 5.0
$\text{SO}_4^{2-} + 8 \text{ e}^- + 9 \text{ H}^+ = \text{HS}^- + 4 \text{ H}_2\text{O}$	0 to -2.5
$\text{H}^+ + \text{ e}^- = 0.5 \text{ H}_2 (\text{g})$	-2.5 to -3.7
$(\text{CN}_2\text{O})_n = n/2 \text{ CO}_2 (\text{g}) + n/2 \text{ CH}_4 (\text{g})$	-2.5 to -3.7

HMoO_4^- , accompanying reduction of iron and manganese. The principal cause of this secondary phenomenon is the desorption of metals and ligands that occurs when the adsorbents (*i.e.*, mostly iron and manganese oxides) to which they are bound become unstable and dissolve. Typically, the metals released in this fashion, including iron and manganese, are soon re-adsorbed by solids that are stable at low pE (*e.g.*, clay minerals or organic matter) and become exchangeable surface species.

These surface changes have an obvious influence on the availability (migration potential) of the chemical elements involved, particularly phosphorus. If a contaminant was involved in this dissolution/ exchange set of reactions, it would be expected that the contaminants would be less strongly associated with the solid phase.

As pE becomes negative, sulfur reduction can take place. If contaminant metals and radionuclides, such as Cr(VI), Pu (VI), or U(VI), are present in the aqueous phase at high enough concentrations, they can react with bisulfide (HS^-) to form metal sulfides that are quite insoluble. Thus, anoxic conditions can diminish significantly the solubility of some redox-sensitive contaminants.

Redox chemistry may also have a direct affect on contaminant chemistry. It can directly affect the oxidation state of several contaminants, including, arsenic, cobalt, chromium, iodine, molybdenum, neptunium, lead, plutonium, selenium, technetium, and uranium. A change in oxidation in turn affects the potential of some contaminants to precipitate. For example, the reduction of Pu(IV),



makes plutonium appreciably less reactive in complexation [*i.e.*, Pu(III) stability constants are much less than those of Pu(IV)] and sorption/partitioning reactions (Kim, 1986). The reduction of U(VI) to U(III) or U(IV), has the opposite effect, *i.e.*, U(III) or U(IV) form stronger complexes and sorb more strongly to surfaces than U(VI). Reducing environments tend to make chromium, similar to uranium, less mobile, and arsenic more mobile.

Therefore, changes in redox may increase or decrease the tendency for reconcentration of contaminants, depending on the chemical composition of the aqueous phase and the contaminant in question. However, if the redox status is low enough to induce sulfide formation, reprecipitation of many metals and metal-like radionuclides can be expected. Redox-mediated reactions are incorporated into most geochemical codes and can be modeled conceptually. The resultant speciation distribution calculated by such a code is used to determine potential solubility controls and adsorption potential. Many redox reactions have been found to be kinetically slow in natural groundwater, and several elements may never reach redox equilibrium between their various oxidation states. Thus, it is more difficult to predict with accuracy the migration potential of redox-sensitive species.

2.2.3 Sorption

When a contaminant is associated with the solid phase, it is not known if it was adsorbed on to the surface of a solid, absorbed into the structure of a solid, precipitated as a 3-dimensional molecular structure on the surface of the solid, or partitioned into the organic matter (Sposito, 1989). Dissolution/ precipitation and adsorption/desorption are considered the most important processes affecting metal and radionuclide interaction with soils and will be discussed at greater lengths than absorption and organic matter partitioning.

- Dissolution/precipitation is more likely to be the key process where chemical nonequilibrium exists, such as at a point source, an area where high contaminant concentrations exist, or where steep pH or redox gradients exist.
- Adsorption/desorption will likely be the key process controlling contaminant migration in areas where chemical equilibrium exists, such as in areas far from the point source.

A generic term devoid of mechanism and used to describe the partitioning of aqueous phase constituents to a solid phase is sorption. Sorption encompasses all of the above processes. It is frequently quantified by the partition coefficient, K_d , that will be discussed below (Section 2.3.1).

In many natural systems, the extent of sorption is controlled by the electrostatic surface charge of the mineral phase. Most soils have net negative charges. These surface charges originate from permanent and variable charges. The permanent charge results from the substitution of a lower valence cation for a higher valence cation in the mineral structure, where as the variable charge results from the presence of surface functional groups. Permanent charge is the dominant charge of 2:1 clays, such as biotite and montmorillonite. Permanent charge constitutes a majority of the charge in unweathered soils, such as exist in temperate zones in the United States, and it is not affected by solution pH. Permanent positive charge is essentially nonexistent in natural rock and soil systems. Variable charge is the dominant charge of aluminum, iron, and manganese oxide solids and organic matter. Soils dominated by variable charge surfaces are primarily located in semi-tropical regions, such as Florida, Georgia, and South Carolina, and tropical regions. The magnitude and polarity of the net surface charge changes with a number of factors, including pH. As the pH increases, the surface becomes increasingly more negatively charged. The pH where the surface has a zero net charge is referred to as the pH of zero-point-of-charge, pH_{zpc} (Table 2.3). At the pH of the majority of natural soils (pH 5.5 to 8.3), calcite, gibbsite, and goethite, if present, would be expected to have some, albeit little, positive charge and therefore some anion sorption capacity.

Table 2.3. pH of zero-point-of-charge, pH_{zpc} . [After Stumm and Morgan (1981) and Lehninger (1970)].

Material	pH_{zpc}
Gibbsite $[\text{Al}(\text{OH})_3]$	5.0
Hematite ($\alpha\text{-Fe}_2\text{O}_3$)	6.7
Goethite ($\alpha\text{-FeOOH}$)	7.8
Silica (SiO_2)	2
Feldspars	2 to 2.4
Kaolinite $[\text{Al}_2\text{Si}_2\text{O}_5(\text{OH})_4]$	4.6
COOH	1.7 to 2.6 ¹
NH_3	9.0 to 10.4 ¹

¹ These values represent the range of pK_a values for amino acids.

2.2.3.1 Adsorption

Adsorption, as discussed in this report, is the net accumulation of matter at the interface between a solid phase and an aqueous-solution phase. It differs from precipitation because it does not include the development of a 3-dimensional molecular structure. The matter that accumulates in 2-dimensional molecular arrangements at the interface is the adsorbate. The solid surface on which it accumulates is the adsorbent.

Adsorption on clay particle surfaces can take place via 3 mechanisms. In the first mechanism, an inner-sphere surface complex is in direct contact with the adsorbent surface and lies within the Stern Layer (Figure 2.1). As a rule, the relative affinity of a contaminant to sorb will increase with its tendency to form inner-sphere surface complexes. The tendency for a cation to form an inner-sphere complex in turn increases with increasing valence (*i.e.*, more specifically, ionic potential¹) of a cation (Sposito, 1984).

The second mechanism creates an outer-sphere surface complex that has at least 1 water molecule between the cation and the adsorbent surface. If a solvated ion (*i.e.*, an ion with water molecules surrounding it) does not form a complex with a charged surface functional group but instead neutralizes surface charge only in a delocalized sense, the ion is said to be adsorbed in the diffuse-ion swarm, and these ions lie in a region called the diffuse sublayer (Figure 2.1). The diffuse-ion swarm and the outer-sphere surface complex mechanisms of adsorption involve exclusively ionic bonding, whereas inner-sphere complex mechanisms are likely to involve ionic, as well as covalent, bonding.

The mechanisms by which anions adsorb are inner-sphere surface complexation and diffuse-ion swarm association. Outer-sphere surface complexation of anions involves coordination to a protonated hydroxyl or amino group or to a surface metal cation (*e.g.*, water-bridging mechanisms) (Gu and Schulz, 1991). Almost always, the mechanism of this coordination is hydroxyl-ligand exchange (Sposito, 1984). In general, ligand exchange is favored at pH levels less than the zero-point-of-charge (Table 2.3). The anions CrO_4^{2-} , Cl^- , and NO_3^- , and to lesser extent HS^- , SO_4^{2-} , and HCO_3^- , are considered to adsorb mainly as diffuse-ion and outer-sphere-complex species.

¹ The ionic potential is the ratio of the valence to the ionic radius of an ion.

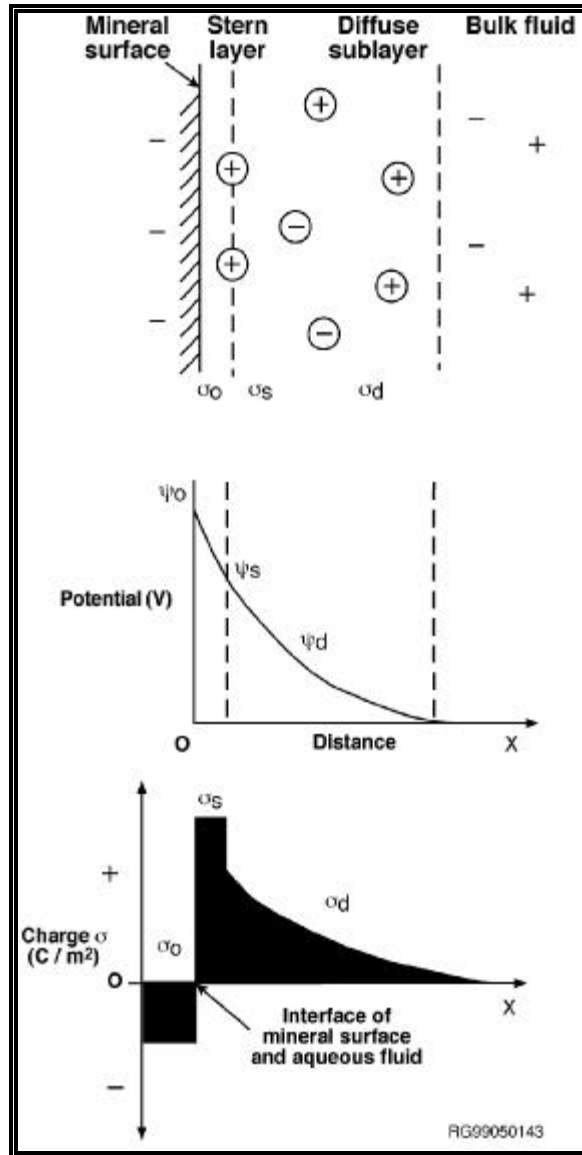


Figure 2.1. Diffuse double layer and surface charge of a mineral surface. (σ_0 , σ_s , and σ_d represent the surface charge at the surface, Stern layer, and diffuse layer, respectively; ψ_0 , ψ_s , and ψ_d represent the potential at the surface, Stern layer, and diffuse layer, respectively.)

As noted previously, the relative affinity of an adsorbent for a free-metal cation will generally increase with the tendency of a cation to form inner-sphere surface complexes, which in turn increases with higher ionic potential of a cation (Sposito, 1989). Based on these considerations and laboratory observations, the relative-adsorption affinity of metals has been described as follows (Sposito, 1989):



With respect to transition metal cations, however, ionic potential is not adequate as a single predictor of adsorption affinity, since electron configuration plays a very important role in the complexes of these cations. Their relative affinities tend to follow the Irving-Williams order:



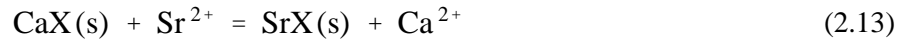
The molecular basis for this ordering is discussed in Cotton and Wilkinson (1972).

Adsorption of dissolved contaminants is very dependent on pH. As noted previously in the discussion of the pH of zero-point-of-charge, pH_{zpc} (Table 2.3), the magnitude and polarity of the net surface charge of a mineral changes with pH (Langmuir, 1997; Stumm and Morgan, 1981). At pH_{zpc} , the net charge of a surface changes from positive to negative. Mineral surfaces become increasingly more negatively charged as pH increases. At $\text{pH} < \text{pH}_{\text{zpc}}$, the surface becomes protonated, which results in a net positive charge and favors adsorption of contaminants present as dissolved anions. Because adsorption of anions is coupled with a release of OH^- ions, anion adsorption is greatest at low pH and decreases with increasing pH. At $\text{pH} > \text{pH}_{\text{zpc}}$, acidic dissociation of surface hydroxyl groups results in a net negative-charge which favors adsorption of contaminants present as dissolved cations. Because adsorption of cations is coupled with a release of H^+ ions, cation adsorption is greatest at high pH and decreases with decreasing pH. It should be noted that some contaminants may be present as dissolved cations or anions depending on geochemical conditions. In soil/groundwater systems containing dissolved carbonate, U(VI) may be present as dissolved cations (*e.g.*, UO_2^{2+}) at low to near-neutral pH values or as anions [*e.g.*, $\text{UO}_2(\text{CO}_3)_3^{4-}$] at near neutral to high pH values. The adsorption of U(VI) on iron oxide minerals (Waite *et al.*, 1994) is essentially 0 percent at pH values less than approximately 3, increases rapidly to 100 percent in the pH range from 5 to 8, and rapidly decreases to 0 percent at pH values greater than 9. This adsorption behavior for U(VI) (see Volume II) is reflected in the K_d values reported in the literature for U(VI) at various pH values.

It should also be noted that the adsorption of contaminants to soil may be totally to partially reversible. As the concentration of a dissolved contaminant declines in groundwater in response to some change in geochemistry, such as pH, some of the adsorbed contaminant will be desorbed and released to the groundwater.

2.2.3.1.1 Ion Exchange

One of the most common adsorption reactions in soils is ion exchange. In its most general meaning, an ion-exchange reaction involves the replacement of 1 ionic species on a solid phase by another ionic species taken from an aqueous solution in contact with the solid. As such, a previously sorbed ion of weaker affinity is exchanged by the soil for an ion in aqueous solution. Most metals in aqueous solution occur as charged ions and thus metal species adsorb primarily in response to electrostatic attraction. In the cation-exchange reaction:



Sr^{2+} replaces Ca^{2+} from the exchange site, X. The equilibrium constant (K_{ex}) for this exchange reaction is defined by the equation:

$$K_{\text{ex}} = \frac{\{\text{SrX(s)}\} \{\text{Ca}^{2+}\}}{\{\text{CaX(s)}\} \{\text{Sr}^{2+}\}} \quad (2.14)$$

There are numerous ion-exchange models and they are described by Sposito (1984) and Stumm and Morgan (1981). The original usage of K_d , often referred to as the thermodynamic K_d , is a special case of Equation 2.14. When one of the cations, such as Sr as the ^{90}Sr contaminant, is present at trace concentrations, the amount of Ca on the exchange sites CaX(s) remains essentially constant, as does Ca^{2+} in solution. These two terms in Equation 2.14 can thus be replaced by a constant and

$$K_d = \frac{\{\text{SrX(s)}\}}{\{\text{Sr}^{2+}\}} \quad (2.15)$$

The ranges of cation exchange capacity (CEC, in milliequivalents/100 g) exhibited by several clay minerals are listed in Table 2.4 based on values tabulated in Grim (1968).

2.2.3.2 Precipitation

The precipitation reaction of dissolved species is a special case of the complexation reaction in which the complex formed by 2 or more aqueous species is a solid. Precipitation is particularly important to the behavior of heavy metals (*e.g.*, nickel and lead) in soil/groundwater systems. As an example, consider the formation of a sulfide precipitate with a bivalent radionuclide cation (M^{2+}):



Table 2.4. Cation exchange capacities (CEC) for several clay minerals (Grim, 1968).

Mineral	CEC (milliequivalents/100 g)
Chlorite	10 - 40
Halloysite · 2H ₂ O	5 - 10
Halloysite · 4H ₂ O	40 - 50
Illite	10 - 40
Kaolinite	3 - 15
Sepiolite-Attapulgite-Palygorskite	3 - 15
Smectite	80 - 150
Vermiculite	100 - 150

The equilibrium constant, $K_{r,T}$, corresponding to Equation 2.16 is:

$$K_{r,T} = \frac{\{M(HS)_2(s)\}}{\{M^{2+}\} \{HS^-\}^2} = \frac{1}{\{M^{2+}\} \{HS^-\}^2} \quad (2.17)$$

By convention, the activity of a pure solid phase is set equal to unity (Stumm and Morgan, 1981). The solubility product, $K_{sp,T}$, corresponding to dissolution form of Equation 2.16 is thus:

$$K_{sp,T} = \{M^{2+}\} \{HS^-\}^2 . \quad (2.18)$$

Precipitation of radionuclides is not likely to be a dominant reaction in far-field (*i.e.*, a distance away from a point source) or non-point source plumes because the contaminant concentrations are not likely to be high enough to push the equilibrium towards the right side of Equation 2.16. Precipitation or coprecipitation is more likely to occur in the near field as a result of high salt concentrations in the leachate and large pH or pE gradients in the environment. Coprecipitation is the simultaneous precipitation of a chemical element with other elements by any mechanism (Sposito, 1984). The 3 broad types of coprecipitation are inclusion, absorption, and solid solution formation.

Solubility-controlled models assume that a known solid is present or rapidly forms and controls the solution concentration in the aqueous phase of the constituents being released. Solubility models are thermodynamic equilibrium models and typically do not consider the time (*i.e.*, kinetics) required to dissolve or completely precipitate. When identification of the likely controlling solid is difficult or when kinetic constraints are suspected, empirical solubility experiments are often performed to gather data that can be used to generate an empirical solubility release model.¹ A solubility limit is not a constant value in a chemically dynamic system. That is, the solubility limit is determined by the product of the thermodynamic activities of species that constitute the solid (see Equation 2.18). If the system chemistry changes, especially in terms of pH and/or redox state, then the individual species activities likely change. For example, if the controlling solid for plutonium is the hydrous oxide Pu(OH)₄, the solubility product, K_{sp}, (as in Equation 2.18) is the plutonium activity multiplied by the hydroxide activity taken to the fourth power, *i.e.*, {Pu}{OH}⁴ = solubility product. The solubility product is fixed, but the value of {Pu} and {OH} can vary. In fact, if the pH decreases 1 unit ({OH} decreases by 10), then for K_{sp} to remain constant, {Pu} must increase by 10⁴, all else held constant. A true solubility model must consider the total system and does not reduce to a fixed value for the concentration of a constituent under all conditions. Numerous constant concentration (*i.e.*, empirical solubility) models are used in performance assessment activities that assume a controlling solid and fix the chemistry of all constituents to derive a fixed value for the concentration of specific contaminants. The value obtained is only valid for the specific conditions assumed.

When the front of a contaminant plume comes in contact with uncontaminated groundwater, the system enters into nonequilibrium conditions. These conditions may result in the formation of insoluble precipitates which are best modeled using the thermodynamic construct, K_{sp} (*i.e.*, the solubility product described in Equation 2.18). Precipitation is especially common in groundwater systems where the pH sharply increases. Additionally, soluble polymeric hydroxo solids of metallic cations tend to form as the pH increases above 5 (Morel and Hering, 1993). At pH values greater than 10, many transition metals and transuranic hydroxide species become increasingly more soluble. The increase in solubility results from the formation of anionic species, such as Fe(OH)₄⁻, UO₂(CO₃)₂²⁻, or UO₂(CO₃)₃⁴⁻. A demonstration calculation of the solubility of U(VI) as a function of pH is given in Chapter 5. As the pH of the plume decreases from values greater than 11 to ambient levels below approximately pH 8, some metal hydroxo solids, such as NpO₂ (s) and Fe(OH)₃ (s), may precipitate. The solubility behaviors of the contaminants included in the first phase of this project are discussed in detail in the geochemistry background sections in Volume II of this report.

¹ An empirical solubility release model is a model that is mathematically similar to solubility, but has no identified thermodynamically acceptable controlling solid.

2.3 Sorption Models

2.3.1 Constant Partition Coefficient (K_d) Model

The constant partition coefficient, K_d , is a measure of sorption and is defined as the ratio of the quantity of the adsorbate (*i.e.*, metal or radionuclide) adsorbed per unit mass of solid to the quantity of the adsorbate remaining in solution at equilibrium. For the reaction



the mass action expression for K_d (typically in units of ml/g) is

$$K_d = \frac{A_i}{C_i} \quad (2.20)$$

where A = free or unoccupied surface adsorption sites,
 C_i = total dissolved adsorbate remaining in solution at equilibrium ($\mu\text{g/ml}$), and
 A_i = adsorbate on the solid at equilibrium ($\mu\text{g/g}$).

Describing the K_d in terms of this simple reaction assumes that A is in great excess with respect to C_i and that the activity of A_i is equal to 1. The K_d term is valid only for a particular adsorbent and applies only to those aqueous chemical conditions (*e.g.*, adsorbate concentration, solution/electrolyte matrix, temperature) in which it was measured. Also inherent in the K_d term are the assumptions that the system is reversible and is independent of the adsorbate concentration in the aqueous phase.

Essentially all of the assumptions associated with the thermodynamically defined K_d value (Equation 2.20) are violated in the common protocols used to measure K_d values for use in contaminant transport codes. Typically, the K_d for a given adsorbent is determined in the laboratory using soil from the study area and actual or simulated groundwater to which an adsorbate is added at some trace concentration. The values of C_i and A_i are operationally defined as the adsorbate concentrations measured in the fractions that passed through or were retained by, respectively, filtration by some known filter pore size, such as 0.45- μm diameter. An important practical limitation of the measurement of K_d values is that the total concentration or radioactivity of the adsorbate is measured, thereby treating the adsorbate as a single species. This assumption is not an inherent requirement, but it is generally applied for convenience. A hypothetical example of the species measured in a neptunium K_d experiment are presented in Equation 2.21:

$$K_d = \frac{\sum_{n=1}^{\infty} \{ \text{NpO}_2\text{X(s)} \} + \{ \text{NpO}_2\text{Y(s)} \} + \{ \text{NaNpO}_2(\text{CO}_3)(\text{s}) \} + \{ \text{Na}_3\text{NpO}_2(\text{CO}_3)_2(\text{s}) \} + \dots}{\sum_{n=1}^{\infty} \{ \text{NpO}_2^+ \} + \{ \text{NpO}_2(\text{OH})_2^+ \} + \{ \text{NpO}_2(\text{OH})^-(\text{aq}) \} + \{ \text{NpO}_2(\text{CO}_3)_2^{2-} \} + \dots} \quad (2.21)$$

where { } indicate activity, and X and Y are 2 different mineral species. The solid phase in this example contains 4 solid neptunium species, including the species adsorbed to species X and Y and the species precipitated as $\text{NaNpO}_2(\text{CO}_3)$ and $\text{Na}_3\text{NpO}_2(\text{CO}_3)_2$. The dissolved phase in this example contains 4 neptunium species including NpO_2^+ , $\text{NpO}_2(\text{OH})_2^-$, $\text{NpO}_2(\text{OH})^-$ (aq), and $\text{NpO}_2(\text{CO}_3)_2^{2-}$. Using common laboratory techniques, experimentalist would not be able to measure the concentrations of each of these dissolved and solid phases. Consequently, the experimentalist can not distinguish between adsorbed and precipitated species. In this example, there are more than just 1 dissolved and sorbed species, thereby violating an important assumption underlying the K_d value. Furthermore, many solutes have been observed to sorb more readily than desorb from mineral or organic surfaces, a phenomena referred to as hysteresis.

In chemistry, the term conditional K_d is often used (Jenne, 1977) to identify experimentally derived partition coefficients that may not necessarily denote an equilibrium value or require some of the other assumptions inherent in the more rigorous use of the K_d term. The definition of conditional K_d is given in Equation 2.22:

$$\text{Conditional } K_d = \frac{\sum_{n=1}^{\infty} A_i}{\sum_{n=1}^{\infty} C_i} \quad (2.22)$$

where A_i = sorbed species
 C_i = dissolved species.

Compared to Equation 2.20, Equation 2.22 more clearly represents the example represented by Equation 2.21. No attempt will be made in this text to distinguish between the true thermodynamic and the conditional K_d .

An important limitation of the constant K_d model is that it does not address sensitivity to changing conditions. If the groundwater properties (*e.g.*, pH and solution ionic strength) change, a different K_d value should be used in the model. This limitation will be discussed further in Section 2.2.3.2.

Chemical retardation, R_f , is defined as,

$$R_f = \frac{v_p}{v_c}, \quad (2.23)$$

where v_p = velocity of the water through a control volume
 v_c = velocity of contaminant through a control volume.

The chemical retardation term does not equal unity when the solute interacts with the soil; almost always the retardation term is greater than 1 due to solute sorption to soils. In rare cases, the retardation factor is actually less than 1, and such circumstances are thought to be caused by anion exclusion (Section 2.8). To predict the effects of retardation, sorption processes must be described in quantitative terms. The K_d provides such a quantitative estimate. Knowledge of the K_d and of media bulk density and porosity for porous flow, or of media fracture surface area, fracture opening width, and matrix diffusion attributes for fracture flow, allows calculation of the retardation factor. For porous flow with saturated moisture conditions, the R_f is defined as

$$R_f = 1 + \frac{\rho_b}{n_e} K_d \quad (2.24)$$

where ρ_b = porous media bulk density (mass/length³)
 n_e = effective porosity of the media at saturation.

For 1-dimensional advection-dispersion flow with chemical retardation, the transport equation can be written as

$$\frac{\partial C_i}{\partial t} = \frac{\left[D_x \frac{\partial^2 C_i}{\partial x^2} - v_x \frac{\partial C_i}{\partial x} \right]}{R_f(i)} \quad (2.25)$$

where C_i = concentration of contaminant species I in solution (mass/length³),
 D_x = dispersion coefficient of species I (length²/time),
 v_x = pore velocity of groundwater (length/time), and
 $R_f(i)$ = retardation factor for species i.

For simplicity, radioactive decay has been omitted from Equation 2.25.

When the K_d term is incorporated into the retardation factor, R_f , as in Equation 2.24, the R_f term is also devoid of sorption mechanism, *i.e.*, adsorption, absorption, or precipitation can not be distinguished from one another as the mechanism by which the contaminants partitioned to the solid phase. Furthermore, incorporating the K_d term into the R_f term assumes implicitly that the reactions go to equilibrium and are reversible and that the chemical environment along the solute flow path does not vary in either space or time (Muller *et al.*, 1983). Although these assumptions rarely hold true in the natural environment, single-value model parameters are generally employed, with the justification that the approach builds conservatism into the analysis. Additionally, the paucity of geochemical data at most sites precludes a more rigorous conceptual model (Section 2.3.3).

2.3.2 Parametric K_d Model

Clearly, the greatest limitation of using K_d values to calculate retardation terms (Equation 2.24) is that it describes solute partitioning between the aqueous and solid phases for only 1 set of environmental conditions. Such homogeneity does not exist in nature and therefore greatly compromises the usefulness of the constant. For example, when the aqueous phase chemistry was varied, americium K_d values in a Hanford sediment ranged from 0.2 to 53 ml/g, roughly a 200-fold range (Delegard and Barney, 1983). Additional variability in the americium K_d values, albeit less, were observed when slightly different Hanford sediments were used: 4.0 to 28.6 ml/g (Delegard and Barney, 1983: Solution 1). Using similar aqueous phases but diverse soils, Sheppard *et al.* (1976) measured americium K_d values ranging from 125 to 43,500 ml/g.

Another practical conceptual model for adsorption is called the parametric K_d model. The K_d value in this model varies as a function of empirically derived relationships with aqueous and solid phase independent parameters. Thus, it has the distinct advantage of being more robust and removes the burden of determining new K_d values for each environmental condition. Because the value of a K_d term is a function of a large number of variables, it is common to systematically vary several parameters simultaneously in 1 experimental study. Factorial design strategies are most often invoked to determine the systematic change resulting from varying the independent variables on the dependent variables, typically the partition coefficient (Box and Behnken, 1960; Cochran and Cox, 1957; Davies, 1954; Plackett and Burman, 1946). Statistical methods commonly used to derive quantitative predictor equations include standard linear or nonlinear regression (Snedecor and Cochran, 1967), stepwise regression (Hollander and Wolfe, 1973), and adaptive-learning networks (Mucciardi *et al.*, 1979, 1980). All these techniques have been used to develop empirical relationships describing K_d values in terms of other variables (Routson and Serne, 1972; Serne *et al.*, 1973; Routson *et al.*, 1981; Delegard and Barney, 1983).

The empirical predictor equations commonly take the form of a nonlinear polynomial expression. For example, after evaluating solutions consisting of several sodium salts, organic chelates, and acids, Delegard and Barney (1983) derived with the following expression for an americium K_d value:

$$\text{Log } K_d (\text{Americium}) = 2.0 + 0.1[\text{NaOH}] - 26.8[\text{HEDTA}] + 153.4[\text{HEDTA}]^2 \quad (2.26)$$

Numerous salts were found to have no significant effect on americium K_d values and therefore were not included in the expression. Delegard and Barney (1983) also evaluated higher exponential and logarithmic terms and determined that these terms did not improve the predictive capabilities of the expression (*i.e.*, the regression coefficients were not significant at $P \leq 0.05$).

It is critical that parametric K_d equations, such as Equation 2.26, be used to calculate K_d values for systems only within the range of the independent variables used to create the equation. In the case of Equation 2.26, the range of independent variables used to generate the model were selected to simulate a plume emanating from a steel-lined concrete tank that contained strong

caustic and high sodium contents. Using Equation 2.26 to generate americium K_d values for a plume low in pH and sodium concentrations would not be appropriate.

These types of statistical relationships are devoid of causality and therefore provide no certain information on the mechanism by which the radionuclide partitioned to the solid phase, whether it be by adsorption, absorption, or precipitation. For example, the statistical analyses may suggest a very strong relationship between pH and the K_d term, when the actual sorption process may be controlled by iron oxide adsorption. Because pH and the surface charge of iron oxides are covariants, a statistical relationship could be calculated, suggesting that sorption is solely caused by pH.

The parametric K_d model can be used in the retardation factor term (Equation 2.24) and the transport equation (Equation 2.25). When used in the transport equation, the code must also keep track of the current value of the independent variables (*e.g.*, [NaOH] and [HEDTA])¹ for the examples described in Equation 2.26) at each point in space and time to continually update the concentration of the independent variables affecting the K_d value. Thus, the code must track many more parameters, and some numerical solving techniques (*e.g.*, closed-form analytical solutions) can no longer be used to perform the integration necessary to solve for contaminant concentration. Generally, computer codes that can accommodate the parametric K_d model use a chemical subroutine to update the K_d value used to determine the R_f , when called by the main transport code. The added complexity in solving the transport equation with the parametric K_d sorption model and its empirical nature may be the reasons this approach has been used sparingly.

2.3.3 Isotherm Adsorption Models

Some adsorption studies are conducted in a systematic fashion to evaluate the effects of various parameters on K_d . The results of a suite of experiments evaluating the effect of contaminant concentration on adsorption, while other parameters are held constant, are called an “adsorption isotherm.” For soils, it is common knowledge that contaminant adsorption can deviate from the linear relationship required by the K_d construct discussed in Section 2.3.1. If it was possible to keep increasing the amount of contaminant in solution contacting soil, all adsorption sites would become saturated at some contaminant concentration and the linear relationship between contaminant adsorbed to contaminant in solution would no longer hold. Isotherm models are used to describe the case where sorption relationships deviate from linearity. For many short-lived radionuclides, the mass present never reaches quantities large enough to start loading surface adsorption sites to the point that the linear K_d relationship is not accurate. However, long-lived radionuclides and stable elements, such as RCRA-regulated metals, can be found in leachates and groundwaters near waste sources at concentrations large enough to affect the saturation of surface adsorption sites.

¹ HEDTA is N-(2-hydroxyethyl) ethylenediaminetetraacetic acid.

In situations where the amount of contaminant loaded on the available adsorption sites is large enough to impact the linear adsorption construct, isotherm models are often invoked. Three adsorption isotherm models used frequently are the Langmuir, Freundlich, and Dubinin-Radushkevich models.

The Langmuir model was originally proposed to describe adsorption of gas molecules onto homogeneous solid surfaces (crystalline materials) that exhibit one type of adsorption site (Langmuir, 1918). Many investigators have tacitly extended the Langmuir adsorption model to describe adsorption of solution species onto solid adsorbents including heterogeneous solids such as soils. The Langmuir model for adsorption is

$$A_i = \frac{K_L A_m C_i}{1 + K_L C_i} \quad (2.27)$$

where A_i = amount of adsorbate adsorbed per unit mass of solid
 K_L = Langmuir adsorption constant related to the energy of adsorption
 A_m = maximum adsorption capacity of the solid
 C_i = equilibrium solution concentration of the adsorbate.

Substituting $1/B$ for K_L , one obtains

$$A_i = \frac{A_m C_i}{B + C_i} \quad (2.28)$$

A plot of values for A_i (y-axis) versus values of C_i (x-axis) passes through the origin and is nearly linear at low values of C_i . As C_i increases, A_i should approach A_m . Taking the reciprocal of Equation 2.28 and multiplying both sides of the equation by $A_i \cdot A_m$ yields

$$A_i = -B \frac{A_i}{C_i} + A_m \quad (2.29)$$

Then, by plotting A_i on the y-axis and (A_i/C_i) on the x-axis, one can determine the value of $-B$ from the slope of the best fit line and the value of A_m from the intercept. Sposito (1984) and Salter *et al.* (1981a) cite several instances where the Langmuir isotherm has successfully fit trace adsorption by natural substrates. Further Sposito (1984) and Salter *et al.* (1981b) discuss modifications of the Langmuir model to accommodate 2 distinct sites and competition of 2 adsorbates (the nuclide and the ion it replaces on the adsorbent) which further extend this conceptual model's usefulness on natural substrates. In the parlance of Giles *et al.* (1974) [also see Sposito (1984)], the Langmuir adsorption isotherm is the L-curve. For L-curve isotherms, the initial slope of A_i (amount of solute adsorbed per unit mass of solid) [plotted on the y-axis] versus C_i (equilibrium solution concentration of the adsorbate) [plotted on the x-axis] is large, but the slope decreases as C_i increases. This forms the concave shaped curve shown in Figure 2.2. The various curves depicted in Figure 2.2 are discussed in greater detail later in this section.

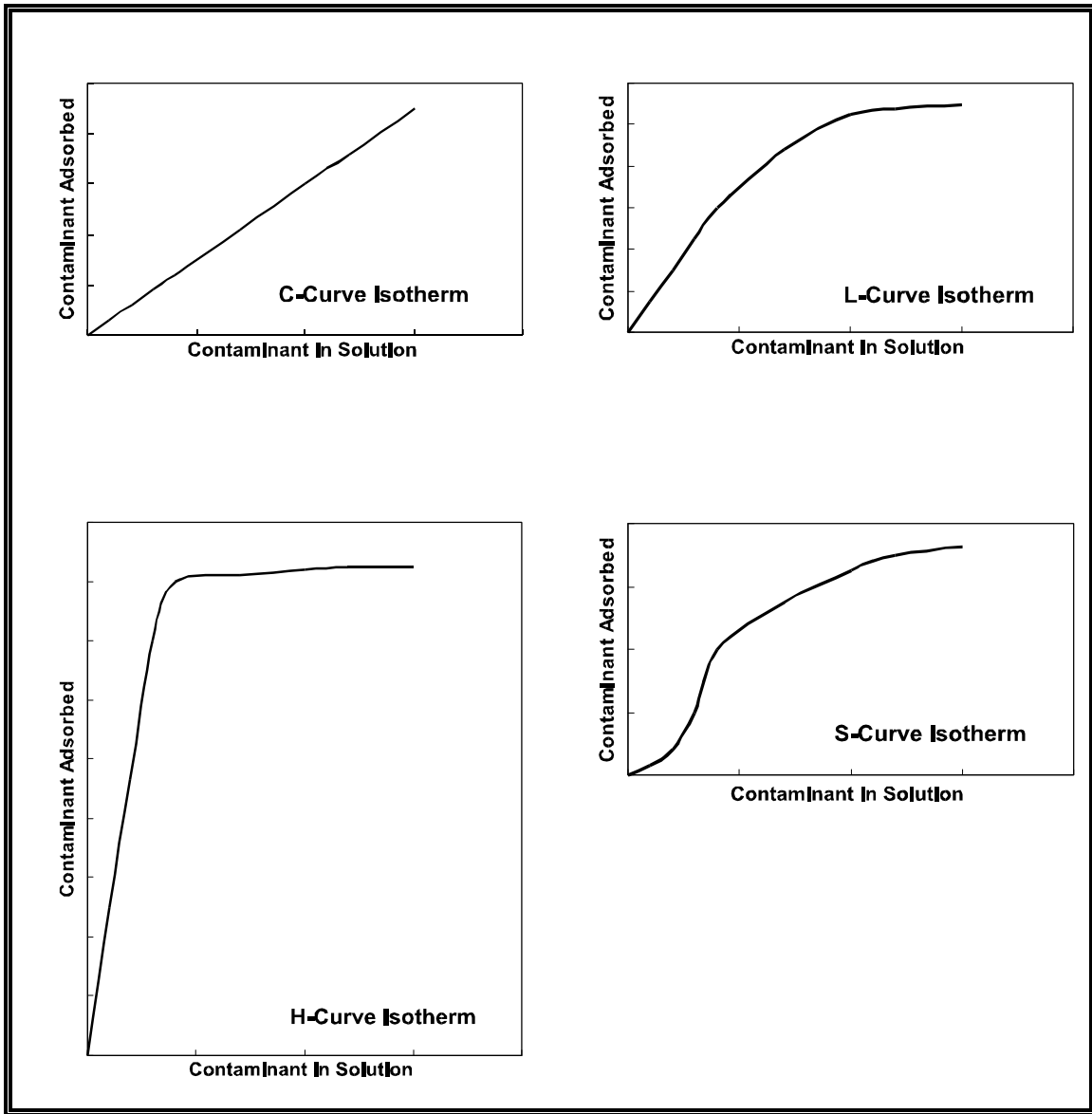


Figure 2.2. Four types of adsorption isotherm curves shown schematically in parlance of Giles *et al.* (1974).

The Freundlich isotherm model (Freundlich, 1926) is defined as:

$$A_i = K_F C_i^N \quad (2.30)$$

where A_i = amount of adsorbate adsorbed per unit mass of solid
 C_i = equilibrium solution concentration of the adsorbate
 K_F = Freundlich adsorption constant
 N = constant.

The Freundlich equation is sometimes written with the exponent in Equation 2.30 being $1/N$ instead of N . The Freundlich model does not account for finite adsorption capacity at high concentrations of solute, but when considering trace constituent adsorption, ignoring such physical constraints is usually not critical. The Freundlich isotherm can be transformed to a linear equation by taking the logarithms of both sides of Equation 2.30:

$$\log A_i = \log K_F + N \log C_i \quad (2.31)$$

When $\log A_i$ is plotted on the y-axis and $\log C_i$ on the x-axis, the best-fit straight line has a slope of N , and $\log K_F$ is its intercept. When $N=1$, the Freundlich isotherm, represented by Equation 2.31 reduces to a linear relationship. Because A_i/C_i is the ratio of the amount of solute adsorbed to the equilibrium solution concentration (the definition of K_d), the Freundlich K_F is equivalent to the value of K_d .

Because adsorption isotherms at very low solute concentrations are often linear, either the Freundlich isotherm with N equaling 1 or the Langmuir isotherm with $K_L \cdot C_i$ much greater than 1 fits the data. The value of N for the adsorption of many radionuclides is often significantly different from 1, such that nonlinear isotherms are observed. In such cases, the Freundlich model is a better predictor than the Langmuir model. Sposito (1984) shows how the Freundlich isotherm is equivalent to the Langmuir isotherm where the parameter K_F is log normally distributed. Sposito (1984) also stresses that the Freundlich isotherm only applies to data obtained at low values of C_i (concentration of contaminant in the equilibrium solution).

A third adsorption model that has been used recently in nuclide studies is the Dubinin-Radushkevich isotherm (Dubinin and Radushkevich, 1947). This model is applicable for the adsorption of trace constituents. Should the adsorbent surface become saturated or the solute exceed its solubility product, the model is inappropriate. The Dubinin-Radushkevich model is more general than the Langmuir model, because it does not require either homogeneous adsorption sites or constant adsorption potential. Its mathematical form is

$$A_i = A_m e^{-K_{DR} \epsilon^2} \quad (2.32)$$

where A_i = observed amount of adsorbate adsorbed per unit mass
 A_m = sorption capacity of adsorbent per unit mass

- K_{DR} = Dubinin-Radushkevich adsorption constant
 ϵ = $RT \ln(1 + 1/C_i)$
 R = gas constant
 T = temperature (in Kelvin)
 C_i = equilibrium solution concentration of the adsorbate.

The Dubinin-Radushkevich equation can be transformed to

$$\ln A_i = \ln A_m - K_{DR} \epsilon^2 \quad (2.33)$$

A plot of $\ln A_i$ (y-axis) versus ϵ^2 (x-axis) allows the estimation of $\ln A_m$ as the intercept and $-K_{DR}$ as the slope of the resultant straight line. Ames *et al.* (1982) successfully used this model to describe adsorption of uranium and cesium onto basalt and its weathering products.

All 3 isotherm models can be compared against data from experiments that systematically vary the mass of a trace constituent or radionuclide while holding all other parameters as constant as possible. It is important to consider the total mass of the element present, including all stable and other radioactive isotopes, when evaluating isotherms. It is incorrect to calculate isotherms based on only one isotope if the system includes several (both stable and radioactive) for a particular element. For convenience, isotherm experiments tend to consider only the total concentration or radioactivity content and thus lumps all species for a given isotope.

It can be argued that all 3 isotherm models are based on physicochemical processes or mechanisms. If the experiments are performed and characterized rigorously to assure equilibrium conditions and constancy of variables aside from the trace constituent concentration, then the resultant isotherm constants undoubtedly have some relationship to adsorption capacities and to site adsorption energies. On the other hand, any suite of experiments that can be plotted as amount adsorbed versus amount in solution at the time of measurement can also be analyzed using these models to see whether predictive equations can be determined. The latter empirical approach is a step up in sophistication over the constant K_d model.

Giles *et al.* (1974) state that isotherm shapes are largely determined by the adsorption mechanism, and thus can be used to explain the nature of adsorption. The S-curve (Figure 2.2) is explained by Giles *et al.* (1974) as adsorption where the presence of the individual solute molecules bound to the solid interact with each other. This increases the strength of the individual solute bonds to the solid surface when the solid has low contaminant loading. Thus, for a brief period during adsorption, the first bound molecules enhance adsorption of the next molecules that bind to the solid. The slope of the isotherm increases from the lowest concentration of contaminant where surface coverage is so sparse that adsorbed molecules cannot interact. At some point, the sites become laden with contaminant and the slope of the adsorption isotherm starts decreasing again. Sposito (1984) gives another plausible explanation for the S-curve, wherein complexing solution ligands compete with the surface sites for the contaminant until the complexing ligands are

complexed with the contaminant and additional contaminant is free to adsorb with less or no complexant competition.

The L-curve (Figure 2.2) is the classical Langmuir curve where the loading of contaminant on the solid starts to decrease the adsorption slope as sites become saturated. The adsorption of many RCRA-regulated metals and long-lived radionuclides on soils have been successfully described by Langmuir isotherms. Giles *et al.* (1974) shows that the L-shaped curve is found for systems where the activation energy for the adsorption/desorption of each adsorbate is unaffected by the other adsorbates and solvent (water) in the systems. Rai and Zachara (1984) include one compilation of Langmuir isotherms for RCRA-regulated metals.

The H-curve (Figure 2.2) is an extreme version of the L-curve isotherm. The H-curve describes adsorption of “high-affinity” adsorbates onto solid adsorbents. The activation energy of the desorption of the analyte of interest is much larger than other species in the solution.

The C-curve (constant slope) (Figure 2.2) suggests that the number of available sorption sites remains constant throughout the whole range of solute concentrations (whereas the K_d model applies to low solute concentrations) or the available surface expands proportionally with the amount of material adsorbed up to the point where all adsorption sites are filled. Giles *et al.* (1974) discuss two conceptual models on how the available sorption sites can expand in proportion to the adsorbed mass. The model where the adsorbent is microporous and the adsorbate has a much higher affinity for the adsorbent surfaces than the water is most germane for soils. The adsorbates enter the microporous solid and act like a molecular wedge to open up more sorption sites through continued penetration.

It is difficult to assess whether one should put much weight on isotherm shape constructs discussed by Giles *et al.* (1974) as a vehicle to elaborate on adsorption mechanisms. The number of discrete crystalline minerals and amorphous phases and coatings present in soils as well as the multitude of inorganic and organic ligands found or expected in soil solutions combine to make a quantitative description of contaminant adsorption and the controlling mechanisms a formidable activity. To quote Sposito (1984, pg. 122), “The adherence of experimental sorption data to an adsorption isotherm provides no evidence as to the actual mechanism of the sorption process in soils and sediments.” We value this statement and suggest that isotherms are just one step more sophisticated than the constant K_d construct in delineating or quantifying adsorption of contaminants.

It must be stressed that isotherm models, as expressed by Equations 2.27, 2.30, and 2.32, explicitly consider dependency of the partition coefficient on only the solution concentration of the contaminant of interest. Isotherm models do not consider dependence on other solid and solution parameters that can influence adsorption, such as those discussed in Volume II for each contaminant of interest.

The incorporation of adsorption isotherm models into transport codes is relatively easy. Each of the aforementioned isotherm equations can be rearranged to calculate a partition coefficient, K_d , that is a function of C , the solution concentration of the radionuclide, and 1 or 2 constants. As the transport model solves for C , substitution of an equation that depends only upon C (and derivable constants) for the K_d in the retardation factor (see Equations 2.23 and 2.24) should be straightforward. For simple cases, analytical closed-form solutions are possible, or numerous numerical approximation schemes can be used. Thus, with little additional work or increases in computer storage requirements, most transport codes can be formulated to predict radionuclide migration with an adsorption isotherm model. It should be repeated, however, that this approach accounts for the dependency of K_d on only one parameter, the concentration of the radionuclide. If the mass of contaminant in the environment is low, and complicating factors such as complexing agents and type S sorption behavior are not expected, all 3 adsorption isotherms discussed above are readily simplified to the constant K_d model.

2.3.4 Mechanistic Adsorption Models

Mechanistic models explicitly accommodate for the dependency of K_d values on contaminant concentration, competing ion concentration, variable surface charge on the adsorbent, and solute species solution distribution. Incorporating mechanistic, or semi-mechanistic, adsorption concepts into transport models is attempted because the models become more robust and, perhaps more importantly from the standpoint of regulators and the public, scientifically defensible. However, less attention will be directed to these adsorption models because we judge them of little practical use for the majority of site-screening applications. The complexity of installing these mechanistic adsorption models into existing transport codes is difficult to accomplish. Additionally, mechanistic adsorption models also require a more intense and costly data collection effort than will likely be available to the majority of EPA, DOE, and NRC contaminant transport modelers and site remediation managers. A brief description of the state of the science is presented below. References to excellent review articles have been included in the discussion to provide the interested reader with additional information.

Experimental data on interactions at the mineral-electrolyte interface can be represented mathematically through 2 different approaches: (1) empirical models and (2) mechanistic models. An empirical model can be defined as a mathematical description of the experimental data without any particular theoretical basis. For example, the K_d , Freundlich isotherm, Langmuir isotherm, Langmuir Two-Surface Isotherm, and Competitive Langmuir construct are considered empirical models by this definition (Sposito, 1984). Mechanistic models refer to models based on thermodynamic concepts such as reactions described by mass action laws and material balance equations. Four of the most commonly used mechanistic models include the Helmholtz, Gouy-Chapman, Stern, and Triple Layer models (Sposito, 1984). The empirical models are often mathematically simpler than mechanistic models and are suitable for characterizing sets of experimental data with a few adjustable parameters, or for interpolating between data points. On the other hand, mechanistic models contribute to an understanding of the chemistry at the interface and are often useful for describing data from complex multicomponent systems for

which the mathematical formulation (*i.e.*, functional relationships) for an empirical model might not be obvious. Mechanistic models can also be used for interpolation and characterization of data sets in terms of a few adjustable parameters (Westall, 1986). However, it is important to realize that adjustable parameters are required for both mechanistic and empirical models, except the K_d model. The need to include adjustable parameters in order to apply/solve mechanistic models compromises their universal application.

Any complete mechanistic description of chemical reactions at the mineral-electrolyte interface must include a description of the electrical double layer (Figure 2.1). While this fact has been recognized for years, a satisfactory description of the double layer at the mineral-electrolyte interface still does not exist. Most electrical double layer models were written for specific conditions and are only accurate under limited environmental conditions. For instance, the Stern model is a better model for describing adsorption of inner-sphere complexes, whereas the Gouy-Chapman model is a better model for describing outer-sphere or diffuse swarm adsorption (Sposito, 1984; Westall, 1986) (Figure 2.1).

Truly mechanistic models are rarely, if ever, applied to complex natural soils (Schindler and Sposito, 1991; Sposito, 1984; Westall and Hohl, 1980; Westall, 1986; Westall, 1994). The primary reason for this is because the surfaces of natural mineral are very irregular and difficult to characterize. These surfaces consist of different microcrystalline structures and/or coatings of amorphous phases that exhibit quite different and complex chemical properties when exposed to solutions. Thus, examination of the surface by virtually any experimental method yields only averaged characteristics of the surface and the interface. Parsons (1982) discussed the surface chemistry of single crystals of pure metals and showed that the potential of zero charge of different crystal faces of the same pure metal can differ by over 400 mV. For an oxide surface, this difference was calculated by Westall (1986) to be energetically equivalent to a variation in the pH of zero-point-of-charge (pH_{zpc}) of more than 6 pH units. This example indicated that an observable macroscopic property of a polycrystalline surface might be the result of a combination of widely different microscopic properties and that characterizations of these surfaces will remain somewhat operational in nature.

Another fundamental problem encountered in characterizing reactions at the mineral-electrolyte interface is the coupling between electrostatic and chemical interactions, which makes it difficult to distinguish the effects of one from the effects of the other. Westall and Hohl (1980) have shown that many models for reactions at the mineral-electrolyte interface are indeterminate in this regard.

2.4 Effects of Unsaturated Conditions on Transport

The major pathway for contaminant transport in arid areas is through unsaturated soils. Although considerable effort has been expended over the past few years to quantify the mobility of contaminants and determine factors that influence contaminant mobility, little work has been done to investigate the transport of radionuclides under conditions of partial saturation.

At unsaturated moisture conditions, the pores are partially filled with air and water. The water in the pores is partly held in place by attractive forces of capillarity. A key hydrologic measurement in unsaturated (vadose zone) soils is the soil-water matric potential (or suction). Matric potential is defined as, the amount of work that must be done per unit of soil solution in order to transport, reversibly and isothermally, an infinitesimal quantity of water from a pool of soil solution at a given elevation above the water table (and at atmospheric pressure) to the soil pores at the same elevation and pressure (SSSA, 1997). When the work (or energy) is expressed on a weight basis, the matric potential is expressed in units of length (*i.e.*, m or cm). Matric potential is always negative (*i.e.*, energy is gained in going from a saturated solution to unsaturated soil pores, because of adsorptive forces and capillarity of porous material). Matric suction is the absolute value of matric potential and is used for convenience to express the matric forces (potentials) as positive values. By definition, at the water table, both the matric potential and matric suction are zero.

Unsaturated flow properties include the unsaturated hydraulic conductivity and the water retention characteristics (relationship between water content and matric suction values). Analogous to saturated flow where the advective flux¹ is the product of the saturated hydraulic conductivity and the gradient of the hydrostatic head,² the advective flow in unsaturated sediments is the product of the unsaturated conductivity and the matric potential (or suction) gradient. The suction gradient defines the direction of flow (from areas of low to high suction). At most vadose zone sites there have been no direct measurements of either the unsaturated conductivity or water retention characteristics for sediments. Generally only water contents have been measured (often by neutron logging) in boreholes or from split-spoon samples.

When the soil is saturated, nearly all pores are filled and hydraulic conductivity is at a maximum. As the soil becomes unsaturated, some of the pores become air-filled and the conductive cross-sectional areas are decreased. In addition, the first pores to empty are the largest and most conductive and tortuosity is increased for any water molecule that is still actively advecting through the porous media (*i.e.*, the water must find less direct pathways around these empty pores). In unsorted soils, the large pores that resulted in high conductivity at saturation become barriers to liquid flow between smaller pores during unsaturated flow. Hence, the transition from saturated to unsaturated flow may result in a steep drop in hydraulic conductivity of several orders of magnitude as the tension increase from 0 to 1 bar. At higher tensions (*i.e.*, more unsaturation), conductivity may be so low that steep pressure gradients are required for any appreciable soil water flow to occur. An interesting corollary of the pore size-conductivity relationship is that at, or near, saturation, a sandy soil conducts water more rapidly than a clay soil with many micropores. When the soils are unsaturated, however, many of the micropores in the clay soil remain filled, and consequently, the hydraulic conductivity in the clay soil does not decrease nearly as sharply as it does in sandy soil under the same tension. If the soil water does

¹ The flux density is the volume of water flowing through a cross-section area per unit time.

² The hydraulic gradient is the head drop per unit distance in the flow direction.

not move, then the contaminant in, or contacted by, the soil water does not move except by diffusion (Section 2.6), which is a relatively slow process (Rancon, 1973).

In modeling contaminant transport in unsaturated conditions, Equation 2.24 takes the form:

$$R_f = 1 + \frac{\rho_b}{\theta} K_d \quad (2.34)$$

where θ , the volumetric water content of the soil (cm^3 water/ cm^3 total), replaces n (cm^3 void space/ cm^3 total), soil porosity, in Equation 2.24. Equation 2.27 explicitly assumes that the extent to which contaminants sorb to soils, the K_d value, is constant as a function of the volumetric water content. This relationship is convenient for modeling; however, its validity is not certain. There have been experiments to test this assumption, and the results have been mixed (Gee and Campbell, 1980; Knoll, 1960; Lindenmeier *et al.*, 1995; Nielsen and Biggar, 1961; Nielsen and Biggar, 1962; Routson and Serne, 1972).

There are theoretical reasons for believing that K_d values vary as a function of volumetric water content. First, as the soil becomes increasingly unsaturated there will be a smaller percentage of the total exchange sites in contact with the aqueous phase. For example, if only half of the exchange sites of a soil come into contact with the aqueous phase, then the effective exchange capacity of the soil is only half of that, had all the available exchange sites come into contact with the aqueous phase. Therefore, as less mineral surface is exposed to the aqueous phase, the lower the effective exchange capacity becomes because less of the surface is exposed to the solute of interest. On the other hand, the clay fraction of the soil constitutes the largest exchange capacity and smallest pore sizes. Because the smaller pores are involved in unsaturated flow, there may be little measurable effect on the exchange capacity of the soil in unsaturated conditions. Another reason for believing that K_d values would vary with degree of saturation is because in the unsaturated systems the aqueous phase is in closer contact with the soil surfaces. Solutes in the middle of large pores have less interaction with soil surfaces than solutes nearer to the soil surfaces. In unsaturated conditions, the middle of large pores tend to be empty, resulting in a greater percentage of pore water being in close contact with the soil surface. Finally, the ionic strength of the aqueous phase tends to increase closer to the clay surfaces. Thus, as a soil dehydrates, the system tends to have a higher ionic strength. The K_d value for many cations tends to decrease with increases in ionic strength.

The average size of individual pores is larger for coarse- versus fine-textured soils, despite the finer-grained soils having a larger total porosity. In saturated soil, all of the pore space is water-filled; the pores are continuous or “connected,” and generally water conducting. As a saturated soil is desaturated, the larger pores drain first, and air becomes a barrier to water flow. Water flow in unsaturated soils may occur as film flow along the particle surface, or as “matrix flow” through smaller, water-filled pores. The unsaturated flow regime is expected to differ in unsaturated coarse- versus fine-textured soils, with film flow dominating the former, and matrix flow the latter. This conceptualizations is illustrated in Figure 2.3. Recent improvements in

imaging technologies [*i.e.*, magnetic resonance imaging (MRI) and X-ray microtomography] have increased our ability to directly distinguish the distribution of water, such as films at the particle surface, pendular water forming a meniscus at the intersection of two particles, and water held in small pores. Improved imaging of the water distribution in unsaturated soils is increasing fundamental understanding of the unsaturated flow regime.

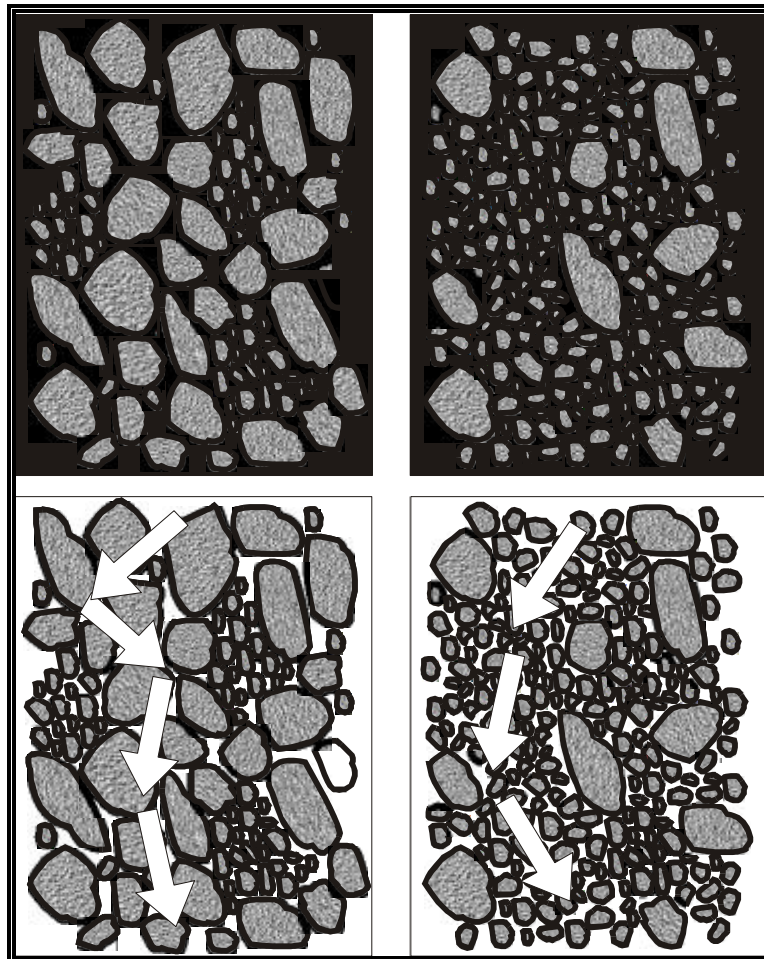


Figure 2.3. Schematic diagram for conceptual model of water distribution in saturated (top two figures) and unsaturated soils (bottom two figures) suggesting differences in the unsaturated flow regime (indicated by arrows) for soils with varying texture. [The two figures on left represent coarse-textured soils, whereas the two figures on the right represent fine-textured soils. Soil particles, air, and water are shown, respectively, in stippled gray, white, and black.]

As a soil is progressively desaturated, retained water is held with increasingly greater “suction,” expressed as the matric or negative pressure potential. Hydraulic conductivity, K_h (m/sec) reflects the ease of water flow through the media and decreases with decreasing moisture saturation (*i.e.*, greater resistance to flow at lower water contents). Hydraulic conductivity is also highly dependent on soil texture. Relationships between hydraulic conductivity, matric potential, and water content are well-established (Hillel, 1998; Jury *et al.*, 1991). The spatial variability of hydraulic conductivity and the effect on solute transport in saturated soils have been the subject of modeling investigations (*e.g.*, Dagan, 1984; Gelhar and Axness, 1983; Tompson and Gelhar, 1990). Various modeling approaches are reviewed by Koltermann and Gorelick (1996) and compared to field data by Sudicky (1986). For unsaturated soils, research has focussed on scaling, and the effect of spatially variable hydraulic conductivity on water flow, infiltration, and drainage (Hopmans *et al.*, 1988; Nielsen *et al.*, 1973; Peck *et al.*, 1977; Warrick and Amoozegar-Fard, 1979).

In unsaturated soils, the pathway for water flow can become more tortuous, and water held in films and in small pores can be “disconnected” with respect to the flow regime. In reviewing water flow and transport in the vadose zone, Nielsen *et al.* (1986) noted that in addition to water held within aggregates, immobile water may exist in thin liquid films around soil particles, in dead-end pores, or as relatively isolated regions associated with unsaturated flow. Immobile water is also apparent in saturated systems. Most investigations that consider mass transfer between mobile and immobile water regions have been conducted in saturated systems.

Immobile water is manifest as hydraulic heterogeneity, and is typically characterized with a “dual porosity” or “two-region” model (Coats and Smith, 1964; Haggerty and Gorelick, 1995; van Genuchten and Wierenga, 1976). The liquid phase is partitioned into mobile and immobile (stagnant or micro-porosity) regions, where advective solute transport is limited to the mobile water phase. The mobile water fraction, ϕ_m , is defined as the volume fraction of water associated with the mobile domain, θ_m , relative to the total water content, θ_v (*i.e.*, $\phi_m = \theta_m/\theta_v$). Transport in and out of the immobile water domain is diffusion-limited. A small degree of hydraulic heterogeneity can be characterized by increased hydrodynamic dispersion (Pickens *et al.*, 1981).

However, a 2-region flow regime is required as the fraction of stagnant water increases. The importance of particle scale properties (Ball *et al.*, 1990), specifically mass transfer between mobile and immobile water regions (Haggerty and Gorelick, 1995), in affecting larger-scale transport has been noted. Compared to the standard advection-dispersion model with sorption, physical models accounting for mobile-immobile water described better reactive solute transport in a field-scale natural gradient tracer study (Goltz and Roberts, 1986), although other factors contributing to non-ideal behavior may also be important (Brusseu, 1994).

The development of heterogeneous unsaturated flow, in non-aggregated porous media was suggested in several studies comparing the transport of non-sorptive tracers at various degrees of moisture saturation (Biggar and Nielsen, 1962; Bond and Wierenga, 1990; Nielsen and Biggar, 1961). The fraction of immobile water increased from 4 to 40 percent when water content was

decreased from 71 to 55 percent moisture saturation in a disturbed sand column (Gaudet *et al.*, 1977). It is important to note one study with contrasting results where a decrease in dispersion (heterogeneity) was observed when moisture content was reduced from 100 to 97 and 93 percent (Jardine *et al.*, 1993). This was observed in undisturbed cores and the effect was attributed to the elimination of macropore flow for the slightly unsaturated conditions. Changes in hydraulic heterogeneity at lower water contents were not evaluated.

Recent studies of unsaturated sands (Gamerding *et al.*, 1998, Gamerding and Kaplan, 1999) confirmed the findings of Gaudet *et al.* (1977). The development of an increasing fraction of immobile water (*i.e.*, decreasing ϕ_m) is illustrated in Figure 2.4 for sandy soils (filled diamond and square symbols). Data for a fine-textured soil (loamy fine sand, represented by the filled triangle in Figure 2.4) with a high ϕ_m is consistent with the conceptual model (above) that water held in the smaller pores of unsaturated fine-texture soils remains conductive.

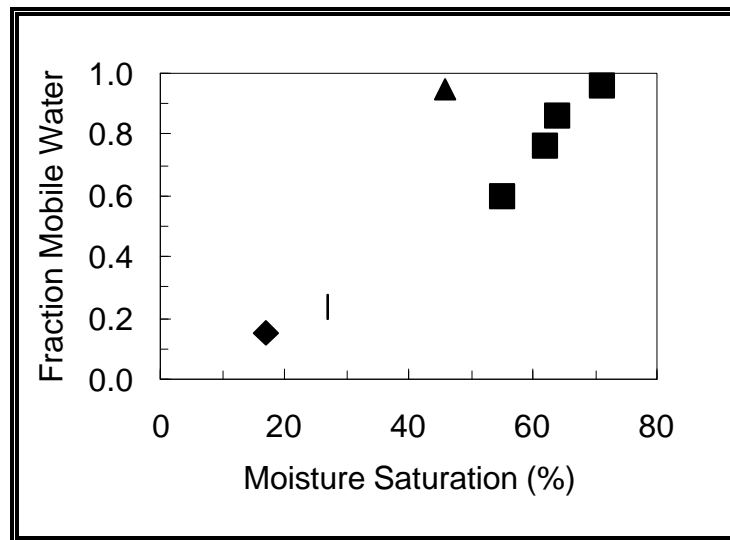


Figure 2.4. Development of hydraulic heterogeneity (decreasing ϕ_m) in unsaturated, non-aggregated soils with decreasing moisture saturation. [Filled diamond and square symbols represent data for sandy soils from Gamerding and Kaplan (1999) and Gaudet *et al.* (1977), respectively. The filled triangle symbol is data for finer-textured loamy fine sand from Bond and Wierenga (1990).]

The unsaturated flow regime is expected to differ in soils dominated by coarse-textured particles in contrast to those with fine-textured particles. As shown schematically in Figure 2.3, the flow regime will consist of film flow along the surfaces of large particles, versus matrix flow through small pores formed by fine particles. Hydraulic conductivity varies with soil texture and decreases with decreasing moisture saturation. Hydraulic heterogeneity resulting from a 2-region, mobile-immobile water, flow domain, increases in unsaturated soils. Limited data suggest a dependence on soil texture for non-aggregated soils where the heterogeneity is not apparent for saturated conditions.

In summary, the development of hydraulic heterogeneity in non-aggregated unsaturated soils has long been identified. However, the implications for the sorptive and transport behavior of contaminants are unknown. Current transport models account for lower, and spatially variable, hydraulic conductivity in unsaturated soils. Hydraulic heterogeneity resulting from mobile-immobile water domains has been considered when modeling transport in saturated systems. Fewer investigations have considered unsaturated systems.

2.5 Effects of Chemical Heterogeneity on Transport

In context of contaminant adsorption and transport, chemical heterogeneity refers in this report to the variability in particle surface reactivity. Iron oxide minerals are abundant in the subsurface environment and mineral coatings consisting of Fe(III)-oxides can be a significant source of reactivity for contaminant adsorption in a variety of soil systems [*e.g.*, Smith and Jenne (1991) as summarized by Tompson *et al.* (1996)]. The effect of chemical heterogeneity arising from spatially variable Fe(III)-oxide abundance has been considered in modeling the transport of cobalt (Brusseau and Zachara, 1993) and reactive transport of uranyl-citrate (Tompson *et al.*, 1996) and Co-EDTA (Szecsody *et al.*, 1998a, 1998b) complexes. Modeling studies of reactive solute transport in saturated systems have shown that chemical heterogeneities result in non-ideal transport behavior (Bosma *et al.*, 1993, Sugita *et al.*, 1995).

Different approaches for representing chemical heterogeneity (*i.e.*, spatial distribution of sorption sites) have been considered when combining processes in reactive flow and transport models for saturated systems (Szecsody *et al.*, 1998a, 1998b; Tompson *et al.*, 1996). The effect of a homogeneous versus a heterogeneous (spatially variable) distribution of reactive sites was compared in simulations of reactivity in batch (non-flowing) and column systems (Szecsody *et al.*, 1998b). While reactive site heterogeneity had a small effect in batch systems, it was highly significant in columns. A major conclusion was that particle-scale heterogeneities significantly influenced the interactions of sorptive (and reactive) solutes during advective flow (Szecsody *et al.*, 1998b).

2.5.1 Coupled Hydraulic and Chemical Heterogeneity

The absence of well-controlled laboratory investigations of contaminant transport in physically and chemically heterogeneous porous media has been noted (Brusseau and Zachara, 1993). The increased importance of particle scale heterogeneity in flowing versus non-flowing systems has implications for the advance from saturated to unsaturated solute transport. Variability in accessibility to reactive sites by mobile solutes is expected to increase with increased tortuosity. Predictive models that incorporate heterogeneity usually focus on reactive site abundance (Szecsody *et al.*, 1998a; Thompson *et al.*, 1996), although the length of Fe(III)-oxide inclusions has been considered (Szecsody *et al.*, 1998a). In an unsaturated soil, the distribution and abundance of reactive sites is considered to be the same as when the soil is saturated. However, the observed increase in hydraulic heterogeneity with decreased moisture saturation suggests greater variability in access to reactive sites, and thus an even greater significance of particle scale chemical heterogeneity during transport in unsaturated soils. Models which consider spatially variable reaction capacity and accessibility have been developed for saturated porous media flow (Reichle *et al.*, 1998).

Unsaturated systems have received less attention, with few investigations considering the combined effects of hydraulic and chemical heterogeneity. Russo (1989a,b) evaluated spatially variable hydraulic conductivity from a different perspective, considering the effect of solution properties on soil properties which included hydraulic conductivity and water content. The spatial variability of pesticide transport and sorption in unsaturated soil was evaluated in field, laboratory column, and batch experiments (Elabd *et al.*, 1986; Jury *et al.*, 1986). Although average K_d values from batch and column experiments were similar, there was no correlation between values measured in batch (non-flowing) and column systems (Jury *et al.*, 1986). For 18 of the 36 samples, retardation in laboratory columns with undisturbed field cores was greater than predicted from the batch K_d value (Elabd *et al.*, 1986). Non-sorptive tracer (*e.g.*, chloride) transport did not show the same degree of heterogeneity as the pesticides, suggesting sorption variability in addition to flow heterogeneity (Jury *et al.*, 1986). This research indicates that sorption during unsaturated transport is not accurately predicted from measurements in batch systems.

An important issue for modeling transport in a chemically heterogeneous system is the correlation between reactivity and other parameters that are used to characterize the medium. Correlations between reactivity and permeability (or hydraulic conductivity) are often used, but the appropriate form of the correlation for specific systems can be debated (Tompson *et al.*, 1996). Data to support specific correlations between particle size and particle surface reactivity are sparse. Consequently, approximate negative correlations are often used (Burr *et al.*, 1994; Tompson, 1993; Tompson *et al.*, 1996), or alternative possibilities of negative, positive, or no correlation are evaluated (Bosma *et al.*, 1993, 1996; Tompson, 1993;).

Experimental evidence for a negative correlation between particle size and the sorption of organic chemicals has been demonstrated (Barber *et al.*, 1992; Karickhoff *et al.*, 1979; Schwarzenbach and Westall, 1981). However, the findings of Ball *et al.* (1990) for the Canadian Forces Base

Borden Aquifer soils do not support this trend. A significant, but weak, correlation between strontium sorption and “ln K_n” was observed for the Borden Aquifer soils (Robin *et al.*, 1991). Preferential sorption of strontium to the fine-textured soil fraction and with micaceous minerals of the coarsest fraction of Chalk River aquifer soils from Ontario, Canada was observed by Pickens *et al.* (1981).

The importance of grain scale properties in determining the sorption and transport of reactive solutes and the need for systematic study of factors that affect correlation for specific porous media and reactions is evident. Due to the increasing complexity of unsaturated systems, the success of simply extending relationships that are developed in saturated systems is questionable. Fundamental research in unsaturated systems with measurement of relevant parameters relating media properties to chemical heterogeneity and reactive transport is needed.

In summary, the relationships between soil texture, porosity, moisture saturation, hydraulic heterogeneity and sorption are complex. Hydraulic heterogeneity in unsaturated soils results from disconnectivity of pore water which can be caused by thin liquid films around soil particles, dead-end pores, or relatively isolated regions associated with unsaturated flow. The proportion of disconnected or immobile water increases with decreasing moisture saturation (Figure 2.4). The unsaturated flow regime is thought to depend on the soil texture, where film flow is more likely to dominate in unsaturated coarse- textured soils, and matrix flow through small pores prevailing in fine-textured soils.

2.6 Diffusion

The transport of matter in the absence of bulk flow is referred to as diffusion. The flux of matter due to diffusion is proportional to the concentration gradient and is a molecular process. In general terms, the flux, J_{ix}, of component I in the x direction is

$$J_{ix} = -D \frac{dC_i}{dx} \quad (2.35)$$

where D = proportionality constant or diffusion coefficient with the dimensions of length²/time
 C_i = concentration of constituent i.

The J_{ix} has the dimensions of moles/length²/time, and the negative sign indicates that flow of constituent I in the x direction is also in the direction of lower I concentration. In an infinitely dilute aqueous solution, the movement is quantified by the diffusion coefficient, D. For most simple aqueous species, D is about 10⁻⁹ m²/s or 10⁻⁵ cm²/s.

Atkinson (1983), Atkinson *et al.* (1986), and Atkinson and Nickerson (1988) present a useful conceptual model for describing the transport of contaminants through a porous media such as soil. The authors consider that the transport is a combination of both physical processes, such as diffusion, and chemical processes, such as precipitation/solubility and adsorption/desorption. In

the constrained geometry of a porous media, such as soil, the D is reduced compared to the D in free aqueous solution. The D for a species within a porous media is defined as D_p and is equal to

$$D_p = \frac{D \delta}{\tau^2} \quad (2.36)$$

where δ = constrictivity of the porous media
 τ = tortuosity of the porous media.

For experimentalists, it is convenient to measure the average flux of a contaminant per unit area of the porous media in relation to the concentration gradient of the contaminant in the aqueous phase. The concentration gradient in the aqueous phase is influenced by the volume fraction of the void space in the porous media (the porosity, n_e). This leads to another equation that defines the "intrinsic" diffusion coefficient, D_i :

$$D_i = D_p n_e = \frac{D n_e \delta}{\tau^2} \quad (2.37)$$

A key assumption herein is that all the porosity in the porous media is interconnected and thus can contribute to diffusion of the contaminant. All three parameters, porosity (n_e), constrictivity (δ), and tortuosity (τ), characterize the physical contribution to diffusion through the porous media.

The chemical contributions to diffusion can potentially be quite varied, such as ion exchange, specific adsorption, precipitation, and lattice substitution. If a very simple chemical process is assumed, reversible surface adsorption having fast kinetics and a linear isotherm (*i.e.*, K_d), then diffusion of a reactive contaminant can be characterized by an apparent diffusion coefficient, D_a :

$$D_a = \frac{D_i}{\alpha'} = \frac{D_p n_e}{\alpha'} = \frac{D n_e \delta}{\tau^2 \alpha'} \quad (2.38)$$

where α' = capacity factor or ratio of the moles per unit volume of water-saturated solid, C_s , to the moles per unit volume of liquid, C_l .

The capacity factor is related to the K_d by the equation

$$\alpha' = n_e + \rho_b K_d \quad (2.39)$$

where ρ_b = dry bulk density of the porous media.

Also note that α'/n_e is the familiar retardation factor used in transport modeling:

$$\frac{\alpha'}{n_e} = R_f = 1 + \frac{\rho_b K_d}{n_e} \quad (2.40)$$

It should be noted that these simple relationships are strictly only valid for reversible, linear adsorption reactions with fast kinetics. This point is often overlooked and should not be. Nevertheless, such simplifying assumptions allow for some interesting analysis of common laboratory data and experiments.

Equation 2.40 has been incorporated into the transport equation:

$$\frac{\partial C}{\partial t} = \frac{D}{R_f} \frac{\partial^2 C}{\partial x^2} \quad (2.41)$$

where R_f = retardation factor, as defined in Equations 2.23 or 2.24
t = time.

Note that Equation 2.41, which is strictly for transport by diffusion, is similar to Equation 2.25, which describes contaminant migration due to advective flow.

Therefore, the apparent diffusion coefficients, D_a , for reactive constituents account for the chemical retardation as well as the physical hindrance to contaminant mobility caused by the small pore sizes and tortuosity of the soil.

2.7 Subsurface Mobile Colloids

2.7.1 Concept of 3-Phase Solute Transport

Contaminant transport models generally treat the subsurface environment as a 2-phase system in which contaminants are distributed between a mobile aqueous phase and an immobile solid phase (*e.g.*, soil). Contaminants with a high affinity for sorbing to rock or vadose zone soils are assumed to be retarded relative to the rate of groundwater flow. However, an increasing body of evidence indicates that under some subsurface conditions, components of the solid phase may exist as colloids¹ that may be transported with the flowing water. Association of contaminants with this additional mobile phase may enhance not only the amount of contaminant that is transported, but also the rate of contaminant transport. Most current approaches to predicting contaminant transport ignore this mechanism not because it is obscure or because the mathematical algorithms have not been developed (Corapcioglu and Kim, 1995; Mills *et al.*, 1991), but because little information is available on the occurrence, the mineralogical properties, the physicochemical properties, or the conditions conducive to the generation of mobile colloids.

¹ A colloid is any fine-grained material, sometimes limited to the particle-size range of <0.00024 mm (*i.e.*, smaller than clay size), that can be easily suspended (Bates and Jackson, 1979). In its original sense, the definition of a colloid included any fine-grained material that does not occur in crystalline form. The geochemistry of colloid systems is discussed in detail in sources such as Yariv and Cross (1979) and the references therein.

There are 2 primary problems associated with studying colloid-facilitated transport of contaminants under natural conditions. First, it is difficult to collect colloids from the subsurface in a manner which minimizes or eliminates sampling artifacts. Sampling artifacts can arise when groundwater is pumped too rapidly, yielding particles that would otherwise remain immobile in the aquifer (Backhus *et al.*, 1993; McCarthy and Degueudre, 1993; Powell and Puls, 1993). Colloids may also be generated during sampling by exposing groundwater containing readily oxidizable metals, such as Fe(II), to atmospheric conditions and causing the precipitation of fine grain-sized hydrous oxide colloids (Backhus *et al.*, 1993; McCarthy and Degueudre, 1993; Ryan and Gschwend, 1990). Secondly, it is difficult to unambiguously delineate between the contaminants in the mobile-aqueous and mobile-solid phases (Buffle *et al.*, 1992; Degueudre *et al.*, 1989; McCarthy and Degueudre, 1993; Puls, 1990). Using ultrafiltration techniques to accomplish this goal is not entirely satisfactory because it provides only indirect evidence, is subject to a number of artifacts, and usually requires high analytical precision at very low contaminant concentrations (Buffle *et al.*, 1992; Danielsson, 1982; Degueudre *et al.*, 1989; McCarthy and Degueudre, 1993).

2.7.2 Sources of Groundwater Mobile Colloids

Subsurface mobile colloids originate from (1) the dispersion of surface or subsurface soils, (2) decementation of secondary mineral phases, and (3) homogeneous precipitation of groundwater constituents (McCarthy and Degueudre, 1993). First, colloidal particles can be dispersed and become mobile in aquifers as a result of changes in the groundwater chemistry, such as a decrease in ionic strength or changes in ionic composition from a calcium- to a sodium-dominated chemistry. The effect of sodium and ionic strength on colloid suspension stability is interactive such that the dispersive quality of sodium is enhanced at low salt levels (Kaplan *et al.*, 1996).

Geochemical or microbiological changes that result in dissolution of cementing phases, such as iron oxides and calcium carbonate can result in release of colloids. For example, Gschwend *et al.* (1990) observed 10 to 100 mg/l of silica colloids in groundwater receiving recharge from evaporation ponds and a fly ash basin. The infiltrate was enriched in carbon dioxide that dissolved the soil-cementing carbonate mineral, thus releasing the silica colloids. The third source of groundwater mobile colloids is homogeneous precipitation. Changes in groundwater geochemical conditions such as pH, major element composition, redox potential, or partial pressures of CO₂ can induce supersaturation and coprecipitation of colloidal particles. The precipitates can include major elements such as oxides of iron and manganese, calcium carbonates, and iron sulfides, as well as minor elements such as carbonates and sulfides of metals and radionuclides. Mobile colloid precipitates may form when soluble contaminants are introduced into a system resulting in their exceeding the solubility product. For example, Gschwend and Reynolds (1987) observed precipitation of ferrous phosphate colloids (1 to 10 mg/l of 100 nm-sized particles) down gradient of a sewage infiltration site. Solubility calculations suggested that the dissolved phosphate ions from the sewage and reduced iron in the aquifer exceeded the solubility product of ferrous phosphate, resulting in the formation of insoluble colloids. Other studies have documented the formation of iron oxide colloids in groundwater as a result of changes in pH and oxygenation that

caused the solubility limit of Fe(III) oxides to be exceeded (Liang *et al.*, 1993). Many strongly hydrolyzing radionuclides also form submicron-sized particles. Increases in solution pH have been shown to induce the formation of plutonium-, uranium-, and americium-oxide colloids in carbonate systems (Ho and Miller, 1986; Kim, 1986).

2.7.3 Case Studies of Mobile-Colloid Enhanced Transport of Metals and Radionuclides

Although the concept of colloid-facilitated transport is often invoked to account for anomalies between predicted and observed transport of contaminants, little field or experimental verification of this potentially important phenomenon is available (McCarthy and Degueudre, 1993). There have been a few field studies describing colloid-facilitated transport and these studies have provided only circumstantial evidence that this is in fact the actual mechanism responsible for the enhanced transport of contaminants (Buddemeier and Hunt, 1988; Degueudre *et al.*, 1989; Kaplan *et al.*, 1994a; Kaplan *et al.*, 1995a; Penrose *et al.*, 1990).

Although laboratory studies at Los Alamos National Laboratory (LANL) predicted that the movement of actinides in subsurface environments would be limited to less than a few meters, both americium and plutonium were detectable in monitoring wells as far as 3,390 m down gradient from the point source (Penrose *et al.*, 1990). Almost all of the americium and plutonium in the groundwater at the 3,390 m well were associated with colloids 0.025 to 0.45 μm in diameter. Similarly, based on laboratory measurements using site-specific soils and a 2-phase solute transport code, americium, curium, plutonium, and uranium were expected to travel less than 10 m in the F-Area of the Savannah River Site; the contaminants were found associated with groundwater colloids 1,200 m away from the point source (Kaplan *et al.*, 1994a). To a lesser extent, chromium, copper, nickel, and lead were also detected directly on suspended groundwater particles collected from the F-Area study site (Kaplan, 1994b, 1995a). The reader is cautioned that, because most transport predictions do not account for preferred flow paths, the interpretation that colloid-facilitated migration is the best explanation for such enhanced migration is still being debated.

2.8 Anion Exclusion

Dissolved chloride, bromide, and nitrate are usually reported to travel through natural systems or soil columns at the same rate as, or faster than, water (James and Rubin, 1986; McMahan and Thomas, 1974). Anion exclusion, the mechanism by which anions move faster than water, occurs when the diffuse double layer, an extension of a particle's negative surface charge into the surrounding solution, repulses anions (Sposito, 1984). By excluding anions from the diffuse double layer, where water is relatively immobile, the system restricts anions to the faster moving pore water, resulting in an average rate of anion transport that is greater than the average pore water velocity defined by Darcy's Law (James and Rubin, 1986; McMahan and Thomas, 1974). Anion exclusion is more pronounced with higher cation exchange capacity (*i.e.*, negative charge) of the soil or rock. For example, smectites ($\text{CEC} \approx 3$ meq/g) exhibit anion exclusion to a greater degree than do the kaolinite ($\text{CEC} \approx 0.2$ meq/g) minerals (McMahan and Thomas, 1974).

The implication of anion exclusion for anionic contaminants (*e.g.*, nitrates, chloride, chromate, pertechnetate) and anionic complexes [*e.g.*, $\text{UO}_2(\text{CO}_3)_2^{2-}$] is that they may be able to travel through the subsurface at a rate greater than water. There is some indirect evidence that anion exclusion may exist for pertechnetate. In an unsaturated column study, pertechnetate breakthrough (C/C_0 , 0.5) occurred at 0.95 pore volumes, whereas for tritium, a conservative tracer, breakthrough occurred at 1.02 pore volumes; that is, pertechnetate may have traveled 5 percent faster than tritium (Gee and Campbell, 1980). Chloride breakthrough in these columns occurred at 0.80 pore volumes, or 22 percent faster than tritium, providing evidence that the transport of chloride may be affected by anion exclusion.

2.9 Summary

The objective of this chapter is to present a primer on the key geochemical processes affecting contaminant transport in subsurface environments. References to important review articles and books are included for each of the major subject areas: aqueous geochemical processes, sorption, diffusion, subsurface mobile colloids, and anion exclusion. These processes are summarized in Table 2.5.

Particular attention is directed at describing the geochemical processes affecting chemical retardation. A brief discussion of mechanistic and semi-empirical adsorption models. Incorporating mechanistic and semi-mechanistic adsorption concepts into transport models is desirable because the models become more robust and scientifically defensible. However, mechanistic models are rarely, if ever, applied to field-scale problems. The reasons for this are the following: (1) mechanistic models require a more intense data collection effort than will likely be available to the majority of transport modelers, licensee requestors, or responsible parties; (2) installing these mechanistic adsorption models into existing transport codes is quite complex; and (3) mechanistic adsorption models require full characterization of the mineral surfaces, information that is impossible to obtain in natural heterogeneous soils. Importantly, these models provide a paradigm for using simpler models, such as the conditional K_d model.

Conditional K_d values can be derived from laboratory or field experiments. Unlike the thermodynamic K_d term, they are less rigorously defined in that the conditional K_d values are not necessarily limited to a single aqueous species and single solid phase. This broader definition lends itself more readily to natural systems, while at the same time resulting in several technical issues and complexities. The understanding of the important geochemical factors affecting the transport of the contaminants of interest is critical for site-specific calculations.

Table 2.5. Summary of chemical processes affecting attenuation and mobility of contaminants.

Process	Mechanism	Enhancement of Attenuation or Mobility of Contaminant?	Key Facts
Aqueous Complexation	Reaction where an aqueous molecular unit (ion) acts as a central group to attract and form a close association with other atoms or molecules	May enhance attenuation or mobility, depending on contaminant and geochemical conditions	<ul style="list-style-type: none"> • Function of pH and redox • Complexation may lower the potential for adsorption and/or increase solubility, both of which can enhance potential for mobility • Complexes may more readily bond to soils and thus retard migration • Organic ligands from humic materials can be present in significant concentrations and dominate contaminant complexation in some systems
Redox Reactions	Reaction where electrons are transferred completely from one species to another	May enhance attenuation or mobility, depending on contaminant and geochemical conditions	<ul style="list-style-type: none"> • Change in redox status changes aqueous speciation which may increase or decrease adsorption and solubility • If redox status is sufficiently low to induce precipitation of sulfide minerals, reprecipitation of some contaminants may be expected • More difficult to predict mobility of redox-sensitive species because many redox reactions are kinetically slow in natural groundwater, and several elements may never reach equilibrium between their various valence states

Table 2.5. Continued.

Process	Mechanism	Enhancement of Attenuation or Mobility of Contaminant?	Key Facts
Adsorption and Ion Exchange	Special case of a complexation reaction where there is a net accumulation of a contaminant at the interface between a solid phase and an aqueous-solution phase; does not include the development of a 3-dimensional molecular structure	Enhances Attenuation	<ul style="list-style-type: none"> • Occurs primarily in response to electrostatic attraction • Very dependent on pH and mineralogy • Anion adsorption is greatest at low pH and decreases with increasing pH • Cation adsorption is greatest at high pH and decreases with decreasing pH. • Some contaminants may be present as cations or anions depending pH • Totally-to-partially reversible; decline in contaminant concentration in groundwater may result in desorption and release of adsorbed contaminant to groundwater • Likely key process controlling contaminant mobility in areas where chemical equilibrium exists
Precipitation	Special case of a complexation reaction in which the complex formed by 2 or more aqueous species is a solid with 3-dimensional molecular structure	Enhances Attenuation	<ul style="list-style-type: none"> • Very dependent on pH and redox • Totally-to-partially reversible; decline in contaminant concentration in groundwater may result in dissolution of precipitated contaminant to groundwater • Likely process where chemical nonequilibrium exists, an area where high contaminant concentrations exist, or where steep pH and/or redox gradients exist

Table 2.5. Continued.

Process	Mechanism	Enhancement of Attenuation or Mobility of Contaminant?	Key Facts
Diffusion	Molecular process of transport of matter in the absence of bulk flow	Enhances Mobility	<ul style="list-style-type: none"> • Flux of matter due to diffusion is proportional to concentration gradient
Subsurface Colloids	Contaminants associated with suspended fine-grained material (smaller than clay size) that may be transported with flowing groundwater	Enhances Mobility	<ul style="list-style-type: none"> • Little information on occurrence, mineralogical and physicochemical properties, or conditions conducive to the generation of mobile colloids • May originate from the dispersion of soils, decementation of secondary mineral phases, and/or precipitation of groundwater constituents • Difficult to collect colloids from subsurface in a manner that minimizes or eliminates sampling artifacts • Difficult to unambiguously delineate between the contaminants in the mobile-aqueous and mobile-solid phases
Anion Exclusion	Occurs when the diffuse double layer, an extension of a particle's negative surface charge into the surrounding solution, repulses anions	Enhances Mobility	<ul style="list-style-type: none"> • By excluding anions from the diffuse double layer, where water is relatively immobile, anions restricted to the faster moving pore water, resulting in an average rate of anion transport greater than the average pore water velocity defined by Darcy's Law • more pronounced with higher cation exchange capacity (<i>i.e.</i>, negative charge) of the soil or rock

3.0 Methods, Issues, and Criteria for Measuring K_d Values

3.1 Introduction

The partition (or distribution) coefficient, K_d ,¹ is a measure of sorption of contaminants to soils and is defined as the ratio of the quantity of the adsorbate adsorbed per unit mass of solid to the amount of the adsorbate remaining in solution at equilibrium. It is the simplest, yet least robust model available. There are 5 general methods used to measure K_d values: laboratory batch method, *in-situ* batch method, laboratory flow-through (or column) method, field modeling method, and K_{oc} method. Each method has advantages and disadvantages, and perhaps more importantly, each method has its own set of assumptions for calculating K_d values from experimental data. Consequently, it is not only common, but expected that K_d values measured by different methods will produce different values.

A number of issues exist concerning the measurement of K_d values and the selection of K_d values from the literature. These issues include: using simple versus complex natural geologic materials as adsorbents, field variability, the “gravel issue,” the “colloid issue,” and the particle concentration effect. Soils are a complex mixture containing solid, gaseous, and liquid phases. Each phase contains several different constituents. The use of simplified systems containing single mineral phases and aqueous phases with 1 or 2 dissolved species have provided valuable paradigms for understanding sorption processes in more complex, natural systems. However, the K_d values generated from these simple systems are generally of little value for importing directly into transport models. Values for transport models should be generated from materials from or similar to the study site. The “gravel issue” is the problem that transport modelers face when converting laboratory-derived K_d values based on experiments using the less than 2-mm fraction into values that can be used in systems containing particles greater than 2 mm in size. No standard methods exist to address this issue. The “colloid issue” was discussed previously in Section 2.7. Some investigators have observed that K_d values determined in the laboratory often decrease as the ratio of solid to solution used in the measurements increases. This particle concentration effect is puzzling, because a K_d value should not depend from a theoretical perspective on the solid-to-solution ratio. Investigators have offered several explanations involving physical/chemical processes and/or experimental artifacts for the observed dependency.

Spatial variability provides additional complexity to understanding and modeling contaminant retention to subsurface soils. The extent to which contaminants partition to soils often changes as field mineralogy and chemistry changes. Thus, a single K_d values is often not sufficient for an entire study site and should change as important environmental conditions change. It is therefore important to be able to identify and measure the effect of ancillary environmental parameters that influence contaminant sorption. Three approaches used to vary K_d values in transport codes are the K_d look-up table approach, the parametric K_d approach, and the mechanistic K_d approach.

¹ A list of acronyms, abbreviations, symbols, and notation is given in Appendix A. A list of definitions is given in Appendix B

The extent to which these approaches are presently used and the ease of incorporating them into flow models varies greatly.

The objective of this chapter is to provide an overview of the different methods of measuring and determining K_d values used in site-specific contaminant transport and risk assessment calculations. Issues regarding the selection of K_d values from the literature for use in screening calculations are discussed.

3.2 Methods for Determining K_d Values

There are 5 methods of determining K_d values: (1) laboratory batch method, (2) *in-situ* batch method, (3) laboratory flow-through (or column) method, (4) field modeling method, and (5) K_{oc} method (EPA, 1991; Ivanovich *et al.*, 1992; Jackson and Inch, 1989; Johnson *et al.*, 1995; Karickhoff *et al.*, 1979; Landstrom *et al.*, 1982; Lyman *et al.*, 1982; Roy *et al.*; 1991; Serkiz *et al.*, 1994; Sposito, 1984; van Genuchten and Wierenga; 1986). Each method provides an estimate of the propensity of a contaminant to sorb to the solid phase. However, the techniques used and the assumptions underlying each method are quite different. Consequently, K_d values for a given system that were measured by different methods commonly have values ranging over an order of magnitude (Gee and Campbell, 1980; Relyea, 1982). This subsection will describe the different methods and compare their implicit and explicit assumptions.

The K_d model originates from thermodynamic chemistry (see detailed discussion in Chapter 2) (Alberty, 1987). It is a measure of sorption and is defined as the ratio of the quantity of the adsorbate adsorbed per gram of solid to the amount of the adsorbate remaining in solution at equilibrium. For the reaction



the mass action expression is the partition coefficient (K_d , ml/g):

$$K_d = \frac{A_i}{C_i} \quad (3.2)$$

where A = concentration of free or unoccupied surface adsorption site on a solid phase (mol/ml),

C_i = total dissolved adsorbate concentration remaining in solution at equilibrium (mol/ml or $\mu\text{g/ml}$), and

A_i = concentration of adsorbate on the solid at equilibrium (mol/g or $\mu\text{g/g}$).

Equation 3.2 is valid only when A is in great excess with respect to C_i and the activity of A_i is equal to unity. For saturated conditions and non-polar organic constituents, sorption from the aqueous phase to the porous media of the subsurface can be treated as an equilibrium-partitioning

process when solute concentrations are low (*e.g.*, either $\leq 10^{-5}$ molar, or less than half the solubility, whichever is lower) (EPA, 1989). Partitioning often can be described using the above linear isotherm.

Also inherent in the thermodynamic definition of the K_d term are the assumptions that the reaction is independent of the contaminant concentration in the aqueous phase and that the system is reversible, *i.e.*, that the desorption rate is equal to the adsorption rate. The thermodynamic K_d term describes a precisely defined system, including fixed pH and temperature, with one type of adsorption site, A, and one type of dissolved aqueous species, C_i . Although the thermodynamic K_d term is overly restrictive for use in natural heterogeneous systems, it provides an important paradigm to base empiricised K_d terms. The assumptions that need to be made to empiricise this construct vary between analytical methods.

3.2.1 Laboratory Batch Method

Batch studies represent the most common laboratory method for determining K_d values (ASTM, 1987; EPA, 1991; Roy *et al.*, 1991). Figure 3.1 illustrates an EPA (1991) procedure for measuring a batch K_d value. A well characterized soil of known mass (M_{sed}) is added to a beaker. A known volume (V_w) and concentration (C_0) of an aqueous contaminant solution is added to the soil in the beaker. The beaker is sealed and mixed until sorption is estimated to be complete, typically 1 to 7 days. When possible, the person conducting the study should ascertain the actual time required to reach sorption equilibrium. The solutions are centrifuged or filtered, and the remaining concentration of the contaminant (C_i) in the supernatant is measured. The concentration of adsorbate sorbed on the solid phase (A_i , sometimes noted as q_i) is then calculated by Equation 3.3:

$$A_i = q_i = \frac{V_w (C_0 - C_i)}{M_{\text{sed}}} \quad (3.3)$$

Equation 3.3 is used to calculate the numerator of the K_d term (Equation 3.2) and the denominator, C_i , of the K_d term is measured directly in the laboratory. Thus,

$$K_d = \frac{V_w (C_0 - C_i)}{M_{\text{sed}} C_i} \quad (3.4)$$

For organic compounds that can degrade into other compounds, it should be noted that the difference in solution concentrations in Equation 3.3 represents both adsorption and degradation. Therefore, the calculated K_d for organic compounds of this type can overestimate the amount of true adsorption. If container blanks are not included in the batch test matrix, adsorption of a contaminant to the container is included in the calculated K_d . Care must be taken when interpreting batch K_d test results.

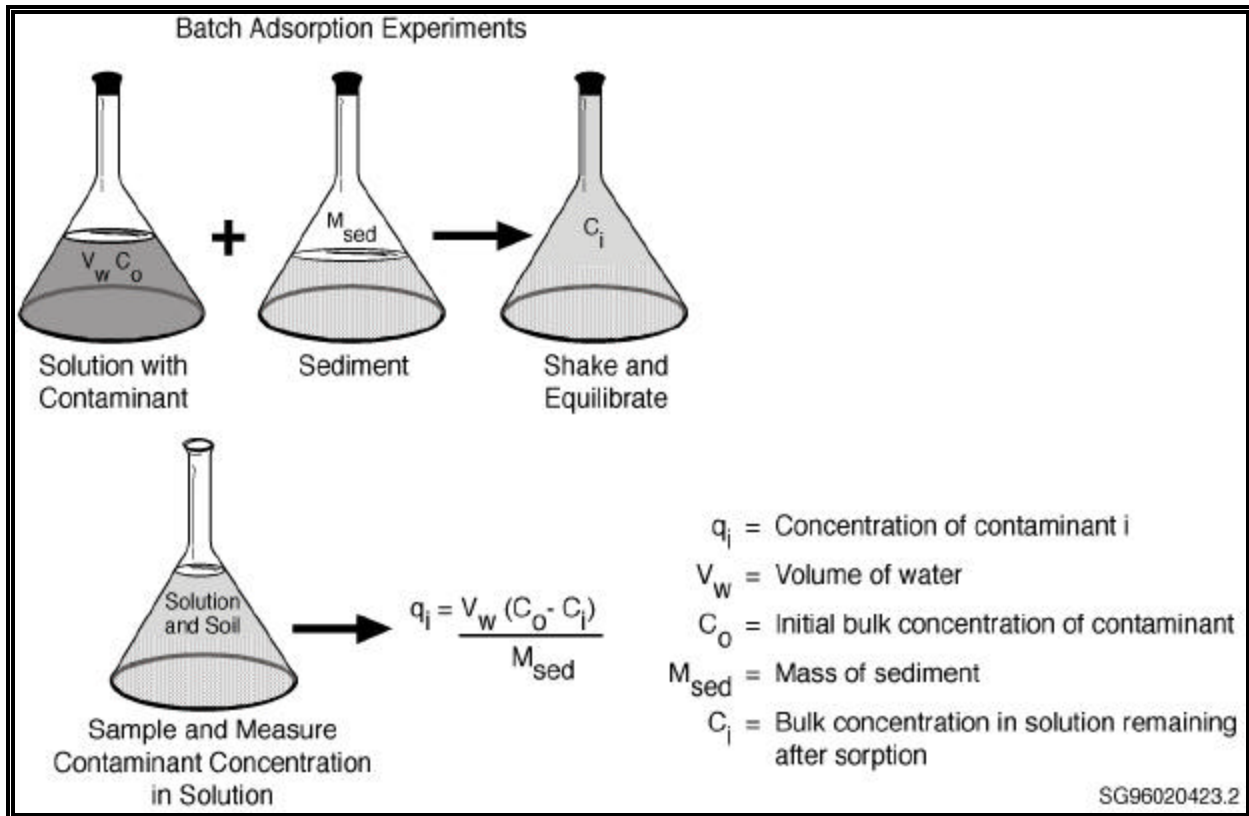


Figure 3.1. Procedure for measuring a batch K_d value (EPA, 1991).

It is important to note that the interpretation of results from batch K_d sorption tests generally allow no distinction to be made on how the sorbate (*i.e.*, contaminant) is associated with the sorbent (*i.e.*, soil). The sorbate may be truly adsorbed by ion exchange, chemisorption, bound to complexes that are themselves sorbed on the solid, and /or precipitated. If the K_d values are going to be used in transport calculations that already account for precipitation processes, it is imperative that the K_d values only include the decrease in dissolved concentrations of the sorbate due to adsorption. That is, the user must be certain that the experiments were performed correctly to prevent significant removal of the sorbate by precipitation reactions. Otherwise, the estimated retardation can be significantly overestimated.

There are several variations of this general procedure, each variation addressing the specific needs of the system. It is necessary to have some latitude in the method because of limits due to analytical chemistry considerations. For instance, for contaminants in which very low sorption is expected, a larger ratio of solid to liquid may increase the small difference in the term $(C_0 - C_i)$. Conversely, for contaminants in which high sorption is expected, a lower ratio of solid to liquid may be desirable. For gamma-ray emitting contaminants, it is possible to directly count the

activity on the equilibrated solid and in the solution, such that the K_d can be directly determined as opposed to relying on the difference in activity (*i.e.*, concentration) in the solution phase only.

One of the most common variations of the EPA method is to conduct a series of batch tests that are identical except for varying of the concentration of the dissolved contaminant, C_i . The K_d for the resulting isotherm is typically calculated from the slope of a C_i versus A_i plot. As discussed in Section 2.3.3, adsorption isotherm experiments are often conducted to evaluate the effect of contaminant concentration on adsorption, while other parameters are held constant. For soils, it is common knowledge that contaminant adsorption can deviate from the linear relationship required by the K_d construct. This approach obviously requires more work, but can provide a more accurate estimate.

Other variations of the batch K_d procedure deal with the ratio of solids to liquid, liquid composition, and contaminant concentration. A detailed description of a batch K_d procedure is included in Appendix C.

Contaminant transport modelers are often interested in the K_d value of a contaminant in a specific groundwater plume (*e.g.*, an acidic plume) in contact with a specific soil. In such a case, an experimenter would spike the contaminant into a representative groundwater, as opposed to pure water. Additionally, the experimenter would attempt to equilibrate the soils with the background aqueous solution (*e.g.*, the acidified groundwater) before bringing the soil in contact with the contaminant of interest. The reason for this latter step is to isolate the adsorption/desorption reaction of interest between the contaminant and soil. By pre-equilibrating the soil first with the acidic plume water (without the contaminants present), all the extraneous chemical reactions should be near equilibrium. Then, when the contaminant is added, its reaction is isolated.

The batch method is popular because the equipment, cost, and time requirements are low and the methodology is quite simple. However, the seemingly elementary operations mask numerous subtleties resulting in variability of data (EPA, 1991; Roy *et al.*, 1991; Serne and Relyea, 1981). One of the most comprehensive exercises to evaluate interlaboratory precision and identify important procedural details was conducted by 9 laboratories (Serne and Relyea, 1981). General guidelines on groundwater compositions, radionuclides, and procedural details were given to participants in this exercise. The measured K_d values were surprisingly varied for 2 of 3 contaminants investigated. As much as 3 orders of magnitude difference were determined in cesium (1.3 ± 0.4 to 880 ± 160 ml/g) and plutonium (70 ± 36 to $63,000 \pm 19,000$ ml/g). Conversely, the strontium K_d values measured in the 9 laboratories were within an order of magnitude of each other, 1.4 ± 0.2 to 14.9 ± 4.6 ml/g. Serne and Relyea (1981) concluded that the cause of the variability of the plutonium and cesium K_d values was due to: (1) method of tracer addition to solution, (2) solution-to-solid ratio, (3) initial tracer concentration in influent solution, (4) particle size distribution, (5) solid-solution separation method, (6) sample containers, and (7) temperature. The authors discussed in detail each of these parameters that are generally not controlled in batch K_d methods.

Essentially all of the assumptions associated with the thermodynamic K_d value (Equation 3.2) are violated in the common batch K_d value. The natural soils used in these studies are not completely defined or quantified with respect to their mineralogy and organic phases. The background aqueous phases that are spiked with the adsorbate are typically not pure water and are rarely completely characterized, especially in the case when natural groundwater are used as the background aqueous phase. The background aqueous phases often contain the dominant electrolytes of the study site or actual uncontaminated groundwater from the study site, consisting of several dissolved and perhaps colloidal species. Furthermore, the sorption/desorption process of adsorbates from soils is typically not reversible, *i.e.*, hysteresis is observed, such that desorption occurs at a slower rate than sorption (Sposito, 1994). However, the batch K_d term can be of much greater value to the contaminant transport modeler than the thermodynamic value if the soil and the aqueous phase closely represent the natural system being modeled. Importantly, such a complex system, though not completely characterized, provides the best available estimate of the extent to which a sorbate partitions to a given soil in the presence of the electrolytes present in the experiment. This issue of measuring K_d values in complex- versus simple-systems is further discussed in Section 3.3.1.

One significant limitation inherent in the batch method is that commonly used analytical instruments can not differentiate between species of a given contaminant. For example, the atomic absorption (AA) spectrophotometer can measure total cadmium in the aqueous phase but can not identify each of its species [*e.g.*, Cd^{2+} , $\text{CdSO}_4^{\text{aq}}$, CdCl^{aq} , *etc.*]. Multiple species typically exist in groundwater and the effect of their individual K_d values have a profound effect on the overall K_d value. For example, consider a system that consists of a contaminant or radionuclide with 2 equal concentration species that are kinetically slow at converting between each composition state; one with a K_d of 0 ml/g and the second with a K_d of 1,000 ml/g. The laboratory batch method would yield an intermediate K_d of about 30 ml/g in an experiment with a solution-to-solid ratio of 30. A demonstration calculation illustrating this issue is given in Figure 3.2. Using the K_d value 30 ml/g in subsequent mass transport calculations would not be conservative because 50 percent of the radionuclide would move at the speed of the carrier solution. For this reason, when there is any suspicion that multiple species with significantly differing K_d values may be present, a second sorption methodology, such as the flow-through method (Section 3.2.3), should be run to search for early breakthrough.

Assumptions:

- Total concentration, C_0 , of contaminant I in the original solution is 1,000 mg/ml.
- Batch test is performed with 1 g of clay soil contacting 30 ml of the original solution.
- The total concentration C_0 is equally divided between two species, A and B, of contaminant I.
- The true K_d values for species A and B are 0 and 1,000 ml/g, respectively.
- Kinetic barriers exist that affect their interconversion between these two composition states over the time period of the test.

Equations and Calculation:

Rearranging the equation

$$K_d = \frac{V_w (C_0 - C_i)}{M_{\text{sed}} C_i}$$

to solve for the concentration of species X of contaminant I (C_{Xi}) (*i.e.*, C_{Ai} and C_{Bi} , where C_A and C_B at end of test), one gets

$$C_{Xi} = \frac{C_{0,X} V_w}{K_{d,X} M_{\text{sed}} + V_w}$$

For C_{Ai} , we know that there is no adsorption. Therefore, $C_{Ai} = C_{0,A} = 0.5 \cdot C_0 = 500$ mg/ml.

For C_{Bi} , we calculate from the above equation for C_{Xi} :

$$C_{Bi} = \frac{500 \times 30}{(1,000 \times 1) + 30} = \frac{15,000}{1,030} = 14.56$$

C_i for total solution is

$$C_{Ai} + C_{Bi} = 500 + 14.56 = 514.56$$

Therefore, if one does not realize that multiple contaminant species are present which do not rapidly interconvert, the overall K_d for the total contaminant would be

$$K_d = \left(\frac{1,000 - 514.56}{514.56} \right) \frac{30}{1} = 28.30 \approx 28$$

Figure 3.2. Demonstration calculation showing affect on overall K_d by multiple species that have different individual K_d values and are kinetically slow at interconverting between each composition state.

3.2.2 *In-situ* Batch Method

A method developed out of the desire to produce an *in-situ* K_d value has been used to a limited extent (Jackson and Inch, 1989; Johnson *et al.*, 1995; Landstrom *et al.*, 1982; McKinley and Alexander, 1993; Read *et al.*, 1991). The procedure used in this method is somewhat similar to that of the laboratory batch K_d method described in Section 3.2.1. A core sample containing a paired solid and aqueous phase is removed directly from an aquifer. The aqueous phase is separated from the solid phase by centrifugation or filtration and then analyzed for the solute concentration, C_i . The solid is then analyzed for the concentration of the contaminant associated with the solid phase, A_i .

Clearly, the advantage of this approach compared to the laboratory K_d method is that the precise solution chemistry and solid phase mineralogy is used for the modeling. Furthermore, the pore water removed from the core material may have had sufficient time to equilibrate and therefore true equilibrium may be attained. The disadvantages are somewhat less apparent but none the less appreciable. The concentration of most metal contaminants on the soil surfaces is typically quite low, in the mg/kg range. It should be noted moreover that the minimum detection limit for radionuclides on solid surfaces is even lower. The most common instruments available to measure metal concentrations on surfaces, energy dispersive x-ray analysis (EDX), or x-ray fluorescence, typically has detection limits in the order of 10,000 and 100 mg/kg, respectively. Another method of measuring A_i is to dissolve the solid phase with acid and then measure the resulting solution by inductively coupled plasma spectroscopy (ICP), inductively coupled plasma/mass spectroscopy (ICP/MS), and/or atomic adsorption spectroscopy (AA) techniques. This latter technique may provide a lower (*i.e.*, better) detection limit. In addition to the detection limit problem, it is not possible by any of these methods to distinguish between sorption and precipitation - processes which are treated quite differently in transport models. Furthermore, some trace metals are present in crystalline lattice sites of minerals present in soils. These molecules are not readily controlled by adsorption/desorption and should not be included in the q_i term. An in-depth discussion of the limitations of the *in-situ* batch method is presented by McKinley and Alexander (1993). For anthropogenic radionuclides present at trace levels, it is possible to assume that precipitation and lattice site contributions are nil and that the total mass/activity measured on the solid does represent adsorption/desorption-controlled molecules. In this scenario, a field *in-situ* K_d may be accurate.

One rather successful application of this technique was recently reported by Johnson *et al.* (1995). They compared laboratory and field batch K_d values of uranium along a transect through a pH gradient of pH 3.0 to 5.6. The field results yielded K_d values that ranged from 0.4 to greater than 15,000 ml/g for approximately 36 samples. The K_d values generated by the laboratory batch technique were generally lower, ranging from 0.08 to greater than 10,000 ml/g. The K_d values determined by both methods varied as a function of soil pH at the study site. When both sets of values were incorporated into a transport code, the results were not significantly different, *i.e.*, both methods were essentially equally good at predicting contaminant retardation in the study site.

3.2.3 Laboratory Flow-Through Method

The laboratory flow-through (or column) method of determining K_d values is the second most commonly used method (EPA, 1991; Relyea, 1982; Van Genuchten and Wierenga, 1986). A solution containing known amounts of a contaminant is introduced into a column of packed soil of known bulk density (*i.e.*, mass of soil per unit volume of column, g/ml) and porosity (*i.e.*, volume of pore space per unit volume of column, ml/ml) (Figure 3.3). The effluent concentration is monitored as a function of time. A known amount of a nonadsorbing tracer may also be introduced into the column and its time-varying concentration provides information about the pore-water velocity. The resulting data is plotted as a break-through curve (Figure 3.3). The velocity of each constituent (*i.e.*, tracer and contaminant) is calculated as the length of the column divided by the constituent's mean residence time.

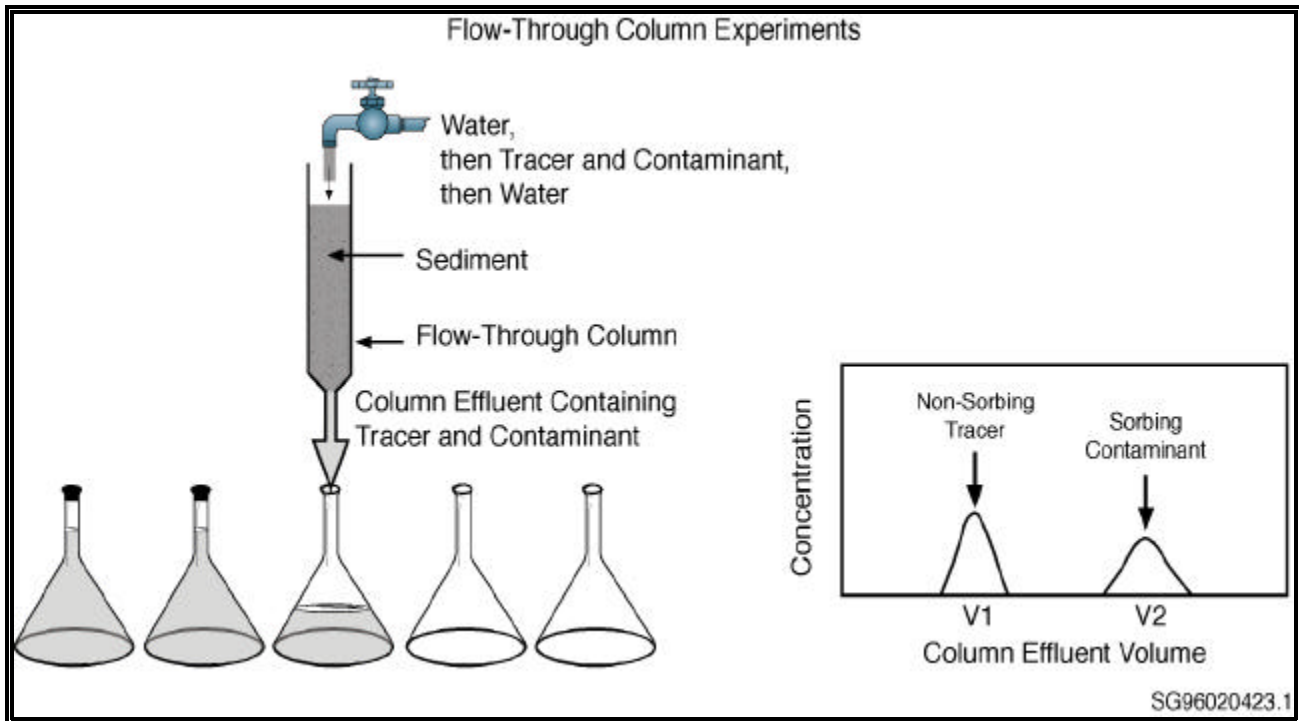


Figure 3.3. Procedure for measuring a column K_d value.

The mean residence time for a pulse input is calculated as follows (Relyea, 1982):

$$t_{\text{pulse}} = \frac{\int_{t_{\text{min}}}^{t_{\text{max}}} t C_i dt}{\int_{t_{\text{min}}}^{t_{\text{max}}} C_i dt} \quad (3.5)$$

where t_{pulse} = mean residence time for a pulse input (hr), t_{max} is the end of the break-through curve (hr),
 t_{min} = beginning of the break-through curve (hr),
 C_i = constituent concentration [(g or curies)/ml], and
 t = time (hr).

The relative concentrations of a constituent at the input source and in the effluent based on a pulse input are shown schematically in the top left and right of Figure 3.4. The mean residence time for a step (continual steady-state) input is calculated as follows:

$$t_{\text{step}} = \frac{\int_{C_{\text{min}}}^{C_{\text{max}}} t dC}{\int_{C_{\text{min}}}^{C_{\text{max}}} C_i dt} \quad (3.6)$$

where t_{step} = mean residence time for a step input/release (hr),
 C_{max} = maximum concentration measured in the effluent [(g or curies)/ml], and
 C_{min} = minimum concentration measured at the beginning of breakthrough [(g or curies)/ml].

When the effluent curve is ideal, t_{step} equals the time when the breakthrough curve reaches 0.5 or 50 percent breakthrough (*i.e.*, $C_i/C_o=0.5$). The relative concentrations of a constituent at the input source and in the effluent based on a step input are shown schematically in the bottom left and right of Figure 3.4.

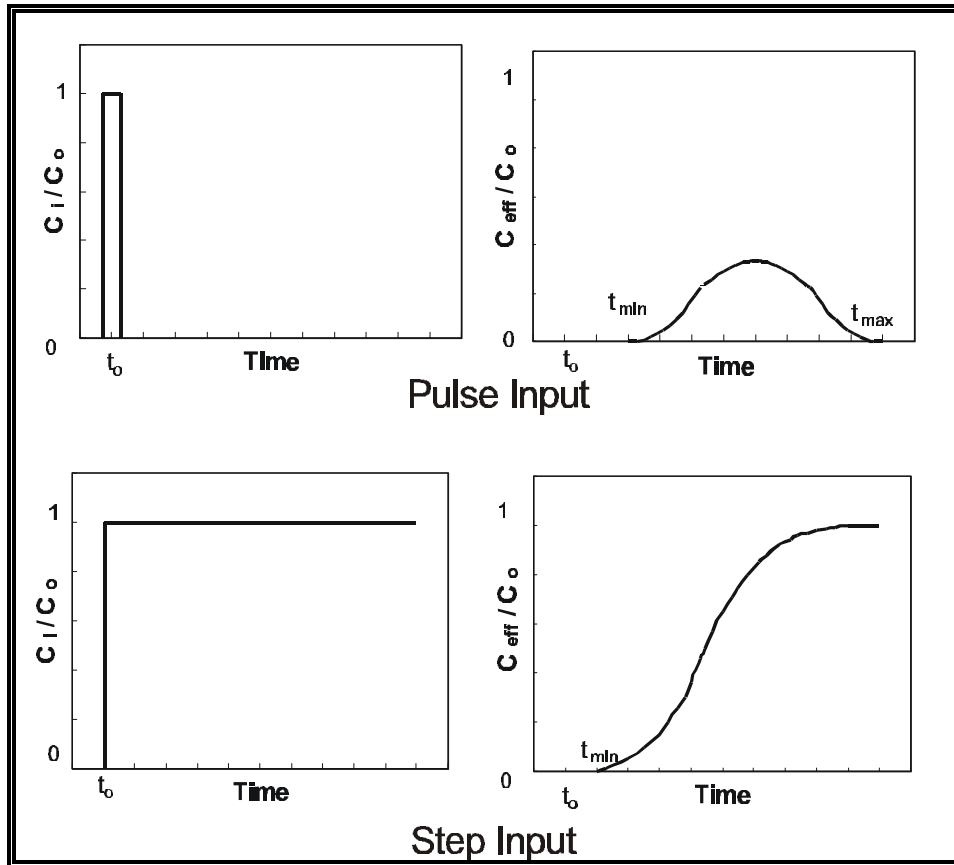


Figure 3.4. Schematic diagram showing the relative concentrations of a constituent at the input source (figures on left) and in the effluent (figures on right) as a function of time for a pulse versus step input. [C_o , C_i , and C_{eff} refer, respectively, to the concentration of the constituent at t_0 and the concentrations of the constituents in the input and effluent.]

The retardation factor (R_f) is the ratio of the pore-water velocity (v_p , cm/hr) to the contaminant velocity (v_c , cm/hr):

$$R_f = \frac{v_p}{v_c} \quad (3.7)$$

The pore-water velocity is operationally defined as the velocity of the nonadsorbing tracer.

The K_d value can be calculated directly from the retardation factor (R_f) and soil properties. Depending upon the environmental conditions in which the contaminant moves and interacts with the soil, the retardation factor can be correlated to the partition coefficient in a number of different ways. At least 4 formulations of the retardation factor have been proposed [see reviews in Bouwer (1991) and Whelan *et al.* (1987, 1996)]. These include the following:

$$R_f = \frac{n}{n_e} + \frac{K_d \rho_b}{n_e} \quad (3.8)$$

$$R_f = 1 + \frac{K_d \rho_b}{n_e} \quad (3.9)$$

$$R_f = 1 + \frac{K_d \rho_b}{n} \quad (3.10)$$

$$R_f = 1 + \frac{K_d \rho_b}{\theta} \quad (3.11)$$

where n = total porosity (cm^3 pore/ cm^3 total volume),
 n_e = effective porosity (cm^3 pore/ cm^3 total volume),
 θ = volumetric water content in the vadose zone (cm^3 water/ cm^3 total volume), and
 ρ_b = bulk density (g soil/ cm^3 total volume).

Total porosity is the ratio of the air/water volume to the total soil. The effective porosity differs from the total porosity in that the numerator is the volume of only those pore spaces that water can travel through, excluding such void volumes as exist within aggregates or dead-end pore spaces. Equation 3.10 was the original equation relating K_d to R_f . It was developed on an empirical basis for use in chemical engineering and was first applied to groundwater situations by Higgins (1959) and Baetslé (1967). Equations 3.8-3.11 were derived from the general transport equation, which is the differential equation describing solute concentration changes in relation to time, distance, dispersion coefficient, water velocity, soil bulk density, porosity, mass of solute per unit dry mass of soil, and degradation of solute (Bouwer, 1991).

Equation 3.8 assumes that the soil has 2 types of pore spaces, those that permit flow to occur (n_e), and those pore spaces that do not permit flow to occur ($n - n_e$). The contaminant in Equation 3.8 is assumed to migrate through the interconnected pore spaces, diffuse into dead-end pore spaces, and instantaneously adsorb to or desorb from the soil matrix where fluid is and is not flowing. Equation 3.8 also assumes that the solute concentration in the dead-end pore spaces is equivalent to the solute concentration in the free-flowing spaces. Equation 3.8 has the appearance of being more comprehensive than the other equations, but it does not allow the contaminant to travel with the same speed as the fluid (*i.e.*, nonadsorbing case), unless the total and effective porosities are equal. Experience has shown that Equation 3.8 does not adequately reflect real-world phenomena, suggesting deficiencies in our understanding of the geohydrochemical processes

impacting contaminant movement in the subsurface environment (Whelan *et al.*, 1987). Furthermore, in field studies, total porosity (n) can be measured directly, whereas effective porosity (n_e) can only be calculated from equations based on assumptions that are difficult to defend (Freeze and Cherry, 1979).

Equation 3.9 includes the same processes as Equation 3.8, except that the contaminant does not diffuse into the dead-end pore spaces. Many models use Equation 3.9 in their formulations. van Genuchten and Wierenga (1986) suggest the use of Equation 3.10. Equation 3.10 includes the same phenomena as Equation 3.9 except that the porous medium contains no dead-end pore spaces. Again, the merit of its use over Equation 3.9 is that the measurable parameter n is included in the formulation and not the calculated parameter n_e . Equation 3.8, 3.9, and 3.10 describe chemical retardation in the saturated zone, whereas Equation 3.11 describes chemical retardation in the unsaturated, or vadose, zone. As with Equation 3.10, contaminant transport and retardation in Equation 3.11 occurs only in the free-flowing pore space. Bouwer (1991) promotes the use of Equation 3.11 but defines the θ term more generally as the water that is moving, whether in unsaturated or saturated conditions. In his derivation of Equation 3.11, Bouwer suggests that the θ term also be used to quantify the mobile phases of water. Along with van Genuchten and Wierenga (1986), he also contends that the use of Equation 3.11 allows better distinction between retardation effects due to sorption and acceleration effects due to preferential flow or anion exclusion.

Flow-through column experiments are appealing in that they allow observation of contaminant migration rates in the presence of hydrodynamic effects (*e.g.*, dispersion, colloidal transport, *etc.*), and chemical phenomena (*e.g.*, multiple species, reversibility, *etc.*). Ideally, flow-through column experiments would be used exclusively for determining K_d values, but equipment costs, time constraints, experimental complexity, and data reduction uncertainties discourage widespread use. One common problem in using column studies to measure K_d values is that the breakthrough curves are asymmetric. Such curves cannot be interpreted using Equations 3.8, 3.9, 3.10, or 3.11. They require more complicated equations for solving for K_d (Brusseau and Rao, 1989; van Genuchten and Alves, 1982; van Genuchten and Wierenga, 1986).

One of the unique characteristics of measuring K_d values from column experiments is that nonequilibrium conditions can be imposed. Especially under conditions in which the solute has slow adsorption kinetics [*e.g.*, those that may occur with uranium (Sposito, 1994)] or when groundwater flow is fast, a measure of adsorption at equilibrium may over-estimate the extent to which sorption occurs under actual field conditions. When either of these conditions are known to exist in a study site, researchers should conduct column experiments at the flow rate existing in the field, thereby creating realistic conditions.

Relyea (1982) provided an excellent review on the theoretical and experimental application of the laboratory flow-through method of determining K_d values. He reported that retardation factors measured in column experiments depended on the water velocity and column dimension. For short columns and slow water velocities, diffusion can become a major transport mechanism

resulting in lower retardation factors and lower K_d values. At high velocities the effective pore volume of a sample can decrease for short columns. High water velocities can also result in lower retardation factors as a result of the solute not having sufficient time to adsorb to the soil, *i.e.*, chemical equilibrium was not obtained. The effects of column length, mass of solute added to column, diameter ratio of particle to column, and ratio of column diameter to column width on the measured K_d value were also presented by Relyea (1982).

3.2.4 Field Modeling Method

Field studies can provide accurate indications of the time of travel of the contaminant because the concentrations of a dissolved contaminant are measured directly from samples taken from monitoring wells. The field modeling method of estimating a K_d value, also called the field calibration method, uses a transport model and existing groundwater monitoring data. This process, which is referred to as calibrating a groundwater transport model to K_d values, involves treating the K_d value as an adjustable parameter (or dependent variable) while simulating contaminant concentrations determined at monitoring wells. Groundwater calibration captures the essence of the problem in the field. This is an iterative process that frequently requires the adjusting the values for several other input parameters, such as effective porosity, dispersion, and flow rate, to yield meaningful K_d values. The minimum information that is needed for such a calculation is the contaminant concentration at the source term, date of release, groundwater flow path, groundwater flow rate, contaminant concentration at a monitoring well, distance between source-release and monitoring well, dispersion coefficient, and source term. The retardation of the chemical is then estimated as the ratio of the pore-water velocity to the contaminant velocity (Equation 3.7). The pore-water velocity, v_p , can be based on Darcy's law (Freeze and Cherry, 1979) where

$$v_p = \frac{v_d}{n_e} \quad (3.12)$$

where v_d = Darcy velocity
 n_e = effective porosity

However, 2 key drawbacks to this technique is that it is highly site specific and very model dependent. Additionally, many assumptions have to be made about the water flow in the study site including uniform flow and flow path. Not obvious, is that the K_d value calculated by this method greatly improves with more data. A detailed description of the theory of calculating K_d values by this method and some examples of this approach are presented in Chapter 4.

3.2.5 K_{oc} Method

The extent to which an organic contaminant partitions between the solid and solution phases is determined by several physical and chemical properties of the contaminant and soil (Lyman *et al.*, 1982). Since most sorption of hydrophobic organic substances is to the natural organic matter present in sediments or soils, the usual approach is to assume that all sorption is to that matter and

to invoke a partition coefficient between organic carbon (K_{oc}) or organic matter (K_{om}) and water (Seth *et al.*, 1999). Hydrophobic solutes appear to bind readily and rapidly with the outer surface region in a few hours to a few days and then diffuse slowly into (and out of) the hydrophobic interior region and narrow cavities in the sediment or soil organic matter during time periods of weeks (Seth *et al.*, 1999). An empirical approach that has had wide acceptance in the scientific community is the organic-carbon partitioning coefficient (K_{oc}) method introduced by Karickhoff *et al.* (1979).

For this method, sorption of an organic contaminant, such as polynuclear aromatic hydrocarbon (PAH), is assumed to occur only to the organic material in the soil. The partitioning between the solid and solution phases is expressed as:

$$K_d = K_{oc} f_{oc} \quad (3.13)$$

where K_{oc} = ratio of the contaminant concentration on the organic matter on a dry weight basis to its dissolved concentration in the surrounding fluid (ml/g) and
 f_{oc} = fraction of organic carbon in the soil (mg/mg).

Importantly, the K_{oc} method is only applicable for estimating organic compound partitioning. Gschwend and Wu (1985) report that if precautions are taken to eliminate or account for nonsettling microparticles or organic macromolecules which remain in the aqueous phase during laboratory sorption tests, the observed organic-carbon partitioning coefficient have been found to remain constant over a wide range of environmental and experimental conditions. However, recent studies by Chiou *et al.* (1998) and Seth *et al.* (1999) indicate that for any given chemical, an inherent variability in K_{oc} values is expected as a result of different environmental conditions and equilibrium times. Dragun (1988) identified the following conditions when this approach is less accurate:

- When the organic fraction, f_{oc} , is less than 1.0 percent¹ (LaGrega, 1994) or greater than 20 percent (EPA, 1988)
- When there are large amounts of swelling clays present (*e.g.*, montmorillonite)
- When the partitioning organic compound is polar
- When mechanisms other than simple partitioning contribute to adsorption (*e.g.*, cation-exchange, anion-exchange)
- When a substantial time is required to reach equilibrium

The organic content of most soils falls in the range of 0.2 to 3.0% (LaGrega, 1994).

¹ Other limits have been suggested for the minimum organic fraction, f_{oc} , such as less than 0.1 percent (EPA, 1989) or less than a few tenths of a percent (Pignatello, 1989).

The commonest correlation for K_{oc} is with the octanol-water partition coefficient (K_{ow}) for which extensive databases and reliable estimation methods exist (Seth *et al.*, 1999). A simplified relationship between these two parameter is given by Equation 3.14.

$$K_{oc} = \alpha K_{ow} \quad (3.14)$$

where α = correlation coefficient (unitless).

LaGrega (1994) reports a value of ($\alpha = 0.63$) as a commonly used value while Seth *et al.* (1999) calculate a value of ($\alpha = 0.35$) with a variation in α by a factor of 2.5 in either direction. Seth *et al.* (1999) also suggested that K_{oc} estimates be viewed as a distribution, which includes uncertainties about attainment of equilibrium and the variability in the composition of organic matter present in soils and sediments, rather than as a single point value.

Streng and Peterson (1989) applied the principle of the K_{oc} model to estimating the partition coefficients for organic compounds on soils. They defined the K_d for organic compounds through the combination of the K_{oc} model and a parametric model (discussed in Section 3.4.2) based on the concentrations of organic material (C_{om} , percent w/w), clay (C_{clay} , percent w/w), silt (C_{silt} , percent w/w) and sand (C_{sand} , percent w/w) as dependent variables:

$$K_d = 10^{-4} K_{oc} [57.735(C_{om}) + 2.0(C_{clay}) + 0.4(C_{silt}) + 0.005(C_{sand})] . \quad (3.15)$$

Equation 3.15 has the disadvantage of requiring more input parameters than Equations 3.13 and 3.14, but it provides an innovative approach for estimating the K_d of organic compounds.

3.3 Issues Regarding Measuring and Selecting K_d Values

3.3.1 Using Simple Versus Complex Systems to Measure K_d Values

Soils are a complex mixture of solid, gaseous, and liquid phases. Each phase contains several different constituents. Sposito (1989) estimated that the aqueous phase of a typical soil easily contains between 100 and 200 different soluble complexes, many of them involving metal cations and organic ligands (Table 3.1). The main effect of pH on these complexes, as is evident in Table 3.1, is to favor free metal cations and protonated anions at low pH and carbonate or hydroxyl complexes at high pH. The number of soluble complexes are also likely to be greater in systems with elevated pH and organic matter concentrations. The solid phase in natural soils typically contains more than 10 different constituents, including minerals, microbes, oxides, naturally occurring organic matter, and organic, carbonate and/or oxide (e.g., iron, aluminum, and manganese) coatings. The gas phase is quite different from that of above ground air as a result of its interaction with the other phases and effects of pressure, temperatures, and microbial activity (Sposito, 1989). For instance, the carbon dioxide levels is commonly several orders of magnitude greater in soils than in above ground air (Wood and Petratis, 1984).

Table 3.1. Representative chemical species in acidic and basic soil solutions (after Sposito, 1989).

Cation	Principal Species ¹	
	Acid Soils	Alkaline Soils
Aluminum	Al-org, ² AlF ²⁺ , AlOH ²⁺	Al(OH) ₄ ⁻ , Al-org
Cadmium	Cd ²⁺ , CdSO ₄ ^o (aq), CdCl ⁺	Cd ²⁺ , CdCl ⁺ , Cd SO ₄ ^o (aq), CdHCO ₃ ⁺
Calcium	Ca ²⁺ , CaSO ₄ ^o (aq), Ca-org	Ca ²⁺ , Ca SO ₄ ^o (aq), CaHCO ₃ ⁺
Chromium(III)	CrOH ²⁺	Cr(OH) ₄ ⁻
Chromium(VI)	CrO ₄ ²⁻	CrO ₄ ²⁻
Copper(II)	Cu-org, Cu ²⁺	CuCO ₃ ^o (aq), Cu-org, CuB(OH) ₄ ⁺ , Cu[B(OH) ₄] ₄ ^o (aq)
Iron(II)	Fe ²⁺ , FeSO ₄ ^o (aq), FeH ₂ PO ₄ ⁺	FeCO ₃ ^o (aq), Fe ²⁺ , FeHCO ₃ ⁺ , FeSO ₄ ^o (aq)
Iron(III)	FeOH ²⁺ , Fe(OH) ₃ ^o (aq), Fe-org	Fe(OH) ₃ ^o (aq), Fe-org
Lead	Pb ²⁺ , Pb-org, PbSO ₄ ^o (aq), PbHCO ₃ ⁺	Pb ²⁺ , PbHCO ₃ ⁺ , Pb-org, Pb(CO ₃) ₂ ²⁻ , PbOH ⁺
Magnesium	Mg ²⁺ , MgSO ₄ ^o (aq), Mg-org	Mg ²⁺ , MgSO ₄ ^o (aq), MgCO ₃ ^o (aq)
Manganese(II)	Mn ²⁺ , MnSO ₄ ^o (aq), Mn-org	Mn ²⁺ , MnSO ₄ ^o (aq), MnCO ₃ ^o (aq), MnHCO ₃ ⁺ , MnB(OH) ₄ ⁺
Molybdenum(VI)	H ₂ MoO ₄ ^o (aq), HMoO ₄ ⁻	HMoO ₄ ⁻ , MoO ₄ ²⁻
Nickel	Ni ²⁺ , NiSO ₄ ^o (aq), NiHCO ₃ ⁺ , Ni-org	NiCO ₃ ^o (aq), NiHCO ₃ ⁺ , Ni ²⁺ , NiB(OH) ₄ ⁺
Potassium	K ⁺	K ⁺ , KSO ₄ ⁻
Silicon	H ₄ SiO ₄ ^o (aq)	H ₄ SiO ₄ ^o (aq)
Sodium	Na ⁺	Na ⁺ , NaHCO ₃ ^o (aq), NaSO ₄ ⁻
Zinc	Zn ²⁺ , ZnSO ₄ ^o (aq), Zn-org	ZnHCO ₃ ⁺ , ZnCO ₃ ^o (aq), Zn-org, Zn ²⁺ , ZnSO ₄ ^o (aq), ZnB(OH) ₄ ⁺

¹ Complexes for each cation are listed in the order of their relative concentrations from greatest to lowest concentration.

² Org = Organic complexes (*e.g.*, fulvic acid complexes).

Scientists will conduct geochemical studies with pure phases, such as goethite, quartz, or montmorillonite to work in well-defined systems. They may also choose not to work with actual groundwater, but instead work with a “synthesized groundwater,” such as a calcium chloride solution or a calcium chloride/sodium chloride solution. Again, the intent is to work in a chemically well-defined system with as few constituents as possible. Experiments conducted under simplified systems have provided information about the mechanisms by which solutes interact with solid surfaces (Sposito, 1984; Sposito, 1989), information that otherwise would not be possible to obtain from experiments conducted with natural heterogeneous soils and groundwater.

Ideally, for site-specific calculations, the transport modeler should use sorption values determined for site-specific materials at site-specific conditions. In the absence of such data, the modeler often selects a K_d value taken from the literature that was measured under similar conditions as existing at the study site. However, as discussed in Chapter 2 (Section 2.2.3), very subtle properties of the solid and aqueous phases can have a profound affect on a contaminants K_d . For example, only 1 percent (w/w) organic matter existing as surface coatings in a South Carolina surface soil completely masked the surface properties of the underlying minerals (Kaplan *et al.*, 1993). The organic coatings imposed a much greater sorption potential than would have been expected based on mineralogical considerations. Similarly, the surface properties of the soils just below these soils were entirely dominated by iron-oxide coatings (Seaman *et al.*, 1995). The effect of the iron-oxide coatings was to create a solid phase that was dominated by pH dependent charge surfaces. These subsurface soils adsorbed large amounts of anions because the pH was below the zero-point-of-charge [discussed in Chapter 2 (Section 2.2.3)] of the iron oxides, pH ~8. Subtle changes in the aqueous composition in a batch K_d test may also have a profound affect on the measured K_d value (Delegard and Barney, 1983). Thus, it is essential for the modeler selecting K_d values to recognize which solid and aqueous phase components have a strong affect on the sorption of the contaminant of interest. Identifying these important components is the subject of Volume II.

3.3.2 Field Variability

The purpose of any soil sample is to obtain information about a particular soil. The sample itself is seldom, if ever, the entire soil mass in which one is interested. In statistics, this larger aggregate of material, in which we are ultimately interested, is called the “population.” Information from the sample is of interest only insofar as it yields information about the population, and the information may or may not be representative, depending on how the sample is selected.

The population itself may be large or small, or even a part of what the modeler considers a larger population. For contaminant transport modeling, the population is commonly defined by either stratigraphic units or soil texture. The justification supporting the use of these definitions is based both on practical and scientific considerations. Soil texture and stratigraphy can be easily and inexpensively determined from well-log data and the close correlation of a number of hydrological and chemical properties with soil textures is well documented (Petersen *et al.*, 1996). A some-

what better definition of soil populations would be the cation- or anion-exchange capacity of the soils. However, this option is appreciably more expensive and is valuable only for defining K_d populations. The soil texture data are also used for defining water flow populations.

The intensity with which a soil must be sampled to estimate with given accuracy some characteristic, such as K_d value, will depend on the magnitude of the variation within the soil population under consideration. The more heterogeneous the population, the more intense must be the sampling rate to attain a given precision. In general, although differences have been found to exist among lithographic units, considerable variation may be expected within the units for such characteristics as pH, phosphorous, potassium, sodium, conductivity, volume weight, permeability and porosity (Peterson and Calvin, 1986). In some instances, the variation within contiguous units is so great that it is not feasible to estimate differences between the units with any satisfactory degree of precision. For most characteristics, the variation, both within and among units, decreases, with increasing depth in the profile (Peterson and Calvin, 1986). Hence, subsurface environments generally need to be sampled less than surface soils to attain comparable accuracy (Mackay *et al.*, 1986; Warrick and Nielsen, 1980). Mackay *et al.* (1986) reported that a number of soil properties, including K_d values, changed more vertically than laterally.

3.3.3 The “Gravel Issue”

Because most K_d values are measured in laboratory studies, the sample size has an upper mass limit of about 100 g soil (and often 10 g with the increased emphasis of waste minimization and high disposal costs for laboratory wastes) in batch K_d measurements and several kilograms of soil in column studies. Both tests also have particle size limitations. The batch K_d is typically limited to the less than 2-mm size fraction (Appendix C, ASTM, 1987; EPA, 1991; Roy *et al.*, 1991). This size fraction was selected for a number of reasons that are both practical and scientific in nature. The less than 2-mm fraction has historically been defined as the soil fraction and the greater than 2-mm fraction as the rock fraction. The less than 2-mm fraction is also convenient for most standard glassware used in batch K_d tests (Figure 3.1). Another practical consideration is that greater uniformity of the soil sample and therefore of the measured K_d value can be achieved if the range of particle sizes used in the test is limited. Finally, the smallest fraction is the most chemically reactive fraction due to its high specific surface area (m^2/g). The particle size used in column studies is also commonly limited to the less than 2-mm fraction. This size fraction was selected for similar reasons as for the batch studies and to compare results between the 2 common methods. However, Relyea (1982) indicated that the less than 2-mm size fraction should only be used in columns greater than 80 mm in diameter. He indicates that to avoid local velocity effects (*e.g.*, channeling or a radial velocity gradient), the column diameter should be at least 30 to 40 times the particle diameter of the solids used to pack the column.

The “gravel issue” is the problem that transport modelers face when converting laboratory-derived K_d values based on experiments conducted with the less than 2-mm fraction into values that can be used in systems containing particles greater than 2 mm in size. As mentioned above, the less than 2-mm fraction is the more chemically reactive fraction due primarily to its large

surface area. There are many subsurface soils dominated by cobbles, gravel, or boulders. To base the K_d values on the less than 2-mm size fraction, which may constitute less than 1 percent of the soil volume, would grossly overestimate the actual K_d of the aquifer. Including large soil particles in a K_d determination will increase the cost of laboratory equipment and perhaps more importantly will result in K_d values with large error terms because of the great variability of the particle size distribution in subsamples of a single soil.

Two general approaches have been proposed to address the “gravel issue.” The first is to assume that all particles greater than 2 mm have a $K_d = 0$ ml/g. As an example, if 75 percent (w/w) of a formation is composed of particles greater than 2 mm and the K_d value of the less than 2-mm size fraction was 100 ml/g, then the K_d value used in the model would be 25 ml/g. Although the assumption underlying this approach is incorrect, the extent to which sorption occurs on these larger particles may be small. This approach is likely to yield a more accurate value in systems dominated by cobbles, gravel, and boulders.

The second approach is to normalize laboratory-derived K_d values by surface area. Thus, instead of having units of

$$\frac{\frac{\mu\text{g metal}}{\text{g sediment}}}{\frac{\mu\text{g metal}}{\text{ml solution}}} = \frac{\text{ml}}{\text{g}}, \quad (3.16)$$

the laboratory K_d value would have units of

$$\frac{\frac{\text{g metal}}{\text{m}^2 \text{ sediment}}}{\frac{\mu\text{g metal}}{\text{ml solution}}} = \frac{\text{ml}}{\text{m}^2}, \quad (3.17)$$

(Kaplan *et al.*, 1995b). Theoretically, this latter approach is more satisfying because it permits some sorption to occur on the >2-mm fraction and the extent of the sorption is proportional to the surface area. The underlying assumption in this approach is that the mineralogy is similar in the less than 2- and greater than 2-mm fractions and that the sorption processes occurring in the smaller fraction are similar to those that occur in the larger fraction. Because sorption is a surface area phenomena (Equation 3.16), as opposed to a weight phenomena (Equation 3.17), normalizing the data to surface area has logic, and is commonly done in soil (Sposito, 1989) and colloid chemistry (Alberty, 1987). The drawback to this approach is that an additional measurement is needed to calculate the newly defined K_d value in the laboratory. Specific surface area measurement is a rather common and simple procedure (Carter *et al.*, 1986). This approach

to the “gravel issue” also requires a means to convert available soil texture data, which are often available from well-hole logs or outcroppings of the formation, into surface area data.

3.3.4 The “Colloid Issue”

The “colloid issue,” as it pertains to measuring K_d values, is the problem experimentalists have in separating the aqueous from the solid phases during a laboratory batch K_d measurement (see Chapter 2). Typically centrifugation or filtration are used to accomplish this. If contaminants are sorbed to tiny particles that remain in suspension after the separation step, the experimenter will incorrectly assign the sorbed contaminant to the dissolved phase, C_i (Equation 3.2). This will result in underestimating the true K_d value. This is an especially important problem for contaminants that sorb strongly to solids, especially organic matter. Organic matter has a much lower density than clay (*i.e.*, $\sim 1.05 \text{ g/cm}^3$ for organic matter versus $\sim 2.6 \text{ g/cm}^3$ clays) and therefore the common centrifugation protocol may not be sufficient to separate the phases. Also, organic matter may exist as extremely small particles, or molecules, $\sim 0.005 \mu\text{m}$ in diameter. Thus, when a great deal of organic matter is present in a soil, or when only a trace amount of organic matter has a profound affect on the measured K_d , additional precautions must be followed (Gschwend and Wu, 1985). For example, Gschwend and Wu (1985) reported that they were able to increase the partitioning coefficient, which is related to the K_d term (see Section 3.2.3), of polychlorinated biphenyl by 3 orders of magnitude by very carefully removing unsettled organic particles from suspension.

Using a centrifuge to make the solid and solution phase separations can also result in the formation of a very thin zone at the liquid surface where surface tension holds fine-grained particles at the top of the solution. The experimentalist should look for such problems and avoid sampling the surface of the clarified liquid. When pipets are used to remove supernatant solution, the pipet should be inserted sufficient distance below the surface to avoid drawing in suspended particles, but to a distance where the pipet tip is above the settled solids-liquid interface to avoid drawing in previously settled fines.

For these reasons, many experimentalists prefer to filter the supernatant solution after centrifugation. Filtration does have its problems, however. Filtering a small volume of supernatant solution can bias the contaminant’s concentration if the filter membrane adsorbs solute species. The type of filter membrane used effects the potential for adsorption. In our experience polyethylene or other plastic-based filter membranes are more inert than cellulosic-based membranes. Filter membranes can also be “pre-treated” with the supernatant solution by discarding the first aliquot and filtering a second aliquot that is saved for analysis. If the filter membrane does adsorb the analyte of interest, the amount adsorbed usually rapidly diminishes as the volume of solution filtered increases. Thus discarding the first aliquot of filtered solution and using subsequent aliquots for analysis lowers the chances of biasing final K_d values.

Another problem associated with colloids, is that the traditional 2-phase solute transport model does not account for contaminants moving in association with mobile colloids. This subject is

discussed in Chapter 2 (Section 2.5.1). Briefly, contaminants with a high affinity for sorbing to rock or vadose zone soils are assumed to be retarded relative to the rate of groundwater flow. However, an increasing body of evidence indicates that under some subsurface conditions, components of the solid phase may exist as colloids that may be transported with the flowing water. Association of contaminants with this additional mobile phase may enhance not only the amount of the contaminant that is transported, but also the rate of contaminant transport. Most current approaches to predicting contaminant transport ignore this mechanism not because it is obscure or the mathematical algorithms have not been developed (Corapcioglu and Kim, 1995; Mills *et al.*, 1991), but because little information is available on the occurrence, the mineralogical properties, the physicochemical properties, or the conditions conducive to the generation of mobile colloids. There have been numerous examples in which mobile colloids have been implicated as the vector responsible for enhanced transport (Kaplan *et al.*, 1994a,b; Kaplan *et al.*, 1995a; reviewed by McCarthy and Degueudre, 1993).

3.3.5 Particle Concentration Effect

Many investigators have observed that K_d values determined in the laboratory often exhibit a dependence with respect to the ratio of solid to solution used in the measurements. As recently discussed by Oscarson and Hume (1998), this dependence is puzzling. From a theoretical perspective, the K_d value should not depend on the solid-to-solution ratio, because the definition of the K_d model (see Equation 2.20) normalizes the ratio of the solute sorbed to the solid to the solute concentration left in solution based on the mass of solid and solution used for the measurement. Thus the K_d has units of volume/mass, such as typically ml/g.

Investigators have often found that K_d values measured for many contaminants for a given soil-groundwater system decrease as the solid-to-solution ratio increases. For example, this particle concentration effect on K_d values has been observed by O'Conner and Connolly (1980), Oscarson and Hume (1998), Honeyman and Santschi (1988), Meier *et al.* (1987), and others. The same trend with respect to particle concentration has also been observed for K_d values for organic contaminants [*e.g.*, see Gschwend and Wu (1985) and Voice *et al.* (1983)].

Investigators have offered several explanations for the observed dependency. These explanations can be categorized into two groups: (1) "real" physical/chemical processes, and (2) experimental artifacts. One rationalization offered in the "real" category is that the particle concentration effect is thought to be caused by particle-particle interactions. In systems with higher solids content, these interactions are perhaps physically blocking some adsorption sites from the adsorbing solutes and thus causing decreased adsorption, or creating electrostatic interferences such that the electrical surface charges on the closely packed particles diminish attractions between the adsorbing solutes and surfaces of individual grains. In terms of physical effects, individual particles in a slurry having a high solid-to-solution ratio may have a greater tendency to coagulate and flocculate into larger particles that have less available surface adsorption sites than individual grains and thus can adsorb less adsorbate. This phenomenon is likely exacerbated by diffusion processes that in short-term laboratory measurements, do not allow sufficient time for

the adsorbate to diffuse to the internal surface adsorption sites. The net effect is a K_d measurement with a lower value when a high solid-to-solution ratio is present, because not enough time was allocated for the water/soil system to reach a final equilibrium state. Thus there are possible experimental artifacts even within the context of this “real” process explanation.

Plausible experimental artifacts also include less efficient separation of the solid phase from high solids-content slurries, such that more colloidal size particles laden with adsorbate remain in the solution phase and the associated adsorbate gets included in the analysis of the solution phase. Complexing agents may desorb and/or dissolve from the solids, and in turn compete with the adsorbate for the available sorption surface sites. Soluble organic carbon is a common example of this process. Such effects increase when higher solid contents are used. Other artifacts include changes in the aqueous system that are caused by mass transfer from the larger quantity of solids but are not recorded during these measurements. Another consideration in the category of possible experimental artifacts for the solid-to-solution effect is improper data reduction. McKinley and Jenne (1991) suggest that the so-called particle concentration effect often goes away when adsorption data are replotted as adsorption isotherms, where the mass of solute adsorbed per mass of solid and the concentration of solute in the equilibrium solution are plotted on the y- and x-axes, respectively.

The explanations for the particle concentration (solid-to-solution ratio) effect are numerous and still rather perplexing [see summaries by Oscarson and Hume (1998) and Jenne (1998a)]. Jenne (1998a,b) includes valuable discussion on this “solids concentration effect.” He also presents some recommendations that should be followed when performing adsorption experiments and identifies several key issues that should be addressed by future adsorption research. One practical position that has been supported by EPRI (1991) is to conduct adsorption experiments as close as possible to the conditions that exist at the site where contaminant mobility is being simulated and assessed. In most cases, this recommendation would require that K_d values determined by flow-through column testing would be preferred over batch measurements conducted at low solid-to-solution ratios.

As noted above, it has been suggested that K_d values may decrease with increasing solid-to-solution ratios. If this is a real effect, application of K_d values based on a batch experiment conducted with a solid-to-solution ratio significantly less than those that would exist in the field would therefore overestimate the magnitude of contaminant sorption and underestimate the extent of contaminant migration.

3.4 Methods of Acquiring K_d Values from the Literature for Screening Calculations

3.4.1 K_d Look-Up Table Approach: Issues Regarding Selection of K_d Values from the Literature

Clearly, the greatest limitation of using a K_d value to calculate a retardation term (Equations 3.8, 3.9, 3.10, and 3.11) is that it describes solute partitioning between the aqueous and solid phases

for only 1 set of environmental conditions. K_d values are known to vary greatly with only slight changes in the composition of the solid and aqueous phases and these conditions often vary greatly in 1 study site. For example, when the aqueous chemistry for a batch K_d measurement was varied, americium K_d values in a Hanford sediment ranged from 0.2 to 53 ml/g, greater than a 200-fold difference (Delegard and Barney, 1983). Additional variability in the americium K_d values were observed when slightly different Hanford sediments were used: 4.0 to 28.6 ml/g (Delegard and Barney, 1983). Similarly, Sheppard *et al.* (1976) measured americium K_d values ranging from 125 to 43,500 ml/g using identical aqueous phases but different soils.

An alternative approach to a constant K_d model is one in which the K_d value varies as a function of a select group of environmental conditions (Delegard and Barney, 1983; Routson and Serne, 1972; Strenge and Peterson, 1989). The easiest variable K_d model to interface with a transport code is one based on a look-up table. For look-up tables, separate K_d values are assigned to a matrix of discrete categories defined by chemically important environmental parameters (Strenge and Peterson, 1989; Whelan *et al.*, 1992). Strenge and Peterson (1989) used 9 categories defined by soil pH and texture in the Multimedia Environmental Pollutant Assessment System (MEPAS) code. The 3 soil texture classes were <10 percent, 10 to 30 percent, >30 percent clay/organic matter/oxide content. The 3 pH classes were >9, 5 to 9, and <5. The 9 cells defined by the pH and soil texture classes contained literature-derived K_d values and where data was not available, estimated values were included in the table. The inorganic contaminants in the K_d look-up table were actinium, aluminum, americium, antimony, arsenic, asbestos, barium, beryllium, borate, cadmium, calcium hypochlorite, calcium oxide, carbon, cerium, chlorate, chromium (III), chromium (VI), cobalt, copper, curium, europium, fluoride, hydrogen fluoride, iodine, iron, krypton, lead, lead oxide, lithium hydroxide, lithium ion, magnesium, manganese, mercury, molybdenum, neptunium, nickel, niobium, nitrate, nitric acid, nitrogen dioxide, palladium, phosphate ion, phosphorus, plutonium, polonium, potassium hydroxide, potassium ion, protactinium, radium, ruthenium, samarium, selenium, silicate ion, silver, sodium ion, strontium, sulfate, sulphur, thallium, thorium, tin, tritium, uranium, vanadium, yttrium, zinc compounds, zinc, and zirconium.

For any literature-derived K_d value, it is essential to clearly understand the selection criteria and the logic used to estimate K_d values not found in the literature. For instance, Strenge and Peterson (1989) reported a wide range of literature K_d values for several cells, typically greater than 10-fold and sometimes greater than a 100-fold difference between minimum and maximum values. The values included in the MEPAS look-up table were the minimum values found in the literature. They justified this criteria because they wanted to build conservatism into the code. Conservatism is traditional when addressing the extent of contaminant migration and associated health effects, but may be erroneous if the modeling calculations are being used to address remediation options, such as pump-and-treat remediation. Conservatism for remediation calculations would tend to error on the side of under estimating the extent of contaminant desorption that would occur in the aquifer once pump-and-treat of soil flushing treatments commenced. Such an estimate would provide an upper limit to time, money, and work required to extract a contaminant from a soil. This would be accomplished by selecting a K_d from the

upper range of literature K_d values. Thus, the K_d values in MEPAS would not provide a conservative estimate for clean-up efforts .

Other important issues regarding the use of literature-derived K_d values are illustrated in Table 3.2. In any K_d look-up table, a small number of ancillary parameters must be selected to define the cells. pH and soil texture were the ancillary parameters used in the MEPAS code. These are excellent general categories for a large number of contaminants, however, they are of only secondary importance to a large number of other contaminants. For example, the amount of vermiculite, which is a 2:1 layer silicate mineral common in the United States, especially in the west and mid-west, is arguable the single most important ancillary parameter affecting cesium sorption (Douglas, 1989). Redox state is another example of an ancillary parameter that is extremely important relative to affecting the removal from redox-sensitive contaminants solution [this is actually a precipitation process and not an adsorption phenomena (Ames and Rai, 1978; Rai and Zachara, 1984; Sposito, 1989)]. Some important redox sensitive contaminants include arsenic, chromium, molybdenum, neptunium, plutonium, selenium, technetium, and uranium. The K_d values of uranium in the 9 MEPAS categories range from 0 to 500 ml/g (Table 3.2).

Table 3.2. Example of a K_d (ml/g) look-up table for uranium, uranium(VI), and uranium(IV).

Material	pH								
	≥ 9			5 - 9			≤ 5		
Fines ¹ (%)	<10	10-30	>30	<10	10-30	>30	<10	10-30	>30
U ²	0	5	50	0	50	500	0	5	50
U(IV) ³	200	500	1,000	100	250	500	20	30	50
U(VI) ³	0	1	2	1	2	5	2	5	20

¹ Fines (%) = sum of percentages of clay, organic matter, and hydrous-oxide in soil
² Reference: Streng and Peterson (1989)
³ Authors' opinion based on values reported in Ames and Rai (1978), Ames and McGarrah (1980), Cloninger *et al.* (1980), Cloninger and Cole (1981), Serne and Relyea (1981), and Rai and Zachara. (1984).

By including an additional ancillary parameter of oxidation state, appreciably greater accuracy can be assigned to K_d values. For U(VI), the 9 categories may be assigned K_d values in the range of 0 to 20 ml/g, whereas, as for U(IV), the 9 categories may be assigned K_d values in the range of 20 to 1,000 ml/g. In this example, oxidation state is obviously a more important ancillary parameter than soil texture and in systems with pH values greater than 5, oxidation state is more important

than pH. The reduced form of U, U(IV), has a much greater K_d value than U(VI) because the former is known to precipitate from solution. The rather low uranium K_d values reported by Streng and Peterson (1989) are somewhat misleading in that they represent, as mentioned above, minimum values identified in the literature. These values would be entirely inappropriate for modeling U(IV) transport. Thus, an important point to this discussion is that no single set of ancillary parameters, such as pH and soil texture, is universally appropriate for defining categories in K_d look-up tables for all contaminants. Instead, the ancillary parameters used in look-up tables must be based on the unique chemical properties of each contaminant.

An apparent inconsistency in Table 3.2 is that the minimum values selected by Streng and Peterson (1989) for the uranium data are greater than those for U(VI). This inconsistency is not due to differences in literature used to estimate these values. Instead it arises from differences in how K_d values are estimated for cells in which no data are available.¹ This illustrates another important reason for clearly understanding the criteria and process used in selecting data incorporated into a look-up table. Clearly, differences in the criteria and process used to select K_d values can result in appreciable different values included in a look-up table; in this example, as much as 3 orders of magnitude.

3.4.2 Parametric K_d Approach

The parametric K_d approach is similar to that of the K_d look-up table approach in that it varies K_d values used in a transport model as a function of important ancillary parameters. It differs from the K_d look-up table in that it uses a regression equation to define the K_d values instead of using discrete categories. The K_d value in this model varies as a function of empirically derived relationships with aqueous and solid phase independent parameters. Thus, it has the distinct advantage over look-up tables of having a continuum of K_d values.

Factorial design experiments are most often used to determine the systematic change resulting from varying the independent variables (*e.g.*, pH, soil texture, and redox status) on the dependent variables (uranium K_d) (Box and Behnken, 1960; Cochran and Cox, 1957; Davies, 1954; Plackett and Burman 1946). Statistical methods commonly used to derive quantitative predictor equations include standard linear or nonlinear regression (Snedecor and Cochran, 1967), stepwise regression

¹ Streng and Peterson (1989) generated most of the values in the pH>9 categories by multiplying the K_d values from the pH 5 to 9 category by 0.1. A significant quantity of K_d values exist in the literature for the latter pH category. The “0.1 factor” was based on consistent, but flawed logic that metal contaminants are less likely to sorb because their cationic valence decreases by $[M^{a+}(OH)_x]^{a-x}$. It is now known that hydrolysis species adsorb as well as or better than free cations (M^{a+}). Also many contaminants precipitate at higher pH values, giving the appearance of increased K_d values. There are a few exceptions in pH >9 systems: $Zr(OH)_5$ species that may not adsorb as well as Zr^{4+} , and $UO_2(CO_3)_2^{2-}$ and $UO_2(CO_3)_3^{4-}$ species do not adsorb as well as the UO_2^{2+} and UO_2OH^+ species. The CO_3^{2-} activity increases as pH increases so complexes get more important at elevated pH levels.

(Hollander and Wolfe, 1973), and adaptive-learning networks (Mucciardi *et al.*, 1979, 1980). All these techniques have been used to develop empirical relationships describing K_d values in terms of other variables (Delegard and Barney, 1983; Routson and Serne, 1972; Serne *et al.*, 1973; Routson *et al.*, 1981).

The empirical predictor equations commonly take the form of a nonlinear polynomial expression. For example, after evaluating solutions consisting of several sodium salts, organic chelates, and acids, Delegard and Barney (1983) came up with the following expression for an americium K_d value:

$$\text{Log } K_d (\text{Americium}) = 2.0 + 0.1[\text{NaOH}] - 26.8[\text{HEDTA}] + 153.4[\text{HEDTA}]^2 \quad (3.18)$$

where HEDTA is N-(2-hydroxyethyl) ethylenediaminetetraacetic acid. Numerous salts were found to have no significant effect on americium K_d values and therefore were not included in the expression. Delegard and Barney (1983) also evaluated higher exponential and logarithmic terms and determined that these terms did not improve the predictive capabilities of the expression (*i.e.*, the regression coefficients were not significant at $P \leq 0.05$).

It is critical that parametric K_d equations, such as Equation 3.18, be used to calculate K_d values for systems within the range of the independent variables used to create the equation. In the case of Equation 3.18, the range of independent variables used to generate the model were selected to simulate a plume beneath the Hanford Site in Richland, Washington. Using Equation 3.18 to generate americium K_d values for a plume low in pH and Na concentrations would not be appropriate.

These types of statistical relationships are devoid of causality and therefore provide no certain information regarding the mechanism by which the contaminant partitioned to the solid phase, whether it be by adsorption, absorption, or precipitation. For example, the statistical analyses may suggest a very strong relationship between pH and the K_d term, when the actual sorption process may be controlled by iron oxide adsorption. Because pH and iron-oxide charge are covariates, a statistical relationship may suggest that sorption is due to pH, when in fact, suggesting that sorption is solely caused by pH.

The parametric K_d model is used in the transport equation, the code must also keep track of the current value of the independent variables (*e.g.*, [NaOH] and [HEDTA] for the examples described in Equation 3.18) at each point in space and time to continually update the concentration of the independent variables affecting the K_d value. Thus, the code must track many more parameters, and some numerical solving techniques (*e.g.*, closed-form analytical solutions) can no longer be used to perform the integration necessary to solve for concentration. Generally, computer codes that can accommodate the parametric K_d model use a chemical subroutine to update the K_d value used to determine the R_f , when called by the main transport code. The added complexity in solving the transport equation with the parametric K_d sorption model and its empirical nature may be the reasons this approach has been used sparingly.

3.4.3 Mechanistic Adsorption Models

Mechanistic models explicitly accommodate for the dependency of K_d values on contaminant concentration, competing ion concentration, variable surface charge on the adsorbent, and solute species solution distribution. Incorporating mechanistic, or semi-mechanistic, concepts into models is attempted because the models become more robust and, perhaps more importantly from the standpoint of regulators and the public, scientifically defensible. The complexity of installing these mechanistic adsorption models into existing transport codes is difficult to accomplish. Additionally, these models also require a more intense and costly data collection effort than will likely be available to the majority of contaminant transport modelers who are conducting screening calculations. Descriptions of the state of this science, with references to excellent review articles, are presented in Chapter 2 and 5. A review of the methodology associated with the determination of the constants for use in these mechanistic models, however, is beyond the scope of this project. A review of the mechanistic adsorption models contained in EPA's MINTEQA2 geochemical reaction code is also presented in Chapter 5.

3.5 Summary

The objective of this chapter is to describe methods used to measure K_d values. The advantages and disadvantages and the assumptions underlying each method were discussed, and are summarized in Table 3.3. A number of issues regarding the selection of K_d values from the literature for screening calculations are also addressed in this chapter. Specific issues discussed included the use of simple versus complex systems to measure K_d values, field variability, the "gravel issue," and the "colloid issue."

Clearly, the greatest limitation of using a K_d value to calculate a retardation term is that it is only applicable to a single set of environmental conditions. Consequently, researchers have generated K_d values that varies as a function of ancillary environmental parameters. They include the look-up table K_d , the parametric K_d , and the mechanistic K_d . Models generated for parametric K_d values have typically been for rather limited environmental conditions. Mechanistic K_d values are limited to uniform solid and aqueous systems with little application to the heterogenous soils that exist in the natural environment. The easiest and the most common variable K_d model to interface with a transport code is the look-up table. No single set of ancillary parameters, such as pH and soil texture, is universally appropriate for defining categories in K_d look-up tables. Instead, the ancillary parameters must vary in accordance to the geochemistry of the contaminant. It is essential that the modeler fully understand the criteria and process used for selecting the values incorporated in such a table. Just as important is to understand the logic used to estimate K_d values not found in the literature. Differences in the criteria and process used to select K_d values can result in appreciable different K_d values.

It is incumbent upon the transport modeler to understand the strengths and weaknesses of the different K_d methods and perhaps more importantly the underlying assumption of the methods in order to properly select K_d values from the literature. The K_d values reported in the literature for

any given contaminant may vary by as much as *6 orders of magnitude*. An understanding of the important geochemical processes and knowledge of the important ancillary parameters affecting the sorption chemistry of the contaminant of interest is necessary for selecting appropriate K_d value(s) for contaminant transport modeling.

Table 3.3. Advantages, disadvantages, and assumptions of different methods used to determine K_d and the assumptions in applying these K_d values to contaminant transport models.

Methods for Determining K_d				
Batch ¹	<i>In-Situ</i> Field Batch	Flow-Through	Field Modeling	K_{oc} ²
Minimum Input Data ³				
<ul style="list-style-type: none"> • M_{sed} • C_i • C_0 • V_w 	<ul style="list-style-type: none"> • C_i • A_i (or q_i) 	<ul style="list-style-type: none"> • C_o • $n, \theta,$ or n_e • $\rho_{particle}$⁴ • $>10 C_{effluent}$ data points • C_o tracer • Time 	<ul style="list-style-type: none"> • $C_{release}$ • C_{well} • Time • Distance • v_w • $n, \theta,$ or n_e • Diffusion or dispersion coefficients 	<ul style="list-style-type: none"> • K_{oc} • f_{oc}
Advantages				
<ul style="list-style-type: none"> • Inexpensive • Quick 	<ul style="list-style-type: none"> • <i>In-situ</i> measurements • Equilibrium conditions • Aqueous and solid phases are precisely those of the modeled system 	<ul style="list-style-type: none"> • Can measure sorption at field flow rates, <i>i.e.</i>, at non-steady state conditions • Can measure hydrodynamic effects (<i>e.g.</i>, dispersion, colloidal transport, <i>etc.</i>) on R_f, and subsequently incorporate into K_d value • Can measure effects of chemical phenomena (<i>e.g.</i>, multiple species, reversibility, <i>etc.</i>) on R_f and K_d values. 	<ul style="list-style-type: none"> • Derived K_d has the precise geochemical conditions and flow conditions of the study site 	<ul style="list-style-type: none"> • Fairly accurate indirect method • Often can use look-up tables to get K_{oc} value • f_{oc} is an easy measurement • K_{oc} can be correlated with K_{ow} which has been measured for many different chemicals

Table 3.3. Continued.

Methods for Determining K_d				
Batch ¹	<i>In-Situ</i> Field Batch	Flow-Through	Field Modeling	K_{oc} ²
Disadvantages				
<ul style="list-style-type: none"> • Provides estimate of chemical processes at equilibrium; flow conditions are not always at equilibrium • Physics involved not considered • Better mixing in batch than in nature • Typically uses larger ratio of solution/soil than exist in nature • Experiments measure <u>adsorption</u> instead of <u>desorption</u>, the dominant process in transport; desorption is typically much slower than adsorption • Speciation of different forms not considered 	<ul style="list-style-type: none"> • Expensive to collect samples • Commonly have high detection limits (undesirable) for measuring contaminant on solid phase (A_s, q_s) • Site-specific data • Cannot unequivocally differentiate between, adsorbed, precipitated, and structural constituents 	<ul style="list-style-type: none"> • Commonly flow-through system is not at equilibrium and therefore results cannot be applied to other flow conditions • Directly measure R_f, then back out K_d; therefore must make assumptions about relation between K_d and R_f⁵ • Measured K_d values commonly vary with water velocity and column dimensions • Requires relatively expensive equipment • Requires a lot of time • Complex experiment to conduct • Data are commonly not well behaved, <i>i.e.</i>, asymmetric or peakless break-through curves • Can investigate some secondary processes affecting contaminant transport, such as effects of unsaturated flow, colloid-facilitated contaminant transport, mobile vs immobile water phases 	<ul style="list-style-type: none"> • K_d is truly site specific • K_d is transport model specific • Need to make many assumptions about the water flow including uniform flow, direction, and path length that affect the calculated K_d value • Measure R_f, then back out K_d; many assumptions go into relating K_d to R_f • May or may not be in equilibrium, therefore not a thermodynamic K_d • K_d value greatly improves with more field data collected • Calculations can be quite involved 	<ul style="list-style-type: none"> • For organic compounds only • More hydrophobic the contaminant compound, more accurate the K_d; vice versa with hydrophilic compounds

Table 3.3. Continued.

Methods for Determining K_d				
Batch ¹	<i>In-Situ</i> Field Batch	Flow-Through	Field Modeling	K_{oc} ²
Assumptions in Calculating K_d				
<ul style="list-style-type: none"> • Adsorption rate = desorption rate • Only 1 type of surface adsorption site, A • Only 1 type of aqueous dissolved species, C_i • $A \gg A_i$ • Activity of $A_i=1$ • Equilibrium has been achieved during mixing period • No adsorbate on suspended colloids • No precipitation of adsorbate due to C_0 concentration exceeding solubility 	<ul style="list-style-type: none"> • Same as for batch K_d • Measurement of adsorbed contaminant, A_i (q_i), can differentiate between adsorbed, precipitated, and structural constituents 	<ul style="list-style-type: none"> • Must assume a relationship between R_f and K_d⁵ • Water flow and dispersion coefficient is constant 	<ul style="list-style-type: none"> • Must assume a relationship between R_f and K_d • Know n_e or n • Must know the flow path and velocity of plume • Sorption is uniform in the study size 	<ul style="list-style-type: none"> • Same as for laboratory batch K_d • Organic contaminant sorbs (partition) only to organic matter in soil, no sorption occurs to inorganic phases

Table 3.3. Continued.

Methods for Determining K_d				
Batch ¹	<i>In-Situ</i> Field Batch	Flow-Through	Field Modeling	K_{oc} ²
Assumptions in Applying Measured K_d to Transport Model				
<ul style="list-style-type: none"> • Adsorption of solute is linear, <i>i.e.</i>, it is independent of C_i • Adsorption of solute is reversible • Solute movement is slow enough that equilibrium conditions exist between the solute and soil • Geochemical conditions (presence and concentration of background electrolytes and solid phases) of batch experiment are identical to those in aquifer • Temperature and pressure conditions of batch experiment are identical to those in the aquifer • Mixing in aquifer is as thorough as in batch experiment • Difference between the soil/water ratio in the aquifer and batch experiment is not important to K_d value 	<ul style="list-style-type: none"> • Same as for laboratory batch K_d (except fourth point not relevant to <i>in-situ</i> batch method) 	<ul style="list-style-type: none"> • It is more common to enter the R_f value derived from experiment than the K_d value into transport code; consequently, do not need to make any assumptions about the relationship between R_f and K_d • If R_f value from column experiment is entered into transport code and the flow conditions of the experiment are similar to those in the site being modeled, then no assumptions need to be made regarding affect of nonequilibrium conditions 	<ul style="list-style-type: none"> • None 	<ul style="list-style-type: none"> • Same as for laboratory batch K_d
<p>¹ See Equation 3.4</p> <p>² See Equation 3.13</p> <p>³ A = Concentration of free or unoccupied surface adsorption site on a solid phase; C_i = the total dissolved adsorbate concentration remaining in solution at equilibrium; f_{oc} = fraction of soil that is organic carbon; $C_{release}$ = concentration of solute at time of release; C_{well} = concentration of solute in monitoring well; M_s = soil mass; A_i = the concentration of adsorbate on the solid at equilibrium; n = total porosity; n_e = effective porosity; V_w = solution volume; ρ_b = bulk density; $\rho_{particle}$ = particle density; θ = water saturation.</p> <p>⁴ $\rho_{particle}$ is used to calculate bulk density (ρ_b); $\rho_b = [\rho_{particle} (1 - n)]$.</p> <p>⁵ See Equations 3.8, 3.9, 3.10, and 3.11.</p>				

4.0 Groundwater Calibration Assessment Based on Partition Coefficients: Derivation and Examples

4.1 Introduction

Partition (or distribution) coefficient, K_d ,¹ values are utilized in transport and risk assessment modeling because of their simplicity in (1) understanding, (2) measuring, and (3) providing closed-form, explicit, analytical solutions to the advective-dispersive equations. Whelan (1996) presented a discussion that illustrates the inherent difficulties associated with utilizing partition coefficients as the sole parameter to define the geochemical properties of a solute as it migrates through a subsurface environment. Multiple definitions for K_d values have been identified, including those based on thermodynamics (*e.g.*, Gibbs free energy of formation), experiments (*e.g.*, batch and flow-through tests), and theory (*e.g.*, isotherms). Each of these procedures identifies a different value for the same parameter, which is supposed to describe the same phenomena. Although K_d values can be thermodynamically defined, their meaning becomes less clear in the real world. As such, K_d values can be estimated using transport models. This process, called calibrating a groundwater transport model to K_d values, involves treating the K_d value as the adjustable parameter (or dependent variable) while simulating known monitored contaminant data. Groundwater calibration captures the essence of the problem in the field. This is an iterative process that frequently requires that the magnitude of a number of other input parameters, such as effective porosity, dispersion, and flow rate, be adjusted to yield meaningful K_d values. A K_d value represents one of the calibration parameters because its magnitude is subject to not only the laboratory analyses but also to the heterogeneity in the field and different ways it is used in the mathematical constructs of different models.

4.2 Calibration: Location, Arrival Time, and Concentration

When calibrating a groundwater model to monitored information (*e.g.*, concentrations at a monitoring well), the model must predict the correct arrival time at the correct location, matching the magnitude of the monitored concentration. Therefore, time, location and magnitude are 3 crucial elements associated with any calibration exercise, and K_d impacts two of them (*i.e.*, travel time and magnitude). Location is predetermined by the user with respect to monitoring wells, receptor locations, *etc.* Once the distances have been defined, the calibration requires modifications to parameters that govern travel times and concentration levels. Parameters, which influence water and contaminant movement, are varied within acceptable ranges in an attempt to recreate conditions in the field. As the model complexity increases, the number of parameters that the analyst can vary increases, and the calibration process becomes increasingly more complicated. Figure 4.1 illustrates the relative relationships between input-data quality, output uncertainty, and types of problems addressed by each level of assessment. As Figure 4.1 indi-

¹ A list of acronyms, abbreviations, symbols, and notation is given in Appendix A. A list of definitions is given in Appendix B

cates, the computational requirements tend to be less at the earlier stages of an assessment when available data are less, and, correspondingly, the uncertainty with the output results tends to be greater. As the assessment progresses, improved site-characterization data and conceptualization of the problem increase, thereby reducing the overall uncertainty in risk estimates.

Figure 4.1 also illustrates some of the characteristics and relationships between screening-level (ranking), “analytical” (prioritization and preliminary assessments), and numerical (detailed) models.

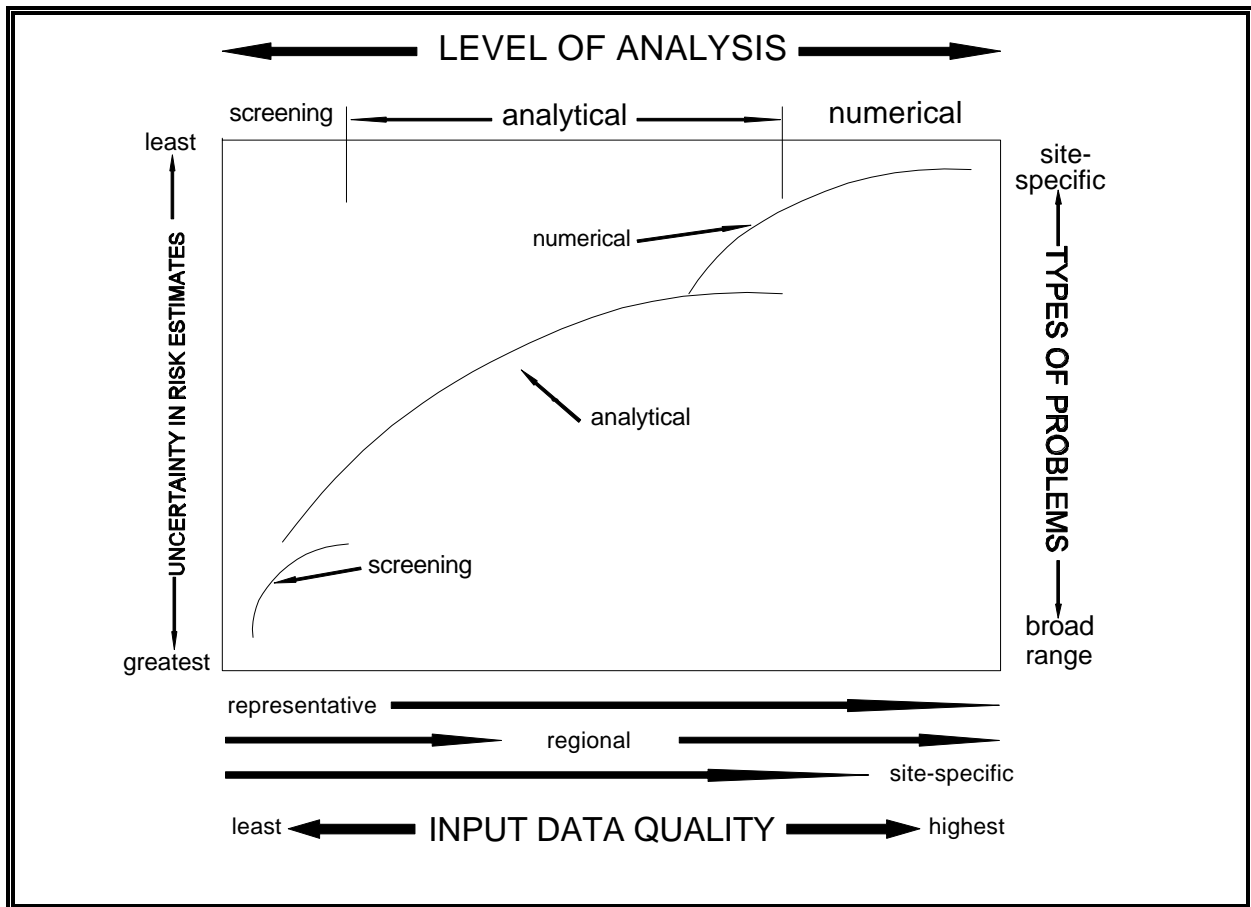


Figure 4.1. Relative relationships between input-data quality, output uncertainty, and types of problems addressed by each level of assessment.

Screening models are used to identify environmental concerns. These models, often based on a structured-value approach, are designed to be used with regional/representative information. Models such as the Hazard Ranking System (HRS) (EPA, 1984, 1992b) divide site and release characteristics into predetermined categories that are assigned a point value based on answers to questions. The score from such systems is useful to determine if a situation requires further analysis, but not to provide a method for estimating actual concentrations or impacts in the environment.

Detailed analyses require a highly specialized assessment of potential impacts. Detailed analyses are usually reserved for the most complex models, are data intensive, and are based on the expertise of the analyst. These detailed assessment models are used to address complex problems and concerns that are relatively well-defined. Models for detailed analyses tend to focus on special sets of problems and special types of situations. Although detailed assessment tools are appropriate for their intended application, extension beyond the site-specific application is often difficult or cost prohibitive. Typical models include MODFLOW (McDonald and Harbaugh, 1988) and CFEST (Cole *et al.*, 1988).

Analytically/semianalytically/empirically based models (designated as “analytical” models in Figure 4.1) can be utilized for prioritization or preliminary assessments and exist between initial-screening and highly specialized numerical models. These physics-based models are the most versatile as they do not have the data constraints associated with the numerical models. The analytical models may contain some numerical computations, hence the semianalytical designation. As Figure 4.1 illustrates, the analytical models are designed to provide environmental evaluations over a wide range of applications. Groundwater models that fall into this category include AT123D (Yeh, 1981), GROUND and GRDFLX (Codell *et al.*, 1982), and MEPAS (Buck *et al.*, 1995; Whelan *et al.*, 1992). The analytical-assessment models are codes with physics-based algorithms whose components can be utilized in a detailed (*i.e.*, numerical) or an initial-screening (*i.e.*, ranking/prioritization) assessment, where data and circumstances warrant.

The calibration process is an interactive one. Because data tend to be limiting, there are generally multiple ways in which parameters can be combined so the simulation results match monitored information. With increasing number of monitored data available, less combinations of the modeling parameters are possible to match the monitored information. In addition, many of these “matches” can assign unrealistic values to parameters; therefore, the number of acceptable possible combinations becomes even more limited. When calibrating, parameters can only be varied within ranges that physically make sense for the site and its conditions. If unrealistic output is a result of the analysis, then the (1) conceptual site model has to be re-evaluated, (2) input data must be re-examined, and/or (3) model must be re-evaluated to ensure that the assessment does not violate the assumptions, limitations, and constraints associated with the mathematical constructs of the code.

Each code has its own mathematical equations upon which it is based. A calibration exercise is performed to meet the constructs of these equations. Analytical models tend to be easier to work

with because of their closed-form, explicit solutions. With an analytical model, some initial calculations can be made that can provide an initial starting point for the calibration process; this process also illustrates how retardation factors (and ultimately K_d) influence the calibration process. As noted earlier, the intent of the calibration process is to get a contaminant from a source to the monitored location (*e.g.*, monitoring well) at the proper time with the appropriate concentration. In addition, the amount of mass monitored in the environment must be conserved, that is, the amount of mass predicted by the model to be in the environment should match the amount of mass monitored in the environment.

Travel times are influenced by the retardation factor, pore-water velocity, and dispersivity, although other parameters can also influence the outcomes. The retardation factor can be directly impacted by K_d . In the vadose zone, soil type and moisture content influence pore-water velocity, and in the saturated zone, soil type and effective porosity influence pore-water velocity. Longitudinal dispersivity normally influences the time to peak but by no more than 10 percent, although more is possible. Concentrations are generally influenced by the contaminant flux rate (or total mass released into the environment), mixing distances (dilution), pore-water velocity (dilution), retardation factor (K_d), and dispersivity (dispersion). If the size of the source is not well known, the areal extent of contamination influences concentration levels for spatially near-field problems. In any modeling exercise, the analyst will know some of the general characteristics of the parameters. Typically, the parameters that are used to calibrate the model are not known exactly; therefore, they can be modified within an appropriate range to help the analyst capture the essence of the problem.

4.3 Illustrative Calculations to Help Quantify K_d Using Analytical Models

If K_d forms the basic premise for retarding the movement of contaminants in a subsurface environment in the mathematical algorithms of a groundwater transport code, then the K_d permeates all of the contaminant transport calculations. Different computer codes may use different mathematical constructs, but the influence of K_d is usually very pronounced. The K_d value influences the calculations for determining the (1) contaminant travel time, (2) mass of contamination at the source or in a plume, and (3) distribution of the concentration in the environment. As an illustration of the impact that the K_d parameter can have in transport calculations, the influences of K_d on an analytical solution to the advective-dispersive equation are explored.

4.3.1 Governing Equations

The 1-dimensional advective, 3-dimensional dispersive equation with first-order degradation/decay can be expressed as follows:

$$\frac{\partial C_i}{\partial t} + v \frac{\partial C_i}{\partial x} = D_x^* \frac{\partial^2 C_i}{\partial x^2} + D_y^* \frac{\partial^2 C_i}{\partial y^2} + D_z^* \frac{\partial^2 C_i}{\partial z^2} - \lambda C_i \quad (4.1)$$

in which

$$v^* = \frac{v_p}{R_f} \quad (4.2)$$

$$v_p = \frac{v_d}{n_e} \quad (4.3)$$

$$R_f = 1 + \frac{\rho_b K_d}{n_e} \quad \text{saturated} \quad (4.4)$$

$$R_f = 1 + \frac{\rho_b K_d}{\theta_{vz}} \quad \text{vadose} \quad (4.5)$$

$$K_d = \frac{A_i}{C_i} \quad (4.6)$$

$$D^* = \frac{D_{\text{mech}} + D_{\text{mol}}}{R_f} \quad (4.7)$$

$$D_{\text{mech}} = \alpha v_p \quad (4.8)$$

where C_i = dissolved concentration
 v^* = contaminant velocity
 D^* = dispersion coefficient in the x, y, and z directions adjusted for retardation with the retardation factor
 λ = first-order degradation/decay coefficient
 v_p = pore-water velocity
 v_d = Darcy velocity
 R_f = retardation factor
 n_e = effective porosity
 ρ_b = bulk density
 θ_{vz} = moisture content in the vadose zone
 K_d = partition (distribution) coefficient
 A_i = adsorbed contaminant concentration on the soil particles
 D_{mech} = mechanical dispersion
 D_{mol} = molecular diffusion coefficient

α = dispersivity in the x, y, or z direction

The solution of advective-dispersive equation for an instantaneous release through a point source in a saturated zone, which is uniformly mixed in the vertical direction, at a distance (x) down gradient from the center of the source is as follows (Codell *et al.*, 1982; Fischer *et al.*, 1979; Whelan *et al.*, 1996; Yeh and Tsai, 1976; Yeh 1981):

$$C_i = \delta' X_{Gf} Y_{Gf} Z_{Gf} \quad (4.9)$$

where δ' = mass-related constant
 X_{Gf} , Y_{Gf} , and Z_{Gf} = Green's functions (which are orthogonal) in the x, y, and z directions, respectively
 X_{Gf} = Green's function corresponding to flow direction

in which

$$\delta' = \frac{M_{rel}}{R_f n_e} \quad (4.10)$$

$$X_{Gf} = \left(\frac{1}{4 \pi D_x^* t} \right)^{1/2} \exp(-\lambda t) \exp \left[- \left(\frac{(x - v_p^* t)^2}{4 D_x^* t} \right) \right] \quad (4.11)$$

$$Y_{Gf} = \left(\frac{1}{4 \pi D_y^* t} \right)^{1/2} \exp \left[- \left(\frac{y^2}{4 D_y^* t} \right) \right] \quad (4.12)$$

$$Z_{Gf} = \frac{1}{h_m} \quad (4.13)$$

where M_{rel} = released mass
 y = off-centerline distance
 h_m = mixing-zone thickness

and all other parameters retain their previous definitions.

The impact that the retardation factor and, hence, K_d has on the calculated value of the concentration at the receptor location can be profound, as illustrated by the number of locations that these terms appear in the governing equations.

4.3.2 Travel Time and the Partition Coefficient

As previously noted, it is very important to ensure that the contaminant arrives at the monitoring location at the appropriate time, and K_d can have a profound impact on the travel time. The advective travel time of the contaminant is defined as the distance x traveled divided by the contaminant velocity:

$$t_T = \frac{x}{v^*} \quad (4.14)$$

where t_T = total advective travel time of the contaminant

If a contaminant is traveling from a contaminated source through a vadose zone, through a saturated zone to a monitoring location, the total advective travel time is the summation of the travel times through the vadose (t_{vz}) and saturated (t_{sz}) zones:

$$t_T = t_{vz} + t_{sz} = \left(\frac{H_1 R_{f1}}{v_{p1}} \right) + \left(\frac{x_2 R_{f2}}{v_{p2}} \right) \quad (4.15)$$

where H_1 = thickness of the vadose zone
subscripts 1 and 2 = vadose and saturated zones, respectively

Substituting the definitions for retardation factor gives a slightly modified equation:

$$t_T = \frac{(H_1) \left(1 + \frac{\rho_{b1} K_{d1}}{\theta_{vz}} \right)}{v_{p1}} + \frac{(x_2) \left(1 + \frac{\rho_{b2} K_{d2}}{n_2} \right)}{v_{p2}} \quad (4.16)$$

This equation demonstrates the potential impact that K_d has on the travel time. Because K_d is assumed to be constant over the distanced traveled, a constant, ξ , can be defined, which represents the ratio of the partition coefficients between the vadose and saturated zones:

$$\xi = \frac{K_{d1}}{K_{d2}} \quad (4.17)$$

Substituting ξ into the total travel time equation gives the travel time as a function of the saturated zone's partition coefficient:

$$t_T = \left(\frac{H_1}{v_{p1}} \right) \left(1 + \left(\frac{\rho_{b1} \xi}{\theta_{vz}} \right) K_{d2} \right) + \left(\frac{x_2}{v_{p2}} \right) \left(1 + \left(\frac{\rho_{b2}}{n_{e2}} \right) K_{d2} \right) \quad (4.18)$$

Rearranging this equation and solving for K_{d2} gives:

$$t_T = \left(\frac{H_1}{v_{p1}} \right) + \left(\frac{H_1 \rho_{b1} \xi}{v_{p1} \theta_{vz}} + \frac{x_2 \rho_{b2}}{v_{p2} n_{e2}} \right) (K_{d2}) + \left(\frac{x_2}{v_{p2}} \right) \quad (4.19)$$

$$K_{d2} = \frac{t_T - (H_1/v_{p1}) - (x_2/v_{p2})}{\left(\frac{H_1 \rho_{b1} \xi}{v_{p1} \theta_{vz}} \right) + \left(\frac{x_2 \rho_{b2}}{v_{p2} n_{e2}} \right)} \quad (4.20)$$

This equation can be used to estimate initial values for the partition coefficients in the vadose and saturated zones, which will help ensure that the contaminant reaches the monitoring location at the appropriate time. These values can also be compared to literature or experimental values to see if they are consistent. If not, then the conceptual site model must be re-analyzed to ensure that the proper problem has been captured or that the appropriate data are being utilized.

4.3.3 Mass and the Partition Coefficient

The partition coefficient can be used to help estimate the mass of contamination that exists at the source or in a plume. The reported soil contamination in the vadose zone is usually expressed as the adsorbed concentration (A_i) and typically has units of mg/kg, which is also expressed as ppm (parts per 10^6). The aqueous concentration (C_i), using K_d as a conversion factor, can be calculated as follows:

$$C_i = \frac{A_i}{K_d} \quad (4.21)$$

The mass associated with the adsorbed phase in the vadose zone can be estimated as:

$$M_{ads} = V_{source} A_i (1 - n) \rho_{particle} \quad (4.22)$$

where M_{ads} = mass associated with the adsorbed phase in the vadose zone
 V_{source} = volume associated with the contaminated source
 n = total porosity
 $\rho_{particle}$ = particle density

The mass associated with the aqueous phase in the vadose zone can be estimated as:

$$M_{aq} = \frac{V_{source} A_i \theta_{vz}}{K_d} \quad (4.23)$$

where M_{aq} = mass associated with the aqueous phase in the vadose zone

The total mass associated with the vadose zone represents the summation of the mass associated with the adsorbed and aqueous phases, assuming no free product:

$$M_{\text{vadose}} = (M_{\text{ads}} + M_{\text{aq}})_{\text{vadose}} \quad (4.24)$$

where M_{vadose} = total mass associated with the vadose zone

The reported aqueous contamination in the saturated zone is usually expressed as the dissolved concentration C_i and typically has units of mg/l, which is also expressed as ppm (parts per 10^6). The mass associated with the aqueous phase in the saturated zone can be estimated as:

$$M_{\text{aq}} = V_{\text{source}} C_i n \quad (4.25)$$

The mass associated with the adsorbed phase in the saturated zone can be estimated as:

$$M_{\text{ads}} = V_{\text{source}} C_i K_d (1 - n) \rho_{\text{particle}} \quad (4.26)$$

The total mass in the vadose zone represents the summation of the mass associated with the adsorbed and aqueous phases, assuming no free product:

$$M_{\text{saturated}} = (M_{\text{ads}} + M_{\text{aq}})_{\text{saturated}} \quad (4.27)$$

where $M_{\text{saturated}}$ = total mass associated with the saturated zone

The total mass in the system is the summation of the masses in the vadose and saturated zones:

$$M_{\text{Total}} = M_{\text{vadose}} + M_{\text{saturated}} \quad (4.28)$$

If the environmental contamination in the vadose zone is expressed as a total mass in the waste site (or layer) per dry weight of soil, the dissolved and adsorbed concentrations can be calculated as follows (Whelan *et al.*, 1987):

$$C_i = \frac{C_{\text{Tp}} \rho_b}{\theta_{\text{vz}} + \rho_b K_d} \quad (4.29)$$

$$A_i = \frac{C_{\text{Tp}} \rho_b K_d}{\theta_{\text{vz}} + \rho_b K_d} \quad (4.30)$$

where C_{Tp} = total mass at the site per dry weight of soil

If the environmental contamination is expressed as a total mass per total volume of the waste site (or soil layer), the dissolved and adsorbed concentrations can be calculated as follows (Whelan *et al.*, 1987):

$$C_i = \frac{C_T}{\theta_{vz} + \rho_b K_d} \quad (4.31)$$

$$A_i = \frac{C_T K_d}{\theta_{vz} + \rho_b K_d} \quad (4.32)$$

where C_T = total mass at the site per total site volume

4.3.4 Dispersion and the Partition Coefficient

The 1-dimensional, dispersive equation in the lateral direction can be expressed as

$$\frac{\partial C_i}{\partial t} = D_y^* \frac{\partial^2 C_i}{\partial y^2} \quad (4.33)$$

where all of the terms are as previously defined. For an instantaneous release from a unit area in an aquifer of infinite lateral extent, the time-varying concentration as a function of lateral distance off the center line can be expressed as follows:

$$C_i = \left(\frac{M_A}{\sigma_{sd} (2 \pi)^{1/2}} \right) \exp \left[- \left(\frac{y^2}{2 \sigma_{sd}^2} \right) \right] \quad (4.34)$$

in which

$$\sigma_{sd} = \left(2 D_y^* t \right)^{1/2} = \left(\frac{2 D_y t}{R_f} \right)^{1/2} \quad (4.35)$$

$$D_y = \alpha_y v_p \quad (4.36)$$

where M_A = instantaneous mass released per unit area (*i.e.*, instantaneous point-source release)
 σ_{sd} = standard deviation associated with the Gaussian solution

Note that the standard deviation (*i.e.*, the degree of lateral spreading) is a function of the retardation factor and, hence, K_d .

To gain an understanding of the impact of the retardation factor (and K_d) on simple advective-dispersive systems, the impact of retardation at a location, x , can be discerned by substituting the time, t , with the advective travel time, as follows:

$$t = \frac{x R_f}{v_p} \quad (4.37)$$

$$\sigma_{sd} = (2 \alpha_y x)^{1/2} \quad (4.38)$$

The standard deviation that indicates the degree of spread at location x is independent of the retardation factor and K_d . This phenomenon is expected because when combined with flow in the longitudinal direction, advection impacts the effects of dispersion in the lateral direction. In effect, advection transports the contaminant in the longitudinal direction, so there is no infinite dispersion at any location in the lateral direction. Hence, Gaussian plumes grow as they migrate down gradient. Unlike the contaminant travel time, the dispersive phenomenon is not closely tied to K_d .

4.4 Modeling Sensitivities to Variations in the Partition Coefficient

Because the retardation factor and partition coefficient permeate many aspects associated with the mathematical algorithms for contaminant transport in the subsurface environment, K_d can have a significant impact on the outcome of any modeling exercise. Under certain circumstances though, K_d can have very little impact on the outcome. The next 2 sections discuss the conditions under which partition coefficients influence the outcome.

1. Relationship Between Partition Coefficients and Risk -- This section explores the situations under which variations in K_d can have a significant influence on simulated groundwater concentrations and, hence, risk.
2. Partition Coefficient as a Calibration Parameter in Transport Modeling -- This section presents an illustrative example of a calibration exercise where the calibration parameter is the partition coefficient.

4.4.1 Relationship Between Partition Coefficients and Risk

The K_d parameter potentially has a very large impact on the mobility of constituents in a subsurface environment. When combined with other phenomena (*e.g.*, degradation/decay, dispersion, pore-water velocity), K_d can have a significant impact by redistributing the contaminant both spatially and temporally.

For example, when the K_d parameter is sufficiently large, the contaminant moves slowly from the source to the receptor. Because significant levels of contaminant have not reached the receptor

within the receptor's lifetime, the risks over the lifetime are low. If the value of the K_d parameter is increased (*i.e.*, its mobility decreased even further), the risks are still low because the contaminant still has not reached the receptor. However, if the K_d parameter is sufficiently small, the contaminants arrive very quickly, and the receptors are exposed within their lifetime.

Different methods were presented in the previous section for determining K_d , and 4 different retardation factors were presented, which were based on K_d . Because different models use different formulations for the retardation factor, pore-water velocity, or contaminant velocity, the same K_d will produce different simulation results by the different models. As one can imagine, there are no accurate generalizations that can be made with regard to defining K_d ; as such, it tends to represent a calibration parameter in computer models. Because any modeling exercise (conceptually, physically, and mathematically) represents a simplification of the real world, many phenomena unknown or misunderstood are lumped into the parameters upon which modeling is based. K_d represents one of those parameters, where known and many unknown phenomena are lumped; as such, K_d tends to lose some of its meaning in the modeling world, although it retains its full meaning in the laboratory.

In the laboratory, K_d is determined under carefully controlled conditions; all aspects of the experiments are controlled to ensure accuracy in the experimental exercise. The real world does not afford the luxury of controlling the environment; therefore, the conditions surrounding the sorption phenomenon must be estimated. Unfortunately, site conditions may not be adequately described by sampling. Moreover, the identification of a single representative K_d value for a site may be impossible due to the large heterogeneities of the site's subsurface system.

4.4.2 Partition Coefficient as a Calibration Parameter in Transport Modeling

Calibrations do not necessarily ensure that the simulated results capture the essence of the transport phenomena. For example, Figures 4.2 and 4.3 present the results of a calibration using the MEPAS model to monitored data.¹ Each figure presents time-varying ⁹⁰Sr concentrations. Figure 4.2 presents MEPAS simulation with a K_d equaling 0.4 ml/g (*i.e.*, solid line and no symbols) and a simulation with K_d equaling 0.8 ml/g (*i.e.*, solid line with open triangles). The solid triangle represents the monitored data, identifying in a concentration of 220 pCi/l at year 27. As Figure 4.2 shows, the "0.8" calibration is precise and passes directly through the monitored data (*i.e.*, an exact match). The "0.4" simulation does not appear to capture the essence of the problem, as it predicts a concentration of 55,600 pCi/l at year 27. The "0.4" simulation seems to have over predicted the concentration by over 2 orders of magnitude. The significant difference in the peak concentration between the 2 simulations were the result of a minor change in K_d (*i.e.*, changes in the tenths place).

¹ The MEPAS simulations were based on actual site data published in Lewis *et al.* (1994) for the CERCLA hazardous waste site ST-19. Only the contaminant information was changed. Radionuclides were never present at the site; they are only used here as an illustrative example.

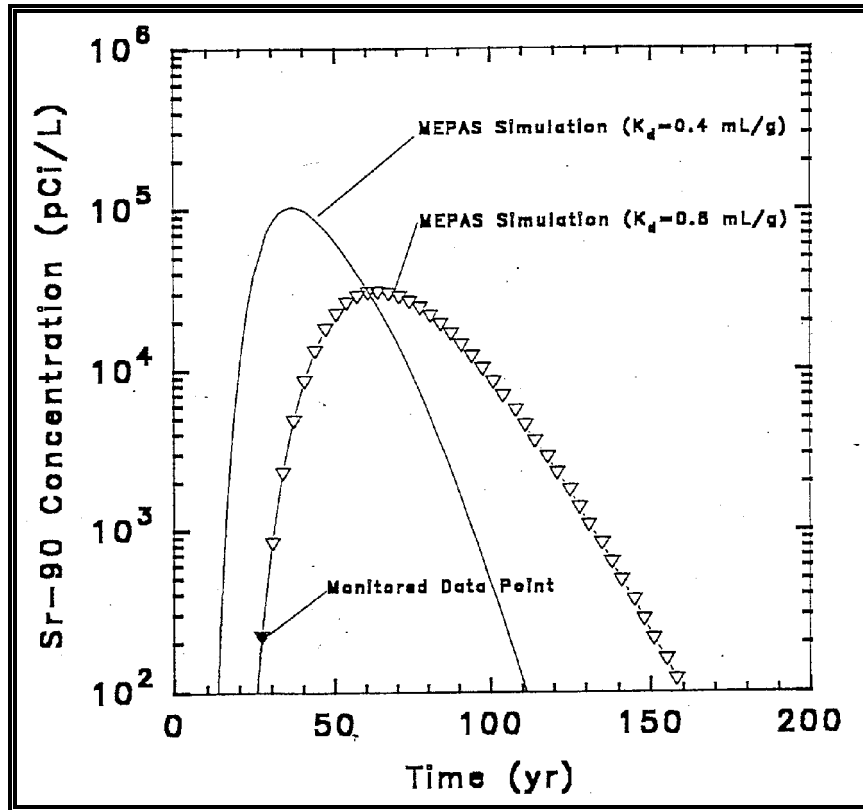


Figure 4.2. Example illustrating a MEPAS ^{90}Sr calibration with K_d equaling 0.8 ml/g and 1 monitored-data point.

Figure 4.3 presents the entire curve that is defined by monitored data, which includes the single data point from Figure 4.2. The monitored data in Figure 4.3 are presented as solid circular symbols. When all of the time-varying monitored data are considered in the assessment, the MEPAS simulation with a K_d equaling 0.4 ml/g appears to have captured the essence of the shape of the monitored data more accurately than the results associated with the 0.8 ml/g simulation. Although the “0.4” simulation does not precisely capture the entire shape of the monitored-data curve, it has captured the peak information, which usually is considered to be most important. Figure 4.3 illustrates the difficulty of calibrating a groundwater model to a single data point or a set of points that are not well distributed in time. Although the “0.8” simulation captured the single data point, it completely missed the peak concentrations and the time to peak. Because only 1 monitored data point is used in the calibration, an unlimited number of curves could have been simulated to pass through the monitored data point.

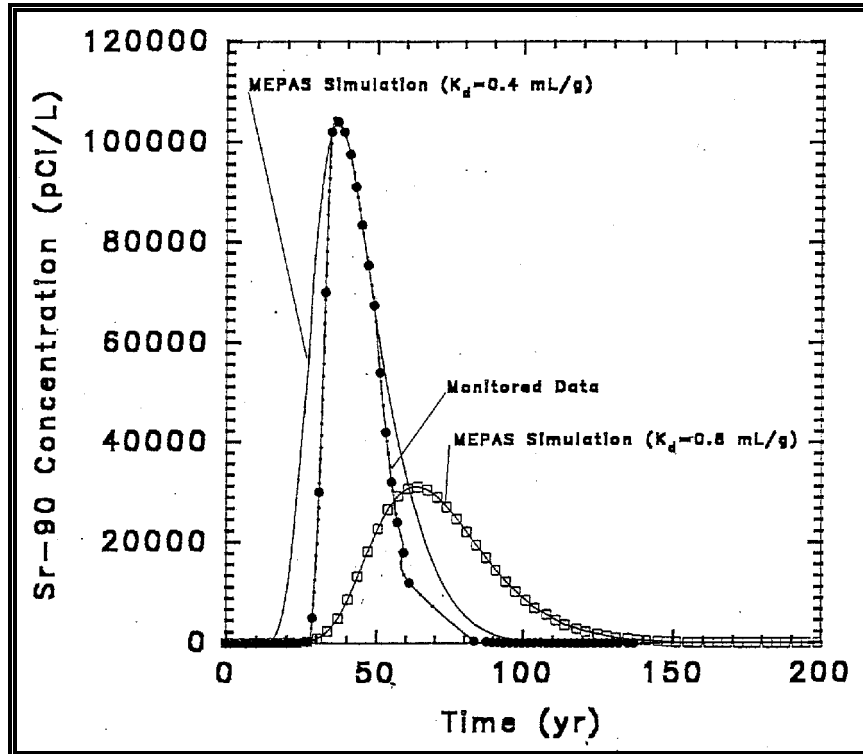


Figure 4.3. Example illustrating MEPAS ^{90}Sr calibrations with K_d equaling 0.4 and 0.8 ml/g and several monitored-data points.

Figure 4.3 illustrates that minor changes in K_d (*i.e.*, in the tenths place) can result in significant changes in simulation results. The concentrations between simulations at year 27 varied by over 2 orders of magnitude. The peak concentration decreased from 104,000 pCi/l to 31,000 pCi/l by increasing the K_d by only 0.4 ml/g. One simulation is over 5 times the drinking water limit of 20,000 pCi/l, while the other simulation is nearly equal to this limit. If the “0.8” results were assumed to be correct, the assessment would have underestimated the impacts by a factor of 3.4. Although the difference between 0.4 and 0.8 mg/l does not appear to be large, these results do illustrate the difficulties in using K_d and other parameters in the calibration process. These results also suggest that the discrepancy between “calibrated” simulations and limited data could be much larger (*i.e.*, orders of magnitude).

4.5 Summary

Various sections in this report have illustrated that there are many definitions for K_d (*e.g.*, theoretical, analytical, experimental, thermodynamic, *etc.*), all resulting with different values. The results presented in Figures 4.2 and 4.3 should represent a sobering reminder of the difficulties associated with groundwater assessments using partition coefficients. In many instances, a groundwater simulation is performed with no calibration at a site using K_d values that

have been obtained from “peer-reviewed” literature. The analyst tries to match soil types and environmental conditions with their site when “selecting” an appropriate K_d . It must be emphasized that these K_d values are unrelated to the actual site and only represent the laboratory conditions reported in the literature; they do not represent actual conditions at the site under investigation. The peer-reviewed values only provided an idea as to the possible magnitude associated with the K_d value. Different geochemical conditions, some known and unknown, exist between the actual site and those reported in the literature. The difficulty in using existing literature numbers is that the phrase “peer-reviewed literature” tends to lend too much credibility to these potentially inappropriate K_d values.

5.0 Application of Chemical Reaction Codes

5.1. Background

Determination of species distributions for dissolved major and trace constituents, including radionuclides, is necessary to understand the processes that control the chemistry of soil-water systems. Several processes will control the thermodynamic activities of dissolved species and, to some extent, their mobility in surface and ground waters and bioavailability to man. These processes are described in detail in Chapter 2 and references cited therein. The processes include the following:

- Aqueous complexation
- Oxidation/reduction
- Adsorption/desorption
- Mineral precipitation/dissolution

The distribution of aqueous species in a multi-component chemical system, such as those in soil-water environments, can only be reliably calculated from a combination of accurate analyses of water compositions and a competent chemical reaction model. Computerized chemical reaction models based on thermodynamic principles may be used to calculate these processes depending on the capabilities of the computer code and the availability of thermodynamic and/or adsorption data for aqueous and mineral constituents of interest. Use of thermodynamic principles to calculate geochemical equilibria in soil-water systems is well established and described in detail in many reference books, such as Bolt and Bruggenwert (1978), Garrels and Christ (1965), Langmuir (1997), Lindsay (1979), Morel (1983), Nordstrom and Munoz (1985), Sposito (1989, 1994), Stumm and Morgan (1981), and others. The reader is referred to these sources for detailed discussions and examples of specific applications relative to the thermodynamic principles and equations that govern these calculations.

Because of the great importance of the aqueous speciation, adsorption, and solubility processes relative to the concentrations and mobility of contaminants that may leach from waste, an understanding of the capabilities and application of chemical reaction models is essential. This understanding is additionally important because these models are used for both the scientific and legal aspects of risk and performance assessment studies of waste disposal and mitigation of environmental contamination.

The purpose of this chapter is to provide a brief conceptual overview of chemical reaction codes and their use in addressing technical defensibility issues associated with data from K_d studies. Particular attention is given to the capabilities of EPA's MINTEQA2 code, including the types of conceptual models the code contains to quantify adsorption. Issues pertaining to the availability of databases for these adsorption models and the status of the MINTEQA2 aqueous speciation and solubility database for radionuclides are also discussed.

5.1.1 Definition of Chemical Reaction Modeling

Chemical reaction models/codes are referred to by several terms in the literature. The term may include either of the adjectives “chemical” or “geochemical,” often depending on the technical field of expertise of the author and/or anticipated audience. Additionally, the models/codes can be referred to as reaction, equilibrium, speciation, or mass transfer¹ (and others) models/codes, although some of these terms refer to submodel capabilities. Throughout this report, the terms “chemical reaction models” and “chemical reaction codes” will be used as collective terms for all variations of these models and codes.

A chemical reaction model is defined here as the integration of mathematical expressions describing theoretical concepts and thermodynamic relationships on which the aqueous speciation, oxidation/reduction, precipitation/dissolution, and adsorption/desorption calculations are based. A chemical reaction code refers to the translation of a chemical reaction model into a sequence of statements in a particular computer language. We define a competent chemical reaction model as a model that contains all the necessary submodels and important aqueous complexes, solids and gases for the important elements of interest required to adequately interpret a given data set.

Most chemical reaction models are based on equilibrium conditions, and contain limited or no kinetic equations in any of their submodels. Some processes, such as aqueous speciation and cation or anion exchange, are closely approximated by equilibrium conditions over short time frames of hours to days. On the other hand, kinetic factors may limit other processes, such as some precipitation/dissolution and redox-sensitive reactions, from reaching equilibrium over reaction periods of tens of years or more. Moreover, without information or assumptions regarding the rate of release of the contaminant of interest from its source term, such as contaminated soils or a decommissioning site, modeling calculations cannot provide an estimate of the total mass (*i.e.*, mass present in aqueous solution plus associated mineral phases) of a contaminant released in the environment under review. At best, chemical modeling based on equilibrium conditions may provide estimates of bounding limits for some processes depending on the reactions being considered. Because of the limited availability of kinetic data and incorporation of kinetic algorithms into chemical reaction codes, this is an important area for future experimental studies and development of chemical reaction models. Readers are referred to references on reviews of chemical reaction models cited later in this chapter for more details on this issue.

Because thermodynamic data typically do not have the resolution to distinguish among different isotopic forms of contaminant-containing aqueous species or solids, geochemical modeling

¹ *Mass transfer* is the transfer of mass between 2 or more phases that includes an aqueous solution, such as the mass change resulting from the precipitation of a mineral or adsorption of a metal on a mineral surface. In contrast, *mass transport* is the time-dependent movement of one or more solutes during fluid flow.

calculations do not provide any information on the distribution of the different contaminant isotopes present in the aqueous, gaseous, or associated solid phases. However, in most situations, radionuclide isotopes will react the same as natural (stable) isotopes of the element. By assuming ideal isotopic mixing or exchange, one can estimate the distribution of any selected isotopes among the bulk elemental distribution.

5.1.2 Reviews of Chemical Reaction Models

Numerous reviews of chemical reaction codes have been published. Some of the more extensive reviews include those by Jenne (1981), Kincaid *et al.* (1984), Mercer *et al.* (1981), Nordstrom *et al.* (1979), Nordstrom and Ball (1984), Nordstrom and Munoz (1985), Potter (1979), and others. These reviews have been briefly described in Serne *et al.* (1990). The reviews discuss issues such as:

- Basic mathematical and thermodynamic approaches that are required to formulate the problem of solving geochemical equilibria in aqueous solutions
- Applications for which these codes have been developed and used, such as the modeling of adsorption equilibria, complexation and solubility of trace metals, equilibria in brine solutions and high-temperature geothermal fluids, mass transfer, fluid flow and mass transport, and redox balance of aqueous solutions
- Selection of thermodynamic data and development of thermodynamic databases
- Limitations of chemical reaction codes, such as the testing of the equilibrium assumption, application of these models to high-ionic strength aqueous solutions (*e.g.*, the ion association versus ion interaction conceptual models), the reliability of thermodynamic databases, and the use of validation to identify inadequacies in the conceptual models developed with chemical codes.

Table 5.1 provides a sampling of some chemical reaction codes that have been described in the literature and mentioned in published proceedings, such as Erdal (1985), Jackson and Bourcier (1986), Jacobs and Whatley (1985), Jenne (1979), Loeppert *et al.* (1995), Melchior and Bassett (1990), and the reviews cited above. The reader is directed to these published proceedings and reviews for the appropriate reference to the documentation of each code. Although this list of chemical reaction models is not meant to be complete and continues to expand each year, it demonstrates the diversity of codes that exist, and, in some cases, the evolution of some codes.

Table 5.1. Chemical reaction models described in the literature.

ADSORP	EQUIL	MINTEQ	SOILCHEM
AION	EQUILIB	MINTEQA1	SOLGASWATE
ALCHEMI	EVAPOR	MINTEQA2	R
AQ/SALT	FASTCALC	MIRE	SOLMNEQ
ASAME	FASTPATH	MIX2	SOLMNEQ.88
BALANCE	GEOCHEM	NOPAIR	SOLVEQ
C-Salt	GEOCHEM-PC	PATH	SYSTAB
CHEMIST	GIBBS	PATHCALC	THERMAL
CHEMTRN	GMIN	PATHI	WATCH1
CHES	HALTAFALL	PHREEQE	WATCHEM
COMICS	HARPHRQ	PHRQPITZ	WATEQ
DISSOL	HITEQ	REDEQL	WATEQ2
ECES	HYDRAQL	REDEQL.EPAK	WATEQ3
ECHEM	IONPAIR	REDEQL2	WATEQ4F
EHMSYS	KATKHE	RIVEQL	WATEQF
EQ3	KATKLE1	SEAWAT	WATEQFC
EQ3NR	MICROQL	SENECA	WATSPEC
EQ6	MINEQL	SENECA2	
EQBRAT	MINEQL2	SIAS	

Nordstrom and Ball (1984) discuss the issue of why so many chemical reaction codes exist. They attribute this diversity of codes to (1) the lack of availability, (2) inadequate documentation, (3) difficulty of use of some chemical codes, and (4) the wide variety of calculational requirements that include aqueous speciation, solubility, and/or adsorption calculations for aqueous systems that range from simple, chemical systems associated with laboratory experiments to complex, multi-component systems associated with natural environments. No single code can do all of the desired calculations in a perfectly general way. Typically the more general and comprehensive a geochemical code is, the more difficult and costly it is to use. Another factor may be that scientists are inherently reluctant to use any computer code that they and their immediate coworkers have not written.

5.1.3 Speciation-Solubility Versus Reaction Path Codes

Jenne (1981) divides chemical reaction codes into 2 general categories: aqueous speciation-solubility codes and reaction path codes. All of the aqueous speciation-solubility codes may be

used to calculate aqueous speciation/complexation,¹ and the degree of saturation (*i.e.*, saturation index) of the speciated composition of the aqueous solution with respect to the solids in the code's thermodynamic database. Some aqueous speciation-solubility codes also include the capabilities to calculate mass transfer between a single initial and final state, that results from mineral precipitation/dissolution and/or adsorption/desorption reactions. Chemical reaction codes, such as WATEQ, REDEQL, GEOCHEM, MINEQL, MINTEQ, and their later versions, are examples of codes of this type.

Reaction path codes include the capabilities to calculate aqueous speciation and the degree of saturation of aqueous solutions, but also permit the simulation of mass transfer due to mineral precipitation/dissolution or adsorption onto adsorbents as a function of reaction progress. Typical applications include the modeling of chemical changes associated with the interaction of a mineral assemblage and ground water (*e.g.*, INTERA, 1983, and Delany, 1985) or the release of radionuclides from a proposed glass waste form (*e.g.*, Bourcier, 1990) as a function of time. Computationally, 1 unit of reaction progress means that 1 unit of gaseous or solid reactant (*e.g.*, radioactive waste source term) has reacted with an aqueous solution in contact with solid phases with which the solution is already in equilibrium. At each step of reaction progress, the code calculates the changes or path of mineral and gaseous solubility equilibria that are constraining the composition of the aqueous solution, the masses of minerals precipitated and/or dissolved to attain equilibrium, and the resulting composition of the aqueous solution. Examples of reaction path codes include the PHREEQE, PATHCALC, and the EQ3/EQ6 series of codes.

5.1.4 Adsorption Models in Chemical Reaction Codes

Various adsorption models have been incorporated into a small number of chemical reaction codes to calculate the mass of a dissolved component adsorbing on a user-specified mineral phase, such as iron hydroxide that coat mineral grains in soil. The adsorption modeling capabilities in these codes have been briefly reviewed by others (*e.g.*, Goldberg, 1995, and Davis and Kent, 1990) and will not be duplicated here. The options vary from code to code. Adsorption models incorporated into chemical reaction codes include non-electrostatic, empirical models as well as the more mechanistic and data intensive, electrostatic, surface complexation models. Examples of non-electrostatic models include the partition (or distribution) coefficient (K_d), Langmuir isotherm, Freundlich isotherm, and ion exchange models. The electrostatic, surface complexation models (SCMs) incorporated into chemical reaction codes include the diffuse layer model (DLM)

¹ *Complexation* (*i.e.*, complex formation) is any combination of dissolved cations with molecules or anions containing free pairs of electrons. *Species* refers to actual form in which a dissolved molecule or ion is present in solution. Definitions are taken from Stumm and Morgan (1981).

A list of acronyms, abbreviations, symbols, and notation is given in Appendix A. A list of definitions is given in Appendix B

[or diffuse double layer model (DDLDM)], constant capacitance model (CCM), Basic Stern model, and triple layer model (TLM).

Some of the chemical reaction codes identified in the reviews by Goldberg (1995) and Davis and Kent (1990) as having adsorption models include HARPHRE (Brown *et al.*, 1991), HYDRAQL (Papelis *et al.*, 1988), SOILCHEM (Sposito and Coves, 1988), and the MINTEQA series of chemical reaction codes, including MINTEQA2 (Allison *et al.*, 1991) developed for the U.S. Environmental Protection Agency (EPA). Compared to other codes, MINTEQA2 contains some of the most extensive options for modeling adsorption, including all of the models listed above, except for the Basic Stern model. The MINTEQA2 adsorption model options are discussed further in Section 5.2, and their associated equation and reaction formulations as coded within MINTEQA2 are described in Section 5.3. It should be noted that the partition coefficient (K_d), Langmuir, and Freundlich models incorporated into MINTEQA2 are formulated in terms of species activities,¹ and not the more traditional approach of total concentrations of dissolved metal. This variation in modeling approach and the rationale for its use are discussed in Section 5.2.

Some of these models are briefly described in Chapter 2. The reader is also referred to reference texts by Langmuir (1997), Morel (1983), Sposito (1984), and Stumm and Morgan (1981) for more detailed background descriptions, associated equations and data needs, and model comparisons pertaining to these adsorption models.

As noted in Chapter 2, the electrostatic, surface complexation models, although robust, are not expected to have a significant impact on contaminant transport and risk assessment modeling due to their significant data needs and more complex equation formulations. Detailed descriptions, comparisons, and derivations of the relevant equations and reactions associated with these models are described in Westall and Hohl (1980), Morel *et al.* (1981), Barrow and Bowden (1987), Davis and Kent (1990), and others. The data needs and associated derivation (*i.e.*, parameterization) of model constants are discussed by Morel *et al.* (1981), Turner (1991), and Goldberg (1995). The electrostatic models were developed to provide a mechanistic description of adsorption reactions in systems containing a pure single phase of an amorphous or crystalline metal oxide. Numerous studies have demonstrated their success in predicting adsorption of trace metals in such simplified systems (*e.g.*, Turner, 1993). Application of such adsorption models to natural systems where the reactive surfaces include a combination of impure phases, clays, and humic materials are limited. The adsorption behavior of such systems unfortunately cannot be modeled assuming that the

¹ In general terms, the *activity* of an ion is its effective concentration that determines its behavior to other ions with which it might react. The activity of an ion is equal to its concentration only in infinitely dilute solutions, and is related to its analytical concentration by an activity coefficient, γ . Activities, activity coefficients, and associated thermodynamic relationships are discussed in detail in texts such as Glasstone (1972), Lewis and Randall (1961), Morel (1983), Sposito (1984), and Stumm and Morgan (1981).

adsorptive properties of a phase mixture, such as soil, can be readily predicted by adding the adsorption constants for the individual solid phases in some normalized fashion.

Numerous papers have been published relative to the application of non-electrostatic and electrostatic adsorption models to modeling the migration of radionuclides released from high (HLW) and low level (LLW) radioactive waste disposal facilities. These include reviews and references cited therein by Serne and Muller (1987) and Turner (1993,1995) for application to HLW disposal and Serne *et al.* (1990) for application to LLW disposal issues. The reader should also be aware of an extensive literature review by Berry (1992a,b,c) of adsorption studies conducted in the United Kingdom and the international community on sorption relative to the release and transport of radionuclides in the near¹ and far field. The literature review is published as 3 reports. The first report summarizes studies funded by the United Kingdom (UK) Nirex and Department of the Environment (UK DoE). The second report contains an extensive bibliography, including reference citations and complete abstracts, of United Kingdom and international publications on the subject area. The third report compares the objectives and approaches used in studies funded by Nirex and UK DoE to those in related studies undertaken by the international community.

5.1.5 Output from Chemical Reaction Modeling

The results from chemical reaction codes vary depending on the capabilities, design of the output report, and user-selected options for each code. The output may be in the form of a report directed to a printer, and/or a total or partial report stored as an ASCII (American Standard Code for Information Interchange)-formatted file for future use in word processing or spreadsheet software or as input for other scientific application software. The output can be extensive depending on the options used for the modeling calculations and the level of output report requested by the user.

The output report from MINTEQA2 chemical reaction code (Allison *et al.*, 1991) will be used as a typical example. The MINTEQA2 code was developed by EPA and is described in greater detail in Section 5.2. For each modeling calculation, the output can include the following:

- Documentation and constraints applied to the calculation
 - Name of the data file and the date and time of modeling calculations
 - Documentation to describe modeling calculation
 - Listing of the model parameters used to control the calculations (*e.g.*, maximum number of permitted iterations, method for calculating activity coefficients, alkalinity option, units used for input of water composition, temperature), level of output report (*e.g.*, short versus long report), and type of selected adsorption algorithm

¹ The “near field” is that portion of a contaminant plume that is near the point source and whose chemical composition is significantly different from that of the uncontaminated portion of the aquifer. The “far field” refers to that which is not the “near field.”

- Listing of the input water composition
 - Listing of any controls (*e.g.*, pH, Eh, redox equilibria) applied to the calculation
 - Listing of any additions or modifications made as part of the input file to the code's thermodynamic database
 - Listing of any adsorption reactions and associated constants used for adsorption reaction calculations
 - Listing of any solid phases and associated masses considered for mass transfer calculations
 - Listing of any gases whose solubility will control the concentration of a dissolved constituent (*e.g.*, solubility of CO₂ gas to fix the total concentration of dissolved carbonate)
- Results of aqueous speciation calculations
 - Number of iterations required for the aqueous speciation calculation to converge
 - Calculated concentrations, activities, activity coefficients, equilibrium constants as modified for ionic strength and temperature for each aqueous species extracted from the code's thermodynamic database and included in the calculation
 - Charge imbalance before and after calculation of aqueous speciation
 - Listing of the distribution of important (*i.e.*, greater than 1 percent of the total concentration of a dissolved component) uncomplexed and complexed aqueous species for each valence form of each dissolved component (See "Glossary" for technical definition of "component.")
- Results of solubility calculations
 - Degree of saturation of the starting water composition relative to equilibrium solubility of every solid in the code's thermodynamic database containing the components included in that water analysis
 - Listing of the reaction stoichiometries and associated temperature-corrected equilibrium constants for each solid phase included in the calculation
- Results of mass transfer calculations at each stage of calculations where a solubility and/or adsorption equilibrium condition is reached
 - Repeat of all speciation results for new calculated water composition
 - Repeat of the solubility results for new calculated water composition
 - Calculated mass of each element in dissolved, precipitated, and/or adsorbed states for new calculated water composition

Parts of example output reports from MINTEQ are listed and explained in detail in Allison *et al.* (1991) and Peterson *et al.* (1987a).

5.1.6 Assumptions and Data Needs

Chemical reaction models may be used to predict the concentrations of elements, such as uranium, that may be present in an aqueous solution. This type of modeling calculation requires the user to select either a solubility or an adsorption reaction to constrain the maximum concentration limit of a contaminant or any other dissolved constituent. The modeling process is based on the following assumptions and data needs for the environment of interest:

- For a solution-concentration limit based on a solubility reaction, the mineral phase selected as the solubility control for the contaminant of interest must have known thermodynamic data (*e.g.*, solubility constant). The selection of the solid phase must be technically defensible in that the phase is known to exist in analogous aqueous environments and have rates of precipitation and dissolution that are not limited by kinetics.
- For a solution-concentration limit based on an adsorption reaction,¹ the substrate (*e.g.*, an iron-oxyhydroxide coating) selected as the adsorption control for the contaminant of interest must be technically defensible relative to the soil or sediment being modeled. The adsorption parameters must be known for the contaminant of interest and its major competing ions for the substrate and the range of appropriate environmental conditions.
- The reactions or conditions that control the pH, redox conditions, and concentrations of complexing ligands (*e.g.*, dissolved carbonate) for the derived aqueous solution must be assumed and technically defensible.
- The model must have an adequate thermodynamic database that includes all the necessary aqueous species, redox reactions, minerals, and sorption substrates for the contaminant of interest and for the other constituents of environmental importance.
- The composition of water (in particular, pH, Eh, and alkalinity) contacting the contaminant-containing phases must be known.
- Most chemical modeling calculations will be limited to equilibrium conditions, because of the general absence of kinetic rate values for the aqueous speciation, solubility, and/or sorption reactions involving the contaminant of interest and other constituents of environmental importance. Equilibrium (actually steady state) conditions are likely in the far field, but are less likely in the near-field environment or at the boundaries of contaminant plumes.

¹ When using the partition coefficient (K_d) or Freundlich adsorption models, the predicted solution-concentration limits are only valid when modeling trace concentrations of a contaminant of interest.

5.1.7 Symposiums on Chemical Reaction Modeling

Both the diversity and interdependency of research efforts associated with chemical reaction modeling are effectively demonstrated by the papers presented at several symposiums held on this subject. Some of these conferences are listed in Table 5.2.

The symposiums typically include papers on a range of subjects, such as theoretical advancements; model and code development, including documentation; application studies of equilibrium and mass transfer codes, transport and coupled codes, and surface processes; database development, including thermodynamic data, kinetic data, and data on organic compounds; modeling sensitivities; and model validation.¹

The reader is encouraged to peruse these proceedings. The proceedings' papers show that the development of chemical reaction models is concurrent with the expansion and improvement of thermodynamic databases for aqueous species and solids and for adsorption, as well as with application studies that test the validity of these models and their associated databases.

Table 5.2. Examples of technical symposiums held on development, applications, and data needs for chemical reaction modeling.

Published Proceedings	Date of Symposium	Location	Sponsorship
Jenne (1979)	Sept. 11-13, 1978	Miami Beach, Florida	Amer. Chem. Soc.
Erdal (1985)	June 20-22, 1984	Los Alamos, New Mexico	U.S. Department of Energy (DOE) and U.S. Nuclear Regulatory Commission (NRC)
Jacobs and Whatley (1985)	Oct. 2-5, 1984	Oak Ridge, Tennessee	NRC
Jackson and Bourcier (1986)	Sept. 14-17, 1986	Fallen Leaf Lake, California	DOE and LLNL
Melchior and Bassett (1990)	Sept. 25-30, 1988	Los Angeles, California	Amer. Chem. Soc.
Loeppert <i>et al.</i> (1995)	Oct. 23-24, 1990	San Antonio, Texas	Soil Sci. Soc. Amer. and Amer. Soc. Agron.

¹ *Model validation* is the integrated test of the accuracy with which a geochemical model and its thermodynamic database simulate actual chemical processes. In contrast, *code verification* is the test of the accuracy with which the subroutines of the computer code perform the numerical calculations.

5.2 MINTEQA2 Chemical Reaction Code

5.2.1 Background

The MINTEQA2 computer code and its predecessor versions are described by Allison *et al.* (1991, MINTEQA2), Brown and Allison (1987, MINTEQA1), Peterson *et al.* (1987a, MINTEQ), and Felmy *et al.* (1984, MINTEQ). The MINTEQ code was developed with EPA funding. It was originally constructed by combining the mathematical structure of the MINEQL code (Westall *et al.*, 1976) with the thermodynamic database and geochemical attributes of the WATEQ3 code (Ball *et al.*, 1981a).

The MINTEQA2 code is used in conjunction with a thermodynamic database to calculate complex chemical equilibria among aqueous species, gases, and solids, and between dissolved and adsorbed states. Conceptually, the code can be considered as having the following 4 submodels: (1) aqueous speciation, (2) solubility, (3) precipitation/dissolution, and (4) adsorption. These submodels include calculations of aqueous speciation/complexation, oxidation-reduction, gas-phase equilibria, solubility and saturation state (*i.e.*, saturation index), precipitation/dissolution of solid phases, and adsorption. The MINTEQA2 code incorporates a Newton-Raphson iteration scheme to solve the set of mass-action and mass-balance expressions.

The reader is referred to the references and user guides listed above for details regarding the use of the MINTEQ code, types and examples of geochemical equilibria calculations possible with this code, the basic equations on which the model is based, and examples of input and output files.

5.2.2 Code Availability

MINTEQA2 (Version 3.11) is the most current version of MINTEQ available from EPA. It is compiled to execute on a personal computer (PC) using the MS-DOS computer operating system. The MINTEQA2 software package distributed by EPA also includes PRODEFA2, which is an user-interactive code used to create and modify input files for MINTEQA2.¹ The user is referred to the description of PRODEFA2 in Allison *et al.* (1991).

Copies of the files containing the source and executable codes for MINTEQA2 and PRODEFA2, thermodynamic databases, example input data sets, and documentation are available by mail from

¹ Versions of MINTEQ modified to operate on DOS and Macintosh personal computer systems are also available from commercial sources.

Center for Exposure Assessment Modeling (CEAM)
U.S. Environmental Protection Agency
Office of Research and Development
Environmental Research Laboratory
960 College Station Road
Athens, Georgia 30605-2720

These files may also be downloaded using the Internet by accessing CEAM's home page. The address of the CEAM home page is

ftp://ftp.epa.gov/epa_ceam/wwwhtml/ceamhome.htm

The MINTEQA2 code and documentation are located under "software products" in "...CEAM *software products* and related *descriptive information* is..." The CEAM home page may also be accessed via EPA's home page at

<http://www.epa.gov>

by selecting "software" in "EPA Data Systems and Software," and then "Center for Exposure Assessment Modeling."

Training courses are commonly held on the use of chemical reaction modeling techniques and the application of the MINTEQA2 code. In the past, MINTEQ training has been provided to EPA and NRC by their supporting national laboratory and private contractors. Allison Geoscience Consultants, Inc.¹ have, for example, conducted several MINTEQA2 modeling workshops. The Pacific Northwest National Laboratory (Peterson *et al.*, 1987a) has provided MINTEQA2 training to the NRC. Short course announcements from the Environmental Education Enterprises, Inc. (E³)² for environmental science and engineering training also included MINTEQ workshops.

5.2.3 Aqueous Speciation Submodel

The MINTEQA2 code can be considered as having the following 4 parts: (1) an aqueous speciation submodel, (2) solubility submodel, (3) precipitation/dissolution submodel, and

¹ The use of commercial business and product names is for descriptive purposes only, and does not imply endorsement by EPA or PNNL.

Allison Geoscience Consultants, Inc., 3920 Perry Lane, Flowery Branch, Georgia 30542.

² Environmental Education Enterprises, Inc. (E³), 2764 Sawbury Boulevard, Columbus, Ohio 43235-4580.

(4) adsorption submodel. The aqueous speciation submodel is fundamental to all other submodels. It first uses the MINTEQA2 thermodynamic database to calculate the activities of the uncomplexed and complexed aqueous species for an initial water composition. The activities of individual aqueous species are corrected for ionic strength using the Davies or extended Debye-Hückel equations.

The aqueous speciation of a dissolved contaminant can only be determined using thermodynamic calculations such as those formulated in the aqueous speciation submodel of chemical reaction codes. Except for pH, which is the negative of the logarithm of the activity of the uncomplexed H^+ aqueous ion, the user typically supplies the total concentrations of a chemical constituent in an input file for a chemical reaction code. Most common analytical techniques measure the total concentrations of a dissolved constituent such as uranium, and not the concentration of any of its many individual species such as UO_2^{2+} , UO_2OH^+ , $UO_2(CO_3)_2^{2-}$, $UO_2SO_4^-(aq)$, or $UO_2PO_4^-$.

Aqueous speciation, and hence the testing of solubility hypotheses in the solubility submodel, is only reliable if the quality of the chemical analysis of the water is adequate. The description of the water composition is usually obtained by direct measurement of major cations and anions, pH, Eh, and trace constituents. As a quality check of the water chemical analysis, the MINTEQA2 code calculates the cation/anion balance for each speciated water composition. The cation/anion balance is calculated using the equation

$$\text{Cation/Anion Balance(\%)} = \frac{[\text{Anions (equiv./l)} - \text{Cations (equiv./l)}]}{[\text{Anions (equiv./l)} + \text{Cations (equiv./l)}]} \times 100. \quad (5.1)$$

For simple groundwater compositions and accurate analytical work, the cation/anion balance should not exceed a few percent (Hem, 1985).

The importance of complexation is discussed in Chapter 2 and elsewhere, such as Langmuir (1997), Lindsay (1979), Morel (1983), and Stumm and Morgan (1981). Complexation of dissolved metals with ligands, such as carbonate, will increase the total concentration of a dissolved metal in a soil-water system, and affect its availability for sorption and migration in geochemical systems. The output from the MINTEQA2 aqueous speciation submodel identifies, based on the data in the code's thermodynamic database, the distribution (*i.e.*, dissolved masses) of uncomplexed and complexed aqueous species for the constituents included in the input water composition.

5.2.3.1 Example of Modeling Study

Krupka and Serne (1998) used the MINTEQA2 code to analyze solubility limits for contaminants that may be released from a hypothetical low-level radioactive waste (LLW) disposal facility being considered in a NRC performance assessment test case analysis. The species distributions plotted for dissolved U(VI) in Figure 5.1 were taken from the MINTEQA2 calculations by Krupka and Serne. They provide a good example of the type of information

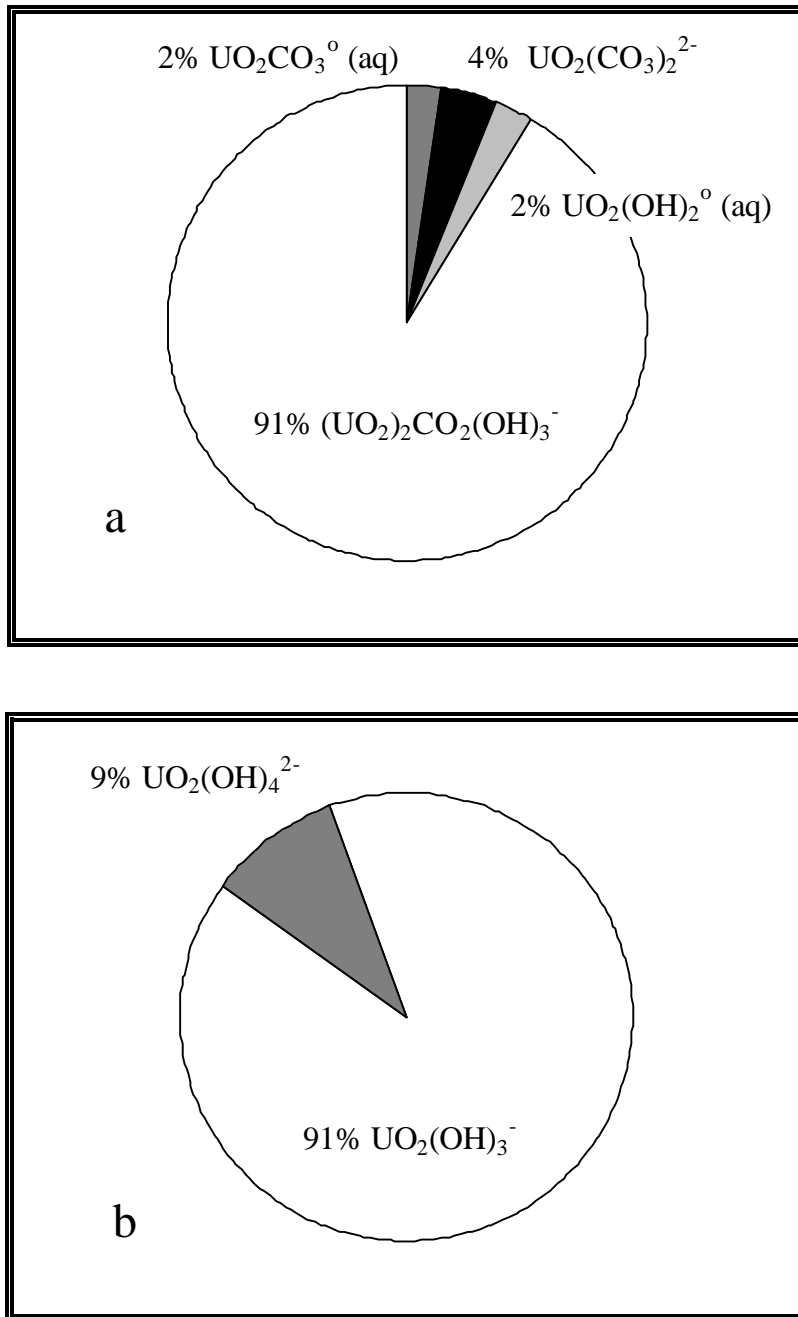


Figure 5.1. Distribution of dominant U(VI) aqueous species for leachates buffered at pH 7.0 by local ground water (Figure 5.1a) and at pH 12.5 by cement pore fluids (Figure 5.1b). [Adapted from MINTEQA2 modeling results of Krupka and Serne (1998).]

provided by the aqueous speciation submodel. Figure 5.1a shows the distribution of dominant species (*i.e.*, greater than 1 percent of total dissolved mass) of dissolved U(VI), respectively, for leachates buffered at pH 7.0 by the local ground water. This distribution can be contrasted to that in Figure 5.1b which shows the distribution of dominant U(VI) species at pH 12.5 by pore fluids derived from ground-water interactions with cementitious materials in the hypothetical LLW disposal facility. At pH 7.0, the speciation of dissolved U(VI) is dominated by uranyl carbonate complexes. At very basic pH conditions, the anionic uranyl hydrolysis species dominate the chemistry of dissolved U(VI). The speciation results clearly demonstrate that major differences can occur in the speciation of a dissolved metal as a function of different solution chemistries, such as pH.

5.2.3.2 Application to Evaluation of K_d Values

As noted in Chapter 2 and published references, such as Morel (1983), Sposito (1989, 1994), Stumm and Morgan (1981), and others, the ionic nature and composition of the dominant aqueous species for a contaminant are important factors relative to its adsorption behavior on reactive mineral surfaces. Moreover, as demonstrated in the example given above, the ionic nature and composition of the dominant aqueous species are dependent on the composition, pH, and redox conditions of a surface or ground water.

If thermodynamic data exist for the important aqueous species of a contaminant of interest, chemical reaction models *provide the most cost and time effective means of predicting the dominant aqueous species* that could exist for practically any water composition. The rate at which these calculations can be done is limited only by the rate at which a user can enter the input data, given the fast speeds of processors used in modern personal computers. The user can rapidly evaluate whether the dominant species is(are) cationic or anionic, as well as how their compositions might be affected by complexation with dissolved ligands such as carbonate and phosphate. If there is uncertainty relative to the pH evolution or ligand content of a water, the user may then quickly modify the input value(s) and complete a series of sensitivity analyses to determine how the ionic charges and compositions of the dominant aqueous species change.

This information can then be used to substantiate the conceptual model that is being used for adsorption for a particular contaminant. For example, if 90 percent of the mass of a dissolved contaminant is present in anionic form, is this consistent with low or high K_d values that one might find reported in the literature? If the calculations indicate strong complexation with dissolved sulfate, are the default K_d values in transport or risk assessment models, such as MEPAS, conservative estimates relative to this specific site chemistry? If toxicology studies indicate that an uncomplexed species, such as Cu^{2+} , is the important actor relative to bioavailability, how does this affect the predicted risk when the aqueous speciation calculations indicate that 99 percent of the mass of dissolved copper is present as a carbonate complex in a given water? Chemical reaction models provide an effective tool for calculating the responses in aqueous speciation to different conceptual models that one might consider for soil-water systems.

For example, Kaplan *et al.* (1998) conducted laboratory batch K_d experiments to study the effects of background geochemistry on the sorption of U(VI) on natural sediments. The MINTEQA2 code was used to calculate the aqueous speciation of U(VI) in a groundwater before and after equilibrium with sediments. The modeling results indicated dissolved U(VI) was present as essentially all aqueous anionic U(VI)-carbonate complexes [*e.g.*, $\text{UO}_2(\text{CO}_3)_3^{4-}$] at high pH conditions. Studies by Waite *et al.* (1994) and others have shown that these complexes, due to their anionic nature, tend to sorb appreciably less to sediments than cationic U(VI) complexes which are present at lower pH conditions.

5.2.4 Solubility Submodel

After calculating the aqueous speciation for a given water composition, solubility-equilibria hypotheses are tested. Ion activity products (IAP) are calculated from the activities of the component (or basis) species,¹ using the stoichiometries of the solubility reactions for minerals and other solids in the thermodynamic database. These activity products are then compared to the equilibrium constants ($K_{r,T}$)² stored in the database for the solubilities for the same solids, to test the assumption that certain of the dissolved constituents in the aqueous solution are in equilibrium with particular solid phases. Saturation indices, $[\log (\text{IAP}/K_{r,T})]$, are calculated to determine if the water is at

$$\text{Equilibrium:} \quad \text{Log} (\text{IAP}/K_{r,T}) \approx 0 , \quad (5.2)$$

$$\text{Oversaturated:} \quad \text{Log} (\text{IAP}/K_{r,T}) > 0 , \quad (5.3)$$

or

$$\text{Undersaturated:} \quad \text{Log} (\text{IAP}/K_{r,T}) < 0 , \quad (5.4)$$

with respect to a specified solid phase. This information allows one to ascertain permissible equilibrium solubility controls for dissolved constituents in that water. This water may be a surface or ground water, or a laboratory solution used for solubility or K_d measurements.

¹ Component (or basis) species are the “basis entities or building blocks from which all species in the system can be built” (Allison *et al.*, 1991). Examples include Mg^{2+} , UO_2^{2+} , CO_3^{2-} , and SO_4^{2-} for magnesium, hexavalent uranium [U(VI)], inorganic carbon, and oxidized sulfur [S(VI)], respectively. The set of components in MINTEQA2 is predefined. They are a set of linearly independent aqueous species in terms of which all aqueous speciation, redox, mineral, and gaseous solubility reactions in the MINTEQA2 thermodynamic database are written.

² Mineral solubility reactions in the MINTEQA2 database are written as formation (*i.e.*, precipitation) reactions. The solubility product, $K_{sp,T}$, (see Chapter 2), which is a commonly used term in the literature, refers to the equilibrium constant, $K_{r,T}$, for a mineral solubility reaction written as a dissolution reaction.

5.2.4.1 Example of Modeling Study

Figure 5.2 shows the saturation indices calculated by Krupka *et al.* (1983)¹ for the mineral rutherfordine (UO_2CO_3) for published analyses of solution samples taken from laboratory uranium solubility studies. The saturation index results demonstrate that these solution samples calculate to be at or very near equilibrium with respect to rutherfordine based on the available thermodynamic data for this mineral and U(VI) aqueous species included in the modeling calculations. Rutherfordine may have therefore precipitated during the course of the solubility studies reported in the cited literature.

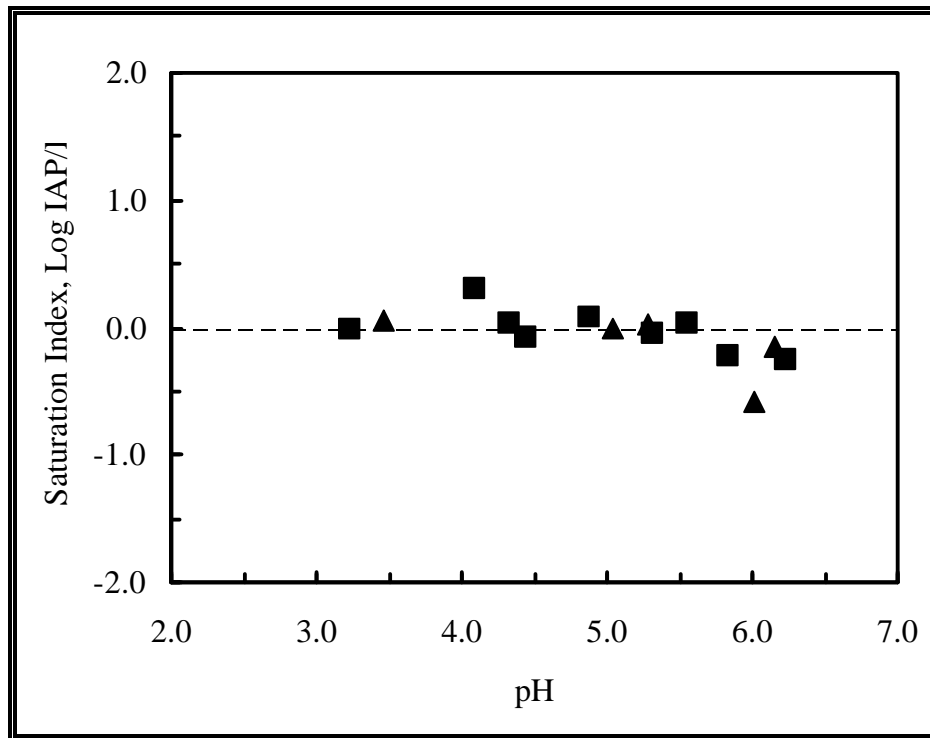


Figure 5.2. Saturation Indices calculated for rutherfordine (UO_2CO_3) as a function of pH for solution analyses from Sergeyeva *et al.* (1972). [Adapted from WATEQ4 modeling results of Krupka *et al.* (1983). The filled square and triangle symbols refer, respectively, to solutions analyses from 25 and 50°C experiments by Sergeyeva *et al.* (1972)]

¹ Although Krupka *et al.* (1983) used the WATEQ4 chemical reaction code, their results are analogous to the types of saturation index calculations permitted with the MINTEQ2A code.

5.2.4.2 Application to Evaluation of K_d Values

Chemical reaction codes can be used to analyze the adequacy of laboratory measurements of K_d values for a particular soil-water system. As noted in Chapter 3, solubility limits have sometimes been exceeded during the process of making laboratory measurements of K_d values. This can result when the concentration of the contaminant spike introduced to the equilibration vessel is too great and/or when the initial chemical conditions, such as pH, vary greatly during the course of the measurements.

By modeling the aqueous speciation and saturation indices for the initial and final compositions of aqueous solutions present in the K_d experiments, the user can test if any solubility limits were exceeded during the measurements. In those cases where a contaminant-containing solid is precipitated, the determined K_d values are measurements of both solubility and adsorption processes and will result in an over-prediction of contaminant attenuation (via only adsorption processes) in the soil-water system.

Kaplan *et al.* (1998) conducted laboratory batch K_d experiments to study the effects of background geochemistry on the sorption of U(VI) on natural sediments. MINTEQA2 calculations indicated that dissolved U(VI) was present as essentially all aqueous anionic U(VI)-carbonate complexes. Waite *et al.* (1994) and others have shown that these complexes, due to their anionic nature, tend to sorb appreciably less to sediments than cationic U(VI) complexes present at lower pH values. However, the K_d values measured by Kaplan *et al.* (1998) increased from 1.07 to 2.22 ml/g as the pH increased from 8.17 to 9.31, and were >400 ml/g at $\text{pH} \geq 10.3$. Kaplan *et al.* (1998) used MINTEQA2 saturation index calculations to show that the apparent increase in U(VI) K_d values was due to the precipitation of uranium-containing solids and not to U(VI) adsorption to the sediment.

5.2.5 Precipitation/Dissolution Submodel

The results from the solubility model are in turn used by the MINTEQA2 as input for the precipitation/dissolution submodel. Application of this submodel is optional. The user may select this submodel and its different options to predict the mass of a solid phase(s) that precipitates or dissolves in the modeled system. The mass transfer submodel determines the mass of a solid phase(s) (*e.g.*, a contaminant-containing solid or a mineral present in a soil) that precipitates from a ground water or dissolves from a soil-water system. If a given water composition calculates to be oversaturated, $[\log (\text{IAP}/K_{r,T}) > 0]$, with respect to a solid phase(s) considered in the modeling problem, the mass transfer model will decrease (*i.e.*, precipitate a solid phase) the masses of the appropriate dissolved constituents until the water composition is at equilibrium, $[\log (\text{IAP}/K_{r,T}) = 0]$, with respect to that solid phase(s). The MINTEQA2 output lists the mass of solid precipitated per a set volume of the system being modeled. If a given water composition calculates to be undersaturated, $[\log (\text{IAP}/K_{r,T}) < 0]$, with respect to a solid phase(s) selected in the modeling problem, the mass transfer model will increase (*i.e.*, dissolve a solid phase) the

masses of the appropriate dissolved constituents until the water composition is at equilibrium with respect to that solid phase(s) or until the user-specified finite mass of that solid has been completely dissolved. For those solids originally designated as having finite masses, the MINTEQA2 output gives the masses per set system volume of any of these solids remaining at final equilibrium.

5.2.5.1 Example of Modeling Study

The solubility limits calculated by Krupka and Serne (1998) demonstrate one of several applications for a precipitation/dissolution submodel. Maximum concentration limits for dissolved americium, neptunium, nickel, plutonium, radium, strontium, thorium, and uranium were calculated using MINTEQA2 for 2 ground-water environments associated with a hypothetical LLW disposal system. The 2 limiting environments included: (1) a cement buffered system, wherein the leachate pH is controlled at values above 10 by the effective buffering capacity of the concrete, and (2) a ground-water buffered system, wherein the leachate pH and related solution parameters are dominated by the local ground-water system.

Figure 5.3 shows the maximum concentrations calculated by Krupka and Serne (1998) for total dissolved uranium as a function of pH. The predicted concentration limits are based on the equilibrium solubilities of schoepite [$\text{UO}_2(\text{OH})_2 \cdot \text{H}_2\text{O}$] and uranophane [$\text{Ca}(\text{H}_3\text{O})_2(\text{UO}_2)_2(\text{SiO}_4)_2 \cdot 3\text{H}_2\text{O}$]. These 2 solids were selected based on published phase-stability information and knowledge of the geochemistry of contaminant aqueous systems. Schoepite precipitates readily in short-duration laboratory experiments conducted at ambient temperatures. Because the concentration of dissolved uranium in equilibrium with schoepite is higher than the solubilities of other uranium solids that precipitate under these conditions or in nature, concentration limits based on schoepite are therefore expected to be highly conservative. The presence of alkali and/or alkaline earth ions at high pH conditions results in the precipitation of alkali/alkaline earth uranyl compounds that control the solubility of uranium at concentrations lower than those resulting from equilibrium with schoepite. Therefore, the solubility of uranophane may provide a more realistic solubility limit for dissolved uranium, especially at high pH conditions. Uranophane is known to exist in uranium-loaded cementitious mixtures and thus may be a realistic solubility control for dissolved uranium in cement dominated systems.

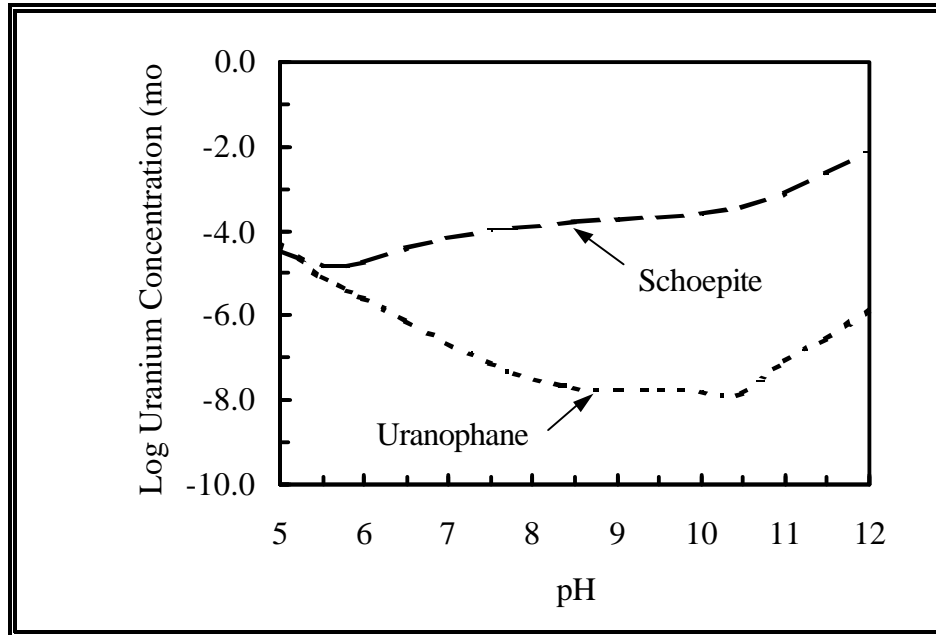


Figure 5.3. Maximum concentration limits calculated for total dissolved uranium as a function of pH based on the equilibrium solubilities of schoepite and uranophane.

5.2.5.2 Application to Evaluation of K_d Values

Chemical reaction codes can be used to calculate bounding, technically-defensible maximum concentration limits for dissolved contaminants as a function of key composition parameters (e.g., pH) of any specified soil-water system. The concentration of a dissolved contaminant predicted with default or site specific K_d values used in transport or risk assessment models may exceed the concentration limit based on solubility relationships. In these instances, the solubility-limited concentration may provide a more realistic bounding value than one based on a K_d value for the assessment calculation, and could have an important impact on the estimated level of risk. If a calculated concentration limit is based on the solubility of a mineral that is known to precipitate under analogous chemical conditions and over reasonable time frames, then the user knows that the dissolved concentrations of this contaminant in an actual, open soil-water system cannot exceed these values and will most likely be significantly less than these values due to adsorption and/or coprecipitation processes.

Moreover, as with the aqueous speciation calculations discussed in Section 5.2.3, mass transfer calculations can be rapidly and inexpensively repeated using a chemical reaction code to determine

their sensitivity to a wide range of chemical parameters for a soil-water systems. This includes easily measured parameters, such as pH, and analytical values that might have a wide range of uncertainty, such as the concentration of a dissolved complexant.

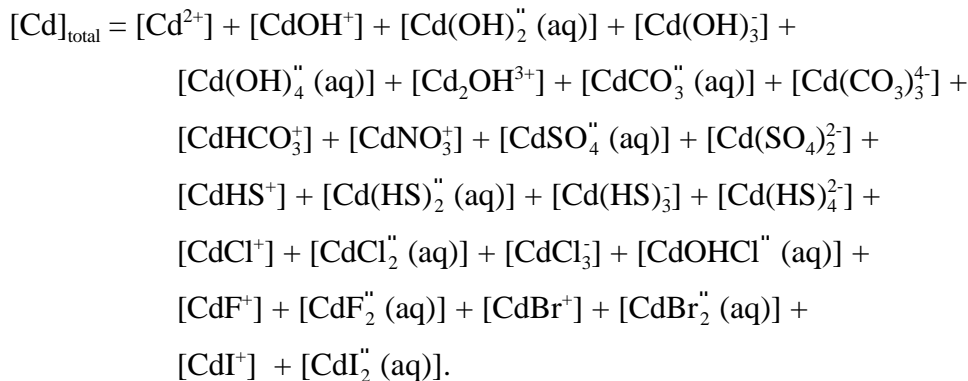
5.2.6 Adsorption Submodel

The MINTEQA2 also includes a submodel to calculate the adsorption of dissolved constituents onto the surfaces of solid phases that can be selected by the code user. The MINTEQA2 code includes 7 adsorption model options. These are:

- Non-electrostatic adsorption models
 - Activity partition coefficient (K_d^{act}) model
 - Activity Langmuir model
 - Activity Freundlich model
 - Ion exchange model
- Electrostatic adsorption models
 - Constant capacitance model (CCM)
 - Diffuse layer model (DLM)
 - Triple layer models (TLM).

The equations and reactions that support these models, as coded in MINTEQA2, are described in greater detail in Section 3. These descriptions and associated equations are adapted from Allison *et al.* (1991).

The K_d^{act} , Langmuir, and Freundlich models in MINTEQA2 are formulated in terms of species activities, and not the more traditional approach of total concentrations of dissolved metal. In the latter case, the total concentrations of a dissolved metal M would equal the sum of the concentrations of all of its dissolved complexed and uncomplexed species. For example, using the species listed in the MINTEQA2 thermodynamic database, the total concentrations of dissolved cadmium, $[\text{Cd}]_{\text{total}}$, in the absence of any organic complexants in the water, could include the following species:



In the presence of organic complexants, $[Cd]_{total}$ could also include, in addition to the cadmium species listed above, the concentrations of aqueous cadmium complexes containing citrate, acetate, EDTA, HEDTA, or other organic complexes.

A total concentration approach would therefore assume that all species of metal M adsorb with equal strength. Experimental data suggest, however, that only certain aqueous species react with the surfaces of a mineral [*e.g.*, Waite *et al.* (1994)]. Based on this assumption, these non-electrostatic models have been reformulated, as those coded in MINTEQA2, in terms of the activities of adsorbing species to provide activity-based models. The purpose of this approach is to reduce the dependency of the model parameters to effects from ionic strength and aqueous complexation of the adsorbing metal by effectively allowing the adsorption of only selected aqueous species of each metal.

Limitations remain, however, regarding these activity formulations of the K_d^{act} , Langmuir, and Freundlich models which restricts their range of applicability. These non-electrostatic adsorption models do not consider: charge balance on surface sites and adsorbed species, electrostatic forces between the adsorbing species and charge surface of the mineral, and reactions between the mineral and dissolved constituents other than the adsorbing metal. The effect of these processes changes with variations in the composition of an aqueous solution. These processes are, however, incorporated into the more robust, but more data intensive, electrostatic “surface complexation” adsorption model options in MINTEQA2.

The MINTEQA2 code includes the reaction components and formalisms necessary to enter the required adsorption data for any of the adsorption models. The code does not however have an adsorption database for these models. The user must provide the set of surface reactions and the associated equilibrium constants as part of the input data set. MINTEQA2 requires that this information be supplied relative to the adsorption of constituents onto specific mineral phases, such as amorphous ferric hydroxide $[Fe(OH)_3 (am)]$, and not a multi-mineral phase material, such as a soil or crushed rock. Examples of MINTEQA2 input files that include the adsorption modeling option are included in the data files distributed by EPA, and are also listed in Allison *et al.* (1991 Appendix D) and Peterson *et al.* (1987a). These examples demonstrate the major data requirements for some of the adsorption model options in MINTEQA2.

5.2.6.1 Examples of Modeling Studies

Modeling studies by Peterson *et al.* (1986), Davis and Runnells (1987), Loux *et al.* (1989), and Turner *et al.* (1993) are examples of the use of MINTEQ adsorption model options. Peterson *et al.* (1986) and Davis and Runnells (1987) studied ground-water contamination associated with waste impoundments for uranium mill tailings using laboratory and computer modeling techniques. Peterson *et al.* (1986) modeled the adsorption of arsenic, chromium, lead, selenium, and zinc using the triple layer model (TLM) in MINTEQ. Their conceptual model was based on the assumption that adsorption of these metals occurred only on amorphous ferric hydroxide $[Fe(OH)_3 (am)]$ that precipitated and dissolved during the course of their experiments.

Adsorption parameters for the TLM for amorphous ferric hydroxide were taken from published sources. The results of the adsorption calculations were in good agreement with some results from their laboratory experiments.

Davis and Runnels (1987) used MINTEQ to successfully model the behavior of zinc observed in laboratory column experiments. They assumed that the concentration of dissolved zinc measured in their solution samples was controlled by adsorption on amorphous ferric hydroxide [Fe(OH)₃ (am)] that precipitated as a result of pH changes occurring in their experiments. The adsorption of zinc on Fe(OH)₃ (am) was calculated using the TLM in MINTEQ. Davis and Runnels describe the selection of adsorption parameters used for the TLM.

Loux *et al.* (1989) used the MINTEQA2 code to model the pH-dependent partitioning of 8 cationic constituents by precipitation and/or adsorption on a sandy aquifer material in an oxidizing environment. The constituents of interest included barium, beryllium, cadmium, copper, nickel, lead, thallium, and zinc. Adsorption of these elements was based on amorphous iron oxide as the only reactive adsorption surface and calculated using the diffuse layer model (DLM). The adsorption parameters and associated reactions for the diffuse layer model were taken from Dzombak (1986). The modeling results were compared to laboratory data for the aquifer material spiked with the trace metals. The predicted concentrations based on the diffuse layer model for adsorption of lead, nickel, and zinc, provided a good description of the pH behavior observed for the spiked samples. The concentrations of the other trace metals were not adequately predicted by the model. These differences were attributed to limitations in the model and/or available thermochemical data.

Turner *et al.* (1993) used the TLM in MINTEQA2 code to model adsorption data for U(VI) on goethite [α -FeO(OH)]. The FITEQL code was used for adsorption parameter optimization. Their study illustrates the extensive parameter-fitting process that the user must complete to use complex electrostatic adsorption models, such as the TLM.

5.2.6.2 Application to Evaluation of K_d Values

Chemical reaction models *cannot be used to predict a K_d value*. The user must supply the adsorption parameters when using any of the adsorption model options. Typically, the data required to derive the adsorption parameters needed as input for adsorption submodels in chemical reaction codes are more extensive than information reported in a laboratory batch K_d study. However, if the parameters have been determined for a particular constituent for a surface complexation model, a chemical reaction model, such as MINTEQA2, can be used to calculate the masses of a constituent that are dissolved or adsorbed and how changes in geochemical conditions, such as pH, affect its adsorption behavior. The user can then derive a K_d using the calculated dissolved and adsorbed masses of the constituent.

The EPA (EPA, 1992a, 1996) has used the MINTEQA2 model and this approach to estimate K_d values for several metals under a variety of geochemical conditions and metal concentrations to

support several waste disposal issues. The EPA in its “Soil Screening Guidance” determined MINTEQA2-estimated K_d values for barium, beryllium, cadmium, Cr(III), Hg(II), nickel, silver, and zinc as a function of pH assuming adsorption on a fixed mass of iron oxide (EPA, 1996; RTI 1994). The calculations assumed equilibrium conditions, and did not consider redox potential or metal competition for the adsorption sites. In addition to these constraints, EPA (1996) noted that this approach was limited by the potential sorbent surfaces that could be considered and availability of thermodynamic data. Their calculations were limited to metal adsorption on iron oxide, although sorption of these metals to other minerals, such as clays and carbonates, is well known.

The data needed to use surface complexation adsorption models are more extensive than those from K_d studies. More importantly, the data for surface complexation models are based on adsorption on pure mineral phases, such as α - Al_2O_3 , γ - Al_2O_3 , böhmite, goethite, magnetite, lepidocrocite, ferrihydrite, SiO_2 , biotite, or kaolinite. Natural soils are more complicated, commonly containing mixtures of more than 10 pure minerals and amorphous mineral coatings. Unless a user can technically defend the assumption that the adsorption of a specific contaminant is dominated in a specific soil-water system, for example, by goethite reactive surfaces, the user is still left with the challenge of extrapolating these modeling results for pure mineral substrates to complex heterogeneous soil-water systems. This issue has been and will continue to be the subject of intensive study, but is not likely to be resolved in the short term or impact contaminant migration and risk assessment modeling soon.

5.2.7 MINTEQA2 Databases

The MINTEQA2 model includes an extensive thermodynamic database that is integrated with the aqueous speciation, solubility, and precipitation/dissolution submodels. The content and equations governing the values stored in the thermodynamic database are described below. MINTEQA2 does not have per se an integrated adsorption submodel database. The adsorption reactions and associated model parameters are supplied by the user as part of each input file. However, as discussed below, the current MINTEQA2 software package is supplied with a limited data file for the diffuse layer model (DLM).

5.2.7.1 Thermodynamic Database

The MINTEQA2 thermodynamic database is considered by many to be one of the most extensive databases for modeling the aqueous speciation and solubility of contaminants and geologically-significant constituents (*e.g.*, magnesium, silica, aluminum, *etc.*) in low-temperature, soil-water systems. To understand the fundamental data needs for a thermodynamic database of a chemical reaction code, the basic equations underlying the thermodynamic parameters stored in the MINTEQA2 thermodynamic database will be reviewed in the next section. The content of the MINTEQA2 thermodynamic database as distributed by EPA will be reviewed and then compared relative to the priority constituents considered in the scope of work for this project.

5.2.7.1.1 Basic Equations

Thermodynamic data used by MINTEQA2 are stored in the form of equilibrium constants ($K_{r,298}^{\circ}$) and enthalpies (heats) of reaction ($\Delta H_{r,298}^{\circ}$) for aqueous speciation, oxidation/reduction, mineral solubility, and gas solubility reactions. The reference temperature for the MINTEQA2 database, as with most geochemical models, is 298 K (25 °C). Equilibrium constants ($\log K_{r,T}^{\circ}$) may be based on values that have been experimentally-determined or calculated from Gibbs free energies of reaction ($\Delta G_{r,T}^{\circ}$) units of cal/mol according to the equation:

$$\log K_{r,T}^{\circ} = \frac{-\Delta G_{r,T}^{\circ}}{2.303 R T} \quad (5.5)$$

where T = temperature in degrees Kelvin,
 R = gas constant (1.9872 cal/mol·K)

Values for $\Delta G_{r,T}^{\circ}$ are calculated from published values for the Gibbs free energy of formation ($\Delta G_{f,298}^{\circ}$) for each product and reactant in the aqueous speciation or solubility reaction by the equation:

$$\Delta G_{r,298}^{\circ} = \sum \Delta G_{f,298}^{\circ} (\text{products}) - \sum \Delta G_{f,298}^{\circ} (\text{reactants}) . \quad (5.6)$$

To calculate aqueous speciation and solubilities at temperatures other than 25°C, the equilibrium constants are recalculated by the MINTEQA2 code to the temperature T of interest using the van't Hoff relation:

$$\log K_{r,T}^{\circ} = \log K_{r,298}^{\circ} - \frac{\Delta H_{r,298}^{\circ}}{2.303 R} \left(\frac{1}{T} - \frac{1}{298} \right) . \quad (5.7)$$

Values for enthalpies of reaction are calculated from published enthalpy of formation values ($\Delta H_{f,298}^{\circ}$) using the equation:

$$\Delta H_{r,298}^{\circ} = \sum \Delta H_{f,298}^{\circ} (\text{products}) - \sum \Delta H_{f,298}^{\circ} (\text{reactants}) . \quad (5.8)$$

Values for $\Delta H_{r,298}^{\circ}$ cannot be calculated for some reactions, because $\Delta H_{f,298}^{\circ}$ values have not been determined for 1 or more reaction products and/or reactants. In these cases, the MINTEQA2 code assumes that

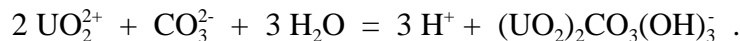
$$\log K_{r,T}^{\circ} \approx \log K_{r,298}^{\circ} . \quad (5.9)$$

Because of the limitations in using the van't Hoff relation for extrapolations over a wide range of temperature, applications of the MINTEQA2 code are limited to temperatures less than 100°C.

5.2.7.1.2 Structure of Thermodynamic Database Files

Typically, each aqueous species, redox, mineral, and gas solubility reaction is represented by 2 fix-formatted lines in the thermodynamic database files supplied with MINTEQA2. A third line is sometimes included when the stoichiometry of a reaction is complex. The first file line includes the identification number, formula descriptor, $\Delta H_{r,298}^{\circ}$ (if available), $\log K_{r,298}^{\circ}$, charge, and related data for each reaction. The second line includes the reaction stoichiometry information formulated in terms of the MINTEQA2 components. Each reaction is entered as a formation reaction; that is, the components react to form the “more complex” species, such as an aqueous complex or mineral phase. The hydrogen stoichiometric component of each reaction is balanced with the components H^+ and H_2O . The hydroxyl species, OH^- , is not used as a component, but is “formed” in a separate reaction in MINTEQA2.

Based on the protocol used for the MINTEQA2 thermodynamic database, the formation reaction for the uranyl mixed hydroxide/carbonate aqueous species, $(UO_2)_2CO_3(OH)_3^-$, is



The corresponding entry in the MINTEQA2 database (in fixed format fields) for this reaction and its associated thermochemical data is

```
8931405 UO2)2CO3OH)3 -14.3940 -0.8969 0.000 0.000-1.00 4.00 0.00 651.0868
2.00 4 2.000 893 1.000 140 3.000 2 -3.000 330
```

For more detailed format information on the MINTEQA2 database files, the reader is referred to the documentation in Allison *et al.* (1991, Appendix A).

5.2.7.1.3 Database Components

The thermodynamic database in the original MINTEQ code (Felmy *et al.*, 1984) was taken from the WATEQ3 code (Ball *et al.*, 1981a). Therefore, many of the inorganic reactions and associated thermodynamic values in the MINTEQA2 database can be traced back to the database supplements and sources described in publications documenting the WATEQ series of chemical reactions codes (Ball *et al.*, 1981a, WATEQ2; Ball *et al.*, 1981b, WATEQ3; Plummer *et al.*, 1976, WATEQ; Truesdell and Jones, 1973, WATEQ; Truesdell and Jones 1974, WATEQ).

The thermodynamic database of the current version of MINTEQA2 includes the original MINTEQ database plus modifications and additions completed on contracts with EPA funding. Some of these supplements include, for example, those completed at PNNL, such as the addition of reactions for aqueous species, gases, and solids containing cyanide and antimony by Sehmel

(1989) and those containing chromium, mercury, selenium, and thallium by Deutsch and Krupka.¹ Documentation for these database supplements are not listed in Brown and Allison (1987, MINTEQA1) or Allison *et al.* (1991, MINTEQA2), and may not be publicly available.

The elements for which the MINTEQA2 thermodynamic database has aqueous speciation, mineral solubility, and/or gas solubility reactions are listed in Table 5.3. The second and third columns of this table list the component species used for these elements and the redox reactions, if any, included in MINTEQA2 for different valence states of a particular element. The reader should note that the database does not contain reactions and associated thermodynamic values for specific isotopes of a particular element. The calculated reactions for a soil-water system assumes the total mass of each element.

Although the list of elements in Table 5.3 is substantial, this table and/or a listing of the database files does not indicate if the database of a chemical reaction code, especially for key contaminants, is adequate (*i.e.*, completeness of reactions and quality of associated thermodynamic values) and up-to-date. The user essentially has this important responsibility. One should expect that, as the period of time between the publication of a code's documentation and its use in an application study increases, the thermodynamic database becomes dated and revisions may be warranted.

Table 5.4 lists the organic ligands for which the MINTEQA2 thermodynamic database has aqueous speciation reactions.² Because of the limited availability of thermodynamic data for metal-organic complexes important to contaminated soil-water systems, as compared to inorganic aqueous complexes, the MINTEQA2 database, as with all chemical reaction codes, is limited. It does not contain complexation reactions for all metals with each of the organic ligands listed in Table 5.4. The reader will need to do a computer search of the MINTEQA2 ASCII file containing these reactions to determine the extent of the organic complexation reactions for each metal.

5.2.7.1.4 Status Relative to Project Scope

The contaminants chosen for study in this project include chromium, cadmium, cesium, tritium (³H), lead, plutonium, radon, strontium, thorium, and uranium. Because the MINTEQA2 thermodynamic database does not contain reactions for specific isotopes, an appraisal of the database content to aqueous speciation and solubility reactions containing tritium is not

¹ Deutsch, W. J., and K. M. Krupka. September 1985. MINTEQ Geochemical Code: Compilation of Thermodynamic Database for the Aqueous Species, Gases, and Solids Containing Chromium, Mercury, Selenium, and Thallium. Unpublished report prepared by Pacific Northwest Laboratory for the U.S. Environmental Protection Agency in Athens, Georgia.

² Although important to contaminant disposal and remediation activities (*i.e.*, "mixed wastes") in the United States, computer modeling of the complexation of contaminant metals with organic complexes was excluded from the scope of the current project due to funding limits.

appropriate. As will be discussed in Volume II of this report, the concentrations of dissolved tritium will be affected by exchange reactions involving hydrogen-containing species dissolved in the soil-water system.

Of the remaining elements, the MINTEQA2 thermodynamic database contains aqueous speciation and solubility reactions for chromium, including the valence states Cr(II), Cr(III), and Cr(VI); cadmium; lead; strontium; and uranium, including the valence states U(III), U(IV), U(V), and U(VI). Except for uranium, the adequacy of the database for these listed elements is not known. Data supplied by Deutsch and Krupka¹ in 1985 is the probable basis for the chromium reactions and associated thermodynamic data. The reactions for cadmium, lead, and strontium may be those taken from the WATEQ-series of codes and supplied with the original MINTEQ code by Felmy *et al.* (1984). It is not known if these have been revised or supplemented since that time.

The reactions and associated thermodynamic data for uranium aqueous species and solid phases were those supplied with the original MINTEQ code. They were taken from those added to WATEQ3 (Ball *et al.*, 1981a) and are based primarily on the compilation of uranium thermodynamic data by Langmuir (1978). Langmuir's review has been superseded by the comprehensive review and compilation of uranium thermodynamic data given in Wanner and Forrest (1992). This compilation represents a significant improvement and update to the values in Langmuir *et al.* (1978), including for U(VI) carbonate and hydrolysis species that are important in soil-water systems with pH values greater than 5.

Of the elements included in the project scope, the thermodynamic database distributed by EPA with MINTEQA2 does not contain reactions and associated thermodynamic data for aqueous species and solids containing cesium, plutonium, radon, and thorium. Published compilations of thermodynamic data for aqueous species, solids, and gases containing these elements are available, such as an Langmuir and Herman (1980), Lemire and Tremaine (1980), Peterson *et al.* (1987b), Phillips *et al.* (1988), Smith and Martell (1976 and more recent supplements), Smith *et al.* (1997), Wagman *et al.* (1982), and others. These sources can be used as good starting points for adding reactions for cesium, plutonium, radon, and thorium to the MINTEQA2 database. However, because these sources are becoming dated, additional reviews of the more recent thermodynamic literature would be needed to supplement them and generate more up-to-date compilations for these elements. Other compilations of thermodynamic data for these elements include databases compiled by geochemical modeling groups elsewhere in the United States and other countries. When documented, these databases are useful sources of information.

¹ Deutsch, W. J., and K. M. Krupka. September 1985. MINTEQ Geochemical Code: Compilation of Thermodynamic Database for the Aqueous Species, Gases, and Solids Containing Chromium, Mercury, Selenium, and Thallium. Unpublished report prepared by Pacific Northwest Laboratory for the U.S. Environmental Protection Agency in Athens, Georgia.

Table 5.3. Component species in MINTEQA2 thermodynamic database.

Element	Component Species	Valence States
Ag	Ag ⁺	
Al	Al ³⁺	
As	H ₃ AsO ₃ ^o (aq), H ₃ AsO ₄ ^o (aq)	As(III), As(V)
B	H ₃ BO ₃ ^o (aq)	
Ba	Ba ²⁺	
Br	Br ⁻	
C	CO ₃ ²⁻ , CN ⁻ , OCN ⁻	
Ca	Ca ²⁺	
Cd	Cd ²⁺	
Cl	Cl ⁻	
Cr	Cr ²⁺ , Cr(OH) ₂ ⁺ , CrO ₄ ²⁻	Cr(II), Cr(III), Cr(VI)
Cu	Cu ⁺ , Cu ²⁺	Cu(I), Cu(II)
F	F ⁻	
Fe	Fe ²⁺ , Fe ³⁺	Fe(II), Fe(III)
Electron	e ⁻	
H	H ⁺ , H ₂ O (l)	
Hg	Hg ₂ ²⁺ , Hg(OH) ₂ ^o (aq)	Hg(I), Hg(II)
I	I ⁻	
K	K ⁺	
Li	Li ⁺	
Mg	Mg ²⁺	

Table 5.3. Continued.

Element	Component Species	Valence States
Mn	Mn^{2+} , Mn^{3+}	Mn(II), Mn(III)
N	NH_4^+ , NO_2^- , NO_3^- , CN^- , OCN^-	N(-III), N(III), N(V)
Na	Na^+	
Ni	Ni^{2+}	
P	PO_4^{3-}	
Pb	Pb^{2+}	
Rb	Rb^{2+}	
S	HS^- , S° , SO_4^{2-}	S(-II), S(VI)
Sb	Sb(OH)_3° (aq), Sb(OH)_6^-	Sb(III), Sb(V)
Se	HSe^- , HSeO_3^- , SeO_4^{2-}	Se(-II), Se(IV), Se(VI)
Si	$\text{H}_4\text{SiO}_4^\circ$ (aq)	
Sr	Sr^{2+}	
Tl	Tl^+ , Tl(OH)_3° (aq)	Tl(I), Tl(III)
U	U^{3+} , U^{4+} , UO_2^+ , UO_2^{2+}	U(III), U(IV), U(V), U(VI)
V	V^{2+} , V^{3+} , VO^{2+} , VO_2^+	V(II), V(III), V(IV), V(V)
Zn	Zn^{2+}	

Table 5.4. Organic ligands in MINTEQA2 thermodynamic database.

Organic Constituents / Complexants	
acetate	methylamine
butyrate	2-methyl pyridine
iso-butyrate	3-methyl pyridine
citrate	4-methyl pyridine
diethylamine	n-butylamine
dimethylamine	nitrilotriacetate ³⁻
EDTA ⁴⁻	phthalate
ethylenediamine	propanoate
formate	salicylate
fulvate	tartrate
glutamate	tri-methylamine
glycine	tributylphosphate
hexylamine	valerate
humate	iso-valerate
iso-propylamine	
n-propylamine	

It should be noted that the thermodynamic database distributed with EPA's MINTEQA2 software package does not include reactions and thermodynamic data for aqueous species and solids containing americium, cobalt, neptunium, niobium, radium, and technetium. Although these radionuclides are not part of the scope of this project, they may be important with respect to contamination and remediation at some sites in the United States and/or performance assessments of proposed LLW and HLW disposal facilities or decommissioning sites. Except for niobium, published compilations of thermodynamic data for these elements, especially for americium (Silva *et al.*, 1995) and technetium (Rard, 1983), exist that can be used to supplement the MINTEQA2 database. The thermodynamic data for aqueous species and solids containing niobium are extremely limited which precludes adequate modeling of aqueous/solid phase equilibria for niobium in soil-water systems.

The thermodynamic database of MINTEQA2 was augmented by Krupka and Serne (1998) for aqueous species and solids containing several radionuclide elements of interest to NRC. These database modifications were based on data files provided by D. Turner¹ who had added these

¹ Center for Nuclear Waste Regulatory Analyses (CNWRA), Southwest Research Institute, San Antonio, Texas

reactions and thermodynamic data to his version of MINTEQA2. The database additions included MINTEQ-formatted reactions, associated thermodynamic data (*i.e.*, $\log K_{r,298}^{\circ}$ and $\Delta H_{r,298}^{\circ}$) and ancillary information (*e.g.*, identification number, formula, charge, mass, reaction stoichiometry) for aqueous species and solids containing americium, neptunium, plutonium, radium, technetium, thorium, and uranium. The database changes for uranium are based on the compilation by Wanner and Forest (1992), and supersede those listed in the MINTEQA2 database as obtained from EPA. Additional revisions to the thermodynamic data for these radionuclide elements were identified by Krupka and Serne (1998) and added to the MINTEQA2 files. These database modifications have not undergone an in depth examination relative to quality-assurance considerations.

5.2.7.1.5 Issues Related to Database Modifications

Successful application of chemical reaction models to quantify contaminant release and transport in soil-water systems is dependent on the development of adequate and internally consistent thermodynamic databases. The thermodynamic databases of chemical reaction codes are typically revised or supplemented based on specific project needs and the availability of thermodynamic data for aqueous species, gases, and solids containing the constituents of interest.

Although an extensive number of tabulations and critical reviews [*e.g.*, see references in Serne *et al.* (1990, Table 3.2)] of thermodynamic data for inorganic complexes and solids have been published during the last 20 years, the selection of "best" values from these publications is a technically and logistically challenging effort. Some of the issues and problems associated with the selection of thermodynamic data are described in detail in Potter (1979), Nordstrom and Munoz (1985), and Smith and Martell (1995). The critical evaluation and selection of a thermodynamic database requires an understanding of general solution chemistry and the phase assemblages of minerals and related amorphous solids associated with a particular cationic and/or anionic constituent. The investigator developing the model's database must also be cognizant of the criteria initially used to review and select the original data for the published tabulations.

Because thermodynamic data tabulations usually contain an inadequate amount of reviewed thermodynamic data for aqueous species of trace metals, available tabulations are typically deficient for modeling contaminated soil-water systems. Researchers are thus faced with the difficult responsibility of assembling thermodynamic data from other possibly less-credible publications, borrowing values from extant chemical reaction models, and/or conducting their own reviews of published thermodynamic data. Because there is a growing reliance on thermodynamic review efforts completed by coworkers and other research organizations, documentation supporting these reviews and the rationale for selecting each datum that is "accepted" for a model's database are extremely important with respect to (1) defining the credibility of the database, (2) achieving an internally consistent database, (3) minimizing duplication in future review efforts, and (4) describing the selection criteria and calculation methods used in selecting the best values.

5.2.7.2 Sorption Database

The MINTEQA2 code is not designed to have a thermochemical database, analogous to the thermodynamic database, that is integrated with the adsorption submodel and its 7 model options. The adsorption reactions and associated model parameters need to be supplied by the user as part of each input file. This process and example input files are discussed in Allison *et al.* (1991).

However, the current MINTEQA2/PRODEFA2 software package is supplied with a limited adsorption data file for use with the diffuse layer adsorption model option. Data files are not supplied for any of the other adsorption model options. The data file, formatted in ASCII, is named *FEO-DLM.dbs*. It includes surface reactions and associated intrinsic conditional surface complexation constants applicable to the diffuse layer model for the adsorption of the trace metals Ba^{2+} , Be^{2+} , Ca^{2+} , Cd^{2+} , Cu^{2+} , Ni^{2+} , Pb^{2+} , and Zn^{2+} , and the ligands $\text{H}_3\text{AsO}_3^\ominus$ (aq), $\text{H}_3\text{AsO}_4^\ominus$ (aq), $\text{H}_3\text{BO}_3^\ominus$ (aq), PO_4^{3-} , and SO_4^{2-} onto 2 types of iron-oxide sites. The adsorption constants are based on data published by Dzombak (1986).¹

5.2.7.2.1 Status Relative to Project Scope

Of the elements chosen for study in this project, cadmium and lead are the only 2 elements included in the diffuse layer adsorption model data file supplied with MINTEQA2. As mentioned above, this file is restricted to adsorption onto 2 types of iron-oxide sites, and is therefore not applicable for the adsorption of these metals to other mineral reactive surfaces. None of the other contaminants, including chromium, cesium, plutonium, radon, strontium, thorium, or uranium, are supported by this data file.

The MINTEQA2/PRODEFA2 software package includes no adsorption database files for the activity partition coefficient (K_d^{act}), activity Langmuir isotherm, activity Freundlich isotherm, ion exchange, constant capacitance, or triple layer adsorption models.

5.2.7.2.2 Published Database Sources

No published compilations are known to exist for adsorption constants for the activity partition coefficient (K_d^{act}), activity Langmuir isotherm, activity Freundlich isotherm, and ion exchange adsorption models used in MINTEQA2. Numerous individual data sets have been published for the adsorption of many individual contaminants on specific mineral substrates, such as TiO_2 or goethite. Typically, these data are parameterized using 1 or more of the surface complexation models. Compilations and review of these studies was beyond the scope of this project.

Smith and Jenne (1988) (and related papers by Dzombak and Hayes, 1992, and Smith and Jenne, 1992) compiled and evaluated published values for triple layer model constants for the adsorption

¹ Personal communication from N. T. Loux at the U.S. Environmental Protection Agency in Athens, Georgia.

of numerous constituents on α -FeO(OH), amorphous iron(III) hydrous oxide, and δ -MnO₂ solids. This study was conducted for the U.S. Environmental Protection Agency (Athens, Georgia) for use in modeling the migration of contaminants in ground-water systems. Their compilation included intrinsic constants and associated reaction stoichiometries for the adsorption of species containing the following constituents:

- For adsorption onto Fe(III) hydrous oxides: Ag, As(V), Ba, CO₃, Ca, Cd, Co, Cr(VI), Cu(II), Fe(II), Hg(II), Mg, Mn(II), Np(V), Pb, Pu(IV), Sb(III), Sb(V), Se(VI), Se(IV), S, SO₄, Th(I), U(VI), and Zn
- For adsorption onto δ -MnO₂: Ag, Ba, Ca, Cd, Co, Cu(II), Fe(II), Hg(II), Mg, Mn(II), Pb, Th(I), and Zn.

Turner (1995) compiled and critically reviewed adsorption data reported in the literature for surface complexation models. He then used a uniform approach to parameterize these data using the diffuse layer, constant capacitance, and triple layer surface complexation models. His study was conducted in support of research funded by NRC to study the potential migration of radionuclides associated with the geologic disposal of commercial high level radioactive waste. Turner (1993) previously described the use of the MINTEQA2 chemical reaction code to model adsorption of radionuclides. Turner (1995) reported model constants for:

- Americium(III) on α -Al₂O₃, γ -Al₂O₃, and amorphous SiO₂
- Neptunium(V) on α -Al₂O₃, γ -Al₂O₃, boehmite (γ -AlOOH), goethite [α -FeO(OH),] magnetite (Fe₃O₄), lepidocrocite [γ -FeO(OH)], ferrihydrite (5Fe₂O₃ · 9H₂O), amorphous SiO₂, biotite mica [K(Mg,Fe)₃(Al,Fe)Si₃O₁₀(OH,F)₂], and kaolinite [Al₂Si₂O₅(OH)₄]
- Plutonium(IV) on goethite
- Plutonium(V) on γ -Al₂O₃ and goethite
- Thorium on γ -Al₂O₃ and amorphous SiO₂
- Uranium(VI) on α -Al₂O₃, magnetite, ferrihydrite, goethite, quartz (SiO₂), and kaolinite
- Carbon on ferrihydrite.

We are not aware of any other major published compilations of adsorption thermochemical data for use with MINTEQA2. Moreover, it is very possible that individual investigators have compiled and parameterized their own databases of adsorption constants based on the needs of their individual research projects. General access, especially in these days of cost recovery, and quality assurance issues will likely prohibit the use of many such individual data files.

5.3 Adsorption Model Options in MINTEQA2

The MINTEQA2 chemical reaction code includes 7 adsorption model options. Each of these adsorption models and their associated equations and reactions are briefly described below. MINTEQA2 includes the following non-electrostatic adsorption models

- Activity partition coefficient (K_d^{act}) model
- Activity Langmuir model
- Activity Freundlich model
- Ion exchange model

and electrostatic adsorption models

- Diffuse layer model
- Constant capacitance model
- Triple layer models.

The following descriptions and associated equations are adapted from the MINTEQA2 documentation by Allison *et al.* (1991). When using the adsorption model options, readers are cautioned to read the MINTEQA2 documentation carefully relative to correct entry and formulation of model reactions and associated constants.

It should be noted that the non-electrostatic models in MINTEQA2 are formulated in terms of species activities, and not the more traditional approach of total concentrations of dissolved metal. The purpose of this approach is to reduce the dependency of the model parameters to effects from ionic strength and aqueous complexation of the adsorbing metal.

Limitations remain, however, regarding these activity formulations which restricts the range of applicability of these non-electrostatic models. These non-electrostatic adsorption models do not consider: charge balance on surface sites and adsorbed species, electrostatic forces between the adsorbing species and charged surface of the mineral, and reactions between the mineral and dissolved constituents other than the adsorbing metal. The effect of these processes changes with variations in the composition of an aqueous solution. These processes are, however, incorporated into the more robust, but more data intensive, electrostatic “surface complexation” adsorption models. The following descriptions of the electrostatic adsorption models incorporated into MINTEQA2 are cursory. The reader is referred to sources, such as Westall and Hohl (1980), Morel *et al.* (1981), Barrow and Bowden (1987), and Davis and Kent (1990), for detailed descriptions, comparisons, and derivations of the relevant equations and reactions associated with these models.

5.3.1 *Electrostatic Versus Non-Electrostatic Models*

Hydrous oxides of iron, manganese, and aluminum and amorphous aluminosilicates that exist as discrete mineral grains or surface coatings on other minerals in soils are assumed to be primary adsorbents for trace metals ions. These solid phases have variable surface charges and exhibit amphoteric behavior. The solids have a net positive charge at pH values below their point of zero charge (PZC) and a net negative charge at pH values above the PZC (see Chapter 2).

These surface charges create electrostatic potentials extending into the surrounding solutions. Dissolved aqueous species that have a charge of the same polarity as the surface will be repelled, while aqueous species with a charge opposite to that of the surface will be attracted (adsorbed). The electrostatic potentials associated with charged surfaces may therefore affect the adsorption of dissolved species on these surfaces. Unlike the non-electrostatic adsorption models, the electrostatic models include a component that accounts for the electrostatic potentials at the charged surface. The mass action equations of electrostatic adsorption models include terms that modify the activities of adsorbing species approaching charged surfaces by the electrical work necessary to penetrate the zone of electrostatic potentials (ψ 's) associated with the mineral surface. The 3 electrostatic models in MINTEQA2 differ primarily in the types of surface species that are allowed within specific physical locations or layers extending away from the surface and in the parameters that each model uses.

The 3 electrostatic models in MINTEQA2 deal with adsorption as surface complexation reactions analogous to aqueous complexation reactions in solution. In the descriptions of the MINTEQA2 adsorption models that follow, surface sites are represented in the adsorption reactions and mass action expressions as SOH groups, where S refers to the mineral structure and adsorption site located at the solid-liquid interface. Some ions, such as H^+ , OH^- , and a variety of trace metal ions are assumed to be adsorbed by complexation with these surface sites.

In the triple layer model (TLM), the most complicated of the 3 electrostatic adsorption models in MINTEQA2, the space around the solid surface is represented in surface complexation adsorption models as 3 semi-infinite layers or zones between the solid surface and the solution (Figure 5.4). These zones are separated by the α , β , and d planes. Starting at the mineral surface, The α plane represents the first interface between the solid surface and the aqueous phase. Generally, only the H^+ and OH^- ions are allowed to penetrate the α layer to interact with the solid surface. Beyond the α plane, farther from the mineral surface, is the β plane which ends at the boundary of the diffuse zone, the d plane. Dissolved ions, such as macro constituents (*e.g.*, Na^+ , Ca^{2+} , and SO_4^{2-}) and trace constituents ions that are adsorbing onto the solid surface are allowed into the β layer. The third layer is the diffuse zone where the ions are not influenced strongly by electrostatic charge on the solid surface. The ions in this region are considered to be counterions that neutralize any residual charge caused by the surface and adsorbed ions in the β layer. Continuing further from the mineral surface, the d layer blends into the bulk solution.

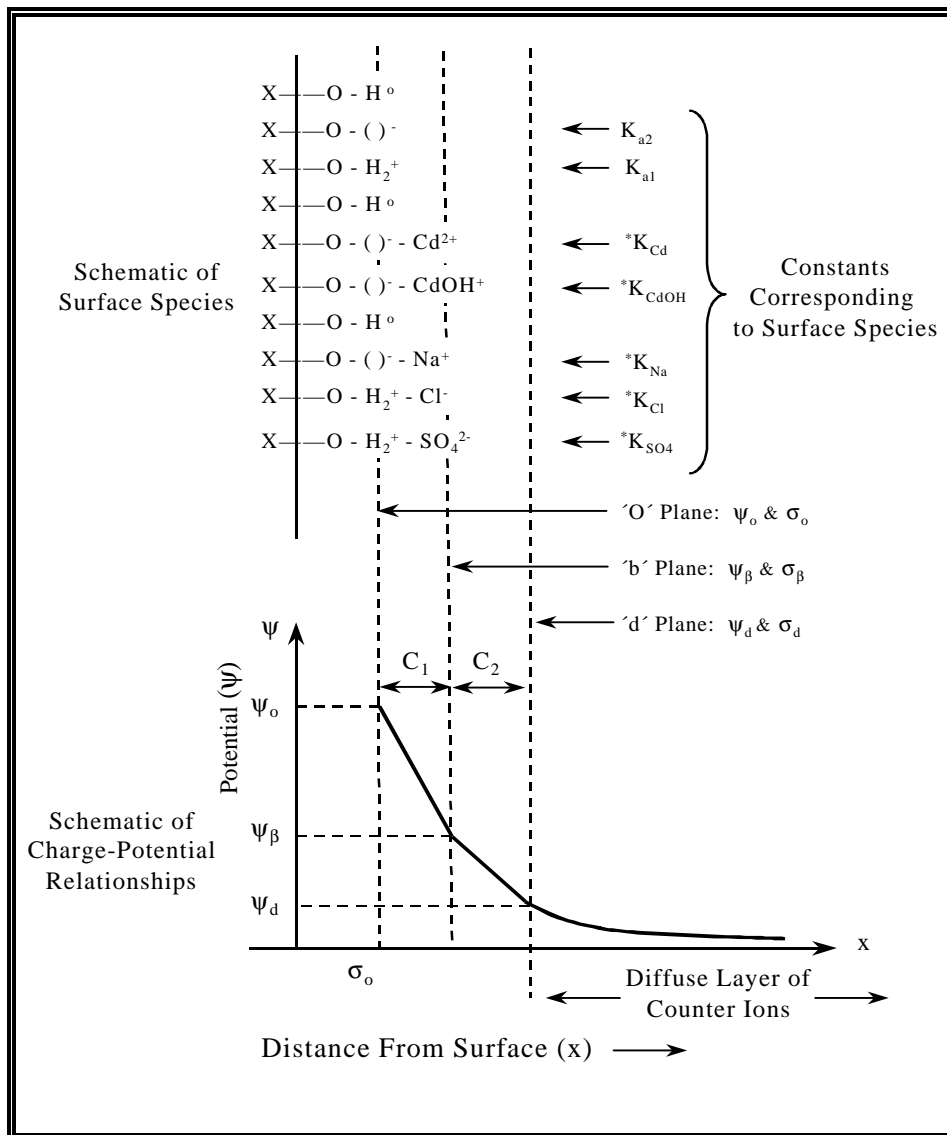


Figure 5.4. Schematic representation of the triple layer model showing surface species and surface charge-potential relationships. [Taken from Peterson *et al.* (1987a). Brackets in the *o* plane indicated deprotonated surface sites.]

The conceptual models for the constant capacitance (Figure 5.5) and diffuse layer models are simplified to only 2 zones separated by the o and d planes. The difference between these 2 adsorption models is in the function relating total surface charge, T_o , to surface potential ψ_o (discussed in Sections 5.3.6 and 5.3.7). This function [$\psi(x)$ in Figure 5.5)] is linear and exponential, respectively, in the constant capacitance and diffuse layer models. It should be noted that parameters subscripted with “ o ” in that 2-layer models are not equivalent to the o plane parameters defined for the triple layer model due to differences in the definition of the o plane.

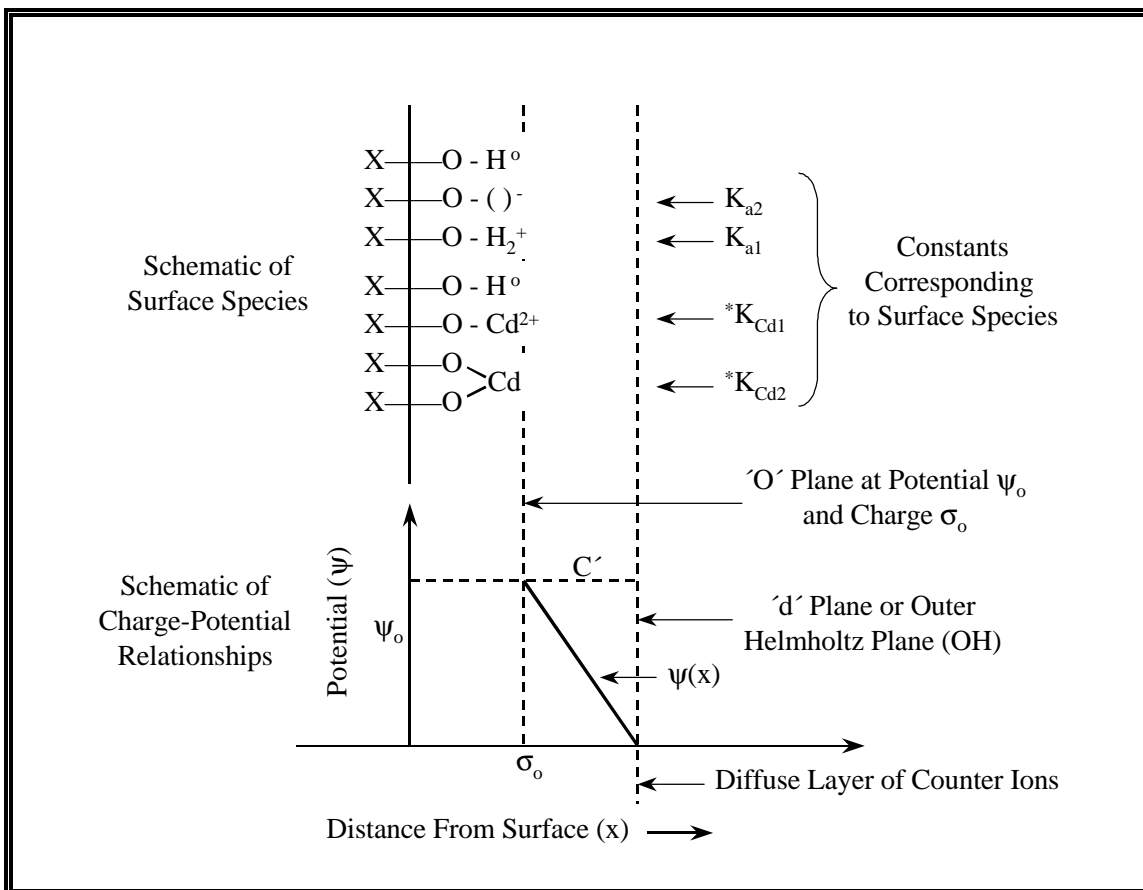


Figure 5.5. Schematic representation of the constant capacitance layer model showing surface species and surface charge-potential relationships. [Taken from Peterson *et al.* (1987a). Brackets in the o plane indicated deprotonated surface sites.]

In all 3 models, a charge, σ , associated with the surface is assumed to be balanced by a charge (σ_d) associated with the diffuse layer d of counterions such that

$$\sigma + \sigma_d = 0 . \quad (5.10)$$

In the constant capacitance and diffuse-layer models, all adsorbed ions contribute to the surface charge. However, the net charge σ due to adsorption in the triple layer model is the sum of the charges associated with 2 rather than 1 adsorbing plane. These include the innermost α plane and the β plane, which are characterized by charges σ_α and σ_β , respectively. Thus, for the triple layer model, the net surface charge is given by

$$\sigma_\alpha + \sigma_\beta = \sigma \quad (5.11)$$

which is balanced by the charge in the diffuse layer such that

$$(\sigma_\alpha + \sigma_\beta) + \sigma_d = 0 . \quad (5.12)$$

Because the electrical potential gradients extending away from the mineral's surface result from the surface charge, the specifically adsorbed potential determining ions also govern distributions of counterions in the diffuse layer.

Activities of ions in solution and near the surface are influenced by the presence of electrostatic potentials arising from the surface charge. The activity difference between ions near the surface and those far away is the result of electrical work required to move them across the potential gradient between the charged surface and the bulk solution. The activity change between these zones is related to the ion charge, z , and the electrical potential, ψ , near the surface and can be expressed using the exponential Boltzmann expression,

$$\{X_s^z\} = \{X^z\} [e^{-\psi F/RT}]^z \quad (5.13)$$

where z = charge of ion X,
 $\{X_s^z\}$ = activity of an ion X of charge z near the surface,
 $\{X^z\}$ = activity of ion X in bulk solution beyond the influence of the charged surface,
 $e^{-\psi F/RT}$ = Boltzmann factor,
 F = Faraday constant,
 R = ideal gas constant, and
 T = absolute temperature in Kelvin.

The general algorithm is similar for all 3 electrostatic models in MINTEQA2. Each model is only briefly described below. The surface reactions for the electrostatic models in MINTEQA2 are written with the Boltzmann factor included as a reactant component with a stoichiometric factor appropriate for the reaction. Although these electrostatically-related components are included in the mass action equations, they are not analogous to the chemical components defined in

MINTEQA2 and have no analytical totals for their input values. Their total charges are determined from equations that are unique to each electrostatic model and potential. The activity coefficients for the Boltzmann factor components are set to unity in MINTEQA2.

Adsorption reactions are entered as part of MINTEQA2 input files. The MINTEQA2 code, as noted previously, has no integrated adsorption database. The adsorption reactions and associated equilibrium constants are written in terms of the neutral surface site, SOH. They are entered as formation reactions, analogous to the aqueous complexation and mineral solubility reactions included in the thermodynamic database. Published adsorption reactions and associated constants are, however, sometimes referenced to the protonated surface site SOH_2^+ for adsorbing anions and the deprotonated site SO^- for adsorbing cations. In these cases, the user must modify the published reaction and equilibrium constant data in terms of MINTEQA2 components to use them in a MINTEQA2 input file.

5.3.2 Activity Partition Coefficient (K_d) Model

The traditional partition coefficient, K_d , adsorption model (see Chapter 2) is defined as the ratio of the concentration of metal bound on the surface of the solid to the total concentration of metal dissolved in the liquid phase at equilibrium as in

$$K_d = \frac{\text{Amount of element sorbed on solid} / \text{solid mass}}{\text{Amount of element dissolved in solution} / \text{solution volume}}. \quad (5.14)$$

This process can be expressed as the surface adsorption reaction



where SOH = unreacted surface site,
M = a dissolved metal M, and
SOH·M = adsorption site occupied by a component or surface-bound metal M.

The convention used for symbols in the adsorption model equations discussed in this chapter follows that used by Allison *et al.* (1991). Although the basic adsorption equations are comparable to those listed in Chapter 2, the symbols may differ slightly.

The mass action expression for this reaction is

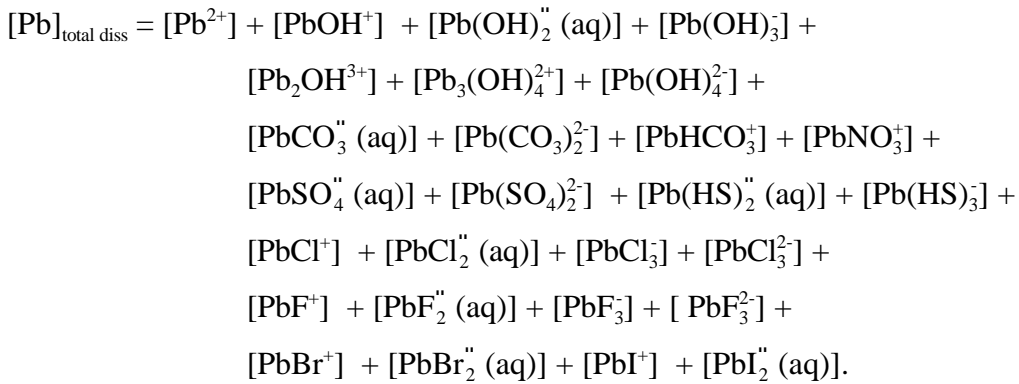
$$K_d = \frac{[\text{SOH}\cdot\text{M}]}{[\text{M}]_{\text{total diss}}} \quad (5.16)$$

where $[\text{SOH}\cdot\text{M}]$ = concentration of adsorption sites occupied by a component M or surface-bound metal per unit mass of adsorbing solid

$[M]_{\text{total diss}} =$ total concentration of dissolved M at equilibrium.

Following common convention for thermodynamic nomenclature, reaction species indicated within [] refer to concentrations, and those indicated within { } refer to activities. Equation 5.16 assumes that the concentration of unreacted surface sites, SOH, are in great excess relative to the total concentration of dissolved metal and the activity of SOH is equal to 1.

As mentioned previously, the traditional K_d assumes that all species of metal M absorb with equal strength, and $[M]_{\text{total diss}}$ includes all aqueous species containing metal M. For example, using the species listed in the MINTEQA2 thermodynamic database, the total concentrations of dissolved lead, $[Pb]_{\text{total diss}}$, in the absence of any organic complexants in the water, could include the following species:



In the presence of organic complexants, $[Pb]_{\text{total diss}}$ would also include, in addition to the lead species listed above, the concentrations of aqueous lead citrate, acetate, EDTA, HEDTA, and other organic complexes.

Because experimental data suggest that only certain aqueous species react with the surface of a mineral, the traditional K_d model is reformulated in MINTEQA2 in terms of the activities of species to provide the activity K_d^{act} model.

In MINTEQA2, the mass action expression for the activity K_d^{act} model is

$$K_d^{\text{act}} = \frac{\{\text{SOH}\cdot\text{M}\}}{\{\text{M}\}} = \frac{[\text{SOH}\cdot\text{M}]}{\gamma_M[\text{M}]} \quad (5.17)$$

where $\{\text{M}\} =$ free activity of the uncomplexed “bare” cation of M in the equilibrium solution,
 $\gamma_M =$ activity coefficient of dissolved species M

The quantity $\{\text{SOH}\cdot\text{M}\}$ is defined as equal to $[\text{SOH}\cdot\text{M}]$. This assumption is made because there is no generally accepted method for calculating activity coefficients for unreacted or reacted adsorption sites. The parameter K_d^{act} can be considered the equilibrium constant for the surface

reaction described in Equation 5.15. This model assumes that there is an unlimited supply of unreacted adsorption sites and the mineral surface cannot become saturated regardless of how much M adsorbs.

5.3.3 Activity Langmuir Model

The concentration-based Langmuir adsorption model has the constraint that the number of surface sites available for adsorption is limited. This is the only difference between the Langmuir and K_d adsorption models. The partition coefficient, K_d , model is linear with respect to the total concentration of a dissolved metal, whereas the Langmuir model is non-linear. The user must specify the concentration of available adsorption sites as part of the input file. The Langmuir equation for adsorption is defined by

$$[\text{SOH} \cdot \text{M}] = \frac{K_L [\text{SOH}]_{\text{total}} [\text{M}]_{\text{total diss}}}{1 + K_L [\text{M}]_{\text{total diss}}} \quad (5.18)$$

where K_L = Langmuir adsorption constant,
 $[\text{SOH} \cdot \text{M}]$ = amount of adsorbed metal M per unit mass of adsorbing solid,
 $[\text{SOH}]_{\text{total}}$ = total concentration of available surface adsorption sites, and
 $[\text{M}]_{\text{total diss}}$ = total concentration of dissolved metal M at equilibrium.

The surface adsorption reaction used for the Langmuir model is identical to that for the K_d model



The equilibrium constant, K_L^{act} , for this reaction can be expressed in terms of activities as

$$K_L^{\text{act}} = \frac{\{\text{SOH} \cdot \text{M}\}}{\{\text{M}\} \{\text{SOH}\}} = \frac{\gamma_{\text{SOH} \cdot \text{M}} [\text{SOH} \cdot \text{M}]}{\gamma_{\text{M}} [\text{M}] \gamma_{\text{SOH}} [\text{SOH}]} \quad (5.20)$$

As discussed previously, the activity coefficients pertaining to unreacted and reacted surface sites in this and the other adsorption models in MINTEQA2 are assigned values of unity. Equation 5.20 can then be rewritten as

$$K_L^{\text{act}} = \frac{[\text{SOH} \cdot \text{M}]}{\gamma_{\text{M}} [\text{M}] [\text{SOH}]} \quad (5.21)$$

The mass balance equation for the available surface sites is

$$[\text{SOH}]_{\text{total}} = [\text{SOH} \cdot \text{M}] + [\text{SOH}] \quad (5.22)$$

By combining Equations 5.21 and 5.22 in terms of $[\text{SOH}]_{\text{total}}$ and $[\text{SOH} \cdot \text{M}]$, one obtains the Langmuir relationship in terms of activities

$$[\text{SOH} \cdot \text{M}] = \frac{K_L^{\text{act}} [\text{SOH}]_{\text{total}} \gamma_m [\text{M}]}{1 + K_L^{\text{act}} \gamma_m [\text{M}]} \quad (5.23)$$

By substituting K_L^{act} with K_L and setting γ_m to a value of 1, Equation 5.23 reduces to the concentration Langmuir model expressed in Equation 5.18.

To use MINTEQA2 to model competition between different metals for adsorption on the available surface sites, one must define the separate adsorption reactions on the surface. For the competitive Langmuir model for the competing metals M_1, M_2, \dots, M_n , separate reactions with associated mass balance expressions need to be formulated using Equations 5.19-5.21 such that



·
·



Geochemical modeling and plotting techniques may be used to derive constants for the activity Langmuir model from experimentally-measured, concentration-based K_L data. One must first determine if the concentration-based Langmuir model fits the experimental data by using the linear form of Equation 5.18

$$\frac{[\text{M}]_{\text{total diss}}}{[\text{SOH} \cdot \text{M}]} = \frac{1}{K_L [\text{SOH}]_{\text{total}}} + \frac{[\text{M}]_{\text{total diss}}}{[\text{SOH}]_{\text{total}}} \quad (5.27)$$

A plot of $[\text{M}]_{\text{total diss}}/[\text{SOH} \cdot \text{M}]$ versus $[\text{M}]_{\text{total diss}}$ will result in a straight line with the slope $1/[\text{SOH}]_{\text{total}}$ and intercept $1/K_L[\text{SOH}]_{\text{total}}$ if the data fit the Langmuir isotherm. The value for the concentration-based K_L is obtained by dividing this slope by the intercept. Geochemical modeling is then used to calculate the aqueous speciation of metal M for the composition of the aqueous solution in which the K_L data were determined. The K_L^{act} value can then be derived from an analogous plot in which the calculated activities $\{M\}$ for metal M are plotted in place of the concentration term $[M]$.

5.3.4 Activity Freundlich Model

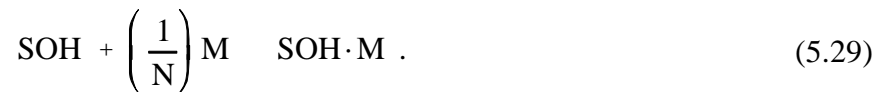
The concentration-based Freundlich equation for adsorption is defined by

$$[\text{SOH}\cdot\text{M}] = K_F [\text{M}]_{\text{total diss}}^{1/N} \quad (5.28)$$

where K_F = Freundlich adsorption constant,
 $[\text{SOH}\cdot\text{M}]$ = amount of adsorbed metal M per unit mass of adsorbing solid,
 $[\text{M}]_{\text{total diss}}$ = total concentration of dissolved metal M at equilibrium, and
 N = a constant.

The Freundlich equation is sometimes written with the exponent in Equation 5.28 being N instead of $1/N$. The Freundlich model assumes, like the K_d adsorption model, an unlimited supply of unreacted adsorption sites. For the special case where N equals 1, the mass action equations for the Freundlich and K_d models are identical.

The Freundlich model can be considered as a surface adsorption reaction where the stoichiometric coefficient for the adsorbed metal M equals $1/N$ as in



The equilibrium constant, K_F^{act} , for this reaction can be expressed in terms of activities as

$$K_F^{\text{act}} = \frac{\{\text{SOH}\cdot\text{M}\}}{\{\text{M}\}^{1/N} \{\text{SOH}\}} \quad (5.30)$$

Like the activity K_d^{act} model, there is no mass balance on surface sites, and, assuming an excess of sites with respect to adsorbed metal M, the concentration, $[\text{SOH}]$, and activity $\{\text{SOH}\}$, of the unreacted surface sites are assumed equal and set to 1. Under these conditions and assuming $\{\text{SOH}\cdot\text{M}\}$ equals $[\text{SOH}\cdot\text{M}]$ as with the activity K_d^{act} and Langmuir models, Equation 5.30 becomes

$$K_F^{\text{act}} = \frac{[\text{SOH}\cdot\text{M}]}{\{\text{M}\}^{1/N}} \quad (5.31)$$

which is similar to the K_d^{act} model except that the stoichiometric coefficient $1/N$ of the adsorbing species of metal M.

An approach using geochemical modeling and plotting techniques similar to that described for the activity Langmuir model may be used to calculate constants for the activity Freundlich model from experimentally-measured, concentration-based K_F data. One must first determine if the Freundlich model fits the experimental data by using the logarithmic form of the Freundlich mass action Equation 5.28

$$\log [\text{SOH}\cdot\text{M}] = \log K_F + \left(\frac{1}{N} \right) \log [\text{M}]_{\text{total diss}} . \quad (5.32)$$

If the data fit the model, a plot of $\log [\text{SOH}\cdot\text{M}]$ versus $\log [\text{M}]_{\text{total diss}}$ will result in a straight line with the slope $1/N$ and intercept $\log K_F$. Geochemical modeling is then used to calculate the aqueous speciation of metal M for the composition of the aqueous solution in which the K_F data were determined. The K_F^{act} value can then be derived by plotting the calculated activities $\{M\}$ for the adsorbing species of metal M in place of the concentration term $[\text{M}]_{\text{total diss}}$.

5.3.5 Ion Exchange Model

Ion exchange sorption is defined as the process by which a dissolved ion M_2 is exchanged for an ion M_1 that already occupies a surface sorption site and ion M_1 is in turn released back into solution. The ion exchange reaction can be expressed as



where M_1 = the ion initially occupying the exchange site,
 M_2 = the ion replacing M_1 on the exchange site;
 $\text{SOH}\cdot\text{M}_1$ = surface sites occupied by ion M_1
 $\text{SOH}\cdot\text{M}_2$ = surface sites occupied by ion M_2 , and
 a and b = stoichiometric coefficients.

The equilibrium constant (selectivity coefficient), K_{ex} , for the exchange reaction expressed as

$$K_{\text{ex}} = \frac{\{M_1\}^a \{\text{SOH}\cdot\text{M}_2\}^b}{\{M_2\}^b \{\text{SOH}\cdot\text{M}_1\}^a} = \frac{\gamma_{M_1}^a [M_1]^a [\text{SOH}\cdot\text{M}_2]^b}{\gamma_{M_2}^b [M_2]^b [\text{SOH}\cdot\text{M}_1]^a} . \quad (5.34)$$

The constant K_{ex} can be written in terms of concentrations by replacing activity of each species with the product of concentration and activity coefficient. The activity coefficients for the occupied sites, $\text{SOH}\cdot\text{M}_n$, are set equal to one as was assumed for the previous adsorption models in MINTEQA2.

5.3.6 Diffuse Layer Model

For the diffuse-layer model, the total charge, T_{σ_o} , for plane o is calculated as

$$T_{\sigma_o} = 0.1174 I^{1/2} \sinh(Z\psi_o F/2RT) \quad (5.35)$$

where Z = valency of the symmetrical electrolyte (which we take as unity),
 I = ionic strength, and

all other parameters are defined as in Equation 5.13.

Examples of surface reactions are listed below for protonation and deprotonation reactions as well as for a divalent cation M^{2+} . Boltzmann factors are represented in the mass action as components.

The surface reaction and corresponding mass action expression for the protonation reaction are, respectively,



and

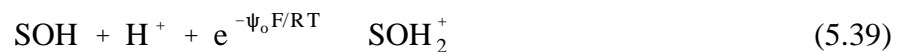
$$K = \frac{\{\text{SOH}_2^+\}}{\{\text{SOH}\} \{\text{H}_s^+\}} \quad (5.37)$$

where H_s^+ denotes a hydronium ion near the surface.

The activity coefficients for the surface species SOH_2^+ and SOH are assumed to be equal to unity. The activity of H_s^+ must be corrected for the energy change required to move from the bulk solution to the charged surface. This activity change is represented by expressing $\{\text{H}_s^+\}$ in terms of the activity of the bulk solution hydronium ion $\{\text{H}^+\}$ and associated exponential Boltzmann expression for a charge z of 1 as

$$\{\text{H}_s^+\} = \{\text{H}^+\} e^{-\psi_0 F/RT} \quad (5.38)$$

Substituting this expression for $\{\text{H}_s^+\}$ in Equations 5.36 and 5.37, one obtains the following surface reaction and mass action equation expressed in terms of the Boltzmann factor



and

$$K = \frac{\{\text{SOH}_2^+\}}{\{\text{SOH}\} \{\text{H}^+\} [e^{-\psi_0 F/RT}]} \quad (5.40)$$

The stoichiometry for the corresponding de-protonation reaction is



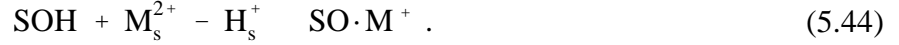
Substituting for $\{\text{H}_s^+\}$ as above results in the following de-protonation surface reaction and mass action equation



and

$$K = \frac{\{SO^-\} \{H^+\} [e^{-\psi_o F/RT}]}{\{SOH\}} \quad (5.43)$$

The stoichiometry for a surface reaction involving a multivalent species, such as a divalent cation M^{2+} , is



The mass action expression for this type of adsorption reaction also includes the charge and stoichiometry for the adsorbing ion. Substituting for $\{M_s^{2+}\}$ and for $\{H_s^+\}$ in Equation 5.44, one obtains the following mass action expressions

$$K = \frac{\{SO \cdot M^+\} \{H_s^+\}}{\{SOH\} \{M_s^{2+}\}} = \frac{\{SO \cdot M^+\} \{H^+\} [e^{-\psi_o F/RT}]}{\{SOH\} \{M^{2+}\} [e^{-\psi_o F/RT}]^2} \quad (5.45)$$

$$K = \frac{\{SO \cdot M^+\} \{H^+\}}{\{SOH\} \{M^{2+}\} [e^{-\psi_o F/RT}]} \quad (5.46)$$

Mass action expressions for other surface reactions are formulated in a similar manner.

5.3.7 Constant Capacitance Model

The constant capacitance model is a special case of the diffuse layer model, applicable in theory only to systems at high, constant ionic strength. The constant capacitance model is similar to the diffuse layer model in that they both define specific adsorption of all ions on the o plane. Except for the values of the equilibrium constants, the mass action and charge balance equations are identical for these 2 adsorption models. Therefore, the surface reactions and mass action expressions described above for the diffuse layer model also apply to the constant capacitance model.

The difference in these 2 models is in the function relating total surface charge, T_{σ_o} , to surface potential ψ_o . In the constant capacitance model, Equation 5.35 is approximated by

$$T_{\sigma_o} \approx C \psi_o \quad (5.47)$$

where C is a constant capacitance term. Although the constant capacitance and diffuse layer models are implemented similarly, the capacitance term C is often treated as a fitting parameter rather than as a measured characteristic of the system.

5.3.8 Triple Layer Model

The triple layer model (Figure 5.4) includes 2 adsorbing planes instead of 1 plane as conceptualized in the diffuse layer and constant capacitances models. As implemented in MINTEQA2, the *o* plane, the inner most zone, only includes the protonation and deprotonation (*i.e.*, gain or loss of H⁺) reactions at the surface sites. The *β* plane includes other specifically adsorbed ions with charge σ_β and potential ψ_β in that zone. The diffuse layer or '*d*' plane, which is the outer most zone, includes non-specifically adsorbed ions affected by ψ_d potentials. The capacitances between the *o* and *β* planes and the *β* and *d* planes are designated C_1 and C_2 , respectively. The user must provide values for both capacitance terms.

The total charges, T_{σ_o} , T_{σ_β} , and T_{σ_d} , associated with *o*, *β*, and *d* planes, respectively, in the triple-layer model are defined as

$$T_{\sigma_o} = C_1(\psi_o - \psi_\beta) \quad (5.48)$$

$$T_{\sigma_\beta} = C_1(\psi_\beta - \psi_o) + C_2(\psi_\beta - \psi_d) \quad (5.49)$$

$$T_{\sigma_d} = C_2(\psi_d - \psi_\beta) \quad (5.50)$$

where ψ_o = electrostatic potential at the *o* plane,
 ψ_β = electrostatic potential at the *β* plane, and
 ψ_d = electrostatic potential at the *d* plane.

Surface reactions as expressed in the triple layer model differ from those used for the diffuse layer and constant capacitance models only in that their mass action expressions include the proper stoichiometry for the electrostatic components representing the *β* and *o* planes. The *d* plane, which as no specific adsorption, is therefore not a factor in the stoichiometry.

The surface protonation and deprotonation reactions for the triple layer model, except for their associated equilibrium constant values, are identical to those given above for the diffuse layer models. Examples of surface reactions and mass action expressions for the adsorption of a mono- and divalent cations and a monovalent anion adapted from Allison *et al.* (1991) are given below for the triple layer model. They show the stoichiometric coefficients for the electrostatic components representing the *β* and *o* planes.

The surface reaction for the adsorption of the monovalent metal cation M^+ is



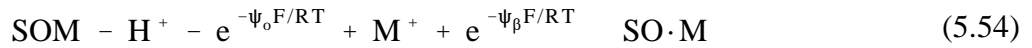
In the triple layer model, H_s^+ and M_s^+ occur in the α and β planes, respectively. Therefore,

$$\{H_s^+\} = \{H^+\} [e^{-\psi_\alpha F/RT}] \quad (5.52)$$

and

$$\{M_s^+\} = \{M^+\} [e^{-\psi_\beta F/RT}] . \quad (5.53)$$

Substituting these expressions into Equation 5.51, the following MINTEQA2 reaction and mass action expression are obtained



and

$$K = \frac{\{SO \cdot M\} \{H^+\} [e^{-\psi_\alpha F/RT}]}{\{SOH\} \{M^+\} [e^{-\psi_\beta F/RT}]} . \quad (5.55)$$

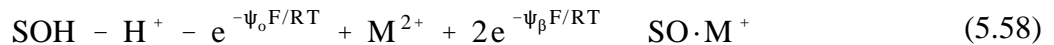
The surface reaction for the adsorption of the divalent metal cation M^{2+} is



For the divalent cation adsorbed in the β plane,

$$\{M_s^{2+}\} = \{M^{2+}\} [e^{-\psi_\beta F/RT}]^2 \quad (5.57)$$

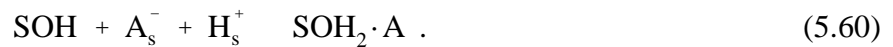
Substituting this expression in the reaction above gives the following MINTEQA2 reaction and mass action expression



and

$$K = \frac{\{SO \cdot M^+\} \{H^+\} [e^{-\psi_\alpha F/RT}]}{\{SOH\} \{M^{2+}\} [e^{-\psi_\beta F/RT}]^2} . \quad (5.59)$$

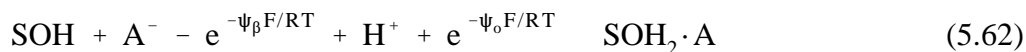
The surface reaction for the adsorption of the monovalent anion A^- is



This reaction results in the formation of a neutral surface complex. For the anion adsorbed in the β plane

$$\{A_s^-\} = \{A^-\} [e^{-\psi_\beta F/RT}]^- . \quad (5.61)$$

Substituting this into the above anion adsorption reaction, one obtains the following MINTEQA2 reaction and mass action expression



and

$$K = \frac{\{\text{SOH}_2 \cdot A\} [e^{-\psi_\beta F/RT}]}{\{\text{SOH}\} \{A^-\} \{H^+\} [e^{-\psi_o F/RT}]} . \quad (5.63)$$

The formulation of reactions and mass action expressions for other adsorbing cations and anions is similar to those examples given above.

5.4 Summary

Chemical reaction models are valuable computational tools that may be used to analyze the macro-chemical processes (*e.g.*, aqueous complexation, redox, solubility, and adsorption equilibrium) affecting the composition of a soil-water system being studied in the laboratory, field lysimeter, or field site. They also be used to provide some bounding calculations for predicting the changes in chemistry that will result when 1 or more of these processes are imposed on a soil-water system.

Numerous chemical reaction models exist. The MINTEQA2 computer code was developed with EPA funding and is currently distributed by EPA in a form that executes on personal computers. MINTEQA2 includes aqueous speciation, solubility (*i.e.*, saturation indices), precipitation/dissolution, and adsorption submodels. MINTEQA2's adsorption submodel includes 4 non-electrostatic [activity partition coefficient (K_d^{act}), activity Langmuir, activity Freundlich, and ion exchange] models and 3 electrostatic (diffuse layer, constant capacitance, and triple layer) adsorption model options.

MINTEQA2 and other similar chemical reaction models can be used in indirect ways to support evaluations of K_d values and related contaminant migration and risk assessment modeling. These applications include the following:

- Calculation of aqueous speciation to determine the ionic state and composition of the dominant species for a dissolved contaminant present in a soil-water system
- Calculation of bounding, technically-defensible maximum concentration limits for contaminants (based on solubility constraints) as a function of key composition parameters (*e.g.*, pH) of any specific soil-water system

- Analysis of data from laboratory measurements of K_d values to determine if any solubility limits were exceeded during the experiments.

Chemical reaction models, however, cannot be used to predict a K_d value. The user must supply the adsorption parameters when using any of the adsorption model options. However, MINTEQA2 may be used to predict the chemical changes that result in the aqueous phase from adsorption using any of 7 adsorption model options.

The MINTEQA2 model includes an extensive thermodynamic database that is integrated with the aqueous speciation, solubility, and precipitation/dissolution submodels. Of the elements included in the project scope, the thermodynamic database distributed by EPA with MINTEQA2 does not contain reactions and associated thermodynamic data for aqueous species and solids containing cesium, plutonium, radon, and thorium. Published compilations of thermodynamic data for aqueous species, solids, and gases containing these elements are available that can be used as starting points for upgrading the MINTEQA2 database to include cesium, plutonium, radon, and thorium aqueous species and solids. MINTEQA2 does not have per se an integrated adsorption submodel database. The adsorption reactions and associated model parameters must be supplied by the user as part of each input file.

6.0 REFERENCES

- Alberty, R. A. 1987. *Physical Chemistry*. Seventh Edition, John Wiley and Sons, New York, New York.
- Allison, J. D., D. S. Brown, and K. J. Novo-Gradac. 1991. *MINTEQA2/PRODEFA2, A Geochemical Assessment Model for Environmental Systems: Version 3.0 User's Manual*. EPA/600/3-91/021, U.S. Environmental Protection Agency, Athens, Georgia, March 1991.
- Ames, L. L., and J. E. McGarrah. 1980. *Basalt Radionuclide Distribution Coefficient Determinations, FY1979 Annual Report*. PNL-3146, Pacific Northwest Laboratory, Richland, Washington.
- Ames, L. L., J. E. McGarrah, B. A. Walker, and P. F. Salter. 1982. "Sorption of Uranium and Cesium by Hanford Basalts and Associated Secondary Smectite." *Chemical Geology*, 35:205-225.
- Ames, L. L., and D. Rai. 1978. *Radionuclide Interactions with Soil and Rock Media*. EPA 520/6-78-007, U.S. Environmental Protection Agency, Office of Radiation Programs, Las Vegas, Nevada.
- ASTM (American Society of Testing and Materials). 1987. "24-hour Batch-Type Measurement of Contaminant Sorption by Soils and Sediments." In *Annual Book of ASTM Standards, Water and Environmental Technology, Volume 11.04*, pp. 163-167, Philadelphia, Pennsylvania.
- ASTM (American Society of Testing and Materials). 1988. "Determining a Sorption Constant (K_{oc}) for an Organic Chemical in Soil and Sediments." In *Annual Book of ASTM Standards, Water and Environmental Technology, Volume 11.04*, pp. 731-737, Philadelphia, Pennsylvania.
- Atkinson, A. 1983. "Mathematical Modeling of Leaching From Porous Nuclear Waste-Forms." *Radioactive Waste Management and the Nuclear Fuel Cycle*, 3:371-386.
- Atkinson, A., K. Nelson, and T. M. Valentine. 1986. "Leach Test Characterization of Cement-Based Nuclear Waste Forms." *Nuclear and Chemical Waste Management*, 6:241-253.
- Atkinson, A., and A. K. Nickerson. 1988. "Diffusion and Sorption of Cesium, Strontium, and Iodine in Water-Saturated Cement." *Nuclear Technology*, 81:100-113.

- Backhus, D. A., J. N. Ryan, D. M. Groher, J. K. MacFarlane, and P. M. Gschwend. 1993. "Sampling Colloids and Colloid-Associated Contaminants in Ground Water." *Ground Water*, 31:466-479.
- Baetslé, L. H. 1967. "Migration of Radionuclides in Porous Media." In *Progress in Nuclear Energy, Series XII, Health Physics*, A.M.F. Duhamel (ed.), pp. 707-730, Pergamon Press, Elmsford, New York.
- Ball, J. W., E. A. Jenne, and M. W. Cantrell. 1981a. *WATEQ3: A Geochemical Model with Uranium Added*. Open-File Report 81-1183, U.S. Geological Survey, Menlo Park, California.
- Ball, J. W., and D. K. Nordstrom. 1998. "Critical Evaluation and Selection of Standard State Thermodynamic Properties for Chromium Metal and Its Aqueous Ions, Hydrolysis Species, Oxides, and Hydroxides." *Journal of Chemical and Engineering Data*, 43:895-918.
- Ball, J. W., D. K. Nordstrom, and E. A. Jenne. 1981b. *Additional and Revised Thermochemical Data and Computer Code for WATEQ2--A Computerized Chemical Model for Trace and Major Element Speciation and Mineral Equilibria of Natural Waters*. Water Resources Investigations WRI 78-116 (second printing), U.S. Geological Survey, Menlo Park, California.
- Ball, W. P., C. H. Buehler, T. C. Harmon, D. M. Mackay, and P. V. Roberts. 1990. "Characterization of a Sandy Aquifer Material at the Grain Scale." *Journal of Contaminant Hydrology*, 5:253-295.
- Barber, L. B., II., E. M. Thurman, and D. D. Runnells. 1992. "Geochemical Heterogeneity in a Sand and Gravel Aquifer: Effect of Sediment Mineralogy and Particle Size on the Sorption of Chlorobenzenes." *Journal of Contaminant Hydrology*, 9:35-54.
- Barrow, N. J., and J. W. Bowden. 1987. "A Comparison of Models for Describing the Adsorption of Anions on a Variable Charge Mineral Surface." *Journal of Colloid and Interface Science*, 119:236-250.
- Bates, R. L., and J. A. Jackson (eds.). 1980. *Glossary of Geology*. American Geological Institute, Falls Church, Virginia.
- Berry, J. A. 1992a. *A Review of Sorption of Radionuclides Under the Near- and Far-Field Conditions of an Underground Radioactive Waste Repository. Part I*. DoE/HMIP/RR/92/061 (Parts I). Harwell Laboratory, Oxfordshire, United Kingdom.

- Berry, J. A. 1992b. *A Review of Sorption of Radionuclides Under the Near- and Far-Field Conditions of an Underground Radioactive Waste Repository. Part II.* DoE/HMIP/RR/92/061 (Parts II). Harwell Laboratory, Oxfordshire, United Kingdom.
- Berry, J. A. 1992c. *A Review of Sorption of Radionuclides Under the Near- and Far-Field Conditions of an Underground Radioactive Waste Repository. Part III.* DoE/HMIP/RR/92/061 (Parts III). Harwell Laboratory, Oxfordshire, United Kingdom.
- Biggar, J. W., and D. R. Nielsen. 1962. "Miscible Displacement: II. Behavior of Tracers." *Soil Science Society of America Journal*, 26:125-128.
- Bolt, G. H., and M. G. M. Bruggenwert (eds.). 1978. *Soil Chemistry. A. Basic Elements.* Developments in Soil Science 5A, Elsevier Scientific Publishing Company, New York, New York.
- Bond, W. J., and P. J. Wierenga. 1990. "Immobile Water During Solute Transport in Unsaturated Sand Columns." *Water Resources Research*, 26:2475-2481.
- Bosma, W. J. P., and S. E. A. T. Van der Zee. 1993. "Transport of Reacting Solute in a One-dimensional Chemically Heterogeneous Porous Medium." *Water Resources Research*, 29:117-131.
- Bosma, W. J. P., S. E. A. T. Van der Zee, and C. J. Van Duijn. 1996. "Plume Development of a Nonlinearly Adsorbing Solute in Heterogeneous Porous Formations." *Water Resources Research*, 32:1569-1584.
- Bourcier, W. L. 1990. *Geochemical Modeling of Radionuclide Waste Glass Dissolution Using EQ3/6: Preliminary Results and Data Needs.* UCID-21869, Lawrence Livermore National Laboratory, Livermore, California.
- Bouwer, J. 1991. "Simple Derivation of the Retardation Equation and Application to Preferential Flow and Macrodispersion." *Ground Water*, 29:41-46.
- Box, G. E. P., and D. W. Behnken. 1960. "Some New Three Level Designs for the Study of Quantitative Variables." *Technometrics*, 2:455-475.
- Brown, P. L., A. Haworth, S. M. Sharland, and C. J. Tweed. 1991. *HARPHRQ: A Geochemical Speciation Program Based on PHREEQE.* Report NSS/R188, Harwell Laboratory, Harwell Laboratory, Oxfordshire, United Kingdom.
- Brown, D. S., and J. D. Allison. 1987. *MINTEQA1, an Equilibrium Metal Speciation Model: User's Manual.* EPA/600/3-87/012, U.S. Environmental Protection Agency, Athens, Georgia.

- Brusseau, M. L. 1994. "Transport of Reactive Contaminants in Heterogeneous Porous Media." *Reviews of Geophysics*, 32:285-313.
- Brusseau, M. L., and P. S. C. Rao. 1989. "Sorption Nonideality During Organic Contaminant Transport in Porous Media." *CRC Critical Reviews in Environmental Control*, 19:33-99.
- Brusseau, M. L., and J. M. Zachara. 1993. "Transport of Co^{2+} in a Physically and Chemically Heterogeneous Porous Media." *Environmental Science and Technology*, 27:1937-1939.
- Buck, J. W., G. Whelan, J. G. Droppo, Jr., D. L. Strenge, K. J. Castleton, J. P. McDonald, C. Sato, and G. P. Streile. 1995. *Multimedia Environmental Pollutant Assessment System (MEPAS): Application Guidance -- Guidelines for Evaluating MEPAS Input Parameters for Version 3.1*. PNL-10395, Pacific Northwest National Laboratory, Richland, Washington.
- Buddemeir, R. W., and J. R. Hunt. 1988. "Transport of Colloidal Contaminants in Groundwater: Radionuclide Migration at the Nevada Test Site." *Applied Geochemistry*, 3:535-548.
- Buffle, J., D. Perret, and M. Newman. 1992. "The Use of Filtration and Ultrafiltration for Size Fractionation of Aquatic Particles, Colloids, and Macromolecules." In *Environmental Particles. Part II. Sampling and Characterization of Particles of Aquatic Systems*, J. Buffle and H. Van Leeuwen (eds.), pp. 171-230, Lewis Publishers, Chelsea, Michigan.
- Burr, D. T., E. A. Sudicky, and R. L. Naff. 1994. "Nonreactive and Reactive Solute Transport in Three-dimensional Heterogeneous Porous Media: Mean Displacement, Plume Spreading, and Uncertainty." *Water Resources Research*, 30:791-815.
- Carter, S. L., M. M. Mortland, and W. D. Kemper. 1986. "Specific Surface." In *Methods of Soil Analysis -- Part I: Physical and Mineralogical Methods*, A. Klute (ed.), Second Edition, pp. 413-422, Soil Science Society of America, Madison, Wisconsin.
- Carslaw, H. S., and J. C. Jaeger. 1959. *Conduction of Heat in Solids*. Oxford University Press, London, England.
- Chiou, Cary T., Susan E. McGroddy, and Daniel E. Kile. 1998. "Partition Characteristics of Polycyclic Aromatic Hydrocarbons on Soils and Sediments." *Environmental Science and Technology*, 32:264-269
- Cloninger, M. O., and C. R. Cole. 1981. *Reference Analysis on the Use of Engineered Barriers for Isolation of Spent Nuclear Fuel in Granite and Basalt*. PNL-3530, Pacific Northwest Laboratory, Richland, Washington.

- Cloninger, M. O., C. R. Cole, and J. F. Wahburn. 1980. *An Analysis on the Use of Engineered Barriers for Geologic Isolation of Spent Fuel in a Referenced Salt Repository*. PNL-3356, Pacific Northwest Laboratory, Richland, Washington.
- Coats, K. H., and B. D. Smith. 1964. "Dead-End Pore Volume and Dispersion in Porous Media." *Society of Petroleum Engineers Journal*, 4:73-84.
- Cochran, G. W., and G. M. Cox. 1957. *Experimental Design*. Second Edition, Wiley, New York, New York.
- Codell, R. B., K. T. Key, and G. Whelan. 1982. *A Collection of Mathematical Models for Dispersion in Surface Water and Groundwater*. NUREG-0868, U.S. Nuclear Regulatory Commission, Washington, DC.
- Cole, C. R., S. B. Yabusaki, and C. T. Kincaid. 1988. *CFEST-SC -- Coupled Fluid, Energy, and Solute Transport Code, SuperComputer Version*. Battelle, Pacific Northwest Laboratory, Richland, Washington.
- Corapcioglu, M. Y., and S. Kim. 1995. "Modeling Facilitated Contaminant Transport of Mobile Bacteria." *Water Resource Research*, 31:2639-2647.
- Cotton, F. A., and G. Wilkinson. 1972. *Advanced Inorganic Chemistry, A Comprehensive Text*. Third Edition. John Wiley and Sons, Inc., New York.
- Dagan, G. 1984. "Solute Transport in Heterogeneous Porous Formations." *Journal of Fluid Mechanics*, 145:151-177.
- Danielsson, L. G. 1982. "On the Use of Filters for Distinguishing Between Dissolved and Particulate Fractions in Natural Waters." *Water Research*, 16:179-182.
- Davies, O. L. 1954. *Design and Analysis of Industrial Experiments*. Hafner, New York, New York.
- Davis, J. A., and D. B. Kent. 1990. "Surface Complexation Modeling in Aqueous Geochemistry." In *Mineral-Water Interface Geochemistry*, M. F. Hochella, Jr. and A. F. White (eds.), pp. 177-260, Reviews in Mineralogy, Volume 23, Mineralogical Society of America, Washington, D.C.
- Davis, A., and D. D. Runnells. 1987. "Geochemical Interactions Between Acidic Tails Fluid and Bedrock: Use of the Computer Model MINTEQ." *Applied Geochemistry*, 2:231-241.

- Dayal, R., H. Arora, and N. Morcos. 1983. *Estimation of Cesium-137 Release from Waste/Cement Composites Using Data from Small-Scale Specimen*. NUREG/CR-3382, Nuclear Regulatory Commission, Washington, D.C.
- Dean, J. A. (ed.). 1973. *Lange's Handbook of Chemistry*. McGraw-Hill, New York, New York.
- Degeldre, C., G. Longworth, V. Mowlin, and P. Vilks. 1989. *Grimsel Colloid Exercise. An International Intercomparison Exercise on the Sampling and Characterization of Groundwater Colloids*. Technical Report 39, Paul Scherrer Institut-Bericht, Wurenlingen und Villigen, Switzerland.
- Delany, J. M. 1985. *Reaction of Topopah Spring Tuff with J-13 Water: A Geochemical Modeling Approach Using the EQ3/6 Reaction Path Code*. UCRL-53631 DE86 013226, Lawrence Livermore National Laboratory, Livermore, California.
- Delegard, C. H., and G. S. Barney. 1983. *Effects of Hanford High-Level Waste Compounds on Sorption of Cobalt, Strontium, Neptunium, Plutonium, and Americium of Hanford Sediments*. RHO-RE-ST-1 P, Rockwell Hanford Operations, Richland, Washington.
- Delegard, C. H., S. A. Gallagher, and R. B. Kasper. 1981. *Saturated Column Leach Studies: Hanford 216Z-Z-1A Sediment*. RHO-SA-210, Rockwell Hanford Operations, Richland, Washington.
- Douglas, L. A. 1989. "Vermiculites." In *Minerals in Soil Environments*, J. B. Dixon and S. B. Week (eds.), Second Edition. pp. 635-674, Soil Science Society of America, Madison, Wisconsin.
- Dragun, J. 1988. *Soil Chemistry of Hazardous Materials*. Hazardous Materials Control Research Institute, Silver Spring, Maryland.
- Dubin, M. M., and L. V. Radushkevich. 1947. "Equation of the Characteristic Curve of Activated Charcoal." *Proceedings of the Academy of Sciences, Physical Chemistry Section, U.S.S.R.*, 55:331-333.
- Dzombak, D. A. 1986. *Toward a Uniform Model for the Sorption of Inorganic Ions on Hydrated Oxides*. Ph.D. Dissertation, Massachusetts Institute of Technology, Boston, Massachusetts.
- Dzombak, D. A., and K. F. Hayes. 1992. "Comment on 'Recalculation, Evaluation, and Prediction of Surface Complexation Constants for Metal Adsorption on Iron and Manganese Oxides.'" *Environmental Science and Technology*, 26:1251-1253.

- Elabd, H., and W. A. Jury. 1986. "Spatial Variability of Pesticide Adsorption Parameters." *Environmental Science and Technology*, 20:256-260.
- EPA (U.S. Environmental Protection Agency). 1984. *Uncontrolled Hazardous Waste Site Ranking System, A User's Manual*. HW-10, U.S. Environmental Protection Agency, Washington, D.C.
- EPA (U.S. Environmental Protection Agency). 1988. *Superfund Exposure Assessment Manual*. EPA/540/1-88/001, U.S. Environmental Protection Agency, Washington, D.C.
- EPA (U.S. Environmental Protection Agency). 1989. *Transport and Fate of Contaminants in the Subsurface*. EPA/625/4-89/019, U.S. Environmental Protection Agency, Cincinnati, Ohio.
- EPA (U.S. Environmental Protection Agency). 1991. *Site Characterization for Subsurface Remediation*. EPA/625/4-91/026, Office of Research and Development, U.S. Environmental Protection Agency, Cincinnati, Ohio.
- EPA (U.S. Environmental Protection Agency). 1992a. *Background Document for Finite Source Methodology for Wastes Containing Metal*. HWEP-S0040, U.S. Environmental Protection Agency, Office of Solid Waste, Washington, D.C.
- EPA (U.S. Environmental Protection Agency). 1992b. "U.S. Environmental Protection Agency, 40 CFR 300, Appendix A, Uncontrolled Hazardous Waste Site Ranking System: A User's Manual." *Federal Register*, 47, No. 137, July 16, 1982.
- EPA (U.S. Environmental Protection Agency). 1993. "Environmental Characteristics of EPA, NRC, and DOE Sites Contaminated with Radioactive Substances." EPA 402-R-93-011, U.S. Environmental Protection Agency, Office of Radiation and Indoor Air (6603J), Office of Solid Waste and Emergency Response, Washington, D.C.
- EPA (U.S. Environmental Protection Agency). 1996. *Soil Screening Guidance: Technical Background Document*. EPA/540/R-96/018, U.S. Environmental Protection Agency, Washington, D.C.
- EPRI (Electric Power Research Institute). 1991. *Use of Batch and Column Methodologies to Assess Utility Waste Leaching and Subsurface Chemical Attenuation*. EPRI EN-7313, Electric Power Research Institute, Palo Alto, California.
- Erdal, B. R., Chairman. 1985. *Workshop on Fundamental Geochemistry Needs for Nuclear Waste Isolation*. US DOE CONF8406134, National Technical Information Service, Springfield, Virginia.

- Felmy, A. R., D. C. Girvin, and E. A. Jenne. 1984. *MINTEQ: A Computer Program for Calculating Aqueous Geochemical Equilibria*. EPA-600/3-84-032 (NTIS PB84-157148), Pacific Northwest Laboratory, Richland, Washington.
- Fischer, H. B., E. J. List, R. C.Y. Koh, J. Imberger, and N. H. Brooks. 1979. *Mixing in Inland and Coastal Waters*. Academic Press, New York, New York.
- Freeze, R. A., and J. A. Cherry. 1979. *Groundwater*. Prentice-Hall, Englewood Cliffs, New Jersey.
- Friedlander, G., J. W. Kennedy, and J. M. Miller. 1966. *Nuclear and Radiochemistry. Second Edition*. John Wiley and Sons, Inc., New York, New York.
- Freundlich, H. 1926. *Colloid and Capillary Chemistry*. Methuen, London, England.
- Gamerding, A. P., D. I. Kaplan, and C. T. Resch. 1998. *Uranium(VI) Sorption and Transport in Unsaturated, Subsurface Hanford Site Sediments – Effect of Moisture Content and Sediment Texture*. PNNL-11975, Pacific Northwest National Laboratory, Richland, Washington.
- Gamerding, A. P., and D. I. Kaplan. 1999. “Application of a Continuous-Flow Centrifugation Method and Determination of Heterogeneous Solute Transport in Disturbed, Unsaturated Sediments.” *Water Resources Research*, (in review).
- Garrels, R. M., and C. L. Christ. 1965. *Solutions, Minerals, and Equilibria*. Freeman, Cooper, and Company, San Francisco, California.
- Gaudet, J. P., H. Jegat, G. Vachaud, and P. J. Wierenga. 1977. “Solute Transfer, with Exchange Between Mobile and Stagnant Water, Through Unsaturated Sand.” *Soil Science Society of America Journal*, 41:665-671.
- Gee, G. W., and A. C. Campbell. 1980. *Monitoring and Physical Characterization of Unsaturated Zone Transport - Laboratory Analysis*. PNL-3304, Pacific Northwest Laboratory, Richland, Washington.
- Gee, G. W., A. C. Campbell, P. J. Wierenga, and T. L. Jones. 1981. *Unsaturated Moisture and Radionuclide Transport: Laboratory Analysis and Modeling*. PNL-3616, Pacific Northwest Laboratory, Richland, Washington.
- Gelhar, L. W., and C. L. Axness. 1983. “Three-Dimensional Stochastic Analysis of Macrodispersion in Aquifers.” *Water Resources Research*, 19:161-180.

- Giles, C. H., D. Smith, and A. Huitson. 1974. "A General Treatment and Classification of the Solute Adsorption Isotherm. I. Theoretical." *Journal of Colloid and Interface Science*, 47:755-765.
- Glasstone, S. 1972. *Thermodynamics for Chemists*. Robert E. Krieger Publishing Company, Huntington, New York.
- Goldberg, S. 1995. "Adsorption Models Incorporated into Chemical Equilibrium Models." In *Chemical Equilibrium and Reaction Models*, R. H. Loeppert, A. P. Schwab, and S. Goldberg (eds.), pp. 75-95, Special Publication Number 42, Soil Science Society of America, Inc., Madison, Wisconsin.
- Goltz, M. N., and P. V. Roberts. 1986. "Interpreting Organic Solute Transport Data from a Field Experiment Using Physical Nonequilibrium Models." *Journal of Contaminant Hydrology*, 1:77-93.
- Grim, R. E. 1968. *Clay Mineralogy*. McGraw-Hill Book Company, New York, New York.
- Gschwend, P. M., D. Backhus, J. K. MacFarlane, and A. L. Page. 1990. "Mobilization of Colloids in Groundwater Due to Infiltration of Water at Coal Ash Disposal Site." *Journal of Contaminant Hydrology*, 6:307-320.
- Gschwend, P. M., and M. C. Reynolds. 1987. "Monodispersed Ferrous Phosphate Colloids in an Anoxic Groundwater Plume." *Journal of Contaminant Hydrology*, 1:309-327.
- Gschwend, P. M. and S. Wu. 1985. "On the Constancy of Sediment-Water Partition Coefficients of Hydrophobic Organic Pollutants." *Environmental Science and Technology*, 19:90-96.
- Gu, B., and R. K. Schulz. 1991. *Anion Retention in Soil: Possible Application to Reduce Migration of Buried Technetium and Iodine*. NUREG/CR-5464, U.S. Nuclear Regulatory Commission, Washington, D.C.
- Haggerty, R., and S. M. Gorelick. 1995. "Multiple-Rate Mass Transfer for Modeling Diffusion and Surface Reactions in Media with Pore-scale Heterogeneity." *Water Resources Research*, 31:2383-2400.
- Hem, J. D. 1985. *Study and Interpretation of the Chemical Characteristics of Natural Water*. Water Supply Paper 2254, U. S. Geological Survey, Alexandria, Virginia.
- Higgins, G. H. 1959. "Evaluation of the Groundwater Contamination Hazard from Underground Nuclear Explosives." *Journal of Geophysical Research*, 64:1509-1519.
- Hillel, D. 1998. *Environmental Soil Physics*. Academic Press, San Diego, California.

- Ho, C. H., and N. H. Miller. 1986. "Formation of Uranium Oxide Sols in Bicarbonate Solutions." *Journal of Colloid and Interface Science*, 113:232-240.
- Hollander, M., and D.A. Wolfe. 1973. *Nonparametric Statistical Methods*. Wiley, New York, New York..
- Honeyman, B. D., and P. H. Santschi. 1988. "Metals in Aquatic Systems." *Environmental Science and Technology*, 22:862-871.
- Hopmans, J. W., H. Schukking, and P. J. J. F. Torfs. 1988. "Two-Dimensional Steady State Unsaturated Water Flow in Heterogeneous Soils with Autocorrelated Soil Hydraulic Properties." *Water Resources Research*, 24:2005-2017.
- INTERA (INTERA Environmental Consultants, Inc.). 1983. *Geochemical Models Suitable for Performance Assessment of Nuclear Waste Storage: Comparison of PHREEQE and EQ3/EQ6*. ONWI-473, INTERA Environmental Consultants, Inc., Houston, Texas.
- Ivanovich, M., A. G. Latham, G. Longworth, and M. Gascoyne. 1992. "Applications to Radioactive Waste Disposal Studies." In *Uranium-Series Disequilibrium. Applications to Earth, Marine, and Environmental Systems*, M. Ivanovich and R. S. Harmon (eds.), pp. 583-630, Oxford University Press, Oxford, England.
- Jackson, K. J., and W. L. Bourcier (technical organizers). 1986. *Proceedings of the Workshop on Geochemical Modeling*. CONF-8609134, National Technical Information Service, Springfield, Virginia.
- Jackson, R. E., and K. J. Inch. 1989. "The In-situ Absorption of Sr-90 in a Sand Aquifer at the Chalk River Nuclear Laboratories." *Journal of Contaminant Hydrology*, 4: 27-50.
- Jacobs, G. K., and S. K. Whatley (eds.). 1985. *Proceedings of the Conference on the Application of Geochemical Models to High-level Nuclear Waste Repository Assessment*. NUREG/CR-0062 (ORNL/TM-9585), Oak Ridge National Laboratory, Oak Ridge, Tennessee.
- James, R. V., and J. Rubin. 1986. "Transport of Chloride Ion in a Water-Unsaturated Soil Exhibiting Anion Exclusion." *Soil Science Society of America Journal*, 50:1142-1149.
- Jardine, P. M., G. K. Jacobs, and G. V. Wilson. 1993. "Unsaturated Transport Processes in Undisturbed Heterogeneous Porous Media: I. Inorganic Contaminants." *Soil Science Society of America Journal*, 57:945-953.

- Jenne, E. A. 1977. "Trace Element Sorption by Sediments and Soils - Sites and Processes." In *Symposium on Molybdenum in the Environment*, W. Chappel and K. Petersen (eds.), pp. 425-553, M. Dekker, Inc., New York, New York.
- Jenne, E. A. (ed.). 1979. *Chemical Modeling in Aqueous Systems. Speciation, Sorption, Solubility, and Kinetics*. Symposium Series 93, American Chemical Society, Washington, D.C.
- Jenne, E. A. 1981. *Geochemical Modeling: A Review*. PNL-3574, Pacific Northwest Laboratory, Richland, Washington.
- Jenne, E. A.. 1998a. "Adsorption of Metals by Geomedia: Data Analysis, Modeling, Controlling Factors, and Related Issues." In *Adsorption of Metals by Geomedia. Variables, Mechanisms, and Model Applications*, E. A. Jenne (ed.), p. 2-73, Academic Press, San Diego, California.
- Jenne, E. A. 1998b. "Priorities for Future Metal Adsorption Research." In *Adsorption of Metals by Geomedia. Variables, Mechanisms, and Model Applications*, E. A. Jenne (ed.), p. 549-560, Academic Press, San Diego, California.
- Johnson, W. H., S. M. Serkiz, L. M. Johnson, and S. B. Clark. 1995. "Uranium Partitioning Under Acidic Conditions in a Sandy Soil Aquifer." Paper presented at the Waste Management '95 Symposium, Tucson, Arizona, February 26 - March 2, 1995.
- Jury, W. A., H. Elabd, and M. Resketo. 1986. "Field Study of Napropamide Movement Through Unsaturated Soil." *Water Resources Research*, 22:749-755.
- Jury, W. A., W. R. Gardner, and W. H. Gardner. 1991. *Soil Physics*. John Wiley and Sons, Inc. New York, New York.
- Kaplan, D. I., P. M. Bertsch, and D. C. Adriano. 1995a. "Enhanced Transport of Contaminant Metals Through an Acidic Aquifer." *Ground Water*, 33:708-717.
- Kaplan, D. I., P. M. Bertsch, D. C. Adriano, and W. P. Miller. 1993. "Soil-Borne Mobile Colloids as Influenced by Water Flow and Organic Carbon." *Environmental Science and Technology*, 27:1193-1200.

- Kaplan, D. I., P. M. Bertsch, D. C. Adriano, and K. A. Orlandini. 1994a. "Actinide Association with Groundwater Colloids in a Coastal Plain Aquifer." *Radiochimica Acta*, 66/67:181-187.
- Kaplan, D. I., D. B. Hunter, P. M. Bertsch, S. Bajt, and D. C. Adriano. 1994b. "Application of Synchrotron X-Ray Fluorescence Spectroscopy and Energy Dispersive X-Ray Analysis to Identify Contaminant Metals on Groundwater Colloids." *Environmental Science & Technology*, 28:1186-1189.
- Kaplan, D. I., T. L. Gervais, and K. M. Krupka. 1998. "Uranium(VI) Sorption to Sediments Under High pH and Ionic Strength Conditions." *Radiochimica Acta*, 80:201-211.
- Kaplan, D. I., and R. J. Serne. 1995. *Distribution Coefficient Values Describing Iodine, Neptunium, Selenium, Technetium, and Uranium Sorption to Hanford Sediments*. PNL-10379, Supplement 1, Pacific Northwest Laboratory, Richland, Washington.
- Kaplan, D. I., R. J. Serne, and M. G. Piepho. 1995b. *Geochemical Factors Affecting Radionuclide Transport Through Near and Far Fields at a Low-Level Waste Disposal Site*. PNL-10379, Pacific Northwest National Laboratory, Richland, Washington.
- Kaplan, D. I., M. E. Sumner, P. M. Bertsch, and D. C. Adriano. 1996. "Chemical Conditions Conducive to the Release of Mobile Colloids from Ultisol Profiles." *Soil Science Society of America Journal*, 60:269-274.
- Karickhoff, S. W., D. S. Brown, and T. A. Scott. 1979. "Sorption of Hydrophobic Pollutants on Natural Sediments." *Water Research*, 13:231-248.
- Kim, J. J. 1986. "Chemical Behavior of Transuranic Elements in Aquatic Systems." In *Handbook on the Physics and Chemistry of the Actinides*, A. J. Freeman and C. Keller (eds.), pp. 413-455, Elsevier Science Publ., Amsterdam, Netherlands.
- Kincaid, C. T., J. R. Morrey, and J. E. Rogers. 1984. *Geohydrochemical Models for Solute Migration. Volume 1: Process Description and Computer Code Selection*. EPRI EA-3417, Volume 1, Battelle, Pacific Northwest Laboratories, Richland, Washington.
- Knoll, K. C. 1960. *Adsorption of Strontium by Soils Under Saturated and Unsaturated Flow Conditions*. HW-67830, General Electric Company, Hanford Atomic Products Operation, Richland, Washington.
- Koltermann, C. E., and S. M. Gorelick. 1996. "Heterogeneity in Sedimentary Deposits: A Review of Structure-Imitating, Process-Imitating, and Descriptive Approaches." *Water Resources Research*, 32:2617-2658.

- Krupka, K. M., E. A. Jenne, and W. J. Deutsch. 1983. *Validation of the WATEQ4 Geochemical Model for Uranium*. PNL-4333, Pacific Northwest Laboratory, Richland, Washington.
- Krupka, K. M. and J. R. Morrey. 1985. MINTEQ Geochemical Reaction Code: Status and Applications. In *Proceedings of the Conference on the Application of Geochemical Models to High-level Nuclear Waste Repository Assessment*, G. K. Jacobs and S. K. Whatley (eds.), pp. 46-53, NUREG/CR-0062 (ORNL/TM-9585), Oak Ridge National Laboratory, Oak Ridge, Tennessee.
- Krupka, K. M. and R. J. Serne. 1998. *Effects on Radionuclide Concentrations by Cement/Ground-Water Interactions in Support of Performance Assessment of Low-Level Radioactive Waste Disposal Facilities*. NUREG/CR-6377 (PNNL-11408), Pacific Northwest National Laboratory, Richland, Washington.
- LaGrega, M.D. 1994. *Hazardous Waste Management*. McGraw-Hill, Inc., New York, New York.
- Landström, O., C. E. Klockars, O. Persson, K. Andersson, B. Torstenfelt, B. Allard, S. Å. Larsson, and E. L. Tullborg. 1982. "A Comparison of In-situ Radionuclide Migration Studies in the Studsvik Area and Laboratory Measurements." In *Scientific Basis for Nuclear Waste Management V*, W. Lutze (ed.), pp. 697-706, Materials Research Society Symposia Proceedings, Volume 11, North Holland, New York, New York.
- Langmuir, D. 1978. "Uranium Solution-Mineral Equilibria at Low Temperatures with Applications to Sedimentary Ore Deposits." *Geochimica et Cosmochimica Acta*, 42:547-569.
- Langmuir, D. 1997. *Aqueous Environmental Geochemistry*. Prentice Hall, Upper Saddle River, New Jersey.
- Langmuir, D., and J. S. Herman. 1980. "The Mobility of Thorium in Natural Waters at Low Temperatures." *Geochimica Cosmochimica Acta* 44:1753-1766.
- Langmuir, I. 1918. "The Adsorption of Gases on Plane Surfaces of Glass, Mica, and Platinum." *Journal of the American Chemical Society*, 40:1361-1403.
- Lehninger, A. L. 1970. *Biochemistry*. Worth Publishers, Inc., New York, New York.
- Lemire, R. J., and P. R. Tremaine. 1980. "Uranium and Plutonium Equilibria in Aqueous Solutions to 200°C." *Journal of Chemical and Engineering Data*, 25:361-370.
- Lewis, G. N., and M. Randall. 1961. *Thermodynamics*. Revised by K. S. Pitzer and L. Brewer, McGraw-Hill Book Company, New York, New York.

- Lewis, R. E., T. T. Jarvis, M. R. Jarvis, and G. Whelan. 1994. *Eielson Air Force Base Operable Unit 2 Baseline Risk Assessment*. PNL-8752, Pacific Northwest Laboratory, Richland, Washington.
- Liang, L., J. F. McCarthy, L. W. Jolley, J. A. McNabb, and T. L. Mehlhorn. 1993. "Iron Dynamics: Observations of Transformation During Injection of Natural Organic Matter in a Sandy Aquifer." *Geochimica et Cosmochimica Acta*, 57:1987-1999.
- Lindenmeier, C. W., R. J. Serne, J. L. Conca, A. T. Owen, and M. I. Wood. 1995. *Solid Waste Leach Characteristics and Contaminant-Sediment Interactions Volume 2: Contaminant Transport Under Unsaturated Moisture Contents*. PNL-10722, Pacific Northwest Laboratory, Richland, Washington.
- Lindsay, W. L., 1979. *Chemical Equilibria in Soils*. John Wiley and Sons, New York, New York.
- Loeppert, R. H., A. P. Schwab, and S. Goldberg (eds.). 1995. *Chemical Equilibrium and Reaction Models*. Special Publication Number 42, Soil Science Society of America, Inc., Madison, Wisconsin.
- Loux, N. T., D. S. Brown, C. R. Chafin, J. D. Allison, and S. M. Hassan. 1989. "Chemical Speciation and Competitive Cationic Partitioning on a Sandy Aquifer Material." *Journal of Chemical Speciation and Bioavailability*, 1:111-125.
- Lyman, W. J., W. F. Reehl, and D. H. Rosenblatt. 1982. *Handbook of Chemical Property Estimation Methods -- Environmental Behavior of Organic Compounds*. McGraw-Hill, New York, New York.
- Mackay, D. M., W. P. Ball, and M. G. Durant. 1986. "Variability of Aquifer Sorption Properties in a Field Experiment on Groundwater Transport of Organic Solutes: Methods and Preliminary Results." *Journal of Contaminant Hydrology*, 1:119-132.
- McCarthy, J. F., and D. Degueudre. 1993. "Sampling and Characterization of Colloids and Particles in Groundwater for Studying their Role in Contaminant Transport." In *Environmental Particles*, J. Buffle and J. P. van Leeuwen (eds.), pp. 247-315. Lewis Publishers, Boca Raton, Florida.
- McDonald, M. G., and A. W. Harbaugh. 1988. *A Modular Three-Dimensional Finite-Difference Groundwater Flow Model*. U.S. Geological Survey Techniques of Water Resources Investigations, Book 6, Chapter A1, U.S. Geological Survey, Reston, Virginia.

- McKinley, I. G., and W. R. Alexander. 1993. "Assessment of Radionuclide Retardation: Uses and Abuses of Natural Analogue Studies." *Journal of Contaminant Hydrology*, 13:249-259.
- McKinley, J. P., and E. A. Jenne. 1991. "Experimental Investigation and Review of the "Solids Concentration" Effect in Adsorption Studies." *Environmental Science and Technology*, 25:2082-2087.
- McMahon, M. A., and J. W. Thomas. 1974. "Chloride and Tritiated Water Flow in Disturbed and Undisturbed Soils Cores." *Proceedings Soil Science Society of America*, 38:727-732.
- Meier, H., E. Zimmerhacki, G. Zeitler, P. Menge, and W. Hecker. 1987. "Influence of Liquid/Solid Ratios in Radionuclide Migration Studies." *Journal of Radioanalytical and Nuclear Chemistry*, 109:139-151.
- Melchior, D. C., and R. L. Bassett (eds.). 1990. *Chemical Modeling in Aqueous Systems II*. Symposium Series 416, American Chemical Society, Washington, D.C.
- Mercer, J. W., C. R. Faust, W. J. Miller, and F. J. Pearson, Jr. 1981. *Review of Simulation Techniques for Aquifer Thermal Energy Storage (ATES)*. PNL-3769, Pacific Northwest Laboratory, Richland, Washington.
- Mills, W. B., S. Liu, and F. K. Fong. 1991. "Literature Review and Model (COMET) for Colloid/Metals Transport in Porous Media." *Ground Water*, 29:199-208.
- Morel, F. M. M. 1983. *Principles of Aquatic Chemistry*. John Wiley and Sons, New York, New York.
- Morel, F. M. M., and J. G. Hering. 1993. *Principles and Applications of Aquatic Chemistry*. John Wiley and Sons, Inc., New York, New York.
- Morel, F. M. M., J. G. Yeasted, and J. C. Westall. 1981. "Adsorption Models: A Mathematical Analysis in the Framework of General Equilibrium Calculations." In *Adsorption of Inorganics at Solid-Liquid Interfaces*, M. A. Anderson and A. J. Rubin (eds.), pp. 263-294, Ann Arbor Science Publishers, Inc., Ann Arbor, Michigan.
- Morrey, J. R., C. T. Kincaid, and C. J. Hostetler. 1986. *Geohydrochemical Models for Solute Migration. Volume 3: Evaluation of Selected Computer Codes*. EPRI EA-3417, Volume 3, Battelle, Pacific Northwest Laboratories, Richland, Washington.
- Mucciardi, A. N., I. J. Booker, E. C. Orr, and D. Cleveland. 1979. "Statistical Investigation of the Mechanics Controlling Radionuclide Sorption, Part II." In *Second Contractor Information Meeting. Task 4*. R. J. Serne (ed.), Vol. 2, pp 333-425, PNL-SA-7352, Pacific Northwest Laboratory, Richland, Washington.

- Mucciardi, A. N., T. C. Johnson, and J. Saunier. 1980. "Statistical Investigation of the Mechanics Controlling Radionuclide Sorption, Part III." In *Third Contractor Information Meeting. Task 4*, J. F. Relyea (ed.), Vol. 1, pp. 1-75, PNL-SA-8571, Pacific Northwest Laboratory, Richland, Washington.
- Muller, A. B., D. Langmuir, and L. E. Duda. 1983. "The Formulation of an Integrated Physico-chemical-Hydrologic Model for Predicting Waste Nuclide Retardation in Geologic Media." In *Scientific Basis for Nuclear Waste Management VI*, D. G. Brookins (ed.), pp. 547-564, Materials Research Society Symposia Proceedings, Volume 15, North Holland, New York, New York.
- Nielsen, D. R., and J. W. Biggar. 1961. "Miscible Displacement in Soils: I. Experimental Information." *Soil Science Society of America Journal*, 25:1-5.
- Nielsen, D. R., and J. W. Biggar. 1962. "Miscible Displacement in Soils: II. Behavior of Tracers." *Proceedings Soil Science Society of America*, 26:125-128.
- Nielsen, D. R., J. W. Biggar, and K. T. Erh. 1973. "Spatial Variability of Field-Measured Soil-Water Properties." *Hilgardia*, 42:215-259.
- Nielsen, D. R., M. T. van Genuchten, and J. W. Biggar. 1986. "Water Flow and Solute Transport Processes in the Unsaturated Zone." *Water Resources Research*, 22:895-1085.
- Nordstrom, D. K., and J. W. Ball. 1984. "Chemical Models, Computer Programs and Metal Complexation in Natural Waters." In *Complexation of Trace Metals in Natural Waters*, C. J. M. Kramer and J. C. Duinker (eds.), pp. 149-169, Martinus Nijhoff/Dr. J. W. Junk Publishing Co., Netherlands.
- Nordstrom, D. K., and J. L. Munoz. 1985. *Geochemical Thermodynamics*. The Benjamin/Cummings Publishing Co., Inc., Menlo Park, California.
- Nordstrom, D. K., L. N. Plummer, T. M. L. Wigley, T. J. Woley, J. W. Ball, E. A. Jenne, R. L. Bassett, D. A. Crerar, T. M. Florence, B. Fritz, M. Hoffman, G. R. Holdren, Jr., G. M. Lafon, S. V. Mattigod, R. E. McDuff, F. Morel, M. M. Reddy, G. Sposito, and J. Thraillkill. 1979. "Comparison of Computerized Chemical Models for Equilibrium Calculations in Aqueous Systems." In *Chemical Modeling in Aqueous Systems. Speciation, Sorption, Solubility, and Kinetics*, E. A. Jenne (ed.), pp. 857-892, American Chemical Society Symposium Series 93, Washington, D.C.

- O'Conner, D. J., and J. P. Connolly. 1980. "The Effect of Concentration of Adsorbing Solids on the Partition Coefficient." *Water Research*, 14:1517-1523.
- Oscarson, D. W., and H. B. Hume. 1998. "Effect of Solid:Liquid Ratio on the Sorption of Sr^{2+} and Cs^+ on Bentonite." In *Adsorption of Metals by Geomedia. Variables, Mechanisms, and Model Applications*, E. A. Jenne (ed.), p. 277-289, Academic Press, San Diego, California.
- Papelis, C., K. F. Hayes, and J. O. Leckie. 1988. *HYDRAQL: A Program for the Computation of Chemical Equilibrium Composition of Aqueous Batch Systems Including Surface-Complexation Modeling of Ion Adsorption at the Oxide/Solution Interface*. Technical Report No. 306, Department of Civil Engineering, Stanford University, Stanford, California.
- Parsons, R. 1982. "Surface Properties of Oxides." *Journal of Electroanalytical Chemistry*, 118:2-18.
- Peck, A. J., R. J. Luxmoore, and J. L. Stolzy. 1977. "Effects of Spatial Variability of Soil Hydraulic Properties in Water Budget Modeling." *Water Resources Research*, 13:348-354.
- Penrose, W. R., W. L. Plozer, W. H. Essington, D. M. Nelson, and K. A. Orlandini. 1990. "Mobility of Pu and Am Through a Shallow Aquifer in a Semiarid Region." *Environmental Science & Technology*, 24:228-234.
- Petersen, L. W., P. Moldrup, O. H. Jacobsen, and D. E. Rolston. 1996. "Relations Between Specific Surface Area and Soil Physical and Chemical Properties." *Soil Science*, 161:9-21.
- Peterson, R. G., and L. D. Calvin. 1986. "Sampling." In *Methods of Soil Analysis, Part 1. Physical and Mineralogical Methods*, A. Klute (ed.), American Society of Agronomy, Inc., Madison, Wisconsin.
- Peterson, S. R., C. J. Hostetler, W. J. Deutsch, and C. E. Cowan. 1987a. *MINTEQ User's Manual*. NUREG/CR-4808 (PNL-6106), Pacific Northwest Laboratory, Richland, Washington.
- Peterson, S. R., W. J. Martin, and R. J. Serne. 1986. *Predictive Geochemical Modeling of Contaminant Concentrations in Laboratory Columns and in Plumes Migrating from Uranium Mill Tailings Waste Impoundments*. NUREG/CR-4520 (PNL-5788), prepared by the Pacific Northwest Laboratory, Richland, Washington.
- Peterson, S. R., B. E. Opitz, M. J. Graham, and L. E. Eary. 1987b. *An Overview of the Geochemical Code MINTEQ: Application to Performance Assessment for Low-Level Wastes*. PNL-6112, Pacific Northwest Laboratory, Richland, Washington.

- Phillips, S. L., F. V. Hale, L. F. Silvester, and M. D. Siegel. 1988. *Thermodynamic Tables for Nuclear Waste Isolation. Aqueous Solutions Database*. NUREG/CR-4864 (LBL-22860), Volume 1, Lawrence Berkeley Laboratory, Lawrence, California.
- Pickens, J. F., R. E. Jackson, K. J. Inch, and W. F. Merritt. 1981. "Measurement of Distribution Coefficients Using a Radial Injection Dual-Tracer Test." *Water Resources Research*, 17:529-544.
- Pignatello, J. J. 1989. "Sorption Dynamics of Organic Compounds in Soils and Sediments." In *Reactions and Movement of Organic Chemicals in Soils*, B. L. Sawhney and K. Brown (eds.), pp. 45-80. SSSA Special Publication 22, Soil Science Society of America, Inc., Madison, Wisconsin.
- Plackett, R. L., and J. P. Burman. 1946. "The Design of Optimum Multifactorial Experiments." *Biometrika*, 33:305-325.
- Plummer, L. N., B. F. Jones, and A. H. Truesdell. 1976, *WATEQF - A FORTRAN IV Version of WATEQ, A Computer Program for Calculating Chemical Equilibrium of Natural Waters*. Water Resources Investigations WRI 76-13, U.S. Geological Survey, Reston, Virginia.
- Potter, R. W., III. 1979. "Computer Modeling in Low Temperature Geochemistry." *Reviews of Geophysics and Space Physics*, 17:850-860.
- Powell, R. M., and R. W. Puls. 1993. "Passive Sampling of Groundwater Monitoring Wells Without Purging: Multilevel Well Chemistry and Tracer Disappearance." *Journal of Contaminant Hydrology*, 12:51-77.
- Puls, R. W. 1990. "Colloidal Consideration in Groundwater Sampling and Contaminant Transport Predictions." *Nuclear Safety*, 31:58-65.
- Rai, D., A. R. Felmy, and J. L. Ryan. 1990. "Uranium(IV) Hydrolysis Constants and Solubility Product of $\text{UO}_2 \cdot x\text{H}_2\text{O}(\text{am})$." *Inorganic Chemistry*, 29:260-254.
- Rai, D., and J. M. Zachara. 1984. *Chemical Attenuation Rates, Coefficients, and Constants in Leachate Migration. Volume 1: A Critical Review*. EPRI EA-3356, Volume 1, Electric Power Research Institute, Palo Alto, California.
- Rancon, D. 1973. "The Behavior in Underground Environments of Uranium and Thorium Discharged by the Nuclear Industry." In *Environmental Behavior of Radionuclides Released in the Nuclear Industry*. IAEA-SM-172/55, pp. 333-346, International Atomic Energy Agency, Vienna, Austria.

- Rard, J. A. 1983. *Critical Review of the Chemistry and Thermodynamics of Technetium and Some of its Inorganic Compounds and Aqueous Species*. UCRL-53440, Lawrence Livermore National Laboratory, Livermore, California.
- Read, D, P. J. Hooker, M. Ivanovich, and A. E. Milodowski. 1991. "A Natural Analogue Study of an Abandoned Uranium Mine in Cornwall, England." *Radiochimica Acta*, 52/53:349-356.
- Reichle, R., W. Kinzelbach, and H. Kinzelbach. 1998. "Effective Parameters in Heterogeneous and Homogeneous Transport Models with Kinetic Sorption." *Water Resources Research*, 34:583-594.
- Relyea, J. F. 1982. "Theoretical and Experimental Considerations for the Use of the Column Method for the Use of the Column Method for Determining Retardation Factors." *Radioactive Waste Management and the Nuclear Fuel Cycle*, 3(2):151-166.
- Ritger, P. D., and N. J. Rose. 1968. *Differential Equations with Applications*. McGraw Hill, New York, New York.
- Robin, M. J. L., E. A. Sudicky, R. W. Gillham, and R. G. Kachanoski. 1991. "Spatial Variability of Strontium Distribution Coefficients and Their Correlation with Hydraulic Conductivity in the Canadian Forces Base Borden Aquifer." *Water Resources Research*, 27:2619-2632.
- Routson, R. C., and R. J. Serne. 1972. *One-Dimensional Model of the Movement of Trace Radioactive Solute Through Soil Columns - The PERCEL Model*. BNWL-1718, Pacific Northwest Laboratory, Richland, Washington.
- Routson, R. C., G. S. Barney, R. H. Smith, C. H. Delegard, and L. Jensen. 1981. *Fission Product Sorption Parameters for Hanford 200-Area Sediment Types*. RHO-ST-35, Rockwell Hanford Operations, Richland, Washington.
- Roy, W. R., I. G. Drapac, S. F. J. Chou, and R. A. Griffin. 1991. *Batch-type Procedures for Estimating Soil Adsorption of Chemicals*. EPA/530-SW-87-006-F, Office of Solid Waste and Emergency Response, U.S. Environmental Protection Agency, Washington, D.C.
- RTI (Research Triangle Institute). 1994. *Chemical Properties for Soil Screening Levels. Draft Report*. Prepared for the Environmental Protection Agency, Office of Emergency and Remedial Response, Washington, D.C.
- Russo, D. 1989a. "Field-Scale Transport of Interacting Solutes Through the Unsaturated Zone 2. Analysis of the Spatial Variability of the Field Response." *Water Resources Research*, 25:2487-2495.

- Russo, D. 1989b. "Field-Scale Transport of Interacting Solutes Through the Unsaturated Zone 1. Analysis of the Spatial Variability of the Transport Properties." *Water Resources Research*, 25:2475-2485.
- Ryan, J. M., and P. M. Gschwend. 1990. "Colloid Mobilization in Two Atlantic Coastal Plain Aquifers: Field Studies." *Water Resources Research*, 26:307-322.
- Salter, P. F., L. L. Ames, and J. E. McGarragh. 1981a. *The Sorption Behavior of Selected Radionuclides on Columbia River Basalts*. RHO-BWI-LD-48, Rockwell Hanford Operations, Richland, Washington.
- Salter, P. F., L. L. Ames, and J. E. McGarragh. 1981b. *Sorption of Selected Radionuclides on Secondary Minerals Associated with the Columbia River Basalts*. RHO-BWI-LD-43, Rockwell Hanford Operations, Richland, Washington.
- Schindler, P. W., and G. Sposito. 1991. "Surface Complexation at (Hydro)oxide Surfaces." In *Interactions at the Soil Colloid-Soil Solution Interface*, G. H. Bolt, M. F. DeBoodt, M. H. B. Hayes, and M. B. Mc Bride (eds.), pp. 115-145, Kluwer Academic Press, New York, New York.
- Schwarzenbach, R. P., and J. Westall. 1981. "Transport of Nonpolar Organic Compounds from Surface Water to Groundwater. Laboratory Sorption Studies." *Environmental Science and Technology*, 15:1360-1367.
- Scott, H. D., R. E. Phillips, and R. F. Paetzold. 1974. "Diffusion of Herbicides in One Adsorbed Phase." *Proceedings Soil Science Society of America*, 38:558-562.
- Seaman, J. C., P. M. Bertsch, and W. P. Miller. 1995. "Ionic Tracer Movement Through Highly Weathered Sediments." *Journal of Contaminant Hydrology*, 20:127-143.
- Sehmel, G. A. 1989. *Cyanide and Antimony Thermodynamic Database for the Aqueous Species and Solids for the EPA-MINTEQ Geochemical Code*. PNL-6835, Pacific Northwest Laboratory, Richland, Washington.
- Sergeyeva, E. I., A. A. Nikitin, I. L. Khodakovskiy, and G. B. Naumov. 1972. "Experimental Investigation of Equilibria in the System $\text{UO}_3\text{-CO}_2\text{-H}_2\text{O}$ in 25-200°C Temperature Interval." *Geochemistry International*, 9:900-910.
- Serkiz, S. M. And W. H. Johnson. 1994. *Uranium Geochemistry in Soil and Groundwater at the F and H Seepage Basins (U)*. EPD-SGS-94-307, Westinghouse Savannah River Company, Savannah River Site, Aiken, South Carolina.

- Serne, R. J., R. C. Arthur, and K. M. Krupka. 1990. *Review of Geochemical Processes and Codes for Assessment of Radionuclide Migration Potential at Commercial LLW Sites*. NUREG/CR-5548 (PNL-7285), Pacific Northwest Laboratory, Richland, Washington.
- Serne, R. J., and A. B. Muller. 1987. "A Perspective on Adsorption of Radionuclides onto Geologic Media." In *The Geological Disposal of High Level Radioactive Wastes*, D. G. Brookins (ed.), pp. 407-443, Theophrastus Publications, S.A., Athens, Greece.
- Serne, R. J., and J. F. Relyea. 1981. "The Status of Radionuclide Sorption-Desorption Studies Performed by the WRIT Program." In *The Technology of high-Level Nuclear Waste Disposal*, Volume 1, pp. 203-254, DOE/TIC-621, Technical Information Center, U.S. Department of Energy, Oak, Ridge, Tennessee.
- Serne, R. J., R. C. Routson, and D. A. Cochran. 1973. *Experimental Methods for Obtaining PERCOL Model Input Verification Data*. BNWL-1721, Pacific Northwest Laboratory, Richland, Washington.
- Seth, Rajesh, Donald MacKay, and Jane Muncke. 1999. "Estimating the Organic Carbon Partition Coefficient and its Variability for Hydrophobic Chemicals." *Environmental Science and Technology*, 33:2390-2394.
- Sheppard, J. C., J. A. Kittrick, and T. L. Hart. 1976. *Determination of Distribution Ratios and Diffusion Coefficients of Neptunium, Americium, and Curium in Soil-Aquatic Environments*. RTO-221-T-12-2, Rockwell Hanford Operations, Richland, Washington.
- Sheppard, S. C., M. I. Sheppard, and W. G. Evenden. 1990. "A Novel Method Used to Examine Variation in Tc Sorption Among 34 Soils, Aerated and Anoxic." *Journal of Environmental Radioactivity*, 11:215.
- Silva, R. J., G. Bidoglio, M. H. Rand, P. B. Robourch, H. Wanner, and I. Puigdomenech. 1995. *Chemical Thermodynamics Series, Volume 2: Chemical Thermodynamics of Americium*. Elsevier Science, New York, New York.
- Smith, R. M., and A. E. Martell. 1976. *Critical Stability Constants. Volume 4: Inorganic Complexes*. Plenum Press, New York, New York.
- Smith, R. M., and A. E. Martell. 1995. "The Selection of Critical Stability Constants." In *Chemical Equilibrium and Reaction Models*, R. H. Loeppert, A. P. Schwab, and S. Goldberg (eds.), Special Publication Number 42, Soil Science Society of America, Inc., Madison, Wisconsin.
- Smith, R. M., A. E. Martell, and R. J. Motekaitis. 1997. *NIST Critically Selected Stability Constants of Metal Complexes Database. Version 4. Users Guide*. NIST Standard

- Reference Database 46, National Institute of Standards and Technology, Gaithersburg, Maryland.
- Smith, R. W., and E. A. Jenne. 1991. "Recalculation, Evaluation, and Prediction of Surface Complexation Constants for Metal Adsorption on Iron and Manganese Oxides." *Environmental Science and Technology*, 25:525-531.
- Smith, R. W. and E. A. Jenne. 1992. "Response to 'Comment on "Recalculation, Evaluation, and Prediction of Surface Complexation Constants for Metal Adsorption on Iron and Manganese Oxides."'" *Environmental Science and Technology*, 26:1253-1254.
- Smith, R. W. and E. A. Jenne. 1991. "Recalculation, Evaluation, and Prediction of Surface Complexation Constants for Metal Adsorption on Iron and Manganese Oxides." *Environmental Science and Technology*, 25:525-531.
- Smith, R. W. and E. A. Jenne. 1988. *Compilation, Evaluation, and Prediction of Trip-Layer Model Constants for Ions on Fe(III) and Mn(IV) Hydrous Oxides*. PNL-6754, Pacific Northwest Laboratory, Richland, Washington.
- Snedecor, G. W., and W. G. Cochran. 1967. *Statistical Methods*. Sixth Edition, Iowa State University Press, Ames, Iowa.
- Sposito, G. 1984. *The Surface Chemistry of Soils*. Oxford University Press, New York, New York.
- Sposito, G. 1989. *The Chemistry of Soils*. Oxford University Press, New York, New York.
- Sposito, G. 1994. *Chemical Equilibria and Kinetics in Soils*. Oxford University Press, New York, New York.
- Sposito, G., and J. Coves. 1988. *SOILCHEM: A Computer Program for the Calculation of Chemical Speciation in Soils*. Kearny Foundation for Soil Science, University of California, Riverside, California.
- SSSA (Soil Science Society of America). 1997. *Glossary of Soil Science Terms*. Soil Science Society of America, Madison, Wisconsin.
- Streng, D. L., and S. R. Peterson. 1989. *Chemical Data Bases for the Multimedia Environmental Pollutant Assessment System (MEPAS): Version 1*. PNL-7145, Pacific Northwest Laboratory, Richland, Washington.
- Stumm, W. (ed.). 1987. *Aquatic Surface Chemistry. Chemical Processes at the Particle-Water Interface*. John Wiley and Sons, New York, New York.

- Stumm, W., and J. J. Morgan. 1981. *Aquatic Chemistry. An Introduction Emphasizing Chemical Equilibria in Natural Waters*. John Wiley and Sons, New York, New York.
- Sudicky, E. A. 1986. "A Natural Gradient Experiment on Solute Transport in a Sand Aquifer: Spatial Variability of Hydraulic Conductivity and its Role in the Dispersion Process." *Water Resources Research*, 22:2069-2082.
- Sugita, F., R. W. Gillham, and C. Mase. 1995. "Pore Scale Variation in Retardation Factor as a Cause of Nonideal Reactive Breakthrough Curves. 2. pore Network Analysis." *Water Resources Research*, 31:113-119.
- Szecsody, J. E., A. Chilakapati, J. M. Zachara, and A. L. Garvin. 1998. "Influence of Iron Oxide Inclusion Shape on Co II/III EDTA Reactive Transport Through Spatially Heterogeneous Sediment." *Water Resources Research*, 34:2501-2514.
- Szecsody, J. E., J. M. Zachara, and P. L. Bruckhart. 1994. "Adsorption-dissolution Reactions Affecting the Distribution and Stability of Co (II) EDTA in Iron Oxide-Coated Sand." *Environmental Science and Technology*, 28(9):1706-1716.
- Szecsody, J. E., J. M. Zachara, A. Chilakapati, P. M. Jardine, and A. S. Ferency. 1998. "Importance of Flow and Particle-Scale Heterogeneity on Co II/III EDTA Reactive Transport." *Journal of Hydrology*, 209:112-136.
- Tompson, A.F.B., A. L. Schafer, and R.W. Smith. 1996. "Impacts of Physical and Chemical Heterogeneity on Contaminant Transport in a Sandy Porous Medium." *Water Resources Research*, 32:801-818.
- Tompson, A. F. B. 1993. "Numerical Simulation of Chemical Migration in Physically and Chemically Heterogeneous Porous Media." *Water Resources Research*, 29:3709-3726.
- Tompson, A. F. B., and L. W. Gelhar. 1990. "Numerical Simulation of Solute Transport in Three-Dimensional Randomly Heterogeneous Porous Media." *Water Resources Research*, 26:2541-2562.
- Truesdell, A. H., and B. F. Jones. 1973. *WATEQ, A Computer Program for Calculating Chemical Equilibria of Natural Waters*. USGS-WRD-73-007, U.S. Geological Survey, Washington, D.C.
- Truesdell, A. H., and B. F. Jones. 1974. "WATEQ, A Computer Program for Calculating Chemical Equilibria of Natural Waters." *U.S. Geological Survey Journal of Research*, 2:233-248.

- Turner, D. R. 1991. *Sorption Modeling for High-level Waste Performance Assessment: A Literature Review*. CNWRA 91-011, Center for Nuclear Waste Regulatory Analysis, San Antonio, Texas.
- Turner, D. R. 1993. *Mechanistic Approaches to Radionuclide Sorption Modeling*. CNWRA 93-019, Center for Nuclear Waste Regulatory Analysis, San Antonio, Texas.
- Turner, D. R. 1995. *Uniform Approach to Surface Complexation Modeling of Radionuclide Sorption*. CNWRA 95-001, Center for Nuclear Waste Regulatory Analysis, San Antonio, Texas.
- Turner, D. R., T. Griffin, and T. B. Dietrich. 1993. "Radionuclide Sorption Modeling Using the MINTEQA2 Speciation Code." In *Scientific Basis for Nuclear Waste Management XVI*, C. G. Interrante and R. T. Pabalan (eds.), pp. 783-789, Materials Research Society Symposium Proceedings, Volume 294, Materials Research Society, Pittsburgh, Pennsylvania.
- van Genuchten, M. Th., and W. J. Alves. 1982. *Analytical Solutions of the One-Dimensional Convective-Dispersive Solute Transport Equation*. Technical Bulletin No. 1661, U.S. Department of Agriculture, Washington, D.C.
- van Genuchten, M. Th., and P. J. Wierenga. 1976. "Mass Transfer Studies in Sorbing Porous Media. I. Analytical Solutions." *Soil Science Society of America Journal*, 40:473-480.
- van Genuchten, M. Th., and P. J. Wierenga. 1986. "Solute Dispersion Coefficients and Retardation Factors." In *Methods of Soil Analysis -- Part 1: Physical and Mineralogical Methods*, A. Klute (ed.), Second Edition, Chapter 44, pp. 1025-1054, Soil Science Society of America, Madison, Wisconsin.
- Voice, T. C., C. P. Rice, and W. J. Weber. 1983. "Effect of Solids Concentration on the Sorptive Partitioning of Hydrophobic Pollutants in Aquatic Systems." *Environmental Science and Technology*, 17:513-518.
- Wagman, D. D., W. H. Evans, V. B. Parker, R. H. Shumm, I. Halow, S. M. Bailey, K. L. Churney, and R. L. Nuttall. 1982. "The NBS Tables of Chemical Thermodynamic Properties. Selected Values for Inorganic and C1 and C2 Organic Substances in SI Units." *Journal of Physical and Chemical Reference Data* 11(Supplement No. 2):1-392.
- Waite, T. D., J. A. Davis, T. E. Payne, G. A. Waychunas, and N. Xu. 1994. "Uranium(VI) Adsorption to Ferrihydrite: Application of a Surface Complexation Model." *Geochimica et Cosmochimica Acta*, 58(24):5465-5478.
- Wanner, H., and I. Forest (eds.). 1992. *Chemical Thermodynamics Series, Volume 1: Chemical Thermodynamics of Uranium*. (I. Grenthe, J. Fuger, R. J. M. Konings, R. J. Lemire, A. B.

- Muller, C. Nguyen-Trung, and H. Wanner, review team), North-Holland, Elsevier Science Publishing Company, Inc., New York, New York.
- Warrick, A. W., and A. Amoozegar-Fard. 1979. "Infiltration and Drainage Calculation Using Spatially Scaled Hydraulic Properties." *Water Resources Research*, 15:1116-1120.
- Warrick, A. W., and D. R. Nielsen. 1980. "Spatial Variability of Soil Physical Properties in the Field." In *Applications of Soil Physics*, D. Hillel (ed.), Chapter 13, pp. 319-345, Academic Press, New York, New York.
- Westall, J. C. 1986. "Reactions at the Oxide-Solution Interface: Chemical and Electrostatic Models." In *Geochemical Processes at Mineral Surfaces*, J. A. Davis and K. F. Hayes (eds.), pp. 54-78, ACS Symposium Series 323, American Chemical Society, Washington, D.C.
- Westall, J. C. 1994. "Modeling of the Association of Metal Ions With Heterogeneous Environmental Sorbents." In *Scientific Basis for Nuclear Waste Management Vol. XVIII. Part 2*, T. Murakami and R. C. Ewing (eds.), pp. 937-950, Materials Research Society Symposia Proceedings, Volume 353, Materials Research Society, Pittsburgh, Pennsylvania.
- Westall, J. C., and H. Hohl. 1980. "A Comparison of Electrostatic Models for the Oxide/Solution Interface." *Advances in Colloid and Interface Science*, 12:265-294.
- Westall, J. C., J. L. Zachary, and F. M. M. Morel. 1976. *MINEQL, A Computer Program for the Calculation of Chemical Equilibrium Composition of Aqueous Systems*. Technical Note 18, Department of Civil Engineering, Massachusetts Institute of Technology, Cambridge, Massachusetts.
- Whelan, G. 1996. *Use of Distribution Coefficients in Transport Modeling and Risk Assessments*. Letter Report, Pacific Northwest National Laboratory, Richland, Washington.
- Whelan, G., J. W. Buck, D. L. Streng, J. G. Droppo, Jr., B. L. Hoopes, and R. J. Aiken. 1992. "An Overview of the Multimedia Assessment Methodology MEPAS." *Hazardous Waste and Hazardous Materials*, 9(2):191-208.
- Whelan, G., J. P. McDonald, and C. Sato. 1996. *Multimedia Environmental Pollutant Assessment System (MEPAS): Groundwater Pathway Formulations*. PNNL-10907, Pacific Northwest National Laboratory, Richland, Washington.
- Whelan, G., D. L. Streng, J. G. Droppo, Jr., B. L. Steelman, and J. W. Buck. 1987. *The Remedial Action Priority System (RAPS): Mathematical Formulations*. PNL-6200, Pacific Northwest Laboratory, Richland, Washington.

Wildung, R. E., T. R. Garland and D. A. Cataldo. 1977. "Accumulation of Technetium by Plants." *Health Physics*, 32:314-317.

Wood, W. W., and J. Petratis. 1984. "Origin and Distribution of Carbon Dioxide in the Unsaturated Zone of the Southern High Plains of Texas." *Water Resources Research*, 20:1193-1208.

Yariv, S., and H. Cross. 1979. *Geochemistry of Colloid Systems*. Springer-Verlag, New York, New York.

Yeh, G. T., and Y. Tsai. 1976. "Analytical Three-Dimensional Transient Modeling of Effluent Discharges." *Water Resources Research*, 12:533-540.

Yeh, G. T. 1981. *AT123D: Analytical Transient One, Two, and Three Dimensional Simulation of Waste Transport in the Aquifer System*. ORNL-5602, Oak Ridge National Laboratory, Oak Ridge, Tennessee.

APPENDIX A

Acronyms, Abbreviations, Symbols, and Notation

Appendix A

Acronyms, Abbreviations, Symbols, and Notation

A.1.0 Acronyms And Abbreviations

AA	Atomic absorption
ASCII	American Standard Code for Information Interchange
ASTM	American Society for Testing and Materials
CCM	Constant capacitance (adsorption) model
CDTA	Trans-1,2-diaminocyclohexane tetra-acetic acid
CEAM	Center for Exposure Assessment Modeling at EPA's Environmental Research Laboratory in Athens, Georgia
CEC	Cation exchange capacity
CERCLA	Comprehensive Environmental Response, Compensation, and Liability Act
DLM	Diffuse (double) layer (adsorption) model
DDLm	Diffuse double layer (adsorption) model
DOE	U.S. Department of Energy
DTPA	Diethylenetriaminepentacetic acid
EDTA	Ethylenediaminetriacetic acid
EDX	Energy dispersive x-ray analysis
EPA	U.S. Environmental Protection Agency
EPRI	Electric Power Research Institute
HEDTA	N-(2-hydroxyethyl) ethylenedinitrilotriacetic acid
HLW	High level radioactive waste
IAEA	International Atomic Energy Agency
ICP	Inductively coupled plasma
ICP/MS	Inductively coupled plasma/mass spectroscopy
IEP (or iep)	Isoelectric point
LLNL	Lawrence Livermore National Laboratory, U.S. DOE
LLW	Low level radioactive waste
MCL	Maximum Contaminant Level
MEPAS	Multimedia Environmental Pollutant Assessment System
MS-DOS®	Microsoft® disk operating system (Microsoft and MS-DOS are register trademarks of Microsoft Corporation.)
NPL	Superfund National Priorities List
NRC	U.S. Nuclear Regulatory Commission
NWWA	National Water Well Association
OERR	Office of Remedial and Emergency Response, U.S. EPA
ORIA	Office of Radiation and Indoor Air, U.S. EPA
OSWER	Office of Solid Waste and Emergency Response, U.S. EPA

PC	Personal computers operating under the MS-DOS® and Microsoft® Windows operating systems (Microsoft® Windows is a trademark of Microsoft Corporation.)
PNL	Pacific Northwest Laboratory. In 1995, DOE formally changed the name of the Pacific Northwest Laboratory to the Pacific Northwest National Laboratory.
PNNL	Pacific Northwest National Laboratory, U.S. DOE
PZC	Point of zero charge
RCRA	Resource Conservation and Recovery Act
SCM	Surface complexation model
SDMP	NRC's Site Decommissioning Management Plan
TDS	Total dissolved solids
TLM	Triple-layer adsorption model
UK	United Kingdom (UK)
UK DoE	United Kingdom Department of the Environment
UNSCEAR	United Nations Scientific Committee on the Effects of Atomic Radiation

A.2.0 List of Symbols for the Elements and Corresponding Names

Symbol	Element	Symbol	Element	Symbol	Element
Ac	Actinium	Gd	Gadolinium	Po	Polonium
Ag	Silver	Ge	Germanium	Pr	Praseodymium
Al	Aluminum	H	Hydrogen	Pt	Platinum
Am	Americium	He	Helium	Pu	Plutonium
Ar	Argon	Hf	Hafnium	Ra	Radium
As	Arsenic	Hg	Mercury	Rb	Rubidium
At	Astatine	Ho	Holmium	Re	Rhenium
Au	Gold	I	Iodine	Rh	Rhodium
B	Boron	In	Indium	Rn	Radon
Ba	Barium	Ir	Iridium	Ru	Ruthenium
Be	Beryllium	K	Potassium	S	Sulfur
Bi	Bismuth	Kr	Krypton	Sb	Antimony
Bk	Berkelium	La	Lanthanum	Sc	Scandium
Br	Bromine	Li	Lithium	Se	Selenium
C	Carbon	Lu	Lutetium	Si	Silicon
Ca	Calcium	Lw	Lawrencium	Sm	Samarium
Cb	Columbium	Md	Mendelevium	Sn	Tin
Cd	Cadmium	Mg	Magnesium	Sr	Strontium
Ce	Cerium	Mn	Manganese	Ta	Tantalum
Cf	Californium	Mo	Molybdenum	Tb	Terbium
Cl	Chlorine	N	Nitrogen	Tc	Technetium
Cm	Curium	Na	Sodium	Te	Tellurium
Co	Cobalt	Nb	Niobium	Th	Thorium
Cr	Chromium	Nd	Neodymium	Ti	Titanium
Cs	Cesium	Ne	Neon	Tl	Thallium
Cu	Copper	Ni	Nickel	Tm	Thulium
Dy	Dysprosium	No	Nobelium	U	Uranium
Er	Erbium	Np	Neptunium	V	Vanadium
Es	Einsteinium	O	Oxygen	W	Tungsten
Eu	Europium	Os	Osmium	W	Wolfram
F	Fluorine	P	Phosphorus	Xe	Xenon
Fe	Iron	Pa	Protactinium	Y	Yttrium
Fm	Fermium	Pb	Lead	Yb	Ytterbium
Fr	Francium	Pd	Palladium	Zn	Zinc
Ga	Gallium	Pm	Promethium	Zr	Zirconium

A.3.0 List of Symbols and Notation

α	Dispersivity in the x, y, or z direction
α'	Capacity factor or ratio of the moles per unit volume of water-saturated solid, C_s , to the moles per unit volume of liquid, C_l
γ	Activity coefficient
δ	Constrictivity of the porous media
δ'	Mass-related constant
ϵ	Parameter in Dubinin-Radushkevich isotherm model equal to “ $RT \ln(1 + 1/C_i)$ ”
λ	First-order degradation/decay coefficient
θ	Volumetric water content
θ_m	Volume fraction of water associated with the mobile domain
θ_v	Total water content
θ_{vz}	Moisture content in the vadose zone
μ	Mobility
ρ_b	Bulk density
ρ_{particle}	Particle density
σ	Net charge associated with the surface of adsorbing mineral as conceptualized in electrostatic adsorption models
σ_d	Charge associated with the diffuse layer d of counterions as conceptualized in electrostatic adsorption models
σ_β	Charge associated with the β layer as conceptualized in electrostatic adsorption models
σ_o	Charge associated with the o layer as conceptualized in electrostatic adsorption models
σ_s	Surface charge at the Stern layer
σ_{sd}	Standard deviation associated with the Gaussian solution
τ	Tortuosity of the porous media
v_x	Pore velocity in direction x
ϕ	Porosity
ϕ_ϵ	Effective porosity
ϕ_m	Mobile water fraction as defined by the ratio of the volume fraction of water associated with the mobile domain, θ_m , to the total water content, θ_v
ψ	Electrical potential
ψ_d	Potential at the diffuse layer
ψ_o	Potential at the surface (plane o)
ψ_s	Potential at the Stern layer
A	Concentration of free or unoccupied surface absorption site on a solid phase
ads	Adsorption
A_i	Concentration of adsorbate (or species) I on the solid phase at equilibrium
A_m	Adsorption capacity of adsorbent per unit mass
am	Amorphous

aq	Aqueous
C	Radioactivity of tracer on sediment
C	Constant capacitance term
CEC	Cation exchange capacity
C_i	Concentration of adsorbate (or species) I in solution at equilibrium
C_l	Moles per unit volume of liquid
C_{om}	Concentration of organic material
C_s	Moles per unit volume of water-saturated solid
C_T	Total mass at the site per total site volume
C_{Tp}	Total mass at the site per dry weight of soil
D	Proportionality constant or diffusion coefficient
D^*	Dispersion coefficient in the x, y, and z directions adjusted for retardation with the retardation factor
D_a	Apparent diffusion coefficient
D_e	Effective diffusion coefficient
D_i	Intrinsic diffusion coefficient
D_{mech}	Mechanical dispersion
D_{mol}	Molecular diffusion coefficient
D_p	Diffusion coefficient for a species within a porous media
D_x	Dispersion coefficient in direction x
e^-	Free electron
$e^{-\psi F/RT}$	Boltzmann factor
Eh	Redox potential of an aqueous system relative to the standard hydrogen electrode
F	Faraday constant, 23,060.9 cal/V·mol
f_{oc}	Fraction (w/w) of organic material in soil
$\Delta G_{f,298}^\circ$	Gibbs free energy of formation at 298 K
$\Delta G_{f,T}^\circ$	Gibbs free energy of formation at temperature T
$\Delta G_{r,298}^\circ$	Gibbs free energy of reaction at 298 K
$\Delta G_{r,T}^\circ$	Gibbs free energy of reaction at temperature T
3H	Tritium
H_1	Thickness of the vadose zone
h_m	Mixing-zone thickness
$\Delta H_{f,298}^\circ$	Enthalpy (or heat) of formation at 298 K
$\Delta H_{f,T}^\circ$	Enthalpy (or heat) of formation at temperature T
$\Delta H_{r,298}^\circ$	Enthalpy (or heat) of reaction at 298 K
$\Delta H_{r,T}^\circ$	Enthalpy (or heat) of reaction at temperature T
I	Ionic strength
IAP	Ion activity product
J_{ix}	Flux of species I in direction x
K	A constant in the Langmuir, Freundlich and Dubinin-Radushkevich isotherm models
K_{DR}	Concentration-based, conditional equilibrium constant calculated from Dubinin-Radushkevich adsorption isotherm

K_d	Concentration-based partition (or distribution) coefficient
K_d^{act}	Activity-based partition coefficient
K_{dis}	Dissolution equilibrium constant
K_{ex}	Exchange reaction constant
K_F	Concentration-based, conditional equilibrium constant calculated from Freundlich adsorption isotherm
K_F^{act}	Activity-based, conditional equilibrium constant calculated from Freundlich adsorption isotherm
K_L	Concentration-based, conditional equilibrium constant calculated from Langmuir adsorption isotherm
K_L^{act}	Activity-based, conditional equilibrium constant calculated from Langmuir adsorption isotherm
K_{oc}	Organic-carbon partition coefficient
K_{om}	Organic-matter partition coefficient
$K_{r,298}$	Equilibrium constant at 298 K
$K_{r,T}$	Equilibrium constant at temperature T
$K_{\text{sp},T}$	Solubility product
l	Liter
M	Generic term for metal or radionuclide constituent
m	Meter
M_A	Instantaneous mass released per unit area
M_{ads}	Mass of constituent I associated with the adsorbed phase in the vadose zone
M_{aq}	Mass of constituent I associated with the aqueous phase in the vadose zone
M_{rel}	Released mass
$M_{\text{saturated}}$	Total mass of constituent I associated with the saturated zone
M_{sed}	Sediment mass
M_{Total}	Total combined mass of constituent I in the vadose and saturated zones
M_{vadose}	Total mass of constituent I associated with the vadose zone
ml	Milliliter
mol	Mole
mV	Millivolt
N	Constant in the Freundlich isotherm model
n	Total porosity
n_e	Effective porosity
pE	Negative common logarithm of the free-electron activity
pH	Negative logarithm of the hydrogen ion activity
pH_{zpc}	pH for zero point of charge
R	Ideal gas constant, 1.9872 cal/mol·K
R_f	Retardation factor
s	Solid phase species
SI	Saturation index, as defined by $\log(IAP/K_{r,T})$
SOH	Unreacted surface site occupied by a hydroxyl group

SOH·M	Used in the non-electrostatic adsorption models for an adsorption site occupied by component M or surface-bound metal
SO·M	Used in the electrostatic adsorption models for an adsorption site occupied by component M or surface-bound metal
T	Absolute temperature, usually in Kelvin unless otherwise specified
T_o	Total surface charge for plane o
t	Time
t_{max}	End of the break-through curve during a column experiment
t_{min}	Beginning of the break-through curve during a column experiment
t_{pulse}	Mean residence time of a solute during a column experiment for a pulse release
t_T	Total advective travel time of the contaminant
t_{ss}	Mean residence time of a solute during a column experiment for a steady-state release
t_{step}	Mean residence time for a step input/release
TDS	Total dissolved solids
V_{source}	Volume associated with the contaminated source
V_w	Volume of water (or adsorbate solution)
v^*	Contaminant velocity
v_c	Contaminant velocity
v_d	Darcy velocity
v_p	Pore-water velocity
X_{Gf}, Y_{Gf}, Z_{Gf}	Green's functions (which are orthogonal) in the x, y, and z directions, respectively
x	Distance in the x direction
y	Off-centerline distance
Z	Valence state
z	Charge of ion
{ }	Activity
[]	Concentration

APPENDIX B

Definitions

Appendix B

Definitions

Absorption - partitioning of a dissolved species into a solid phase.

Adsorption - partitioning of a dissolved species onto a solid surface.

Adsorption Edge - the pH range where solute adsorption sharply changes from ~10% to ~90%.

Actinon - name occasionally used, especially in older documents, to refer to ^{219}Rn which forms from the decay of actinium.

Activity - the effective concentration on an ion that determines its behavior to other ions with which it might react. An activity of ion is equal to its concentration only in infinitely dilute solutions. The activity of an ion is related to its analytical concentration by an activity coefficient, γ .

Alkali Metals - elements in the 1A Group in the periodic chart. These elements include lithium, sodium, potassium, rubidium, cesium, and francium.

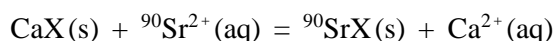
Alpha Particle - particle emitted from nucleus of atom during one type of radioactive decay. Particle is positively charged and has two protons and two neutrons. Particle is physically identical to the nucleus of the ^4He atom (Bates and Jackson 1980).

Alpha Recoil - displacement of an atom from its structural position, as in a mineral, resulting from radioactive decay of the release an alpha particle from its parent isotope (*e.g.*, alpha decay of ^{222}Rn from ^{226}Ra).

Amphoteric Behavior - the ability of the aqueous complex or solid material to have a negative, neutral, or positive charge.

Basis Species - see component species.

Cation Exchange - reversible adsorption reaction in which an aqueous species exchanges with an adsorbed species. Cation exchange reactions are approximately stoichiometric and can be written, for example, as



where X designates an exchange surface site.

Cation Exchange Capacity (CEC) - the sum total of exchangeable cations that a sediment can adsorb.

Code Verification - test of the accuracy with which the subroutines of the computer code perform the numerical calculations.

Colloid - any fine-grained material, sometimes limited to the particle-size range of <0.00024 mm (*i.e.*, smaller than clay size), that can be easily suspended (Bates and Jackson 1979). In its original sense, the definition of a colloid included any fine-grained material that does not occur in crystalline form.

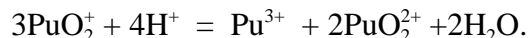
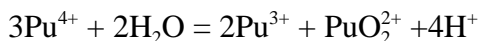
Complexation (Complex Formation) - any combination of dissolved cations with molecules or anions containing free pairs of electrons.

Component Species - “basis entities or building blocks from which all species in the system can be built” (Allison et al. 1991). They are a set of linearly independent aqueous species in terms of which all aqueous speciation, redox, mineral, and gaseous solubility reactions in the MINTEQA2 thermodynamic database are written.

Detrital Mineral - “any mineral grain resulting from mechanical disintegration of parent rock” (Bates and Jackson 1979).

Deuterium (D) - stable isotopes ^2H of hydrogen.

Disproportionation - is a chemical reaction in which a single compound serves as both oxidizing and reducing agent and is thereby converted into more oxidized and a more reduced derivatives (Sax and Lewis 1987). For the reaction to occur, conditions in the system must be temporarily changed to favor this reaction (specifically, the primary energy barrier to the reaction must be lowered). This is accomplished by a number of ways, such as adding heat or microbes, or by radiolysis occurring. Examples of plutonium disproportionation reactions are:



Electron Activity - unity for the standard hydrogen electrode.

Far Field - the portion of a contaminant plume that is far from the point source and whose chemical composition is not significantly different from that of the uncontaminated portion of the aquifer.

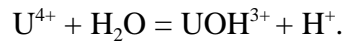
Fulvic Acids - breakdown products of cellulose from vascular plants (also see humic acids). Fulvic acids are the alkaline-soluble portion which remains in solution at low pH and is of

lower molecular weight (Gascoyne 1982).

Humic Acids - breakdown products of cellulose from vascular plants (also see fulvic acids).

Humic acids are defined as the alkaline-soluble portion of the organic material (humus) which precipitates from solution at low pH and are generally of high molecular weight (Gascoyne 1982).

Hydrolysis - a chemical reaction in which water reacts with another substance to form two or more new substances. For example, the first hydrolysis reaction of U^{4+} can be written as



Hydrolytic Species - an aqueous species formed from a hydrolysis reaction.

Ionic Potential - ratio (z/r) of the formal charge (z) to the ionic radius (r) of an ion.

Isoelectric Point (iep) - pH at which a mineral's surface has a net surface charge of zero. More precisely, it is the pH at which the particle is electrokinetically uncharged.

Lignite - a coal that is intermediate in coalification between peat and subbituminous coal.

Marl - an earthy substance containing 35-65% clay and 65-35% carbonate formed under marine or freshwater conditions

Mass Transfer - transfer of mass between two or more phases that includes an aqueous solution, such as the mass change resulting from the precipitation of a mineral or adsorption of a metal on a mineral surface.

Mass Transport - time-dependent movement of one or more solutes during fluid flow.

Mire - a small piece of marshy, swampy, or boggy ground.

Model Validation - integrated test of the accuracy with which a geochemical model and its thermodynamic database simulate actual chemical processes.

Monomeric Species - an aqueous species containing only one center cation (as compared to a polymeric species).

Near Field - the portion of a contaminant plume that is near the point source and whose chemical composition is significantly different from that of the uncontaminated portion of the aquifer.

Peat - an unconsolidated deposit of semicarbonized plant remains in a water saturated environment.

Polynuclear Species - an aqueous species containing more than one central cation moiety, *e.g.*, $(\text{UO}_2)_2\text{CO}_3(\text{OH})_3^-$ and $\text{Pb}_4(\text{OH})_4^{4+}$.

Protium (H) - stable isotope ^1H of hydrogen.

Retrograde Solubility - solubility that decreases with increasing temperature, such as those of calcite (CaCO_3) and radon. The solubility of most compounds (*e.g.*, salt, NaCl) increases with increasing temperature.

Species - actual form in which a dissolved molecule or ion is present in solution.

Specific Adsorption - surface complexation via a strong bond to a mineral surface. For example, several transition metals and actinides are specifically adsorbed to aluminum- and iron-oxide minerals.

Sol - a homogeneous suspension or dispersion of colloidal matter in a fluid.

Solid-Solution Phase - a solid material in which a minor element is substituted for a major element in a mineral structure.

Thoron - name occasionally used, especially in older documents, to refer to ^{220}Rn which forms from the decay of thorium.

Tritium (T) - radioactive isotope ^3H of hydrogen.

Tritium Units - units sometimes used to report tritium concentrations. A tritium unit (TU) is equivalent to 1 atom of ^3H (tritium) per 10^{18} atoms of ^1H (protium). In natural water that produces 7.2×10^{-3} disintegrations per minute per milliliter (dpm/ml) of tritium, 1 TU is approximately equal to 3.2 picocuries/milliliter (pCi/ml).

APPENDIX C

**Standard Method Used At
Pacific Northwest National Laboratory
For Measuring Laboratory Batch K_d Values**

Appendix C

Standard Method Used At Pacific Northwest National Laboratory For Measuring Laboratory Batch K_d Values

The standard method reproduced below is used by the authors of this report and their coworkers at the Pacific Northwest National Laboratory in Richland, Washington for the measurement of K_d values. It is adapted from the procedure described in Relyea et al. (1980).¹

1.0 Applicability

This procedure describes the method for measuring radionuclide distribution coefficients (K_d 's) of geologic material. This procedure includes descriptions for analyses of unconsolidated, loosely consolidated, consolidated porous, and intact, impermeable geological materials.

2.0 Definitions

- Cold wash: Contact of solid sample with nonradioactive groundwater for purposes of establishing chemical equilibrium with nontracer aqueous constituents.
- Tracer: Radioactive element added to groundwater solution to indicate migration and retardation events.
- Spiked groundwater: Groundwater with tracer.
- Blank tube: Centrifuge tube containing spiked groundwater but no solids.
- Radiation Work Procedure (RWP): This is a set of instructions for safe handling of radioactive material in the laboratory. The RWP covers a number of topics and shall be read and understood before performing any work in the laboratory.

3.0 Responsible Staff

- Task leader
- Cognizant staff

¹ Relyea, J. F., R. J. Serne, and D. Rai. 1980. *Methods for Determining Radionuclide Retardation Factors: Status Report*. Pacific Northwest Laboratory, Richland, Washington

4.0 Procedure

4.1 Materials

pH meter
pH combination electrode 0-14 pH
Magnetic stirrer
Stir bars
Scintillation vials
pH buffers
Groundwater
No. 18 stainless steel sieve (1 mm)
No. 50 sieve (0.3 mm)
Mortar and pestle
Analytical balance (accuracy within ± 0.01 g) - Refer to operation manual specific to balance for use instructions.
50 ml polycarbonate centrifuge tubes with screw caps
Teflon tape
Groundwater
Orbit shaker
Centrifuge
Vacuum pipets
0.45-micrometer polycarbonate membrane filters
Radioactive tracer
Plastic bags

4.2 Safety Precautions

In using radioactive substances and/or solutions protective clothing should be used to reduce the possibility of contamination. Each laboratory is supplied with a radiation work procedure (RWP) which outlines the types and quantities of radionuclides permitted with instructions for handling. Record the number of the RWP in the laboratory record book.

4.3 Sample Characterization

Before the K_d study perform the following analyses to characterize solid and groundwater samples (perform groundwater analysis within one month prior to study). Include the following:

4.3.1 For groundwater

- pH
- bulk chemistry (Ca, Mg, Na, K, Cl, NO₃, SO₄, CO₃, HCO₃)

4.3.2 For solids

- Mineralogy
- Surface area
- Cation exchange capacity
- Moisture content
- Particle size analysis

Procedures which may be used to determine the above parameters are referenced at the end of this document. Record all results.

4.4 Sample Preparation

4.4.1 Groundwater

- 4.4.1.1 Filter groundwater through a 0.45- μ m polycarbonate membrane before it is used in a batch K_d measurement.
- 4.4.1.2 If retardation parameters (such as pH, ionic strength, and complexing ligand concentration) are to be studied, chemically analyze the synthetic or altered groundwater after preparation and filtration and record results.

4.4.2 Solid

- 4.4.2.1 Unconsolidated Material. To remove particles greater than one millimeter (>1.0 mm), the sample shall be wet-sieved with groundwater by passing the sample through a No. 18 stainless steel sieve. If tests with the material are to be conducted in an inert atmosphere or in a controlled atmosphere, rock samples are to be prepared under those same atmospheric conditions. This requires minimum contact of the rock with air from the time it is removed from the earth until the time the experiment is concluded. This condition holds for Sections 4.5.2.2 and 4.5.2.3. The particle size shall be determined and reported with results from Section 4.3.
- 4.4.2.2 Loosely Consolidated Material. The sample shall be disaggregated by an ultrasonic method or by hand with a mortar and pestle. A portion of the intact material shall be preserved for dynamic testing. Disaggregation

shall proceed no farther than that required to reduce the sample to its natural grain size. Fresh surfaces will be exposed to weathering, but this procedure should reduce fracturing of particles to a minimum. Remove particles >1.0 mm as in Section 4.5.2.1. The particle size distribution after disaggregation shall be reported with results in Section 4.3.

- 4.4.2.3 Consolidated Porous Material (and intact, impermeable rock). A portion of the intact sample shall be preserved (and maintained under conditions that simulate those in situ) for dynamic testing. The remaining sample is to be crushed to pass through a No. 18 sieve (<1 mm). Crushing must be accomplished by means that minimize the introduction of extraneous material, such as metal filings, into the sample. The sample should then be wet sieved through a No. 50 sieve (0.30 mm) to obtain particle sizes between 0.30 mm and 1.00 mm.
- 4.4.2.4 After samples have been sized (Sections 4.5.2.1, 4.5.2.2 or 4.5.2.3), they must be homogenized to insure that the same particle size distribution is obtained for each subsample to be studied.

4.4.3 Equilibrium

- 4.4.3.1 Prepare 50 ml polycarbonate centrifuge tubes with screw caps by obtaining and recording tare weights and assigning identifications which are unique to each sample tube.
- 4.4.3.2 After homogenizing, 1-g ($1.0 \text{ g} \pm 0.01 \text{ g}$) samples are to be weighed (and weights recorded) into centrifuge tubes. Wrap centrifuge tube threads with Teflon tape to prevent leaks.
- 4.4.3.3 Thirty-milliliters of filtered, nonspiked (no radioactive tracer) groundwater is added to each tube, including blanks with no soil, for a “cold” wash. The tube caps are to be replaced before the tubes are placed on a shaker for a gentle overnight agitation (about one oscillation per second).
- 4.4.3.4 Next centrifuge the tubes to separate solids and liquids. Remove the solutions with a vacuum pipettes to prevent removal of the rock sample (some liquid will remain in the tube).
- 4.4.3.5 Repeat the wash procedure twice more for a total of three cold (nonradioactive) washes. Before the centrifuge step on the third wash, measure and record the pH of the solid-solution. If the pH has changed from its natural equilibrium value as measured in the field, the rock

sample and groundwater have not yet re-established equilibrium. Continue to wash until the pH is stable. A change in pH is most likely to occur with samples of crushed rock (Section 4.4.2.3) because fresh surfaces (either rock or cementing agents) have been exposed.

- 4.4.4 After removal of the third wash solution, each tube must be reweighed and the weight must be recorded to determine the volume of excess solution left in each sample. Secure the cap of each tube to prevent evaporation, which would result in an increased salt concentration in the remaining solution. The excess solution volume is found by dividing the excess solution weight by the solution density.

4.5 Addition of Tracer

- 4.5.1 The adding of tracer to a solution represents a critical step in the execution of radionuclide migration studies. Two items must be carefully considered: (1) the total amount of tracer added must be soluble in the volume of solution used and (2) the chemical composition of the groundwater or synthetic groundwater must remain unchanged, except for the addition of the radionuclide(s) to be studied.
- 4.5.2 Dry the tracers so that excess acid or base in the stock solution is removed. Do not dry volatile tracers in acid media or they will be lost. The chemical produced by drying must be soluble in the solutions used in experimentation. (An incorrect procedure would be to dry plutonium basic media that would produce an insoluble PuO_2 or $\text{Pu}[\text{OH}]_4$ precipitate.)
- 4.5.3 Exception to the dry-addition rule must be made in some cases for radionuclides that have multiple oxidation states. When drying might change the tracer stock solution's oxidation state--such as Pu(VI) to Pu(IV)--tracer should be added to solution in as small a volume as possible with as little excess salt and acid or base as possible. Otherwise, a dry, soluble, salt-free tracer shall be added to groundwater.
- 4.5.4 Allow the tracer solution to sit for at least one week under conditions to be used in the experiment (in equilibrium with air if the aquifer is in equilibrium with air, or under controlled atmosphere conditions if the aquifer is not in equilibrium with air). Make any necessary adjustments to pH during the equilibration time. Solution is to be filtered (0.45 μm) after equilibration prior to contact with the geologic material.
- 4.5.5 Calculate and record the amount of tracer (mol/l) present in the groundwater just prior to contact with the geologic material. Additionally, report any carrier isotope of the element added with the tracer and any natural occurrence of the element in groundwater.

4.6 Rock and Groundwater Contact

- 4.6.1 Thirty milliliters (30 ml) of filtered groundwater containing the radioactive tracer is added to each sample tube containing one gram (1 g) of solid. In addition, 30 ml of spiked groundwater is placed in each of three empty (blank) centrifuge tubes (prewashed as in Section 4.4.3). The blank tubes are needed to detect sorption of tracer by centrifuge tube walls.
- 4.6.2 After replacing the tube caps, the tubes are placed in plastic bags (5 to 20 tubes per bag) to contain any contamination caused by leaky tubes. Next, the tubes are placed on a shaker (for linear reciprocating shaker, place tubes horizontally) so that the solid-solution mixture makes maximum contact. Set the shaking speed to 0.8 to 1.2 oscillations per second to ensure mixing of solid and liquid but to reduce grinding of particles.
- 4.6.3 If time is not a parameter being studied, then contact between solid and liquid is to be seven days (7 days). Record the actual contact time allowed. The samples are then removed from the shaker and the tubes are visually checked for leaks (decontaminate if necessary and discard leaky tubes).
- 4.6.4 The blank and sample tubes are centrifuged for twenty minutes (20 min) at 10,000 g ($g = 980 \text{ cm/sec}^2$) or more, and fifteen milliliters (15 ml) of effluent is filtered through a pre-washed 0.45 μm polycarbonate-membrane-type filter. (Pre-wash with groundwater from Section 2.2 to remove foreign particles and soluble impurities). Analyze filtered effluent samples for tracer activity. Next, the effluent is decanted from the blanks into cleanly washed tubes and the empty blank tubes are analyzed for tracer activity adsorbed on tube walls. If tracer activity on blank tube walls is greater than 10 percent of the total blank activity (determined in Section 4.7.3), do not use the blank influent activity for K_d calculation. If the activity sorbed on blank walls is significantly greater than 10 percent (using a one-tailed “t” test and combined counting error and statistical variation between blanks), directly count the activity of the sample. Methods for both cases follow.

5.0 Batch K_d Calculations

5.1 When tracer is not sorbed by blank tube wall

- 5.1.1 Data needed for K_d calculation are: (1) excess solution volume, V_{excess} (ml) left from the third cold wash (weight of excess solution divided by solution density); (2) mass of solid aquifer material, M_{sed} (g); (3) volume of groundwater with radioactive tracer added, V_{spike} (ml); (4) activity or concentration of tracer in the

effluent solution, C_{effluent} (dpm/ml); and (5) the tracer activity or concentration in the influent blank, C_{blank} , (dpm/ml).

5.1.2 The tracer concentration on the solid phase, A_i (or q_i), is:

$$A_i = q_i = \frac{(C_{\text{blank}} \times V_{\text{spike}}) - C_{\text{effluent}}(V_{\text{spike}} + V_{\text{excess}})}{M_{\text{sed}}} \quad (1)$$

The K_d is then given by:

$$K_d = \frac{(C_{\text{blank}} \times V_{\text{spike}}) - C_{\text{effluent}}(V_{\text{spike}} + V_{\text{excess}})}{C_{\text{effluent}} \times M_{\text{sed}}} \quad (2)$$

5.2 When tracer is sorbed by blank tube wall (Gamma or X-ray Emitting Isotopes)

5.2.1 If the radioactive tracer is adsorbed on the walls of blank tubes, determine the tracer adsorbed by the solid by direct measurement. Use a traceable standard made with the same type of geologic material as used in the test.

5.2.2 For this procedure, after the sediment and traced groundwater have contacted for at least 7 days, the samples are centrifuged to separate solids from liquids, then the liquid effluent is decanted from the sample tube using a vacuum pipette, and the sample is weighed to determine the excess effluent solution volume (V_{excess}). The solid sample is then dried (it should be “air dried” in the same manner as when originally weighed, either in air or in a controlled atmosphere) and transferred to a clean polycarbonate centrifuge tube. The weight of the dry sample M_{sed} (g) is then determined and radiocounting of the dry sample is performed for tracer activity, C (dpm), using the same detector, sample position, and radioanalytical techniques as used for the attenuation standard prepared in Section 5.2.1.

5.2.3 Determine the effluent tracer activity, C_{effluent} (dpm/ml), in geometries that are traceable to a standard. The K_d can then be calculated from:

$$K_d = \frac{C - (C_{\text{effluent}} \times V_{\text{excess}})}{C_{\text{effluent}} \times M_{\text{sed}}} \quad (3)$$

5.3 When tracer is sorbed by blank tube wall (α - or β -Emitting Isotopes)

5.3.1 If the radioactive tracer is adsorbed by sample container walls, only the effluent activity can be determined simply and directly. Two options are available for determination of the activity adsorbed by the rock sample. One method is to remove both the solid sample and effluent from the original container and to strip the isotope from the container wall by some means. Mass balance will allow calculation of the K_d if one knows the amount of radionuclide in the effluent on the tube wall and the total radionuclide initially added. A second method is to chemically remove the radionuclide from the rock sample and count it.

Problems with the first method include the possibility that some of the solid may adhere to the wall and raise the apparent activity of the nuclide adsorbed by the container. Removal of the solid sample may also cause leaching of the container wall and result in an apparent low activity for nuclides adsorbed by the container. This can be minimized by using tubes made of material most appropriate to your sample; consider Teflon, glass, or various plastics to minimize adherence.

The second method is subject to incomplete removal of the nuclide from the solid or loss of material during any additional steps required for extraction, or both.

6.0 Reporting Results from Radionuclide Migration Experiments

6.1 The following generic K_d coding form (Table 1) includes the information to be obtained. (The different data categories and abbreviations are described in Section 6.2.)

6.2 Explanation of K_d Coding Form

6.2.1 Category I. Reference

- A. *Name* of the person who performed experiments
- B. *Date* that the experiment was started.
- C. *Comments* regarding deviations from procedure, anomalies that occurred during the process, other pertinent information.

Table 1. Generic K_d coding form.

Reference	Experimental Details	Geologic Media	Aqueous Phase	Nuclide	Adsorption Function
A. Name	A. Method	A. Name	A. BEG	A. ISO	A. K_d
B. Date Started	B. State	B. Origin	B. Macro	B. CONC	B. Units
C. Comments	C. Ratio	C. Total	C. Trace	C. SPE	C. Direction
	D. Time	D. Mineral	D. END	D. ADD	D. NUM
	E. Temperature	E. CO_3		E. Loading	
	F. ATM	F. OX			
	G. SEP	G. CEC			
	H. Analyze	H. AEC			
	I. RAD	I. SA			

6.2.2 Category II. Experimental Details

- A. *Method* refers to batch, axial filter, column, intact core, channel chromatography, and so forth. For batch method, add more detail as to whether cold washes and blank corrections were used. For example, use mnemonics such as
- “BATCH (3W, BC) = batch, three cold washes, with blank tube sorption correction”
- “BATCH (OW) = batch, zero cold washes and no correction.”
- B. *State* of geologic media such as crushed 40 μm ; intact core 2.5 cm dia x 5 cm; tablet 1 cm x 0.5 cm; crushed 30-80 μm , etc.
- C. *Ratio* of solids to solution for batch K_d ; for columns include pore velocity or column velocity (for example, 1 PV = 1 cm/hr, CV = 0.5 cm/hr) and porosity and column bulk density; PR = porosity, BD = bulk density.
- D. *Time* of contact such as shaking time for batch system or residence time in flow through columns (h) = hours, (d) = days.

- E. *Temp* is the temperature of the experiment in °C.
- F. *ATM* is the equilibrating atmosphere air, N₂, Ar, 10 percent CO₂ - 90 percent Ar, and so forth.
- G. *SEP* stands for separation technique; did you use filters (give median pore size) or centrifugation (include approximate g's)?
- “FIL(.4) = filter 0.4 m”
- “CEN(50) = centrifuged at 50 g's where g = 980 cm/sec² units.”
- H. *Analyze* states whether the K_d is determined by analyzing (or counting) liquids only or solid and liquid:
- “L/L = liquids only”
- “S/L = solid and liquid”
- I. *RAD* is a list of all radioisotopes that were run simultaneously in the experiment. Example: “Sr, Cs, Tc” means these isotopes were run together.

6.2.3 Category III. Geologic Media

- A. *Name*. Use the generic name of the rock or mineral, *e.g.*, basalt, granite, montmorillonite.
- B. *Origin*. Include a geographic description and some formation information, *e.g.*, Eleana shale, Sentinel Gap basalt, Argillaceous Shale Wards #404561.
- C. *Total*. Identify the chemical composition as oxides (SiO₂, Al₂O₃TiO₂, FeO, Fe₂O₃, MnO, CaO, MgO, K₂O, Na₂O, P₂O₅ in percent.
- D. *Minerals*. Identify the minerals present in the rock sample, listing the major ones first, the minor ones last, in the order of the composition percentages in which they appear (largest first). If there are quantitative estimates, add this information as percent and tr = 5 percent.
- E. *CO₃* = carbonate content of rock.
- F. *OX* = hydrous Fe, Mn, Al oxides content of rock.

- G. *CEC* = cation exchange content of material; units = meq/100g. Specify pH of system (typically pH = 7).
- H. *AEC* = anion exchange content of material; units = meq/100g. Specify pH of system.
- I. *SA* = surface area; use “EG” for ethylene glycol, “BET” for gas adsorption, use units m²/g, for example: EG(1.3).

6.2.4 Category IV. Aqueous Phase

- A. *BEG* signifies measurements made prior to tracer adsorption.
- B. *Macro* constituents include:
 - pH
 - Eh (units vs. S.H.E.)
 - Na⁺
 - Ca²⁺
 - K⁺
 - Mg²⁺
 - Cl⁻
 - HCO₃⁻; CO₃²⁻
 - SO₄²⁻
 - SiO₄
- C. *Trace* constituents include:
 - NO₃, ppm
 - Organic carbon
 - B
 - Trace metals or anything else measured.
- D. *END* signifies measurements (if performed) taken at the same time as K_d determined.

6.2.5 Category V. Nuclide

- A. *ISO*. Isotope used such as ²³⁷Pu, ^{95m}Tc.
- B. *CONC*. Concentration added to groundwater in M = molarity. Include any carrier if present.

- C. *SPE*. Species or valence state added, if known. Also state whether the valence state distribution was determined after equilibration state, *e.g.*, “Pu(VI) BEG; Pu(IV) 15 percent, Pu(V) 50 percent, Pu(VI) 10 percent END” (which means that the original spike was 100 percent Pu(VI), and after shaking the final distribution was as shown).
- D. *ADD* describes how the tracer was added to the groundwater; DRY means evaporated to dryness and groundwater added; WET/PH/3DFO.4 means a small aliquot of liquid tracer was added to the groundwater, the pH of the system was re-adjusted to the appropriate value and shaken for 3 days to filtration through 0.4 μm filters before usage.
- “DRY/1DC50” means the dried spike was brought back into solution equilibrated for one day, and centrifuged at 50 g’s before usage.
- E. *Loading* describes (a) the percent of total exchange capacity of the adsorbent filled with the nuclide of interest or (b) the mass of nuclide adsorbed/mass of adsorbent at the condition when the K_d measurement is performed. This value can be calculated from knowledge of the cation or anion exchange capacity in case (a) and from mass balance considerations. One must know the original mass of the nuclide used in each experiment.

6.2.6 Category VI. Adsorption Function

- A. K_d . Place the value for K_d . If a retardation factor is determined in a flow-through column as a function of water velocity, designate by the symbol RF.

Where several measurements were made, also give the standard deviation, such as

“ $75 \pm 12 = a K_d$ ”
 “(RF) $60 \pm 30 = \text{retardation factor}$ ”

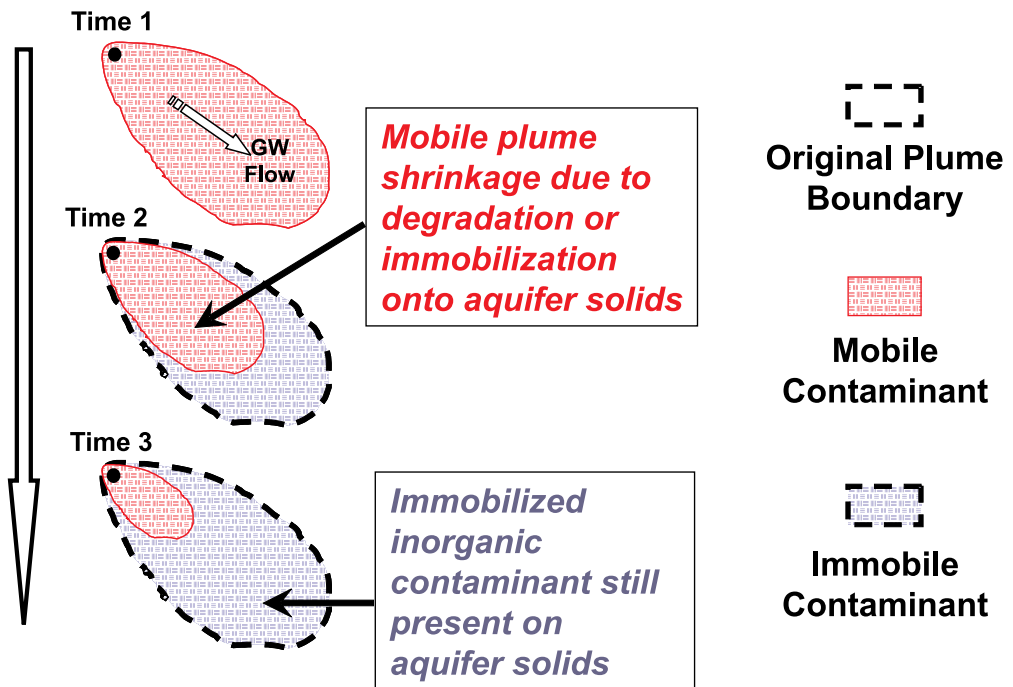
- B. *Units*. ml/g or ml/m².
- C. *Direction*.
 ADS = adsorption direction
 DES = desorption direction
 ADS-DES = A spike addition to a column.
- D. *NUM* = number of observations used to derive data point, for example:
 3 = triplicate samples.

ATTACHMENT 11

Monitored Natural Attenuation of Inorganic Contaminants in Ground Water

Volume 1 Technical Basis for Assessment

Evolution of Inorganic Contaminant Plume



Monitored Natural Attenuation of Inorganic Contaminants in Ground Water

Volume 1 - Technical Basis for Assessment

Edited by
Robert G. Ford
Richard T. Wilkin
Robert W. Puls

U.S. Environmental Protection Agency
Office of Research and Development
National Risk Management Research Laboratory
Ada, Oklahoma 74820

Project Officer
Robert G. Ford
Ground Water and Ecosystems Restoration Division
National Risk Management Research Laboratory
Ada, Oklahoma 74820

National Risk Management Research Laboratory
Office of Research and Development
U.S. Environmental Protection Agency
Cincinnati, Ohio 45268

Notice

The U.S. Environmental Protection Agency through its Office of Research and Development managed the research described here under EPA Contract No. 68-C-02-092 to Dynamac Corporation, Ada, Oklahoma, through funds provided by the U.S. Environmental Protection Agency's Office of Air and Radiation and Office of Solid Waste and Emergency Response. It has been subjected to the Agency's peer and administrative review and has been approved for publication as an EPA document. Mention of trade names or commercial products does not constitute endorsement or recommendation for use.

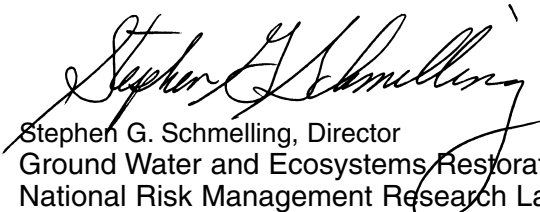
All research projects making conclusions or recommendations based on environmental data and funded by the U.S. Environmental Protection Agency are required to participate in the Agency Quality Assurance Program. This project did not involve the collection or use of environmental data and, as such, did not require a Quality Assurance Plan.

Foreword

The U.S. Environmental Protection Agency is charged by Congress with protecting the Nation's land, air, and water resources. Under a mandate of national environmental laws, the Agency strives to formulate and implement actions leading to a compatible balance between human activities and the ability of natural systems to support and nurture life. To meet this mandate, EPA's research program is providing data and technical support for solving environmental problems today and building a science knowledge base necessary to manage our ecological resources wisely, understand how pollutants affect our health, and prevent or reduce environmental risks in the future.

The National Risk Management Research Laboratory is the Agency's center for investigation of technological and management approaches for preventing and reducing risks from pollution that threatens human health and the environment. The focus of the Laboratory's research program is on methods and their cost-effectiveness for prevention and control of pollution to air, land, water, and subsurface resources; protection of water quality in public water systems; remediation of contaminated sites, sediments and ground water; prevention and control of indoor air pollution; and restoration of ecosystems. NRMRL collaborates with both public and private sector partners to foster technologies that reduce the cost of compliance and to anticipate emerging problems. NRMRL's research provides solutions to environmental problems by: developing and promoting technologies that protect and improve the environment; advancing scientific and engineering information to support regulatory and policy decisions; and providing the technical support and information transfer to ensure implementation of environmental regulations and strategies at the national, state, and community levels.

This publication has been produced as part of the Laboratory's strategic long-term research plan. It is published and made available by EPA's Office of Research and Development to assist the user community and to link researchers with their clients. Understanding site characterization to support the use of monitored natural attenuation (MNA) for remediating inorganic contaminants in ground water is a major priority of research and technology transfer for the U.S. Environmental Protection Agency's Office of Research and Development and the National Risk Management Research Laboratory. This document provides technical recommendations regarding the development of conceptual site models and site characterization approaches useful for evaluating the effectiveness of the natural attenuation component of ground-water remedial actions.



Stephen G. Schmelling, Director
Ground Water and Ecosystems Restoration Division
National Risk Management Research Laboratory

Contents

Notice	ii
Foreword	iii
Figures	viii
Tables	ix
Acknowledgments	x
Executive Summary	xi
Section I - Conceptual Background for Natural Attenuation	
IA. Background and Purpose	1
IA.1 Document Organization	1
IA.2 Purpose of Document	1
IA.3 Applicable Regulatory Criteria	2
IA.4 Policy Framework for Use of MNA	2
IB. Relevant Distinctions in Site Characterization for MNA of Inorganic Contaminants.....	4
IC. Tiered Analysis Approach to Site Characterization	5
IC.1 Tier I.....	6
IC.2 Tier II.....	7
IC.3 Tier III.....	7
IC.4 Tier IV	8
ID. Role of Modeling in the Tiered Analysis Approach.....	10
ID.1 Developing a Conceptual Model.....	10
ID.2 Types of Models.....	11
ID.2.1 Simple Calculations	11
ID.2.2 Mass Transport Models.....	12
ID.2.3 Speciation Models.....	12
ID.2.4 Reaction Models	12
ID.2.5 Reactive Transport Models	12
ID.3 Modeling and the Tiered Analysis Approach	13
ID.3.1 Tier I – Demonstration of Contaminant Removal from Ground Water.....	13
ID.3.2 Tier II – Determine Mechanism and Rate of Attenuation	13
ID.3.3 Tier III – Demonstrate Capacity and Stability of Removal Mechanism	13
ID.3.4 Tier IV – Long-Term Performance Monitoring	14
ID.4 Choosing Modeling Software.....	14
ID.4.1 Public Domain vs. Commercial Software.....	14
ID.4.2 Sources of Software.....	14
ID.4.3 Thermodynamic Data	16
ID.5 Accounting for Uncertainty.....	17
ID.6 Model Calibration and Verification	17
IE. Long-Term Performance Monitoring and Site Closure.....	18
IE.1 Duration and Monitoring Frequency.....	19
IE.2 Monitoring of Aquifer Solids.....	19
IE.3 Monitoring Types.....	19

IE.4	Monitoring Locations.....	20
IE.5	Modification of the Performance Monitoring Plan.....	22
IE.6	Periodic Reassessment of Contaminant Removal Technologies.....	22
IF.	References.....	23
 Section II - Technical Basis for Natural Attenuation in Ground Water		
IIA.	Physical Transport Mechanisms.....	26
IIA.1	Basics of Ground-Water Flow and Solute Movement.....	26
IIA.2	Colloidal Transport of Inorganic Contaminants.....	27
IIA.2.1	Implications for Monitored Natural Attenuation.....	27
IIB.	Contaminant Sorption to Aquifer Solids.....	28
IIB.1	Adsorption.....	29
IIB.1.1	Reactive Mineral Phases Involved in Adsorption.....	29
IIB.1.2	Surface Functional Groups on Aquifer Solids and the Impact on Surface Charge.....	31
IIB.1.3	Weak and Strong Adsorption Regimes.....	32
IIB.2	Precipitation.....	33
IIB.2.1	Precipitation from Solution.....	33
IIB.2.2	Coprecipitation.....	35
IIB.2.3	Surface Precipitation.....	35
IIB.2.4	Mineral Transformation.....	36
IIB.3	Implications for Natural Attenuation Assessment.....	36
IIC.	Microbial Impacts on Inorganic Contaminant Attenuation.....	36
IIC.1	Characteristics of Aquifer Microbiology.....	37
IIC.2	Microbial Controls on Subsurface Redox State.....	37
IIC.3	Impacts on Contaminant Speciation and Attenuation.....	39
IIC.3.1	Contaminant Oxidation-reduction Reactions.....	39
IIC.3.2	Biosorption and Intracellular Bioaccumulation.....	39
IIC.3.3	Methylation and Demethylation.....	40
IIC.4	Implications for Natural Attenuation Assessment.....	40
IID.	References.....	40
 Section III - Site Characterization to Support Evaluation of MNA		
IIIA.	Site Hydrogeology.....	43
IIIA.1	Characterization Objectives.....	43
IIIA.2	Geologic Characterization.....	44
IIIA.2.1	Saturated Porous Media.....	44
IIIA.2.2	Saturated Fractured Media.....	44
IIIA.3	Hydrologic Characterization.....	45
IIIA.4	Ground-Water/Surface-Water Interactions.....	47
IIIA.5	Hydrogeologic Data Interpretation.....	47
IIIA.5.1	Attenuation Rate Estimates.....	48
IIIA.5.2	Contaminant Flux.....	48
IIIA.5.3	Source Term Characteristics.....	50
IIIB.	Contaminant Quantification, Distribution and Speciation.....	50
IIIB.1	Aqueous Characterization Approaches.....	50
IIIB.1.1	Filtration.....	51
IIIB.2	Solid Phase Characterization Approaches.....	52
IIIB.2.1	Sampling and Fractionation.....	53
IIIB.2.2	Total Amount.....	53
IIIB.2.3	Structurally Defined Form.....	54
IIIB.2.4	Operationally Defined Form.....	55
IIIB.2.4.1	Sequential Extractions.....	55

III B.2.4.2 Sequential Extraction Considerations.....	58
III B.2.5 Attenuation Capacity.....	59
III B.3 Model Representations to Interpret Contaminant Sorption Observations.....	61
III B.3.1 Distribution Coefficient/partition Coefficient, K_d	61
III B.3.2 The Langmuir Model.....	61
III B.3.3 The Freundlich Isotherm.....	61
III B.3.4 Mechanistic Models for Predicting Sorption - Surface Complexation.....	62
III B.3.5 Mineral Solubility.....	63
III B.3.5.1 Coprecipitation Reactions.....	64
III B.3.5.2 Thermodynamic Data	65
III C.Characterization of System Redox and Underlying Microbial Processes.....	66
III C.1 Process Identification.....	66
III C.1.1 Redox Measurements.....	67
III C.2 Capacity	68
III C.3 Stability	69
III C.4 Microbial Community Characterization	70
III C.4.1 Standard and Emerging Techniques.....	70
III C.4.2 Molecular Characterization	70
III C.4.3 Sampling Considerations	71
III C.5 Implications for Natural Attenuation Assessment	71
III D.References.....	72

Figures

Figure 1.1	Conceptual distinction between organic versus inorganic contaminant plume behavior where natural processes are active within the ground-water aquifer.....	5
Figure 1.2	Conceptual depiction of the data collection effort to demonstrate whether sorption to aquifer solids attenuates contaminant transport in ground water.....	6
Figure 1.3	Example of a network design for performance monitoring, including target zones for monitoring effectiveness with respect to specific remedial objectives.	15
Figure 2.1	Conceptual view of attenuation as the interaction of the contaminant with aquifer constituents to form a product resulting in attenuation.....	25
Figure 2.2	Cross-sectional view of differences in solute migration due to differences in hydraulic conductivity with accompanying differences in ground-water velocity and the spreading of the solute front caused by dispersion.....	26
Figure 2.3.	Representation of an aquifer mineral surface with (a) an outer-sphere surface complex; (b) an inner-sphere surface complex; (c) a multinuclear surface complex or a surface precipitate; and (d) absorption, or solid state diffusion and substitution of the sorbate in the mineral structure.....	28
Figure 2.4	Examples of contaminant-specific sorption processes that may lead to attenuation of the ground-water plume.....	29
Figure 2.5	Diagrammatic sketch of the structure of 1:1 and 2:1 phyllosilicate minerals.	30
Figure 2.6	Surface charge of some hydroxides from pH 2 to 10 measured in different electrolyte solutions shown in parentheses; positive and negative surface charge shown above and below the x-axis, respectively.....	31
Figure 3.1	Geologic block diagram and cross section depicting a stream environment.	45
Figure 3.2	Potential effects of changes in ground-water flow direction on temporal trends in contaminant concentrations.....	46
Figure 3.3	Elements of a conceptual site model for monitored natural attenuation of inorganic contaminants.	49
Figure 3.4	Illustration of two approaches for determining attenuation rate constants within a contaminant plume.	50
Figure 3.5	pH-dependent solubility trend of orpiment predicted using two different Gibbs free energy of formation values.	65

Tables

Table 1.1	Synopsis of site characterization objective to be addressed throughout the tiered analysis process and potential supporting data types and/or analysis approaches associated with each tier	9
Table 1.2	Example software packages for modeling groundwater flow and mass transport	15
Table 1.3	Example software packages for speciation in inorganic geochemical systems	15
Table 1.4	Example software packages for modeling reactive transport in inorganic geochemical systems.	16
Table 1.5	Example internet sources of thermodynamic data useful in constructing geochemical models	16
Table 1.6	Objectives for performance monitoring of MNA.....	18
Table 2.1	Important functional groups in humic substances that impact surface charging behavior and contaminant binding.....	32
Table 2.2	Major mineral classes in aquifers and soils	34
Table 2.3	Relationships among Q, K, and Ω	35
Table 2.4	Range of hydrogen concentrations for a given terminal electron-accepting process that can be used for classification of the redox status within the contaminant plume	38
Table 3.1	Sequential extraction procedure of Tessier et al. (1979)	56
Table 3.2	Summary of reagents used to selectively dissolve iron oxides and sulfides	57
Table 3.3	BCR extraction scheme applied to 1 gram of sample	58
Table 3.4	Synopsis of the various surface complexation models (SCMs) commonly employed to describe solute partitioning to solid surfaces	62
Table 3.5	Ground-water redox parameters and measurement approaches	67
Table 3.6	Methods that may be employed for estimating the oxidation and reduction capacity for solid materials (from USEPA, 2002)	68
Table 3.7	Standard and emerging techniques for microbial community characterization	70

Acknowledgments

This document represents a collective work of many individuals with expertise in the policy and technical aspects of selecting and implementing cleanup remedies at sites with contaminated ground water. Preparation of the various components of this document was undertaken by personnel from the USEPA Office of Research and Development (ORD), Office of Superfund Remediation and Technology Innovation (OSRTI), and Office of Radiation and Indoor Air (ORIA), as well as technical experts whose participation was supported under USEPA Contract No. 68-C-02-092 to Dynamac Corporation, Ada, Oklahoma, through funds provided by ORIA and OSRTI. Contributing authors are listed below along with their affiliation:

Contributing Author	Affiliation
Richard T. Wilkin	USEPA/ORD, National Risk Management Research Laboratory, Ada, OK 74820
Kenneth Lovelace	USEPA/OSWER/OSRTI, Washington, DC 20460 (deceased)
Stuart Walker	USEPA/OSWER/OSRTI, Washington, DC 20460
Ronald Wilhelm	USEPA/OAR/ORIA, Washington, DC 20460
Steven Acree	USEPA/ORD, National Risk Management Research Laboratory, Ada, OK 74820
Steve Mangion	USEPA/ORD/OSP, Region 1, Boston, MA 02114
Robert W. Puls	USEPA/ORD, National Risk Management Research Laboratory, Ada, OK 74820
Ann Azadpour-Keeley	USEPA/ORD, National Risk Management Research Laboratory, Ada, OK 74820
Robert G. Ford	USEPA/ORD, National Risk Management Research Laboratory, Cincinnati, OH 45268
Patrick V. Brady	Sandia National Laboratories, Geochemistry Department (MS-0750), Albuquerque, New Mexico 87185
James E. Amonette	Pacific Northwest National Laboratory, Fundamental Science Directorate, Richland, WA 99352
Paul M. Bertsch	University of Kentucky, College of Agriculture, Lexington, KY 40506
Craig Bethke	University of Illinois, Department of Geology, Urbana, IL 61801
Douglas B. Kent	U.S. Geological Survey, McKelvey Building (MS-465), Menlo Park, CA 94025

Critical and constructive reviews were provided by Jim Weaver (USEPA/ORD National Exposure Research Laboratory, Athens, GA), George Redden (Idaho National Laboratory, Battelle Energy Alliance), and Sue Clark (Washington State University, Chemistry Department). Pat Bush (Ada, OK) is acknowledged for her technical editing to provide consistency in formatting and grammar. Martha Williams (Contract #68-W-01-032) assisted with final editing and formatting for publication. This effort is dedicated to the memory of Kenneth Lovelace, whose insight and patience made it a reality.

Executive Summary

The term “monitored natural attenuation,” as used in this document and in the Office of Solid Waste and Emergency Response (OSWER) Directive 9200.4-17P, refers to “the reliance on natural attenuation processes (within the context of a carefully controlled and monitored site cleanup approach) to achieve site-specific remediation objectives within a time frame that is reasonable compared to that offered by other more active methods.” When properly employed, monitored natural attenuation (MNA) may provide an effective knowledge-based remedy where a thorough engineering analysis informs the understanding, monitoring, predicting, and documenting of the natural processes. In order to properly employ this remedy, the Environmental Protection Agency needs a strong scientific basis supported by appropriate research and site-specific monitoring implemented in accordance with the Agency's Quality System. The purpose of this series of documents, collectively titled “Monitored Natural Attenuation of Inorganic Contaminants in Ground Water,” is to provide a technical resource for remedial site managers to define and assess the potential for use of site-specific natural processes to play a role in the design of an overall remedial approach to achieve cleanup objectives.

The current document represents the first volume of a set of three volumes that address the technical basis and requirements for assessing the potential applicability of MNA as part of a ground-water remedy for plumes with non-radionuclide and/or radionuclide inorganic contaminants. Volume 1, titled “Technical Basis for Assessment,” consists of three sections that describe 1) the conceptual background for natural attenuation for inorganic contaminants, 2) the technical basis for attenuation of inorganic contaminants in ground water, and 3) approaches to site characterization to support evaluation of MNA. Emphasis is placed on characterization of immobilization and/or degradation processes that may control contaminant attenuation, as well as technical approaches to assess performance characteristics of the MNA remedy. A tiered analysis approach is presented to assist in organizing site characterization tasks in a manner designed to reduce uncertainty in remedy selection while distributing costs to address four primary issues:

1. Demonstration of active contaminant removal from ground water & dissolved plume stability;
2. Determination of the mechanism and rate of attenuation;
3. Determination of the long-term capacity for attenuation and stability of immobilized contaminants; and
4. Design of performance monitoring program, including defining triggers for assessing MNA failure, and establishing a contingency plan.

Detailed discussion is provided on the importance of acquiring site-specific data that define ground-water hydrogeology and chemistry, the chemical and mineralogical characteristics of aquifer solids, and the aqueous and solid phase chemical speciation of contaminants within the ground-water plume boundary. Technical distinctions are drawn between characterization efforts to evaluate the applicability of MNA as part of a cleanup remedy for organic versus inorganic contaminants. Emphasis is placed on the need to collect site-specific data supporting evaluation of the long-term stability of immobilized inorganic contaminants. Also included is discussion on the role of analytical models as one of the tools that may be employed during the site characterization process. This discussion is intended to provide context to contaminant-specific site characterization approaches recommended in the remaining two volumes of this document.

This document is limited to evaluations performed in porous-media settings. Detailed discussion of performance monitoring system design in fractured rock, karst, and other such highly heterogeneous settings is beyond the scope of this document. Ground water and contaminants often move preferentially through discrete pathways (e.g., solution channels, fractures, and joints) in these settings. Existing techniques

may be incapable of fully delineating the pathways along which contaminated ground water migrates. This greatly increases the uncertainty and costs of assessments of contaminant migration and fate and is another area of continuing research. As noted in OSWER Directive 9200.4-17P, "MNA will not generally be appropriate where site complexities preclude adequate monitoring." The directive provides additional discussion regarding the types of sites where the use of MNA may be appropriate.

This document focuses on monitoring the saturated zone, but site characterization and monitoring for MNA or any other remedy typically would include monitoring of all significant pathways by which contaminants may move from source areas and contaminant plumes to impact receptors (e.g., surface water and indoor air).

Nothing in this document changes Agency policy regarding remedial selection criteria, remedial expectations, or the selection and implementation of MNA. This document does not supersede any guidance. It is intended for use as a technical reference in conjunction with other documents, including OSWER Directive 9200.4-17P, "Use of Monitored Natural Attenuation at Superfund, RCRA Corrective Action, and Underground Storage Tank Sites" (<http://www.epa.gov/swerust1/directiv/d9200417.pdf>).

Section I

Conceptual Background for Monitored Natural Attenuation

Kenneth Lovelace, Stuart Walker, Ronald Wilhelm, Robert Puls, Robert G. Ford, Richard T. Wilkin, Steven Acree, Steve Mangion, Patrick V. Brady, Craig Bethke

IA. Background and Purpose

IA.1 Document Organization

The purpose of this document is to provide a framework for assessing the potential application of monitored natural attenuation as part of the remedy for inorganic contaminant plumes in ground water. It is organized into three volumes that provide: Volume 1 - a general overview of the framework and technical requirements for application of Monitored Natural Attenuation (MNA); Volume 2 - contaminant-specific discussions addressing potential attenuation processes and site characterization requirements for non-radionuclides, and Volume 3 - contaminant-specific discussions addressing potential attenuation processes and site characterization requirements for radionuclides. Volume 1 is divided into three sections that address the regulatory and conceptual background for natural attenuation, the technical basis for natural attenuation of inorganic contaminants, and site characterization approaches to support assessment and application of MNA. The contaminant-specific chapters in Volumes 2 and 3 provide an overview of contaminant geochemistry, applicable natural attenuation processes, and specific site characterization requirements. Criteria for selecting specific contaminants for these detailed overviews are described below.

The non-radionuclide contaminants selected for this document include: arsenic (As), cadmium (Cd), chromium (Cr), copper (Cu), lead (Pb), nickel (Ni), nitrate, perchlorate, and selenium (Se). The selection of these contaminants by USEPA was based on several criteria. First, a 1994 booklet containing information regarding common chemicals found at Superfund sites throughout the nation was consulted (USEPA, 1994). The most commonly found inorganic contaminants were included for consideration in this document. Another document specific to metal-contaminated Superfund sites (USEPA, 1995) identified arsenic (As), cadmium (Cd), chromium (Cr), and lead (Pb) as primary contaminants of concern based on toxicity, industrial use, and frequency of occurrence at Superfund sites. Second, selection was based on chemical behavior considering chemical traits such as: toxicity, ion charge (cation vs. anion), transport behavior (conservative vs. non-conservative), and redox chemistry to cover a broad range of geochemical behavior (USEPA, 1999a; USEPA, 1999b; USEPA, 2004). Finally, USEPA regional staff were asked to nominate inorganic contaminants that occurred frequently or that were problematic in their Regions. The above list of nine inorganic contaminants was selected from this process.

The radionuclide contaminants selected for this document include: americium (Am), cesium (Cs), iodine (I), neptunium (Np), plutonium (Pu), radium (Ra), radon (Rn), technetium (Tc), thorium (Th), tritium, strontium (Sr), and uranium (U). The selection of these contaminants by EPA was based on two criteria. First, a selected element had to be one of high priority to the site remediation or risk assessment activities of the USEPA (USEPA, 1993; USEPA, 2002). Second, selection was based on chemical behavior considering chemical traits such as: toxicity, cations, anions, conservatively transported, non-conservatively transported, and redox sensitive elements (USEPA, 1999b; USEPA, 2004). By using these characteristics of the contaminants, the general geochemical behavior of a wide range of radionuclide contaminants could be covered as well as the chemical classes that make up the Periodic Table. In addition, this selection accounts for many daughter and fission product contaminants that result from radioactive decay. This is important as the decay of radioisotopes can produce daughter products that may differ both physically and chemically from their parents. The selection of radionuclide contaminants for this document is representative of these characteristics.

IA.2 Purpose of Document

This document is intended to provide a technical resource for determining whether MNA is likely to be an effective remedial approach for inorganic contaminants¹ in ground water. This document is intended to be used during the remedial investigation and feasibility study phases of a Superfund cleanup, or during the equivalent phases of a RCRA Corrective Action (facility investigation and corrective measures study, respectively). The decision to select MNA as the remedy (or part of the remedy) will be made in a Superfund Record of Decision (ROD) or a RCRA Statement of Basis (or RCRA permit).

The USEPA expects that users of this document will include USEPA and State cleanup programs and their contractors, especially those individuals responsible for evaluating alternative cleanup methods for a given site or facility. The overall policy for use of MNA in OSWER cleanup programs is described in the April 21, 1999 OSWER Directive titled, "Use of Monitored Natural Attenuation at Superfund, RCRA Corrective Action and Underground Storage Tank Sites" (Directive No. 9200.4-17P).

¹ The term "inorganic contaminants" is used in this document as a generic term for metals and metalloids (such as arsenic); and also refers to radiologic as well as non-radiologic isotopes.

Both radiological and non-radiological inorganic contaminants are discussed in this document. There are two reasons for this. First, except for radioactive decay, the potential attenuation processes affecting inorganic contaminants are the same for both contaminant types. Second, several OSWER directives clarify the USEPA's expectation that the decision-making approach and cleanup requirements used at CERCLA sites will be the same for sites with radiological and non-radiological inorganic contaminants, except where necessary to account for the technical differences between the two types of contaminants. Also, the 1999 OSWER Directive specified that the decision process for evaluating MNA as a potential remediation method should be the same for all OSWER cleanup programs.

This document is intended to provide an approach for evaluating MNA as a possible cleanup method for contaminated ground water. Although the focus of the document is on ground water, the unsaturated zone is discussed as a source of contaminants to ground water. Emphasis is placed on developing a more complete evaluation of the site through development of a conceptual site model² based on an understanding of the attenuation mechanisms, the geochemical conditions governing these mechanisms, the capacity of the aquifer to sustain attenuation of the contaminant mass and prevent future contaminant migration, and indicators that can be used to monitor MNA performance.

This document focuses on technical issues and is not intended to address policy considerations or specific regulatory or statutory requirements. The USEPA expects that this document will be used in conjunction with the 1999 OSWER Directive (USEPA, 1999c). Users of this document should realize that different Federal and State remedial programs may have somewhat different remedial objectives. For example, the CERCLA and RCRA Corrective Action programs generally require that remedial actions: 1) prevent exposure to contaminated ground water, above acceptable risk levels; 2) minimize further migration of the plume; 3) minimize further migration of contaminants from source materials; and 4) restore ground-water conditions to cleanup levels appropriate for current or future beneficial uses, to the extent practicable. Achieving such objectives could often require that MNA be used in conjunction with other "active" remedial methods. For other cleanup programs, remedial objectives may be focused on preventing exposures above acceptable levels. Therefore, it is imperative that users of this document be aware of and understand the Federal and State statutory and regulatory requirements, as well as policy considerations that apply to a specific site for which this document will be used to evaluate MNA as a remedial option. As a general practice, individuals responsible for evaluating remedial alternatives should check with the over-

² A conceptual site model is a three-dimensional representation that conveys what is known or suspected about contamination sources, release mechanisms, and the transport and fate of those contaminants. The conceptual model provides the basis for assessing potential remedial technologies at the site. "Conceptual site model" is **not** synonymous with "computer model"; however, a computer model may be helpful for understanding and visualizing current site conditions or for predictive simulations of potential future conditions.

seeing regulatory agency to identify likely characterization and cleanup objectives for a particular site prior to investing significant resources.

Use of this document is generally inappropriate in complex fractured bedrock or karst aquifers. In these situations the direction of ground water flow can not be predicted directly from the hydraulic gradient, and existing techniques may not be capable of identifying the pathway along which contaminated groundwater moves through the subsurface. Understanding the contaminant flow field in the subsurface is essential for a technically justified evaluation of an MNA remedial option. MNA will not generally be appropriate where site complexities preclude adequate monitoring (USEPA, 1999c).

Because documentation of natural attenuation requires detailed site characterization, the data collected can be used to compare the relative effectiveness of other remedial options and natural attenuation. The technical information contained in this document can be used as a point of reference to evaluate whether MNA by itself, or in conjunction with other remedial technologies, is sufficient to achieve site-specific remedial objectives.

IA.3 Applicable Regulatory Criteria

All remedial actions at CERCLA sites must be protective of human health and the environment and comply with applicable or relevant and appropriate requirements (ARARs) unless a waiver is justified. Cleanup levels for response actions under CERCLA are developed based on site-specific risk assessments, ARARs, and/or to-be-considered material (TBCs). The determination of whether a requirement is applicable, or relevant and appropriate, must be made on a site-specific basis (see 40 CFR §300.400(g)).

"EPA expects to return usable ground waters to their beneficial uses whenever practicable" (see 40 CFR §30 0.430(a)(1)(iii)(F)). In general, drinking water standards provide relevant and appropriate cleanup levels for ground waters that are a current or potential source of drinking water. However, drinking water standards generally are not relevant and appropriate for ground waters that are not a current or potential source of drinking water (see 55 FR 8732, March 8, 1990). Drinking water standards include federal maximum contaminant levels (MCLs) and/or non-zero maximum contaminant level goals (MCLGs) established under the Safe Drinking Water Act (SDWA), or more stringent state drinking water standards. Other regulations may also be ARARs as provided in CERCLA §121(d)(2)(B).

IA.4 Policy Framework for Use of MNA

The term "monitored natural attenuation" is used in this document when referring to a particular approach to remediation. MNA is defined in the 1999 OSWER Directive as follows:

"...the reliance on natural attenuation processes (within the context of a carefully controlled and monitored site cleanup approach) to achieve site-

specific remediation objectives within a time frame that is reasonable compared to that offered by other more active methods. The 'natural attenuation processes' that are at work in such a remediation approach include a variety of physical, chemical, or biological processes that, under favorable conditions, act without human intervention to reduce the mass, toxicity, mobility, volume, or concentration of contaminants in soil or groundwater. These in-situ processes include biodegradation; dispersion; dilution; sorption; volatilization; radioactive decay; and chemical or biological stabilization, transformation, or destruction of contaminants. (USEPA, 1999c, page 3.)

Even though several physical, chemical, and biological processes are included in the above definition, the 1999 OSWER Directive goes on to state a preference for those processes that permanently degrade or destroy contaminants, and for use of MNA for stable or shrinking plumes, as noted below:

"When relying on natural attenuation processes for site remediation, EPA prefers those processes that degrade or destroy contaminants. Also, EPA generally expects that MNA will only be appropriate for sites that have a low potential for contaminant migration." (USEPA, 1999c, page 3.)

*"MNA should not be used where such an approach would result in either plume migration or impacts to environmental resources that would be unacceptable to the overseeing regulatory authority. **Therefore, sites where the contaminant plumes are no longer increasing in extent, or are shrinking, would be the most appropriate candidates for MNA remedies.**" (USEPA, 1999c, page 18.)*

Control of contaminant sources is also an important aspect of EPA's policy. The actual policy language is given below:

*"Control of source materials is the most effective means of ensuring the timely attainment of remediation objectives. **EPA, therefore, expects that source control measures will be evaluated for all contaminated sites and that source control measures will be taken at most sites where practicable.** At many sites it will be appropriate to implement source control measures during the initial stages of site remediation ("phased remedial approach"), while collecting additional data to determine the most appropriate groundwater remedy." (USEPA, 1999c, page 22.)*

The 1999 OSWER Directive also provides a few general guidelines for use of MNA as a remedial approach for inorganic contaminants. The key policy concerns are that the specific mechanisms responsible for attenuation of inorganic contaminants should be known at a particular site, and the stability of the process should be evaluated and shown to be protective under anticipated changes in site

conditions. The actual policy language is given below:

MNA may, under certain conditions (e.g., through sorption or oxidation-reduction reactions), effectively reduce the dissolved concentrations and/or toxic forms of inorganic contaminants in groundwater and soil. Both metals and non-metals (including radionuclides) may be attenuated by sorption³ reactions such as precipitation, adsorption on the surfaces of soil minerals, absorption into the matrix of soil minerals, or partitioning into organic matter. Oxidation-reduction (redox) reactions can transform the valence states of some inorganic contaminants to less soluble and thus less mobile forms (e.g., hexavalent uranium to tetravalent uranium) and/or to less toxic forms (e.g., hexavalent chromium to trivalent chromium). Sorption and redox reactions are the dominant mechanisms responsible for the reduction of mobility, toxicity, or bioavailability of inorganic contaminants. It is necessary to know what specific mechanism (type of sorption or redox reaction) is responsible for the attenuation of inorganics so that the stability of the mechanism can be evaluated. For example, precipitation reactions and absorption into a soil's solid structure (e.g., cesium into specific clay minerals) are generally stable, whereas surface adsorption (e.g., uranium on iron-oxide minerals) and organic partitioning (complexation reactions) are more reversible. Complexation of metals or radionuclides with carrier (chelating) agents (e.g., trivalent chromium with EDTA) may increase their concentrations in water and thus enhance their mobility. Changes in a contaminant's concentration, pH, redox potential, and chemical speciation may reduce a contaminant's stability at a site and release it into the environment. Determining the existence, and demonstrating the irreversibility, of these mechanisms is important to show that a MNA remedy is sufficiently protective.

In addition to sorption and redox reactions, radionuclides exhibit radioactive decay and, for some, a parent-daughter radioactive decay series. For example, the dominant attenuating mechanism of tritium (a radioactive isotopic form of hydrogen with a short half-life) is radioactive decay rather than sorption. Although tritium does not generate radioactive daughter products, those generated by some radionuclides (e.g., Am-241 and Np-237 from Pu-241) may be more toxic, have longer half-lives, and/or be more mobile than the parent in the decay series. Also, it is important that the near surface or

³ When a contaminant is associated with a solid phase, it is usually not known if the contaminant is precipitated as a three-dimensional molecular coating on the surface of the solid, adsorbed onto the surface of the solid, absorbed into the structure of the solid, or partitioned into organic matter. "Sorption" will be used in this Directive to describe, in a generic sense (i.e., without regard to the precise mechanism) the partitioning of aqueous phase constituents to a solid phase.

surface soil pathways be carefully evaluated and eliminated as potential sources of external direct radiation exposure.⁴

Inorganic contaminants persist in the subsurface because, except for radioactive decay, they are not degraded by the other natural attenuation processes. Often, however, they may exist in forms that have low mobility, toxicity, or bioavailability such that they pose a relatively low level of risk. Therefore, natural attenuation of inorganic contaminants is most applicable to sites where immobilization or radioactive decay is demonstrated to be in effect and the process/mechanism is irreversible. (USEPA, 1999c, pages 8-9.)

The 1999 OSWER Directive provides the context for the Agency's expectations for evaluating the feasibility of employing MNA as part of a cleanup remedy for contaminated ground water. As indicated by the sections from the Directive that are transcribed above, it also points out specific issues concerning what constitutes natural attenuation for inorganic contaminants. In practice, most of the technical experience developed to date has primarily dealt with evaluations of MNA as applied to remediation of organic contaminant plumes. While this experience provides some perspective for the scope of site characterization that may be warranted to evaluate MNA for inorganic contaminants, there are some important distinctions that bear on the types of required data and the approaches available to obtain these data. The following section elaborates these distinctions in order to provide context for the technical aspects relevant to MNA for inorganic contaminants and the steps needed to implement a technically defensible site characterization effort.

IB. Relevant Distinctions in Site Characterization for MNA of Inorganic Contaminants

As stated within the OSWER Directive on MNA (USEPA, 1999c), natural attenuation processes are those that 'reduce mass, toxicity, mobility, volume or concentration of contaminants'. Inorganic contaminants discussed within this document include both non-radioactive and radioactive constituents. For radioactive contaminants, radioactive decay processes result in the reduction of risk derived from radiation exposure. The rates of radioactive decay (characterized by the decay half-life) are known for the radioisotopes of concern, thus facilitating this aspect of site characterization. Guidelines for assessing the feasibility of MNA as a component of ground-water cleanup for radio-

nuclides are provided in Volume 3 of this document. For non-radioactive inorganic contaminants and radionuclides possessing long decay half-lives, *immobilization* within the aquifer via sorption to aquifer solids provides the primary means for attenuation of the ground-water plume. In general, an inorganic contaminant can be transferred between solid, liquid, or gaseous phases present within the aquifer, but the contaminant will always be present. Contaminant immobilization will prevent transport to sensitive receptors at points of compliance. There are limited examples where *degradation* of inorganic contaminants may be a viable attenuation process (e.g., biological degradation of nitrate or perchlorate), but degradation is not a viable process for most of the inorganic contaminants discussed in this document. For inorganic contaminants subject to degradation or reductive transformation processes, the supporting site characterization will likely be consistent with the approach employed to assess MNA for organic contaminant plumes (e.g., USEPA, 1998; USEPA, 2001; see also specific discussions for nitrate and perchlorate in Volume 2). The following discussion provides context for the potential significance of immobilization as a means for natural attenuation of inorganic contaminants in ground water.

There is an important distinction between site characterization as applied to assessment of MNA for organic and inorganic contaminants. For organic contaminants, site characterization typically is focused towards determining the mechanism of contaminant degradation and the capacity of site conditions to sustain degradation for treatment of the mass of contaminant within the plume. This analysis may include identification of ground-water characteristics and degradation byproducts that are characteristic for contaminant degradation. Thus, much of the emphasis on site characterization for MNA of organic contaminants has been directed towards the collection and analysis of ground-water samples. In some cases, this characterization effort may have been supplemented with the analysis of contaminant degradation behavior through the use of microcosm experiments employing aquifer solids collected within the plume boundary. For inorganic contaminants in which immobilization onto aquifer solids provides the primary means for attenuation of the ground-water plume, characterization of the solid substrate within the aquifer plays a more significant role during site assessment. In this case risk reduction in ground water is realized through the sorption of the inorganic contaminant onto aquifer solids in combination with the long-term stability of the immobilized contaminant to resist remobilization due to changes in ground-water chemistry. The importance of this distinction between natural attenuation for organic and inorganic contaminants is emphasized in Figure 1.1. In essence, for inorganic contaminants one can consider the existence of two distinct 'plumes' within the boundary of the ground-water plume: 1) the dissolved or "mobile" plume (including dissolved contaminant and contaminant associated with mobile colloids), and 2) the solid phase or "immobile" plume resulting from sorption of the contaminant to aquifer solids (Figure 1.1). Thus, for inorganic contaminants there are two overriding objectives to address through site characterization:

⁴ External direct radiation exposure refers to the penetrating radiation (i.e., primarily gamma radiation and x-rays) that may be an important exposure pathway for certain radionuclides in near surface soils. Unlike chemicals, radionuclides can have deleterious effects on humans without being taken into or brought in contact with the body due to high-energy particles emitted from near surface soils. Even though the radionuclides that emit penetrating radiation may be immobilized due to sorption or redox reactions, the resulting contaminated near surface soil may not be a candidate for a MNA remedy as a result of this exposure risk.

- 1) Demonstration of removal of the inorganic contaminant from the dissolved phase leading to a stable or shrinking ground-water plume and,
- 2) Demonstration of stabilization of the inorganic contaminant immobilized onto aquifer solids such that future re-mobilization will not occur to a level that threatens health of environmental receptors.

Evaluating the overall success of natural attenuation for inorganic contaminant remediation will require demonstrating that the rate and capacity for inorganic contaminant attenuation meets regulatory objectives and, in addition, that inorganic contaminant immobilization is sustainable to the extent that future health risks are eliminated. The latter requirement necessitates identifying the chemical speciation of the inorganic contaminant partitioned to the solid phase. This information is critical towards identifying the process controlling attenuation and evaluating the long-term stability of the immobilized contaminant relative to observed or anticipated changes in ground-water chemistry.

Site characterization to support evaluation of MNA as a remedial alternative will involve assessment of contaminant transport in the aquifer. In general terms, this process will include assessment of ground-water hydrology and the biogeochemical processes that control contaminant migration within the plume. Defining the processes that control contaminant immobilization (or degradation) along the paths of ground-water flow will necessitate collection of a range of data that define the dynamics of system hydrology, the chemical characteristics of ground water, and the properties of the aquifer solids. In order to screen out sites that

are inappropriate for selection of MNA, it is recommended that collection of site-specific data be conducted in stages that serve to minimize expenditures while providing insight into the potential existence of natural processes that may attenuate contaminant migration. Description of a tiered analysis approach for organizing site characterization tasks is provided in the following section.

IC. Tiered Analysis Approach to Site Characterization

Site characterization to support evaluation and selection of MNA as part of a cleanup action for inorganic contaminant plumes in ground water will involve a detailed analysis of site characteristics controlling and sustaining attenuation. The level of detailed data that may be required to adequately characterize the capacity and stability of natural processes to sustain plume attenuation will likely necessitate significant resource outlays. Thus, it is recommended that site characterization be approached in a step-wise manner to facilitate collection of data necessary to progressively evaluate the existing and long-term effectiveness of natural attenuation processes within the aquifer. Implementation of a *tiered analysis approach* provides an effective way to screen sites for MNA that is cost effective because it prioritizes and limits the data that is needed for decision making at each screening step. Conceptually a tiered analysis approach seeks to progressively reduce uncertainty as site-specific data are collected. The decision-making approach presented in this document includes three decision tiers that require progressively greater information on which to assess the likely effectiveness of MNA as a remedy for

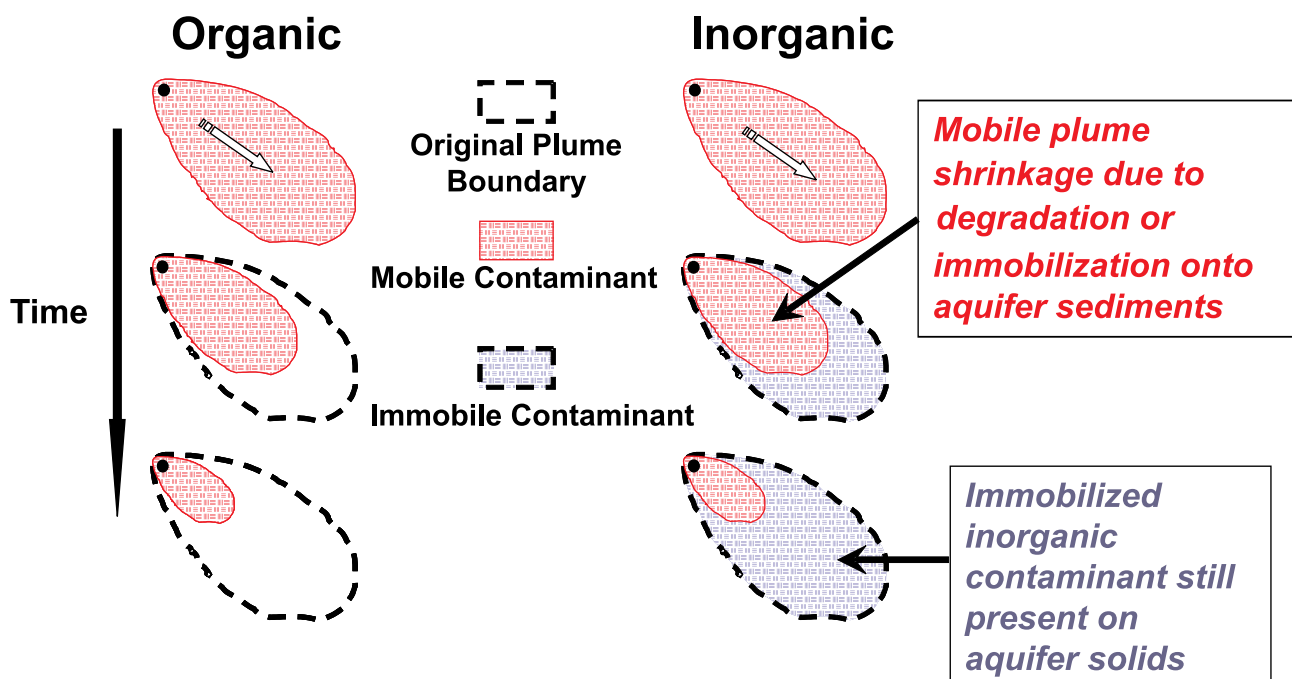


Figure 1.1 *Conceptual distinction between organic versus inorganic contaminant plume behavior where natural processes are active within the ground-water aquifer. Natural attenuation of inorganic contaminants is viable only if the immobilized contaminant remains stable and resistant to remobilization during changes in ground-water chemistry.*

inorganic contaminants in ground water. The fourth tier is included to emphasize the importance of determining appropriate parameters for long-term performance monitoring, once MNA has been selected as part of the remedy. Data collection and evaluation within the tiered analysis approach would be structured as follows:

- I. Demonstration that the ground-water plume is not expanding and that sorption of the contaminant onto aquifer solids is occurring where immobilization is the predominant attenuation process;
- II. Determination of the *mechanism and rate* of the attenuation process;
- III. Determination of the *capacity* of the aquifer to attenuate the mass of contaminant within the plume and the *stability* of the immobilized contaminant to resist re-mobilization, and;
- IV. Design performance monitoring program based on the mechanistic understanding developed for the attenuation process, and establish a contingency plan tailored to site-specific characteristics.

Elaboration on the objectives to be addressed and the types of site-specific data to be collected under each successive tier is provided below.

IC.1 Tier I

The objective under Tier I analysis would be to eliminate sites where site characterization indicates that the ground-water plume is continuing to expand in aerial or vertical extent. For contaminants in which sorption onto aquifer solids is the most feasible attenuation process, an additional objective would be to demonstrate contaminant uptake onto aquifer solids. Analysis of ground-water plume behavior at this stage is predicated on adequate aerial and vertical delineation of the plume boundaries. Characterization of ground-water plume expansion could then be supported through analysis of current and historical data collected from monitoring wells installed along the path of ground-water flow. An increasing temporal trend in contaminant concentration in ground-water at monitoring locations down gradient from a source area is indicative that attenuation is not occurring sufficient to prevent ground-water plume expansion. Determination of contaminant sorption onto aquifer solids could be supported through the collection of aquifer cores coincident with the locations of ground-water data collection and analysis of contaminant concentrations on the retrieved aquifer solids. Illustration of the type of data trend anticipated for a site where sorption actively attenuates contaminant transport is provided in Figure 1.2. The spatial distribution in aqueous and solid contaminant

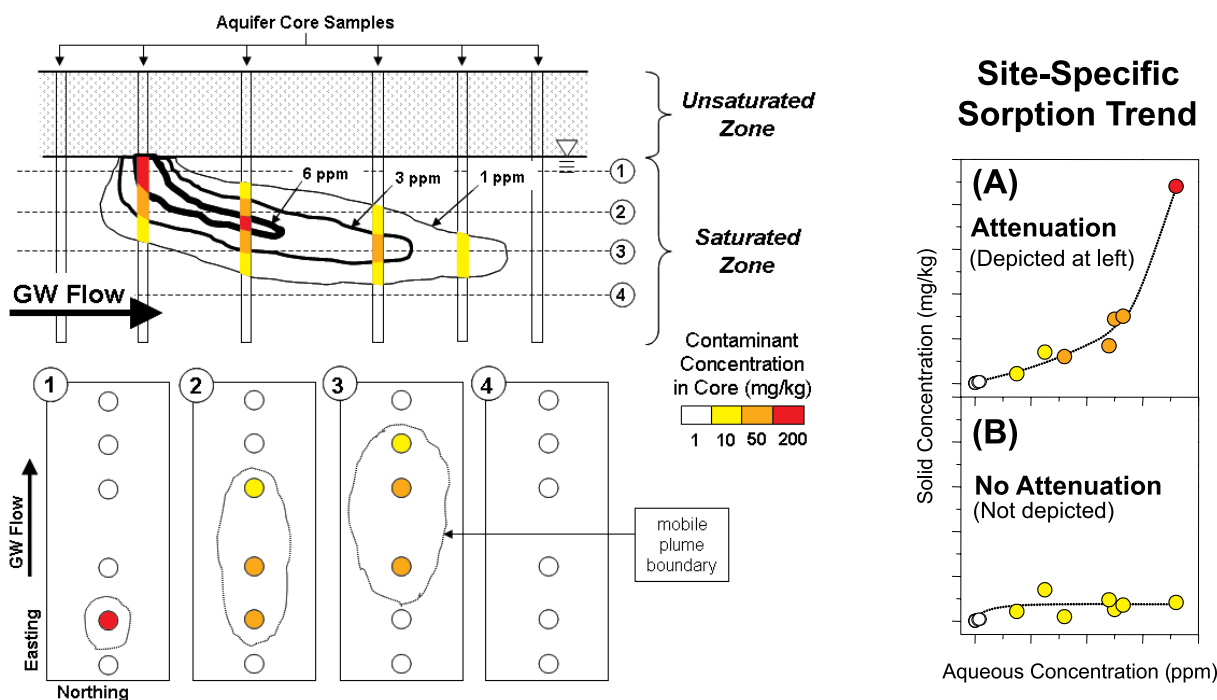


Figure 1.2 Conceptual depiction of the data collection effort to demonstrate whether sorption to aquifer solids attenuates contaminant transport in ground water. The left side of the diagram provides a cross-sectional view of the spatial distribution of the contaminant concentration in ground water and co-located aquifer solids for a site where sorption attenuates contaminant transport. The trend in aqueous and solid contaminant concentrations for this scenario is depicted in Panel (A) to the right. Panel (B) depicts the relationship between aqueous and solid contaminant concentrations for a site where sorption does not attenuate contaminant transport.

concentrations for a site where sorption attenuates contaminant migration is depicted on the left side of the illustration. Anticipated relationships between aqueous and solid contaminant concentrations for sites with and without active contaminant attenuation via sorption are depicted on the right side of the illustration in Panels (A) and (B), respectively. Specifically, where sorption onto aquifer solids is occurring, there should be an increasing trend in solid phase contaminant concentrations as a function of increasing aqueous concentration. In contrast, no change in solid phase contaminant concentrations as a function of increasing aqueous concentration is indicative that attenuation is not occurring. Ultimately, sites that demonstrate ground-water plume expansion and a lack of contaminant sorption (for contaminants subject to sorption) would be eliminated from further consideration of MNA as part of the cleanup remedy.

IC.2 Tier II

The objective under Tier II analysis would be to eliminate sites where further analysis shows that attenuation rates are insufficient for attaining cleanup objectives established for the site within a timeframe that is reasonable compared to other remedial alternatives. (see USEPA, 1999c, pages 19-21, for a discussion of “reasonable timeframe for remediation”.) Data collection and analysis performed for Tier II would indicate whether MNA processes are capable of achieving remediation objectives, based on current geochemical conditions at the site. This data collection effort would also be designed to support identification of the specific mechanism(s) controlling contaminant attenuation.

An estimate of attenuation rates for inorganic contaminants will typically involve calculation of the apparent transfer of mass from the aqueous to the solid phase, based on sampling of ground water and/or aquifer solids. It is recommended that these estimates be based as much as possible on field measurements rather than modeling predictions. A recommended approach is to identify hydrostratigraphic units for the site and develop a ground water flow model which can be used to estimate ground water seepage velocities in each of these units (Further information on ground water flow models is provided in Section I.D.) These seepage velocities can be combined with measured contaminant concentrations to estimate mass flux (mass per time per area) for each contaminant, in each hydrostratigraphic unit. The necessary data might include physical parameters such as hydraulic conductivities within the aquifer and hydraulic gradients. Changes in mass flux can then be used to estimate mass loss from the aqueous phase since the last sampling event, which is assumed to be the apparent attenuation rate. (Further information on estimating attenuation rates is provided in Section IIIA.5.)

Determination of attenuation mechanism will depend on collection of data to define ground-water chemistry, aquifer solids composition and mineralogy, and the chemical speciation of the contaminant in ground water and associated aquifer solids. This will entail a significant effort in the site-specific data collection effort, but provides the

underpinning for further evaluation of the performance of MNA to be addressed in subsequent stages of the site characterization process. The goal of this characterization effort is to identify the aqueous and solid phase constituents within the aquifer that control contaminant attenuation. This data collection effort may include collection of field water quality data (e.g., pH, dissolved oxygen, alkalinity, ferrous iron, and dissolved sulfide), laboratory measurements of ground-water and aquifer solids chemical composition, microbial characteristics and/or mineralogy of the aquifer solids (as relevant to degradation or immobilization), and the chemical speciation of the contaminant in ground-water and/or the aquifer solids. Contaminant speciation refers to both oxidation state characterizations [e.g., As(III) vs. As(V)] as well as specific associations with chemical constituents in aquifer solids (e.g., precipitation of Pb carbonate vs. adsorption of Pb to iron oxides). Evaluations of the sub-surface microbiology may be necessary in situations where biotic processes play a direct or indirect role in governing contaminant attenuation. Indirect microbial influence on contaminant attenuation includes situations in which the predominant characteristics of the ground-water chemistry are controlled by microbial oxidation-reduction reactions. This situation may be more predominant in plumes in which readily degradable organic contaminants, such as hydrocarbons or chlorinated solvents, are also present. Ultimately, mechanistic knowledge of the attenuation process along with a detailed knowledge of the ground-water flow field provides the basis for subsequent evaluations to assess the long-term capacity of the aquifer to sustain contaminant attenuation.

IC.3 Tier III

The objective under Tier III would be to eliminate sites where site data and analysis show that there is insufficient capacity in the aquifer to attenuate the contaminant mass to ground-water concentrations that meet regulatory objectives or that the stability of the immobilized contaminant is insufficient to prevent re-mobilization due to future changes in ground-water chemistry. Possible factors that could result in an insufficient capacity for attenuation include:

1. changes in ground-water chemistry result in slower rates of attenuation,
2. insufficient mass flux of aqueous constituents that participate in the attenuation reaction, and/or
3. insufficient mass of solid constituents in aquifer solids that participate in the attenuation reaction.

These factors pertain to situations where either degradation or immobilization is the primary attenuation process. For immobilized contaminants, factors to consider relative to the long-term stability of the attenuated contaminant include changes in ground-water chemistry that could result in release of the contaminant from aquifer solids due to desorption from solid surfaces or dissolution of precipitates. For example, contaminant desorption could be caused by changes in ground-water pH, since the degree of adsorption is typically sensitive to this parameter. Alternatively, dissolution of a contaminant attenuated as a carbonate

precipitate may result from decreases in ground-water pH and alkalinity.

Assessment of attenuation capacity will depend on knowledge of the flux of contaminants and associated reactants in ground-water, as well as the mass distribution of reactive aquifer solids along ground-water flow paths. In order to conduct this type of evaluation, adequate information is needed on the heterogeneity of the ground-water flow field, and the spatial and/or temporal variability in the distribution of aqueous and solids reactants within the plume. For situations where ground-water chemistry is governed by microbial processes, seasonal variations may exert an indirect influence on the effective capacity within the aquifer at any point in time. The general approach that can be taken is to estimate the attenuation capacity within the plume boundaries and compare this capacity with the estimated mass flux of aqueous phase contaminants emanating from source areas based on site-specific data. Exploring alternatives to minimize contaminant release from source areas may prove beneficial for sites that possess insufficient capacity to adequately attenuate the ground-water plume. Ultimately, this points to the critical importance of a detailed characterization of the system hydrology.

Assessment of the stability of an immobilized contaminant can be evaluated through a combination of laboratory testing and chemical reaction modeling within the context of existing and anticipated site conditions. Both analysis approaches can be developed based on the information gathered during Tier II efforts to characterize the specific attenuation process active within the ground-water plume. Through Tier II analysis, a specific attenuation reaction was defined that identified critical reaction parameters such as the identity of dissolved constituents that participated in the process. In addition, mechanistic understanding of the overall reaction provides the context for evaluating site conditions or dissolved constituents that may interfere with or reduce the efficiency of the attenuation reaction. For example, sites where the contaminant plume is reducing (e.g., sulfate-reducing conditions) while ambient ground-water is oxidizing may be susceptible to future influxes of dissolved oxygen. In this situation, the attenuation process may be due to precipitation of sulfides under sulfate-reducing conditions within the plume. Future exposure of these sulfides to oxygen may result in dissolution of the sulfide precipitate along with release of the contaminant back into ground water. Alternatively, sites where attenuation is predominated by contaminant adsorption onto existing aquifer solids may be sensitive to future influx of dissolved constituents due to land use changes that alter either the source or chemical composition of ground-water recharge. The sensitivity to contaminant re-mobilization can be assessed via laboratory tests employing aquifer solids collected from within the plume boundaries that can be exposed to solutions that mimic anticipated ground-water chemistries (e.g., ambient ground-water samples or synthetic solutions in which the concentrations of specific dissolved constituents can be systematically varied). A supplementary avenue to test contaminant stability could include use of chemical reaction models with adequate parameterization to replicate

both the attenuation reaction as well as changes in water composition that may interfere with attenuation. The utility of this type of modeling analysis would be the ability to efficiently explore contaminant solubility under a range of hypothetical ground-water conditions in order to identify the ground-water parameters to which the attenuation reaction may be most sensitive.

It is feasible to consider implementation of MNA as a component of the ground-water remedy if the analysis conducted through the previous Tiers indicates that the aquifer within the plume boundaries supports natural attenuation processes with sufficient efficiency, capacity, and stability. The technical knowledge obtained through identification of the specific attenuation mechanism and the sensitivity of the attenuation process to changes in ground-water chemistry can then be employed in designing a monitoring program that tracks continued performance of the MNA remedy.

IC.4 Tier IV

The objective under Tier IV analysis is to develop a monitoring program to assess long-term performance of the MNA remedy and identify alternative remedies that could be implemented for situations where changes in site conditions could lead to remedy failure. Site data collected during characterization of the attenuation process will serve to focus identification of alternative remedies that best match site-specific conditions. The monitoring program will consist of establishing a network of wells: 1) that provide adequate aerial and vertical coverage to verify that the ground-water plume remains static or shrinks, and 2) that provide the ability to monitor ground-water chemistry throughout the zones where contaminant attenuation is occurring. It is recommended that the performance monitoring program include assessment of the consistency in ground-water flow behavior, so that adjustments to the monitoring network could be made to evaluate the influence of potential changes in the patterns of ground-water recharge to or predominant flow direction within the plume. In addition to monitoring ground-water parameters that track the attenuation reaction, periodic monitoring of parameters that track non-beneficial changes in ground-water conditions is also recommended. Monitoring the attenuation reaction will include continued verification of contaminant removal from ground water, but will also include tracking trends in other reactants that participate in the attenuation reaction (possible examples include pH, alkalinity, ferrous iron, and sulfate). For sites in which contaminant immobilization is the primary attenuation process, periodic collection of aquifer solids may be warranted to verify consistency in reaction mechanism. It is recommended that the selection of ground-water parameters to be monitored also include constituents that provide information on continued stability of the solid phase with which an immobilized contaminant is associated. Examples of this type of parameter might include ferrous iron or sulfate to track dissolution of iron oxides or sulfide precipitates, respectively. Non-contaminant performance parameters such as these will likely serve as "triggers" to alert site managers to potential remedy failure or performance losses, since the attenuation reaction will

respond to these changed conditions. Since increases in mobile contaminant concentrations may be delayed relative to changes in site conditions, these monitoring parameters may improve the ability of site managers to evaluate and address the potential for ground-water plume expansion.

In summary, the tiered analysis process provides a means to organize the data collection effort in a cost-effective manner that allows the ability to eliminate sites at intermediate stages of the site characterization effort. A general synopsis of the objectives along with possible analysis approaches and/or data types to be collected under each tier is provided in Table 1.1. The types of data collected early in the site characterization process would typically be required for selection of appropriate engineered remedies, including characterization of the system hydrology, ground-water chemistry, contaminant distribution, and the aqueous

speciation of the contaminant. These system characteristics can have direct influence on the selection of pump-and-treat or in-situ remedies best suited to achieve cleanup objectives for inorganic contaminants. This limits any loss on investment in site characterization for sites where selection of MNA as part of the ground-water remedy is ultimately determined not viable. The primary objective of progressing through the proposed tiered site analysis steps is to reduce uncertainty in the MNA remedy selection.

The remaining discussion in this section of Volume 1 will elaborate on two issues that have been introduced above, specifically the use of models in site characterization and general factors to consider for implementation of a long-term performance monitoring program. These topics are addressed at this juncture to allow greater focus to discussions later in this volume pertaining specifically to

Table 1.1 Synopsis of site characterization objective to be addressed throughout the tiered analysis process and potential supporting data types and/or analysis approaches associated with each tier.

Tier	Objective	Potential Data Types and Analysis
I	Demonstrate active contaminant removal from ground water	<ul style="list-style-type: none"> Ground-water flow direction (calculation of hydraulic gradients); aquifer hydrostratigraphy Contaminant concentrations in ground water and aquifer solids General ground-water chemistry data for preliminary evaluation of contaminant degradation
II	Determine mechanism and rate of attenuation	<ul style="list-style-type: none"> Detailed characterization of system hydrology (spatial and temporal heterogeneity; flow model development) Detailed characterization of ground-water chemistry Subsurface mineralogy and/or microbiology Contaminant speciation (ground water & aquifer solids) Evaluate reaction mechanism (site data, laboratory testing, develop chemical reaction model)
III	Determine system capacity and stability of attenuation	<ul style="list-style-type: none"> Determine contaminant & dissolved reactant fluxes (concentration data & water flux determinations) Determine mass of available solid phase reactant(s) Laboratory testing of immobilized contaminant stability (ambient ground water; synthetic solutions) Perform model analyses to characterize aquifer capacity and to test immobilized contaminant stability (hand calculations, chemical reaction models, reaction-transport models)
IV	Design performance monitoring program and identify alternative remedy	<ul style="list-style-type: none"> Select monitoring locations and frequency consistent with site heterogeneity Select monitoring parameters to assess consistency in hydrology, attenuation efficiency, and attenuation mechanism Select monitored conditions that “trigger” re-evaluation of adequacy of monitoring program (frequency, locations, data types) Select alternative remedy best suited for site-specific conditions

attenuation processes (Volume 1, Section II) and the types of site characterization data needed for their identification (Volume 1, Section III). The following discussion provides perspective on the role of model applications in the site characterization process, the types of models that might be employed to help meet the objectives set forth under each tier, and potential limitations in the availability and adequacy of available model codes.

ID. Role of Modeling in the Tiered Analysis Approach

Design of the site characterization effort and analysis of site-specific data in support of assessing the suitability of MNA as a component of the ground-water remedy is dependent on development of a Conceptual Site Model (CSM) that identifies site conditions and processes that influence contaminant transport. The CSM also provides the underpinning for selecting and developing model applications that provide a set of tools for evaluating transport processes, reaction mechanisms, attenuation capacity within the aquifer, and the sensitivity of the attenuation process to changes in site conditions. The types of models that may be employed as part of the site characterization process include simple calculations, speciation models, reaction models, transport models, and reactive transport models. Most modeling undertaken in support of an application will be quantitative, involving computer programs that require special skills to run correctly. The contaminated natural system being modeled is physically-, chemically-, and biologically-complex, and the modeler must have a thorough knowledge of the processes that affect the specific contaminants of concern. Site-specific data collected to define the physical, chemical, and biological characteristics of the aquifer are required to calibrate components of the analytical models and test the validity of model predictions. Deriving meaningful modeling results is likely to require expenditure of significant amounts of time, and entail considerable expense. This planning should occur early in the site assessment process, so that the modeling can be integrated with the evaluation of the site and the appropriate data can be collected.

To obtain the best results at the least expense, it is important to develop a valid modeling plan before beginning the modeling itself. Developing such a plan will likely require the combined talents of a group of specialists, including those familiar with the site and those with expertise in applying quantitative modeling of physical, chemical, and biological systems to real-world problems. This section is devoted to giving general perspective to the design and implementation of the modeling strategy. In addition to the following discussion, the reader is also referred to the document entitled "Documenting Ground-Water Modeling at Sites Contaminated with Radioactive Substances" (USEPA, 1996).

ID.1 Developing a Conceptual Model

Initially, the CSM is developed based on a general knowledge of ground-water hydrogeology, ground-water geochemistry, and known properties of the specific contaminant. With acquisition of data that maps out the spatial and temporal

heterogeneity of the subsurface system, the CSM can be updated. In general, there are more physical, chemical, and biological processes operating in the subsurface of any given site than can reasonably be accounted for in a modeling study. The modeling effort begins with the careful identification of the processes that play significant roles in contaminant migration and attenuation at the site. In this way a conceptual model emerges that will eventually be coded into the input streams of the software packages that will produce the modeling results. If a correct and robust conceptual model is not derived, the modeling results, no matter how detailed or expensive, will contribute little to understanding the site, and will not be supportive of the MNA application.

While it is important to begin modeling with a well-planned conceptual model, the conceptual model may evolve as modeling and collection of site-specific data proceeds. The processes of observation and measurement and of modeling are, in practice, closely interconnected. Initial observation and measurement suggests a conceptual model, which supports development of quantitative models. The results from application of these quantitative models, in turn suggest additional important observations and measurements, which better constrain model design and implementation. In this way, the conceptual model is updated in an iterative fashion, as progressively more is learned about the site. The most significant step in developing a conceptual model of natural attenuation at the site is to identify the transport and reaction mechanisms that significantly affect the mobility of contaminants there. Once these mechanisms have been identified, the logical components that will comprise the conceptual model can be selected.

The evaluation of transport refers to analysis of the flow of ground-water through the aquifer. The rate and direction of ground-water flow will be governed by the physical characteristics of the aquifer solids as well as the factors controlling inputs of water into the aquifer. Spatial and temporal heterogeneity or variability in these factors determines details of the mathematical construction of analytical models used to evaluate fluid and contaminant migration through the aquifer. In characterizing transport, it is important to ask questions such as:

- Does groundwater migrate through the bulk aquifer matrix, through fractures or heterogeneities in the matrix, or both?
- Does solute diffusion from areas of rapid flow to those with stagnant conditions affect contaminant transport on a scale finer than the envisioned numerical gridding, so that a dual porosity model is required?
- Should the medium be considered homogeneous or heterogeneous on the scale envisioned for the nodal blocks in the numerical gridding?
- Are medium properties best assigned deterministically, or according to a stochastic algorithm?
- Is hydrodynamic dispersion described well in a Fickian sense (i.e., in terms of dispersivity, according to Fick's law), by differential advection through a numerical gridding, or in both ways?

- How can the model be calibrated to reflect as accurately as possible transport rates through the subsurface?
- What additional data need to be collected to characterize flow and calibrate the transport model? Such data might include the distribution of hydraulic head, the evolution of the contaminant plume through time, and the results of tracer tests.

Evaluation of contaminant migration in ground water relies on determination of the types of chemical reactions that control contaminant degradation or immobilization. Thus, determination of specific reaction mechanisms that may be active within a ground-water plume provides the basis for constructing analytical models employed to evaluate performance of the attenuation process and project contaminant transport into the future. To characterize the reaction mechanisms driving attenuation, it is necessary to ask questions such as:

- Does the contaminant adsorb to solid surfaces? If so, onto what surfaces, and as what type of surface complex? Does it desorb readily?
- Is the contaminant chemically oxidized or reduced? Is the reaction catalyzed by mineral surfaces, or promoted by microbial activity? If so, what is the catalyst or microbial species?
- Does the contaminant precipitate as a solid phase? If it does, what is the phase, and what is its solubility?
- Might complexation of the contaminant with chemical constituents in solution affect its mobility?

A conceptual model can be thought of as a combination of the logical components describing the various aspects of transport and reaction at a site. For example, choice of how to represent hydrodynamic dispersion, the equations to account for sorption of contaminant species onto solid surfaces, rate laws describing the kinetics of redox reactions, and equations defining rates of microbial metabolism all contribute to the conceptual model. Since a conceptual model is no more than the sum of its components, and an analytical model is simply the realization of a conceptual model, the final modeling results are no better than the components selected.

ID.2 Types of Models

There are several types of models that may prove useful for characterizing attenuation processes at a site. In general, in approaching a specific question, it is most expedient to begin working with the simplest applicable model, adding complexity to the study as necessary. It is wise to avoid the temptation to begin by constructing the “ultimate” model, one that accounts for all aspects of transport and reaction at a site. Highly complex models are difficult to work with, expensive to produce, and difficult to interpret. A more efficient strategy is to begin with simple models of various aspects of the system, combining these as necessary into progressively more complex models, until reaching a satisfactory final result, one that reproduces the salient aspects of the system’s behavior without introducing unnecessary complexity.

ID.2.1 Simple Calculations

Simple calculations performed by hand or via computer applications may provide an important component to the overall modeling strategy. For purposes of this document, two modeling approaches that fall under this category include simplified calculation approaches to evaluate a range of process outcomes and specific mathematical formulas used to calculate input parameters needed for implementation of more complex transport or reaction models. An example of a simplified calculation approach would be the calculation of the mass of contaminant and the mass of reactant within a predefined volume of the aquifer for the purpose of assessing if sufficient reactant mass is available for an identified attenuation process. This type of calculation is simplified in the sense that one may assume that the rate of the reaction is unimportant. Thus, while this type of calculation provides a general sense of the relative degree to which the aquifer could support attenuation, it does not likely provide a sufficiently accurate representation of the actual efficiency of the attenuation process. However, the utility of this calculation approach is to provide some perspective as to the relative importance of investing resources to fully characterize reactant mass or flux. Several examples of the second category of this model type, specific mathematical formulas, are provided at the following USEPA website - <http://www.epa.gov/athens/learn2model/part-two/onsite/index.html>. This website provides on-line access to a suite of prepackaged tools (or “calculators”) for performing site assessment calculations. Several examples relevant to site characterization advocated within this document include:

- “Hydraulic Gradient Calculation” for assessing the direction(s) of ground-water flow employing head measurements in wells spaced horizontally across the site;
- “Vertical Gradients” for assessing the potential for vertical water transport within the aquifer based on head measurements in closely-spaced, vertically nested wells with identical screen lengths;
- “Vertical Gradients with Well Screen Effects” for assessing the influence of variable screen lengths in vertically nested wells on the calculated vertical gradient; and
- “Average Borehole Concentrations” to illustrate the potential impact on contaminant concentrations measured for samples collected from a single long-screened well in an aquifer with a depth-varying concentration and a depth-varying hydraulic conductivity field.

These simplified models support analysis of the adequacy of the location and construction of ground-water wells, which underpins the adequacy of the monitoring design to provide samples and data reflective of the site-specific conditions. They may also be used to provide reasonable estimates for parameters needed as input to more complex mass transport or reactive transport models. Since both modeling approaches provide a means for preliminary assessment of site data and potentially improving design of the monitoring network, they play an important role in the site characterization effort.

ID.2.2 Mass Transport Models

Mass transport models seek to describe the flow of ground water at a site, and the transport of chemical species within the flow. Mass transport models are generally implemented as transient simulations in one, two, or three dimensions. Strictly speaking, a mass transport model considers the migration of non-reacting species. In reality, many mass transport codes can consider simple reaction scenarios, such as partitioning of a species onto the solid surface according to a constant partitioning factor. Mass transport models can seldom be relied upon for describing natural attenuation, because they lack sophisticated knowledge of chemical and biological processes, but are nonetheless valuable in evaluating a site's potential for MNA. The models are well developed and straightforward to run; they are useful tools for simulating the rate and pattern of groundwater flow at a site.

Mass transport modeling might be applied to figure the transit time of contaminants within the site, absent attenuating processes. The models find use in applying the results of tracer tests to calibrate the flow field. Some reactive transport models (described below) accept externally determined flow fields as input, so running a mass transport model may be a required preliminary to a full reactive transport model.

ID.2.3 Speciation Models

Speciation models seek to describe the distribution of chemical mass between solution, minerals, mineral surfaces, gases, and biomass. Models of this class are useful because they can predict the conditions under which contaminants might be attenuated by sequestration, and those in which they are likely to be mobile in the ground-water flow. For example, a speciation model might demonstrate that a contaminant is likely to adsorb to the surface of a component of the aquifer solids over the pH range of interest. Or, the model might show that the contaminant will tend to complex strongly with dissolved chemical species, leaving it mobile and resistant to attenuation.

Speciation models are implemented via the assumption that the modeled system is in chemical equilibrium or, more commonly, partial chemical equilibrium. A model can be configured to account for:

- Reactions among species in solution, including protonation-deprotonation, redox, and complexation reactions.
- Adsorption reactions onto solid surfaces, possibly including minerals and organic matter.
- Precipitation and dissolution reactions, to predict whether a mineral is saturated in solution, or undersaturated or supersaturated.
- Gas solubility reactions, to account for the dissolution of coexisting gases into solution, or the loss of gas species from solution.

Where redox reactions play a critical role in the attenuation reaction, it may be important to use a speciation model that can account for redox disequilibrium. Microbial respiration, for

example, is driven by the transfer of electrons from donating to accepting chemical constituents, including the inorganic contaminant. It may be critical, therefore, to characterize the redox state of ground water at a site in an accurate and meaningful manner to fully evaluate redox-driven reactions that influence contaminant attenuation. Redox reactions in shallow ground water rarely attain a state of equilibrium (e.g., Lindberg and Runnells, 1984), which limits the utility of analytical models that describe the distribution of chemical species in ground water based on a single parameter such as dissolved oxygen (DO) concentration or Eh (e.g., as measured using a DO or platinum electrode, respectively). Geochemical models that describe redox in terms of a single parameter may be limited in their accuracy and/or flexibility in describing the redox characteristics of the ground-water system. An alternative approach to the model design would be to employ a flexible description of redox in a state of chemical disequilibrium (e.g., as discussed in Bethke, 1996, Chapter 6.). This type of modeling approach allows the user to specify for each element the mass found in the various possible redox states and reports the energy (i.e., the Nernst Eh) associated with the half reaction for each pairing of the element's oxidized and reduced states.

ID.2.4 Reaction Models

Reaction models are similar to speciation models in that they consider the distribution of chemical mass, but have the additional ability of modeling the chemical evolution of the system. Like speciation models, it is commonly necessary to use a reaction model with a flexible description of redox disequilibrium, as well as suitable models to describe adsorption and precipitation reactions. Where appropriate, the model should be able to account for the kinetics of species sorption, redox reactions, mineral precipitation and dissolution, or microbial metabolism. Examples of the application of reaction models in an MNA application include:

- Sequestration of contaminants onto a mineral surface as the mineral forms, such as the complexation of heavy metals in mine drainage onto ferrihydrite.
- Precipitation of contaminant-bearing minerals, according to a kinetic rate law appropriate for the chemical conditions at the site.
- Immobilization of a contaminant by oxidation or reduction, according to a kinetic rate law.
- Biotransformation of a contaminant by microbial life, using a rate equation for fermentation or cellular respiration appropriate for conditions at the site.

ID.2.5 Reactive Transport Models

Reactive transport models, as the name suggests, are the coupling of reaction models to transport models. Unlike a reaction model, a reactive transport model predicts not only the reactions that occur in the ground-water flow, but the distribution of those reactions across the site through time. A reactive transport model of a site may have several advantages over a simple reaction model, including:

- The ability to account for heterogeneity at the site, such as an uneven distribution of a sorbing mineral, variation in

pH conditions, or the differential development of microbial populations.

- The ability to describe evolution of a contaminant plume through space and time.

Reactive transport modeling is a relatively complex and time-consuming undertaking, since it combines the data needs and uncertainties inherent in modeling reaction as well as transport, and because the calculation procedure may require a significant amount of computing time. It may be the capstone of the modeling effort, but is seldom the best tool for initial scoping of the attenuation capabilities at a site. Such modeling, on the other hand, may play an important role in the site characterization effort, because it represents the integration of all of the components of the conceptual model.

ID.3 Modeling and the Tiered Analysis Approach

As described in Section IC of this document, a tiered analysis approach is recommended for organizing the collection of site-specific data and providing a means for screening out sites inappropriate for selection of MNA as part of the ground-water remedy. Previously, possible applications of models of varying complexity throughout the tiered analysis process were provided in Table 1.1. The following discussion provides additional context for evaluating the potential role of model applications during the site characterization process.

ID.3.1 Tier I – Demonstration of Contaminant Removal from Ground Water

The application of models under Tier I pertains primarily to initial characterization of hydrology and evaluating whether measured ground-water characteristics may support immobilization processes. Assessment of hydrology may include calculation of horizontal or vertical gradients to assess the predominant direction(s) of ground-water flow. This information could be used to guide installation of monitoring points within the aquifer for collection of ground-water and aquifer solids samples. Evaluation of contaminant immobilization potential may involve use of chemical data collected from ground-water and/or aquifer solids samples as input into a speciation model to assess the potential for contaminant precipitation or adsorption onto aquifer solids. For example, speciation calculations based on measurements of alkalinity and dissolved lead within the ground-water plume may indicate saturation or oversaturation with respect to precipitation of lead carbonate. Conversely, measurements of ground-water chemistry and extractable iron concentrations in aquifer solids could serve as parameter inputs into a speciation model with the capability of describing contaminant adsorption onto iron oxides. It is recommended that these latter calculations be used as secondary lines of evidence in support of site-specific measurements that demonstrate active sorption of the contaminant onto aquifer solids within the plume.

ID.3.2 Tier II – Determine Mechanism and Rate of Attenuation

Modeling at this stage in the evaluation process should be closely integrated with observational study. In studying the mechanism of contaminant removal from ground water, careful attention should be paid to assuring collection of sufficient data to fully define the components of the conceptual model. For example:

- If a precipitating phase is identified by x-ray diffraction, spectroscopy, or electron microscopy, it will be necessary to characterize the phase's solubility.
- If reaction with solid surfaces is identified as an important attenuation process, it will be necessary to collect sufficient data to properly parameterize an adsorption model that describes the specific mechanism of adsorption, as described in Section IIIB.
- It may be necessary to establish a kinetic rate law describing precipitation of the contaminant into solid phases, or its adsorption onto solid surfaces, where these reactions may occur at different rates throughout the plume due to the concentrations of aqueous or solid reactants.

In determining the rate of the attenuation process, modeling may be used to describe chemical fluxes in the system and rate of species uptake or production during chemical reaction. Modeling might be specifically employed to estimate the time frame required to sequester the contamination sufficiently to meet cleanup objectives, where the attenuation reactions are kinetically controlled.

ID.3.3 Tier III – Demonstrate Capacity and Stability of Removal Mechanism

Model applications under Tier III would be directed toward assessment of the capacity of the aquifer to attenuate the mass of contaminant within the ground-water plume and the long-term stability of an immobilized contaminant. Reaction models and/or reactive transport models might be employed to evaluate the extent of contaminant removal throughout the plume. Use of these model types allows assessment of rate-dependent reactions and/or the influence of decreases in the flux of reactants due to changes in concentration or ground-water flow that might occur over time. These same models may be employed to evaluate ground-water conditions that may remobilize contaminants sorbed to aquifer solids. These evaluations may prove most useful for situations in which laboratory testing may be less practical. For example, model simulations may be employed to examine the stability of the attenuated contaminant for hypothetical situations not reflected in existing ambient ground water. For example, modeling might be applied for a number of specific purposes:

- To test the chemical feasibility of specific remobilization scenarios, such as infiltration of pristine groundwater, a shift in oxidation state (perhaps due to waterlogging), or a change in pH (due to soil acidification, for example).

- To figure reactant fluxes required to remobilize the contaminant.
- To evaluate the possible effects of chelating agents, such as organic acids, in the groundwater.

These model applications provide a means to project system behavior under conditions that do not currently exist, but could feasibly develop. They provide a source of information that further reduces the uncertainty of reliance on MNA as a permanent remedy.

ID.3.4 Tier IV – Long-Term Performance Monitoring

Under Tier IV of the analysis process, modeling provides a tool for designing a long-term monitoring plan, as well as a contingency remedy for cases where unanticipated changes in site conditions leads to failure of the MNA remedy. Modeling tasks that might be performed at this stage include:

- Optimizing the location of monitoring wells for long-term observation.
- Optimizing the frequency of sample collection events based on knowledge of ground-water flow dynamics at the site.
- Identifying critical chemical parameters to monitor based on model simulations to examine the sensitivity of attenuation process rate or capacity to changes in ground-water composition.
- Identifying critical parameters to monitor based on model simulations to evaluate conditions leading to contaminant re-mobilization.

These model applications provide a means for designing the monitoring program to best evaluate remedy performance and provide site managers with a context for evaluating possible decreases in the efficiency of the attenuation process.

ID.4 Choosing Modeling Software

Once a modeling strategy has been developed and a conceptual model defined, a computer software package (or packages) will be needed to compute the modeling results. A number of software packages exist for modeling physical, chemical, and biological processes in natural systems. No single package is best for all problems; one seeks the package or packages that best satisfies the objectives of the site characterization process. Significantly, software packages designed for analyzing problems of the MNA of organic contaminants (e.g., Bioplume III; USEPA, 1997) are generally not suitable for studying the fate of inorganic contaminants. The first step in selecting software involves identification of packages incorporating features needed to evaluate the conceptual model. The selection process should amount to more than compiling a checklist of features. It is important to determine if the features work well for the situation in question.

It is critical to consider the efficiency of the software, not only in computing time, but the time required to configure each run and render the modeling results in a suitable graphical

form. One should, therefore, inspect carefully the documentation from potentially suitable packages, and run test cases. In evaluating a commercial package, insist on inspecting the documentation before buying. Avoid licensing software without being allowed a trial period, or a period during which the software may be returned for a full refund.

ID.4.1 Public Domain vs. Commercial Software

Modeling software falls into two categories, public domain and commercial. Public domain codes can generally be downloaded over the internet or purchased for a minimal charge; some codes are obtained by personal request addressed to the developer. A public domain code has a number of potential advantages: there is little or no up-front cost; the source code is in many cases available, allowing the modeler to correct bugs and add features; and there may be a body of experienced users available for consultation or troubleshooting at minimal or no charge. A commercial code also has potential advantages: it may be written by a group of professional programmers; there may be people assigned to support users, offer training, and fix bugs; documentation may be superior; there is more likely to be an intuitive user interface; the code may be easier to use than public domain alternatives; and it may offer superior graphics for rendering results. In general, distributors of commercial codes hope they can convince customers that the up-front costs of their product will be offset in the long run by quality and savings, principally by improving the productivity of the people involved in the modeling process, and by speeding project completion.

ID.4.2 Sources of Software

A considerable number of software packages that can be applied to the analysis of inorganic contaminant attenuation in ground water are available in the public domain and from commercial sources. Tables 1.2–1.4 list examples of various types of commonly applied packages and their sources. Additional packages may be found by searching the internet, and from software retailers such as Rockware, Inc. (www.rockware.com) and Scientific Software Group (www.scisoftware.com). New software packages appear frequently, others fall into disuse or are no longer supported and updated, and new releases of the various packages add features and fix bugs. As such, no attempt is made in this document to provide exhaustive listings of software packages applicable to MNA assessments, nor to judge the suitability or compile the features of various packages. In evaluating software, the reader will be well served by considering in light of his or her own needs only the most recent available information. The following discussion provides some issues to consider during selection of a software package.

Issues to consider during selection of a mass transport model and a representative list of commonly applied models (Table 1.2):

- Whether the model operates in two or three dimensions, or both.
- Whether the model can account for dispersion in the manner chosen.

- If the model accounts for saturated flow (flow below the water table), unsaturated flow (above the water table), or both.
- The deterministic or stochastic method or methods the model can use to represent heterogeneity in the properties of the medium (hydraulic conductivity, dispersivity, and so on) across the modeling domain.

Issues to consider during selection of a geochemical speciation model and a representative list of commonly applied models (Table 1.3):

- A flexible description of redox state. A disequilibrium scheme in which each redox couple can be set to its own redox potential is commonly required.

- The ability to account for sorption or surface complexation in a manner appropriate for the site.

Issues to consider during selection of a reaction model, in addition to those relevant for a speciation model, and a representative list of commonly applied models (Table 1.3):

- An accounting for the kinetics of redox reactions, whether occurring in the fluid phase, catalytically on mineral surfaces, or promoted by enzymes.
- The ability to account for the kinetics of mineral precipitation and dissolution reactions invoked as an attenuation mechanism, using appropriate rate laws.
- A model of microbial metabolism based on valid chemical principles. The metabolic model should treat the

Table 1.2 Example software packages for modeling groundwater flow and mass transport.

Software	Source
FEFLOW	Groundwater Modeling, Inc. www.ssg-int.com/
GMS	Environmental Modeling Systems, Inc. www.ems-i.com/GMS/gms.html
Modflow-2000	U. S. Geological Survey water.usgs.gov/nrp/gwsoftware/modflow.html
Visual Modflow	Waterloo Hydrogeology www.visual-modflow.com
GroundWater Vistas	www.groundwater-vistas.com

Table 1.3 Example software packages for speciation in inorganic geochemical systems. Each of these packages except Wateq4F also has at least some capability for modeling reaction processes.

Software	Source
Chess	Ecole des Mines de Paris chess.ensmp.fr/
Eq3/6	Lawrence Livermore National Laboratory www.llnl.gov/IPandC/technology/software/softwaretitles/eq36.php
Mineql+	Environmental Research Software http://www.mineql.com/
MinteqA2	U.S. EPA http://www.epa.gov/ceampubl/mmedia/minteq/
Phreeq-C	U.S. Geological Survey wwwbrr.cr.usgs.gov/projects/GWC_coupled/phreeqc/index.html
The Geochemist's Workbench®	University of Illinois www.geology.uiuc.edu/Hydrogeology
Visual Minteq	KTH (Sweden) www.lwr.kth.se/english/OurSoftware/Vminteq/index.htm
Wateq4F	U.S. Geological Survey water.usgs.gov/software/wateq4f.html

metabolism as a balanced chemical reaction, accounting for not only consumption of substrate species, but generation of product species. The software should also account for how the amount of energy available in the environment affects metabolic rate, and for the growth and decay of biomass.

Issues to consider during selection of a reactive transport model, in addition to the points raised above about mass transport, speciation, and reaction models, and a representative list of commonly applied models (Table 1.4):

- Whether the model can work in one, two, or three dimensions.
- Compatibility of the model with the mass transport and reaction models chosen. For example, can the reactive transport model import a flow field predicted by the mass transport model?
- Time to solution, since reactive transport modeling can require considerable amounts of computing time.

ID.4.3 Thermodynamic Data

Most software packages are configured to accept any external database, provided that it is presented in the proper format. A number of databases have been compiled for various purposes, and many of these are available already formatted to be read directly into one or more of the widely distributed geochemical models. A list of various internet sites from which thermodynamic data can be downloaded in various formats is provided in Table 1.5. Additional databases might be located by consulting web pages and the latest documentation for the various geochemical modeling packages, and by searching the internet. Since updates to posted databases may be conducted infrequently, it may be worthwhile to verify the database incorporates currently accepted thermodynamic data based on a review of the technical literature.

Table 1.4 Example software packages for modeling reactive transport in inorganic geochemical systems.

Software	Source
Crunch	Lawrence Livermore Laboratory www.csteefel.com/
HYTEC	Ecole des Mines de Paris www.cig.ensmp.fr/~vanderlee/hytec/index.html
PHAST	U. S. Geological Survey wwwbrr.cr.usgs.gov/projects/GWC_coupled/phast/index.html
Phreeq-C	U.S. Geological Survey wwwbrr.cr.usgs.gov/projects/GWC_coupled/phreeqc/index.html
The Geochemist's Workbench® Professional ¹	University of Illinois www.geology.uiuc.edu/Hydrogeology

¹ The "Xt" package in previous releases.

Table 1.5 Example internet sources of thermodynamic data useful in constructing geochemical models.

Source	URL
Ecole des Mines de Paris	ctdp.ensmp.fr/
Japan Nuclear Cycle Development Institute	migrationdb.inc.go.jp/
Murdoch University (Australia)	iess.murdoch.edu.au/iess/iess_home.htm
National Institute of Standards and Technology	webbook.nist.gov/
Nuclear Energy Agency (France)	www.nea.fr/html/dbtdb/
University of Illinois	www.geology.uiuc.edu/Hydrogeology/hydro_thermo.htm
University of Illinois at Chicago	tigger.uic.edu/~mansoori/TRL.html

ID.5 Accounting for Uncertainty

For a model constructed in support of an MNA application, there are a number of sources of uncertainty, including:

- Error in chemical analyses. The accuracy and completeness of chemical analyses vary widely. Routine chemical analyses performed by commercial laboratories are in many cases of insufficient quality to support geochemical and reactive transport modeling. Several useful checks for internal consistency are available in the American Water Works Association “Standard Methods” volume (Clesceri et al., 1998), and computer programs (e.g., Aq•QA, www.aqqa.com) are available for performing these tests automatically. Geochemical modeling applications require complete chemical analyses, including not only the contaminants of interest, but the major ion chemistry, pH, and distribution of metals among their mobile redox states.
- Error in determining hydrologic parameters. Measuring representative values of hydrologic parameters such as hydraulic conductivity and dispersivity can be difficult, because these values may change with the scale on which they are observed. Laboratory measurements, therefore, may give different results than well tests (e.g., slug and bail tests, pumping tests), which may in turn differ from values representative of the site as a whole. Measured hydrologic parameters are important, but may need to be calibrated to observations from the site, including perhaps the rate of plume advance or the migration of a tracer injected into the subsurface.
- Sample choice and dataset size. Significant error can be introduced by sampling bias, although this bias is not always obvious or even avoidable. Laboratory measurements of hydrologic properties, for example, are commonly made on samples that can be recovered intact, even though the fractured or poorly consolidated portions of the medium, left unsampled, control flow. Fluid samples may be taken from monitoring wells completed in highly conductive layers, where they can be extracted rapidly, leaving unaccounted significant quantities of residual contamination in slightly less conductive layers. Finally, the number of samples available or monitoring wells constructed is in some cases too small to comprise a statistically significant dataset.
- Incompleteness and inaccuracy of the thermodynamic database. To provide meaningful results, a geochemical or reactive transport model has to include each of the aqueous species, minerals, gases, and adsorbed species important at the site, and the data for these species need to be accurate. The thermodynamic databases available for geochemical study vary widely in breadth and accuracy.
- Error in model components. Each of the components of which the model is constructed is a potential source of error. Components likely to contribute to error include kinetic rate laws, surface complexation (sorption) models, and descriptions of the effects of microbial metabolism.

- Conceptual errors. Perhaps most significantly, model results can be affected by failure to conceptualize the problem completely and accurately. If an important process is not accounted for, or accounted for in an inaccurate fashion, the modeling results will likely be rendered useless.

The modeler accounts for uncertainty by experimenting with the model to discover which sources of uncertainty affect the results significantly. This uncertainty can subsequently be reduced, for example, by making new measurements or refining critical observations. Another source of uncertainty is the limited possibility to obtain measured site-specific values for some of the model parameters due to the complexity of the geochemical model. It is recommended that the results of uncertainty analysis be provided for the purpose of site decisions. This information would include the sources and potential ranges of all input data along with the origin of input data (i.e., review of technical literature, model calibration, field testing, or estimation).

ID.6 Model Calibration and Verification

Developing a quantitative model of contaminant attenuation in the subsurface may entail considerable uncertainty. Parameters needed to constrain the model are seldom known precisely, parameter inputs may not be available and require estimation, and the conceptual model itself may need refinement. Due to these uncertainties, it is necessary to calibrate the model to observations, and to verify that the model behaves in a manner that adequately describes the natural system. The processes of calibration and verification are closely related, since calibration brings the model into alignment with observed data. A model that (1) utilizes to the greatest extent possible parameter values specific to the site, and (2) is calibrated to the observed evolution and distribution of the contaminant plume, therefore, is most likely to be readily verified. It is recommended that steps taken to calibrate the model application be documented and provided for review in order to build confidence in the use of this assessment tool.

Model verification requires that the model predict an independent set of observations, i.e., a set separate from those used for calibration. For example, a model that predicts the attenuation of chromate by chemical reduction might be “fit” on the basis of a plume or section thereof, and subsequently used to predict the behavior of another plume at the same site. The initial fitting would presumably involve arriving at reasonably precise estimates of the most uncertain inputs – in this case reduction rates, electron donor loads, and so on. If the subsequent independent prediction accurately reflects field observations, this result would lend credence to the model. Here, “accurate reflection” of field predictions probably means predicting correctly the speed at which the plume is retreating and estimating the rate of overall contaminant mass reduction to within a factor no greater than five. Predictions that do not achieve this level of accuracy should prompt further refinement of the model.

This discussion has been intended to point out that models may serve as a useful tool that can be employed as part of the evaluation process for selection of MNA as a remedy.

However, the complexity of the modeling effort and the potential level of uncertainty associated with model predictions indicate that pursuit of more direct lines of evidence is critical to the tiered analysis process. The acquisition of these data will depend on establishing a network of monitoring locations throughout the aquifer. The site-specific data collected from these monitoring locations provide the means to identify the attenuation process and assess the performance characteristics of the MNA remedy. As with any technology used as part of a cleanup remedy, continued assessment of remedy performance is critical for ensuring attainment of cleanup goals. The following discussion provides context for the eventual design of the performance monitoring program leading to site closure for situations in which MNA provides a viable component to the ground-water remedy.

IE. Long-Term Performance Monitoring and Site Closure

The performance of the MNA remedy must be monitored to determine compliance with site-specific remedial objectives identified in remedy decisions. This long-term monitoring is often the largest expenditure incurred in the course of cleanup and, for this reason alone, should be considered at the earliest stages of remedial investigation. Because the time horizons for successful implementation of an MNA remedy are often expected to be long, it is critical that particular attention is paid to long-term monitoring plans. Detailed discussions of the performance monitoring framework and monitoring plan development have recently been published (USEPA, 2003). Although that discussion focuses on attenuation of common organic contaminants, the framework and many of the principles governing plan development are also applicable to inorganic constituents. However, there are conceptual differences with respect to the outcome of the MNA remedy for inorganic contaminants. With the exception of situations where degradation reactions transform harmful contaminants (e.g., nitrate or perchlorate) into innocuous constituents, contaminant mass is not reduced during MNA for inorganic contaminants. The MNA process results in relocation, dispersion, and ultimately chemical conversion of the original source zone. Therefore, the purposes of performance monitoring

are to demonstrate degradation to innocuous materials and immobilization of contaminants. It is recommended that site closure be considered only after degradation and immobilization within the risk level specified in the remedy decision are demonstrated and shown to have long term stability.

Development of a performance monitoring plan is site specific in nature. Monitoring objectives and quantifiable performance criteria are developed to evaluate temporal and spatial remedy performance with respect to the site-specific remedial action objectives. Much of the monitoring to demonstrate performance of the MNA remedy will fall into three basic categories: 1) ambient monitoring to assess background contaminant levels and the status of relevant ambient geochemical indicators (e.g., E_H , pH); 2) process monitoring to assure the progress of chemical attenuation; and 3) monitoring to detect plume expansion.

Within this framework, the OSWER Directive 9200.4-17P (USEPA, 1999c) provides eight specific objectives to be met by the performance monitoring program of an MNA remedy (Table 1.6). The objectives usually will be met by implementing a performance monitoring program that measures contaminant concentrations, geochemical parameters, and hydrologic parameters (e.g., hydraulic gradients). Much of the monitoring will be focussed on ground water. However, periodic monitoring of aquifer solids, through soil coring, will be warranted in most situations. These data will be used to evaluate the chemical behaviour of the contaminant in the subsurface over time, including:

- Changes in three-dimensional plume boundaries,
- Changes in the redox state that may indicate changes in the rate and extent of natural attenuation,
- Reduction in the capacity of aquifer materials for contaminant immobilization, and
- Mobile contaminant mass and concentration reductions indicative of progress toward contaminant removal objectives.

Contaminant behavior can then be evaluated to judge the effectiveness of the MNA remedy and the adequacy of the monitoring program.

Table 1.6 Objectives for performance monitoring of MNA (USEPA, 1999c).

1)	Demonstrate that natural attenuation is occurring according to expectations,
2)	Detect changes in environmental conditions (e.g., hydrogeologic, geochemical, microbiological, or other changes) that may reduce the efficacy of any of the natural attenuation processes,
3)	Identify any potentially toxic and/or mobile transformation products,
4)	Verify that the plume(s) is not expanding down gradient, laterally or vertically,
5)	Verify no unacceptable impact to down gradient receptors,
6)	Detect new releases of contaminants to the environment that could impact the effectiveness of the natural attenuation remedy,
7)	Demonstrate the efficacy of institutional controls that were put in place to protect potential receptors, and
8)	Verify attainment of remediation objectives.

IE.1 Duration and Monitoring Frequency

As stated in the OSWER Directive (USEPA, 1999c), performance monitoring should continue until remediation objectives have been achieved, and longer if necessary to verify that the site no longer poses a threat to human health or the environment. Typically, monitoring is continued for a specified period after remediation objectives have been achieved to ensure that concentration levels are stable and remain below target levels. In order to demonstrate stability, verification of the achievement of target levels under conditions where the aquifer geochemistry has reestablished a chemical steady state with respect to ambient ground-water geochemistry will be needed. The magnitude of the chemical gradient between the impacted and non-impacted portions of the aquifer provides a reference point for evaluating establishment of steady-state conditions. A monitoring strategy to verify the attainment of remedial objectives and provide for termination of monitoring and site closure generally should be formulated during the development of the performance monitoring plan and updated, as necessary, prior to implementation.

Monitoring frequency should be specified in the performance monitoring plan. In addition, the plan may specify an approach and technical criteria that could be used to increase or reduce the frequency as conditions change. Such criteria would scale monitoring frequency to match MNA performance and the level of understanding and confidence in the conditions that control attenuation at a given site. The most appropriate frequency for ground-water sampling is site specific and depends on several factors including:

- The rate at which contaminant concentrations may change due to ground-water flow and natural attenuation processes,
- The degree to which the causes of this variability are known,
- The types of evaluations to be performed and the importance of the type of data in question, and
- The location(s) of possible receptors relative to the plume.

In addition, the most appropriate frequency may vary in different areas of the site based on site-specific conditions and the intended use of the data. Similar principles are applied in determining the most appropriate frequency for sampling of aquifer solids.

With respect to the initial frequency of ground-water sampling under the performance monitoring program, quarterly monitoring may often be an appropriate frequency to establish baseline conditions over a period of time sufficient to observe seasonal trends, responses to recharge, and to confirm attenuation rates for key contaminants. Quarterly monitoring for several years provides baseline data to determine trends at new monitoring points and test key hypotheses of the conceptual site model.

More frequent monitoring of ground-water elevations may be warranted, particularly during the establishment of baseline conditions, to improve the characterization of ground-water flow patterns. In addition, more frequent monitoring may be needed to observe changes in ground-water flow patterns in response to other site activities, such as the start or cessation of ground-water extraction in off-site water supply wells, source control activities, and other significant changes in the hydrologic system.

IE.2 Monitoring of Aquifer Solids

The aquifer material may serve as the reactive media to which many inorganic contaminants become partitioned and immobilized. Therefore, periodic re-assessment of the capacity of aquifer materials for contaminant immobilization, including immobilization of radioactive contaminants and any harmful products of radioactive decay, often is a critical step in performance monitoring. There are three aspects to this solid-phase characterization to be addressed through collection of field data and laboratory testing:

- Determination of the chemical process(es) resulting in contaminant immobilization,
- Determination of the capacity of the un-reacted aquifer material for contaminant immobilization, and
- Determination of the stability of the reacted aquifer material with respect to contaminant release.

Characterization of aquifer material requires collection of core material within the existing contaminant plume and down gradient and side gradient to the plume. Characterization within the existing plume is used to identify the immobilization process(es) and capacity, while down gradient and side gradient characterization is used to re-assess the potential and capacity for immobilization in the event of plume expansion. In general, this characterization involves identification of the aquifer mineralogy to determine the abundance and spatial distribution of reactive solid component(s) and the distribution of the contaminant among the identified components.

The spatial extent and density of sampling points will be dictated by the degree of heterogeneity of the aquifer material both within and outside of the existing plume boundary. The frequency of sampling will be dictated by the rate of the immobilization process with respect to fluid transport and the dynamics of fluid flow and chemistry. In general, sampling frequency will be greater within the plume boundary where immobilization is active. The frequency of sampling outside of the plume boundary will be dictated by the proximity of receptors and the time frame for reaching remedial objectives relative to the rate of weathering processes that may change the composition or mineralogy of the aquifer material.

IE.3 Monitoring Types

The majority of the monitoring performed to determine the effectiveness of the MNA remedy may be classified under three general headings:

- Monitoring of conditions outside of the plume boundaries (ambient monitoring),
- Monitoring of natural attenuation processes (process monitoring), and
- Monitoring to detect plume expansion and verify the lack of impact to receptors (migration monitoring).

Other types of monitoring include periodic evaluations of the effectiveness of any institutional controls specified in the remedy decision documents and, ultimately, verification of the attainment of all remedial objectives.

Ambient monitoring should be performed outside of the boundaries (e.g., hydraulically up gradient, side gradient, and down gradient) of the contaminant plume. The purpose of this monitoring is to establish background conditions and to provide an indication of the potential for additional plume migration in situations where redox state and the capacity of aquifer materials for contaminant immobilization are dominant controls on migration. The extent and duration of ambient monitoring will be influenced by the sensitivity of aquifer chemistry to changes in recharge water quality and processes that may change its composition.

Process monitoring is used to verify that attenuation is occurring according to prediction. If process monitoring indicates that attenuation is not occurring as expected, a change in cleanup approach may be warranted. Process monitoring is contaminant-specific and might include, for example, measurement of ground-water redox state or pH to assure the existence of conditions favorable for natural attenuation via reduction-oxidation processes or pH-dependent sorption as well as the monitoring of contaminants. Process monitoring parameters are discussed in the contaminant-specific sections in Volumes 2 and 3 of this document. Process monitoring should also take into account any impacts of ongoing or prior active treatment on subsequent ambient attenuation processes. For example, such impacts may include gradual shifts in system redox as water levels and/or electron donor/acceptor levels change after, respectively, pump and treat or in situ bioremediation have been halted.

Monitoring to detect plume expansion (migration monitoring) and any impacts to receptors is another important aspect of the performance monitoring program. This monitoring objective may be met through multi-level monitoring performed at or near the side gradient and down gradient plume boundaries, beneath the plume, and near any other compliance boundaries specified in remedy decision documents in conjunction with monitoring of possible receptor locations (e.g., potable water wells or locations of ecological receptors) to directly verify the lack of impacts. Monitoring locations between the plume and compliance boundaries or possible receptors should be close enough to the plume that a contingency plan can be implemented before the contaminant can move past the point of compliance or impact receptors. Identifying locations for monitoring wells designed to detect migration ultimately relies on a site-specific assessment of contaminant migration and fate. Additional

insight may be obtained from site-specific transport model predictions, where model use is conducted iteratively with the site characterization process so that model predictions are both tested and influence future data collection.

IE.4 Monitoring Locations

At many sites, the performance monitoring program will be three-dimensional in nature due in large measure to the effects of site-specific hydrogeology on contaminant migration. Typical target zones for monitoring a contaminant plume (Figure 1.3) include:

- Original source areas - within and immediately down gradient of source areas (Process Monitoring)

The monitoring objectives include the detection of any further contaminant releases to ground water that may occur and demonstration of reductions in contaminant concentrations in ground water over time. In situations where the original source is contained, increased contamination or new contaminants could be indicative of containment system failure.

- Transmissive zones with highest contaminant concentrations or hydraulic conductivity (Process Monitoring)

A change in conditions in these zones, such as an increase in contaminant mass, change in redox state, increased ground-water velocity, or exceedance of the aquifer capacity for immobilization, may lead to relatively rapid plume expansion.

- Distal or fringe portions within the plume (Process and Migration Monitoring)

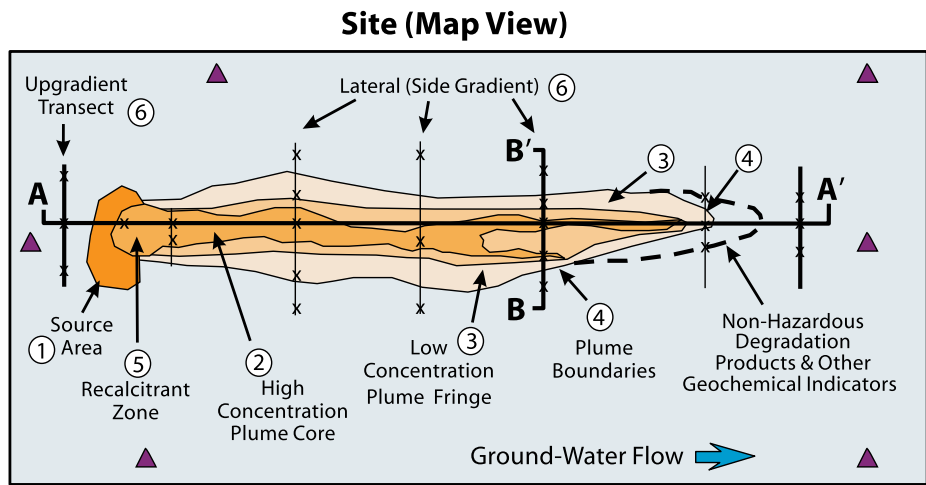
These are areas where reduction of contaminant concentrations in ground water to levels required by remedial action objectives may be attained most rapidly or where plume expansion may be observed most readily.

- Outside the plume, including areas near plume boundaries and other compliance boundaries (Migration Monitoring)

Multi-level monitoring points, reflecting vertical differences in subsurface conditions, generally will be warranted at the side gradient, down gradient, and vertical plume boundaries; between these boundaries and possible receptors; and at any other compliance boundaries specified in remedy decision documents. Monitoring of receptor locations should also be included to directly verify that no impacts occur.

- Zones in which contaminant reductions in ground water appear to be less than predicted (Process Monitoring)

These are the areas where attaining cleanup standards within time frames specified in the remedy decision documents may be impeded due to site conditions (e.g., higher than anticipated concentrations of residual source materials, redox conditions, or exceedance of the capacity for immobilization). Such areas, if present, will be delineated through evaluation of data obtained throughout the performance



Target Monitoring Zones

1. Source area
2. Contaminated zones of highest concentrations and mobility
3. Plume fringes
4. Plume boundaries
5. Recalcitrant zone determined from historical trends
6. Upgradient and sidegradient locations

- x Monitoring well cluster
- ▲ Piezometer
- x-x-x- Transect of well clusters

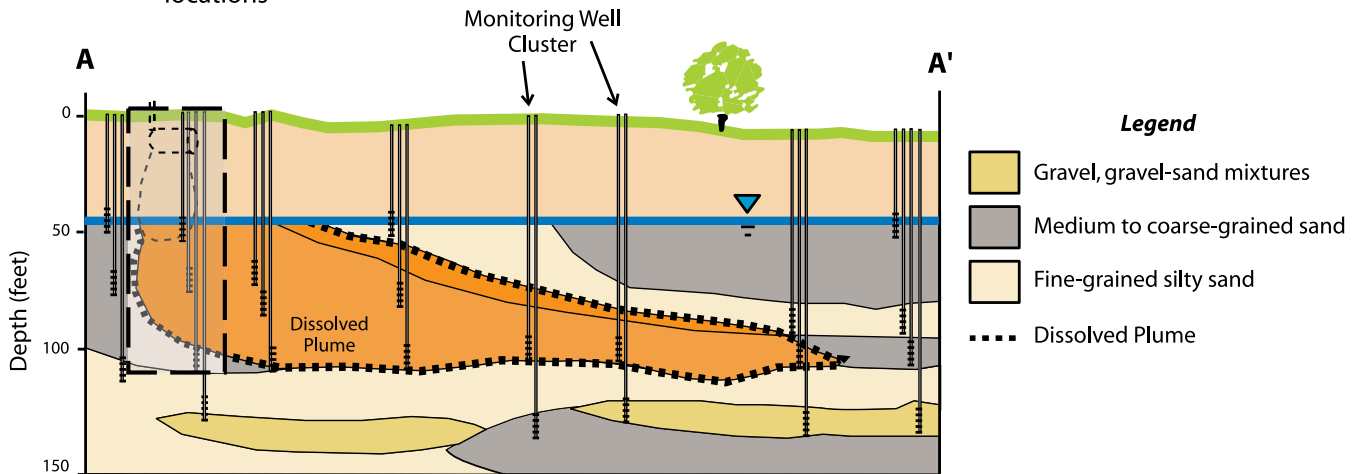


Figure 1.3 Example of a network design for performance monitoring, including target zones for monitoring effectiveness with respect to specific remedial objectives.

monitoring period. These areas may require additional characterization to determine if additional remedial actions are necessary to reduce contaminant concentrations to desired levels.

- Areas representative of uncontaminated settings (Ambient Monitoring)

Sampling locations for monitoring the redox state and immobilization capacity of aquifer materials include points that

are adjacent to but outside the plume. Data from these monitoring locations will often be needed to assess the continuation of favorable conditions for attenuation. Since assumptions concerning the redox state and attenuation capacity affect interpretation of data from the plume, such assumptions should be periodically evaluated like other aspects of the conceptual site model. Therefore, multiple monitoring points generally should be used to determine the variability of these parameters outside the plume.

- Areas supporting the monitoring of site hydrology

At some sites, monitoring of ground-water elevations at locations additional to those used for the monitoring of chemical parameters may be needed to determine if changes in ground-water flow rates and directions are occurring. Appropriate locations for placing piezometers will often include positions that are up gradient, side gradient, and down gradient of the contaminant plume, as well as in zones above and below the plume and near surface water bodies.

IE.5 Modification of the Performance Monitoring Plan

The monitoring plan should be a dynamic document that is modified as conditions change or the conceptual site model is revised to reflect new information. Decisions regarding remedy effectiveness and the adequacy of the monitoring program will generally result in either:

- Continuation of the monitoring program without modification;
- Modification of the monitoring program;
- Implementation of a contingency or alternative remedy; or
- Verification that remedial objectives have been met with subsequent termination of the monitoring program.

Continuation of the program without modification would be supported by contaminant concentrations behaving according to remedial expectations while ground-water flow and geochemical parameters remain within ranges indicative of continued contaminant immobilization. Modification of the program, including increases or decreases in monitoring parameters, frequency, or locations, may be warranted to reflect changing conditions or improved understanding of natural attenuation processes at the site. In addition, modification generally would be warranted whenever remedy modifications are implemented, such as implementation of additional source removal or hydraulic control for plume migration.

In situations where hydrologic and geochemical parameters are stable and the contaminant concentrations in ground water are decreasing as predicted, reductions in sampling frequency (e.g., semi-annual, annual, or less frequent) will often be warranted for process monitoring. For example, five years of quarterly monitoring showing predictable decreases in mobile contaminant concentrations might be the basis for decreasing the frequency to a semi-annual or annual basis at some sites. Ten years of semi-annual or annual monitoring that shows predictable decreases in mobile contaminant mass might likewise be the basis for additional decreases in frequency, depending on site conditions. Conversely, unexpected increases or lack of predicted decreases in contaminant concentrations may trigger additional characterization to determine the reasons for the behavior, increased monitoring of pertinent parameters, re-evaluation of the conceptual site model, and, potentially, the implementation of a contingent or alternative remedy.

Changes in the frequency of monitoring to detect plume expansion may also be warranted as process monitoring is modified. However, the frequency of such monitoring should not be decreased to the point where insufficient time would be available for implementation of an effective contingency plan in the event of MNA remedy failure.

Criteria for modifying the monitoring program, including the type and amount of data needed to support the evaluation, should be discussed and agreed to by stakeholders. Site-specific criteria should be developed to define conditions that indicate the appropriateness of increased or decreased monitoring, additional characterization, re-evaluation of the conceptual site model, implementation of a contingency or alternative remedy, and termination of performance monitoring.

Another reason for altering the monitoring program is the development of more advanced monitoring technologies. Because long-term monitoring costs are substantial, every advantage of technological advances in monitoring efficiencies should be considered. This might best be done by assessing monitoring technology every 3 to 5 years to identify "off-the-shelf" monitoring approaches/equipment that can improve accuracy and lower costs. National technology verification programs are often a good source of such information.

IE.6 Periodic Reassessment of Contaminant Removal Technologies

In addition to the routine monitoring of MNA remedy performance, it is recommended that periodic consideration be given to any technological advances in the efficiencies of source removal for inorganic contaminants. Implementation of more efficient technologies may result in reductions in the time frames for performance monitoring with associated reductions in cost as well as improvements in performance. Many sites may benefit from a Periodic Remedial Technology Assessment (PRTA) conducted at regular intervals (e.g., 5 years) throughout the performance monitoring program. The PRTA should consist of a rigorous literature search and engineering assessment of the field implementation of new technologies. It should involve a survey of cleanup efficiencies achieved by new technologies at sites similar to the one under consideration. The survey should rely on the results of national or state technology verification programs (e.g., USEPA Environmental Technology Verification Program, www.epa.gov/etv/; Interstate Technology & Regulatory Council, www.itrcweb.org). The PRTA should either indicate the absence of more suitable alternatives or suggest a faster path to site closure. The criteria for technology selection should be clearly stated during the development of the evaluation plan. The goal of this review should be identification of technologies that have a very high probability of achieving at least order-of-magnitude reductions in contaminant mass and/or achievement of MCLs in ground water by means acceptable to stakeholders. A reasonable metric should be successful implementation of the technology as judged by impartial bench marking criteria at several sites where site closure has been achieved.

1F. References

- Bethke, C.M. *Geochemical Reaction Modeling, Concepts and Applications*, Oxford University Press, New York, NY (1996).
- Clesceri, L.S., A.E. Greenberg, and A.D. Eaton. *Standard Methods for the Examination of Water and Wastewater*, 20th Edition, American Public Health Association, Washington DC (1998).
- USEPA. *Environmental Characteristics of EPA, NRC, and DOE Sites Contaminated with Radioactive Substances*, EPA 402-R-93-011, Office Radiation and Indoor Air, Washington DC (1993).
- USEPA. *Common Chemicals Found at Superfund Sites*, EPA/OSWER No. 9203, Office of Solid Waste and Emergency Response, Washington DC (1994).
- USEPA. *Contaminants and Remedial Options at Selected Metal-Contaminated Sites*, EPA/540/R-95/512, Washington DC (1995).
- USEPA. *Documenting Ground-Water Modeling at Sites Contaminated with Radioactive Substances*, EPA/540/R-96/003, Office of Radiation and Indoor Air, Office of Solid Waste and Emergency Response, Washington DC (1996). (<http://www.epa.gov/radiation/docs/clean-up/540-r-96-003.pdf>)
- USEPA. *Technical Protocol for Evaluating Natural Attenuation of Chlorinated Solvents in Ground Water*, EPA/600/R-98/128, Office of Research and Development, Washington DC (1998). (<http://www.epa.gov/ada/download/reports/protocol.pdf>)
- USEPA. *Understanding Variation in Partition Coefficient, Kd, Values: Volume I - Kd Model, Measurement Methods, and Application of Chemical Reaction Codes*, EPA 402-R-99-004A, Office of Radiation and Indoor Air, Washington DC (1999a).
- USEPA. *Understanding Variation in Partition Coefficient, Kd, Values: Volume II - Geochemistry and Available Kd Values for Selected Inorganic Contaminants*, EPA 402-R-99-004B, Office of Radiation and Indoor Air, Washington DC (1999b).
- USEPA. *Use of Monitored Natural Attenuation at Superfund, RCRA Corrective Action, and Underground Storage Tank Sites*, EPA/OSWER No. 9200.4-17P, Office of Solid Waste and Emergency Response, Washington DC (1999c).
- USEPA. *Evaluation of the Protocol for Natural Attenuation of Chlorinated Solvents: Case Study at the Twin Cities Army Ammunition Plant*, EPA/600/R-01/025, Office of Research and Development, Washington DC (2001). (http://www.epa.gov/ada/download/reports/epa_600_r01_025.pdf)
- USEPA. *Common Radionuclides Found at Superfund Sites*, EPA 540/R-00-004, Office of Radiation and Indoor Air, Washington DC (2002a).
- USEPA. *Workshop on Monitoring Oxidation-Reduction Processes for Ground-water Restoration*, EPA/600/R-02/002, Office of Research and Development, Washington DC (2002b).
- USEPA. *Understanding Variation in Partition Coefficient, Kd, Values: Volume III - Review of Geochemistry and Available Kd Values for Americium, Arsenic, Curium, Iodine, Neptunium, Radium, and Technetium*, EPA 402-R-99-004C, Office of Radiation and Indoor Air, Washington DC (2004).

Section II

Technical Basis for Natural Attenuation in Ground Water

**Richard T. Wilkin, Steven Acree, Steve Mangion, Patrick V. Brady, Robert G. Ford,
Robert W. Puls, Paul M. Bertsch, Douglas B. Kent, Ann Azadpour-Keeley,
James E. Amonette, Craig Bethke**

In determining whether MNA is applicable to a site, the properties of the site and the properties of the contaminant are analyzed in order to identify the specific process (or processes) causing contaminant attenuation. Inorganic contaminant transport in the subsurface will be governed by the site-specific characteristics of ground-water flow and the chemical interactions between the contaminant and aquifer solids along the path (or paths) of fluid flow. The overall extent of contaminant attenuation will be governed by the velocity of ground-water flow relative to the rates of chemical reactions that attenuate contaminant transport. The types and rates of chemical reactions that result in contaminant attenuation will be controlled by the availability of constituents within the aquifer that interact with the contaminant in a manner that results in contaminant immobilization or

transformation. In simple terms, one can view the product of the reaction between the contaminant and aquifer constituents (or reactants) as the specific form of attenuation. Examples of possible attenuation reactions are provided in Figure 2.1 to illustrate this conceptual viewpoint and the types of processes that may be active at a given site. The reactants in the attenuation process may be present in dissolved form or associated with aquifer solids (e.g., aquifer minerals or microbes). Thus, assessment for MNA will necessitate collection of site-specific data that define the processes controlling contaminant transport. In order to provide context for the types of data that may be required to address this assessment objective, this section will provide a review of the physical and biogeochemical processes that govern contaminant transport in ground water.

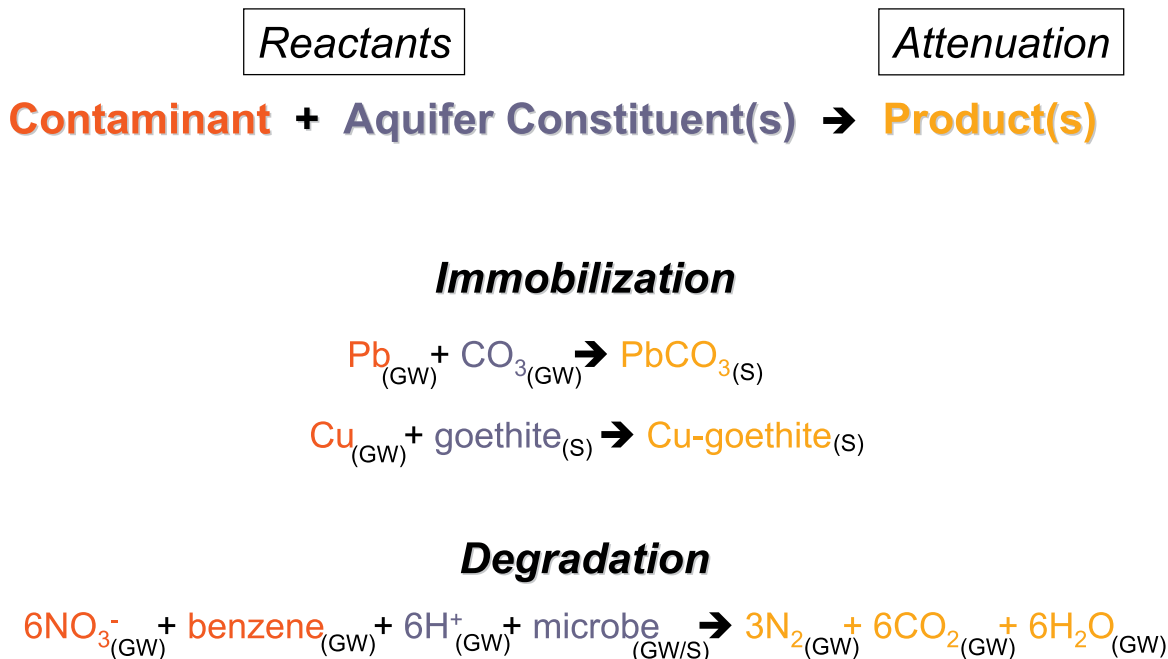


Figure 2.1 Conceptual view of attenuation as the interaction of the contaminant with aquifer constituents to form a product resulting in attenuation. Subscript designations “(GW)” and “(S)” indicate, respectively, whether the reactant(s) and product(s) are in ground water or associated with immobile aquifer solids. For the degradation reaction, N_2 and CO_2 are likely present as dissolved gases; “goethite” is the name of a commonly occurring iron oxyhydroxide mineral in aquifers.

IIA. Physical Transport Mechanisms

IIA.1 Basics of Ground-Water Flow and Solute Movement

Ground water is rarely static and moves from areas of ground-water recharge (i.e., high hydraulic head) to areas of discharge (i.e., low hydraulic head). In a porous medium, ground-water flow generally obeys Darcy's law with velocity proportional to the hydraulic conductivity and hydraulic gradient. In such settings, the average interstitial flow velocity, or seepage velocity (V_s), is the rate at which water moves through the pore spaces of the medium. Under natural conditions, ground-water movement is relatively slow with rates ranging from less than a foot per year to several feet per day (USEPA, 1991). Seepage velocities for the various aquifer materials at a site may often be estimated using:

$$V_s = Ki/n_e$$

where,

K = the hydraulic conductivity of the medium

i = the magnitude of the hydraulic gradient

n_e = the effective porosity or fraction of the medium occupied by interconnected pore space.

In general, the seepage velocity at most sites is expected to vary spatially due to heterogeneity in aquifer material properties and temporally due to fluctuations in hydraulic gradients.

The dominant processes that result in subsurface solute movement in this dynamic environment are advection and dispersion. Advection is the movement of a solute with the bulk movement of ground water (Freeze and Cherry, 1979) and generally is the primary solute transport mechanism at sites with moderate to high ground-water flow rates. Mechanical dispersion results in mixing of ground water during advection reducing dissolved solute concentrations within the plume and causing some solute molecules to travel faster and some to travel slower than the average ground-water velocity. A more detailed discussion of dispersion is provided by Gelhar (1993) and Gelhar et al. (1992). The result at the macro scale is that a solute will spread to occupy a larger portion of the flow field in the direction of ground-water flow and in transverse (perpendicular) directions than that due solely to advection. However, limitations in the ability to obtain direct measurements of dispersion relegate its determination primarily as a fitting parameter during calibration of a ground-water flow model for site-specific applications. At the field scale, stratification (with associated differences in the hydraulic conductivity of geologic materials) and fluctuations in hydraulic gradient often result in much greater differences in the movement of solutes relative to estimates based on the average ground-water flow velocity (Figure 2.2). Thus, relative to site-specific evaluation of contaminant transport, assessment of the degree of variability in the distribution of hydraulic conductivity within the aquifer and time-dependent changes in the magnitude and direction(s) of the hydraulic gradient most likely plays a more critical role under the site characterization effort.

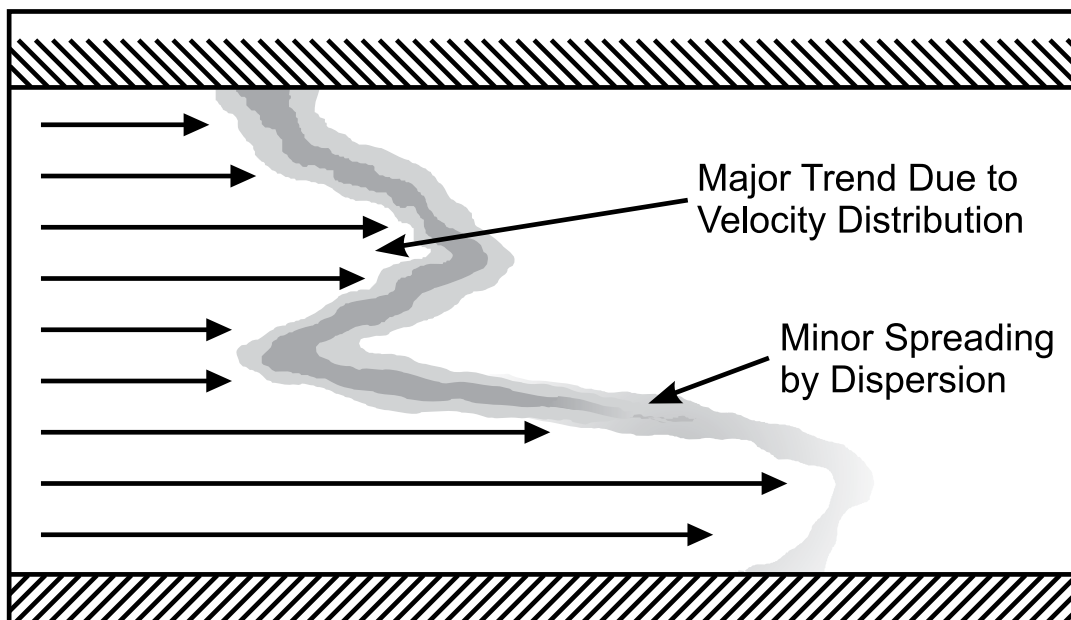


Figure 2.2 Cross-sectional view of differences in solute migration due to differences in hydraulic conductivity with accompanying differences in ground-water velocity and the spreading of the solute front caused by dispersion (Keeley, 1989).

IIA.2 Colloidal Transport of Inorganic Contaminants

The association of contaminants with suspended colloidal material in ground water is a possible transport mechanism and a complicating factor for accurate estimations of the natural attenuation of contaminants in subsurface systems. The mobile colloidal phase must be highly reactive, of sufficient quantity, and stable for periods of time (i.e., remain in suspension due to physical or chemical perturbations to the aquifer) to enable the transport of a significant mass of contaminants. Research to date indicates colloidal facilitated transport of contaminants in ground waters, surface waters and in the unsaturated zone. Evidence suggests that colloidal transport of contaminants may be significant for some species under some hydrogeological conditions. It is important therefore for sampling methods, transport models, and site assessments to consider and be sensitive to this transport mechanism.

Colloids are generally considered to be particles with diameters less than 10 microns (Stumm and Morgan, 1981). Based on theoretical considerations, Yao et al. (1971) and O'Melia (1980) have estimated that the most mobile colloidal particles in filtration studies in porous media may range from 0.1 to 1.0 μm . These include both organic and inorganic materials. Recent estimates of colloidal concentrations in ground water range as high as 63 mg L^{-1} (Buddemeier and Hunt, 1988), 60 mg L^{-1} (Ryan and Gschwend, 1990), and 20 mg L^{-1} (Puls and Eychaner, 1990). In addition to a high surface area per unit mass, colloidal particles such as organic carbon particles, clay minerals and iron oxides are also extremely reactive sorbents for inorganic contaminants. If mobile in subsurface systems, these colloids can effect the migration of contaminants for much larger distances than many transport models would predict, because sorbing contaminants spend a significant fraction of time associated with mobile rather than immobile solids, and because colloid transport can be primarily along large diameter, fast flow paths.

Colloidal material may be released from the soil or geologic matrix and transported large distances given favorable hydrological and geochemical conditions. Changes in solution chemistry resulting from environmental pollution or changes in ground water recharge chemistry can bring about changes in the aqueous saturation state in the subsurface leading to precipitation of new colloid-sized inorganic solids that are entrained within flowing ground water, or can cause the dissolution of matrix cementing agents, promoting the release of colloid-sized particles. In addition, changes in the concentrations of solutes that affect colloid surface charge, such as pH or organic anions, can change the stability of colloids. An excellent review of the mechanisms of colloidal release, transport, and stability was published by McCarthy and Zachara (1989). Reference to field and laboratory studies provide examples of situations representative of sites with subsurface contamination where periods of colloid mobilization may exist. For example, Gschwend and Reynolds (1987) demonstrated that submicron ferrous phosphate colloids were suspended and presumably mobile

in a sand and gravel aquifer. The colloids were formed from sewage-derived phosphate and iron released from aquifer solids due to reduction and dissolution of ferric iron from the soil. Thompson et al. (2006) have also demonstrated that microbially-driven redox cycling of iron bound to soils may also lead to release of colloidal solids via indirect impacts on water chemistry. In this instance, the mobilized colloidal fraction was dominated by organic carbon solids.

However, field observations also point to the transience of colloid mobilization in the subsurface. Nightingale and Bianchi (1977) observed that ground-water turbidity may increase for periods of time due to mobilization of colloidal solids coincident with time-varying recharge events. These observed turbidity increases were abated with time as the aquifer returned to steady-state conditions. In addition, Baumann et al. (2006) observed high colloid concentrations in leachate from landfills, but colloid concentrations decreased rapidly in ground water down gradient from the landfill. Their observations suggested that the change of hydrochemical conditions at the interface, from a reducing, high ionic strength environment inside of the disposal sites to an oxidizing, low ionic strength environment in the ground water (together with physical filtration effects for the larger particles) was an effective chemical barrier for colloid migration. Thus, it appears that while colloid mobilization (along with associated contaminants) probably does occur, colloid migration is not likely to serve as a dominant mechanism for contaminant migration encountered at contaminated sites.

IIA.2.1 Implications for Natural Attenuation Assessment

Many studies have documented that colloidal transport can occur under some hydrogeological conditions. As noted above, very few studies have shown that transport of contaminants via colloidal transport in the subsurface accounts for the predominant mass of mobile contaminant at a site. Where colloidal transport may be significant from a human health standpoint is with highly toxic elements. From a site characterization perspective, assessing the significance of colloid-facilitated contaminant transport will depend on the adequacy of well installation materials and construction approaches, as well as the approaches to sampling ground water. Since well installation results in disturbance of the subsurface solids, initial development to removed fine-grained, disturbed aquifer materials from within and adjacent to the well screen is a critical step prior to initiating retrieval of ground-water samples. In addition, stabilization criteria employed as indicators of the retrieval of representative ground-water samples may need to be adjusted if it is important to rule out colloid transport as a contaminant migration method. For this situation, more strict limits may need to be placed on turbidity stabilization observations, resulting in longer pumping times and/or significantly lower pumping rates (e.g., Jensen and Christensen, 1999).

In addition, it is recommended that the chemical composition of the colloidal materials be identified at sites where field data suggests colloid-facilitated contaminant transport.

This step is warranted to rule out possible sources of sample contamination or artifacts resulting from sample collection or processing. For example, the presence of iron oxide colloids may be observed for reduced ground-water samples containing elevated concentrations of ferrous iron [e.g., >5 ppm Fe(II)] that are exposed to oxygen during collection or handling. In this case, the likely source of colloidal iron oxides is due to rapid oxidation and precipitation of ferrous iron after the ground water has been pumped from the subsurface. In general, the rigid and complex procedures needed to insure sample quality for identification of ground-water colloids may be difficult to implement within the overall characterization effort (e.g., Dai et al., 2002).

Ultimately, the resources expended to this effort need to be balanced with the effort to characterize site hydrology as well as the subsurface processes that may control contaminant degradation or sorption to aquifer solids. In order to provide context to the types of data that may be needed to identify specific sorption processes active within the plume, the following sections provide detail on the types of mechanisms that may result in contaminant immobilization.

As previously outlined in Section I, the processes leading to contaminant attenuation may include those that cause reduction of contaminant mass (i.e., degradation and radioactive decay) or cause immobilization of the contaminant via sorption to aquifer solids. For a majority of the inorganic contaminants encountered at contaminated sites, some form of immobilization will likely dominate the attenuation process. The following discussion will provide detail on the types of sorption processes that may result in contaminant attenuation. This discussion will illustrate the factors or parameters that are a component of the sorption

reaction in order to provide context to the types of measurements needed to support identification of the site-specific attenuation process and its performance characteristics (discussed below in Section III of this volume). In addition, the impact that microbial processes exert on the subsurface geochemistry will be discussed in order to provide context to factors that may dictate site-specific conditions within a contaminant plume.

IIB. Contaminant Sorption to Aquifer Solids

The primary, and in most instances, the only process involved in the natural attenuation of inorganic contaminants is through partitioning to the solid phase. The process of contaminant transfer from the aqueous to the solid phase is generally referred to as *sorption* and involves three primary mechanisms (Sposito, 1986): *adsorption*, which is the accumulation of matter at the interface between the aqueous phase and a solid adsorbent without the development of a three-dimensional molecular arrangement; *precipitation*, which is the growth of a solid phase exhibiting a molecular unit that repeats itself in three dimensions; and *absorption*, which is the diffusion of an aqueous or adsorbed chemical species into a solid phase (Figure 2.3). From the standpoint of monitored natural attenuation, the mechanisms of most relevance will be dependent on contaminant and site specific characteristics, such as the surface reactivity, solubility, and redox sensitivity of the contaminant, as well as the type and abundance of reactive mineral phases and the ground-water chemistry.

More detailed discussion is provided below on the various sorption processes introduced in the preceding paragraph. As a point of reference, representative examples of sorption processes for specific contaminants are provided in Figure 2.4.

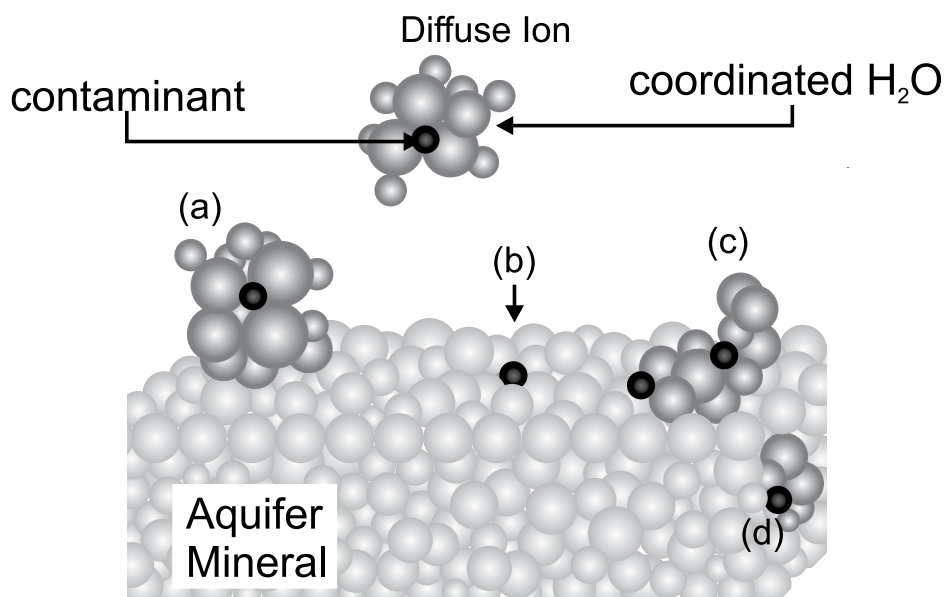


Figure 2.3 Representation of an aquifer mineral surface with (a) an outer-sphere surface complex; (b) an inner-sphere surface complex; (c) a multinuclear surface complex or a surface precipitate; and (d) absorption, or solid state diffusion and substitution of the sorbate in the mineral structure (after Sposito, 1984).

IIB.1 Adsorption

Adsorption processes are typically categorized by the relative binding strength of interaction between the adsorbate (species in solution) and the adsorbent (aquifer solid). There is a range of binding strength for contaminant adsorption that depends on characteristics of the adsorbate, sorbent, and ground-water chemistry. However, discussions of binding strength are generally couched in terms of “weak” or “strong” adsorption processes, albeit a common convention in chemistry would categorize both the covalent and electrostatic interactions involved in adsorption as ‘strong’ intermolecular forces (Israelachvili, 1994). One microscopic distinction borrowed from the characterization of soluble ion pairs that is commonly used to delineate weak and strong adsorption involves the solvation properties of the adsorbate (Westall, 1986; Stumm, 1992). If solvating water molecules are interposed between the cation or anion and the surface, the adsorption complex is referred to as *outer sphere* and is considered to be weak. Conversely, if upon adsorption the adsorbate loses waters of hydration such that there are no water molecules interposed between the cation or anion and the surface, the adsorption complex is referred to as *inner sphere* and is considered to be strong (Sposito, 1984). The propensity of a cation or anion to form either an inner-sphere or outer-sphere surface complex is a function of the adsorbate, the surface functional groups of the adsorbent, and aqueous phase chemistry (e.g., pH and ionic strength).

IIB.1.1 Reactive Mineral Phases Involved in Adsorption

Important adsorbent phases commonly found in the environment include phyllosilicate minerals, metal oxyhydroxide phases, sulfide phases, and natural organic matter (Dixon and Schulze, 2002). Many phyllosilicate minerals possess a permanent negative charge as a result of the substitution of lower valence cations, i.e., Mg(II), Fe(II), Li(I) for Al(III) in the octahedral layer and/or Al(III) for Si(IV) in the tetrahedral layer (referred to as isomorphic substitution). There are two main classes of phyllosilicate minerals based on layer structure (Figure 2.5). The 1:1 mineral layer type is comprised of one Si tetrahedral layer and one Al octahedral layer, which in soils and aquifers is commonly represented by the mineral kaolinite having the general formula $[\text{Si}_4]\text{Al}_4\text{O}_{10}(\text{OH})_8 \cdot n\text{H}_2\text{O}$. Kaolinite and related minerals generally have insignificant degrees of cation substitution within their octahedral and tetrahedral layers, and, thus generally possess a very low permanent negative charge. The 2:1 mineral type is comprised of one Al octahedral layer interposed between two Si tetrahedral layers comparable to the mica structures (Figure 2.5). The 2:1 layer class is represented by a variety of minerals, which are classified based on the location (tetrahedral vs. octahedral layer) and relative amount of isomorphic substitution. The three major mineral classes within the 2:1 layer type are illite ($\text{M}_x[\text{Si}_{6.8}\text{Al}_{1.2}](\text{Al}_3\text{Fe}_{0.25}\text{Mg}_{0.75})\text{O}_{20}(\text{OH})_4$), vermiculite ($\text{M}_x[\text{Si}_7\text{Al}](\text{Al}_3\text{Fe}_{0.5}\text{Mg}_{0.5})\text{O}_{20}(\text{OH})_4$), and smectite ($\text{M}_x[\text{Si}_8]\text{Al}_{3.2}\text{Fe}_{0.2}\text{Mg}_{0.6}\text{O}_{20}(\text{OH})_4$), which display different levels

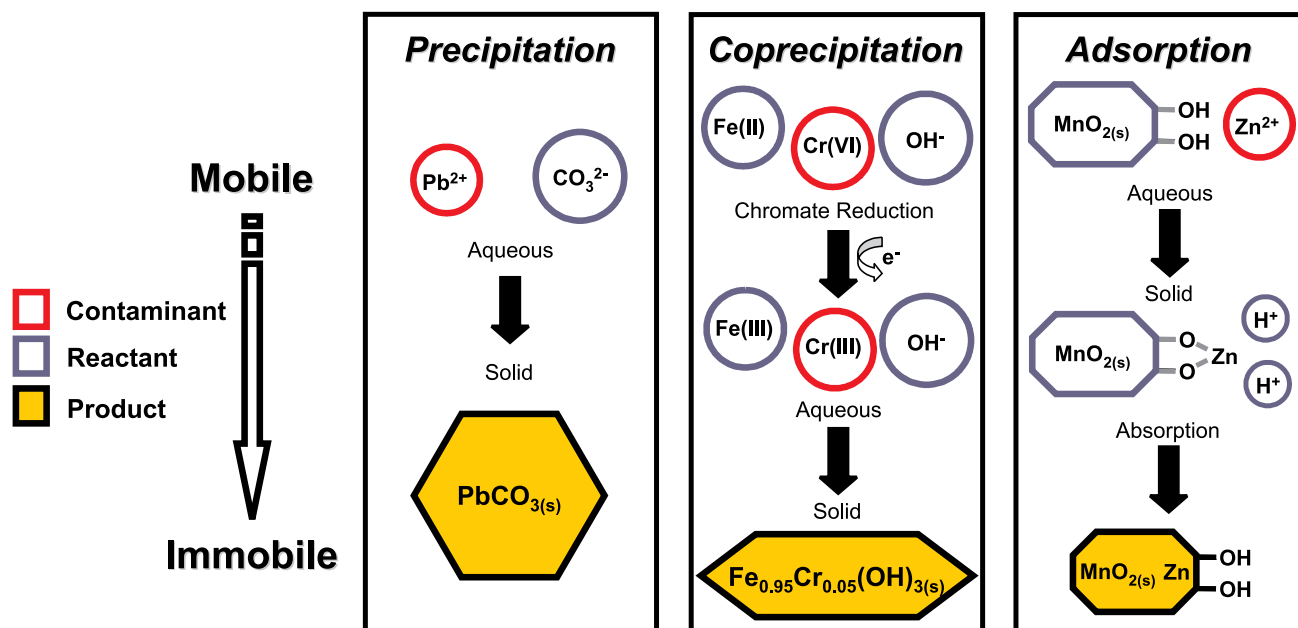


Figure 2.4 Examples of contaminant-specific sorption processes that may lead to attenuation of the ground-water plume. Color coding is employed to distinguish the contaminant (red), aqueous or solid phase reactants (blue), and the product (yellow) of the reaction leading to contaminant attenuation. Absorption is illustrated as a possible sequential process that follows the adsorption of a contaminant onto a mineral component within aquifer solids.

of cation substitution in their tetrahedral and octahedral layers. The permanent negative charge imparted to 2:1 clay minerals by isomorphic substitution is typically balanced through exchange reactions involving major cations in ground water (e.g., Na^+ , K^+ , Ca^{2+} , or Mg^{2+} ; represented by " M_x " in the formulas listed above).

Contaminant sorption to phyllosilicates may occur via ion exchange or surface complexation with surface functional groups (see examples labeled "surface complex" and "ion exchange" in Figure 2.5). Due to differences in the levels of isomorphic substitution for the 1:1 and 2:1 clay mineral classes, ion exchange is usually only significant for 2:1 phyllosilicates. In addition to siloxane oxygen atoms along the basal plane, phyllosilicates possess two types of terminal ionizable OH groups, aluminol and silanol, protruding from the edge surface. These edge OH groups can form both inner- and outer-sphere complexes with metal cations and oxyanions depending on the pH of the bathing solution and on the specific characteristics of the cation or oxyanion (represented as "surface complex" in Figure 2.5).

The most important surface reactive phases for both cationic and anionic contaminants in many soil and subsurface systems are the metal oxyhydroxide phases. These phases are characterized by hexagonal or cubic close-packed O or OH anions with $\text{Fe}^{2+,3+}$, Al^{3+} , and/or $\text{Mn}^{3+,4+}$ occupying octahedral sites. These oxides are present as discrete phases

and as complex mineral assemblages, being co-associated with phyllosilicates and primary minerals as coatings or with humic macromolecules. In soils and sediments the crystallinity of these phases typically varies from poorly ordered to well crystalline forms and grain size from the nanometer to micrometer scale. Among the most common Fe-oxyhydroxide phases found in soils and sediments are the poorly ordered phase ferrihydrite ($\text{Fe}_2\text{O}_3 \cdot n\text{H}_2\text{O}$), and the moderate to well crystalline phases, goethite ($\alpha\text{-FeOOH}$), and hematite ($\alpha\text{-Fe}_2\text{O}_3$). The most common Al oxyhydroxide phase found in soils and sediments is gibbsite ($\gamma\text{-Al(OH)}_3$). Additionally, poorly ordered aluminosilicates can be important reactive phases in certain soils and these include the very poorly ordered allophanes (Si/Al ratios 1:2 to 1:1) and the paracrystalline phase, imogolite ($\text{SiO}_2 \cdot \text{Al}_2\text{O}_3 \cdot 2\text{H}_2\text{O}$). While Mn oxyhydroxides are less prevalent than Fe- and Al-oxyhydroxides in soils and sediments they are very important phases in terms of surface mediated redox reactions and because of their propensity for high metal sorption. The mineralogy of Mn is complicated by the range in Mn-O bond lengths resulting from extensive substitution of Mn^{2+} and Mn^{3+} for Mn(IV). Thus, there exists a continuous series of stable and metastable compositions from MnO to MnO_2 forming a large variety of minerals. Among the more common Mn-oxyhydroxides are pyrolusite ($\beta\text{-MnO}_2$), the hollandite-cryptomelane family ($\alpha\text{-MnO}_2$), todorokite, and birnessite ($\sigma\text{-MnO}_2$).

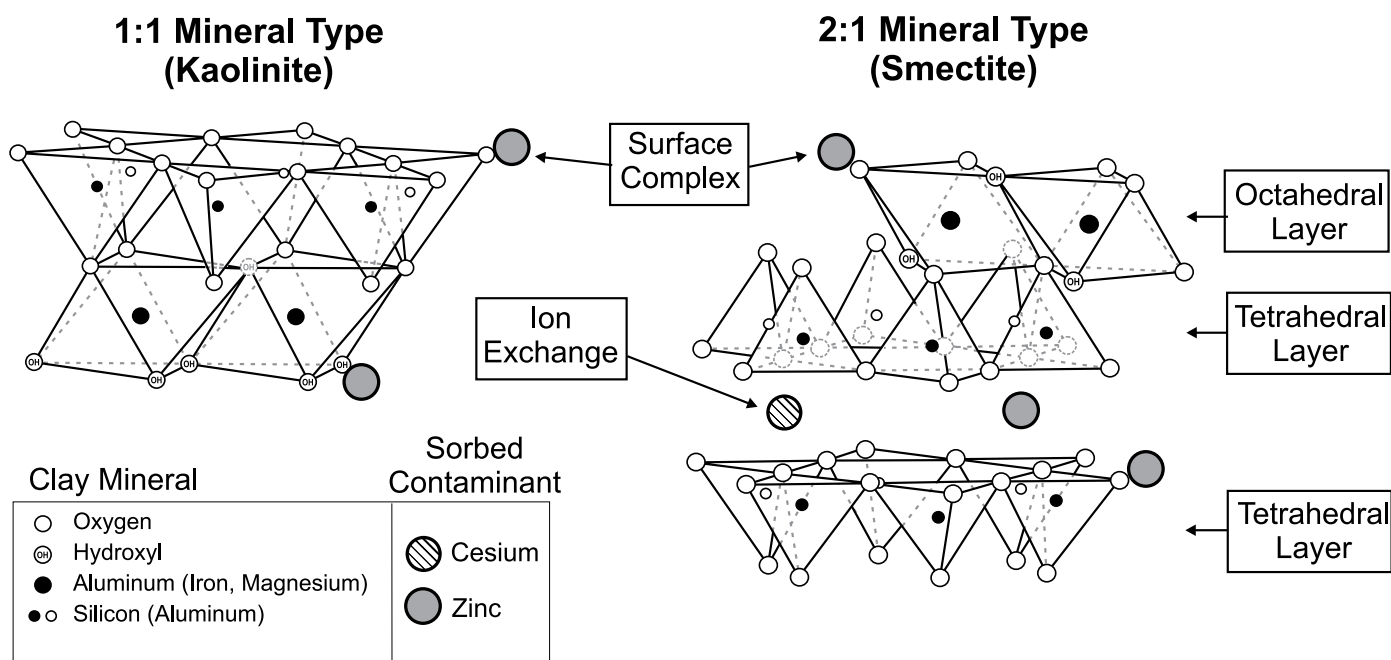


Figure 2.5 Diagrammatic sketch of the structure of 1:1 and 2:1 phyllosilicate minerals. Also shown are hypothetical sorption reactions for zinc and cesium (ion exchange represented as " M_x " in structural formulas for 2:1 phyllosilicates shown in text).

IIB.1.2 Surface Functional Groups on Aquifer Solids and the Impact on Surface Charge

The reactive surface functional group for all of the metal oxyhydroxide phases is the inorganic OH moiety exposed on the outer periphery of these minerals. The reactivity of a specific metal oxyhydroxide is dependent on the surface area (S_A), surface-site density (N_S), the degree of coordination of the OH group to the bulk structure, and the point of zero charge (PZC). The charge on the mineral surface may impose either attractive or repulsive contributions to the overall adsorption reaction, depending on the type of charge possessed by the adsorbate. The properties of the sorbent that impact adsorption are controlled by both the grain size and specific structure of the oxyhydroxide phase.

The surface charge of oxyhydroxide minerals and edge sites on phyllosilicates is derived from the protonation and ionization of exposed surface hydroxyl groups, represented by $\equiv \text{SOH}_n^{n-1}$, where S represents the structural metal cation (e.g., Fe, Al, Mn) over a stoichiometric range from $n=0, 1$, or 2. Thus, as a function of pH, the surface functional groups can be generally described with the following idealized nomenclature: $\equiv \text{SOH}_2^+$, $\equiv \text{SOH}^0$, and $\equiv \text{SO}^-$. The exact charge associated with the various surface functional groups is difficult to measure, so the main purpose of employing this nomenclature is to illustrate that surface charge varies as a function of ground-water chemistry. The gradual change in surface charging with pH for some common minerals is illustrated in Figure 2.6 and a discussion of surface site charging is provided below.

Natural organic matter comprised of complex polymers called humic substances, represents another very important reactive phase in aquifer solids. A variety of functional groups are present in humic substances, and, like OH functional groups of the inorganic metal oxyhydroxides, these also are characterized by pH dependent charging mechanisms. The primary functional groups associated with humic substances in terms of surface charge are carboxyl and phenolic groups, however the less abundant amino, imidazole, and sulfhydryl groups may play an important role in the sorption of certain contaminant metals when present at trace levels (Table 2.1).

Based on the previous discussion, it is apparent that the charge on aquifer solids can be grouped into two classes associated with the mechanisms that give rise to electrical charge associated with mineral surfaces or with organic functional groups. These two classes are commonly referred to as permanent (or constant) charge and variable charge.

- Constant charge - Constant charge is the predominant charge in phyllosilicate clays. Because, for the most part, these isomorphic substitutions occur during mineral formation, this charge deficit is fixed in the lattice structure and is hence unaffected by changes in electrolyte concentration or pH of the soil solution.
- Variable (pH dependent) charge - Variable charge is the predominant charge for oxyhydroxide minerals such as hematite, goethite, and gibbsite, as well as

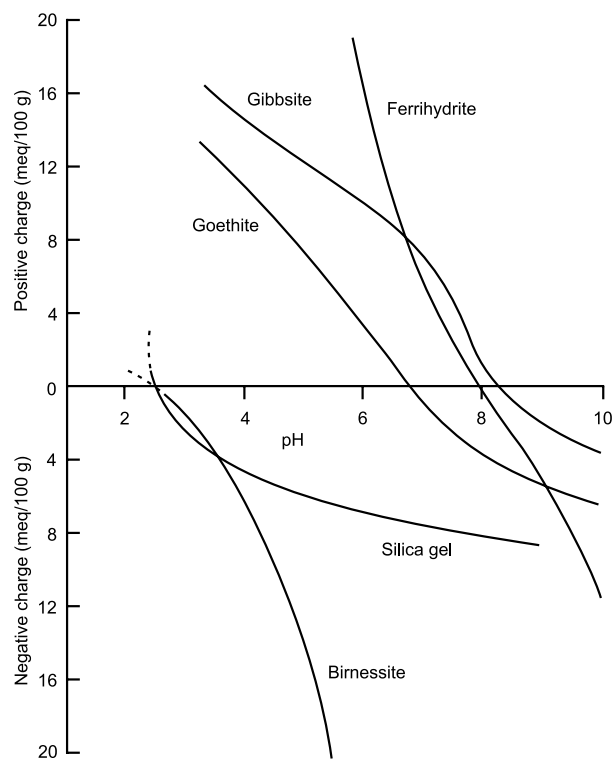
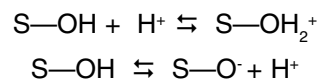


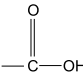
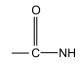
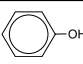
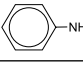
Figure 2.6 Surface charge of some hydroxides from pH 2 to 10 measured in different electrolyte solutions shown in parentheses; positive and negative surface charge shown above and below the x-axis, respectively. Ferrihydrite [$\text{Fe}(\text{OH})_3 \cdot n\text{H}_2\text{O}$] (0.001 M NaNO_3) from Hsi and Langmuir (1985); gibbsite [$\text{Al}(\text{OH})_3$] and silica gel [$\text{SiO}_2 \cdot n\text{H}_2\text{O}$] (1.0 M CsCl) based on Greenland and Mott (1978); goethite [$\alpha\text{-FeOOH}$] (0.005 M CsCl) based on Greenland and Mott (1978) (see also Hsi, 1981); birnessite ($\sigma\text{-MnO}_2$) (0.001 M NaNO_3) based on Catts and Langmuir (1986).

for humic substances. The metal ions in the vicinity of the surface of metal oxyhydroxide minerals are coordinatively unsaturated, i.e. they are lewis acids, and coordinate with water molecules, which subsequently dissociate a proton leading to a surface layer of metal hydroxide functional groups. This process also occurs at the edges of phyllosilicate clays giving rise to SiOH (silanol) and AlOH (aluminol) functional groups. These surface hydroxyl groups can become positively or negatively charged by binding or dissociating a proton (i.e., protonation-deprotonation reactions):



Thus, the prevalent surface charge in aquifer solids will be dependent on the pH of ground water and the types and concentrations of ions that balance the permanent charge association with phyllosilicates. The extent to which

Table 2.1 Important functional groups in humic substances that impact surface charging behavior and contaminant binding.

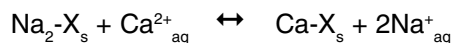
Functional Group	Structural Formula
Amino	-NH ₃
Carboxyl	
Carbonyl	
Alcoholic hydroxyl	-OH
Phenolic hydroxyl	
Imidazole	
Sulfhydryl	-SH

protonation or deprotonation occurs is also a function of the metal ion and the local binding environment of the metal hydroxide surface group. The highly electropositive Si⁴⁺ in silanols precludes the protonation of the surface hydroxyl and this functional group can only dissociate a proton under pH conditions generally encountered in ground water. Aluminols, on the other hand, can be either positively or negatively charged. Various types of hydroxyls of differing reactivity have been identified spectroscopically at the surface of metal oxides.

The charge of aquifer minerals is always electrically balanced by interactions with ions of an opposite charge (counter-ions). We can define two broad classes of weak and strong interactions (outer and inner-sphere) that act to neutralize the charge developed at soil mineral surfaces.

IIB.1.3 Weak and Strong Adsorption Regimes

Weak adsorption regime - Within the weak adsorption regime, simple ion exchange is the most common mechanism and involves the electrostatic attraction of an ionic species by a negative or positive charge emanating from a mineral surface or from functional groups associated with humic substances (Sposito, 1981). Long before the structures of reactive soil minerals were determined, it was observed that, under certain circumstances, there was a reversible and stoichiometric (based on charge) replacement of major cations in soils equilibrated with concentrated neutral salt solutions according to the reaction:



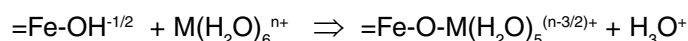
Soil and sediment materials are typically characterized by their cation exchange capacity (CEC), which is defined as the quantity of cations reversibly adsorbed per unit weight of mineral and typically expressed as cmol kg⁻¹. The cation exchange capacity of 2:1 phyllosilicate clays tends to be constant over a wide pH range, since ionizable edge groups are relatively minor on a surface area basis compared to

the permanent charge associated with planar sites. For 2:1 phyllosilicates, cations hydrated to differing degrees are located in the interlayer space and can be displaced by other competing cations through ion exchange reactions (see Figure 2.5). In principle, cation exchange reactions involve both inner and outer sphere complexation with planar sites, although except for the special case discussed below for large weakly hydrated monovalent cations, such as K⁺ and Cs⁺, both are readily reversible. Both inner and outer sphere complexes can also form with O functional groups associated with organic macromolecules and O and OH atoms associated with metal oxyhydroxides, but only the outer sphere complexes are considered weak adsorption. The major difference between phyllosilicates having substantial isomorphous substitution and metal oxyhydroxides and humic substances, is that the CEC is highly pH dependent, increasing with increasing pH. Since reactive mineral phases in soils and sediments are composed of complex assemblages of phyllosilicates, oxyhydroxides, and humic substances, CEC is always a pH dependent property.

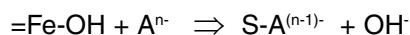
Strong adsorption regime - As discussed above, simple ion exchange is the predominant adsorption mechanism for phyllosilicate clays. A major exception to this is the inner-sphere sorption of larger unhydrated cations, such as K⁺ and Cs⁺ to oxygen atoms of two opposing siloxane ditrigonal cavities of collapsed layers of weathered micaceous minerals, such as illite, which can be classified as an 'irreversible' adsorption or as an absorption process.

At this point it is important to discuss the concept of the reversibility of adsorption. From the perspective of chemical thermodynamics, the definition of a 'reversible' process is one where the initial state of the system can be restored with no observable effects in the system *and* its surroundings (Holman, 1980). The use of the term 'irreversible' from the standpoint of adsorption mechanisms is relative and does not strictly adhere to the thermodynamic (or chemical) definition in all cases. The fixation of Cs⁺ in illitic minerals is conceptually thought to proceed via an initial ion exchange reaction followed by an interlayer collapse (fast) or through the slower migration into interlayer sites in collapsed layers (absorption). Once Cs⁺ is fixed within the interlayer of the clay mineral, its release is not readily reversible via displacement with competing solutes, i.e., through ion exchange mechanisms. Thus, the release of fixed Cs⁺ is subsequently controlled by a process such as mineral dissolution. In this sense, the original fixation process is irreversible, since contaminant release would result from a mechanism other than the reversal of the original adsorption mechanism.

The formation of a chemical bond between an adsorbate and a functional group on the adsorbent also falls within the category of a strong adsorption regime. In general, breaking chemical bonds requires more energy than overcoming electrostatic interactions. Metal adsorption to OH functional groups of oxyhydroxide phases through surface complexation can be illustrated by the following surface reaction (Stumm, 1992; McBride, 2000):



Thus, specific adsorption of cations increases the positive charge at the mineral surface when $n > 1$, which is generally the case for transition elements, and results in the net release of H^+ ions to the soil solution. Adsorption of anions from solution occurs by ligand exchange of a OH or H_2O at the surface functional group according to the following reaction (solution anion represented by A^{n-}):



Anion adsorption is favored by low pH, which leads to protonation of surface functional groups and makes them better leaving groups in the ligand exchange reaction.

IIB.2 Precipitation

Mineral-water reactions occur as ground water moves through porous media. These reactions may result in the removal of aquifer components due to mineral dissolution or result in the buildup to oversaturation and consequent precipitation of secondary minerals. As an outcome of mineral-water reactions along a flow path, fluid compositions and the mineralogical makeup of the solid phase will continuously evolve towards a stable or equilibrium state. Mineral precipitation processes in aquifer systems are an important group of immobilization mechanisms for inorganic contaminants in ground water.

Full treatment of precipitation processes, including coverage of relevant thermodynamic and kinetic concepts, is outside the scope of this document. The reader is referred to numerous standard textbooks in geochemistry, soil science, and aquatic chemistry (e.g., Lindsay, 1979; Stumm, and Morgan, 1981; Drever, 1982; Sposito, 1989; Stumm 1992; Morel and Hering, 1993; McBride, 1994; Sparks, 1995; Langmuir, 1997; Lasaga, 1999). The purpose of this section is to introduce key concepts and issues regarding the potential impact precipitation reactions may exert on contaminate attenuation. In general, mineral precipitation in relation to contaminant immobilization can be discussed in the context of four widely studied processes:

- Precipitation from solution: Nucleation and growth of a solid phase exhibiting a molecular unit that repeats itself in three dimensions. Homogeneous nucleation occurs from bulk solution and heterogeneous nucleation occurs on the surfaces of organic or mineral particles. Heterogeneous nucleation is thought to be more important in natural systems that are rich in reactive inorganic and biological surfaces. Precipitation may result in the formation of sparingly soluble hydroxides, carbonates, and, in anoxic systems, sulfides. Many precipitation reactions have a strong dependence on pH.
- Coprecipitation: Incorporation of an element as a trace or minor constituent within a precipitating phase. In this case, the contaminant substitutes for a more concentrated component in the crystal lattice (isomorphous substitution). This process is distinct from adsorption due to incorporation of the contaminant within the bulk structure of the major mineral phase. Examples of coprecipitation include Cr(III) in hydrous ferric oxide, Cd(II) in calcium carbonate, and As(III) in iron sulfide.

- Surface precipitation: A precipitation process intermediate between surface complexation and precipitation from bulk solution. Surface precipitation represents the continuous growth of particles formed via heterogeneous nucleation. Macroscopic studies of adsorption of some solutes, particularly di-valent and tri-valent cations, suggest that precipitation occurs at surfaces under conditions where the solid is apparently undersaturated based on solution concentrations (Dzombak and Morel, 1990).
- Mineral transformation: Adsorbed contaminants can become incorporated into minerals that form as a result of recrystallization or mineral transformation processes in soils and sediments. Transformation reactions may be accelerated or retarded by the contaminant, and in some cases mineral transformation may result in the exclusion of the impurity contaminant from the solid phase. Examples include incorporation of anions, such as As(V), into hydrous ferric oxide and transformation to Fe oxyhydroxides (e.g., Ford, 2002), coprecipitation of metals with iron monosulfide and transformation to iron disulfide (e.g., Lowers et al., 2007), and layered double hydroxides (typically with Al) as intermediates between adsorbed/surface precipitated metal ions like Ni and Zn, and metal-ion-containing aluminosilicates (e.g., Ford, 2007).

The relative importance of these processes will be determined by contaminant characteristics as well as site-specific characteristics of the plume ground-water chemistry and aquifer solids. These individual processes are discussed in more detail below.

IIB.2.1 Precipitation from Solution

Solution precipitation or crystallization can be divided into two main processes: nucleation and crystal growth. Nucleation occurs prior to growth of a mineral crystal. Both nucleation and growth processes require a system to be oversaturated in the new phase. The probability of nucleation occurring increases exponentially with the degree of oversaturation. Nucleation of a new phase is often facilitated in the presence of a surface (heterogeneous nucleation) compared to bulk solution (homogeneous nucleation). Because nucleation and growth are processes that compete for dissolved solutes, at high degrees of oversaturation the rate of nucleation may be so fast that all excess solute is partitioned into crystal nuclei. In contrast, lower levels of oversaturation can result in the growth of existing crystals without nucleation. Well-formed or euhedral crystals typically develop slowly via growth from solution at low degrees of oversaturation. During crystal growth various chemical reactions can occur at the surface of the growing mineral, such as adsorption, ion exchange, diffusion, and formation of surface precipitates. In general, the rate of crystal growth is controlled either by transport of solutes to the growing surface (i.e., transport controlled), by reactions at the surface (i.e., surface controlled), or a combination of these factors.

For the most abundant cations present in aquifers and soils, such as Al, Si, Fe, Mn, Ca, and Mg, precipitation of mineral forms is common and will in many cases control concentrations observed in solution. At contaminated sites, concentrations of ground-water contaminants are typically several orders of magnitude below the concentrations of the dominant solutes in water. At low concentrations, sorption, surface precipitation, or formation of a dilute solid solution (coprecipitation) may be the more probable removal processes for contaminant species (McBride, 1994). However, precipitation of iron-bearing or aluminum-bearing minerals, for example, can have an important affect on the transport and fate of metal and metalloid contaminants. Major mineral precipitate classes encountered in aquifers and soils are listed in Table 2.2.

The tendency for a system to support a specific precipitation or dissolution reaction can be evaluated through comparison of the equilibrium solubility constant for a given solid phase to the ion activity product calculated using ground-water chemical data. The relative magnitude of the values of the equilibrium solubility product and the calculated ion

activity product provides a measure of the saturation state of ground water relative to mineral precipitation or dissolution. A conventional method for expressing the ground-water saturation state is by calculation of the saturation index, SI, which is given by (Stumm and Morgan, 1981):

$$SI = \Delta G_r^0/RT + \ln Q = \ln Q/K_r$$

where ΔG_r^0 is the standard state free energy change of the reaction, R is the gas constant, T is temperature in degrees Kelvin, Q is the reaction quotient (or ion activity product), and K_r is the temperature- and pressure-dependent equilibrium constant of a reaction. Another term used frequently in place of the saturation index is the relative saturation, $\Omega = Q/K_r$. At chemical equilibrium, $\Delta G_r^0 = 0$, $Q = K_r$, and $\Omega = 1$. In this special case, the solution of interest is in equilibrium with the mineral and no dissolution or precipitation should take place. Where $\Delta G_r^0 < 0$, the mineral cannot precipitate from solution and the thermodynamic driving force is such that mineral dissolution should occur. Where $\Delta G_r^0 > 0$, the mineral will likely precipitate if there are no limiting kinetic factors (Table 2.3).

Table 2.2 Major mineral classes in aquifers and soils.

Mineral Class	Primary Mineral	Contaminant Precipitate
Hydroxides	Al(OH) ₃ , gibbsite Fe(OH) ₃ , hydrous ferric oxide FeO(OH), goethite FeO(OH), lepidocrocite	Cu(OH) ₂ Cr(OH) ₃ Zn(OH) ₂
Oxides	Fe ₃ O ₄ , magnetite Fe ₂ O ₃ , hematite MnO ₂ , pyrolusite SiO ₂ , quartz	UO ₂ , uraninite
Carbonates	CaCO ₃ , calcite/aragonite FeCO ₃ , siderite MnCO ₃ , rhodochrosite	CdCO ₃ , otavite ZnCO ₃ , smithsonite PbCO ₃ , cerussite
Sulfates	BaSO ₄ , barite CaSO ₄ ·2H ₂ O, gypsum	PbSO ₄ , anglesite RaSO ₄
Sulfides	FeS, mackinawite FeS ₂ , pyrite/marcasite	PbS, galena NiS, millerite HgS, cinnabar ZnS, sphalerite
Phyllosilicates	Al ₄ (OH) ₈ Si ₄ O ₁₀ , kaolinite K _{1.5} Al ₂ (OH) ₂ Si _{2.5} Al _{1.5} O ₁₀ , illite	Ni ₃ Si ₂ O ₅ (OH) ₄ , nepouite Na _{0.3} Zn ₃ (Si,Al) ₄ O ₁₀ (OH) ₂ ·4H ₂ O, sauconite

The ion activity product is a useful probe to evaluate the potential for contaminant precipitation. Some caution, however, is recommended in interpreting solution indicators as evidence for the presence of a particular precipitated solid within the plume. The observation that an ion activity product is equal to a corresponding solubility product is not unequivocal evidence that a given phase is at equilibrium or even present in the system (Sposito, 1984). Similarly, an ion activity product that is greater than a corresponding solubility product cannot be taken as confirmation that precipitation is occurring. To understand the state of a system with respect to precipitation and dissolution, it is recommended that the presence of the relevant solid phases be evaluated in addition to measuring the concentrations of solutes that participate in a precipitation reaction suspected to occur within the ground-water plume.

Table 2.3 Relationships among Q , K_r , and Ω .

Process	Saturation Index, $\log(Q/K_r)$	Relative Saturation, Ω	Q , K_r
Mineral dissolution	Negative	< 1	$Q < K_r$
Mineral precipitation	Positive	> 1	$Q > K_r$
Equilibrium	0	1	$Q = K_r$

IIB.2.2 Coprecipitation

Contaminant plumes are often characterized by concentrations of dissolved solids in excess of that found in ambient ground water. These elevated dissolved solids may be derived as a component of the contaminant source or due to the dissolution of soil or aquifer solids during plume transport. Examples of these processes include interactions of acid wastes with aquifer solids leading to dissolution of aquifer minerals (e.g., carbonates or oxyhydroxides) or the development of reducing conditions driven by microbial degradation of organic contaminants that result in reductive dissolution of iron-bearing minerals. With downgradient transport, changes in ground-water chemistry or interaction with unimpacted aquifer solids may lead to precipitation of these major ground-water constituents out of solution. Contaminants may be removed from ground water at the location where precipitation of these major ground-water constituents occurs. This process is called coprecipitation, since the contaminant is sequestered within a newly formed precipitate, but only as a trace structural component within the precipitate. Examples of major precipitate classes with a coprecipitated contaminant include oxyhydroxides (e.g. $Fe_{1-x}Cr_x(OH)_3(s)$), carbonates (e.g., $Ca_{1-x}Cd_xCO_3(s)$), sulfides (e.g., $Fe_{1-x}Ni_xS_2(s)$), and phyllosilicates. The contaminant may be coprecipitated in a cationic or anionic form depending on ground-water chemistry and the nature of the precipitating phase.

For coprecipitates (or solid solutions) the concentration of the contaminant in ground water in contact with a precipitate may be reduced significantly below that observed for ground water in which the concentration of the contact is governed by the solubility of a precipitate in which the contaminant is a major structural component (e.g., $Ca_{1-x}Cu_xCO_3(s)$, coprecipitate vs. $CuCO_3(s)$, pure precipitate). For example, the partial molal Gibbs free energy of a binary mixture can be expressed as the sum of two components: a mechanical mixing term and a free energy of mixing term ($\Delta G_{mixture}$):

$$\bar{G}_{mixture} = (X_1\bar{G}_1 + X_2\bar{G}_2) + \Delta G_{mixture}$$

where X_1 and X_2 are the mole fractions of two components in a binary mixture. The $\Delta G_{mixture}$ term contains an ideal component that depends on X_1 and X_2 and a non-ideal component dependent on X_1 , X_2 , and activity coefficients in the solid phase (γ_1 and γ_2):

$$\Delta G_{mixture} = RT[X_1 \ln X_1 + X_2 \ln X_2] + RT[X_1 \ln \gamma_1 + X_2 \ln \gamma_2]$$

For an ideal solid solution, $\gamma_1 = \gamma_2 = 1$, so that $RT[X_1 \ln \gamma_1 + X_2 \ln \gamma_2] = 0$. Ideal mixing may be approached where the amount of substitution is very low (a dilute solid solution) or where the mixing cations are closely matched in size and charge. In this case, the $\Delta G_{mixture}$ function is a symmetrical parabola having a minimum at $X_1 = X_2 = 0.5$. Hence as a general rule, the free energy of binary mixtures is less than that of the pure, end-member components. It follows that the solubility of an ion can be lowered in a mixed ionic compound relative to the solubility of the pure compound.

Remobilization of a coprecipitated contaminant will be governed by the overall stability of the host precipitate, which may be controlled by ground water parameters such as pH and/or redox state. In most cases, the identification of a coprecipitation process cannot be made with a single line of evidence. Observations of decreased contaminant concentrations concurrent with decreases in the concentrations of major ground-water constituents such as Ca, Fe, or dissolved sulfide may be indicative of a coprecipitation event. It is recommended that this evidence be supplemented with solid phase characterization approaches, such as chemical extractions or microanalytical techniques, to confirm that coprecipitation is an attenuation mechanism.

IIB.2.3 Surface Precipitation

Surface precipitation may result when adsorption leads to high sorbate coverage at the mineral-water interface. Surface precipitation can be thought of as an intermediate stage between surface complexation and bulk precipitation of the sorbing ion in solution (Farley et al., 1985; Ford et al., 2001). At low concentrations of the sorbing metal at the mineral surface, surface complexation is the dominant process. As the concentration of the sorbate increases, the surface complexation concentration increases to the point where nucleation and growth of a surface precipitate occurs. Surface precipitation can be viewed as a special

case of coprecipitation where the mineral interface is a mixing zone for ions of surface precipitate and those of the underlying substrate. It is generally believed that surface precipitation can occur from solutions that would appear to be undersaturated relative to precipitate formation based on considering solution saturation indices. The reason for this may be due in part to different equilibrium constants for surface precipitation versus precipitation from solution, or may be related to the way the mineral-water interface is modeled (Sverjensky, 2003). For example, the dielectric constant of water and therefore activity coefficients in bulk solution may be different from activity coefficients near a mineral surface. Again, the identification of a surface precipitation process cannot be made only with solution data. Solid phase characterization data, such as chemical extractions or microanalytical techniques, are needed to confirm that surface precipitation plays a role as an attenuation mechanism.

IIB.2.4 Mineral Transformation

In many cases the solids that precipitate in near surface environments are not the most thermodynamically stable phases. For example, hydrous ferric oxide, ferrihydrite, is metastable relative to the iron oxyhydroxide goethite. The preponderance of metastability in near surface environments is a consequence of the slowness of chemical reactions at temperatures typical of surficial environments. Kinetics, therefore, play an integral role in ground-water and soil geochemistry. Mineral transformation is one example of how metastable precipitates evolve toward more stable mineral phases within an aquifer. Ultimately, contaminants that are initially adsorbed onto or coprecipitated with these metastable precipitates are likely to become more resistant to remobilization if they are incorporated into the more stable transformation product.

The Ostwald Step Rule is often obeyed in low-temperature mineral formation. Precipitation of less stable and more soluble phases is followed by transformation to progressively more stable and less soluble phases. This behavior stems from the preferential formation of materials with fast precipitation kinetics over nucleation and growth of phases with slow kinetics (Stumm, 1992). Differences in precipitation kinetics are often tied to structural complexity of the precipitating mineral. Relatively simple structures are able to form rapidly whereas ordered structures, although more stable, require longer time periods to develop. Precursor phases are usually poorly crystalline and they may be chemically dissimilar to the final stable mineral. Examples that follow the Ostwald Step Rule include the precipitation of ferrihydrite and transformation to more stable iron oxyhydroxides (goethite) and iron oxides (hematite), the precipitation of mackinawite and transformation to pyrite, and the precipitation of amorphous aluminosilicates such as allophane and transformation to halloysite and kaolinite. Transformation pathways result from solution mediated processes or solid-phase transitions (Steefel and van Cappellen, 1990).

The iron monosulfide-to-iron disulfide transformation has been widely studied in the laboratory and in the field. In this

example of a mineral transformation process, mackinawite (Fe_{1-x}S) precipitates as concentrations of dissolved sulfide and ferrous iron accumulate in pore water. It has been determined that in sulfate-reducing environments, pore water concentrations of ferrous iron and sulfide are controlled by the solubility of mackinawite. Mackinawite, however, is metastable with respect to the iron disulfides, pyrite and marcasite. The rate of transformation from mackinawite to pyrite or marcasite depends on pH and redox conditions. Metals that coprecipitate with mackinawite are likely incorporated into pyrite, which is more stable over a wide pH range and in anoxic conditions. The rate at which this transformation occurs will be governed by chemical conditions including the coprecipitation or adsorption of contaminants and other dissolved constituents from solution. Site characterization aspects relating to mineral transformation processes as an immobilization mechanism will involve determining the spatial concentration distribution of precursor phases and their more stable transformation products along with contaminant associations using mineralogical and wet chemical characterization tools.

IIB.3 Implications for Natural Attenuation Assessment

The sorption processes discussed in the preceding paragraphs may act in isolation or together to arrest contaminant migration within the aquifer. Factors that dictate which process is likely to dominate contaminant attenuation include chemical properties of the contaminant, chemical characteristics of the ground water, and properties of the aquifer solids. Due to the complexities of directly identifying the immobilized form of the contaminant, it is likely that multiple lines of evidence will be needed to adequately discern the controlling attenuation reaction. These lines of evidence will include the evaluation of patterns in ground-water chemistry that point to potential precipitation or coprecipitation reactions, evaluation of aquifer solids to determine patterns in contaminant and solid component associations, and the use of chemical speciation or reaction models to assess if ground-water and aquifer solid characteristics are consistent with observed contaminant attenuation. Additional perspective on possible sorption processes for specific contaminants is provided in the contaminant-specific chapters included in Volume 2 and 3 of this document.

IIC. Microbial Impacts on Inorganic Contaminant Attenuation

The chemical characteristics of ground water and properties of the aquifer mineral components are, in part, influenced by microbial reactions. Microbial activity within the aquifer may also play a more direct role in controlling contaminant speciation and migration. The influence of microbial reactions may be more pronounced in contaminant plumes that also contain degradable organic contaminants such as hydrocarbons or chlorinated solvents. In these instances, the plume geochemistry may differ significantly from that observed in ambient ground water at a site. If microbial reactions play a significant role in contaminant attenuation, it may be necessary to gather information on the degree that

these reactions control the concentrations and distributions of reactants that participate in contaminant attenuation, as well as the capacity of the aquifer to sustain microbial activity within the plume. In order to provide perspective on the potential influence of the subsurface microbiology, the following discussion provides an overview of general characteristics of subsurface microbiology, the influence of microbial activity on the redox state within the plume, and the types of contaminant attenuation reactions that may be directly mediated by microorganisms.

IIC.1 Characteristics of Aquifer Microbiology

Microbial reactions can alter the geochemical structure of the subsurface (Newman and Banfield, 2002), and it is becoming increasingly important to characterize these processes in terms of the natural attenuation of inorganic contaminants. Microorganisms inhabiting the subsurface environment exhibit a remarkable array of metabolic capabilities enabling them to use organic or inorganic matter as energy sources and propagate under aerobic or anaerobic conditions. A large part of a microorganism's metabolism is devoted to the generation of adenosine triphosphate (ATP), an "energy currency" that is used by the microorganism for cell synthesis. Microorganisms derive energy through the oxidation of organic compounds or chemically-reduced inorganic ions and compounds. The electrons or hydrogen atoms resulting from oxidation are transferred in most microorganisms by an electron transport chain to an electron acceptor which, in the case of aerobic respiration, is oxygen. Some microorganisms are capable of anaerobic respiration, whereby the electron acceptor is not O_2 but chemically-reducible inorganic compounds such as NO_3^- , SO_4^{2-} , CO_2 , Fe^{3+} , or iron/manganese oxyhydroxides. A third type of metabolism, called "fermentation," involves intra-molecular oxidation/reduction without an externally supplied terminal electron acceptor. Fermentation reactions are not considered here because they do not involve metal transformations.

The metabolic diversity manifested by microorganisms is key to their being agents of geochemical change in the subsurface (Ehrlich, 1995). Subsurface biota are usually categorized as either heterotrophic or chemolithotrophic according to the following criteria:

- Heterotrophic microorganisms - Heterotrophs include bacteria (single- or multi-celled organisms lacking internal membrane structures), fungi (mycelial or single-celled organisms possessing a cell wall but no photosynthetic capability), protozoa (unicellular, microscopic animals such as amoebae), and archaeobacteria (a newly discovered group of organisms possessing a unique cell envelope, membrane structure and ribosomal RNA, distinguishing them from all other microorganisms). Heterotrophs derive energy from the oxidation of organic compounds and obtain most of their carbon from these compounds. Some heterotrophs respire aerobically while others respire anaerobically, requiring the availability of oxygen or other reducible compounds to serve as electron acceptors.

- Chemolithotrophic microorganisms - Some genera of bacteria and archaeobacteria are chemolithotrophs. These microorganisms derive energy from the oxidation of inorganic compounds (for example, Fe^{2+} , HS^- , and H_2) and obtain their carbon as CO_3^{2-} , HCO_3^- or CO_2 . Some chemolithotrophs are aerobic using O_2 as an electron acceptor while others respire anaerobically using chemically reducible inorganic matter as an electron acceptor (Newman, 2001). An example of this type of metabolism is carried out by methanogens, which oxidize H_2 using CO_2 as an electron acceptor to form CH_4 . Reactions carried out by chemolithotrophic microorganisms must derive sufficient energy from the oxidation/reduction reactions to fix carbon (that is, reduce CO_3^{2-} , HCO_3^- or CO_2 to organic carbon) and phosphorylate ADP.

In the aquifer below the vadose zone the populations and numbers of microorganisms vary significantly due to limitations to available oxygen. If the aquifer is shallow and is recharged through cracks and fissures, the water may be nutrient-rich and oxygenated resulting in an abundance of different microorganisms whose numbers can reach 10^6 per gram. Lower population numbers would be expected in aquifers where the supply of dissolved oxygen from surface recharge is limited. Deep aquifers are generally more depleted with respect to nutrients (unless contaminated) and oxygen causing the numbers and diversity of microorganisms to decline and often be limited to bacteria and archaeobacteria. This finding has been supported, during the last 15–20 years, by carefully controlled drilling studies undertaken to evaluate the microbiology of deep, impermeable rock strata (Ghiorse, 1997; Kerr, 2002).

IIC.2 Microbial Controls on Subsurface Redox State

Since microorganisms chemically transform aquifer constituents such as dissolved oxygen, iron [aqueous and solid forms of Fe(III) and Fe(II)], and sulfur [aqueous species such as sulfate and dissolved sulfide], their metabolic reactions may exert significant influence on the redox geochemistry within the plume. As previously discussed, redox conditions within the aquifer may govern precipitation-dissolution reactions that control contaminant precipitation or coprecipitation, as well as the types and concentration of aquifer solids that may serve as adsorbents. From this perspective, some knowledge about the microbial populations as a function of space and time within the plume may be necessary to understand the existing redox status of the aquifer and make projections about how it may evolve. For heterotrophic microorganisms, the electrons or reducing equivalents (hydrogen or electron-transferring molecules) produced during degradation of organic compounds must be transferred to a terminal electron acceptor (TEA). Observations of microbial systems have led to the development of a classification system that groups microorganisms into three categories according to predominant TEAs:

- Aerobic bacteria — Bacteria which can only utilize molecular oxygen as a TEA. Without molecular oxygen, these bacteria are not capable of degradation.

- Facultative aerobes/anaerobes — Bacteria which can utilize molecular oxygen or when oxygen concentrations are low or nonexistent, may switch to nitrate, manganese oxides or iron oxides as electron acceptors.
- Anaerobes — Bacteria which cannot utilize oxygen as an electron acceptor and for which oxygen is toxic. Though members may utilize nitrate or other electron acceptors, it can be said that they generally utilize sulfate or carbon dioxide as electron acceptors.

In any environment in which microbial activity occurs, there is a progression from aerobic to anaerobic conditions (ultimately methanogenic) with an associated change in the redox status of the system. There is a definite sequence of electron acceptors used in this progression through distinctly different redox states. The rate, type of active microbial population, and level of activity under each of these environments are controlled by several factors. These include the concentration of the electron acceptors, substrates which can be utilized by the bacteria, and specific microbial populations leading to the progression of an aquifer from aerobic to methanogenic conditions (Salanitro, 1993). This results in a loss of organic carbon and various electron acceptors from the system as well as a progression in the types and physiological activity of the indigenous bacteria.

If microbial activity is high, the aquifer environment would be expected to progress rapidly through these conditions. The following scenario outlines a general sequence of events in which aerobic metabolism of preferential carbon sources would occur first. The carbon source may be from organic contaminant sources or other more readily degradable carbon which has entered the system previously or simultaneously with the contamination event.

- Oxygen-Reducing to Nitrate-Reducing Conditions – Once available oxygen is consumed, active aerobic populations begin to shift to nitrate respiration. Denitrification will continue until available nitrate is depleted, or usable carbon sources become limiting.
- Nitrate-Reducing to Manganese-Reducing Conditions – Once nitrate is depleted, populations which reduce manganese may dominate. Bacterial metabolism of substrates utilized by manganese-reducing populations will continue until the concentration of manganese oxide becomes limiting.
- Manganese-Reducing to Iron-Reducing Conditions – When manganese oxide becomes limiting, iron reduction becomes the predominant reaction mechanism. Available evidence suggests that iron reduction does not occur until all Mn(IV) oxides are depleted. In addition, bacterial Mn(IV) respiration appears to be restricted to areas where sulfate is nearly or completely absent.
- Iron-Reducing to Sulfate-Reducing Conditions – Iron reduction continues until substrate or carbon limitations allow sulfate-reducing bacteria to become active.

Sulfate-reducing bacteria then dominate until usable carbon or sulfate limitations impede their activity.

- Sulfate-Reducing to Methanogenic Conditions – Once usable carbon or sulfate limitations occur, methanogenic bacteria are able to dominate.

Development of a general knowledge of the redox status of the aquifer throughout the plume is important relative to understanding the processes contaminant attenuation (or lack thereof) within the plume, as well as changes in the capacity for or stability of contaminant attenuation with the return to ambient conditions. There are several approaches to evaluating the redox state of the aquifer. One common approach is to monitor the oxidation-reduction potential in ground water using a platinum electrode with recalculation of the measured electrode potential as Eh. However, due to the lack of internal redox equilibrium in natural systems (Morris and Stumm, 1967) and limitations to electrode potential measurements in a complex matrix such as ground water, this measurement should be supplemented with other site-specific determinations. One supplemental approach to assessing redox status is the determination of concentrations of specific redox sensitive species such as oxygen, Fe(II), hydrogen sulfide, or methane as qualitative guides to the redox status of ground water (Lindberg and Runnells, 1984; USEPA, 2002). These measurements provide a means to generally characterize the ground water as oxic, suboxic, or anoxic and may provide more direct evidence of the occurrence of iron-reducing, sulfate-reducing or methanogenic conditions. Another approach that may be used to indicate the terminal electron acceptor process (TEAP) which dominates within the plume is measurement of the hydrogen (H₂) concentration in ground water (Lovely and Goodwin, 1988). Hydrogen concentration for the various TEAPs are shown in Table 2.4 (Chapelle et al., 1995).

Table 2.4 Range of hydrogen concentrations for a given terminal electron-accepting process that can be used for classification of the redox status within the contaminant plume.

Terminal Electron Accepting Process	Hydrogen (H ₂) Concentration (nanomoles per liter)
Denitrification	<0.1
Iron (III) Reduction	0.2 to 0.8
Sulfate Reduction	1 to 4
Methanogenesis	5 to 20

The focus of this discussion has been on the influence of microbial activity on the redox status of ground water, which governs the types of aqueous and solid phase reactants that may be involved in contaminant attenuation. The following discussion elaborates on the influence of microbial reactions on the chemical speciation of inorganic contaminants.

IIC.3 Impacts on Contaminant Speciation and Attenuation

Microbe/metal interactions result in immobilization, mobilization, or transformation by extracellular precipitation reactions, intracellular accumulation, oxidation and reduction reactions, methylation and demethylation, and extracellular binding and complexation. Many of these processes play an important role in achieving natural attenuation through immobilization or degradation. Many transformations of metals and metalloids are carried out by subsurface microorganisms for the purpose of obtaining energy for growth and reproduction; however, these transformations may not result in decreasing the mobility or toxicity of the metal. Some microbial transformations are carried out specifically to detoxify their environment, suggesting that microbes have an enormous capacity to sustain life. Therefore, the role of microbes in the subsurface is multifaceted. The principal mechanisms employed by microorganisms to transform metals and metalloids in the subsurface environment are:

- Oxidation and reduction reactions resulting from microbial respiratory activities (Lovely, 1993; Ahmann et al., 1994);
- Biosorption by cell walls, cell membranes and exopolymers and intracellular bioaccumulation (Beveridge, 1989); and
- Methylation and demethylation (Oremland et al., 1991; Bentley et al., 2002).

These microbial mechanisms are described with emphasis on reactions involved in natural attenuation of metals and radionuclides.

IIC.3.1 Contaminant Oxidation-reduction Reactions

Oxidation-reduction (redox) processes are chemical reactions that involve a transfer of electrons between reactants and products and consequently a change in the oxidation state of elements that can either be oxidized to higher valence states or reduced to lower valence states. Changes in the valence state of a particular element can result in the following:

- Change in speciation resulting in lower or higher toxicity
- Change in speciation resulting in lower element solubility (immobilization) or increased solubility (mobilization)
- Change in speciation that impacts adsorption/desorption behavior

The contaminants for which redox-mediated processes may lead to attenuation include elements that can occur in multiple oxidation states under environmentally relevant conditions. Thus, a transition metal such as Cr is redox-active since two stable oxidation states (VI and III) are readily observed in aqueous solution, whereas Ni is not redox-active as only one oxidation state (II) occurs in

aqueous solutions at ambient conditions. (More detailed discussions on the redox activity of individual contaminants are provided in Volume 2.)

Oxidation-reduction (redox) reactions, which can be carried out by both heterotrophic and chemolithotrophic microorganisms, are either energy-generating or enzymatically-catalyzed without coupling to energy generation. Microbially catalyzed, energy generating redox reactions tend to be rapid and the metal transformations so extensive that the geological influence is often substantial. One example that results in the attenuation of metals is the reduction of soluble SO_4^{2-} by *Desulfovibrio* and *Desulfotomaculum* species involving oxidation of organic matter or H_2 for energy and use of sulfate as a terminal electron acceptor (Lovely, 1993). This redox reaction yields dissolved sulfide that can chemically react with a number of soluble, divalent metals producing insoluble metal sulfides. In some cases, the microbially-generated sulfide may chemically reduce an inorganic contaminant. For example, dissolved sulfide may result in reduction of arsenate to arsenite. Examples of enzymatically-catalyzed redox reactions that immobilize metals for attenuation in the subsurface are the reduction of mobile Cr(VI) to the less toxic and less mobile Cr(III) (Palmer and Wittbrodt, 1991) and reduction by some microorganisms of Se(VI) or Se(IV) to insoluble Se(0) (Ehrlich, 1995).

IIC.3.2 Biosorption and Intracellular Bioaccumulation

Biosorption, a form of contaminant *adsorption*, is the binding of inorganic ions to the outer surface of a microorganism by ion exchange, van der Waals attractions, or chemical reactions between the metal ion and cell wall, cell membrane, excreted metabolites, or exopolymers. Biosorption is not dependent on metabolism by the microbial cell. Intracellular bioaccumulation, or *absorption*, is the transport of metals across the cell wall and membrane and subsequent retention of the metals within the cell. Bioaccumulation is metabolism dependent because the transport process requires energy.

The outer surfaces of microorganisms are chemically complex with each group of organisms possessing differing cell wall, membrane, and expolymeric structures. These structures are composed of macromolecules having functional groups including carboxylates, amines, imidazole, phosphate, sulfhydryl, sulfate, hydroxyl and others. Usually the microbes exhibit a net negative charge owing to the abundance of carboxylate and phosphate groups, however, positively charged amines and imidazole functional groups impart polyfunctional characteristics to the cell surface. Most inorganic contaminant binding occurs after initial complexation and neutralization of the chemically active site. This stoichiometric interaction between contaminant ions and active sites within the wall acts as a nucleation site for the deposition of additional ions from solution in a manner similar to surface precipitation onto aquifer minerals. The deposition product then grows in size within the intermolecular spaces of the wall fabric until it is physically

constrained by the polymeric meshwork of the wall. Therefore, the amount of contaminants bound to the outer surfaces of organisms can be considerably greater than that accounted for by the number of charges available because binding occurs not only by ion exchange type reactions and covalent bonding to charged functional groups, but by precipitation and reduction reactions (Beveridge, 1989).

As with mineral surfaces in the aquifer solids, pH plays a critical role in the binding of inorganic contaminants. At low pH values cationic metal binding is diminished because negative charges on functional groups become protonated, reducing the negative charge density of the organism's surface. Although the quantitative role of extracellular binding in controlling the concentration of inorganic contaminants in the subsurface is not well defined, it does play a larger part in metal mobility than intracellular metal accumulation. The relative contribution of microbial binding processes to the overall immobilization of the contaminant within the plume is largely unknown. However, a simple comparison of the relative mass of microbes versus reactive minerals in aquifer solids would suggest that microbial binding plays a minor role.

IIC.3.3 Methylation and Demethylation

Microbial interactions with some inorganic contaminants considered in this document result in the transfer of methyl groups onto these elements by a process known as methylation. This process may result in either the increased toxicity or mobility of some inorganic contaminants. Bio-methylation of metal(loid)s takes place when suitable organisms are present under anaerobic conditions with high concentration of available metal(loid)s and methyl donors. These conditions may exist in contaminated ground water (e.g., derived from landfill leachate). An example of this type of process is the methylation of inorganic selenium to dimethylselenide, a volatile product. Methylation of selenium decreases rather than increases its toxicity and probably represents a detoxification reaction that occurs readily in aerobic soils and sediments. Arsenate can also be methylated by some bacteria and filamentous fungi. Biosynthesis of organic compounds containing arsenic such as arsenocholine, arsenobetaine, and arsenosugars also occurs among various bacteria, algae, and many higher organisms (Andreae and Klumpp, 1979).

IIC.4 Implications for Natural Attenuation Assessment

Based on the previous discussion, it is apparent that the subsurface microbial community could influence inorganic contaminant transport. For many of the contaminants discussed in this document, microbial reactions will primarily exert an indirect influence on contaminant attenuation by governing the types, distribution, and concentrations of aqueous and solid phase reactants. However, microbial activity may constitute a more direct impact on contaminant speciation, including changes in the redox state of contaminants such as arsenic or selenium. From this perspective, it is recommended that the site characterization effort incor-

porate analysis of the extent to which microbial processes may govern ground-water chemistry within the plume. This is more critical at sites where the co-occurrence of readily degradable organic contaminants result in ground-water conditions significantly different than those observed in ambient ground water. For these situations, information on the mechanism, rate, capacity, and stability of contaminant attenuation may need to be evaluated within the context of the behavior of the organic component of the plume.

IID. References

- Ahmann, D., A.L. Roberts, L.R. Krumholz, and F.M.M. Morel. Microbes grow by reducing arsenic. *Nature* 371: 750 (1994).
- Andreae M.O. and D. Klumpp. Biosynthesis and release of organoarsenic compounds by marine algae. *Environmental Science and Technology* 13: 738-741 (1979).
- Baumann, T., P. Fruhstorfer, T. Klein, and R. Niessner. Colloid and heavy metal transport at landfill sites in direct contact with groundwater. *Water Research* 40: 2776-2786 (2006).
- Bentley, R. and T.G. Chasteen. Microbial methylation of metalloids: arsenic, antimony, and bismuth. *Microbiology and Molecular Biology Reviews* 66: 250-271 (2002).
- Beveridge, T.J. Role of cellular design in bacterial metal accumulation and mineralization. *Annual Reviews in Microbiology* 43: 147-171 (1989).
- Buddemeier, R. W. and J.R. Hunt. Transport of colloidal contaminants in ground water: Radionuclide migration at the Nevada Test site. *Applied Geochemistry* 3: 535-548 (1988).
- Catts, J. G. and D. Langmuir. Adsorption of Cu, Pb, Zn by delta-MnO₂: Applicability of the site binding-surface complexation model. *Applied Geochemistry* 1: 255-264 (1986).
- Chapelle, F.H., P.B. McMahon, N.M. Dubrovsky, R.F. Fujii, E.T. Oaksford, and D.A. Vroblesky. Deducing the distribution of terminal electron-accepting processes in hydrologically diverse groundwater systems. *Water Resources Research* 31: 359-371 (1995).
- Dai, M., J.M. Kelley, and K.O. Buesseler. Sources and migration of plutonium in groundwater at the Savannah River Site. *Environmental Science and Technology* 36: 3690-3699 (2002).
- Dixon, J.B. and D.G. Schulze (Eds.). *Soil Mineralogy with Environmental Applications*. Soil Science Society of America, Madison, WI (2002).
- Drever, J.I. *The Geochemistry of Natural Waters*. Prentice-Hall, Englewood Cliffs, NJ (1982).
- Dzombak, D.A. and F.M.M. Morel. *Surface Complexation Modeling; Hydrous Ferric Oxide*. John Wiley & Sons, New York, NY (1990).
- Ehrlich, H.L. *Geomicrobiology*, 3rd edition. Marcel Dekker, New York, NY (1995).

- Farley, K.J., D.A. Dzombak, and F.M.M. Morel. A surface precipitation model for the sorption of cations on metal oxides. *Journal of Colloid and Interface Science* 106: 226-242 (1985).
- Ford, R.G. Rates of hydrous ferric oxide crystallization and the influence on coprecipitated arsenate. *Environmental Science and Technology* 36: 2459-2463 (2002).
- Ford, R.G., A.C. Scheinost, and D.L. Sparks. Frontiers in metal sorption/precipitation mechanisms on soil mineral surfaces. *Advances in Agronomy* 74: 41-62 (2001).
- Ford, R.G. Structural dynamics of metal partitioning to mineral surfaces. In *Natural Attenuation of Trace Element Availability in Soils*. R. Hamon, M. McLaughlin and D. Stevens (Eds.), SETAC Press, Pensacola, FL (2007).
- Freeze, R.A. and J.A. Cherry. *Groundwater*. Prentice-Hall, Englewood Cliffs, NJ (1979).
- Gelhar, L.W. *Stochastic Subsurface Hydrology*. Prentice-Hall, Englewood Cliffs, NJ (1993).
- Gelhar, L.W., C. Welty, and K.R. Rehfeldt. A critical review of data on field-scale dispersion in aquifers. *Water Resources Research* 28: 1955-1974 (1992).
- Ghiorse, W.C. Subterranean life. *Science* 275: 789-790 (1997).
- Greenland, D.J. and C.J.B. Mott. Surfaces of soil particles. In *Chemistry of Soil Constituents*. D.J. Greenland and M.H.B. Hayes (Eds.), John Wiley, Chichester, UK (1978).
- Gschwend, P.M. and M.D. Reynolds. Monodisperse ferrous phosphate colloids in an anoxic groundwater plume. *Journal of Contaminant Hydrology* 1: 309-327 (1987).
- Holman, J.P. Reversible processes and cycles. In *Thermodynamics*. F.J. Cerra and J.W. Bradley (Eds.), McGraw-Hill, New York, NY, pp. 200-203 (1980).
- Hsi, C.D. and D. Langmuir. Adsorption of uranyl onto ferric oxyhydroxides: Application of the surface complexation site-binding model. *Geochimica et Cosmochimica Acta* 49: 1931-1941 (1985).
- Israelachvili, J.N. Interactions involving polar molecules. In *Intermolecular and Surface Forces*. Academic Press Inc., San Diego, CA, pp. 48-82 (1994).
- Keeley, J.F. *Ground Water Issue, Performance Evaluations of Pump-and-Treat Remediations*, EPA/540/4-89/005, U.S. Environmental Protection Agency, Ada, OK (1989).
- Kerr, R.A. Deep life in the slow, slow lane. *Science* 296: 1056 (2002).
- Langmuir, D. *Aqueous Environmental Geochemistry*. Prentice-Hall, Upper Saddle River, NJ (1997).
- Lasaga, A.C. *Kinetic Theory in the Earth Sciences*. Princeton University Press, Princeton, NJ (1999).
- Lindberg, R.D. and D.D. Runnells. Ground water redox reactions: An analysis of equilibrium state applied to Eh measurements and geochemical modeling. *Science* 225: 925-927 (1984).
- Lindsay, W.L. *Chemical Equilibria in Soils*. John Wiley & Sons, New York, NY (1979).
- Lowers, H.A., G.N. Breit, A.L. Foster, J. Whitney, J. Yount, Md.N. Uddin, and Ad.A. Muneem. Arsenic incorporation into authigenic pyrite, Bengal Basin sediment, Bangladesh. *Geochimica et Cosmochimica Acta* 71: 2699-2717 (2007).
- McBride, M.B. Chemisorption and precipitation reactions. In *Handbook of Soil Science*. M.E. Summer (Ed.), CRC Press, Boca Raton, FL (2002).
- McBride, M.B. *Environmental Chemistry of Soils*. Oxford University Press, New York, NY (1994).
- McCarthy, J.F. and J.M. Zachara. Subsurface transport of contaminants. *Environmental Science and Technology* 5: 496-502 (1989).
- Morel, F.M.M. and J.G. Hering. *Principles and Applications of Aquatic Chemistry*. John Wiley & Sons, New York, NY (1993).
- Morris, J.C. and W. Stumm. In *Equilibrium Concepts in Natural Waters Systems*. W. Stumm (Ed.), American Chemical Society, Washington DC (1967).
- Newman, D.K. and J.F. Banfield. Geomicrobiology: how molecular-scale interactions underpin biogeochemical systems. *Science* 296: 1071-1077 (2002).
- Newman, D.K. How bacteria respire minerals. *Science* 292: 1312-1313 (2001).
- Nightingale, H.I. and W.C. Bianchi. Ground water turbidity resulting from artificial recharge. *Ground Water* 15: 146-152 (1977).
- O'Melia, C.R. Aquasols: The behavior of small particles in aquatic systems. *Environmental Science and Technology* 14: 1052-1060 (1980).
- Oremland, R.S., C.W. Culbertson, and M.R. Winfrey. Methylmercury decomposition in sediments and bacterial cultures: Involvement of methanogens and sulfate reducers in oxidative demethylation. *Applied and Environmental Microbiology* 57: 130-137 (1991).
- Palmer, C.D. and P.R. Wittbrodt. Processes affecting the remediation of chromium-contaminated sites. *Environmental Health Perspectives* 92: 25-40 (1991).
- Puls, R.W. and J.H. Eychaner. Sampling ground water for inorganics - pumping rate, filtration, and oxidation effects. In *Fourth National Outdoor Action Conference on Aquifer Restoration*, National Water Well Association, Dublin, OH (1990).
- Ryan, J.N. and P.M. Gschwend. Colloid mobilization in two Atlantic coastal plain aquifers. *Water Resources Research* 26: 307-322 (1990).
- Salanitro, J.P. The role of bioattenuation in the management of aromatic hydrocarbon plumes in aquifers. *Ground Water Monitoring and Remediation* 13: 150-161 (1993).
- Sparks, D. *Environmental Soil Chemistry*. Academic Press, San Diego, CA (1995).

-
- Sposito, G. Cation exchange in soils: An historical and theoretical perspective. In *Chemistry in the Soil Environment*, American Society of Agronomy, Madison, WI, pp. 13-30 (1981).
- Sposito, G. *The Surface Chemistry of Soils*. Oxford University Press, New York, NY (1984).
- Sposito, G. *The Chemistry of Soils*. Oxford University Press, New York, NY (1989).
- Sposito, G. Distinguishing adsorption from surface precipitation. In *Geochemical Processes at Mineral Surfaces*. J.A. Davis and K.F. Hayes (Eds.), American Chemical Society Symposium Series 323, pp. 217-228 (1986).
- Steeffel, C.I. and P. van Cappellen. A new kinetic approach to modeling water-rock interaction: The role of nucleation, precursors, and Ostwald ripening. *Geochimica et Cosmochimica Acta* 54: 2657-2677 (1990).
- Stumm, W. and J.J. Morgan. *Aquatic Chemistry*. John Wiley & Sons, New York, NY (1981).
- Stumm, W. *Chemistry of the Solid-Water Interface*. John Wiley & Sons, New York, NY (1992).
- Sverjensky, D.A. Standard states for the activities of mineral surface sites and species. *Geochimica et Cosmochimica Acta* 67: 17-28 (2003).
- Thompson, A., O.A. Chadwick, S. Boman, and J. Chorover. Colloid mobilization during soil iron redox oscillations. *Environmental Science and Technology* 40: 5743 -5749 (2006).
- USEPA. *Seminar Publication Site Characterization for Sub-surface Remediation*, EPA/625/4-91/026, U.S. Environmental Protection Agency, Cincinnati, OH (1991).
- USEPA. *Workshop on Monitoring Oxidation-reduction Processes for Ground-water Restoration*, EPA/600/R-02/002, Office of Research and Development, Washington DC (2002).
- Westall, J. Reactions at the oxide-solution interface: Chemical and electrostatic models. In *Geochemical Processes and Mineral Surfaces*. J.A. Davis and K.F. Hayes (Eds.), American Chemical Society Symposium Series 323, pp. 54-78 (1986).
- Yao, K., M.T. Habibian, and C.R. O'Melia. Water and waste water filtration: concepts and applications. *Environmental Science and Technology* 5: 1105-1112 (1971).

Section III

Site Characterization to Support Evaluation of MNA

Richard T. Wilkin, Steven Acree, Steve Mangion, Patrick V. Brady, James E. Amonette, Paul M. Bertsch, Douglas B. Kent, Robert W. Puls, Ann Azadpour-Keeley, Robert G. Ford

In determining whether MNA is applicable to a site, characterization data are collected to define site hydrogeology and the reaction(s) that result in contaminant attenuation. Characterization of attenuation reactions will involve identification of the reactants that control contaminant immobilization or degradation. The reactants may be of aqueous and/or solids forms, with solid reactants potentially consisting of aquifer solids or microbes. Once the specific reaction mechanism is identified, site characterization will then proceed to determination of the capacity of ground-water conditions to sustain the attenuation reaction and assessment of the stability of immobilized contaminants to resist remobilization due to changes in ground-water chemistry. The types of samples collected from within the plume boundary will include ground water and aquifer solids. Analyses of these samples will include those more commonly employed to understand the overall geochemical context of subsurface chemistry, as well as more specialized analyses used to identify the chemical speciation of the contaminant in dissolved or solid form. Simple observations of the distribution of the contaminant between solid and liquid forms will be insufficient to identify the specific reaction process. A mechanistic understanding of the reaction is needed in order to assess the overall performance characteristics of the attenuation process. This section will provide an overview of the analytical techniques that are used to provide evidence for processes and chemical speciation in the subsurface.

IIIA Site Hydrogeology

Hydrogeology is the foundation of the conceptual model for natural attenuation (National Research Council, 2000). Three-dimensional characterization of the ground-water flow field and the changes that occur through time are crucial to understanding the transport and, ultimately, the fate of contaminants. Discussions of hydrogeologic site characterization in this document draw freely from USEPA (2003) and are largely limited to evaluations performed in saturated porous-media settings, such as unconsolidated aquifer materials. Although similar concepts are sometimes applicable in other geologic settings, such as fractured rock formations, ground water often moves primarily through discrete pathways at these sites. In such highly anisotropic settings, the direction of ground-water flow and contaminant transport often cannot be determined within a sufficient degree of certainty to support assessments of natural attenuation rates or processes. Assessment of contaminant

transport and fate in these and other highly heterogeneous settings is an area of continuing research and is beyond the scope of this discussion. In similar fashion, hydrogeologic characterization of vadose zone materials is not specifically addressed in this section. Flow conditions are often more complex in the vadose zone than in similar saturated media. However, characterization of the hydrogeologic properties of the vadose zone, as well as the saturated zone, will be necessary at some sites. A general discussion of vadose zone characterization for contaminant transport assessments is found in USEPA (1991; 1993a; 1993b).

IIIA.1 Characterization Objectives

Much of the spatial variability in observed contaminant concentrations is the result of geologic heterogeneity. Differences in the geologic properties of aquifer materials from the micro-scale (e.g., grain-size distribution) to the field scale (e.g., stratigraphy) result in differences in hydraulic conductivity and the directions and rates of ground-water flow. Three-dimensional hydraulic gradients that occur due to the site-specific characteristics of ground-water recharge and discharge are also dominant controls on flow. Together, the differences in the hydraulic conductivity of different aquifer materials, hydraulic gradients, and the changes in gradients that often occur in response to natural or anthropogenic changes in ground-water discharge and recharge control the directions and rates of ground-water flow.

Detailed hydrogeologic characterization is essential for evaluating natural attenuation processes and rates, as well as for specification of the locations and frequencies for performance monitoring. The first step in characterizing contaminant transport, and, therefore the processes that may result in attenuation, is the determination of the path or paths of ground-water transport along which the contaminant will migrate. At a minimum, the hydrogeologic database should be sufficient to:

- Define geologic and hydrologic controls on the ground-water flow field (e.g., transmissive units, preferential pathways, and barriers to flow);
- Quantify flow rates and directions and their spatial and temporal variations;
- Support characterization of contaminant sources, the distribution of contaminants of concern, and the effects of dominant natural attenuation processes; and
- Identify possible receptors.

The scale and intensity of this characterization is determined by site-specific conditions (e.g., variability in geology and hydrology and the acceptable level of uncertainty in the outcome of the evaluations).

III.A.2 Geologic Characterization

III.A.2.1 Saturated Porous Media

The key geologic factors that control ground-water flow at sites where secondary porosity features such as fractures, including faults, joints, and partings along bedding planes, are not present include site stratigraphy and lithologic characteristics. Stratigraphy is the science concerned with the form, composition, thickness, areal extent, sequence, and correlation of both consolidated and unconsolidated geologic materials. It defines the framework of the ground-water flow field and constrains the pathways for contaminant migration (USEPA, 1991). Lithology is the description of the physical and mineralogic characteristics of geologic materials. Physical characteristics that control flow include grain-size distribution, grain shape, and packing. As discussed in other sections, mineral composition and coatings affect inorganic constituent distribution through a variety of chemical reactions including cation exchange, substitution, precipitation, dissolution, acid-base reactions, complexation and redox reactions (USEPA, 1991). Grain-size distribution, grain shape, and packing (i.e., arrangement) of grains influence the hydraulic conductivity, total porosity, and effective porosity of the geologic materials.

At many sites, evaluation of sedimentary depositional environments is an especially useful framework for the understanding of site stratigraphy and the distribution of lithologic controls on ground-water flow. Sedimentary facies (i.e., sedimentary bodies that are internally similar in characteristics) determine the three-dimensional geometries, connectivity, and heterogeneity of aquifer units and barriers to flow (Galloway and Sharp, 1998) in many porous-media settings. Ground water can move preferentially through coarser-grained materials, resulting in varying degrees of heterogeneity in flow patterns and contaminant transport. Interconnected facies of relatively coarse-grained materials may provide preferential pathways for contaminant migration. An example of a naturally occurring preferential pathway would be a deposit of interconnected sands of high hydraulic conductivity bounded by deposits of finer-grained materials. In similar fashion, anthropogenic features such as buried utility corridors and heterogeneous fill materials may also result in the formation of preferential pathways for ground-water flow or impediments to flow. However, even within a given preferential pathway, ground water may move in sinuous paths due, in part, to small-scale differences in hydraulic conductivity of the materials or to temporally variable, three-dimensional hydraulic gradients.

Interconnected transmissive materials may be separate and distinct pathways for contaminant movement. For example, the degree of hydrologic connection between different sedimentary facies depicted in Figure 3.1 is small. Monitoring points in different facies may appear to be similar and may be hydraulically down gradient of one another without sig-

nificant ground-water flow and contaminant transport from one unit to the next. This is explicitly illustrated in Figure 3.1 where two wells are screened at similar depth below the water table along the pathway of ground-water transport. The two screens are placed within two different facies that likely possess different magnitudes of hydraulic conductivity (i.e., Well 1 screened in a higher conductivity material in the “medium to coarse-grained sand” vs. Well 2 screened in a lower conductivity in the “fine-grained silty sand”). The difference in hydraulic conductivity between these two facies may prevent a direct line of transport from Well 1 to Well 2. In such cases, apparent contaminant attenuation between monitoring points (i.e., due to lower concentration observed in Well 2) may be an artifact of sample location and not representative of actual conditions. Inferences about natural attenuation based on apparent decreases in contaminant concentration in the down gradient direction are likely to be incorrect in these situations unless ground-water flow paths are determined and monitored. This level of characterization is often difficult to accomplish using small numbers of monitoring points.

Three-dimensional characterization will be needed to evaluate and predict the effects of natural attenuation processes (e.g., advection, dispersion, diffusion, and sorption processes) on contaminants at many sites. Data required to construct the site geologic framework include stratigraphic and lithologic data obtained from geologic cores and supplemented with information from surface and, particularly, borehole geophysical methods. Innovative characterization technologies, such as the cone penetrometer and geologic sampling using direct-push methods, offer the potential for cost-effectively evaluating the geologic controls on ground-water flow and their variability in greater detail than previously possible without obtaining continuous cores during traditional drilling. Regardless of the chosen technology, the choice of sampling locations needed as a basis for evaluations of natural attenuation processes depends on factors such as the site-specific geology, contaminant characteristics, degree of physical, chemical, and biological heterogeneity, and the locations of points of compliance and or critical down gradient exposure points.

III.A.2.2 Saturated Fractured Media

In rock or consolidated materials, features such as fractures often control ground-water flow. The primary factors affecting flow through fractured media are the density and orientations of fractures, the effective aperture width of the fractures, and properties of the rock matrix (Schmelling and Ross, 1989). An adequate characterization of a fractured rock system would generally include information on fracture orientation (i.e., strike and dip), aperture widths, fracture locations, and interconnection; hydraulic head throughout the contaminated volume; the distribution of rock porosity and permeability; sources of ground water and contaminants; contaminant distribution; and chemical interactions with the rock matrix. Chemical weathering of the rock and the subsequent mineralogic changes that occur along fractures can also be especially important controls on the fate and transport of inorganic contaminants.

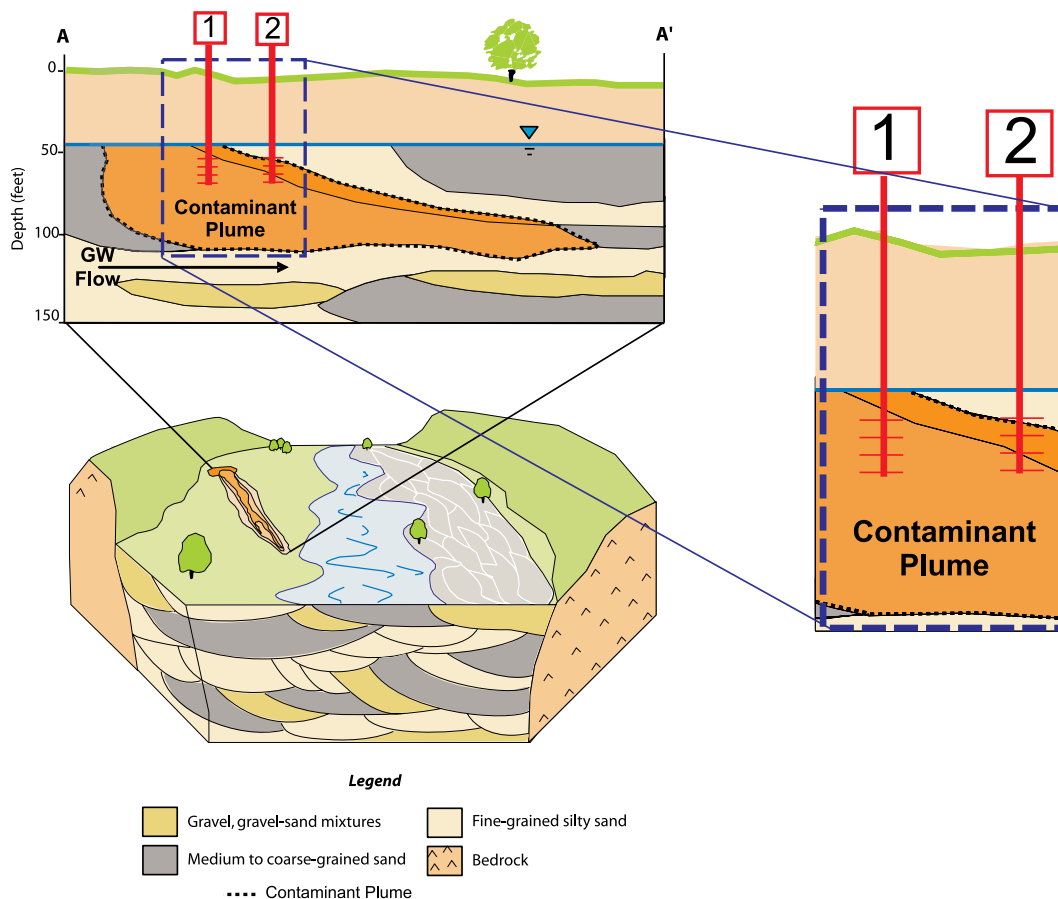


Figure 3.1 *Geologic block diagram and cross section depicting a stream environment. In this setting, numerous facies of channel materials are surrounded by finer-grained materials of lower hydraulic conductivity (modified from USEPA, 2003). Two monitoring wells, labeled [1] and [2], are shown in red. A magnified portion of the aquifer cross-section is shown to the right to clarify that the well screens are placed within two different facies possessing differing hydraulic conductivities.*

Many important features, such as fracture patterns, can often be determined by standard surficial geologic mapping techniques. Much additional data concerning subsurface conditions can also be obtained using downhole and surface geophysical methods. However, sufficient characterization to support natural attenuation process evaluations with the level of certainty needed to satisfy data quality objectives will be neither technically nor economically feasible at the scale of many sites.

III.A.3 Hydrologic Characterization

Knowledge of the geologic framework provides much information needed to define the features that control ground-water flow. However, data regarding the hydraulic properties (e.g., hydraulic conductivities and effective porosities) of the aquifer materials and their distribution are needed to allow quantitative estimates of such parameters as ground-water flow rates, contaminant fluxes, and contaminant attenuation rates. Much of the necessary data regarding hydraulic properties will generally be acquired through hydraulic tests performed in the field (e.g., pumping tests, slug tests, packer

tests, and tracer tests). Additional information regarding geologic and hydrologic site characterization concepts and techniques may be obtained from a variety of sources (e.g., Butler, 1998; Kruseman and de Ridder, 1989; USEPA, 1991; USEPA, 1993a; USEPA, 1998).

Hydrologic characterization of the ground-water flow system also requires an understanding of natural and anthropogenic sources for recharge, the characteristics of discharge, and the hydraulic gradients that are the result. Recharge sources include precipitation, surface-water bodies, irrigation, and losses from potable water distribution systems. Important locations of ground-water discharge include water production wells, springs, wetlands, and surface-water bodies. The locations and rates of ground-water recharge and discharge are important factors in determining site-specific hydraulic gradients and, therefore, the directions and rates of flow. Hydraulic gradients may be three dimensional in nature with strong vertical as well as horizontal components in many cases. This often results in a dynamic, three-dimensional flow system.

Temporal variations in either natural or anthropogenic recharge or discharge may result in fluctuations in both the horizontal and vertical components of hydraulic gradients, the directions/rates of contaminant migration, contaminant loading to ground water, and, potentially, redox conditions. These fluctuations may lead to changes in the geometry of the plume that should be considered during evaluations of natural attenuation and monitoring plan development. For example, seasonal changes in precipitation may result in non-uniform changes in water table elevations due to differences in recharge related to topography, different soil types, or land uses. This may result in seasonal changes in hydraulic gradients or discharge locations. Rapid and sustained changes in ground-water flow velocity are common in flood plains, particularly near large rivers that have major changes in the river stage. In some situations, changes in contaminant loading to ground water may also occur due to increased recharge through contaminated vadose zone materials or elevation of the water table into

these materials. Longer-term patterns associated with sequences of unusually wet or dry years may also influence ground-water velocity over correspondingly longer time periods.

Anthropogenic influences on site hydrology, such as changes in ground-water withdrawal or irrigation rates and patterns, may have similar effects on plume behavior but occur on frequencies other than those corresponding to precipitation patterns. Irrigation or municipal water supply wells that pump intermittently can affect ground-water flow patterns in a complex manner that may be difficult to assess. In addition, land use changes that alter patterns of recharge, discharge, or withdrawal may be important sources of variability in the ground-water flow field that should be routinely considered during the life of an MNA remedy. The illustration in Figure 3.2 provides an example where the off-site installation and activation of an irrigation well can result in movement of the ground-water plume in

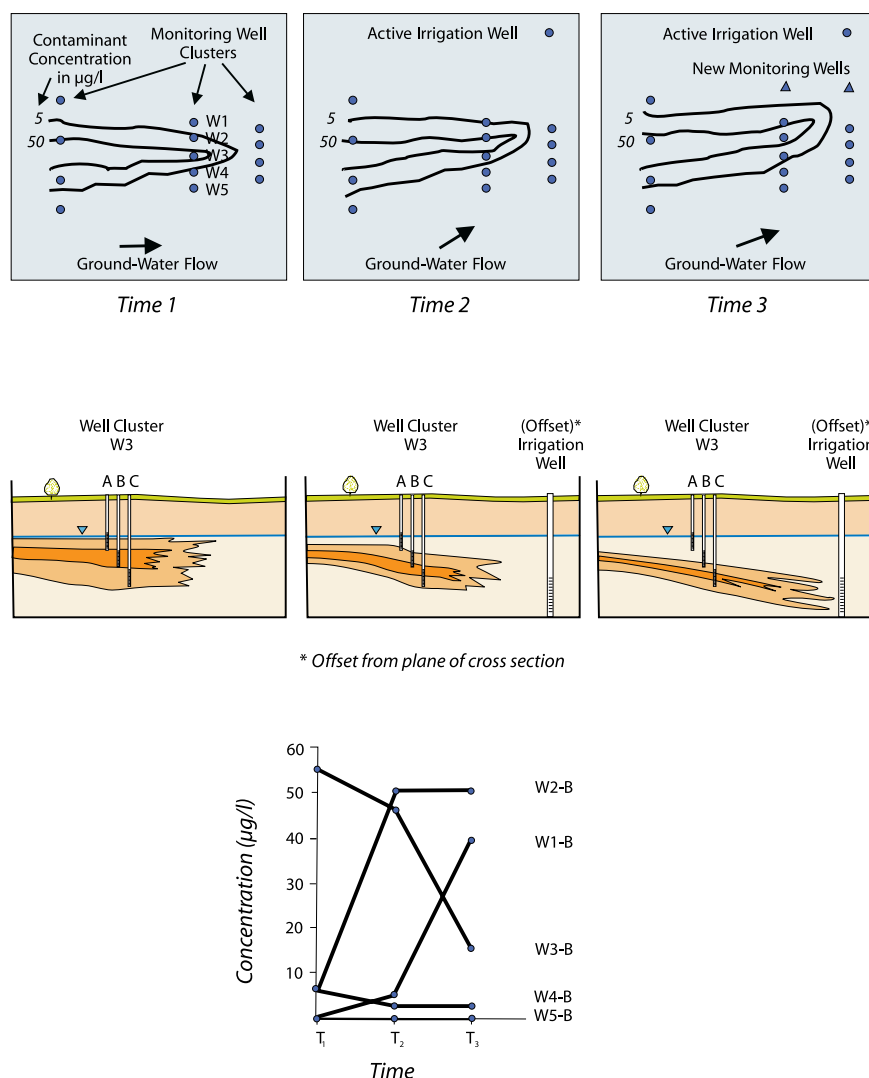


Figure 3.2 Potential effects of changes in ground-water flow direction on temporal trends in contaminant concentrations (USEPA, 2003).

response to this new ground-water withdrawal from the aquifer. In this situation, a decrease in contaminant concentration at a well screen originally placed within a portion of the plume with highest concentrations could be mistaken for evidence of an attenuation process. This misinterpretation in contaminant concentration trend can be prevented through periodic re-examination of the hydraulic gradient distribution within the monitored portion of the aquifer. In addition, these observations also provide guidance on how to adjust the location of monitoring points within the aquifer to insure that the entire plume is being monitored.

Elevations of surface-water bodies and ground-water elevation data periodically obtained from a network of wells and piezometers screened at appropriate depths within the contaminated aquifer units and surrounding units are essential elements of hydrologic analyses. Additional data for assessing ground-water flow include land use information such as the locations, rates, and schedules of irrigation; local precipitation data; and pumping rates and schedules for nearby wells. These data and the resulting estimates of hydraulic gradients are used in conjunction with interpretations of the hydraulic properties of subsurface materials and locations of contaminant sources to evaluate potential changes in contaminant loading, transport and attenuation rates, and transport directions with time. The evaluations should be three-dimensional in nature, including horizontal and vertical components of hydraulic gradients that result in three-dimensional contaminant transport.

In many cases, frequent (e.g., weekly or monthly) monitoring of ground-water and surface-water elevations may be warranted, particularly during early phases of monitoring, to improve the characterization of ground-water flow patterns. In some cases, monitoring of these parameters on a very frequent basis using automated recording equipment may be needed to determine the effects of variability in recharge and discharge rates or locations. Once the effects are determined, the information would be used in the specification of appropriate long-term monitoring frequencies. These data may also indicate changes in hydraulic gradients that warrant more frequent monitoring of chemical parameters. Based on the results of such assessments, monitoring frequencies may be adjusted to adequately capture the fundamental features of the observed trends. In general, several years of monitoring data are often necessary for estimation of the site variability in the ground-water flow field.

IIIA.4 Ground-Water/Surface-Water Interactions

Ground-water/surface-water interactions are of particular importance at sites where surface-water bodies are present. The hydrologic, as well as geochemical conditions, in areas where ground water discharges to or is recharged by surface water often differ markedly from those in the main body of the plume and may require intensive monitoring to determine the effect on remedial goals (Winter, 2000). Locations where ground water discharges to surface water may vary both temporally and spatially due to changing hydrologic conditions (Winter et al., 1998; USEPA, 2005a). Tools to characterize the hydraulic relationships between

ground water and surface water include piezometers, devices for the direct measurement of ground-water flux and velocity, geophysical methods, and certain geochemical techniques. These tools may be used to define areas of plume discharge into the surface-water body, quantify rates of discharge, and to aid in the selection of monitoring point locations for determining the impact of the discharging water on the sediments and surface-water quality. Multilevel monitoring is generally required to characterize the interactions of ground water and surface water features. For situations where the contaminant plume intersects the transition zone between ground water and surface water, information on the distribution of ground-water discharge/recharge can be used in the selection of monitoring points to characterize chemical characteristics of the transition zone. Characterization of the transition zone can be employed to assess and demonstrate that contaminant concentrations in discharging ground water or accumulated in surface water sediments do not negatively impact human or ecological receptors. Additional discussions of methods for hydrologic characterization of ground-water/surface-water interactions and monitoring of the potential for contaminated ground-water discharge to surface water may be found in various sources, including USEPA (2000a).

IIIA.5 Hydrogeologic Data Interpretation

The data obtained during hydrogeologic characterization are used in conjunction with information on contaminant sources, distribution, and behavior; redox conditions; and possible receptors to develop a conceptual model describing site conditions (Figure 3.3). A three-dimensional conceptual site model incorporating temporal changes is generally necessary to provide a framework for interpreting the site data, judging the significance of changes in site conditions, and predicting the range of future behavior of the source and plume. Understanding plume formation and behavior is the basis for evaluating whether an MNA remedy may be able to achieve site remedial goals within given time frames. Conceptual site models are expressed tangibly in text, maps (e.g., chemical isoconcentration maps and potentiometric surface maps), cross sections (e.g., hydrogeologic and chemical distributions), plots of temporal trends, and other graphical formats, and should be formulated in terms of mathematical calculations describing the plume and site. The conceptual model is a dynamic tool that is continually challenged, evaluated, and refined as new data are obtained. The data and analyses necessary for formulation of an adequate three-dimensional conceptual model for describing the effects of natural attenuation processes depend on site-specific conditions.

The development of quantitative models (i.e., mathematical models) based on the conceptual site model is often an important part of site characterization and remedy selection for MNA. These quantitative models may be as simple as equations for estimation of ground-water flow rates (e.g., Darcy's law), or as complex as numerical models of ground-water flow and contaminant fate and transport. Such calculations are used to help understand site processes, locate monitoring points, estimate attenuation rates, and evaluate possible effects of different conditions on plume

behavior. Quantitative models require particular types of data, and the data collection effort should be designed considering the requirements of the chosen model(s) and site-specific characterization objectives.

The conceptual site model for natural attenuation is the site-specific qualitative and quantitative description of the transport and fate of contaminants with respect to receptors and the geologic, hydrologic, biologic, and geochemical factors that control contaminant distribution (USEPA, 2003). The model expresses the understanding of the structure, processes, and factors that affect plume development and behavior. It is built on assumptions and hypotheses that have been tested using site-specific data.

IIIA.5.1 Attenuation Rate Estimates

The spatial and temporal distribution of the contaminant within the ground-water plume will depend on source location, the spatial distribution and velocity of water flow (or diffusion where advective flux is slow), and the abundance and biotic/abiotic reactivity of aqueous and solid phase biogeochemical components along the paths of water flow. The extent to which biogeochemical processes will cause contaminant attenuation during transport will depend on the relative rates of both fluid transport and chemical reactions (Morgan and Stone, 1985). For example, contamination will likely be negligible for systems in which the timescale for water flow within a hypothetical reaction volume is much shorter than the timeframe for significant reaction to take place. Conversely, significant attenuation may be observed for contaminants in systems where reactions occur rapidly relative to the timescale for fluid transport. The latter situation is commonly assumed to apply to ground-water systems, but this needs to be confirmed during site characterization. This is particularly important for near-surface systems that may experience large variability in water flux and fluid velocities (e.g., Conant Jr., 2004).

Attenuation rate constant calculations can be an important tool for evaluating the feasibility of natural attenuation at a contaminated site, e.g., as part of the Tier II screening analysis. Specific applications identified in U.S. EPA guidelines (USEPA, 1999) include use in characterization of plume trends, as well as estimation of the time required for achieving remediation goals. As illustrated by Newell et al. (2002) different types of attenuation rate data may be obtained for a given site and careful consideration should be given to the appropriate use of the first-order rate constants derived from these data.

The illustrations in Figure 3.4 provide two examples of attenuation rate constant data that may be collected within the plume. The overall extent of plume attenuation can be estimated by examining contaminant concentrations at a series of wells within the ground-water flow system (Panel A). In this instance, the influence of dispersion on contaminant concentrations as a function of distance must be determined through comparison with a conservative dissolved tracer. The duration of a plume at a given location can be estimated through analysis of contaminant concentration trends with time (Panel B). This can be

used to estimate the time required to reach ground-water remediation goals. In both cases, the overall determination of whether the ground-water plume is expanding, showing relatively little change, or shrinking (in three dimensions) will depend on the analysis of multiple well transects (concentration vs. distance) or well points (concentration vs. time) in order to provide appropriate spatial coverage. Since the directions and rates of ground-water flow can vary in time, the determination of concentration-based rate constants may be subject to errors of a magnitude determined to be unacceptable for site characterization. In order to reduce this level of potential error, one may determine mass-based rate constants provided details on the spatial and temporal variability of hydraulic flux is also well characterized. Newell et al. (2002) should be consulted for further details on the application and limitations of the various approaches for estimation of rate constants.

IIIA.5.2 Contaminant Flux

While contaminant concentration is a determining factor for human or ecological risk, this metric does not provide a measure of contaminant mass and distribution within the system of interest. Determination of a contaminant mass balance is critical for determining changes in contaminant mass or speciation during subsurface transport. For organic contaminants, a mass balance calculation aids determination of whether contaminant degradation or sorption is occurring. For inorganic contaminants, a mass balance is required to assess changes in chemical speciation and mobility. The mass balance is inclusive of liquid and solid matrices (e.g., aquifer sediments) within the boundaries of the conceptual model. The distribution of contaminant mass is important with respect to defining remedial objectives and assessing remedial performance.

Contaminant flux (M) is defined as the product of contaminant concentration (C) in the mobile phase (water and mobile colloids) and the volumetric flow of the mobile phase (Q):

$$M = C * Q$$

Contaminant flux can be calculated for point locations or cross-sectional areas perpendicular to water flux depending on the level of heterogeneity in water flow or contaminant concentration distribution (Einarson and Mackay, 2001; Buscheck et al., 2004). For inorganic contaminants, this general equation represents the flux of all contaminant species at a given point in time. Since a mobile inorganic contaminant can change chemical form, it may be useful or necessary to further define contaminant flux for individual contaminant species relevant to site-specific conditions.

$$M_i = C_i * Q$$

Contaminant transport occurs along water flow paths in the subsurface. Therefore, the first step to determining contaminant flux is developing an understanding of system hydrology. With the establishment of a water budget for the site (i.e., water flux distribution), then a mass budget can be developed to establish contaminant flux across relevant system boundaries.

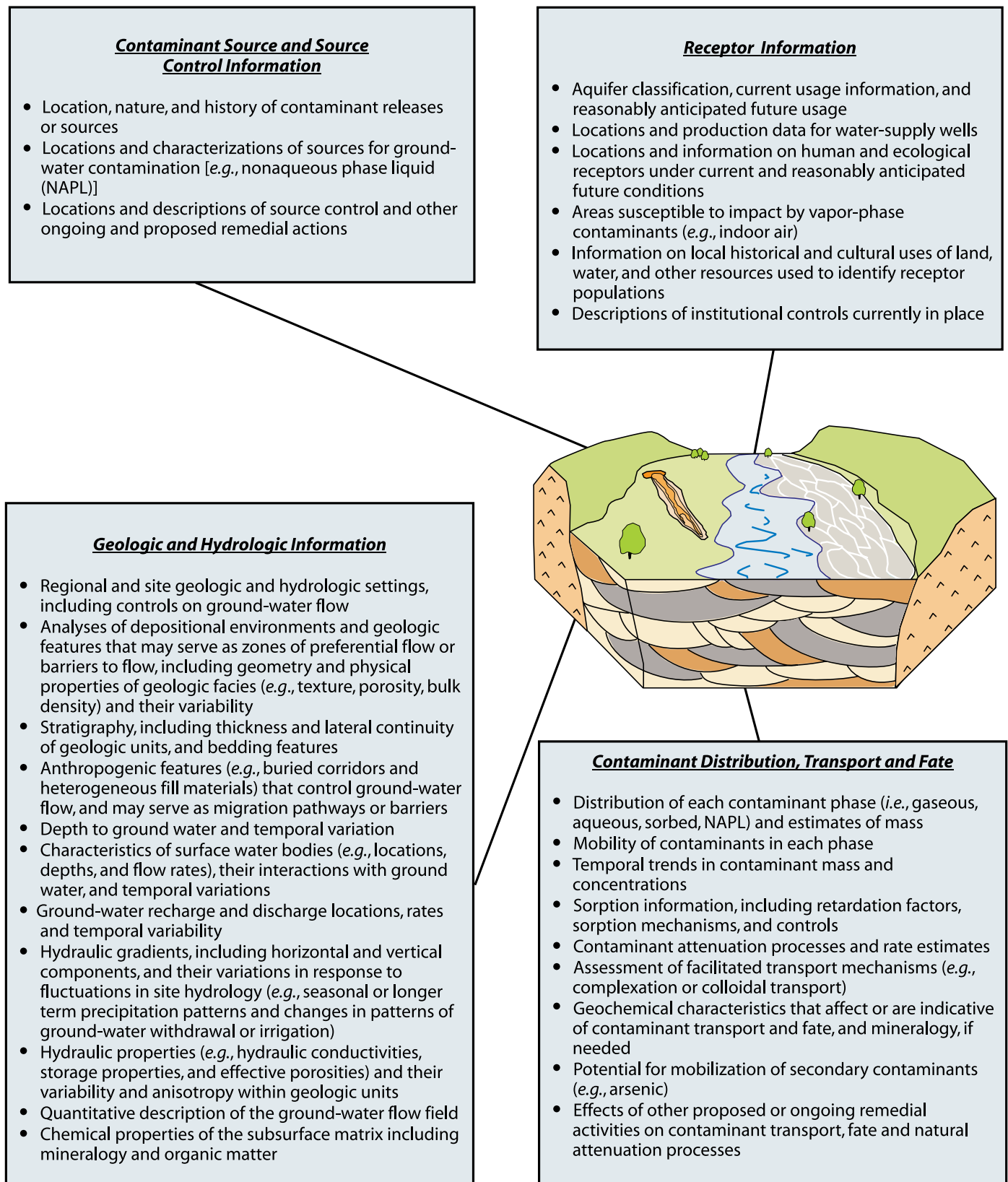


Figure 3.3 Elements of a conceptual site model for monitored natural attenuation of inorganic contaminants (modified from USEPA, 2003).

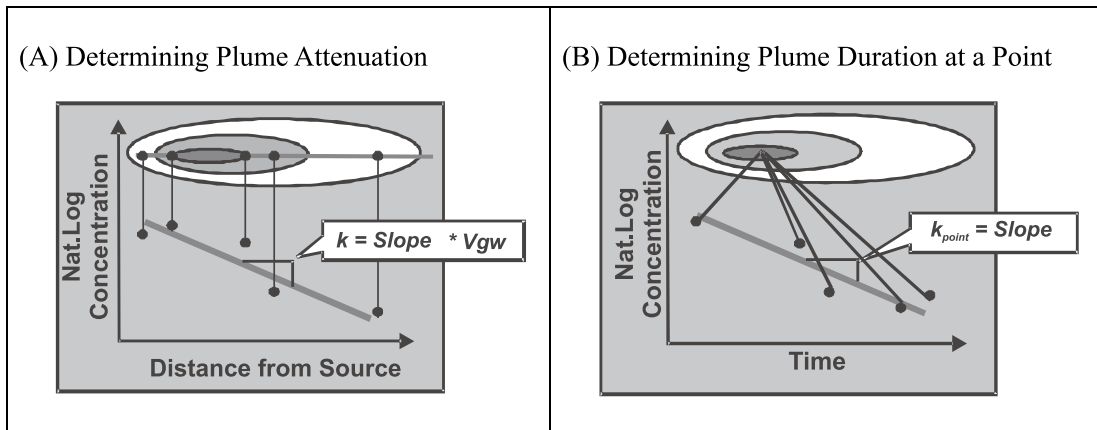


Figure 3.4 *Illustration of two approaches for determining attenuation rate constants within a contaminant plume. Critical assumptions underlie the applicability of these two analysis approaches: 1) analysis depicted in Panel A presumes that a plume centerline exists and that five monitoring wells are sufficient to define it, and 2) analysis depicted in Panel B presumes that the plume is stable. Both assumptions are to be verified through acquisition of supporting spatial and temporal data in order to reduce the uncertainty in rate estimates.*

IIIA.5.3 Source Term Characteristics

In addition to the geologic factors that influence ground-water transport, the chemical and physical characteristics of the source term can play a significant role in determining the physical dimensions of the ground water plume. The dimensions of the mobile plume may be impacted by characteristics of the contaminant source such as the total mass and rate of release of contaminant into the saturated zone within the aquifer. Active treatment of the source zone may also impact plume characteristics, particularly in cases where engineered remedies within the source zone introduce chemical reactants, stimulate microbial processes, or influence ground-water flow. Finally, the chemical characteristics of the contaminant source materials may impact the contaminant transport either directly through chemical reactions that influence aqueous speciation (e.g., Pb complexation by EDTA to form solution species) or indirectly by influencing ground-water chemistry (e.g., via biodegradation of organic co-contaminants such as fuel hydrocarbons or chlorinated solvents). In some instances, microbial reactions that are stimulated by the presence of organic contaminants may result in conditions beneficial to inorganic contaminant attenuation within the plume, e.g., generation of sulfate-reducing conditions that result in precipitation of metal sulfides. While this process may be beneficial to inorganic contaminant immobilization, the site investigation needs to include consideration of the long-term stability of the immobilized contaminant for a site at which the aquifer is generally oxic outside of the plume boundaries. This discussion serves to highlight the importance of factoring in evaluation of contaminant source characteristics and the management of the source area relative to down gradient plume behavior.

IIIB. Contaminant Quantification, Distribution and Speciation

Determination of the attenuation mechanism, assessment of aquifer capacity to attenuate contaminant mass, and the evaluation of the long-term stability of immobilized contaminants will necessitate analytical measurements conducted on aqueous and solid samples collected from within the plume. The types of measurements will include determination of total element concentrations as well as determination of aqueous and solid phase speciation of the contaminant and reactants involved in the attenuation reaction. The measurements will likely be applied to samples collected over a range of locations and times in order to adequately characterize the spatial and temporal variability of aquifer conditions within the plume. The following discussion will provide an overview of the types of measurements that may be required to evaluate the adequacy of site-specific attenuation reactions. The discussion will first address aqueous phase measurements followed by solid phase measurement techniques.

IIIB.1 Aqueous Characterization Approaches

Characterization of ground water will include assessment of the overall chemical conditions as well as the chemical speciation of the contaminant. Determination of the overall chemical conditions within the plume (e.g., redox status discussed in Section IIIC) sets the context for evaluating reactions that lead to contaminant attenuation. Chemical measurements to assess redox status of ground water can be achieved through a combination of field- and laboratory-based methods. Evaluation of the types and distribution of ions in ground water can adequately be addressed via laboratory measurements on properly preserved samples.

These data are typically required to assess what type(s) of sorption reactions control contaminant immobilization. Likewise, determination of contaminant degradation products is needed to verify attenuation is occurring. An underlying assumption for all analysis types is that the approaches to sample collection and preservation are adequate to maintain the intact chemical characteristics of the ground-water sample. Insuring the adequacy of sample collection protocols can be realized, in part, through adherence to recommendations for well installation and low-flow well sampling procedures (USEPA, 1994; USEPA, 1996). It is also recommended that the design of the well monitoring network consider temporal as well as spatial variability that may influence chemical measurements. For example, variations in ground-water levels may result in variations in ground-water redox chemistry. These considerations are explored more holistically in USEPA (2003), which should be consulted both from the perspective of designing the initial ground-water characterization plan as well as the long-term performance monitoring plan.

In general, a variety of water samples should be collected at the same time to allow analysis for metals, common anions, alkalinity, total dissolved carbon, dissolved oxygen, and pH. In some systems, assessment of oxidation-reduction potential (ORP) using a Pt electrode may be desirable for qualitative assessment of variability between screened intervals within the plume. For metals and anions, the use of ultra-clean sample bottles is essential to avoid artifacts, and these can be checked through the inclusion of trip blank samples consisting of deionized water or tap water in the same types of containers.

For preservation, samples for metal analysis are usually acidified immediately upon collection to pH 2 using either HNO₃ or HCl to avoid precipitation of oxide phases. Samples for anion analysis are not treated with acid, as this may swamp the anion of interest during the ion chromatography analysis. Subsamples of the same sample taken for anion analysis can be used for alkalinity determinations, as this quantity is robust. Measurements of dissolved oxygen and pH are best taken in the field using a closed flow cell instrumented with electrodes for in-line measurement. For most samples (especially total dissolved carbon), chilling to 4 °C as soon as possible after collection is useful, although changes of temperature for dissolved gas measurements are not recommended. Methods used for determination of total concentrations of metals in aqueous samples are usually the same as used for destructive analysis of solids with elimination of the digestion step. Oxidation-state determinations can be made on the basis of reactions with chromophores [e.g., *s*-diphenyl carbazide for Cr(VI), phenanthroline or ferrozine for Fe(II)] and determination of absorbance in the UV-Vis region of the spectrum. Field kits and ion-selective electrodes are available for many of these determinations as well as for pH and dissolved oxygen. Common anions are usually determined in the laboratory using ion chromatography or capillary electrophoresis.

Colorimetry involves specific complexation of the atom of interest in solution by a strongly absorbing compound

having a high absorptivity at an accessible wavelength (i.e., a chromophore) and subsequent measurement of the absorptivity of the solution. Atomic absorption, emission, and fluorescence rely on the same electronic transitions involving valence-shell electrons of unbound atoms. With absorption, the amount of light lost in exciting electrons into unbound states is measured, whereas with emission and fluorescence, the amount of light emitted when these electrons return to the ground state is measured. Emission and fluorescence differ in the manner by which the electrons are excited—emission involves thermal excitation of the sample by injection into a flame (flame photometry) or a plasma (ICP-AES), whereas fluorescence uses photon excitation. The sensitivity of colorimetry, AAS, AES, and AFS are roughly comparable (ppm to ppb), although ICP-AES has the advantage of being able to analyze multiple elements more easily with fewer matrix interferences and across a wider concentration range than the other techniques. With ICP-MS, the masses of individual atoms are measured using a mass spectrometer, the intake of which is coupled to a plasma where the atoms are thermally ionized. This technique has many advantages including a wide dynamic range, ability to analyze all elements heavier than He, few matrix or spectral interferences, and the ability to measure isotopic ratios. Specific recommendations on contaminant speciation measurements and supporting ground-water chemistry data are provided within individual non-radionuclide contaminant chapters included in Volume 2 of this document.

IIIB.1.1 Filtration

While regulatory requirements stipulate that unfiltered ground-water samples be analyzed to support regulatory decisions at a contaminated site, it may be necessary to also collect filtered samples to help interpret the process(es) controlling contaminant mobility. The use of 0.45 µm pore size filter paper is common as an arbitrary cutoff point to differentiate between dissolved and particulate phases in water samples. However, caution is recommended when using this approach, particularly for Fe and Al and other elements that may be associated with Fe or Al particles (including associated contaminants) that could pass through 0.45 µm filter membranes. The use of filter membranes with pore sizes of 0.1 µm or less will generally provide a better assessment of the dissolved vs. particulate load of ground water.

Analytical methods have typically used 0.45 µm filters to differentiate between dissolved and particulate phases. If the intent of such determinations is an evaluation of truly dissolved concentrations, which would be important for geochemical modeling purposes, the inclusion of colloidal material less than 0.45 µm will result in incorrect values. Conversely, if the purpose of sampling is to estimate 'mobile' contaminant species in solution, significant underestimations of mobility may result, due to colloidal facilitated transport by particles, which are filtered out by 0.45 µm filtration. Kim et al. (1984) found the majority of the concentrations of rare earth elements to be associated with colloidal species that had passed a 0.45 µm filter. Wagemann and Brunskill

(1975) found more than a two-fold difference in total iron and aluminum values between 0.05 and 0.45 μm filters of the same type. Some aluminum compounds were observed to pass through a 0.45 μm filter, but were retained on a 0.10 μm filter (Hem and Roberson, 1967). DeVitre et al. (1987) found approximately 35% of the particulate bound manganese in the 0.015 to 0.10 μm size fraction in anoxic lake waters. Kennedy and Zellweger (1974) found errors of an order of magnitude or more in the determination of dissolved concentrations of aluminum, iron, manganese and titanium using 0.45 μm filtration as an operational definition for "dissolved". Sources of error were attributed to filter passage of fine-grained clay particles. De Mora and Harrison (1983) provided an excellent review on the subject of physical separation techniques for trace metal speciation.

During sample collection in anoxic or suboxic systems, iron oxidation and precipitation may occur prior to filtration and result in the removal from solution of previously dissolved species due to instantaneous sorption by the precipitate (Puls and Eychaner, 1990). Filter loading and clogging of pores with fine particles may also occur, introducing filtration errors due to reductions in effective pore size (Danielsson, 1982). Sheldon and Sutcliffe (1969) found that virtually all filters remove particles smaller than the stated pore size. In experiments with seawater and latex particles, using light scattering techniques, Johnson and Wangersky (1985) demonstrated that a high proportion of materials dispersed at sizes smaller than the filter pore size will interact with the filter surface. These interactions are dependent upon size, particle concentration, colloid surface chemistry, electrolyte concentration and composition, nature and concentration of adsorbents, chemical properties of the filter surface, and the frequency of collisions of dispersed particles with the filter surfaces.

Contaminants may exist as dissolved species, precipitated solids, polymeric species or be adsorbed to inorganic or organic particles of colloidal dimensions. Based on the above discussions, the filtration of ground water samples for metal analyses using 0.45 μm filters may not provide accurate data either for geochemical modeling or for contaminant migration estimates. Some mobile species are likely to be removed by 0.45 μm filtration prior to chemical analysis, while other particulate-associated metals will pass through the filters and be incorrectly considered 'dissolved'. A principle objective in sampling to test a geochemical speciation model is to obtain estimates of the free ion activities of the major, minor, and trace elements of interest. Since there are relatively few easily performed analytical procedures for making these estimates, an alternative is to test the analytically determined dissolved concentrations with model predictions, including both free and complexed species.

Collection of ground-water samples and measurement of their chemical properties will be necessary irregardless of whether degradation or attenuation is the primary attenuation mechanism. Characterization of aquifer solids may be necessary to support evaluation of degradation

processes, but primarily when knowledge of specific microbial processes or identification of abiotic solid phase reductants is needed to constrain attenuation rate and capacity evaluations. In contrast, for contaminants in which immobilization is the primary (or only) viable attenuation mechanism, collection and characterization of aquifer solids is a specific requirement.

IIIB.2 Solid Phase Characterization Approaches

Determination of aquifer solids mineralogy and solid phase contaminant speciation is critical to identification of the contaminant immobilization process. Contaminant speciation is inclusive of oxidation state of the immobilized contaminant as well as the solid phase component(s) with which it is associated. Determination of contaminant solid phase speciation can be approached in two ways, structurally and operationally. Structural determination uses instrumental procedures (spectroscopy, microscopy) to identify and quantify the discrete phases present. This information, together with accumulated knowledge of their thermodynamic properties and the rates at which they precipitate/adsorb and dissolve/desorb, is employed to assess the capacity of the aquifer to sustain contaminant attenuation and evaluate the long-term stability of immobilized contaminants. The challenges associated with the structural approach include 1) difficulty in identifying specific phases at concentrations near or below instrumental detection limits, 2) need for good sampling statistics (e.g., a large number of micron-sized measurements are needed to ensure that the site is adequately represented), 3) inadequacy of available thermodynamic and kinetic data to evaluate reaction mechanisms, and 4) cost of instrumentation and model applications that may be employed during evaluation of aqueous and solid phase chemical data.

The operational approach, on the other hand, classifies contaminant form solely in terms of reactivity. Contaminated materials are contacted with solutions that simulate, in a short period of time, subsurface conditions expected over much longer time intervals. The amount of contaminant released by the material as a result of this contact is measured. In some instances, the rate of release is also quantified either by in-situ measurements or successive extractions. Examples of the operational approach include chemical extractions using a variety of solutions and procedures, and bioavailability studies that measure uptake by organisms directly. Sequential chemical extractions, in which contaminated materials are treated with successively harsher solutions, have found wide use in site characterization and several standard methods are available for specific situations (Tessier et al., 1979; Yanase et al., 1991). While highly relevant, bioavailability studies are rarely conducted because of the high cost and long time periods required. Operational determination of contaminant form avoids many of the problems associated with the structural approach, but still requires the development of substantial and expensive databases that correlate the amounts and rates of contaminant release during laboratory contact studies with actual contaminant reactivity under field conditions.

IIIB.2.1 Sampling and Fractionation

Collection of samples is the first step in determination of contaminant distribution within the source area and down gradient plume. The most important consideration is that the samples collected give a fair representation of the size and extent of the contamination. Enough samples must be collected to provide statistical certainty to any set of results. As soils and sediments are heterogeneous, minimum sample sizes of about 50 g are needed at each sampling point. These are mixed thoroughly before taking 1- to 10-g subsamples for analysis. In some instances, mixing of samples from different sampling points to provide composite samples can be done to decrease analytical costs, but this practice also tends to decrease the precision with which the geographical extent of the contamination can be determined. To avoid the possibility of bias, and to retain the ability to interpolate results, sampling points should be laid out on a three-dimensional grid that takes into account any pre-existing knowledge of the underlying stratigraphy. Samples may be collected in several rounds, starting with a coarse grid to identify the overall extent of the contamination and possible "hot" spots. Successive sampling rounds using finer grid sizes on subsets of the original coarse grid can be used to provide further data about regions of interest.

Aquifer samples can be collected using a variety of methods. In all cases, however, the goal will be to collect materials to allow for lithologic logging, to provide representative samples for laboratory investigations and for submission to analytical laboratories. The samples must meet the appropriate data quality objectives as identified in the project-specific Quality Assurance Plan (QAP). In all cases, aquifer materials should be collected with local, State, and Federal requirements in mind.

The procedures to follow for collection of soil and sediment samples will depend on the degree to which environmental availability is to be assessed. Aquifer materials can be collected, for example, using hollow-stem auger or hydraulic percussion methods. These are generally well-tested methods applicable to a wide variety of environments. With these methods various types of sample liners may be used, such as plastic or brass sleeves. The sleeves can be cut and capped to preserve materials and facilitate their transport. If oxidation-reduction processes are believed to be an important component of attenuation mechanism(s), special attention must be given to preserving the redox status of materials after they are retrieved from the subsurface. For example, if anoxic materials are collected they must be frozen after collection or stored in evacuated or inert-gas-purged containers in order to preserve primary mineralogy (USEPA, 2002; USEPA, 2006).

For total analyses, little care need be taken and the samples, once collected, can be air-dried and stored before analysis. The availability of many metals, however, depends greatly on their oxidation state, and this may change with time in storage due to microbial activity or exposure to air. Drying of samples can also affect the availability of some elements, e.g., due to irreversible (or slowly reversible) changes in

the structure of illitic and vermiculitic clay minerals during drying. A realistic assessment of current availability, therefore, will attempt to make the measurement as soon after collection as possible using samples that have been stored under conditions that maintain their redox and moisture status at the levels seen in the field (USEPA, 2006). The best procedures for preserving samples thus involve, at a minimum, storage of field-moist samples at 4 °C in airtight plastic bags from which the air has been squeezed. In instances where oxidation state is critical, injection of N₂(g) or Ar(g) into the bore hole, and collection of cores in thick plastic cylinders that are immediately capped and transferred into anoxic chambers for further processing or storage is advised. Lowering the temperature to 4 °C slows microbial activity substantially. Freezing the samples may result in lysing of microbial cells and can create a different organic mixture in the soils than was present at the time of sampling.

In preparation for actual analysis, some particle-size fractionation may be needed for easy sample handling and enhanced sensitivity. As a result of surface-area considerations, the most reactive fraction of soils and sediments is that having particle sizes less than about 50 µm (i.e., silt and clay). Gravel (particles > 2 mm) and cobbles can generally be removed by sieving with little or no impact on the analytical results. The sand fraction (50-2000 µm) is generally left intact, as its removal by wet-sieving creates more problems than it solves. Careful records need to be kept of the mass and volume of the fractions removed so that analytical results on the remaining fractions can be scaled to field conditions. Fractionation on the basis of properties other than particle size can be done to concentrate specific minerals, and this may prove beneficial in some instances (Laird and Dowdy, 1994).

IIIB.2.2 Total Amount

Determination of the total quantity of a metal contaminant present is generally performed on "bulk" sample sizes of at most a few grams. In instances where the total amount of contamination is very low and detection limits are encountered, analysis by electron or X-ray microscopic techniques can be performed in which specific particles containing the contaminant are identified. With the microscopic approach, sample sizes of µg to mg are common, and scaling to field concentrations is difficult.

The bulk analysis techniques are distinguished on the basis of whether they are sample destructive or nondestructive. The sample-destructive techniques require digestion of the sample using strong acid or base to destroy the original compounds present and release the elements in a soluble state. Once in the soluble state, the concentration of the contaminant is determined by spectroscopic means after nebulization or injection into a flame or plasma connected to a suitable detector. The most common detection techniques include colorimetry, atomic absorption spectrometry (AAS), atomic emission spectroscopy (AES) using either flame (photometry) or an inductively coupled plasma (ICP-AES), atomic fluorescence spectroscopy (AFS), and inductively coupled plasma mass spectrometry (ICP-MS).

Colorimetry involves specific complexation of the atom of interest in solution by a strongly absorbing compound having a high absorptivity at an accessible wavelength (i.e., a chromophore) and subsequent measurement of the absorptivity of the solution. Atomic absorption, emission, and fluorescence rely on the same electronic transitions involving valence-shell electrons of unbound atoms. With absorption, the amount of light lost in exciting electrons into unbound states is measured, whereas with emission and fluorescence, the amount of light emitted when these electrons return to the ground state is measured. Emission and fluorescence differ in the manner by which the electrons are excited—emission involves thermal excitation of the sample by injection into a flame (flame photometry) or a plasma (ICP-AES), whereas fluorescence uses photon excitation. The sensitivity of colorimetry, AAS, AES, and AFS are roughly comparable, although ICP-AES has the advantage of being able to analyze multiple elements more easily with fewer matrix interferences and across a wider concentration range than the other techniques. With ICP-MS, the masses of individual atoms are measured using a mass spectrometer, the intake of which is coupled to a plasma where the atoms are thermally ionized. This technique has many advantages including a wide dynamic range (pptr to ppm), ability to analyze all elements heavier than He, few matrix or spectral interferences, and the ability to measure isotopic ratios.

The nondestructive analysis techniques generally rely on inner-shell electronic transitions or nuclear transitions for elemental identification and thus are less reliant on decomposition of the sample into individual atoms. Nevertheless, a homogeneous sample consisting of particle sizes of $<2\ \mu\text{m}$ and presenting a flat surface is needed for best results. Thus, although the sample is not completely destroyed in preparation, it is altered by grinding to achieve the particle size needed. The most common of these techniques is X-ray fluorescence (XRF), which can use high-energy photons from an X-ray tube or radioactive source to excite electrons in the atoms of interest. The light emitted by these atoms upon return to the ground state is then detected using an X-ray detector such as a gas-filled proportional counter, scintillation detector, or solid-state semiconductor detector. X-ray emission spectroscopy is similar to XRF except that it uses high-energy particles (electrons, protons, or alpha particles) to excite the atoms rather than photons. In general, detection limits are in the ppm range for solids although X-ray emission spectroscopy is more sensitive for lighter elements ($z < 30$) and X-ray fluorescence is more sensitive for heavier elements ($z > 45$) (Amonette and Sanders, 1994).

Microscopic methods of elemental analysis are generally more expensive than the bulk techniques, but can prove of great use in identification of specific contaminant phases and their associations with minerals. Electron microscopy images particles through scattering of an electron beam. At the same time, the electron beam is stimulating the emission of X-rays by the sample and detection of these (as in X-ray fluorescence) allows simultaneous multielemental analysis of the material being imaged. Scanning electron microscopy (SEM) can be used with samples of any thick-

ness, whereas transmission electron microscopy (TEM) requires preparation of samples on the order of 30-150 nm thick often in the form of thin sections. Conventional SEM and TEM require high vacuum for the analysis, due to the short pathlength of electrons in air, but new developments of the environmental SEM allows analysis of samples at pressures approaching ambient thus allowing observation of wet specimens for short periods of time. With the development of synchrotron X-ray sources, a microscopic technique based on X-ray fluorescence is available for high-value specimens. X-ray microscopy (XRM) has spatial resolution near $1\ \mu\text{m}$, and because of the very high photon fluxes available can achieve detection limits in the ppb range, better than any other X-ray technique. The XRM technique can be coupled with X-ray absorption spectrometry (XAS) to determine oxidation states and local structural information. Although primarily a research tool at the moment, XRM may prove quite useful for phase identification of critical samples when other techniques fail.

IIIB.2.3 Structurally Defined Form

One approach to the determination of environmental availability relies on identification of the discrete contaminant-bearing phases that are present and combining this information with phase-relevant thermodynamic or kinetic data using a geochemical model. Identification and quantification of the discrete phases present is gained through a combination of elemental, structural, and in some instances, solubility analysis. Techniques for structural analysis measure the arrangement of atoms both local to the contaminant and in extended structures. The combination of structural and elemental information uniquely determines a thermodynamic phase with specific properties.

The primary technique for structural analysis is X-ray diffraction (XRD), which relies on measuring the coherent scattering of a collimated beam of X-rays by the sample as a function of angle to the beam. The technique requires some degree of repetitive structural unit having dimensions on the order of the wavelength of the X-rays. Scattering from parallel planes of atoms separated by regular spacings yields an interference or diffraction pattern. The spacings at which constructive interference occurs (d) yield high intensity in the diffraction pattern and can be calculated from the angle of incidence (θ) and the wavelength of the X-ray (λ) using the Bragg equation, $d = n\lambda/2\sin\theta$, where n is an integer. The set of d -spacings and relative intensities measured for a compound are unique and can be compared with those for thousands of other compounds stored in a large database. In soils and sediments, however, mixtures of compounds occur and overlapping patterns for different compounds can make identification difficult in many instances. Also, XRD is sensitive down to about 1-5% by weight, and thus is not well-suited for identification of trace phases typical of contaminants in soils and sediments. To some extent, these drawbacks can be overcome by fractionating the sample to eliminate interfering compounds and to concentrate the contaminant-bearing phases. Diffraction also occurs with electron beams, as these have wave properties (albeit with shorter wavelengths than X-rays). Electron diffraction is used in TEM analysis to identify phases at the same time

they are being imaged and their elemental compositions determined by X-ray emission. Diffraction techniques do not work well for poorly ordered phases, as these phases yield very broad peaks that have little value for identification purposes.

Vibrational spectroscopic techniques can be used in some instances to identify poorly ordered phases, as these methods detect molecular vibrations that depend on bond energies and atomic masses rather than long-range atomic order. The two major types of vibrational spectroscopy are infrared absorption and Raman scattering. Infrared absorption spectroscopy requires a long-wavelength (ca. 1-100 μm) source of light and measures the fraction of this light that is absorbed by the sample. Water absorbs strongly in much of this region, and so samples are best analyzed when dry, unless internal reflectance techniques are used. The long wavelengths used, however, are well suited for interferometry in which the incident beam is split in two and recombined after delaying one beam by a known path length. The resulting interference spectrum, collected as a function of path length difference, is then converted using a Fourier transform to yield an absorption spectrum in terms of wavelength. Because the entire spectrum is collected at all times, rather than scanning through each wavelength individually, the Fourier-transform approach (i.e., FTIR) is the most efficient means of collecting an infrared absorption spectrum.

Raman scattering spectroscopy measures the loss or gain in energy of monochromatic light as a result of interactions with molecular bonds. In theory, incident light of any wavelength can be used to measure these changes, and so some of the limitations of infrared absorption spectroscopy are avoided, such as the need to study dry samples. However, Raman scattering yields a weak signal, and fluorescence from the sample may interfere when incident light in the visible region is used. The recent development of Fourier-transform Raman spectroscopy using laser light in the near infrared region (ca 1 μm wavelength) has provided enough incident light intensity with minimal fluorescence to make Raman practical for many samples.

Vibrational spectroscopic techniques, while sensitive to local bond strengths, are rarely as definitive as XRD because the same types of bonds are found in most inorganic compounds (e.g., oxide, hydroxyl, sulfate, carbonate, etc.) and the differences among compounds are often subtle. This approach, however, can be used to positively identify solid solutions of poorly ordered materials, such as $(\text{Fe,Cr})(\text{OH})_3$ (Amonette and Rai, 1990), based on shifts in bond energies due to substitution. Vibrational techniques also find use for identifying orientation and bonding of sorbed contaminants that exist in ground water as oxyanions (e.g., arsenic; Eggleston et al., 1998).

Under certain circumstances, solubility can be used to determine or at least confirm the environmentally relevant phase controlling the availability of an inorganic contaminant. These circumstances require collection of equilibrium solubility data across a range of pH (or some other primary solubility-controlling variable), in which the concentrations of the contaminant as well as other key species involved in

formation of aqueous complexes with the contaminant are measured. Based on these data, and known thermodynamic solubilities of the putative contaminant phase, a solubility diagram can be constructed and compared with that for known phases. It is critical that equilibrium be attained or thermodynamic calculations will not be valid. Thus systems that approach equilibrium slowly may not be suitable. Rai et al. (1984) reviewed this approach and its applicability to twenty-one environmentally relevant elements.

IIIB.2.4 Operationally Defined Form

A more direct approach to assessing environmental availability of a contaminant, involves determining the conditions under which it can be dissolved and therefore mobilized into the ground water. This empirical approach presupposes nothing about the chemical form of the contaminant and thus has little predictive value in the event that ground water conditions change. Nevertheless, it offers much in the way of addressing economically the degree to which a total concentration of a contaminant poses an environmental risk.

The primary technique used is that of sequential selective extractions, with each successive extracting solution offering a harsher solution environment than the one that preceded it. The general assumption is that the earlier in the sequence that the contaminant is released, the higher is its environmental availability. Sequential extraction approaches are discussed in more detail in Sections IIIB.2.4.1 and IIIB.2.4.2.

The sequential (selective) extraction approach can be improved by incorporating measurements of the rate of release during each step in the procedure. This can be done by successive extractions for shorter time periods using the same reagent, by measurement of small aliquots taken from the extraction solutions at different times during the extractions, or by a continuous-flow extraction using a specially designed flow cell similar to that of Wollast and Chou (1985) used in mineral weathering studies. Despite the apparent need, the kinetic approach has not been widely applied to estimation of environmental availability of contaminants, although it has been suggested for use in assessing the availability of U in soils (Amonette et al., 1994b).

IIIB.2.4.1 Sequential Extractions

Sequential extraction methods will perhaps be the most practicable approaches for demonstrating contaminant partitioning in the solid phase and for providing information for substantiating proposed attenuation mechanisms. These methods can be particularly useful because they provide quantitative information on the capacity of a given material to attenuate inorganic contaminants. They are also advantageous because large numbers of samples can be analyzed and compared, unlike methods that involve spectroscopy and microscopy. However, as a cautionary note, sequential extraction methods are not without limitations. It must be acknowledged that results of sequential extraction tests are operationally defined and users of these tests must be aware of potential artifacts, as will be pointed out in the following discussion.

Sequential extraction procedures consist of subjecting a given quantity of soil or aquifer sample to a series of increasingly aggressive reagents under specified conditions. An underlying assumption is that the release of components in earlier extractions implies a higher potential for environmental mobility than components released later in the extraction sequence. A conceptual model of the sequential extraction approach is that solid materials consist of specific mineral fractions that can be extracted selectively by using appropriate reagents and experimental conditions. As mineral fractions are selectively dissolved, any element that they contain will release into solution and in this way the “speciation” of particulate trace metals can be determined. If it is determined that the majority of a contaminant of concern is present, for example, in the operationally-defined carbonate fraction, then geochemical modeling efforts might be appropriately focused on the factors that govern long-term stability of carbonate minerals.

Perhaps the most often followed or modified chemical extraction procedure is that of Tessier et al. (1979). Other approaches are outlined, for example, in Dragun (1988) and Yong et al. (1993). In the Tessier et al. (1979) method, five distinct extraction procedures are used to recover metals from the following sediment/soil fractions: 1) exchangeable sites; 2) carbonate minerals; 3) metal oxyhydroxides; 4) organic matter; and, 5) the residual fraction (Table 3.1). Metals associated with loosely bound sites (weak electrostatic attraction) are released by extraction in concentrated salt solutions. Divalent metal chloride salts prepared at a concentration of 1 molar are often used in this first step (e.g., CaCl₂ or MgCl₂). After extraction for a set period of

time and mixing rate, the supernatant solution is analyzed using spectroscopic methods and the concentration of an element in solution is related back to a mass fraction of that element associated with operationally defined exchangeable sites. Metals associated with carbonate minerals are removed in a second step by wet chemical extraction in a sodium acetate-acetic acid buffer solution. This buffer (pH 5) is effective in dissolving calcite, an abundant carbonate mineral found in natural systems. Iron and manganese oxides are removed with hot hydroxylamine hydrochloride solution. Organic compounds, such as humic acids and fulvic acids, are targeted with acidic, oxidizing reagents (hydrogen peroxide plus nitric acid; note that other published extraction methodologies employ basic conditions to “selectively” remove organic matter, for example, 3 M KOH). The residual fraction is typically determined from a concentrated nitric acid digestion or total analysis (by complete digestion or by X-ray fluorescence spectroscopy) after subtracting out the fraction of metal extracted in steps 1 through 4. The residual fraction is considered to represent the fraction of metals present in tightly bound matrices, for example, in aluminosilicate matrices that are not effectively dissolved with any of the reagents used in steps 1-4.

This extraction scheme has been adapted for testing and validation against natural matrix standards by the Radioactivity Group of the National Institute of Standards (NIST) Ionizing Radiation Division (<http://physics.nist.gov/Divisions/Div846/Gp4/enviro.html>). This work represents an effort to support metrology improvements in the radiochemistry community through research and development of low-level radionuclide Standard Reference Materials (SRMs) and

Table 3.1 Sequential extraction procedure of Tessier et al. (1979).

Step	Target Fraction	Chemicals/Conditions
Step 1: Exchangeable	Ionically bound metals and metalloids	1 M magnesium chloride (pH = 7.0) 1 hour, room temperature
Step 2: Carbonates	Metals/metalloids with carbonate minerals (e.g., calcite, dolomite)	1 M sodium acetate plus acetic acid (pH = 5.0) 4 hours, room temperature
Step 3: Fe and Mn oxides/ hydroxides	Metals/metalloids with iron and manganese hydroxides	0.04 M hydroxylamine hydrochloride in 25% (v/v) acetic acid (pH ~ 2) 6 hours, 96°C
Step 4: Organic matter	Metals/metalloids bound to natural organic matter (e.g., humic and fulvic acids)	0.02 M nitric acid, 18% hydrogen peroxide (pH = 2) 2 hours, 85 °C
Step 5: Residual	Aluminosilicate minerals, pyrite	16 N nitric acid 2 hours, 140 °C

Notes: Initial sample weight is generally 1 gram. This initial mass is used to report all metals fractions in terms of metal weight per gram of dry sediment. Samples are generally dried (aerobically or anaerobically) to a constant mass, gently ground and homogenized in an agate mortar. Samples should be constantly agitated during each extraction step. Extractions are conveniently carried out using polypropylene or Teflon centrifuge tubes. Initial and final pH values should be measured and recorded. Supernatant solutions are collected and analyzed by atomic absorption spectroscopy, inductively coupled plasma emission spectroscopy, or other suitable methods. Between steps, samples are centrifuged (typically 5000 to 10000 rpm, 30 minutes) and rinsed with deionized water (5-10 mL).

measurement quality assurance. The Radioactivity Group has undertaken a systematic study to test the relative selectivity of a Tessier-based extraction scheme for the speciation of a suite of radionuclides and stable elements (Schultz et al. 1998a; 1998b; 1998c; 1999). These tests have been conducted with a suite of natural matrix standards (soils and sediments) developed by NIST for the purpose of validating radiochemical methods. While the adoption of this extraction scheme may not be suitable for all sample matrices (see discussion below), the development of a uniform reference database relative to the performance for a given extraction scheme provides a valuable starting point for adapting an extraction scheme(s) better suited for site-specific conditions. The availability of certified SRMs for testing extraction schemes is critical for assessing data quality across analytical laboratories that may be utilized to support site characterization.

In sulfate-reducing systems, the iron sulfides mackinawite (FeS) and pyrite (FeS₂) may be potential hosts to a variety of metals. Huerta-Díaz and Morse (1990) presented a sequential extraction method for the determination of metal partitioning in iron sulfides. Their method involves the sequential leaching of samples using 1 M HCl to recover a “reactive” fraction (FeS; equivalent to acid volatile fraction discussed below), 10 M HF to recover the silicate fraction, and finally concentrated HNO₃ to recover the pyrite fraction. Moore et al. (1988) investigated the partitioning of metals

in reducing sulfidic systems using sequential extraction techniques. They chose to use a three-step procedure: 1) 0.25 M hydroxylamine hydrochloride in 25% acetic acid to remove metals bound to oxyhydroxides of Fe and Mn and carbonates; 2) 0.1 M sodium pyrophosphate at pH 10 to recover the organic fraction; and 3) the sulfide fraction was recovered using potassium chlorate plus hydrochloric acid. These fractions were compared with total metal concentrations determined by digestion of samples in HF plus perchloric acid.

Numerous reagents and extraction schemes have been developed for iron minerals in soils and sediments (e.g., Mehra and Jackson, 1960; Chao and Zhou, 1983; Walker, 1983; Canfield, 1989; Ryan and Gschwend, 1991; Kostka and Luther, 1994). Because of the importance of iron minerals for sequestering metals and metalloids in the environment, it is worthwhile to summarize the most commonly used wet chemical techniques for iron, and the oxide and sulfide minerals dissolved using these various reagents (Table 3.2). Slight variations in technique can have profound influences on the outcome of chemical extractions, for example, whether 1 M or 4 M hydrochloric acid is used (e.g., Chao and Zhou, 1983). Consequently, in all cases where sequential extraction methods are employed it will be necessary to clearly document the types of reagents used, extraction times, temperature, and laboratory procedures. Validation of laboratory procedures by spiking

Table 3.2 Summary of reagents used to selectively dissolve iron oxides and sulfides.

Extractant	Composition	pH	Time (h)	Fe minerals Extracted
Ascorbate ¹	0.17 M sodium citrate; 0.6 M sodium bicarbonate; 0.023 M ascorbic acid	8	24	ferrihydrite
HCl ¹⁻³	0.5–6 M hydrochloric acid	<2	1	ferrihydrite mackinawite
Hydroxylamine hydrochloride ¹⁻⁴	0.04 M hydroxylamine hydrochloride in 25% (v/v) acetic acid, 96 °C	<2	6	ferrihydrite mackinawite
Oxalate ⁵	0.2 M ammonium oxalate/ 0.2 M oxalic acid	2.5	48	ferrihydrite lepidocrocite magnetite (partial) mackinawite
Dithionite ^{1,2,6,7}	0.11 M sodium bicarbonate/0.27 M sodium citrate, add 0.5 grams sodium dithionite at 80 °C, repeat dithionite addition	5-7	4	ferrihydrite goethite (partial) hematite (partial) magnetite (partial)
Ti-citrate ⁸	0.05 M Ti(III) citrate EDTA-bicarbonate	7	2	ferrihydrite goethite hematite (partial)
Chromous chloride ^{9,10}	1 M Cr(II) chloride in 0.5 M hydrochloric acid; reagent prepared using a Jones reductor	<2	1	pyrite mackinawite elemental sulfur

Notes: see references for experimental details; ¹Kostka and Luther (1994); ²Canfield (1989); ³Chao and Zhou (1983); ⁴Tessier et al. (1979); ⁵Schwertmann (1964); ⁶Mehra and Jackson (1960); ⁷Walker (1983); ⁸Ryan and Gschwend (1991); ⁹Zhabina and Volkov (1978); ¹⁰Tack et al. (1997).

extraction experiments with known quantities of minerals and assessment of recovery will be needed in most cases to evaluate and verify assumptions related to sequential extraction approaches (see, for example, Chao and Zhou, 1983; Kostka and Luther, 1994; Keon et al., 2001). In this way, the results of sequential extraction experiments can depart from purely operational definitions and approach the point where such results can be confidently applied to assess mineral-contaminant associations.

Over the past 10 years, the European environmental research community has developed a three-step sequential extraction scheme, the so-called BCR method (formerly the Community Bureau of Reference, now referred to as The Standards, Measurements and Testing Programme of the European Commission; see Rauret et al., 1999). The extraction scheme has been evaluated using standard reference materials (CRB 601, sediment; CRM 483, sewage sludge amended soil) by multiple laboratories (Ure et al., 1993; Quevauviller et al., 1997; Rauret et al., 1999). In step 1 of the BCR scheme, metals present in ionic forms, bound to carbonates, and in exchangeable forms are separated (Table 3.3). In step 2, metals bound to amorphous iron and manganese oxides are leached, while in step 3 metals bound to organic matter and sulfides are selectively dissolved (Table 3.3). The use of prescribed procedures and standard reference materials to verify performance is an important development and a potential advantage of the BCR extraction approach.

Assessments of environmental risk may be more suitably focused on the water soluble and exchangeable soil fractions, i.e., the most labile metal/metalloid forms released in the first step of the sequential extraction schemes described above. While total metals contents and pseudo

Table 3.3 BCR extraction scheme applied to 1 gram of sample.

Step	Reagents/Conditions	Target Fraction
Step 1	40 mL of 0.11 M acetic acid; 16 h at room temperature	Ionic, exchangeable, carbonates
Step 2	40 mL of 0.50 M hydroxylamine hydrochloride plus 0.05 M nitric acid, 16 h at room temperature	Amorphous iron and manganese oxides
Step 3	10 mL 8.8 M hydrogen peroxide at room temperature for 1 h plus 1 h at 85 °C, reduce solution volume to near dryness; 50 mL 1 M ammonium acetate adjusted to pH 2 with nitric acid; 16 h at room temperature	Organic matter, sulfides

Notes: see Rauret et al. (1999) for detailed experimental procedures.

metals contents (sum of all extractable forms) are valuable in defining the extent of metal buildup in contaminated soils and sediments, these fractions may be less useful for assessing environmental and ecological impacts (Gupta et al., 1996). Use of single-step extraction tests with salt solutions of CaCl₂ and NaNO₃ for the determination of the most readily bioavailable metal fraction is discussed, for example, by Maiz et al. (1997) and Gupta et al. (1996). Although single-step procedures may be useful in developing models of ecological risk, these procedures will generally not be adequate in developing the necessary understanding of attenuation mechanisms and long-term contaminant behavior needed to adopt monitored natural attenuation as a site remedy.

In most cases, assessment and monitoring of natural attenuation processes for inorganic contaminants will require some type of sequential extraction procedure in Tier II. Tier II and Tier III sequential extraction efforts might be carried out to: i) further refine the conceptual model of natural attenuation; ii) increase the spatial resolution of metal partitioning data at a site; and, iii) validate extraction procedures by spiking extraction experiments with known quantities of reference minerals to assess method performance and test assumptions regarding solid phase partitioning. The selection of a sequential extraction procedure must take into consideration site-specific factors, such as physical soil/aquifer characteristics, redox conditions, and contaminant type. Examples of sequential extraction approaches on a contaminant-specific basis are presented in the element-specific chapters in Volume 2 of this document. It is possible that several procedures might be tried before an optimal method is selected at any site. Samples for sequential extraction tests should be collected near the source region and at points moving down gradient through the contaminant plume and at points past the down gradient and lateral plume fronts. Vertical resolution should cover the area most impacted by the contaminant plume but vertical sampling should also encompass subjacent and superjacent regions of the aquifer. These spatial data will be needed in order to develop a model of contaminant uptake along the flow-path. Sequential extraction procedures should be carried out prior to any active remediation and they may be a useful component of annual site monitoring activities.

IIIB.2.4.2 Sequential Extraction Considerations

Many examples of selective extraction recipes can be found in the literature. The choice of procedure will necessarily involve consideration of project objectives and site-specific details. Moreover, the pros and cons of using sequential extraction methods for determining metals speciation in the solid phase have been extensively discussed and debated in the literature (e.g., Kheboian and Bauer, 1987; Belzile et al., 1989; Nirel et al., 1990; Tessier and Campbell, 1991). Sequential extractions clearly provide a very practical methodology for getting at critical information about where metals reside in a sample that can be linked to bioavailability and geochemistry of contaminant metals. Further, a considerable amount of work has gone into verifying the selective extraction methods for specific elements of interest

(e.g., Gruebel et al., 1988). On the other hand, a number of complicating factors can strongly direct the outcome of sequential extraction procedures and the interpretation of results with regard to potential metal mobility. The two most identifiable experimental problems with sequential extraction procedures are the non-selectivity of extractants and potential trace element redistribution among phases during extraction (e.g., Rendell et al., 1980; Rapin et al., 1986). For example, metals that are released during extraction can potentially re-adsorb to other surfaces present in the sample at the time of extraction, or the extracting solution itself can impact geochemical conditions that favor metal removal by re-adsorption or precipitation. As noted previously in Section IIIB.3.1, extraction results are operationally defined and they are influenced by factors such as choice of reagents, extraction time, and solid to solution ratios.

An example of an extraction artifact relating to arsenic is described in Wilkin and Ford (2002). Extraction of samples with dilute hydrochloric acid is commonly adopted to assess metal and metalloid partitioning to the acid-volatile sulfide (AVS) fraction of soils and sediments. This extraction test is also used to estimate potential metal toxicity of aquatic sediments (DiToro et al., 1990; Allen et al., 1993; USEPA, 2000b). The method takes advantage of the comparatively high solubility of metal monosulfides like FeS, PbS, CdS, and ZnS at low pH. However, insoluble metal sulfides of Cu and Hg are not effectively dissolved in hydrochloric acid (e.g., Mikac et al., 2000). Furthermore, arsenic chemistry in sulfidic systems contrasts with that of divalent metals in that the solubility of arsenic sulfides like orpiment (As_2S_3) increases with pH; solubility minima for orpiment are found at low pH. This means that at the low pH conditions typical of HCl extractions, precipitation of arsenic sulfide is favored. Two potential artifacts complicate the use of low pH extractions for As solid-phase partitioning in sediments containing acid-volatile sulfides. If orpiment is present in sediment, it will not be efficiently dissolved with hydrochloric acid. A more serious problem, however, relates to interpretations of arsenic extraction data. During acid-extraction, arsenic may be released from labile sediment components, i.e., loosely bound or sorbed sites. If AVS is present, arsenic sulfide is expected to precipitate at low pH and thereby significantly impact arsenic partitioning by transferring arsenic from a labile and potentially bioavailable fraction to what would be considered, using conventional interpretations, a refractory, bio-unavailable fraction (i.e., a fraction insoluble in hydrochloric acid).

A second example of element redistribution during chemical extraction procedures relating to lead is described in Gerth (1990) and Ford et al. (1999). In these studies metal partitioning to iron hydroxide was evaluated using a 2 h extraction with ammonium oxalate. The procedure takes advantage of the rapid dissolution of ferrihydrite in ammonium oxalate relative to other more stable transformation products of ferrihydrite, such as goethite. However, an insoluble Pb-oxalate phase was identified as an end-product of the chemical extraction. The formation of this insoluble phase was clearly a consequence of the choice of reagents used in the extraction procedure. Again without knowledge

of this artifact, interpretation of extraction results would have likely guided the conclusion that lead was immobile and non-bioavailable, which in fact may or may not be the case. The magnitude of extraction non-selectivity and/or extraction artifacts can be assessed through the addition of specific mineral components targeted by the individual extraction steps. These internal reference materials can be synthesized in a manner that includes the contaminant in a sorbed form. Synthesis methods for many of the solid phase components targeted by the various proposed extraction protocols are included in the cited references. The inclusion of this form of quality control into the overall extraction methodology will increase the level of confidence in these analytical data.

IIIB.2.5 Attenuation Capacity

The capacity of geological materials to attenuate contaminants has been a subject of extensive research. The static or batch adsorption method has often been used to assess the capacity of soils and aquifer materials to remove metal components from the aqueous phase. The ease of carrying out batch-adsorption tests clearly factors into the popularity of this testing strategy. In this method, aqueous solutions are mixed with a given mass of solid material for a set period of time. The aqueous solution is next separated from the solid adsorbent material, typically by filtration, and chemically analyzed to determine changes in solute concentrations. The concentration of a dissolved component before reaction with the adsorbent minus the concentration after reaction is used to calculate the mass of the component that has been removed by adsorption (or some other removal process). The approach is simple yet numerous experimental parameters impact the results of a given batch-adsorption test (USEPA, 1992; USEPA, 1999; Jenne, 1998).

For inorganic species of concern, critical experimental parameters include contact time, solution pH, method of mixing, solid:solution ratio, and the concentration of other dissolved components in the solution (e.g., Barrow and Shaw, 1979; Roy et al., 1986). Solution composition is of critical importance since dissolved constituents in the background matrix of the ground water can influence contaminant partitioning either through competition for sorption sites or modification of the surface charge of the aquifer matrix. In addition, due to chemical interactions between the aquifer matrix and the solution in which it is suspended, it is important that solution matrix employed closely mimics the in-situ conditions from which the aquifer matrix was collected. For example, exposure of reduced sediments to a solution matrix containing molecular oxygen will likely cause significant changes in the mineralogical composition of the aquifer matrix during the time period of the batch test (USEPA, 2006). The results from a test performed in this manner provide no meaningful data relative to the assessment of in-situ sorption properties.

The methods used to prepare samples for use in laboratory-based studies, including batch-adsorption tests, can have a profound influence on test results. For example, oven-drying

samples, although useful for homogenizing materials and for obtaining accurate dry weights, in most cases affects the chemical properties of sediments and may influence the results of batch-adsorption procedures. This affect will vary from material to material but may be the consequence of surface area changes that come about after drying, mineral transformations that occur at elevated temperatures or result from oxidation reactions. Consequently, oven-drying is generally not an advisable practice to accelerate material drying. Air-drying is more preferable although this method may take a longer period of time (several days). Air-drying can be considered to be a partial drying procedure to bring the moisture content of a material to near equilibrium with the atmosphere under which drying is taking place. The duration of air-drying should be kept to the minimum time possible and the progress should be tracked with methods such as weighing. Anaerobic soils provide a special case. Drying of such materials must be carried out in a anaerobic chamber or glove box. Drying of anaerobic materials can be accelerated by using a stream of dry, high-purity (oxygen-free) inert gas.

Batch-adsorption tests should be carried out under constant-temperature conditions (e.g., ± 3 °C) and should attempt to mimic site chemical conditions. The influence of pH on batch-adsorption tests is extremely important and the effect of pH will vary depending on the nature of the adsorbent and the solute of interest. Measurements of the equilibrium pH of the soil-water suspension should be given along with adsorption results. For anaerobic systems, batch tests and pH measurements should be carried out in a glove box so that air-sensitive soil components do not oxidize and influence contaminant sorption (USEPA, 2006). Methods for ensuring proper mixing of solid and solution mixtures and selection of appropriate solid:solution ratios are discussed for example in USEPA (1992).

Results of batch-adsorption tests are conveniently analyzed using linear regression tools and adsorption isotherm equations that relate the amount of solute adsorbed to the equilibrium concentration of the solute. Two of the more frequently used adsorption models employ the Langmuir Equation (Section IIIB.3.2) and the Freundlich Equation (Section IIIB.3.3). The choice of one of these adsorption models or other possible adsorption equations will typically stem from the simplicity of the equation and from statistical reasoning using the regression coefficient. These equations can be used to quantitatively describe adsorption data and be “plugged” into reaction transport models used to develop site models (see Section ID).

Dynamic, continuous flow column experiments are a more detailed and desirable method for obtaining metal uptake and desorption potential. In column experiments, aquifer materials are packed into a column apparatus, typically a glass chromatography column equipped with Teflon end-plate assemblies. Columns typically contain sampling ports at the influent and effluent ends and preferably along the length of the column. The sampling ports are designed to allow for water sampling along the center axis

of the column. Representative solutions are then pumped through the column using for example a high-performance liquid chromatography pump at a flow rate selected to approximate an average seepage velocity expected in the field. Effluent solutions and sampling ports along the column are then monitored with respect to contaminant concentrations, geochemical parameters (e.g., pH, redox potential), and volume of solution eluted from the column. These data allow for the construction of contaminant breakthrough curves based on the reduced contaminant concentrations ($C_{\text{effluent}}/C_{\text{input}}$) and sample pore volume. The results of column tests can be augmented by the application of mineralogical characterization techniques to allow for the identification of reaction products that can lead to insight regarding uptake mechanisms and provide an improved basis for predicting long-term trends.

The results of static-batch and dynamic-column tests ultimately will be fed into a mathematical model (i.e., a surface complexation model, or Freundlich adsorption isotherm) to develop a quantitative description of contaminant sorption to and desorption from aquifer materials. Examples of this methodology are presented for example in Dunnivant et al. (1992) and Kent et al. (1995), studies that explore the transport of cadmium and chromium/selenium, respectively, in aquifer systems.

In context of using laboratory- or field-derived data as input to computer modeling codes, Bethke and Brady (2000) have recently pointed out potential problems with the “ K_d ” or single parameter distribution coefficient approach. When sorption is suspected as being the dominant attenuation mechanism, these authors argue that the simple distribution coefficient will in many cases not adequately describe contaminant movement through aquifer systems, especially for the ionic species typical of inorganic contaminants of concern in this document. The distribution coefficient simply gives the ratio of a metal ion’s sorbed concentration (mol/g sediment) to its dissolved concentration (mol/cm³). Alternatively, Freundlich or Langmuir adsorption isotherms or surface complexation models are available to more accurately model field observations. The advantage of the isotherm approach is that adsorption trends can be tied specifically to materials collected from a specific site, yet the method is empirical and it must be acknowledged that extrapolation of results can not be made outside of measured ranges. The surface complexation model does indeed provide a more realistic description of ion adsorption from fundamental principles, yet available databases for surface complexation constants are limited. Almost all applications of surface complexation modeling efforts use hydrous ferric oxide as the dominant sorbing material, this may not be appropriate for all sites.

IIIB.3 Model Representations to Interpret Contaminant Sorption Observations

While thermodynamic equilibrium-based geochemical models are useful for providing boundary conditions for estimating the extent of contaminant partitioning to aquifer solid phases, the kinetics and reversibility of the sorption

process are factors that warrant consideration on a site-specific basis if monitored natural attenuation is proposed as a remedial strategy for inorganic contaminants. Another important consideration is that a purely thermodynamic treatment of partitioning is a purely macroscopic description and therefore, is not dependent on an atomic or a molecular scale model which may be employed to represent sorption reactions occurring within the aquifer (Sposito, 1981).

There are two general approaches to modeling contaminant sorption behavior, namely empirical and mechanistic models. Empirical models provide a mathematical description of observed experimental data without necessarily invoking a theoretical basis or microscopic model for the observed relationship. Mechanistic models seek to describe a system based on thermodynamic principles. In theory, the mechanistic approach is desirable because it is more robust and widely applicable in that the effects of changes in ionic strength and pH within a system are fully integrated into the models. On the other hand, mechanistic models require a rather complete chemical and physical description of the system to be modeled and thus are still less commonly used than the empirical models. In general, mathematical descriptions of contaminant sorption to solid surfaces capture the electrostatic and/or chemical forces (or some combination thereof) that result in a net attraction of dissolved contaminants to the solid surface. Empirical models are derived to describe sorption trends irrespective of the specific mechanisms, e.g., electrostatic/chemical forces, involved in the partitioning process. In contrast, mechanistic models attempt to describe the relationship between properties of the solid surface and the net attraction/repulsion of the dissolved contaminant.

IIIB.3.1 Distribution Coefficient/Partition Coefficient, K_d

The partition coefficient, K_d , is the simplest model for predicting sorption in soil systems. It is defined as the ratio of the quantity of adsorbate sorbed per unit mass of solid to the quantity of adsorbate in solution at equilibrium:

$$K_d = q/C$$

where q = concentration of adsorbate on the solid at equilibrium ($\mu\text{g/g}$) and C = total dissolved concentration remaining in solution ($\mu\text{g/ml}$).

This approach assumes that the system is reversible and that sorption is independent of the adsorbate concentration in the aqueous phase. Like all the empirical models the constant K_d value does not account for changing physical and chemical conditions in the soil. An extension of the constant K_d is the parametric K_d model where the dependence of K_d of a particular contaminant on various physical and chemical properties of the system is determined by stepwise linear regression analysis and polynomial expressions are developed that express K_d as a function of the relevant soil and aqueous conditions. The parametric K_d approach is preferable in that it allows for the K_d value to vary dependant on prevalent conditions, however, it arguably involves as complete an analytical characterization of

the system as the mechanistic models while still remaining an empirical approach.

The basic tenant of the constant K_d approach, i.e., that partitioning is a linear function of concentration, has been shown to be invalid in many instances. Adsorption isotherm models have been used by soil scientists to model situations where adsorption deviates from linearity. The two most commonly used models are the Langmuir and Freundlich adsorption isotherm models.

IIIB.3.2 The Langmuir Model

The Langmuir model was originally developed to describe the adsorption of gas molecules on a homogenous solid surface. The assumptions underlying the model are that every adsorption site is equivalent, and that the ability of a site to bind the adsorbate is independent of whether neighboring sites are occupied. The Langmuir equation is expressed as:

$$q = \frac{bKC}{1+KC}$$

Where q is the concentration of adsorbate on the solid and C is the concentration in solution, b is the maximum number of available sites for adsorption (assumes monolayer coverage) and K is a constant related to binding strength. The Langmuir equation can be rearranged to a linear form:

Let $K_d = q/C$
 then $K_d = bK - Kq$

and a plot of K_d versus q should be linear with a slope of $-K$ and intercept of b .

Sposito (1984) reports that it is not uncommon for the relationship between K_d and q to be convex to the q axis rather than linear. This type of isotherm has been fit with a two site Langmuir isotherm:

$$q = \frac{b_1K_1C}{1+K_1C} + \frac{b_2K_2C}{1+K_2C}$$

The adherence of an adsorption isotherm to a two site Langmuir model has been interpreted as evidence for two discrete binding sites on the solid phase, however, no mechanistic interpretation can really be inferred from the goodness of fit of sorption data to these isotherms.

IIIB.3.3 The Freundlich Isotherm

The Freundlich isotherm has the form:

$$q = AC_i^\beta$$

Where A and β are adjustable parameters and β can have a value between 0 and 1. Hence a plot of $\log q$ vs. $\log C$ should be a straight line with an intercept of $\log A$ and slope of β . Note that when $\beta = 1$, then the Freundlich equation reduces to the linear K_d .

Sorption isotherms have been widely used to describe and predict adsorption of a contaminant in soil and sediment systems, however, as stated previously they are purely

empirically derived relationships and the validity of the calculated parameters can only be expected to hold within the bounds of the experimental data used to create the initial isotherm. They also provide no mechanistic interpretation of the reactions governing the solubility of a contaminant in a system; they are insensitive to the mode of sorption (i.e. precipitation or adsorption). In view of these facts mechanistic models of the soil sediment system have been developed. The mechanistic approach uses thermodynamic relationships to model aqueous speciation and electric double layer theory to model changes in surface charge as a function of pH, electrolyte concentration and valence. Mechanistic models are potentially much more robust than adsorption isotherm approaches and, once the model has been established, potentially much more powerful in their predictive capabilities with respect to changing physical and chemical conditions within the system.

IIIB.3.4 Mechanistic Models for Predicting Sorption - Surface Complexation

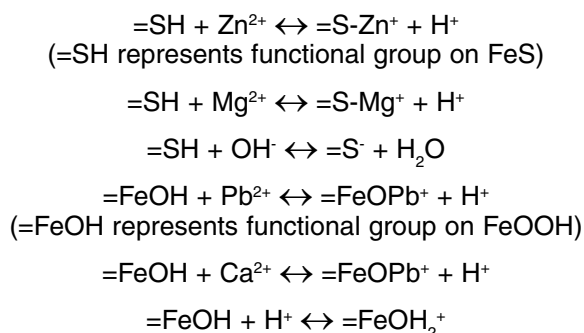
A variety of mechanistic approaches have been applied to provide a molecular description of adsorption in soil-water systems. A number of approaches are based on a mathematical description of the distribution of ions in the vicinity of a charged surface, and the surface charge and potential in the interfacial region. These mathematical models, termed surface complexation models (SCMs), capture the influence of electrostatic forces between the solid surface and charged ions within solution as well as the influence of chemical interactions between these two entities that leads to the formation of coordinative bonds. The various models that are commonly employed to describe surface complexation reactions differ in their description of the distribution of charge at the solid-water interface and how ions are distributed in the aqueous layer that bathes the solid surface. Details of the various models are available from several sources and should be consulted by those unfamiliar with the implementation of surface complexation modeling to describe contaminant solid-solution speciation (e.g., Sposito, 1984; Davis and Kent, 1990; Stumm, 1992; Goldberg, 1995). A brief synopsis of the various models is provided in Table 3.4. In general, two different types of surface complexes are proposed in the various models: 1) inner-sphere surface complexes in which the contaminant forms a bond with a surface functional group, and 2) outer-sphere surface complexes where the contaminant partitions to the surface via electrostatic attraction (similar to the process of ion exchange).

A key difference between SCMs and empirical models is the employment of thermodynamic concepts to model chemical reactions occurring at the solid surface. By proposing specific chemical reactions for the partitioning of solution ions to the solid surface it becomes feasible to account for the influence of the bulk solution composition such as pH, which can exert an influence on both surface charge as well as solute speciation. In addition, the bulk water composition can influence contaminant sorption via the presence of ions in solution that compete for available surface sites. Examples of surface complexation reactions that may be

Table 3.4 Synopsis of the various surface complexation models (SCMs) commonly employed to describe solute partitioning to solid surfaces.

Surface Complexation Model	Description of Solute Partitioning to Solid Surface	Influence of Surface Charge
Constant Capacitance Model (CCM)	Inner-sphere complexes	Exponential electrostatic term that modifies value of surface complexation constant
Diffuse Layer Model (DLM)	Inner-sphere complexes	Exponential electrostatic term that modifies value of surface complexation constant
Triple Layer Model (TLM)	Inner- and outer-sphere complexes	Two exponential electrostatic terms that modify values of inner-sphere and outer-sphere surface complexation constants
Nonelectrostatic Model (NEM)	Inner-sphere complexes	None

postulated within an SCM are as follows:



A mass action equation can then be written for each of these reactions (similar to solution complexation reactions) and solved to calculate *conditional* surface complexation constants. For SCMs that account for the influence of electrostatic interactions, the conditional surface complexation constant is typically modified via multiplication by an exponential electrostatic factor in order to calculate an *intrinsic* surface complexation constant.

The reactions describing ion partitioning to a solid surface provide the physicochemical context for assessing changes in sorption that may accompany changes in ground-water chemistry. Several observations are evident from the example reactions shown above:

- 1) pH can influence the speciation of surface functional groups as well as the surface charge,
- 2) ion sorption can influence surface charge, and
- 3) major ions in solution (e.g., Mg^{2+} and Ca^{2+}) can compete with the contaminants of concern (e.g., Zn^{2+} and Pb^{2+}) for available sorption sites.

Thus, an SCM provides one with the ability to project how changes in solution chemistry can impact contaminant uptake; a significant limitation of empirical partitioning relationships. While this flexibility provides a powerful tool for examining the evolution of a contaminant plume, current implementations of most SCMs is limited by the heterogeneous nature of solid surfaces within an aquifer (types of sorption sites) and the ability to predict surface charging behavior. Recent efforts have been employed to develop nonelectrostatic surface complexation constants for site-specific descriptions of subsurface contaminant transport (e.g., Kohler et al., 2004). This approach will most likely be successful for contaminants that predominantly form strong chemical bonds with available solid surfaces.

IIIB.3.5 Mineral Solubility

Characterization of the solid phase will, in most cases, be an integral component of monitored natural attenuation assessment and application. Some insight regarding the mineralogical composition of aquifer systems can be obtained by analyzing solution compositions. Investigations of mineral solubility in aquifer systems usually concentrate on the question: does a mineral control the concentration of a particular element, and, if so, what is the identity of the mineral? In order to answer these questions, geochemical models are frequently employed to calculate ion activities and mineral saturation indices. In aquifer systems, some chemical reactions are sufficiently fast that equilibrium relationships are immediately attained. For example, protonation/deprotonation reactions of acids and bases and ion pairing reactions are fast chemical reactions. Other reactions, in particular those reactions involving solids, can proceed so slowly that equilibrium is not attained even after decadal time periods. Yet, equilibrium is a practical reference point and equilibrium relationships are useful for predicting reactions that are likely or unlikely to occur.

Mineral solubility is influenced by the ionic strength of solution. Unless conditional equilibrium constants are employed, solution activity models are a necessary component of geochemical modeling efforts. Activity models account for the non-ideal behavior of solute ions in aqueous solutions. Non-ideal behavior is a consequence of electrostatic interactions between water molecules and charged solute ions. Methods for computing individual ion activity coefficients are presented in numerous textbooks (e.g., Stumm and Morgan, 1981; Nordstrom and Munoz, 1986). For

most ground water studies of low ionic strength waters, the extended Debye-Hückel equation or the Davies equation will provide reasonable activity models. In these equations, activity coefficients are estimated based on input values for solution ionic strength and temperature. For concentrated waters that are high in total dissolved solids, virial methods such as the Pitzer model are available for estimating ion activity coefficients (Langmuir, 1997).

The unit of concentration for dissolved species most frequently used for aqueous solutions is molality, m_i (mol/kg). Analytical concentrations are often expressed in mass based units, e.g., ppm (parts per million). A useful conversion is:

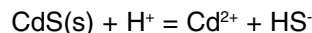
$$\text{Conc. in ppm} = \text{Conc. in mol/kg} \times \frac{\text{formula weight in g/mol} \times 1000}{\text{molality}}$$

The effective concentration or activity of a dissolved species, a_i , is given by:

$$a_i = (\gamma_i m_i) / (\gamma_i^0 m_i^0)$$

Where γ_i is the ion-specific activity coefficient and $(\gamma_i^0 m_i^0)$ refers to the standard state, which for aqueous solutions is typically chosen as an ideal, 1 molal solution, i.e., both γ_i^0 and m_i^0 are equal to 1.

In order to evaluate whether a ground water is oversaturated, undersaturated, or at equilibrium with a particular phase, geochemical speciation models are of practical use. As an example, consider the solubility expression for cadmium sulfide (greenockite):



The mass-action expression that applies to the equilibrium is:

$$K_r = \frac{a_{Cd^{2+}} a_{HS^-}}{a_{CdS} a_{H^+}} = 10^{-14.4}$$

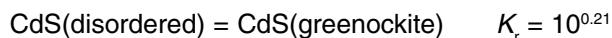
Ground water may or may not be at saturation with respect to greenockite, depending on whether the phase is indeed present, available surface area, residence time of water, and kinetic factors that may impede dissolution and/or precipitation. If the water is at equilibrium, then the ion activity product, Q , should be the same as the equilibrium constant, i.e.,

$$Q = \frac{a_{Cd^{2+}} a_{HS^-}}{a_{H^+}} = K_r = 10^{-14.4}$$

where the activity of CdS is taken to be unity. Calculation of the saturation index (SI) for a water can then be used to determine if the solution is undersaturated, at equilibrium, or oversaturated with respect to precipitation (see Section IIB.2.1, Table 2.3).

It is important to point out that solubility products for precipitates, such as cadmium sulfide, depend on whether the solid is freshly precipitated (typically disordered) or crystalline (well ordered). At 25 °C, Daskalakis and Helz (1992) report a solubility product of $10^{-14.36}$ for crystalline cadmium sulfide (greenockite). Wang and Tessier (1999)

give a value of a freshly prepared CdS precipitate of $10^{-14.15}$. Hence, freshly precipitated cadmium sulfide is metastable with respect to greenockite since:



and

$$\Delta G_r^0 = -\alpha RT \log K = -1.20 \text{ kJ/mol}$$

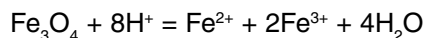
If it is possible to calculate activities of free ions from a given water analysis, then it is a relatively simple matter to calculate the degree saturation of a large number of possible mineral phases, keeping in mind that temperature and ionic strength are needed to correct the ion activity product.

In the example above, pH and the molal concentrations and ion activity coefficients for Cd^{2+} and HS^- are needed in order to compute the ion activity product. If complexes of cadmium are present, then $m_{\text{Cd}^{2+}}$ is not the same as the total concentration of dissolved cadmium. If we consider only mononuclear bisulfide complexes,

$$m_{\text{Cd}, \text{total}} = m_{\text{Cd}^{2+}} + m_{\text{CdHS}^+} + m_{\text{Cd}(\text{HS})_2^0} + m_{\text{Cd}(\text{HS})_3^-}$$

Depending on the solution composition, cadmium complexes with chloride, bicarbonate, hydroxide, or sulfate may be important in addition to bisulfide complexes. Similarly, m_{HS^-} is not the same as the total concentration or analytical concentration of dissolved sulfide. Both protonated and deprotonated forms of sulfide and complexed forms of sulfide may be present. Speciation calculations, therefore, are critically dependent on the completeness and quality of thermodynamic constants in the thermodynamic database used for geochemical modeling (see Section ID).

In cases where mineral solubility is controlled in part by redox conditions, calculation of the saturation index is not straightforward. For example, when an aqueous solution has attained saturation with respect to a mineral such as the iron oxide magnetite (Fe_3O_4), then the reaction



is at reversible equilibrium when

$$\frac{a_{\text{Fe}^{2+}} a_{\text{Fe}^{3+}}^2 a_{\text{H}_2\text{O}}^4}{a_{\text{H}^+}^8} = 10^{4.2} = K_r$$

Magnetite solubility depends therefore on pH and redox. It follows that to calculate the saturation index for magnetite, activities of both the ferrous and ferric ions are needed input variables. Accurate measurement of ferric iron concentration at circumneutral pH is a notoriously difficult task. There are several ways to approach this problem:

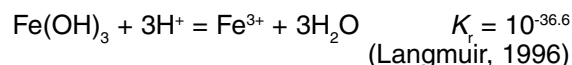
- Measure separately both Fe(II) and Fe(III) in a water sample and estimate activity coefficients in order to calculate the activities of Fe^{2+} and Fe^{3+}
- Use Eh as a master redox variable to fix Fe(II):Fe(III) ratios
- Measure Fe(II), calculate Fe(III) by assuming control by the solubility of Fe_2O_3 , FeOOH , or $\text{Fe}(\text{OH})_3$
- Use some other measured redox pair to fix Fe(II)/Fe(III)

There are methods available to determine separately the concentration of ferrous iron and ferric iron (e.g., To et al., 1999); however, these methods are most effective for use in low pH waters, such as aquatic systems impacted by mine wastes. At near-neutral pH, the concentration of Fe(III) is typically very low so that analytical detection limits constrain the use of direct measurements.

The second method is to use the measured Eh of a water to estimate the Fe(II)/Fe(III) ratio in solution. Applying the Nernst equation to the iron(II/III) couple, we have

$$E = E^0 - \frac{RT}{nF} \ln \Pi a_i^{v_i} = 0.770 - 0.0592 \log \frac{a_{\text{Fe}^{2+}}}{a_{\text{Fe}^{3+}}}$$

Using this approach, Fe(II)/Fe(III) can be calculated from a potential measurement using a platinum electrode. Nordstrom et al. (1979) conclude that this approach is most effective at pH < 6 and at total iron concentrations exceeding 10^{-6} molal. A third method is to assume that the solubility of a ferric-bearing mineral controls the activity of Fe^{3+} . For example, consider the solubility expression of hydrous ferric oxide:



So that,

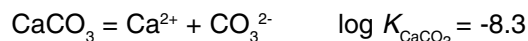
$$\log a_{\text{Fe}^{3+}} = \log K - 3 \log a_{\text{H}_2\text{O}} - 3\text{pH} \cong -36.6 - 3\text{pH}$$

In this example, the activity of Fe^{3+} can be estimated based on a measurement of pH. In the last example, a separate redox pair, e.g., As(III)/As(V), can be used to fix the Fe(II)/Fe(III) ratio in solution by applying the Nernst equation. The correctness of any one of these approaches relies on how closely the assumptions are obeyed for a given system.

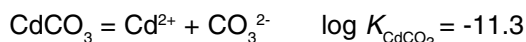
IIIB.3.5.1 Coprecipitation Reactions

The concept of a solid solution implies an isomorphic substitution, for example, regular substitution of Mn for Ca in a carbonate mineral. Minerals formed in the environment often contain substitutional impurities and coprecipitation is likely to be a primary natural attenuation mechanism. Thermodynamic models of solid solutions indicate that the solubility of a component becomes greatly reduced as that component becomes a constituent in a solid phase. In other words, solid solutions in binary systems, for example, are less soluble (more stable) than pure end-member compositions. A considerable effort has gone into understanding the thermodynamic and kinetic factors that control the formation of solid solutions from aqueous solutions (e.g., Lippmann, 1977; Busenberg and Plummer, 1989; Glynn et al., 1990; Glynn and Reardon, 1990).

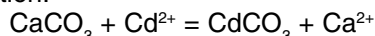
Laboratory and field studies indicate that cadmium is effectively removed by calcareous materials (e.g., Dudley et al., 1988; Davis et al., 1987). The solid solution $(\text{Ca,Cd})\text{CO}_3$ is complete and the endmember solubility products differ by three orders of magnitude at room temperature:



and



Combining these solubility expressions we obtain an exchange reaction:



The equilibrium constant for this type of reaction is often referred to as a distribution constant, D , and is given by the quotient of the solubility products of CaCO_3 and CdCO_3 :

$$D = \frac{a_{\text{CdCO}_3}}{a_{\text{CaCO}_3}} \cdot \left(\frac{a_{\text{Cd}^{2+}}}{a_{\text{Ca}^{2+}}} \right)^{-1} = \frac{K_{\text{CaCO}_3}}{K_{\text{CdCO}_3}} = 10^3$$

The activity ratio of the solids by definition can be replaced by the ratio of the mole fractions multiplied by activity coefficients:

$$D = \left(\frac{X_{\text{CdCO}_3}}{X_{\text{CaCO}_3}} \right) \cdot \left(\frac{\gamma_{\text{CdCO}_3}}{\gamma_{\text{CaCO}_3}} \right) \cdot \left(\frac{a_{\text{Ca}^{2+}}}{a_{\text{Cd}^{2+}}} \right)$$

Therefore, the amount of substitution of Cd into calcium carbonate is a function of the solubility product ratio of CaCO_3 to CdCO_3 , the solution activity ratio of Cd^{2+} to Ca^{2+} , and a term that represents activity coefficients of the solid solution components:

$$\left(\frac{X_{\text{CdCO}_3}}{X_{\text{CaCO}_3}} \right) = \frac{K_{\text{CaCO}_3}}{K_{\text{CdCO}_3}} \cdot \left(\frac{a_{\text{Cd}^{2+}}}{a_{\text{Ca}^{2+}}} \right) \cdot \left(\frac{\gamma_{\text{CdCO}_3}}{\gamma_{\text{CaCO}_3}} \right)$$

In general practice the first two terms, solubility product ratio and the solution activity ratio, are straightforward to obtain. Activity coefficients in the solid phase in most cases differ markedly from 1. In principle, the activity term can be determined experimentally by measuring the mole fraction ratio over a range of solution activity ratios at constant temperature.

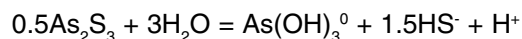
An analysis of solution concentration data alone will generally not be adequate to confirm any precipitation or coprecipitation mechanism of attenuation. Multiple lines of evidence, including solution and solid-phase data, which supports a specific natural attenuation mechanism will in most cases be necessary to pursue monitored natural attenuation as a partial or sole cleanup remedy.

IIIB.3.5.2 Thermodynamic Data

Site characterization and remedial investigations that involve contaminant transport in the environment are usually accomplished, in part, with geochemical modeling. Consequently, thermodynamic properties are essential components to geochemical modeling efforts. Normally, the thermodynamic constants used in modeling exercises are taken from published compilations of such properties (e.g., Wagman et al., 1982). In some cases these compilations contain minimal documentation as to the source or quality of compiled data. In other cases, compilations contain outdated information. Users of thermodynamic databases can easily be misled into believing that modern databases are up to date in terms of data quality and completeness.

As an example to illustrate problems noted above, a specific example of orpiment ($\text{As}_2\text{S}_3(\text{s})$) is discussed. Eary (1992) listed a number of values of the Gibbs free energy of formation, ΔG_f° , of orpiment, each from a separate lit-

erature source. The values tabulated by Eary (1992) range from -168.8 kJ/mol to -90.7 kJ/mol. This wide range in Gibbs free energy values equates to equilibrium constants describing orpiment dissolution and precipitation that can span almost 7 orders of magnitude. For example, consider the solubility expression for orpiment to form arsenite in solution:



An equilibrium constant for this reaction can be computed from the ΔG_f° values for orpiment given above and fixed values of ΔG_f° for $\text{H}_2\text{O}(\text{l})$, $\text{As}(\text{OH})_3^0$, and HS^- of -639.8 kJ/mol, -237.18 kJ/mol, and 12.05 kJ/mol, respectively. The more negative ΔG_f° value for orpiment gives a log K value for the above reaction of -30.5 , while the greater value gives a log K value of -23.7 . The pH dependent trend of orpiment solubility resulting from these differing log K values is shown in Figure 3.5. The solubility diagram is constructed at $\Sigma\text{H}_2\text{S}$ concentration of $10^{-5.5}$ m, so that thioarsenite species have a negligible contribution to orpiment solubility (Wilkin et al., 2003). It is clear that depending on the log K value employed in reaction modeling, solutions will have vastly different saturation indices and one would reach different conclusions about possible attenuation mechanisms for arsenic.

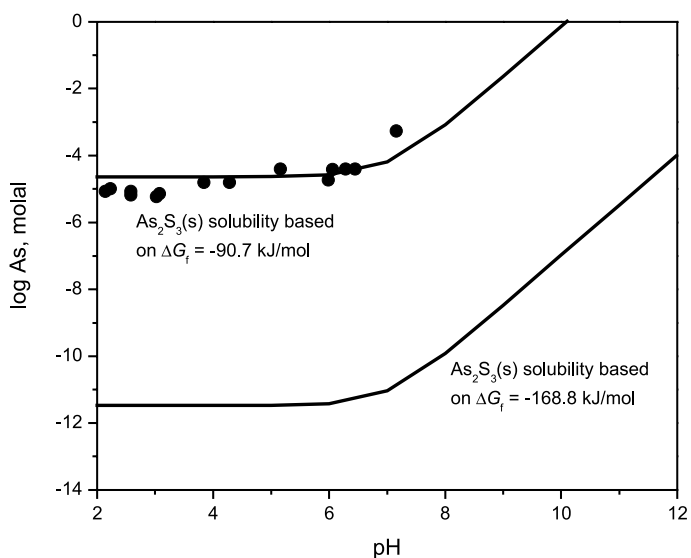


Figure 3.5 pH-dependent solubility trend of orpiment predicted using two different Gibbs free energy of formation values (see text). The model curves correspond to a constant $\Sigma\text{H}_2\text{S}$ concentration of $10^{-5.5}$ m. The data points are measured solubility data taken from Webster (1990). The experimental data are consistent with a ΔG_f° for orpiment of approximately -90 kJ/mol, yet most thermodynamic compilations adopt a value of -168.8 kJ/mol. Application of the lower value will vastly over predict the stability of orpiment.

Which value of ΔG_i^0 for orpiment is more appropriate? The most recent solubility and calorimetric studies seem to support a ΔG_i^0 formation value close to -90 kJ/mol for crystalline orpiment (Webster, 1990; Eary, 1992; Johnson et al., 1980). The key point is that users of geochemical models should be familiar with the sources of thermodynamic data used and attempt to evaluate whether constants in thermodynamic compilations are in reasonable agreement with recent experimental evidence or whether there may be discrepancies that could impact how model results are interpreted.

IIIC. Characterization of System Redox and Underlying Microbial Processes

Oxidation-reduction processes affect the chemical composition of ground water and impact the aqueous and solid phase chemical speciation of inorganic contaminants. Thus, characterizing the redox status of ground water systems will likely play an important role in understanding controls on contaminant attenuation. As stated previously in Section IIC, the subsurface microbiology within a plume will, in part, influence the predominant redox characteristics of the system. Microbial processes may influence the redox chemistry of important components within the aquifer, such as iron and sulfur, participating as reactants within attenuation reactions that result in contaminant immobilization or degradation. Thus, it is recommended that site characterization include both assessment of the prevailing subsurface redox chemistry impacting contaminant transport, as well as more explicit analysis of specific microbial processes for sites at which the plume conditions support microbial activity that differs from ambient conditions. For example, a more detailed microbial community analysis may be warranted in order to improve the reliability of assessing attenuation capacity for sites where contaminant source characteristics govern aquifer geochemistry within the down gradient plume. The following discussion provides approaches and tools available to characterize the overall redox status of site ground water, as well as the specific microbial communities that support the observed redox chemistry within the plume.

IIIC.1 Process Identification

Identification of a redox-mediated attenuation process starts with knowledge of the aqueous and solid-phase species present. Although analysis of the contaminant concentration in ground water at various distances from the source can indicate attenuation, inclusion of data for pH, E_H , major solutes, and redox-sensitive species such as Fe^{2+} , O_2 , and H_2S is needed to demonstrate that redox processes may be involved.

Further evidence for redox-mediated processes may be derived from determination of the mineral species present. The absence of Fe and Mn oxides and the presence of Fe sulfides, for example, suggest that the aquifer is predominantly reducing, whereas the inverse of this situation suggests an oxidizing aquifer. A variety of techniques can be used for mineral identification and is detailed elsewhere

in this document (Section IIIB.2). A major consideration related to mineralogical characterization relates to the preservation of original mineralogy in aquifer materials by preventing contact with oxygen during sample collection and removal of pore water. For example, iron-bearing minerals may exist in a reduced state within the saturated zone. Yet such minerals that are stable in reducing environments are subject to significant alteration upon exposure to oxygen. Solid phase structural and chemical transformations are commonly mediated or facilitated by the pore water. Thus, removal of pore water may act to retard or impede transformation. In order to preserve redox characteristics of samples collected in the field, cores materials should be immediately capped and frozen. Sample freezing can be accomplished either by submersing in liquid nitrogen or placement in a portable freezer located in the field. Following transport to a laboratory setting, frozen materials should be thawed under an oxygen-free or inert atmosphere, e.g., within an anaerobic glove box. Extended periods of storage should be avoided, since sample mineralogy will alter with time during approach to a new equilibrium state. Procedures for the collection and processing of aquifer solids to minimize alterations to mineralogy are outlined in several EPA documents (USEPA, 2002; USEPA, 2005b; USEPA, 2006).

In some situations, intense local microbial activity may be entirely responsible for the redox status of the aquifer. The nature of the active microbial population (e.g., iron-reducing, sulfate-reducing, or sulfur-oxidizing bacteria) can often be inferred from geochemical data. Thus, trends in the concentration of organic substrates (soluble organic C) and their metabolites (e.g., H_2 , H_2S , CH_4 , CO_2 , NO_2^- , HS^- , Fe^{2+}) can indicate whether and which microorganisms are active in a particular subsurface region. In some instances, direct and specific determination of microbial population by culturing or genetic analysis (e.g., messenger ribonucleic acid profiles) of aquifer solids extracts may be warranted.

Although the best support for a particular redox process comes from direct examination of reactants and products at the site, a strong case for the process can be made with laboratory tests using core materials taken from the site. These tests involve batch or column studies in which the geochemical inputs and conditions are comparable to those at the actual site, and evidence for the process is obtained from analysis of the solution phase (supernate or effluent) during the test and of the solid phases at its conclusion. Attenuation obviously must be demonstrated through the solution-phase data, and direct identification of the attenuated form of the contaminant provided from the solid-phase data. As described below, this same general approach with suitable modifications can be used to determine capacity, kinetics, and stability.

IIIC.1.1 Redox Measurements

Measurement of redox parameters in ground water is inherently challenging due to the fact that a steep redox gradient is often present between the sampling location (subsurface) and the location where the particular measurement is made

(surface). Consequently, special care must be taken to preserve the redox integrity of ground-water samples. In some cases water samples can be preserved by using inert gases or by acidification because oxidation rates generally decrease substantially with decreasing pH. In other cases where sample preservation is not possible or practical, it is recommended that analyses be carried out in the field at the time of sample collection (e.g., for dissolved oxygen and Eh). Summaries of methods used to determine redox status can be found in, for example, USEPA (2002), Baedecker and Cozzarelli (1992), and Walton-Day et al. (1990). Table 3.5 provides a list of parameters that can be used to assess the redox status of ground water systems.

Other laboratory approaches include selective dissolution of reactive fractions (see Section IIIB.2.4.1). For example, reactive Fe²⁺ (i.e., that which is sorbed as well as that present in sulfides carbonates, hydroxides, and green rusts) can be estimated by extraction with 0.5 M HCl followed by complexation with ferrozine (Roden and Zachara, 1996; Amonette et al., 2000). From the oxidizing side, Mn(III,IV) oxides and poorly ordered Fe(III) (hydr)oxides can be de-

termined by extraction with hydroxylamine solutions (Chao, 1972; Chao and Zhou, 1983; Ross, 1985).

The direct reactions and laboratory tests, however, measure only the redox-buffering capacity at a single point in time. Microbial activity, through conversion of organic C, can create and replenish the reductive capacity of a site. Thus, more accurate measurements of reductive capacity may necessitate consideration of inputs of dissolved constituents from source areas or up gradient portions of the aquifer such as dissolved organic C, as well as terminal electron acceptors such as oxygen, nitrate, and sulfate, in order to assess ability of the microbial community to maintain or degrade the redox capacity of a site.

IIIC.2 Capacity

Once the operative redox-mediated attenuation process has been identified, an assessment of its capacity to attenuate the contaminant is needed. The primary soluble electron donor in most ground waters is dissolved organic carbon, although, under some circumstances, sulfide (H₂S, and HS⁻)

Table 3.5 Ground-water redox parameters and measurement approaches.

Parameter	Measurement Approach
Oxidation-reduction potential (ORP)	Combination platinum electrode with Ag/AgCl reference electrode; KCl filling solution. Electrode performance is determined using reference solutions (e.g., Zobell's solution, hydroquinone).
Dissolved oxygen	Membrane-covered electrodes; colorimetric tests, modified Winkler titration. Electrode performance is determined using air-saturated water and sodium sulfite solutions.
Dissolved hydrogen	Sample collection in glass vessel and analysis by gas chromatography/reduced gas analyzer.
Iron speciation	Ferrous iron determined by colorimetric analysis (e.g., ferrozine, 1,10-phenanthroline). Ferric iron determined by adding reducing agent and measuring ferrous iron, and/or by determination of total iron and subtracting Fe(II). Measurement made in the field or preservation required.
Sulfur speciation	Sulfate and other sulfoxyanions (sulfite, thiosulfate) are typically determined by ion chromatography or capillary electrophoresis. Sulfide can be determined by colorimetric, gravimetric, coulometric, or voltametric methods. Measurement made in the field or preservation required.
Nitrogen speciation	Colorimetric, chromatographic, and potentiometric methods available for nitrate, nitrite, and ammonium. Preservation of sample is recommended.
Arsenic speciation	Anion exchange, chromatographic, and hydride generation methods are available for arsenite, arsenate, and several organic forms of arsenic. Preservation is recommended.
Chromium speciation	Colorimetric, exchange, and voltametric methods are available for determination of Cr(VI) and Cr(III).
Selenium speciation	Selenium oxyanions can be determined by ion chromatography or capillary electrophoresis. Preservation of sample is recommended.

and Fe²⁺ species can dominate. Important electron acceptors include oxygen, nitrate, nitrite, and sulfate. Thus, in addition to the contaminant, ground-water analyses should include measurements of these constituents. Equally important is a hydrological assessment of ground water flow rates, which, when combined with the concentration data, allows an estimate of the average influx of oxidants or reductants to the site. In addition, quantification of the accessible redox-buffering capacity of the aquifer solids may be important, since these solids may represent a significant fraction of the capacity of the aquifer. Methods for characterizing the oxidation capacity and reducing capacity of aquifer solids are listed in Table 3.6. These methods represent examples of approaches that have been tested and documented in the literature. For site-specific applications of these methods, some method development or modification may be required to obtain optimal results (USEPA, 2002).

Laboratory tests can be performed in which a known oxidant [e.g., O_{2(aq)} or Cr(VI)] or reductant [e.g., H₂S_(aq)] is reacted with the aquifer solids under controlled environmentally relevant conditions (Fruchter et al., 1996; Istok et al., 1999). The quantity of this reagent consumed by reaction is then expressed in terms of the mass or volume of the aquifer

solids. Rough estimates of maximum reductive capacity present in a soil can also be obtained from digestions using acidic Cr(VI) solutions. Thus, adaptations of Cr(VI) titration methods for organic C in soils (e.g., Nelson and Sommers, 1996) are suitable as they include the contributions of Fe(II) and sulfides to overall reductive capacity. Other laboratory approaches include selective dissolution of reactive fractions (see Section IIIB.2.4.1) with the assignment of a specific mass-based oxidation/reduction capacity to the phase quantified by extraction. For example, reactive Fe²⁺ (i.e., that which is sorbed as well as that present in sulfides carbonates, hydroxides, and green rusts) can be estimated by extraction with 0.5 M HCl followed by complexation with ferrozine (Roden and Zachara, 1996; Amonette et al., 2000). From the oxidizing side, Mn(III,IV) oxides and poorly ordered Fe(III) (hydr)oxides can be determined by extraction with hydroxylamine solutions (Chao, 1972; Chao and Zhou, 1983; Ross, 1985).

The direct reactions and laboratory tests, however, measure only the redox-buffering capacity at a single point in time. Microbial activity, through conversion of organic C, can create and replenish the reductive capacity of a site. Thus, more accurate measurements of reductive capacity

Table 3.6 Methods that may be employed for estimating the oxidation and reduction capacity for solid materials (from USEPA, 2002).

Method	Source	Comments
Cr(II) (oxidation capacity)	(Barcelona and Holm, 1991a) (Barcelona and Holm, 1991b) (Barcelona and Holm, 1992)	Most aggressive but oxygen-free atmosphere recommended; high estimate
Digestion with Ti(III)-EDTA (oxidation capacity)	(Ryan and Gschwend, 1991)	Developed for extraction of Fe oxides; applicability limited to iron oxide dominated sediments
Titration/digestion with dithionite solution (oxidation capacity)	(Loeppert and Inskeep, 1996) (Williams et al., 2000)	Valid for only specific remedial technology; targets Fe oxides
Chemical Oxygen Demand by digestion with acid dichromate (reduction capacity)	(USEPA, 1979) (Barcelona and Holm, 1991a) (Barcelona and Holm, 1991b) (Barcelona and Holm, 1992)	Precipitate coatings if pH not buffered; high estimate
Digestion in hydrogen peroxide solution (reduction capacity)	(Nelson and Sommers, 1996)	Developed for quantifying organic matter content
Dissolved oxygen consumption in air-saturated water (reduction capacity)	(Williams et al., 2000)	Dynamic column test with mathematical simulation; test design must minimize gas diffusion from external sources; time-consuming, but realistic

may necessitate consideration of inputs such as dissolved organic C, as well as terminal electron acceptors such as oxygen, nitrate, and sulfate, in order to assess ability of the microbial community to maintain or degrade the redox capacity of a site. For this analysis, it may be necessary to evaluate microbial response to dissolved constituent inputs through sampling of aquifer solids for the purpose of conducting microcosm studies to examine microbial activity and/or contaminant attenuation. Recommendations for the design and implementation of microcosm studies are provided in USEPA (1998). Evaluation of microcosm response to variations in electron donor/acceptor concentrations in solution, relative to contaminant attenuation, provides means for directly assessing the limits in these reactant concentrations under which attenuation remains viable. For situations in which contaminant degradation is the primary attenuation process, microcosm measurements will likely include determination of trends in contaminant loss as well as the increase of degradation products. For situations in which contaminant immobilization dominates, it is recommended that microcosm characterization include determination of the quantity and solid phase speciation of contaminant sorption. The degree to which microcosm studies replicate subsurface conditions within the plume may be assessed through comparison of similarities (or lack thereof) between measured aqueous and solid phase chemical parameters based on measurement of aquifer microcosm properties (e.g., water chemistry, mineralogy).

An additional line of evidence to support capacity assessments includes development of a reaction or reactive transport model that incorporates quantitative description of the processes that control contaminant attenuation. Requirements for model construction and parameter inputs have previously been specified in Section ID. The utility of this type of analysis is the ability to quickly assess a range of ground-water conditions that may influence the efficiency of modeled attenuation reactions. However, as previously noted, the degree of uncertainty in model predictions will be constrained by the accuracy of parameter inputs to represent aquifer conditions within the plume. Thus, verification of model performance is warranted to demonstrate the ability of the model to reproduce measured ground-water conditions prior conducted model tests of aquifer capacity to support attenuation.

IIIC.3 Stability

If a redox-mediated attenuation mechanism has been identified and a reasonable estimate of the capacity of the aquifer to attenuate the contaminant has been made, evaluation of the stability of immobilized contaminants is needed to assess the potential for contaminant remobilization due to anticipated changes in ground-water chemistry. This component of the site characterization effort may include direct measurements of contaminant stability via laboratory- or field-based evaluations, which could be supplemented with implementation of reaction or reactive-transport models that explicitly consider the solid-phase speciation of the contaminant. The ultimate goal of this effort is to gauge the response of the aquifer, from the perspective of contami-

nant remobilization, to changes in aquifer redox status that may be driven by future increases in the influx of dissolved components such as oxygen or the cessation of microbial processes that accompany decreased influx of degradable organic contaminants.

Contaminant stability may be estimated through laboratory tests constructed using aquifer solids collected from within the zone of contaminant attenuation. Controlled tests could be then be devised that evaluate contaminant response to changes in specific ground-water parameters that may result in release of the contaminant from aquifer solids. For sites in which the ground-water chemistry differs significantly within the plume compared to up gradient or ambient conditions, this may entail exposure of the aquifer solids to ambient ground-water samples. Alternative approaches may include systematic variation of one or more parameters identified as being critical to the stability of the form in which the contaminant is immobilized. For example, this may involve systematic variation in ground-water sample pH over a range that captures current conditions as well as anticipated conditions that may be reflected by the pH measured in background wells installed within the aquifer. Other parameters that might be assessed include those that reflect conditions that might develop as a result of potential land-use changes, including influxes of dissolved constituents that might compete for adsorption sites and/or may form soluble complexes with the contaminant. An alternative approach to assessing the stability of an immobilized contaminant may include the implementation of in-situ studies using single-well push-pull tests (Istok et al., 1997; Haggerty et al., 1998; Senko et al., 2002). These tests can similarly be devised to evaluate contaminant response to changes in ground-water chemistry through manipulation of specific parameters via mixing of synthetic solutions with ground water retrieved from the well and subsequently re-injected into the aquifer. The re-injected water is then allowed to react with the aquifer solids for short periods of time (days to weeks), and then several pore volumes are withdrawn and analyzed to assess the fate of the contaminant and/or analyze potential by-products that result during a re-mobilization reaction. Comparison of reagent concentrations with those of a non-reactive tracer injected with the reagent can be use to evaluate the degree of mixing between water sources with the reaction zone and to assess the overall rate of reaction.

As noted previously, modeling studies may provide a supplementary line of evidence to assess the sensitivity of the immobilized contaminant to changes in ground-water chemistry. This type of analysis provides an indirect means to gauge contaminant response, as well as a means to assess the impact of other ground-water characteristics that may not be practically assessed via direct measurements. However, as previously noted, the degree of uncertainty in model predictions will be constrained by the accuracy of reaction expressions and parameter inputs to represent aquifer conditions within the plume. Ultimately, these tests may require more explicit analysis of the microbial community that supports existing conditions or mediates future changes to redox conditions within the boundary of the

plume. Approaches to identify and quantify active microbial communities within the subsurface are discussed below.

IIIC.4 Microbial Community Characterization

Microbiological evidence to support the natural attenuation of inorganic contaminants as a remedial alternative in ground water involves the characterization of microbial population size, diversity, composition, physiological and genetic/phylogenetic traits. This section addresses techniques used for the characterization of subsurface microbial communities. In addition, some microbiological sampling practices for the assessment of ground water are discussed and emerging methodologies are identified.

IIIC.4.1 Standard and Emerging Techniques

Analyses focused on the composition and diversity of bacterial community structures cannot rely on traditional microbiological procedures alone. This is especially critical in subsurface ecological systems because the vast majority of the microbial communities that reside in that environment have not been cultivated using culture-dependent methods (Amann et al., 1995). Although the importance of emerging molecular approaches in subsurface microbiology will be stressed later in this section, a successful program will likely include a combination of culture-independent methods as well as traditional cultivation strategies. Often, molecular tools are applied to pure culture isolates harvested from defined media. In other words, traditional selective and enrichment techniques are used to develop specific microbial communities to be further characterized with molecular monitoring (i.e., genes coding for 16S rRNAs [16S rDNA] to identify potential gene expressions). Since standard microbiological techniques are readily available in most environmental laboratories, only a brief discussion of them is provided here (see also Table 3.7).

- Most probable-number (MPN) technique is a standard methodology used to estimate the number of specific physiological types of bacteria. Usually, a modified basal medium is amended with a carbon substrate and electron acceptors for total heterotrophic aerobes or anaerobes, denitrifying, iron-reducing, sulfate-reducing, and methanogenic bacteria (Fedorak et al., 1987; Lovley, 1991; Mahne and Tiedje, 1995; Chapelle et al., 2002; Tanner, 1989). A three-tube dilution series is often used to provide a 10-fold dilution. The same regiment is applied to semi-solid media to provide plate counts.
- Acridine orange direct count (AODC) is the most versatile technique for yielding a count of the total intact cells without differentiation for viability (Ghiorse and Balkwill, 1983). Differential staining for live vs. dead can be used via the Bac-light™ method (Loyd and Anthony, 1995).
- Phospholipid ester-linked fatty acids (PLFA) is a popular assay used to identify “biomarkers” to provide a quantitative insight into three important attributes of microbial communities including viable biomass, community structure, and metabolic activity (Lehman et al.,

1995). An estimation of non-viable populations can be accompanied through the measurement of diglyceride fatty acids (DGFA). Both assays are independent of the bias inherent in classical culturing techniques providing a more accurate estimation of in-situ microbial populations. The lipid biomarker analysis is, however, incapable of identifying every microbial species in an environmental sample because many species contain over-lapping PFLA.

- Community-level physiological profile (CLPP) can be carried out using Biolog-GN plates (Biolog, Inc., Hayward, CA). This “phenotypic fingerprinting” assay is useful for screening bacterial isolates and consortia to establish correlation between their activity and composition.
- rRNAa can be used for the determination of microbial biomass (Loyd and Anthony, 1995).

Table 3.7 Standard and emerging techniques for microbial community characterization.

Method	Type of Information
Most probable-number (MPN)	Enumeration, Cultural
Acridine orange direct counts (AODC)	Enumeration, Morphological Cultural
Phospholipid ester-linked fatty acids (PLFA)	Enumeration, Biochemical
Community-level physiological profile (CLPP)	Physiological

Microcosms are routinely prepared using subsurface cores and ground-water samples for the characterization of microbial communities. Recently, there has been an increased interest in the use microcosms to perform molecular community fingerprinting such as denaturing gradient gel electrophoresis due to the generation of a sufficient cell mass.

IIIC.4.2 Molecular Characterization

Within the last decade, a variety of culture-independent genetic analyses have been used to complement traditional culture-dependent methods (enrichment and isolation). Many of these molecular biological methods rely on 16S rDNA sequences, including in-situ hybridization (Amann et al., 1990; Amann et al., 1995), direct amplification of 16S rDNA, and additional analysis using community “DNA fingerprinting” such as temperature gradient gel electrophoresis (TGGE) (Felske et al., 1998), denaturing gradient gel electrophoresis (DGGE) (Muyzer et al. 1993), restriction fragment length polymorphism (RFLP) (Martinez-Murcis et al., 1995), single-strand conformation polymorphism (SSCP) (Lee et al., 1996), terminal RFLP (Clement et al., 1998), or 16S rDNA cloning-sequencing (Wise et al., 1997). To date, most of the results obtained by using molecular

techniques have been provided by cloning-sequencing of 16S rDNA fragments. Although 16S rDNA cloning-sequencing is successful on the reconnaissance of microbial diversity by detecting infrequent sequences from various habitats, thereby avoiding limitations of traditional cultivation techniques, it is time-consuming and problematic for multiple sample analysis. Since the cloning approach cannot provide an immediate overview of the community structure, many environmental laboratories apply DGGE to detect population shifts. DGGE can be used for simultaneous analysis of multiple samples obtained at various time intervals to detect microbial community changes; an advantageous feature in studying microbial ecology and MNA.

These methods characterize differing aspects of the subsurface microbial community, which may be used alone or in combination to further delineate the impact of microbial processes on ground-water chemistry. DGGE provides a simple approach to obtaining profiles of microbial communities and identifying temporal and spatial variations which occur in response to various environmental conditions (Muyzer et al., 1993). It is also possible to infer the phylogeny of community members by DNA sequence analysis of re-amplified fragments, after they are excised from the gel, where bands corresponding to each microorganism can be separated through DGGE. Fluorescent in-situ hybridization (FISH) provides a powerful tool for directly studying organisms within the environment by providing information on cell morphology, phylogenetic affiliation and the ability to quantify organisms (Amann et al., 1990; Amann et al., 1995). During the last few years numerous efforts have been made to increase the sensitivity of FISH, including multi-labeled polynucleotide probes (Pernthaler et al., 2002). The RFLP approach involves electrophoretic analysis where DNA is detected with probes after Southern blotting. RFLP is applied broadly since it has a good predictive power and can rapidly identify phylogenetic relatedness of clusters of very closely related or even identical strains. It can screen large numbers of isolates to identify a much smaller subset of representative types to be resolved by 16S rRNA sequencing. Although RFLP generates a complex set of rDNA bands that can be used to group closely related strains, it does not provide the distance between strains that are not closely related, as does rRNA sequencing. In contrast, the T-RFLP approach uses restriction enzymes, coupled with PCR, in which only fragments containing a fluorescent tag are detected. The use of T-RFLP is advantageous as a rapid screening tool and does not require culturing or a genetic database.

IIIC.4.3 Sampling Considerations

Hydrogeologic conditions are of overriding significance in designing and conducting subsurface microbiological sampling programs because the selection of equipment and the location of sampling points are necessarily subject to site-specific conditions. With regard to the type of sample (core or water), core samples provide more information in defining the horizontal and vertical distribution of microbes even though they are intrinsically disruptive and prohibit

repeated sampling at the same location. Ground-water samples, on the other hand, can be obtained from the same well repeatedly but may not quantitatively or qualitatively reflect conditions in the aquifer. Since there are uncertainties that mandate caution in the extrapolation of information obtained from either type of sample, a thorough characterization may require both water and core samples.

In studies addressing the origin and nature of subsurface microbes, an important consideration is the extent organisms cultured or manipulated in the laboratory represent the intrinsic microbial community. Therefore, microbiologists are challenged when collecting not only representative but also microbially uncontaminated samples. To minimize contamination, after a core is obtained using strict aseptic methods, care should be taken not to disturb or contaminate the sample. Processing should be performed as quickly as possible under anaerobic and aseptic conditions while in the field. Surface layers of the core should be scraped away using a sterile sampling device and discarded so that only the center of the core is packaged in doubled sterile sample bags. The portion used for DNA/PLFA analyses must be rapidly frozen with liquid nitrogen and stored at -70°C . Another portion should be flushed with inert gases (N_2 or Ar), sealed in canning jars and placed inside cans containing oxygen-scavenging catalyst packets (Gas Pak; BBL Inc., Franklin Lakes, N.J.), and stored at 4°C for microbial counts and cultural techniques for analysis within 24 hours. Frozen (-70°C) genomic DNA can be extracted from core sample using an UltraClean soil DNA kit (MoBio, Solana, CA).

Ground-water samples will be unfiltered for microbial counts and cultural techniques and filtered for DNA/PLFA analysis. Community analysis involving "DNA fingerprinting" requires ultrafiltration of ground water (50 to 100 L) using inorganic (Anodisc™, Whatman) filters (0.2 μm pore size). The filter is placed in sterile bag and rapidly freeze dried with liquid nitrogen. Since PCR bias can be introduced, particularly during cell lysis and PCR amplification, a physical method such as bead mill homogenization should be used to effectively lyse all cell types, including those that are most recalcitrant to physical and enzymatic treatments (More et al., 1994).

IIIC.5 Implications for Natural Attenuation Assessment

Ultimately, the extent and degree of site characterization to define the redox status of the aquifer will represent a balance between technical information needs and the cost associated with the different proposed data collection or evaluation schemes. The primary objective of site characterization is to identify the mechanism leading to contaminant attenuation at a given site. Emphasis of this characterization effort should be given to direct measurements of ground water conditions and solid phase characteristics of the aquifer that result from these conditions. Measurements and/or tests conducted with subsurface samples retrieved within the zones where attenuation occurs will provide the most direct means to evaluate on-going reaction processes. This knowledge will guide approaches

to assess the capacity of the aquifer to sustain contaminant attenuation within the plume and to evaluate the long-term stability of immobilized contaminants. Evaluations conducted on subsurface samples also have the benefit of implicitly incorporating characteristics/factors of ground water and aquifer solids that may be difficult to adequately parameterize within analytical models.

IIID. References

- Allen, H.E., G. Fu, and B. Deng. Analysis of acid-volatile sulfide (AVS) and simultaneously extracted metals (SEM) for the estimation of potential toxicity in aquatic sediments. *Environmental Toxicology and Chemistry* 12: 1441-1453 (1993).
- Amann, R.I., L. Krumholz, and D.A. Stahl. Fluorescent-oligonucleotide probing of whole cells for determinative, phylogenetic, and environmental studies in microbiology. *Journal of Bacteriology* 172: 762-770 (1990).
- Amann, R.I., W. Ludwig, and K.H. Schleifer. Phylogenetic identification and in situ detection of individual microbial cells without cultivation. *Microbiology Review* 59: 143-169 (1995).
- Amonette, J.A. and R.W. Sanders. Nondestructive techniques for bulk elemental analysis. In *Quantitative Methods in Soil Mineralogy*. J.E. Amonette and L.W. Zelazy (Eds.), Soil Science Society of America, Madison, WI (1994).
- Amonette, J.A. Methods for determination of mineralogy and environmental availability. In *Soil Mineralogy with Environmental Applications*. J.B. Dixon and D.G. Schulze (Eds.), Soil Science Society of America, Madison, WI (2002).
- Amonette, J.E. and D. Rai. Identification of noncrystalline (Fe,Cr)(OH)₃ by infrared spectroscopy. *Clays and Clay Minerals* 38: 129-136 (1990).
- Amonette, J.E. Iron redox chemistry of clays and oxides: environmental applications. In *Electrochemical Properties of Clays*, CMS Workshop Lectures Volume 10 A. Fitch (Ed.), The Clay Minerals Society, Aurora, CO, pp. 89-146 (2004).
- Amonette, J.E., G.R. Holdren, K.M. Krupka, and C.W. Lindenmeier. Assessing the environmental availability of uranium in soils and sediments. NUREG/CR-6232, PNL-9750. U.S. Nuclear Regulatory Commission, Washington DC (1994).
- Amonette, J.E., D.J. Workman, D.W. Kennedy, J.S. Fruchter, and Y.A. Gorby. Dechlorination of carbon tetrachloride by Fe(II) associated with goethite. *Environmental Science and Technology* 34: 4606-4613 (2000).
- Barcelona, M.J. and T.R. Holm. Oxidation-reduction capacities of aquifer solids. *Environmental Scientific Technology* 25: 1565-1572 (1991a).
- Barcelona, M.J. and T.R. Holm. Oxidation-reduction capacities of aquifer solids. *Environmental Science and Technology* 25: 2540 (1991b).
- Barcelona, M.J. and T.R. Holm. Oxidation-reduction capacities of aquifer solids. *Environmental Science and Technology* 26: 2538-2539 (1992).
- Barrow, N.J. and T.C. Shaw. Effects of soil:solution ratio and vigour of shaking on the rate of phosphate adsorption by soil. *Journal of Soil Science* 30: 67-76 (1979).
- Belzile, N., P. Lecomte, and A. Tessier. Testing readsorption of trace elements during partial chemical extractions of bottom sediments. *Environmental Science and Technology* 23: 1015-1020 (1989).
- Bethke, C.M. and P.V. Brady. How the K_d approach undermines ground water cleanup. *Ground Water* 38: 435-443 (2000).
- Bish, D.L. Quantitative X-ray diffraction analysis of soils. In *Quantitative Methods in Soil Mineralogy*. J.E. Amonette and L.W. Zelazy (Eds.), Soil Science Society of America, Madison, WI (1994).
- Brady, P.V., M.V. Brady, and D.J. Borns. *Natural Attenuation: CERCLA, RBCA's, and the Future of Environmental Remediation*. Lewis Publishers, Boca Raton, FL (1997).
- Buscheck, T.E., N. Nijhawan, and K. O'Reilly. Mass flux estimates to assist remediation decision-making. In *2003 Proceedings of the Seventh International In Situ and On-Site Bioremediation Symposium (Orlando, FL; June 2003)*. V.S. Magar, and M.E. Kelley (Eds.), Batelle Press, Columbus, OH (2004).
- Busenberg, E. and L.N. Plummer. Thermodynamics of magnesian calcite solid-solutions at 25°C and 1 atm total pressure. *Geochimica et Cosmochimica Acta* 53: 1189-1208 (1989).
- Butler, J.J. *Design, Performance, and Analysis of Slug Tests*. Lewis Publishers, Boca Raton, FL (1998).
- Canfield, D.E. Reactive iron in marine sediments. *Geochimica et Cosmochimica Acta* 53: 619-632 (1989).
- Chao, T.T. and L. Zhou. Extraction techniques for selective dissolution of amorphous iron oxides from soils and sediments. *Soil Science Society of America Journal* 47: 225-232 (1983).
- Chao, T.T. Selective dissolution of manganese oxides from soils and sediments with acidified hydroxylamine hydrochloride. *Soil Science Society of America Proceedings* 36: 764-768 (1972).
- Chapelle, F.H., K. O'Neill, P.M. Bradley, B.A. Methe, S.A. Ciufo, L.L. Knobel, and D.R. Lovley. A hydrogen-based subsurface microbial community dominated by methanogens. *Nature* 415: 312-314 (2002).
- Clement, B.G., L.E. Kehl, K.L. DeBord, and C.L. Kitts. Terminal restriction fragment patterns (TRFPs), a rapid, PCR-based method for the comparison of complex bacterial communities. *Journal of Microbiological Methods* 31: 135-142 (1998).
- Conant Jr., B. Delineating and quantifying ground water discharge zones using streambed temperatures. *Ground Water* 42: 243-257 (2004).

- Danielsson, L.G. On the use of filters for distinguishing between dissolved and particulate fractions in natural waters. *Water Research* 16: 179-182 (1982).
- Daskalakis, K.D. and G.R. Helz. Solubility of CdS(greenockite) in sulfidic waters at 25°C. *Environmental Science and Technology* 26: 2642-2648 (1992).
- Davis, J.A. and D.B. Kent. Surface complexation modeling in aqueous geochemistry. In *Mineral-Water Interface Geochemistry*. M.F. Hochella Jr. and A.F. White (Eds.), Mineralogical Society of America, Washington DC (1990).
- Davis, J.A., C.C. Fuller, and A.D. Cook. A model for trace metal sorption processes at the calcite surface: Adsorption of Cd²⁺ and subsequent solid-solution formation. *Geochimica et Cosmochimica Acta* 51: 1477-1490 (1987).
- DeMora, S.J. and R.M. Harrison. The use of physical separation techniques in trace metal speciation studies. *Water Research* 7: 723-733 (1983).
- DeVitre, R.R., F. Bujard, C. Bernard, and J. Buffle. A novel in situ cascade ultrafiltration unit specifically designed for field studies of anoxic waters. *International Journal of Environmental Analytical Chemistry* 31: 145-163 (1987).
- Dragun, J. *The Soil Chemistry of Hazardous Materials*. Hazardous Materials Control Research Institute, Silver Spring, MD (1988).
- Dudley, L.M., J.E. McLean, R.C. Sims, and J.J. Jurniak. Sorption of cadmium and copper from the water soluble fraction of an acid mine waste by two calcareous soils. *Soil Science* 145: 207-214 (1988).
- Dunnivant, F.M., P.M. Jardine, D.L. Taylor, and J.F. McCarthy. Cotransport of cadmium and hexachlorobiphenyl by dissolved organic carbon through columns containing aquifer materials. *Environmental Science and Technology* 26: 360-368 (1992).
- Eary, L.E. The solubility of amorphous As₂S₃ from 25 to 90°C. *Geochimica et Cosmochimica Acta* 56: 2267-2280 (1992).
- Eggleston, C.M., S. Hug, W. Stumm, B. Sulzberger, and M. Afonso. Surface complexation of sulfate by hematite surfaces; FTIR and STM observations. *Geochimica et Cosmochimica Acta* 62: 585-593 (1997).
- Einarson, M.D. and D.M. Mackay. Predicting impacts of groundwater contamination. *Environmental Science and Technology* 35: 66A-73A (2001). (Supporting Information available at http://pubs.acs.org/subscribe/journals/esthag/35/supmat/files/es66A.fil/Einarson_SI.pdf)
- Fedorak, P.M., K.M. Semple, and D.W.S. Westlake. A statistical comparison of two culturing methods from enumerating sulfate-reducing bacteria. *Journal of Microbiological Methods* 7: 19-27 (1987).
- Felske, A., A.D. Akkermans, and W.M. DeVos. Quantification of 16S rRNAs in complex bacterial community by multiple competitive reverse transcription-PCR in temperature gradient gel electrophoresis fingerprints. *Applied and Environmental Microbiology* 64: 4581-4587 (1998).
- Ford, R.G., K.M. Kemner, and P.M. Bertsch. Influence of sorbate-sorbent interactions on the crystallization kinetics of nickel- and lead-ferrihydrite coprecipitates. *Geochimica et Cosmochimica Acta* 63: 39-48 (1999).
- Fruchter, J.S., J.E. Amonette, C.R. Cole, Y.A. Gorby, M.D. Humphrey, J.D. Istok, F.A. Spane, J.E. Szecsody, S.S. Teel, V.R. Vermeuel, M.D. Williams, and S.B. Yabusaki. In situ redox manipulation field injection test report-Hanford 100-H Area. PNNL-11372/UC-602. Pacific Northwest National Laboratory, Richland, WA (1996).
- Galloway, W.E. and J.M. Sharp, Jr. Characterizing aquifer heterogeneity within terrigenous clastic depositional systems. In *SEPM Concepts in Hydrogeology and Environmental Geology No. 1: Hydrogeologic Models of Sedimentary Aquifers*. G.S. Fraser and J.M. Davis (Eds.), Society for Sedimentary Geology, Tulsa, OK (1998).
- Gerth, J. Unit-cell dimensions of pure and trace metal-associated goethites. *Geochimica et Cosmochimica Acta* 55: 455-460 (1990).
- Ghiorse, W.C. and D.L. Balkwill. Enumeration and morphological characterization of bacteria indigenous to subsurface environments. *Developments in Industrial Microbiology* 24: 213-244 (1983).
- Gihwala, D. and M. Peisach. Analysis using prompt gamma-ray emission. In *Elemental Analysis by Particle Accelerators*. Z.B. Alfassi and M. Peisach (Eds.), CRC Press, Boca Raton, FL (1992).
- Gilkes, R.J. Transmission electron microscope analysis of soil materials. In *Quantitative Methods in Soil Mineralogy*. J.E. Amonette and L.W. Zelazy (Eds.), Soil Science Society of America, Madison, WI (1994).
- Glynn, P.D. and E. Reardon. Solid-solution aqueous solution equilibria: Thermodynamic theory and representation. *American Journal of Science* 290: 164-201 (1990).
- Glynn, P.D., E. Reardon, L.N. Plummer, and E. Busenberg. Reaction paths and equilibrium end-points in solid-solution aqueous-solution systems. *Geochimica et Cosmochimica Acta* 54: 267-282 (1990).
- Goldberg, S. Adsorption models incorporated into chemical equilibrium models. In *Chemical Equilibrium and Reaction Models*. R.H. Loeppert, A.P. Schwab, and S. Goldberg (Eds.), Soil Science Society of America, Madison, WI (1995).
- Goldberg, S. Use of surface complexation models in soil chemical systems. *Advances in Agronomy* 47: 233-329 (1992).
- Gruebel, K.A., J.A. Davis, and J.O. Leckie. The feasibility of using sequential extraction techniques for arsenic and selenium in soils and sediments. *Soil Science Society of America Journal* 52: 390-397 (1988).

- Gupta, S.K., M.K. Vollmer, and R. Krebs. The importance of mobile, mobilisable and pseudo total heavy metal fractions in soil for three-level risk assessment and risk management. *Science of the Total Environment* 178: 11-20 (1996).
- Haggerty, R., M.H. Schroth, and J.D. Istok. Simplified method of "push-pull" test data analysis for determining in situ reaction rate coefficients. *Ground Water* 36: 314-324 (1998).
- Helmke, P.A. Neutron activation analysis. In *Methods of Soil Analysis*. A.L. Page et al. (Eds.), Agronomy Monograph 9, American Society of Agronomy and Soil Science Society of America, Madison, WI (1982).
- Hem, J.D. and C.E. Roberson. Form and stability of aluminum hydroxide complexes in dilute solution. U.S. Geological Survey, Water Supply Paper 1967 (1967).
- Huerta-Diaz, M. and J.W. Morse. A quantitative method for determination of trace metals concentrations in sedimentary pyrite. *Marine Chemistry* 29: 119-144 (1990).
- Istok, J.D., J.E. Amonette, C.R. Cole, J.S. Fruchter, M.D. Humphrey, J.E. Szecsody, S.S. Teel, V.R. Vermeul, M.D. Williams, and S.B. Yabusaki. In situ redox manipulation by dithionite injection: Intermediate-scale laboratory experiments. *Ground Water* 37: 884-889 (1999).
- Istok, J.D., M.D. Humphrey, M.H. Schroth, M.R. Hyman, and K.T. O'Reilly. Single-well, "push-pull" test for in situ determination of microbial activities. *Ground Water* 35: 619-631 (1997).
- Jenne, E.A. Adsorption of metals by geomedia: Data analysis, modeling, controlling factors, and related issues. In *Adsorption of Metals by Geomedia*. E.A. Jenne (Ed.), Academic Press, San Diego, pp. 1-73 (1998).
- Johnson, B.D. and P.J. Wangersky. Seawater filtration: Particle flow and impact considerations. *Limnology and Oceanography* 30: 966-971 (1985).
- Johnson, G.K., G.N. Papatheodorou, and C.E. Johnson. The enthalpies of formation and high-temperature thermodynamic functions of As_4S_4 and As_2S_3 . *Journal of Chemical Thermodynamics* 1980: 545-557 (1980).
- Kalkwarf, D.R. Solubility classification of airborne products from uranium ores and tailings piles. NUREG/CR-0530, Pacific Northwest Laboratory, Richland, WA (1979).
- Kalkwarf, D.R. Solubility classification of airborne uranium products collected at the perimeter of the Allied Chemical plant, Metropolis, Illinois. NUREG/CR-1316, Pacific Northwest Laboratory, Richland, WA (1980a).
- Kalkwarf, D.R. Solubility classification of airborne uranium products from LWR-Fuel plants. NUREG/CR-1428, Pacific Northwest Laboratory, Richland, WA (1980b).
- Kennedy, V.C. and G.W. Zellweger. Filter pore-size effects on the analysis of Al, Fe, Mn, and Ti in water. *Water Resources Research* 10: 785-790 (1974).
- Kent, D.B., J.A. Davis, L.C.D. Anderson, and B.A. Rea. Transport of chromium and selenium in a pristine sand and gravel aquifer: Role of adsorption processes. *Water Resources Research* 31: 1041-1050 (1995).
- Keon, N.E., C.H. Swartz, D.J. Brabander, C. Harvey, and H.F. Hemond. Validation of an arsenic sequential extraction method for evaluating mobility in sediments. *Environmental Science and Technology* 35: 2778-2784 (2002).
- Kheboian, C. and C.F. Bauer. Accuracy of selective extraction procedures for metal speciation in model aquatic sediments. *Analytical Chemistry* 59: 1417-1423 (1987).
- Kim, J.I., G. Buckau, F. Baumgartner, H.C. Moon, and D. Lux. Colloid generation and the actinide migration in Gorleben groundwaters. In *Scientific Basis for Nuclear Waste Management*, v. 7. G.L. McVay (Ed.), Elsevier, NY (1984).
- Kohler, M., G.P. Curtis, D.E. Meece, and J.A. Davis. Methods for estimating adsorbed uranium(VI) and distribution coefficients of contaminated sediments. *Environmental Science and Technology* 38: 240-247 (2004).
- Kostka, J.E. and G.W. Luther. Partitioning and speciation of solid phase iron in saltmarsh sediments. *Geochimica et Cosmochimica Acta* 58: 1701-1710 (1994).
- Kruseman, G.P. and N.A. de Ridder. *Analysis and Evaluation of Pumping Test Data*. International Institute for Land Reclamation and Improvement, Wageningen, The Netherlands (1989).
- Laird, D.A. and R.H. Dowdy. Preconcentration techniques in soil mineralogical analyses. In *Quantitative Methods in Soil Mineralogy*. J.E. Amonette and L.W. Zelazny (Eds.), Soil Science Society of America, Madison, WI (1994).
- Langmuir, D. *Aqueous Environmental Geochemistry*. Prentice-Hall, Upper Saddle River, NJ (1997).
- Lee, D.H., Y.-G. Zo, and S.-J. Kim. Nonradioactive method to study genetic profiles of natural bacterial communities by PCR-single strand-conformation polymorphism. *Applied and Environmental Microbiology* 62: 3112-3120 (1996).
- Lehman, R.M., F.S. Colwell, D.B. Ringelberg, and D.C. White. Combined microbial community-level analyses for quality assurance of terrestrial subsurface cores. *Microbiological Methods* 22: 263-281 (1995).
- Lippmann, F. The solubility products of complex minerals, mixed crystals, and three-layer clay minerals. *Neues Jahrbuch für Mineralogie Abhandlung* 130: 243-263 (1977).
- Loeppert, R.H. and W.P. Inskeep. Iron. In *Methods of Soil Analysis: Part 3 - Chemical Methods*. D.L. Sparks (Ed.), Soil Science Society of America, Madison, WI, pp. 639-664 (1996).
- Lovley, D.R. Dissimilatory Fe(III) and Mn(IV) reduction. *Microbiology Review* 55: 259-287 (1991).
- Loyd, D. and J.H. Anthony. Vigour, vitality and viability of microorganisms. *FEMS Microbiology Letters* 133: 1-7 (1995).

- Mahne, I. and J.M. Tiedji. Criteria and methodology for identifying respiratory denitrifiers. *Applied and Environmental Microbiology* 61: 1110-1115 (1995).
- Maiz, I., M.V. Esnaola, and E. Millán. Evaluation of heavy metal availability in contaminated soils by a short sequential extraction procedure. *Science of the Total Environment* 206: 107-115 (1997).
- Martinez-Murcis, A.J., S.G. Acinas, and F. Rodriguez-Valeria. Evaluation of prokaryotic diversity by restrictase digestion of 16S rDNA directly amplified from hypersaline environments. *FEMS Microbial Ecology* 14: 219-232 (1995).
- Mikac, N., S. Niessen, B. Ouddane, and J. Fischer. Effects of acid volatile sulfides on the use of hydrochloric acid for determining solid-phase associations of mercury in sediments. *Environmental Science and Technology* 34: 1871-1876 (2000).
- Moore, J.N., W.H. Ficklin, and C. Johns. Partitioning of arsenic and metals in reducing sulfidic sediments. *Environmental Science and Technology* 22: 432-437 (1988).
- More, M.I., J.B. Herrick, M.C. Silva, W.C. Ghiorse, and E.L. Madsen. Quantitative cell lysis of indigeous microorganisms and rapid extraction of microbial DNA from sediment. *Applied and Environmental Microbiology* 60: 1572-1580 (1994).
- Morgan J.J. and A.T. Stone. Kinetics of chemical processes of importance in lacustrine environments. In *Chemical Processes in Lakes*. W. Stumm (Ed.), John Wiley & Sons, Inc., New York, NY, pp. 389-426 (1985).
- Muyzer, G., E.C. DeWaal, and A.G. Uitterlinden. Profiling of complex microbial populations by denaturing gradient gel electrophoresis analysis of polymerase chain reaction-amplified genes coding for 16S rRNA. *Applied and Environmental Microbiology* 59: 695-700 (1993).
- National Research Council. Natural Attenuation for Groundwater Remediation. Committee on Intrinsic Remediation, Water Science and Technology Board, Board on Radioactive Waste Management. National Academy Press, Washington DC (2000).
- Nelson, D.W. and L.E. Sommers. Total carbon, organic carbon, and organic matter. In *Methods of Soil Analysis. Part 3: Chemical Methods*. D.L. Sparks (Ed.), Soil Science Society of America, Madison, WI (1996).
- Nirel, P.M.V. and F.M.M. Morel. Pitfalls of sequential extractions. *Water Research* 24: 1055-1056 (1990).
- Nordstrom, D.K. and J.L. Munoz. *Geochemical Thermodynamics*. Blackwell Scientific Publications, Palo Alto, CA (1986).
- Nordstrom, D.K., E.A. Jenne, and J.W. Ball. Redox equilibria of iron in acid mine waters. In *American Chemical Society Symposium Series 93, Chapter 3*. E.A. Jenne (Ed.), American Chemical Society, Washington DC (1979).
- Pernthaler, A., C.M. Preston, J. Pernthaler, F.E. DeLong, and R. Amann. A comparison of fluorescently labeled oligonucleotide and polynucleotide probes for the detection of pelagic marine bacteria and archaea. *Applied and Environmental Microbiology* 68: 661-667 (2002).
- Puls, R.W. and J.H. Eychaner. Sampling ground water for inorganics - pumping rate, filtration, and oxidation effects. In *Fourth National Outdoor Action Conference on Aquifer Restoration, Ground Water Monitoring and Geophysical Methods*, National Water Well Association, Dublin, OH, pp. 313-327 (1990).
- Quevauviller, Ph., G. Rauret, J.F. López-Sánchez, R. Rubio, A. Ure, and H. Muntau. Certification of trace metal extractable contents in a sediment reference material (CRM 601) following a three-step sequential extraction procedure. *Science of the Total Environment* 205: 223-234 (1997).
- Rai, D. et al. Chromium reactions in geologic materials. EA-5741, Battelle Pacific Northwest Laboratories for Electric Power Research Institute, Palo Alto, California (1988).
- Rai, D. et al. Chemical attenuation rates, coefficients, and constants in leachate migration, Volume 1: A critical review. EA-3356, Battelle Pacific Northwest Laboratories for Electric Power Research Institute, Palo Alto, California (1984).
- Rai, D., R.J. Serne, and D.A. Moore. Solubility of plutonium compounds and their behavior in soils. *Soil Science Society of America Journal* 44: 490-495 (1980).
- Rapin, F., A. Tessier, P.G.C. Campbell, and R. Carignan. Potential artifacts in the determination of metal partitioning in sediments by a sequential extraction procedure. *Environmental Science and Technology* 20: 836-840 (1986).
- Rauret, G., J.F. López-Sánchez, A. Sahuquillo, R. Rubio, C. Davidson, A. Ure, and Ph. Quevauviller. Improvement of the BCR three step sequential extraction procedure prior to the certification of new sediment and soil reference materials. *Journal of Environmental Monitoring* 1: 57-61 (1999).
- Rendell, P.S., G.E. Batley, and A.J. Cameron. Adsorption as a control of metal concentrations in sediment extracts. *Environmental Science and Technology* 14: 314-318 (1980).
- Roden, E.E. and J.M. Zachara. Microbial reduction of crystalline iron(III) oxides: Influence of oxide surface area and potential for cell growth. *Environmental Science and Technology* 30: 1618-1628 (1996).
- Ross, G.J., C. Wang, and P.A. Schuppli. Hydroxylamine and ammonium oxalate solutions as extractants for iron and aluminum from soils. *Soil Science Society of America Journal* 49: 783-785 (1985).
- Roy, W.R., J.J. Hassett, and R.A. Griffin. Competitive interactions of phosphate and molybdate on arsenate adsorption. *Soil Science* 142: 203-210 (1986).

- Ryan, J.N. and P.M. Gschwend. Extraction of iron oxides from sediments using reductive dissolution by titanium(III). *Clays and Clay Minerals* 39: 509-518 (1991).
- Sass, B.M. and D. Rai. Solubility of amorphous chromium(III)-iron(III) hydroxide solid solutions. *Inorganic Chemistry* 26: 2228-2232 (1987).
- Sawhney, B.L. and D.E. Stilwell. Dissolution and elemental analysis of minerals, soils, and environmental samples. In *Quantitative Methods in Soil Mineralogy*. J.E. Amonette and L.W. Zelazy (Eds.), Soil Science Society of America, Madison, WI (1994).
- Schmelling, S.G. and R.R. Ross. Superfund Ground Water Issue, Contaminant Transport in Fractured Media: Models for Decision Makers, EPA/540/4-89/004. U.S. Environmental Protection Agency, Ada, OK (1989).
- Schultz M.K., S. Biegalski, K.G.W. Inn, L. Yu, W.C. Burnett, J. Thomas, and G. Smith. Optimizing the removal of carbon phases in soils and sediments for sequential extractions by coulometry. *Journal of Environmental Monitoring* 1: 183-190 (1999).
- Schultz M.K., W.C. Burnett, and K.G.W. Inn. Evaluation of a sequential extraction method for determining actinide fractionation in soils and sediments. *Journal of Environmental Radioactivity* 40: 155-174 (1998a).
- Schultz M.K., W.C. Burnett, G. Smith and K.G.W. Inn. Geochemical partitioning of actinides using sequential chemical extractions: Comparison to stable elements. *Journal of Radioanalytical and Nuclear Chemistry* 234: 251-256 (1998b).
- Schultz M.K., W.C. Burnett, K.G.W. Inn, Z. Lin, G. Smith, S. Biegalski, and J.J. Filliben. Identification of radionuclide partitioning in soils and sediments: Determination of best settings for the exchangeable fraction of the NIST standard sequential extraction protocol. *Journal of Applied Radiation and Isotopes* 49: 1289-1293 (1998c).
- Senko, J.M., J.D. Istok, J.M. Sufliata, and L.R. Krumholz. In-situ evidence for uranium immobilization and remobilization. *Environmental Science and Technology* 36: 1491-1496 (2002).
- Sheldon, R.W. and W.H. Sutcliffe. Retention of marine particles by screens and filters. *Limnology and Oceanography* 17: 494-498 (1969).
- Sheppard, J.C., M.J. Campbell, and J.A. Kittrick. Retention of Neptunium, Americium, and Curium by diffusible soil particles. *Environmental Science and Technology* 13: 680-684 (1979).
- Sparks, D. *Environmental Soil Chemistry*. Academic Press, San Diego, CA (1995).
- Sposito, G. *The Surface Chemistry of Soils*. Oxford University Press, New York, NY (1984).
- Stumm, W. and J.J. Morgan. *Aquatic Chemistry*. John Wiley & Sons, New York, NY (1981).
- Tack, F.M., F. Lapauw, and M.G. Verloo. Determination and fractionation of sulphur in a contaminated dredged sediment. *Talanta* 44: 2185-2192 (1997).
- Tanner, R.S. Monitoring sulfate-reducing bacteria: comparison of enumeration media. *Journal of Microbiological Methods* 10: 83-90 (1989).
- Tessier, A. and P.G.C. Campbell. Comment on "Pitfalls of sequential extractions" by P.M.V. Nirel and F.M.M. Morel. *Water Research* 25: 115-117 (1991).
- Tessier, A., P.G.C. Campbell, and M. Bison. Sequential extraction procedure for the speciation of particulate trace metals. *Analytical Chemistry* 51: 844-851 (1979).
- To, T.B., D.K. Nordstrom, K.M. Cunningham, J.W. Ball, and R.B. McCleskey. New method for the direct determination of dissolved Fe(III) concentration in acid mine waters. *Environmental Science and Technology* 33: 807-813 (1999).
- Ure, A.M., Ph. Quevauviller, H. Munteau, and B. Griepink. Speciation of heavy metals in soils and sediments. An account of the improvement and harmonization of extraction techniques undertaken under the auspices of the BCR of the commission of the European Communities. *International Journal of Environmental and Analytical Chemistry* 51: 135-151 (1993).
- USEPA. Chemical Oxygen Demand. *Methods for Chemical Analysis of Water and Wastes*, EPA Method 410.4, EPA/600/4-79-020 (1979).
- USEPA. Seminar Publication: Site Characterization for Subsurface Remediation, EPA/625/4-91/026, U.S. Environmental Protection Agency, Cincinnati, OH (1991).
- USEPA. *Batch-type Procedures for Estimating Soil Adsorption of Chemicals*. Technical Resource Document, EPA/530/SW-87/006-F, Office of Solid Waste and Emergency Response, Washington DC (1992).
- USEPA. *Subsurface Characterization and Monitoring Techniques: A Desk Reference Guide, Volume 1: Solids and Ground Water*, EPA/625/R-93/003a, U.S. Environmental Protection Agency, Washington DC 20460 (1993a).
- USEPA. *Subsurface Characterization and Monitoring Techniques: A Desk Reference Guide, Volume 2: The Vadose Zone, Field Screening and Analytical Methods*, EPA/625/R-93/003, U.S. Environmental Protection Agency, Washington DC (1993b).
- USEPA. *Ground Water Sampling -- A Workshop Summary*, EPA/600/R-94/205, Office of Research and Development, Ada, OK (1994). (<http://www.epa.gov/ada/download/reports/gwwkshop.pdf>)
- USEPA. *Low-Flow (Minimal Drawdown) Ground-Water Sampling Procedures*, EPA/540/S-95/504, Office of Research and Development, Washington DC (1996). (<http://www.epa.gov/ada/download/issue/lwflw2a.pdf>)
- USEPA. *Site Characterization Library, Volume 1*, EPA/600/C-98/001, U.S. Environmental Protection Agency, Las Vegas, NV (1998).
- USEPA. *Technical Protocol for Evaluating Natural Attenuation of Chlorinated Solvents in Ground Water*, EPA/600/R-98/128, Office of Research and Development

- ment, Washington DC (1998). (<http://www.epa.gov/ada/download/reports/protocol.pdf>)
- USEPA. *Understanding Variation in Partition Coefficient, K_d, Values: Volume I - K_d Model, Measurement Methods, and Application of Chemical Reaction Codes*, EPA 402-R-99-004A, Office of Radiation and Indoor Air, Washington DC (1999).
- USEPA. *Proceedings of the Ground-Water/Surface-Water Interactions Workshop*, EPA/542/R-00/007, U.S. Environmental Protection Agency, Washington DC (2000a).
- USEPA. *An SAB Report: Review of an Integrated Approach to Metals Assessment in Surface Waters and Sediments*, EPA-SAB-EPEC-00-005, U.S. Environmental Protection Agency, Washington DC (2000b).
- USEPA. *Workshop on Monitoring Oxidation-reduction Processes for Ground-water Restoration*, EPA/600/R-02/002, Office of Research and Development, Cincinnati, OH (2002). (http://www.epa.gov/ada/download/reports/epa_600_r02_002.pdf)
- USEPA. *Performance Monitoring for Natural Attenuation Remedies in Ground Water*, OSWER 9355.4-25, U.S. Environmental Protection Agency, Washington DC (2003).
- USEPA. *The Impact of Ground Water-Surface Water Interactions on Contaminant Transport with Application to an Arsenic Contaminated Site*, EPA/600/S-05/002, U.S. Environmental Protection Agency, Cincinnati, OH (2005a).
- USEPA. *Field Study of the Fate of Arsenic, Lead, and Zinc at the Ground-Water/Surface-Water Interface*, EPA/600/R-05/161, Office of Research and Development, Cincinnati, OH (2005b). (<http://www.epa.gov/ada/download/reports/600R05161/600R05161.pdf>)
- USEPA. *Mineralogical Preservation of Solid Samples Collected from Anoxic Subsurface Environments*, EPA/600/R-06/112, Office of Research and Development, Cincinnati, OH (2006). (<http://www.epa.gov/ada/download/issue/600R06112.pdf>)
- Wagemann, R. and G.J. Brunskill. The effect of filter pore-size on analytical concentrations of some trace elements in filtrates of natural water. *International Journal of Environmental and Analytical Chemistry* 4: 75-84 (1975).
- Wagman, D.D., W.H. Evans V.B. Parker, R.H. Schumm, I. Halow, S.M. Bailey, K.L. Churney, and R.L. Nuttall. The NBS tables of chemical thermodynamic properties. *Journal of Physical Chemical Reference Data* 11, 1-392 (1982).
- Walker, A.L. The effects of magnetite on oxalate- and dithionite-extractable iron. *Soil Science Society of America Journal* 47: 1022-1026 (1983).
- Wang, F. and A. Tessier. Cadmium complexation with bisulfide. *Environmental Science and Technology* 33: 4270-4277 (1999).
- Webster, J.G. The solubility of As₂S₃ and speciation of As in dilute and sulphide-bearing fluids at 25 and 90°C. *Geochimica et Cosmochimica Acta* 54: 1009-1017 (1990).
- Westall, J. Reactions at the oxide-solution interface: Chemical and electrostatic models. In *Geochemical Processes and Mineral Surfaces*. J.A. Davis and K.F. Hayes (Eds.), American Chemical Society Symposium Series 323, American Chemical Society, Washington DC, pp. 54-78 (1986).
- Wilkin, R.T. and R.G. Ford. Use of hydrochloric acid for determining solid-phase arsenic partitioning in sulfidic sediments. *Environmental Science and Technology* 36: 4921-4927 (2002).
- Wilkin, R.T., D. Wallschläger, and R.G. Ford. Speciation of arsenic in sulfidic waters. *Geochemical Transactions* 4: 1-7 (2003).
- Williams, M.D., V.R. Vermeul, J.E. Szecsody, and J.S. Fruchter. 100-D Area In Situ Redox Treatability Test for Chromate-Contaminated Groundwater. PNNL-13349, Pacific Northwest National Laboratory, Richland, WA (2000).
- Winter, T.C., J.W. Harvey, O.L. Franke, and W.M. Alley. Ground water and surface water: a single resource. U.S. Geological Survey Circular 1139 (1998).
- Winter, T.C. Interaction of ground water and surface water. In *Proceedings of the Ground-Water and Surface-Water Interactions Workshop*, EPA/542/R-00/007, U.S. Environmental Protection Agency, Washington DC (2000).
- Wise, M.G., J.V. McArthur, and L.J. Shimkets. Bacterial diversity of a Carolina bay as determined by 16S rRNA gene analysis: confirmation of novel taxa. *Applied and Environmental Microbiology* 63: 1505-1514 (1997).
- Yanase, N., T. Nightingale, T. Payne, and P. Duerden. Uranium distribution in mineral phases of rock by sequential extraction procedure. *Radiochimica Acta* 52/53: 387-393 (1991).
- Yong, R.N., R. Galvez-Cloutier, and Y. Phadungchewit. Selective sequential extraction analysis of heavy-metal retention in soil. *Canadian Geotechnical Journal* 30: 834-847 (1993).
- Zhabina, N.N. and I.I. Volkov. A method of determination of various sulfur compounds in sea sediments and rocks. In *Environmental Biogeochemistry and Geomicrobiology*, v. 3. W. Krumbein (Ed.), Ann Arbor Science Publishers, Ann Arbor, MI, pp. 735-746 (1978).



United States
Environmental Protection
Agency

National Risk Management
Research Laboratory
Cincinnati, OH 45268

Official Business
Penalty for Private Use
\$300

EPA/600/R-07/139
October 2007

Please make all necessary changes on the below label,
detach or copy, and return to the address in the upper
left-hand corner.

If you do not wish to receive these reports CHECK HERE ;
detach, or copy this cover, and return to the address in the
upper left-hand corner.

PRESORTED STANDARD
POSTAGE & FEES PAID
EPA
PERMIT No. G-35



Recycled/Recyclable

Printed with vegetable-based ink on
paper that contains a minimum of
50% post-consumer fiber content
processed chlorine free

EPA/600/R-03/139 Monitored Natural Attenuation of Inorganic Contaminants in Ground Water - Volume 1

**The following are attachments to the testimony of Scott M. Payne,
PhD, PG and Ian Magruder, M.S..**

ATTACHMENT 12

A Critical Review of Data on Field-Scale Dispersion in Aquifers

LYNN W. GELHAR

Department of Civil Engineering, Massachusetts Institute of Technology, Cambridge

CLAIRE WELTY

Department of Civil and Architectural Engineering, Drexel University, Philadelphia, Pennsylvania

KENNETH R. REHFELDT

Illinois State Water Survey, Champaign

A critical review of dispersivity observations from 59 different field sites was developed by compiling extensive tabulations of information on aquifer type, hydraulic properties, flow configuration, type of monitoring network, tracer, method of data interpretation, overall scale of observation and longitudinal, horizontal transverse and vertical transverse dispersivities from original sources. This information was then used to classify the dispersivity data into three reliability classes. Overall, the data indicate a trend of systematic increase of the longitudinal dispersivity with observation scale but the trend is much less clear when the reliability of the data is considered. The longitudinal dispersivities ranged from 10^{-2} to 10^4 m for scales ranging from 10^{-1} to 10^5 m, but the largest scale for high reliability data was only 250 m. When the data are classified according to porous versus fractured media there does not appear to be any significant difference between these aquifer types. At a given scale, the longitudinal dispersivity values are found to range over 2-3 orders of magnitude and the higher reliability data tend to fall in the lower portion of this range. It is not appropriate to represent the longitudinal dispersivity data by a single universal line. The variations in dispersivity reflect the influence of differing degrees of aquifer heterogeneity at different sites. The data on transverse dispersivities are more limited but clearly indicate that vertical transverse dispersivities are typically an order of magnitude smaller than horizontal transverse dispersivities. Reanalyses of data from several of the field sites show that improved interpretations most often lead to smaller dispersivities. Overall, it is concluded that longitudinal dispersivities in the lower part of the indicated range are more likely to be realistic for field applications.

INTRODUCTION

The phenomenon of dispersive mixing of solutes in aquifers has been the subject of considerable research interest over the past 10 years. Characterizing the dispersivity at a particular field site is essential to any effort in predicting the subsurface movement and spreading of a contaminant plume at that location. Both theoretical and experimental investigations have found that field-scale dispersivities are several orders of magnitude greater than lab-scale values for the same material; it is generally agreed that this difference is a reflection of the influence of natural heterogeneities which produce irregular flow patterns at the field scale. Consequently, laboratory measurements of dispersivity cannot be used to predict field values of dispersivity. Instead field-scale tracer tests are sometimes conducted to estimate dispersivity at a particular site.

Early efforts to document the scale dependence of dispersivity [Lallemand-Barres and Peaudecerf, 1978; Anderson, 1979; Pickens and Grisak, 1981; Beims, 1983; Nereiniaks, 1985] were based on field values of dispersivity reported in the literature and the test scales associated with those values. These studies were useful in that they indeed documented field evidence of the scale effect, but they were lacking in that they did not assess the reliability of the data presented. Because we felt that the data would be more

meaningful if their variable quality was recognized, we assembled the dispersivity data along with related information from the original sources and evaluated the reliability or quality of these data [Gelhar *et al.*, 1985]. The graphical results of that work have been widely used by both practitioners and theoreticians, often without appropriate consideration of the reliability of the data. For example, recent theoretical developments based on fractal concepts [Philip, 1986; Wheatcraft and Tyler, 1988; Neuman, 1990] have relied on information similar to that in the work by Gelhar *et al.* [1985] but those studies disregarded the issue of the reliability of the data. We feel that it is important to update the dispersivity information including results from recent comprehensive field experiments and at the same time focus on the interpretations of the reliability of the data. With these goals in mind, this work develops the following: (1) an outline of the theoretical description of dispersive mixing in porous media; (2) a tabular summary of existing data on values of field-scale dispersivity and related site information reported in the literature; (3) an evaluation of the reliability or quality of these values based on clearly delineated criteria; and (4) discussion and interpretation of the applied and theoretical implications of the data.

THEORETICAL CONCEPTS OF FIELD-SCALE DISPERSIVE MIXING

The mass balance equation governing the transport of an ideal chemically nonreactive conservative solute by a homo-

Copyright 1992 by the American Geophysical Union.

Paper number 92WR00607.
0043-1397/92/92WR-00607\$05.00



geneous fluid (constant density and viscosity) that flows through a rigid saturated porous medium is commonly expressed as [e.g., Bear, 1972; de Marsily, 1986]

$$\frac{\partial c}{\partial t} + v_i \frac{\partial c}{\partial x_i} = \frac{\partial}{\partial x_i} \left(D_{ij} \frac{\partial c}{\partial x_j} \right) \quad i, j = 1, 2, 3 \quad (1)$$

where c is the solute concentration, v_i is the seepage velocity component in the x_i direction, and D_{ij} are the components of the dispersion coefficient tensor. The right-hand side of (1) represents the net dispersive transport which is presumed to be Fickian, i.e., the dispersive mass flux is proportional to the concentration gradient. Some investigators [e.g., Robertson and Barraclough, 1973; Bredehoeft and Pinder, 1973] alternatively define the dispersion coefficient tensor including the porosity n as $D_{ij}^* = nD_{ij}$. When it was clear that D_{ij}^* was used in a study, we converted to the more common form used in (1). The mean flow direction is taken to be x_1 , with $v_1 = v$, $v_2 = v_3 = 0$. Assuming that x_1 , x_2 , and x_3 are principal directions, the dispersivity is simply the ratio of the appropriate component of the dispersive coefficient tensor divided by the magnitude of the seepage velocity, v . To distinguish the field-scale dispersivities from laboratory values, the field-scale values are designated by the uppercase letter A [see Gelhar and Axness, 1983] and, to allow for anisotropy of transverse dispersion, a third dispersivity coefficient is used as follows:

$$D_{11} = A_L v \quad D_{22} = A_T v \quad D_{33} = A_V v \quad (2)$$

where A_L is the longitudinal macrodispersivity (field scale), and A_T is the horizontal transverse macrodispersivity, and A_V is the vertical transverse macrodispersivity.

The classical equation (1) with macrodispersivities (2) is standardly used for applied modeling of field-scale solute transport. The macrodispersivities are considered to be a property of some region of the aquifer. Although the macrodispersivity may be a function of space, in most applications it is assumed constant over a region of the aquifer that encompasses the entire plume both horizontally and vertically. Real solute plumes are observed to be three-dimensional [LeBlanc, 1982; Perlmutter and Lieber, 1970; MacFarlane et al., 1983] and often of limited vertical extent. Although the classical equation is three-dimensional, the two-dimensional form is most commonly applied. Reasons for the use of the two-dimensional form of the equation include lack of three-dimensional data and in the case of numerical models, restrictions on the size of data arrays in the model. Seldom is the two-dimensional form justified on the basis of site conditions or plume observations.

A number of theoretical studies have proposed methods of describing field-scale dispersive mixing. All of the theories view field-scale dispersion as being produced by some kind of small-scale heterogeneity or variability of the aquifer. At present there is considerable debate concerning how to parameterize the variability and model field-scale solute transport. Assuming a perfectly layered aquifer, one group [Molz et al., 1983, 1986] suggests measuring the variability in detail and modeling the transport in each layer with local-scale dispersivities, thus eliminating the need for a field-scale dispersivity. Again assuming a layered aquifer, a second group suggests the use of a scale-dependent or time-dependent field-scale dispersivity [e.g., Pickens and Grisak,

1981; Dieulin, 1980]. A third group [e.g., Gelhar and Axness, 1983; Dagan, 1982; Neuman et al., 1987] has examined more general three-dimensional heterogeneity with stochastic methods and concluded the classical equation with constant field-scale dispersivities is applicable to describe transport over large distances. These stochastic approaches incorporate the effects of practically unknowable small-scale variations in flow by means of macrodispersivities which are used in a deterministic transport model describing the large-scale variations in flow by means of the convection terms. Nonetheless, under what circumstances a field-scale dispersivity can be used to describe field-scale solute transport is still an open question. Until the issue is resolved, the field-scale dispersivity concept can be regarded as a working hypothesis which has a sound theoretical basis and finds wide application.

FIELD DATA ON DISPERSIVITY

Summary of Observations

A literature review was conducted to collect reported values of dispersivity from published analyses of field-scale tracer tests and contaminant transport modeling efforts. The literature sources and pertinent data characterizing each reviewed study are summarized in Table 1 which includes information on 59 different field sites. The information compiled from each study includes site location, description of aquifer material, average aquifer saturated thickness, hydraulic conductivity or transmissivity, effective porosity, mean pore velocity, flow configuration, dimensionality of monitoring network, tracer type and input conditions, length scale of the test or problem, reported values of longitudinal and horizontal and vertical transverse dispersivities, and classification of the reliability of the reported data. Blank entries indicate that the information was not provided in the cited documents. This table summarizes information for purposes of comparison only. More detail regarding a particular study may be found in the original sources.

Aquifer characteristics. As indicated by the second through sixth columns from the left, the study sites represent a wide variety of aquifer conditions and settings. Summarized in these columns is information on aquifer material, saturated thickness, hydraulic conductivity or transmissivity, and velocity. The aquifer thickness for each site is the arithmetic average of the range at that site. Hydraulic conductivity and transmissivity values show the range reported at the site. Reported values for effective porosity vary from 0.5% (for fractured media) to 60% (for porous media). When a value was reported as "porosity," we interpreted this as the effective porosity (interconnected pore space), the value used in analysis of the advection-dispersion equation. Where porosity was reported as "total porosity," we have indicated this in the table. The velocity column indicates the mean pore or seepage velocity at a site. In some cases the values were calculated from information provided on average specific discharge, q , and effective porosity, n , as $v = q/n$. Velocities ranged from 0.0003 to 200 m/d.

Methods of determining dispersivity. The seventh through tenth columns from the left summarize the method used to determine the dispersivity for each site. The seventh, eighth, and ninth columns from the left describe experimental conditions: flow configuration, monitoring, tracer and

input; the tenth column from the left summarizes methods of data interpretation. Dispersivity values were calculated or inferred from one of two types of subsurface solute transport events: large-scale, uncontrolled contamination (naturally occurring or human-induced) events, or controlled tracer tests.

Uncontrolled events are characterized by a source input history that is unknown, transport of contaminants by the ambient flow of groundwater, and solute plumes that often extend over regional scales (hundreds of meters). We describe naturally occurring events as "environmental" tracers, implying chemical constituents associated with uncontrolled natural changes occurring in groundwater before the start of a study. Examples of naturally occurring events include tritium in groundwater from recharge containing atmospheric bomb tritium, seawater intrusion, and mineral dissolution. These events are indicated in the "tracer and input" column by the notation "environmental" along with the type of chemical species reported. Examples of human-induced contamination events include leaks and spills to groundwater from landfills, storage tanks, surface impoundments, and infiltration basins. These types of events are indicated by the notation "contamination" in the tracer and input column. Values of dispersivity for uncontrolled events are commonly determined by fitting a one-, two-, or three-dimensional solute transport model to historical data; i.e., values of dispersivity are altered until model output matches historical solute concentration measurements.

The main features distinguishing controlled tracer tests from uncontrolled ones is that in the former, both the quantity and duration of solute input are known. This is indicated by "step" (continuous input of mass) or "pulse" ("instantaneous" or slug input) in the "tracer and input" column. Controlled tracer tests may be conducted under ambient groundwater flow conditions (also referred to as natural gradient tests), or under conditions where the flow configuration is induced by pumping or recharge. The type of test is reported in the "flow configuration" column. Induced flow configurations include radial, two-well, and forced uniform flow. In radial flow tracer tests, a pulse or step input of tracer is injected at a recharge well and the time distribution of tracer is recorded at an observation well (diverging radial flow test), or the tracer is injected at an observation well and the time distribution is recorded at a distant pumping well (converging radial flow test). In a two-well test, both a recharge well and pumping well are operating; tracer is injected at the recharge well and tracer breakthrough is observed at the pumping well. Recirculation of the water (containing tracer) from the pumping well to the recharge well is often employed. "Forced uniform flow" refers to the flow regime at the Bonnaud site in France, where a uniform flow field was generated between two lines of equally spaced wells, one line recharging and one line pumping, with both screened to the full depth of the aquifer. A discussion of the advantages and disadvantages of different types of tracer tests is presented by *Welty and Gelhar* [1989].

A number of methods have been used to evaluate the data from controlled tracer tests, as indicated by column headed "method of data interpretation." These include fitting of one-, or two- or three-dimensional solute transport analytical solutions, and the method of spatial moments. It should be noted that since the velocity is nonuniform for both radial

and two-well tracer tests, analysis of the data must account for this effect to determine dispersivity properly for such cases. Nonuniform velocity effects have also been observed in ambient flow tracer tests.

The types of tracers used to determine dispersivity at each site are summarized in the "tracer and input" column along with the input conditions. A variety of chemical and microbiological tracers have been employed for controlled tracer tests. Discussions of the suitability of different chemical and microbial species for tracer tests are presented by *Davis et al.* [1980, 1985] and *Betson et al.* [1985]. A primary consideration in designing a controlled tracer test is whether the species is conservative or nonconservative. A conservative tracer is one that moves with the same velocity as the groundwater and does not undergo radioactive decay, adsorption, degradation, chemical reaction (or in the case of microorganisms, death). If any of these effects are present, they must be accounted for in evaluation of the dispersivity. Another factor important in the choice of a tracer is that it is not present in naturally occurring groundwater, or that it is injected at concentrations much higher than natural background levels.

The "monitoring" column indicates whether two- or three-dimensional monitoring was employed at a site. By two-dimensional monitoring we mean depth-averaged (vertically mixed). Three-dimensional monitoring implies point samples with depth. This information is noted because vertical mixing in an observation well influences the concentration of tracer in a water sample. Several studies [*Meyer et al.*, 1981; *Pickens and Grisak*, 1981] have shown that when a tracer is not injected over the full aquifer depth, vertically mixed samples underestimate the tracer concentration and as a result the longitudinal dispersivity is overestimated. This occurs because the tracer occupies only a portion of the vertical thickness. When a sample from the entire thickness is taken, the true tracer concentration is diluted in the well with tracer-free water. If an attempt is made to interpret the diluted ("measured") concentration, the dispersivity will be overestimated. At many sites there was no indication whether point or fully mixed sampling was performed. From examination of the cases where three-dimensional measurements of solute concentrations were made, it is clear that vertical mixing of the tracer as it travels through the aquifer is often very small [*Sudicky et al.*, 1983; *LeBlanc*, 1982; *Freyberg*, 1986; *Garabedian et al.*, 1988, 1991].

Field dispersivities and scale. The "scale of test" column represents the distance traveled from the source for ambient conditions, or the distance between injection and observation wells for the case of an induced flow configuration. The values of dispersivity reported at the indicated scale are given in the second column from the right. Data from the 59 sites yielded 106 values of longitudinal dispersivity, since often multiple investigations or multiple experiments by one investigator were performed at one site. A plot of the longitudinal dispersivity values as a function of scale is presented in Figure 1. The arithmetic average was plotted in cases where a range was reported either for the scale or dispersivity in Table 1. In some cases, values of dispersivity for individual layers were reported as well as an average "aquifer" value. In these cases the latter value was plotted for the given scale. The symbols on Figure 1 indicate whether the dispersivity value is for fractured media (open symbols, 18 values) or porous media (solid symbols, 88

TABLE 1. Summary of

Reference and Site Name	Aquifer Material	Average Aquifer Thickness, m	Hydraulic Conductivity (m/s) or Transmissivity (m ² /s)	Effective Porosity, %	Velocity, m/d	Flow Configuration
<i>Adams and Gelhar</i> [1991], § Columbus, Mississippi	very heterogeneous sand and gravel	8	10 ⁻⁵ to 10 ⁻³ m/s	35	0.03–0.5	ambient
<i>Ahlstrom et al.</i> [1977], Hanford, Washington	glaciofluvial sands and gravels	64	5.7 × 10 ⁻⁴ to 3.0 × 10 ⁻² m/s			ambient
<i>Bentley and Walter</i> [1983], WIPP	fractured dolomite	5.5		18	0.3	two-well recirculating
<i>Bierschenk</i> [1959] and <i>Cole</i> [1972], Hanford, Washington	glaciofluvial sands and gravels	64	1.7 × 10 ⁻¹ m ² /s	10	26 31	ambient
<i>Bredehoeft and Pinder</i> [1973], Brunswick, Georgia	limestone	50	6.5 × 10 ⁻⁷ to 8.6 × 10 ⁻⁷ m ² /s	35		radial converging
<i>Claasen and Cordes</i> [1975], Amargosa, Nevada	fractured dolomite and limestone	15	5 × 10 ⁻² to 11 × 10 ⁻² m ² /s	6–60	0.14–3.4	two-well recirculating
<i>Daniels</i> [1981, 1982], Nevada Test Site	alluvium derived from tuff	500	1.7 × 10 ⁻⁵ m/s		0.04	radial converging
<i>Dieulin</i> [1981], Le Cellier (Lozere, France)	fractured granite	20	3 × 10 ⁻⁴ to 9 × 10 ⁻⁴ m/s	2–8	3	radial converging
<i>Dieulin</i> [1980], Torcy, France	alluvial deposits	6	3 × 10 ⁻⁴ m/s		0.5	ambient
<i>Egboka et al.</i> [1983], Borden	glaciofluvial sand	7–27	10 ⁻⁵ to 10 ⁻⁷ m/s	38	0.01–0.04	ambient
<i>Fenske</i> [1973], Tatum Salt Dome, Mississippi	limestone	53	4.7 × 10 ⁻⁶ m/s	23	1.2	radial diverging
<i>Freyberg</i> [1986], Borden	glaciofluvial sand	9	7.2 × 10 ⁻⁵ m/s	33 (total)	0.09	ambient
<i>Fried and Ungemach</i> [1971], Rhine aquifer	sand, gravel, and cobbles	12			9.6	radial diverging
<i>Fried</i> [1975], Rhine aquifer (salt mines) southern Alsace, France	alluvial; mixture of sand, gravel, and pebbles with clay lenses	125	10 ⁻³ m/s			ambient
<i>Fried</i> [1975], Lyons, France (sanitary landfill)	alluvial, with sand and gravel and slightly stratified clay lenses	20			5.0	ambient
<i>Garabedian et al.</i> [1988] Cape Cod, Massachusetts	medium to coarse sand with some gravel overlying silty sand and till	70	1.3 × 10 ⁻³ m/s	39	0.43	ambient
<i>Gelhar</i> [1982], Hanford, Washington	brecciated basalt interflow zone					two-well without recirculation
<i>Goblet</i> [1982], site B, France	fractured granite	50	10 ⁻⁵ to 10 ⁻⁷ m/s		84	radial converging
<i>Grove</i> [1977], NRTS, Idaho	basaltic lava and sediments	76	1.4 × 10 ⁻¹ to 1.4 × 10 ¹ m ² /s	10		ambient
<i>Grove and Beetem</i> [1971], Eddy County (near Carlsbad), New Mexico	fractured dolomite	12		12	3.5	two-well recirculating
<i>Gupta et al.</i> [1975], Sutter Basin, California	sandstone, shale, sand, and alluvial sediments					ambient
<i>Halevy and Nir</i> [1962] and <i>Lenda and Zuber</i> [1970], Nahal Oren, Israel	dolomite	100		3.4	4.0	radial converging
<i>Harpaz</i> [1965], southern coastal plain, Israel	sandstone with silt and clay layers	90			14	radial diverging
<i>Helweg and Labadie</i> [1977], Bonsall subbasin, California						ambient
<i>Hoehn</i> [1983], lower Glatt Valley, Switzerland	layered gravel and silty sand	25	9.2 × 10 ⁻⁴ to 6.6 × 10 ⁻³ m/s		3.4 1.8 1.2 8.6 4.1 1.7	ambient

Field Observations

Monitoring	Tracer and Input*	Method of Data Interpretation	Scale of Test, m	Dispersivity $A_L/A_T/A_V, \dagger$ m	Classification of Reliability of $A_L/A_T/A_V$ (I, II, III)‡
three-dimensional	Br ⁻ (pulse)	spatial moments	200	7.5	II
two-dimensional	³ H (contamination)	two-dimensional numerical model	20,000	30.5/18.3	III
two-dimensional	PFB, SCN (step)	one-dimensional quasi-uniform flow solution [Grove and Beetem, 1971]	23	5.2	III
two-dimensional	fluorescein (pulse)	one-dimensional uniform flow solution	3,500 4,000	6 460	III III
two-dimensional	Cl ⁻ (contamination)	two-dimensional numerical model	2,000	170/52	III
two-dimensional	³ H (pulse)	one-dimensional quasi-uniform flow solution [Grove and Beetem, 1971]	122	15	III
two-dimensional	³ H (contamination)	radial flow type curve [Sauty, 1980]	91	10-30	III
two-dimensional	Cl ⁻ , I ⁻ (pulse)	radial flow type curve [Sauty, 1980]	5	0.5	II
two-dimensional (resistivity)	Cl ⁻ (pulse)	one-dimensional uniform flow solution	15	3	III
three-dimensional	³ H (environmental)	one-dimensional uniform flow solution	600	30-60	III
	³ H (pulse)	one-dimensional uniform flow solution	91	11.6	III
three-dimensional	Br ⁻ , Cl ⁻ (pulse)	spatial moments	90	0.43/0.039	I
	Cl ⁻ (pulse)	one-dimensional radial flow numerical model	6	11	III
three-dimensional	Cl ⁻ (contamination)	two-dimensional numerical model	800	15/1	III
two-dimensional	EC (contamination)	two-dimensional numerical model	600-1000	12/4	III
three-dimensional	Br ⁻ (pulse)	spatial moments	250	0.96/0.018/ 0.0015	I
two-dimensional	¹³¹ I (pulse)	one-dimensional nonuniform flow solution along streamlines [Gelhar, 1982]	17.1	0.60	I
two-dimensional	RhWt, SrCl (pulse)	one-dimensional uniform flow solution including borehole flushing effects	17	2	III
two-dimensional	Cl ⁻ (contamination)	two-dimensional numerical model	20,000	91/91	III
two-dimensional	³ H (step)	one-dimensional quasi-uniform flow solution [Grove and Beetem, 1971]	55	38.1	III
	Cl ⁻ (environmental)	three-dimensional numerical model	50,000	80-200/ 8-20	III
two-dimensional	⁶⁰ Co (pulse)	one-dimensional uniform flow solution	250	6	II
two-dimensional	Cl ⁻ (step)	one-dimensional radial flow solution	28	0.1-1.0	II
	TDS (contamination)	two-dimensional numerical model	14,000	30.5/9.1	III
two-dimensional	uranine (pulse)	one-dimensional uniform flow solution for layers	4.4 4.4 4.4 10.4 10.4 10.4	0.1 0.01 0.2 0.3 0.04 0.7	III III III III

TABLE 1.

Reference and Site Name	Aquifer Material	Average Aquifer Thickness, m	Hydraulic Conductivity (m/s) or Transmissivity (m ² /s)	Effective Porosity, %	Velocity, m/d	Flow Configuration
<i>Hoehn and Santschi</i> [1987], lower Glatt Valley, Switzerland	layered gravel and silty sand	27.5	8.1×10^{-5} to 6.6×10^{-3} m/s		1.5	ambient
					3.2	
					5.6	ambient
					3.9	
<i>Huyakorn et al.</i> [1986], Mobile, Alabama	layered medium sand	21.6		0.35	3.2	
						two-well without recirculation
<i>Iris</i> [1980], Campuget (Gard), France	alluvial deposits	9	3.6×10^{-3} m ² /s		0.05	radial diverging
<i>Ivanovitch and Smith</i> [1978], Dorset, England	fractured chalk		2.2×10^{-3} m/s (fast pulse)	0.5	57.6	radial converging
	chalk		3.6×10^{-4} m/s (slow pulse)	2.3	9.6	radial converging
<i>Kies</i> [1981], New Mexico State University, Las Cruces	fluvial sands		9.55×10^{-5} m/s	42 (total)		ambient
<i>Klotz et al.</i> [1980], Dormach, Germany	fluvioglacial gravels	14			20	radial converging
<i>Konikow</i> [1976], Rocky Mountain Arsenal	alluvium			30		ambient
<i>Konikow and Bredehoeft</i> [1974], Arkansas River valley (at La Junta, Colorado)	alluvium, inhomogeneous clay, silt, sand and gravel		2.4×10^{-4} to 4.2×10^{-3} m/s	20		ambient
<i>Kreft et al.</i> [1974], Poland	sand	2.5	3.1×10^{-5} to 1.5×10^{-4} m/s; 1.2×10^{-4} m ² /s	24	29	radial converging
<i>Kreft et al.</i> [1974], Zn-Pb deposits, Poland	fractured dolomite	57	2.5×10^{-4} to 4.7×10^{-4} m/s	2.4	7.5	radial converging
	fractured dolomite	48	2.5×10^{-4} to 4.7×10^{-4} m/s	2.4	100	radial converging
<i>Kreft et al.</i> [1974], sulfur deposits, Poland	limestone	7	1.1×10^{-4} m/s	12.3	10	radial converging
	limestone	7	1.1×10^{-4} m/s	12.3	10.8	radial converging
<i>Lau et al.</i> [1957], University of California, Berkeley	sand and gravel with clay lenses	1.5	9×10^{-4} m/s	30	7	radial diverging
<i>Lee et al.</i> [1980], Perch Lake, Ontario, (lake bed)	sand		3.2×10^{-5} m/s		0.14	ambient
<i>Leland and Hillel</i> [1981], Amherst, Massachusetts	fine sand and glacial till	0.75	2.4 to 3×10^{-5} m/s	40	0.3–0.6	ambient
<i>Mercado</i> [1966], Yavne region, Israel	sand and sandstone with some silt and clay	80	2.1×10^{-8} to 2.4×10^{-8} m ² /s	23.3	0.84–3.4	radial diverging/converging
<i>Meyer et al.</i> [1981]; Koeberg Nuclear Power Station, South Africa	sand	20			0.12	ambient
<i>Molinari and Peaudecerf</i> [1977] and <i>Sauty</i> [1977], Bonnaud, France	sand	3	8.3×10^{-4} to 1.1×10^{-3} m ² /s		2.7	forced uniform
					1.0	
					2.4	
					1.0	
					2.0	
<i>Moltyaner and Killey</i> [1988a, b], Twin Lake aquifer (Chalk River)	fluvial sand			40.8 (total)	1.2	ambient
<i>Naymik and Barcelona</i> [1981], Meredosia, Illinois (Morgan County)	unconsolidated sand and gravel	27	2.2×10^{-2} to 4.3×10^{-2} m ² /s			ambient

(continued)

Monitoring	Tracer and Input*	Method of Data Interpretation	Scale of Test, m	Dispersivity $A_L/A_T/A_V, \dagger$ m	Classification of Reliability of $A_L/A_T/A_V$ (I, II, III)‡
two-dimensional	uranine (pulse)	temporal moments	4.4	1.1	II
two-dimensional	^3H (environmental)	temporal moments	10.4 100 110 500	1.2 6.7 10.0 58.0	II III III III
two-dimensional	Br^- (pulse)	two-dimensional numerical model	38.3	4.0	I
three-dimensional	heat (pulse)	two-dimensional radial numerical model	40	3/1.5	II
	^{82}Br (pulse)	one-dimensional uniform flow solution	8	3.1	III
	^{82}Br (pulse)	one-dimensional uniform flow solution	8	1.0	III
two-dimensional	NO_3^- (pulse)	two-dimensional uniform flow solution	25	1.6/0.76	III
two-dimensional	^{82}Br , uranine (pulse)	one-dimensional uniform flow solution	10	5, 1.9	II
	Cl^- (contamination)	two-dimensional numerical model	13,000	30.5	III
two-dimensional	dissolved solids (contamination)	two-dimensional numerical model	18,000	30.5/9.1	III
two-dimensional	^{131}I (pulse)	one-dimensional uniform flow solution	5-6	0.18	II
	^{131}I (pulse)	one-dimensional uniform flow solution	22	44-110	II
	^{131}I (pulse)	one-dimensional uniform flow solution	21.3	2.1	II
	^{58}Co (pulse)	one-dimensional uniform flow solution	27	2.7-27	II
	^{58}Co (pulse)	one-dimensional uniform flow solution	41.5	20.8	II
	Cl^- (step)	one-dimensional radial numerical model	19	2-3	I
three-dimensional	Cl^- (pulse)	one-dimensional uniform flow solution	≤ 6	0.012	II
three-dimensional	Cl^- (pulse)	two-dimensional uniform flow solution	4	0.05-0.07	III
three-dimensional	^{60}Co , Cl^- (step)	one-dimensional radial flow solution	≤ 115 (observation wells)	0.5-1.5 (injection phase)	I
three-dimensional	^{131}I (pulse)	one-dimensional uniform flow solution for layers	2-8	0.01, 0.03, 0.01, 0.05 for layers; 0.42 for depth average	III
two-dimensional	I^-	two-dimensional uniform flow solution	13	0.79	I
	^3H		13	1.27	I
	^{131}I		13	0.72	I
	^{131}I		26	2.23	I
	^{131}I		33.2	1.94/0.11	I
	^{131}I (pulse)		32.5	2.73/0.11	I
three-dimensional	^{131}I (pulse)	two-dimensional uniform flow solution	40	0.06-0.16/ · · / 0.0006-0.002	II
two-dimensional	NH_3 (contamination)	two-dimensional numerical model	16.4	2.13-3.35/ 0.61-0.915	III

TABLE 1.

Reference and Site Name	Aquifer Material	Average Aquifer Thickness, m	Hydraulic Conductivity (m/s) or Transmissivity (m ² /s)	Effective Porosity, %	Velocity, m/d	Flow Configuration
<i>New Zealand Ministry of Works and Development</i> [1977] Heretaunga aquifer, New Zealand: Roys Hill site	gravel with cobbles	100	0.29 m ² /s	22	150–200	ambient
Flaxmere site 2	alluvium (gravels)	120	0.37 m ² /s	22	20–25	ambient
Hastings City rubbish dump	alluvium (gravels)		0.14, 0.35 m ² /s		20	ambient
<i>Oakes and Edworthy</i> [1977], Clipstone, United Kingdom	sandstone	44	2.4 × 10 ⁻⁶ to 1.4 × 10 ⁻⁴ m/s	32–48	5.6, 4.0 9.6	radial diverging radial converging
<i>Papadopulos and Larson</i> [1978], Mobile, Alabama	medium to fine sand interspersed with clay and silt	21	5 × 10 ⁻⁴ m/s (horizontal) and 5.1 × 10 ⁻⁵ m/s (vertical)	25	0.05	radial diverging
<i>Pickens and Grisak</i> [1981], Chalk River	sand	8.5	2 × 10 ⁻⁵ to 2 × 10 ⁻⁴ m/s	38	0.15	two-well recirculating
	sand	8.5	2 × 10 ⁻⁵ to 2 × 10 ⁻⁴ m/s	38	0.15	radial diverging/converging
<i>Pinder</i> [1973], Long Island	glacial outwash	43	7.5 × 10 ⁻⁴ m/s	35	0.43	regional
<i>Rabinowitz and Gross</i> [1972], Roswell Basin, New Mexico	fractured limestone	61	1.1 × 10 ⁻² to 2.9 × 10 ⁻¹ m ² /s	1	11–21	regional
<i>Rajaram and Gelhar</i> [1991], Borden	glaciofluvial sand	9	7.2 × 10 ⁻⁵ m/s	33 (total)	0.09	ambient
<i>Roberts et al.</i> [1981], Palo Alto bay lands	sand, gravel, and silt	2	1.25 × 10 ⁻³ m ² /s (lower aquifer); 5.0 × 10 ⁻⁴ m ² /s (upper aquifer)	25	15.5 12.0 3.5 25.6 7.9	radial diverging
<i>Robertson</i> [1974] and <i>Robertson and Barraclough</i> [1973], NRTS, Idaho	basaltic lava and sediments	76	1.4 × 10 ⁻¹ to 1.4 × 10 ¹ m ² /s	10	1.5–8	regional
<i>Robson</i> [1974, 1978], Barstow, California	alluvial sediments	27	2.1 × 10 ⁻⁴ to 1 × 10 ⁻² m ² /s	40		two-well recirculating
				40	3	regional
<i>Robson</i> [1978], Barstow, California	alluvial sediments	30.5	5 × 10 ⁻⁴ m/s	40		regional
<i>Rousselot et al.</i> [1977], Byles–Saint Vulbas near Lyon, France	clay, sand, and gravel	12	6.5 × 10 ⁻³ to 1.5 × 10 ⁻² m/s	14	18 2.1–18 1.8–5.9 46.7, 16 24	radial converging
<i>Sauty</i> [1977], Corbas, France	sand and gravel	12			125, 100 15.5, 78 6.9	radial converging
<i>Sauty et al.</i> [1978], Bonnaud, France	sand	3	8.3 × 10 ⁻⁴ to 1.1 × 10 ⁻³ m ² /s			radial diverging
<i>Segol and Pinder</i> [1976], Cutler area, Biscayne Bay aquifer, Florida	fractured limestone and calcareous sandstone	30.5	0.45 × 10 ⁻² m/s (horizontal) and 0.09 × 10 ⁻⁴ m/s (vertical)	25	20	ambient
<i>Sudicky et al.</i> [1983], Borden	glaciofluvial sand	7–27	4.8 × 10 ⁻⁵ to 7.6 × 10 ⁻⁵ m/s	38	0.07– 0.25	ambient
<i>Sykes et al.</i> [1982, 1983], Borden	sand		5.8 to 7.2 × 10 ⁻⁵ m/s	35		ambient
<i>Sykes et al.</i> [1983], Mobile, Alabama	sand, silt, and clay	21	5 × 10 ⁻⁴ m/s (horizontal) and 2.5 × 10 ⁻⁵ m/s (vertical)	25	0.05	radial diverging

(continued)

Monitoring	Tracer and Input*	Method of Data Interpretation	Scale of Test, m	Dispersivity $A_L/A_T/A_V, \dagger$ m	Classification of Reliability of $A_L/A_T/A_V$ (I, II, III)‡
three-dimensional	^{131}I , RhWt, ^{82}Br , Cl^- , <i>E. Coli</i> (pulse)	three-dimensional uniform flow solution	54-59	1.4-11.5/ 0.1-3.3/ 0.04-0.10	II
three-dimensional	RhWt, ^{82}Br (pulse)	three-dimensional uniform flow solution	25	0.3-1.5/ · · ·/0.06	II
three-dimensional	Cl^- (contamination)	three-dimensional uniform flow solution	290	41/10/0.07	III
two-dimensional	^{82}Br (pulse)	radial flow numerical model	6 3	0.16, 0.38 0.31	II II
two-dimensional	Cl^- , I^- (pulse)		6 3	0.6 0.6	II II
two-dimensional	heat (step)	two-dimensional numerical model	57.3	1.5	II
three-dimensional	^{51}Cr (step)	one-dimensional quasi-uniform flow solution	8	0.5	III
three-dimensional	^{131}I (step)	one-dimensional radial flow solution	3	0.03	III
three-dimensional	Cr^{+6} (contamination)	two-dimensional numerical model	1,000	21.3/4.2	III
two-dimensional	^3H (environmental)	one-dimensional uniform flow solution	32,000	20-23	III
three-dimensional	Br^- , Cl^- (pulse)	spatial moments	90	0.50/0.05/ 0.0022	I
two-dimensional	Cl^- (step)	one-dimensional uniform flow solution	11 20 40 16 43	5 2 8 4 11	III III III III III
two-dimensional	Cl^- (contamination)	two-dimensional numerical model	20,000	910/1370	III
two-dimensional	Cl^- (step)	one-dimensional quasi-uniform flow solution	6.4	15.2	III
two-dimensional	TDS (contamination)	two-dimensional numerical model	10,000	61/18	III
three-dimensional	TDS (contamination)	two-dimensional numerical model (vertical section)	3,200	61/· · ·/0.2	III
two-dimensional	I^- (pulse)	one-dimensional uniform flow solution for layers	9.3 5.3 10.7 7.1	6.9 0.3, 0.7 0.46, 1.1 0.37	II III III II
two-dimensional	I^- (pulse)	one-dimensional uniform flow solution for layers	25 50 150 13	11, 1.25 25, 6.25 12.5 1.0	III III II II
two-dimensional	heat (step)	one-dimensional radial flow solution	490	6.7/· · ·/0.67	III
three-dimensional	Cl^- (environmental)	two-dimensional numerical model			
three-dimensional	Cl^- (pulse)	three-dimensional uniform flow solution	11 0.75	0.08/0.03 0.01/0.005	II II
three-dimensional	Cl^- (pulse)	two-dimensional numerical model	700	7.6/· · ·/0.31	III
three-dimensional	heat (step)	three-dimensional numerical model	57.3	0.76/· · ·/0.15	II

TABLE 1.

Reference and Site Name	Aquifer Material	Average Aquifer Thickness, m	Hydraulic Conductivity (m/s) or Transmissivity (m ² /s)	Effective Porosity, %	Velocity, m/d	Flow Configuration
Vaccaro and Bolke [1983], Spokane aquifer, Washington and Idaho	glaciofluvial sand and gravel	152	9×10^{-5} m ² /s to 6.5 m ² /s	7–40	0.003–2.8	ambient
Valocchi et al. [1981], Palo Alto bay lands	sand, gravel, and silt	2	1.25×10^{-3} m ² /s (lower aquifer); 5.0×10^{-4} m ² /s (upper aquifer)	25	27	radial diverging
Walter [1983], WIPP	fractured dolomite	7	8.0×10^{-5} m ² /s	0.7 and 11 (along separate paths)	4.7, 2.4	radial converging
Webster et al. [1970], Savannah River Plant, South Carolina	crystalline, fractured schist and gneiss	76	3.6×10^{-7} m/s		1.3 21.4	two-well recirculating
Werner et al. [1983], Hydrothermal Test Site, Aeffigen, Switzerland	gravel	20	6×10^{-3} m/s	17	9.1	ambient
Wiebenga et al. [1967] and Lenda and Zuber [1970], Burdekin Delta, Australia	sand and gravel	6.1	5.5×10^{-3} m/s	32	29	radial converging
Wilson [1971] and Robson [1974], Tucson, Arizona	unconsolidated gravel, sand, and silt		5.75×10^{-3} m ² /s	38		two-well without recirculation radial diverging
Wood [1981], Aquia Formation, southern Maryland	sand	1,000	2.9×10^{-4} to 8.7×10^{-4} m ² /s	35	0.0003–0.0007	ambient
Wood and Ehrlich [1978] and Bassett et al. [1980], Lubbock, Texas	sand and gravel	17	3.2×10^{-3} to 4.4×10^{-3} m ² /s		78	radial converging

*TDS denotes total dissolved solids; EC, electrical conductivity; PFB, pentafluorobenzoate; MTFMB, metatetrafluoromethylbenzoate; MFB, metafluorobenzoate; Para-FB, parafluorobenzoate; RhWT, rhodamine-WT dye; and SCN, thiocyanate.

† A_L denotes longitudinal dispersivity; A_T , horizontal transverse dispersivity; and A_V , vertical transverse dispersivity. Reported values for A_L , A_T , and A_V are separated by slashes. Absence of slashes means that values were reported for A_L only. A comma or a dash separating entries means that multiple values or a range of values, respectively, were reported for a particular dispersivity component.

‡For description of classification criteria, see text.

§E. E. Adams and L. W. Gelhar, Field study of dispersion in a heterogeneous aquifer: Spatial moments analysis (submitted to *Water Resources Research*, 1991).

||Porosity-corrected dispersivity value.

values). The type of event evaluated is indicated by a circle (tracer test, 83 values), triangle (contamination event, 15 values), or square (environmental tracer, eight values). The total numbers of values of dispersivity for each type of medium and test are shown in Table 2. Any reported values of horizontal transverse dispersivity or vertical transverse dispersivity are also listed in the dispersivity column of Table 1. For the cases examined, 24 values of horizontal transverse dispersivity and nine values of vertical transverse dispersivity were reported. In nearly all cases, the horizontal values were found to be 1–2 orders of magnitude less than the longitudinal values, and the vertical values smaller by another order of magnitude.

Evaluation of Dispersivity Data

From Figure 1, it appears that longitudinal dispersivity increases with scale. Field observations of dispersivity ranged from 0.01 m to approximately 5500 m at scales of 0.75 m to 100 km. The longitudinal dispersivity for the two types of aquifer material (porous versus fractured media) tends to

scatter over a similar range, although at a smaller scale fractured media seem to show higher values. At each scale there is at least a two-order-of-magnitude range in dispersivity. Because we noted a number of problems with data and their interpretation as we gathered them for Table 1, we would regard any conclusions about Figure 1 with skepticism until further qualifying statements can be made about the data points. Typical problems that we found with the studies reported in Table 1 include the following: data analysis not matched to flow configuration; mass input history unknown; nonconservative effects of tracer not accounted for; dimensionality of the monitoring not matched to the dimensionality of the analysis; and assumption of distinct geologic layers in analysis when their actual presence was not documented. Based on these problems, we decided to rate the data as high (I), medium (II), or low (III) reliability according to the criteria set forth below. Table 3 lists the criteria used to designate either high- or low-reliability data. No specific criteria were defined for the intermediate classification; it encompasses the dispersivity

(continued)

Monitoring	Tracer and Input*	Method of Data Interpretation	Scale of Test, m	Dispersivity $A_L/A_T/A_V, \dagger$ m	Classification of Reliability of $A_L/A_T/A_V$ (I, II, III)‡
	Cl^- (contamination)	two-dimensional numerical model	43,400	91.4/27.4	III
	Cl^- (step)	two-dimensional numerical model	16	1.0/0.1	I
two-dimensional	MTFMB, PFB, MFB, para-FB (pulse)	one-dimensional uniform flow solution	30	10–15	III
two-dimensional	^{85}Sr ^{85}Br (pulse)	one-dimensional quasi-uniform flow solution	538	134	III
three-dimensional	heat (step)	one-dimensional numerical model	700 37 105 200	130–234 131 208 234	III III III III
	^{131}I , ^3H (pulse)	one-dimensional uniform flow solution	18.3	0.26	II
three-dimensional	Cl^- (step)	one-dimensional quasi-uniform flow solution	79.2	15.2	III
two-dimensional	Cl^- (step)	one-dimensional radial flow solution	4.6	0.55	III
	Na^+ (environmental)	one-dimensional uniform flow solution	10^5	5,600–40,000	III
two-dimensional	I^- (pulse)	one-dimensional radial flow solution	1.52	0.015	II

values that do not fall into the high or low groups. These classifications do not place strict numerical confidence limits on reported dispersivities, but rather are intended to provide an order-of-magnitude estimate of the confidence we place on a given value. In general, we consider high-reliability dispersivity values to be accurate within a factor of 2. Low-reliability values are considered to be no more accurate than within 1 or 2 orders of magnitude. Intermediate reliability falls somewhere between the extremes. We wish to make a distinction between the judgment of the reliability of the reported dispersivity and the worth of a study. Often, the purpose of a study was for something other than the determination of dispersivity. Our classification of dispersivity is not intended as a judgment on the quality of a study as a whole, but rather to provide us with some criteria with which to screen the large number of data values obtained. By then examining the more reliable data, conclusions which evolve from the data will be more soundly based and alternative interpretations may become apparent.

High-reliability dispersivity data. For a reported dispersivity value to be classified as high reliability, each of the following criteria must have been met.

1. The tracer test was either ambient flow with known input, diverging radial flow, or a two-well pulse test (without recirculation). These three test configurations produce breakthrough curves which are sensitive to the dispersion coefficient and appear to work well in field applications [Welty and Gelhar, 1989]. The radial converging flow test is generally considered less satisfactory than the diverging test because breakthrough curves at the pumping well for the converging test frequently exhibit tailing, which complicates the interpretation of these tests. Some researchers attribute this behavior to two or more discrete geologic layers and try to reproduce the observed breakthrough curve by superposition of breakthrough curves in each layer, where the properties of each layer may differ [e.g., Ivanovitch and Smith, 1978; Sauty, 1977]. The problem with this interpretation is that there are typically numerous heterogeneities on a small scale that cannot be attributed solely to identifiable layers. One possible explanation of the tailing in radial convergent tests is sometimes termed "borehole flushing," where the tail of the breakthrough curve is attributed to the slow flushing of the input slug of tracer out of the injection borehole by the ambient groundwater flow. Goblet [1982] measured the slow flushing of tracer out of the

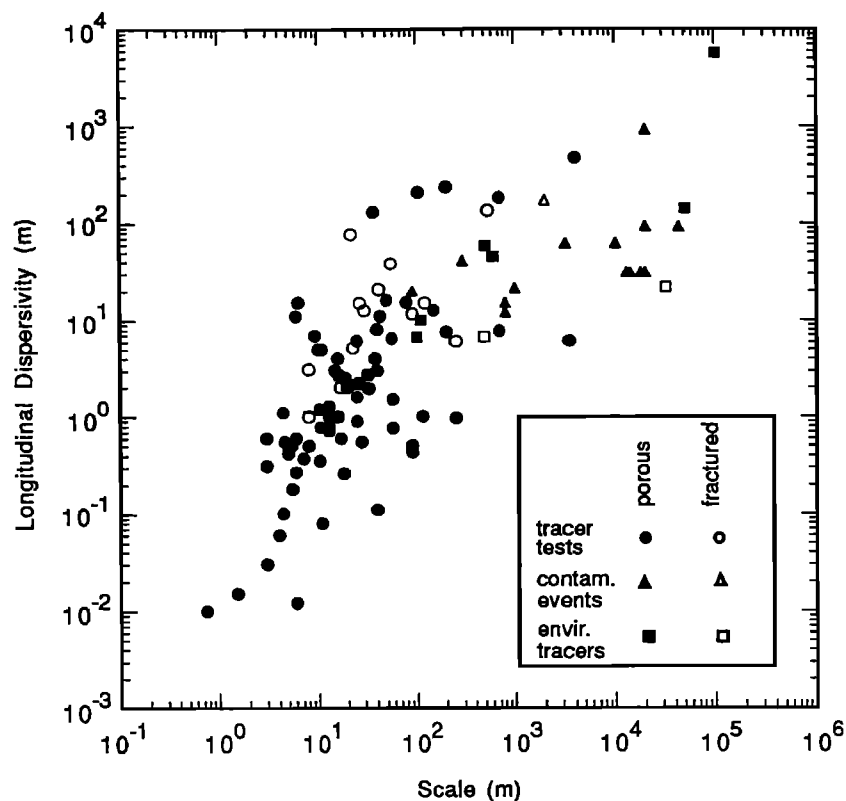


Fig. 1. Longitudinal dispersivity versus scale of observation identified by type of observation and type of aquifer. The data are from 59 field sites characterized by widely differing geologic materials.

borehole and modeled the effect as an exponentially decreasing input. His solution reproduced the tailing observed at the pumping well. In cases where borehole flushing was observed and accounted for, dispersivities obtained from a radial convergent flow test were not excluded from the high-reliability category.

2. The tracer input must be well defined. Both the input concentration and the temporal distribution of the input concentrations must be known (measured). If not, the input is another unknown in the solution of the advection-dispersion equation, and we are less confident in the resulting value of dispersivity.

3. The tracer must be conservative. A reactive or non-conservative tracer complicates the governing equations and resulted in additional parameters that must be estimated. Consequently, we are less confident in the resulting dispersivity. Tracers such as Cl^- , I^- , Br^- , and tritium were considered to be conservative.

4. The dimensionality of the tracer concentration measurements was appropriate. A tracer introduced into an aquifer will spread in three spatial dimensions. High-reliability dispersivities were judged to be those where three-dimensional monitoring was used in all cases except where the aquifer tracer had been injected and measured over the full depth of the aquifer; in this case two-dimensional monitoring was acceptable. In all other cases, where the dimension of the measurement was either not reported or where two-dimensional measurements were used where three-dimensional measurements should have been used, the dispersivity values were judged to be of lower reliability.

5. The analysis of the concentration data was appropriate. Since the interpretation of the tracer data is necessarily linked to the type of tracer test to which the interpretation method is applied, these two features of the field studies were evaluated together. The three general categories of data interpretation can be grouped as follows: (1) breakthrough curve analysis, usually applied to uniform ambient flow tests and radial flow tests [e.g., Sauty, 1980]; (2) method of spatial moments, applied to uniform ambient flow tests [Freyberg, 1986]; and (3) numerical methods, applied to contamination events [e.g., Pinder, 1973; Konikow and Bredehoeft, 1974].

A common difficulty with the interpretation of concentration data using breakthrough curve matching to determine dispersivity is the assumption that the dispersivity is constant. The field data assembled in this review suggest that this assumption is not valid, at least for small-scale tests (tens of meters). At larger scales (hundreds of meters) an asymptotic constant value of dispersivity is predicted by some theories. However, at most sites the displacement distance after which the dispersivity is constant is not

TABLE 2. Numbers of Dispersivities for Different Types of Tests and Media

Media Type	Tracer Type			Total
	Artificial	Contamination	Environmental	
Porous	68	14	6	88
Fractured	15	1	2	18
Total	83	15	8	106

TABLE 3. Criteria Used to Classify the Reliability of the Reported Dispersivity Values

Classification	Criteria
High reliability	Tracer test was either ambient flow, radial diverging flow, or two-well instantaneous pulse test (without recirculation). Tracer input was well defined. Tracer was conservative. Spatial dimensionality of the tracer concentration measurements was appropriate. Analysis of the tracer concentration data was appropriate.
Low reliability	Two-well recirculating test with step input was used. Single-well injection-withdrawal test with tracer monitoring at the single well was used. Tracer input was not clearly defined. Tracer breakthrough curve was assumed to be the superposition of breakthrough curves in separate layers. Measurement of tracer concentration in space was inadequate. Equation used to obtain dispersivity was not appropriate for the data collected.

known. Data for which no a priori assumptions were made regarding the dispersivity were considered to be highly reliable.

A second major problem with many of the analyses reviewed was that a one- or two-dimensional solution to the advection-dispersion equation was used when the spreading of the plume under consideration was three-dimensional in nature. High-reliability dispersivities were those for which the dimensionality of the solute plume, the solute measurements, and the data analyses were consistent.

Low-reliability dispersivity data. A reported dispersivity was classified as being of low reliability if one of the following criteria was met.

1. The two-well recirculating test with a step input was used. The problem with this configuration is that, except for very early time where concentrations are low, the breakthrough curve is not strongly influenced by dispersion, but rather is determined by the different travel times along the flow paths established by injection and pumping wells [Welty and Gelhar, 1989]. As a result, the two-well test with a step input is generally insensitive to dispersion. For this reason all tests of this type were considered to produce data of low reliability.

2. The single-well injection-withdrawal test was used with tracer monitoring at the pumping well. A difficulty encountered in the small-scale, single-well, injection-withdrawal test (where water is pumped into and out of one well) is that if observations are made at the production well, the dispersion process observed is different from one of unidirectional flow. The problem stems from the fact that macrodispersion near the injection well is due to velocity differences associated with layered heterogeneity of the hydraulic conductivity. In the single-well test with observations made at the production well, the effect observed is that of reversing the velocity of the water. If the tracer travels at different velocities in layers as it radiates outward, it will also travel with the same velocity pattern as it is drawn back

to the production well. As a result, the mixing process is partially reversible and the dispersivity would be underestimated relative to the value for unidirectional flow. Heller [1972] has carried out experiments which demonstrate the reversibility effect on a laboratory scale.

3. The tracer input was not clearly defined. When a contamination event or environmental tracer is modeled, the tracer input (both quantity and temporal distribution) is not well defined and becomes another unknown in solving the advection-dispersion equation.

4. The tracer breakthrough curve was assumed to be the superposition of breakthrough curves in separate layers when there was little or no evidence of such layers at the field site. These studies generally assume that the porous medium is perfectly stratified, which, especially at the field scale, may not be a valid assumption. At a small scale (a few meters) where the existence of continuous layers may be a reasonable assumption, the dispersivity of each layer does not represent the field-scale parameter. The field-scale dispersivity is a result of the spreading due to the different velocities in each layer.

5. The measurement of tracer concentration in space was inadequate. Under ambient flow conditions the tracer is usually distributed in three-dimensional space, but if the measurements are two-dimensional then the actual tracer cloud cannot be analyzed lacking the appropriate data. If the tracer is introduced over the entire saturated thickness, then two-dimensional measurements would be adequate.

6. The equation used to obtain dispersivity was not appropriate for the data collected. Various assumptions regarding flow and solute characteristics are made in obtaining a solution to the advection-dispersion equation. To apply a particular solution to the data from a field experiment, the assumptions in that solution must be consistent with the experimental conditions. One common example is the case of applying a one-dimensional (uniform velocity) flow solution to a radial flow test in which the converging (or diverging) flow field around the pumping or injection well is clearly nonuniform.

Results of classification. From the classification process, 14 dispersivity values were judged to be of high reliability. The sites where these values were determined include Borden, Ontario, Canada; Otis Air Force Base, Cape Cod, Massachusetts; Hanford, Washington; Mobile, Alabama; University of California, Berkeley; Yavne region, Israel; Bonnaud, France (six tests); and Palo Alto bay lands. There were 61 values judged to be of low reliability for one or more of the reasons discussed above; 31 sites provided data judged to be of intermediate value. Figure 2 depicts the longitudinal dispersivity data replotted with symbols reflecting the reliability classification; the largest symbols indicate data judged to be of highest reliability.

The general compilation of all dispersivity data in Figure 1 indicates that dispersivity might increase indefinitely with scale, but after critically evaluating the data in terms of reliability as shown in Figure 2, it is evident that this trend cannot be extrapolated with confidence to all scales. The largest high-reliability dispersivity value is 4 m (Mobile, Alabama) and the largest scale of high-reliability values is 250 m (Cape Cod, Massachusetts). It is not clear from these data whether dispersivity increases indefinitely with scale or whether the relationship becomes constant for very large scales, as would be predicted by some theories. This points

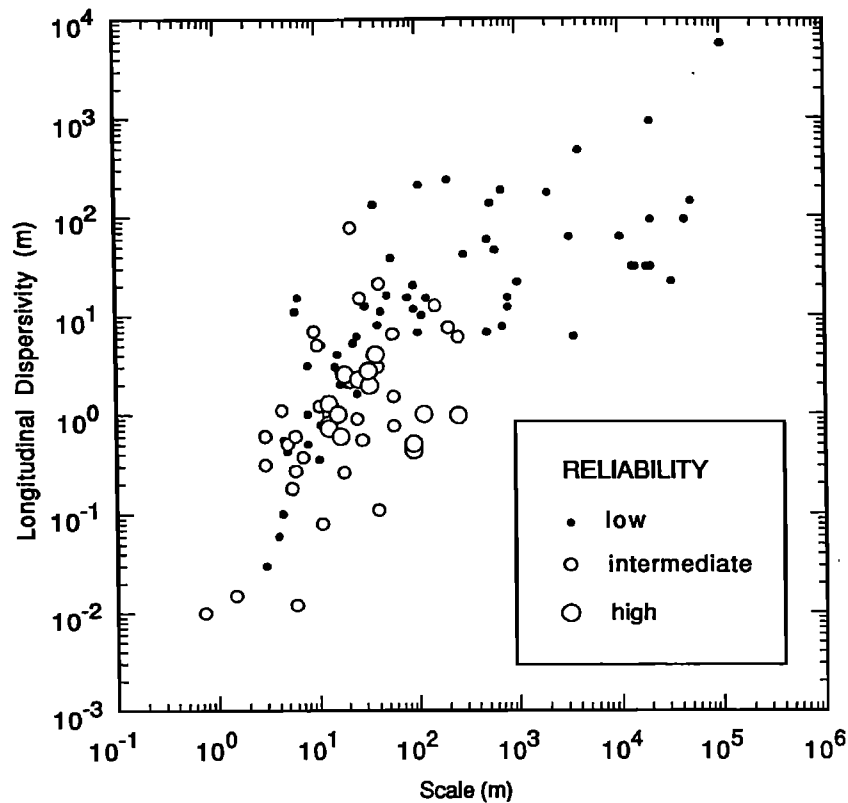


Fig. 2. Longitudinal dispersivity versus scale with data classified by reliability.

to a need for reliable data at scales larger than 250 m. Whether conducting controlled tracer tests at these very large scales is feasible is open to question.

When the reliability of the data is considered, the apparent difference between fractured and porous media at small scales (Figure 1) is regarded to be less significant because none of the fractured media data are of high reliability.

Reanalyses of Selected Dispersivity Data

In cases where the concentration data collected were of high reliability but the method of analysis could be improved, we reevaluated the data to determine a dispersivity value which we judged to be of higher reliability. The details of these analyses are reported by *Welty and Gelhar* [1989]. The results are summarized here.

Corbas, France. The data from this converging radial flow tracer test are reported by *Sauty* [1977]. These data are of particular interest because tests were conducted at three different scales in the same aquifer material; tracer was injected at 25, 50, and 150 m from a pumping well. *Sauty* [1977] evaluated these data using uniform flow solutions to the one-dimensional advection-dispersion equation. At the two smaller-scale tests, he assumed a two-layer scheme, although this assumption was not supported by geologic evidence. For this reason the data at the smaller scales were rated to be of lower reliability than the data at 150 m. We reevaluated these data using a solution that accounts for nonuniform, convergent radial flow effects and that makes no assumptions about geologic layers [*Welty and Gelhar*, 1989]. The values of dispersivity reported by *Sauty* at 25 m are 11 m and 1.25 m for the two hypothesized layers; we calculated

a value of 2.4 m without the assumption of layers. At 50 m, *Sauty* calculated dispersivity values of 25 m and 6.25 m for the two layers; we calculate an overall value of 4.6 m. At a scale of 150 m, *Sauty* calculated a dispersivity value of 12.5 m without the assumption of layers; our calculation of 10.5 m is in close agreement. Our calculations indicate that dispersivity increases with scale, accounting for nonuniform flow effects and without the arbitrary assumption of geologic layers.

Savannah River Plant, Georgia. *Webster et al.* [1970] evaluated data from a two-well recirculating test using the methodology of *Grove and Beetem* [1971]. This analysis assumes uniform flow along stream tubes and sums individual breakthrough curves along the stream tubes to obtain a composite breakthrough curve. A dispersivity value of 134 m at a scale of 538 m was obtained using this method. We reevaluated the data using the methodology of *Gelhar* [1982] which accounts for nonuniform flow effects. We obtained a dispersivity value of 47 m from our analysis. We have more confidence in this value because the analysis more accurately represents the actual flow configuration.

Tucson, Arizona. The data reported by *Wilson* [1971] for a two-well test were also evaluated by *Robson* [1974] using a *Grove and Beetem*-type analysis. *Wilson* reported a value of longitudinal dispersivity of 15.2 m at a scale of 79.2 m. Using a nonuniform flow solution based on that of *Gelhar* [1982], we calculated a value of longitudinal dispersivity of 1.2 m, an order of magnitude smaller than that of *Robson*. Again, we have more confidence in this value because the analysis more accurately reflects the actual flow situation.

Columbus, Mississippi. The natural gradient tracer test at the Columbus site (*E. E. Adams and L. W. Gelhar*, Field

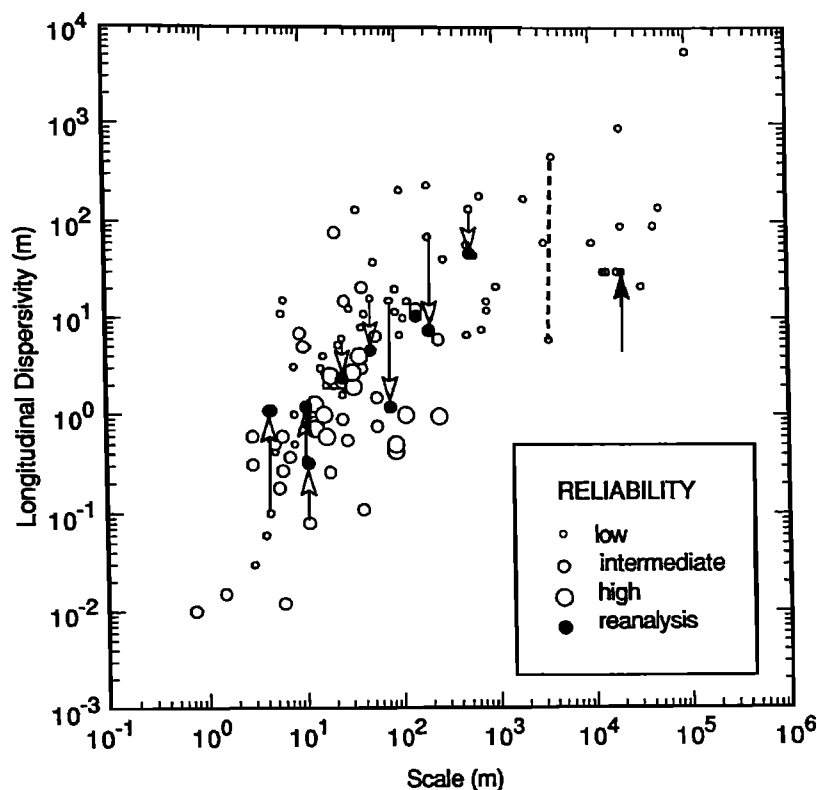


Fig. 3. Longitudinal dispersivity versus scale of observation with adjustments resulting from reanalyses. Arrows indicate reported values at tails and corresponding values from reanalyses at heads. Dashed line connects two dispersivity values determined at the Hanford site.

study of dispersion in a heterogeneous aquifer: Spatial moments analysis, submitted to *Water Resources Research*, 1991; hereinafter Adams and Gelhar, submitted manuscript, 1991) is unique in that the large-scale ambient flow field exhibits strong nonuniformity and the aquifer is very heterogeneous. A superficial spatial moments interpretation, ignoring the flow nonuniformity, indicated a longitudinal dispersivity of around 70 m, whereas a more refined analysis that explicitly includes the influence of flow nonuniformity yields a dispersivity of around 7 m (Adams and Gelhar, submitted manuscript, 1991). This refined estimate is regarded to be of intermediate reliability because of the uncertainty regarding the mass balance at the Columbus site.

From the above reanalyses, all values of dispersivity calculated were smaller than the original values. We have higher confidence in these values because they are associated with solutions to the advection-dispersion equation with more realistic assumptions. In all cases we would rate the new values to be of intermediate reliability instead of low reliability. The reevaluated data are shown as solid symbols on Figure 3 connected to their original values by vertical arrows.

Based on the above reanalyses, we suspect that it is most likely that improved analyses would reduce many of the lower-reliability dispersivities in Figure 2. However, there are a few cases for which more appropriate observations and/or interpretations would most likely lead to larger dispersivities. For example, the Twin Lake natural gradient tracer test [Moltyaner and Killely, 1988a, b] was interpreted by using breakthrough curves at individual boreholes con-

structed as the average of breakthrough curves in three somewhat arbitrarily defined layers. We suspect that this kind of localized observation will produce a significantly lower dispersivity than would result from a spatial moments analysis which considers the overall spreading of the plume. The magnitude of the possible increase in the dispersivity cannot be assessed because the sampling network did not completely encompass the plume at the Twin Lake site.

Another example is that of the first Borden site natural gradient experiment [Sudicky *et al.*, 1983] which was analyzed using an analytical solution with spatially constant dispersivities. In the near-source region where dispersivities are actually increasing with displacement, this approach will tend to underestimate the magnitude of the dispersivity. Gelhar *et al.* [1985] reanalyzed the first Borden experiment using the method of spatial moments and found that the longitudinal dispersivity at 11 m was 2–4 times that found by Sudicky *et al.* [1983]. The resulting increase in the dispersivity is illustrated in Figure 3 connected to the original point by a vertical line. Because of the incomplete plume sampling and plume bifurcation in this test (only the "slow zone" was analyzed), this point is still regarded to be of intermediate reliability.

Dispersivities at small displacements will also be underestimated if based on breakthrough curves measured in localized samplers in individual layers. Such effects are likely, for example, in the Perch Lake [Lee *et al.*, 1980] and Lower Glatt Valley [Hoehn, 1983] interpretations. Later interpretation of the Lower Glatt Valley data using temporal moments [Hoehn and Santschi, 1987] shows values an order of

magnitude larger; these are connected with the original values by vertical lines in Figure 3.

As a further illustration of the uncertainty in the longitudinal dispersivity values in Figure 2, consider the data for the Hanford site. The tracer test [Bierschenk, 1959; Cole, 1972] interpreted from breakthrough curves at two different wells at roughly the same distance (around 4000 m) from the injection point produced values differing by 2 orders of magnitude (see dashed line in Figure 3). This difference illustrates the difficulty in interpreting point breakthrough curves in heterogeneous aquifers, even at this large displacement. The numerical simulations of the contamination plume [Ahlstrom et al., 1977] extending to 20,000 m used a dispersivity of 30.5 m (100 feet) as identified by the bold arrow in Figure 3. Evidently this round number (100 feet) was popular in several different simulations of contaminant plumes.

In none of the cases of simulations of contamination events is there any explicit information on how the dispersivity values were selected or in what sense the values may be optimal. Consequently it is not possible to quantify the uncertainty in dispersivity values based on contamination event simulations. However, experience suggests that, because of the possible tendency to select large dispersivities which avoid the numerical difficulties associated with large grid Peclet numbers, some of the dispersivity values based on contaminant plumes are likely to be biased toward higher values. Such overestimates would occur mainly at larger scales.

The results of these reanalyses provide an explicit indication of the uncertainty in the dispersivity values in Figure 2 and suggest that for large displacements the low-reliability dispersivities are likely to decrease whereas for small displacements some increases can be expected.

Transverse Dispersivities

Although the data on transverse dispersivity are much more limited, they reveal some features which are important in applications. The data on horizontal and vertical transverse dispersivities are summarized in Figures 4 and 5, which show these parameters as a function of scale of observation. The data are portrayed in terms of reliability classification with the largest symbols identifying the high-reliability points.

In the case of the horizontal dispersivity, there appears to be some trend of increasing dispersivity with scale but this appearance results from low-reliability data which finds their origin largely in contaminant event simulations using two-dimensional depth-averaged descriptions. In these contamination situations the sources are often ill-defined; if the actual source area is larger than that represented in the model there will be greater transverse spreading which would incorrectly be attributed to transverse dispersion.

In the case of vertical transverse dispersion (Figure 5), the data are even more limited and certainly do not imply any significant trend with overall scale. Note that there are only two points of high reliability, those corresponding to the Borden [Freyberg, 1986] and Cape Cod [Garabedian et al., 1988, 1991] sites. The estimate of the vertical transverse dispersivity for the Borden site is from the recent three-dimensional analysis of Rajaram and Gelhar [1991]. The vertical transverse dispersivity is seen to be much smaller than the horizontal transverse dispersivity, apparently reflecting the roughly horizontal stratification of hydraulic conductivity encountered in permeable sedimentary materi-

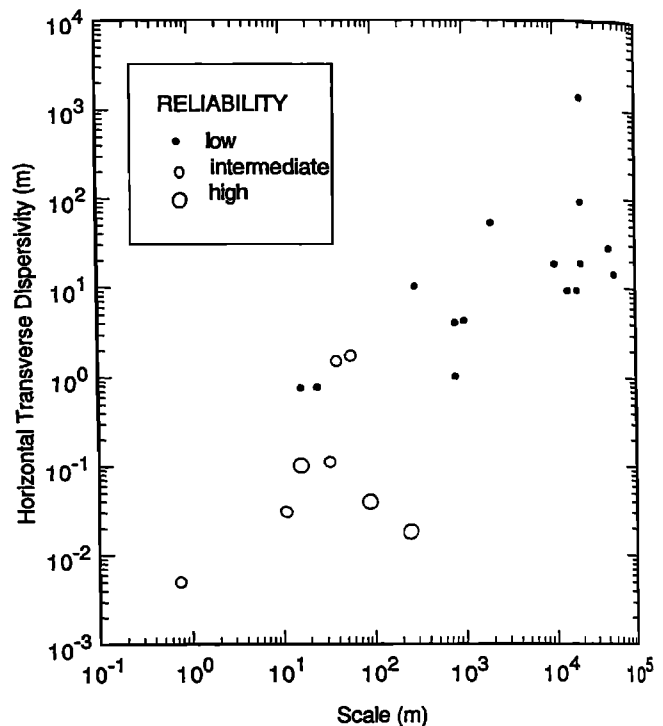


Fig. 4. Horizontal transverse dispersivity as a function of observation scale.

als. All of the vertical dispersivities are less than 1 m and high-reliability values are only a few millimeters, this being the same order of magnitude as the local transverse dispersivity for sandy materials.

The ratio of longitudinal dispersivity to the horizontal and vertical transverse dispersivities is shown in Figure 6. This form of presentation is used because it is common practice to select constant values for the ratio of longitudinal to transverse dispersivities. For one thing, this plot illustrates the popularity of using, in numerical simulations, a horizontal transverse dispersivity which is about one third of the longitudinal dispersivity (the horizontal dashed line in Figure 6). There does not appear to be any real justification for using this ratio. We are not aware of any simulation work which systematically demonstrates the appropriateness of this value for the horizontal transverse dispersivity. The two high-reliability points show an order of magnitude higher ratio of longitudinal to horizontal transverse dispersivities. The vertical dashed lines in Figure 6 are used to identify three-dimensionally monitored sites for which all three principal components of the dispersivity tensor have been estimated. In all of these cases, the vertical transverse dispersivity is 1–2 orders of magnitude smaller than the horizontal transverse dispersivity. This behavior further emphasizes the small degree of vertical mixing which is frequently encountered in naturally stratified sediments. This small degree of vertical mixing is clearly an important consideration in many applications, such as the design of observation networks to monitor contamination plumes and the development of remediation schemes. Consequently, in order to model many field situations realistically, it will be necessary to use three-dimensional transport models which adequately represent the small but finite vertical mixing.

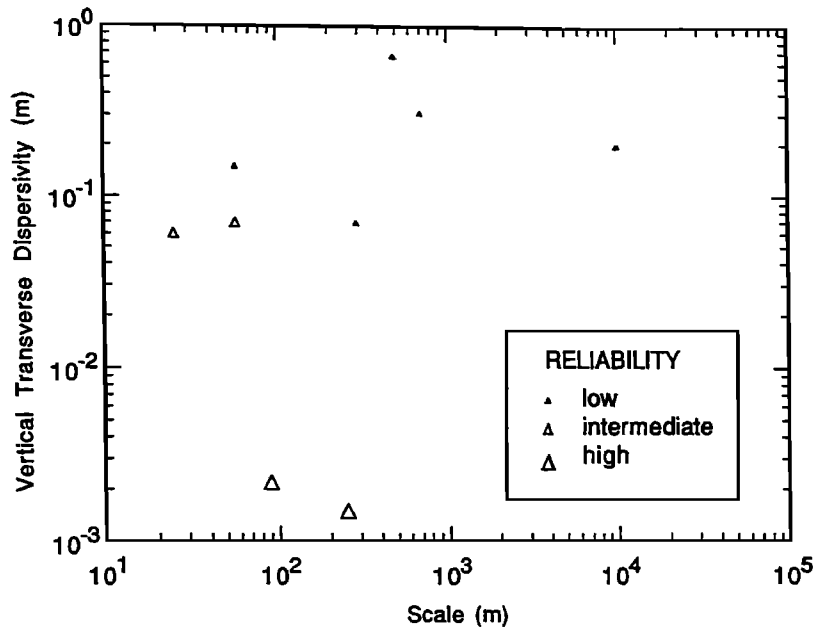


Fig. 5. Vertical transverse dispersivity as a function of observation scale.

INTERPRETATIONS

This review of field observations of dispersive mixing in aquifers demonstrates several overall features which are evident from the graphical and tabular information developed here. Taken in aggregate, without regard for reliability, the data indicate a clear trend of systematic increase of longitudinal dispersivity with scale. In terms of aquifer type (porous versus fractured media) the data at smaller scale may seem to be higher for fractured media but, in view of the lower reliability of the fractured media data, this difference is of minimal significance.

When the data on longitudinal dispersivity are classified according to reliability, the pattern regarding scale dependence of dispersivity is less clear (see Figure 2). There are no

high-reliability points at scales greater than 300 m and the high-reliability points are systematically in the lower portion of the scattering of data. The lack of high-reliability data at scales greater than 300 m reflects the fact that the data beyond that scale are almost exclusively from contamination simulations or environmental tracer studies for which the solute input is typically ill-defined. Because of the very long period of time required to carry out controlled input tracer experiments at these larger scales, such experiments have not been undertaken.

Although the data shown in Figure 2 suggest that some overall trend of increasing dispersivity with scale is plausible, it does not seem reasonable to conclude that a single universal line [Neuman, 1990] can be meaningfully identified

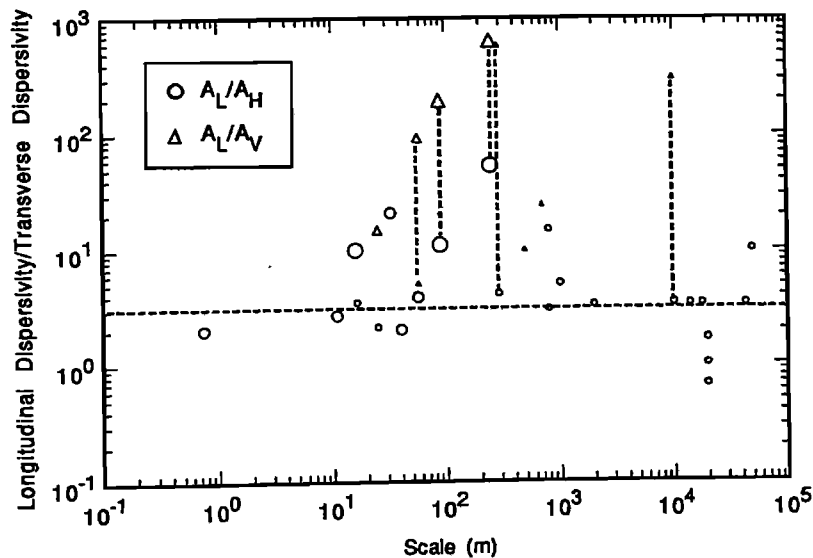


Fig. 6. Ratio of longitudinal to horizontal and vertical transverse dispersivities; largest symbols are high reliability and smallest symbols are low reliability. Vertical dashed lines connecting two points indicate sites where all three principal components of the dispersivity tensor have been measured. Horizontal dashed line indicates a ratio of $A_L/A_T = 1/3$, which has been widely used in numerical simulations.

by applying standard linear regression to all of the data. Rather we would expect a family of curves reflecting different dispersivities in aquifers with different degrees of heterogeneity. At a given scale, the longitudinal dispersivity typically ranges over 2–3 orders of magnitude. This degree of variation can be explained in terms of the established stochastic theory [e.g., Gelhar and Axness, 1983; Dagan, 1984] which shows that the longitudinal dispersivity is proportional to the product of the variance and the correlation scale of the natural logarithm of hydraulic conductivity. A compilation of data on these parameters [Gelhar, 1986] shows that they vary over a range that can easily explain the range of variation in Figure 2. The theoretical results for the developing dispersion process [Gelhar et al., 1979; Dagan, 1984; Gelhar, 1987; Naff et al., 1988] show that the longitudinal dispersivity initially increases linearly with displacement distance and gradually approaches a constant asymptotic value [see Gelhar, 1987, Figure 9]. One could visualize the behavior of Figure 2 as being the result of superimposing several such theoretical curves with different parameters characterizing aquifer heterogeneity.

The results of reanalyses for several of the individual sites serve to illustrate explicitly the uncertainty involved in the estimates of longitudinal dispersivity. The reanalyses indicate that, for the most part, improved analysis will lead to decreases in the longitudinal dispersivity except possibly for very small displacements where limited localized sampling can produce underestimates of the bulk spreading and mixing. In cases where the dispersivity estimates were based on numerical simulations of contamination events, the degree of uncertainty is likely large and ill-determined, but bias in some of the estimates toward the high side seems most likely.

From an applications perspective, the information assembled here should serve as a strong cautionary note about routinely adopting dispersivities from Figure 2 or a linear regression representation through the data. We feel that the preponderance of evidence favors the use of dispersivity values in the lower half of the range at any given scale. If values in the upper part of the range are adopted, excessively large dilution may be predicted and the environmental consequences misrepresented. In the case of transverse dispersivities, it is particularly important to recognize the very low vertical transverse dispersivities that have been observed at several sites. As a result, many contamination plumes will exhibit very limited vertical mixing with high concentrations at a given horizon. The recognition of such features is of obvious importance in designing monitoring schemes and implementing aquifer remediation. Horizontal transverse dispersivities are typically an order of magnitude smaller than the longitudinal dispersivity whereas vertical transverse dispersivities are another order of magnitude lower.

From a research perspective, the data reviewed here suggest a need for some skepticism regarding "universal" models which represent the scattered data of varying reliability by a single straight line. The presumption of such a universal model ignores the fact that different aquifers will have different degrees of heterogeneity at a given scale. The data suggest that there is a scale dependence of longitudinal dispersivity but reliable data must be developed at larger scales in order to establish the nature of the dependence. Clearly, there is a need for very large scale, long-term, carefully planned experiments extending to several kilometers.

Acknowledgments. The work was supported in part by the Electric Power Research Institute (EPRI), project 2485-5, which was a joint effort of the Massachusetts Institute of Technology (MIT) and the Tennessee Valley Authority (TVA). This portion of the work was done at MIT under contract TV-61664A with TVA. The work was also supported by the National Science Foundation, grant CES-8814615.

REFERENCES

- Ahlstrom, S. W., H. P. Foote, R. C. Arnett, C. P. Cole, and R. J. Serne, Multicomponent mass transport model: Theory and numerical implementation (discrete-particle-random-walk-version), *Rep. BNWL-2127*, Battelle Pac. Northwest Lab., Richland, Wash., 1977.
- Anderson, M. P., Using models to simulate the movement of contaminants through groundwater flow systems, *CRC Crit. Rev. Environ. Control*, 9, 97–156, 1979.
- Bassett, R. L., et al., Preliminary data from a series of artificial recharge experiments at Stanton, Texas, *U.S. Geol. Surv. Open File Rep.*, 81-0149, 1980.
- Bear, J., *Dynamics of Fluids in Porous Media*, Elsevier Scientific, New York, 1972. (Reprinted by Dover, New York, 1988.)
- Beims, U., Planung, Durchführung und Auswertung von Gütepumpversuchen, *Z. Angew. Geol.*, 29(10), 482–490, 1983.
- Bentley, H. W., and G. R. Walter, Two-well recirculating tracer tests at H-2: Waste Isolation Pilot Plant (WIPP), southwest New Mexico, draft paper, Hydro Geochem., Inc., Tucson, Ariz., 1983.
- Betson, R. P., J. M. Boggs, S. C. Young, W. R. Waldrop, and L. W. Gelhar, Macrodispersion experiment (MADE): Design of a field experiment to investigate transport processes in a saturated groundwater zone, *Rep. EPRI EA-4082*, Elec. Power Res. Inst., Palo Alto, Calif., June 1985.
- Bierschenk, W. H., Aquifer characteristics and ground-water movement at Hanford, *Rep. HW-60601*, Hanford At. Products Oper., Richland, Wash., 1959.
- Bredehoeft, J. D., and G. F. Pinder, Mass transport in flowing groundwater, *Water Resour. Res.*, 9(1), 144–210, 1973.
- Claasen, H. C., and E. H. Cordes, Two-well recirculating tracer test in fractured carbonate rock, Nevada, *Hydrol. Sci. Bull.*, 20(3), 367–382, 1975.
- Cole, J. A., Some interpretations of dispersion measurements in aquifers, *Groundwater Pollution in Europe*, edited by J. A. Cole, pp. 86–95, Water Research Association, Reading, England, 1972.
- Dagan, G., Stochastic modeling of groundwater flow by unconditional and conditional probabilities, 2, The solute transport, *Water Resour. Res.*, 18(4), 835–848, 1982.
- Dagan, G., Solute transport in heterogeneous porous formations, *J. Fluid Mech.*, 145, 151–177, 1984.
- Daniels, W. R. (Ed.), Laboratory field studies related to the radionuclide migration project, *Progress Rep. LA-8670-PR*, Los Alamos Sci. Lab., Los Alamos, N. M., 1981.
- Daniels, W. R. (Ed.), Laboratory field studies related to the radionuclide migration project (draft), *Progress Rep. LA-9192-PR*, Los Alamos Sci. Lab., Los Alamos, N. M., 1982.
- Davis, S. N., G. M. Thompson, H. W. Bentley, and G. Stiles, Groundwater tracers—A short review, *Ground Water*, 18(1), 14–23, 1980.
- Davis, S. N., D. J. Campbell, H. W. Bentley, and T. J. Flynn, An introduction to groundwater tracers, *Rep. EPA/600/2-85/022*, Environ. Prot. Agency, Washington, D. C., 1985. (Available as *NTIS PB86-100591* from Natl. Tech. Inf. Serv., Springfield, Va.)
- de Marsily, G., *Quantitative Hydrogeology*, Academic, San Diego, Calif., 1986.
- Dieulin, A., Propagation de pollution dans un aquifere alluvial: L'effet de parcours, doctoral dissertation, Univ. Pierre et Marie Curie-Paris VI and l'Ecole Natl. Super. des Mines de Paris, Fontainebleau, France, 1980.
- Dieulin, A., Lixiviation in situ d'un gisement d'uranium en milieu granitique, *Draft Rep. LHM/RD/81/63*, Ecole Natl. Super. des Mines de Paris, Fontainebleau, France, 1981.
- Egboka, B. C. E., J. A. Cherry, R. N. Farvolden, and E. O. Frind, Migration of contaminants in groundwater at a landfill: A case study, 3, Tritium as an indicator of dispersion and recharge, *J. Hydrol.*, 63, 51–80, 1983.
- Fenske, P. R., Hydrology and radionuclide transport, monitoring well HT-2m, Tatum Dome, Mississippi, *Proj. Rep. 25, Tech. Rep.*

- NVD-1253-6, Cent. for Water Resour. Res., Desert Res. Inst., Univ. of Nev. Syst., Reno, 1973.
- Freyberg, D. L., A natural gradient experiment on solute transport in a sand aquifer, 2, Spatial moments and the advection and dispersion of nonreactive tracers, *Water Resour. Res.*, 22(13), 2031-2046, 1986.
- Fried, J. J., *Groundwater Pollution*, Elsevier, New York, 1975.
- Fried, J. J., and P. Ungemach, Determination in situ du coefficient de dispersion longitudinale d'un milieu poreux naturel, *C. R. Acad. Sci., Ser. 2*, 272, 1327-1329, 1971.
- Garabedian, S. P., L. W. Gelhar, and M. A. Celia, Large-scale dispersive transport in aquifers: Field experiments and reactive transport theory, *Rep. 315*, Ralph M. Parsons Lab. for Water Resour. and Hydrodyn., Mass. Inst. of Technol., Cambridge, 1988.
- Garabedian, S. P., D. R. LeBlanc, L. W. Gelhar, and M. A. Celia, Large-scale natural gradient tracer test in sand and gravel, Cape Cod, Massachusetts, 2, Analysis of tracer moments for a nonreactive tracer, *Water Resour. Res.*, 27(5), 911-924, 1991.
- Gelhar, L. W., Analysis of two-well tracer tests with a pulse input, *Rep. RHO-BW-CR-131 P*, Rockwell Intl., Richland, Wash., 1982.
- Gelhar, L. W., Stochastic subsurface hydrology from theory to applications, *Water Resour. Res.*, 22, 135S-145S, 1986.
- Gelhar, L. W., Stochastic analysis of solute transport in saturated and unsaturated porous media, *NATO ASI Ser., Ser. E*, 128, 657-700, 1987.
- Gelhar, L. W., and C. L. Axness, Three dimensional stochastic analysis of macrodispersion in aquifers, *Water Resour. Res.*, 19(1), 161-180, 1983.
- Gelhar, L. W., A. L. Gutjahr, and R. L. Naff, Stochastic analysis of macrodispersion in a stratified aquifer, *Water Resour. Res.*, 15(6), 1387-1397, 1979.
- Gelhar, L. W., A. Mantoglou, C. Welty, and K. R. Rehfeldt, A review of field-scale physical solute transport processes in saturated and unsaturated porous media, *EPRI Rep. EA-4190*, Elec. Power Res. Inst., Palo Alto, Calif., Aug. 1985.
- Goblet, P., Interpretation d'expériences de tracage en milieu granitique (site B), *Rep. LHM/RD/82/11*, Cent. d'Inf. Geol., Ecole Natl. Super. des Mines de Paris, Fontainebleau, France, 1982.
- Grove, D. B., The use of Galerkin finite-element methods to solve mass transport equations, *Rep. USGS/WRD/WRI-78/011*, U.S. Geol. Surv., Denver, Colo., 1977. (Available as *NTIS PB 277-532* from Natl. Tech. Inf. Serv., Springfield, Va.)
- Grove, D. B., and W. A. Beetem, Porosity and dispersion constant calculations for a fractured carbonate aquifer using the two-well tracer method, *Water Resour. Res.*, 7(1), 128-134, 1971.
- Gupta, S. K., K. K. Tanji, and J. N. Luthin, A three-dimensional finite element ground water model, *Rep. UCAL-WRC-C-152*, Calif. Water Resour. Cent., Univ. of Calif., Davis, 1975. (Available as *NTIS PB 248-925* from Natl. Tech. Inf. Serv., Springfield, Va.)
- Halevy, E., and A. Nir, Determination of aquifer parameters with the aid of radioactive tracers, *J. Geophys. Res.*, 67(5), 2403-2409, 1962.
- Harpaz, Y., Field experiments in recharge and mixing through wells, *Underground Water Storage Study Tech. Rep. 17*, Publ. 483, Tahal-Water Plann. for Isr., Tel Aviv, 1965.
- Heller, J. P., Observations of mixing and diffusion in porous media, *Proc. Symp. Fundam. Transp. Phenom. Porous Media*, 2nd, 1-26, 1972.
- Helweg, O. J., and J. W. Labadie, Linked models for managing river basin salt balance, *Water Resour. Res.*, 13(2), 329-336, 1977.
- Hoehn, E., Geological interpretation of local-scale tracer observations in a river-ground water infiltration system, draft report, Swiss Fed. Inst. Reactor Res. (EIR), Würenlingen, Switzerland, 1983.
- Hoehn, E., and P. H. Santschi, Interpretation of tracer displacement during infiltration of river water to groundwater, *Water Resour. Res.*, 23(4), 633-640, 1987.
- Huyakorn, P. S., P. F. Anderson, F. J. Motz, O. Güven, and J. G. Melville, Simulations of two-well tracer tests in stratified aquifers at the Chalk River and the Mobile sites, *Water Resour. Res.*, 22(7), 1016-1030, 1986.
- Iris, P., Contribution à l'étude de la valorisation énergétique des aquifères peu profonds, thèse de docteur-ingenieur, Ecole des Mines de Paris, Fontainebleau, France, 1980.
- Ivanovitch, M., and D. B. Smith, Determination of aquifer parameters by a two-well pulsed method using radioactive tracers, *J. Hydrol.*, 36(1/2), 35-45, 1978.
- Kies, B., Solute transport in unsaturated field soil and in groundwater, Ph.D. dissertation, Dep. of Agron., N. M., State Univ., Las Cruces, 1981.
- Klotz, D., K. P. Seiler, H. Moser, and F. Neumaier, Dispersivity and velocity relationship from laboratory and field experiments, *J. Hydrol.*, 45(3/4), 169-184, 1980.
- Konikow, L. F., Modeling solute transport in ground water, in *Environmental Sensing and Assessment: Proceedings of the International Conference*, article 20-3, Institute for Electrical and Electronic Engineers, Piscataway, N. J., 1976.
- Konikow, L. F., and J. D. Bredehoeft, Modeling flow and chemical quality changes in an irrigated stream-aquifer system, *Water Resour. Res.*, 10(3), 546-562, 1974.
- Kreft, A., A. Lenda, B. Turek, A. Zuber, and K. Czauderna, Determination of effective porosities by the two-well pulse method, *Isot. Tech. Groundwater Hydrol., Proc. Symp.*, 2, 295-312, 1974.
- Lallemande-Barres, A., and P. Peaudecerf, Recherche des relations entre la valeur de la dispersivité macroscopique d'un milieu aquifère, ses autres caractéristiques et les conditions de mesure, *Bull. Bur. Rech. Geol. Min., Sect. 3, Ser. 2, 4*, 1978.
- Lau, L. K., W. J. Kaufman, and D. K. Todd, Studies of dispersion in a radial flow system, Canal Seepage Research: Dispersion Phenomena in Flow Through Porous Media, *Progress Rep. 3, I.E.R. Ser. 93, Issue 3*, Sanit. Eng. Res. Lab., Dep. of Eng. and School of Public Health, Univ. of Calif., Berkeley, 1957.
- LeBlanc, D. R., Sewage plume in a sand and gravel aquifer, Cape Cod, Massachusetts, *U.S. Geol. Surv. Open File Rep.*, 82-274, 35 pp., 1982.
- Lee, D. R., J. A. Cherry, and J. F. Pickens, Groundwater transport of a salt tracer through a sandy lakebed, *Limnol. Oceanogr.*, 25(1), 46-61, 1980.
- Leland, D. F., and D. Hillel, Scale effects on measurement of dispersivity in a shallow, unconfined aquifer, paper presented at Chapman Conference on Spatial Variability in Hydrologic Modeling, AGU, Fort Collins, Colo., July 21-23, 1981.
- Lenda, A., and A. Zuber, Tracer dispersion in groundwater experiments, in *Isot. Hydrol. Proc. Symp. 1970*, 619-641, 1970.
- MacFarlane, D. S., J. A. Cherry, R. W. Gilham, and E. A. Sudicky, Migration of contaminants at a landfill: A case study, 1, Groundwater flow and plume delineation, *J. Hydrol.*, 63, 1-29, 1983.
- Mercado, A., Recharge and mixing tests at Yavne 20 well field, *Underground Water Storage Study Tech. Rep. 12, Publ. 611*, Tahal-Water Plann. for Isr., Tel Aviv, 1966.
- Meyer, B. R., C. A. R. Bain, A. S. M. DeJesus, and D. Stephenson, Radiotracer evaluation of groundwater dispersion in a multi-layered aquifer, *J. Hydrol.*, 50(1/3), 259-271, 1981.
- Molinari, J., and P. Peaudecerf, Essais conjoints en laboratoire et sur le terrain en vue d'une approche simplifiée de la prévision des propagations de substances miscibles dans les aquifères réels, paper presented at Symposium on Hydrodynamic Diffusion and Dispersion in Porous Media, Int. Assoc. for Hydraul. Res., Pavis, Italy, 1977.
- Moltyaner, G. L., and R. W. D. Killey, Twin Lake tracer tests: Longitudinal dispersion, *Water Resour. Res.*, 24(10), 1613-1627, 1988a.
- Moltyaner, G. L., and R. W. D. Killey, Twin Lake tracer tests: Transverse dispersion, *Water Resour. Res.*, 24(10), 1628-1637, 1988b.
- Molz, F. J., O. Güven, and J. G. Melville, An examination of scale-dependent dispersion coefficients, *Ground Water*, 21, 715-725, 1983.
- Molz, F. J., O. Güven, J. G. Melville, R. D. Crocker, and K. T. Matteson, Performance, analysis, and simulation of a two-well tracer test at the Mobile site, *Water Resour. Res.*, 22(7), 1031-1037, 1986.
- Naff, R. L., T.-C. J. Yeh, and M. W. Kemblowski, A note on the recent natural gradient tracer test at the Borden site, *Water Resour. Res.*, 24(12), 2099-2103, 1988.
- Naymik, T. G., and M. J. Barcelona, Characterization of a contaminant plume in ground water, Meredosia, Illinois, *Ground Water*, 19(5), 517-526, 1981.
- Netretnieks, I., Transport in fractured rocks, paper presented at the

- 17th International Congress on the Hydrology of Rock of Low Permeability, Intl. Assoc. of Hydrogeol., Tucson, Ariz., Jan. 7-12, 1985.
- Neuman, S. P., Universal scaling of hydraulic conductivities in geologic media, *Water Resour. Res.*, 26(8), 1749-1758, 1990.
- Neuman, S. P., C. L. Winter, and C. M. Newman, Stochastic theory of field-scale dispersion in anisotropic porous media, *Water Resour. Res.*, 23(3), 453-466, 1987.
- New Zealand Ministry of Works and Development, Water and Soil Division, Movement of contaminants into and through the Here-taunga Plains aquifer, report, Wellington, 1977.
- Oakes, D. B., and D. J. Edworthy, Field measurement of dispersion coefficients in the United Kingdom, in *Ground Water Quality, Measurement, Prediction, and Protection*, pp. 327-340, Water Research Centre, Reading, England, 1977.
- Papadopoulos, S. S., and S. P. Larson, Aquifer storage of heated water: II, Numerical simulation of field results, *Ground Water*, 16(4), 242-248, 1978.
- Perlmutter, N. M., and M. Lieber, Dispersal of plating wastes and sewage contaminants in the groundwater and surface water: South Farmingdale-Massapequid area, Nassau County, New York, *U.S. Geol. Surv. Water Supply Pap.*, 1879-G, 1970.
- Philip, J. R., Issues in flow and transport in heterogeneous porous media, *Transp. Porous Media*, 1, 319-338, 1986.
- Pickens, J. F., and G. E. Grisak, Scale dependent dispersion in a stratified granular aquifer, *Water Resour. Res.*, 17(4), 1191-1211, 1981.
- Pinder, G. F., A Galerkin-finite element simulation of groundwater contamination on Long Island, *Water Resour. Res.*, 9(6), 1657-1669, 1973.
- Rabinowitz, D. D., and G. W. Gross, Environmental tritium as a hydrometeorologic tool in the Roswell Basin, New Mexico, *Tech. Completion Rep. OWRR:A-037-NMEX*, N. M. Water Resour. Res. Inst., Las Cruces, 1972.
- Rajaram, H., and L. W. Gelhar, Three-dimensional spatial moments analysis of the Borden tracer test, *Water Resour. Res.*, 27(6), 1239-1251, 1991.
- Roberts, P. V., M. Reinhard, G. D. Hopkins, and R. S. Summers, Advection-dispersion-sorption models for simulating the transport of organic contaminants, paper presented at *International Conference on Ground Water Quality Research*, Rice Univ., Houston, Tex., 1981.
- Robertson, J. B., Digital modeling of radioactive and chemical waste transport in the Snake River Plain aquifer of the National Reactor Testing Station, Idaho, *U.S. Geol. Surv. Open File Rep.*, IDO-22054, 1974.
- Robertson, J. B., and J. T. Barraclough, Radioactive and chemical waste transport in groundwater of National Reactor Testing Station: 20-year case history and digital model, *Underground Waste Manage. Artif. Recharge Prepr. Pap. Int. Symp. 2nd*, 1, 291-322, 1973.
- Robson, S. G., Feasibility of digital water quality modeling illustrated by application at Barstow, California, *U.S. Geol. Surv. Water Resour. Invest.*, 46-73, 1974.
- Robson, S. G., Application of digital profile modeling techniques to ground-water solute transport at Barstow, California, *U.S. Geol. Surv. Water Supply Pap.*, 2050, 1978.
- Rousselot, D., J. P. Sauty, and B. Gaillard, Etude hydrogéologique de la zone industrielle de Blyes-Saint-Vulbas, rapport préliminaire no. 5: Caractéristiques hydrodynamiques du système aquifère, *Rep. Jal 77/33*, Bur. de Rech. Geol. et Min., Orleans, France, 1977.
- Sauty, J. P., Contribution à l'identification des paramètres de dispersion dans les aquifères par interprétation des expériences de tracage, dissertation, Univ. Sci. et Med. et Inst. Natl. Polytech. de Grenoble, Grenoble, France, 1977.
- Sauty, J. P., An analysis of hydrodispersive transfer in aquifers, *Water Resour. Res.*, 16(1), 145-158, 1980.
- Sauty, J. P., A. C. Gringarten, and P. A. Landel, The effects of thermal dispersion on injection of hot water in aquifers, paper presented at *Invitational Well-Testing Symposium*, Lawrence Berkeley Lab., Berkeley, Calif., 1978.
- Segol, G., and G. F. Pinder, Transient simulation of saltwater intrusion in southeastern Florida, *Water Resour. Res.*, 12(1), 65-70, 1976.
- Sudicky, E. A., J. A. Cherry, and E. O. Frind, Migration of contaminants in groundwater at a landfill: A case study, 4, A natural-gradient dispersion test, *J. Hydrol.*, 63, 81-108, 1983.
- Sykes, J. F., S. B. Pahwa, R. B. Lantz, and D. S. Ward, Numerical simulation of flow and contaminant migration at an extensively monitored landfill, *Water Resour. Res.*, 18(6), 1687-1704, 1982.
- Sykes, J. F., S. B. Pahwa, D. S. Ward, and D. S. Lantz, The validation of SWENT, a geosphere transport model, in *Scientific Computing*, edited by R. Stapleman et al., pp. 351-361, IMAES/North-Holland, Amsterdam, 1983.
- Vaccaro, J. J., and E. L. Bolke, Evaluation of water quality characteristics of part of the Spokane aquifer, Washington and Idaho, using a solute transport digital model, *U.S. Geol. Surv. Open File Rep.*, 82-769, 1983.
- Valocchi, A. J., P. V. Roberts, G. A. Parks, and R. L. Street, Simulation of the transport of ion-exchanging solutes using laboratory-determined chemical parameter values, *Ground Water*, 19(6), 600-607, 1981.
- Walter, G. B., Convergent flow tracer test at H-6: Waste isolation pilot plant (WIPP), southeast New Mexico (draft), Hydro Geochem, Inc., Tucson, Ariz., 1983.
- Webster, D. S., J. F. Procter, and J. W. Marine, Two-well tracer test in fractured crystalline rock, *U.S. Geol. Surv., Water Supply Pap.*, 1544-I, 1970.
- Welty, C., and L. W. Gelhar, Evaluation of longitudinal dispersivity from tracer test data, *Rep. 320*, Ralph M. Parsons Lab. for Water Resour. and Hydrodyn., Mass. Inst. of Technol., Cambridge, 1989.
- Werner, A., et al., Nutzung von Grundwasser für Wärmepumpen, Versickerungstest Aeffigen, Versuch 2, 1982/83, Water and Energy Manage. Agency of the State of Bern, Switzerland, 1983.
- Wheatcraft, S. W., and S. W. Tyler, An explanation of scale-dependent dispersivity in heterogeneous aquifers using concepts of fractal geometry, *Water Resour. Res.*, 24(4), 566-578, 1988.
- Wiebenga, W. A., et al., Radioisotopes as groundwater tracers, *J. Geophys. Res.*, 72(16), 4081-4091, 1967.
- Wilson, L. G., Investigations on the subsurface disposal of waste effluents at inland sites, *Res. Develop. Progress Rep. 650*, U.S. Dep. of Interior, Washington, D. C., 1971.
- Wood, W., A geochemical method of determining dispersivity in regional groundwater systems, *J. Hydrol.*, 54(1/3), 209-224, 1981.
- Wood, W. W., and G. G. Ehrlich, Use of baker's yeast to trace microbial movement in ground water, *Ground Water*, 16(6), 398-403, 1978.

L. W. Gelhar, Ralph M. Parsons Laboratory, Department of Civil Engineering, Massachusetts Institute of Technology, Cambridge, MA 02139.

K. R. Rehfeldt, Illinois State Water Survey, 2204 Griffith Drive, Champaign, IL 61820.

C. Welty, Department of Civil and Architectural Engineering, Drexel University, Philadelphia, PA 19104.

(Received April 8, 1991;
revised March 4, 1992;
accepted March 12, 1992.)

ATTACHMENT 13

**HYDROGEOLOGIC ASSESSMENT REPORT
FLY ASH POND AND BOTTOM ASH POND
MEREDOSIA POWER STATION
800 SOUTH WASHINGTON STREET
MEREDOSIA, ILLINOIS**

Prepared for:

AMERENENERGY MEDINA VALLEY COGEN, LLC
St. Louis, Missouri

Prepared by:

GEOTECHNOLOGY, INC.
St. Louis, Missouri

Project No. J024917.01

December 13, 2016





HYDROGEOLOGIC ASSESSMENT REPORT
FLY ASH POND AND BOTTOM ASH POND
MEREDOSIA POWER STATION
800 SOUTH WASHINGTON STREET
MEREDOSIA, ILLINOIS

TABLE OF CONTENTS

	<u>Page</u>
1.0 INTRODUCTION	1
2.0 PHYSICAL SETTING	2
3.0 REGIONAL GEOLOGY	2
3.1 Bedrock Stratigraphy	2
3.2 Surficial Geology	3
3.3 Surface Water.....	3
3.4 Groundwater	4
3.4.1 Private Water Supply Wells.....	5
3.4.2 Public Water Supply Wells.....	5
3.4.3 Oil and Gas Wells	5
4.0 SUBSURFACE INVESTIGATION.....	6
4.1 Subsurface Investigations	6
4.2 Subsurface Conditions	7
5.0 HYDROGEOLOGY	8
5.1 Groundwater Classification	8
5.2 Groundwater Monitoring	8
5.3 Groundwater Flow	8
5.4 Groundwater Geochemistry	8
5.5 Contaminants of Concern	9
5.6 Groundwater Modeling.....	10
5.6.1 HELP Model	10
5.6.2 MODFLOW and MT3DMS	10
5.6.3 Boron and Arsenic Loading to the Illinois River.....	11
6.0 CONCLUSIONS.....	13
7.0 REFERENCES	13
8.0 LICENSED PROFESSIONAL SIGNATURE/SEAL	15

HYDROGEOLOGIC ASSESSMENT REPORT
FLY ASH POND AND BOTTOM ASH POND
MEREDOSIA POWER STATION
800 SOUTH WASHINGTON STREET
MEREDOSIA, ILLINOIS

TABLE OF CONTENTS

-continued-

TABLES

	<u>Table</u>
Water Supply Well Summary	1
Groundwater Gauging Data Summary	2
Analytical Data Summary.....	3

ILLUSTRATIONS

	<u>Plate</u>
Site Location and Topography.....	1
Site Plan and Boring/Monitoring Well Locations	2
Bedrock Geology Map.....	3
Potable Water Well Search Radius	4
Subsurface Stratigraphy Cross Section Plan.....	5
Generalized Subsurface Profile - Section A-A'	6
Generalized Subsurface Profile - Section B-B'	7
Groundwater Elevation Contours – November 2010.....	8
Groundwater Elevation Contours – December 2010.....	9
Groundwater Elevation Contours – September 2011	10
Groundwater Elevation Contours – October 2011.....	11
Groundwater Elevation Contours – March 2012	12
Groundwater Elevation Contours – June 2012	13
Groundwater Elevation Contours – September 2012	14
Groundwater Elevation Contours – August 2015.....	15
Groundwater Elevation Contours – December 2015.....	16
Groundwater Elevation Contours – February 2016.....	17
Boron Concentration Map – August 2015	18
Boron Concentration Map – December 2015	19
Boron Concentration Map – February 2016	20
Arsenic, Iron, and Manganese Analytical Results – February 2016.....	21



J024917.01

HYDROGEOLOGIC ASSESSMENT REPORT
FLY ASH POND AND BOTTOM ASH POND
MEREDOSIA POWER STATION
800 SOUTH WASHINGTON STREET
MEREDOSIA, ILLINOIS

TABLE OF CONTENTS

-continued-

APPENDICES

	<u>Appendix</u>
Potable Water Well Data	A
Boring Logs	B
Statistical Analysis Plots.....	C
HELP Groundwater Model Data	D
MODFLOW and MT3DMS Model Data	E
Illinois River Loading Data	F

HYDROGEOLOGIC ASSESSMENT REPORT
FLY ASH POND AND BOTTOM ASH POND
MEREDOSIA POWER STATION
800 SOUTH WASHINGTON STREET
MEREDOSIA, ILLINOIS

1.0 INTRODUCTION

AmerenEnergy Median Valley Cogen, LLC (Ameren) has retained Geotechnology, Inc. (Geotechnology) to provide design services for the closures of a fly ash pond and a bottom ash pond at their Meredosia, Illinois power station. We understand that the closure rules for the Meredosia ash ponds are similar to those defined for ash pond closures at Ameren's Hutsonville Power Station - Hutsonville, Illinois in January 2011 under Illinois Administrative Code (IAC) Title 35, Part 840, Subpart A: *Closure of Ash Pond D, Hutsonville Power Station*. These rules address the hydrogeologic site investigation, groundwater monitoring, groundwater collection and discharge, final slopes and stabilization, final cover system, closure plan, and post-closure maintenance and care.

The Meredosia Power Station in Morgan County, Illinois is owned by AmerenEnergy Medina Valley Cogen, LLC and operated by the Ameren Energy Generating Company from 1948 to 2011, when the power station was closed. The Meredosia Power Station has three coal combustion product impoundments including: the Bottom Ash Pond, the Fly Ash Pond and the Old Ash Pond. The Old Ash Pond was previously closed.

This document comprises the Hydrogeologic Assessment and includes a review and update of previous hydrogeologic assessment documents prepared by others for the Meredosia Power Station. Additionally, subsurface data collected from the October 2015 subsurface investigation and monitoring well installation activities are incorporated into this assessment. Hydrogeologic assessment data was compiled from previously presented information including the March 2013 Phase I Hydrogeological Assessment Report prepared by Natural Resource Technology Environmental Consultants (NRT)¹ and the November 2009 Site Characterization and Groundwater Monitoring Plan for CCP Impoundments prepared by Rapps Engineering and Applied Science (Rapps)².

¹ *Phase I Hydrogeological Assessment Report, Coal Combustion Product Impoundments, Meredosia Power Station, Morgan County, Illinois*; prepared by Natural Resource Technology, Inc. for Ameren Energy Generating Company; Project No. 2124, dated March 19, 2013.

² *Site Characterization and Groundwater Monitoring Plan For CCP Impoundments, Ameren Energy Generating Company, Meredosia Power Station, Morgan County, Illinois*; prepared by Rapps Engineering and Applied Science for Ameren Services; dated November 2009.

2.0 PHYSICAL SETTING

The Meredosia Power Station is located at 800 South Washington Street, Meredosia, Illinois. The Fly Ash and Bottom Ash Ponds are located southwest of the former coal pile and plant facilities. The site location and topography are shown on Plate 1. An aerial photograph site plan showing existing structures, ash ponds, and monitoring well/boring locations is included as Plate 2. The Meredosia Power Station is located in the floodplain of the Illinois River which borders the site to the west.

The Meredosia Power Station ash ponds are located in the south half of Section 21 and the north half of Section 28, T.16N, R.13W. The Bottom Ash Pond was constructed in 1972 with a design surface area of 11 acres, a height of 24 feet, and a volume of approximately 90 acre-feet. The Fly Ash Pond was constructed in 1968 and has a design surface area of 44.8 acres, a height of 24 feet, and a volume of approximately 500 acre-feet.

3.0 REGIONAL GEOLOGY

The Meredosia Power Station is located near the western edge of the Springfield Plain Subsection of the Till Plains Section, Central Lowland Province, Interior Plains Physiographic Region. The Interior Plains Physiographic Region extends across the Laurentian craton of central North America. It is comprised of the Great Plains and Central Lowland Provinces. The Central Lowlands Province to the east formed from eroded sediments from the topographically-higher Great Plains Province to the west (Fenneman, 1922).

The Till Plains Section of the Central Lowland Province is subdivided into seven areas in Illinois. Four of the subdivisions are in Illinoian-aged drift (Willman et al., 1975). The Springfield Plain comprises the western half of the Illinoian-aged till plain. It is level to undulatory and exhibits relatively shallow drainages. The southern boundary is observed where the drift thins and the underlying bedrock control becomes prominent. It is characterized by smoothed features and glacial landforms. The Illinois River forms the northwestern border of the Springfield Plain.

3.1 Bedrock Stratigraphy. The Meredosia Power Station and surrounding areas within the Illinois River valley are underlain by Mississippian System bedrock of the Lower Valmeyeran Series which consists of the Meppen Limestone, Fern Glen formation, and the Burlington-Keokuk Limestone (Kolata, 2005). A bedrock geology map of the site and surrounding areas is included as Plate 3.

Willman et al. (1975) describe the Meppen Limestone as a tan or buff, very fine-grained dolomitic limestone or calcareous dolomite. The formation is slightly crinoidal and contains calcite geodes up to 2-inches in diameter. The maximum thickness of this formation is

approximately 22 feet. The Fern Glen formation consists of calcareous shale, limestone, and dolomite. Dolomitic portions of the formation are partially argillaceous. The limestone portions of the formation contain nodules of greenish-gray chert. The thickness of the formation can range from approximately 50 to 100 feet. The Burlington formation of the Burlington-Keokuk Limestone is described as a “very pure, coarsely crystalline, crinoidal, light gray limestone in medium to thick beds.” The Burlington formation also contains beds of fine-grained, brownish-gray, dolomitic limestone. The formation is approximately 100 to 150 feet thick in Illinois. The Keokuk formation of the Burlington-Keokuk Limestone is composed of beds of fossiliferous, crinoidal limestone interbedded with fine-grained limestone, argillaceous dolomite, and calcareous gray shale. The Keokuk formation is approximately 60 to 80 feet thick in Illinois.

3.2 Surficial Geology. The Meredosia Power Station is situated within the Illinois River valley. The overburden soils consist of channel and floodplain deposits of the Cahokia formation underlain by glacial outwash deposits belonging to the Henry formation. Fine-grained lacustrine deposits of the Equality formation are present in the subsurface, but are discontinuous. These formations occur throughout Illinois in valley bottoms and floodplains as channel deposits in present-day rivers and streams.

The Cahokia Alluvium consists mainly of poorly-sorted silt, clay, and silty sand, but locally contains lenses of sand and gravel. The upper part consists of overbank silt and clays. The lower portion consists of coarse-textured sand and lateral accretion deposits. The Cahokia formation may be up to 20 feet thick in the area of the Meredosia Power Station (Berg and Kempton, 1987).

The Henry formation consists of glacial sand and gravel outwash. The Henry formation is subdivided into three members that differ in lithology: the Batavia Member (outwash plains), the Mackinaw Member (valley trains), and the Wasco Member (ice-contact deposits) (Willman and Frye, 1970; Willman et al., 1975). Based on information from well logs, the thickness of the Henry formation ranges from 60 to 84 feet in the area of the Meredosia Power Station.

The Equality formation consists of bedded silt and clay deposits in glacial and post-glacial lakes. Gravel, sand, and organic deposits occur in lenses that intertongue with the Henry formation. In the area of the Meredosia Power Station, the Equality formation overlies the Henry formation and generally occurs as lenses or patches not exceeding 20 feet thick.

Geotechnology has conducted subsurface explorations of the overburden soils at the Meredosia Power Station. The subsurface exploration and laboratory testing efforts are discussed further in Section 4.0.

3.3 Surface Water. The major surface water body in the vicinity of the Meredosia Power Station is the Illinois River, which flows from the north-northeast to the south-southwest, and borders the west side of the site. The normal pool elevation of the Illinois River is approximately



421.0 feet³. Information from the U.S. Army Corps of Engineers indicates the Illinois River flood stage is 435.0 feet above mean sea level (MSL). The record high stage was 446.69 feet above MSL on May 26, 1943, and the record low stage was 418.40 feet above MSL on January 11, 1940.

Meredosia Lake is a backwater lake located north of the Village of Meredosia within the Illinois River valley and within the Meredosia National Wildlife Refuge. Meredosia Lake is approximately 1.5 miles north of the Meredosia Power Station. Smith Lake is located approximately 1-mile south of the Meredosia Power Station and is connected to Seaman’s Pond. Westerly-flowing streams drain the uplands to the east of the Meredosia Power Station. Easterly-flowing streams and drainage channels drain the floodplain across the Illinois River to the west of the Meredosia Power Station.

3.4 Groundwater. Groundwater within and near the Illinois River valley is obtained from the sand and gravel deposits of the Henry formation and to a lesser extent from wells drilled into the Mississippian-age Burlington-Keokuk Limestone and Salem Limestone. A summary of the water supply wells identified within 1-mile of the Meredosia Power Station is presented in Table 1 below. The water supply well information is included as Appendix A. The approximate locations of the water supply wells are depicted on Plate 4.

TABLE 1 – WATER SUPPLY WELL SUMMARY				
Owner	Wells	On/Off Site	Type	Status
CIPS*	42	On Site	Water Supply	Abandoned (except 4)
National Starch	15	Off Site	Water Supply	Unknown
Village of Meredosia	6	Off Site	Public Supply	In Use
IDOT	4	Off Site	Test Borings	Not Wells
W.R. Grace	2	Off Site	Water Supply	Unknown
T.A. Terminal	2	Off Site	Water Supply	Unknown
Illinois Road Contractors	1	Off Site	Water Supply	Unknown

*Central Illinois Public Service Company

The water supply wells were located using the Illinois State Geological Survey (ISGS) *Illinois Water Well (ILWATER) Internet Map Service*, the Illinois State Water Survey’s *Domestic Wells Database*, the Illinois Environmental Protection Agency (IEPA) web-based Geographic Information System (GIS) files, Illinois Department of Health (IDPH) records, and Morgan County Health Department records.

³ Elevations herein refer to the mean sea level datum in feet (msl-ft).

3.4.1 Private Water Supply Wells. Approximately 62 private water supply wells and 4 non-well test borings were identified within 1-mile of the Meredosia Power Station. Twenty of the private water supply wells are off-site. The status of the wells are unknown at this time, but are assumed to be in-use. The twenty off-site private water supply wells are up-gradient or cross-gradient from the site and are not anticipated to be impacted from the site. Groundwater sampling and testing results further support that the twenty off-site water supply wells are not expected to be impacted.

The other 42 private water supply wells are located at the Meredosia Power Station. According to site records, personnel interviews, and field reconnaissance, 38 of the on-site water supply wells have been abandoned. Two wells are no longer used, but have not been abandoned. One well is shut down and one currently supplies water to the restrooms/showers on the site. Once the former power plant is demolished and the ash pond closure activities are complete, these four supply wells will be abandoned in accordance with 77 Illinois Administrative Code 920.120. Additional water needs at the Meredosia Power Station are provided by the Village of Meredosia public water supply.

3.4.2 Public Water Supply Wells. According to the mapping sources referenced in Section 3.4.1, public water supply wells are not located within 1-mile of the Meredosia Power Station. The closest public water supply wells to the Meredosia Power Station belong to the Village of Meredosia. The six public water supply wells are situated approximately 1.2 miles to the north-northeast. Although the wells are beyond 1-mile from the facility, the locations are depicted on Plate 4 and the water supply well information is included in Appendix A for reference.

Per the IEPA database, two of the Village of Meredosia public water supply wells have a minimum setback of 400 feet and a second setback of 1,000 feet due to the Phase I Wellhead Protection Area (WHPA). A third Village of Meredosia public water supply well has a Phase II WHPA, which has an extended area of protection that includes the recharge area or geographic area surrounding the well that supplies potable water to a community.

3.4.3 Oil and Gas Wells. Oil and gas wells within a 1-mile radius of the Meredosia Power Station were identified using the Illinois State Geological Survey *Illinois Oil and Gas Resources (ILOIL) Internet Map Service*. ILOIL contained records for three wells within the search radius, but the status of the three wells was listed as dry, abandoned and plugged.

4.0 SUBSURFACE INVESTIGATION

4.1 Subsurface Investigations. From October 19 through October 26, 2010, Geotechnology advanced 15 borings at the Meredosia Power Station. Ten of the borings (B-1 through B-10) were drilled in support of a global stability evaluation, while the remaining five borings were completed as Monitoring Wells APW-1 through APW-5 in support of groundwater monitoring activities. The borings were drilled using a truck-mounted CME 550 rotary drill rig equipped with 4-1/4-inch hollow stem augers. The borings were drilled to depths ranging from 25 to 60 feet below land surface (bls). Standard Penetration Tests (SPT) were performed using an automatic hammer and split spoon sampler. The locations of the borings and monitoring wells are included on Plate 2.

From September 28 through October 1, 2015, Geotechnology advanced four additional borings at the site using a truck-mounted CME 550 rotary drill rig equipped with 4-1/4-inch hollow stem augers. The borings were drilled to depths ranging from 17 to 40 feet bls. SPTs were performed using an automatic hammer and split spoon sampler. Monitoring Wells APW-6 through APW-9 were installed in the borings in support of ongoing groundwater monitoring activities. Copies of the boring logs are included as Appendix B. The locations of the monitoring wells are included on Plate 2.

Monitoring Wells APW-6 through APW-9 were constructed using 10 feet of 2-inch-diameter 0.010-inch slotted PVC screen and riser to the surface. The monitoring wells were completed at the surface with above-ground steel covers set in a concrete pad. The monitoring wells were developed in accordance with industry practice and registered with the IDPH and the IEPA.

An engineer from Geotechnology provided technical direction during field exploration, observed drilling and sampling, assisted in obtaining samples and prepared descriptive logs of the material encountered. The boring logs represent conditions observed at the time of exploration.

Unless noted on the boring logs, the lines designating the changes between various strata represent approximate boundaries. The transition between materials may be gradual or may occur between recovered samples. The stratification given on the boring logs, or described herein, is for use by Geotechnology in its analyses and should not be used as the basis of design or construction cost estimates without realizing that there can be variation from that shown or described.

4.2 Subsurface Conditions. Native soils consisting of brown and gray, very soft to medium stiff, silt and clay were encountered below the fill in Boring B-1 and Monitoring Well APW-9, and at the ground surface in Boring B-5. Native soils consisting of black, clayey sand with trace gravel were encountered below the fill in Boring B-2.

A stratum of very soft to medium stiff, brown, black, and gray clay with traces of sand and wood was encountered below the fill in Borings B-3 and B-8, below the native soils in Borings B-1, B-2, and B-5, and at the ground surface in Borings B-4, B-9, APW-2, APW-3, APW-4, and APW-7. This soil stratum ranged in thickness from approximately 8 to 17 feet bls.

The clay layer described above was underlain by a stratum of granular and cohesive alluvial soils (except for Boring APW-4). The granular alluvium generally consisted of loose, gray, clayey sand with gravel. The cohesive alluvium generally consisted of very soft to medium stiff, gray and brown, clayey silt, silty clay, and sandy clay. This soil stratum ranges in thickness from approximately 5 to 11 feet bls in borings where it is encountered.

Alluvium was encountered below the fill soils in Borings B-6 and B-7, and at the ground surface in Boring B-10 and Monitoring Wells APW-6 and APW-8. This stratum is interpreted as alluvium placed in a buried valley that had been cut down through the soil stratum described above. The granular portions of this alluvium infill generally consisted of very loose, gray, silty sand. The cohesive portions generally consisted of very soft to very stiff, gray, silty clay with sand and silt seams. This soil stratum was at least 28 feet thick where encountered.

The native soils described above are interpreted as belonging to the Cahokia Alluvium, and were underlain by sand deposits interpreted as belonging to the Henry formation. Generalized east-west and north-south subsurface profiles based on the soil boring data at the Meredosia Power Station are included on Plates 6 and 7, respectively. The plan-view of the subsurface profile orientations is included on Plate 5.

During the subsurface exploration activities, groundwater was observed in Borings B-3, B-4, B-5 and B-6 at depths ranging from approximately 18 to 39 feet bls. Groundwater was observed in Monitoring Wells APW-1 through APW-9 at depths ranging from 6 to 32 feet bls at the time of construction. Groundwater levels might not have stabilized before backfilling or well construction activities. Consequently, the indicated groundwater levels might not represent present or future levels. Groundwater levels could vary over time due to the effects of the Illinois River, seasonal variation in precipitation, or other factors not evident at the time of exploration.

5.0 SITE HYDROGEOLOGY

5.1 Groundwater Classification. The Illinois Class I groundwater standards are applicable to the Meredosia Power Station. The Illinois Class I groundwater is generally defined and groundwater that is capable of being potable.

5.2 Groundwater Monitoring. The groundwater monitoring network at the Meredosia Power Station consists of one up-gradient monitoring well (APW-1) and eight down-gradient monitoring wells (APW-2 through APW-9). The approximate locations of the monitoring wells are included on Plate 2. The monitoring wells are screened in the uppermost aquifer which generally consists of saturated, fine to coarse sand. The monitoring well depths range from 17 to 40 feet bls. Monitoring well construction diagrams from Monitoring Wells APW-1 through APW-9 are included in Appendix B. A total of 11 groundwater monitoring events have been conducted at the Meredosia Power Station since December 2010. The groundwater monitoring events have been conducted quarterly since the third quarter of 2015. Future groundwater monitoring events are anticipated to be conducted quarterly until trend analysis indicates less frequent monitoring is acceptable. A summary of the monitoring well gauging data is included as Table 2. A summary of the groundwater laboratory analytical results collected to date is included as Table 3.

5.3 Groundwater Flow. Based on the monitoring well gauging data in Table 2, the groundwater flow direction at the Meredosia Power Station is to the west-northwest toward the Illinois River. Groundwater flow direction may be influenced by the stage of the Illinois River. Groundwater elevation contour maps for the 10 groundwater monitoring events are included as Plates 8 through 16. These events include a range of climate conditions including flood and dry timeframes. *Note: Only gauging events with data from at least five monitoring wells are included.*

5.4 Groundwater Geochemistry. A total of 11 groundwater sampling events have been conducted at the Meredosia Power Station since December 2010. The parameters analyzed include those listed in Section 5.1 in addition to field parameters pH, specific conductivity, and temperature. The analytical testing data are summarized in Table 3. The historical groundwater data collected prior to 2015 consists of dissolved parameter concentrations only. During the time these data were collected, laboratory analysis for dissolved concentrations was the applicable standard of care. The use of dissolved parameter concentration results in the statistical analysis for this Hydrogeologic Assessment report was the only historical data available for the site and was based on the precedent set by the Hutsonville Ash Pond D Closure which was approved by the IEPA. The recent three quarterly sampling events (3Q15, 4Q15, and 1Q16) were analyzed for both total and dissolved parameter concentrations. The purpose of the dual analysis was to allow historical data to be compared to current data and to prepare for future statistical analysis using total parameter concentrations. *Note: The historical data provided by others did not*

contain practical quantitation limits (PQLs) or method detection limits (MDLs). The PQLs and MDLs from the February 2016 groundwater sampling event were substituted for the missing data during statistical analysis.

The analytical results were compared to the Illinois Class I groundwater standards. Historical concentrations of arsenic exceeded the Class I groundwater standard in Monitoring Wells APW-3 and APW-4. Currently, (as of February 2016) the arsenic concentration exceeded the Class I groundwater standard in APW-3 only. Concentrations of boron exceeded the Class I groundwater standard in Monitoring Wells APW-2, APW-3, APW-4, APW-6, APW-8, and APW-9. Currently, (as of February 2016) the boron concentration exceeded the Class I groundwater standard (2 ppm) in Monitoring Wells APW-2, APW-3, APW-8, and APW-9. Aerial photographs showing the boron concentration contours for September 2015, December 2015, and February 2016 are included as Plates 18 through 20, respectively. Concentrations of manganese exceeded the Class I groundwater standard in Monitoring Wells APW-2, APW-3, and APW-4. Historical concentrations of iron exceeded the Class I groundwater standards in Monitoring Wells APW-3 and APW-4, but the February 2016 results are below the Class I groundwater standard. A single event anomaly associated with flooding in February 2016 resulted in the concentration of sulfate in Monitoring Well APW-9 being above the Class I groundwater standard. The arsenic and manganese exceedances at each monitoring well for the February 2016 sampling event are included on Plate 21. Changes of oxidation/reduction (redox) potential in the subsurface due to fluctuations in pH make evaluation of manganese and iron concentrations unreliable at this facility. Comparison of manganese and iron to the respective Class I groundwater standard may be inappropriate for this site.

Box and whiskers plots of boron and arsenic are included as Appendix C. Statistical trend analysis plots for boron and arsenic are also included in Appendix C. Statistical trends are decreasing or not significant at a 98% confidence level. The analysis indicates that increasing trends may have been present while the Meredosia Power Station was in operation through 2011, but appear to be decreasing based on the three most recent quarterly monitoring data.

5.5 Contaminants of Concern. Boron and arsenic are the contaminants of concern for the Meredosia Power Station and are also the groundwater indicator parameters. Boron and arsenic are widespread across the site and are generally considered good indicator chemicals for ash pond facilities in Illinois. Due to the elevated levels of boron above background levels in the groundwater near the ash ponds on site, boron will be a primary indicator parameter for the site during remedial actions and ash pond closure activities. Boron and arsenic are relatively stable in the subsurface and are not prone to attenuation.

Other chemicals and water quality parameters such as iron, manganese, pH, and TDS can be affected by redox conditions in the subsurface and are therefore not reliable as indicator parameters at this site. The concentrations of other chemicals may naturally fluctuate through attenuation.

5.6 Groundwater Modeling.

Both a two-dimensional and three-dimensional transient groundwater flow and transport model were used to describe the site. The models were calibrated to match the groundwater elevation and concentration trends observed between 2009 and 2015. Prediction simulations were then performed for no action and for proposed ash pond closure activities. The existing conditions model was used to calibrate the hydrogeologic flow and transport conditions and to evaluate the need for the ponds to be closed. The proposed closure conditions model was created to evaluate the length of time for the boron and arsenic concentrations to decrease to below the IEPA Class I Groundwater standards. Boron and arsenic were chosen because they are indicator contaminants for coal ash leachate, are mobile in groundwater, and are widespread in groundwater across the site.

5.6.1 HELP Model

In order to assess the drainage capabilities of the proposed fly ash and bottom ash pond closures, Geotechnology utilized the USEPA Hydrologic Evaluation of Landfill Performance (HELP) model to simulate conditions at the site. The version of software used was HELP 3.07 (November 1997). A description of inputs and output data is attached in Appendix D of this report. For the purposes of this evaluation, the proposed ash pond cap, ash, and soil cross-section has been divided into six layers.

Model parameters for the layers were the default values for each selected layer type as provided by the HELP software module, or were input by the user (for synthetic materials) with known or manufacturer provided parameters. The model was run without groundwater influx parameters.

The model indicates that steady state conditions (<0.05 inches of head on the sand layer) will be achieved within approximately six months of closure activities at the two ash ponds on site. The data obtained from the HELP model was used as input parameters for MODFLOW and MT3DMS.

5.6.2 MODFLOW and MT3DMS

MODFLOW was developed by the United States Geological Survey (USGS) to solve three-dimensional transient head distributions using finite difference approximations. The model inputs include soil properties, multiple layers, heterogeneities, variable thicknesses, variable gradients, flow boundaries, wells, and can define confined or unconfined flow systems. Assumptions of the program include that groundwater is governed by Darcy's law; the formation behaves as a continuous porous medium; flow is not affected by chemical, temperature, or density gradients; and hydraulic properties are constant within a grid cell.

MT3DMS was developed by the USGS and calculates concentration distributions for a single chemical as a function of time and location using a finite difference solution. Concentration is distributed over a three-dimensional, non-uniform, transient flow field. MT3DMS accounts for advection, diffusion, dispersion, sorption, and first order decay. Assumptions of the module include changes in the concentration field do not affect the flow field; concentrations of solutes do not interact with each other; chemical and hydraulic properties are constant within a cell; sorption is instantaneous and fully reversible; and decay is not reversible.

Flow and transport boundaries, soil properties, and river stage fluctuations were the same for the calibration and prediction scenarios. One prediction scenario was no action and the other included the proposed ash pond closures.

Boron and arsenic concentrations for the current configuration were modeled for 25 years into the future to represent a scenario where the ash ponds were not closed. After 25 years, monitoring well APW-3 (the well with historically highest boron concentrations) stabilized at 16.9 mg/L of boron and 0.208 mg/L of arsenic, which exceed the respective Class I Groundwater standards. APW-2, APW-6, APW-7, and APW-8 also exceeded the Class I Groundwater standards for boron and arsenic at 25 years with no action.

According to the closure scenario model results, boron concentrations will be below the Class I Groundwater standards for each well on site within three years after dewatering and closure of the fly ash and bottom ash ponds, and arsenic concentrations will be below the Class I Groundwater standards for each well on site within six years.

Additional information on the MODFLOW and MT3DMS modeling and modeling results are provided in Appendix E.

5.6.3 Boron and Arsenic Loading to the Illinois River

Groundwater in the vicinity of the fly ash and bottom ash ponds discharges to the Illinois River. A mixing calculation was performed to conservatively estimate the boron and arsenic loading rates to the Illinois River. Calculations are provided in Appendix F.

The loading rate was calculated by multiplying the volume of groundwater flowing into the river by the concentration of boron and arsenic in groundwater.

$$\text{Loading Rate (L)} = \text{Concentration (C)} * \text{Groundwater Discharge Volume (Q)}$$

$$\text{Where } Q = \text{Hydraulic Conductivity (K)} * \text{Hydraulic Gradient (I)} * \text{Area (A)}$$

To be conservative, the highest single concentration in groundwater monitoring wells at the site was initially used in this calculation (C_{max}). A second calculation was performed using the average of the four monitoring wells near the river (APW-2, APW-3, APW-4, and APW-9).

The monitoring wells were not tested for hydraulic conductivity; however, Gibb et al. (1979) published hydraulic conductivity values for wells along the Illinois waterway, which included a site-specific value of 1,200 gallons per day/square foot (gpd/ft²). Both a maximum and an average hydraulic gradient were used. The average hydraulic gradient was based on the ten groundwater gauging events. Two groundwater gauging events were not used because of flooding and inaccessibility of the wells. Removing flooding events provides a more conservative value. The cross sectional area was assumed to be over the entire thickness of the aquifer, and along the entire length of the Fly Ash Pond parallel to the river, plus 50 feet north and south of the pond.

The calculated loading rate was divided by: 1) the 7-day 10-year low flow (Q_{7,10}); and 2) the mean of the average annual flow data at the Meredosia gaging station. This calculation estimates the incremental concentration increase (dB) in the river due to discharge from the Fly Ash Pond. Due to the size of the Illinois River, it is unlikely that boron and arsenic concentrations would initially be distributed across the entire width of the river. Therefore, an additional calculation was performed to determine the incremental concentration increase assuming that mixing occurred within 50 feet of the shoreline. This calculation was performed by multiplying dB by 750 feet/50 feet (750 feet being total river width and 50 feet being the assumed mixing width).

The result of the boron calculation is an incremental increase of 0.0061 mg/L calculated using average concentration, average hydraulic gradient, and mean annual river discharge. This is near the reporting limit for boron as listed by the USEPA in method SW-846, 6010c and below the Public and Food Processing Water Supply Standard of 1.0 mg/L. (35 IAC 302.304). The result of the boron calculation; based on maximum concentration, maximum hydraulic gradient, and the Q_{7,10}; is a conservative estimate of the increase in boron loading to the Illinois River. This result (0.23 mg/L) suggests that a measurable boron increase could occur near shore for worst case conditions at low flow. This value is below the Public and Food Processing Water Supply Standard.

The boron concentrations were calculated at three years after dewatering and closure, which was the time period when boron concentrations were calculated to be below the Class I Groundwater Standards. The calculation indicated potential increases of 0.00014 mg/L and 0.0057 mg/L for the average and worst case conditions, respectively. Both values are below the Public and Food Processing Water Supply Standard of 1.0 mg/L.

The arsenic concentrations were calculated at six years after dewatering and closure, which was the time period when arsenic concentrations were calculated to be below the Class I Groundwater Standards. The calculation indicated potential increases of 0.0000010 mg/L and 0.000045 mg/L for the average and worst case conditions, respectively. Both values are below the Public and Food Processing Water Supply Standard of 1.0 mg/L.

The calculated impacts to the Illinois River for both boron and arsenic are below typical detection limits for analytical testing.

6.0 CONCLUSIONS

Although up to 11 groundwater monitoring events have been conducted at the Meredosia Power Station since December 2010, only three monitoring events have been conducted since the facility ceased operations in 2011. Therefore, statistical analysis of post-closure trends could not be performed. The groundwater analytical and statistical data indicates that the unlined ash ponds are a primary contributor to groundwater impacts based on the location of groundwater exceedances, the types of chemicals common to coals ash exceeding the applicable Class I groundwater standards, gradual reduction of groundwater impacts after plant closure, and contaminant transport modeling. The preliminary data suggests that a reduction in the concentrations of boron and arsenic has occurred since the facility ceased operations. The results of the groundwater modeling further support this preliminary assessment. When the ash ponds are capped the primary pathway (storm water infiltration) for contaminants to impact the groundwater at the site will not be complete. Groundwater modeling indicates that within six years of dewatering and closure, boron and arsenic levels in the residual plume will be below the Class I Groundwater standards.

Additional groundwater monitoring events are planned to further assess the extent of the impacts of ash pond capping activities. Future monitoring events will be sampled for the parameters in accordance with the Meredosia Power Station Groundwater Monitoring Plan (GMP, 2016).

7.0 REFERENCES

Natural Resource Technology Environmental Consultants, Phase I Hydrogeological Assessment Report, Coal Combustion product Impoundments, Meredosia Power Station, Morgan County, Illinois, March 19, 2013.

Rapps Engineering and Applied Science, Site Characterization and Groundwater Monitoring Plan For CCP Impoundments, Ameren Generating Company – Meredosia Power Station, Meredosia, Illinois, November 2009.

Bergstrom, R.E. and Zeisel, A.J. (1957). Groundwater Geology in Western Illinois, South Part: A Preliminary Geologic Report. Illinois State Geological Survey, Circular 232, 28 p.

Collinson, C. (1964). Western Illinois: 28th Ann. Tri-State Field Conf., Quincy, Ill., Ill. Geol. Surv. Guidebook Ser. 6, 30 p.

Fenneman, N. M. (1922). Physiographic provinces and sections in western Oklahoma and adjacent parts of Texas, in United States Geological Survey, *Contributions to Geography of the United States*, 1922.

Freeze, R.A. and Cherry, J.A. (1979). Groundwater. Prentice-Hall, Inc., Englewood Cliffs, N.J. 604 p.

Warner, K.L. (2001). Water-quality assessment of the Lower Illinois River Basin: environmental setting.

Willman, H.B. and Frye, J.C. (1970). Pleistocene Stratigraphy of Illinois: Illinois State Geological Survey, Bulletin 94, 204 p.

Willman, H.B., Atherton, E., Buschbach, T.C., Collinson, C., Frye, J.C., Hopkins, M.E., Lineback, J.A., and Simon, J.A. (1975). Handbook of Illinois Stratigraphy: Illinois State Geological Survey, Bulletin 95, 261 p.

Woller, D.M. (1974). Public Groundwater Supplies in Brown County. Illinois State Water Survey Bulletin 60-5, Urbana, 4 p.

Woller, D.M. and Sanderson, E.W. (1979). Public Groundwater Supplies in Morgan and Scott Counties. Illinois State Water Survey Bulletin 60-27, Urbana, 20 p.

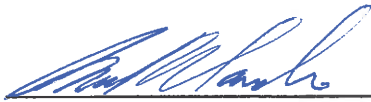
Woller, D.M., Kunz, K.L., and Sanderson, E.W. (1979). Public Groundwater Supplies in Pike County. Illinois State Water Survey Bulletin 60-26, Urbana, 20 p.

Geotechnology, Inc., Groundwater Monitoring Plan, Meredosia Power Station, Ameren, 2016.

Geotechnology, Inc., Groundwater Management Zone Plan, Meredosia Power Station, Ameren, 2016.

8.0 LICENSED PROFESSIONAL SIGNATURE/SEAL

I hereby affirm that the information and design documents contained in this hydrogeologic assessment report are true and accurate to the best of my knowledge and professional opinion.



Rosanna M. Saindon, P.E., Ph.D.
Illinois Licensed Professional Engineer
Project Manager
Geotechnology, Inc.



TABLE 1

J024917.01

**MONITORING WELL SURVEY DATA
MEREDOSIA POWER STATION
MEREDOSIA, ILLINOIS**

Well ID (feet)	Northing (feet)	Easting (feet)	Elevation (feet)		
			Top Vault	Top Casing	Ground
APW-1	1147018.68	2185605.20	449.581	449.261	446.062
APW-2	1148489.69	2182485.19	437.528	436.869	433.966
APW-3	1148118.60	2181973.76	436.782	436.281	433.345
APW-4	1146935.94	2181602.97	435.198	434.859	431.897
APW-5	1146922.64	2183711.11	453.652	453.197	450.476

Coordinates are referenced to Illinois State Plane Coordinates, East Zone - NAD 1983
Elevations are referenced to NAVD 1988

TABLE 2

**MONITORING WELL DATA SUMMARY
MEREDOSIA POWER STATION
MORGAN COUNTY, ILLINOIS**

Well ID	Ground Surface Elevation	Bottom of Well Elevation	Screen Length (ft)	Top of Casing Elevation ¹	Groundwater Measurements		
					Date	Depth to Water (ft)	Groundwater Surface Elevation
APW-1	446.06	420.90	10.00	449.26	11/17/10	18.35	430.91
					12/13/10	19.15	430.11
					03/14/11	18.30	430.96
					06/24/11	10.80	438.46
					09/15/11	17.30	431.96
					10/28/11	19.60	429.66
					03/26/12	21.55	427.71
					06/18/12	21.34	427.92
					09/17/12	23.45	425.81
					08/25/15	12.10	437.16
					12/21/15	18.22	431.04
APW-2	433.97	410.60	10.00	436.87	02/18/16	13.54	435.72
					11/17/10	13.00	423.87
					12/13/10	13.14	423.73
					03/14/11	8.30	428.57
					09/15/11	12.65	424.22
					10/28/11	13.60	423.27
					03/26/12	13.27	423.60
					06/18/12	14.46	422.41
					09/17/12	15.59	421.28
					08/25/15	9.67	427.20
					12/21/15	9.05	427.82
APW-3	433.35	410.30	10.00	436.28	02/18/16	8.21	428.66
					11/17/10	13.52	422.76
					12/13/10	13.35	422.93
					03/14/11	5.70	430.58
					09/15/11	13.90	422.38
					10/28/11	14.60	421.68
					03/26/12	12.80	423.48
					06/18/12	13.95	422.33
					09/17/12	15.92	420.36
					08/25/15	11.10	425.18
					12/21/15	4.79	431.49
APW-4	431.90	405.80	6.50	434.86	02/18/16	8.74	427.54
					11/17/10	9.15	425.71
					12/13/10	9.25	425.61
					09/15/11	9.20	425.66
					10/28/11	10.00	424.86
					03/26/12	9.90	424.96
					06/18/12	10.95	423.91
					09/17/12	12.36	422.50
					08/25/15	6.13	428.73
					12/21/15	5.47	429.39
					02/18/16	4.92	429.94
APW-5	450.48	420.20	10.00	453.20	12/21/15	21.90	430.00
					11/17/10	25.60	427.60
					12/13/10	25.40	427.80
					03/14/11	22.60	430.60
					06/24/11	14.70	438.50
					09/15/11	23.40	429.80
					10/28/11	24.50	428.70
					03/26/12	27.20	426.00
					06/18/12	27.30	425.90
					09/17/12	29.18	424.02
					08/25/15	18.55	434.65
APW-6	448.60	420.60	9.68	451.90	12/21/15	23.68	429.52
					02/18/16	19.42	433.78
APW-7	435.00	418.50	9.70	438.70	02/18/16	18.35	433.55
					12/21/15	9.15	429.55
APW-8	460.50	421.40	9.68	463.90	02/18/16	6.95	431.75
					12/21/15	34.56	429.34
APW-9	445.00	415.70	9.68	448.10	02/18/16	31.60	432.30
					12/21/15	18.23	429.87
					02/18/16	17.76	430.34

¹Elevations reported in feet above mean sea level.

TABLE 3
GROUNDWATER ANALYTICAL DATA SUMMARY
MEREDOSIA POWER STATION
MEREDOSIA, ILLINOIS

WELL ID	SAMPLE DATE	PARAMETER												
		Antimony (d)	Arsenic (d)	Arsenic (t)	Barium (d)	Barium (t)	Beryllium (d)	Beryllium (t)	Boron (d)	Boron (t)	Cadmium (d)	Cadmium (t)	Chloride (d)	Chromium (d)
APW-1	12/13/2010	<0.006	<0.004	NA	<0.005	NA	<0.004	NA	<0.004	NA	<0.004	NA	<0.004	1
	5/24/2011	<0.003	<0.001	NA	0.01	NA	<0.001	NA	0.13	NA	<0.001	NA	<0.004	5.6
	5/24/2011	<0.003	<0.001	NA	0.017	NA	<0.001	NA	0.14	NA	<0.001	NA	<0.004	13
	10/28/2011	<0.003	<0.001	NA	0.019	NA	<0.001	NA	0.098	NA	<0.001	NA	<0.004	6.8
	3/26/2012	<0.003	<0.001	NA	0.011	NA	<0.001	NA	0.11	NA	<0.001	NA	<0.004	20
	6/18/2012	<0.003	<0.001	NA	0.02	NA	<0.001	NA	0.097	NA	<0.001	NA	<0.004	45
	9/17/2012	<0.003	<0.001	NA	0.013	NA	<0.001	NA	0.055	NA	<0.001	NA	<0.004	39
	8/25/2015	<0.001	<0.001	0.004	0.014	0.032	<0.0005	<0.0005	0.066	0.071	<0.002	<0.002	54	<0.005
	12/21/2015	<0.001	<0.001	0.003	0.014	0.03	<0.0005	<0.0005	0.074	0.079	<0.002	<0.002	62	<0.005
	2/18/2016	<0.004	0.004	0.004	0.012	0.06	<0.0005	<0.0005	0.112	0.076	<0.002	<0.002	50	<0.005
APW-2	12/13/2010	<0.006	0.004	NA	<0.005	NA	<0.004	NA	2.11	NA	<0.004	NA	<0.004	33
	3/24/2011	<0.003	NA	0.004	NA	0.055	NA	<0.001	NA	<0.001	NA	50	<0.004	50
	9/15/2011	<0.003	NA	0.003	NA	0.042	NA	<0.001	NA	<0.001	NA	41	<0.004	41
	10/28/2011	<0.003	NA	0.004	NA	0.045	NA	<0.001	NA	<0.001	NA	42	<0.004	42
	3/26/2012	<0.003	NA	0.004	NA	0.046	NA	<0.001	NA	<0.001	NA	47	<0.004	47
	6/18/2012	<0.003	NA	0.004	NA	0.051	NA	<0.001	NA	<0.001	NA	50	<0.004	50
	9/17/2012	<0.003	NA	0.004	NA	0.048	NA	<0.001	NA	<0.001	NA	44	<0.004	44
	10/28/2011	<0.003	NA	0.004	NA	0.048	NA	<0.001	NA	<0.001	NA	44	<0.004	44
	12/21/2015	<0.001	<0.001	0.002	0.003	0.074	0.093	<0.0005	<0.0005	2.05	<0.002	<0.002	36	<0.005
	2/18/2016	<0.001	0.007	0.001	0.014	0.057	0.0654	<0.0005	<0.0005	2.66	<0.002	<0.002	30	<0.005
APW-3	12/13/2010	<0.006	0.148	NA	<0.005	NA	<0.001	NA	30.2	NA	<0.004	NA	54.5	<0.001
	3/24/2011	<0.003	0.17	NA	0.05	NA	<0.001	NA	28	NA	<0.001	NA	54	<0.004
	9/15/2011	<0.003	0.21	NA	0.042	NA	<0.001	NA	32	NA	<0.001	NA	44	<0.004
	10/28/2011	<0.003	0.22	NA	0.045	NA	<0.001	NA	35	NA	<0.001	NA	47	<0.004
	3/26/2012	<0.003	0.19	NA	0.048	NA	<0.001	NA	31	NA	<0.001	NA	54	<0.004
	6/18/2012	<0.003	0.31	NA	0.041	NA	<0.001	NA	36	NA	<0.001	NA	58	<0.004
	9/17/2012	<0.003	0.31	NA	0.041	NA	<0.001	NA	36	NA	<0.001	NA	58	<0.004
	10/28/2011	<0.003	0.21	NA	0.072	0.082	<0.0005	<0.0005	25.3	27	<0.002	<0.002	27	<0.005
	12/21/2015	<0.001	0.19	0.07	0.066	0.074	<0.0005	<0.0005	24.2	24.9	<0.002	<0.002	26	<0.005
	2/18/2016	<0.001	0.143	0.138	0.0605	0.0690	<0.0005	<0.0005	23.1	23.7	<0.002	<0.002	25	<0.005
APW-4	12/13/2010	<0.006	0.063	NA	<0.004	NA	<0.004	NA	2.55	NA	<0.004	NA	41	<0.001
	3/24/2011	<0.003	0.15	NA	0.085	NA	0.002	NA	4.5	NA	<0.001	NA	50	0.007
	9/15/2011	<0.003	0.18	NA	0.095	NA	0.002	NA	6.3	NA	<0.001	NA	63	<0.004
	10/28/2011	<0.003	0.18	NA	0.095	NA	0.002	NA	6.3	NA	<0.001	NA	63	<0.004
	3/26/2012	<0.003	0.29	NA	0.048	NA	<0.001	NA	3.9	NA	<0.001	NA	38	<0.004
	6/18/2012	<0.003	0.16	NA	0.048	NA	<0.001	NA	4.3	NA	<0.001	NA	49	<0.004
	9/17/2012	<0.003	0.16	NA	0.044	NA	<0.001	NA	4.3	NA	<0.001	NA	49	<0.004
	10/28/2011	<0.003	0.16	NA	0.044	NA	<0.001	NA	4.3	NA	<0.001	NA	49	<0.004
	12/21/2015	<0.001	0.03	0.032	0.053	0.063	<0.0005	<0.0005	1.81	1.89	<0.002	<0.002	33	<0.005
	2/18/2016	<0.001	0.018	0.02	0.057	0.077	<0.0005	<0.0005	1.96	2.22	<0.002	<0.002	24	<0.005
APW-5	12/13/2010	<0.006	0.0086	0.0151	0.0706	0.176	<0.0005	0.0007	1.33	1.62	<0.002	<0.002	26	<0.005
	3/24/2011	<0.003	<0.004	NA	<0.005	NA	<0.004	NA	0.118	NA	<0.004	NA	3	<0.001
	6/24/2011	<0.003	<0.001	NA	0.009	NA	<0.001	NA	0.17	NA	<0.001	NA	2.8	<0.004
	9/24/2011	<0.003	<0.001	NA	0.01	NA	<0.001	NA	0.22	NA	<0.001	NA	2.6	<0.004
	10/28/2011	<0.003	<0.001	NA	0.006	NA	<0.001	NA	0.35	NA	<0.001	NA	1	<0.004
	3/26/2012	<0.003	NA	<0.001	NA	0.009	NA	<0.001	NA	0.31	<0.001	NA	2.5	<0.004
	6/18/2012	<0.003	NA	<0.001	NA	0.01	NA	<0.001	NA	0.41	<0.001	NA	4.6	<0.004
	9/17/2012	<0.003	NA	<0.001	NA	0.009	NA	<0.001	NA	0.32	<0.001	NA	2.9	<0.004
	8/25/2015	<0.001	<0.001	0.008	0.011	0.042	<0.0005	<0.0005	0.109	0.119	<0.002	<0.002	9	<0.005
	12/21/2015	<0.001	<0.001	0.001	0.012	0.018	<0.0005	<0.0005	0.092	0.116	<0.002	<0.002	6	<0.005
APW-6	2/18/2016	0.0006	0.0003	0.0010	0.0113	0.0151	<0.0005	<0.0005	0.118	0.165	<0.002	<0.002	9	<0.005
	12/21/2015	<0.001	<0.001	0.001	0.015	0.017	<0.0005	<0.0005	0.246	0.244	<0.002	<0.002	6	<0.005
	2/18/2016	<0.001	<0.001	0.001	0.015	0.017	<0.0005	<0.0005	0.246	0.244	<0.002	<0.002	6	<0.005
	12/21/2015	<0.001	<0.001	0.002	0.028	0.042	<0.0005	<0.0005	0.245	0.26	<0.002	<0.002	28	<0.005
	2/18/2016	<0.001	0.0003	0.0010	0.0202	0.0384	<0.0005	<0.0005	0.109	0.0986	<0.002	<0.002	30	<0.005
	12/21/2015	<0.001	0.001	0.002	0.083	0.09	<0.0005	<0.0005	10.8	11	<0.002	<0.002	13	0.01
	2/18/2016	0.0006	0.0012	0.0013	0.0729	0.0788	<0.0005	<0.0005	10.3	11.1	<0.002	<0.002	12	0.0070
	12/21/2015	<0.001	<0.001	0.002	0.017	0.028	<0.0005	<0.0005	0.5	0.531	<0.002	<0.002	16	<0.005
	2/18/2016	0.0008	0.0013	0.0007	0.025	0.0425	<0.0005	<0.0005	4.42	5.12	<0.002	<0.002	19	<0.005
	Class GW Standards		NE	0.010	NE	2	NE	0.004	NE	2	NE	0.005	NE	200

Results are reported as mg/L or parts per million (ppm)
 Concentrations are based on the following:
 NA = Not Analyzed
 NE = Not Established
 TDS = Total Dissolved Solids
 (d) = dissolved concentration
 (t) = total concentration

TABLE 3
GROUNDWATER ANALYTICAL DATA SUMMARY
MEREDOSIA POWER STATION
MEREDOSIA, ILLINOIS

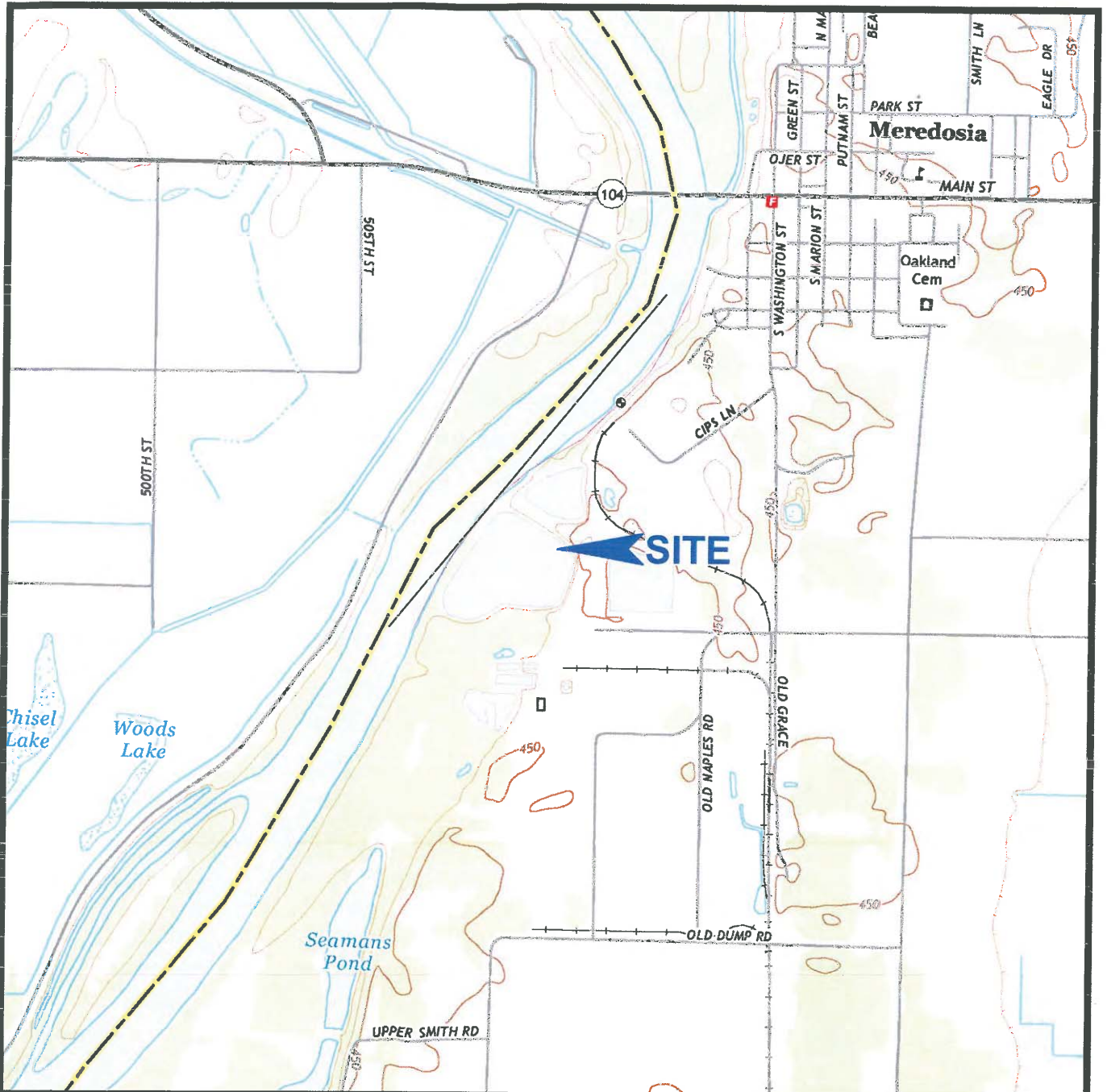
WELL ID	PARAMETER 1															
	Chromium (d)	Cobalt (d)	Cobalt (t)	Copper (d)	Copper (t)	Cyanide	Fluoride (d)	Iron (d)	Iron (t)	Lead (d)	Lead (t)	Manganese (d)	Manganese (t)	Mercury (d)	Mercury (t)	
APW-1	NA	<0.05	NA	<0.025	NA	NA	<0.1	NA	0.02	<0.005	NA	<0.015	NA	<0.0002	NA	
	NA	<0.02	NA	<0.03	NA	<0.05	<0.25	NA	0.03	<0.01	NA	<0.08	NA	<0.002	NA	
	NA	<0.02	NA	<0.03	NA	<0.05	<0.25	NA	0.03	<0.01	NA	<0.08	NA	<0.002	NA	
	NA	<0.02	NA	<0.03	NA	<0.05	0.26	NA	NA	<0.01	NA	0.05	NA	<0.002	NA	
	NA	<0.02	NA	<0.03	NA	<0.05	0.32	NA	NA	<0.01	NA	0.05	NA	<0.002	NA	
	NA	<0.02	NA	<0.03	NA	<0.05	<0.25	NA	NA	<0.01	NA	0.05	NA	<0.002	NA	
	NA	<0.02	NA	<0.03	NA	<0.05	<0.25	NA	NA	<0.01	NA	0.09	NA	<0.002	NA	
	NA	<0.02	NA	<0.03	NA	<0.05	<0.25	NA	NA	<0.01	NA	0.09	NA	<0.002	NA	
	<0.005	<0.005	0.012	<0.005	0.008	<0.007	<0.1	5.67	0.1	<0.01	0.007	<0.003	<0.002	<0.002	<0.002	NA
	<0.005	<0.005	0.009	<0.005	0.006	<0.007	0.11	4.18	<0.02	<0.01	0.005	<0.003	<0.002	<0.002	<0.002	NA
NA	<0.05	NA	<0.025	NA	<0.05	0.3	NA	<0.20	<0.01	NA	<0.015	NA	<0.002	NA		
NA	<0.05	NA	<0.025	NA	<0.05	0.3	NA	<0.20	<0.01	NA	<0.015	NA	<0.002	NA		
NA	0.004	NA	<0.003	NA	<0.005	<0.25	NA	1.1	<0.01	NA	0.48	NA	<0.002	NA		
NA	0.002	NA	<0.003	NA	<0.005	0.44	NA	0.37	<0.01	NA	0.82	NA	<0.002	NA		
NA	0.003	NA	<0.003	NA	<0.005	0.46	NA	0.46	<0.01	NA	0.79	NA	<0.002	NA		
NA	0.003	NA	<0.003	NA	<0.005	0.32	NA	0.15	<0.01	NA	0.91	NA	<0.002	NA		
NA	0.003	NA	<0.003	NA	<0.005	0.27	NA	0.34	<0.01	NA	0.83	NA	<0.002	NA		
NA	0.003	NA	<0.003	NA	<0.005	0.3	NA	0.3	<0.01	NA	0.96	NA	<0.002	NA		
<0.005	<0.005	<0.005	<0.005	<0.005	<0.007	0.29	2.06	0.19	<0.01	0.011	0.69	NA	<0.002	NA		
<0.005	<0.005	<0.005	<0.005	<0.005	<0.007	0.29	2.19	0.24	<0.01	0.011	0.86	NA	<0.002	NA		
<0.050	<0.050	<0.050	<0.050	0.015	<0.007	0.31	0.297	0.18	<0.010	0.004	0.92	NA	<0.0020	<0.0020	NA	
NA	<0.05	NA	<0.025	NA	<0.01	0.25	NA	0.1	<0.005	NA	0.169	NA	<0.002	NA		
NA	<0.02	NA	<0.003	NA	<0.005	0.36	NA	0.65	<0.01	NA	0.45	NA	<0.002	NA		
NA	<0.02	NA	<0.003	NA	<0.005	0.49	NA	0.41	<0.01	NA	0.28	NA	<0.002	NA		
NA	<0.02	NA	<0.003	NA	<0.005	0.54	NA	0.33	<0.01	NA	0.25	NA	<0.002	NA		
NA	<0.02	NA	<0.003	NA	<0.005	0.32	NA	0.48	<0.01	NA	0.3	NA	<0.002	NA		
NA	<0.02	NA	<0.003	NA	<0.005	0.29	NA	0.39	<0.01	NA	0.4	NA	<0.002	NA		
NA	<0.02	NA	<0.003	NA	<0.005	0.29	NA	0.43	<0.01	NA	0.4	NA	<0.002	NA		
<0.005	<0.005	<0.005	<0.005	<0.005	<0.007	0.2	2.38	0.475	<0.01	0.001	0.432	NA	<0.002	<0.002	NA	
<0.050	<0.050	<0.050	<0.050	<0.050	<0.007	0.23	1.93	1.38	<0.01	<0.001	0.632	NA	<0.002	<0.002	NA	
NA	<0.05	NA	<0.025	NA	<0.01	0.39	NA	<0.1	<0.005	NA	3.1	NA	<0.002	NA		
NA	<0.02	NA	<0.003	NA	<0.005	0.73	NA	5.9	<0.01	NA	3.4	NA	<0.002	NA		
NA	<0.02	NA	<0.003	NA	<0.005	0.79	NA	6.6	<0.01	NA	5.4	NA	<0.002	NA		
NA	<0.02	NA	<0.003	NA	<0.005	0.47	NA	14	<0.01	NA	2.8	NA	<0.002	NA		
NA	<0.02	NA	<0.003	NA	<0.005	0.45	NA	16	<0.01	NA	2.9	NA	<0.002	NA		
<0.005	<0.005	<0.005	<0.005	<0.005	<0.007	0.37	13.8	11.8	<0.01	<0.001	2.14	NA	<0.002	<0.002	NA	
0.0228	<0.005	0.0079	<0.005	0.0203	<0.007	0.30	27.5	2.16	<0.010	0.136	2.3	NA	<0.002	<0.002	NA	
NA	<0.05	NA	<0.025	NA	<0.01	0.13	NA	<0.1	<0.005	NA	1.72	NA	<0.0020	<0.0020	NA	
NA	<0.02	NA	<0.003	NA	<0.005	<0.25	NA	0.012	<0.001	NA	0.015	NA	<0.002	NA		
NA	<0.02	NA	<0.003	NA	<0.005	0.36	NA	0.01	<0.001	NA	0.01	NA	<0.002	NA		
NA	<0.02	NA	<0.003	NA	<0.005	0.36	NA	0.01	<0.001	NA	0.01	NA	<0.002	NA		
NA	<0.02	NA	<0.003	NA	<0.005	<0.25	NA	<0.01	<0.001	NA	0.04	NA	<0.002	NA		
NA	<0.02	NA	<0.003	NA	<0.005	<0.25	NA	<0.01	<0.001	NA	0.04	NA	<0.002	NA		
0.009	<0.005	0.05	<0.005	0.023	<0.007	<0.1	11.2	<0.02	<0.001	0.018	0.04	NA	<0.002	<0.002	NA	
<0.050	<0.050	0.0035	<0.005	0.0015	<0.007	<0.1	1.4	<0.02	<0.001	0.002	0.003	NA	<0.002	<0.002	NA	
<0.050	<0.050	<0.050	<0.050	<0.050	<0.007	0.08	0.888	<0.200	<0.010	0.016	0.009	NA	<0.0020	<0.0020	NA	
<0.050	<0.050	<0.050	<0.050	<0.050	<0.007	0.15	0.05	<0.02	<0.001	0.001	0.017	NA	<0.0020	<0.0020	NA	
<0.050	<0.050	<0.050	<0.050	<0.050	<0.007	0.22	2.57	<0.02	<0.001	0.002	0.017	NA	<0.0020	<0.0020	NA	
<0.050	<0.050	<0.050	<0.050	<0.050	<0.007	0.21	1.32	<0.020	<0.010	0.010	0.0549	NA	<0.0020	<0.0020	NA	
0.013	<0.005	<0.005	<0.005	<0.005	<0.007	<0.1	0.809	<0.02	<0.001	0.001	0.003	NA	<0.002	<0.002	NA	
0.0078	<0.050	<0.050	<0.050	<0.050	<0.007	0.23	0.6531	<0.200	<0.010	<0.010	0.0652	NA	<0.0020	<0.0020	NA	
<0.005	<0.005	<0.005	<0.005	<0.005	<0.007	0.59	1.26	<0.02	<0.001	0.002	0.008	NA	<0.002	<0.002	NA	
<0.050	<0.050	<0.050	<0.050	<0.050	<0.007	0.10	0.505	<0.020	<0.010	0.007	0.0579	NA	<0.0020	<0.0020	NA	
Class I GW Standards	NE	1	NE	0.65	NE	0.2	4	NE	5	0.0075	NE	0.15	NE	0.002	NE	

Results are reported as mg/L or parts per million (ppm)
 Concentrations of table obtained from data listed below
 NA = Not Analyzed
 NE = Not Established
 TDS = Total Dissolved Solids
 (d) = dissolved concentration
 (t) = total concentration

TABLE 3
GROUNDWATER ANALYTICAL DATA SUMMARY
MEREDOSIA POWER STATION
MEREDOSIA, ILLINOIS

WELL ID	PARAMETER 1											Zinc (f)			
	Nickel (d)	Nickel (f)	Nitrate	Selenium (d)	Selenium (f)	Silver (d)	Silver (f)	Sulfate	TDS	Thallium (d)	Thallium (f)		Vanadium (d)	Vanadium (f)	Zinc (d)
APW-1	<0.004	NA	3.8	<0.01	NA	<0.005	NA	26.4	132	<0.002	NA	NA	NA	<0.02	NA
	<0.005	NA	3.9	0.02	NA	<0.005	NA	31	80	<0.001	NA	NA	NA	<0.006	NA
	<0.005	NA	4.7	0.06	NA	<0.005	NA	140	140	<0.001	NA	NA	NA	<0.006	NA
	<0.005	NA	1.7	0.002	NA	<0.005	NA	20	190	<0.001	NA	NA	NA	<0.006	NA
	<0.005	NA	2.8	0.002	NA	<0.005	NA	24	150	<0.001	NA	NA	NA	<0.006	NA
	<0.005	NA	5.7	0.001	NA	<0.005	NA	15	180	<0.001	NA	NA	NA	<0.006	NA
	<0.005	NA	2.1	<0.001	NA	<0.005	NA	13	270	<0.001	NA	NA	NA	<0.006	NA
	<0.005	NA	1.6	0.002	NA	<0.005	NA	12	280	<0.001	NA	NA	NA	<0.006	NA
	<0.005	0.021	3.94	<0.04	<0.04	<0.005	NA	12	226	<0.001	<0.001	<0.001	<0.001	<0.001	0.02
	<0.005	0.015	3.43	<0.04	<0.04	<0.005	NA	11	280	<0.001	<0.001	<0.001	<0.001	<0.001	<0.015
<0.005	0.040	0.4	<0.01	<0.01	<0.005	NA	38.2	368	<0.002	<0.010	<0.002	<0.002	<0.002	0.080	
APW-2	0.012	NA	0.02	<0.01	NA	<0.005	NA	41	630	<0.002	NA	NA	NA	<0.02	NA
	0.007	NA	0.04	<0.01	NA	<0.005	NA	25	430	<0.001	NA	NA	NA	<0.006	NA
	0.006	NA	0.04	0.005	NA	<0.005	NA	14	440	<0.001	NA	NA	NA	<0.006	NA
	0.009	NA	0.07	0.001	NA	<0.005	NA	13	460	<0.001	NA	NA	NA	<0.006	NA
	0.011	NA	0.02	0.004	NA	<0.005	NA	18	510	<0.001	NA	NA	NA	0.006	NA
	0.011	NA	<0.02	0.002	NA	<0.005	NA	15	520	<0.001	NA	NA	NA	<0.006	NA
	<0.005	0.005	0.005	<0.04	<0.04	<0.005	NA	27	574	<0.001	<0.001	<0.001	<0.001	<0.001	<0.01
	<0.005	0.005	0.005	<0.04	<0.04	<0.005	NA	27	574	<0.001	<0.001	<0.001	<0.001	<0.001	<0.01
	0.058	0.062	<0.050	<0.040	<0.040	<0.050	NA	19	404	<0.010	<0.010	0.0015	0.0017	<0.010	0.0016
	0.04	NA	0.49	<0.01	NA	<0.005	NA	284	660	<0.002	NA	NA	NA	<0.02	NA
0.01	NA	<0.02	<0.01	NA	<0.005	NA	310	750	<0.001	NA	NA	NA	<0.006	NA	
<0.005	NA	<0.02	<0.01	NA	<0.005	NA	260	680	<0.001	NA	NA	NA	<0.006	NA	
0.006	NA	<0.02	0.002	NA	<0.005	NA	290	650	<0.001	NA	NA	NA	<0.006	NA	
0.006	NA	<0.02	<0.001	NA	<0.005	NA	270	710	<0.001	NA	NA	NA	<0.006	NA	
0.011	NA	<0.02	0.002	NA	<0.005	NA	300	700	<0.001	NA	NA	NA	<0.006	NA	
<0.005	<0.005	<0.005	<0.04	<0.04	<0.005	NA	177	470	<0.001	<0.001	<0.001	<0.001	<0.001	<0.01	
<0.005	<0.005	<0.005	<0.04	<0.04	<0.005	NA	177	470	<0.001	<0.001	<0.001	<0.001	<0.001	<0.01	
<0.050	<0.050	<0.050	<0.040	<0.040	<0.050	NA	192	736	<0.001	<0.001	<0.010	<0.010	<0.010	0.0028	
0.019	NA	0.31	<0.01	NA	<0.005	NA	49.3	418	<0.002	NA	NA	NA	<0.02	NA	
0.019	NA	0.04	0.012	NA	<0.005	NA	53	470	<0.001	NA	NA	NA	<0.006	NA	
0.01	NA	0.29	0.013	NA	<0.005	NA	17	520	<0.001	NA	NA	NA	<0.006	NA	
0.006	NA	<0.02	0.015	NA	<0.005	NA	23	300	<0.001	NA	NA	NA	<0.006	NA	
0.009	NA	0.005	0.005	NA	<0.005	NA	24	360	<0.001	NA	NA	NA	<0.006	NA	
0.01	NA	<0.02	0.03	NA	<0.005	NA	24	360	<0.001	NA	NA	NA	<0.006	NA	
<0.005	<0.005	<0.005	<0.04	<0.04	<0.005	NA	504	<0.001	<0.001	<0.001	<0.001	<0.001	<0.001	<0.01	
<0.005	<0.005	<0.005	<0.04	<0.04	<0.005	NA	504	<0.001	<0.001	<0.001	<0.001	<0.001	<0.001	<0.01	
0.0033	0.0232	<0.050	<0.040	<0.040	<0.050	NA	26	462	<0.001	<0.001	<0.010	<0.010	0.0024	0.0077	
0.007	NA	1.7	<0.01	NA	<0.005	NA	6.1	138	<0.002	NA	NA	NA	<0.02	NA	
0.007	NA	1.9	<0.001	NA	<0.005	NA	17	230	<0.001	NA	NA	NA	<0.006	NA	
0.001	NA	1.4	0.002	NA	<0.005	NA	15	290	<0.001	NA	NA	NA	<0.006	NA	
<0.005	<0.005	<0.005	<0.04	<0.04	<0.005	NA	3	40	<0.001	NA	NA	NA	<0.006	NA	
<0.005	<0.005	<0.005	<0.04	<0.04	<0.005	NA	3	40	<0.001	NA	NA	NA	<0.006	NA	
<0.005	<0.005	<0.005	<0.04	<0.04	<0.005	NA	14	250	<0.001	NA	NA	NA	<0.006	NA	
<0.005	<0.005	<0.005	<0.04	<0.04	<0.005	NA	15	280	<0.001	NA	NA	NA	<0.006	NA	
0.006	NA	2.6	0.002	NA	<0.005	NA	33	290	<0.001	NA	NA	NA	<0.006	NA	
<0.005	0.007	2.03	<0.04	<0.04	<0.005	NA	19	338	<0.001	<0.001	0.017	0.017	<0.01	0.037	
<0.005	0.009	2.1	<0.04	<0.04	<0.005	NA	66	400	<0.001	<0.001	<0.001	<0.001	<0.01	<0.01	
<0.005	0.077	1.85	<0.040	<0.040	<0.050	NA	36	340	<0.010	<0.010	0.0025	0.0025	<0.010	0.0048	
<0.005	0.005	0.72	<0.04	<0.04	<0.005	NA	13	324	<0.001	<0.001	<0.001	<0.001	<0.001	<0.015	
<0.005	<0.005	<0.005	<0.04	<0.04	<0.005	NA	17	364	<0.001	<0.001	<0.001	<0.001	<0.001	<0.015	
<0.005	<0.005	<0.005	<0.04	<0.04	<0.005	NA	35	248	<0.001	<0.001	<0.001	<0.001	<0.001	<0.015	
<0.005	<0.005	<0.005	<0.04	<0.04	<0.005	NA	35	248	<0.001	<0.001	<0.001	<0.001	<0.001	<0.015	
<0.005	<0.005	5.73	0.126	0.135	<0.005	NA	47.2	994	<0.001	<0.001	<0.001	<0.001	<0.001	<0.01	
<0.005	<0.005	5.29	0.102	0.118	<0.005	NA	338	786	<0.001	<0.001	<0.010	<0.010	<0.010	<0.010	
<0.005	0.005	3.25	<0.04	<0.04	<0.005	NA	26.5	716	<0.001	<0.001	<0.001	<0.001	<0.001	<0.01	
<0.005	0.005	3.88	<0.040	<0.040	<0.050	NA	400	1,070	<0.001	<0.001	0.0028	0.0028	<0.001	0.0030	
Class ICG Standards	0.1	NE	10	0.05	NE	0.05	400	1,200	NE	NE	0.049	NE	5	NE	

Results are reported as mg/L or parts per million (ppm).
 Concentrations of metals obtained from the analysis are provided by the
 Concentration above Illinois Class I Groundwater Standards
 NA = Not Analyzed
 NE = Not Established
 TDS = Total Dissolved Solids
 (d) = dissolved concentration
 (f) = total concentration



NOTES

1. Plan adapted from a 7.5 minute U.S.G.S. map for Meredosia, Illinois quadrangle, last revised in 2015.



SCALE IN FEET

Drawn By: WAH	Ck'd By: <i>De</i>	App'vd By: <i>AMS</i>
Date: 5-9-16	Date: <i>7/20/16</i>	Date: <i>7/20/16</i>



Meredosia Power Station
Meredosia, Illinois

**SITE LOCATION
AND TOPOGRAPHY**

Project Number
J024917.01

PLATE 1



NOTES

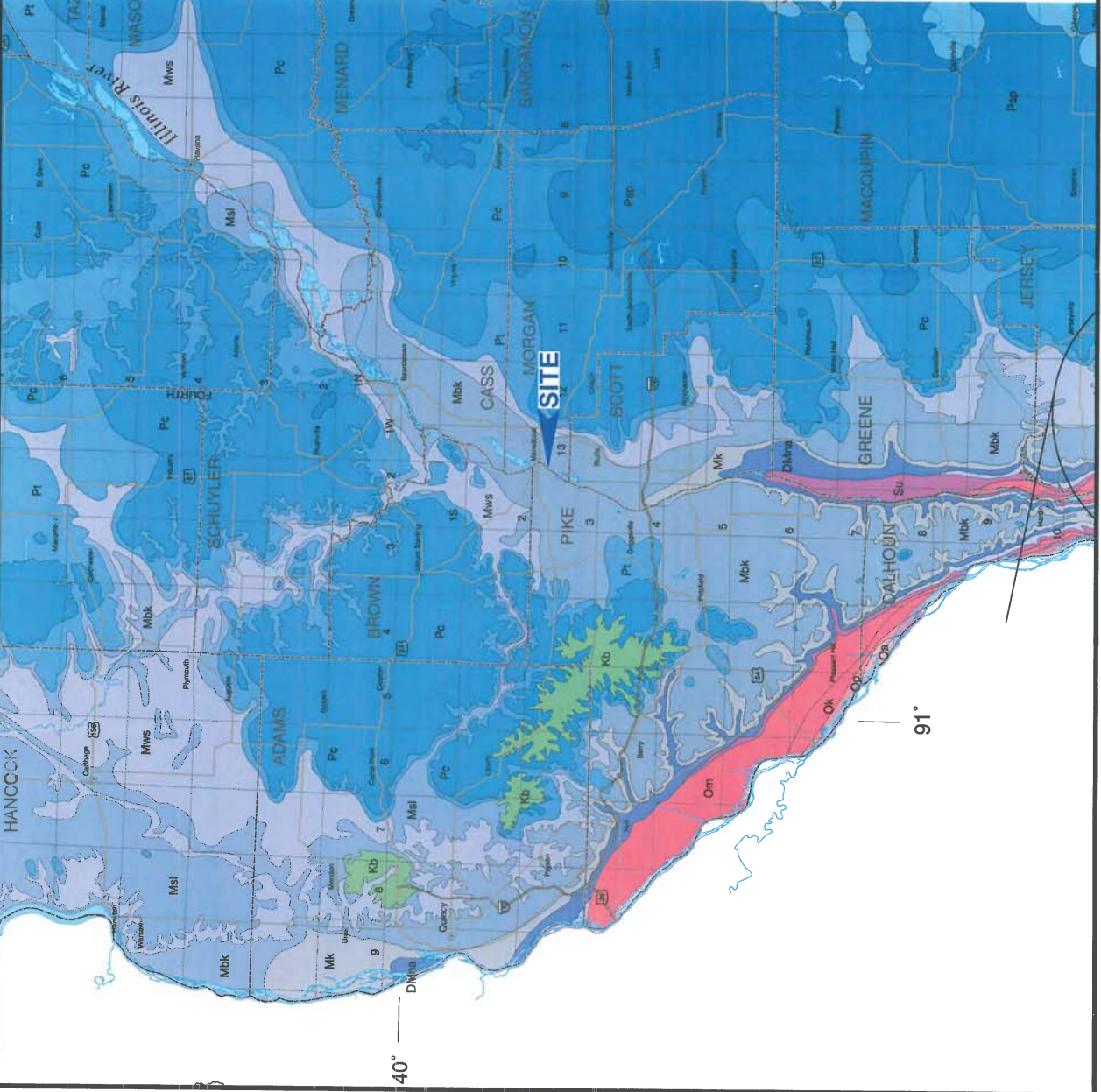
1. Plan adapted from drawings based on topography obtained by AeroView in October 2015 and supplied by the client.
2. Monitoring Wells were located by the project surveyor.

LEGEND

- ▲ Monitoring Well Location
- Soil Boring Location




Drawn By: WAH	CK'd By: [Signature]	Appvd By: AMMS
Date: 5-18-16	Date: 7/20/16	Date: 7/20/16
 FROM THE GROUND UP		
Meredosia Power Station Meredosia, Illinois		
SITE PLAN AND MONITORING WELL LOCATIONS		
Project Number J024917.01		PLATE 2



- Kb Baylis Formation (western Illinois)
- Psp Shelbyville-Palucka Formations undivided
- Pc Carbonate Formation
- Pl Tradewater Formation
- Msg St. Genevieve Limestone
- Msl St. Louis Limestone
- Mbk Meppen Limestone, Fern Glen Formation, and Burlington-Kookuk Limestone
- Mk Glen Park Formation, Henshal Shale, Crippleau Limestone, McCaskey Limestone, Prospect Hill Silstone, and Stars Cave Limestone
- DMms New Albany Shale, Blocher Shale, Sycamore Sandstone, Selmer Shale, Sweetland Creek Shale, Grassy Creek Shale, Severn Shale, and Louisiana Limestone
- Su Sturion System undivided, includes Sexton Creek Limestone, St. Clair Limestone, and Moccasin Springs Formation in southern Illinois; includes Pittsford Limestone, Elwood Dolomite, Kaniksee Dolomite, Sugar Run Dolomite, and Racine Dolomite in northern Illinois; includes Mosaic, Tule des Morts, Blarding, Sweeney, Marcus, and Racine Dolomites in northwestern Illinois
- Om Mazonia Formation or Group, includes Cape Limestone, Cape La Croix Shale, Thebes Sandstone, Orchard Creek Shale, Girardeau Limestone, and St. Charles Limestone; includes Shawnee Shale, Fort Atkinson Limestone, and Shawnee Shale and Neola Formation in northern Illinois; includes Nox Colite in western Illinois
- Ok Kirmasick (Trenton) Limestone and Decatur Formation in southern and western Illinois
- Op Pittsville Group, includes Pecatonica, Moffit, Grand Debar, Nachusa, and Quimby Mill Formations; includes Pleath Limestone in southwestern Illinois
- Oa Arcell Group, includes St. Peter Sandstone, Duaneville Limestone, Joachim Dolomite, and Glenwood Formation; includes Prairie du Chien Group in Jo Daviess County of northwestern Illinois

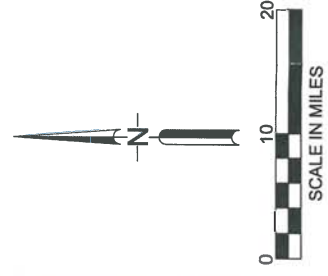
Drawn By: WAH CK'd By: *W* App'd By: *AMS*
 Date: 2-28-16 Date: 7/22/16 Date: 7/22/16


GEOTECHNOLOGY
FROM THE GROUND UP

Meredosias Power Station
 Meredosias, Illinois

BEDROCK GEOLOGY
MAP

Project Number
 J024917.01 **PLATE 3**



NOTES

1. Plan adapted from a July 22, 2012 aerial photograph courtesy of Google Earth.
2. Water well locations from Illinois State Geological Survey Prairie Research Institute.
3. See Appendix A for water well records.
4. Abandoned on-site water supply wells are not shown.

LEGEND

- Water Supply Wells
- On-Site Water Supply Wells to be Abandoned






SCALE IN FEET

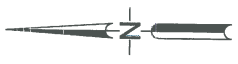
Drawn By: WAH	Checked By: Jbe	App'd By: Am S
Date: 4-21-16	Date: 7/20/16	Date: 7/20/16
Meredosia Power Station Meredosia, Illinois		
POTABLE WATER WELL SEARCH RADIUS		
Project Number J024917.01	PLATE 4	




NOTES

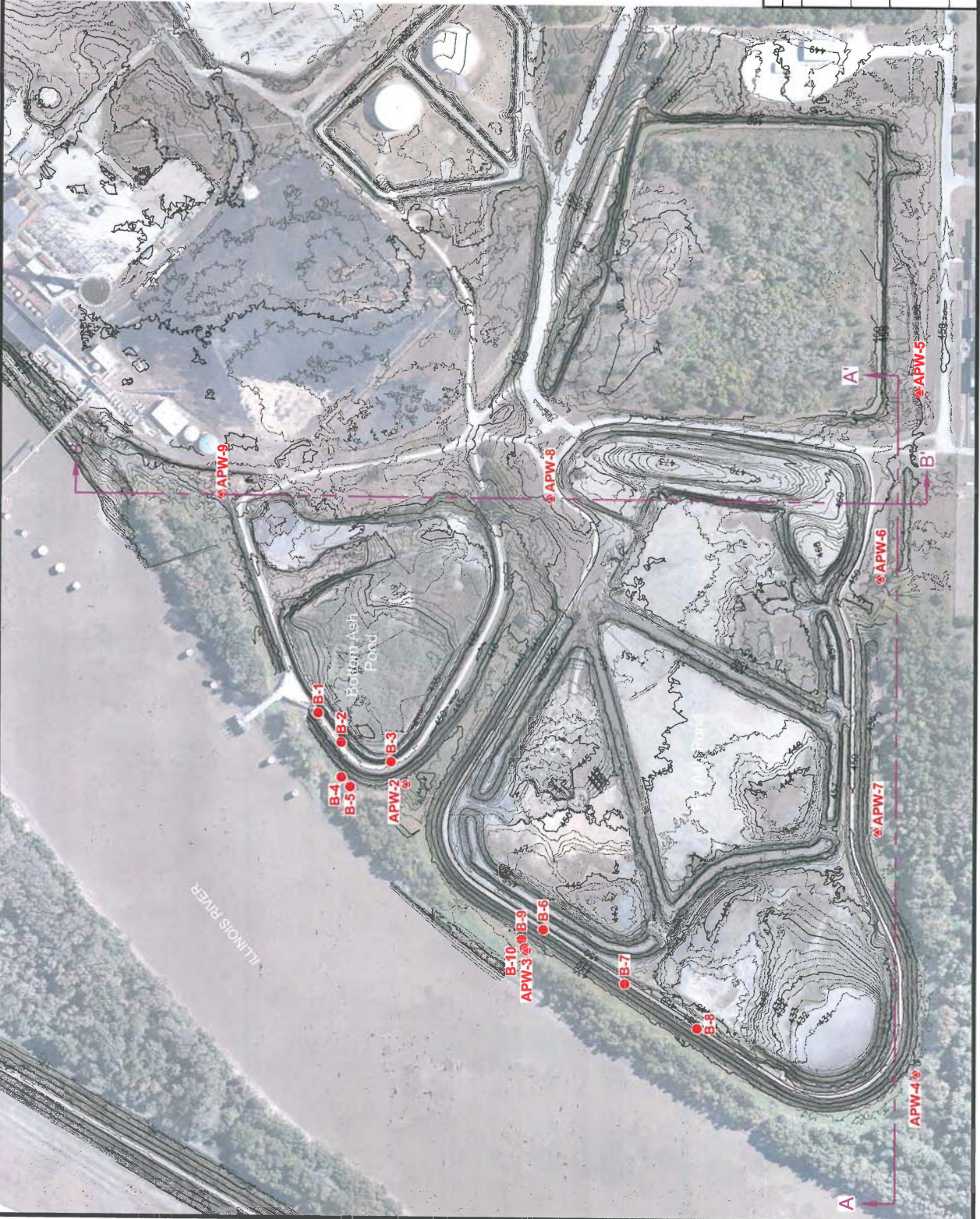
1. Plan adapted from drawings based on topography obtained by AeroView in October 2015 and supplied by the client.
2. Monitoring Wells were located by the project surveyor.
3. Monitoring Well APW-1 is located beyond the limits of this map and is approximately 2000-feet east of Monitoring Well APW-5.

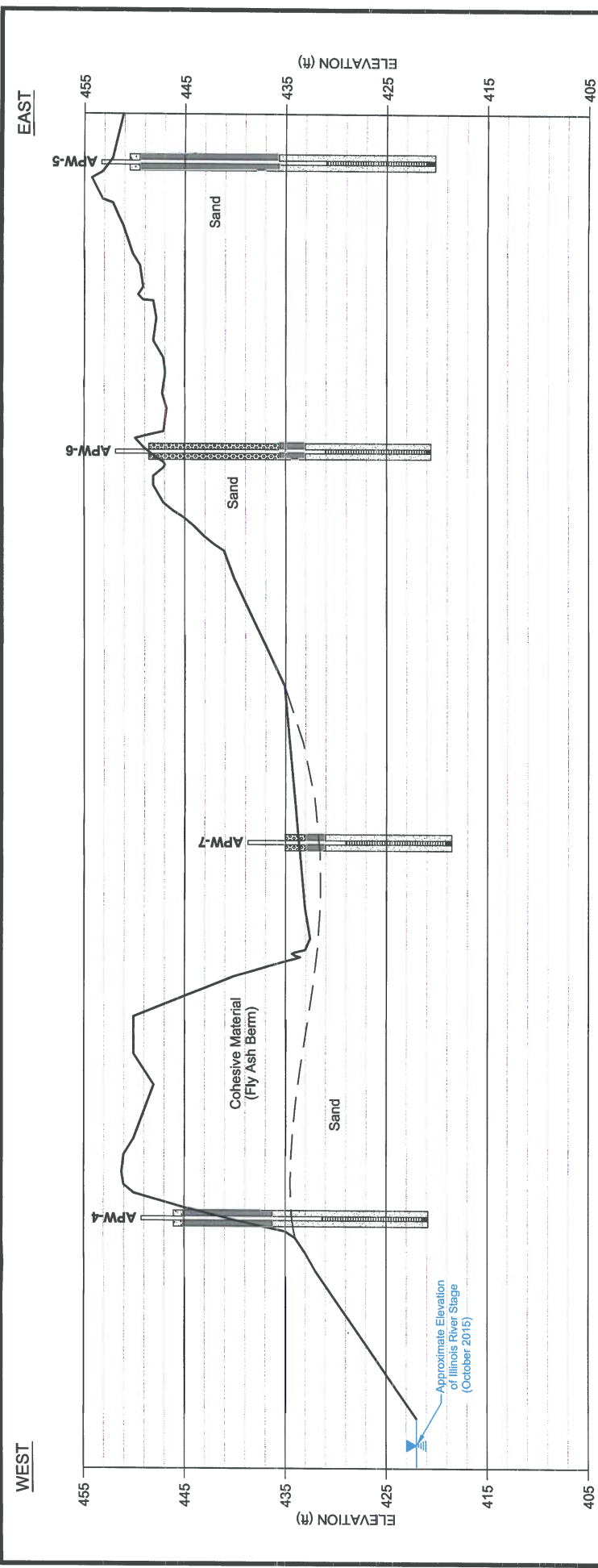
LEGEND

-  Monitoring Well Location
-  Soil Boring Location
-  Subsurface Profile (See Plate 6 and 7 for Cross-Section A-A' and B-B', Respectively)



Drawn By: WAH	CK'd By: 	App'vd By: 
Date: 3-9-16	Date: 7/20/16	Date: 7/20/16
		
Meredosia Power Station Meredosia, Illinois		
SUBSURFACE PROFILE PLAN		
Project Number J024917.01		PLATE 5





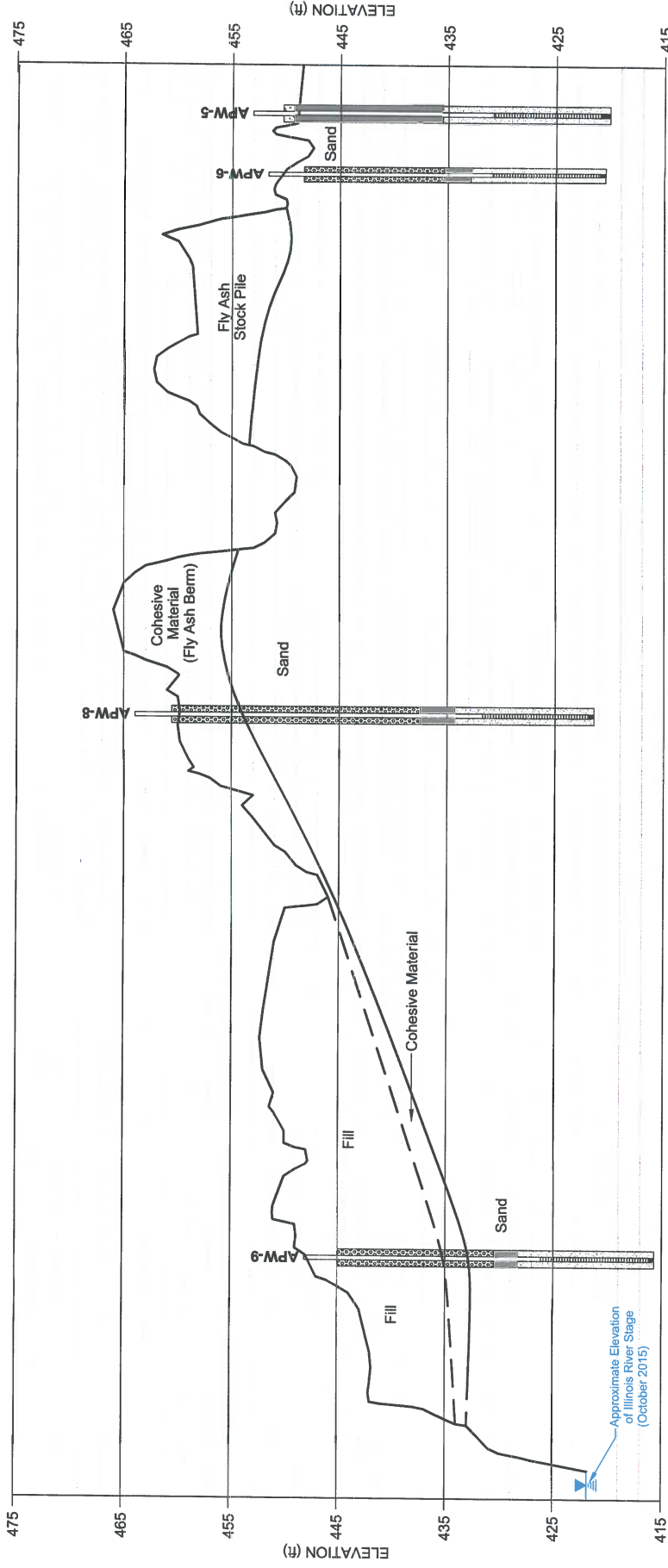
SCALE IN FEET
 Horizontal 1" = 200'
 Vertical 1" = 10'

- NOTES**
1. See PLATE 5 for location of Subsurface Profile A-A'.
 2. Data concerning subsurface conditions have been obtained at boring locations only. Actual conditions at locations between borings may differ from the generalized profile shown here.

Drawn By: WAH	CK'd By: <i>Ue</i>	Appvd By: <i>AMS</i>
Date: 3-9-16	Date: 7/20/14	Date: 7/20/14
Meredosia Power Station Meredosia, Illinois		
GENERALIZED SUBSURFACE PROFILE - SECTION A-A'		
Project Number J024917.01	PLATE 6	

NORTH

SOUTH



NOTES

1. See PLATE 5 for location of Subsurface Profile B-B'.
2. Data concerning subsurface conditions have been obtained at boring locations only. Actual conditions at locations between borings may differ from the generalized profile shown here.

SCALE IN FEET
 Horizontal 1" = 200'
 Vertical 1" = 10'

Drawn By: WAH	CK'd By: <i>ve</i>	Appvd By: <i>AS</i>
Date: 3-7-16	Date: 7/16/16	Date: 7/16/16
Meredosia Power Station Meredosia, Illinois		
GENERALIZED SUBSURFACE PROFILE - SECTION B-B'		
Project Number J024917.01	PLATE 7	

NOTES

1. Plan adapted from drawings based on topography obtained by AeroView in October 2015 and supplied by the client.
2. Monitoring Wells were located by the project surveyor.
3. Monitoring Well APW-1 is located beyond the limits of this map and is approximately 2000-feet east of Monitoring Well APW-5.

LEGEND

- Monitoring Well Location (427.20)
- Groundwater Elevation at Well Location (November 17, 2010)
- 425- Groundwater Elevation Contour



Drawn By: WAH	CK'd By: [Signature]	Appvd By: A*5
Date: 5-18-16	Date: 7/20/16	Date: 7/20/16
Meredosia Power Station Meredosia, Illinois		
GROUNDWATER ELEVATION CONTOURS - NOVEMBER 2010		
Project Number J024917.01	PLATE 8	

NOTES

1. Plan adapted from drawings based on topography obtained by AeroView in October 2015 and supplied by the client.
2. Monitoring Wells were located by the project surveyor.
3. Monitoring Well APW-1 is located beyond the limits of this map and is approximately 2000-feet east of Monitoring Well APW-5.

LEGEND

- Monitoring Well Location (427.20)
- Groundwater Elevation at Well Location (December 13, 2010)
- 425— Groundwater Elevation Contour



Drawn By: WAH	CK'd By: VSC	Appvd By: AM5
Date: 5-18-16	Date: 7/27/16	Date: 7/16/20
GEOTECHNOLOGY FROM THE GROUND UP		
Meredosia Power Station Meredosia, Illinois		
GROUNDWATER ELEVATION CONTOURS - DECEMBER 2010		
Project Number J024917.01	PLATE 9	

NOTES

1. Plan adapted from drawings based on topography obtained by AeroView in October 2015 and supplied by the client.
2. Monitoring Wells were located by the project surveyor.
3. Monitoring Well APW-1 is located beyond the limits of this map and is approximately 2000-feet east of Monitoring Well APW-5.

LEGEND

- Monitoring Well Location (427.20)
- Groundwater Elevation at Well Location (September 15, 2011)
- 425— Groundwater Elevation Contour



Drawn By: WAH	Checked By: [Signature]	Approved By: [Signature]
Date: 5-18-16	Date: 7/20/16	Date: 7/20/16
GEOTECHNOLOGY FROM THE GROUND UP		
Mercedosa Power Station Mercedosa, Illinois		
GROUNDWATER ELEVATION CONTOURS - SEPTEMBER 2011		
Project Number J024917.01	PLATE 10	

NOTES

1. Plan adapted from drawings based on topography obtained by AeroView in October 2015 and supplied by the client.
2. Monitoring Wells were located by the project surveyor.
3. Monitoring Well APW-1 is located beyond the limits of this map and is approximately 2000-feet east of Monitoring Well APW-5.

LEGEND

- Monitoring Well Location (427.20)
- Groundwater Elevation at Well Location (October 28, 2011)
- 425- Groundwater Elevation Contour



Drawn By: WAH	Checked By: [Signature]	App'd By: AAS
Date: 5-18-16	Date: 7/20/16	Date: 7/20/16
Meredosia Power Station Meredosia, Illinois		
GROUNDWATER ELEVATION CONTOURS - OCTOBER 2011		
Project Number J024917.01	PLATE 11	

NOTES

1. Plan adapted from drawings based on topography obtained by AeroView in October 2015 and supplied by the client.
2. Monitoring Wells were located by the project surveyor.
3. Monitoring Well APW-1 is located beyond the limits of this map and is approximately 2000-feet east of Monitoring Well APW-5.

LEGEND

- Monitoring Well Location (427.20)
- Groundwater Elevation at Well Location (March 26, 2012)
- 425— Groundwater Elevation Contour



Drawn By: WAH	Checked By: J. Belle	Approved By: AMS
Date: 5-18-16	Date: 7/12/16	Date: 7/12/16
GEOTECHNOLOGY FROM THE GROUND UP		
Meredosia Power Station Meredosia, Illinois		
GROUNDWATER ELEVATION CONTOURS - MARCH 2012		
Project Number J024917.01	PLATE 12	

NOTES

1. Plan adapted from drawings based on topography obtained by AeroView in October 2015 and supplied by the client.
2. Monitoring Wells were located by the project surveyor.
3. Monitoring Well APW-1 is located beyond the limits of this map and is approximately 2000-feet east of Monitoring Well APW-5.

LEGEND

- Monitoring Well Location (427.20)
- Groundwater Elevation at Well Location (June 18, 2012)
- 425— Groundwater Elevation Contour



Drawn By: WAH	Checked By: [Signature]	Approved By: [Signature]
Date: 5-18-16	Date: 7/20/16	Date: 7/20/16
GEOTECHNOLOGY FROM THE GROUND UP		
Mercedosa Power Station Mercedosa, Illinois		
GROUNDWATER ELEVATION CONTOURS - JUNE 2012		
Project Number J024917.01	PLATE 13	


NOTES

1. Plan adapted from drawings based on topography obtained by AeroView in October 2015 and supplied by the client.
2. Monitoring Wells were located by the project surveyor.
3. Monitoring Well APW-1 is located beyond the limits of this map and is approximately 2000-feet east of Monitoring Well APW-5.

LEGEND

- Monitoring Well Location (427.20)
- Groundwater Elevation at Well Location (September 17, 2012)
- 425— Groundwater Elevation Contour



Drawn By: WAH	Checked By: VLO	Approved By: APAS
Date: 5-18-16	Date: 7/20/16	Date: 7/18/16
 GEOTECHNOLOGY FOR THE GEOTECHNICAL		
Meredosia Power Station Meredosia, Illinois		
GROUNDWATER ELEVATION CONTOURS - SEPTEMBER 2012		
Project Number J024917.01	PLATE 14	

NOTES

1. Plan adapted from drawings based on topography obtained by AeroView in October 2015 and supplied by the client.
2. Monitoring Wells were located by the project surveyor.
3. Monitoring Well APW-1 is located beyond the limits of this map and is approximately 2000-feet east of Monitoring Well APW-5.

LEGEND

- Monitoring Well Location (427.20)
- Groundwater Elevation at Well Location (August 25, 2015)
- 425— Groundwater Elevation Contour



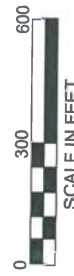
Drawn By: WAH	Checked By: [Signature]	Appvd By: AM5
Date: 5-18-16	Date: 7/26/16	Date: 7/26/16
GEOTECHNOLOGY FROM THE GROUND UP		
Meredosia Power Station Meredosia, Illinois		
GROUNDWATER ELEVATION CONTOURS - AUGUST 2015		
Project Number J024917.01	PLATE 15	


NOTES

1. Plan adapted from drawings based on topography obtained by AeroView in October 2015 and supplied by the client.
2. Monitoring Wells were located by the project surveyor.
3. Monitoring Well APW-1 is located beyond the limits of this map and is approximately 2000-feet east of Monitoring Well APW-5.



LEGEND
 Monitoring Well Location
 Groundwater Elevation at Well Location
 (December 21, 2015)
 425—Groundwater Elevation Contour



Drawn By: WAH	Checked By: V.C.	Approved By: APAS
Date: 3-9-16	Date: 7/20/16	Date: 7/20/16
 GEOTECHNOLOGY <small>FROM THE GROUND UP</small>		
Meredosia Power Station Meredosia, Illinois		
GROUNDWATER ELEVATION CONTOURS - DECEMBER 2015		
Project Number J024917.01		PLATE 16


NOTES

1. Plan adapted from drawings based on topography obtained by AeroView in October 2015 and supplied by the client.
2. Monitoring Wells were located by the project surveyor.
3. Monitoring Well APW-1 is located beyond the limits of this map and is approximately 2000-feet east of Monitoring Well APW-5.



LEGEND

- Monitoring Well Location (427.20)
- Groundwater Elevation at Well Location (February 18, 2016)
- 425—Groundwater Elevation Contour

Drawn By: WAH	Cktd By: Vbe	Appvd By: APMS
Date: 5-18-16	Date: 7/21/16	Date: 7/20/16
 GEO TECHNOLOGY FROM THE SOURCE UP		
Meredosias Power Station Meredosia, Illinois		
GROUNDWATER ELEVATION CONTOURS - FEBRUARY 2016		
Project Number J024917.01	PLATE 17	


NOTES

1. Plan adapted from drawings based on topography obtained by AeroView in October 2015 and supplied by the client.
2. Monitoring Wells were located by the project surveyor.
3. Monitoring Well APW-1 is located beyond the limits of this map and is approximately 2000-feet east of Monitoring Well APW-5.

LEGEND

- Monitoring Well Location (10.8)
- Boron Concentration in Groundwater, (mg/l - ppm) - August 25, 2015
- 10—Boron Concentration Isoleth, (mg/l - ppm)



Drawn By: WAH	Checked By: VJG	Approved By: AWS
Date: 4-21-16	Date: 7/20/16	Date: 7/20/16
 GEOTECHNOLOGY <small>FROM THE GROUND UP</small>		
Meredosia Power Station Meredosia, Illinois		
BORON CONCENTRATION IN GROUNDWATER - AUGUST 2015		
Project Number J024917.01		PLATE 18

NOTES

1. Plan adapted from drawings based on topography obtained by AeroView in October 2015 and supplied by the client.
2. Monitoring Wells were located by the project surveyor.
3. Monitoring Well APW-1 is located beyond the limits of this map and is approximately 2000-feet east of Monitoring Well APW-5.

LEGEND

- Monitoring Well Location (10.8)
- Boron Concentration in Groundwater, (mg/l - ppm) - December 21, 2015
- 10—Boron Concentration Isoleth, (mg/l - ppm)



Drawn By: WAH	Checked By: [Signature]	Appvd By: [Signature]
Date: 4-19-16	Date: 7/20/16	Date: 7/20/16
GEOTECHNOLOGY FROM THE GROUND UP		
Mercedosa Power Station Mercedosa, Illinois		
BORON CONCENTRATION IN GROUNDWATER - DECEMBER 2015		
Project Number J024917.01	PLATE 19	


NOTES

1. Plan adapted from drawings based on topography obtained by AeroView in October 2015 and supplied by the client.
2. Monitoring Wells were located by the project surveyor.
3. Monitoring Well APW-1 is located beyond the limits of this map and is approximately 2000-feet east of Monitoring Well APW-5.

LEGEND

- Monitoring Well Location (10.3)
- Boron Concentration in Groundwater, (mg/l - ppm) - February 18, 2016
- 10—Boron Concentration Isoleth, (mg/l - ppm)



Drawn By: WAH	Checked By: JDB/llc	Approved By: JMS
Date: 4-21-16	Date: 7/20/16	Date: 7/20/16
 GEOTECHNOLOGY <small>FROM THE SURFACE UP</small>		
Meredosia Power Station Meredosia, Illinois		
BORON CONCENTRATION IN GROUNDWATER - FEBRUARY 2016		
Project Number	J024917.01	
	PLATE 20	

NOTES

1. Plan adapted from drawings based on topography obtained by AeroView in October 2015 and supplied by the client.
2. Monitoring Wells were located by the project surveyor.
3. Monitoring Well APW-1 is located beyond the limits of this map and is approximately 2000-feet east of Monitoring Well APW-5.

LEGEND  Monitoring Well Location



APW-2

Feb. 18, 2016	APW-2	0.832
Feb. 18, 2016	APW-2	0.836

APW-3

Feb. 18, 2016	APW-3	0.832
Feb. 18, 2016	APW-3	0.832

APW-4

Feb. 18, 2016	APW-4	1.177
Feb. 18, 2016	APW-4	1.177

APW-7

Feb. 18, 2016	APW-7	0.832
Feb. 18, 2016	APW-7	0.832

APW-8

Feb. 18, 2016	APW-8	0.832
Feb. 18, 2016	APW-8	0.832

APW-5

Feb. 18, 2016	APW-5	0.832
Feb. 18, 2016	APW-5	0.832

APW-6

Feb. 18, 2016	APW-6	0.832
Feb. 18, 2016	APW-6	0.832

APW-9

Feb. 18, 2016	APW-9	0.832
Feb. 18, 2016	APW-9	0.832



Drawn By: WAH	Checked By: <i>Wah</i>	App'd By: <i>APW</i>
Date: 5-18-16	Date: 7/20/16	Date: 7/20/16
GEOTECHNOLOGY FROM THE GROUND UP		
Meredosia Power Station Meredosia, Illinois		
ARSENIC AND MANGANESE EXCEEDANCES - FEBRUARY 2016		
Project Number J024917.01	PLATE 21	

**The following are attachments to the testimony of Scott M. Payne,
PhD, PG and Ian Magruder, M.S..**

APPENDIX A

POTABLE WATER WELL DATA

ILLINOIS STATE GEOLOGICAL SURVEY

Water Well	Top	Bottom
sand, fine; silt & pebbles	0	5
sand, medium grain	5	11
sand, medium grain	11	22
sand, medium; small pebbles	22	32
sand, medium; small pebbles	32	42
sand, medium; small pebbles	42	52
sand, medium; small pebbles	52	62
sand, coarse; medium gravel & rock	62	67
limestone, chert bands; core	67	77
limestone, chert bands; core	77	88
limestone, chert bands; core	88	94
limestone, chert bands; core	94	100
Total Depth		100

Driller's Log filed

Owner Address: ,

Location source: Location from the driller

Permit Date:

Permit #:

COMPANY owner
 FARM Cen. Ill. Pub. Service Co
 DATE DRILLED January 1, 1941 NO. 27
 ELEVATION 4180 COUNTY NO. 00561
 LOCATION 460'N line, 20'W line of NW SE
 LATITUDE 39.82506 LONGITUDE -90.567886
 COUNTY Morgan API 121370056100

21 - 16N - 13W

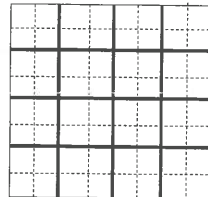
ILLINOIS STATE GEOLOGICAL SURVEY

Water Well	Top	Bottom
fine sand	0	25
medium sand fine gravel	25	40
fine sand	40	48
fine coarse sand & gravel	48	52
fine medium sand	52	65
fine pink sand,	65	81
coarse sand, gravel & small boulders	81	105
Total Depth		105
Static level 38' below casing top which is 0' above GL		
Pumping level 40' when pumping at 503 gpm for 8 hours		
Driller's Log filed		
Owner Address: ,		
Location source: Location from the driller		

Permit Date:

Permit #:

COMPANY owner
 FARM Central Ill. Public Service
 DATE DRILLED December 1, 1960 NO. 4
 ELEVATION 460GL COUNTY NO. 20656
 LOCATION 2003'S line, 577'E line of section
 LATITUDE 39.824389 LONGITUDE -90.565516
 COUNTY Morgan API 121372065600



21 - 16N - 13W

ILLINOIS STATE GEOLOGICAL SURVEY

Water Well	Top	Bottom
sand, brown, medium grain	0	3
sand, brown, medium grain	3	6
sand, brown, fine grain	6	10
sand, brown, coarse grain	10	15
sand, coarse; fine gravel	15	20
sand, brown, medium grain	20	30
sand, medium, small pebbles	30	40
sand, brown, medium grain	40	50
sand, brown, fine grain	50	60
sand, coarse; medium gravel	60	70
sand, brown, fine grain	70	80
sand, coarse; coarse gravel	80	83
limestone, 2 1/8" core	83	86
limestone, 2 1/8" core	86	91
limestone, crystallized bands, very hard	91	96
limestone, 2 1/8" core	96	100
Total Depth		100

Driller's Log filed

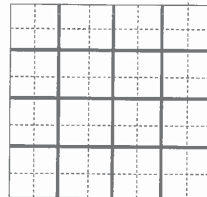
Owner Address: ,

Location source: Location from the driller

Permit Date:

Permit #:

COMPANY owner
FARM Cen. Ill. Pub. Service Co
DATE DRILLED January 1, 1941 **NO. 21**
ELEVATION 433CO **COUNTY NO.** 00555
LOCATION 530'N 315'E SW/c NE SE
LATITUDE 39.824039 **LONGITUDE** -90.564817
COUNTY Morgan **API** 121370055500



21 - 16N - 13W

ILLINOIS STATE GEOLOGICAL SURVEY

Water Well	Top	Bottom
sand, medium, light brown	0	3
sand, medium, clay content	3	6
sand, brown, medium grain	6	10
sand, medium, slight clay content	10	15
sand, brown, fine grain	15	20
sand, brown, fine grain	20	30
sand, coarse; fine gravel	30	40
sand, brown, fine grain	40	50
sand, coarse; fine gravel	50	60
sand, coarse; small gravel	60	70
sand, coarse; coarse gravel	70	80
sand, fine	80	90
sand, fine	90	98
boulders, small	98	99
sand, coarse; small gravel	99	100
Total Depth		100

Driller's Log filed

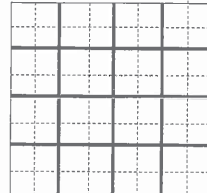
Owner Address: ,

Location source: Location from the driller

Permit Date:

Permit #:

COMPANY owner
FARM Cen. Ill. Pub. Service Co
DATE DRILLED January 1, 1941 **NO. 20**
ELEVATION 4500 **COUNTY NO.** 00554
LOCATION 485'N 350'E SW/c NE SE
LATITUDE 39.823913 **LONGITUDE** -90.564729
COUNTY Morgan **API** 121370055400



21 - 16N - 13W

ILLINOIS STATE GEOLOGICAL SURVEY

Water Well	Top	Bottom
sand, silty, brown	0	3
sand, brown, medium grain	3	10
sand, brown, medium grain	10	20
sand, brown, medium grain	20	30
sand, brown, medium grain	30	40
sand, brown, coarse grain, medium gravel	40	50
sand, coarse, small gravel	50	60
gravel, medium	60	70
gravel, medium	70	80
gravel, medium;sand, medium brown	80	90
medium gravel & sand, traces of lignite	90	100
Total Depth		100

Driller's Log filed

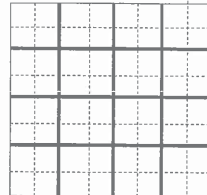
Owner Address: ,

Location source: Location from the driller

Permit Date:

Permit #:

COMPANY owner
FARM Cen. Ill. Pub. Service
DATE DRILLED January 1, 1941 **NO. 11**
ELEVATION 4560 **COUNTY NO.** 00545
LOCATION 420'N 405'E SW/c NE SE
LATITUDE 39.823732 **LONGITUDE** -90.564583
COUNTY Morgan **API** 121370054500



21 - 16N - 13W

ILLINOIS STATE GEOLOGICAL SURVEY

Water Well	Top	Bottom
sand, brown, medium grain	0	5
sand, brown, medium grain	5	7
sand, coarse; fine gravel	7	11
sand, coarse; fine gravel	11	16
sand, medium grain	16	26
sand, medium; medium gravel	26	36
sand, medium; medium gravel	36	46
sand, fine grain	46	56
sand, fine grain	56	66
sand, medium grain	66	76
sand, coarse; medium gravel	76	82
limestone	82	88
limestone	88	91
limestone, interbedded with flint	91	98
limestone	98	100
Total Depth		100

Driller's Log filed

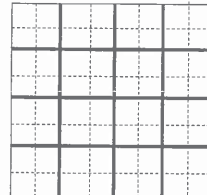
Owner Address: ,

Location source: Location from the driller

Permit Date:

Permit #:

COMPANY owner
FARM Cen. Ill. Pub. Service Co
DATE DRILLED January 1, 1941 **NO. 22**
ELEVATION 4340 **COUNTY NO.** 00556
LOCATION 445'N 230'E SW/c NE SE
LATITUDE 39.823809 **LONGITUDE** -90.565185
COUNTY Morgan **API** 121370055600



21 - 16N - 13W

ILLINOIS STATE GEOLOGICAL SURVEY

Water Well	Top	Bottom
sand, fine grain	0	3
sand, fine grain	3	6
sand, fine grain	6	10
sand, fine grain	10	15
sand, fine grain	15	25
sand, medium, clay content	25	35
sand, coarse, small pebbles	35	45
sand, coarse, small pebbles	45	55
sand, fine grain	55	65
sand, fine grain	65	75
sand, medium grain	75	85
sand, coarse; fine gravel	85	92
sand, coarse; medium gravel (rock)	92	94
limestone (core)	94	100
Total Depth		100

Driller's Log filed

Owner Address: ,

Location source: Location from the driller

Permit Date:

Permit #:

COMPANY owner

FARM Cen. Ill. Pub. Service Co.

DATE DRILLED January 1, 1941

NO. 19

ELEVATION 4440

COUNTY NO. 00553

LOCATION 400'N 270'E SW/c NE SE

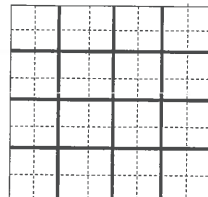
LATITUDE 39.823683

LONGITUDE -90.56508

COUNTY Morgan

API 121370055300

21 - 16N - 13W



Water Well	Top	Bottom
sand, brown, medium grain	0	3
sand, brown, medium grain	3	10
sand, brown, medium grain	10	20
sand, brown, medium grain	20	30
sand, brown, medium grain	30	40
sand, coarse grain, small gravel	40	50
sand, coarse, grain, medium gravel	50	60
sand, coarse grain, small gravel	60	70
sand, coarse grain, small gravel	70	80
sand, coarse, grain, med gvl, tr lignite	80	90
sand, coarse grain, medium gravel	90	100
Total Depth		100

Driller's Log filed

Owner Address: ,

Location source: Location from the driller

Permit Date:

Permit #:

COMPANY owner

FARM Cen. Ill. Pub. Service

DATE DRILLED January 1, 1941

NO. 12

ELEVATION 4570

COUNTY NO. 00546

LOCATION 370'N 360'E SW/c NE SE

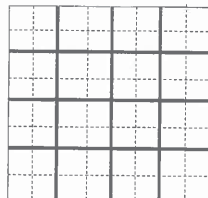
LATITUDE 39.823598

LONGITUDE -90.564781

COUNTY Morgan

API 121370054600

21 - 16N - 13W



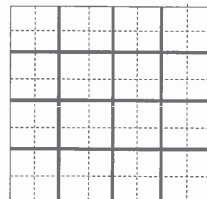
ILLINOIS STATE GEOLOGICAL SURVEY

Water Well	Top	Bottom
silty sand	0	15
coarse sand & gravel	15	30
medium sand & gravel	30	50
gravel, coarse sand	50	60
fine sand	60	67
sand & gravel	67	80
fine sand	80	85
gravel	85	106
rock at	106	106
Total Depth		106
Casing: 12" from -2' to 81'		
20" from 0' to 30'		
Water from sand & gravel at 0' to 0'.		
Static level 27' below casing top which is 2' above GL		
Pumping level 33' when pumping at 503 gpm for 24 hours		
Driller's Log filed		
Owner Address: ,		
Location source: Location from permit		

Permit Date:

Permit #:

COMPANY owner
 FARM CIPS Meredosia Unit 4
 DATE DRILLED May 1, 1974 NO. 5
 ELEVATION 455TM COUNTY NO. 20658
 LOCATION 1700'S line, 300'E line of SE
 LATITUDE 39.823541 LONGITUDE -90.564662
 COUNTY Morgan API 121372065800



21 - 16N - 13W

ILLINOIS STATE GEOLOGICAL SURVEY

Water Well	Top	Bottom
sand, fine grain	0	3
sand, fine grain	3	6
sand, medium grain	6	10
sand, medium grain	10	15
sand, medium; fine gravel	15	25
sand, coarse; medium gravel	25	35
sand, fine grain	35	45
sand, fine grain	45	55
sand, medium; small gravel	55	65
sand, coarse; small gravel	65	75
sand, coarse; medium gravel	75	82
limestone	82	85
limestone	85	95
limestone	95	100
Total Depth		100

Driller's Log filed

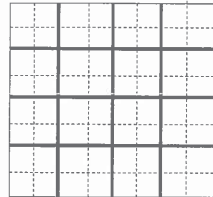
Owner Address: ,

Location source: Location from the driller

Permit Date:

Permit #:

COMPANY owner
 FARM Cen. Ill. Pub. Service Co
 DATE DRILLED January 1, 1941 NO. 23
 ELEVATION 43200 COUNTY NO. 00557
 LOCATION 380'N 160'E SW/c NE SE
 LATITUDE 39.823633 LONGITUDE -90.565487
 COUNTY Morgan API 121370055700



21 - 16N - 13W

ILLINOIS STATE GEOLOGICAL SURVEY

Water Well	Top	Bottom
sand, fine; little clay	0	3
sand, fine grain	3	6
sand, medium grain	6	10
sand, medium grain	10	15
sand, coarse; fine gravel	15	25
sand, coarse; fine gravel	25	35
sand, medium, small pebbles	35	45
sand, coarse; fine gravel	45	55
sand, fine grain	55	65
sand, fine grain	65	75
sand, medium, small pebbles	75	85
sand, coarse; coarse gravel	85	93
limestone core	93	97
limestone, chert bands, core	97	100
Total Depth		100

Driller's Log filed

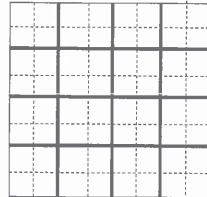
Owner Address: ,

Location source: Location from the driller

Permit Date:

Permit #:

COMPANY owner
 FARM Cen. Ill. Pub. Service Co.
 DATE DRILLED January 1, 1941 NO. 18
 ELEVATION 4430 COUNTY NO. 00552
 LOCATION 335'N 200'E SW/c NE SE
 LATITUDE 39.823507 LONGITUDE -90.565381
 COUNTY Morgan API 121370055200



21 - 16N - 13W

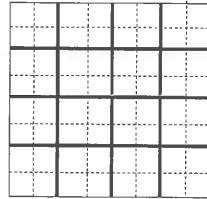
ILLINOIS STATE GEOLOGICAL SURVEY

Water Well	Top	Bottom
fine to medium sand	0	24
medium sand & fine gravel	24	55
fine sand	55	68
sand & gravel	68	73
medium sand, gravel & boulders	73	78
total depth	78	109
Total Depth		109
Casing: 30" from 0' to 30'		
10" from 4' to 84'		
Pumping level 3' when pumping at 165 gpm for 1 hour		
Driller's Log filed		
Owner Address:		
Location source: Location from the driller		

Permit Date:

Permit #:

COMPANY owner
 FARM Central Ill. Public Ser.
 DATE DRILLED November 21, 1957 NO. 3
 ELEVATION 460GL COUNTY NO. 20657
 LOCATION 1643'S line, 473'E line of section
 LATITUDE 39.823391 LONGITUDE -90.565304
 COUNTY Morgan API 121372065700



21 - 16N - 13W

ILLINOIS STATE GEOLOGICAL SURVEY

Water Well	Top	Bottom
sand, medium grain	0	3
sand, brown, medium grain	3	10
sand, brown, medium grain	10	15
sand, medium grain, clay content	15	17
sand, brown, medium grain	17	20
sand, brown, medium grain	20	30
sand, coarse; small gravel	30	40
sand, coarse; small gravel	40	50
sand, coarse; medium gravel	50	60
sand, coarse; medium gravel	60	70
sand, medium grain	70	80
sand, medium grain	80	90
sand, medium grain; medium gravel	90	100
Total Depth		100

Driller's Log filed

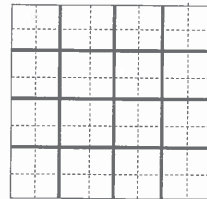
Owner Address: ,

Location source: Location from the driller

Permit Date:

Permit #:

COMPANY owner
 FARM Cen. Ill. Pub. Service Co.
 DATE DRILLED January 1, 1941 NO. 13
 ELEVATION 4560 COUNTY NO. 00547
 LOCATION 305'N 295'E SW/c NE SE
 LATITUDE 39.823421 LONGITUDE -90.565065
 COUNTY Morgan API 121370054700



21 - 16N - 13W

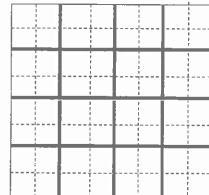
ILLINOIS STATE GEOLOGICAL SURVEY

Water Well	Top	Bottom
sand, silty, brown	0	3
sand, brown, medium grain	3	10
sand, brown, medium grain	10	20
sand, brown, medium grain	20	25
Total Depth		25
Driller's Log filed		
Owner Address: ,		
Location source: Location from the driller		

Permit Date:

Permit #:

COMPANY owner
FARM Cen. Ill. Pub. Service
DATE DRILLED January 1, 1941 **NO. 10**
ELEVATION 4560 **COUNTY NO.** 00544
LOCATION 255'N 350'E SW/c NE SE
LATITUDE 39.823282 **LONGITUDE** -90.564909
COUNTY Morgan **API** 121370054400



21 - 16N - 13W

ILLINOIS STATE GEOLOGICAL SURVEY

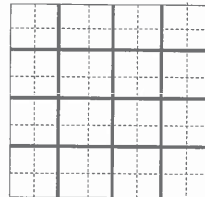
Water Well	Top	Bottom
sand, silty, medium grain	0	1
sand, brown, medium grain	1	7
sand, brown, medium grain	7	10
sand, brown, slight clay content	10	13
sand, brown, slight clay content	13	19
sand, dark brown, medium grain	19	25
Total Depth		25

Driller's Log filed

Permit Date:

Permit #:

COMPANY C.I.P.S.
FARM Cen. Ill. Pub. Service
DATE DRILLED January 1, 1941 **NO. 1**
ELEVATION 4540 **COUNTY NO.** 00535
LOCATION 190'N 410'E SW/c NE SE
LATITUDE 39.823098 **LONGITUDE** -90.564749
COUNTY Morgan **API** 121370053500



21 - 16N - 13W

ILLINOIS STATE GEOLOGICAL SURVEY

Water Well	Top	Bottom
sand, medium grain	0	3
sand, medium grain	3	6
sand, medium grain	6	10
sand, medium grain	10	15
sand, fine grain	15	25
sand, medium; fine gravel	25	35
sand, fine grain	35	45
sand, fine grain	45	50
Total Depth		50

Driller's Log filed

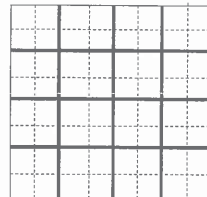
Owner Address: ,

Location source: Location from the driller

Permit Date:

Permit #:

COMPANY owner
 FARM Cen. Ill. Pub. Service Co
 DATE DRILLED January 1, 1941 NO. 26
 ELEVATION 42300 COUNTY NO. 00560
 LOCATION 395'N 45'E SW/c NE SE
 LATITUDE 39.823679 LONGITUDE -90.565885
 COUNTY Morgan API 121370056000



21 - 16N - 13W

ILLINOIS STATE GEOLOGICAL SURVEY

Water Well	Top	Bottom
sand, brown, medium grain	0	3
sand, brown, medium grain	3	10
sand, brown, medium grain	10	20
sand, brown, medium grain	20	30
sand, medium grain; small gravel	30	40
sand, medium grain; small gravel	40	50
sand, medium grain; small gravel	50	60
sand, medium grain; medium gravel	60	70
sand, medium grain; small gravel	70	80
sand, medium grain; small gravel	80	90
sand, medium grain; small gravel	90	100
Total Depth		100

Driller's Log filed

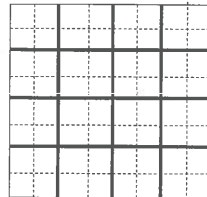
Owner Address: ,

Location source: Location from the driller

Permit Date:

Permit #:

COMPANY owner
 FARM Cen. Ill. Pub. Service Co.
 DATE DRILLED January 1, 1941 NO. 14
 ELEVATION 4560 COUNTY NO. 00548
 LOCATION 240'N 230'E SW/c NE SE
 LATITUDE 39.823245 LONGITUDE -90.565349
 COUNTY Morgan API 121370054800



21 - 16N - 13W

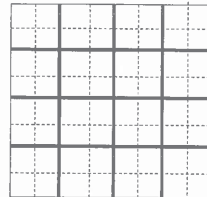
ILLINOIS STATE GEOLOGICAL SURVEY

Water Well	Top	Bottom
sand, silty, brown	0	3
sand, brown, medium grain	3	10
sand, brown, medium grain	10	20
sand, brown, medium grain, small gravel	20	25
Total Depth		25
Driller's Log filed		
Owner Address: ,		
Location source: Location from the driller		

Permit Date:

Permit #:

COMPANY owner
FARM Cen. Ill. Pub. Service
DATE DRILLED January 1, 1941 **NO. 9**
ELEVATION 4560 **COUNTY NO.** 00543
LOCATION 215'N 310'E SW/c NE SE
LATITUDE 39.823173 **LONGITUDE** -90.565083
COUNTY Morgan **API** 121370054300



21 - 16N - 13W

Water Well	Top	Bottom
sand, silty	0	2
sand, brown, medium grain	2	5
sand, brown, medium grain	5	10
sand, brown, medium grain	10	14
sand, brown, medium grain, slight clay	14	15
sand, brown, medium grain	15	20
sand, brown, medium grain	20	25
Total Depth		25

Driller's Log filed

Owner Address: ,

Location source: Location from the driller

Permit Date:

Permit #:

COMPANY owner

FARM Cen. Ill. Pub. Service

DATE DRILLED January 1, 1941

NO. 2

ELEVATION 4540

COUNTY NO. 00536

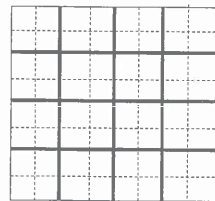
LOCATION 150'N 370'E SW/c NE SE

LATITUDE 39.822992

LONGITUDE -90.564922

COUNTY Morgan

API 121370053600



21 - 16N - 13W

ILLINOIS STATE GEOLOGICAL SURVEY

Water Well	Top	Bottom
sand, fine grain	0	3
sand, medium grain	3	6
sand, fine grain	6	10
sand, fine grain	10	15
sand, medium, small pebbles	15	25
sand, fine grain	25	35
sand, medium grain	35	45
sand, fine grain	45	55
sand, fine grain	55	65
sand, coarse; fine gravel	65	75
sand, coarse; medium gravel	75	81
limestone core	81	86
limestone with chert bands	86	89
limestone	89	91
limestone	91	100
Total Depth		100

Driller's Log filed

Owner Address: ,

Location source: Location from the driller

Permit Date:

Permit #:

COMPANY owner
 FARM Cen. Ill. Pub. Service Co
 DATE DRILLED January 1, 1941 NO. 24
 ELEVATION 43100 COUNTY NO. 00558
 LOCATION 310'N 95'E SW/c NE SE
 LATITUDE 39.823442 LONGITUDE -90.565774
 COUNTY Morgan API 121370055800

21 - 16N - 13W

ILLINOIS STATE GEOLOGICAL SURVEY

Water Well	Top	Bottom
sand, medium grain	0	3
sand, medium grain	3	10
sand, medium grain	10	20
sand, medium grain; small gravel	20	30
sand, medium grain	30	40
sand, coarse; large gravel	40	50
sand, coarse; large gravel	50	56
sand, fine	56	60
sand, fine; small gravel	60	70
sand, fine; small gravel	70	80
sand, coarse; coarse gravel	80	90
gravel, medium, clay content	90	95
limestone	95	96
limestone	96	100
Total Depth		100

Driller's Log filed

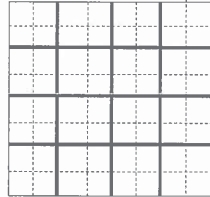
Owner Address: ,

Location source: Location from the driller

Permit Date:

Permit #:

COMPANY owner
 FARM Cen. Ill. Pub. Service Co.
 DATE DRILLED January 1, 1941 NO. 17
 ELEVATION 4460 COUNTY NO. 00551
 LOCATION 270'N 135'E SW/c NE SE
 LATITUDE 39.82333 LONGITUDE -90.565661
 COUNTY Morgan API 121370055100



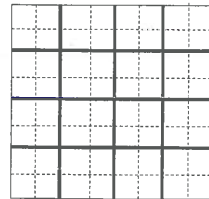
21 - 16N - 13W

Water Well	Top	Bottom
sand, brown, medium grain	0	2
sand, brown, medium grain	2	10
sand, brown, medium grain	10	20
sand, brown, medium grain	20	25
Total Depth		25
Driller's Log filed		
Owner Address: ,		
Location source: Location from the driller		

Permit Date:

Permit #:

COMPANY owner
FARM Cen. Ill. Pub. Service
DATE DRILLED January 1, 1941 **NO. 8**
ELEVATION 45700 **COUNTY NO.** 00542
LOCATION 175'N 270'E SW/c NE SE
LATITUDE 39.823063 **LONGITUDE** -90.565256
COUNTY Morgan **API** 121370054200



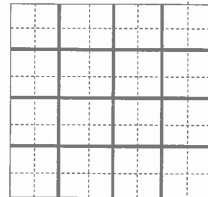
21 - 16N - 13W

Water Well	Top	Bottom
sand, brown, silty	0	3
sand, brown, medium grain	3	5
sand, brown, medium grain	5	10
sand, brown, medium grain	10	20
sand, brown, traces of fine gravel	20	25
Total Depth		25
Driller's Log filed		
Owner Address: ,		
Location source: Location from the driller		

Permit Date:

Permit #:

COMPANY owner
 FARM Cen. Ill. Pub. Service
 DATE DRILLED January 1, 1941 NO. 3
 ELEVATION 4540 COUNTY NO. 00537
 LOCATION 105'N 330'E SW/c NE SE
 LATITUDE 39.822869 LONGITUDE -90.5651
 COUNTY Morgan API 121370053700



21 - 16N - 13W

Water Well	Top	Bottom
sand, brown	0	3
sand, brown, medium grain	3	10
sand, brown, medium grain	10	20
sand, brown, medium grain	20	30
sand, medium grain; small gravel	30	40
sand, medium grain; small gravel	40	50
sand; small gravel	50	60
sand; coarse gravel	60	70
sand, fine grain; traces small gravel	70	80
sand, fine grain	80	90
sand, coarse	90	100
Total Depth		100

Driller's Log filed

Owner Address: ,

Location source: Location from the driller

Permit Date:

Permit #:

COMPANY owner

FARM Cen. Ill. Pub. Service Co.

DATE DRILLED January 1, 1941

NO. 15

ELEVATION 4540

COUNTY NO. 00549

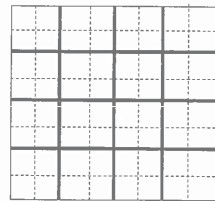
LOCATION 175'N 160'E SW/c NE SE

LATITUDE 39.823068

LONGITUDE -90.565647

COUNTY Morgan

API 121370054900



21 - 16N - 13W

ILLINOIS STATE GEOLOGICAL SURVEY

Water Well	Top	Bottom
sand, brown, medium grain	0	3
sand, brown, medium grain	3	10
sand, brown, medium grain	10	20
sand, brown, medium grain	20	30
sand, medium coarse grain, small gravel	30	40
sand, medium coarse grain, small gravel	40	50
Total Depth		50

Driller's Log filed

Owner Address: ,

Location source: Location from the driller

Permit Date:

Permit #:

COMPANY owner

FARM Cen. Ill. Pub. Service

DATE DRILLED January 1, 1941

NO. 7

ELEVATION 4560

COUNTY NO. 00541

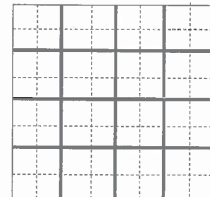
LOCATION 130'N 230'E SW/c NE SE

LATITUDE 39.822943

LONGITUDE -90.565434

COUNTY Morgan

API 121370054100



21 - 16N - 13W

ILLINOIS STATE GEOLOGICAL SURVEY

Water Well	Top	Bottom
sand, silty, brown	0	1
sand, brown, medium grain	1	5
sand, brown, medium grain	5	10
sand, brown, medium grain, slight clay	10	10
sand, brown, medium grain	10	28
sand, medium gravel	28	30
sand, medium gravel, water showing	30	40
sand, medium gravel, water showing	40	50
Total Depth		50

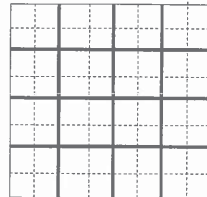
Driller's Log filed

Owner Address: ,
 Location source: Location from the driller

Permit Date:

Permit #:

COMPANY owner
 FARM Cen. Ill. Pub. Service
 DATE DRILLED January 1, 1941 NO. 4
 ELEVATION 4540 COUNTY NO. 00538
 LOCATION 65°N 290°E SW/c NE SE
 LATITUDE 39.82276 LONGITUDE -90.565273
 COUNTY Morgan API 121370053800



21 - 16N - 13W

ILLINOIS STATE GEOLOGICAL SURVEY

Water Well	Top	Bottom
sand, brown, medium grain	0	5
sand, brown, medium grain	5	10
sand, brown, medium grain	10	20
sand, light brown, medium grain	20	30
no record	30	31
sand, coarse; medium gravel	31	35
sand, coarse; medium gravel	35	40
sand, fine grain	40	50
sand, fine grain	50	60
gravel, small, pea size	60	70
sand, coarse; small gravel	70	80
sand, coarse; small gravel	80	86
limestone	86	92
limestone	92	95
limestone	95	100
Total Depth		100

Driller's Log filed

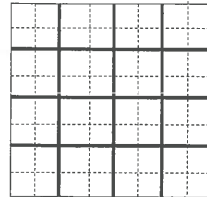
Owner Address: ,

Location source: Location from the driller

Permit Date:

Permit #:

COMPANY owner
FARM Cen. Ill. Pub. Service Co
DATE DRILLED January 1, 1941 **NO. 25**
ELEVATION 4360 **COUNTY NO.** 00559
LOCATION 245'N 25'E SW/c NE SE
LATITUDE 39.823266 **LONGITUDE** -90.566072
COUNTY Morgan **API** 121370055900



21 - 16N - 13W

ILLINOIS STATE GEOLOGICAL SURVEY

Water Well	Top	Bottom
sand, brown, medium grain	0	4
clay, sandy	4	5
sand, brown, medium grain	5	10
sand, brown, medium grain	10	20
sand, medium; medium gravel	20	30
sand, medium; medium gravel	30	40
sand, coarse; medium gravel	40	50
sand, fine; coarse gravel	50	60
sand, fine	60	70
sand; medium gravel	70	80
sand, coarse; small gravel	80	90
sand, coarse; small gravel	90	93
sand, coarse; small gravel	93	95
limestone	95	96
limestone	96	100
Total Depth		100

Driller's Log filed

Owner Address: ,

Location source: Location from the driller

Permit Date:

Permit #:

COMPANY owner

FARM Cen. Ill. Pub. Service Co.

DATE DRILLED January 1, 1941

NO. 16

ELEVATION 4460

COUNTY NO. 00550

LOCATION 190'N 80'E SW/c NE SE

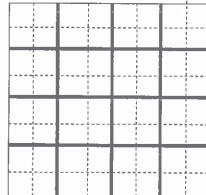
LATITUDE 39.823113

LONGITUDE -90.565919

COUNTY Morgan

API 121370055000

21 - 16N - 13W



ILLINOIS STATE GEOLOGICAL SURVEY

Water Well	Top	Bottom
sand, silty, brown	0	2
sand, brown, medium grain	2	10
sand, brown, medium grain	10	20
sand, brown, medium coarse grain	20	30
sand, brown, small gravel	30	40
sand, medium coarse, medium gravel	40	50
Total Depth		50

Driller's Log filed

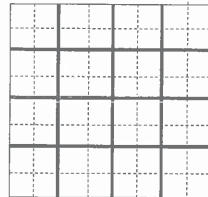
Owner Address: ,

Location source: Location from the driller

Permit Date:

Permit #:

COMPANY owner
 FARM Cen. Ill. Pub. Service
 DATE DRILLED January 1, 1941 NO. 6
 ELEVATION 4540 COUNTY NO. 00540
 LOCATION 85°N 190°E SW/c NE SE
 LATITUDE 39.82282 LONGITUDE -90.565614
 COUNTY Morgan API 121370054000



21 - 16N - 13W

ILLINOIS STATE GEOLOGICAL SURVEY

Water Well	Top	Bottom
sand, silty, brown	0	3
sand, brown, medium grain	3	5
sand, brown, medium grain	5	10
sand, brown, slight clay content	10	15
sand, brown, medium grain	15	20
sand, brown, medium grain	20	29
sand, medium gravel, water showing	29	30
sand, medium grain, medium gravel	30	40
sand, medium grain, medium gravel	40	50
Total Depth		50

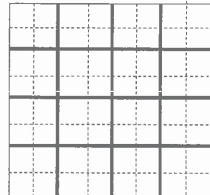
Driller's Log filed

Owner Address: ,
 Location source: Location from the driller

Permit Date:

Permit #:

COMPANY owner
 FARM Cen. Ill. Pub. Service
 DATE DRILLED January 1, 1941 NO. 5
 ELEVATION 454CO COUNTY NO. 00539
 LOCATION 25'N 250'E SW/c NE SE
 LATITUDE 39.822653 LONGITUDE -90.565447
 COUNTY Morgan API 121370053900



21 - 16N - 13W

Water Well	Top	Bottom
sand, medium; silt & pebbles	0	5
sand, medium; fine gravel	5	14
sand, medium; fine gravel	14	24
sand, fine grain	24	34
sand, fine grain	34	44
sand, fine grain	44	54
sand, coarse; small pebbles	54	64
sand, coarse; medium gravel	64	67
limestone (broken), core	67	77
limestone (broken), core	77	87
limestone (broken), core	87	100
Total Depth		100

Driller's Log filed

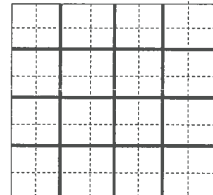
Owner Address: ,

Location source: Location from the driller

Permit Date:

Permit #:

COMPANY owner
FARM Cen. Ill. Pub. Service Co
DATE DRILLED January 1, 1941 **NO. 28**
ELEVATION 417CO **COUNTY NO.** 00562
LOCATION 290'N 180'W SE/c NW SE
LATITUDE 39.823398 **LONGITUDE** -90.566769
COUNTY Morgan **API** 121370056200



21 - 16N - 13W

ILLINOIS STATE GEOLOGICAL SURVEY

Water Well	Top	Bottom
silt, sandy, dark brown	0	3
silt, sandy, dark brown	3	6
sand, medium & silt	6	10
sand, fine, light brown	10	15
sand, medium; fine gravel	15	20
sand, coarse; coarse gravel	20	30
sand, fine; small stones	30	40
sand, fine	40	50
Total Depth		50

Driller's Log filed

Owner Address: ,

Location source: Location from the driller

Permit Date:

Permit #:

COMPANY owner

FARM Cen. Ill. Pub. Service Co

DATE DRILLED January 1, 1941

NO. 29

ELEVATION 4290

COUNTY NO. 00563

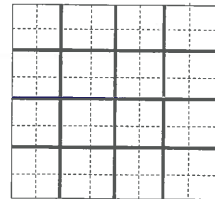
LOCATION 200'N 95'W SE/c NW SE

LATITUDE 39.823148

LONGITUDE -90.566536

COUNTY Morgan

API 121370056300



21 - 16N - 13W

Water Well	Top	Bottom
sand, brown, slight clay content	0	3
sand, brown, medium grain	3	10
sand, brown, medium grain	10	19
sand, coarse; medium gravel	19	20
sand, coarse; medium gravel	20	30
sand, coarse; small gravel	30	40
sand, coarse; medium gravel	40	50
sand, fine	50	60
sand, coarse	60	70
sand, coarse	70	80
sand, coarse	80	89
sand, coarse; small gvl w/tr of lignite	89	90
limestone	90	96
limestone	96	100
Total Depth		100

Driller's Log filed

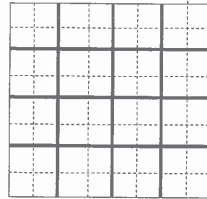
Owner Address: ,

Location source: Location from the driller

Permit Date:

Permit #:

COMPANY owner
FARM Cen. Ill. Pub. Service Co
DATE DRILLED January 1, 1941 **NO.** 30
ELEVATION 44200 **COUNTY NO.** 00564
LOCATION 115'N 5'W SE/c NW SE
LATITUDE 39.822911 **LONGITUDE** -90.566281
COUNTY Morgan **API** 121370056400



21 - 16N - 13W

ILLINOIS STATE GEOLOGICAL SURVEY

Water Well	Top	Bottom
sand fill	0	20
clay	20	30
coarse sand & gravel	30	104
rock at	104	104
Total Depth		104
Casing: 30" STEEL .312 from 0' to 30'		
12" STEEL .375 from 0' to 79'		
Screen: 25' of 12" diameter 6 slot		
Size hole below casing: 38"		
Water from alluvial at 30' to 102'.		
Static level 25' below casing top which is 2' above GL		
Driller's Log filed		
Owner Address: Meredosia, IL		
Location source: Platbook verified		

Permit Date: September 8, 1977

Permit #: 66466

COMPANY Ruester, John T.

FARM Central Ill. Public Ser.Co.

DATE DRILLED April 25, 1978

NO. 6

ELEVATION 448GL

COUNTY NO. 20758

LOCATION 100'S line, 50'W line of SW NE SE

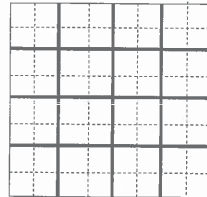
LATITUDE 39.822865

LONGITUDE -90.566098

COUNTY Morgan

API 121372075800

21 - 16N - 13W



Water Well	Top	Bottom
sand, brown, medium grain	0	8
sand, medium, clay content	8	10
sand, brown, medium grain	10	15
sand, brown, medium grain	15	20
sand, brown, medium grain	20	30
sand & medium gravel	30	35
sand, coarse; medium gravel	35	40
sand, coarse; medium gravel	40	45
sand, coarse; fine gravel	45	50
Total Depth		50

Driller's Log filed

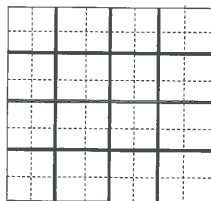
Owner Address: ,

Location source: Location from the driller

Permit Date:

Permit #:

COMPANY owner
 FARM Cen. Ill. Pub. Service Co
 DATE DRILLED January 1, 1941 NO. 31
 ELEVATION 454CO COUNTY NO. 00565
 LOCATION 40'N 70'E SW/c NE SE
 LATITUDE 39.8227 LONGITUDE -90.566074
 COUNTY Morgan API 121370056500



21 - 16N - 13W

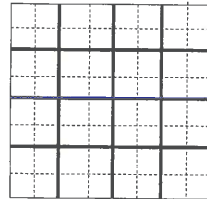
ILLINOIS STATE GEOLOGICAL SURVEY

Water Well	Top	Bottom
fine brown sand	0	30
coarse sand	30	50
medium sand	50	70
fine to medium sand	70	90
sand & gravel	90	105
rock at	105	105
Total Depth		105
Casing: 12" from -1' to 79'		
30" from 0' to 31'		
Water from sand & gravel at 0' to 0'.		
Static level 32' below casing top which is 0' above GL		
Pumping level 39' when pumping at 517 gpm for 22 hours		
Driller's Log filed		
Sample set # 58921 (0' - 103') Received: December 8, 1973		
Owner Address: ,		
Location source: Location from permit		

Permit Date:

Permit #:

COMPANY owner
FARM CIPS Meredosia Power Sta unit 4,#
DATE DRILLED August 30, 1973 **NO.** 5
ELEVATION 445TM **COUNTY NO.** 00639
LOCATION 1300'S line, 500'E line of SE
LATITUDE 39.822448 **LONGITUDE** -90.565551
COUNTY Morgan **API** 121370063900



21 - 16N - 13W

ILLINOIS STATE GEOLOGICAL SURVEY

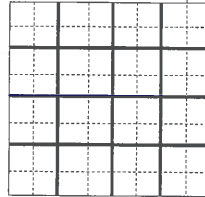
Test Hole	Top	Bottom
crushed stone	0	1
silty sand	1	5
fine sand	5	20
fine to medium sand	20	25
fine to coarse sand	25	35
coarse sand	35	40
med. to coarse sand w/gravel	40	45
fine to medium sand	45	50
fine to coarse sand	50	70
fine to coarse sand w/gravel	70	75
silty, fine to medium sand	75	85
fine to coarse sand	85	95
medium to coarse sand	95	101
fine to coarse sand w/boulders	101	104
Total Depth		104

Sample set # 67974 (5' - 103') Received: July 1, 1994

Owner Address: Meredosia, IL
 Location source: Location from the driller

Permit Date: Permit #: none

COMPANY Brotcke, Paul
 FARM CIPS Power Station
 DATE DRILLED June 21, 1994 NO. 7
 ELEVATION 0 COUNTY NO. 21579
 LOCATION SE NE SE
 LATITUDE 39.823501 LONGITUDE -90.564221
 COUNTY Morgan API 121372157900 21 - 16N - 13W



Noncommunity - Public Water Well	Top	Bottom
fine-medium sand	0	24
medium sand & fine gravel	24	55
fine sand	55	68
sand & gravel	68	73
medium sand, gravel & boulders	73	78
Total Depth		78
Pumping level 0' when pumping at 165 gpm for 1 hour		

Permit Date:

Permit #:

COMPANY

FARM CIPS

DATE DRILLED November 21, 1957

NO. 3

ELEVATION 460

COUNTY NO. 21982

LOCATION NW NE SE

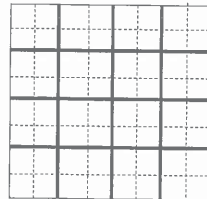
LATITUDE 39.825368

LONGITUDE -90.564994

COUNTY Morgan

API 121372198200

21 - 16N - 13W



Noncommunity - Public Water Well	Top	Bottom
fine sand	0	25
medium sand-fine gravel	25	40
fine sand	40	48
fine-coarse sand & gravel	48	52
fine-medium sand	52	65
fine pink sand	65	81
coarse sand, gravel & small boulders	81	105
Total Depth		105
Static level 38' below casing top which is 0' above GL		
Pumping level 40' when pumping at 503 gpm for 8 hours		

Permit Date:

Permit #:

COMPANY

FARM CIPS

DATE DRILLED December 1, 1960

NO. 4

ELEVATION 460

COUNTY NO. 21981

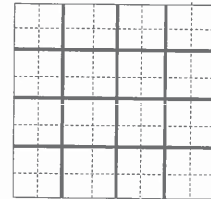
LOCATION NE NE SE

LATITUDE 39.825356

LONGITUDE -90.563863

COUNTY Morgan

API 121372198100



21 - 16N - 13W

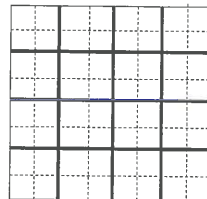
ILLINOIS STATE GEOLOGICAL SURVEY

Noncommunity - Public Water Well	Top	Bottom
fill sand	0	20
fine sand	20	40
medium sand	40	85
medium sand with gravel	85	104
rock at	104	104
Total Depth		104
Casing: 36" STEEL 166.35#/FT from -2' to 30' 16" STEEL 62.58#/FT from -2' to 79'		
Screen: 25' of 16" diameter .05 slot		
Grout: NEAT from 0 to 30.		
Water from sand & gravel at 32' to 104'.		
Static level 32' below casing top which is 2' above GL		
Permanent pump installed at 75' on July 11, 1994, with a capacity of 600 gpm		
Owner Address: 800 S. Washington St. Meredosia, IL		
Location source: Location from permit		

Permit Date: June 9, 1994

Permit #:

COMPANY Brotcke Engineering
 FARM Central IL Public Service C
 DATE DRILLED June 21, 1994 NO. 7
 ELEVATION 0 COUNTY NO. 21613
 LOCATION SE NE SE
 LATITUDE 39.823501 LONGITUDE -90.564221
 COUNTY Morgan API 121372161300



21 - 16N - 13W

ILLINOIS STATE GEOLOGICAL SURVEY

Noncommunity - Public Water Well	Top	Bottom
fill sand	0	20
fine sand	20	40
medium sand	40	85
medium sand w/ gravel	85	104
rock @	104	104
Total Depth		104
Casing: 36" STEEL from -2' to 30'		
16" STEEL from -2' to 79'		
Grout: NEAT from 0 to 30.		
Water from sand & gravel at 32' to 104'.		
Static level 32' below casing top which is 2' above GL		
Permanent pump installed at 75'		
on July 11, 1994, with a capacity of 600 gpm		
Remarks: IEPA well #13700182		
Owner Address:		
Address of well: 800 Washington		
Meredosia, IL		
Location source: Location from the driller		

Permit Date: June 9, 1994

Permit #:

COMPANY Brotcke Engineering

FARM CIPS

DATE DRILLED June 21, 1994

NO. 7

ELEVATION 0

COUNTY NO. 21980

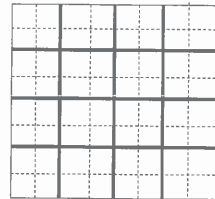
LOCATION SE NE SE

LATITUDE 39.823501

LONGITUDE -90.564221

COUNTY Morgan

API 121372198000



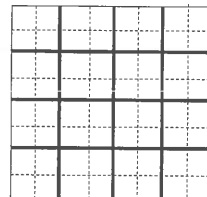
21 - 16N - 13W

Water Well	Top	Bottom
sand	0	40
medium to fine sand	40	70
sand & gravel	70	94
gravel & boulders	94	98
Total Depth		98
Casing: 12" STEEL CASING from 0' to 78'		
Static level 25' below casing top which is 0' above GL		
Pumping level 34' when pumping at 600 gpm for 15 hours		
Owner Address: ,		
Location source: Location from the driller		

Permit Date:

Permit #:

COMPANY owner
 FARM National Starch & Chem. Co
 DATE DRILLED July 7, 1964 NO. 4
 ELEVATION 435GL COUNTY NO. 20802
 LOCATION 1669'N line, 1850'E line of NE
 LATITUDE 39.814322 LONGITUDE -90.570968
 COUNTY Morgan API 121372080200



28 - 16N - 13W

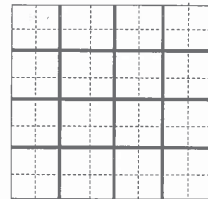
ILLINOIS STATE GEOLOGICAL SURVEY

Water Well	Top	Bottom
ss #31677	0	0
sand	0	20
sand & gravel	20	60
coarse sand & gravel	60	92
Total Depth		92
Casing: 12" ID from -2' to 72'		
Water from at 70' to 90'.		
Static level 25' below casing top which is 0' above GL		
Pumping level 0' when pumping at 500 gpm for 0 hours		
Remarks: see file for detail sample study		
Driller's Log filed		
Sample set # 31677 (0' - 92') Received: October 21, 1958		
Owner Address: ,		
Location source: Location from permit		

Permit Date: September 9, 1958

Permit #:

COMPANY owner
 FARM National Starch Prod.
 DATE DRILLED October 1, 1958 NO. 2
 ELEVATION 442GL COUNTY NO. 00147
 LOCATION 310'N line, 1200'E line of NE
 LATITUDE 39.818045 LONGITUDE -90.568641
 COUNTY Morgan API 121370014700



28 - 16N - 13W

ILLINOIS STATE GEOLOGICAL SURVEY

Water Well	Top	Bottom
sand	0	45
sand & gravel	45	90
Total Depth		90
Casing: 16" STEEL 3/8 WALL from -2' to 65'		
Screen: 25' of 16" diameter .8 slot		
Water from drift at 65' to 90'.		
Owner Address: P.O. Box 197 Meredosia, IL		
Location source: Location from permit		

Permit Date: October 13, 1978

Permit #: 80737

COMPANY owner

FARM National Starch

DATE DRILLED October 24, 1978

NO. 11

ELEVATION 0

COUNTY NO. 20760

LOCATION 1408'N line, 855'E line of NE

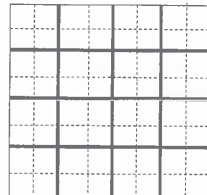
LATITUDE 39.815

LONGITUDE -90.567407

COUNTY Morgan

API 121372076000

28 - 16N - 13W



ILLINOIS STATE GEOLOGICAL SURVEY

Water Well	Top	Bottom
sand	0	40
medium to fine sand	40	70
sand & gravel	70	94
gravel & boulders	94	98
Total Depth		98
Casing: 12" STEEL CASING from 0' to 78'		
Static level 25' below casing top which is 0' above GL		
Pumping level 34' when pumping at 600 gpm for 15 hours		
Owner Address: ,		
Location source: Location from the driller		

Permit Date:

Permit #:

COMPANY owner

FARM National Starch & Chem. Co

DATE DRILLED July 7, 1964

NO. 4

ELEVATION 435GL

COUNTY NO. 20802

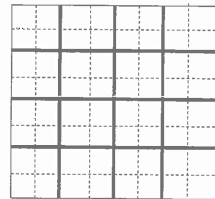
LOCATION 1669'N line, 1850'E line of NE

LATITUDE 39.814322

LONGITUDE -90.570968

COUNTY Morgan

API 121372080200



28 - 16N - 13W

ILLINOIS STATE GEOLOGICAL SURVEY

Semi-Private Water Well	Top	Bottom
top soil	0	2
fine sand	2	17
medium-coarse sand	17	40
medium-coarse gravel	40	62
coarse sand at	62	62
Total Depth		62
Casing: 5" SS SCREEN from 0' to 4' 5" PLAIN CASING from 4' to 62'		
Screen: 4' of 5" diameter .012 slot		
Grout: BENTONITE from 4 to 25.		
Permanent pump installed at 45' on , with a capacity of 10 gpm		
Owner Address: P.O. Box #500 Meredosia, IL		
Address of well: Co. Rd. #1975N		
Location source: Location from permit		

Permit Date: July 16, 1993

Permit #:

COMPANY Dirks, Michael J.

FARM National Starch & Chemical Co.

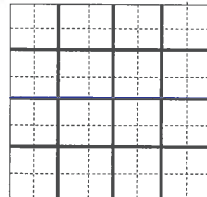
DATE DRILLED July 26, 1993 NO.

ELEVATION 0 COUNTY NO. 21524

LOCATION NW SE NE

LATITUDE 39.814361 LONGITUDE -90.567035

COUNTY Morgan API 121372152400 28 - 16N - 13W



ILLINOIS STATE GEOLOGICAL SURVEY

Water Well	Top	Bottom
sand & gravel	0	89
Total Depth		89
Casing: 16" OD STEEL 3/8"WALL from 0' to 63'		
Screen: 25' of 16" diameter .08 slot		
Water from sand & gravel at 63' to 88'.		
Static level 26' below casing top which is 2' above GL		
Pumping level 33' when pumping at 600 gpm for 8 hours		
Owner Address: Merdosia, IL		
Location source: Location from permit		

Permit Date: October 16, 1977

Permit #: 61809

COMPANY Miller, J.P. Artesian Well Co.

FARM Natl. Starch & Chem.

DATE DRILLED June 21, 1977

NO. 6A

ELEVATION 0

COUNTY NO. 20759

LOCATION 1889'N line, 871'E line of NE

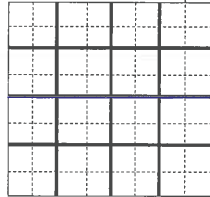
LATITUDE 39.813672

LONGITUDE -90.567465

COUNTY Morgan

API 121372075900

28 - 16N - 13W

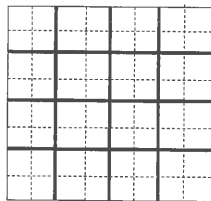


Water Well	Top	Bottom
sand	0	40
medium to fine sand	40	70
sand & gravel	70	94
gravel & boulders	94	98
Total Depth		98
Casing: 12" STEEL CASING from 0' to 78'		
Static level 25' below casing top which is 0' above GL		
Pumping level 34' when pumping at 600 gpm for 15 hours		
Owner Address: ,		
Location source: Location from the driller		

Permit Date:

Permit #:

COMPANY owner
 FARM National Starch & Chem. Co
 DATE DRILLED July 7, 1964 NO. 4
 ELEVATION 435GL COUNTY NO. 20802
 LOCATION 1669'N line, 1850'E line of NE
 LATITUDE 39.814322 LONGITUDE -90.570968
 COUNTY Morgan API 121372080200



28 - 16N - 13W

ILLINOIS STATE GEOLOGICAL SURVEY

Water Well	Top	Bottom
fine sand, not clean	0	18
fine sand, clean	18	60
Total Depth		60
Casing: 16" STEEL 3/8" WALL from 0' to 49'		
8" STEEL 25# from 0' to 52'		
Screen: 10' of 8" diameter 40 slot		
Water from aluvium at 0' to 62'.		
Static level 20' below casing top which is 2' above GL		
Pumping level 25' when pumping at 120 gpm for 2 hours		
Driller's Log filed		
Owner Address: Meredosia, IL		
Location source: Location from permit		

Permit Date: January 1, 1971

Permit #: 10077

COMPANY Diehl Pump and Supply Co.

FARM National Starch

DATE DRILLED January 1, 1971

NO. 2A

ELEVATION 0

COUNTY NO. 00629

LOCATION 2154'N line, 1108'E line of NE

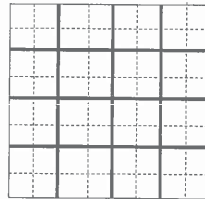
LATITUDE 39.812952

LONGITUDE -90.568313

COUNTY Morgan

API 121370062900

28 - 16N - 13W



ILLINOIS STATE GEOLOGICAL SURVEY

Test Hole	Top	Bottom
drift- sand & gravel	0	96
Total Depth		96
Casing: 16" STEEL 62.58 LB. from 0' to 70'		
Screen: 25' of 16" diameter .08 slot		
Water from drift at 50' to 96'.		
Static level 17' below casing top which is 0' above GL		
Pumping level 24' when pumping at 800 gpm for 8 hours		
Remarks: see file for detail sample study		
Driller's Log filed		
Sample set # 58824 (0' - 95') Received: September 19, 1973		
Owner Address: Meredosia, IL		
Location source: Location from permit		

Permit Date: May 1, 1973

Permit #: 18880

COMPANY Miller, J.P. Artesian Well Co.

FARM National Starch & Chemical

DATE DRILLED May 1, 1973

NO. 9

ELEVATION 0

COUNTY NO. 00638

LOCATION 2600'N line, 1400'E line of NE

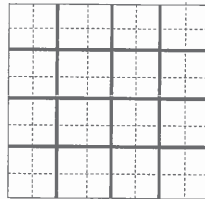
LATITUDE 39.811734

LONGITUDE -90.569358

COUNTY Morgan

API 121370063800

28 - 16N - 13W



ILLINOIS STATE GEOLOGICAL SURVEY

Test Hole	Top	Bottom
ss #55587	0	0
sandy brown clay	0	20
sandy gravel	20	92
Total Depth		92
Casing: 24" STEEL 3/8" WALL from 0' to 50' 12" STEEL 3/8" WALL from 0' to 62'		
Screen: 30' of 12" diameter 50 slot		
Water from drift at 0' to 92'.		
Static level 26' below casing top which is 0' above GL		
Remarks: see file for detail sample study		
Driller's Log filed		
Sample set # 55587 (0' - 93') Received: October 1, 1968		
Owner Address: Meredosia, IL		
Location source: Location from permit		

Permit Date: January 1, 1968

Permit #: NF 4615

COMPANY Diehl Pump and Supply Co.

FARM National Starch

DATE DRILLED August 31, 1968

NO. 8

ELEVATION 0

COUNTY NO. 00422

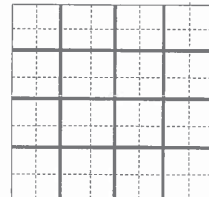
LOCATION 2150'N line, 1400'E line of NE

LATITUDE 39.812976

LONGITUDE -90.569359

COUNTY Morgan

API 121370042200



28 - 16N - 13W

ILLINOIS STATE GEOLOGICAL SURVEY

Non Potable Water Well	Top	Bottom
brown silty sand	0	5
fine sand	5	18
medium to large sand w/1" gravel	18	83
sand w/medium to large gravel	83	85
gravel	85	86
Total Depth		86
Casing: 24" STEEL 94.62#/FT from -2' to 51'		
Screen: 15' of 24" diameter 100 slot		
Grout: CEMENT from 0 to 20.		
Size hole below casing: 42"		
Water from sand & gravel at 0' to 0'.		
Static level 18' below casing top which is 2' above GL		
Pumping level 33' when pumping at 1500 gpm for 8 hours		
Permanent pump installed at 65'		
on September 17, 1996, with a capacity of 1500 gpm		
Owner Address: PO Box 500 Meredosia, IL		
Address of well: S. Washington St. Meredosia, IL		
Add'l loc. info: FALSE		
Process water only		
Location source: Location from permit		

Permit Date: August 28, 1996

Permit #: 137-046

COMPANY Stollhans, Jeff

FARM National Starch & Chem. Co

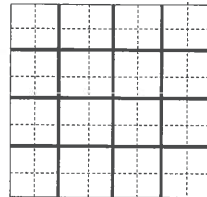
DATE DRILLED September 13, 1996 NO. 16

ELEVATION 0 COUNTY NO. 21769

LOCATION SW SW NE

LATITUDE 39.812578 LONGITUDE -90.570974

COUNTY Morgan API 121372176900 28 - 16N - 13W



ILLINOIS STATE GEOLOGICAL SURVEY

Test Hole	Top	Bottom
ss #55586	0	0
sandy brown clay	0	24
fine sand & gravel	24	69
medium sand & small gravel	69	96
Total Depth		96
Casing: 8" STEEL 3/8" WALL from 0' to 96'		
Screen: 16' of 8" diameter 25 slot		
Water from drift at 0' to 96'.		
Static level 26' below casing top which is 0' above GL		
Driller's Log filed		
Sample set # 55586 (0' - 97') Received: October 1, 1968		
Owner Address: Meredosia, IL		
Location source: Location from permit		

Permit Date: January 1, 1968

Permit #: NF 4614

COMPANY Diehl Pump and Supply Co.

FARM National Starch

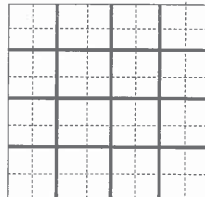
DATE DRILLED August 31, 1968 NO. 7

ELEVATION 0 COUNTY NO. 00421

LOCATION 0'N 0'E SW/c NW SE NE

LATITUDE 39.813492 LONGITUDE -90.569044

COUNTY Morgan API 121370042100 28 - 16N - 13W



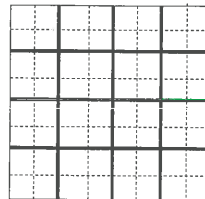
ILLINOIS STATE GEOLOGICAL SURVEY

Test Hole	Top	Bottom
ss #57364	0	0
sandy top soil	0	18
fine sand	18	45
fine sand, small gravel	45	55
fine sand	55	65
fine sand, small gravel	65	93
very large boulders	93	95
rock at	95	95
Total Depth		95
Casing: 26" 3/8 WALL from 0' to 63' 12" 48 POUND from 0' to 68'		
Screen: 25' of 12" diameter 40 slot		
Water from glacial drift at 0' to 95'.		
Static level 25' below casing top which is 2' above GL		
Pumping level 34' when pumping at 1000 gpm for 6 hours		
Remarks: see file for detail sample study		
Driller's Log filed		
Sample set # 57364 (2' - 93') Received: February 4, 1971		
Owner Address: Meredosia, IL		
Location source: Location from permit		

Permit Date: June 24, 1970

Permit #: 10077

COMPANY Diehl Pump and Supply Co.
 FARM National Starch
 DATE DRILLED December 18, 1970 NO. 8
 ELEVATION 0 COUNTY NO. 00628
 LOCATION 1800'N line, 625'E line of NE
 LATITUDE 39.813907 LONGITUDE -90.566585
 COUNTY Morgan API 121370062800



28 - 16N - 13W

ILLINOIS STATE GEOLOGICAL SURVEY

Test Hole	Top	Bottom
ss #54997	0	0
sandy clay	0	21
fine sand, very little gravel	21	60
sand & gravel	60	90
Total Depth		90
Casing: 18" CASING STEEL 3/8" from 0' to 60' 12" STEEL WALL from 0' to 67'		
Screen: 25' of 10" diameter 35 slot		
Size hole below casing: 18"		
Water from glacial drift at 0' to 0'.		
Static level 27' below casing top which is 0' above GL		
Pumping level 47' when pumping at 780 gpm for 3 hours		
Driller's Log filed		
Sample set # 54997 (50' - 91.5') Received: December 14, 1967		
Owner Address: Meredosia, IL		
Location source: Location from permit		

Permit Date: January 1, 1967

Permit #: 3350

COMPANY Diehl Pump and Supply Co.

FARM National Starch

DATE DRILLED February 1, 1968

NO. 6

ELEVATION 0

COUNTY NO. 00396

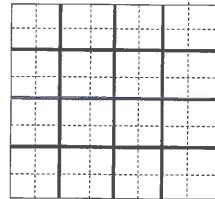
LOCATION 1800'N line, 900'E line of NE

LATITUDE 39.81392

LONGITUDE -90.567569

COUNTY Morgan

API 121370039600



28 - 16N - 13W

ILLINOIS STATE GEOLOGICAL SURVEY

Test Hole	Top	Bottom
ss #60435	0	0
sand	0	40
sand & fine gravel	40	90
rock at	90	90
Total Depth		90
Casing: 16" from -2' to 65'		
Screen: 25' of 16" diameter slot		
Static level 25' below casing top which is 0' above GL		
Pumping level 38' when pumping at 1075 gpm for 2 hours		
Sample set # 60435 (0' - 90') Received: August 30, 1976		
Owner Address: ,		
Location source: Location from permit		

Permit Date: January 20, 1976

Permit #: 44276

COMPANY owner

FARM National Starch & Chem.Co

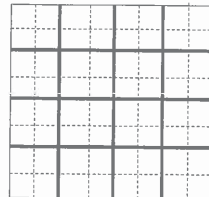
DATE DRILLED February 17, 1976 NO. 10

ELEVATION 0 COUNTY NO. 20682

LOCATION 1403'N line, 332'E line of NE

LATITUDE 39.81499 LONGITUDE -90.565535

COUNTY Morgan API 121372068200 28 - 16N - 13W



ILLINOIS STATE GEOLOGICAL SURVEY

Industrial Water Well	Top	Bottom
fine brown sand	0	40
fine light brown sand	40	55
medium to coarse brown sand & gravel	55	90
Total Depth		91
Casing: 16" BLACK 375 from -2' to 64'		
Screen: 25' of 16" diameter .08 slot		
Grout: CEMENT from 0 to 20.		
Water from sand & gravel at 64' to 91'.		
Static level 28' below casing top which is 2' above GL		
Pumping level 36' when pumping at 800 gpm for 6 hours		
Permanent pump installed at 50'		
on November 10, 1988, with a capacity of 800 gpm		
Owner Address: South Washington St. Meredosia, IL		
Location source: Location from permit		

Permit Date: September 23, 1988

Permit #: 006133

COMPANY Peterson, Steven R.

FARM National Starch-Chemical Co.

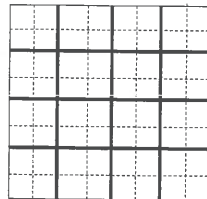
DATE DRILLED October 11, 1988 NO.

ELEVATION 0 COUNTY NO. 21398

LOCATION NE NE NE

LATITUDE 39.817955 LONGITUDE -90.565139

COUNTY Morgan API 121372139800 28 - 16N - 13W



ILLINOIS STATE GEOLOGICAL SURVEY

Industrial Water Well	Top	Bottom
SS #67434 (0'-80.5')	0	0
fine reddish brown sand	0	15
fine-med lt brown to reddish brown sand	15	25
fine-medium light brown sand	25	30
med lt brn sand, some cobbles in samples	30	45
medium light brown sand	45	50
med lt brown sand, lignite in sample	50	55
medium to fine light brown sand	55	60
medium light brown sand	60	80
medium to fine light brown sand	80	81
Total Depth		81
Casing: 8" CARBON STEEL 24.7# from -2' to 58'		
Screen: 20' of 8" diameter 60 slot		
Grout: CONCRETE from 0 to 20.		
Size hole below casing: 34"		
Water from at 24' to 81'.		
Static level 24' below casing top which is 2' above GL		
Pumping level 26' when pumping at 0 gpm for 1 hour		
Permanent pump installed at 50'		
on March 8, 1991, with a capacity of 80 gpm		
Sample set # 67434 (0' - 80.5') Received: April 17, 1981		
Owner Address: S. Washington Meredosia, IL		
Location source: Location from the driller		

Permit Date: January 15, 1991

Permit #: 13736

COMPANY Skouby, Marion

FARM National Starch

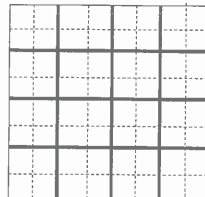
DATE DRILLED February 13, 1991 NO.

ELEVATION 0 COUNTY NO. 21647

LOCATION SW NE NE

LATITUDE 39.816167 LONGITUDE -90.56688

COUNTY Morgan API 121372164700 28 - 16N - 13W

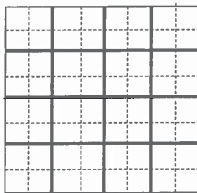


Water Well	Top	Bottom
ss #20134	0	0
sand	0	30
sand, coarse	30	40
Total Depth		40
Casing: 8" from 0' to 0'		
Screen: 10' of " diameter 16 slot		
Driller's Log filed		
Sample set # 20134 (0' - 40') Received: January 1, 1950		
Owner Address: ,		
Location source: Location from the driller		

Permit Date:

Permit #:

COMPANY owner
 FARM Meredosia, Village of
 DATE DRILLED April 1, 1950 NO. 1
 ELEVATION 455GL COUNTY NO. 00514
 LOCATION 900'N line, 3000'E line of section
 LATITUDE 39.831189 LONGITUDE -90.5543
 COUNTY Morgan API 121370051400



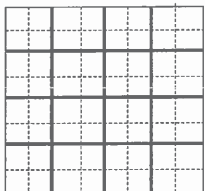
22 - 16N - 13W

Municipal Water Supply	Top	Bottom
no record	0	84
Total Depth		84
Casing: 8" CASING from 0' to 70'		
8" SCREEN from 70' to 84'		
Screen: 14' of 8" diameter 25 slot		
Water from coarse sand at 69' to 84'.		
Owner Address:		
Address of well: 120' NNE of WTP		

Permit Date:

Permit #:

COMPANY Elmer W. Franke/Calhoun Drlg.
FARM Meredosia, Village
DATE DRILLED September 1, 1973 **NO. 3**
ELEVATION 0 **COUNTY NO.** 21944
LOCATION SE NE NW
LATITUDE 39.830881 **LONGITUDE** -90.554188
COUNTY Montgomery **API** 121352194400

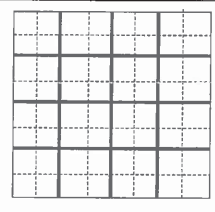


22 - 16N - 13W

Water Well	Top	Bottom
Total Depth		88

Permit Date: Permit #: 37760

COMPANY
 FARM Meredosia Village
 DATE DRILLED NO. 4
 ELEVATION 0 COUNTY NO. 20971
 LOCATION 805'N line, 2950'E line of NE
 LATITUDE 39.83145 LONGITUDE -90.554082
 COUNTY Morgan API 121372097100



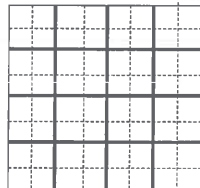
22 - 16N - 13W

Water Well	Top	Bottom
ss #20135	0	0
s, lgt brn, f, rndd, well srted, drty, noncalc	0	5
s, lgt brn, f, rndd, well srted, few calc grns	5	10
s, f, rndd, well srted, few calc grns, clean	10	25
sand, light brown, fine/med, clean, noncalc	25	30
s, lgt brn, f/med, clean, few calc grns	30	35
sand, lgt brn, f/vy crd, clean, mly calc	35	40
Pleistocene	5	40
Total Depth		40
Casing: 8" from 0' to 0'		
Screen: 10' of " diameter 16 slot		
Remarks: see logbook for detail sample study		
Driller's Log filed		
Survey Sample Study filed		
Sample set # 20135 (0' - 40') Received: January 1, 1950		
Owner Address:		
Location source: Location from the driller		

Permit Date:

Permit #:

COMPANY owner
 FARM Meredosia, Village of
 DATE DRILLED April 1, 1950 NO. 2
 ELEVATION 0 COUNTY NO. 00515
 LOCATION 725'S 10'W NE/c NW
 LATITUDE 39.831665 LONGITUDE -90.552929
 COUNTY Morgan API 121370051500



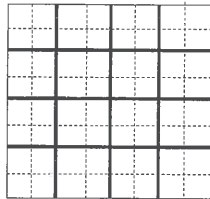
22 - 16N - 13W

Municipal Water Supply	Top	Bottom
no record	0	25
sand & gravel	25	92
Total Depth		92
Casing: 10" CASING from -1' to 72' 10" SCREEN from 72' to 92'		
Screen: 20' of 10" diameter slot		
Water from sand & gravel at 25' to 92'.		
Static level 27' below casing top which is 1' above GL		
Pumping level 32' when pumping at 300 gpm for 3 hours		
Owner Address:		
Address of well: 200' NNW of WTP		

Permit Date:

Permit #:

COMPANY Albrecht Well Drilling Inc
FARM Meredosia, Village
DATE DRILLED September 2, 1980 **NO. 5**
ELEVATION 0 **COUNTY NO.** 21945
LOCATION 612'S line, 2425'E line of section
LATITUDE 39.820473 **LONGITUDE** -90.553748
COUNTY Montgomery **API** 121352194500



22 - 16N - 13W

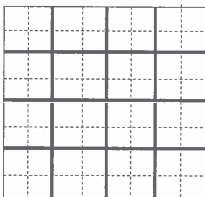
ILLINOIS STATE GEOLOGICAL SURVEY

Engineering Test	Top	Bottom
railroad embankment ballast stone, cinders, & silty clay loam fill drilled 5' to seat augers	0	5
brown silty clay loam moist (v. stiff)	5	8
brown silty clay loam moist (hard)	8	10
dark brown & grey silty clay loam moist (v. stiff)	10	13
dark brown & grey silty clay moist (v. stiff)	13	18
grey clay v. moist (stiff)	18	20
grey & brown clay v. moist (medium)	20	23
grey & brown clay v. moist (stiff)	23	25
grey & brown clay v. moist (medium)	25	28
grey & brown silty clay loam v. moist (stiff)	28	30
grey silty clay v. moist (stiff)	30	33
grey silty clay v. moist (medium)	33	35
grey clay loam wet (soft)	35	38
grey silty clay loam v. moist (soft)	38	40
grey sand (coarse) w/medium pebble gravel wet (v. loose)	40	43
grey sand (coarse) w/some small gravel wet medium	43	45
brown sand (medium) w/some small gravel wet (medium)	45	50
brown sand (medium) wet (medium)	50	53
brown sand (medium-coarse) w/some small gravel wet (medium)	53	55
brown sand (medium-coarse) w/some small gravel wet (dense)	55	58

Permit Date:

Permit #:

COMPANY IL Dept. of Transportation
FARM FAS 2585 P-96-056-85
DATE DRILLED June 9, 1986 **NO. 1 (NW. Abut)**
ELEVATION 438GL **COUNTY NO.** 21245
LOCATION 0'S 0'W NE/c SW SE NW
LATITUDE 39.833731 **LONGITUDE** -90.582965
COUNTY Pike **API** 121492124500



1 - 3S - 2W

brown sand (coarse) w/some small gravel wet (medium)	58	60
brown sand (coarse) w/some medium pebble gravel wet (dense)	60	65
brown sand (medium-coarse) w/some fine pebble gravel wet (dense)	65	70
brown sand (medium-coarse) w/some gravel wet (dense)	70	71.5
Total Depth		71

ILLINOIS STATE GEOLOGICAL SURVEY

Engineering Test	Top	Bottom
brown-brown & grey silty clay loam moist (stiff)	0	7
grey & brown silty clay loam v. moist (medium)	7	9
grey silty clay wet (medium)	9	12
grey silty clay wet (soft)	12	14
grey silty clay wet (medium)	14	17
grey silty clay wet (soft)	17	22
grey clay loam wet (soft)	22	27
grey sand (fine-medium) w/some clay bonding wet (v. loose)	27	29
grey sand (medium-coarse) w/some medium pebble gravel wet (medium)	29	39
grey sand (fine-medium) wet (medium)	39	44
grey sand (medium-coarse) w/some fine pebble gravel wet (medium)	44	49
grey sand (medium-coarse) w/some medium pebble gravel wet (medium)	49	57
grey sand (medium-coarse) w/some medium pebble gravel wet (dense)	57	60.5
Total Depth		60

Permit Date:

Permit #:

COMPANY IL Dept. of Transportation

FARM FAS 2585 Illinois Route 99

DATE DRILLED June 19, 1986

NO. 2 (SE. Abut)

ELEVATION 427GL

COUNTY NO. 21246

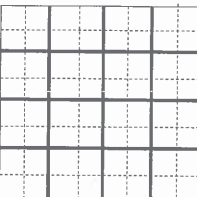
LOCATION SW SE NW

LATITUDE 39.832804

LONGITUDE -90.584075

COUNTY Pike

API 121492124600



1 - 3S - 2W

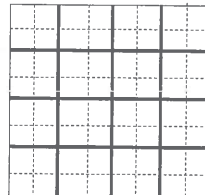
ILLINOIS STATE GEOLOGICAL SURVEY

Engineering Test	Top	Bottom
concrete pavement & subbase material	0	3
dark grey silty clay loam moist (soft)	3	7
dark grey silty clay loam moist (stiff)	7	12
grey & brown silty clay moist (stiff)	12	14
grey sand (fine) wet (v. loose)	14	19
grey sand (fine) wet (loose)	19	22
grey sand (fine) wet (medium)	22	27
grey sand (medium) wet (medium)	27	37
grey sand (medium-coarse) w/some gravel wet (dense)	37	42
grey sand (medium) wet (medium)	42	54
grey sand (medium-coarse) w/some fine pebble gravel wet (dense)	54	59
grey sand (medium-coarse) w/some fine pebble gravel wet (medium)	59	64
grey sand (medium-coarse) w/some fine pebble gravel wet (dense)	64	67
standard 50 tsf bearing achieved. augered and additional 10' to check for possible limestone bedrock	67	70
grey sand w/some gravel throughout wet (medium-dense) from elev.365.7 to 354.7	70	78
Total Depth		78

Permit Date:

Permit #:

COMPANY IL Dept. of Transportation
 FARM FAP 745 Il. Rte. 104
 DATE DRILLED June 3, 1986 NO. 2 (W.Abut)
 ELEVATION 433GL COUNTY NO. 21248
 LOCATION 2640'N line, 2640'W line of section
 LATITUDE 39.831966 LONGITUDE -90.579769
 COUNTY Pike API 121492124800



1 - 3S - 2W

ILLINOIS STATE GEOLOGICAL SURVEY

Engineering Test	Top	Bottom
concrete pavement & subbase material	0	2
brown sand (medium) moist (loose) w/some shells @ 9.5 - 10.5'	2	10.5
grey clay moist (medium)	10.5	14
grey clay moist (stiff)	14	17
grey silty clay v. moist (medium)	17	19
grey sand (fine) wet (loose)	19	22
grey sand (fine) wet (v. loose)	22	24
grey sand (fine) wet (loose)	24	27
grey sand (fine) wet (medium)	27	29
grey sand (fine) wet (loose)	29	31
grey sand (medium) wet (medium)	31	37
grey sand (fine-medium) wet (medium)	37	44
grey fine pebble gravel wet (medium)	44	49
grey gravel (fine-medium pebble) wet (medium)	49	54
brown sand (coarse) w/some gravel wet (dense)	54	59
grey sand (fine) wet (dense)	59	63.5
grey sand (fine) wet (medium)	63.5	65.5
Total Depth		65

Permit Date:

Permit #:

COMPANY IL Dept. of Transportation

FARM FAP 745 Ill. RTE. 104

DATE DRILLED June 2, 1986

NO. 1 (E.Abut)

ELEVATION 436GL

COUNTY NO. 21247

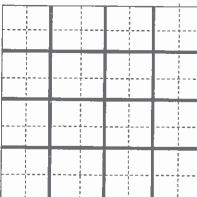
LOCATION

LATITUDE 39.831875

LONGITUDE -90.579775

COUNTY Pike

API 121492124700



1 - 3S - 2W

ILLINOIS STATE GEOLOGICAL SURVEY

Test Hole	Top	Bottom
ss #56380	0	0
fine sand	0	20
fine sand, small gravel	20	45
fine sand, coarse gravel	45	55
fine sand, small gravel	55	71
medium sand, small gravel	71	85
medium sand, large gravel	85	90
Total Depth		90
Casing: 24" 3/8 WALL from 0' to 60' 12" 52 LB. from 0' to 64'		
Screen: 26' of 12" diameter 60 slot		
Water from sand & gravel at 0' to 90'.		
Static level 14' below casing top which is 2' above GL		
Pumping level 32' when pumping at 1000 gpm for 8 hours		
Remarks: see file for detail sample study		
Driller's Log filed		
Sample set # 56380 (0' - 90') Received: August 26, 1969		
Owner Address: Meredosia, IL		
Location source: Location from permit		

Permit Date: June 29, 1969

Permit #: 06700

COMPANY Lorenz D A

FARM W.R. Grace Co.

DATE DRILLED September 11, 1969

NO. DL-3

ELEVATION 0

COUNTY NO. 00607

LOCATION NE NE NE

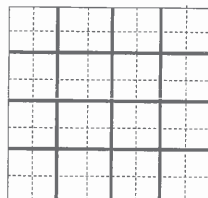
LATITUDE 39.817955

LONGITUDE -90.565139

COUNTY Morgan

API 121370060700

28 - 16N - 13W



ILLINOIS STATE GEOLOGICAL SURVEY

Water Well	Top	Bottom
sand	0	36
sand & gravel	36	67
fine to medium gravel	67	91
Total Depth		91
Casing: 16" STEEL .375 from 3' to 66'		
Screen: 25' of 16" diameter .08 slot		
Water from drift at 66' to 91'.		
Static level 12' below casing top which is 0' above GL		
Pumping level 22' when pumping at 1000 gpm for 8 hours		
Owner Address: P.O. Box 153 Meredosia, IL		
Location source: Location from permit		

Permit Date: May 11, 1979

Permit #: 85480

COMPANY Hakala, Richard L.

FARM Grace, W.R. & Co.

DATE DRILLED May 15, 1979

NO. 4

ELEVATION 0

COUNTY NO. 20770

LOCATION 1980'N line, 450'W line of NW

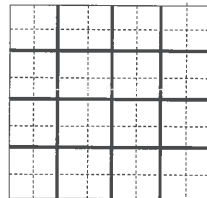
LATITUDE 39.813373

LONGITUDE -90.562736

COUNTY Morgan

API 121372077000

27 - 16N - 13W



ILLINOIS STATE GEOLOGICAL SURVEY

Industrial Water Well	Top	Bottom
fine to medium sand	0	40
medium to coarse sand	40	50
medium sand	50	62
coarse sand to fine gravel	62	73
medium to coarse sand	73	78
fine to medium sand with gravel	78	85
coarse sand & fine to medium gravel	85	90
medium sand to fine gravel	90	91
coarse sand, gravel & boulders	91	95
Total Depth		95
Casing: 24" STEEL from -2' to 65'		
24" STAINLESS STL SCREEN from 65' to 94'		
Screen: 29' of 24" diameter .05 slot		
Grout: NEAT CEMENT from 0 to 20.		
Grout: BENTONITE CHIPS from 20 to 27.		
Grout: SILICA #2 NORTHERN from 27 to 94.		
Water from sand & gravel at 16' to 94'.		
Static level 16' below casing top which is 2' above GL		
Pumping level 40' when pumping at 2503 gpm for 20 hours		
Permanent pump installed at 60'		
on January 25, 2011, with a capacity of 1850 gpm		
Remarks: driller's est. well yield 3000 gpm		
Sample set # 69973 (0' - 95') Received: January 9, 2012		
Owner Address: ,		
Address of well: 1994 Old Grace Road		
Location source: Location from permit		

Permit Date:

Permit #:

COMPANY Water Well Solutions

FARM T.A. Terminal

DATE DRILLED November 23, 2011

NO. 6

ELEVATION

COUNTY NO. 22134

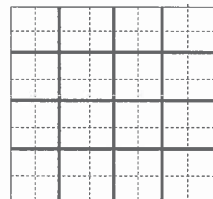
LOCATION NW NW SW

LATITUDE 39.81073

LONGITUDE -90.563186

COUNTY Morgan

API 121372213400



27 - 16N - 13W

ILLINOIS STATE GEOLOGICAL SURVEY

Industrial Water Well	Top	Bottom
fine to medium sand	0	40
medium to coarse sand	40	50
medium sand	50	62
coarse sand to fine gravel	62	73
medium to coarse sand	73	78
fine to medium sand with gravel	78	85
coarse sand & fine to medium gravel	85	90
medium sand to fine gravel	90	91
coarse sand, gravel & flat boulders	91	95
Total Depth		100
Casing: 24" STEEL from -2' to 65'		
24" STAINLESS STL SCREEN from 65' to 94'		
Screen: 29' of 24" diameter .05 slot		
Grout: NEAT CEMENT from 0 to 20.		
Grout: BENTONITE CHIPS from 20 to 27.		
Grout: SILICA #3 NORTHERN from 27 to 94.		
Water from sand & gravel at 20' to 94'.		
Static level 20' below casing top which is 2' above GL		
Pumping level 43' when pumping at 2485 gpm for 24 hours		
Permanent pump installed at 60'		
on January 19, 2011, with a capacity of 1850 gpm		
Remarks: driller's est. well yield 3000 gpm		
Sample set # 69972 (0' - 100') Received: January 9, 2012		
Owner Address: ,		
Address of well: 1994 Old Grace Road		
Location source: Location from permit		

Permit Date:

Permit #:

COMPANY Water Well Solutions

FARM T.A. Terminal

DATE DRILLED November 23, 2011

NO. 5

ELEVATION

COUNTY NO. 22133

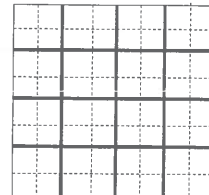
LOCATION NW NW SW

LATITUDE 39.81073

LONGITUDE -90.563186

COUNTY Morgan

API 121372213300

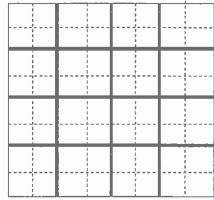


27 - 16N - 13W

Water Well	Top	Bottom
sand fine	0	30
sand coarse	30	50
coarse sand and gravel	50	60
gravel small to large	60	73
Total Depth		73
Casing: 10" STEEL from 0' to 61' " 12' SCREEN from 0' to 73'		
Screen: 12' of 9.5" diameter 50 slot		
Water from sand gravel at 61' to 73'.		
Static level 4' below casing top which is 3' above GL		
Pumping level 15' when pumping at 300 gpm for 2 hours		
Owner Address: Box 328 Jacksonville, IL		
Location source: Platbook verified		

Permit Date: December 11, 1975 Permit #: 43710

COMPANY Chadwick, G. W.
 FARM Ill. Road Contractors Inc.
 DATE DRILLED December 20, 1975 NO.
 ELEVATION 0 COUNTY NO. 20621
 LOCATION SE SE NE
 LATITUDE 39.832804 LONGITUDE -90.571759
 COUNTY Pike API 121492062100



1 - 3S - 2W

**The following are attachments to the testimony of Scott M. Payne,
PhD, PG and Ian Magruder, M.S..**

APPDENDIX B
BORING LOGS

LOG OF BORING 2002 WL J017150.01GEO - MEREDOSIA.GPJ GTINC 0638301.GPJ 12/13/10 AND THE TRANSITION MAY BE GRADUAL. GRAPHIC LOG FOR ILLUSTRATION PURPOSES ONLY.

Surface Elevation: <u>449.0</u>		Completion Date: <u>10/21/10</u>		GRAPHIC LOG	DRY UNIT WEIGHT (pcf) SPT BLOW COUNTS CORE RECOVERY/RQD	SAMPLES	SHEAR STRENGTH, tsf		
Datum <u>msl</u>		STANDARD PENETRATION RESISTANCE (ASTM D 1586)							
DEPTH IN FEET		WATER CONTENT, %							
DESCRIPTION OF MATERIAL		PLI							
	Crushed rock								
	FILL: brown, fine to coarse sand, trace clay lenses								
5		6-16-10	SS1						
		3-11-13-14	SS2						
10		5-7-9	SS3						
		5-9-14	SS4						
15	FILL: black clay with sand	4-4-4	SS5						
	Very soft, gray, interbedded SILT and CLAY with organics - ML/CL	0-0-1	SS6						
20		2-2-3	SS7						
	Medium stiff, gray CLAY - (CH)	92	ST8						
25		87-89	ST9						
30		1-4-4	SS10						
	Loose, gray, clayey SAND with gravel - SP	5-7-7	SS11						
35									
	Loose to medium dense, brown, fine to coarse SAND, trace gravel - SP								

GROUNDWATER DATA

FREE WATER NOT ENCOUNTERED DURING DRILLING

DRILLING DATA

 AUGER 4 1/4" HOLLOW STEM
WASHBORING FROM 15 FEET
MB DRILLER LAH LOGGER
CME 550X DRILL RIG
HAMMER TYPE Auto

Drawn by: KA Checked by: SK App'vd. by: DM
Date: 10/26/10 Date: 12/22/10 Date: 1/4/11



Meredosia Power Station
Meredosia, Illinois

LOG OF BORING: B-1

Project No. J017150.01

REMARKS: Datum: IL State Plane Coordinates, West Zone. N: 1148760.916'
E: 2182703.077'

LOG OF BORING 2002 WL J017150.01GEO - MEREDOSIA.GPJ GTINC 0638301.GPJ 12/13/10 THE TRANSITION MAY BE GRADUAL. GRAPHIC LOG FOR ILLUSTRATION PURPOSES ONLY.

Surface Elevation: <u>449.0</u>		Completion Date: <u>10/21/10</u>				SHEAR STRENGTH, tsf Δ - UU/2 ○ - QU/2 □ - SV 0.5 1.0 1.5 2.0 2.5		
Datum <u>msl</u>						STANDARD PENETRATION RESISTANCE (ASTM D 1586) ▲ N-VALUE (BLOWS PER FOOT)		
						WATER CONTENT, % PLI -----●----- LL 10 20 30 40 50		
DEPTH IN FEET	DESCRIPTION OF MATERIAL	GRAPHIC LOG	DRY UNIT WEIGHT (pcf) SPT BLOW COUNTS CORE RECOVERY/RQD	SAMPLES				
	Loose to medium dense, brown, fine to coarse SAND, trace gravel - SP (continued)							
45			4-5-4	SS12	▲			
50			5-7-9	SS13	▲			
55			9-8-9	SS14	▲			
60	Boring terminated at 60 feet		7-12-15	SS15	▲			
65								
70								
75								

GROUNDWATER DATA

X FREE WATER NOT ENCOUNTERED DURING DRILLING

DRILLING DATA

 AUGER 4 1/4" HOLLOW STEM
 WASHBORING FROM 15 FEET
MB DRILLER LAH LOGGER
CME 550X DRILL RIG
 HAMMER TYPE Auto

Drawn by: KA Checked by: SK App'vd. by: DAI
 Date: 10/26/10 Date: 10/21/10 Date: 1/14/11



Meredosia Power Station
 Meredosia, Illinois

REMARKS: Datum: IL State Plane Coordinates, West Zone. N: 1148760.916'
 E: 2182703.077'

CONTINUATION OF
 LOG OF BORING: B-1

Project No. J017150.01

LOG OF BORING 2002 WL J017150.01 GEO - MEREDOSIA, GPJ GTING 0638301, GPJ 12/21/10 THE TRANSITION MAY BE GRADUAL. GRAPHIC LOG FOR ILLUSTRATION PURPOSES ONLY.

Surface Elevation: <u>449.2</u> Datum <u>msl</u>		Completion Date: <u>10/21/10</u>		SHEAR STRENGTH, tsf					
DEPTH IN FEET	DESCRIPTION OF MATERIAL	GRAPHIC LOG	DRY UNIT WEIGHT (pcf) SPT BLOW COUNTS CORE RECOVERY/RQD	SAMPLES	Δ - UU/2	○ - QU/2	□ - SV		
					0,5	1,0	1,5	2,0	2,5
					STANDARD PENETRATION RESISTANCE (ASTM D 1586)				
					▲ N-VALUE (BLOWS PER FOOT)				
					WATER CONTENT, %				
					PL	LL			
					10	20	30	40	50
	Crushed rock								
	FILL: brown, fine to coarse sand with black clay lenses								
5			5-7-9	SS1	▲				
			6-10-8	SS2	▲				
10			7-8-13	SS3	▲				
			5-5-9	SS4	▲				
15			3-3-3	SS5	▲				
	Black, clayey SAND, trace gravel - SP			ST6					
20									
	Medium stiff, gray CLAY - CH								
25			3-4-4	SS7	▲	●			
30			3-3-3	SS8	▲	●			
	Soft, gray, clayey SILT with sand and clay lenses - ML								
35			2-1-1	SS9	▲	●			
	Loose to medium dense, brown, fine to coarse SAND, trace gravel - SP								
			0-2-4	SS10	▲				

GROUNDWATER DATA

FREE WATER NOT ENCOUNTERED DURING DRILLING
AT 13.6 FEET AFTER 16 HOURS ▼

DRILLING DATA

___ AUGER 4 1/4" HOLLOW STEM WASHBORING FROM 15 FEET
MB DRILLER LAH LOGGER
CME 550X DRILL RIG
HAMMER TYPE Auto

Drawn by: KA Checked by: SM App'vd. by: DM
Date: 10/26/10 Date: 12/21/10 Date: 11/4/11



Meredosia Power Station
Meredosia, Illinois

LOG OF BORING: B-2

Project No. J017150.01

REMARKS: Hole collapsed at 46 feet. Datum: IL State Plane Coordinates, West Zone. N: 1148689.546' E: 2182613.025'

LOG OF BORING 2002 WL J017150.01GEO - MEREDOSIA.GPJ GTINC 0638301.GPJ 12/13/10 THE TRANSITION MAY BE GRADUAL. GRAPHIC LOG FOR ILLUSTRATION PURPOSES ONLY.

Surface Elevation: <u>449.2</u> Datum <u>msl</u>		Completion Date: <u>10/21/10</u>		GRAPHIC LOG	DRY UNIT WEIGHT (pcf) SPT BLOW COUNTS CORE RECOVERY/RQD	SAMPLES	SHEAR STRENGTH, tsf		
DEPTH IN FEET	DESCRIPTION OF MATERIAL	Δ - UU/2 \circ - QU/2 \square - SV 0.5 1.0 1.5 2.0 2.5							
		STANDARD PENETRATION RESISTANCE (ASTM D 1586)							
		\blacktriangle N-VALUE (BLOWS PER FOOT) WATER CONTENT, % PL ----- LL 10 20 30 40 50							
45	Loose to medium dense, brown, fine to coarse SAND, trace gravel - SP (continued)		3-6-6	SS11					
	Boring terminated at 46 feet.								
50									
55									
60									
65									
70									
75									

GROUNDWATER DATA

FREE WATER NOT ENCOUNTERED DURING DRILLING
AT 13.6 FEET AFTER 16 HOURS

DRILLING DATA

AUGER 4 1/4" HOLLOW STEM WASHBORING FROM 15 FEET
MB DRILLER LAH LOGGER
CME 550X DRILL RIG
HAMMER TYPE Auto

Drawn by: KA Checked by: SK App'vd. by: DW
Date: 10/26/10 Date: 12/21/10 Date: 1/4/11



Meredosia Power Station
Meredosia, Illinois

CONTINUATION OF
LOG OF BORING: B-2

Project No. J017150.01

REMARKS: Hole collapsed at 46 feet. Datum: IL State Plane Coordinates, West Zone. N: 1148689.546' E: 2182613.025'

Surface Elevation: <u>449.1</u>		Completion Date: <u>10/21/10</u>		GRAPHIC LOG	DRY UNIT WEIGHT (pcf) SPT BLOW COUNTS CORE RECOVERY/RQD	SAMPLES	SHEAR STRENGTH, tsf				
Datum <u>msl</u>		Δ - UU/2 \circ - QU/2 \square - SV 0.5 1.0 1.5 2.0 2.5									
DEPTH IN FEET	DESCRIPTION OF MATERIAL	STANDARD PENETRATION RESISTANCE (ASTM D 1586)									
		\blacktriangle N-VALUE (BLOWS PER FOOT) WATER CONTENT, % PLI LL 10 20 30 40 50									
	Crushed rock										
	FILL: brown sand with black clay lenses	4-6-8	SS1								
		5-6-9	SS2								
5			ST3								
		8-10-16	SS4								
		8-13-15	SS5								
		6-8-8	SS6								
15	FILL: black clay with sand, trace gravel		SS7								
	Soft to medium stiff, gray CLAY - CH with organics	2-2-2	SS8								
20		86	ST9								
			ST10								
25		1-2-3	SS11								
30	Soft, brown, clayey SILT with sand - ML	1-2-1	SS12								
35	Medium dense, brown, fine to coarse SAND, trace gravel - SP	5-5-7	SS13								

NOTE: STRATIFICATION LINES REPRESENT THE APPROXIMATE BOUNDARIES BETWEEN SOIL TYPES
 LOG OF BORING 2002 WL J017150.01GEO - MEREDOSIA.GPJ GTINC 0638301.GPJ 12/13/10 THE TRANSITION MAY BE GRADUAL. GRAPHIC LOG FOR ILLUSTRATION PURPOSES ONLY.

GROUNDWATER DATA

FREE WATER NOT ENCOUNTERED DURING DRILLING

DRILLING DATA

___ AUGER 4 1/4" HOLLOW STEM
 WASHBORING FROM 15 FEET
MB DRILLER LAH LOGGER
CME 550X DRILL RIG
 HAMMER TYPE Auto

Drawn by: KA Checked by: SK App'vd. by: DW
 Date: 10/26/10 Date: 12/2/10 Date: 1/14/11



Meredosia Power Station
Meredosia, Illinois

LOG OF BORING: B-3

Project No. J017150.01

REMARKS: Datum: IL State Plane Coordinates, West Zone. N: 1148536.604'
E: 2182554.305'

LOG OF BORING 2002 WL J017150.01GEO - MEREDOSIA.GPJ GTINC 0638301.GPJ 12/13/10 THE TRANSITION MAY BE GRADUAL. GRAPHIC LOG FOR ILLUSTRATION PURPOSES ONLY.

Surface Elevation: <u>449.1</u>		Completion Date: <u>10/21/10</u>		SHEAR STRENGTH, tsf Δ - UU/2 ○ - QU/2 □ - SV 0.5 1.0 1.5 2.0 2.5 STANDARD PENETRATION RESISTANCE (ASTM D 1586) ▲ N-VALUE (BLOWS PER FOOT) WATER CONTENT, % PLI ——— 10 20 30 40 50 ——— LL	
Datum <u>msl</u>		GRAPHIC LOG			
DEPTH IN FEET		DESCRIPTION OF MATERIAL			
DRY UNIT WEIGHT (pcf) SPT BLOW COUNTS CORE RECOVERY/RQD		SAMPLES			
45	Medium dense, brown, fine to coarse SAND, trace gravel - SP (continued)	6-7-7	SS14	▲	
50		6-7-9	SS15	▲	
55		5-8-9	SS16	▲	
60	Boring terminated at 60 feet.	8-8-13	SS17	▲	
65					
70					
75					

GROUNDWATER DATA

FREE WATER NOT ENCOUNTERED DURING DRILLING

DRILLING DATA

AUGER 4 1/4" HOLLOW STEM
 WASHBORING FROM 15 FEET
 MB DRILLER LAH LOGGER
 CME 550X DRILL RIG
 HAMMER TYPE Auto

Drawn by: KA Checked by: SK App'vd. by: DW
 Date: 10/26/10 Date: 12/2/10 Date: 1/1/11



Meredosia Power Station
Meredosia, Illinois

CONTINUATION OF
LOG OF BORING: B-3

Project No. J017150.01

REMARKS: Datum: IL State Plane Coordinates, West Zone. N: 1148536.604' E: 2182554.305'


LOG OF BORING 2002 WL J017150.01 GEO - MEREDOSIA.GPJ GTINC 0638301.GPJ 12/13/10 THE TRANSITION MAY BE GRADUAL. GRAPHIC LOG FOR ILLUSTRATION PURPOSES ONLY.

Surface Elevation: <u>431.6</u> Datum <u>msl</u>		Completion Date: <u>10/22/10</u>		GRAPHIC LOG	DRY UNIT WEIGHT (pcf) SPT BLOW COUNTS CORE RECOVERY/RQD	SAMPLES	SHEAR STRENGTH, tsf				
DEPTH IN FEET		DESCRIPTION OF MATERIAL					Δ - UU/2	○ - QU/2	□ - SV		
							0.5	1.0	1.5	2.0	2.5
							STANDARD PENETRATION RESISTANCE (ASTM D 1586)				
PLI		▲ N-VALUE (BLOWS PER FOOT)			WATER CONTENT, %						
		10	20	30	40	50	LL				
5		Soft to medium stiff, brown and gray CLAY - (CH)		[Hatched Pattern]	1-2-2	SS1	▲	●			
	*				ST2		●				
	1-2-3				SS3	▲	●	—			
	0-2-2				SS4	▲	●				
15		Soft, gray, silty CLAY, trace sand - CL		[Hatched Pattern]	0-1-1	SS5	▲	●			
20		Very soft, gray, sandy CLAY with silt - CL			0-0-0	SS6	▲	●			
25		Very loose, brown, fine to coarse SAND, trace gravel - SP		[Dotted Pattern]	0-1-2	SS7	▲				
25		Boring terminated at 25 feet.									

GROUNDWATER DATA
ENCOUNTERED AT 19 FEET ∇

DRILLING DATA
4 1/4" AUGER HOLLOW STEM
 WASHBORING FROM FEET
MB DRILLER LAH LOGGER
CME 550X DRILL RIG
 HAMMER TYPE Auto

REMARKS: * Disturbed sample Datum: IL State Plane Coordinates, West Zone. N: 1148688.82' E: 2182505.605'

Drawn by: KA	Checked by: <i>SK</i>	App'vd. by: <i>DM</i>
Date: 10/26/10	Date: <i>11/2/10</i>	Date: <i>1/4/11</i>
 GEOTECHNOLOGY INC. <small>FROM THE GROUND UP</small>		
Meredosia Power Station Meredosia, Illinois		
LOG OF BORING: B-4		
Project No. J017150.01		

LOG OF BORING 2002 WL J017150.01 GEO - MEREDOSIA.GPJ GTINC 0638301.GPJ 12/22/10 THE TRANSITION MAY BE GRADUAL. GRAPHIC LOG FOR ILLUSTRATION PURPOSES ONLY.

Surface Elevation: <u>431.8</u> Datum <u>msl</u>		Completion Date: <u>10/22/10</u>		GRAPHIC LOG	DRY UNIT WEIGHT (pcf) SPT BLOW COUNTS CORE RECOVERY/RQD	SAMPLES	SHEAR STRENGTH, tsf		
DEPTH IN FEET	DESCRIPTION OF MATERIAL	Δ - UU/2	○ - QU/2				□ - TV		
		0.5	1.0				1.5	2.0	2.5
		STANDARD PENETRATION RESISTANCE (ASTM D 1586)					▲ N-VALUE (BLOWS PER FOOT)		
PLI			WATER CONTENT, %			LL			
		10	20	30	40	50			
5	Medium stiff to soft, brown and gray, silty CLAY - CL						▲	●	
							▲	●	
10	Medium stiff to very soft, brown and gray CLAY - CH						▲	●	
							○	●	
15							▲	●	
20	Very soft, gray, silty CLAY with sand - CL						▲	●	
25	Boring terminated at 25 feet.						▲	●	
30									
35									

GROUNDWATER DATA

ENCOUNTERED AT 23 FEET ∇

DRILLING DATA

___ AUGER 4 1/4" HOLLOW STEM
WASHBORING FROM ___ FEET
MB DRILLER LAH LOGGER
CME 550X DRILL RIG
HAMMER TYPE Auto

Drawn by: KA Checked by: SJC App'vd. by: DW
Date: 10/26/10 Date: 12/22/10 Date: 11/4/11



Meredosia Power Station
Meredosia, Illinois

LOG OF BORING: B-5

Project No. J017150.01

REMARKS: Datum: IL State Plane Coordinates, West Zone. N: 1148661.88' E: 2182476.0360'

LOG OF BORING 2002 WL J017150.01GEO - MEREDOSIA GPJ GTINC 0638301.GPJ 12/13/10 THE TRANSITION MAY BE GRADUAL. GRAPHIC LOG FOR ILLUSTRATION PURPOSES ONLY.

Surface Elevation: <u>450.8</u> Datum <u>msl</u>		Completion Date: <u>10/19/10</u>		GRAPHIC LOG		SHEAR STRENGTH, tsf					
DEPTH IN FEET	DESCRIPTION OF MATERIAL	DRY UNIT WEIGHT (pcf) SPT BLOW COUNTS CORE RECOVERY/RQD	SAMPLES	Δ - UU/2	○ - QU/2	□ - SV	STANDARD PENETRATION RESISTANCE (ASTM D 1586)				
				0.5	1.0	1.5	2.0	2.5	▲ N-VALUE (BLOWS PER FOOT)		
				PLI						WATER CONTENT, %	
						10	20	30	40	50	LL
	Crushed rock										
	FILL: black clay with sand pockets		3-6-10 SS1								
	FILL: brown, fine sand, trace clay		3-8-9 SS2								
5											
	FILL: black ash and sand		4-6-7 SS3								
10											
	FILL: brown, fine sand, trace gravel		6-7-13 SS6								
15											
	Very stiff, gray, silty CLAY with sand - CL		0-5-15 SS7								
20											
	Very loose, gray silty SAND - SM		0-0-0 SS8								
25											
	Very soft to soft, gray, silty CLAY with clay and silt seams - (CL)		0-1-3 SS9								
30											
			0-0-0 SS10								
35											
			0-0-0 SS11								

GROUNDWATER DATA

ENCOUNTERED AT 19.5 FEET ∇

DRILLING DATA

___ AUGER 4 1/4" HOLLOW STEM
WASHBORING FROM ___ FEET
MB DRILLER LAH LOGGER
CME 550X DRILL RIG
HAMMER TYPE Auto

Drawn by: KA Checked by: SA App'vd. by: DW
Date: 10/26/10 Date: 12/22/10 Date: 1/11/11



Meredosia Power Station
Meredosia, Illinois

LOG OF BORING: B-6

Project No. J017150.01

REMARKS: Datum: IL State Plane Coordinates, West Zone. N: 1148066.896'
E: 2182040.954'

NOTE: STRATIFICATION LINES REPRESENT THE APPROXIMATE BOUNDARIES BETWEEN SOIL TYPES
 LOG OF BORING 2002 WL J017150.01GEO - MEREDOSIA GPJ GTINC 0638301.GPJ 12/13/10 THE TRANSITION MAY BE GRADUAL. GRAPHIC LOG FOR ILLUSTRATION PURPOSES ONLY.

Surface Elevation: <u>450.8</u> Datum <u>msl</u>		Completion Date: <u>10/19/10</u>		GRAPHIC LOG	DRY UNIT WEIGHT (pcf) SPT BLOW COUNTS CORE RECOVERY/RQD	SAMPLES	SHEAR STRENGTH, tsf		
DEPTH IN FEET	DESCRIPTION OF MATERIAL	Δ - UU/2 \circ - QU/2 \square - SV 0.5 1.0 1.5 2.0 2.5							
		STANDARD PENETRATION RESISTANCE (ASTM D 1586)							
		▲ N-VALUE (BLOWS PER FOOT)							
			WATER CONTENT, %						
			PL ----- LL 10 20 30 40 50						
	Very soft to soft, gray, silty CLAY with clay and silt seams - (CL) (continued)								
45			1-1-1	SS12	▲				
	Dense, brown, fine to coarse SAND - SP								
50	Boring terminated at 50 feet.		7-13-42	SS13					▲
55									
60									
65									
70									
75									

GROUNDWATER DATA

ENCOUNTERED AT 19.5 FEET ∇

DRILLING DATA

___ AUGER 4 1/4" HOLLOW STEM
 WASHBORING FROM ___ FEET
MB DRILLER LAH LOGGER
CME 550X DRILL RIG
 HAMMER TYPE Auto

Drawn by: KA Checked by: SK App'vd. by: DM
 Date: 10/26/10 Date: 11/1/10 Date: 11/1/11



Meredosia Power Station
Meredosia, Illinois

CONTINUATION OF
LOG OF BORING: B-6

Project No. J017150.01

REMARKS: Datum: IL State Plane Coordinates, West Zone. N: 1148066.896'
E: 2182040.954'

LOG OF BORING 2002 WL J017150.01 GEO - MEREDOSIA.GPJ GTINC 0638301.GPJ 12/13/10 AND THE TRANSITION MAY BE GRADUAL. GRAPHIC LOG FOR ILLUSTRATION PURPOSES ONLY.

Surface Elevation: <u>450.5</u>		Completion Date: <u>10/19/10</u>		GRAPHIC LOG	DRY UNIT WEIGHT (pcf) SPT BLOW COUNTS CORE RECOVERY/RQD	SAMPLES	SHEAR STRENGTH, tsf		
Datum <u>msl</u>		Δ - UU/2	○ - QU/2				□ - SV		
		0,5	1,0				1,5	2,0	2,5
		STANDARD PENETRATION RESISTANCE (ASTM D 1586)							
		▲ N-VALUE (BLOWS PER FOOT)							
		WATER CONTENT, %							
		PL	LL						
		10	20	30	40	50			
DEPTH IN FEET	Crushed rock								
	FILL: black clay, ash and sand	5-8-9	SS1						
	FILL: brown, fine sand	2-6-6	SS2						
		4-6-9	SS3						
	FILL: black sand and ash with clay lenses	3-6-5	SS4						
			SS5						
		3-7-9	SS6						
	Medium stiff, brown, sandy CLAY - CL	6-4-3	SS7						
	Medium stiff to very soft, gray, silty CLAY with sand - CL	3-4-5	SS8						
		87	ST9						
		86							
	95	ST10							
	1-0-0	SS11							
	*	ST12							

GROUNDWATER DATA

FREE WATER NOT ENCOUNTERED DURING DRILLING

DRILLING DATA

 AUGER 4 1/4" HOLLOW STEM WASHBORING FROM 20 FEET
MB DRILLER LAH LOGGER
CME 550X DRILL RIG
HAMMER TYPE Auto

Drawn by: KA Checked by: SK App'vd. by: DM
Date: 10/26/10 Date: 12/22/10 Date: 1/4/11



Meredosia Power Station
Meredosia, Illinois

LOG OF BORING: B-7

Project No. J017150.01

REMARKS: * No recovery in samples SS11 and ST12 Datum: IL State Plane Coordinates, West Zone. N: 1147816.37' E: 2181875.293'

LOG OF BORING 2002 WL J017150.01GEO - MEREDOSIA.GPJ GTINC 0638301.GPJ 12/13/10 THE TRANSITION MAY BE GRADUAL. GRAPHIC LOG FOR ILLUSTRATION PURPOSES ONLY.

Surface Elevation: <u>450.5</u>		Completion Date: <u>10/19/10</u>		GRAPHIC LOG	DRY UNIT WEIGHT (pcf) SPT BLOW COUNTS CORE RECOVERY/RQD	SAMPLES	SHEAR STRENGTH, tsf			
Datum <u>msl</u>		Δ - UU/2 \circ - QU/2 \square - SV 0.5 1.0 1.5 2.0 2.5								
DEPTH IN FEET		STANDARD PENETRATION RESISTANCE (ASTM D 1586)								
		\blacktriangle N-VALUE (BLOWS PER FOOT) WATER CONTENT, % PL ----- LL 10 20 30 40 50								
DESCRIPTION OF MATERIAL		GRAPHIC LOG		DRY UNIT WEIGHT (pcf) SPT BLOW COUNTS CORE RECOVERY/RQD		SAMPLES		SHEAR STRENGTH, tsf		
Medium stiff to very soft, gray, silty CLAY with sand - CL <i>(continued)</i>		[Hatched pattern]				ST13		[Grid with data points]		
sandy								[Grid with data points]		
- 45								[Grid with data points]		
Medium dense to dense, brown, fine to medium coarse SAND - SP								5-8-10		SS14
- 50		7-9-14		SS15		[Grid with data points]				
- 55		13-17-19		SS16		[Grid with data points]				
- 60		Boring terminated at 60 feet,						[Grid with data points]		
- 65								[Grid with data points]		
- 70								[Grid with data points]		
- 75								[Grid with data points]		

GROUNDWATER DATA

FREE WATER NOT ENCOUNTERED DURING DRILLING

DRILLING DATA

 AUGER 4 1/4" HOLLOW STEM
 WASHBORING FROM 20 FEET
MB DRILLER LAH LOGGER
CME 550X DRILL RIG
 HAMMER TYPE Auto

Drawn by: KA Checked by: ge App'vd. by: DM
 Date: 10/26/10 Date: 12/20/10 Date: 1/8/11



Meredosia Power Station
 Meredosia, Illinois

CONTINUATION OF
 LOG OF BORING: B-7

Project No. J017150.01

REMARKS: * No recovery in samples SS11 and ST12 Datum: IL State Plane Coordinates, West Zone. N: 1147816.37' E: 2181875.293'

LOG OF BORING 2002 WL J017150.01GEO - MEREDOSIA.GPJ GTINC 0638301.GPJ 12/13/10 AND THE TRANSITION MAY BE GRADUAL. GRAPHIC LOG FOR ILLUSTRATION PURPOSES ONLY.

Surface Elevation: <u>451.1</u> Datum <u>msl</u>		Completion Date: <u>10/20/10</u>		GRAPHIC LOG	DRY UNIT WEIGHT (pcf) SPT BLOW COUNTS CORE RECOVERY/RQD	SAMPLES	SHEAR STRENGTH, tsf											
DEPTH IN FEET	DESCRIPTION OF MATERIAL	Δ - UU/2	○ - QU/2				□ - SV											
		0.5	1.0				1.5	2.0	2.5									
		STANDARD PENETRATION RESISTANCE (ASTM D 1586)					▲ N-VALUE (BLOWS PER FOOT)											
PLI			WATER CONTENT, %															
10			20			30			40			50			LL			
	Crushed rock																	
	FILL: black clay with sand				5-6-10	SS1												
	FILL: brown sand, trace to some clay				2-4-6	SS2												
5					0-5-7	SS3												
					4-8-12	SS4												
	FILL: black clay with sand				0-4-6	SS5												
						ST6												
15																		
	FILL: gray, clayey sand with black clay lenses				2-4-6	SS7												
					4-3-3	SS8												
	Medium stiff, black to gray CLAY - CH				2-3-4	SS9												
25																		
					0-2-3	SS10												
	Medium stiff to soft, gray clayey SILT with sand - ML				101	ST11												
						SS12												
35																		
					0-0-2	SS13												

GROUNDWATER DATA

FREE WATER NOT ENCOUNTERED DURING DRILLING
AT 9.3 FEET AFTER 0.5 HOURS ▼

DRILLING DATA

___ AUGER 4 1/4" HOLLOW STEM
WASHBORING FROM 20 FEET
MB DRILLER LAH LOGGER
CME 550X DRILL RIG
HAMMER TYPE Auto

Drawn by: KA Checked by: SK App'vd. by: DM
Date: 10/28/10 Date: 12/21/10 Date: 1/14/11



Meredosia Power Station
Meredosia, Illinois

LOG OF BORING: B-8

Project No. J017150.01

REMARKS: Datum: IL State Plane Coordinates, West Zone. N: 1147594.427'
E: 2181738.149'

LOG OF BORING 2002 WL J017150.01 GEO - MEREDOSIA.GPJ GTINC 0638301.GPJ 12/13/10 AND THE TRANSITION MAY BE GRADUAL. GRAPHIC LOG FOR ILLUSTRATION PURPOSES ONLY.

Surface Elevation: <u>451.1</u>		Completion Date: <u>10/20/10</u>		GRAPHIC LOG	DRY UNIT WEIGHT (pcf) SPT BLOW COUNTS CORE RECOVERY/RQD	SAMPLES	SHEAR STRENGTH, tsf			
Datum <u>msl</u>							Δ - UU/2 \circ - QU/2 \square - SV 0.5 1.0 1.5 2.0 2.5			
DEPTH IN FEET		DESCRIPTION OF MATERIAL					STANDARD PENETRATION RESISTANCE (ASTM D 1586)			
							▲ N-VALUE (BLOWS PER FOOT)			
					WATER CONTENT, %					
					PLI LL					
					10 20 30 40 50					
		Medium stiff to soft, gray clayey SILT with sand - ML <i>(continued)</i>								
		Dense to medium dense, brown, fine to coarse SAND with gravel - SP								
45					13-16-16	SS14				
50					7-9-11	SS15				
55		5-7-9	SS16							
60		10-13-14	SS17							
		Boring terminated at 60 feet.								
65										
70										
75										

GROUNDWATER DATA

FREE WATER NOT ENCOUNTERED DURING DRILLING
 AT 9.3 FEET AFTER 0.5 HOURS ∇

DRILLING DATA

 AUGER 4 1/4" HOLLOW STEM
 WASHBORING FROM 20 FEET
MB DRILLER LAH LOGGER
CME 550X DRILL RIG
 HAMMER TYPE Auto

Drawn by: KA Checked by: SK App'vd. by: DW
 Date: 10/26/10 Date: 12/22/10 Date: 1/14/11



Meredosia Power Station
 Meredosia, Illinois

CONTINUATION OF
 LOG OF BORING: B-8

Project No. J017150.01

REMARKS: Datum: IL State Plane Coordinates, West Zone. N: 1147594.427'
 E: 2181738.149'

LOG OF BORING 2002 WL J017150.01GEO - MEREDOSIA.GPJ_GTINC 0638301.GPJ 12/13/10 THE TRANSITION MAY BE GRADUAL. GRAPHIC LOG FOR ILLUSTRATION PURPOSES ONLY.

Surface Elevation: <u>433.6</u>		Completion Date: <u>10/25/10</u>		GRAPHIC LOG	DRY UNIT WEIGHT (pcf) SPT BLOW COUNTS CORE RECOVERY/RQD	SAMPLES	SHEAR STRENGTH, tsf		
Datum <u>msl</u>		Δ - UU/2 \circ - QU/2 \square - SV 0,5 1,0 1,5 2,0 2,5							
DEPTH IN FEET	DESCRIPTION OF MATERIAL	STANDARD PENETRATION RESISTANCE (ASTM D 1586)							
		\blacktriangle N-VALUE (BLOWS PER FOOT) PL ----- LL 10 20 30 40 50							
5	Medium stiff to soft, black and gray CLAY - (CH)	2-3-4	SS1	\blacktriangle	\bullet				
		1-1-1	SS2	\blacktriangle	\bullet				
			ST3		-----				
10		86	ST4	\circ	\bullet				
15	Soft to very soft, gray, silty CLAY with silt seams and sand - CL	0-1-1	SS6	\blacktriangle	\bullet				
20		0-1-2	SS7	\blacktriangle	\bullet				
25		0-0-0	SS8	\blacktriangle	\bullet				
30	Boring terminated at 25 feet.								
35									

GROUNDWATER DATA

FREE WATER NOT ENCOUNTERED DURING DRILLING

DRILLING DATA

AUGER 4 1/4" HOLLOW STEM WASHBORING FROM FEET
 MB DRILLER LAH LOGGER
 CME 550X DRILL RIG
 HAMMER TYPE Auto

Drawn by: KA Checked by: SJC App'vd. by: DW
 Date: 11/3/10 Date: 11/22/10 Date: 11/11/11



Meredosia Power Station
Meredosia, Illinois

LOG OF BORING: B-9

Project No. J017150.01

REMARKS: Datum: IL State Plane Coordinates, West Zone. N: 1148133.361'
E: 2182009.017'

LOG OF BORING 2002 WL J017150.01GEO - MEREDOSIA.GPJ_GTINC 0638301.GPJ_12/2/10 AND THE TRANSITION MAY BE GRADUAL. GRAPHIC LOG FOR ILLUSTRATION PURPOSES ONLY.

Surface Elevation: <u>433.2</u>		Completion Date: <u>10/25/10</u>		GRAPHIC LOG	DRY UNIT WEIGHT (pcf) SPT BLOW COUNTS CORE RECOVERY/RQD	SAMPLES	SHEAR STRENGTH, tsf				
Datum <u>msl</u>		Δ - UU/2 \circ - QU/2 \square - SV 0.5 1.0 1.5 2.0 2.5									
DEPTH IN FEET		DESCRIPTION OF MATERIAL					STANDARD PENETRATION RESISTANCE (ASTM D 1586)				
							\blacktriangle N-VALUE (BLOWS PER FOOT) WATER CONTENT, % PLI 10 20 30 40 50 LL				
5	Medium stiff to soft, brown and gray silty CLAY, trace sand and wood - CL		2-3-3	SS1	\blacktriangle	\bullet					
			2-2-3	SS2	\blacktriangle		\bullet				
			0-2-3	SS3	\blacktriangle		\bullet				
10			0-1-2	SS4	\blacktriangle		\bullet				
			95	ST5	\circ		\bullet				
15			0-1-1	SS6	\blacktriangle						
20	Very loose to medium dense, gray, silty SAND with silty clay seams - SM		8-11-7	SS7			\blacktriangle				
25	Wood Boring terminated at 25 feet.										
30											
35											

GROUNDWATER DATA

ENCOUNTERED AT 12 FEET ∇

DRILLING DATA

___ AUGER 4 1/4" HOLLOW STEM
 WASHBORING FROM ___ FEET
MB DRILLER LAH LOGGER
CME 550X DRILL RIG
 HAMMER TYPE Auto

Drawn by: KA Checked by: SK App'vd. by: DM
 Date: 11/3/10 Date: 12/2/10 Date: 1/4/11



Meredosia Power Station
 Meredosia, Illinois

LOG OF BORING: B-10

Project No. J017150.01

REMARKS: Datum: IL State Plane Coordinates, West Zone. N: 1148120.612'
 E: 2181976.582'

Surface Elevation: 446.06

Completion Date: 10/26/10

Datum msl

Northing: 1147018.68

Easting: 2185605.2

WELL DIAGRAM

DEPTH IN FEET

5

10

15

20

25

30

35

DESCRIPTION OF MATERIAL

Loose, brown, fine SAND - SP

Loose, brown fine to coarse SAND, trace gravel - SP

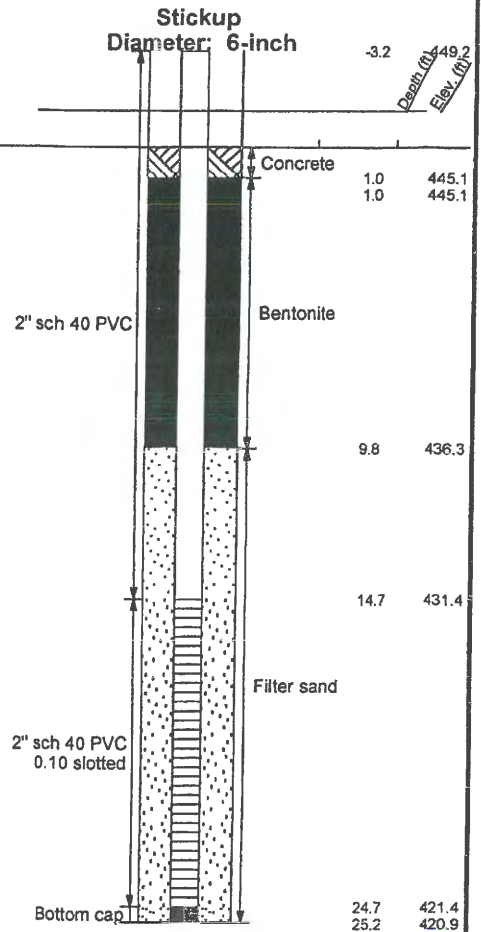
Loose, brown, fine SAND - SP

Boring terminated at 25 feet.

GRAPHIC LOG

DRY UNIT WEIGHT (pcf)
SPT BLOW COUNTS
CORE RECOVERY/RQD

SAMPLES



NOTE: STRATIFICATION LINES REPRESENT THE APPROXIMATE BOUNDARIES BETWEEN SOIL TYPES LOG OF BORING 2002 WL J017150.01 - MEREDOSIA, ILL. G.TINC 0638301.GPJ 1/11/11 - AND THE TRANSITION MAY BE GRADUAL. GRAPHIC LOG FOR ILLUSTRATION PURPOSES ONLY.

GROUNDWATER DATA

ENCOUNTERED AT 13 FEET ∇

REMARKS:

DRILLING DATA

4 1/4" HOLLOW STEM
WASHBORING FROM FEET
MB DRILLER LAH LOGGER
CME 550X DRILL RIG
HAMMER TYPE Auto

Drawn by: KA Checked by: DK App'vd. by: RBP
Date: 11/3/10 Date: 2-17-11 Date: 2/12/11



Ameren Power Generating
Facility
Meredosia, Illinois

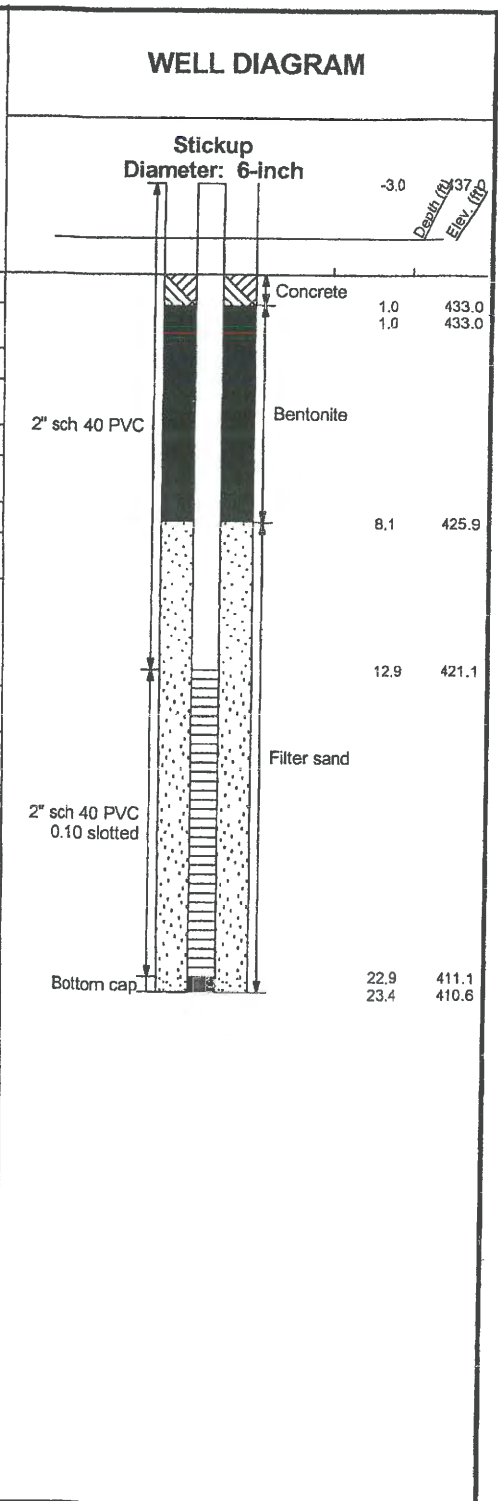
LOG OF BORING: APW-1

Project No. J017150.01

LOG OF BORING 2002 WL J017150.01 - MEREDOSIA.GPJ GTINC 0638301.GPJ 12/22/10 AND THE TRANSITION MAY BE GRADUAL. GRAPHIC LOG FOR ILLUSTRATION PURPOSES ONLY.

Surface Elevation: 433.97 Completion Date: 10/25/10
 Datum msl Northing: 1148489.69
 Easting: 2182485.19

DEPTH IN FEET	DESCRIPTION OF MATERIAL	GRAPHIC LOG	DRY UNIT WEIGHT (pcf) SPT BLOW COUNTS CORE RECOVERY/RQD	SAMPLES
	Soft to medium stiff, brown and gray CLAY, trace sand - CH			
			2-2-2	SS1
			2-2-2	SS2
5			2-2-4	SS3
			0-2-3	SS4
10				
			2-2-3	SS5
15				
	Soft, gray, silty CLAY with shells, trace to some sand - CL		0-1-1	SS6
20				
	Very loose, brown, fine to medium SAND - SP		0-0-1	SS7
25	Boring terminated at 25 feet.			
30				
35				



GROUNDWATER DATA

FREE WATER NOT ENCOUNTERED DURING DRILLING

DRILLING DATA

AUGER 4 1/4" HOLLOW STEM WASHBORING FROM FEET

MB DRILLER LAH LOGGER

CME 550X DRILL RIG

HAMMER TYPE Auto

REMARKS:

Drawn by: KA Checked by: DTK App'vd. by: KSP
 Date: 11/3/10 Date: 2-17-11 Date: 2/17/11

**Ameren Power Generating Facility
Meredosia, Illinois**

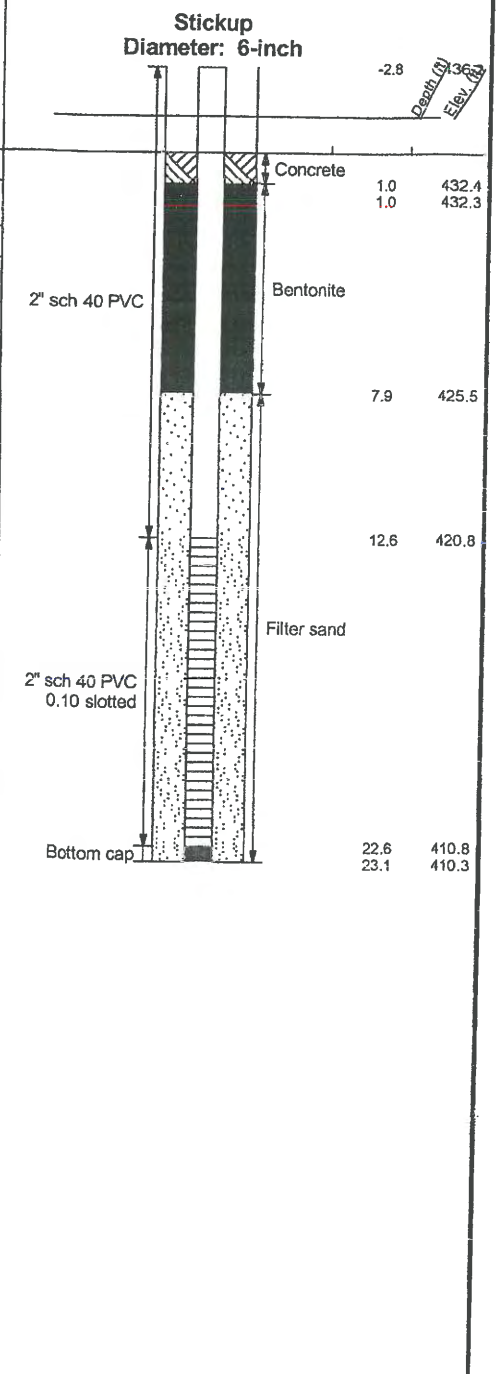
LOG OF BORING: APW-2/MW-2

Project No. J017150.01

Surface Elevation: 433.35 Completion Date: 10/25/10
 Datum msl Northing: 1148118.6
 Easting: 2181973.76

WELL DIAGRAM

DEPTH IN FEET	DESCRIPTION OF MATERIAL	GRAPHIC LOG	DRY UNIT WEIGHT (pcf)	SPT BLOW COUNTS	CORE RECOVERY/RQD	SAMPLES
0-1	Medium stiff, brown and gray CLAY, trace sand and wood - CH	[Hatched pattern]				2-3-3 SS1
1-2						
2-3						2-2-3 SS2
3-4						
4-5						0-2-3 SS3
5-6						
6-7						0-1-2 SS4
7-8						
8-9	Gray, silty CLAY, trace sand - CL	[Hatched pattern]				95 ST5
9-10						
10-11						
11-12						
12-13	Soft, gray, silty SAND with shells and silty clay seams - SM	[Dotted pattern]				0-1-1 SS6
13-14						
14-15						
15-16						
16-17						
17-18						
18-19						
19-20						
20-21						
21-22						
22-23						
23-24						
24-25	Wood					8-11-7 SS7
25-26	Boring terminated at 25 feet.					



NOTE: STRATIFICATION LINES REPRESENT THE APPROXIMATE BOUNDARIES BETWEEN SOIL TYPES LOG OF BORING 2002 WL J017150.01 - MEREDOSIA.GPJ GTINC 0638301.GPJ 12/22/10 AND THE TRANSITION MAY BE GRADUAL. GRAPHIC LOG FOR ILLUSTRATION PURPOSES ONLY.

GROUNDWATER DATA

ENCOUNTERED AT 12 FEET ∇

REMARKS:

DRILLING DATA

___ AUGER 4 1/4" HOLLOW STEM
 WASHBORING FROM ___ FEET
MB DRILLER LAH LOGGER
CME 550X DRILL RIG
 HAMMER TYPE Auto

Drawn by: KA Checked by: DK App'vd. by: RSP
 Date: 11/3/10 Date: 2-17-11 Date: 2/17/11



Ameren Power Generating Facility
 Meredosia, Illinois

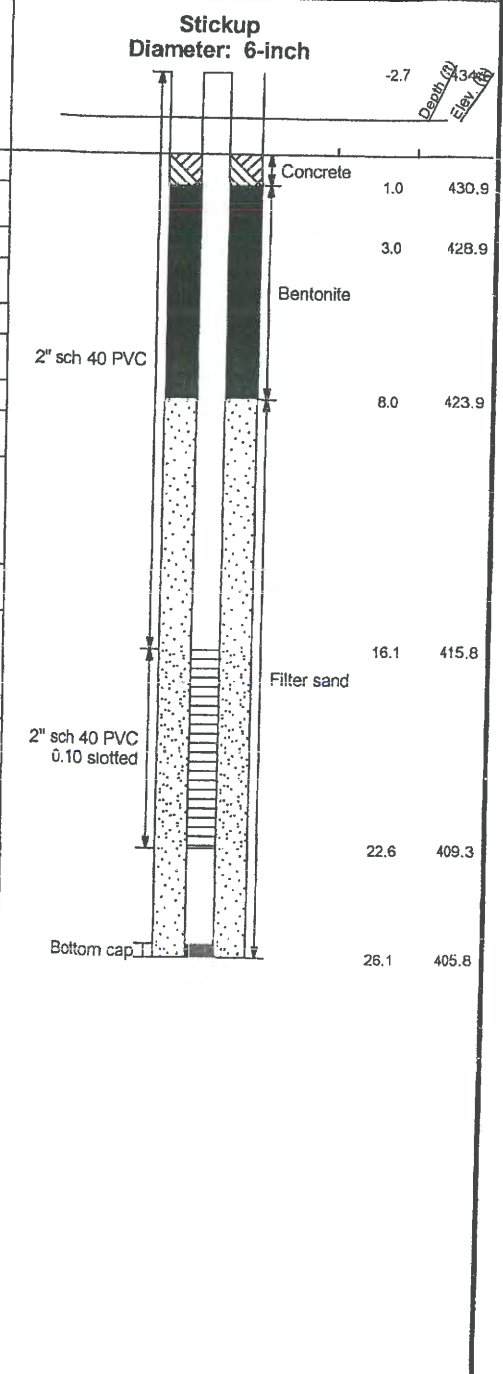
LOG OF BORING: APW-3/B-10

Project No. J017150.01

Surface Elevation: 431.90 Completion Date: 10/26/10
 Datum msl Northing: 1146935.94
 Easting: 2181602.97

WELL DIAGRAM

DEPTH IN FEET	DESCRIPTION OF MATERIAL	GRAPHIC LOG	DRY UNIT WEIGHT (pcf) SPT BLOW COUNTS CORE RECOVERY/RQD	SAMPLES
	Medium stiff to soft, brown and gray CLAY, trace sand and wood - CH			
			0-0-4	SS1
5			2-4-4	SS2
			1-1-1	SS3
10			1-1-2	SS4
	Loose, brown, fine SAND - SP			
15			3-6-7	SS5
20			0-2-2	SS6
25	Boring terminated at 25 feet.		0-0-0	SS7
30				
35				



NOTE: STRATIFICATION LINES REPRESENT THE APPROXIMATE BOUNDARIES BETWEEN SOIL TYPES LOG OF BORING 2002 WL J017150.01 - MEREDOSIA.GPJ GTINC 0638301.GPJ 12/22/10 AND THE TRANSITION MAY BE GRADUAL. GRAPHIC LOG FOR ILLUSTRATION PURPOSES ONLY.

GROUNDWATER DATA

DRILLING DATA

ENCOUNTERED AT 11.5 FEET ∇

4 1/4" HOLLOW STEM
 WASHBORING FROM FEET
MB DRILLER LAH LOGGER
CME 550X DRILL RIG
 HAMMER TYPE Auto

REMARKS:

Drawn by: KA Checked by: DJK App'vd. by: ABP
 Date: 11/3/10 Date: 2-17-11 Date: 2/17/11



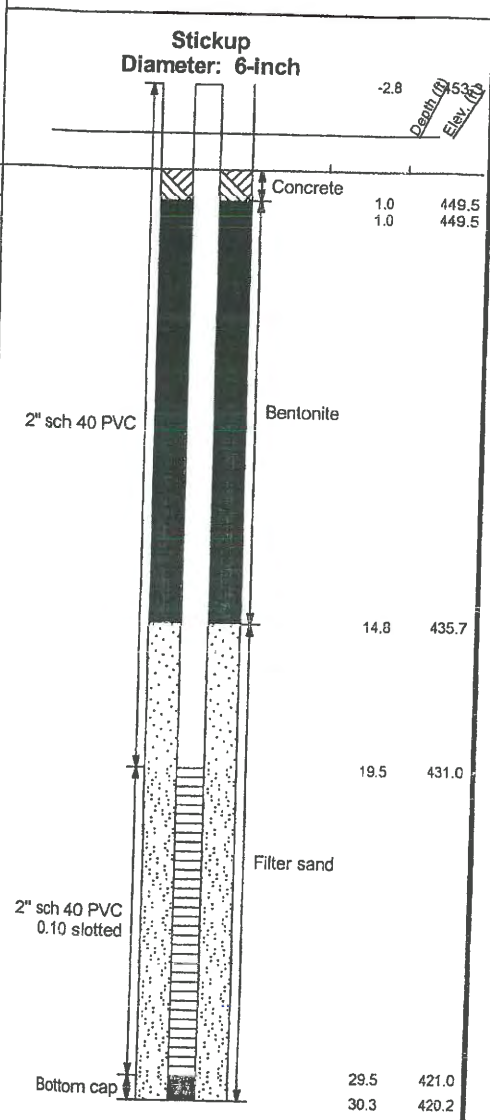
Ameren Power Generating
 Facility
 Meredosia, Illinois

LOG OF BORING: APW-4

Project No. J017150.01

LOG OF BORING 2002 WL J017150.01 - MEREDOSIA.GPJ GTINC.0638301.GPJ 12/22/10 - MEREDOSIA.GPJ 12/22/10 AND THE TRANSITION MAY BE GRADUAL. GRAPHIC LOG FOR ILLUSTRATION PURPOSES ONLY.

Surface Elevation: <u>450.48</u> Datum <u>msl</u>		Completion Date: <u>10/26/10</u> Northing: <u>1146922.64</u> Easting: <u>2183711.11</u>		WELL DIAGRAM	
DEPTH IN FEET	DESCRIPTION OF MATERIAL	GRAPHIC LOG	DRY UNIT WEIGHT (pcf) SPT BLOW COUNTS CORE RECOVERY/RQD	SAMPLES	
	Loose, brown, fine SAND - SP				
			3-3-3	SS1	
			2-2-2	SS2	
5			1-3-4	SS3	
			2-3-3	SS4	
10					
			2-3-4	SS5	
15					
			2-1-2	SS6	
20	Loose, brown, fine to coarse SAND, trace to some gravel - SP				
			3-3-3	SS7	
25					
			1-1-1	SS8	
30	Boring terminated at 30 feet.				
35					



GROUNDWATER DATA

DRILLING DATA

ENCOUNTERED AT 19.5 FEET ∇

___ AUGER 4 1/4" HOLLOW STEM
WASHBORING FROM ___ FEET
MB DRILLER LAH LOGGER
CME 550X DRILL RIG
HAMMER TYPE Auto

REMARKS:

Drawn by: KA Checked by: DK App'vd. by: ABP
Date: 11/3/10 Date: 2-17-11 Date: 2/17/11



Ameren Power Generating Facility
Meredosia, Illinois

LOG OF BORING: APW-5

Project No. J017150.01

LOG OF BORING 2002 WL J024917.01 - MEREDOSIA WELL.GPJ 00 CLONE.ME.GPJ 12/29/15 AND THE TRANSITION MAY BE GRADUAL. GRAPHIC LOG FOR ILLUSTRATION PURPOSES ONLY.

Surface Elevation: 448.55		Completion Date: 10/1/2015		WELL DIAGRAM			
Datum: _____		Latitude: 39.815833					
		Longitude: -90.570556		Stickup = 3.3 ft Diameter: 8 1/2 inch			
DEPTH IN FEET	DESCRIPTION OF MATERIAL	GRAPHIC LOG	DRY UNIT WEIGHT (pcf) SPT BLOW COUNTS CORE RECOVERY/RQD	SAMPLES	Depth (ft) Elev. (ft)		
5 10 15 20 25 30 35	Brown, fine grained SAND - SP		0-3-4	SS1			
			3-4-6	SS2			
			2-3-1	SS3			
			2-2-2	SS4			
			3-3-5	SS5			
			4-5-6	SS6			
			1-3-3	SS7		13.0	435.6
			1-2-3	SS8		15.5	433.1
			4-6-7	SS9		17.5	431.1
			4-3-4	SS10			
			1-2-2	SS11			
	Brown, medium grained SAND - SP						
	Blind drilled - heaving sands						
	Boring terminated at 28 feet.						

GROUNDWATER DATA

ENCOUNTERED AT 18 FEET ∇

REMARKS:

DRILLING DATA

___ AUGER 4 1/4" HOLLOW STEM
WASHBORING FROM ___ FEET
SMP DRILLER SJK LOGGER
CME 550 DRILL RIG
HAMMER TYPE Auto

Drawn by: AGB	Checked by:	App'vd. by:
Date: 10/9/2015	Date:	Date:



Meredosia Power Plant
Ameren Missouri

LOG OF BORING: APW-6

Project No. J024917.01

LOG OF BORING 2002 WL J024917.01 - MEREDOSIA WELL.GPJ_00 CLONE.ME.GPJ_12/29/15 AND THE TRANSITION MAY BE GRADUAL. GRAPHIC LOG FOR ILLUSTRATION PURPOSES ONLY.

Surface Elevation: 435.03		Completion Date: 10/1/2015		GRAPHIC LOG	DRY UNIT WEIGHT (pcf) SPT BLOW COUNTS CORE RECOVERY/RQD	SAMPLES	WELL DIAGRAM		
Datum: _____		Latitude: 39.815833					Stickup = 3.7 ft Diameter: 8 1/2 inch		Depth (ft)
DEPTH IN FEET	DESCRIPTION OF MATERIAL								
	Black, silty CLAY - CL				2-4-3	SS1			
	Brown, silty CLAY - CL				2-3-4	SS2		2.0	433.0
					1-2-1	SS3		4.0	431.0
5	Brown, fine grained SAND - SP				1-1-1	SS4		6.0	429.0
					0-0-1	SS5			
10	Blind drilled - heaving sands								
15									
	Boring terminated at 17 feet.						16.0	419.0	
							16.5	418.5	
20									
25									
30									
35									

GROUNDWATER DATA

ENCOUNTERED AT 6 FEET ∇

REMARKS:

DRILLING DATA

___ AUGER 4 1/4" HOLLOW STEM
WASHBORING FROM ___ FEET
SMP DRILLER SJK LOGGER
CME 550 DRILL RIG
HAMMER TYPE Auto

Drawn by: AGB	Checked by:	App'vd. by:
Date: 10/9/2015	Date:	Date:



Meredosia Power Plant
Ameren Missouri

LOG OF BORING: APW-7

Project No. J024917.01

LOG OF BORING 2002 WL J024917.01 - MEREDOSIA WELL.GPJ_00 CLONE.ME.GPJ_12/29/15 AND THE TRANSITION MAY BE GRADUAL. GRAPHIC LOG FOR ILLUSTRATION PURPOSES ONLY.

Surface Elevation: 460.54		Completion Date: 10/1/2015		GRAPHIC LOG	DRY UNIT WEIGHT (pcf) SPT BLOW COUNTS CORE RECOVERY/RQD	SAMPLES	WELL DIAGRAM		
Datum: _____		Latitude: 39.818611					Stickup = 3.4 ft Diameter: 8 1/2 inch		Depth (ft) Elev. (ft)
DEPTH IN FEET	DESCRIPTION OF MATERIAL								
	Brown, fine grained, poorly graded SAND - SP				3-9-9	SS1			
					7-11-12	SS2			
5					3-4-5	SS3			
					2-3-3	SS4			
					2-3-4	SS5			
10					2-3-5	SS6			
					3-5-9	SS7			
					5-7-7	SS8			
					5-7-8	SS9			
					5-7-8	SS10			
					9-15-16	SS11			
					7-12-13	SS12		23.0	437.5
25					8-13-14	SS13			
					9-10-11	SS14		26.3	434.3
	Brown, medium grained, poorly graded SAND - SP				6-6-9	SS15	28.6	431.9	
30					5-8-9	SS16			
					4-5-6	SS17			
35	Blind drilled - heaving sands								
40	Boring terminated at 40 feet.						38.6	421.9	
							39.1	421.4	

GROUNDWATER DATA

DRILLING DATA

ENCOUNTERED AT 32 FEET ∇

___ AUGER 4 1/4" HOLLOW STEM
WASHBORING FROM ___ FEET
SMP DRILLER SJK LOGGER
CME 550 DRILL RIG
HAMMER TYPE Auto

REMARKS:

Drawn by: AGB Checked by: _____ App'vd. by: _____
Date: 10/9/2015 Date: _____ Date: _____



Meredosia Power Plant
Ameren Missouri

LOG OF BORING: APW-8

Project No. J024917.01

LOG OF BORING 2002 WL_J024917.01 - MEREDOSIA WELL.GPJ_00 CLONE ME.GPJ_12/29/15 AND THE TRANSITION MAY BE GRADUAL. GRAPHIC LOG FOR ILLUSTRATION PURPOSES ONLY.

Surface Elevation: <u>444.97</u>		Completion Date: <u>10/1/2015</u>		GRAPHIC LOG	DRY UNIT WEIGHT (pcf) SPT BLOW COUNTS CORE RECOVERY/RQD	SAMPLES	WELL DIAGRAM			
Datum: _____		Latitude: <u>39.821388</u>					Stickup = 3.1 ft Diameter: 8 1/2 inch		Depth (ft)	Elev. (ft)
DEPTH IN FEET	DESCRIPTION OF MATERIAL									
	FILL: black, silty sand with coal CCR				4-3-2	SS1	2" sch 40 PVC	Bentonite Chips		
					2-3-3	SS2				
5					3-8-8	SS3				
					2-4-1	SS4				
					2-3-10	SS5				
10	Gray SILT - ML				4-3-2	SS6	2" sch 40 PVC 0.010 slotted	Pel-Plug	14.5	430.5
	Brown, fine grained SAND - SP				5-6-5	SS7				
15					3-4-3	SS8				16.7
					3-3-4	SS9				
20	Brown, medium grained SAND - SP				3-3-4	SS10	2" sch 40 PVC 0.010 slotted	Filter Sand	18.8	426.2
					1-2-1	SS11				
					2-2-4	SS12				
25	Blind drilled - heaving sands									
30	Boring terminated at 30 feet.								28.8	416.2
									29.3	415.7
35										

GROUNDWATER DATA

ENCOUNTERED AT 20 FEET ∇

REMARKS:
CCR = Coal Combustion Residuals

DRILLING DATA

 AUGER 4 1/4" HOLLOW STEM
WASHBORING FROM FEET
SMP DRILLER SJK LOGGER
CME 550 DRILL RIG
HAMMER TYPE Auto

Drawn by: AGB Checked by: App'vd. by:
Date: 10/9/2015 Date: Date:



**Meredosia Power Plant
Ameren Missouri**

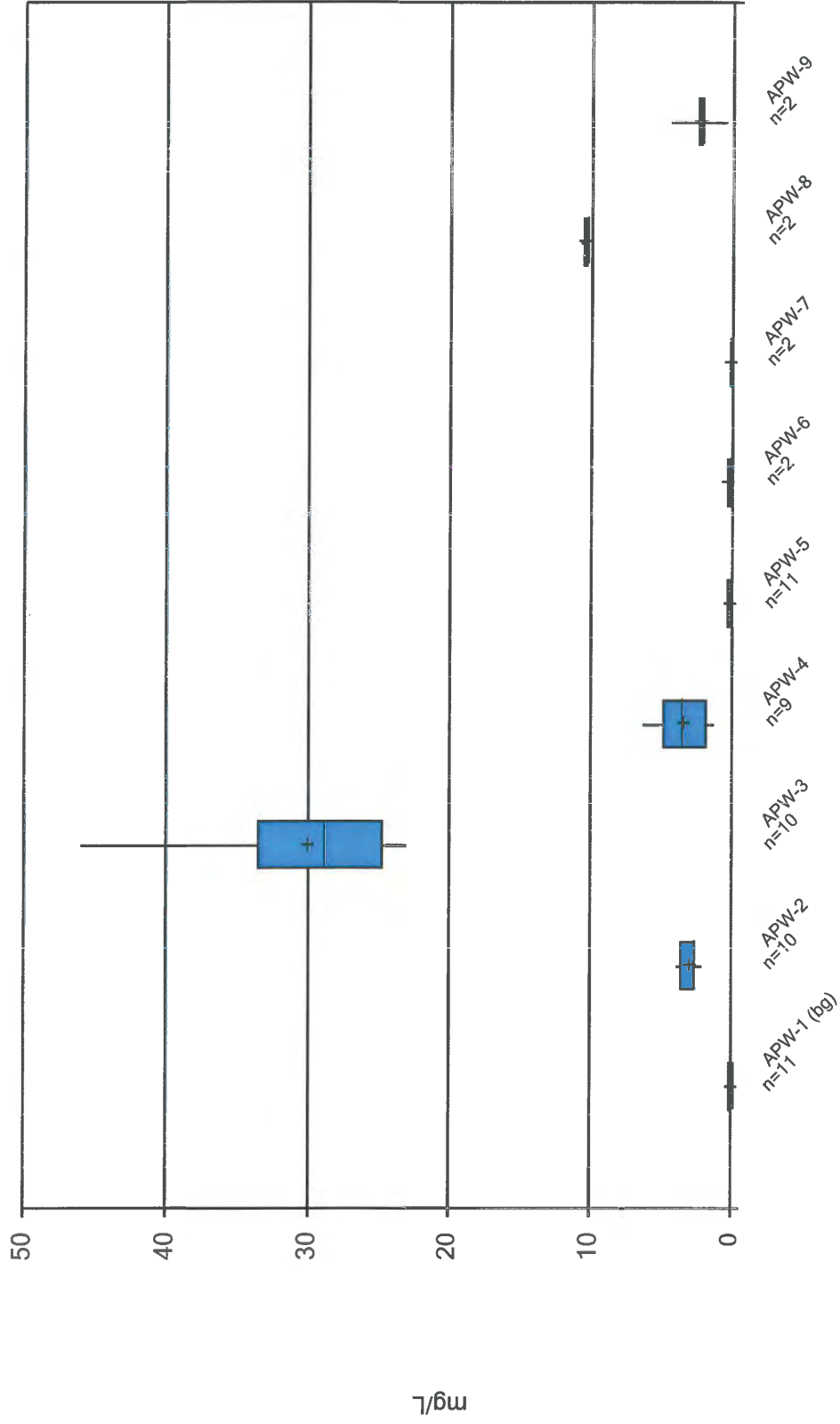
LOG OF BORING: APW-9

Project No. J024917.01

APPENDIX C

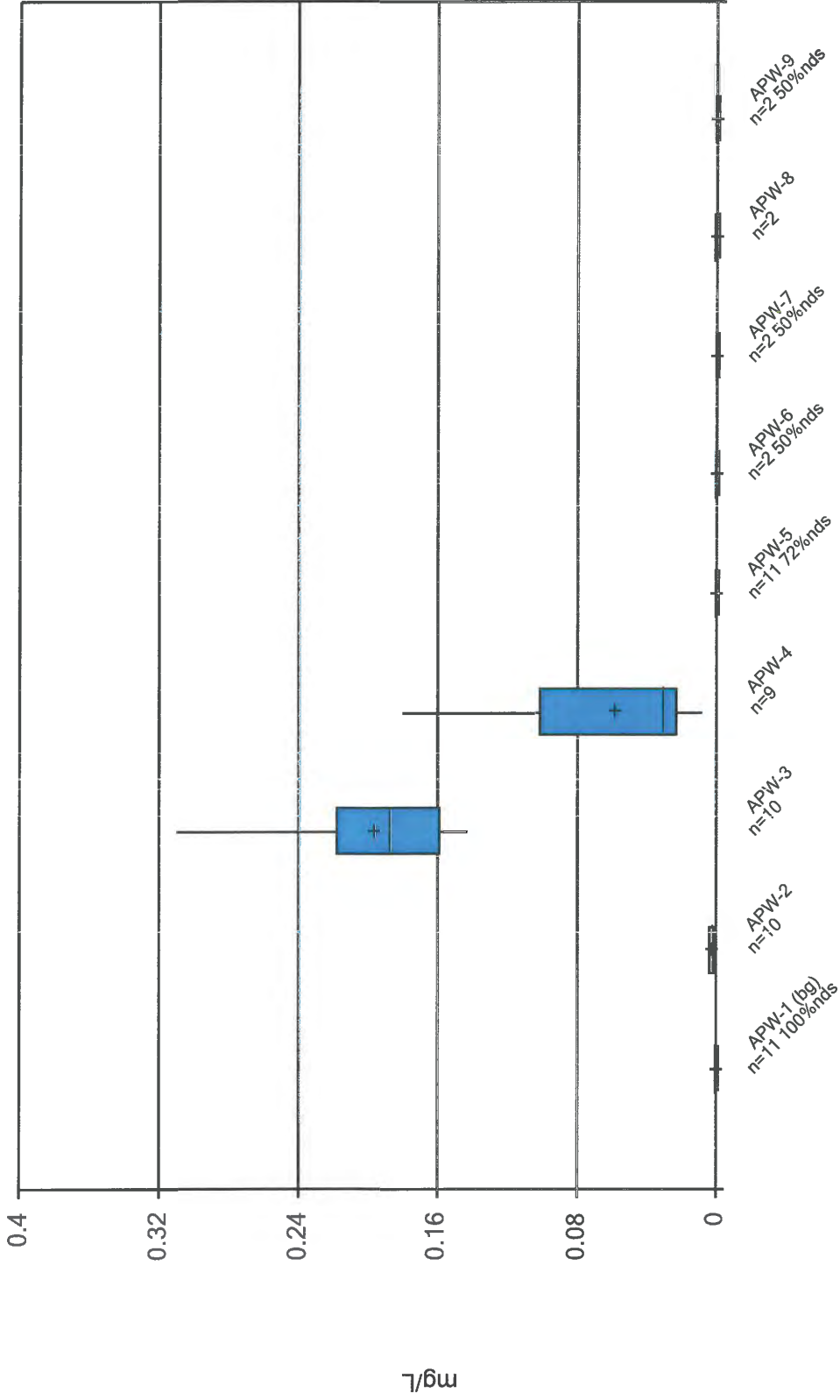
STATISTICAL ANALYSIS PLOTS

Box & Whiskers Plot



Constituent: Boron Dissolved Analysis Run 4/18/2016 3:06 PM
Facility: Meredosa Client: Geotechnology Data File: Final EDD

Box & Whiskers Plot

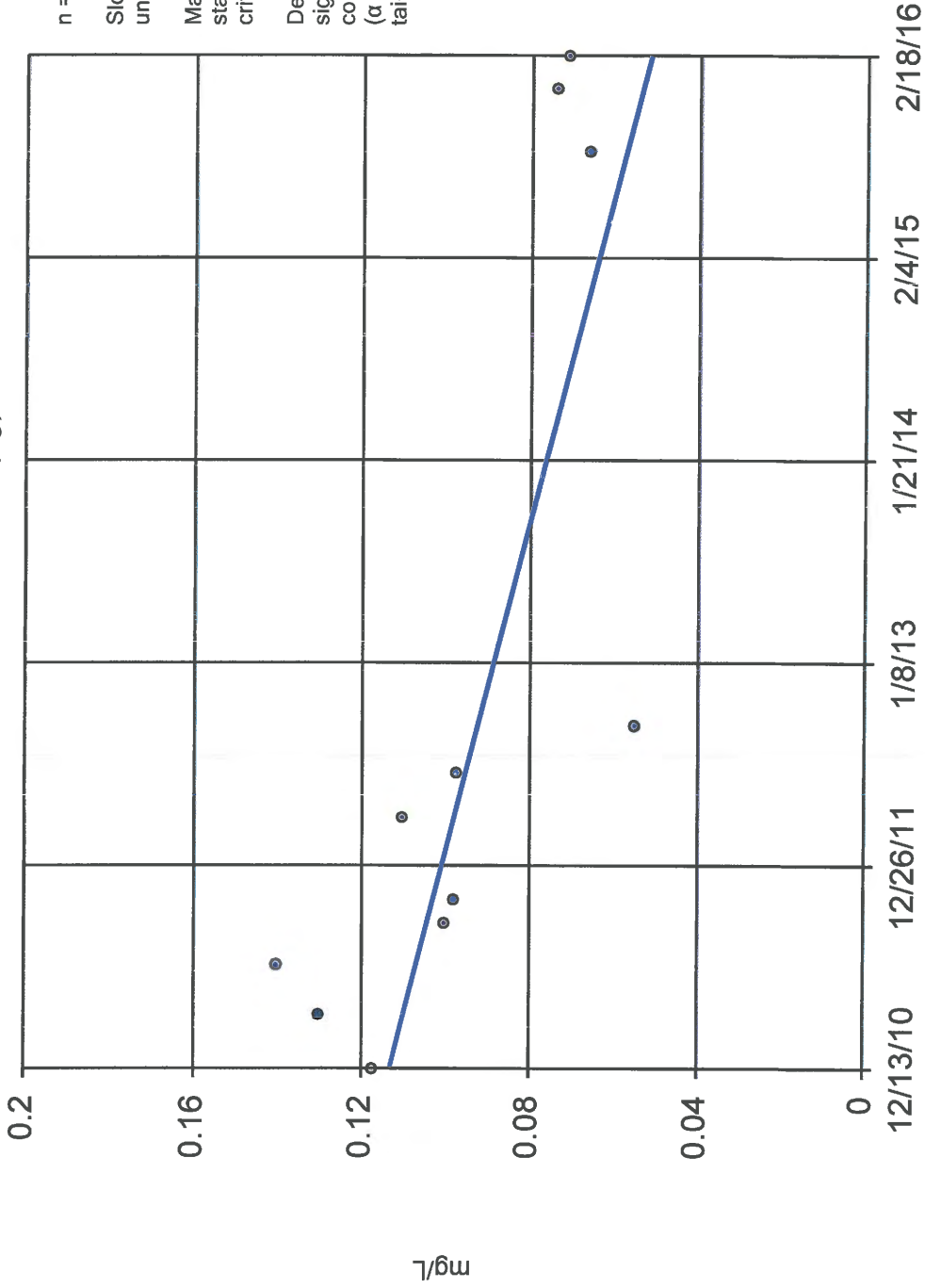


Constituent: Arsenic Dissolved Analysis Run 4/18/2016 3:07 PM

Facility: Meredosia Client: Geotechnology Data File: Final EDD

Sen's Slope Estimator

APW-1 (bg)



n = 11

Slope = -0.01179 units per year.

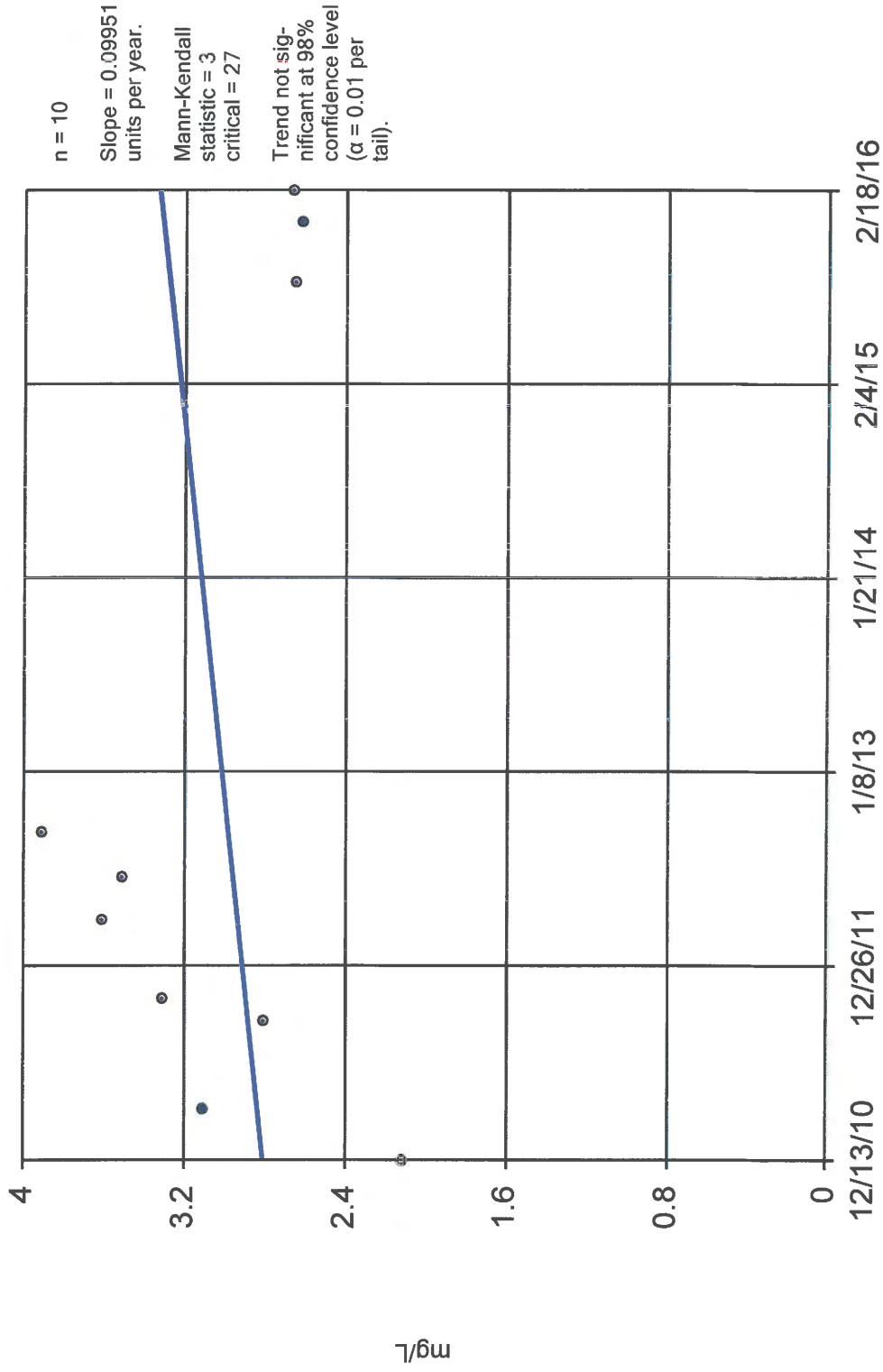
Mann-Kendall statistic = -35 critical = -31

Decreasing trend significant at 98% confidence level ($\alpha = 0.01$ per tail).

Constituent: Boron Dissolved Analysis Run 4/18/2016 3:04 PM

Facility: Meredosia Client: Geotechnology Data File: Final EDD

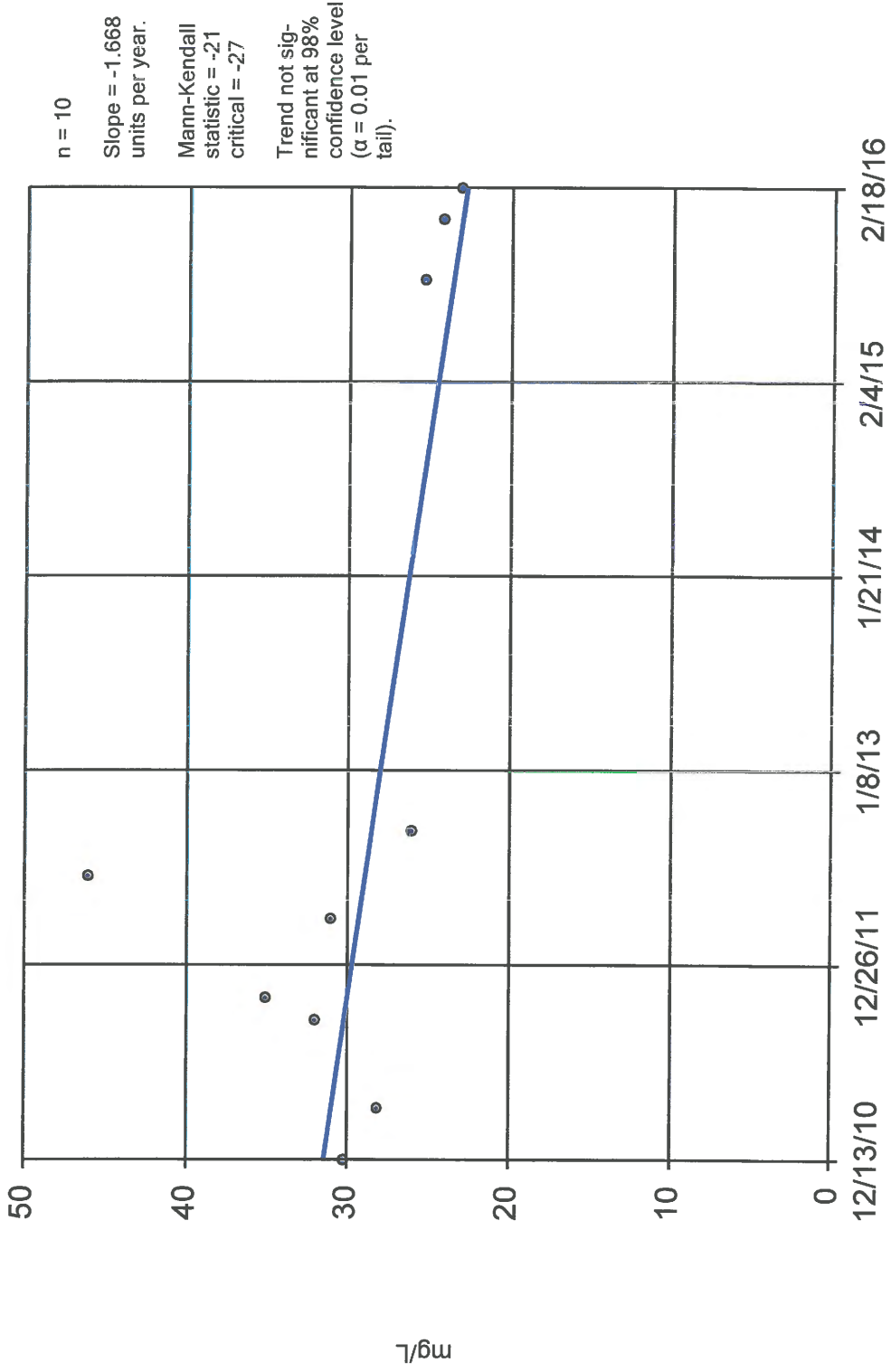
Sen's Slope Estimator APW-2



Constituent: Boron Dissolved Analysis Run 4/18/2016 3:04 PM
Facility: Meredosia Client: Geotechnology Data File: Final EDD

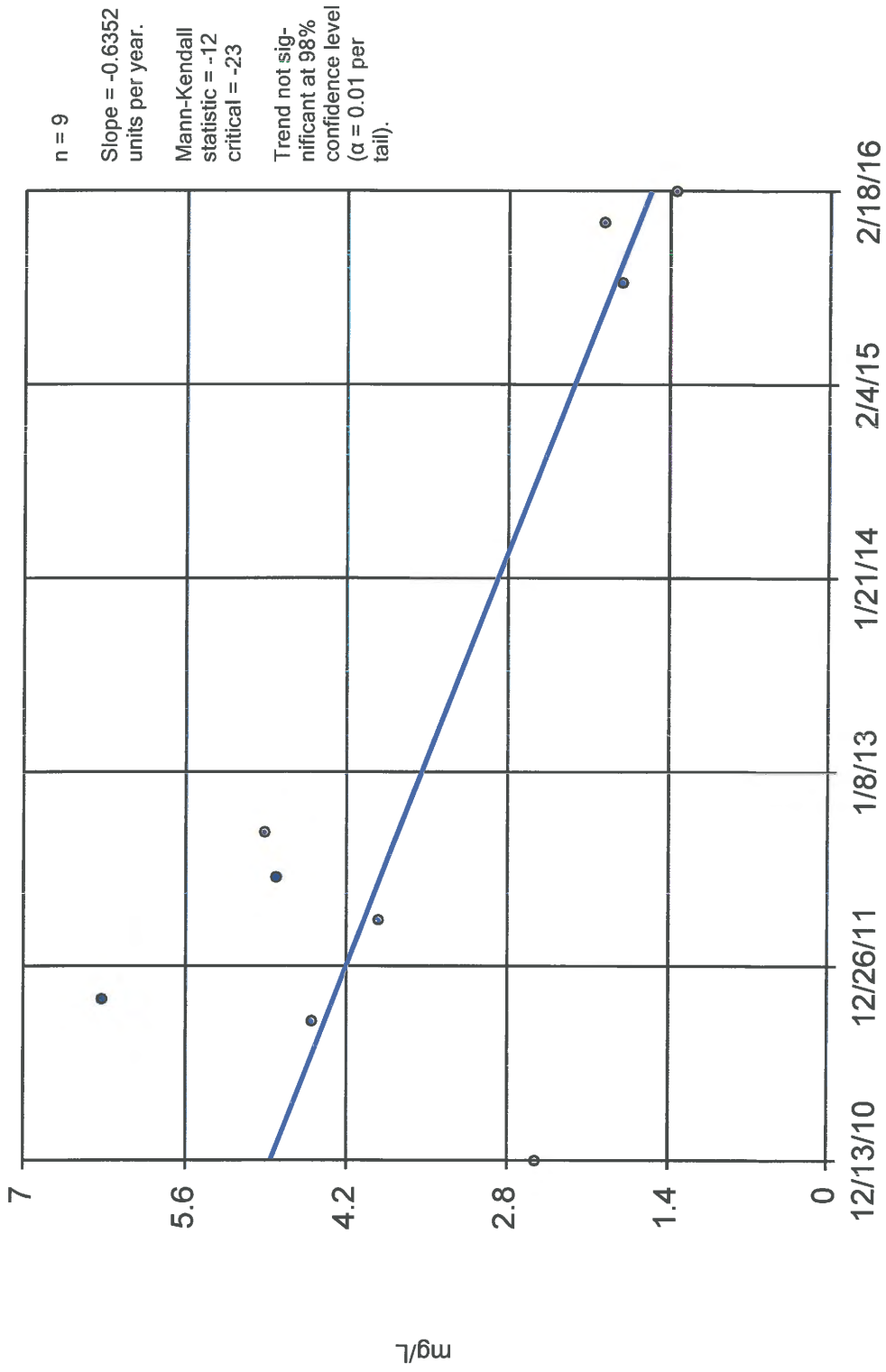
Sen's Slope Estimator

APW-3



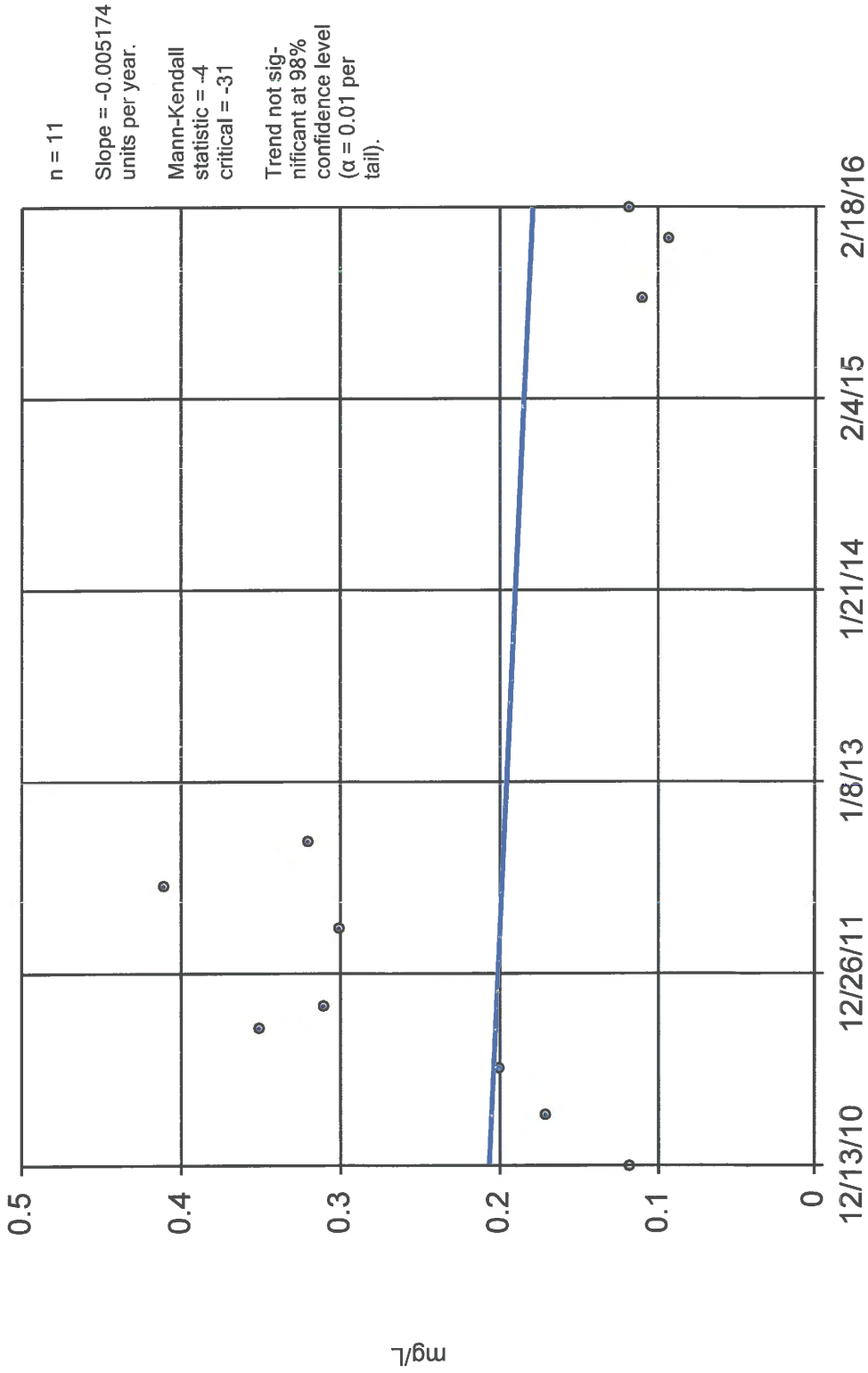
Constituent: Boron Dissolved Analysis Run 4/18/2016 3:04 PM
Facility: Meredosia Client: Geotechnology Data File: Final EDD

Sen's Slope Estimator APW-4



Constituent: Boron Dissolved Analysis Run 4/18/2016 3:04 PM
Facility: Meredosia Client: Geotechnology Data File: Final EDD

Sen's Slope Estimator APW-5

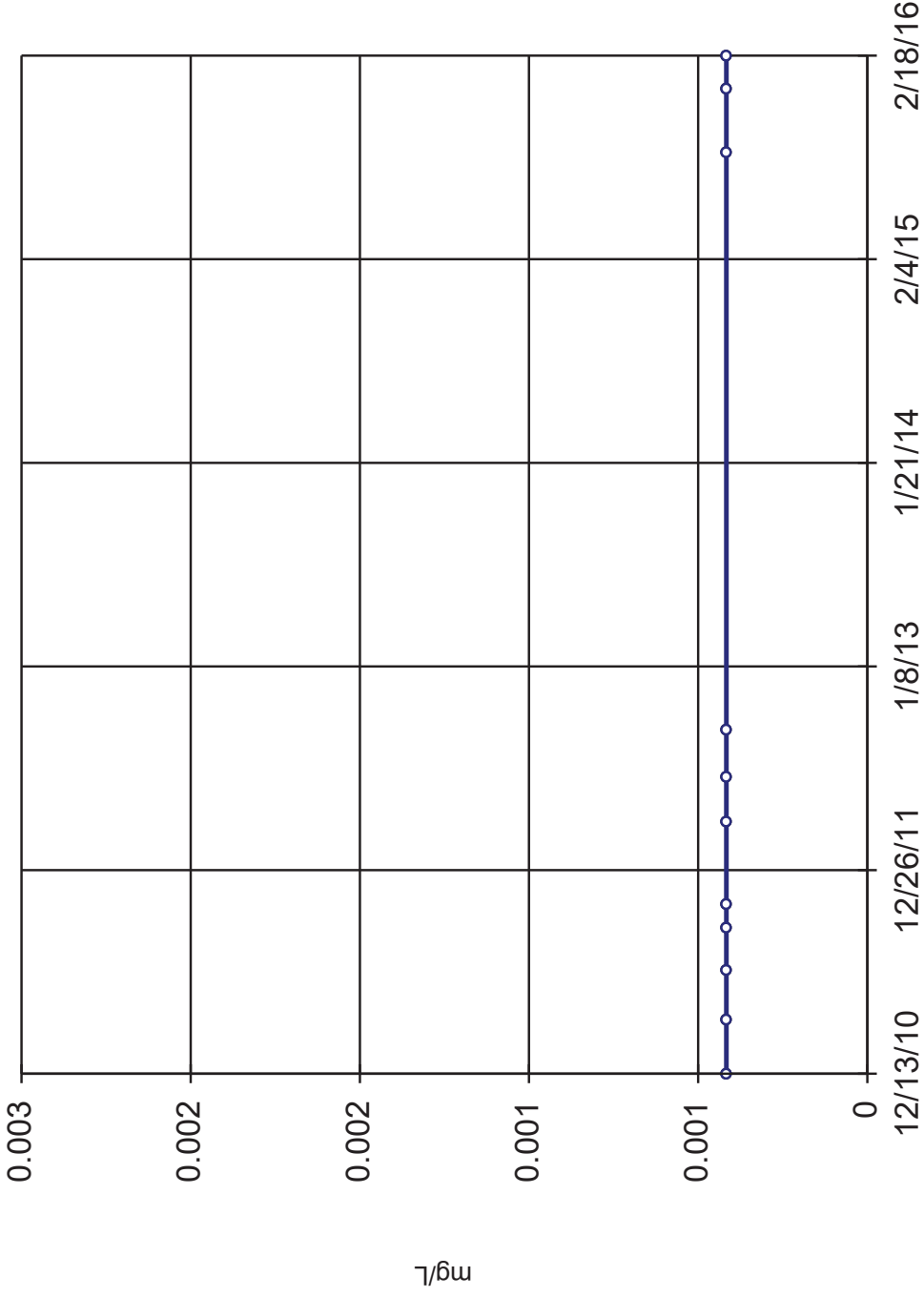


Constituent: Boron Dissolved Analysis Run 4/18/2016 3:05 PM
Facility: Meredosia Client: Geotechnology Data File: Final EDD

Sanitas™ v.9.5.27 Sanitas software licensed to Geotechnology. EPA
Hollow symbols indicate censored values.

Sen's Slope Estimator

APW-1 (bg)



n = 11

Slope = 0
units per year.

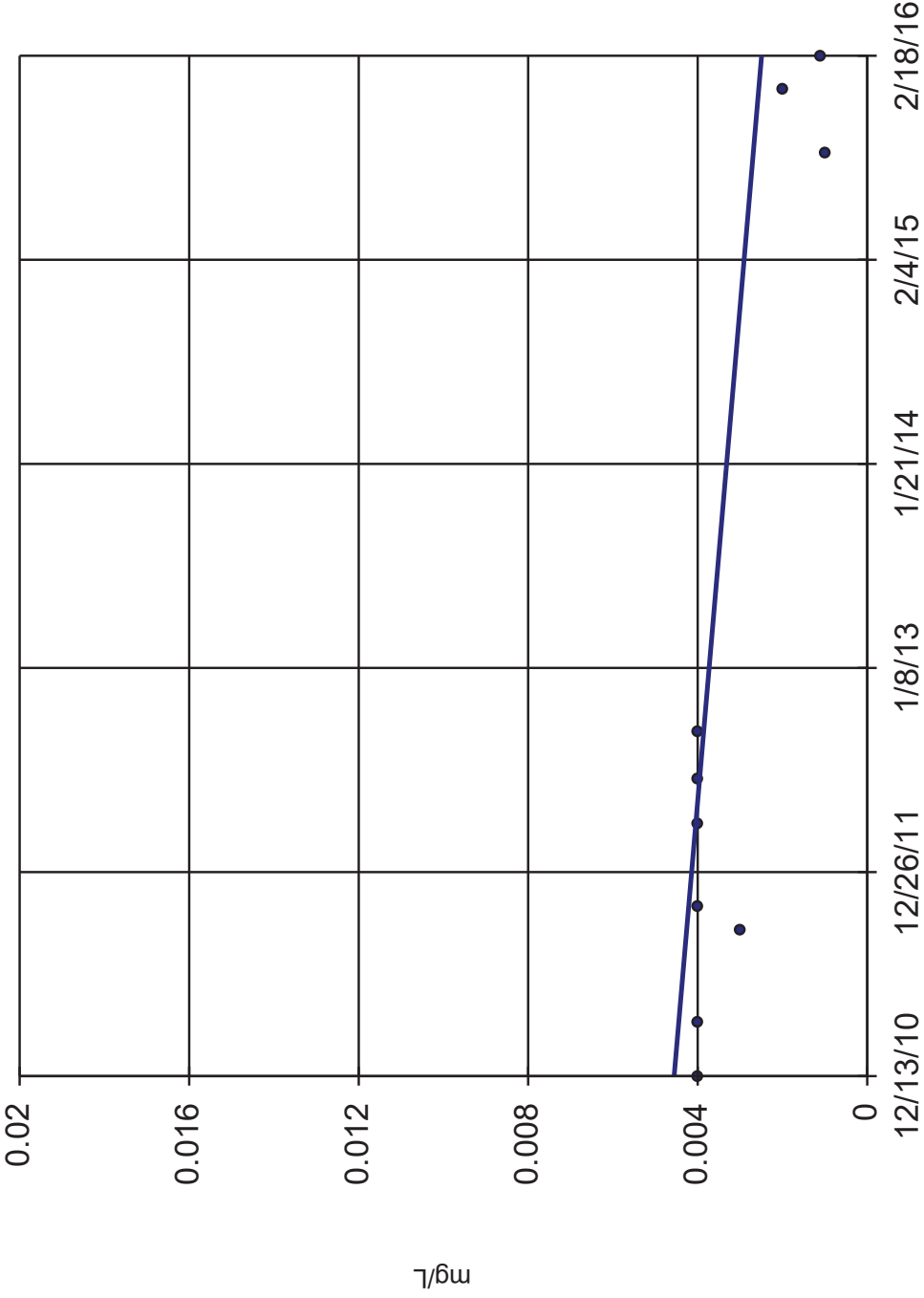
Mann-Kendall
statistic = 0
critical = 31

Trend not sig-
nificant at 98%
confidence level
($\alpha = 0.01$ per
tail).

Constituent: Arsenic Dissolved Analysis Run 10/25/2016 1:31 PM

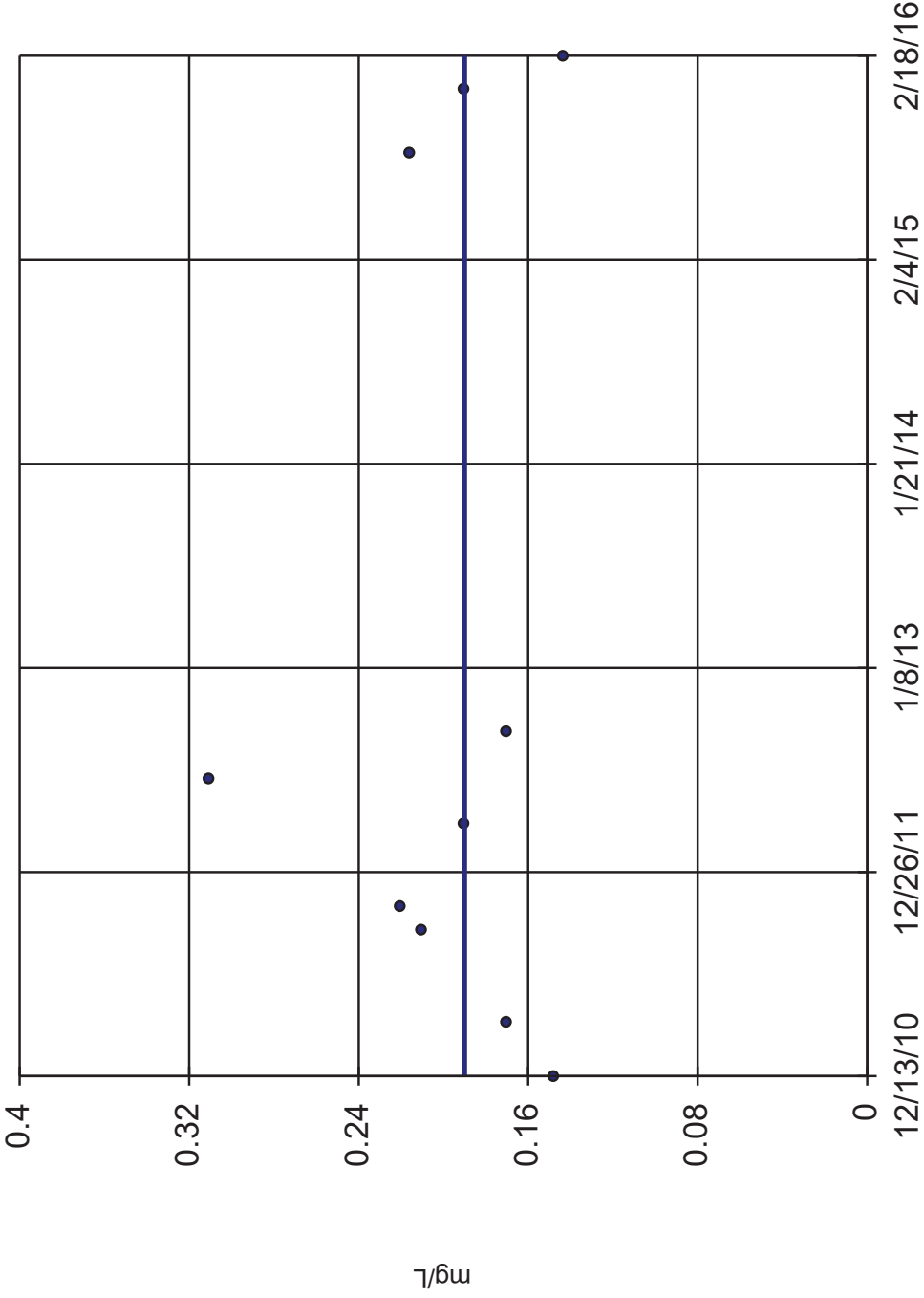
OU3 HBR Client: Geotechnology Data: Final EDD

Sen's Slope Estimator APW-2



Constituent: Arsenic Dissolved Analysis Run 10/25/2016 1:31 PM
OU3 HBR Client: Geotechnology Data: Final EDD

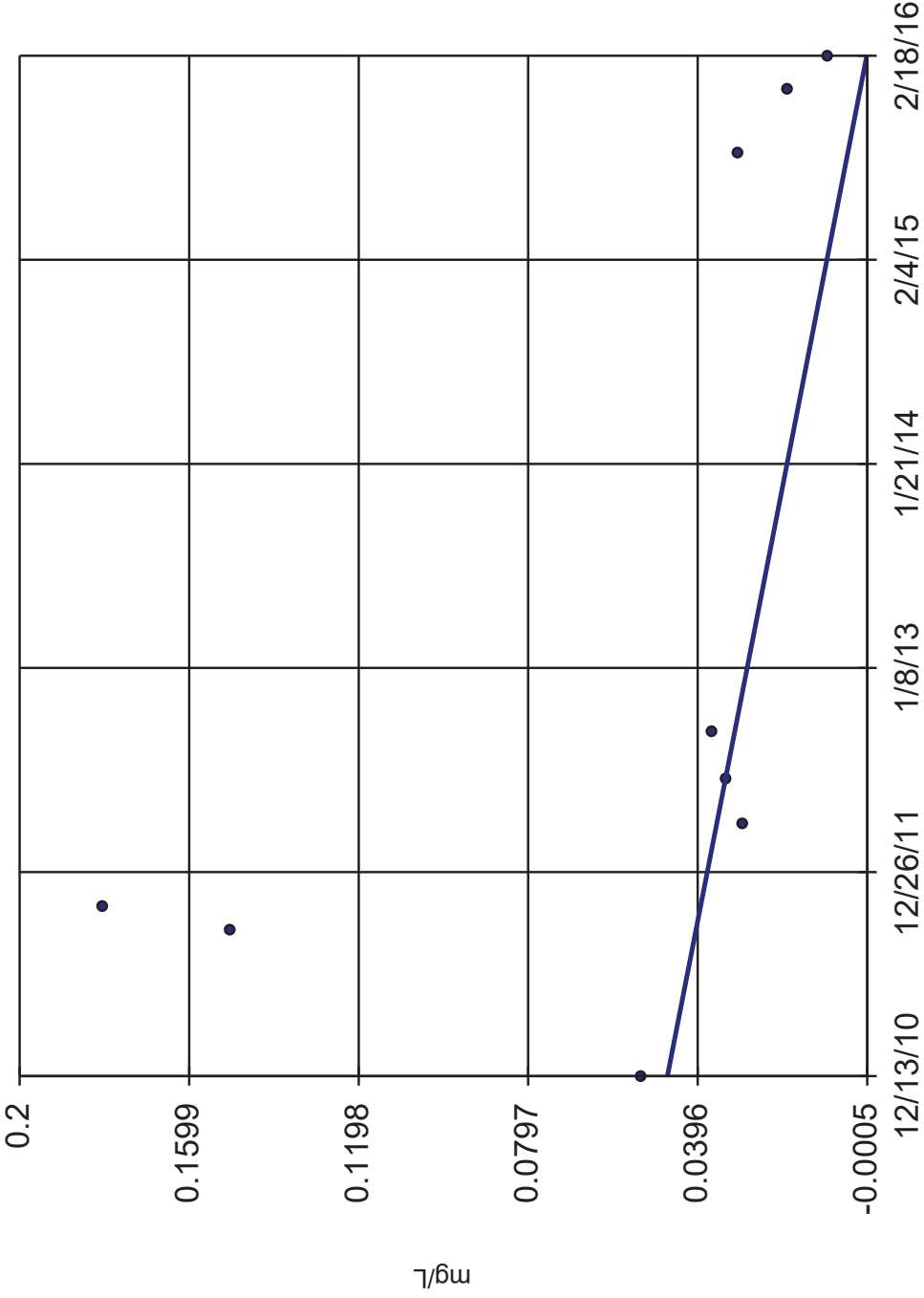
Sen's Slope Estimator APW-3



n = 10
Slope = 0
units per year.
Mann-Kendall
statistic = 1
critical = 27
Trend not sig-
nificant at 98%
confidence level
($\alpha = 0.01$ per
tail).

Sen's Slope Estimator

APW-4



n = 9

Slope = -0.009098 units per year.

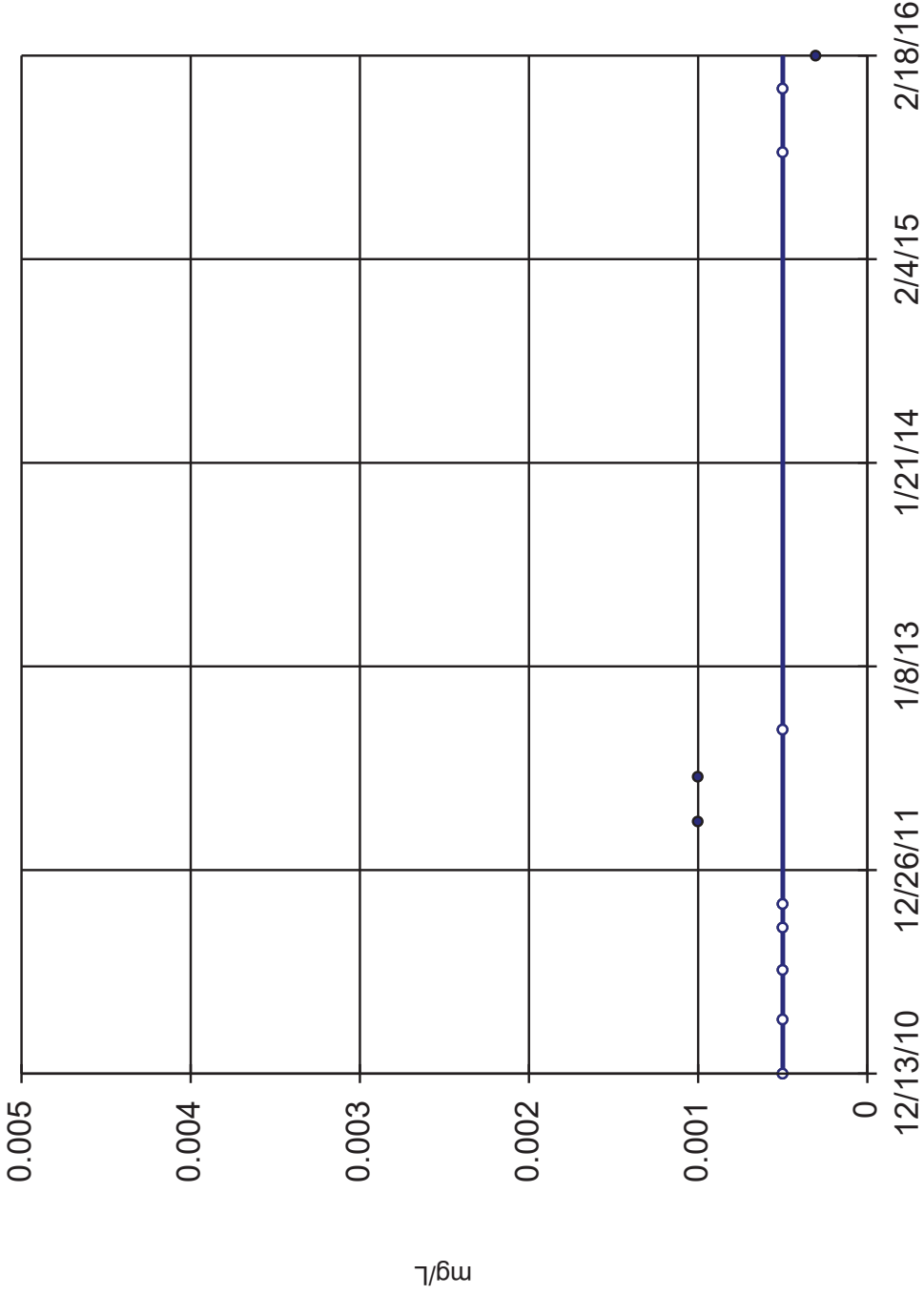
Mann-Kendall statistic = -22 critical = -23

Trend not significant at 98% confidence level ($\alpha = 0.01$ per tail).

Sanitas™ v.9.5.27 Sanitas software licensed to Geotechnology. EPA
Hollow symbols indicate censored values.

Sen's Slope Estimator

APW-5



Constituent: Arsenic Dissolved Analysis Run 10/25/2016 1:32 PM
OU3 HBR Client: Geotechnology Data: Final EDD

APPENDIX D

HELP GROUNDWATER MODEL DATA

In order to assess the drainage capabilities of the proposed Meredosia Ash Pond, Geotechnology utilized the USEPA Hydrologic Evaluation of Landfill Performance (HELP) model to simulate conditions at the site. The version of software used was HELP 3.07 (1 November 1997). For the purposes of this evaluation, the ash pond designed cap has been divided into 6 layers as follows:

- Layer 1 – Closure Turf (Geotextile/Turf Layer)
- Layer 2 – Closure Turf Drainage Layer
- Layer 3 – Membrane (50 mil HDPE)
- Layer 4 – Fly Ash (at elevations above the piezometric surface of the pond, but 100% saturated to reflect conservative conditions at initial placement)
- Layer 5 – Fly Ash (at elevations below the piezometric surface of the pond, at 100% saturation)
- Layer 6 – Fine Silty Sand (conservative for the range of sands encountered)

Model parameters for the layers were the default values for each selected layer type as provided by the HELP software module, or were input by the user (for synthetic materials) with manufacturer provided parameters. Geotechnology utilized user-selected variables of 5 pinholes and 1 installation defect per each acre of membrane material as the modeled values, with a “good” initial installation quality. We assumed the Illinois River was at nominal stage and does not affect the drainage. During future flooding events, groundwater elevation may increase to the point where the lower levels of the ash are rewetted. In the case of a 100-year flood, it is not expected that the conditions in the ash will be as saturated as provided in this model due to the limited time of flooding and relatively low permeability of the ash compared to the underlying native sands.

Geotechnology utilized a user-generated Soil Conservation Service (SCS) Curve Number of 95% and an evaporative zone depth of 0.8 inches for the model based on the site location. Evapotranspiration data were calculated using site latitude, an artificial vegetative surface, and a growing season from April 19 to October 10. Average wind speed at the site was chosen from the Springfield, Illinois National Oceanic and Atmospheric Administration (NOAA) Station, and humidity input was calculated from NOAA data provided for Meredosia, Illinois. Precipitation and temperature coefficients were selected from the HELP database-provided site (Columbia, Missouri) and adjusted for site latitude. The model was run without groundwater influx parameters. The model indicates that steady state conditions (<0.05 inches of head on the sand layer) will be achieved within approximately six months of closure activities at the two ash ponds on site.

RBCA1

0

```

*****
**
**
**          HYDROLOGIC EVALUATION OF LANDFILL PERFORMANCE          **
**          HELP MODEL VERSION 3.07 (1 NOVEMBER 1997)              **
**          DEVELOPED BY ENVIRONMENTAL LABORATORY                  **
**          USAE WATERWAYS EXPERIMENT STATION                    **
**          FOR USEPA RISK REDUCTION ENGINEERING LABORATORY       **
**
*****
*****

```

```

PRECIPITATION DATA FILE:  C:\HELP3\DATA4.D4
TEMPERATURE DATA FILE:   C:\HELP3\DATA7.D7
SOLAR RADIATION DATA FILE: C:\HELP3\DATA13.D13
EVAPOTRANSPIRATION DATA: C:\HELP3\DATA11.D11
SOIL AND DESIGN DATA FILE: C:\HELP3\DATAMER2.D10
OUTPUT DATA FILE:        C:\HELP3\RBCA1.OUT

```

TIME: 11:49 DATE: 4/15/2016

```

*****
TITLE: Meredosia
*****

```

NOTE: INITIAL MOISTURE CONTENT OF THE LAYERS AND SNOW WATER WERE SPECIFIED BY THE USER.

LAYER 1

```

          TYPE 1 - VERTICAL PERCOLATION LAYER
          MATERIAL TEXTURE NUMBER 0
THICKNESS           = 0.60 INCHES
POROSITY            = 0.4170 VOL/VOL
FIELD CAPACITY      = 0.0450 VOL/VOL
WILTING POINT       = 0.0180 VOL/VOL
INITIAL SOIL WATER  = 0.0180 VOL/VOL
EFFECTIVE SAT. HYD. COND. = 0.720000011000E-03 CM/SEC

```

LAYER 2

TYPE 2 - LATERAL DRAINAGE LAYER

RBCA1

	MATERIAL TEXTURE NUMBER	0	
THICKNESS	=	0.20	INCHES
POROSITY	=	0.8500	VOL/VOL
FIELD CAPACITY	=	0.0100	VOL/VOL
WILTING POINT	=	0.0050	VOL/VOL
INITIAL SOIL WATER CONTENT	=	0.0050	VOL/VOL
EFFECTIVE SAT. HYD. COND.	=	0.499999987000E-04	CM/SEC
SLOPE	=	4.00	PERCENT
DRAINAGE LENGTH	=	750.0	FEET

LAYER 3

TYPE 4 - FLEXIBLE MEMBRANE LINER
MATERIAL TEXTURE NUMBER 0

THICKNESS	=	0.05	INCHES
POROSITY	=	0.0000	VOL/VOL
FIELD CAPACITY	=	0.0000	VOL/VOL
WILTING POINT	=	0.0000	VOL/VOL
INITIAL SOIL WATER CONTENT	=	0.0000	VOL/VOL
EFFECTIVE SAT. HYD. COND.	=	0.199999996000E-12	CM/SEC
FML PINHOLE DENSITY	=	5.00	HOLES/ACRE
FML INSTALLATION DEFECTS	=	1.00	HOLES/ACRE
FML PLACEMENT QUALITY	=	3 - GOOD	

LAYER 4

TYPE 1 - VERTICAL PERCOLATION LAYER
MATERIAL TEXTURE NUMBER 30

THICKNESS	=	240.00	INCHES
POROSITY	=	0.5410	VOL/VOL
FIELD CAPACITY	=	0.1870	VOL/VOL
WILTING POINT	=	0.0470	VOL/VOL
INITIAL SOIL WATER CONTENT	=	0.5410	VOL/VOL
EFFECTIVE SAT. HYD. COND.	=	0.499999987000E-04	CM/SEC

LAYER 5

TYPE 1 - VERTICAL PERCOLATION LAYER
MATERIAL TEXTURE NUMBER 30

THICKNESS	=	264.00	INCHES
POROSITY	=	0.5410	VOL/VOL
FIELD CAPACITY	=	0.1870	VOL/VOL
WILTING POINT	=	0.0470	VOL/VOL
INITIAL SOIL WATER CONTENT	=	0.5410	VOL/VOL
EFFECTIVE SAT. HYD. COND.	=	0.499999987000E-04	CM/SEC

LAYER 6

RBCA1

TYPE 3 - BARRIER SOIL LINER
MATERIAL TEXTURE NUMBER 7

THICKNESS = 480.00 INCHES
 POROSITY = 0.4730 VOL/VOL
 FIELD CAPACITY = 0.2220 VOL/VOL
 WILTING POINT = 0.1040 VOL/VOL
 INITIAL SOIL WATER CONTENT = 0.4730 VOL/VOL
 EFFECTIVE SAT. HYD. COND. = 0.520000001000E-03 CM/SEC

GENERAL DESIGN AND EVAPORATIVE ZONE DATA

NOTE: SCS RUNOFF CURVE NUMBER WAS USER-SPECIFIED.

SCS RUNOFF CURVE NUMBER = 95.00
 FRACTION OF AREA ALLOWING RUNOFF = 100.0 PERCENT
 AREA PROJECTED ON HORIZONTAL PLANE = 41.900 ACRES
 EVAPORATIVE ZONE DEPTH = 0.8 INCHES
 INITIAL WATER IN EVAPORATIVE ZONE = 0.012 INCHES
 UPPER LIMIT OF EVAPORATIVE STORAGE = 0.420 INCHES
 LOWER LIMIT OF EVAPORATIVE STORAGE = 0.012 INCHES
 INITIAL SNOW WATER = 0.000 INCHES
 INITIAL WATER IN LAYER MATERIALS = 499.716 INCHES
 TOTAL INITIAL WATER = 499.716 INCHES
 TOTAL SUBSURFACE INFLOW = 0.00 INCHES/YEAR

EVAPOTRANSPIRATION AND WEATHER DATA

NOTE: EVAPOTRANSPIRATION DATA WAS OBTAINED FROM
 MEREDOSIA IL

STATION LATITUDE = 39.83 DEGREES
 MAXIMUM LEAF AREA INDEX = 2.00
 START OF GROWING SEASON (JULIAN DATE) = 109
 END OF GROWING SEASON (JULIAN DATE) = 283
 EVAPORATIVE ZONE DEPTH = 0.8 INCHES
 AVERAGE ANNUAL WIND SPEED = 9.40 MPH
 AVERAGE 1ST QUARTER RELATIVE HUMIDITY = 73.70 %
 AVERAGE 2ND QUARTER RELATIVE HUMIDITY = 67.70 %
 AVERAGE 3RD QUARTER RELATIVE HUMIDITY = 72.80 %
 AVERAGE 4TH QUARTER RELATIVE HUMIDITY = 74.00 %

NOTE: PRECIPITATION DATA WAS SYNTHETICALLY GENERATED USING
 COEFFICIENTS FOR COLUMBIA MISSOURI

NORMAL MEAN MONTHLY PRECIPITATION (INCHES)

JAN/JUL	FEB/AUG	MAR/SEP	APR/OCT	MAY/NOV	JUN/DEC
1.57	1.86	3.19	3.83	4.47	3.76
3.51	2.93	3.64	3.34	2.02	1.95

RBCA1

NOTE: TEMPERATURE DATA WAS SYNTHETICALLY GENERATED USING
COEFFICIENTS FOR COLUMBIA MISSOURI

NORMAL MEAN MONTHLY TEMPERATURE (DEGREES FAHRENHEIT)

JAN/JUL	FEB/AUG	MAR/SEP	APR/OCT	MAY/NOV	JUN/DEC
27.50	32.50	41.70	54.80	64.10	72.90
77.60	76.00	68.40	57.10	43.50	32.90

NOTE: SOLAR RADIATION DATA WAS SYNTHETICALLY GENERATED USING
COEFFICIENTS FOR COLUMBIA MISSOURI
AND STATION LATITUDE = 39.83 DEGREES

MONTHLY TOTALS (IN INCHES) FOR YEAR 1

	JAN/JUL	FEB/AUG	MAR/SEP	APR/OCT	MAY/NOV	JUN/DEC
PRECIPITATION	0.65 1.99	0.98 2.71	4.35 2.91	2.34 5.84	2.09 0.59	5.12 3.18
RUNOFF	0.268 0.076	0.076 0.413	3.142 1.655	0.562 4.155	0.817 0.135	1.215 2.372
EVAPOTRANSPIRATION	0.237 1.966	0.691 2.312	1.145 1.253	1.773 1.680	1.675 0.453	3.834 0.559
LATERAL DRAINAGE COLLECTED FROM LAYER 2	0.0001 0.0001	0.0004 0.0003	0.0023 0.0004	0.0009 0.0011	0.0006 0.0003	0.0007 0.0018
PERCOLATION/LEAKAGE THROUGH LAYER 3	0.0004 0.0007	0.0021 0.0014	0.0071 0.0017	0.0039 0.0041	0.0029 0.0013	0.0032 0.0053
PERCOLATION/LEAKAGE THROUGH LAYER 6	54.4649 4.0537	19.1717 3.4231	12.2311 2.8656	8.0304 2.5884	6.2079 2.2323	4.7599 2.0824

MONTHLY SUMMARIES FOR DAILY HEADS (INCHES)

AVERAGE DAILY HEAD ON TOP OF LAYER 3	0.026 0.031	0.122 0.079	0.487 0.104	0.254 0.259	0.179 0.081	0.209 0.364
STD. DEVIATION OF DAILY HEAD ON TOP OF LAYER 3	0.080 0.107	0.211 0.164	0.299 0.187	0.225 0.285	0.208 0.183	0.197 0.370
AVERAGE DAILY HEAD ON TOP OF LAYER 6	4.633 0.046	0.242 0.039	0.140 0.034	0.095 0.029	0.071 0.026	0.056 0.024

RBCA1

STD. DEVIATION OF DAILY HEAD ON TOP OF LAYER 6 22.615 0.047 0.019 0.009 0.005 0.003
 0.002 0.002 0.001 0.001 0.001 0.001

ANNUAL TOTALS FOR YEAR 1

	INCHES	CU. FEET	PERCENT
PRECIPITATION	32.75	4981177.000	100.00
RUNOFF	14.887	2264236.500	45.46
EVAPOTRANSPIRATION	17.579	2673680.250	53.68
DRAINAGE COLLECTED FROM LAYER 2	0.0089	1348.050	0.03
PERC./LEAKAGE THROUGH LAYER 3	0.033986	5169.242	0.10
AVG. HEAD ON TOP OF LAYER 3	0.1828		
PERC./LEAKAGE THROUGH LAYER 6	122.111244	18572754.000	372.86
AVG. HEAD ON TOP OF LAYER 6	0.4529		
CHANGE IN WATER STORAGE	-121.836	-18530826.000	-372.02
SOIL WATER AT START OF YEAR	499.716	76005376.000	
SOIL WATER AT END OF YEAR	377.881	57474548.000	
SNOW WATER AT START OF YEAR	0.000	0.000	0.00
SNOW WATER AT END OF YEAR	0.000	0.000	0.00
ANNUAL WATER BUDGET BALANCE	-0.0001	-17.406	0.00

MONTHLY TOTALS (IN INCHES) FOR YEAR 2

	JAN/JUL	FEB/AUG	MAR/SEP	APR/OCT	MAY/NOV	JUN/DEC
PRECIPITATION	2.86 3.39	1.75 1.19	3.39 0.84	5.43 5.12	9.02 1.57	6.65 0.67
RUNOFF	0.146 1.386	2.270 0.404	3.338 0.179	2.979 4.267	6.238 0.565	3.405 0.319

	RBCA1					
EVAPOTRANSPIRATION	0.611	0.427	1.316	2.334	3.009	3.243
	1.703	1.084	0.350	1.151	0.628	0.490
LATERAL DRAINAGE COLLECTED FROM LAYER 2	0.0007	0.0001	0.0005	0.0009	0.0012	0.0010
	0.0005	0.0001	0.0016	0.0013	0.0007	0.0027
PERCOLATION/LEAKAGE THROUGH LAYER 3	0.0040	0.0024	0.0032	0.0042	0.0043	0.0035
	0.0020	0.0008	0.0047	0.0043	0.0028	0.0084
PERCOLATION/LEAKAGE THROUGH LAYER 6	1.8995	1.5731	1.6060	1.4391	1.3817	1.2485
	1.2092	1.1317	1.0323	1.0082	0.9299	0.9066

MONTHLY SUMMARIES FOR DAILY HEADS (INCHES)

AVERAGE DAILY HEAD ON TOP OF LAYER 3	0.237	0.131	0.178	0.276	0.288	0.243
	0.132	0.041	0.343	0.294	0.176	0.581
STD. DEVIATION OF DAILY HEAD ON TOP OF LAYER 3	0.214	0.000	0.191	0.232	0.272	0.281
	0.223	0.115	0.327	0.304	0.267	0.230
AVERAGE DAILY HEAD ON TOP OF LAYER 6	0.022	0.020	0.018	0.017	0.016	0.015
	0.014	0.013	0.012	0.011	0.011	0.010
STD. DEVIATION OF DAILY HEAD ON TOP OF LAYER 6	0.001	0.000	0.000	0.000	0.000	0.000
	0.000	0.000	0.000	0.000	0.000	0.000

ANNUAL TOTALS FOR YEAR 2

	INCHES	CU. FEET	PERCENT
PRECIPITATION	41.88	6369823.000	100.00
RUNOFF	25.496	3877910.000	60.88
EVAPOTRANSPIRATION	16.345	2486056.250	39.03
DRAINAGE COLLECTED FROM LAYER 2	0.0114	1726.946	0.03
PERC./LEAKAGE THROUGH LAYER 3	0.044646	6790.513	0.11
AVG. HEAD ON TOP OF LAYER 3	0.2433		
PERC./LEAKAGE THROUGH LAYER 6	15.365823	2337095.750	36.69
AVG. HEAD ON TOP OF LAYER 6	0.0149		
CHANGE IN WATER STORAGE	-15.339	-2332968.000	-36.63
SOIL WATER AT START OF YEAR	377.881	57474548.000	
SOIL WATER AT END OF YEAR	362.542	55141580.000	
SNOW WATER AT START OF YEAR	0.000	0.000	0.00

RBCA1

SNOW WATER AT END OF YEAR	0.000	0.000	0.00
ANNUAL WATER BUDGET BALANCE	0.0000	1.886	0.00

MONTHLY TOTALS (IN INCHES) FOR YEAR 3

	JAN/JUL	FEB/AUG	MAR/SEP	APR/OCT	MAY/NOV	JUN/DEC
PRECIPITATION	2.74 8.48	2.95 0.95	1.91 5.48	2.30 2.08	1.25 2.67	3.82 1.16
RUNOFF	2.459 4.299	2.121 0.054	0.531 3.751	1.093 0.637	0.696 1.542	1.824 0.260
EVAPOTRANSPIRATION	0.096 4.004	0.889 1.227	1.304 1.642	1.204 1.371	0.768 1.250	2.022 0.372
LATERAL DRAINAGE COLLECTED FROM LAYER 2	0.0001 0.0011	0.0021 0.0001	0.0009 0.0006	0.0008 0.0008	0.0010 0.0017	0.0007 0.0003
PERCOLATION/LEAKAGE THROUGH LAYER 3	0.0027 0.0041	0.0070 0.0006	0.0036 0.0025	0.0029 0.0036	0.0031 0.0055	0.0036 0.0023
PERCOLATION/LEAKAGE THROUGH LAYER 6	0.8677 0.6678	0.7468 0.6424	0.7898 0.5990	0.7322 0.5954	0.7255 0.5543	0.6688 0.5595

MONTHLY SUMMARIES FOR DAILY HEADS (INCHES)

AVERAGE DAILY HEAD ON TOP OF LAYER 3	0.138 0.259	0.530 0.030	0.235 0.162	0.204 0.227	0.212 0.377	0.223 0.134
STD. DEVIATION OF DAILY HEAD ON TOP OF LAYER 3	0.030 0.247	0.237 0.078	0.258 0.231	0.253 0.238	0.320 0.310	0.194 0.152
AVERAGE DAILY HEAD ON TOP OF LAYER 6	0.010 0.008	0.009 0.007	0.009 0.007	0.009 0.007	0.008 0.007	0.008 0.006
STD. DEVIATION OF DAILY HEAD ON TOP OF LAYER 6	0.000 0.000	0.000 0.000	0.000 0.000	0.000 0.000	0.000 0.000	0.000 0.000

ANNUAL TOTALS FOR YEAR 3

RBCA1

	INCHES	CU. FEET	PERCENT
PRECIPITATION	35.79	5443552.000	100.00
RUNOFF	19.266	2930366.500	53.83
EVAPOTRANSPIRATION	16.149	2456188.000	45.12
DRAINAGE COLLECTED FROM LAYER 2	0.0102	1553.305	0.03
PERC./LEAKAGE THROUGH LAYER 3	0.041437	6302.389	0.12
AVG. HEAD ON TOP OF LAYER 3	0.2274		
PERC./LEAKAGE THROUGH LAYER 6	8.149208	1239470.120	22.77
AVG. HEAD ON TOP OF LAYER 6	0.0079		
CHANGE IN WATER STORAGE	-7.785	-1184027.870	-21.75
SOIL WATER AT START OF YEAR	362.542	55141580.000	
SOIL WATER AT END OF YEAR	354.618	53936332.000	
SNOW WATER AT START OF YEAR	0.000	0.000	0.00
SNOW WATER AT END OF YEAR	0.140	21218.414	0.39
ANNUAL WATER BUDGET BALANCE	0.0000	2.176	0.00

MONTHLY TOTALS (IN INCHES) FOR YEAR 4

	JAN/JUL	FEB/AUG	MAR/SEP	APR/OCT	MAY/NOV	JUN/DEC
PRECIPITATION	0.80 2.02	2.25 4.10	2.37 3.72	2.92 1.07	4.89 2.94	4.29 2.40
RUNOFF	0.586 0.137	1.541 1.452	1.387 1.793	1.382 0.022	1.789 1.683	1.468 1.930
EVAPOTRANSPIRATION	0.353 1.881	0.761 2.388	1.322 1.942	1.149 0.917	3.297 1.206	3.003 0.461
LATERAL DRAINAGE COLLECTED FROM LAYER 2	0.0001 0.0002	0.0015 0.0007	0.0019 0.0010	0.0006 0.0004	0.0013 0.0020	0.0006 0.0023
PERCOLATION/LEAKAGE THROUGH LAYER 3	0.0027 0.0012	0.0056 0.0025	0.0062 0.0038	0.0024 0.0022	0.0051 0.0068	0.0027 0.0074
PERCOLATION/LEAKAGE THROUGH LAYER 6	0.5398 0.4517	0.4892 0.4385	0.5039 0.4116	0.4772 0.4133	0.4789 0.3914	0.4493 0.3909

RBCA1

 MONTHLY SUMMARIES FOR DAILY HEADS (INCHES)

AVERAGE DAILY HEAD ON TOP OF LAYER 3	0.131 0.064	0.392 0.163	0.424 0.257	0.153 0.141	0.329 0.477	0.160 0.498
STD. DEVIATION OF DAILY HEAD ON TOP OF LAYER 3	0.001 0.145	0.254 0.231	0.274 0.237	0.241 0.168	0.239 0.217	0.205 0.303
AVERAGE DAILY HEAD ON TOP OF LAYER 6	0.006 0.005	0.006 0.005	0.006 0.005	0.006 0.005	0.005 0.005	0.005 0.004
STD. DEVIATION OF DAILY HEAD ON TOP OF LAYER 6	0.000 0.000	0.000 0.000	0.000 0.000	0.000 0.000	0.000 0.000	0.000 0.000

ANNUAL TOTALS FOR YEAR 4

	INCHES	CU. FEET	PERCENT
PRECIPITATION	33.77	5136316.500	100.00
RUNOFF	15.170	2307287.750	44.92
EVAPOTRANSPIRATION	18.679	2840977.500	55.31
DRAINAGE COLLECTED FROM LAYER 2	0.0124	1883.304	0.04
PERC./LEAKAGE THROUGH LAYER 3	0.048741	7413.380	0.14
AVG. HEAD ON TOP OF LAYER 3	0.2659		
PERC./LEAKAGE THROUGH LAYER 6	5.435782	826766.250	16.10
AVG. HEAD ON TOP OF LAYER 6	0.0052		
CHANGE IN WATER STORAGE	-5.527	-840596.500	-16.37
SOIL WATER AT START OF YEAR	354.618	53936332.000	
SOIL WATER AT END OF YEAR	349.231	53116956.000	
SNOW WATER AT START OF YEAR	0.140	21218.414	0.41
SNOW WATER AT END OF YEAR	0.000	0.000	0.00
ANNUAL WATER BUDGET BALANCE	0.0000	-1.668	0.00

RBCA1

MONTHLY TOTALS (IN INCHES) FOR YEAR 5

	JAN/JUL	FEB/AUG	MAR/SEP	APR/OCT	MAY/NOV	JUN/DEC
PRECIPITATION	0.31 0.87	0.76 1.98	4.61 3.38	6.11 2.79	2.96 3.89	7.06 2.30
RUNOFF	0.116 0.103	0.531 0.369	2.830 1.915	3.019 1.795	0.715 2.559	4.162 0.983
EVAPOTRANSPIRATION	0.194 0.767	0.281 1.562	1.802 1.247	3.116 1.254	2.530 1.317	2.893 0.911
LATERAL DRAINAGE COLLECTED FROM LAYER 2	0.0001 0.0001	0.0001 0.0003	0.0016 0.0006	0.0015 0.0008	0.0009 0.0017	0.0011 0.0007
PERCOLATION/LEAKAGE THROUGH LAYER 3	0.0027 0.0006	0.0025 0.0014	0.0054 0.0023	0.0056 0.0029	0.0036 0.0056	0.0040 0.0030
PERCOLATION/LEAKAGE THROUGH LAYER 6	0.3862 0.3365	0.3427 0.3309	0.3694 0.3111	0.3482 0.3122	0.3489 0.2973	0.3338 0.2996

MONTHLY SUMMARIES FOR DAILY HEADS (INCHES)

AVERAGE DAILY HEAD ON TOP OF LAYER 3	0.131 0.037	0.143 0.081	0.364 0.160	0.385 0.189	0.230 0.390	0.267 0.187
STD. DEVIATION OF DAILY HEAD ON TOP OF LAYER 3	0.001 0.108	0.082 0.155	0.272 0.236	0.240 0.259	0.259 0.290	0.266 0.240
AVERAGE DAILY HEAD ON TOP OF LAYER 6	0.004 0.004	0.004 0.004	0.004 0.004	0.004 0.004	0.004 0.003	0.004 0.003
STD. DEVIATION OF DAILY HEAD ON TOP OF LAYER 6	0.000 0.000	0.000 0.000	0.000 0.000	0.000 0.000	0.000 0.000	0.000 0.000

ANNUAL TOTALS FOR YEAR 5

	INCHES	CU. FEET	PERCENT
PRECIPITATION	37.02	5630630.500	100.00
RUNOFF	19.098	2904761.000	51.59
EVAPOTRANSPIRATION	17.872	2718264.500	48.28
DRAINAGE COLLECTED FROM LAYER 2	0.0095	1444.178	0.03

	RBCA1		
PERC./LEAKAGE THROUGH LAYER 3	0.039613	6025.084	0.11
AVG. HEAD ON TOP OF LAYER 3	0.2135		
PERC./LEAKAGE THROUGH LAYER 6	4.016714	610930.187	10.85
AVG. HEAD ON TOP OF LAYER 6	0.0039		
CHANGE IN WATER STORAGE	-3.976	-604767.562	-10.74
SOIL WATER AT START OF YEAR	349.231	53116956.000	
SOIL WATER AT END OF YEAR	345.255	52512188.000	
SNOW WATER AT START OF YEAR	0.000	0.000	0.00
SNOW WATER AT END OF YEAR	0.000	0.000	0.00
ANNUAL WATER BUDGET BALANCE	0.0000	-1.523	0.00

AVERAGE MONTHLY VALUES IN INCHES FOR YEARS 1 THROUGH 5

	JAN/JUL	FEB/AUG	MAR/SEP	APR/OCT	MAY/NOV	JUN/DEC
<u>PRECIPITATION</u>						
TOTALS	1.47 3.35	1.74 2.19	3.33 3.27	3.82 3.38	4.04 2.33	5.39 1.94
STD. DEVIATIONS	1.23 3.00	0.90 1.27	1.19 1.67	1.81 2.03	3.09 1.28	1.43 1.01
<u>RUNOFF</u>						
TOTALS	0.715 1.200	1.308 0.538	2.246 1.859	1.807 2.175	2.051 1.297	2.415 1.173
STD. DEVIATIONS	0.993 1.819	0.970 0.532	1.227 1.270	1.127 1.965	2.384 0.960	1.296 0.950
<u>EVAPOTRANSPIRATION</u>						
TOTALS	0.298 2.064	0.610 1.714	1.378 1.287	1.915 1.275	2.256 0.971	2.999 0.559
STD. DEVIATIONS	0.198 1.185	0.250 0.606	0.248 0.599	0.826 0.282	1.034 0.399	0.656 0.208
<u>LATERAL DRAINAGE COLLECTED FROM LAYER 2</u>						
TOTALS	0.0002 0.0004	0.0008 0.0003	0.0014 0.0008	0.0010 0.0009	0.0010 0.0013	0.0008 0.0016

		RBCA1				
STD. DEVIATIONS	0.0003 0.0004	0.0009 0.0002	0.0007 0.0005	0.0004 0.0003	0.0003 0.0007	0.0002 0.0010
PERCOLATION/LEAKAGE THROUGH LAYER 3						
TOTALS	0.0025 0.0017	0.0039 0.0013	0.0051 0.0030	0.0038 0.0034	0.0038 0.0044	0.0034 0.0053
STD. DEVIATIONS	0.0013 0.0014	0.0022 0.0008	0.0017 0.0012	0.0012 0.0009	0.0009 0.0023	0.0005 0.0027
PERCOLATION/LEAKAGE THROUGH LAYER 6						
TOTALS	11.6316 1.3438	4.4647 1.1933	3.1000 1.0439	2.2054 0.9835	1.8286 0.8810	1.4921 0.8478
STD. DEVIATIONS	23.9518 1.5515	8.2352 1.2838	5.1269 1.0552	3.2834 0.9358	2.4802 0.7930	1.8604 0.7280

 AVERAGES OF MONTHLY AVERAGED DAILY HEADS (INCHES)

DAILY AVERAGE HEAD ON TOP OF LAYER 3						
AVERAGES	0.1323 0.1045	0.2634 0.0789	0.3375 0.2051	0.2543 0.2219	0.2476 0.3002	0.2203 0.3528
STD. DEVIATIONS	0.0747 0.0953	0.1867 0.0524	0.1292 0.0948	0.0871 0.0599	0.0603 0.1649	0.0400 0.1927
DAILY AVERAGE HEAD ON TOP OF LAYER 6						
AVERAGES	0.9350 0.0153	0.0564 0.0136	0.0354 0.0123	0.0260 0.0112	0.0208 0.0104	0.0176 0.0097
STD. DEVIATIONS	2.0672 0.0177	0.1042 0.0146	0.0585 0.0124	0.0387 0.0107	0.0283 0.0093	0.0219 0.0083

 AVERAGE ANNUAL TOTALS & (STD. DEVIATIONS) FOR YEARS 1 THROUGH 5

	INCHES		CU. FEET	PERCENT
PRECIPITATION	36.24	(3.567)	5512299.0	100.00
RUNOFF	18.783	(4.2906)	2856912.50	51.828
EVAPOTRANSPIRATION	17.325	(1.0653)	2635033.25	47.803
LATERAL DRAINAGE COLLECTED FROM LAYER 2	0.01046	(0.00142)	1591.157	0.02887
PERCOLATION/LEAKAGE THROUGH LAYER 3	0.04168	(0.00553)	6340.122	0.11502

RBCA1

AVERAGE HEAD ON TOP OF LAYER 3	0.227 (0.031)		
PERCOLATION/LEAKAGE THROUGH LAYER 6	31.01575 (51.11133)	4717403.000	85.57959
AVERAGE HEAD ON TOP OF LAYER 6	0.097 (0.199)		
CHANGE IN WATER STORAGE	-30.892 (51.0256)	-4698637.00	-85.239

♀

PEAK DAILY VALUES FOR YEARS	1 THROUGH	5
	(INCHES)	(CU. FT.)
PRECIPITATION	2.59	393931.219
RUNOFF	2.144	326045.4060
DRAINAGE COLLECTED FROM LAYER 2	0.00013	20.29407
PERCOLATION/LEAKAGE THROUGH LAYER 3	0.000370	56.22432
AVERAGE HEAD ON TOP OF LAYER 3	0.800	
MAXIMUM HEAD ON TOP OF LAYER 3	1.569	
LOCATION OF MAXIMUM HEAD IN LAYER 2 (DISTANCE FROM DRAIN)	13.3 FEET	
PERCOLATION/LEAKAGE THROUGH LAYER 6	7.397256	1125100.62000
AVERAGE HEAD ON TOP OF LAYER 6	126.484	
SNOW WATER	2.25	342081.3750
MAXIMUM VEG. SOIL WATER (VOL/VOL)		0.5253
MINIMUM VEG. SOIL WATER (VOL/VOL)		0.0148

*** Maximum heads are computed using McEnroe's equations. ***

Reference: Maximum Saturated Depth over Landfill Liner
 by Bruce M. McEnroe, University of Kansas
 ASCE Journal of Environmental Engineering
 Vol. 119, No. 2, March 1993, pp. 262-270.

♀

RBCA1

FINAL WATER STORAGE AT END OF YEAR 5

LAYER	(INCHES)	(VOL/VOL)
1	0.2646	0.4411
2	0.1556	0.7778
3	0.0000	0.0000
4	51.6723	0.2153
5	66.1214	0.2505
6	227.0400	0.4730
SNOW WATER	0.000	

APPENDIX E

MODFLOW AND MT3DMS MODEL DATA

MODFLOW was developed by the United States Geological Survey (USGS) to solve three-dimensional transient head distributions using finite difference approximations. The user can input soil properties, multiple layers, heterogeneities, variable thicknesses, variable gradients, flow boundaries, wells, and can define confined or unconfined flow systems. Major assumptions of the program include that groundwater is governed by Darcy's law; the formation behaves as a continuous porous medium; flow is not affected by chemical, temperature, or density gradients; and hydraulic properties are constant within a grid cell.

MT3DMS calculates concentration distributions for a single chemical as a function of time and location using a finite difference solution. Concentration is distributed over a three-dimensional, non-uniform, transient flow field. MT3DMS accounts for advection, diffusion, dispersion, sorption, and first order decay. Major assumptions of the module include changes in the concentration field do not affect the flow field; concentrations of solutes do not interact with each other; chemical and hydraulic properties are constant within a cell; sorption is instantaneous and fully reversible; and decay is not reversible.

The current configuration was calibrated to groundwater elevation data collected between 2009 and 2015 in the MODFLOW program and the boron and arsenic concentration data was used to calibrate the MT3DMS module. The prediction scenario includes the clean closure and capping of the two ash ponds.

Model Setup

A two layer grid with twelve objects was established with 100-foot grid spacing parallel and perpendicular to the primary flow direction. The grid size was decreased to a 50-foot grid in the vicinity of the ash ponds. Areas adjacent to the flow and transport boundaries, soil properties, and river stage fluctuations were the same for the calibration and prediction scenarios. The upgradient (east) edge of the model was a general head boundary to allow for flow reversals due to the Illinois River fluctuations. The bottom of the aquifer (estimated), north boundary, and south boundary was modeled as no-flow boundaries. The downgradient boundary was a river object to model the Illinois River. The top boundary (land surface) was a specified flux boundary condition to model rainfall infiltration and seepage through the ash ponds.

Simplifying assumptions were made for this model.

- indicator chemicals instantaneously dissolve into water;
- leachate instantaneously migrates to the groundwater;
- leachate concentrations remain constant over time and the source is not depleted;
- the Illinois River has a consistent annual pattern; and
- the cap has an instantaneous effect on the percolation rate.

MODFLOW and MT3DMS Input Values

Layers

The top layer included the two ash pond objects and the topographic surface. This layer was between 2 and 42 feet thick depending on the location of the layer. The bottom layer represented the unconfined sand aquifer and was 50 feet thick.

Soil Parameters

Soil parameters were estimated using published values for the units as observed during drilling activities, from laboratory testing results, or defaults provided within the MODFLOW and MT3DMS program. Soil parameters were refined during model calibration using observed data.

Recharge

Water recharge rates were modeled using results from the HELP model for the proposed closure configuration. Rainfall and infiltration rates were applied across the site using average annual rainfall data from the City of Meredosia.

River Parameters

The Illinois River was represented by a head-dependent flux that required inputs for river stage, width, bed thickness, and bed hydraulic conductivity. River stage data was obtained from the river gauge located adjacent to the site (National Weather Service <http://water.weather.gov/>) from years 2009 to 2015. River stages were split into high stage (March to July) and low stage (August to February) for each year.

Source Concentration

The source concentration of boron and arsenic in the Fly Ash and Bottom Ash Ponds was based on calibration results at the end of 25 years. The Fly Ash Pond boron concentration was modeled as a constant source of 25 mg/L. The Bottom Ash Pond boron concentration was modeled as a constant source of 3 mg/L. Boron and other contaminants dissolve more slowly into water from bottom ash instead of fly ash due to the higher temperatures that form bottom ash stabilizing the chemicals as solids (Cox 1978; Leaching of Boron from Coal Ash). Both the Fly Ash Pond and the Bottom Ash Pond arsenic concentrations were modeled as a constant source of 0.3 mg/L (Want, T. et al. 2005; The Leaching Behavior of Arsenic from Fly Ash). An arsenic concentration leached from bottom ash was not found, therefore, the arsenic concentration in fly ash was used for bottom ash as a conservative value. Retardation and decay were not used to be conservative.

Model Results

Boron and arsenic concentrations for the current configuration were modeled for 25 years to represent a scenario where the ash ponds were not closed. After 25 years, monitoring well APW-3 (the well with historically highest concentrations) stabilized at 16.9 mg/L of boron and 0.208 mg/L of arsenic, which exceed the respective Class I Groundwater standards. As shown in the tables below, APW-2, APW-6, APW-7, and APW-8 also exceeded the Class I Groundwater standards for boron and arsenic at 25 years with no action.

**Boron Concentration in Groundwater
for the No Action Scenario at 25 Years**

Well	Boron (mg/l)
APW-1	0.010
APW-2	10.2
APW-3	16.9
APW-4	0.330
APW-5	0.002
APW-6	7.60
APW-7	8.89
APW-8	12.9
APW-9	0.261

Yellow highlighting indicates a prediction exceeding the Class I Groundwater standard of 2 mg/l.

**Arsenic Concentration in Groundwater
for the No Action Scenario at 25 Years**

Well	Arsenic (mg/l)
APW-1	0.0000689
APW-2	0.181
APW-3	0.208
APW-4	0.00144
APW-5	0.0000943
APW-6	0.0586
APW-7	0.0272
APW-8	0.169
APW-9	0.00413

Yellow highlighting indicates a prediction exceeding the Class I Groundwater standard of 0.010 mg/l.

Within three years after dewatering and complete closure of the two ash ponds on site, modeling results indicate that boron will be below the Class I Groundwater standards at each well on the site. Boron concentrations at each of the monitoring wells after three years are shown in the table below.

**Boron Concentration in Groundwater
for the Ash Pond Closure Scenario at
at 3 years after Closure and Dewatering**

Well	Boron (mg/l)
APW-1	0.056
APW-2	0.124
APW-3	0.955
APW-4	0.011
APW-5	0.033
APW-6	0.067
APW-7	0.030
APW-8	1.17
APW-9	0.014

Within six years after dewatering and complete closure of the two ash ponds on site, modeling results indicate that arsenic will be below the Class I Groundwater standards at each well on the site. Arsenic and boron concentrations at each of the monitoring wells after six years are shown in the tables below.

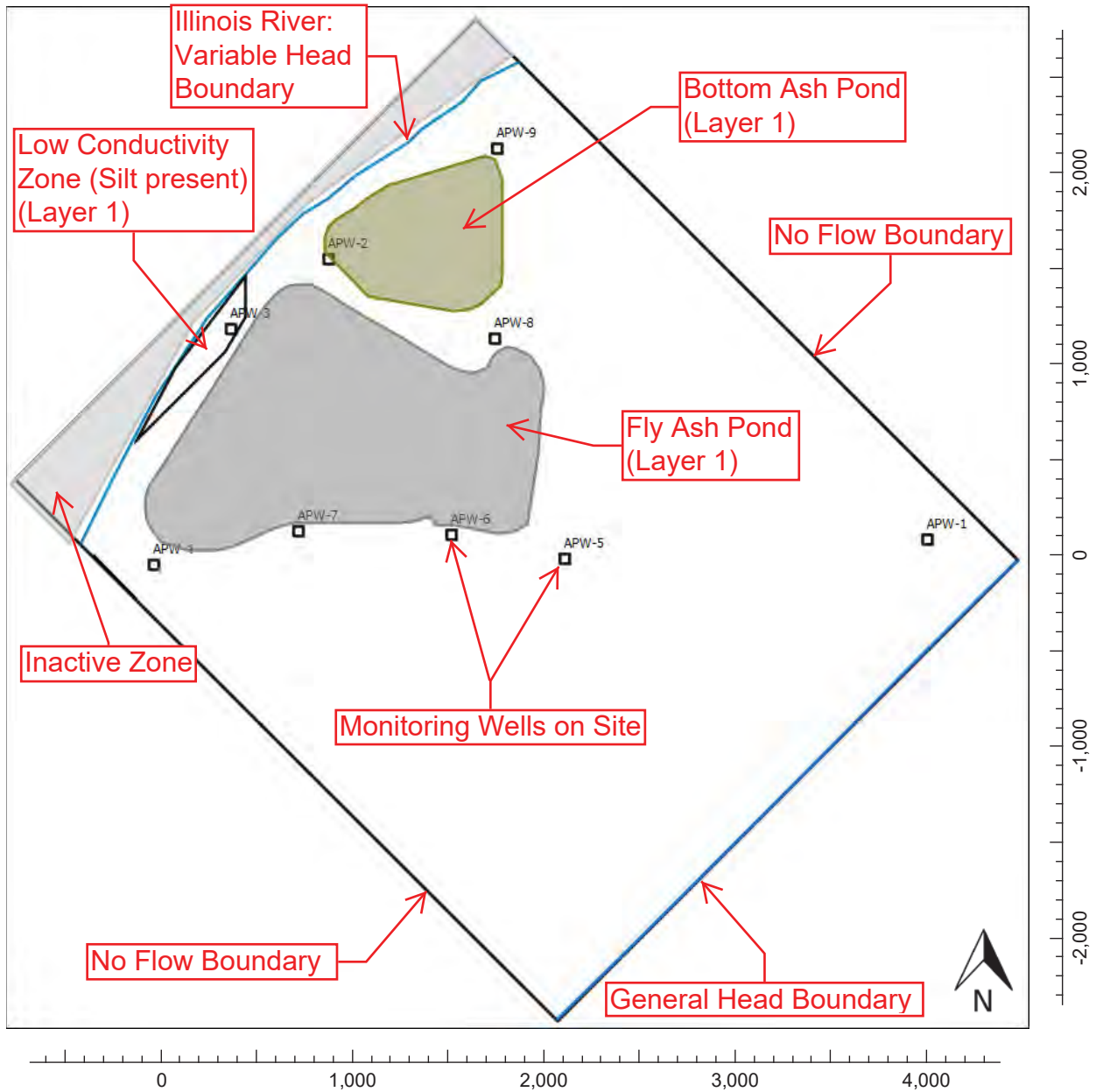
**Arsenic Concentration in Groundwater
for the Ash Pond Closure Scenario at
at 6 years after Closure and Dewatering**

Well	Arsenic (mg/l)
APW-1	0.000165
APW-2	0.0000830
APW-3	0.00924
APW-4	0.0000664
APW-5	0.0000929
APW-6	0.000154
APW-7	0.000262
APW-8	0.0000971
APW-9	0.0000572

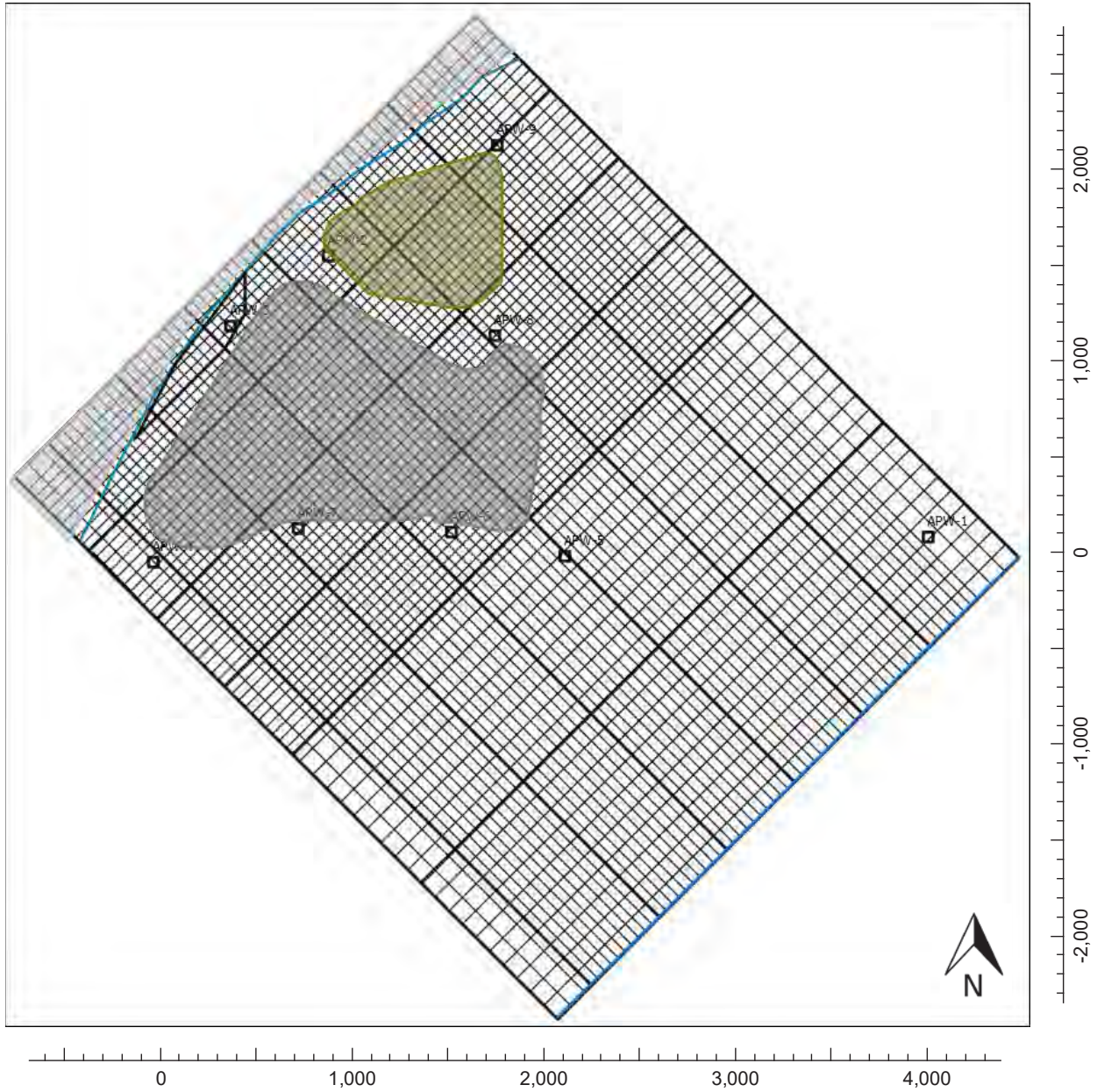
**Boron Concentration in Groundwater
for the Ash Pond Closure Scenario at
at 6 years after Closure and Dewatering**

Well	Boron (mg/l)
APW-1	0.024
APW-2	0.182
APW-3	0.091
APW-4	0.014
APW-5	0.029
APW-6	0.063
APW-7	0.014
APW-8	0.88
APW-9	0.038

MODEL OBJECTS - NO ACTION SCENARIO
MEREDOSIA POWER STATION
MEREDOSIA, ILLINOIS

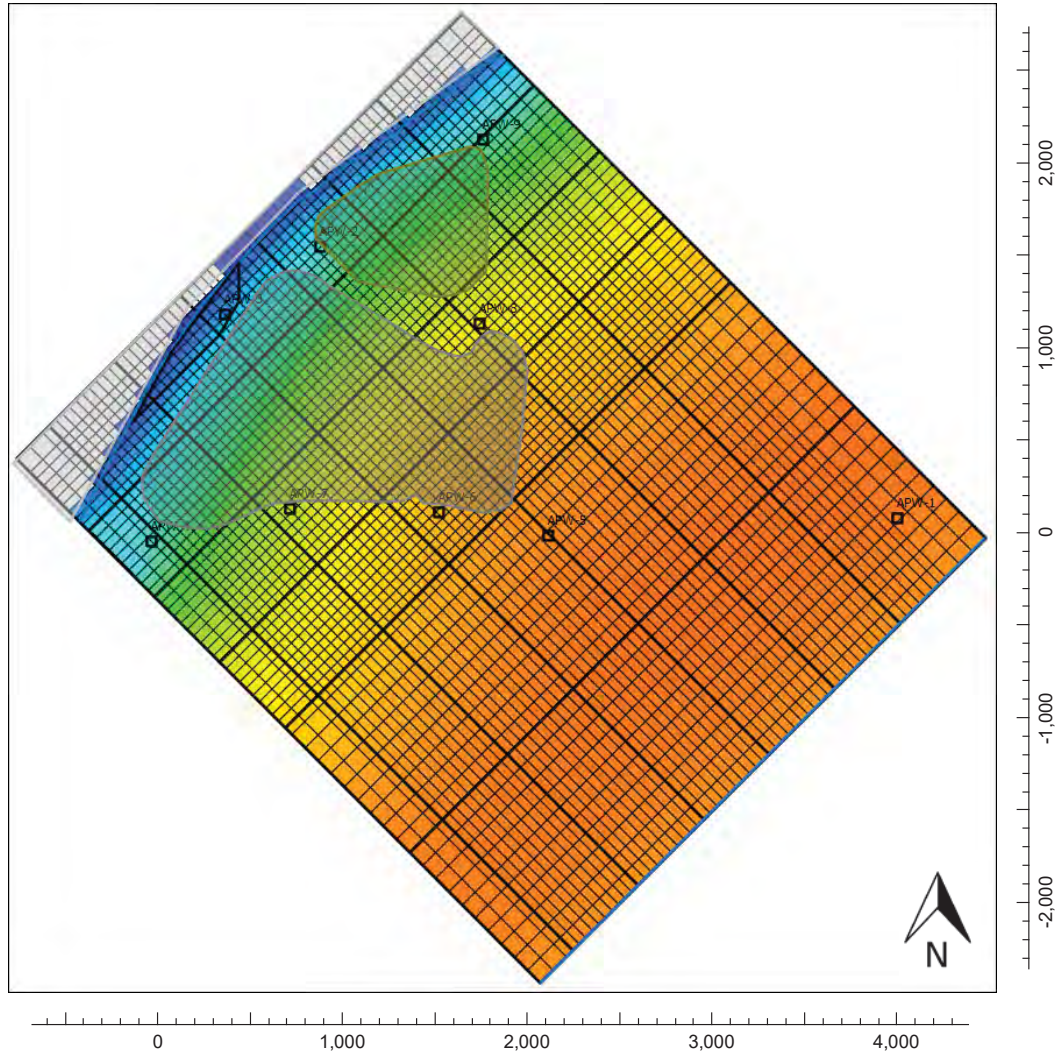
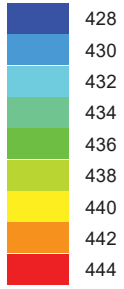


GRID LAYOUT - NO ACTION SCENARIO
MEREDOSIA POWER STATION
MEREDOSIA, ILLINOIS



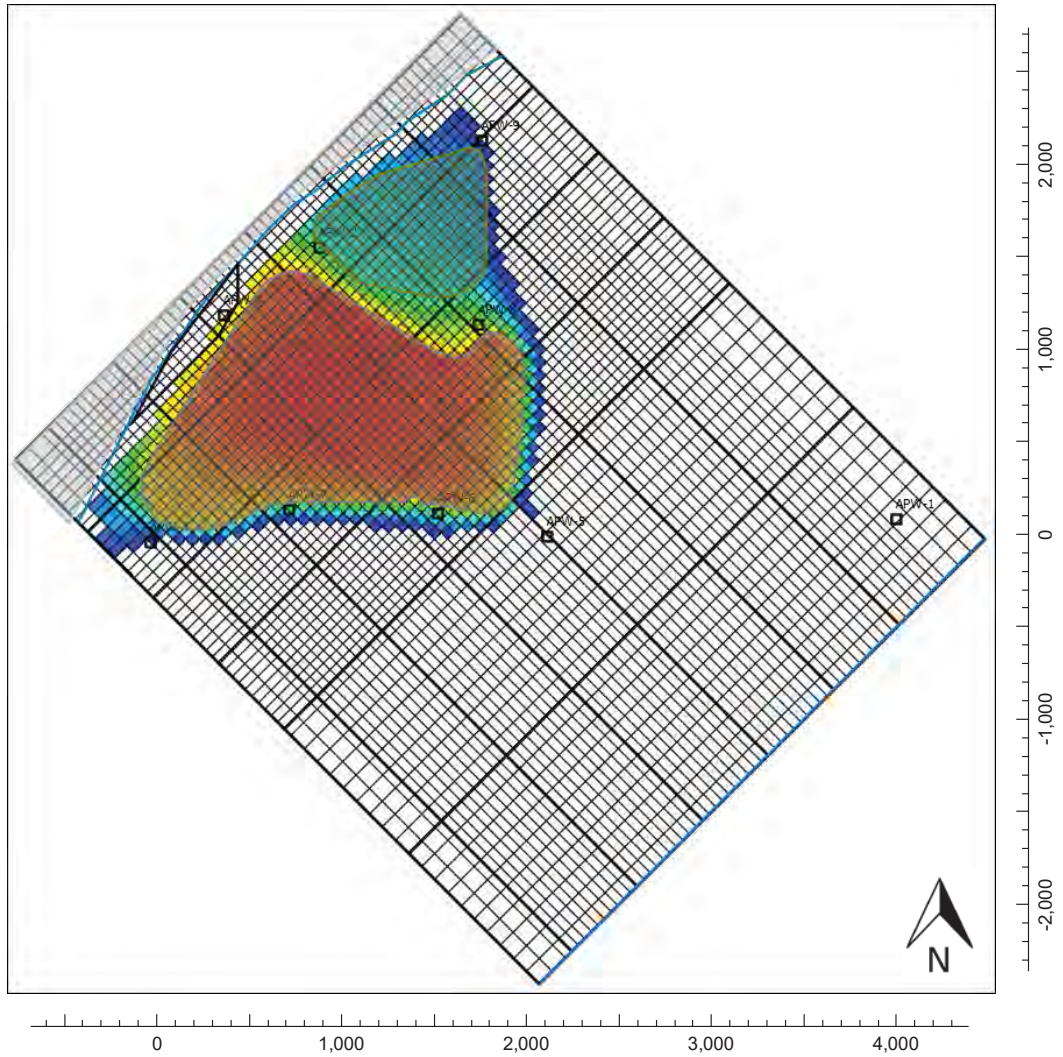
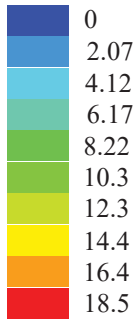
POTENTIOMETRIC HEAD AT 25 YEARS - NO ACTION SCENARIO
MEREDOSIA POWER STATION
MEREDOSIA, ILLINOIS

Color legend (feet above msl)



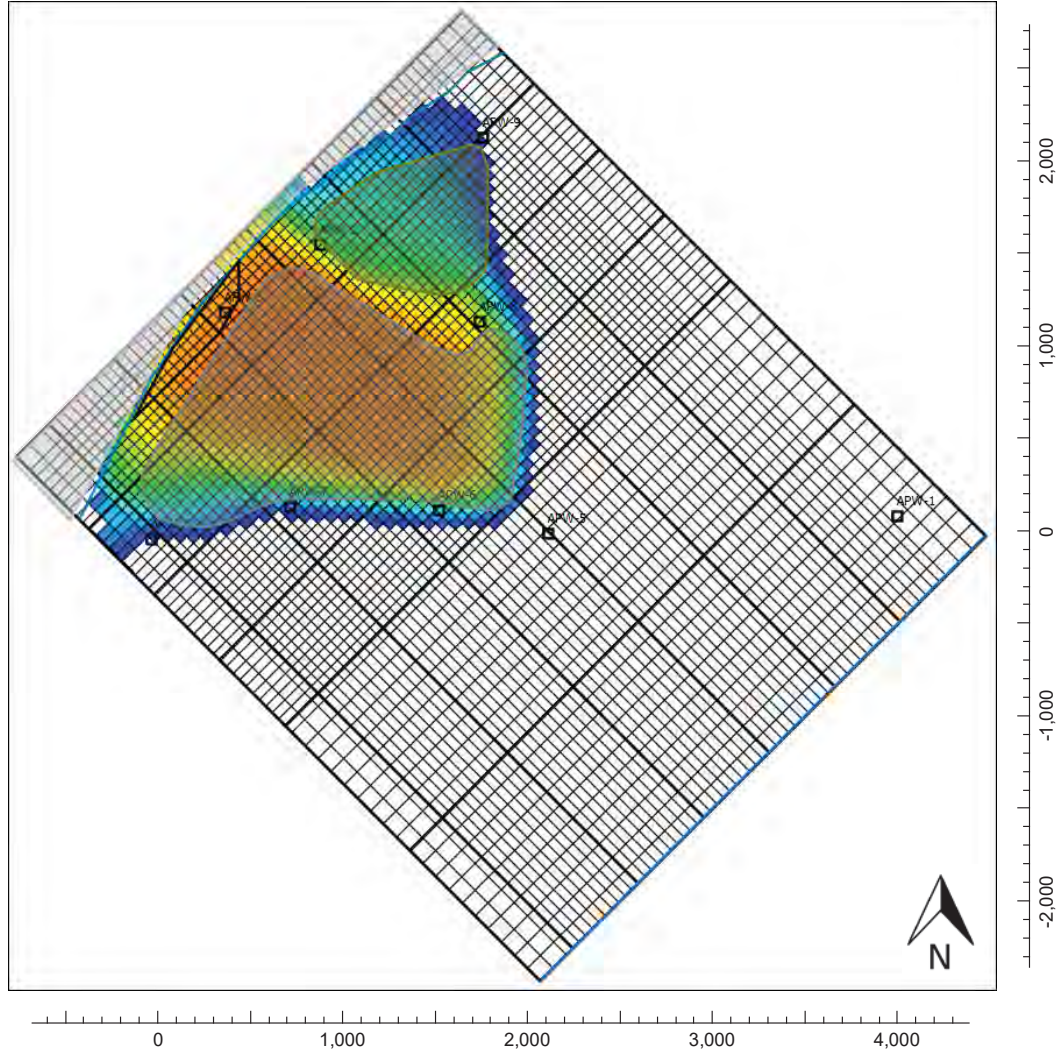
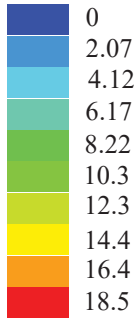
BORON CONCENTRATION IN GROUNDWATER AT 25 YEARS
NO ACTION SCENARIO - LAYER 1
MEREDOSIA POWER STATION
MEREDOSIA, ILLINOIS

Color legend (mg/l)



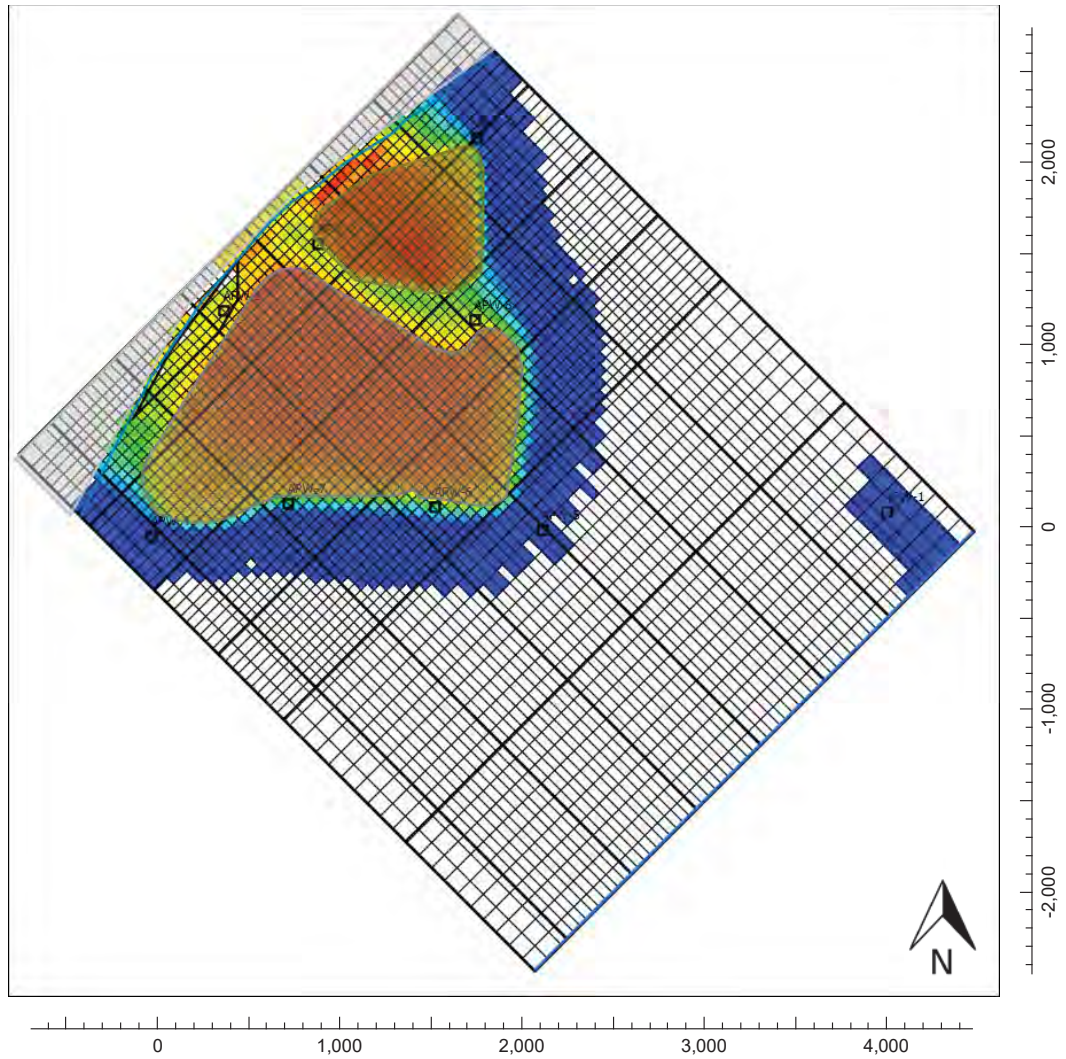
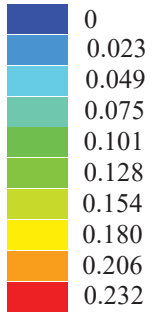
**BORON CONCENTRATION IN GROUNDWATER AT 25 YEARS
NO ACTION SCENARIO - LAYER 2
MEREDOSIA POWER STATION
MEREDOSIA, ILLINOIS**

Color legend (mg/l)



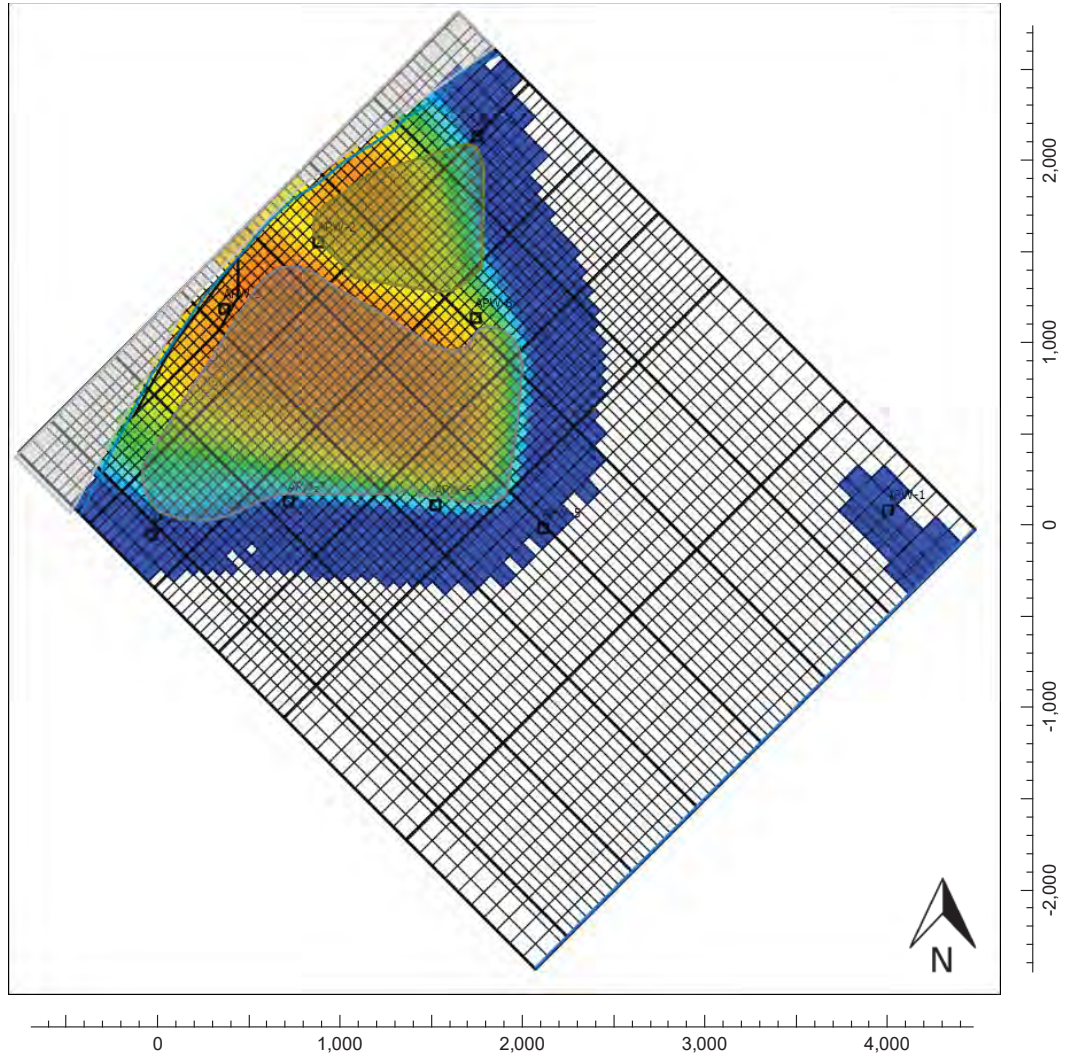
ARSENIC CONCENTRATION IN GROUNDWATER AT 25 YEARS
NO ACTION SCENARIO - LAYER 1
MEREDOSIA POWER STATION
MEREDOSIA, ILLINOIS

Color legend (mg/l)

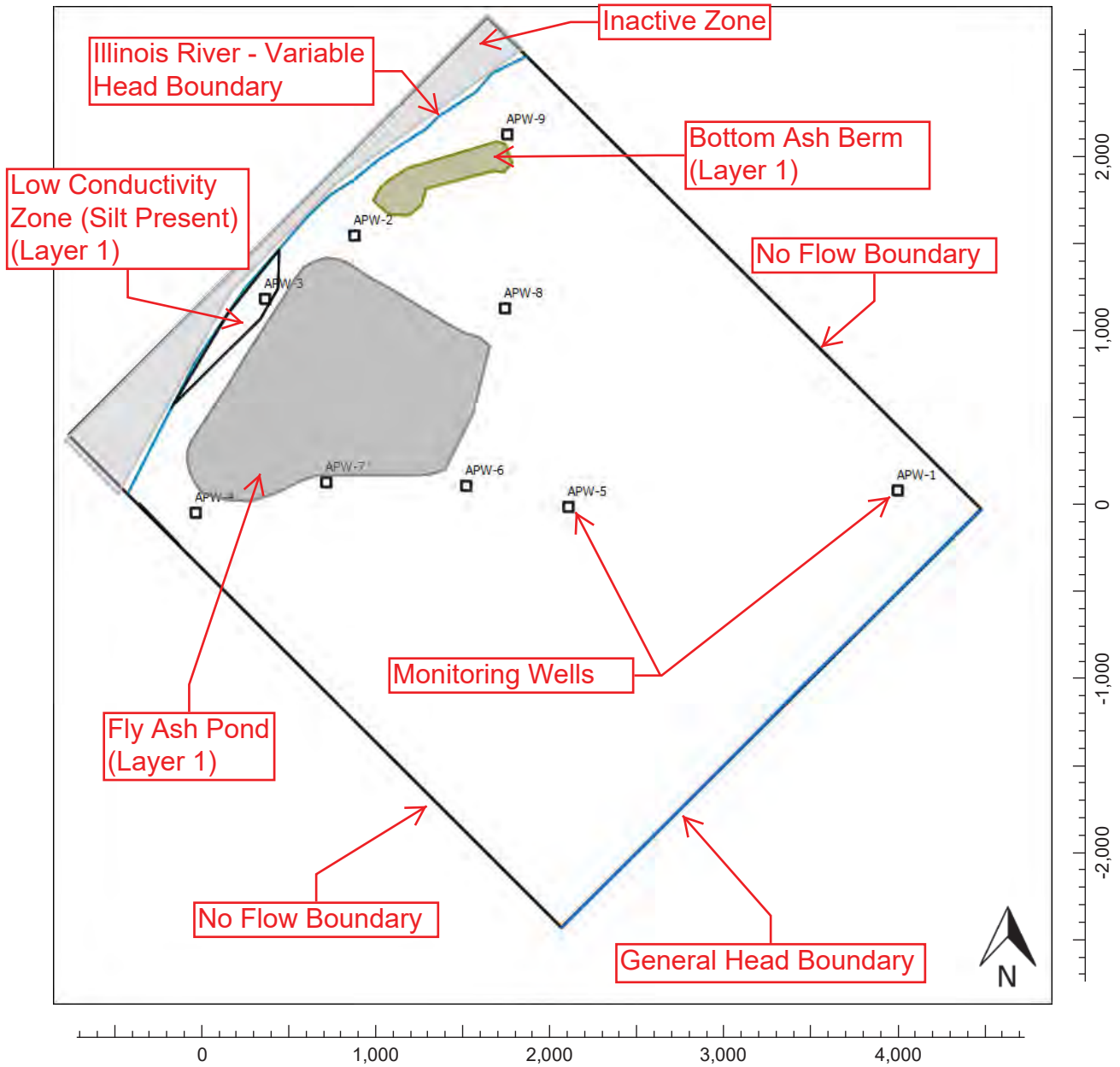


ARSENIC CONCENTRATION IN GROUNDWATER AT 25 YEARS
NO ACTION SCENARIO - LAYER 2
MEREDOSIA POWER STATION
MEREDOSIA, ILLINOIS

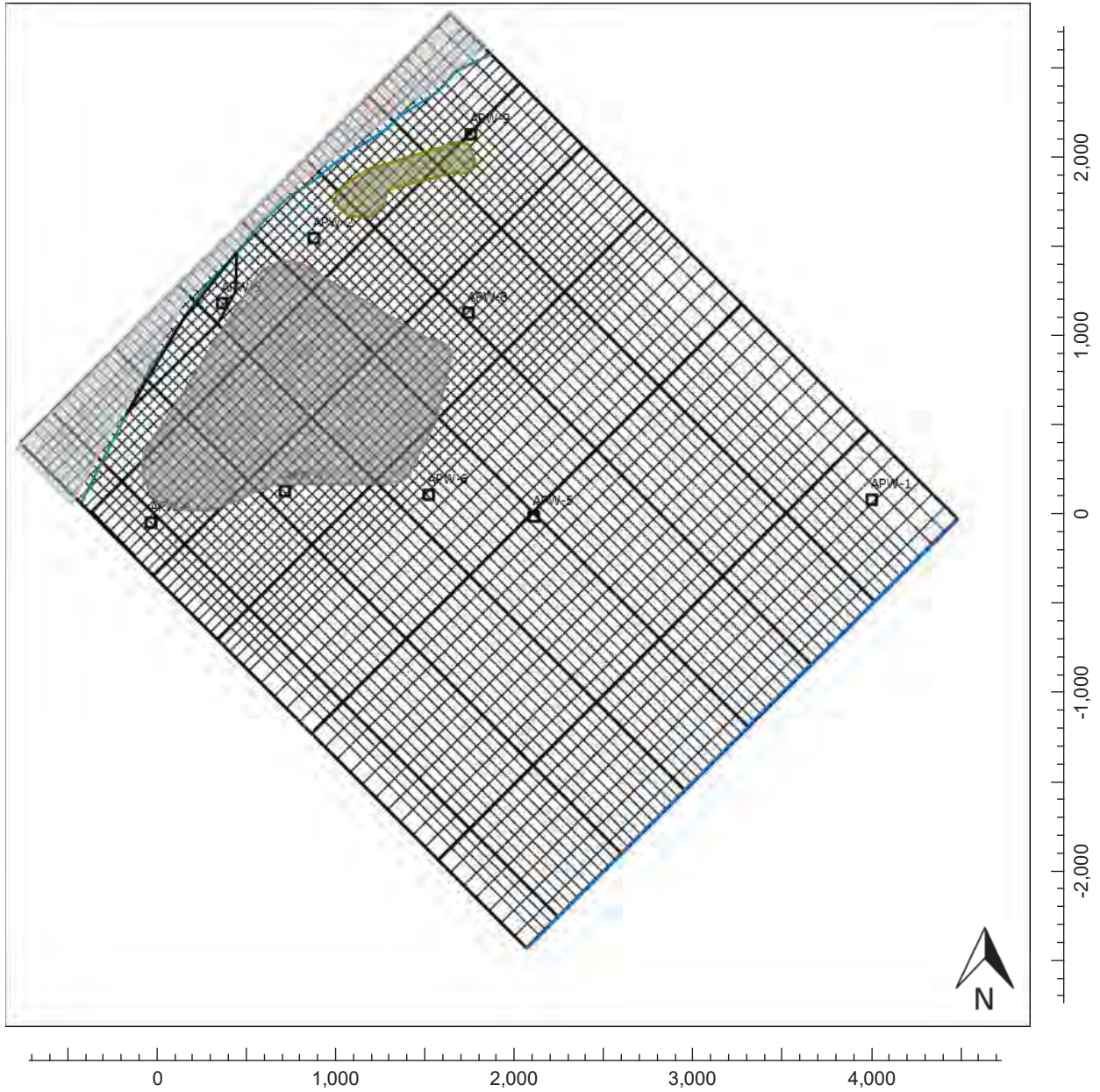
Color legend (mg/l)



MODEL OBJECTS - ASH POND CLOSURE SCENARIO
MEREDOSIA POWER STATION
MEREDOSIA, ILLINOIS

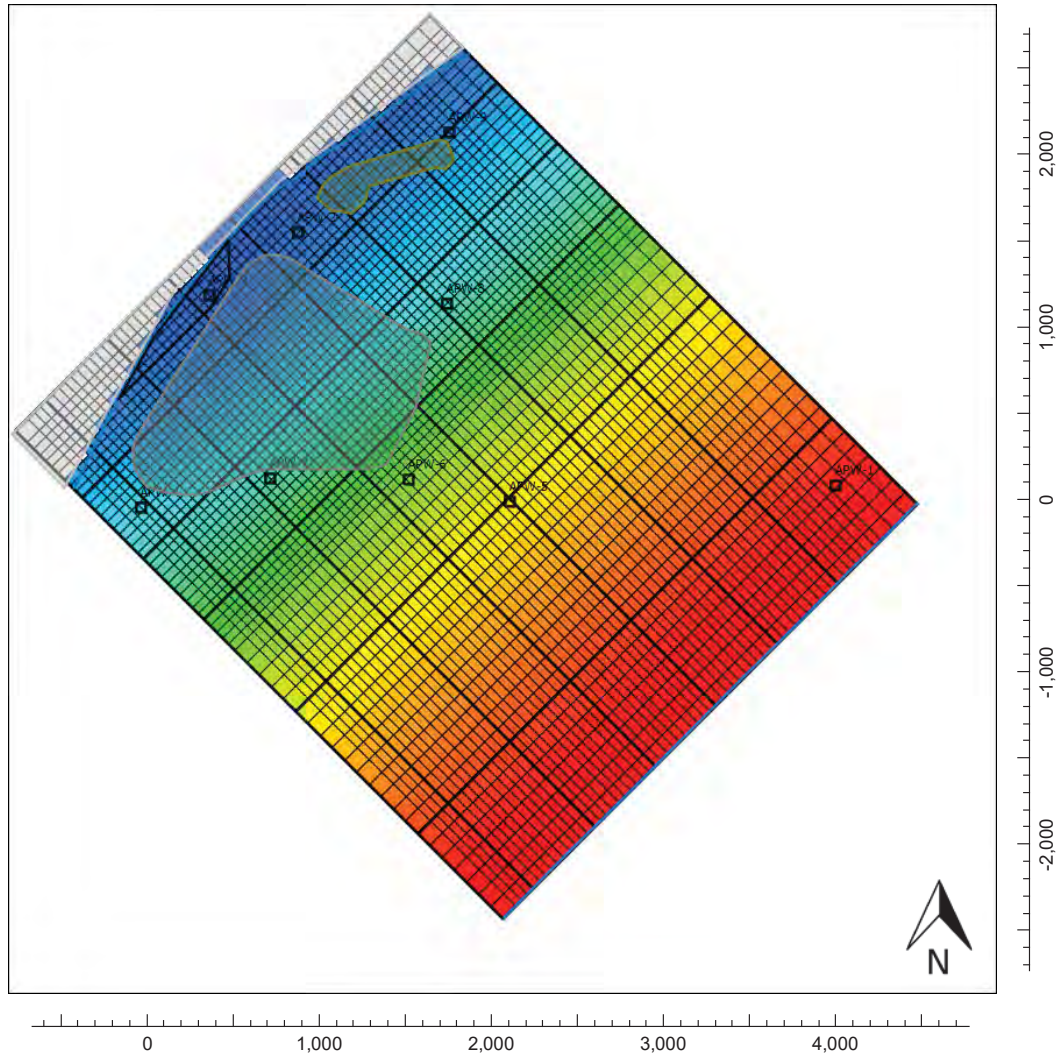
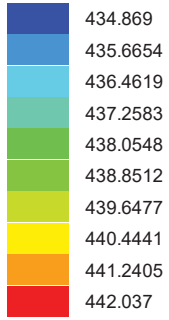


GRID LAYOUT - ASH POND CLOSURE SCENARIO
MEREDOSIA POWER STATION
MEREDOSIA, ILLINOIS



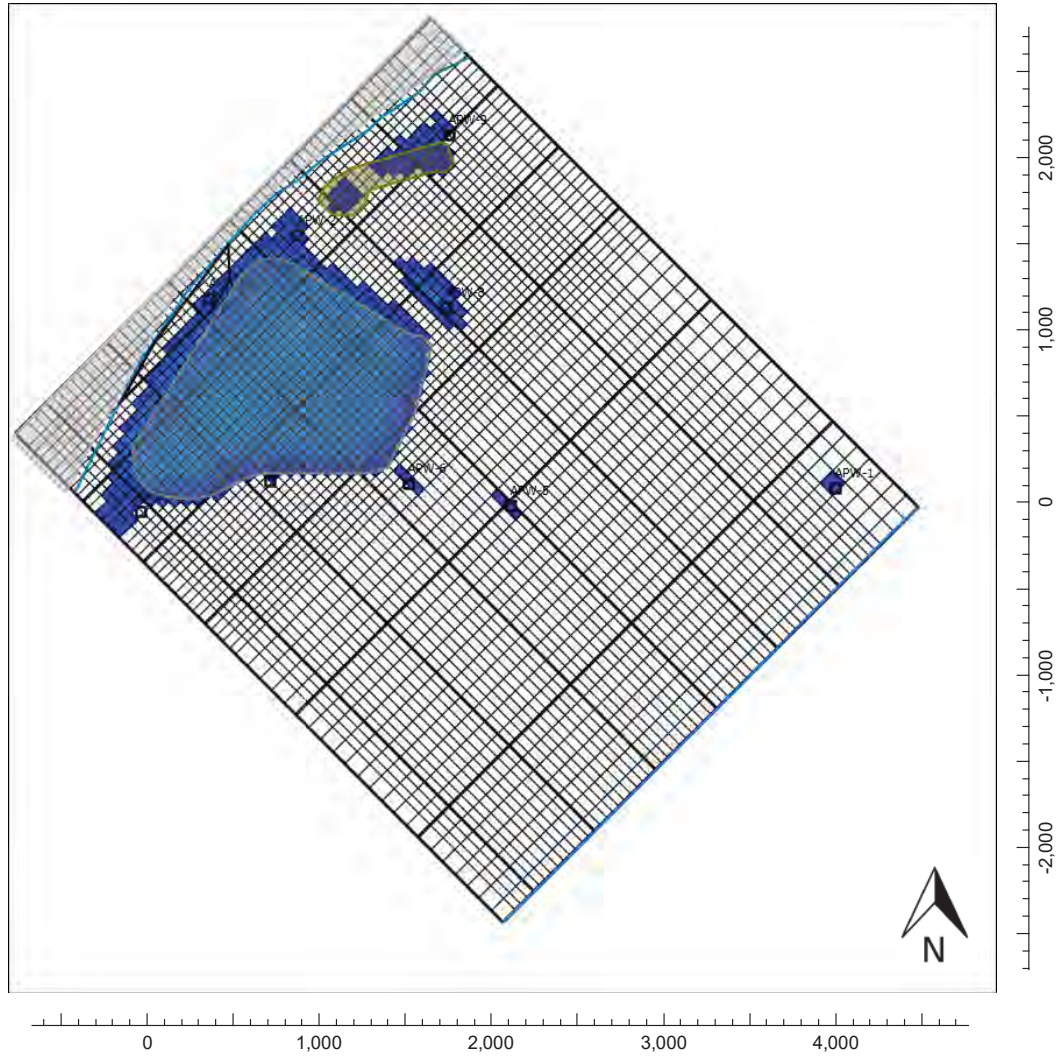
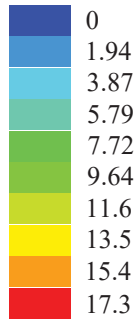
POTENTIOMETRIC HEAD - ASH POND CLOSURE SCENARIO
3 YEARS AFTER CLOSURE AND DEWATERING
MEREDOSIA POWER STATION
MEREDOSIA, ILLINOIS

Color legend (feet above msl)



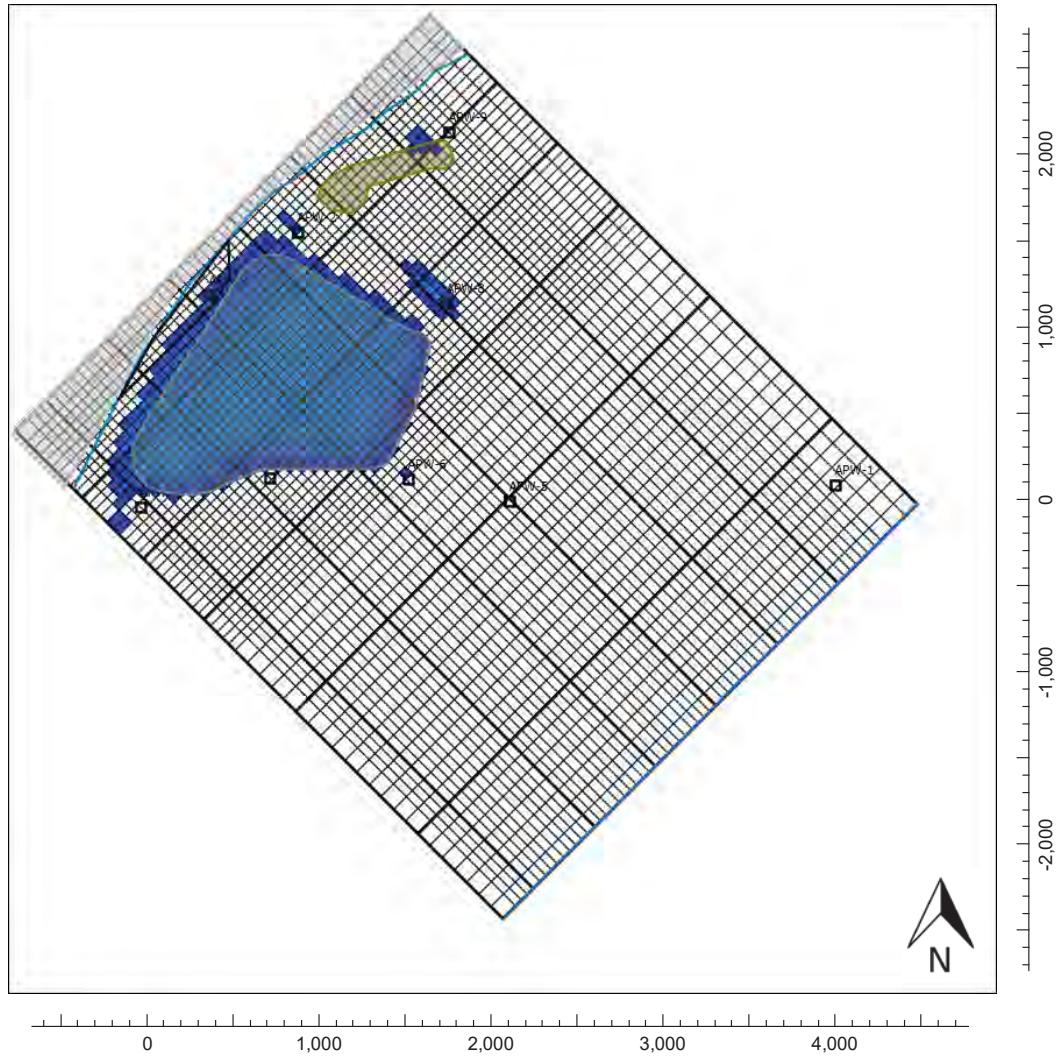
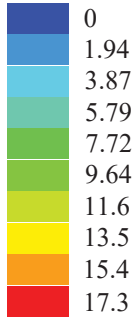
**BORON CONCENTRATION IN GROUNDWATER - ASH POND CLOSURE SCENARIO
3 YEARS AFTER CLOSURE AND DEWATERING - LAYER 1
MEREDOSIA POWER STATION
MEREDOSIA, ILLINOIS**

Color legend (mg/l)



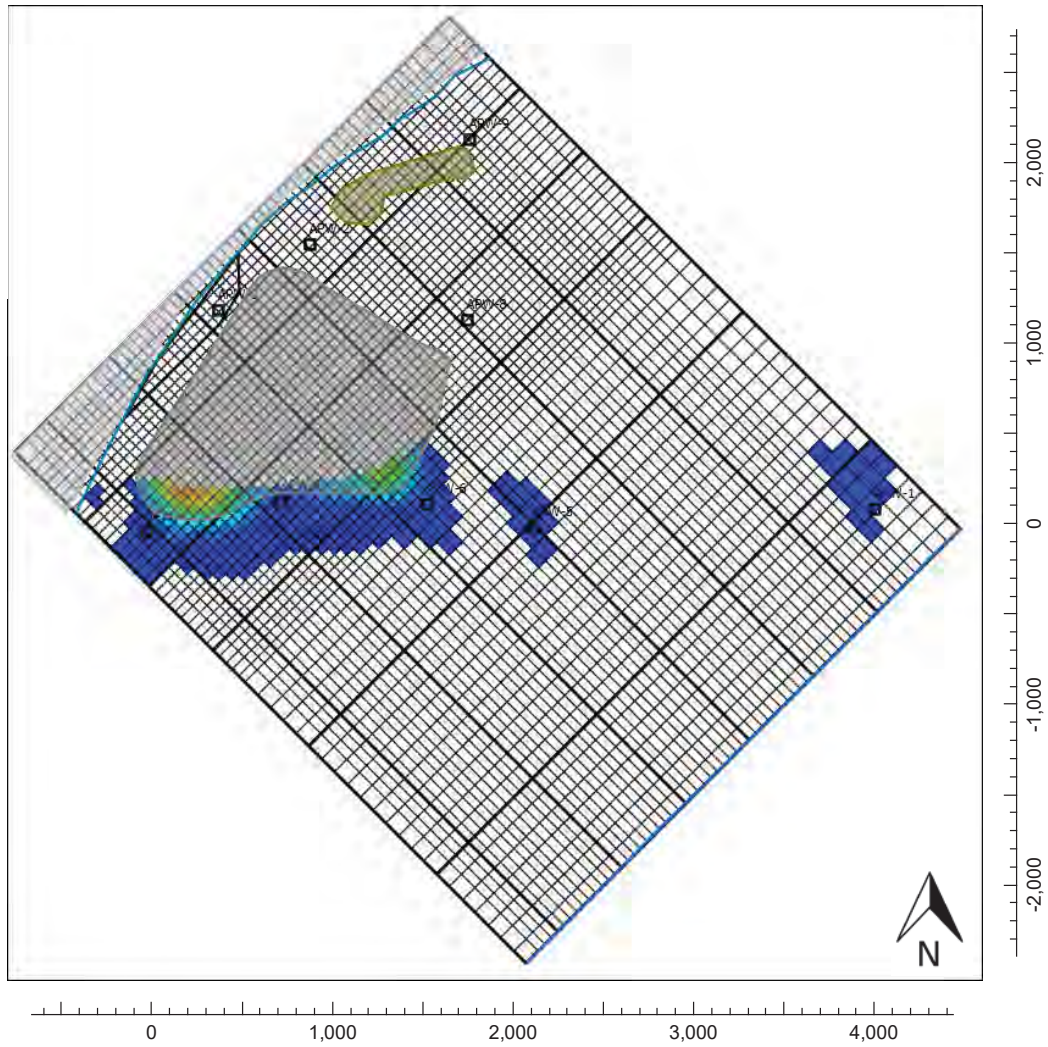
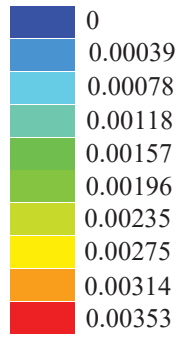
**BORON CONCENTRATION IN GROUNDWATER - ASH POND CLOSURE SCENARIO
3 YEARS AFTER CLOSURE AND DEWATERING - LAYER 2
MEREDOSIA POWER STATION
MEREDOSIA, ILLINOIS**

Color legend (mg/l)



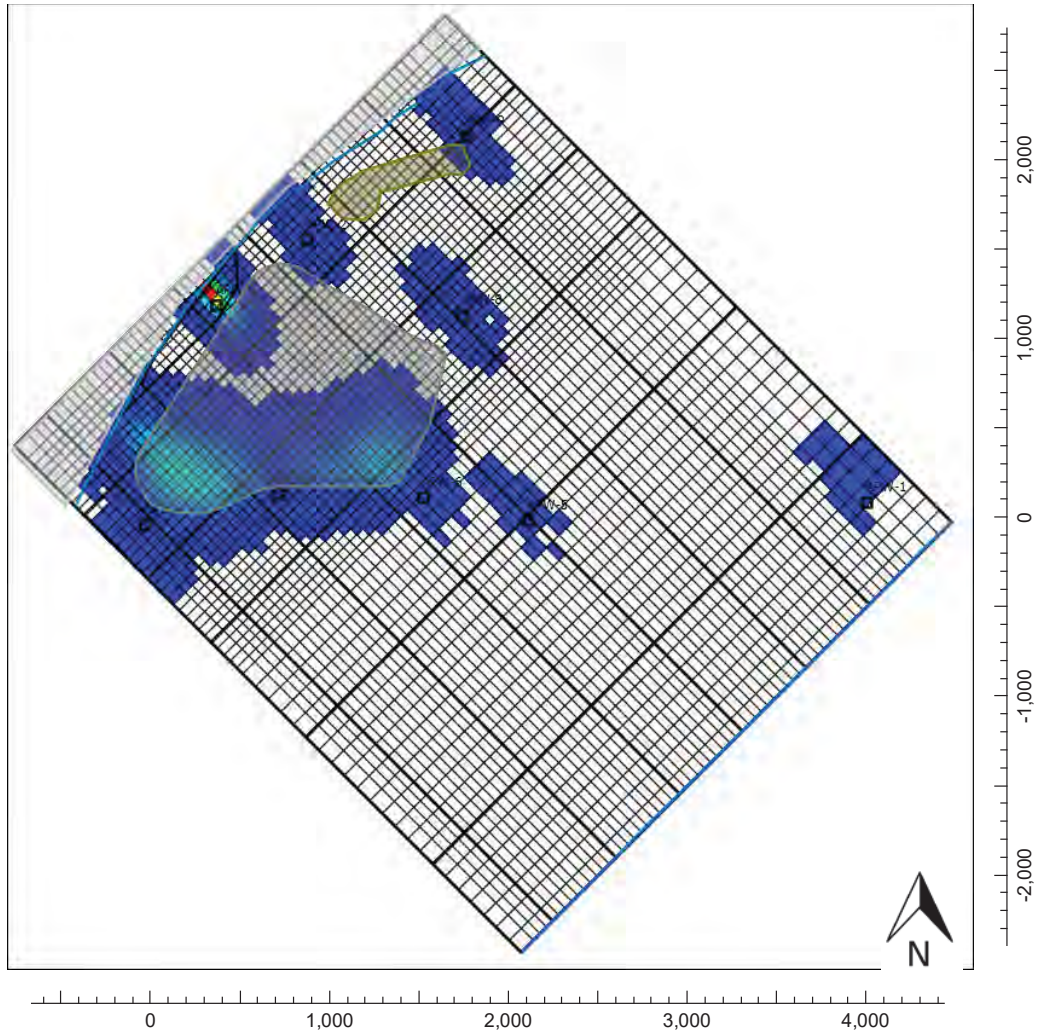
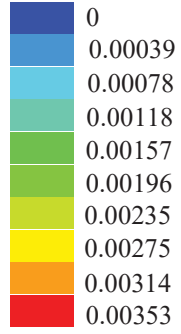
ARSENIC CONCENTRATION IN GROUNDWATER - ASH POND CLOSURE SCENARIO
6 YEARS AFTER CLOSURE AND DEWATERING - LAYER 1
MEREDOSIA POWER STATION
MEREDOSIA, ILLINOIS

Color legend (mg/l)



ARSENIC CONCENTRATION IN GROUNDWATER - ASH POND CLOSURE SCENARIO
6 YEARS AFTER CLOSURE AND DEWATERING - LAYER 2
MEREDOSIA POWER STATION
MEREDOSIA, ILLINOIS

Color legend (mg/l)



APPENDIX F

ILLINOIS RIVER LOADING DATA

**Meredosia Power Plant
Boron Loading in the Illinois River**

J024917.01

Boron Concentrations

Cmax=highest single concentration (mg/L)
Cavg=mean concentration of APWs-2, 3, 4, and 9 (closest to river) (mg/L)

Values from sampling events December 2010 through February 2016	Values from Modflow/MT3DMS Modelling
Boron Cmax 46 mg/L	Boron C _{3yr,max} 1.17 mg/L
Boron Cavg 11.87 mg/L	Boron C _{3yr,avg} 0.276 mg/L

Groundwater Flow

Q=K*A
Q=groundwater discharge volume into river (gpd)
K=hydraulic conductivity, from value in NRT report (gpd/ft²)
Imax=maximum observed hydraulic gradient (ft/ft)
lavg=mean hydraulic gradient (ft/ft)
A=cross section of aquifer, 52 feet thick x 2000 feet long (ft²)

K	1200 gpd/ft ²
Imax	0.00625 ft/ft
lavg	0.00377 ft/ft
A	104,000 ft ²
Qmax	780,000 gpd
Qavg	470,496 gpd

Boron Mass Loading Rate

L=Q*C
L = Boron Loading (gpd*mg/L)

Lmax	35,880,000 gpd*mg/L	Lmax,3yr	912,600 gpd*mg/L
Lavg	5,584,788 gpd*mg/L	Lavg,3yr	129,857 gpd*mg/L

Illinois River Flow

Q_{7,10}=7-day, 10 year low flow, from IL Water Survey 1988 (most recent calculated value)
converted from cfs to gpd with factor of 1cfs = 646190.4 gpd
Qavg=average annual flow from 1936 to 1988, from USGS NWIS
converted from cfs to gpd with factor of 1cfs = 646190.4 gpd

(1) Q _{7,10}	2,390,904,625 gpd
(2) Qavg	13,818,782,542 gpd

Flow through Mixing Zone = 50 feet from shore, river is 750 feet wide = Q_{river}*50 ft/750 ft

(1)Q _{7,10} _{mix}	159,393,642 gpd
(2)Qavg _{mix}	921,252,169 gpd

Boron Concentration Loading

Existing	Boron Loading max (1)	0.225 mg/L
	Boron Loading max (2)	0.0389 mg/L
	Boron Loading avg (1)	0.0350 mg/L
	Boron Loading avg (2)	0.00606 mg/L

**Public and Food Processing Water Supply Standard
1.0 mg/L**

Boron loading is less than the Public and Food Processing Water Supply Standard for the calculated scenarios.

3 Years Post Closure	Boron Loading max (1)	0.00573 mg/L
	Boron Loading max (2)	0.000991 mg/L
	Boron Loading avg (1)	0.000815 mg/L
	Boron Loading avg (2)	0.000141 mg/L

**Meredosia Power Plant
Arsenic Loading in the Illinois River**

J024917.01

Arsenic Concentrations

C_{max}=highest single concentration (mg/L)
C_{avg}=mean concentration of APWs-2, 3, 4, and 9 (closest to river) (mg/L)

Values from sampling events December 2010 through February 2016		Values from Modflow/MT3DMS Modelling	
Arsenic C _{max}	0.31 mg/L	Arsenic C _{6yr,max}	0.0092 mg/L
Arsenic C _{avg}	0.08 mg/L	Arsenic C _{6yr,avg}	0.002 mg/L

Groundwater Flow

Q=K*A
Q=groundwater discharge volume into river (gpd)
K=hydraulic conductivity, from value in NRT report (gpd/ft²)
I_{max}=maximum observed hydraulic gradient (ft/ft)
I_{avg}=mean hydraulic gradient (ft/ft)
A=cross section of aquifer, 52 feet thick x 2000 feet long (ft²)

K	1200 gpd/ft ²
I _{max}	0.00625 ft/ft
I _{avg}	0.00377 ft/ft
A	104,000 ft ²
Q _{max}	780,000 gpd
Q _{avg}	470,496 gpd

Arsenic Mass Loading Rate

L=Q*C
L = Arsenic Loading (gpd*mg/L)

L _{max}	241,800 gpd*mg/L	L _{max,3yr}	7,176 gpd*mg/L
L _{avg}	37,640 gpd*mg/L	L _{avg,3yr}	941 gpd*mg/L

Illinois River Flow

Q_{7,10}=7-day, 10 year low flow, from IL Water Survey 1988 (most recent calculated value)
converted from cfs to gpd with factor of 1cfs = 646190.4 gpd
Q_{avg}=average annual flow from 1936 to 1988, from USGS NWIS
converted from cfs to gpd with factor of 1cfs = 646190.4 gpd

(1) Q _{7,10}	2,390,904,625 gpd
(2) Q _{avg}	13,818,782,542 gpd

Flow through Mixing Zone = 50 feet from shore, river is 750 feet wide = Q_{river}*50 ft/750 ft

(1)Q _{7,10} _{mix}	159,393,642 gpd
(2)Q _{avg} _{mix}	921,252,169 gpd

Arsenic Concentration Loading

Existing	Arsenic Loading max (1)	0.00152 mg/L
	Arsenic Loading max (2)	0.000262 mg/L
	Arsenic Loading avg (1)	0.000236 mg/L
	Arsenic Loading avg (2)	0.0000409 mg/L

**Public and Food Processing Water Supply Standard
0.05 mg/L**

Arsenic loading is less than the Public and Food Processing Water Supply Standard for the calculated scenarios.

6 Years Post Closure	Arsenic Loading max,6yr (1)	0.0000450 mg/L
	Arsenic Loading max,6yr (2)	0.00000779 mg/L
	Arsenic Loading avg,6yr (1)	0.00000590 mg/L
	Arsenic Loading avg,6yr (2)	0.00000102 mg/L

**The following are attachments to the testimony of Scott M. Payne,
PhD, PG and Ian Magruder, M.S..**

ATTACHMENT 14



J024917.01

FLY ASH POND AND BOTTOM ASH POND
MEREDOSIA POWER STATION
800 SOUTH WASHINGTON STREET
MEREDOSIA, ILLINOIS

TABLE OF CONTENTS

Closure Plan

	<u>Attachment</u>
Hydrogeologic Assessment Report	A
Groundwater Monitoring Plan.....	B
Groundwater Management Zone Application	C
Post-Closure Care Plan	D
Construction Quality Assurance Plan.....	E
Construction Specification.....	F
Construction Plans.....	G

**CLOSURE PLAN
FLY ASH POND AND BOTTOM ASH POND
MEREDOSIA POWER STATION
800 SOUTH WASHINGTON STREET
MEREDOSIA, ILLINOIS**

Prepared for:

AMERENENERGY MEDINA VALLEY COGEN, LLC
St. Louis, Missouri

Prepared by:

GEOTECHNOLOGY, INC.
St. Louis, Missouri

Project No. J024917.01

December 9, 2016





CLOSURE PLAN
FLY ASH POND AND BOTTOM ASH POND
MEREDOSIA POWER STATION
800 SOUTH WASHINGTON STREET
MEREDOSIA, ILLINOIS

TABLE OF CONTENTS

	<u>Page</u>
1. INTRODUCTION	1
2. SITE LAYOUT	1
3. SITE HISTORY	1
4. SLOPE STABILITY ANALYSIS	2
5. CLOSURE ACTIVITIES	3
5.1 Grading	4
5.2 ClosureTurf®/HydroTurf® Installation	4
5.3 Surface Water Management.....	4
5.4 Construction Quality Assurance (CQA) Program	4
6. HYDROGEOLOGIC SITE INVESTIGATION.....	5
7. GROUNDWATER	5
7.1 Groundwater Monitoring Program	5
7.2 Groundwater Monitoring System	5
7.3 Groundwater Trend Analysis.....	5
7.4 Mitigation of Statistically Significant Trends.....	5
8. TIME AND COST ESTIMATES.....	6
8.1 Time to Complete Closure	6
8.2 Time to Reach Hydrostatic Equilibrium of Groundwater.....	6
8.3 Remediation Time Frame	6
8.4 Cost of Closure	6
8.5 Cost of Post-Closure Care.....	6
9. REFERENCES	7
10. LICENSED PROFESSIONAL SIGNATURE/SEAL	8



J024917.01

CLOSURE PLAN
FLY ASH POND AND BOTTOM ASH POND
MEREDOSIA POWER STATION
800 SOUTH WASHINGTON STREET
MEREDOSIA, ILLINOIS

TABLE OF CONTENTS
(continued)

PLATES

	<u>Plate</u>
Site Location and Topography.....	1
Aerial Photograph of Site.....	2

APPENDICES

	<u>Appendix</u>
Stability Analysis.....	A

CLOSURE PLAN
FLY ASH POND AND BOTTOM ASH POND
MEREDOSIA POWER STATION
800 SOUTH WASHINGTON STREET
MEREDOSIA, ILLINOIS

1.0 INTRODUCTION

This Closure Plan for the AmerenEnergy Medina Valley Cogen, LLC Meredosia Power Station (Meredosia Power Station) Fly Ash Pond and Bottom Ash Pond Coal Combustion Waste Surface Impoundments has been prepared in general accordance with the requirements of the site-specific rule in 35 Illinois Administrative Code (IAC) Part 840.101 through 840.152 and the United States Environmental Protection Agency (USEPA) regulation at 40 Code of Federal Regulations (CFR) Parts 257 and 261. Supporting documents to this Closure Plan are listed in the Reference Section of this report.

2.0 SITE LAYOUT

The Meredosia Power Station is located at 800 South Washington Street, Meredosia, Illinois. The Fly Ash and Bottom Ash Ponds are located southwest of the coal pile and plant facilities. The site location and topography are shown on Plate 1. The existing structures, ash ponds, and boring/monitoring wells are shown on Plate 2.

3.0 SITE HISTORY

The Meredosia Power Station is located south of Meredosia in Morgan County, Illinois, which is located in west-central Illinois. The Meredosia Power Station ash ponds are located in the south half of Section 21 and the north half of Section 28, T.16N, R.13W. The plant generated electricity from 1948 until February 2012. The plant is located on the floodplain east of the Illinois River. A third ash pond referred to as the “Old Ash Pond” was reportedly closed, and will not be further discussed in this report. Reportedly, the Bottom Ash and Fly Ash Ponds were constructed of native materials.

The Bottom Ash Pond was constructed in 1972 with a design surface area of 11 acres, a height of 24 feet and a volume of approximately 90 acre-feet. The Bottom Ash Pond had received low-volume wastewater, bottom ash and storm water runoff. The site operates under NPDES Permit IL0000116, Outfall 003, which is for the Bottom Ash Pond. Reportedly, the Bottom Ash Pond did not have standing water within two months of the plant closure.



The Fly Ash Pond was constructed in 1968. The Fly Ash Pond has a surface area of 34 acres, a height of 24 feet and a volume of approximately 500 acre-feet. The Fly Ash Pond reportedly received fly ash, low-volume wastewater and storm water runoff. The site operates under NPDES Permit IL0000116, Outfall 004, which is for the Fly Ash Pond. The Fly Ash Pond was reportedly dry by October 2012.

A feasibility analysis was performed regarding the closure options for the Fly Ash and Bottom Ash Ponds on the site. The options included no action, complete clean closure, soil/geosynthetic composite cap, and partial clean closure with a ClosureTurf® cap alternatives. The no closure option was not selected due to the known groundwater impacts at the site and facility decommissioning activities. Clean closure of both ponds was cost and time prohibitive due to ash disposal and subsequent backfilling and grading of the site. The soil/geosynthetic composite cap option was not selected due to the long term maintenance issues, lack of personnel on site to perform maintenance activities, cost, and the longer time frame needed to close the ponds. Partial clean closure of the bottom ash pond, moving the bottom ash to the fly ash pond, and capping the fly ash pond and bottom ash pond berm with ClosureTurf® was selected as an effective and efficient option.

4.0 SLOPE STABILITY ANALYSIS

Slope stability analysis consists of comparing the driving forces within a cross-section of slope to the resisting forces and calculating the factor of safety. Per the Illinois Department Natural Resources (IDNR)¹, embankments should have a minimum factor of safety of 1.5 for long-term static stability, and 1.0 for the pseudo-static condition (seismic condition). Major flood conditions and rapid drawdown conditions were also analyzed due to the proximity of the site to the Illinois River. Slope stability analysis discussion, section profiles, and calculated critical failure arcs at selected locations are presented in Appendix A. Global stability analysis results, at current groundwater elevations in relation to mean sea level (MSL) and design grades for the Fly Ash and Bottom Ash Ponds, are summarized in the following table.

¹ *Rules for Construction and Maintenance of Dams*, Illinois Department of Natural Resources, Office of Water Resources, Springfield, Illinois.



SUMMARY OF STABILITY ANALYSES			
Section Location	Case	Calculated Factor of Safety	Target Factor of Safety
Fly Ash Pond West Embankment	Static Condition Normal River Stage	2.1	1.5
	Static Condition Major Flood Stage (447'MSL)	2.5	1.5
	Rapid Drawdown Major Flood Stage (447'MSL)	1.7	1.2
	Seismic Condition	1.3	1.0
Bottom Ash Pond West Embankment	Static Condition Normal River Stage	1.8	1.5
	Static Condition Major Flood Stage (447'MSL)	1.6	1.5
	Rapid Drawdown Major Flood Stage (447'MSL)	1.7	1.2
	Seismic Condition	1.3	1.0

The stability models for each section at the Fly Ash Pond and Bottom Ash Pond closures have calculated factors of safety greater than or equal to the recommended IDNR target factor of safety for the static and seismic conditions.

5.0 CLOSURE ACTIVITIES

The remedial action for the facility is the relocation and clean closing of the east ash storage pile, capping of the Fly Ash Pond, and the partial clean closure and capping of the Bottom Ash Pond. The Bottom Ash Pond will be closed by the removal of most coal combustion residuals (CCR) to the Fly Ash Pond. The remaining CCR under the roadway and pipeline will be capped in-place. The ash in the east ash storage pile will be removed and placed in the Fly Ash Pond.

The proposed closure activities associated with the remedial action includes grading, installation of high performance high density polyethylene (HDPE) geomembrane, and establishment of surface water control features for the Fly Ash and Bottom Ash Ponds. Closure activities will be performed in accordance with the Closure Plans and Specifications. Quality control will be performed in accordance with the Construction Quality Assurance (CQA) Plan prepared for this project and will be documented by a professional engineer licensed in Illinois.

Refer to the Plans and Specifications completed for this project (CDG, 2016) for details on the closure system.

5.1 Grading. Ash and other material (i.e. embankment soils, bottom ash, and approved demolition debris) will be moved within and between the Fly Ash and Bottom Ash Ponds to achieve design grades. Embankment materials and bottom ash may be used to bring the subgrade to within one foot of design elevations. At least one foot of fly ash will be placed on top of the bottom ash to provide a working surface for ClosureTurf® installation. Ash will be placed at a maximum slope of 1V:10H (10 percent slope). Slopes are designed to promote surface runoff and reduce ponding. The final subgrade surface will be compacted and drum-rolled to provide a smooth surface prior to placement of the high performance HDPE system.

5.2 ClosureTurf®/HydroTurf® Installation. The ClosureTurf®/HydroTurf® system is a low permeability synthetic liner used to control storm water infiltration and limit exposure of the capped material to humans and vectors (i.e. animals). The design grades facilitate storm water runoff to the surface water management features outside the Fly Ash and Bottom Ash Ponds.

The ClosureTurf®/HydroTurf® is generally installed in the following manner (Refer to the CQA Plan for specific installation guidelines):

- The geomembrane component is installed per the manufacturer's requirements including the use of heat welding for seaming.
- The turf component is installed per the manufacturer's requirements including the use of a sewing machine for seaming.
- Sand or hydrobinder infill is placed and hydrated per the manufacturer's requirements.
- The perimeter of the geomembrane and turf components is secured by an anchor trench.

5.3 Surface Water Management. Surface water management features have been incorporated into the final cover design. Surface water features, such as ditches, will be formed in the subgrade to facilitate runoff. The ClosureTurf®/HydroTurf® will be placed over the berms and into ditches. Additional details are provided in the Plans and Specifications (CDG, 2016).

Surface water features are designed to handle runoff from a 20-year precipitation event without damage to the final cover and water ponding.

5.4 Construction Quality Assurance (CQA) Program. Refer to the CQA Plan (Geotechnology, 2016) for details on the project specific CQA program.

6.0 HYDROGEOLOGIC SITE INVESTIGATION

The Hydrogeologic Site Investigation includes a summary of geologic data, hydrogeologic data, and known impacts to the groundwater for the site. Boron and arsenic are typically the best indicator chemicals for coal combustion waste related impacts at the site. Please refer to the separate Hydrogeologic Site Investigation Report (Geotechnology, 2016) for detailed information.

7.0 GROUNDWATER

7.1 Groundwater Monitoring Program. Requirements for the groundwater monitoring program and associated quality assurance are found in the Groundwater Monitoring Plan (Geotechnology, 2016). Quarterly groundwater sampling of the groundwater monitoring system will occur for the first five years after the CQA acceptance report is submitted, and sampling frequencies may be reduced after that time frame. Monitoring data and trend analysis data will be maintained at the offices of Medina Valley Cogen, LLC until a post-closure completion report is accepted by the IEPA.

7.2 Groundwater Monitoring System. Nine monitoring wells (Groundwater Monitoring Program, Plate 2) have been installed in the vicinity of the Fly Ash and Bottom Ash Ponds. These monitoring wells are used for the groundwater monitoring system. Additional monitoring wells are not planned at this time. The monitoring well network will be evaluated two years after completion of the ash pond closures for effectiveness. One monitoring well (APW-1) will be sampled for background values, and eight monitoring wells will be sampled for groundwater assessment. Please refer to the separate Groundwater Monitoring Plan (Geotechnology, 2016) for additional information.

7.3 Groundwater Trend Analysis. Intrawell analysis will be used to assess groundwater trends over time. Please refer to the separate Groundwater Monitoring Plan (Geotechnology, 2016) for additional information.

7.4 Mitigation of Statistically Significant Trends. If statistically significant increasing trends are noted in the groundwater analysis, additional investigation into the cause of the increasing trends will be needed. Refer to the Groundwater Monitoring Plan (Geotechnology, 2016) for additional information.

8.0 TIME AND COST ESTIMATES

8.1 Time to Complete Closure. Completion of closure activities is dependent on weather and final approval of the closure plan by the IEPA. However, closure activities are anticipated to begin and be completed in 2017.

8.2 Time to Reach Class I Groundwater Standards. Boron and arsenic concentrations for the current ash pond configurations were modeled for 25 years to represent a scenario where the ash ponds were not closed. After 25 years, Monitoring Well APW-3 (the well with historically highest boron and arsenic concentrations) stabilized at 16.9 mg/L of boron and 0.208 mg/L of arsenic, which exceeded the respective Class I Groundwater standards. Monitoring Wells APW-2, APW-6, APW-7, and APW-8 also exceeded the Class I Groundwater standards for boron and arsenic at 25 years with no action.

After the dewatering and closure activities of the Fly Ash and Bottom Ash Ponds are complete, it will take approximately three years for boron concentrations and six years for arsenic concentrations to decrease below the Class I Groundwater standards for each well on site according to the model results.

Refer to the Hydrogeologic Site Investigation Report (Geotechnology, 2016) for more information regarding the groundwater modeling.

8.3 Remediation Time Frame. Once the ClosureTurf® caps for the Fly Ash and Bottom Ash Ponds are in place, precipitation will be diverted away from the ash ponds. Infiltration of precipitation into the ash ponds will be reduced or eliminated and further reductions of the concentrations of COCs are anticipated. Boron and arsenic exhibited the highest concentration over the largest area and were used as the indicator contaminants for contaminant transport modeling. Based on the modeling results, the lengths of time required for the concentration of boron and arsenic to decrease below the Class I Groundwater Standards are approximately three years and six years, respectively. Additional contamination transport modeling information is in the Hydrogeologic Site Investigation Report (Geotechnology 2016). Groundwater sampling and post-closure activities are anticipated to be 30 years.

8.4 Cost of Closure. The cost for closure activities related to the closure of the Fly Ash and Bottom Ash Ponds as specified in the drawings and specifications is estimated to be \$10,000,000.

8.5 Cost of Post-Closure Care. The cost for post-closure care activities related to the closure of the Fly Ash and Bottom Ash Ponds as specified in the Post-Closure Plan is estimated to be \$20,000 annually while quarterly groundwater sampling is in progress.



9.0 REFERENCES

CDG, 2016. "Specifications and Construction Plans, Fly Ash and Bottom Ash Ponds Closure, Merodosia Power Station." CDG Engineers Architects Planners, Inc., St. Louis, Missouri, 2016

Geotechnology, Inc., Construction Quality Assurance Plan, Merodosia Power Station, Ameren, 2016.

Geotechnology, Inc., Groundwater Monitoring Plan, Merodosia Power Station, Ameren, 2016.

Geotechnology, Inc., Groundwater Management Zone Plan, Merodosia Power Station, Ameren, 2016.

Geotechnology, Inc., Post-Closure Plan, Merodosia Power Station, Ameren, 2016.

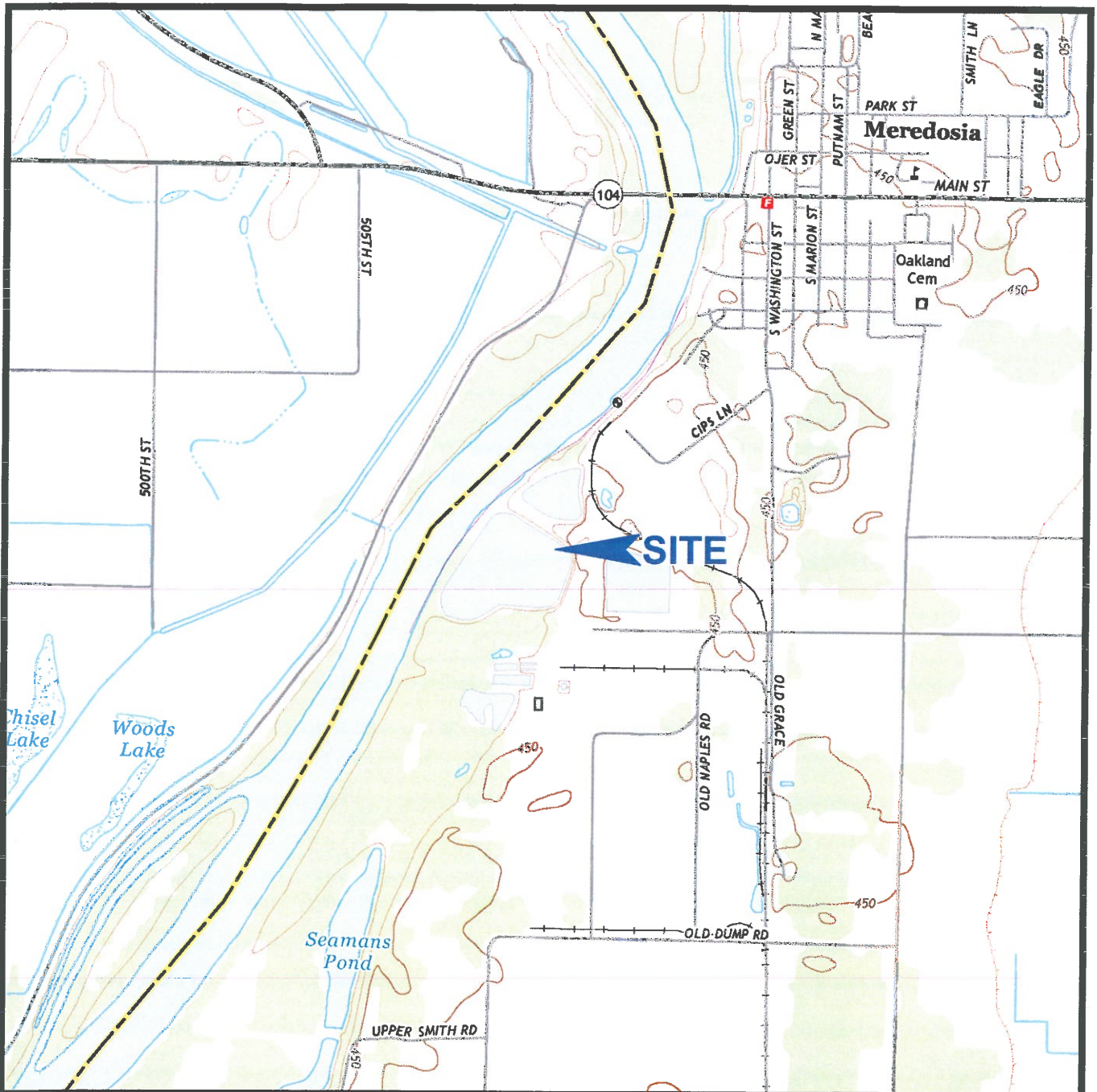
10.0 LICENSED PROFESSIONAL SIGNATURE/SEAL

I hereby affirm that the information and design documents contained in this closure plan are true and accurate to the best of my knowledge and professional opinion.



Rosanna M. Saindon, P.E., Ph.D.
Illinois Licensed Professional Engineer
Project Manager
Geotechnology, Inc.





NOTES

1. Plan adapted from a 7.5 minute U.S.G.S. map for Meredosias, Illinois quadrangle, last revised in 2015.



Drawn By: WAH	Ck'd By: <i>Wah</i>	App'vd By: <i>Ans</i>
Date: 7-20-16	Date: <i>7/20/16</i>	Date: <i>7/21/16</i>



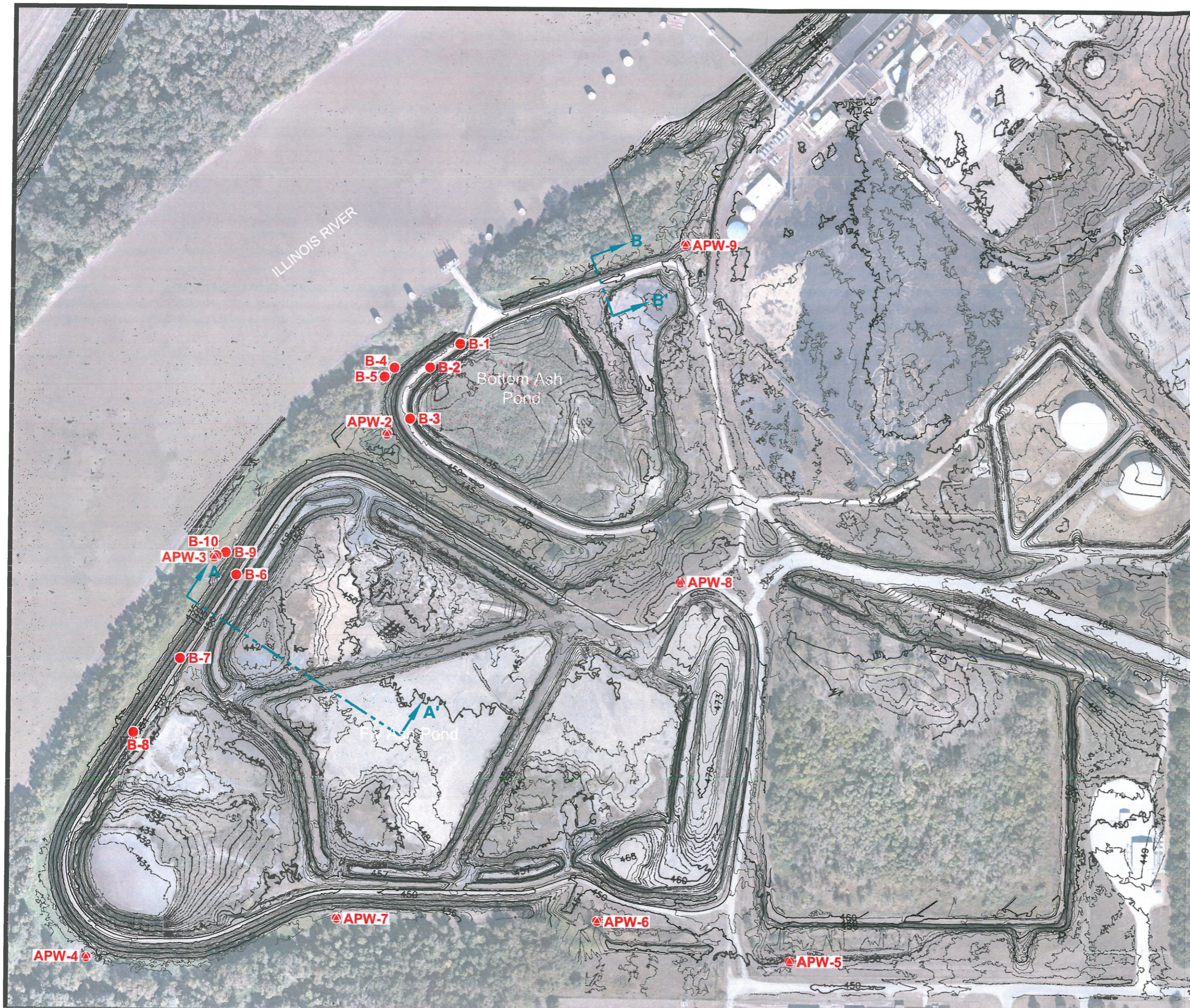
Meredosias Power Station
Meredosias, Illinois

**SITE LOCATION
AND TOPOGRAPHY**

Project Number
J024917.01

PLATE 1





NOTES

1. Plan adapted from drawings based on topography obtained by AeroView in October 2015 and supplied by the client.

LEGEND

-  Monitoring Well Location
-  Soil Boring Location
-  Slope Stability Analysis Cross Section



SCALE IN FEET

Drawn By: WAH	Ck'd By: <i>me</i>	App'vd By: <i>Amos</i>
Date: 7-20-16	Date: 7/20/16	Date: 7/20/16



Meredosia Power Station
Meredosia, Illinois

AERIAL PHOTOGRAPH OF SITE

Project Number
J024917.01

PLATE 2

APPENDIX A

STABILITY ANALYSIS

APPENDIX A

STABILITY ANALYSIS

1.0 PREVIOUS SLOPE STABILITY STUDY

Geotechnology performed a subsurface exploration and global stability evaluation² for the west embankments of the Bottom Ash and Fly Ash Ponds at the subject site in January 2011. Ten borings designated as Borings B-1 through B-10 were drilled during the subsurface exploration. Boring locations are shown on Plate 2. Laboratory testing included moisture contents for cohesive samples and Atterberg limits on selected samples. Also, consolidated-undrained triaxial, unconfined compression and direct shear tests were performed on representative samples. Relevant data from this exploration are incorporated into this report. Copies of the boring logs are presented in Attachment A. Laboratory test results are included in Attachment B.

2.0 SLOPE STABILITY ANALYSIS

Slope stability analysis consists of comparing the driving forces within a cross-section of slope to the resisting forces and determining the factor of safety. Gravity forces tend to move the slope downwards (driving force), while resisting forces, derived from the soil shear strength, tend to keep the slope in place. When the driving force acting on the slope is greater than the resisting force, sliding can occur. The factor of safety of the slope is the ratio of the restraining force divided by the driving force. Generally, when the factor of safety is 1 or less, the slope is considered to be unstable. The accepted standard in local practice and consistent with the Illinois Department of Natural Resources (IDNR) dam safety requirement is a factor of safety of 1.5 for long term static stability of a slope, and 1.0 for pseudo-static conditions (seismic loading).

Slope stability analyses were performed for representative sections of the west embankments of the Bottom Ash and Fly Ash Ponds. We understand that the embankment slopes will remain as-is or will be graded to a slope of 1V:3H (Vertical:Horizontal) or flatter. The locations of the typical cross-sections of the embankments are represented by Sections B-B' and A-A', respectively, and are shown on Plate 2. Soil profile and properties used in the stability analysis were selected based on boring and laboratory test results reported in the 2011 Global Stability Evaluation report and Geotechnology's experience with similar materials. The soil properties used in the models are summarized in the following table:

² *Global Stability Evaluation, Meredosia Power Station, Bottom and Fly Ash Ponds, Meredosia, Illinois*, prepared for Ameren Energy Resources by Geotechnology Inc., Report No. J017150.01, and dated January 4, 2011.

2.1 Effective Stress Parameters

Material	Cohesion (psf)	Friction Angle (deg)	Density (pcf)
Embankment Fill	0	28	115
Silty Clay	50	29	115
Sand	0	39	120
Fly Ash	0	25	112
Bottom Ash	0	28	112

2.2 Total Stress Parameters

Material	Cohesion (psf)	Friction Angle (deg)
Embankment Fill	0	0
Silty Clay	500	14
Sand	0	0
Fly Ash	0	0
Bottom Ash	0	0

Geotechnology performed stability analysis for deep seated, global failure of the embankments. Representative cross-sections of the embankments are shown on the plates included in Appendix C. Since the embankments have been in place for 40 years or more, long-term stability of the embankments was analyzed (i.e. effective stress conditions). Both effective and total stress soil properties were used for the rapid drawdown analysis. Groundwater in the Bottom Ash Pond was varied between El 435³ to 440 for our analyses. Groundwater in the Fly Ash Pond was assumed to be at El 450. For the rapid drawdown case it was assumed that the Illinois River will drain rapidly from its major flood stage of El 447.

A pseudo-static seismic analysis was performed on the embankment sections using a Peak Ground Acceleration (PGA) of 0.1g, which corresponds to a seismic event with a mean return time of 2,500 years. The PGA is based on data provided in Appendix 1 of the dam safety guidelines⁴ published by the IDNR. The Morgenstern-Price procedure was used to compute factors of safety. The computer program SLOPE/W was used to perform the computations. The calculated factors of safety are given in the following table.

³ All elevations herein refer to the mean sea level (msl) datum in feet.

⁴ "Procedural Guidelines for Preparation of Technical Data to be included in Application for Permits for Construction and Maintenance of Dams" issued by Illinois Department of Natural Resources.



SLOPE STABILITY ANALYSIS RESULTS				
Analysis Condition	Calculated Factor of Safety		Target Factor of Safety^a	Reference Plate No.
	Fly Ash Pond Section AA'	Bottom Ash Pond Section BB'		
Steady State Seepage Groundwater Elevation in Ash Pond as noted	2.1 (El 450)	1.8 (El 435)	1.5	1 and 5
Steady State Seepage at Major Flood Stage El 447 Groundwater Elevation in Ash Pond as noted	2.5 (El 450)	1.6 (El 440)	1.5	2 and 6
Rapid Drawdown from Major Flood Stage at El 447 Groundwater Elevation in Ash Pond as noted	1.7 (El 450)	1.7 (El 440)	1.2	3 and 7
Slope with Seismic Forces Mean Return Time 2,500 Years Groundwater Elevation in Ash Pond as noted	1.3 (El 450)	1.3 (El 435)	1.0	4 and 8

^a "Procedural Guidelines for Preparation of Technical Data to be included in Application for Permits for Construction and Maintenance of Dams" issued by Illinois Department of Natural Resources.

IDNR recommends a minimum factor of safety of 1.5 for long-term stability. During an extreme event, such as an earthquake, a factor of safety of 1.0 or more is recommended. Based on the results of our analyses, the Bottom Ash and Fly Ash Pond embankment slopes have adequate factors of safety for global stability.

ATTACHMENT A

**BORING LOGS AND
BORING LOG TERMS AND SYMBOLS**

LOG OF BORING 2002 WL J017150.01 GEO - MEREDOSIA.GPJ GTINC.0538301.GPJ 12/13/10 AND THE TRANSITION MAY BE GRADUAL. GRAPHIC LOG FOR ILLUSTRATION PURPOSES ONLY.

Surface Elevation: <u>449.0</u> Datum <u>msl</u>		Completion Date: <u>10/21/10</u>		GRAPHIC LOG	DRY UNIT WEIGHT (pcf) SPT BLOW COUNTS CORE RECOVERY/RQD	SAMPLES	SHEAR STRENGTH, tsf				
DEPTH IN FEET		DESCRIPTION OF MATERIAL					Δ - UU/2	○ - QU/2	□ - SV		
							0.5	1.0	1.5	2.0	2.5
							STANDARD PENETRATION RESISTANCE (ASTM D 1586)				
		▲ N-VALUE (BLOWS PER FOOT)		WATER CONTENT, %							
				PLI	10	20	30	40	50	LL	
			Crushed rock								
			FILL: brown, fine to coarse sand, trace clay lenses								
5					6-16-10	SS1		▲			
					3-11-13-14	SS2		▲			
10					5-7-9	SS3		▲			
					5-9-14	SS4		▲			
15			FILL: black clay with sand		4-4-4	SS5		▲ ●			
			Very soft, gray, interbedded SILT and CLAY with organics - ML/CL		0-0-1	SS6	▲		●		
20					2-2-3	SS7		▲	●		
25			Medium stiff, gray CLAY - (CH)		92	ST8					
					87	ST9					
30					89	ST9					
			Loose, gray, clayey SAND with gravel - SP		1-4-4	SS10		▲			
35					5-7-7	SS11		▲			
			Loose to medium dense, brown, fine to coarse SAND, trace gravel - SP								

GROUNDWATER DATA

FREE WATER NOT ENCOUNTERED DURING DRILLING

DRILLING DATA

 AUGER 4 1/4" HOLLOW STEM
WASHBORING FROM 15 FEET
MB DRILLER LAH LOGGER
CME 550X DRILL RIG
HAMMER TYPE Auto

Drawn by: KA Checked by: DL App'vd. by: DW
Date: 10/26/10 Date: 12/22/10 Date: 1/11/11



Meredosia Power Station
Meredosia, Illinois

LOG OF BORING: B-1

Project No. J017150.01

REMARKS: Datum: IL State Plane Coordinates, West Zone. N: 1148760.916'
E: 2182703.077'

LOG OF BORING 2002 WL J017150.01GEO - MEREDOSIA.GPJ CTINC 0638301.GPJ 12/23/10 AND THE TRANSITION MAY BE GRADUAL. GRAPHIC LOG FOR ILLUSTRATION PURPOSES ONLY.

Surface Elevation: <u>449.0</u>		Completion Date: <u>10/21/10</u>		GRAPHIC LOG	DRY UNIT WEIGHT (pcf) SPT BLOW COUNTS CORE RECOVERY/RQD	SAMPLES	SHEAR STRENGTH, tsf					
Datum <u>msl</u>							Δ - UU/2	○ - QU/2	□ - SV			
							0.5	1.0	1.5	2.0	2.5	
							STANDARD PENETRATION RESISTANCE (ASTM D 1586)					
DEPTH IN FEET	DESCRIPTION OF MATERIAL				▲ N-VALUE (BLOWS PER FOOT)							
					WATER CONTENT, %							
					PL	10	20	30	40	50	LL	
	Loose to medium dense, brown, fine to coarse SAND, trace gravel - SP (continued)											
45			4-5-4	SS12		▲						
50				5-7-9	SS13		▲					
55				9-8-9	SS14		▲					
60	Boring terminated at 60 feet		7-12-15	SS15			▲					
65												
70												
75												

GROUNDWATER DATA

FREE WATER NOT ENCOUNTERED DURING DRILLING

DRILLING DATA

AUGER 4 1/4" HOLLOW STEM WASHBORING FROM 15 FEET
 MB DRILLER LAH LOGGER
 CME 550X DRILL RIG
 HAMMER TYPE Auto

Drawn by: KA Checked by: Sik App'vd. by: DM
 Date: 10/26/10 Date: 12/23/10 Date: 1/4/11



Meredosia Power Station
Meredosia, Illinois

CONTINUATION OF
LOG OF BORING: B-1

Project No. J017150.01

REMARKS: Datum: IL State Plane Coordinates, West Zone. N: 1148760.916'
E: 2182703.077'

LOG OF BORING 2002.WL J017150.01GEO - MEREDOSIA.GPJ GTINC 0638301.GPJ 12/13/10 THE TRANSITION MAY BE GRADUAL. GRAPHIC LOG FOR ILLUSTRATION PURPOSES ONLY.

Surface Elevation: <u>449.2</u>		Completion Date: <u>10/21/10</u>		GRAPHIC LOG	DRY UNIT WEIGHT (pcf) SPT BLOW COUNTS CORE RECOVERY/RQD	SAMPLES	SHEAR STRENGTH, tsf				
Datum <u>msl</u>		Δ - UU/2 \circ - QU/2 \square - SV 0,5 1,0 1,5 2,0 2,5									
DEPTH IN FEET		DESCRIPTION OF MATERIAL					STANDARD PENETRATION RESISTANCE (ASTM D 1586) ▲ N-VALUE (BLOWS PER FOOT)				
				WATER CONTENT, %							
				PLI ——— LL							
				10 20 30 40 50							
			Crushed rock								
			FILL: brown, fine to coarse sand with black clay lenses								
5					5-7-9	SS1	▲				
					6-10-8	SS2	▲				
					7-8-13	SS3	▲				
10					5-5-9	SS4	▲				
					3-3-3	SS5	▲				
15											
			Black, clayey SAND, trace gravel - SP			ST6					
20											
			Medium stiff, gray CLAY - CH								
25					3-4-4	SS7	▲	●			
					3-3-3	SS8	▲	●			
30											
			Soft, gray, clayey SILT with sand and clay lenses - ML								
35					2-1-1	SS9	▲	●			
			Loose to medium dense, brown, fine to coarse SAND, trace gravel - SP								
					0-2-4	SS10	▲				

GROUNDWATER DATA

FREE WATER NOT ENCOUNTERED DURING DRILLING
AT 13.6 FEET AFTER 16 HOURS ▼

DRILLING DATA

___ AUGER 4 1/4" HOLLOW STEM WASHBORING FROM 15 FEET
MB DRILLER LAH LOGGER
CME 550X DRILL RIG
HAMMER TYPE Auto

Drawn by: KA Checked by: SM App'vd. by: DM
Date: 10/26/10 Date: 10/26/10 Date: 11/11/10



Meredosia Power Station
Meredosia, Illinois

LOG OF BORING: B-2


Project No. J017150.01

REMARKS: Hole collpased at 46 feet. Datum: IL State Plane Coordinates, West Zone. N: 1148689.546' E: 2182613.025'

LOG OF BORING 2002 WL J017150.01GEO · MEREDOSIA.GPJ GTINC 0638301.GPJ 12/23/10 THE TRANSITION MAY BE GRADUAL. GRAPHIC LOG FOR ILLUSTRATION PURPOSES ONLY.

Surface Elevation: <u>449.2</u>		Completion Date: <u>10/21/10</u>		GRAPHIC LOG	DRY UNIT WEIGHT (pcf) SPT BLOW COUNTS CORE RECOVERY/RQD	SAMPLES	SHEAR STRENGTH, tsf														
Datum <u>msl</u>		Δ - UU/2 ○ - QU/2 □ - SV 0.5 1.0 1.5 2.0 2.5																			
DEPTH IN FEET		STANDARD PENETRATION RESISTANCE (ASTM D 1586)																			
		▲ N-VALUE (BLOWS PER FOOT)																			
DESCRIPTION OF MATERIAL		WATER CONTENT, %																			
		PLI ● LL																			
Loose to medium dense, brown, fine to coarse SAND, trace gravel - SP (continued)		<table border="1" style="width: 100%; height: 100%;"> <tr> <td style="width: 20%; text-align: center;">10</td> <td style="width: 20%; text-align: center;">20</td> <td style="width: 20%; text-align: center;">30</td> <td style="width: 20%; text-align: center;">40</td> <td style="width: 20%; text-align: center;">50</td> </tr> <tr> <td style="text-align: center;">▲</td> <td></td> <td></td> <td></td> <td></td> </tr> </table>					10	20	30	40	50	▲									
							10	20	30	40	50										
▲																					
45	Boring terminated at 46 feet.		3-6-6		SS11		<table border="1" style="width: 100%; height: 100%;"> <tr> <td style="width: 20%; text-align: center;">10</td> <td style="width: 20%; text-align: center;">20</td> <td style="width: 20%; text-align: center;">30</td> <td style="width: 20%; text-align: center;">40</td> <td style="width: 20%; text-align: center;">50</td> </tr> <tr> <td></td> <td></td> <td></td> <td></td> <td></td> </tr> </table>					10	20	30	40	50					
10			20	30	40	50															
50	Boring terminated at 46 feet.																				
55																					
60																					
65																					
70																					
75																					

<p>GROUNDWATER DATA</p> <p><input checked="" type="checkbox"/> FREE WATER NOT ENCOUNTERED DURING DRILLING</p> <p>AT <u>13.6</u> FEET AFTER <u>16</u> HOURS <input checked="" type="checkbox"/></p>	<p>DRILLING DATA</p> <p><input type="checkbox"/> AUGER <u>4 1/4"</u> HOLLOW STEM WASHBORING FROM <u>15</u> FEET</p> <p><input type="checkbox"/> MB DRILLER <input type="checkbox"/> LAH LOGGER</p> <p><input type="checkbox"/> CME 550X DRILL RIG</p> <p>HAMMER TYPE <u>Auto</u></p>
<p>REMARKS: Hole collapsed at 46 feet. Datum: IL State Plane Coordinates, West Zone. N: 1148689.546' E: 2182613.025'</p>	

Drawn by: KA	Checked by: <u>SK</u>	App'vd. by: <u>DW</u>
Date: 10/26/10	Date: <u>12/22/10</u>	Date: <u>1/4/11</u>
 GEOTECHNOLOGY <small>FROM THE GROUND UP</small>		
Meredosia Power Station Meredosia, Illinois		
CONTINUATION OF LOG OF BORING: B-2		
Project No. J017150.01		

Surface Elevation: <u>449.1</u>		Completion Date: <u>10/21/10</u>		GRAPHIC LOG		SHEAR STRENGTH, tsf						
Datum <u>msl</u>						Δ - UU/2	○ - QU/2	□ - SV				
						0.5	1.0	1.5	2.0	2.5		
DEPTH IN FEET	DESCRIPTION OF MATERIAL	DRY UNIT WEIGHT (pcf)	SPT BLOW COUNTS	CORE RECOVERY/RQD	SAMPLES	STANDARD PENETRATION RESISTANCE (ASTM D 1586)						
						▲ N-VALUE (BLOWS PER FOOT)						
						WATER CONTENT, %						
						PLI	10	20	30	40	50	LL
	Crushed rock											
	FILL: brown sand with black clay lenses											
5			4-6-8		SS1		▲					
			5-6-9		SS2		▲					
					ST3							
10			8-10-16		SS4		▲					
			8-13-15		SS5		▲					
			6-8-8		SS6		▲					
15	FILL: black clay with sand, trace gravel				SS7							
	Soft to medium stiff, gray CLAY - CH with organics		2-2-2		SS8		▲					
20					ST9		○					
					ST10							
25												
			1-2-3		SS11		▲					
30												
	Soft, brown, clayey SILT with sand - ML		1-2-1		SS12		▲					
35												
	Medium dense, brown, fine to coarse SAND, trace gravel - SP		5-5-7		SS13		▲					

NOTE: STRATIFICATION LINES REPRESENT THE APPROXIMATE BOUNDARIES BETWEEN SOIL TYPES AND THE TRANSITION MAY BE GRADUAL. GRAPHIC LOG FOR ILLUSTRATION PURPOSES ONLY.
LOG OF BORING 2002.WL J017150.01.GEO - MEREDOSIA.GPJ GTINC 0638301.GPJ 12/1/10

GROUNDWATER DATA

FREE WATER NOT ENCOUNTERED DURING DRILLING

DRILLING DATA

___ AUGER 4 1/4" HOLLOW STEM WASHBORING FROM 15 FEET
MB DRILLER LAH LOGGER
CME 550X DRILL RIG
 HAMMER TYPE Auto

Drawn by: KA Checked by: SK App'vd. by: DW
 Date: 10/26/10 Date: 12/2/10 Date: 11/1/11



Meredosia Power Station
Meredosia, Illinois

LOG OF BORING: B-3


Project No. J017150.01

REMARKS: Datum: IL State Plane Coordinates, West Zone. N: 1148536.604' E: 2182554.305'

LOG OF BORING 2002 WL J017150.01GEO - MEREDOSIA.GPJ GTINC 0638301.GPJ 12/1/10 AND THE TRANSITION MAY BE GRADUAL. GRAPHIC LOG FOR ILLUSTRATION PURPOSES ONLY.

Surface Elevation: <u>449.1</u>		Completion Date: <u>10/21/10</u>		GRAPHIC LOG DRY UNIT WEIGHT (pcf) SPT BLOW COUNTS CORE RECOVERY/RQD		SAMPLES		SHEAR STRENGTH, tsf Δ - UU/2 ○ - QU/2 □ - SV 0.5 1.0 1.5 2.0 2.5				
Datum <u>msl</u>		STANDARD PENETRATION RESISTANCE (ASTM D 1586) ▲ N-VALUE (BLOWS PER FOOT)										
DEPTH IN FEET		DESCRIPTION OF MATERIAL						WATER CONTENT, % PLI ————— LL				
45			Medium dense, brown, fine to coarse SAND, trace gravel - SP (continued)									
50												
55												
60			Boring terminated at 60 feet.									
65												
70												
75												

GROUNDWATER DATA <input checked="" type="checkbox"/> FREE WATER NOT ENCOUNTERED DURING DRILLING	DRILLING DATA <input type="checkbox"/> AUGER <u>4 1/4"</u> HOLLOW STEM WASHBORING FROM <u>15</u> FEET <input type="checkbox"/> MB DRILLER <u>LAH</u> LOGGER <input type="checkbox"/> CME 550X DRILL RIG <input type="checkbox"/> HAMMER TYPE <u>Auto</u>
REMARKS: Datum: IL State Plane Coordinates, West Zone. N: 1148536.604' E: 2182554.305'	

Drawn by: KA	Checked by: <i>SLC</i>	App'vd. by: <i>DM</i>
Date: 10/26/10	Date: <i>12/2/10</i>	Date: <i>1/1/11</i>
		
Meredosia Power Station Meredosia, Illinois		
CONTINUATION OF LOG OF BORING: B-3		
Project No. J017150.01		

LOG OF BORING 2002 WL J017150.01.GEO - MEREDOSIA.GPJ GTINC 0638301.GPJ 12/13/10 THE TRANSITION MAY BE GRADUAL. GRAPHIC LOG FOR ILLUSTRATION PURPOSES ONLY.

Surface Elevation: <u>431.6</u>		Completion Date: <u>10/22/10</u>		GRAPHIC LOG	DRY UNIT WEIGHT (pcf) SPT BLOW COUNTS CORE RECOVERY/ROD	SAMPLES	SHEAR STRENGTH, tsf		
Datum <u>msl</u>		Δ - UU/2 \circ - QU/2 \square - SV 0.5 1.0 1.5 2.0 2.5							
DEPTH IN FEET	DESCRIPTION OF MATERIAL	STANDARD PENETRATION RESISTANCE (ASTM D 1586)							
		\blacktriangle N-VALUE (BLOWS PER FOOT) WATER CONTENT, % PLI ————— LL							
5	Soft to medium stiff, brown and gray CLAY - (CH)	1-2-2	SS1	\blacktriangle	\bullet				
		*	ST2		\bullet				
		1-2-3	SS3	\blacktriangle	—●—	—			
10		0-2-2	SS4	\blacktriangle	\bullet				
15	Soft, gray, silty CLAY, trace sand - CL	0-1-1	SS5	\blacktriangle	\bullet				
20	Very soft, gray, sandy CLAY with silt - CL	0-0-0	SS6	\blacktriangle	\bullet				
25	Very loose, brown, fine to coarse SAND, trace gravel - SP	0-1-2	SS7	\blacktriangle					
25	Boring terminated at 25 feet.								

GROUNDWATER DATA

ENCOUNTERED AT 19 FEET ∇

DRILLING DATA

___ AUGER 4 1/4" HOLLOW STEM
 WASHBORING FROM ___ FEET
MB DRILLER LAH LOGGER
CME 550X DRILL RIG
 HAMMER TYPE Auto

REMARKS: * Disturbed sample Datum: IL State Plane Coordinates, West Zone. N: 1148688.82' E: 2182505.605'

Drawn by: KA	Checked by: <i>SK</i>	App'vd. by: <i>DM</i>
Date: 10/26/10	Date: <i>11/2/10</i>	Date: <i>1/4/11</i>



Meredosia Power Station
 Meredosia, Illinois

LOG OF BORING: B-4

Project No. J017150.01

NOTE: STRATIFICATION LINES REPRESENT THE APPROXIMATE BOUNDARIES BETWEEN SOIL TYPES
 LOG OF BORING 2002 WL J017150.01GEO - MEREDOSIA.GPJ GTINC 0638301.GPJ 12/2/10 AND THE TRANSITION MAY BE GRADUAL. GRAPHIC LOG FOR ILLUSTRATION PURPOSES ONLY.

Surface Elevation: <u>431.8</u>		Completion Date: <u>10/22/10</u>		GRAPHIC LOG	DRY UNIT WEIGHT (pcf) SPT BLOW COUNTS CORE RECOVERY/RQD	SAMPLES	SHEAR STRENGTH, tsf				
Datum <u>msl</u>		Δ - UU/2 ○ - QU/2 □ - TV 0.5 1.0 1.5 2.0 2.5									
DEPTH IN FEET	DESCRIPTION OF MATERIAL	STANDARD PENETRATION RESISTANCE (ASTM D 1586)									
		▲ N-VALUE (BLOWS PER FOOT)									
		PLI WATER CONTENT, % LL									
		10	20	30	40	50	LL				
5	Medium stiff to soft, brown and gray, silty CLAY - CL	2-2-3	SS1	▲		●					
		2-2-2	SS2	▲		●					
10	Medium stiff to very soft, brown and gray CLAY - CH	1-1-3	SS3	▲		●					
		89	ST4	○		●					
15		0-0-0	SS5	▲		●					
20	Very soft, gray, silty CLAY with sand - CL	0-0-0	SS6	▲		●					
25	Boring terminated at 25 feet.	0-0-0	SS7	▲		●					
30											
35											

GROUNDWATER DATA

DRILLING DATA

ENCOUNTERED AT 23 FEET ∇

___ AUGER 4 1/4" HOLLOW STEM
 WASHBORING FROM ___ FEET
MB DRILLER LAH LOGGER
CME 550X DRILL RIG
 HAMMER TYPE Auto

REMARKS: Datum: IL State Plane Coordinates, West Zone. N: 1148661.88' E: 2182476.0360'

Drawn by: KA Checked by: SK App'vd. by: DW
 Date: 10/26/10 Date: 12/22/10 Date: 1/4/11



Meredosia Power Station
Meredosia, Illinois

LOG OF BORING: B-5

Project No. J017150.01

NOTE: STRATIFICATION LINES REPRESENT THE APPROXIMATE BOUNDARIES BETWEEN SOIL TYPES AND THE TRANSITION MAY BE GRADUAL. GRAPHIC LOG FOR ILLUSTRATION PURPOSES ONLY.
 LOG OF BORING 2002 WL J017150.01GEO - MEREDOSIA.GPJ GTINC 0638301.GPJ 12/7/10

Surface Elevation: <u>450.8</u>		Completion Date: <u>10/19/10</u>		GRAPHIC LOG	DRY UNIT WEIGHT (pcf) SPT BLOW COUNTS CORE RECOVERY/RQD	SAMPLES	SHEAR STRENGTH, tsf				
Datum <u>msl</u>		Δ - UU/2 \circ - QU/2 \square - SV 0.5 1.0 1.5 2.0 2.5									
DEPTH IN FEET		DESCRIPTION OF MATERIAL					STANDARD PENETRATION RESISTANCE (ASTM D 1586)				
							\blacktriangle N-VALUE (BLOWS PER FOOT) WATER CONTENT, % PLI ————— LL				
				10 20 30 40 50							
		Crushed rock									
		FILL: black clay with sand pockets									
		FILL: brown, fine sand, trace clay			3-6-10	SS1					
5		FILL: black ash and sand			3-8-9	SS2					
		FILL: brown, fine sand, trace gravel			4-6-7	SS3					
10		FILL: black ash and sand				ST4					
		FILL: brown, fine sand, trace gravel				ST5					
15		Very stiff, gray, silty CLAY with sand - CL			6-7-13	SS6					
		Very loose, gray silty SAND - SM									
20		Very soft to soft, gray, silty CLAY with clay and silt seams - (CL)			0-5-15	SS7					
25					0-0-0	SS8					
30					0-1-3	SS9					
35					0-0-0	SS10					
					0-0-0	SS11					

GROUNDWATER DATA

ENCOUNTERED AT 19.5 FEET ∇

DRILLING DATA

___ AUGER 4 1/4" HOLLOW STEM
 WASHBORING FROM ___ FEET
MB DRILLER LAH LOGGER
CME 550X DRILL RIG
 HAMMER TYPE Auto

REMARKS: Datum: IL State Plane Coordinates, West Zone. N: 1148066.896'
E: 2182040.954'

Drawn by: KA Checked by: SA App'vd. by: DW
 Date: 10/26/10 Date: 12/22/10 Date: 1/11/11



Meredosia Power Station
Meredosia, Illinois

LOG OF BORING: B-6

Project No. J017150.01

NOTE: STRATIFICATION LINES REPRESENT THE APPROXIMATE BOUNDARIES BETWEEN SOIL TYPES AND THE TRANSITION MAY BE GRADUAL. GRAPHIC LOG FOR ILLUSTRATION PURPOSES ONLY.
 LOG OF BORING 2002 WL J017150.01 GEO - MEREDOSIA.GPJ GTINC 063B301.GPJ 12/13/10

Surface Elevation: <u>450.8</u>		Completion Date: <u>10/19/10</u>		GRAPHIC LOG	DRY UNIT WEIGHT (pcf) SPT BLOW COUNTS CORE RECOVERY/RQD	SAMPLES	SHEAR STRENGTH, tsf		
Datum <u>msl</u>							Δ - UU/2 \circ - QU/2 \square - SV 0.5 1.0 1.5 2.0 2.5		
DEPTH IN FEET		DESCRIPTION OF MATERIAL					STANDARD PENETRATION RESISTANCE (ASTM D 1586) ▲ N-VALUE (BLOWS PER FOOT)		
					WATER CONTENT, %				
					PLI				
					10 20 30 40 50 LL				
		Very soft to soft, gray, silty CLAY with clay and silt seams - (CL) (continued)							
45					1-1-1	SS12	▲	●	
		Dense, brown, fine to coarse SAND - SP							
50					7-13-42	SS13		▲	
		Boring terminated at 50 feet.							
55									
60									
65									
70									
75									

GROUNDWATER DATA

ENCOUNTERED AT 19.5 FEET ∇

DRILLING DATA

___ AUGER 4 1/4" HOLLOW STEM
 WASHBORING FROM ___ FEET
MB DRILLER LAH LOGGER
CME 550X DRILL RIG
 HAMMER TYPE Auto

REMARKS: Datum: IL State Plane Coordinates, West Zone. N: 1148066.896'
E: 2182040.954'

Drawn by: KA Checked by: SA App'vd. by: DR
 Date: 10/26/10 Date: 11/2/10 Date: 11/4/11



Meredosia Power Station
Meredosia, Illinois

CONTINUATION OF
LOG OF BORING: B-6

Project No. J017150.01

LOG OF BORING 2002 WL J017150.01 GEO. MEREDOSIA.GPJ GTINC 0638301.GPJ 12/14/10 THE TRANSITION MAY BE GRADUAL. GRAPHIC LOG FOR ILLUSTRATION PURPOSES ONLY.

Surface Elevation: <u>450.5</u> Datum <u>msl</u>		Completion Date: <u>10/19/10</u>		GRAPHIC LOG	DRY UNIT WEIGHT (pcf) SPT BLOW COUNTS CORE RECOVERY/RQD	SAMPLES	SHEAR STRENGTH, tsf				
DEPTH IN FEET	DESCRIPTION OF MATERIAL	Δ - UU/2 \circ - QU/2 \square - SV 0.5 1.0 1.5 2.0 2.5									
		STANDARD PENETRATION RESISTANCE (ASTM D 1586)									
		▲ N-VALUE (BLOWS PER FOOT)									
WATER CONTENT, %					PLI	LL					
10 20 30 40 50											
	Crushed rock										
	FILL: black clay, ash and sand	5-8-9	SS1								
	FILL: brown, fine sand	2-6-6	SS2								
5		4-6-9	SS3								
	FILL: black sand and ash with clay lenses	3-6-5	SS4								
10			SS5								
		3-7-9	SS6								
15											
	Medium stiff, brown, sandy CLAY - CL	6-4-3	SS7								
20											
	Medium stiff to very soft, gray, silty CLAY with sand - CL	3-4-5	SS8								
25		87	ST9								
		86									
		95	ST10								
30											
		1-0-0	SS11								
35											
		*	ST12								

GROUNDWATER DATA

FREE WATER NOT ENCOUNTERED DURING DRILLING

DRILLING DATA

— AUGER 4 1/4" HOLLOW STEM
WASHBORING FROM 20 FEET
MB DRILLER LAH LOGGER
CME 550X DRILL RIG
HAMMER TYPE Auto

REMARKS: * No recovery in samples SS11 and ST12 Datum: IL State Plane Coordinates, West Zone. N: 1147816.37' E: 2181875.293'

Drawn by: KA Checked by: SK App'vd. by: DM
Date: 10/26/10 Date: 12/22/10 Date: 1/14/11



Meredosia Power Station
Meredosia, Illinois

LOG OF BORING: B-7

Project No. J017150.01

LOG OF BORING 2002 WL J017150.01 GEO - MEREDOSIA.GPJ GTINC 0638301.GPJ 12/13/10 THE TRANSITION MAY BE GRADUAL. GRAPHIC LOG FOR ILLUSTRATION PURPOSES ONLY.

Surface Elevation: <u>450.5</u>		Completion Date: <u>10/19/10</u>		GRAPHIC LOG	DRY UNIT WEIGHT (pcf) SPT BLOW COUNTS CORE RECOVERY/RQD	SAMPLES	SHEAR STRENGTH, tsf				
Datum <u>msl</u>		Δ - UU/2 ○ - QU/2 □ - SV 0.5 1.0 1.5 2.0 2.5									
DEPTH IN FEET	DESCRIPTION OF MATERIAL	STANDARD PENETRATION RESISTANCE (ASTM D 1586)									
		▲ N-VALUE (BLOWS PER FOOT)									
WATER CONTENT, %											
PLI ——— LL											
10 20 30 40 50											
45	Medium stiff to very soft, gray, silty CLAY with sand - CL <i>(continued)</i> sandy					ST13	●				
50	Medium dense to dense, brown, fine to medium coarse SAND - SP					5-8-10 SS14	▲				
55						7-9-14 SS15	▲				
60	Boring terminated at 60 feet,					13-17-19 SS16	▲				
65											
70											
75											

GROUNDWATER DATA

FREE WATER NOT ENCOUNTERED DURING DRILLING

DRILLING DATA

___ AUGER 4 1/4" HOLLOW STEM
WASHBORING FROM 20 FEET
MB DRILLER LAH LOGGER
CME 550X DRILL RIG
HAMMER TYPE Auto

Drawn by: KA Checked by: SC App'vd. by: DM
Date: 10/26/10 Date: 12/21/10 Date: 1/4/11



Meredosia Power Station
Meredosia, Illinois

CONTINUATION OF
LOG OF BORING: B-7

Project No. J017150.01

REMARKS: * No recovery in samples SS11 and ST12 Datum: IL State Plane Coordinates, West Zone. N: 1147816.37' E: 2181875.293'

Surface Elevation: 451.1

Completion Date: 10/20/10

Datum msl

SHEAR STRENGTH, tsf

Δ - UU/2 ○ - QU/2 □ - SV
 0.5 1.0 1.5 2.0 2.5

STANDARD PENETRATION RESISTANCE

(ASTM D 1586)

▲ N-VALUE (BLOWS PER FOOT)

WATER CONTENT, %

PLI LL

NOTE: STRATIFICATION LINES REPRESENT THE APPROXIMATE BOUNDARIES BETWEEN SOIL TYPES AND THE TRANSITION MAY BE GRADUAL. GRAPHIC LOG FOR ILLUSTRATION PURPOSES ONLY.

DEPTH IN FEET	DESCRIPTION OF MATERIAL	GRAPHIC LOG	DRY UNIT WEIGHT (pcf) SPT BLOW COUNTS CORE RECOVERY/RQD	SAMPLES	SHEAR STRENGTH, tsf					
					Δ - UU/2	○ - QU/2	□ - SV	STANDARD PENETRATION RESISTANCE (ASTM D 1586)		
	Crushed rock									
	FILL: black clay with sand			5-6-10	SS1					
	FILL: brown sand, trace to some clay			2-4-6	SS2					
5				0-5-7	SS3					
				4-8-12	SS4					
10	FILL: black clay with sand			0-4-6	SS5					
					ST6					
15	FILL: gray, clayey sand with black clay lenses			2-4-6	SS7					
				4-3-3	SS8					
20	Medium stiff, black to gray CLAY - CH			2-3-4	SS9					
25				0-2-3	SS10					
30	Medium stiff to soft, gray clayey SILT with sand - ML			101	ST11					
					SS12					
35				0-0-2	SS13					

GROUNDWATER DATA

FREE WATER NOT ENCOUNTERED DURING DRILLING AT 9.3 FEET AFTER 0.5 HOURS ▼

DRILLING DATA

AUGER 4 1/4" HOLLOW STEM WASHBORING FROM 20 FEET
MB DRILLER LAH LOGGER
CME 550X DRILL RIG
 HAMMER TYPE Auto

Drawn by: KA Checked by: SK App'vd. by: DM
 Date: 10/26/10 Date: 12/22/10 Date: 1/4/11



Meredosia Power Station
 Meredosia, Illinois

LOG OF BORING: B-8

Project No. J017150.01

REMARKS: Datum: IL State Plane Coordinates, West Zone. N: 1147594.427'
 E: 2181738.149'

Surface Elevation: 451.1

Completion Date: 10/20/10

Datum msl

SHEAR STRENGTH, tsf

Δ - UU/2 ○ - QU/2 □ - SV
0.5 1.0 1.5 2.0 2.5

STANDARD PENETRATION RESISTANCE

(ASTM D 1586)

▲ N-VALUE (BLOWS PER FOOT)

WATER CONTENT, %

PL |-----●-----| LL
10 20 30 40 50

DEPTH
IN FEET

DESCRIPTION OF MATERIAL

GRAPHIC LOG

DRY UNIT WEIGHT (pcf)
SPT BLOW COUNTS
CORE RECOVERY/RQD

SAMPLES

Medium stiff to soft, gray clayey SILT with sand - ML
(continued)

Dense to medium dense, brown, fine to coarse SAND with
gravel - SP

45

50

55

60

65

70

75

Boring terminated at 60 feet.

13-16-16 SS14

7-9-11 SS15

5-7-9 SS16

10-13-14 SS17

NOTE: STRATIFICATION LINES REPRESENT THE APPROXIMATE BOUNDARIES BETWEEN SOIL TYPES AND THE TRANSITION MAY BE GRADUAL. GRAPHIC LOG FOR ILLUSTRATION PURPOSES ONLY.

GROUNDWATER DATA

FREE WATER NOT
ENCOUNTERED DURING DRILLING
AT 9.3 FEET AFTER 0.5 HOURS

DRILLING DATA

 AUGER 4 1/4" HOLLOW STEM
WASHBORING FROM 20 FEET
MB DRILLER LAH LOGGER
CME 550X DRILL RIG
HAMMER TYPE Auto

Drawn by: KA Checked by: SK App'vd. by: DMV
Date: 10/26/10 Date: 12/22/10 Date: 1/14/11



Meredosia Power Station
Meredosia, Illinois

CONTINUATION OF
LOG OF BORING: B-8

Project No. J017150.01

REMARKS: Datum: IL State Plane Coordinates, West Zone. N: 1147594.427'
E: 2181738.149'


Surface Elevation: <u>433.6</u>		Completion Date: <u>10/25/10</u>		GRAPHIC LOG	DRY UNIT WEIGHT (pcf) SPT BLOW COUNTS CORE RECOVERY/RQD	SAMPLES	SHEAR STRENGTH, tsf				
Datum <u>msl</u>		Δ - UU/2 \circ - QU/2 \square - SV 0.5 1.0 1.5 2.0 2.5									
DEPTH IN FEET		DESCRIPTION OF MATERIAL					STANDARD PENETRATION RESISTANCE (ASTM D 1586)				
							\blacktriangle N-VALUE (BLOWS PER FOOT) WATER CONTENT, % PLI ————— LL				
		Medium stiff to soft, black and gray CLAY - (CH)									
5				2-3-4	SS1	\blacktriangle	\bullet				
				1-1-1	SS2	\blacktriangle	\bullet				
					ST3			— —			
10				86	ST4	\circ	\bullet				
		Soft to very soft, gray, silty CLAY with silt seams and sand - CL									
15				0-1-1	SS6	\blacktriangle	\bullet				
				0-1-2	SS7	\blacktriangle		\bullet			
20				0-0-0	SS8	\blacktriangle	\bullet				
25		Boring terminated at 25 feet.									
30											
35											

NOTE: STRATIFICATION LINES REPRESENT THE APPROXIMATE BOUNDARIES BETWEEN SOIL TYPES AND THE TRANSITION MAY BE GRADUAL. GRAPHIC LOG FOR ILLUSTRATION PURPOSES ONLY.

GROUNDWATER DATA
 FREE WATER NOT ENCOUNTERED DURING DRILLING

DRILLING DATA
___ AUGER 4 1/4" HOLLOW STEM WASHBORING FROM ___ FEET
MB DRILLER LAH LOGGER
CME 550X DRILL RIG
HAMMER TYPE Auto

REMARKS: Datum: IL State Plane Coordinates, West Zone. N: 1148133.361'
E: 2182009.017'

Drawn by: KA	Checked by: <u>SAC</u>	App'vd. by: <u>DM</u>
Date: 11/3/10	Date: <u>11/22/10</u>	Date: <u>11/4/11</u>
 GEOTECHNOLOGY <small>FROM THE GROUND UP</small>		
Meredosia Power Station Meredosia, Illinois		
LOG OF BORING: B-9		
Project No. J017150.01		

LOG OF BORING 2002 WL J017150.01 GEO - MEREDOSIA GPJ GTINC 0638301.GPJ 12/13/10 THE TRANSITION MAY BE GRADUAL. GRAPHIC LOG FOR ILLUSTRATION PURPOSES ONLY.

Surface Elevation: <u>433.2</u>		Completion Date: <u>10/25/10</u>		GRAPHIC LOG	DRY UNIT WEIGHT (pcf) SPT BLOW COUNTS CORE RECOVERY/RQD	SAMPLES	SHEAR STRENGTH, tsf				
Datum <u>msl</u>		Δ - UU/2 \circ - QU/2 \square - SV 0.5 1.0 1.5 2.0 2.5									
DEPTH IN FEET		DESCRIPTION OF MATERIAL					STANDARD PENETRATION RESISTANCE (ASTM D 1586)				
							\blacktriangle N-VALUE (BLOWS PER FOOT) PL ----- LL 10 20 30 40 50				
5		Medium stiff to soft, brown and gray silty CLAY, trace sand and wood - CL			2-3-3	SS1	\blacktriangle	\bullet			
					2-2-3	SS2	\blacktriangle		\bullet		
					0-2-3	SS3	\blacktriangle		\bullet		
10					0-1-2	SS4	\blacktriangle		\bullet		
					95	ST5	\circ		\bullet		
20		Very loose to medium dense, gray, silty SAND with silty clay seams - SM			0-1-1	SS6	\blacktriangle				
25		Wood			8-11-7	SS7		\blacktriangle			
		Boring terminated at 25 feet.									
30											
35											

GROUNDWATER DATA

DRILLING DATA

ENCOUNTERED AT 12 FEET ∇

___ AUGER 4 1/4" HOLLOW STEM
 WASHBORING FROM ___ FEET
MB DRILLER LAH LOGGER
CME 550X DRILL RIG
 HAMMER TYPE Auto

REMARKS: Datum: IL State Plane Coordinates, West Zone. N: 1148120.612'
E: 2181976.582'

Drawn by: KA Checked by: SK App'vd. by: DM
 Date: 11/3/10 Date: 12/2/10 Date: 1/4/11



Meredosia Power Station
Meredosia, Illinois

LOG OF BORING: B-10

Project No. J017150.01

BORING LOG: TERMS AND SYMBOLS

GENERAL NOTES

LEGEND

- Information on each boring log is a compilation of subsurface conditions based on soil or rock classifications obtained from the field as well as from laboratory testing of samples. The strata lines on the logs may be approximate or the transition between the strata may be gradual rather than distinct. Water level measurements refer only to those observed at the times and places indicated, and may vary with time, geologic condition or construction activity.
- Relative composition and Unified Soil Classification designations are based on visual estimates and are approximate only. If laboratory tests were performed to classify the soil, the unified designation is shown in parenthesis.
- Value given in Unit Dry Weight/SPT Column is either a unit dry weight in pounds per cubic foot, if adjacent to a ST sample designation, or blows per 6-inch increment if adjacent to a SS sample designation.

CS	Continuous Sampler
GB	Grab Sample Taken From Auger Cuttings Or Wash Water Return
NX 100 42	NX Rock Core with Percent Recovery/R.Q.D. Given In Adjacent Column
PST	Three Inch Diameter Piston Tube Sample
SS	Split Spoon Sample (Standard Penetration Test)
ST	Three Inch Diameter Shelby Tube Sample
*	Sample Not Recovered
SV	Field Vane Test

ABBREVIATIONS

- UU/2 Shear Strength from Unconsolidated – Undrained Triaxial Test (ASTM D2850)
- QU/2 Shear Strength from Unconfined Compression Test (ASTM D2166)
- SV Shear Strength from Field Vane (ASTM D2573)
- PL Plastic Limit (ASTM D4318)
- LL Liquid Limit (ASTM D4318)

SPLIT – BARREL SAMPLER DRIVING RECORD

Blow Per Foot (N-Value)

25.....	25 blows drove sampler 12 inches after initial 6 inches of seating.
75/10.....	75 blows drove sampler 10 inches after initial 6 inches of seating.
50/S3.....	50 blows drove sampler 3 inches during initial 6 inch seating interval.

- NOTES: 1. To avoid damage to sampling tools, driving is limited to 50 blows during any six inch interval.
2. N-Value (Blow Count) is the standard penetration resistance based on the total number of blows, using a 140-lb hammer with 30-inch free fall, required to drive a split spoon the last two of three, 6-inch drive increments. (Example: 4/7/9, N = 7 + 9 = 16). Values are shown as a summation on grid plot and may be shown as 4/7/9 in Unit Dry Weight – SPT column.

RELATIVE COMPOSITION

Trace.....0-10 %
 With/Some.....11-35 %
 Soil modifier such..... > 35 %
 As silty, clayey, sandy, etc.

STRENGTH OF COHESIVE SOILS

Consistency	Undrained Shear Strength Tons Per Sq. Ft.	Field Test	Approximate N-Value Range
Very Soft.....	less than 0.12	Thumb will penetrate soil more than 1" ..	0 - 1
Soft.....	13 to 0.25	Thumb will penetrate soil about 1"	2 - 4
Medium Stiff.....	0.26 to 0.50	Thumb will penetrate soil about 1/4"	5 - 8
Stiff.....	0.51 to 1.00	Thumb hardly indents soil.....	9 - 15
Very Stiff.....	1.01 to 2.00	Thumb will not indent soil, but readily indented with thumbnail.....	16 - 30
Hard.....	greater than 2.00.....	Thumbnail will not indent soil.....	> 30

DENSITY OF GRANULAR SOILS

Descriptive Term:	N-Value
Very Loose.....	0 - 4
Loose.....	5 - 10
Medium Dense.....	11 - 30
Dense.....	31 - 50
Very Dense.....	> 50

SOIL GRAIN SIZE

U.S. STANDARD SIEVE

12"	3"	3/4"	4	10	40	200				
BOULDERS		COBBLES		GRAVEL		SAND			SILT	CLAY
				COARSE	FINE	COARSE	MEDIUM	FINE		
300	76.2	19.1	4.76	2.00	0.42	0.074	0.002			
SOIL GRAIN SIZE IN MILLIMETERS										

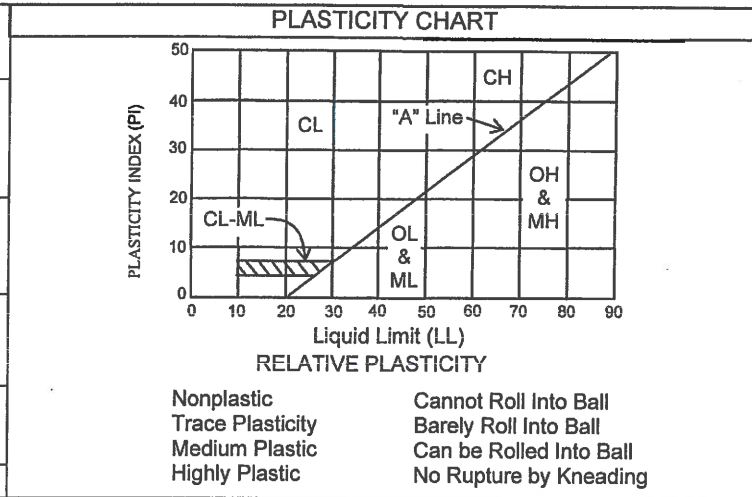
SOIL STRUCTURE

- Calcareous** – Having appreciable quantities of carbonate.
- Fissured** – Containing shrinkage or relief cracks, often filled with sand or silt; usually more or less vertical.
- Slickensided** – Having planes of weakness that appear slick and glossy. The degree of slickensidedness depends upon the spacing of slickensides and the ease of breaking along those planes.
- Layer** -- Inclusion greater than 3 inches thick.
- Seam** – Inclusion 1/8 inch to 3 inches thick extending through the sample

- Parting** – Inclusion less than 1/8 inch thick.
- Pocket** – Inclusion of material of different texture that is smaller than the diameter of the sample.
- Interlayered** – Soil samples composed of alternating layers of different soil types.
- Intermixed** – Soil samples composed of pockets of different soil types and a layered or laminated structure is not evident.
- Laminated** – Soil sample composed of alternating partings or seams of different soil type.

UNIFIED SOIL CLASSIFICATION SYSTEM

MAJOR DIVISIONS			SYM BOL	DESCRIPTION
Coarse-Grained Soils (More than 50% Larger than No. 200 Sieve Size)	Gravel and Gravelly Soils	Clean Gravels Little or no Fines	GW	Well-Graded Gravel, Gravel-Sand Mixture
			GP	Poorly-Graded Gravel, Gravel-Sand Mixture
		Gravels with Appreciable Fines	GM	Silty Gravel, Gravel-Sand-Silt Mixture
	Sand and Sandy Soils	Clean Sands Little or no Fines	SW	Well-Graded Sand, Gravelly Sand
			SP	Poorly Graded Sand, Gravelly Sand
		Sands with Appreciable Fines	SM	Silty Sand, Sand-Silt Mixture
		SC	Clayey Sand, Sand-Clay Mixture	
Fine-Grained Soils (More than 50% Smaller than No. 200 Sieve Size)	Silt and Clays	Liquid Limit Less Than 50	ML	Silt, Clayey Silt, Silty or Clayey Very Fine Sand, Slight Plasticity
			CL	Clay, Sandy Clay, Silty Clay, Low to Medium Plasticity
			OL	Organic Silts, or Silty Clays of Low Plasticity
	Silt and Clays	Liquid Limit More Than 50	MH	Silt, Fine Sandy or Silt Soil with High Plasticity
			CH	Clay, High Plasticity
			OH	Organic Clay of Medium to High Plasticity
	Highly Organic Soils		PT	Peat, Humus, Swamp Soil



VISUAL DESCRIPTION CRITERIA*

TABLE 1: CRITERIA FOR DESCRIBING ANGULARITY OF COARSE-GRAINED PARTICLES

Description	Criteria
Angular	Particles have sharp edges and relatively plane sides with unpolished surfaces
Subangular	Particles are similar to angular description but have rounded edges
Subrounded	Particles have nearly plane sides but have well-rounded corners and edges
Rounded	Particles have smoothly curved sides and no edges

TABLE 2: CRITERIA FOR DESCRIBING PARTICLE SHAPE

Description	Criteria
Flat	Particles with width/thickness X3
Elongated	Particles with length/width X3
Flat and Elongated	Particles meet criteria for both flat and elongated

TABLE 3: CRITERIA FOR DESCRIBING MOISTURE CONDITION

Description	Criteria
Dry	Absence of moisture, dusty, dry to the touch
Moist	Damp, but no visible water
Wet	Visible free water, usually soil is below the water table

TABLE 4: CRITERIA FOR DESCRIBING REACTION WITH HCL

Description	Criteria
None	No visible reaction
Weak	Some reaction, with bubbles forming slowly
Strong	Violent reaction, with bubbles forming rapidly

TABLE 6: CRITERIA FOR DESCRIBING CEMENTATION

Description	Criteria
Weak	Crumbles or breaks with handling or little finger pressure
Moderate	Crumbles or breaks with considerable finger pressure
Strong	Will not crumble or break with finger pressure

TABLE 8: CRITERIA FOR DESCRIBING DRY STRENGTH

Description	Criteria
None	The dry specimen crumbles into powder with mere pressure of handling
Low	The dry specimen crumbles into powder with some finger pressure
Medium	The dry specimen breaks into pieces or crumbles with considerable finger pressure
High	The dry specimen cannot be broken with finger pressure. Specimen will break into pieces between thumb and a hard surface.
Very High	The dry specimen cannot be broken between the thumb and a hard surface

TABLE 9: CRITERIA FOR DESCRIBING DILATANCY

Description	Criteria
None	No visible change in the specimen
Slow	Water appears slowly on the surface of the specimen during shaking and does not disappear or disappears slowly upon squeezing.
Rapid	Water appears quickly on the surface of the specimen during shaking and disappears quickly upon squeezing.

TABLE 10: CRITERIA FOR DESCRIBING TOUGHNESS

Description	Criteria
Low	Only slight pressure is required to roll the thread near the plastic limit. The thread and the lump are weak and soft.
Medium	Medium pressure is required to roll the thread to near the plastic limit. The thread and the lump have medium stiffness
High	Considerable pressure is required to roll the thread to near the plastic limit. The thread and the lump have very high stiffness

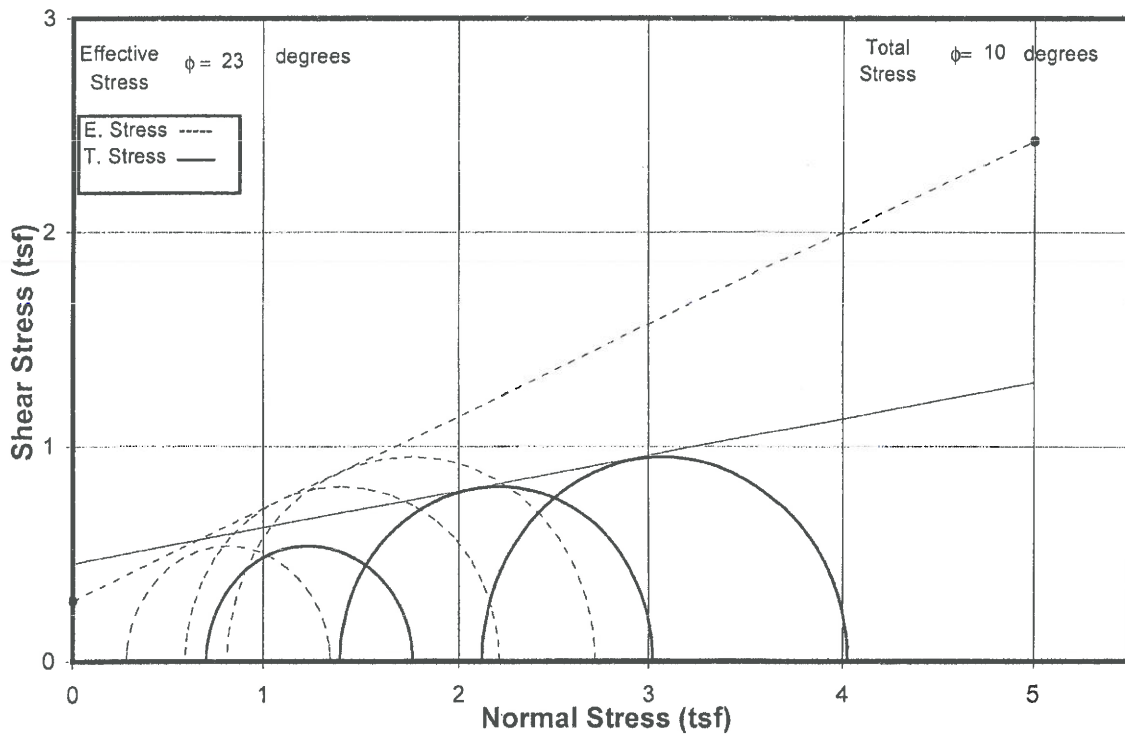
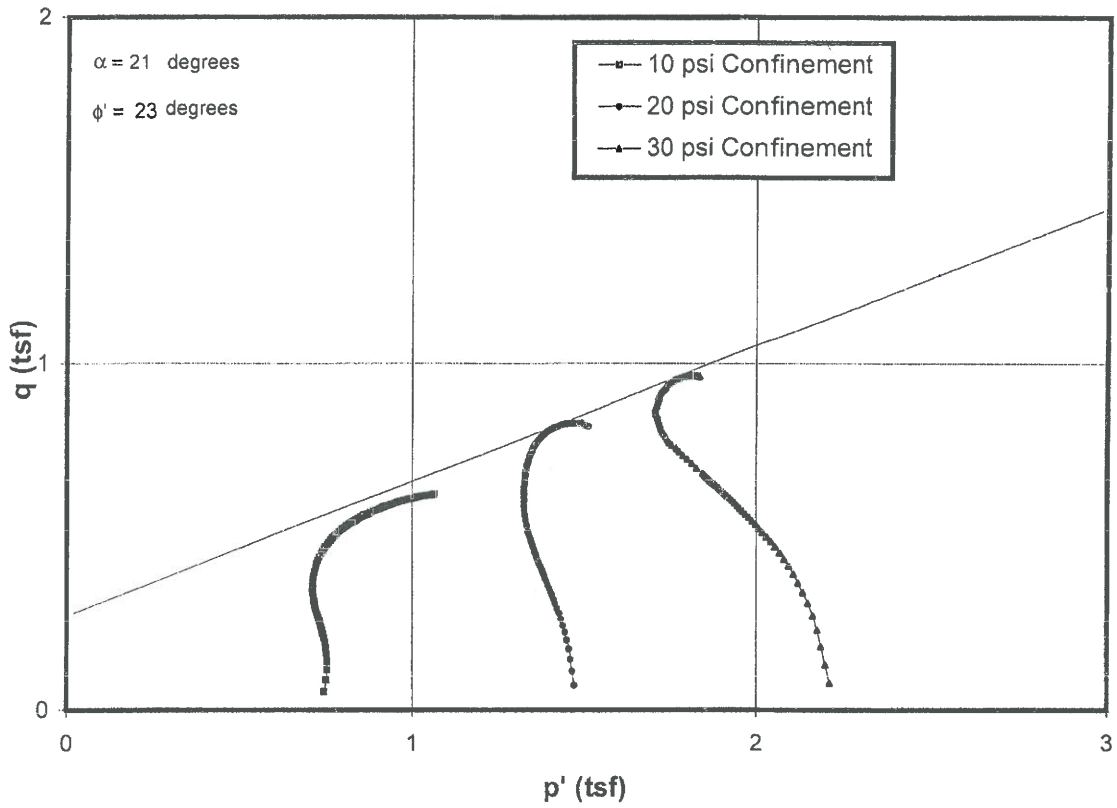
TABLE 12: IDENTIFICATION OF INORGANIC FINE-GRAINED SOILS FROM MANUAL TESTS

Soil Symbol	Dry Strength	Dilatancy	Toughness
ML	None to low	Slow to rapid	Low or thread cannot be formed
CL	Medium to high	None to slow	Medium
MH	Low to medium	None to slow	Low to medium
CH	High to very high	none	High

*NOTES: 1. Tables adapted from ASTM D2488 "Description and Identification of Soils" (Visual-Manual Procedure)
2. Tables 5, 7 and 11 incorporated into other information on this plate.

ATTACHMENT B

LABORATORY TEST RESULTS



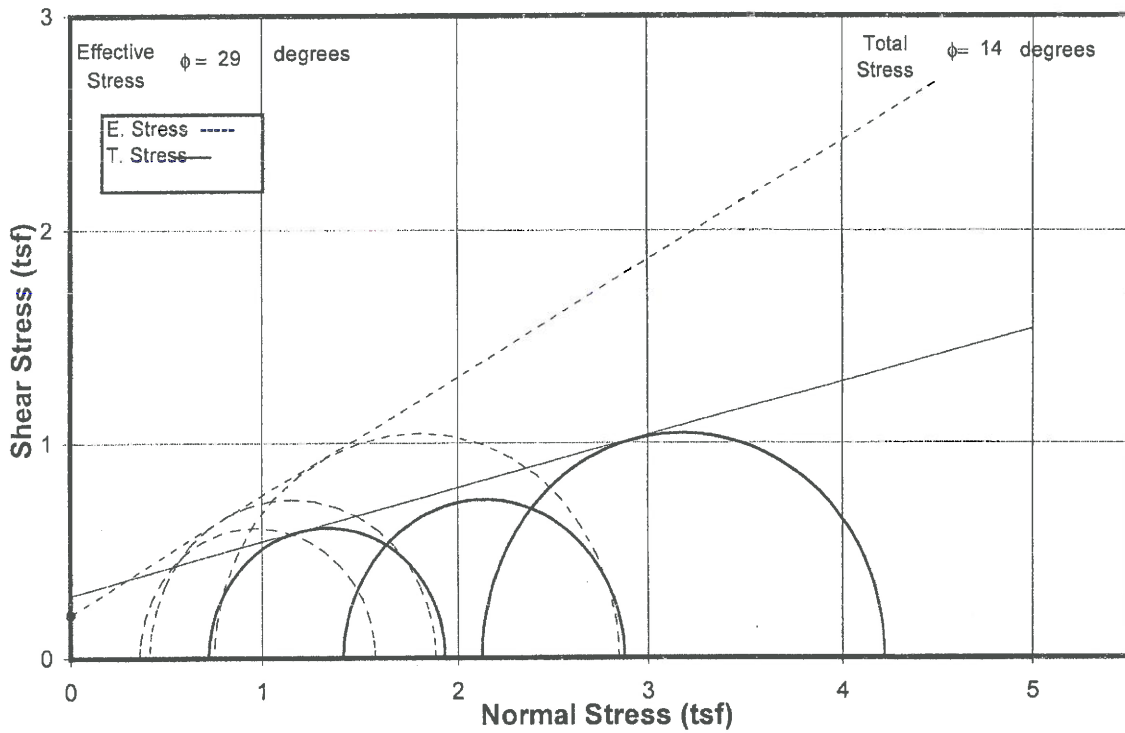
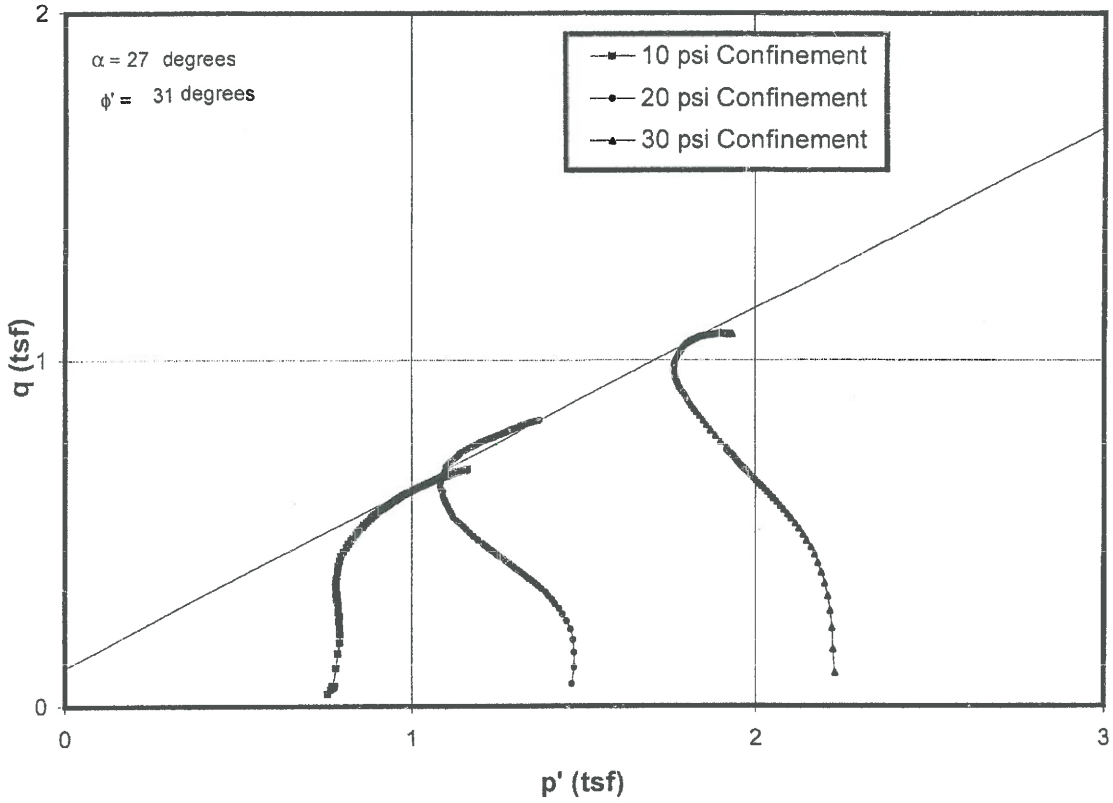
CONSOLIDATED UNDRAINED TRIAXIAL COMPRESSION TEST

ASTM D 4767

Project No.: J017150.01

Boring: B-1

Sample: ST-8, ST-9, ST-9 - Depth: 26, 28, 28



CONSOLIDATED UNDRAINED TRIAXIAL COMPRESSION TEST

ASTM D 4767

Project No.: J017150.01

Boring: B-7

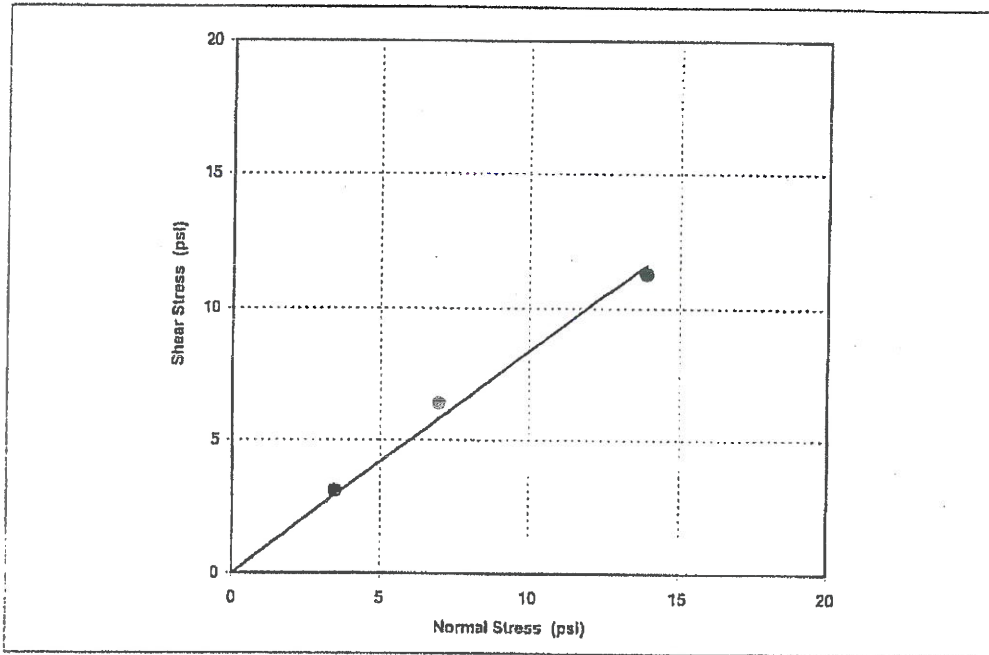
Sample: ST-10, ST-9, ST-9 - Depth: 28, 26, 26

DIRECT SHEAR TEST DATA

ASTM D 3080

Project Number: J017150.01
 Project Name: Ameren-Meredosia
 Project Location: --

Boring Number.: B-1
 Sample Number: SS-11, SS-12
 Sample Depth (ft): 38.5' - 45.0'



Trial Number	Normal Stress (psi)	Shear Stress (psi)	Normal Stress (psf)	Shear Stress (psf)	ϕ (degrees)
1	3.5	3.1	500	445	39.9
2	6.9	6.4	1000	923	
3	13.9	11.3	2000	1626	

Atterberg Limits:

Liquid Limit: --
 Plastic Limit: --
 Plasticity Index: NP

Standard Proctor Results:

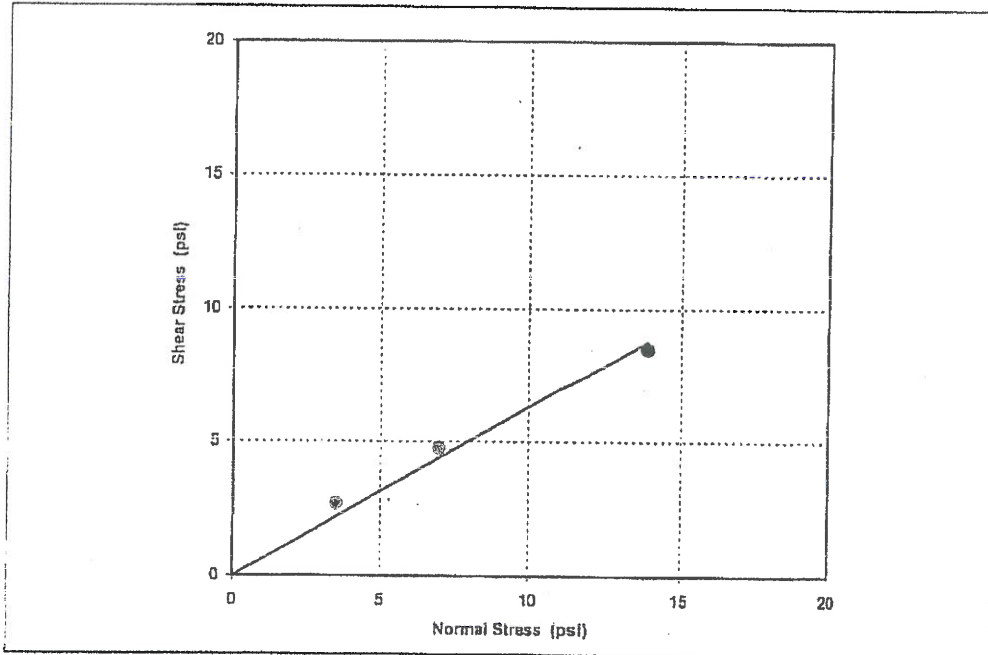
Max. Dry Density: N/A
 Opt. Moisture Content: N/A

Soil Classification: SAND, medium grained, brown, medium dense - (SP)

DIRECT SHEAR TEST DATA

ASTM D 3080

Project Number:	J017150.01	Boring Number.:	B-1
Project Name:	Ameren-Meredosia	Sample Number:	SS-2
Project Location:	—	Sample Depth (ft):	6.0' - 7.5'



Trial Number	Normal Stress (psi)	Shear Stress (psi)	Normal Stress (psf)	Shear Stress (psf)	ϕ (degrees)
1	3.5	2.7	500	389	32.3
2	6.9	4.7	1000	684	
3	13.9	8.5	2000	1218	

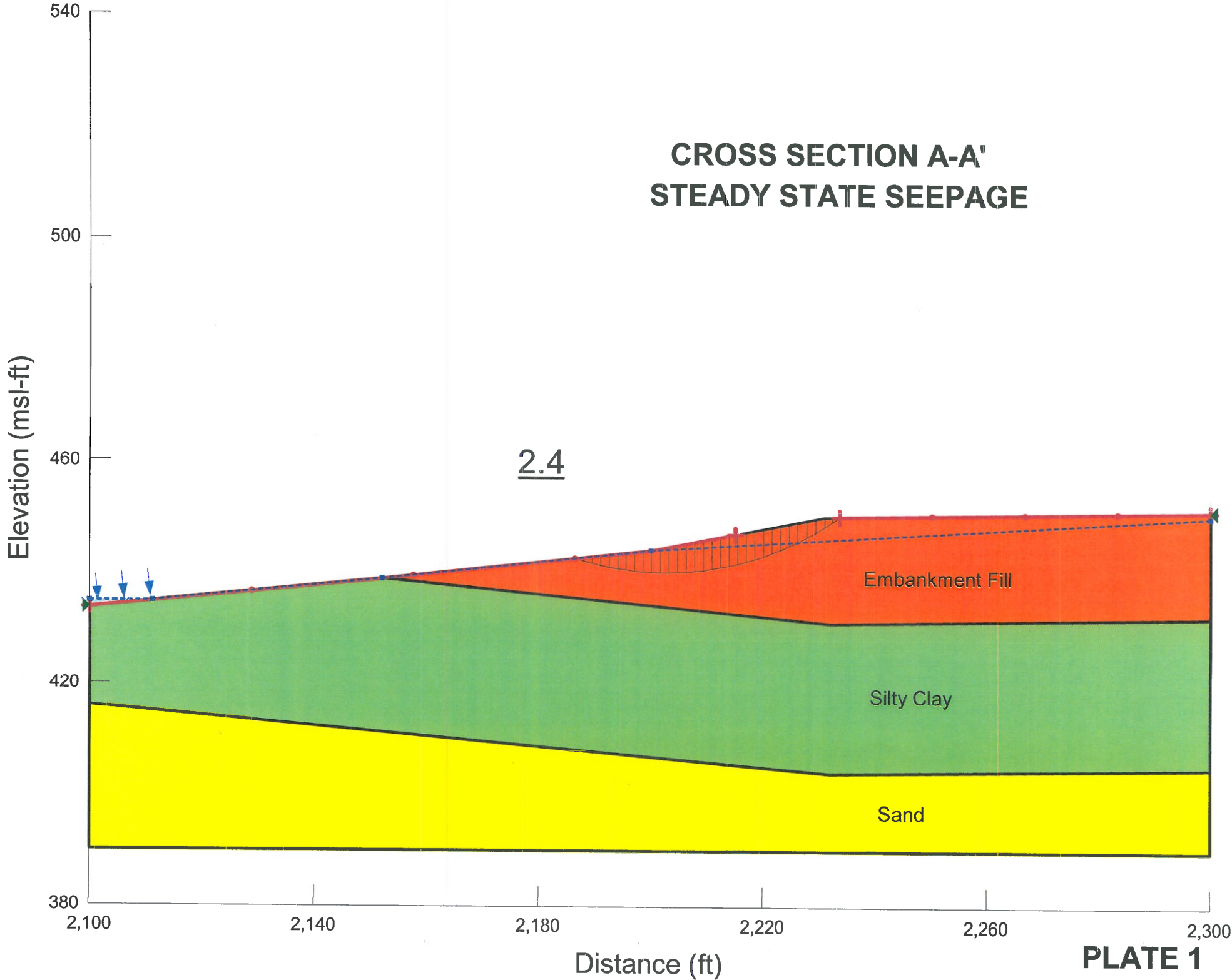
Atterberg Limits: Liquid Limit: — Plastic Limit: — Plasticity Index: NP	Standard Proctor Results: Max. Dry Density: N/A Opt. Moisture Content: N/A
---	---

Soil Classification: SAND, fine grained, brown, loose - (SP)

ATTACHMENT C

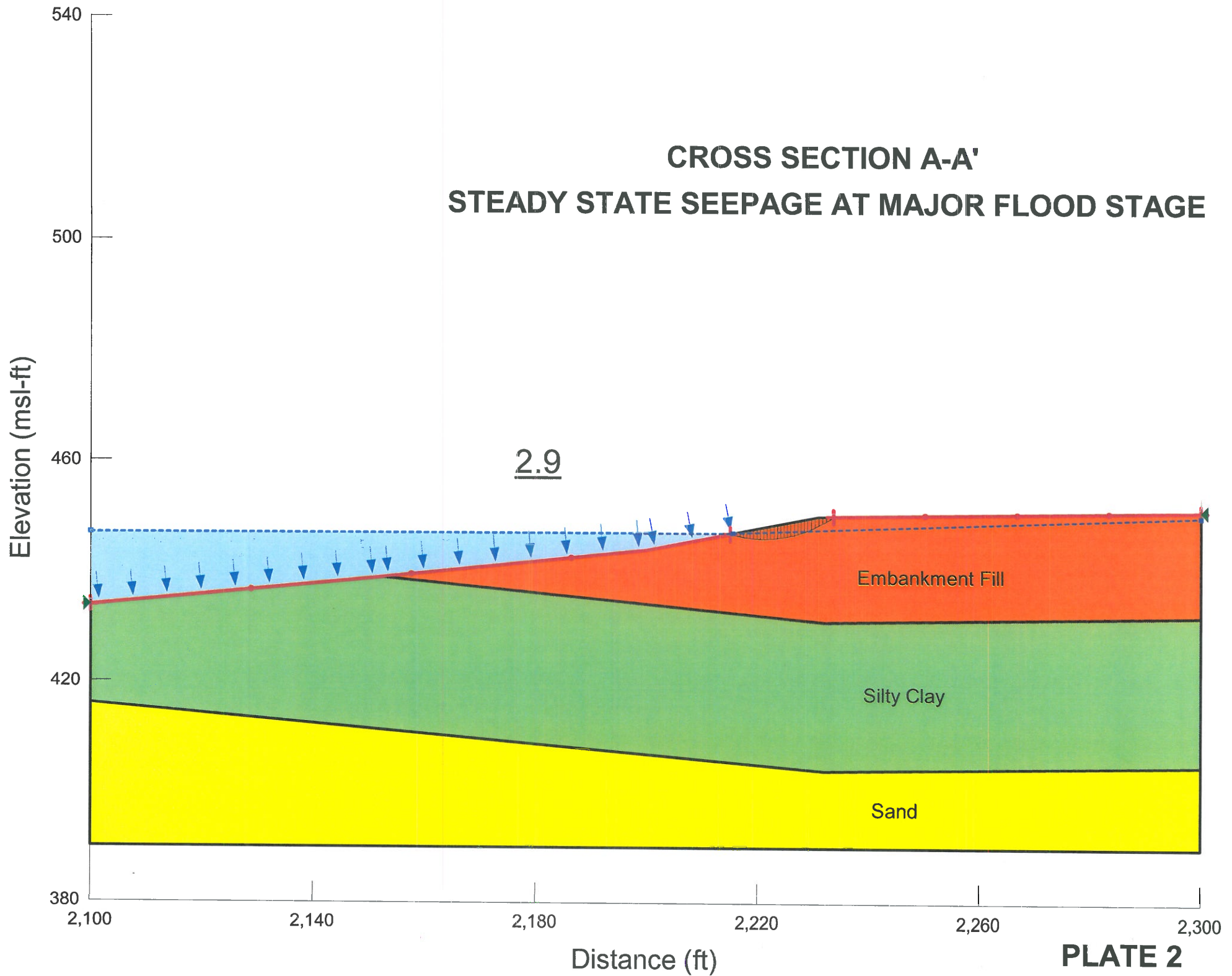
SLOPE STABILITY ANALYSIS RESULTS

CROSS SECTION A-A'
STEADY STATE SEEPAGE



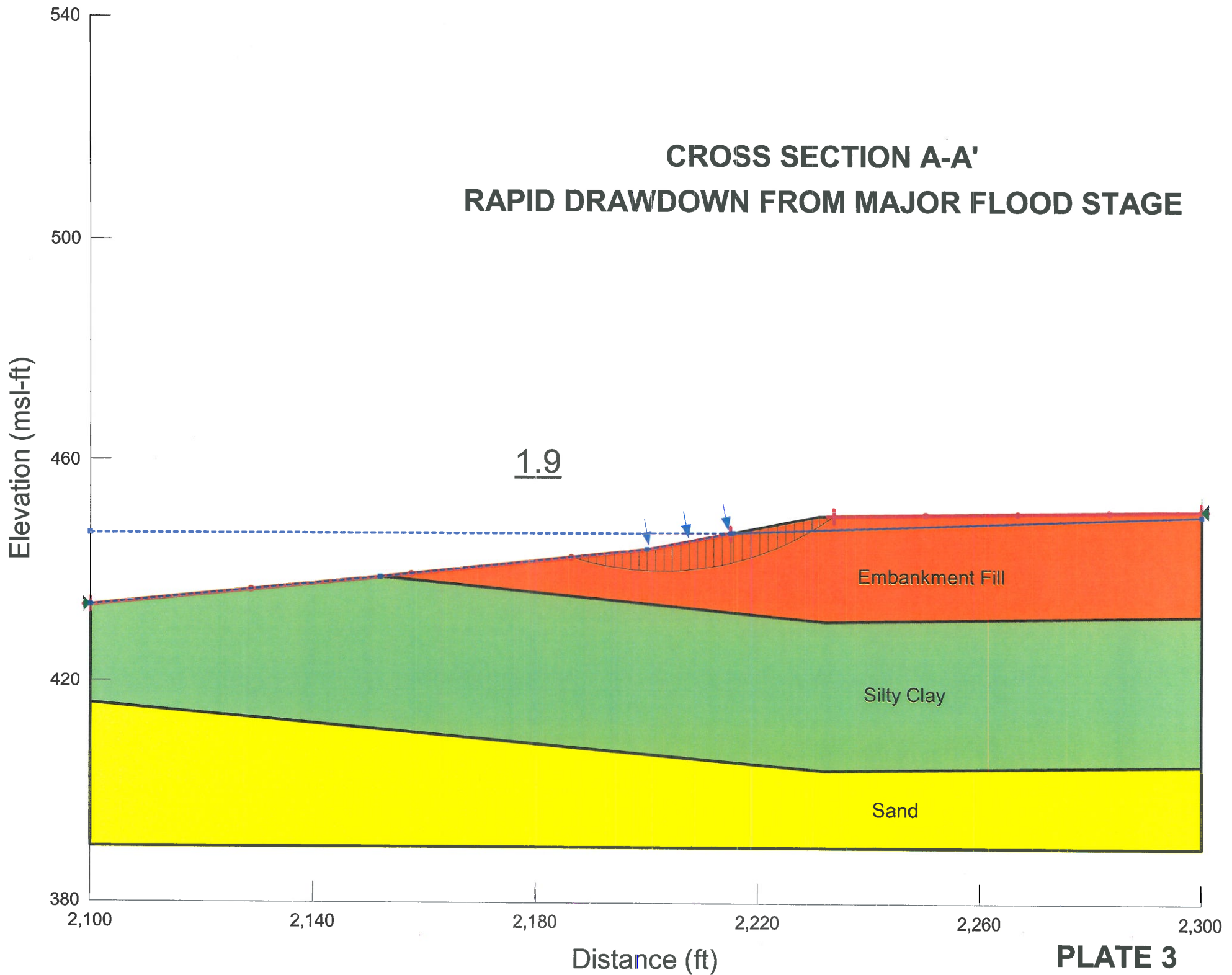
CROSS SECTION A-A'

STEADY STATE SEEPAGE AT MAJOR FLOOD STAGE

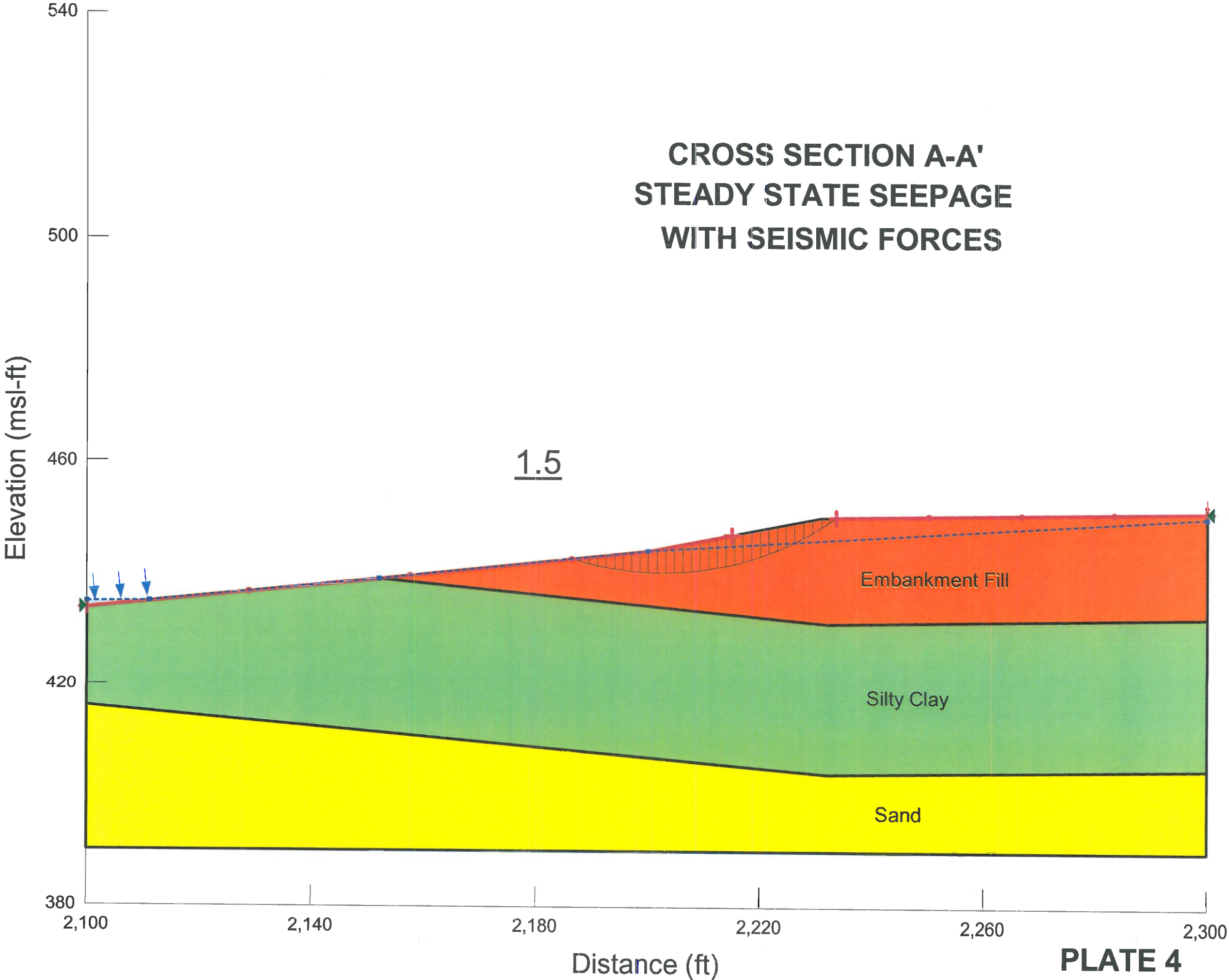


CROSS SECTION A-A'

RAPID DRAWDOWN FROM MAJOR FLOOD STAGE



**CROSS SECTION A-A'
STEADY STATE SEEPAGE
WITH SEISMIC FORCES**



CROSS SECTION B-B' STEADY STATE SEEPAGE

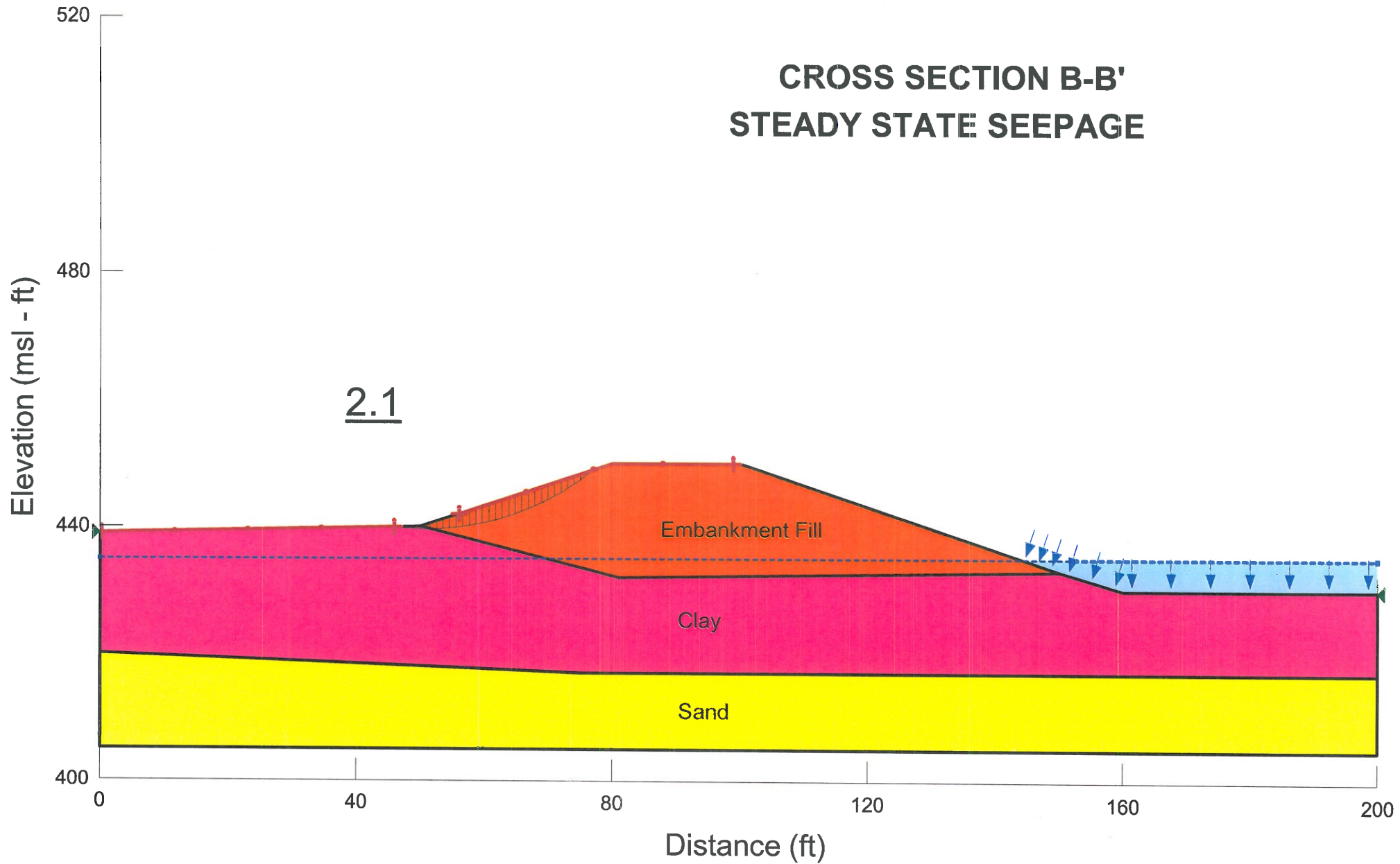


PLATE 5

CROSS SECTION B-B'

STEADY STATE SEEPAGE AT MAJOR FLOOD STAGE

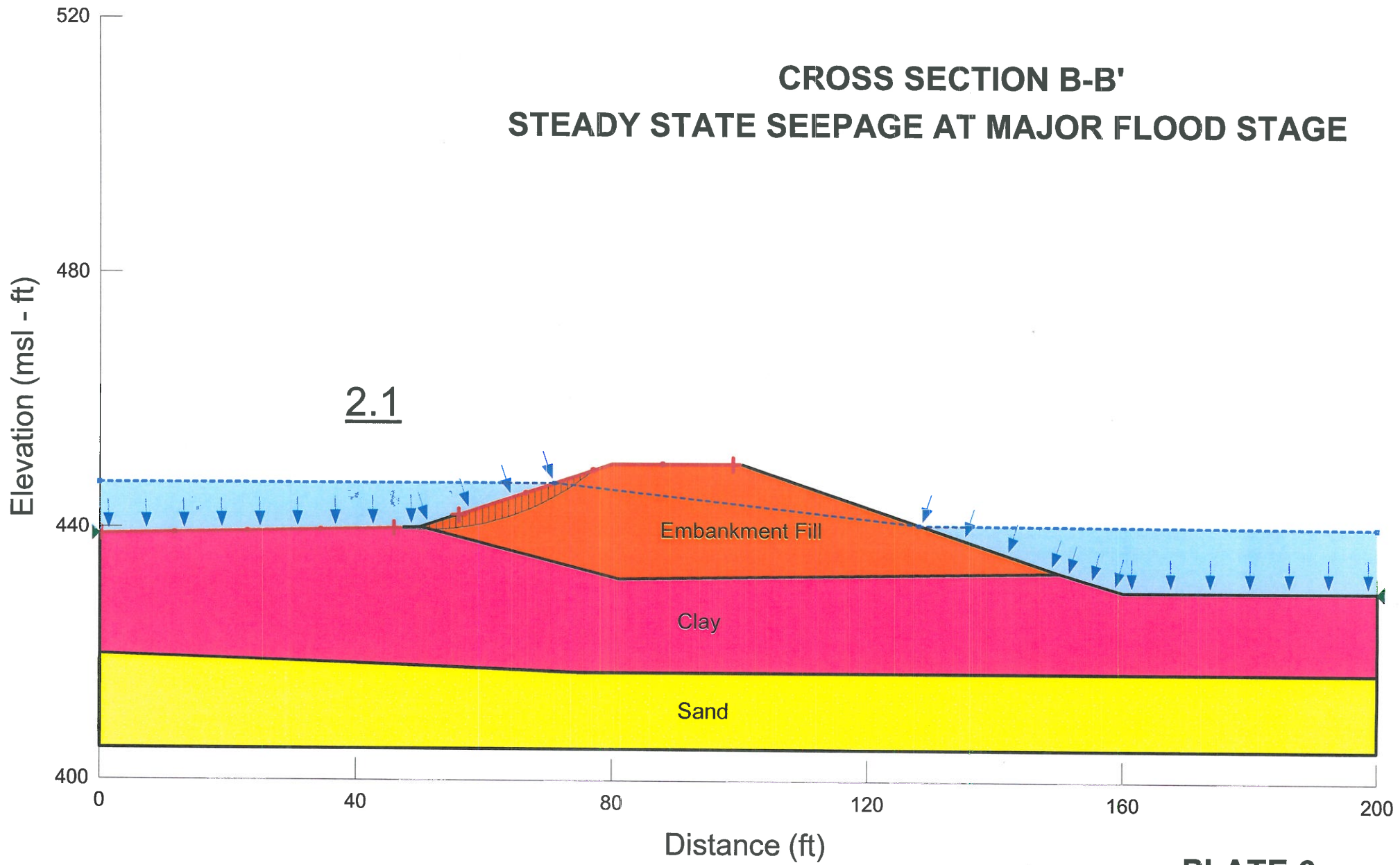


PLATE 6

CROSS SECTION B-B' RAPID DRAWDOWN FROM MAJOR FLOOD STAGE

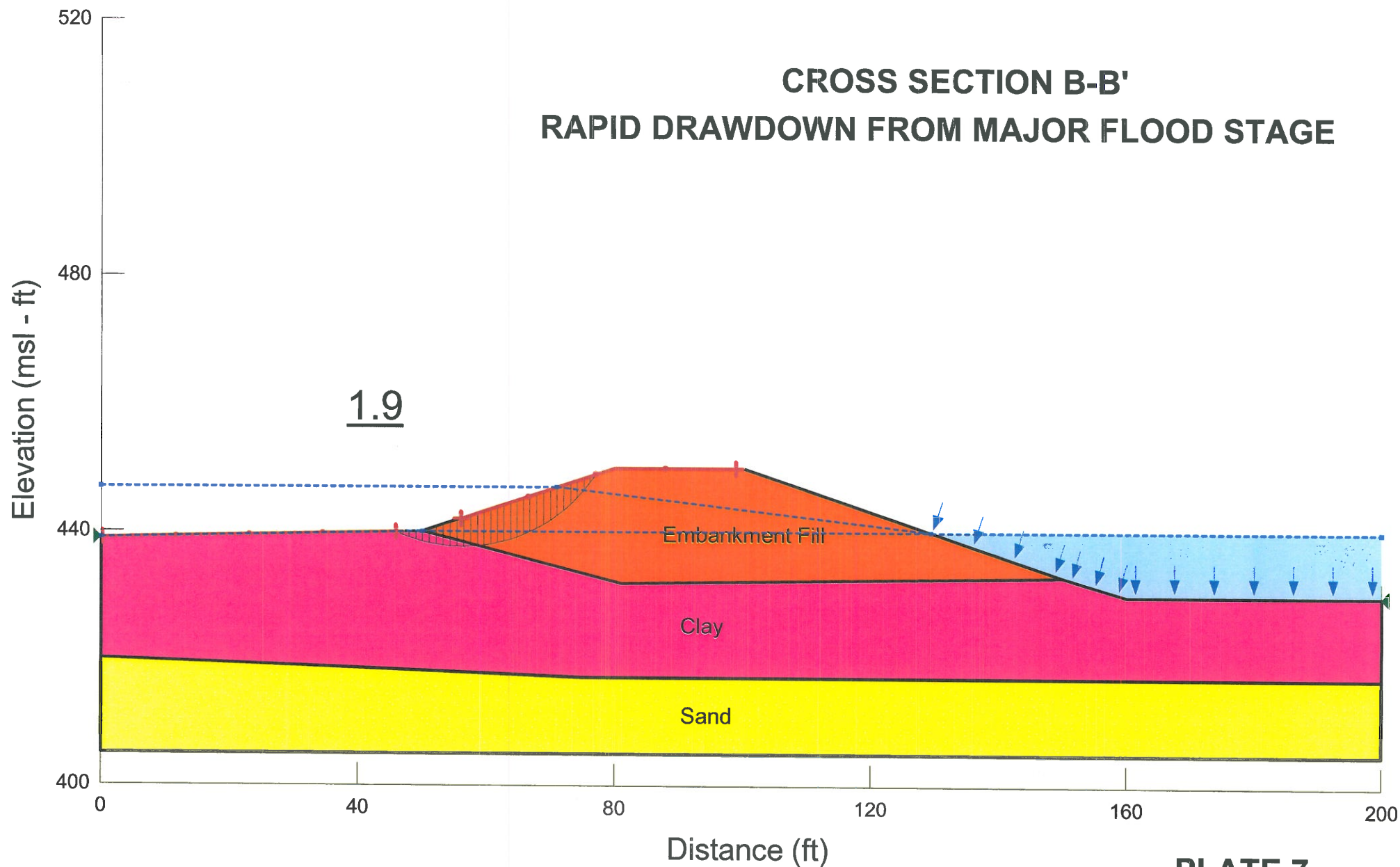


PLATE 7

ATTACHMENT A

ATTACHMENT B

ATTACHMENT C

ATTACHMENT D

ATTACHMENT E

ATTACHMENT F

ATTACHMENT G

ATTACHMENT 15



GEORGIA
DEPARTMENT OF NATURAL RESOURCES

ENVIRONMENTAL PROTECTION DIVISION

Land Protection Branch

**Guidance:
Groundwater Contaminant
Fate and Transport Modeling**

**GEPD/LPB GROUNDWATER CONTAMINANT
FATE AND TRANSPORT MODELING GUIDANCE COMMITTEE**

Chairman.....*Land Protection Branch*
Underground Storage Tank Management Program
Ronald Wallace, P.G., Team Leader

Members.....*Director's Office*
Jim Kennedy, Ph.D., P.G., State Geologist

Land Protection Branch

Response and Remediation Program

Carolyn L. Daniels, P.G., Geologist

Allan Nix, P.G., Geologist

Greg Gilmore, P.G., Geologist

Terry Allison, P.G., Geologist

Gary Davis, P.G., Geologist (*Brownfields
Unit*)

Robin Futch, P.G., Geologist

Susan Kibler, P.G., Geologist

Solid Waste Management Program

Kelly Norwood, Geologist

Hazardous Waste Management Program

Michael Elster, Treatment and Storage Unit
Coordinator

DoHyong Kim, P.E., Environmental Engineer

Becky Ferguson, C.P.G., Geologist

TABLE OF CONTENTS

1.0 INTRODUCTION	5
2.0 DEFINE MODELING OBJECTIVES	5
3.0 DATA REVIEW	6
4.0 CONCEPTUAL SITE MODEL	7
5.0 COMPUTER MODEL SOFTWARE SELECTION	7
6.0 CONSTRUCTION OF THE MODEL	8
6.1 Model Layering	8
6.2 Aquifer and Confining Unit Hydraulic Properties.....	9
6.3 Boundary Conditions	9
6.4 Aquifer Recharge and Discharge.....	9
6.5 Chemical Properties and Transport Processes	10
6.6 Baseline Stresses.....	10
6.7 Steady State or Transient Simulations.....	10
7.0 MODEL CALIBRATION	11
7.1 Method of Model Calibration	11
7.2 Calibration Targets	14
7.3 Calibration Criteria and Quantitation of Calibration	15
7.4 Degree of Model Calibration	17
7.5 Calibration of Analytical Models	18
8.0 DATA SENSITIVITY ANALYSIS	19
9.0 MODEL VERIFICATION AND VALIDATION	20
9.1 Model Verification.....	20
9.2 Model Validation.....	20
10.0 PREDICTIVE SIMULATIONS	21
11.0 UNCERTAINTY OF MODEL PREDICTIONS	23
12.0 PERFORMANCE/POST AUDIT MONITORING AND MODEL REFINEMENT .	23
13.0 MODELING REPORTING REQUIREMENTS	24
14.0 SELECTED REFERENCES/SOURCES	25

LIST OF FIGURES

- Figure 1-1** **Steps in Groundwater Contaminant Fate and Transport Modeling Application**
- Figure 7-1** **History Matching/Calibration Using “Trial and Error” and Automatic Procedures**
- Figure 7-2** **Residual Scatter Plot Example**
- Figure 11-1** **Examples of Graphical Representations of Ranges of Model Predictions**

LIST OF APPENDICES

- APPENDIX A** **Basic Aspects of Hydrogeology**
- APPENDIX B** **Example Data Input Summary Spreadsheets**

1.0 INTRODUCTION

The purpose of this guidance is to provide general guidelines for the application of groundwater contaminant fate and transport models, including the planning and evaluation of models for use at sites with groundwater contamination that are subject to regulation by the Georgia Environmental Protection Division (EPD) under the following statutes:

- Federal Resource Conservation and Recovery Act (RCRA)
- Federal Comprehensive Environmental Response, Compensation, and Liability Act (CERCLA)
- Georgia Hazardous Waste Management Act, O.C.G.A. 12-8-60
- Georgia Hazardous Site Response Act (HSRA), O.C.G.A. 12-8-90
- Georgia Voluntary Remediation Program Act (VRPA), O.C.G.A. 12-8-100
- Georgia Brownfield Act, O.C.G.A. 12-8-200
- Georgia Underground Storage Tank Act, O.C.G.A. 12-13-1
- Georgia Solid Waste Management Act., O.C.G.A. 12-8-20

Regulatory oversight of the above statutes is administered by the following programs within the EPD Land Protection Branch:

- Response and Remediation Program (including the Brownfields Unit)
- Solid Waste Management Program
- Underground Storage Tank Management Program
- Hazardous Waste Management Program
- Hazardous Waste Corrective Action Program

This guidance outlines recommended practices and explains their rationale. However, EPD may not require an entity to follow methods recommended by this or any other guidance document. The entity may however need to demonstrate that an alternate method produces data and information that meet the pertinent requirements. This guidance *is not a substitute for professional judgment*, which must be applied in the selection and application of fate and transport modeling, *nor does it advocate modeling over the collection and interpretation of quality media-specific site data*.

This document describes the process of preparing a fate and transport model for consideration. Each section provides a brief discussion of each step and the rationale for its use. Figure 1-1 outlines the steps that are typically involved in groundwater contaminant fate and transport model application at contaminated sites. Additional steps may be necessary to meet modeling objectives. For example, a site investigation may provide additional data that can be used in the modeling process. The development of a Modeling Work Plan may assist EPD in determining if the proposed modeling is appropriate.

2.0 DEFINE MODELING OBJECTIVES

The objective(s) for the modeling should be specific and measurable. Acceptable objectives for groundwater contaminant fate and transport modeling will vary dependent upon the statute under which a particular site is administrated. The ultimate objective of EPD is protection of human health and the environment. Groundwater contaminant fate and transport modeling is a potential tool that can be used, along with others, to achieve that objective.

The modeling report must demonstrate that the objectives of the specific regulatory program under which the site is administrated, *and* this guidance, have been met by the model.

3.0 DATA REVIEW

Available data should be included as part of a Conceptual Site Model (CSM). Some EPD programs require a summary of the available data be submitted as part of the CSM. The CSM may also identify gaps in the data to be used in modeling. Regardless of how data are presented, the sources and validity of data used in modeling must be documented. Any manipulation (*i.e.*, exclusion, statistical analysis, *etc.*) of data used in modeling must also be thoroughly documented and justified.

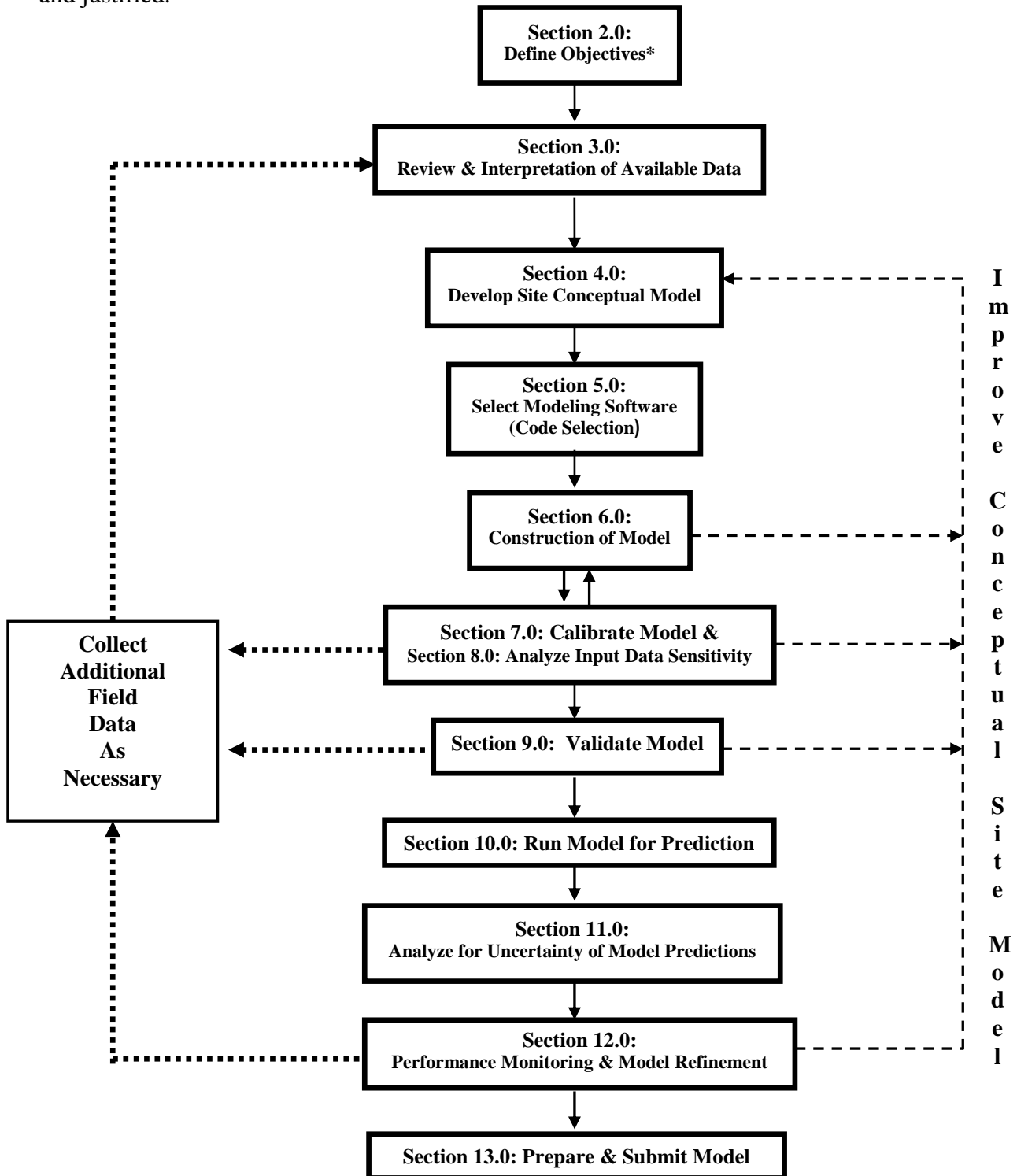


Figure 1-1: Steps in Groundwater Contaminant Fate & Transport Modeling Application

(Modified from Bear, et. al., April 1992)

**Note: At any time in the model application process it may become apparent that objectives should be refined or redefined based on availability of data, inability to calibrate or validate the model, etc.*

4.0 CONCEPTUAL SITE MODEL

Guidance on how to develop a CSM is readily available from other state agencies, federal agencies, and private organizations such as the American Society for Testing and Materials (ASTM; ASTM E1689-95), and will not be covered in detail here. The purpose in developing a CSM is to document physical and chemical site conditions that affect contaminant fate and transport. Developing a CSM may allow EPD to verify that the modeling adequately represents site conditions. In some cases, the CSM required by the Voluntary Remediation Program may be adequate for modeling.

The CSM should be as simple as possible, while retaining sufficient complexity to adequately represent the physical and chemical elements of the system. For instance, a site with a single homogeneous, isotropic, water-bearing unit with one direction of groundwater movement and a single constituent of concern may only require a simple CSM. A site with multiple water-bearing units, more than one direction of groundwater movement and multiple constituents of concern may require a more complex CSM.

A CSM may address, but not necessarily be limited to, site conditions such as:

- One-dimensional or multi-dimensional contaminant transport
- Steady-state or transient conditions
- Unconfined or confined aquifers
- Homogeneous/isotropic or heterogeneous/anisotropic aquifers
- Dip/Attitude of water-bearing unit(s)
- Constant or variable groundwater velocity, hydraulic head, *etc.*
- Variable or constant/uniform, groundwater flow direction/paths
- Contaminant concentrations, dispersion, adsorption/retardation and biodegradation/transformation
- Continuous or instantaneous/finite source
- Variable source concentrations
- Mass transport
- Mixing of water-bearing units
- Chemical specific properties, *etc.*

A CSM should be updated if and as more site-specific data become available, *or* if site conditions change. Some EPD programs [*e.g.*, the Voluntary Remediation Program (VRP)] require the CSM to be periodically updated and reported.

5.0 COMPUTER MODEL SOFTWARE SELECTION

A list of software available for contaminant fate and transport modeling is not included in this guidance. The nature of transport media, contaminant type and distribution, modeling objectives, and the complexity of site conditions require that models should be evaluated on a site-specific basis. Lists of fate and transport models, and supporting guidance, are available from many sources, including:

- U.S. EPA's Center for Subsurface Modeling Support (CSMoS)
- U.S. EPA's Center for Exposure Assessment Modeling in Athens, Georgia
- U.S. Geological Survey (USGS)
- Air Force Center for Environmental Excellence (AFCEE)
- International Groundwater Modeling Center (IGWMC)

The model used may be analytical, numerical, or any combination thereof and should include user documentation that a reviewer could use to set up and run the model and understand model outputs. Georgia EPD will consider models using software developed by the U.S. Environmental

Protection Agency, the U.S. Geological Survey, and the U.S. Departments of Defense or Energy. EPD may consider models developed using other software, if documentation is provided to EPD demonstrating the software has been verified, peer-reviewed and well documented. If the software is required to review the model and the software cannot be obtained without cost, a copy of the software and a license to view the software must be provided to EPD. Any analytical model must meet regulatory and program-specific requirements.

6.0 CONSTRUCTION OF THE MODEL

Inputs should be based on field data and, in some cases, appropriate peer-reviewed literature values. The use of literature values may depend on how sensitive the model is to the particular parameter, whether the approach is conservative (*i.e.*, will result in over-estimated rather than under-estimated contaminant concentrations and contaminant migration), and in some cases, whether there are field methods to reliably obtain the data. Inputs may need to be adjusted to calibrate the model. The modeler should demonstrate that final values lie within a reasonable range (e.g., physically realistic for the conditions). The values of all inputs for each model, node, or cell should be specified in tabular, graphical, or map format. The source of the values should be specified. Any methods used to process field-measured data to obtain model input should be specified and discussed in the report.

The design of the groundwater model should adequately represent the data available for modeling and the conceptual site model, and meet the modeling objectives. Where applicable, the model design should include, but not be limited to:

- Model layering and grids
- Aquifer and confining unit hydraulic properties
- Boundary conditions
- Aquifer recharge and discharge
- Interactions between groundwater and surface water
- Groundwater flow and chemical interactions with the aquifer(s) that cause retardation of constituent movement
- Baseline Stresses such as existing groundwater pumping from wells
- The ability of the model to run steady state or transient simulations or both
- Other pertinent features of the model

Basic aspects of hydrogeology that should be considered in constructing a model are presented in Appendix A of this Guidance.

6.1 Model Layering

Some models consist of a single layer and some consists of multiple layers to represent an aquifer system. Model layers and identification of confined and unconfined aquifers should be consistent with the site hydrogeology represented in the CSM. If the aquifer system consists of multiple layers, and the software can only model a single layer, multiple models may need to be run for each layer in the aquifer system. If a CSM indicates that there are multiple layers within the aquifer system through which contaminant transport may occur, it may be better to use alternate software capable of modeling multiple layers. Grids (where used) should be spaced adequately to provide the required level of model output detail, appropriate aspect ratios, and aligned consistent with boundary conditions.

6.2 Aquifer and Confining Unit Hydraulic Properties

Hydraulic properties are the aquifer properties that regulate the transmission and storage of water and movement of constituents in those media such as:

- Horizontal Hydraulic Conductivity (K_h)
- Vertical Hydraulic Conductivity (K_v)
- Transmissivity (T)
- Total Porosity (n_t)
- Effective Porosity (n_e)
- Saturated Thickness of Aquifer (b)
- Seepage Velocity (V_{sx})
- Darcy Velocity (V_x)
- Specific Yield (S_y)
- Storativity/Storage Coefficient (S)
- Specific Storage
- Streambed Conductance
- Leakance
- Bulk Density (ρ_b)
- pH
- Fraction of Organic Carbon (f_{oc})

Some models may include other hydraulic properties that are not listed above. Hydraulic properties used in the model should be consistent with peer-reviewed publications or field measured values, or both.

Key input parameters for modeling fate and transport of organic and inorganic contaminants are f_{oc} and pH, respectively. Contaminant fate and transport models are often very sensitive to these parameters. Therefore, values of these parameters must be justified and conservative.

6.3 Boundary Conditions

Types of boundaries that should be evaluated include constant head, impermeable, constant flow, variable head, and mixed. Examples of boundaries include: surface water bodies, rivers, geologic structures, injection barriers, and ground water divides. Boundary conditions are represented by mathematical expressions of a state of the physical system that refine the equations of the mathematical model.

Selection of boundary conditions may have profound effects on model simulations. A model may yield biased or erroneous results if wrong boundary conditions are used. Boundaries of the modeled domain should preferably be, or correlate with, existing physical boundaries. Groundwater divides may at times be chosen as domain boundaries, but they are not fixed physical boundaries in that they can change location or disappear as a result of different stresses upon the hydrologic system. Accordingly, the use of a groundwater divide as a model boundary may produce inconsistent or errant results. It is appropriate that only existing natural hydrogeologic boundaries be represented in a model. This is possible in analytical models and large regional numerical models that incorporate distant flow boundaries. However, many smaller site-specific numerical models employ grid systems that require an artificial boundary be specified at the edge of the grid system. In these instances, the grid boundaries should be sufficiently remote from the area of interest so that the artificial boundary does not significantly impact the predictive capabilities of the model. When using artificial boundaries, the effects of boundary conditions on a particular area can be tested by adjusting the boundary conditions to determine the effects on model results.

6.4 Aquifer Recharge and Discharge

Where applicable, aquifer recharge and discharge rates and volumes should be consistent with the CSM and how interactions between groundwater and surface water were modeled. Recharge can be simulated using specified head or flow boundaries, or by specifying recharge to be a surficial layer of a numerical model. Not all modeling programs will allow for input of recharge.

6.5 Chemical Properties and Transport Processes

Physical- and chemical-property values may include, but not necessarily be limited to:

- Retardation Factors (R) and Parameters Used to Calculate Retardation Factors:
 - Aquifer Matrix Bulk Density (ρ_b)
 - Adsorption Coefficient
 - Fraction of Organic Carbon (f_{oc})
 - Normalized Distribution Coefficient for Organic Carbon (K_{oc}),
- Dissolved Plume Solute Half-Life ($t_{1/2}$)
- First Order Chemical Decay Coefficients (λ)
- Dispersion Coefficients (α_x , α_y , and α_z)
- pH

6.6 Baseline Stresses

Baseline stresses are currently operating influences on the hydrogeologic system and can include anthropogenic influences. Baseline stresses may include, but are not limited to:

- Contamination Concentrations
- Source Loading of Contaminants
- Groundwater Pumping or Injection
- Natural or Man Induced Recharge
- Hydraulic Barriers
- Groundwater Interaction with Surface Waters
- Underground Utilities, Structures, Tunnels, and Drainage

Baseline stresses may be constant over time or may change. Values of baseline stresses on the hydrogeological system within the modeled area can also be manipulated during calibration in an attempt to match predicted values from calibration runs with field data.

6.7 Steady State or Transient Simulations

If the model will be used for transient predictive simulations of contaminant fate and transport (*i.e.* predictive simulations that change over time), then the time steps used in the transient predictive simulations should be sufficient to obtain accurate iterative solutions and to adequately simulate variations of contaminant concentrations over time. The model should also simulate maximum possible contaminant concentrations at point of demonstration wells and other pertinent possible receptors. A steady state model can be used if the objective of modeling is to predict what the maximum contaminant concentration may be at the point of interest, regardless of how long it takes the maximum concentration to occur. Steady state modeling should be done in a way to predict the maximum plume concentration. A transient model can be used if the objective of modeling is to predict how long it may take a maximum concentration to occur at a specified location.

7.0 MODEL CALIBRATION

Calibration consists of changing values of model input parameters so that simulated values match measured values within acceptable and pre-established calibration criteria.

7.1 Method of Model Calibration

Calibration should proceed by first changing those parameters with the lowest level of accuracy, and then fine-tuning the simulation by adjusting other parameters. Typically, the model parameters with the greatest uncertainty, including those that are not easily measured or can have significant spatial variability, are used for initial adjustment in calibration. Complexity of the parameter adjustments should increase slowly. Parameters should be adjusted within a reasonable, limited range relative to field measured or literature values or both. Criteria for an acceptable calibration can be defined in a quality assurance plan. The rationale and assumptions used to adjust hydrogeological parameters during calibration should be presented in the modeling report. Calibration requires that field conditions be properly characterized. Lack of proper characterization may result in a calibration to a set of conditions that do not represent actual field conditions.

The model calibration method should include:

- Setting pre-simulation calibration targets and criteria from which to judge the acceptability of the calibration
- Performing the calibration process
- Evaluating the level of calibration based on the stated targets and criteria

The objective of the calibration process is to obtain acceptable agreement between model calculated values and corresponding measured values. The calibration process systematically varies model parameters within predetermined ranges based on site data and professional judgment to obtain this agreement.

Since the goodness-of-fit of the model is defined by comparing simulated values to corresponding measured values, a quantitative measure of this fit needs to be developed. This measure is defined as an objective function.

The overall model calibration process can be conducted in three steps:

- Calibration to a representative steady-state period
- Calibration to a representative transient period
- Verification of calibration to the full study period

The calibration process can proceed by first approximating model parameters using a steady state calibration period. The model parameters from the steady-state calibration can then be used as initial estimates for the transient calibration period to refine the model. Finally, the calibrated model can be run over the entire study period to verify that acceptable agreement between the model and field data has been reached.

In the steady-state mode, all the model parameters are fixed and do not vary with time. Annual averaged groundwater levels can be used or approximated. Simulated contaminant concentrations can be compared to measured concentrations in a stabilized plume. In the transient calibration, the model output for various time steps can be compared to measured time-series values, such as water levels that vary monthly, seasonally, or during the course of a pumping test, and time-series contaminant concentrations of groundwater samples.

The calibration can be done manually or automated. Manual “trial and error” calibration involves making small changes to the input files, running the model, and assessing the improvements made in matching simulated values to corresponding measured values. For numerical models this may include matching hydraulic heads, hydraulic gradients, streamflow gains

and losses, water mass balance, contaminant concentrations, contaminant migration, and contaminant degradation. For analytical models this may include matching seepage velocities and contaminant concentrations.

Trial and error calibration can be time consuming, but it allows the modeler to inject knowledge and understanding of the hydrogeological system into the calibration process. In trial and error calibration, modelers have the ability to continuously change the conceptualization of the system and parameter distributions in order to improve the calibration. The insight and skill of the modeler during a trial and error calibration can control how well a model represents the groundwater system under investigation. In evaluating the adequacy of a model calibration, the conceptual model and the insight of the modeler can be as important as evaluation of quantitative measures of goodness of fit.

A recent development is the automated estimation of parameters by computer algorithms that will optimize the calibration of models. These techniques are based on minimizing an objective function. The larger the computed objective function is, the greater the discrepancy between simulated values and corresponding measured values. A key concept in automatic parameter estimation methods is that a limited set of parameters used in the model is designated to be automatically adjusted. These parameters usually are identified for specific regions of the model that are determined before the calibration process. The parameters and boundary conditions that are not identified for automatic calibration either remain fixed at their initial values or must be calibrated by trial and error.

Automated calibration techniques will find the optimal set of parameter values that result in a minimal value of the objective function. Such techniques can save a modeler time in the calibration process. A drawback to automated calibration is that a computer algorithm only knows as much about the hydrogeological system as the modeler is able to tell it. Sometimes the computer algorithm can move too far from known data in an effort to closely match measured values. The automated techniques can yield unreasonable results if insufficient constraints are supplied.

Contaminant transport models require that the groundwater flow field first be evaluated. Groundwater transport model calibration will require a minimum of two discreet sampling events from an appropriate time interval from the site. Calibrating a groundwater transport model using too few sampling events, or sampling events at short time intervals, can lead to serious errors in predictive calculations. The modeling report must justify the field data used to calibrate a contaminant transport model.

The modeler should avoid the temptation of adjusting model input data on a scale that is smaller than the distribution of field data. This process, referred to as "over calibration", can result in a model that appears to be calibrated but has been based on a dataset that is not supported by field data.

A groundwater model may inadequately assess model calibration. This deficiency may be due to the absence of clearly stated calibration targets and a failure to quantitatively assess the level of calibration achieved. Two common problems are strong indicators of model error:

- The model does a poor job of matching observations
- The optimized parameter values are unrealistic and confidence intervals on the optimized values do not include reasonable values

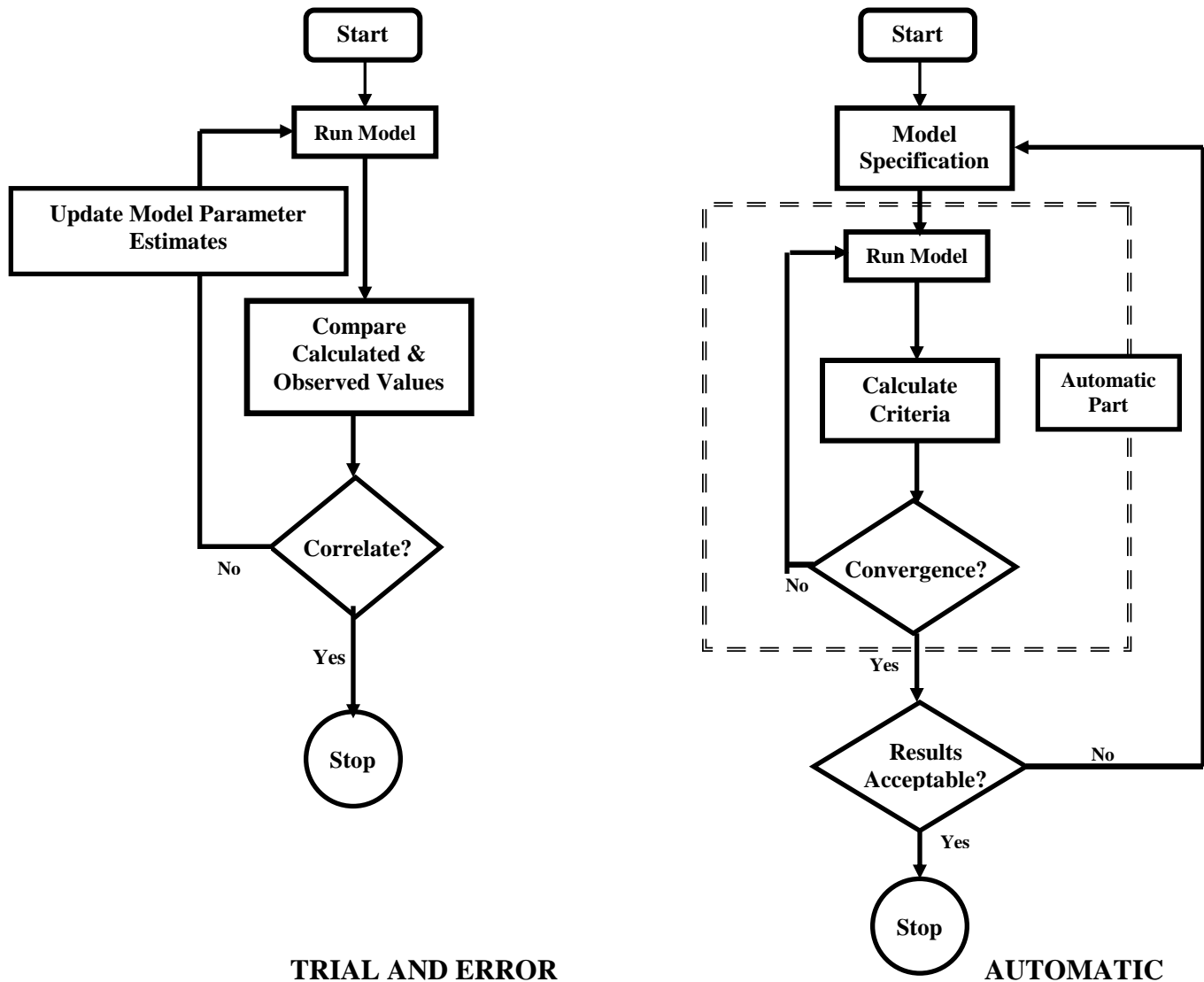


Figure 7-1: History Matching/Calibration Using “Trial and Error” and Automatic Procedures. [Modified from van der Heijde, et. al. (1988) after Mercer and Faust (1981).]

The level of model calibration should be defined:

- Level 1: Simulated value falls within target (highest degree of calibration).
- Level 2: Simulated value falls within two times the calibration criterion.
- Level 3: Simulated value falls within three times the calibration criterion.
- Level N: Simulated value falls within N times the calibration criterion (lowest degree of calibration).

Just because a model is calibrated does not ensure that it is an accurate representation of the hydrogeological system. The appropriateness of the conceptual model of the hydrogeological system is frequently more important than achieving the smallest differences between simulated and measured values. If a groundwater model is to have credibility it must respect what is known about the system hydrogeology. While the measures of calibration might make a model appear to be well-calibrated, the violation of a reasonable conceptual model may make the model a poor model. During model calibration the conceptual model of the hydrogeological system should be evaluated and adjusted as needed.

A model developed according to a well-argued conceptual model with minor adjustments may be superior to a model that has smaller discrepancies between simulated values and corresponding measured values resulting from unjustified manipulation of the parameter values. As calibration proceeds, data gaps often become evident. The modeler may have to redefine the conceptual model and collect more data. When the best calibrated match is achieved, a final input data set should be established and demonstrated to be reasonable and realistic.

The modeling report must document the level of calibration achieved for the model. Documentation of the calibration should include listing of the calibration targets, number of nodes used for calibration, objective functions for calibration targets, and the percentage of the total number of simulated values falling within an objective function. This information should be presented in the report at least in tabular form. The distribution of the levels of calibration should be shown graphically in map form in the modeling report.

7.2 Calibration Targets

A calibrated model simulates historical conditions within an acceptable range of uncertainty, which needs to be defined before the model is calibrated. A groundwater model can be calibrated by comparing simulated values with corresponding measured values. The measured values used for comparison against simulated values are termed calibration targets.

Calibration targets are defined in terms of the type of measurement, its location and date of measurement, and measurement value. An objective function is a measure of the fit between simulated values and corresponding measured values. The model parameters modified during calibration are typically those that have the largest uncertainty and impact the objective function value as they are varied.

Different calibration targets would be used for calibration of analytical and numerical models. For some analytical models, calibration targets may be limited to groundwater seepage velocities and contaminant concentrations. For numerical models calibration targets can include the following:

- Steady state or transient hydraulic heads
- Groundwater-flow direction
- Hydraulic gradient
- Water mass balance
- Streamflows
- Streamflow gains and losses
- Contaminant concentrations
- Contaminant migration rates
- Contaminant migration directions
- Contaminant degradation rates
- Contaminant mass balance

The calibration data set should include measurements over the lateral and vertical extent of the model area. For a flow model these data will often consist of water level measurements from monitoring wells and piezometers. Contaminant concentrations measured in groundwater samples can be used to calibrate a contaminant transport model.

The relative importance of the calibration targets can be incorporated through weighting factors assigned to each class of calibration targets. The weighting factors should represent an estimate of the measurement error for each calibration target. Errors must be an estimate of the underlying accuracies of the measurements and not a measure of variation in the measurements over

time. Weighting factors can be applied to account for factors such as clustering of observations in time or space.

In the case where parameters are well characterized by field measurements, the range over which that parameter is varied in the model should be consistent with the range observed in the field. The calibration target size may be too large and/or the number of targets too few or poorly distributed, thereby introducing additional uncertainty into the model results. Using multiple calibration targets increases the confidence that the model accurately represents the stresses imposed on it.

7.3 Calibration Criteria and Quantitation of Calibration

Calibration is evaluated by analyzing the residuals, or differences between simulated values and corresponding measured values, at specific locations and times. Criteria for achieving and documenting model calibration can be established in a quality assurance plan.

The degree of fit between model simulations and field measurements is the objective function which can be quantified by statistical means. Prior to calibration of the model, appropriate calibration targets should be selected from the available field data. The calibration criteria must be defined along with the rationale for establishing when a model is calibrated, and when calibration efforts should be terminated.

Calibration is by its nature non-unique. Many combinations of model parameters may result in a model that fits the field data. The modeling report must justify the model parameters used in the calibrated model. It is best if the parameters are consistent with measured or literature values or both. If model parameters used in the calibrated model are not consistent with measured or literature values, the modeling report must document how the use of these parameters may compromise the usefulness of the model.

Model calibration is evaluated by considering the magnitude of the residuals and their distribution both statistically and relative to independent variable values such as location and time. There are different quantitative criteria that can be used to demonstrate calibration of a steady-state or transient groundwater model. These may include:

- All hydraulic head residuals are within a pre-established range.
- The average and standard deviation of hydraulic head residuals is below a pre-established value.
- Average and standard deviations of head-dependent boundary flow residuals are below pre-established values.
- Magnitudes and directions of hydraulic head gradient residuals are within a pre-established range.
- All residuals of hydraulic heads between model layers are within a pre-established range.
- Average and standard deviations of residuals of hydraulic heads between model layers are below pre-established values.
- The number of flooded and dry cells within the model domain will be less than a defined percent of the model cells in the active model domain and will be randomly distributed.
- All streamflow and streamflow gain and loss residuals are within a pre-established range.
- Average and standard deviations of streamflow and streamflow gain and loss residuals are below pre-established values.
- Mass balance of the groundwater flow into and out of the modeled system is below a pre-established error value.

- All contaminant concentration residuals are within a pre-established range.
- The average and standard deviation of contaminant concentration residuals is below a pre-established value.

In initial model runs, large residuals or a bias in the distribution of residuals can indicate gross errors in the model, the data, or how values were simulated. For steady-state simulations, residuals would be calculated for specific locations within the model domain. For transient simulations residuals would be calculated for specific locations within the model domain at specific times.

The areal distribution of residuals is also important to determine whether some areas of the model are biased either too high or too low. Positive and negative residuals for hydraulic head, groundwater flow, contaminant concentration, and other calibration targets should be randomly distributed on a geographic and temporal basis.

The objective functions define the acceptable differences between the measured and simulated values for each calibration target. Documenting the degree of model calibration is important since it helps demonstrate how well the model estimates reality. Comparisons between simulated values and corresponding measured values should be presented in maps, tables, or graphs. Locations of point measurements used to set calibration targets should be presented in map form to illustrate the relative locations of targets and nodes. Ideally, a selected calibration value should be measured at a large number of locations, uniformly distributed over the modeled region, and have small associated error.

Hydraulic head measurements or contaminant concentrations can be presented in the form of contour maps and cross sections of observed and simulated values. The general shape of the calibrated potentiometric surface should be similar to observed site conditions including mounds, depressions, and general flow directions. A mass balance of water flow and contaminant mass should be presented for the calibrated model.

Statistical evaluations of residuals should be presented in tabular and graphical formats. An x-y scatter plot of observed versus simulated heads will show the magnitude and bias in residuals. An example of such a plot is shown in Figure 7-2.

There are no universally accepted “goodness-of-fit” criteria that apply in all cases. However, it is important that the modeler make every attempt to minimize the difference between model simulations and measured field conditions. For instance, a criterion for calibration may be that residuals are less than 10 percent of the variability in the field data across the model domain.

Measures of model calibration can be expressed as lumped parameters such as the mean of the absolute value of the differences, root mean square, absolute value of the mean differences, or the mean difference between simulated and measured values. While easy to calculate, lumped parameters are only a gross indication of the calibration because they hide poorly calibrated portions of the model *via* the averaging process. Lumped parameters may give no indication of the spatial variability of calibration results, and therefore should not be used as the only demonstration of model calibration.

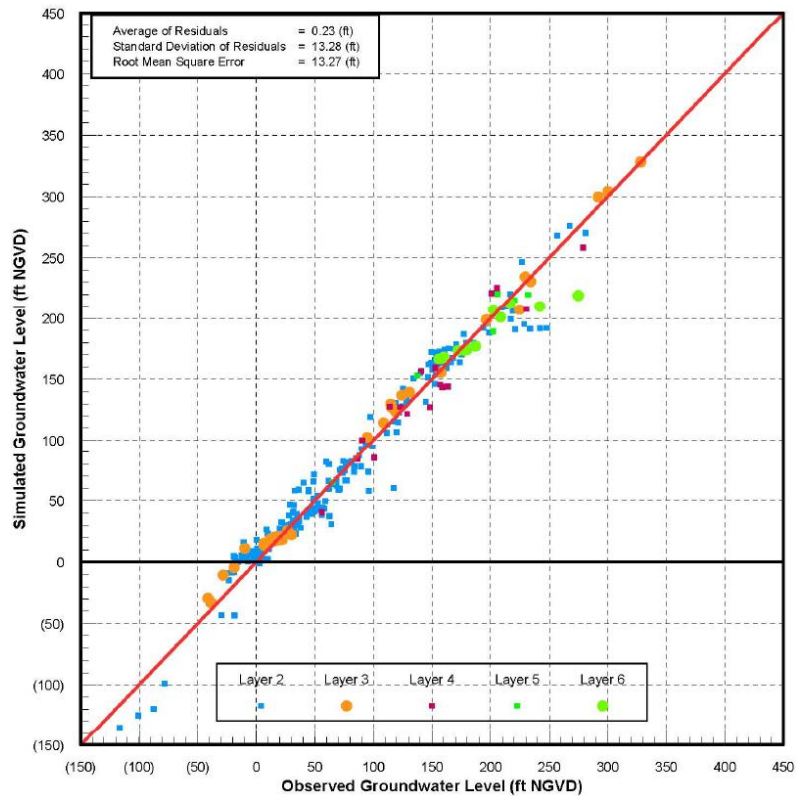


Figure 7-2: Residual Scatter Plot Example

7.4 Degree of Model Calibration

There can be three basic applications of a groundwater model:

- Predictive simulations of groundwater flow and contaminant transport
- Interpretative simulations used as a framework for studying dynamics of the hydrogeological system, identifying data gaps, and planning field data collection efforts
- Generic simulations used to interpret hypothetical conditions of the hydrogeological system

For predictive simulations to be acceptable the groundwater model must be calibrated and calibration of the model must be documented in the modeling report. Interpretative simulations do not necessarily require model calibration and generic simulations can be done when there are no comparative data for model calibration. It may be possible to use un-calibrated numerical or analytical models for interpretative or generic simulations, but not for acceptable predictive simulations.

Numerical groundwater flow and contaminant transport models can usually be calibrated sufficiently to use for acceptable predictive simulations. It may be more difficult to calibrate analytical models due to the limited number of model parameters that can be adjusted to achieve calibration. It may be possible to calibrate an analytical model of a linear groundwater flow system, with relatively short flow paths, in a single-layer aquifer with homogenous aquifer properties and consistent contaminant source concentration and transport properties under steady-state conditions. It may be difficult to calibrate an analytical model of a non-linear groundwater flow system with longer flow paths in a single- or multi-layer aquifer with varying aquifer properties, contaminant concentrations, or contaminant transport properties.

It may not be possible to calibrate a groundwater model because of:

- The type of model developed (analytical versus numerical)
- The complexity of the model (model layers, model dimensions, heterogeneity of hydraulic and contaminant concentration or transport properties, steady-state versus transient capabilities)
- Inadequacy of the conceptual site model
- Insufficient data for model calibration
- A lack of time or project budget for model calibration

If, for any reason, a groundwater model cannot be calibrated, the modeling report must demonstrate that predictive simulations made with the un-calibrated model were sufficiently conservative to allow the modeling results to be used to meet project objectives.

Overly conservative estimates of groundwater flow or contaminant transport may result in higher costs for remedial action scenarios to meet compliance or clean up objectives. Refinement of a groundwater model may avoid such overly conservative estimates. A model may be refined by:

- Using a numerical rather than an analytical model
- Developing a more complex model to accommodate complexities or temporal variations in the hydrogeological system
- Collection of sufficient site-specific data to refine the CSM and to allow for adequate model calibration
- Running transient rather than steady-state simulations
- Allowing sufficient time and project budget for model calibration

In some situations the cost of refining a groundwater model may be a fraction of the cost needed to deal with overly conservative estimates of groundwater flow or contaminant transport.

7.5 Calibration of Analytical Models

The preceding details of Section 7.0 apply best to calibration of sophisticated numerical models. Some of the details can apply to an analytical model, but most analytical models do not have the same or as many aspects of model construction, model input parameters, and boundary conditions with which to make calibration adjustments. It is often said that an analytical model does not have as many “calibration dials” as a numerical model.

Some of the calibration methods described in the section can be applied to an analytical model, but this depends on how many and what types of calibration dials are available in the analytical model. Calibration of an analytical model must be designed based on the available calibration dials.

For instance, the analytical code BIOCHLOR, developed by AFCEE and available on the CSMoS website allows for input of single values of aquifer hydraulic conductivity, hydraulic gradient, aquifer porosity, dispersivity, soil bulk density, and fraction organic carbon. First-order decay coefficients can be specified for two zones within the modeled domain. BIOCHLOR does not allow for multiple aquifers, specification of aquifer thickness and geometry, varying aquifer properties, boundary conditions, recharge, surface water-groundwater interactions, or transient conditions. While a model developed using BIOCHLOR cannot be calibrated to measured hydraulic heads, it could be calibrated by adjusting the input parameters until simulated constituent concentrations reasonably match measured concentrations.

Because of the limited number of calibration dials in an analytical model such as BIOCHLOR, it may not be possible to reasonably adjust input parameters so that simulated constituent concentrations reasonably match measured concentrations. In this case, use of a more sophisticated numerical model with more calibration dials should be considered.

The analytic element modeling (AEM) module of the Groundwater Modeling System (GMS) graphical user interface for MODFLOW allows for specification of more input parameters than BIOCHLOR such as specified head boundaries, aquifer thickness, rivers, recharge, and production wells. The AEM software is limited to single-layer, steady-state models so there may still be limitations in fully depicting a CSM. However, an AEM model can have more calibration dials than a BIOCHLOR model.

Section 7.3 presented information on quantitation of calibration. Because output is limited for some analytical models, quantitation of calibration can be difficult. However, even in an analytical BIOCHLOR model, quantitative comparisons can be made between simulated and measured constituent concentrations. In an AEM model simulated hydraulic heads and stream flows can be quantitatively compared to measured hydraulic heads and stream flows. Consequently, quantitative metrics of calibration residuals can reflect limitations in output from analytical models.

If an analytical model cannot be calibrated to the degree described in this section the modeling report must document that calibration, to the degree it was completed, was sufficient to meet the modeling objectives. Documentation of calibration can include, but may not necessarily be limited to:

- Comparison of simulated concentrations at specific locations to measured concentrations at the same locations (e.g. such as could be done with BIOCHLOR or BIOSCREEN).
- Comparison of simulated hydraulic heads and water fluxes to measured hydraulic heads and water fluxes (e.g. such as could be done with GMS AEM and Visual AEM).
- Comparison of simulated recovery well capture zones to measured recovery well capture zones (e.g., such as could be done with WHAem).
- Comparison of simulated groundwater concentrations resulting from soil leaching to measured groundwater concentrations between leaching areas (e.g. such as could be done with VLEACH or SESOIL).

With an analytical model with limited calibration dials, conservative simulations (*i.e.*, overestimating the rate or extent of constituent movement) can sometimes be run in *lieu* of developing a more complex model with more calibration dials. Documentation of matches between simulated and measured parameters should be done graphically (by means of comparing model output to maps of hydraulic heads or contaminant concentrations) or in tables.

8.0 DATA SENSITIVITY ANALYSIS

Sensitivity analysis is performed to determine the relative impact of changes in model input parameters on model output. Some input parameters are more important in determining model outcome than other parameters. Their relative importance can be influenced by site-specific conditions and the properties of the contaminants being modeled. Sensitivity analysis can also be used to help quantify the uncertainty in model prediction due to uncertainty in an input parameter. For example, if a potentially sensitive parameter is varied over an expected range of possible values, a range of model outcomes is produced, and inferences can be made about uncertainty in the model predictions due to uncertainty in that parameter. For example: f_{oc} can be a sensitive parameter when modeling the fate and transport of organic contaminants as shown in Appendix A in the example using BIOCHLOR. The modeler is also able to select values from the range for use in the final model that are demonstrated to be conservative.

A model is considered sensitive to an input parameter if a small change in the parameter causes a large change in the model prediction. The sensitivity of a given parameter largely depends on its role in the governing equation of the model. However, site-specific conditions, including the properties of the contaminant being modeled, can also impact the relative importance of some input

parameters, so care should be taken to perform the sensitivity analysis for a model that is calibrated for a given site rather than relying on past experience with the model at other sites.

Many input parameters used in fate and transport models actually result from analysis of an observed range of field measurements or from a range of values published in professional journals and reports, so it is clear that many model inputs are subject to uncertainty. Sensitivity analysis attempts to make clear the significance of choosing a particular value from that range of possible values for a given parameter. A procedure for using sensitivity analyses to determine how model output varies as the range of parameter values is used is presented in Foster-Wheeler (1998) and includes the following steps:

- Identify input parameters for which a range of reasonable values exists.
- Conduct model runs varying the value of the target input parameter while holding values of other input parameters constant. Vary the target input value by both increasing it and decreasing it by a small percentage or fraction.
- The number of model runs needed to determine sensitivity of an input parameter will depend on how the parameter is incorporated into the solution of the governing equation. Fewer model runs are needed if the input parameter is used in a linear form than if it is used as an exponent, raised to a power, used as a logarithm, or incorporated into a functional transformation.
- Compare model runs by calculating the percent change in the concentration predicted by the model as the target input parameters are varied to identify the most and least sensitive input parameters for the model.
- If model output is only slightly sensitive to the range of reasonable values used for an input parameter, there is generally little or no need for additional effort to better define the value. On the other hand, if model output is highly sensitive to an input parameter, it may be helpful to obtain more field or laboratory measurements of the parameter, reducing uncertainty in that parameter and consequently reducing uncertainty in the model prediction.

The relative sensitivity of model results to each tested model input parameter and boundary condition must be documented. Failure to conduct a sensitivity analysis and/or provide adequate documentation could invalidate modeling results, leading to the rejection of the entire modeling effort by EPD.

9.0 MODEL VERIFICATION AND VALIDATION

9.1 Model Verification

Model verification is a test of whether the model can be used as a predictive tool, by demonstrating that the calibrated model was an adequate representation of the physical and chemical system. The common test for verification is to run the calibrated model in predictive mode to check whether the prediction reasonably matches the observations of a reserved data set deliberately excluded from consideration during calibration.

9.2 Model Validation

Model validation is intended to ensure that the model represents and correctly reproduces the behavior of the system being modeled. Although model validation does not imply model verification, often validation is interchanged with verification since model results are usually compared to measured data from the system being modeled. If model results are proven to be insensitive to variation of input parameters that cannot be verified, a calibrated but unverified model

may be used to model fate and transport of constituents¹. The validation process consists of applying a calibrated model to a set of input parameter values and boundary conditions separate from the set used for calibration to reproduce an independent set of observations, typically the hydraulic head or solute concentrations over a different time period². If a calibrated model can approximate the measurements from the represented system within an acceptable range, the model is validated as a satisfactory representation of the system.

Depending on the types of models (*i.e.* analytical model and numerical model), the number and extent of calculations and measurements to validate a model would be different. For example, the validation of a simple analytical model can be done by comparing model output to independent calculations using a spreadsheet. Because an analytical model will not account for field conditions that change with time or space, validation parameters for an analytical model may be more limited than those of a numerical model that is used to predict spatial and temporal changes in dissolved constituent concentrations. The validation of numerical models can be done by determining concentrations of dissolved constituents at locations where initial concentrations are not known, and by time-series sampling at locations where initial conditions are known¹. For the model composed of a combination of independent equations, several independent calculations may be needed to validate a single model output¹. A detailed discussion of the validation processes, assumptions, and derivations of groundwater models is beyond the scope of this document. Therefore, the reader should use and document the published references for this information.

10.0 PREDICTIVE SIMULATIONS

Upon completing calibration, sensitivity analysis, and verification of the model, can be used to predict future scenarios. Such simulations may be used to estimate:

- The hydraulic response of a hydrogeological system to changes in groundwater withdrawals, boundary conditions, and recharge
- Migration pathways of contaminants
- Contaminant retardation and decay along migration pathways
- Changes in contaminant concentrations in groundwater due to changes in contaminant source concentration or changes in contaminant mass loading rates to groundwater
- Contaminant mass removal rates as a result of remedial action scenarios
- Concentrations of a contaminant at points of compliance at future moments in time

Predictive simulations may either be run when using a model in steady-state or transient mode. In the steady-state mode all the model parameters are fixed and do not vary with time, whereas in the transient mode certain parameters such as rainfall, evapotranspiration, pumping rates, contaminant source concentrations, contaminant mass loading rates to groundwater, and other parameters are varied to generate variations in hydraulic heads or contaminant concentrations, or both. Predictive simulation conditions that are vastly different from the model calibration and validation conditions, such as high pumping rates or drawdowns, high contaminant concentrations, or vastly different contaminant retardation or decay properties, may invalidate the model as a representation of the hydrogeological system.

Predictive simulations can be:

- Groundwater flow simulations
- Contaminant transport simulations
- A combination of groundwater flow simulation and contaminant transport simulations

¹ American Society for Testing and Materials (ASTM), 1999: RBCA Fate and Transport Models: Compendium and Selection Guidance.

² Michigan Department of Environmental Quality, 2002: Groundwater Modeling Guidance.

Predictive groundwater flow simulations can be run in steady-state mode, where dynamic equilibrium is achieved. Transient groundwater flow simulations can be run to simulate multiple time periods when stresses on the aquifer such as groundwater withdrawals, boundary conditions, and recharge may change.

Predictive contaminant transport simulations may be run until the contaminant plume has reached steady-state (or near steady-state) conditions. Assuming the source and mass loading of the contaminant to groundwater remains constant (or near constant), at some moment in time the contaminant plume will reach a maximum size and the shape of the plume will remain relatively fixed for future times. Running steady-state contaminant transport simulations requires running the groundwater flow simulation in steady-state mode using average hydrogeological conditions. Because the time span of groundwater contaminant travel is usually measured in years, over the span of multiple years the seasonal groundwater flow variations can be averaged out so that performing transport models with a transient groundwater flow model may not be required.

Transient contaminant transport predictive simulations should be used *if* there will be noteworthy changes in groundwater withdrawals, model boundary conditions, or recharge, *or* changes (increases or decreases) in contaminant source concentrations or mass loading rates to groundwater. Transient contaminant transport predictive simulations can also be used to predict the effects of remedial action scenarios on groundwater flow and contaminant concentrations.

Transient numerical simulations would allow aquifer stresses and contaminant source concentrations and mass loading rates to be varied over time. Analytical models typically cannot accommodate temporal variation of parameter inputs. Analytical models require input of specific hydraulic properties, aquifer stresses, contaminant concentrations, contaminant transport properties such as retardation and decay rates, and a simulation time for each individual simulation. Model inputs can be varied incrementally for a series of individual simulations to generate pseudo-transient groundwater flow and contaminant transport simulations.

Pseudo-transient contaminant transport simulations may grossly over- or under-predict groundwater flow or contaminant transport or both. Pseudo-transient simulations should therefore not be used if there may be noteworthy temporal changes to groundwater flow or contaminant source or transport conditions. In such situations, transient numerical simulations would better predict groundwater flow and contaminant transport and would be more likely to achieve modeling objectives. Predictions generated using numerical simulations may also result in lower costs for remedial action scenarios needed to achieve compliance or cleanup goals.

If pseudo-transient analytical models are used to simulate groundwater flow and contaminant transport over varying time intervals, the modeling report must demonstrate that pseudo-transient simulations do not incorrectly predict groundwater movement or under predict contaminant concentrations at modeled locations and time intervals.

Predictive simulations should be viewed as estimates and not as certainties. There is always some uncertainty in predictive models. The simulations are based on the conceptual model, the hydrogeological and contaminant input parameters, and the model algorithms. The model's limitations and assumptions, as well as the differences between field conditions and the conceptual model will result in errors in simulations.

Time periods over which a model is calibrated may be small compared to the length of time used for predictive simulations. Relatively small errors observed during the time period over the model calibration may be greatly magnified during predictive simulations because of the larger time periods used in predictive simulations. The growth in errors resulting from projecting model simulations into the future may need to be evaluated by monitoring field conditions over the time period of the simulation or until appropriate cleanup criteria have been achieved.

11.0 UNCERTAINTY OF MODEL PREDICTIONS

The response of the model to various prediction scenarios should be presented in both narrative and graphical forms. Model predictions should be expressed as a range of possible outcomes, which reflect the uncertainty in model parameter values. The range of uncertainty should be similar to that used for the sensitivity analysis. Expression of model predictions as ranges is illustrated in Figure 11-1.

Predictive simulations may be conservative. That is, given the uncertainty in model input parameters and the corresponding uncertainty, model input values may be selected that result in a “worst-case” simulation. Site-specific data may be used to support more realistic predictive simulations. Site-specific data can be collected to limit the range of uncertainty in predictive simulations and to minimize the conservativeness of such simulations.

The cost of site-specific data collection may be a fraction of the cost of remedial action scenarios needed to deal with overly conservative estimates of groundwater flow or contaminant transport. In situations where long-term remedial action may be necessary, it may be useful to refine and update predictive simulations as additional data are collected and future aquifer stresses or contaminant source concentrations and mass loading rates are observed.

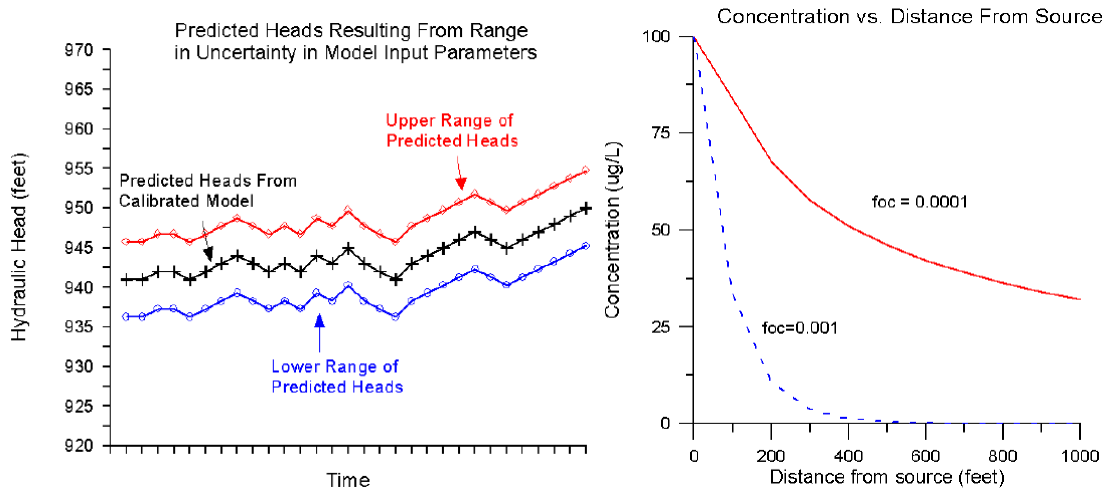


Figure 11-1 Examples of Graphical Representations of Ranges of Model Predictions

If a model was not adequately calibrated or verified, or the complexity of the model would not allow adequate calibration and verification, it must be documented that predictive simulations made with the model were sufficiently conservative (*i.e.*, tend to over-estimate rather than under-estimate contaminant migration) to allow the modeling results to be used.

12.0 PERFORMANCE/POST AUDIT MONITORING AND MODEL REFINEMENT

Groundwater models can be useful tools in simulating hydrogeologic conditions and contaminant concentrations over time. However, small errors in the predictive model may result in large errors when projected forward in time. Performance monitoring is required to compare future conditions with modeled conditions and assess errors in the model. Depending on purpose of the

model, and accuracy of the parameters used for simulation, an effective performance-monitoring plan, with submittal of regularly scheduled progress/performance reports, must be developed.

Errors in groundwater models become evident with the collection of additional data from effective performance monitoring. As additional data becomes available, the model should be refined to more accurately predict future conditions. The refined predictive model should be rerun based on the additional data and any changes to the original predictive model should be discussed in the appropriate progress/performance monitoring reports. A performance/post audit monitoring plan should be provided.

Some common Modeling Errors to Avoid include, but are not limited to:

- Units are inconsistent (For example, using standard and metric units without converting)
- Insufficient field data for calibration
- Insufficient boundary size and/or conditions
- Inaccurate hydrologic assumptions
- Incorrect sign for pumping or recharge
- Typographical errors or general mistakes in input values
- Using unrealistic input data that doesn't match the site
- Excluding data from wells with the highest contamination
- Improper selection and use of source and target wells
- Target wells clustered in only a small portion of the model
- Incorrect assumptions regarding the effect of soil/source removal on source area groundwater contamination. For example, assuming a 50% contamination loss in source well due to removal of overlying soil.
- Forcing data to fit using maximum or minimum ranges of input values
- Acceptance of model output without logical assessment

13.0 MODELING REPORTING REQUIREMENTS

Submittal of a stand-alone report, which may be included as an appendix to another submittal, as support documentation, to EPD will be required for all facilities requesting approval of groundwater modeling results. The report must be an all-encompassing document that contains enough information to allow EPD to duplicate the model if EPD finds that such an effort is necessary. This may require providing EPD with model input files and a table summarizing the input parameter values, the source/justification of these values, and sufficient output sheets to verify modeling objectives have been met. Appendix B provides two examples of such tables for BIOCHLOR and BIOSCREEN.

A groundwater modeling report must contain the following at a minimum:

- A general description of the mode.
- A demonstration that the model is appropriate
- A description of the scope of the model
- A description of the site environmental history
- A description of current groundwater conditions
- A list/table of model input values and their source/justification
- Any input values that are neither site-specific values *nor* reference values must be proven to be conservative
- A description of model calibration procedures
- A description and results of a sensitivity analysis
- A discussion of model results including, but not limited to:

- A discussion on how the plume will change through time and what to expect
- Output data should be presented in both tabular form and a printout of the output pages should be provided
- Supporting maps showing site details and output may provide a means of confirming the stated model objectives have been met, such as:
 - o Isopleth map showing anticipated maximum extent of contaminant plume
 - o Isopleth maps indicating incremental changes in plume configuration through time. Time increments should be based on the modeling objectives and correspond with proposed performance monitoring requirements
- Conclusions and recommendations for confirming the adequacy of the modeling effort or the need for additional modeling

14.0 SELECTED REFERENCES/SOURCES

American Society for Testing and Materials (ASTM). *Standard Guide for Defining Boundary Conditions in Ground-Water Flow Modeling*, ASTM D5609-94, Reapproved 2002.

American Society for Testing and Materials (ASTM). *Standard Guide for Calibrating a Ground-Water Flow Model Application*, ASTM D5981-96, Reapproved 2002.

Aziz, C.E., C.J. Newell, J.R. Gonzales, P. Haas, T.P. Clement, and Y-W, Sun, 2000. *BIOCHLOR, Natural Attenuation Decision Support System – User’s Manual, Version 1.0.*, EPA/600/R-00/008, Office of Research and Development, U.S. EPA (January 2000).

Aziz, C.E., C.J. Newell, and J.R. Gonzales, 2002. *BIOCHLOR, Natural Attenuation Decision Support System, Version 2.2, User’s Manual Addendum*, EPA/600/R-00/008, U.S. EPA (March 2002).

Bakker, M., S.R. Kraemer, W.J. deLange, O.D.L. Stack, 2000. *Analytic Element Modeling of Coastal Aquifers*, EPA/600/R-99/110, U.S. EPA (January 2000).

Bear, Jacob, M.S. Beljin, and R.R. Ross, 1992. *EPA Ground Water Issue - Fundamentals of Ground-Water Modeling*, EPA/540/S-92/005, U.S. EPA, April 1992.

California Environmental Protection Agency, 1995 *Groundwater Modeling for Hydrogeologic Characterization*.

Camp, Dresser & McKee, 2011. *Groundwater Flow Modeling of the Coastal Plain Aquifer System of Georgia*, June 2011.

Domenico, P.A., 1987. *An Analytical Model for Multidimensional Transport of a Decaying Contaminant Species*, Journal of Hydrology, 91:49-58.

Fetter, C.W., Jr., 1980. *Applied Hydrogeology*, Charles E. Merrill Publishing Company, Columbus, OH.

Fetter, C.W., Jr., 1999. *Contaminant Hydrogeology*, 2nd ed., Prentice Hall, Upper Saddle River, NJ.

Foster Wheeler Environmental Corporation, 1998. *RBCA Fate and Transport Models: Compendium and Selection*, ASTM, November 1998.

Freeze, R.A. and J.A. Cherry, 1979. *Groundwater*, Prentice-Hall, Inc., Englewood Cliffs, N.J.

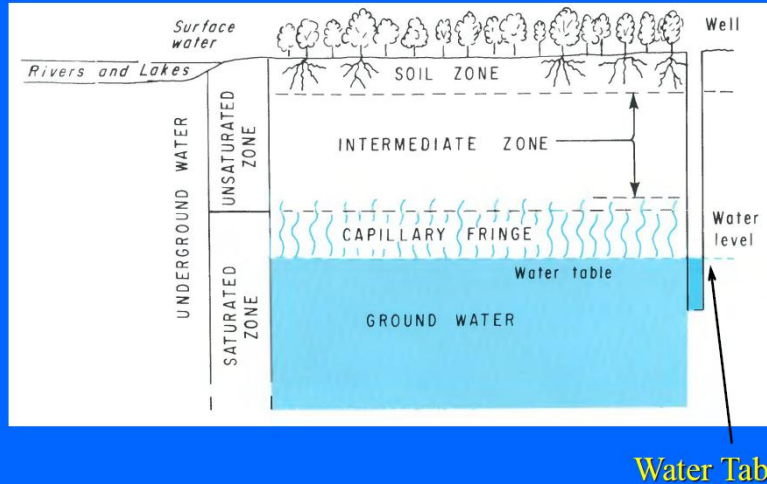
Heath, R.C., 1983. *Basic Ground-Water Hydrology*, United States Geological Survey (USGS) Water-Supply Paper 2220, USGS, Reston, VA.

- Howard, P.H., R.S. Boethling, W.F. Jarvis, W.M. Meylan, and E.M., Michalenko, 1991. *Handbook of Environmental Degradation Rates*, Lewis Publishing, Inc., Chelsea, MI.
- Interstate Technology and Regulatory Council (ITRC), 1999. *Technical/Regulatory Guidelines - Natural Attenuation of Chlorinated Solvents in Groundwater; Principles and Practices*, ISB-3, September 1999.
- Introduction to Fate and Groundwater Modeling Seminar, 1999, Georgia Ground Water Association, Doraville, Georgia
- Michigan Department of Environmental Quality. *Performance Monitoring and Model Refinement*, http://www.michigan.gov/deq/0,4561,7-135-3313_21698-55872--,00.html.
- Newell, C.J., Acree, S.D., Ross, R.R., and Huling, S.G., 1995. *EPA Ground Water Issue - Light Nonaqueous Phase Liquids*, EPA/540/S-95/500, U.S. EPA (July 1995).
- Newell, C.J., McLeod, R.K., and Gonzales, J.R., 1996 and 1997, *BIOSCREEN, Natural Attenuation Decision Support System User's Manual*, Versions 1.3 and 1.4 revisions: U.S. EPA Report No. EPA/600/R-96/087, August 1996 and July 1997.
- Ohio Environmental Protection Agency. *Technical Guidance Manual for Ground Water Investigations*, (Revision 1, November 2007), *Chapter 14: Ground Water Flow and Fate and Transport Modeling*.
- Schmelling, S. G. and R. R. Ross (1989). *EPA Superfund Ground Water Issue - Contaminant Transport in Fractured Media: Models for Decision Makers*, EPA/540/4-89/004, U.S. EPA.
- Solid Waste and Emergency Response, U.S. EPA, 1994. *OSWER Directive #9029.00 Assessment Framework for Groundwater Model Applications*, EPA 500-B-94-003, July 1994.
- Solid Waste and Emergency Response, U.S. EPA, 1994. *Ground-Water Modeling Compendium-Second Edition: Model Fact Sheets, Description and Cost Guidelines*, EPA 50-B-94-004, July 1994.
- United States Environmental Protection Agency (U.S. EPA). *Mid-Atlantic Risk Assessment Risk-Based Screening Level Tables (Generic)*, http://www.epa.gov/reg3hwmd/risk/human/rb-concentration_table//Generic_Tables/index.htm.
- United States Environmental Protection Agency (U.S. EPA). *Mid-Atlantic Risk Assessment Risk-Based Screening Level (RSL) Tables User's Guide*, http://www.epa.gov/reg3hwmd/risk/human/rb-concentration_table/usersguide.htm.
- United States Environmental Protection Agency (U.S. EPA). *EPA On-line Tools for Site Assessment*: http://www.epa.gov/athens/learn2model/part-two/onsite/rintro_onsite.html.
- United States Environmental Protection Agency (U.S. EPA). *Potential Limitations of Four Domenico-Based Fate and Transport Models*, <http://www.epa.gov/ada/csmos/domenico.html>.
- United States Environmental Protection Agency (U.S. EPA), 1989. *Statistical Analysis of Ground-Water Monitoring Data at RCRA Facilities*, EPA/530-SW-89-026. U.S. EPA, April 1989.
- United States Environmental Protection Agency (U.S. EPA), 1996. *Soil Screening Guidance: Technical Background Document*, EPA/540/R95/128. U.S. EPA, May 1996.
- United States Environmental Protection Agency (U.S. EPA), 1996. *Soil Screening Guidance: Users Guide, Second Edition*, Publication 9355.4-23, U.S. EPA, July 1996.

- United States Environmental Protection Agency (U.S. EPA), 1998. *Technical Protocol for Evaluating Natural Attenuation of Chlorinated Solvents in Ground Water*, EPA/600/R-98/128, U.S. EPA, September 1998.
- United States Environmental Protection Agency (U.S. EPA), 1999. *U.S. EPA Remedial Technology Fact Sheet –Monitored Natural Attenuation of Petroleum Hydrocarbons*, EPA/600/F-98/021, U.S. EPA, May 1999.
- United States Environmental Protection Agency (U.S. EPA), 1999. *U.S. EPA Remedial Technology Fact Sheet –Monitored Natural Attenuation of Chlorinated Solvents*, EPA/600/F-98/022, U.S. EPA, May 1999.
- United States Environmental Protection Agency (U.S. EPA), 1999. *Understanding Variation in Partition Coefficient, K_d Values, Vol. 1, The K_d Model, Methods of Measurement, and Application of Chemical Reaction Codes*, EPA 402-R-99-004A, U.S. EPA, August 1999.
- United States Environmental Protection Agency (U.S. EPA), 2002. *Supplemental Guidance for Developing Soil Screening Levels for Superfund Sites*, OSWER 9355.4-24, U.S. EPA, December 2002.
- United States Environmental Protection Agency (U.S. EPA), Technology Innovation and Field Service Division, *Capture Zone Analyses for Pump and Treat Systems Slide Presentation: http://cl-in.org/siteopt/proceedings_04/track_a/wed/07/supporting_slides.pdf, July 2008.*
- van der Heijde, P.K.M., A.I. El-Kadi, and S.A. Williams, 1988. *Groundwater Modeling: An Overview and Status Report*, EPA/600/2-89/028, U.S. EPA, December 1988.
- van der Heijde, P.K.M. and O.A. Elnawawy, 1993. *Compilation of Ground-Water Models*, EPA/600/R-93/118, Office of Research and Development, U.S. EPA, May 1993.

APPENDIX A: Basic Aspects of Hydrogeology

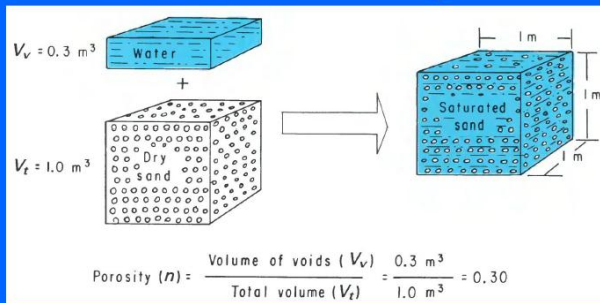
Water Table



USGS Water Supply Paper 2220 (1983)

The water table is where the hydraulic head is equal to one atmosphere. It is the level to which water will rise in a well open to the atmosphere and is below the top of the saturated capillary fringe. The top of the saturated capillary fringe is not the water table. Water in the capillary fringe is held at pressures less than one atmosphere so that capillary water cannot enter a well (*i.e.*, water will not run “uphill” from a pressure of less than one atmosphere to a pressure of one atmosphere).

Total Porosity

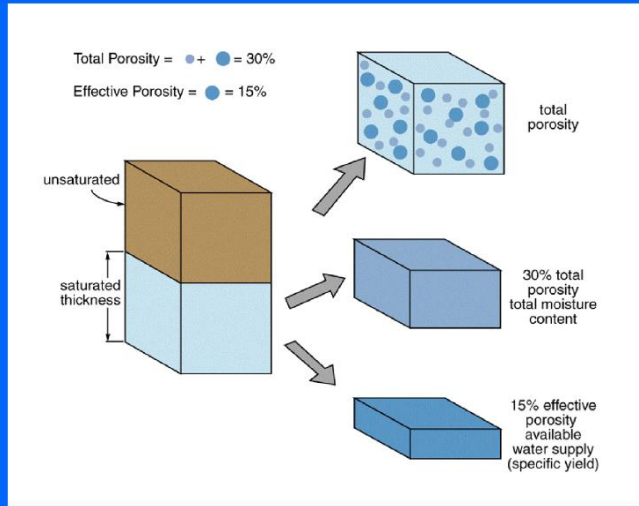


SELECTED VALUES OF POROSITY		
[Values in percent by volume]		
Material	Primary openings	Secondary openings
Equal-size spheres (marbles):		
Loosest packing	48	—
Tightest packing	26	—
Soil	55	—
Clay	50	—
Sand	25	—
Gravel	20	—
Limestone	10	10
Sandstone (semiconsolidated)	10	1
Granite	—	.1
Basalt (young)	10	1

USGS Water Supply Paper 2220 (1983)

Total porosity is the ratio of openings (voids) in a soil or rock to the total volume of the soil or rock. Total porosities of fine-grained materials such as clay can be very high due to the way that individual particles are packed within the soil. Total porosities of rocks are often smaller than total porosities of soils.

Effective Porosity



Effective porosity is the porosity through which groundwater movement occurs. Effective porosity is smaller than total porosity. In coarse-grained materials such as sands and gravels effective porosity may be only slightly less than total porosity (*e.g.*, total porosity = 0.35, effective porosity = 0.30). In fine-grained materials such as silts and clays effective porosity may be much less than total porosity (*e.g.*, total porosity = 0.40, effective porosity = 0.05). Effective porosity is analogous to, but not always equal to, specific yield.

Effective Porosities

TABLE 3-1. DEFAULT VALUES FOR EFFECTIVE POROSITY (Ne) FOR USE IN TIME OF TRAVEL (TOT) ANALYSES

Soil textural classes	Effective porosity of saturation ^a
<u>Unified soil classification system</u>	
GS, GP, GM, GC, SW, SP, SM, SC	0.20 (20%)
ML, MH	0.15 (15%)
CL, OL, CH, OH, PT	0.01 (1%)^b
<u>USDA soil textural classes</u>	
Clays, silty clays, sandy clays	0.01 (1%) ^b
Silts, silt loams, silty clay loams	0.10 (10%)
All others	0.20 (20%)
<u>Rock units (all)</u>	
Porous media (nonfractured rocks such as sandstone and some carbonates)	0.15 (15%)
Fractured rocks (most carbonates, shales, granites, etc.)	0.0001 (0.01%)

EPA/530-SW-89-026 (1989)

Effective porosities are related to the grain size distribution and packing of geologic materials. Finer grained materials such as silts and clays have smaller effective porosities than coarse grained materials such as sand and gravel. Effective porosities of fractured metamorphic, igneous, and sedimentary rocks can be small while effective porosities of solution-opened carbonates can be large.

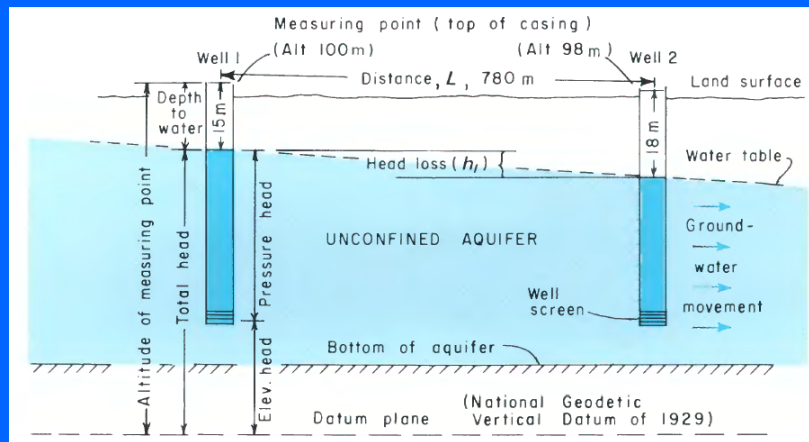
Average Linear Velocity of Groundwater Movement

$$V = (K \times i) / n_e$$

- V = Average Linear Velocity
- K = Hydraulic Conductivity
- i = Hydraulic Gradient
- n_e = Effective Porosity

The equation for average linear velocity of groundwater movement includes hydraulic conductivity (K), hydraulic gradient (i), and effective porosity (n_e). With n_e in the denominator of the equation average linear velocity increases as n_e gets smaller (for a given K and i). For a given K and i , if the n_e through which groundwater can flow is smaller the groundwater must move faster through the pores to maintain the groundwater flux.

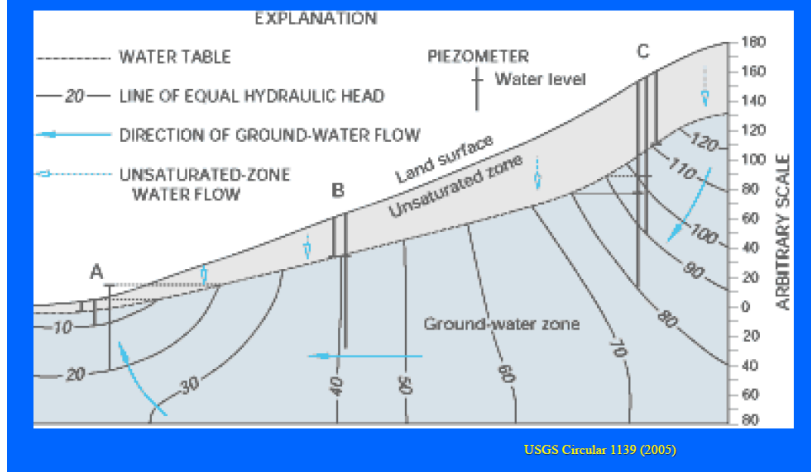
Total Hydraulic Head = Elevation Head + Pressure Head



USGS Water Supply Paper 2220 (1983)

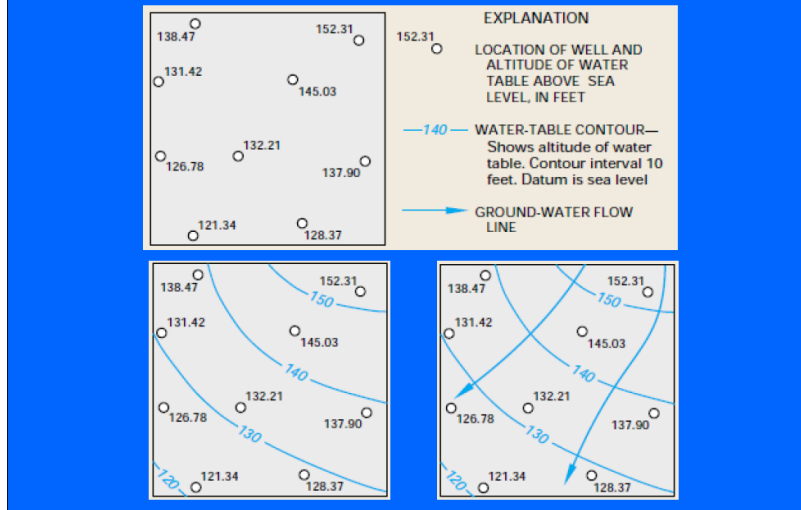
Hydraulic head is equal to elevation head + pressure head. Therefore the hydraulic head will be the same throughout the water column in a well (assuming there is no vertical component of hydraulic gradient). Hydraulic gradient is the hydraulic head loss between two wells divide by the distance between the wells (*i.e.*, hydraulic gradient; $i = \Delta h / \Delta L$).

Hydraulic Gradient Horizontal vs Vertical Components

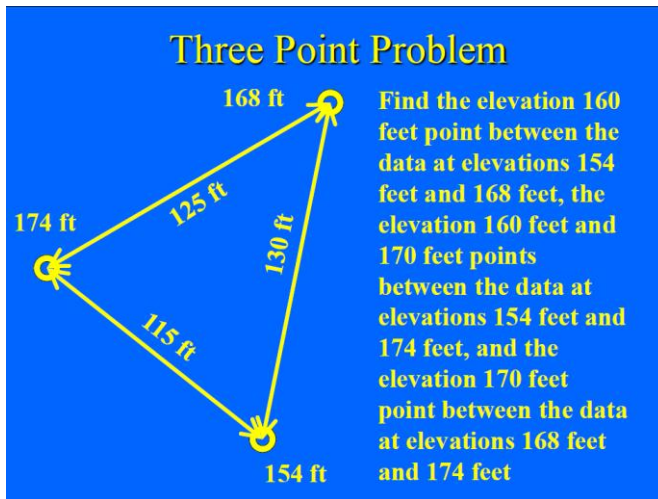


Groundwater moves in all directions at the same time so that there are both horizontal and vertical components of hydraulic gradient. In groundwater recharge and discharge areas there are vertical components of hydraulic gradient. Wells close to each other in recharge and discharge areas may have different hydraulic heads that reflect the vertical component of hydraulic gradient more than the horizontal component of hydraulic gradient. Contouring the hydraulic heads of such wells would incorrectly depict the horizontal component of hydraulic gradient. Hydraulic heads between recharge and discharge areas may be hydrostatic (*i.e.*, the same at each depth in the aquifer) so that there would be no vertical component of hydraulic gradient.

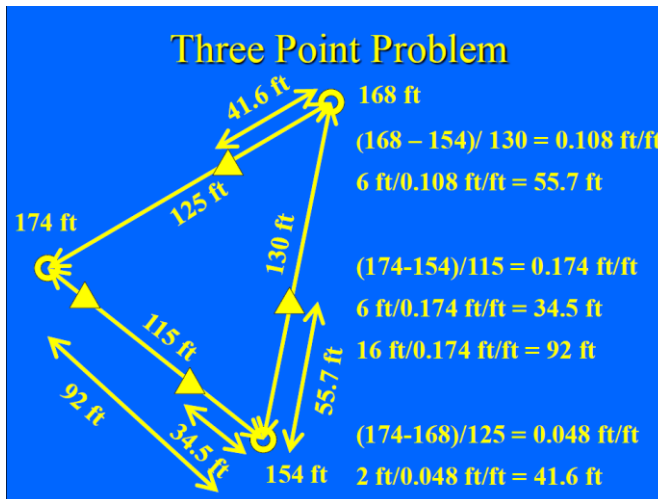
Direction of Groundwater Movement



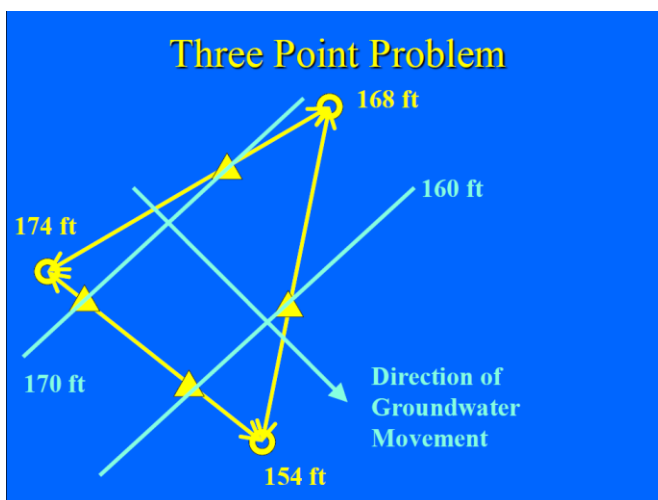
Hydraulic heads in individual wells can be contoured to generate contour lines of equal hydraulic head within the aquifer. Directions of horizontal groundwater movement are perpendicular to the hydraulic head contours. To avoid influences from vertical gradient components, hydraulic head contours should be drawn using hydraulic head data from similar portions of the aquifer (*e.g.*, shallow, middle, deep) in depictions of horizontal groundwater movement.



Three point problem solved to find the elevation 160 feet point between the data at elevations 154 feet and 168 feet, the elevation 160 feet and 170 feet points between the data at elevations 154 feet and 174 feet, and the elevation 170 feet point between the data at elevations 168 feet and 174 feet. Measure the distances between the elevation data points.

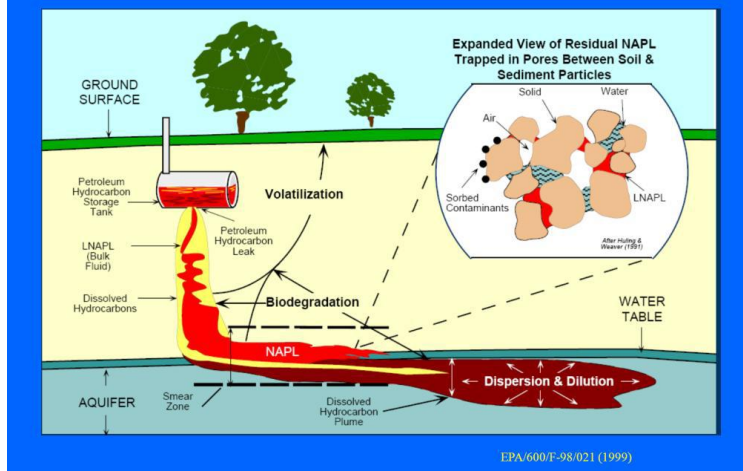


Calculations are done by proportioning distances between the points of known elevation to the distances between points at elevation $154 + 6 = 160 \text{ ft.}$, $154 + 6 = 160 \text{ ft.}$, $154 + 16 = 170 \text{ ft.}$, and $168 + 2 = 170 \text{ ft.}$



Complete the three point problem by connecting 160 feet and 170 feet data points to show groundwater contours at elevations 160 feet and 170 feet, and drawing an arrow perpendicular to the contours to show direction of groundwater movement within the area of available elevation data.

Light Non-Aqueous Phase Liquids (LNAPL)

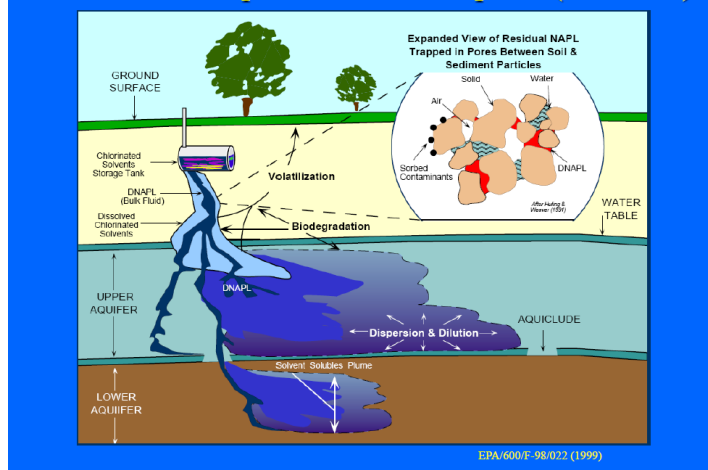


Light non-aqueous phase liquids (LNAPL) have densities less than water (i.e., specific gravity less than 1.00) and therefore float on the water table. Examples of LNAPL are gasoline, diesel fuel, and heating oil. LNAPLs are soluble in water to some degree. Released LNAPLs accumulate on the water table and plumes of dissolved LNAPL move downgradient of the floating LNAPL pool. In geologic materials LNAPL chemicals exist in four phases:

- Free product LNAPL
- LNAPL dissolved in groundwater
- LNAPL chemical adsorbed to organic material in the aquifer matrix
- LNAPL vapors in pore air (if there is any; typically below the water table there isn't any pore air so that the vapor phase of LNAPL does not exist)

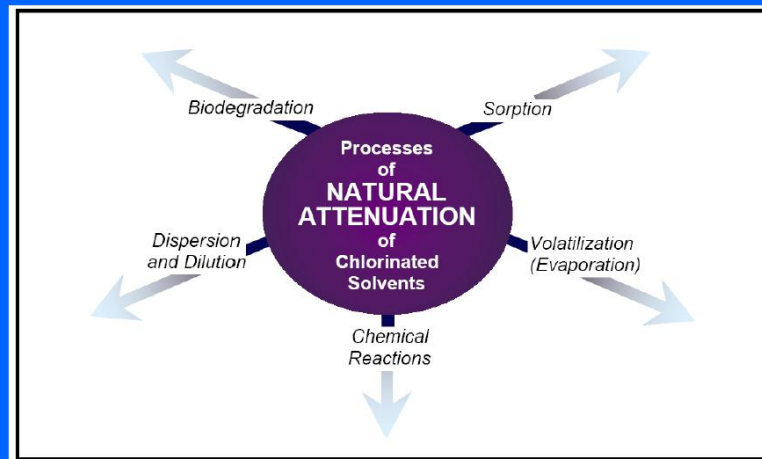
When estimating the extent of LNAPL contamination for remediation, all four phases must be accounted for. For example, if remediation of the dissolved LNAPL is undertaken without considering the adsorbed phase, adsorbed LNAPL chemicals will desorb into the groundwater and keep dissolved concentrations high. Free LNAPL in the formation pores will continue to dissolve into groundwater so that concentrations of dissolved LNAPL will not decrease during remediation.

Dense Non-Aqueous Phase Liquids (DNAPL)



Dense non-aqueous phase liquids (DNAPL) have densities greater than water (i.e., specific gravity greater than 1.00) and therefore sink through the water table until a low-permeability material is encountered to stop the vertical downward migration of DNAPL, or the source of DNAPL for vertical downward migration is depleted. Examples of DNAPL are chlorinated solvents (PCE, TCE), creosote, and coal tar. DNAPLs are also soluble in water to some degree. Released DNAPLs penetrate the water table and plumes of dissolved DNAPL move downgradient of the zone of DNAPL pool. In geologic materials DNAPL chemicals also exist in four phases and when estimating the extent of DNAPL contamination for remediation all four phases must be accounted for. Free phase DNAPL does not move in the direction of hydraulic gradient; the plume of dissolved DNAPL chemicals moves downgradient but DNAPL does not move downgradient. DNAPL moves under the influence of gravity (i.e., downward) and will continue to move downward as long as there are pathways to move through and enough DNAPL to “feed” the movement.

Natural Attenuation Processes

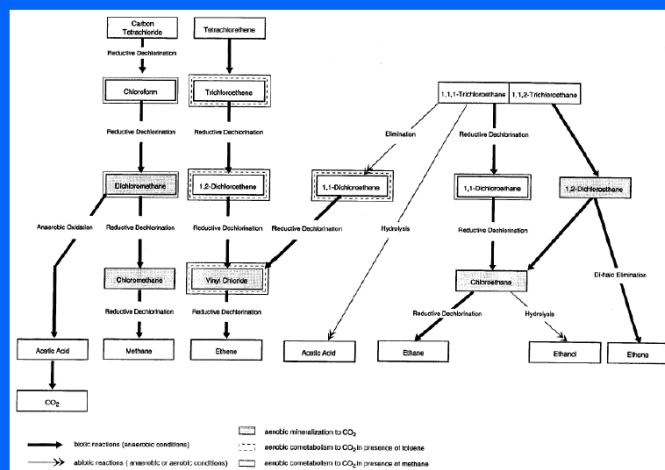


There are several mechanisms for natural attenuation:

- Volatization to pore air
- Sorption to the aquifer matrix
- Mechanical dispersion
- Chemical reactions that immobilize or “deactivate” some chemicals (particularly inorganic chemicals)
- Biodegradation of organic chemicals

Volatization, sorption, and mechanical dispersion are non-destructive attenuation mechanisms while chemical reactions and biodegradation are usually destructive attenuation mechanisms.

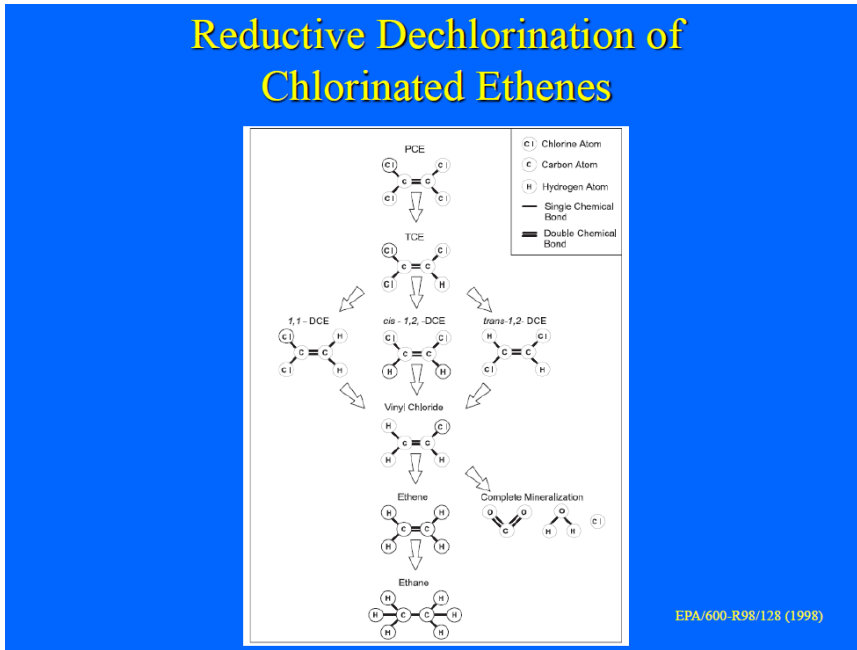
Common Degradation Pathways of Chlorinated Solvents



ITRC Technical /Regulatory Guideline ISB-3 (1999)

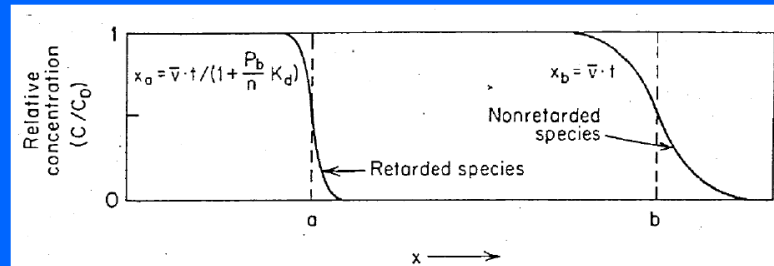
Organic chemicals such as chlorinated ethenes and ethanes degrade to other chemicals. Ethenes have two carbons with a double bond between the carbon atoms (C=C) while ethanes have two carbons with a single bond between the carbon atoms (C-C).

Reductive Dechlorination of Chlorinated Ethenes



In “reductive” dechlorination reductive refers to the reduction of the number of chlorine atoms (as described previously) and the reduction of the oxidation state of the carbon atoms. Each carbon atom must have four “connections” and each molecule must be electronically neutral. In tetrachloroethene there are two carbon atoms and four chlorine atoms. The oxidation states of the chlorine atoms are “-1” so that the four chlorine atoms equals an electronic charge of -4. Therefore each of the two carbon atoms must have a charge of +2 to make the molecule electronically neutral. In trichloroethene there are two carbon atoms, three chlorine atoms, and one hydrogen atom. The oxidation states of the hydrogen atoms are +1, so one hydrogen atom “neutralizes” the charge on one chlorine atom leaving two chlorine atoms with an electronic charge of -2. Therefore each of the two carbon atoms must have a charge of +1, a reduction in oxidation state from +2 to +1. In dichloroethene there are two carbon atoms, two chlorine atoms, and two hydrogen atoms. The two chlorine atoms (-2) neutralize the electronic charge of the two hydrogen atoms (+2) so that the two carbon atoms have a charge of 0, again reducing the oxidation state. In vinyl chloride there are two carbon atoms, one chlorine atom (-1), and three hydrogen atoms (+3) so that the two carbon atoms have a charge of -1. In ethene there are two carbon atoms and four hydrogen atoms (+4) so that the two carbon atoms have a charge of -2 and in ethane there are two carbon atoms and six hydrogen atoms (+6) so that the two carbon atoms have a charge of -3. The most reduced state of carbon is methane, CH₄, where the single carbon atom must have a charge of -4 to neutralize the +4 charge of the four hydrogen atoms.

Retardation of Adsorbed and Non-adsorbed Constituents



Constituent concentration profiles in the porous media at time t with constituent inputs at concentration C_0 at $t > 0$

Groundwater, Freeze, R.A. and J.A. Cherry, Prentice Hall 1979

Some dissolved constituents react with the aquifer matrix so that movement of the constituents is retarded relative to the movement of groundwater. The concentration profile, caused by dispersion, of a retarded constituent will lag behind the concentration profile of a non-retarded constituent.

Retardation Factor

$$V/V_c = 1 + (\rho_b/n) \times K_d$$

- V = Average Linear Velocity of Groundwater Movement
- V_c = Velocity of the Constituent $C/C_0 = 0.5$ Point on the Concentration Profile
- ρ_b = Bulk Density of Aquifer Matrix
- n = Total Porosity of Aquifer Matrix
- K_d = Distribution Coefficient (units of L^3/M)
- $K_d = \frac{\text{Mass of Constituent on the Solid Phase}}{\text{Concentration of Constituent in Solution}}$

Mathematics of the retardation factor: Variables include bulk density of the aquifer matrix, total (not effective) porosity of the aquifer matrix, and the distribution coefficient which is the ratio between the mass of constituent on the solid matrix of the aquifer and the concentration of the constituent in groundwater. The larger the distribution coefficient the more constituent there is on the aquifer matrix relative to the groundwater concentration.

Retardation Factor

- When the constituent is not adsorbed by aquifer materials (i.e., $K_d = 0$), $V/V_c = 1$, the velocity of groundwater movement equals the velocity of constituent movement, and the constituent is not retarded
- Constituents that are not adsorbed are referred to as conservative constituents; examples are Cl^- , NO_3^- , and ClO_4^-
- When the constituent is adsorbed (i.e., $K_d > 0$), $V/V_c > 1$, $V > V_c$, and the constituent is retarded relative to groundwater movement

The retardation factor is 1 for conservative constituents that are not adsorbed on the aquifer matrix, have a distribution coefficient of zero, and are therefore not retarded. Conservative constituents that don't react with the aquifer matrix include chloride, nitrate, and perchlorate. For constituents that react with the aquifer matrix and are adsorbed, the distribution coefficient is larger than zero, the retardation factor is greater than one, and the dissolved constituent moves more slowly than the average linear velocity of groundwater movement.

Effect of K_d on Contaminant Transport

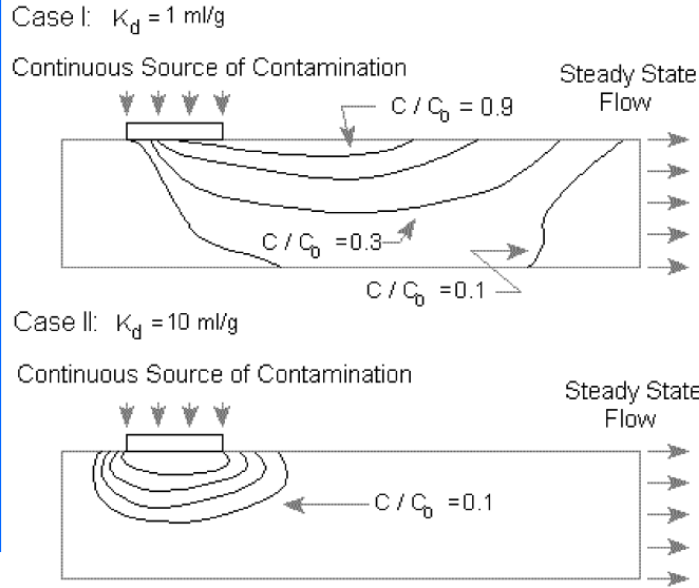


Illustration of how distribution coefficient and retardation affects movement of dissolved constituents in groundwater. With a smaller distribution coefficient plumes move further in a given time than with a larger distribution coefficient

Distribution Coefficient for Inorganic Constituents (K_d)

- K_d depends on the pH of the groundwater

Metal	Estimated K_d (L/kg)*		
	pH = 4.9	pH = 6.8	pH = 8.0
Antimony ^a		4.5E+01	
Arsenic (+3) ^b	2.5E+01	2.9E+01	3.1E+01
Barium	1.1E+01	4.1E+01	5.2E+01
Beryllium	2.3E+01	7.9E+02	1.0E+05
Cadmium	1.5E+01	7.5E+01	4.3E+03
Chromium (+3)	1.2E+03	1.8E+06	4.3E+06
Chromium (+6) ^b	3.1E+01	1.9E+01	1.4E+01
Cyanide ^c		9.9E+00	
Mercury (+2)	4.0E-02	5.2E+01	2.0E+02
Nickel	1.6E+01	6.5E+01	1.9E+03
Selenium ^b	1.8E+01	5.0E+00	2.2E+00
Silver	1.0E-01	8.3E+00	1.1E+02
Thallium ^b	4.4E+01	7.1E+01	9.6E+01
Vanadium ^a		1.0E+03	
Zinc	1.6E+01	6.2E+01	5.3E+02

* From USEPA Soil Screening Guidance, 1996. There are many sources and ranges of values available including the U.S. EPA Mid-Atlantic Risk-Based Screening Level Tables (RSL) which are updated periodically and may be the preferred source for said values by some EPD programs.

Distribution coefficients of inorganic constituents depend on the pH of the groundwater. Higher pH (less acidity) does not always mean a larger distribution coefficient (look at hexavalent chromium and selenium).

Distribution Coefficient for Organic Constituents (K_{oc})

- $K_d = K_{oc} \times f_{oc}$ where
 K_{oc} = organic carbon-water partition coefficient
 f_{oc} = fraction organic carbon on uncontaminated aquifer material
- An $f_{oc} = 1$ is 1,000,000 ppm organic carbon
- Example K_{oc} s at 20° C (in L/kg)*
 Perchloroethene 426 Trichloroethene 130
 Dichloroethene 125 Vinyl Chloride 29.6
- K_{oc} is temperature dependent

* From Biochlor User's Manual ver. 1.0. Note that there are many sources and ranges of values available. Note that U.S. EPA Region 3 have risk-based screening level (RSL) tables that list K_{oc} values that are updated periodically and may be the preferred values for use by some EPD programs.

Distribution coefficients of organic constituents are equal to the organic carbon-water partition coefficient, a property of the constituent, times the fraction of organic carbon in the uncontaminated aquifer matrix (i.e., the amount of organic carbon available to adsorb the organic constituent). Fraction organic carbon is different than concentration of total organic carbon (TOC). A fraction organic carbon of 1 is a TOC concentration of 1,000,000 ppm, a fraction organic carbon of 0.1 is a TOC concentration of 100,000 ppm, and a fraction organic carbon of 0.01 is a TOC concentration of 10,000 ppm. Organic carbon-water partition coefficient is temperature dependent, particularly for volatile organic compounds

First Order Decay

- First Order Decay Equation

$$C_2 = C_1 e^{-\lambda \Delta t}$$
- First Order Decay Coefficient

$$\lambda = (\ln C_1 - \ln C_2) / \Delta t = 0.693 / t_{1/2}$$
- Half Lives (years)
 Perchloroethene 0.58 – 9.9 Trichloroethene 0.77 – 13.9
 Dichloroethene 0.21 - 3.9 Vinyl Chloride 0.27 – 5.8
- First Order Decay Coefficients (units of 1/yr)
 Perchloroethene 0.07 - 1.20 Trichloroethene 0.05 - 0.9
 Dichloroethene 0.18 - 3.3 Vinyl Chloride 0.12 - 2.6

Constituents can decay by first order decay. The first order decay equation is exponential with time in the exponent. The first order decay coefficient is related to the half-life of the dissolved constituent. While the retardation factor equation is linear, the first order decay equation is exponential. A larger retardation factor allows more half lives for contaminant attenuation. If an initial concentration is 600 µg/L, the travel time to a target is 5 years, and the half life is 1 year, the concentration at the target would be $600 \mu\text{g/L} \times 0.5 \times 0.5 \times 0.5 \times 0.5 \times 0.5 = 18.75 \mu\text{g/L}$. This would be above an MCL of 5 µg/L. If the retardation was twice as large, the travel time to the target would be 10 years and the concentration at the target would be $600 \mu\text{g/L} \times 0.5 \times 0.5 \times 0.5 \times 0.5 \times 0.5 \times 0.5 \times 0.5 \times 0.5 = 0.59 \mu\text{g/L}$. This would be below an MCL of 5 µg/L. In this example a factor of 2 in the retardation factor resulted in a factor of about 32 in the constituent concentration at the target. This is why getting retardation correct in an assessment is important

Sensitivity of K_d of Organic Constituents to f_{oc}

- Fate and transport models are typically very sensitive to input values of fraction organic carbon used to calculate retardation factors for organic contaminants
- Sensitivity to f_{oc} in a BIOCHLOR fate and transport model for chlorinated ethenes

$$f_{oc} = 0.01 \text{ (10,000 ppm)}$$

$$f_{oc} = 0.001 \text{ (1,000 ppm)}$$

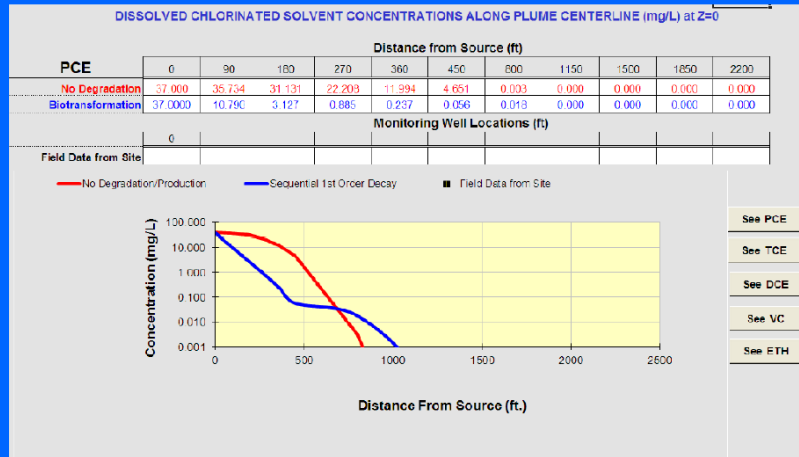
Fate and transport models of organic constituents are very sensitive to the fraction organic carbon used in the calculations.

Examples: Sensitivity of Biochlor to f_{oc} Values

BIOCHLOR Model Setup for $f_{oc} = 0.01$ (10,000 ppm)

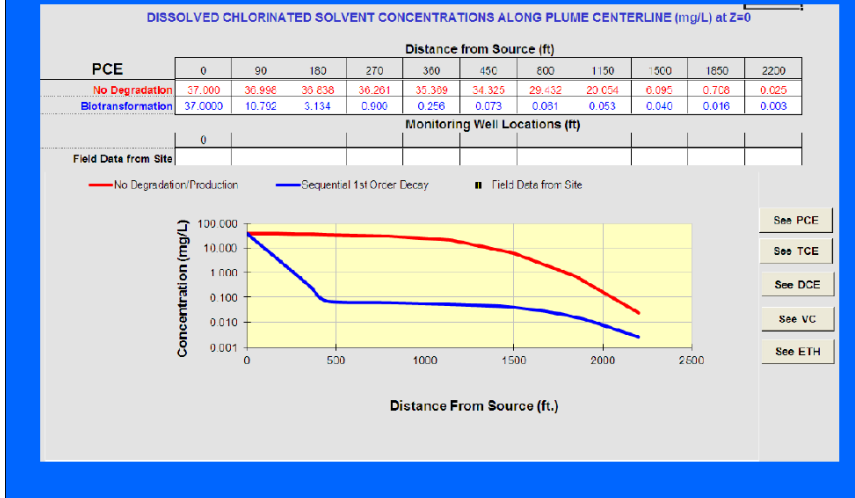
BIOCHLOR model for fate and transport of chlorinated ethenes set up with a fraction organic carbon of 0.01 (10,000 ppm TOC).

PCE Plume Movement With $f_{oc} = 0.01$ (10,000 ppm)



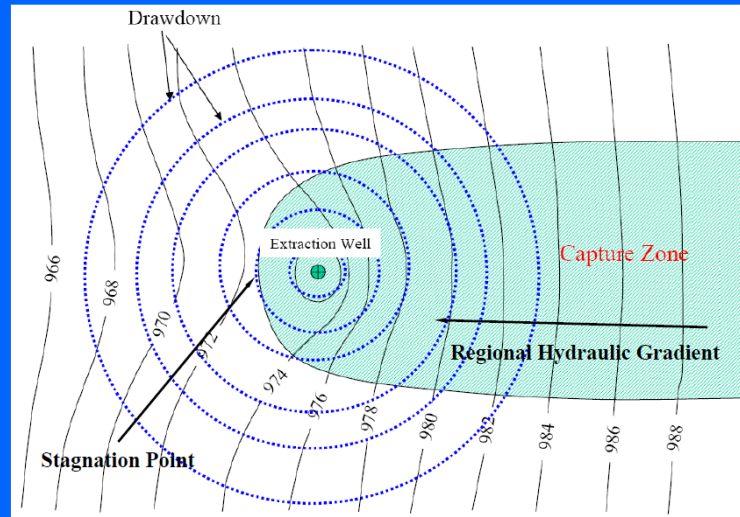
With a fraction organic carbon of 0.01 the model predicts that detectable PCE will travel less than 1,150 feet from the source.

PCE Plume Movement with $f_{oc} = 0.001$ (1,000 ppm)



With a fraction organic carbon of 0.001 the model predicts detectable PCE will travel more than 2,200 feet from the source.

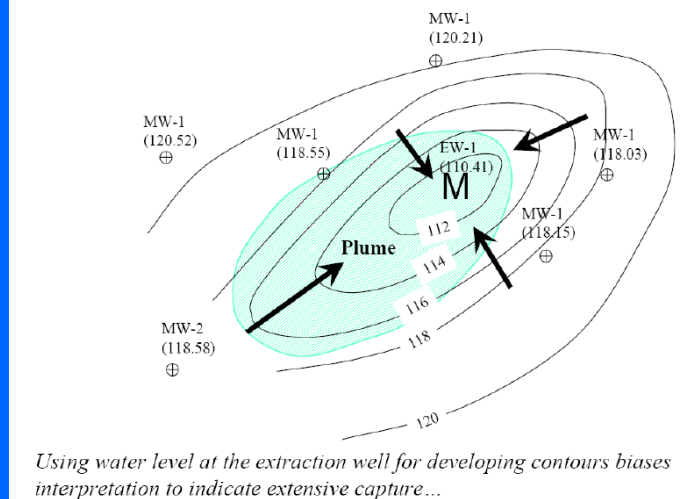
Drawdown and Capture Are Not The Same



http://clu-in.org/sites/default/files/track_a/wed/07/supporting_slides.pdf

An extraction well will create a cone-of-depression where water levels are drawn down. The cone-of-depression is not the same as the capture zone of the extraction well. The cone-of-depression must be superimposed on the regional groundwater flow field to determine the capture zone. The well capture zone will extend up the regional hydraulic gradient beyond the cone-of-depression. The capture zone will extend downgradient to the stagnation point where groundwater is no longer is captured by the extraction well. The stagnation point is within the downgradient extent of the cone-of-depression. In other words, the capture zone extends further upgradient than the cone-of-depression and does not extend as far downgradient as the cone-of-depression.

Water Level Interpretation Using Measurement from Extraction Well

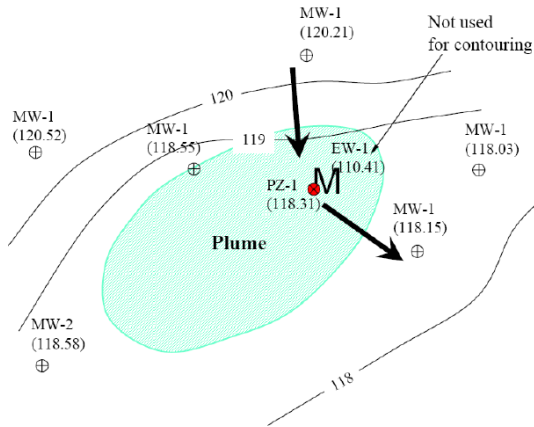


Using water level at the extraction well for developing contours biases interpretation to indicate extensive capture...

http://clu-in.org/sites/default/files/track_a/wed/07/supporting_slides.pdf

When determining capture zones of extraction wells, hydraulic heads in extraction wells should not be used to draw potentiometric surface contours or determine directions of groundwater movement. Water levels in extraction wells are lower than in the aquifer around the extraction well due to friction head-losses as groundwater enters the wells. The hydraulic head at well EW-1 (110.41 feet) is lower than the hydraulic head of the aquifer around well EW-1, and including the water level at EW-1 in the potentiometric surface map, over-estimates the extraction well capture zone.

Water Level Interpretation Using Measurement at Piezometer near Extraction Well



With piezometer data to indicate actual water level in aquifer near the extraction well, no clear-cut capture zone is apparent...

http://clu-n.org/siteopt/proceedings_04/track_a/wed/07/supporting_slides.pdf

A piezometer near well EW-1 indicated a hydraulic head of 118.31 feet, much higher than the hydraulic head in the extraction well. The potentiometric surface map properly drawn using the hydraulic head at the piezometer rather than the extraction well depicts a much different (in fact nonexistent) extraction well capture zone.

APPENDIX B: Example Data Input Spreadsheets

Example Data Summary Sheet for BIOSCREEN Model

(from Introduction to Fate and Groundwater Modeling Seminar, 1999, Georgia Ground Water Association, Doraville, Georgia)

Input Parameters for BIOSCREEN (Newell et al., 1996; 1997)

Input Parameter	Symbol	Value	Unit	Remarks
1. HYDROGEOLOGY				
Seepage velocity or	Vs	54.8	ft/yr	Calculated in BIOSCREEN spreadsheet
Hydraulic conductivity	K	3.42E-04	cm/sec	Geometric mean of slug tests performed at the site (See Section 6.2 and Appendix I)
Hydraulic gradient	I	0.031	ft/ft	Averaged value calculated from Figure 13 contours
Porosity	n	0.2	dim. less	Estimated for clayey sand saprolitic soils on site (Shelby tube; See laboratory data sheets in Appendix II)
2. DISPERSION				
Longitudinal dispersivity	alpha x	17	ft	Calculated in BIOSCREEN spreadsheet
Transverse dispersivity	alpha y	1.7	ft	Calculated in BIOSCREEN spreadsheet
Vertical dispersivity	alpha z	0	ft	Calculated in BIOSCREEN spreadsheet
or Estimated Plume Length	Lp	450	ft	Estimated from Figure 5
3. ADSORPTION				
Retardation Factor	R	1.2	dim. less	Calculated in BIOSCREEN spreadsheet
or Soil Bulk Density	rho	1.6	kg/L	Based on grain size analysis (See Appendix II) and EPD Figure 5
Partition Coefficient	Koc	81	L/kg	Montgomery (1991)
Fraction Organic Carbon	foc	0.0003	dim. less	Field samples <30 mg/kg, so minimum value used (See lab data sheets, Appendix III)
4. BIODEGRADATION				
1st Order Decay Coefficient or	lambda	0.35	per year	Calculated in BIOSCREEN spreadsheet
Solute half-life	t-half	2.00	year	Conservative value
or Instan. Reaction Model				
Delta Oxygen	ΔO		mg/L	Not measured for this site
Delta Nitrate	ΔNO3		mg/L	Not measured for this site
Observed Ferrous Iron	Fe2+		mg/l	Not measured for this site
Delta Sulfate	ΔSO4		mg/L	Not measured for this site
Observed Methane	CH4		mg/L	Not measured for this site

Input Parameters for BIOSCREEN (Newell et al., 1996; 1997)

Input Parameter	Symbol	Value	Unit	Remarks
5. GENERAL				
Model Area Length		670	ft	Distance from source to intermittent stream
Model Area Width		100	ft	Measured from Figure 5
Simulation Time		9	yr	Assumed petroleum release in 1990
6. SOURCE DATA				
Source Thickness in Sat. Zone				
Source Zones:				
	Width (ft)	Conc. (mg/L)		
Zone 1	25	0.032		See Figure 5
Zone 2	20	6.5		Geomet. mean of 1000, and 1.0 ug/l (Figure 5)
Zone 3	10	59.77		Geo. mean of 59.77, and 1 mg/l contours, MWs 1, 10D, & 9 (Fig 5)
Zone 4	20	6.5		Free product concentration at source
Zone 5	25	0.032		Assumed mirror image of Zone 2
				Assumed mirror image of Zone 1
Source Half Life (see Help)				
Instan. Reaction		1st Order	yr	
Soluble Mass		Infinite	kg	Most conservative
7. FIELD DATA FOR COMPARISON				
	Conc. (mg/L)	Dist. from source (ft)		
Monitoring well B-4	59.77	0		Figure 5 - free product
Monitoring Well MW-16	5.3	150		Figure 5
Monitoring Well MW-9	1.8	278		Figure 5

Note: Input values and remarks shown above are examples only. References to figures do not refer to figures contained within this guidance document. Furthermore, the source of, and justification for, input values used in modeling effort should be included in the “Remarks” column.

Example Data Summary Sheet for BIOCHLOR Model
 (from Biochlor Natural Attenuation Decision Support System User's Manual, Version 1.0)

Cape Canaveral Air Station, Florida

DATA TYPE	Parameter	Value	Source of Data																																			
Hydrogeology	<ul style="list-style-type: none"> Hydraulic Conductivity: Hydraulic Gradient: Effective porosity: 	1.8 x 10 ⁻² (cm/sec) 0.0012 (ft/ft) 0.2	<ul style="list-style-type: none"> Slug-tests results Static water level measurements Estimated 																																			
Dispersion	<ul style="list-style-type: none"> Longitudinal Dispersivity: Transverse Dispersivity: Vertical Dispersivity: 	40 4 0 (ft)	<ul style="list-style-type: none"> Intermediate value for 800-1200 ft. plume (from Gelhar et al. (1992)) 0.1 x long. dispersivity Assume vertical dispersivity is zero since depth of source is approx. depth of aquifer 																																			
Adsorption	<ul style="list-style-type: none"> Individual Retardation Factors Common Retardation Factor Aquifer Matrix Bulk Density foc: Koc: 	PCE: 7.1 TCE: 2.9 c-DCE: 2.8 VC: 1.4 ETH: 5.3 2.9 1.6 (kg/L) 0.184% PCE: 426 (L/kg) TCE: 130 (L/kg) c-DCE: 125 (L/kg) VC: 29.6 (L/kg) ETH: 302 (L/kg)	<ul style="list-style-type: none"> Calculated from $R=1+K_{oc} \cdot f_{oc} \cdot \rho_b/n$ Median value Estimated Lab analysis Literature correlation using solubilities at 20 °C 																																			
Biotransformation	Biotransformation Rate Coefficients, (1/yr) PCE----> TCE TCE---->c-DCE c-DCE---->VC VC----> ETH	2.0 1.0 0.7 0.4	<ul style="list-style-type: none"> Based on calibration to field data using a simulation time of 32 years (field data collected in 1997). Started with literature values and then adjusted model to fit field data 																																			
General	<ul style="list-style-type: none"> Modeled Area Length: Modeled Area Width: Simulation Time: 	1085 (ft) 700 (ft) 33 (yrs)	<ul style="list-style-type: none"> Based on area of affected ground-water plume From 1965 (first release) to 1998 																																			
Source Data	<ul style="list-style-type: none"> Source Thickness: Source Widths (ft) Source Concentrations (mg/L) 	56(ft) <table border="1"> <thead> <tr> <th></th> <th><u>Area 1</u></th> <th><u>Area 2</u></th> <th><u>Area 3</u></th> </tr> </thead> <tbody> <tr> <td>105</td> <td>175</td> <td>298</td> <td></td> </tr> </tbody> </table> <table border="1"> <thead> <tr> <th></th> <th><u>Area 1</u></th> <th><u>Area 2</u></th> <th><u>Area 3</u></th> </tr> </thead> <tbody> <tr> <td>PCE</td> <td>0.056</td> <td>0.007</td> <td>0.001</td> </tr> <tr> <td>TCE</td> <td>15.8</td> <td>0.316</td> <td>0.01</td> </tr> <tr> <td>c-DCE</td> <td>98.5</td> <td>1.0</td> <td>0.01</td> </tr> <tr> <td>VC</td> <td>3.080</td> <td>0.089</td> <td>0.009</td> </tr> <tr> <td>ETH</td> <td>0.030</td> <td>0.013</td> <td>0.003</td> </tr> </tbody> </table>		<u>Area 1</u>	<u>Area 2</u>	<u>Area 3</u>	105	175	298			<u>Area 1</u>	<u>Area 2</u>	<u>Area 3</u>	PCE	0.056	0.007	0.001	TCE	15.8	0.316	0.01	c-DCE	98.5	1.0	0.01	VC	3.080	0.089	0.009	ETH	0.030	0.013	0.003	<ul style="list-style-type: none"> Based on geologic logs and monitoring data (see figure A.5 for TCE Example) Modeled source area as variable source Source concentrations are aqueous concentrations 			
	<u>Area 1</u>	<u>Area 2</u>	<u>Area 3</u>																																			
105	175	298																																				
	<u>Area 1</u>	<u>Area 2</u>	<u>Area 3</u>																																			
PCE	0.056	0.007	0.001																																			
TCE	15.8	0.316	0.01																																			
c-DCE	98.5	1.0	0.01																																			
VC	3.080	0.089	0.009																																			
ETH	0.030	0.013	0.003																																			
Actual Data	Distance From Source (ft): PCE Conc. (mg/L): TCE Conc. (mg/L): c-DCE (mg/L): VC (mg/L): ETH (mg/L):	<table border="1"> <thead> <tr> <th></th> <th><u>560</u></th> <th><u>650</u></th> <th><u>930</u></th> <th><u>1085</u></th> </tr> </thead> <tbody> <tr> <td><0.001</td> <td>ND</td> <td><0.001</td> <td><0.001</td> <td></td> </tr> <tr> <td>0.220</td> <td>0.0165</td> <td>0.0243</td> <td>0.019</td> <td></td> </tr> <tr> <td>3.48</td> <td>0.776</td> <td>1.200</td> <td>0.556</td> <td></td> </tr> <tr> <td>3.080</td> <td>0.797</td> <td>2.520</td> <td>5.024</td> <td></td> </tr> <tr> <td>0.188</td> <td>ND</td> <td>0.107</td> <td></td> <td></td> </tr> <tr> <td></td> <td>0.150</td> <td></td> <td></td> <td></td> </tr> </tbody> </table>		<u>560</u>	<u>650</u>	<u>930</u>	<u>1085</u>	<0.001	ND	<0.001	<0.001		0.220	0.0165	0.0243	0.019		3.48	0.776	1.200	0.556		3.080	0.797	2.520	5.024		0.188	ND	0.107				0.150				<ul style="list-style-type: none"> Based on 1997 observed concentrations at site near centerline of plume
	<u>560</u>	<u>650</u>	<u>930</u>	<u>1085</u>																																		
<0.001	ND	<0.001	<0.001																																			
0.220	0.0165	0.0243	0.019																																			
3.48	0.776	1.200	0.556																																			
3.080	0.797	2.520	5.024																																			
0.188	ND	0.107																																				
	0.150																																					
OUTPUT	Centerline Concentration:	See Figures A.7, A.8																																				
	Array Concentration:	See Figure A.9																																				

Note: Input values and remarks shown are examples only. References to figures do not refer to figures contained within this guidance document. Furthermore, the source of, and justification for, input values used in your modeling effort should be included in the "Remarks" column.

**The following are attachments to the testimony of Scott M. Payne,
PhD, PG and Ian Magruder, M.S..**

ATTACHMENT 16



EPA-600/R-09/151
December 2009

Characterization of Coal Combustion Residues from Electric Utilities – Leaching and Characterization Data



Characterization of Coal Combustion Residues from Electric Utilities – Leaching and Characterization Data

D. Kosson¹, F. Sanchez¹,
P. Kariher², L.H. Turner³, R. Delapp¹, P. Seignette⁴

¹**Vanderbilt University**
Department of Civil and Environmental Engineering
Nashville, TN 37235

²**ARCADIS**
4915 Prospectus Drive, Suite F
Durham, NC 27713

³**Turner Technology, LLC**
Nashville, TN 37205

⁴**Energy Research Centre of the Netherlands**

Contract No. EP-C-09-027
Work Assignment No. 0-7

Prepared for:
Susan A. Thorneloe
U.S. Environmental Protection Agency
Office of Research and Development
National Risk Management Research Laboratory
Air Pollution Prevention and Control Division
Research Triangle Park, NC 27711

ACKNOWLEDGMENTS

Authors are grateful to the input provided by G. Helms, U.S. EPA, Office of Solid Waste and Emergency Response (Washington, D.C.) in helping with the research design and application of improved leaching test methods to provide better characterization data for fly ash and other coal combustion residues.

Overall project planning and integration was carried out jointly by D.S. Kosson and F. Sanchez (Vanderbilt University), and P. Kariher (ARCADIS).

R. Delapp and D. McGill of Vanderbilt University were responsible for the chemical analyses of the leachate samples except for mercury analysis. All other laboratory testing including physical and chemical analysis, sample digestion, and leaching tests of fly ash and other coal combustion residues was conducted by ARCADIS. Technical assistance was provided by A. Garrabrants of Vanderbilt University. Solid phase chromium analysis by X-ray Absorption Fine Structure was carried out under the direction of N.D. Hutson (U.S. EPA). Database management and data presentation technical assistance was provided by L.H. Turner (Turner Technology, LLC) and P. Seignette (Energy Research Centre of the Netherlands).

K. Ladwig and the Electric Power Research Institute (EPRI) are gratefully acknowledged for assistance in obtaining coal combustion residue samples and providing information from the EPRI database on coal combustion residues.

S. Thorneloe provided technical direction for this research. In addition, she was responsible for obtaining samples, communication, and report writing.

ABSTRACT

This report evaluates changes in composition and constituent release by leaching that may occur to fly ash and other coal combustion residues (CCRs) in response to changes in air pollution control technology at coal-fired power plants. The addition of flue-gas desulfurization (FGD) systems, selective catalytic reduction, and activated carbon injection to capture mercury and other pollutants will shift mercury and other pollutants from the stack gas to fly ash, FGD gypsum, and other air pollution control residues. The objective is to understand the fate of mercury and other constituents of potential concern (COPC) in air pollution control residues and support EPA's broader goal of ensuring that emissions being controlled in the flue gas at power plants are not later being released to other environmental media.

This report includes data on 73 CCRs [34 fly ashes, 20 flue gas desulfurization (FGD) gypsum, 7 "other" FGD residues (e.g., scrubbers without oxidation or with inhibited oxidation), and 8 blended CCRs "as managed" (e.g., scrubber sludge mixed with fly ash and lime prior to disposal)]. Each of the CCRs sampled has been analyzed for a range of physical properties, total elemental content, and leaching characteristics for mercury, aluminum, antimony, arsenic, barium, boron, cadmium, chromium, cobalt, lead, molybdenum, selenium and thallium.

The leach testing methods that were used in this research consider the impact on leaching of management conditions. These methods are intended to address concerns raised by the National Academy of Science and the EPA's Science Advisory Board with the use of single-point pH tests. Because of the range of field conditions that CCRs are managed during disposal or use as secondary (or alternative) materials, it is important to understand the leaching behavior of materials over the range of plausible field conditions that can include acid mine drainage and co-disposal of fly ash and other CCRs with pyrites or high-sulfur coal rejects. The methods have also been developed into draft protocols for inclusion in EPA's waste testing guidance document, SW-846, which would make them available for more routine use.

(<http://www.epa.gov/osw/hazard/testmethods/sw846/index.htm>)

The major conclusions from this research include:

- There is great variability in both the range of total constituent concentration values and in leaching values (orders of magnitude). In comparing these results to health indicator values such as the maximum concentration limit or toxicity characteristic, there are multiple COPCs of potential concern.
- Distinctive patterns in leaching behavior have been identified over a range of pH values that would plausibly be encountered for CCR management.
- Total constituent content is not a good indicator of leaching which has been found to be a function of the characteristics of the material (pH) and field conditions in which the material is managed.
- The maximum eluate concentration from leaching test results varies over a wide range in pH and is different for different CCR types and elements. This indicates that there is not a single pH for which testing is likely to provide confidence in release estimates over a wide range of disposal and beneficial use options, emphasizing the benefit of multi-pH testing. Furthermore, for CCRs, the rate of constituent release to the environment is affected by leaching conditions (in some cases dramatically so), and that leaching

evaluation under a single set of conditions will, in many cases, lead to inaccurate conclusions about expected leaching in the field.

The intended use for the data in this report is to support future risk and environmental assessments of the CCRs studied. A follow-up report is planned which will use these data in conducting a probabilistic assessment of mercury and other COPCs release rates based on the range of plausible management scenarios for these materials in either disposal or beneficial use situations. The data summarized in this report will also be made available electronically through a leaching assessment tool (LeachXS Lite[®]) that can be used to develop source-term inputs needed for using groundwater transport and fate models. The leaching assessment tool will also provide means for data management in viewing data resulting from the of the improved leaching test methods.

Characterization of Coal Combustion Residues III

GLOSSARY OF TERMS

ACI	Activated Carbon Injection
Al	Aluminum
AL	Action Level
APC	Air Pollution Control
APPCD	Air Pollution Prevention and Control Division
As	Arsenic
ASTM	American Society for Testing and Materials
B	Boron
Ba	Barium
BDL	Below Detection Limit
BET	Brunauer, Emmett and Teller (method for estimating surface area)
CAIR	Clean Air Interstate Rule
CAMR	Clean Air Mercury Rule
Cd	Cadmium
CCRs	Coal Combustion Residues
CCV	Continuing Calibration Verification
Co	Cobalt
COPCs	Constituents of Potential Concern
Cr	Chromium
CV	Coefficient of Variation
CVAA	Cold Vapor Atomic Adsorption
DIC	Dissolved Inorganic Carbon
DOC	Dissolved Organic Carbon
DOE	United States Department of Energy
DI	Deionized (i.e., deionized water)
DRC	Dynamic Reaction Chamber
dw	dry weight basis
DWEL	Drinking Water Equivalent Level
EPA	United States Environmental Protection Agency
EPRI	Electric Power Research Institute
ESP	Electrostatic Precipitator

GLOSSARY OF TERMS - CONTINUED

ESP-CS	Cold-side Electrostatic Precipitator
ESP-HS	Hot-side Electrostatic Precipitator
FF	Fabric Filter (baghouse)
FGD	Flue Gas Desulfurization
FID	Flame Ionization Detector
FO	Forced Oxidation
FSS	Fixated Scrubber Sludge
FSSL	Fixated Scrubber Sludge with Lime
Gyp-U	Unwashed Gypsum
Gyp-W	Washed Gypsum
Hg	Mercury
HHV	Higher Heating Value
Ho	Holmium
ICP-OES	Inductively Coupled Plasma Optical Emission Spectrometry
ICP-MS	Inductively Coupled Plasma-Mass Spectrometry
ICV	Initial Calibration Verification
In	Indium
IO	Inhibited Oxidation
IOx	Inhibited Oxidation (this abbreviation used in some figures to improve clarity)
LF	Landfill
LOI	Loss On Ignition
LS	Liquid-to-Solid Ratio (LS ratio)
M	Molar
Max	Maximum
MCL	Maximum Contaminant Level (for drinking water)
MDL	Method Detection Limit
Mg Lime	Magnesium Enriched Lime (often also referred to as “mag-lime”)
Min	Minimum
ML	Minimum Level of Quantification
Mo	Molybdenum

Characterization of Coal Combustion Residues III

GLOSSARY OF TERMS - CONTINUED

NETL	National Energy Technology Laboratory (DOE)
NIOSH	National Institute of Occupational Safety and Health
NO	Natural Oxidation
NO _x	Nitrogen Oxides
NSPS	New Source Performance Standards
OC/EC	Organic Carbon/Elemental Carbon
ORD	Office of Research and Development (EPA)
OSWER	Office of Solid Waste and Emergency Response (EPA)
PAC	Powdered Activated Carbon
Pb	Lead
PJFF	Pulse-Jet Fabric Filter
PM	Particulate Matter
PRB	Sub-bituminous coal mined in Wyoming's Powder River Basin
PS	Particulate Scrubber
QA/QC	Quality Assurance/Quality Control
RCRA	Resource Conservation and Recovery Act
RFA	Reference Fly Ash
SAB	EPA Science Advisory Board
SCA	Specific Collection Area
Sb	Antimony
ScS	Scrubber Sludge
SCR	Selective Catalytic Reduction
SNCR	Selective Non-Catalytic Reduction
SDA	Spray Dryer Absorber
Se	Selenium
SI	Surface Impoundment
SO ₂	Sulfur Dioxide
SOFA	Separated Overfire Air
SPLP	Synthetic Precipitation Leaching Procedure
SRM	Standard Reference Material
S/S	Stabilization/Solidification

GLOSSARY OF TERMS - CONTINUED

SWDA	Solid Waste Disposal Act
TC	Toxicity Characteristic
TCLP	Toxicity Characteristic Leaching Procedure
Tl	Thallium
XAFS	X-Ray Absorption Fine Structure
XRF	X-Ray Fluorescence

EXECUTIVE SUMMARY

This report is the third in a series to evaluate changes in composition and constituent release by leaching that may occur to fly ash and other coal combustion residues (CCRs) in response to changes in air pollution control technology at coal-fired power plants. The addition of flue-gas desulfurization (FGD) systems, selective catalytic reduction, and activated carbon injection to capture mercury and other pollutants will shift mercury and other pollutants from the stack gas to fly ash, FGD gypsum, and other air pollution control residues. The Air Pollution Prevention and Control Division (APPCD) of EPA's Office of Research and Development (ORD) is conducting research to evaluate potential leaching and other cross media transfers of mercury and other constituents of potential concern (COPCs) resulting from the management of CCRs resulting from wider use of state-of-the-art air pollution control technology. This research was cited as a priority in EPA's Mercury Roadmap¹ to ensure that one environmental problem is not being traded for another. The objective is to understand the fate of mercury and other COPCs in air pollution control residues and support EPA's broader goal of ensuring that emissions being controlled in the flue gas at power plants are not later being released to other environmental media.

Approximately 40% of the 126 million tons of CCRs produced in the U.S. as of 2006 were utilized in agricultural, commercial, and engineering applications. The remainder (i.e., 75 million tons) was managed in either landfills or impoundments. The physical and chemical characteristics of CCRs make them potentially suitable as replacements for materials used in a wide range of products including cement, concrete, road base, and wallboard. Use of CCRs as an alternative to virgin materials helps conserve natural resources and energy, as well as decrease the amount of CCRs being land disposed.

In developing data to characterize the leaching potential of COPCs from the range of likely CCRs resulting from use of state-of-the-art air pollution control technology, improved leaching test methods have been used². The principle advantage of these methods is that they consider the impact on leaching of management conditions. These methods address concerns raised by National Academy of Science and EPA's Science Advisory Board with the use of single-point pH tests. Because of the range of field conditions that CCRs are managed during disposal or use as secondary (or alternative) materials, it is important to understand the leaching behavior of materials over the range of plausible field conditions that can include acid mine drainage and co-disposal of fly ash and other CCRs with pyrites or high-sulfur coal rejects^{3, 4}. The methods have

¹ EPA (2006). EPA's Roadmap for Mercury, EPA-HQ-OPPT-2005-0013. U.S. Environmental Protection Agency, <http://www.epa.gov/mercury/pdfs/FINAL-Mercury-Roadmap-6-29.pdf> (accessed August 21, 2009).

² Improved leaching test methods described in (Kosson et al., 2002) have been developed as draft SW-846 protocols. These methods consider the effect of varying environmental conditions on waste constituent leaching.

³ National Academy of Sciences (2006). *Managing Coal Combustion Residues in Mines*, Washington, D.C.

⁴ Sanchez, F.; Keeney, R.; Kosson, D., and Delapp, R. Characterization of Mercury-Enriched Coal Combustion Residues from Electric Utilities Using Enhanced Sorbents for Mercury Control, EPA-600/R-06/008, Feb. 2006; <http://www.epa.gov/ORD/NRMRL/pubs/600r06008/600r06008.pdf>.

also been developed into draft protocols for inclusion in EPA's waste testing guidance document, SW-846, which would make them available for more routine use.

(<http://www.epa.gov/osw/hazard/testmethods/sw846/index.htm>).

The selected testing approach was chosen for use because it evaluates leaching over a range of values for two key variables [pH and liquid-to-solid ratio (LS)] that both vary in the environment and affect the rate of constituent release from waste. The range of values used in the laboratory testing encompasses the range of values expected to be found in the environment for these parameters. Because the effect of these variables on leaching is evaluated in the laboratory, prediction of leaching from the waste in the field is expected to be done with much greater reliability.

The categories into which samples have been grouped are fly ash, flue gas desulfurization (FGD) gypsum, "other" FGD residues (such as from spray drier absorbers), blended CCRs "as managed" (mixtures of fly ash and scrubber residues with and without added lime or mixture of fly ash and gypsum), and wastewater filter cake. In the first report from this research⁵, results of leaching from fly ash were reported for mercury, arsenic, and selenium. Report 2 provided leaching results for an expanded list of materials and COPCs to include mercury, aluminum, antimony, arsenic, barium, boron, cadmium, chromium, cobalt, lead, molybdenum, selenium and thallium⁶. In the current report (Report 3), analyses of eluates from CCR samples presented in Report 1 have been included for the expanded list of COPCs. Report 3 also includes the data previously reported in Report 2, and leach test results for an additional 38 CCRs. A total of 73 samples were evaluated, and all results are presented in the current report to facilitate comparisons (Table ES-1).

⁵ Sanchez, F.; Keeney, R.; Kosson, D., and Delapp, R. Characterization of Mercury-Enriched Coal Combustion Residues from Electric Utilities Using Enhanced Sorbents for Mercury Control, EPA-600/R-06/008, Feb. 2006; <http://www.epa.gov/ORD/NRMRL/pubs/600r06008/600r06008.pdf>.

⁶ Sanchez, F.; Kosson, D.; Keeney, R.; Delapp, R.; Turner, L.; Kariher, P.; Thorneloe, S. Characterization of Coal Combustion Residues from Electric Utilities Using Wet Scrubbers for Multi-Pollutant Control; EPA-600/R-08/077, July 2008; <http://www.epa.gov/nrmrl/pubs/600r08077/600r08077.pdf>.

Characterization of Coal Combustion Residues III

Table ES-1. Identification of CCRs evaluated and included in this Report.

Samples Evaluated	Report 1*	Report 2**	Additional Samples Collected	Total in Report 3
Fly Ash	12	5	17	34
FGD Gypsum	-	6	14	20
“Other” FGD Residues	-	5	2	7
Blended CCRs “as managed”	-	7	1	8
Wastewater Treatment Filter Cake	-		4	4

* Sanchez, F.; Keeney, R.; Kosson, D., and Delapp, R. Characterization of Mercury-Enriched Coal Combustion Residues from Electric Utilities Using Enhanced Sorbents for Mercury Control, EPA-600/R-06/008, Feb. 2006; <http://www.epa.gov/ORD/NRMRL/pubs/600r06008/600r06008.pdf>.

**Sanchez, F.; Kosson, D.; Keeney, R.; Delapp, R.; Turner, L.; Kariher, P.; Thorneloe, S. Characterization of Coal Combustion Residues from Electric Utilities Using Wet Scrubbers for Multi-Pollutant Control; EPA-600/R-08/077, July 2008; <http://www.epa.gov/nrmrl/pubs/600r08077/600r08077.pdf>.

Each of the CCRs sampled has been analyzed for a range of physical properties, total elemental content, and leaching characteristics. Laboratory leach data are compared to field observations from industry and EPA data from sampling of impoundments and landfills. The laboratory leach results are also compared to reference indicators to provide context for the data including:

- The toxicity characteristic (TC), which is a threshold for hazardous waste determinations;
- The maximum concentration limit (MCL), which is used for protecting drinking water; and,
- The drinking water equivalent level (DWEL), which is used to be protective for non carcinogenic endpoints of toxicity over a lifetime of exposure⁷.

These comparisons to reference indicators do not consider dilution and attenuation factors (collectively referred to in this report as attenuation factors) that arise as a consequence of disposal or beneficial use designs and transport from the point of release to the potential receptor. Minimum attenuation factors needed to reduce maximum leach concentrations (based on laboratory test results) to less than MCL or DWEL values are provided to illustrate the importance of consideration of attenuation factors during evaluation of management options.

The intended use for the data in this report is to support future risk and environmental assessments of the CCRs. A follow-up report is planned which will use these data in conducting a probabilistic assessment of mercury and other COPCs release rates based on the range of plausible management scenarios for these materials in either disposal or beneficial use situations.

The data summarized in this report will be made available electronically through a leaching assessment tool that can be used to develop source-term inputs needed for using groundwater

⁷DWEL was developed for chemicals that have a significant carcinogenic potential and provides risk managers with evaluation on non-cancer endpoints, but infers that carcinogenicity should be considered the toxic effect of greatest concern (<http://www.epa.gov/safewater/pubs/gloss2.html#D>).

transport and fate models⁸. The leaching assessment tool will provide easier access to the leach data for a range of CCRs and potential field conditions. The tool can be used to develop more detailed leach data as input to more refined assessments of CCRs and support environmental decision-making that will ensure protection of human health and the environment.

Summary of Conclusions

In Table ES-2 and Table ES-3, the total metals content of the fly ash and FGD gypsum samples evaluated is provided along with the leach test results. Reference indicators (i.e., TC, MCL, and DWEL) are also provided to provide some context in understanding the leach results. It is critical to bear in mind that the leach test results represent a distribution of potential constituent release concentrations from the material as disposed or used on the land. The data presented do not include any attempt to estimate the amount of constituent that may reach an aquifer or drinking water well. Leachate leaving a landfill is invariably diluted in ground water to some degree when it reaches the water table, or constituent concentrations are attenuated by sorption and other chemical reactions in groundwater and sediment. Also, groundwater pH may be different from the pH at the site of contaminant release, and so the solubility and mobility of leached contaminants may change when they reach groundwater. None of these dilution or attenuation processes is incorporated into the leaching values presented. Thus, comparisons with regulatory health values, particularly drinking water values, must be done with caution. Groundwater transport and fate modeling would be needed to generate an assessment of the likely risk that may result from the CCRs represented by these data.

In reviewing the data and keeping these caveats in mind, conclusions to date from the research include:

1. Review of the fly ash and FGD gypsum (Table ES-2 and Table ES-3) show a range of total constituent concentration values, but a much broader range (by orders of magnitude) of leaching values, in nearly all cases. This much greater range of leaching values only partially illustrates what more detailed review of the data shows: that for CCRs, the rate of constituent release to the environment is affected by leaching conditions (in some cases dramatically so), and that leaching evaluation under a single set of conditions may, to the degree that single point leach tests fail to consider actual management conditions, lead to inaccurate conclusions about expected leaching in the field.
2. Comparison of the ranges of totals values and leachate data from the complete data set supports earlier conclusions^{9, 10, 11} that the rate of constituent leaching cannot be reliably estimated based on total constituent concentration.

⁸ The leaching assessment tool, LeachXS Lite®, will be available for inclusion in the CCR docket (December 2009).

⁹ Senior, C; Thorneloe, S.; Khan, B.; Goss, D. Fate of Mercury Collected from Air Pollution Control Devices; Environmental Management, July 2009, 15-21.

¹⁰ U.S. EPA, Characterization of Mercury-Enriched Coal Combustion Residuals from Electric Utilities Using Enhanced Sorbents for Mercury Control, EPA-600/R-06/008, Feb. 2006; <http://www.epa.gov/ORD/NRMRL/pubs/600r06008/600r06008.pdf>.

Characterization of Coal Combustion Residues III

3. The maximum eluate concentration from leaching test results varies over a wide range in pH and is different for different CCR types and elements. This indicates that there is not a single pH for which testing is likely to provide confidence in release estimates over a wide range of disposal and beneficial use options, emphasizing the benefit of multi-pH testing.
4. From the more complete data in this report, distinctive patterns in leaching behavior have been identified over the range of pH values that would plausibly be encountered for CCR disposal, depending on the type of material sampled and the element. This reinforces the above conclusions based on the summary data.
5. Summary data in Table ES-2 on the leach results from evaluation of 34 fly ash samples across the plausible management pH domain of 5.4 to 12.4, indicates leaching concentration ranges over several orders of magnitude as a function of pH and ash source:
 - the leach results at the upper end of the concentration ranges exceeded the TC values for As, Ba, Cd, Cr, and Se.
 - the leach results at the upper end of the concentration ranges exceeded the MCL or DWEL for Sb, As, Ba, B, Cd, Cr, Pb, Mo, Se, and Tl.
6. Summary data in Table ES-3 on the leach results from evaluation of 20 FGD gypsum samples across the plausible management pH domain of 5.4 to 12.4, indicates leaching concentration ranges over several orders of magnitude as a function of pH and FGD gypsum source:
 - the leach results at the upper end of the concentration ranges exceeded the TC values for Cd and Se.
 - the leach results at the upper end of the concentration ranges exceeded the MCL or DWEL for Sb, As, B, Cd, Cr, Mo, Se, and Tl.
7. The variability in total content and the leaching of constituents within a material type (e.g., fly ash, gypsum) is such that, while leaching of many samples exceeds one or more of the available reference indicators, many of the other samples within the material type may be lower than the available regulatory or reference indicators. Additional or more refined assessment of the dataset may allow some distinctions regarding release potential to be made among particular sources of some CCRs, which may be particularly useful in evaluating CCRs in reuse applications.

Work is underway to develop a fourth report that presents such additional analysis of the leaching data to provide more insight into constituent release potential for a wider range of scenarios, including beneficial use applications. This will include calculating potential release

¹¹U.S. EPA, Characterization of Coal Combustion Residuals from Electric Utilities Using Wet Scrubbers for Multi-Pollutant Control; EPA-600/R-08/077, July 2008; <http://www.epa.gov/nrmrl/pubs/600r08077/600r08077.pdf>.

rates over a specified time for a range of management scenarios including use in engineering and commercial applications using probabilistic assessment modeling¹².

In interpreting the results provided in this report, please note that the CCRs analyzed in this report are not considered to be a representative sample of all CCRs produced in the U.S. For many of the observations, only a few data points were available. It is hoped that through broader use of the improved leach test methods (as used in this report), that additional data from CCR characterization will become available. That will help better define trends associated with changes in air pollution control at coal-fired power plants.

¹² Sanchez, F. and D. S. Kosson, 2005. Probabilistic approach for estimating the release of contaminants under field management scenarios. *Waste Management* 25(5), 643-472 (2005).

Characterization of Coal Combustion Residues III

Table ES-2. Leach results for $5.4 \leq \text{pH} \leq 12.4$ and at “own pH¹³” from evaluation of thirty-four fly ashes.

	Hg	Sb	As	Ba	B	Cd	Cr	Co	Pb	Mo	Se	Tl
Total in Material (mg/kg)	0.01 – 1.5	3 – 14	17 – 510	590 – 7,000	NA	0.3 – 1.8	66 – 210	16 – 66	24 – 120	6.9 – 77	1.1 – 210	0.72 – 13
Leach results (µg/L)	<0.01 – 0.50	<0.3 – 11,000	0.32 – 18,000	50 – 670,000	210 – 270,000	<0.1 – 320	<0.3 – 7,300	<0.3 – 500	<0.2 – 35	<0.5 – 130,000	5.7 – 29,000	<0.3 – 790
TC (µg/L)	200	-	5,000	100,000	-	1,000	5,000	-	5,000	-	1,000	-
MCL (µg/L)	2	6	10	2,000	7,000 DWEL	5	100	-	15	200 DWEL	50	2

Note: The shade is used to indicate where there could be a potential concern for a metal when comparing the leach results to the MCL, DWEL, or TC. Note that MCL and DWEL values represent well concentrations; leachate dilution and attenuation processes that would occur in groundwater before leachate reaches a well are not accounted for, and so MCL and DWEL values are compared to leaching concentrations here to provide context for the test results and initial screening.

Table ES-3. Leach results for $5.4 \leq \text{pH} \leq 12.4$ and at “own pH” from evaluation of twenty FGD gypsums.

	Hg	Sb	As	Ba	B	Cd	Cr	Co	Pb	Mo	Se	Tl
Total in Material (mg/kg)	0.01 – 3.1	0.14 – 8.2	0.95 – 10	2.4 – 67	NA	0.11 – 0.61	1.2 – 20	0.77 – 4.4	0.51 – 12	1.1 – 12	2.3 – 46	0.24 – 2.3
Leach results (µg/L)	<0.01 – 0.66	<0.3 – 330	0.32 – 1,200	30 – 560	12 – 270,000	<0.2 – 370	<0.3 – 240	<0.2 – 1,100	<0.2 – 12	0.36 – 1,900	3.6 – 16,000	<0.3 – 1,100
TC (µg/L)	200	-	5,000	100,000	-	1,000	5,000	-	5,000	-	1,000	-
MCL (µg/L)	2	6	10	2,000	7,000 DWEL	5	100	-	15	200 DWEL	50	2

Note: The shade is used to indicate where there could be a potential concern for a metal when comparing the leach results to the MCL, DWEL, or TC. Note that MCL and DWEL values represent well concentrations; leachate dilution and attenuation processes that would occur in groundwater before leachate reaches a well are not accounted for, and so MCL and DWEL values are compared to leaching concentrations here to provide context for the test results and initial screening.

¹³ “Own pH” is defined as the end-point (equilibrium) eluate pH when a CCR is extracted with DI water at liquid to solid ratio of 10 mL/g, and is measured as part of leach testing as a function of pH.

TABLE OF CONTENTS

Acknowledgments.....	i
Abstract.....	ii
Glossary of terms.....	iv
Executive Summary.....	viii
Table of Contents.....	xv
List of Tables.....	xviii
List of Figures.....	xix
1. Introduction.....	1
1.1. Regulatory Context.....	5
1.1.1. Waste Management.....	5
1.1.2. Air Pollution Control.....	5
1.2. Configurations of U.S. Coal Fired Power Plants and Multi-pollutant Control Technologies.....	6
1.2.1. Current Air Pollution Control Technologies.....	7
1.2.2. Wet Scrubbers, NO _x Controls and Multi-pollutant Controls.....	9
1.2.3. Mercury Control Using Sorbent Injection.....	10
1.2.4. Mercury Control by Conventional PAC Injection.....	12
1.2.5. Mercury Control by Halogenated PAC Injection.....	13
1.3. Coal Combustion Residues.....	13
1.4. Residue Management Practices.....	14
1.4.1. Beneficial Use.....	14
1.4.2. Land Disposal.....	15
1.5. Leaching Protocol.....	17
2. Materials and Methods.....	21
2.1. CCR Materials for Evaluation.....	21
2.2. Leaching Assessment Protocols.....	34
2.2.1. Alkalinity, Solubility and Release as a Function of pH (SR002.1).....	34
2.2.2. Solubility and Release as a Function of LS Ratio (SR003.1).....	35
2.3. Analytical Methods.....	35
2.3.1. Surface Area and Pore Size Distribution.....	35
2.3.2. pH and Conductivity.....	35

Characterization of Coal Combustion Residues III

2.3.3. Moisture Content	36
2.3.4. Carbon Content - Organic Carbon/Elemental Carbon Analyzer	36
2.3.5. Dissolved Inorganic Carbon (DIC) and Dissolved Organic Carbon (DOC)	36
2.3.6. Mercury (CVAA, Method 3052, and Method 7473)	37
2.3.7. Other Metals (ICP-MS, ICP-AES, Method 3052, Method 6020, and Method 6010)	37
2.3.7.1. ICP-MS Analysis (SW-846 Method 6020).....	39
2.3.7.2. ICP-OES Analysis (SW-846 Method 6010).....	40
2.3.8. X-Ray Fluorescence (XRF)	42
2.3.9. XAFS	44
2.3.10. Determination of Hexavalent Chromium (Cr ⁶⁺) and Total Chromium Species in CCR Eluates.....	44
2.3.11. MDL and ML for Analytical Results.....	44
2.4. Quality Assurance assessment	45
2.4.1. Homogenization of Individual CCR Samples and Aliquots for Analyses.....	45
2.4.2. Leaching Test Methods and Analytical QA/QC.....	45
2.4.3. Improving QA/QC Efficiency.....	46
2.4.4. Data Management	47
2.5. Interpretation and Presentation of Laboratory Leaching Data.....	49
2.5.1. Interpretation of Mechanisms Controlling Constituent Leaching	49
2.5.2. Field pH Probability Distribution	52
3. Results and Discussion	54
3.1. Total Elemental Content	54
3.2. Laboratory Leaching Test Results	86
3.2.1. Typical Characteristic Leaching Behavior as a Function of pH.....	87
3.2.1.1. Fly Ash without Hg Sorbent Injection.....	88
Main characteristics leaching behavior (Figure 41 and Figure 42)	88
Effect of coal type (Figure 38, Figure 39, and Figure 40)	90
Effect of NO _x control (SNCR vs. SCR, Figure 43)	90
Effect of fabric filter vs. CS-ESP (Figure 44).....	91
Chromium speciation in selected fly ash samples and eluates (Figure 45)	91
3.2.1.2. Fly ash without and with Hg Sorbent Injection Pairs	106
3.2.1.3. Gypsum, Unwashed and Washed	111
3.2.1.4. Scrubber Sludge.....	118

Characterization of Coal Combustion Residues III

3.2.1.5. Spray Dryer Absorber Residues	121
3.2.1.6. Blended CCRs (Mixed Fly Ash and Scrubber Sludge/Mixed Fly Ash and Gypsum).....	124
3.2.1.7. Waste Water Filter Cake.....	127
3.2.2. Comparisons of the Ranges of Constituent Concentrations from Laboratory Testing (Minimum Concentrations, Maximum Concentrations, and Concentrations at the Materials' Own pH).....	130
3.2.3. Leaching Dependency on Total Content.....	146
3.2.4. pH at the Maximum Concentration Value versus the Materials' Own pH.....	153
3.2.5. Comparison of Constituent Maximum Concentrations and Concentrations at the Materials' Own pH from Laboratory Testing Grouped by Material Type with Measurements of Field Samples and the EPA Risk Report Database	162
3.2.6. Attenuation Factors Needed to Reduce Estimated Leachate Concentrations to Less Than Reference Indicators	177
4. Summary of Results, Conclusions and Recommendations.....	180
5. References.....	184
Appendices.....	189
A. Facility Descriptions and CCR Sample Locations.....	A-1
B. Quality Assurance Project Plan	B-1
C. Solid Phase Characterization of CCR Samples	C-1
D. Total Content by Digestion.....	D-1
E. Total Content by XRF.....	E-1
F. CCR Leaching Test Results	F-1
G. CCR pH Titration Curves	G-1
H. Hexavalent Chromium and Total Chromium Analyses by Arcadis & ERG	H-1
I. Summary of Statistics (Min/Max/Own pH value)	I-1
J. Summary of Statistics (Percentiles).....	J-1
K. Outliers.....	K-1
L. Attenuation Factors.....	L-1

ANNEX – Analytical QA/QC (all data on a DVD)

LIST OF TABLES

Table ES-1. Identification of CCRs evaluated and included in this Report. x

Table ES-2. Leach results for $5.4 \leq \text{pH} \leq 12.4$ and at “own pH” from evaluation of thirty-four fly ashes. xiv

Table ES-3. Leach results for $5.4 \leq \text{pH} \leq 12.4$ and at “own pH” from evaluation of twenty FGD gypsums. xiv

Table 1. General characteristics of coals burned in U. S. power plants (EPA, 2005). 6

Table 2. Projected coal-fired capacity by air pollution control configuration as per data collection in 1999 (EPA, 2005). 8

Table 3. Beneficial uses of CCRs (ACAA, 2007). 16

Table 4. Summary of facility configurations, CCR sample types and sample codes. 22

Table 5. CCR samples evaluated in this study, grouped by residue type, coal type and air pollution control configuration. 26

Table 6. MDL and ML of analysis of DIC and DOC. 37

Table 7. ICP instrument used for each element. 38

Table 8. Method detection limits (MDLs) and minimum level of quantification (ML) for ICP-MS analysis on liquid samples. 40

Table 9. Method detection limits (MDLs) and minimum level of quantification (ML) for ICP-OES analysis on liquid samples. 41

Table 10. XRF detection limits. 43

Table 11. Data quality indicator goals. 47

Table 12. Identification of CCRs evaluated and included in this Report. 181

Table 13. Fly Ash - Laboratory leach test eluate concentrations for $5.4 \leq \text{pH} \leq 12.4$ and at “own pH” from evaluation of thirty-four fly ash samples. 183

Table 14. FGD Gypsum - Laboratory leach test eluate concentrations for $5.4 \leq \text{pH} \leq 12.4$ and at “own pH” from evaluation of twenty FGD gypsum samples. 183

LIST OF FIGURES

Figure 1. Flow diagram describing processing and nomenclature of FGD scrubber residues and samples included in this study. 3

Figure 2. Illustration of available technology for multi-pollutant control at coal-fired power plants. 10

Figure 3. Coal-fired boiler with sorbent injection and spray cooling (Senior et al., 2003). 11

Figure 4. Flow diagram for power plant with a hot ESP, carbon injection, and a compact hybrid particulate collector (Senior et al., 2003). 12

Figure 5. Uses of CCRs based on 2006 industry statistics (ACAA, 2007). 17

Figure 6. An example of eluate concentrations as a function of pH from SR002.1. 51

Figure 7. An example of eluate concentrations as a function of LS ratio from SR003.1. 52

Figure 8. Probability distributions for field pH. Summary statistics for the field data and the probability distribution are provided to the right of the graph (EPA, 2000; EPA, 2007b; EPRI, 2006). 53

Figure 9. Aluminum. Comparison of total elemental content by digestion (Methods 3052 and 6020). 57

Figure 10. Arsenic. Comparison of total elemental content by digestion (Methods 3052 and 6020). 58

Figure 11. Barium. Comparison of total elemental content by digestion (Methods 3052 and 6020). 59

Figure 12. Cadmium. Comparison of total elemental content by digestion (Methods 3052 and 6020). 60

Figure 13. Cobalt. Comparison of total elemental content by digestion (Methods 3052 and 6020). 61

Figure 14. Chromium. Comparison of total elemental content by digestion (Methods 3052 and 6020). 62

Figure 15. Mercury. Comparison of total elemental content by digestion (Method 7470). 63

Figure 16. Mercury. Comparison of total elemental content by digestion (Method 7473). 64

Figure 17. Molybdenum. Comparison of total elemental content by digestion (Methods 3052 and 6020). 65

Figure 18. Lead. Comparison of total elemental content by digestion (Methods 3052 and 6020). 66

Figure 19. Antimony. Comparison of total elemental content by digestion (Methods 3052 and 6020). 67

Figure 20. Selenium. Comparison of total elemental content by digestion (Methods 3052 and 6020). 68

Characterization of Coal Combustion Residues III

Figure 21. Thallium. Comparison of total elemental content by digestion (Methods 3052 and 6020).	69
Figure 22. Aluminum. Comparison of total elemental content by XRF.....	70
Figure 23. Barium. Comparison of total elemental content by XRF.....	71
Figure 24. Carbon. Comparison of total elemental content.....	72
Figure 25. Calcium. Comparison of total elemental content by XRF.	73
Figure 26. Chloride. Comparison of total elemental content by XRF.....	74
Figure 27. Fluoride. Comparison of total elemental content by XRF.	75
Figure 28. Iron. Comparison of total elemental content by XRF.	76
Figure 29. Potassium. Comparison of total elemental content by XRF.....	77
Figure 30. Magnesium. Comparison of total elemental content by XRF.....	78
Figure 31. Sodium. Comparison of total elemental content by XRF.....	79
Figure 32. Phosphorous. Comparison of total elemental content by XRF.	80
Figure 33. Sulfur. Comparison of total elemental content by XRF.....	81
Figure 34. Silicon. Comparison of total elemental content by XRF.....	82
Figure 35. Strontium. Comparison of total elemental content by XRF.....	83
Figure 36. Thallium. Comparison of total elemental content by XRF.	84
Figure 37. Total calcium content (by XRF) and own pH for fly ash samples.....	85
Figure 38. pH dependent leaching results. Fly ash samples from facilities without mercury sorbent injection [bituminous low sulfur coal].	92
Figure 39. pH dependent leaching results. Fly ash samples from facilities without mercury sorbent injection [bituminous medium and high sulfur coal].	94
Figure 40. pH dependent leaching results. Fly ash samples from facilities without mercury sorbent injection [sub-bituminous and lignite coal].....	96
Figure 41. pH dependent leaching results. Selected results to illustrate characteristic leaching behavior.....	98
Figure 42. pH dependent leaching results. Selected results to illustrate characteristic leaching behavior of calcium, magnesium, strontium, iron, and sulfur.	100
Figure 43. Effect of NO _x controls - none (or by-passed; samples DFA, EFB, FFA, TFA), SNCR (samples GFA, SHB) or SCR (all other samples) for facilities burning Eastern Bituminous coal and using CS-ESP for particulate control.	101
Figure 44. Effect of fabric filter vs. CS-ESP (fabric filter without NO _x control, sample CFA; with SNCR, sample AFA; CS-ESP without NO _x control, samples DFA, EFB, FFA, TFA; with SNCR, samples GFA, SHB) for facilities burning Eastern Bituminous coal.....	103

Figure 45. Chromium speciation results. Bituminous coal: Facility B with SCR (BFA), with SCR-BP (DFA); Facility K with SCR (KFA); Facility A with SNCR (AFA), with SNCR-BP (CFA). Sub-bituminous coal: Facility J with SCR (JAB)..... 105

Figure 46. pH dependent leaching results. Fly ash samples from facility pairs with and without mercury sorbent injection. 109

Figure 47. pH dependent leaching results. Gypsum samples unwashed (sample codes __U) and washed (sample codes __W) from facilities using low and medium sulfur bituminous coals. 112

Figure 48. pH dependent leaching results. Gypsum samples unwashed (sample codes __U) and washed (sample codes __W) from facilities using high sulfur bituminous coal. 114

Figure 49. pH dependent leaching results. Gypsum samples unwashed (sample codes __U) and washed (sample codes __W) from facilities using sub-bituminous and lignite bituminous coals. 116

Figure 50. pH dependent leaching results. Scrubber sludges. 119

Figure 51. pH dependent leaching results. Spray dryer residue samples (sub-bituminous coal). 122

Figure 52. pH dependent leaching results. Facility A samples (low S east-bit., fabric filter, limestone, natural oxidation). SNCR-BP. Fly ash (CFA); scrubber sludge (CGD); blended fly ash and scrubber sludge (“as managed,” CCC). 125

Figure 53. pH dependent leaching results. Filter cake samples..... 128

Figure 54. Aluminum. Comparison of maximum, minimum and own pH concentrations observed in SR002.1 and SR003.1 eluates over the pH domain $5.4 \leq \text{pH} \leq 12.4$. SDA samples were from facilities burning sub-bituminous coal..... 132

Figure 55. Arsenic. Comparison of maximum, minimum and own pH concentrations observed in SR002.1 and SR003.1 eluates over the pH domain $5.4 \leq \text{pH} \leq 12.4$. SDA samples were from facilities burning sub-bituminous coal..... 133

Figure 56. Boron. Comparison of maximum, minimum and own pH concentrations observed in SR002.1 and SR003.1 eluates over the pH domain $5.4 \leq \text{pH} \leq 12.4$. SDA samples were from facilities burning sub-bituminous coal..... 134

Figure 57. Barium. Comparison of maximum, minimum and own pH concentrations observed in SR002.1 and SR003.1 eluates over the pH domain $5.4 \leq \text{pH} \leq 12.4$. SDA samples were from facilities burning sub-bituminous coal..... 135

Figure 58. Cadmium. Comparison of maximum, minimum and own pH concentrations observed in SR002.1 and SR003.1 eluates over the pH domain $5.4 \leq \text{pH} \leq 12.4$. SDA samples were from facilities burning sub-bituminous coal. 136

Figure 59. Cobalt. Comparison of maximum, minimum and own pH concentrations observed in SR002.1 and SR003.1 eluates over the pH domain $5.4 \leq \text{pH} \leq 12.4$. SDA samples were from facilities burning sub-bituminous coal..... 137

Characterization of Coal Combustion Residues III

Figure 60. Chromium. Comparison of maximum, minimum and own pH concentrations observed in SR002.1 and SR003.1 eluates over the pH domain $5.4 \leq \text{pH} \leq 12.4$. SDA samples were from facilities burning sub-bituminous coal.	138
Figure 61. Mercury. Comparison of maximum, minimum and own pH concentrations observed in SR002.1 and SR003.1 eluates over the pH domain $5.4 \leq \text{pH} \leq 12.4$. SDA samples were from facilities burning sub-bituminous coal.	139
Figure 62. Molybdenum. Comparison of maximum, minimum and own pH concentrations observed in SR002.1 and SR003.1 eluates over the pH domain $5.4 \leq \text{pH} \leq 12.4$. SDA samples were from facilities burning sub-bituminous coal.	140
Figure 63. Lead. Comparison of maximum, minimum and own pH concentrations observed in SR002.1 and SR003.1 eluates over the pH domain $5.4 \leq \text{pH} \leq 12.4$. SDA samples were from facilities burning sub-bituminous coal.	141
Figure 64. Antimony. Comparison of maximum, minimum and own pH concentrations observed in SR002.1 and SR003.1 eluates over the pH domain $5.4 \leq \text{pH} \leq 12.4$. SDA samples were from facilities burning sub-bituminous coal.	142
Figure 65. Selenium. Comparison of maximum, minimum and own pH concentrations observed in SR002.1 and SR003.1 eluates over the pH domain $5.4 \leq \text{pH} \leq 12.4$. SDA samples were from facilities burning sub-bituminous coal.	143
Figure 66. Thallium. Comparison of maximum, minimum and own pH concentrations observed in SR002.1 and SR003.1 eluates over the pH domain $5.4 \leq \text{pH} \leq 12.4$. SDA samples were from facilities burning sub-bituminous coal.	144
Figure 67. pH. Comparison of maximum, minimum and own pH observed in SR002.1 and SR003.1 eluates over the pH domain $5.4 \leq \text{pH} \leq 12.4$. SDA samples were from facilities burning sub-bituminous coal.	145
Figure 68 and Figure 69. Aluminum and Arsenic. Maximum eluate concentration ($5.4 \leq \text{pH} \leq 12.4$) as a function of total content by digestion.	147
Figure 70 and Figure 71. Barium and Cadmium. Maximum eluate concentration ($5.4 \leq \text{pH} \leq 12.4$) as a function of total content by digestion.	148
Figure 72 and Figure 73. Cobalt and Chromium. Maximum eluate concentration ($5.4 \leq \text{pH} \leq 12.4$) as a function of total content by digestion.	149
Figure 74 and Figure 75. Mercury and Molybdenum. Maximum eluate concentration ($5.4 \leq \text{pH} \leq 12.4$) as a function of total content by digestion.	150
Figure 76 and Figure 77. Lead and Antimony. Maximum eluate concentration ($5.4 \leq \text{pH} \leq 12.4$) as a function of total content by digestion.	151
Figure 78 and Figure 79. Selenium and Thallium. Maximum eluate concentration ($5.4 \leq \text{pH} \leq 12.4$) as a function of total content by digestion.	152
Figure 80. An example of pH identity plot. Dashed red lines are used to indicate the pH domain of 5.4 to 12.4.	154
Figure 81 and Figure 82. Aluminum and Arsenic. pH identity plots.	155
Figure 83 and Figure 84. Boron and Barium. pH identity plots.	156

Figure 85 and Figure 86. Cadmium and Cobalt. pH identity plots..... 157

Figure 87 and Figure 88. Chromium and Mercury. pH identity plots..... 158

Figure 89 and Figure 90. Molybdenum and Lead. pH identity plots..... 159

Figure 91 and Figure 92. Antimony and Selenium. pH identity plots..... 160

Figure 93. Thallium. pH identity plots..... 161

Figure 94. Aluminum. Comparison of maximum concentrations observed in SR002.1 and SR003.1 eluates over the pH domain $5.4 \leq \text{pH} \leq 12.4$, own pH concentrations from SR002.1 at LS = 10mL/g, and reference data ranges derived from the EPRI database of field leachate and pore water concentrations (EPRI SI – surface impoundments; EPRI LF – landfills) and the EPA Risk Report (EPA, 2007b)..... 164

Figure 95. Arsenic. Comparison of maximum concentrations observed in SR002.1 and SR003.1 eluates over the pH domain $5.4 \leq \text{pH} \leq 12.4$, own pH concentrations from SR002.1 at LS = 10mL/g, and reference data ranges derived from the EPRI database of field leachate and pore water concentrations (EPRI SI – surface impoundments; EPRI LF – landfills) and the EPA Risk Report (EPA, 2007b)..... 165

Figure 96. Boron. Comparison of maximum concentrations observed in SR002.1 and SR003.1 eluates over the pH domain $5.4 \leq \text{pH} \leq 12.4$, own pH concentrations from SR002.1 at LS = 10mL/g, and reference data ranges derived from the EPRI database of field leachate and pore water concentrations (EPRI SI – surface impoundments; EPRI LF – landfills) and the EPA Risk Report (EPA, 2007b)..... 166

Figure 97. Barium. Comparison of maximum concentrations observed in SR002.1 and SR003.1 eluates over the pH domain $5.4 \leq \text{pH} \leq 12.4$, own pH concentrations from SR002.1 at LS = 10mL/g, and reference data ranges derived from the EPRI database of field leachate and pore water concentrations (EPRI SI – surface impoundments; EPRI LF – landfills) and the EPA Risk Report (EPA, 2007b)..... 167

Figure 98. Cadmium. Comparison of maximum concentrations observed in SR002.1 and SR003.1 eluates over the pH domain $5.4 \leq \text{pH} \leq 12.4$, own pH concentrations from SR002.1 at LS = 10mL/g, and reference data ranges derived from the EPRI database of field leachate and pore water concentrations (EPRI SI – surface impoundments; EPRI LF – landfills) and the EPA Risk Report (EPA, 2007b)..... 168

Figure 99. Cobalt. Comparison of maximum concentrations observed in SR002.1 and SR003.1 eluates over the pH domain $5.4 \leq \text{pH} \leq 12.4$, own pH concentrations from SR002.1 at LS = 10mL/g, and reference data ranges derived from the EPRI database of field leachate and pore water concentrations (EPRI SI – surface impoundments; EPRI LF – landfills) and the EPA Risk Report (EPA, 2007b)..... 169

Figure 100. Chromium. Comparison of maximum concentrations observed in SR002.1 and SR003.1 eluates over the pH domain $5.4 \leq \text{pH} \leq 12.4$, own pH concentrations from SR002.1 at LS = 10mL/g, and reference data ranges derived from the EPRI database of field leachate and pore water concentrations (EPRI SI – surface impoundments; EPRI LF – landfills) and the EPA Risk Report (EPA, 2007b)..... 170

Characterization of Coal Combustion Residues III

Figure 101. Mercury. Comparison of maximum concentrations observed in SR002.1 and SR003.1 eluates over the pH domain $5.4 \leq \text{pH} \leq 12.4$, own pH concentrations from SR002.1 at LS = 10mL/g, and reference data ranges derived from the EPRI database of field leachate and pore water concentrations (EPRI SI – surface impoundments; EPRI LF – landfills) and the EPA Risk Report (EPA, 2007b)..... 171

Figure 102. Molybdenum. Comparison of maximum concentrations observed in SR002.1 and SR003.1 eluates over the pH domain $5.4 \leq \text{pH} \leq 12.4$, own pH concentrations from SR002.1 at LS = 10mL/g, and reference data ranges derived from the EPRI database of field leachate and pore water concentrations (EPRI SI – surface impoundments; EPRI LF – landfills) and the EPA Risk Report (EPA, 2007b)..... 172

Figure 103. Lead. Comparison of maximum concentrations observed in SR002.1 and SR003.1 eluates over the pH domain $5.4 \leq \text{pH} \leq 12.4$, own pH concentrations from SR002.1 at LS = 10mL/g, and reference data ranges derived from the EPRI database of field leachate and pore water concentrations (EPRI SI – surface impoundments; EPRI LF – landfills) and the EPA Risk Report (EPA, 2007b). 173

Figure 104. Antimony. Comparison of maximum concentrations observed in SR002.1 and SR003.1 eluates over the pH domain $5.4 \leq \text{pH} \leq 12.4$, own pH concentrations from SR002.1 at LS = 10mL/g, and reference data ranges derived from the EPRI database of field leachate and pore water concentrations (EPRI SI – surface impoundments; EPRI LF – landfills) and the EPA Risk Report (EPA, 2007b)..... 174

Figure 105. Selenium. Comparison of maximum concentrations observed in SR002.1 and SR003.1 eluates over the pH domain $5.4 \leq \text{pH} \leq 12.4$, own pH concentrations from SR002.1 at LS = 10mL/g, and reference data ranges derived from the EPRI database of field leachate and pore water concentrations (EPRI SI – surface impoundments; EPRI LF – landfills) and the EPA Risk Report (EPA, 2007b)..... 175

Figure 106. Thallium. Comparison of maximum concentrations observed in SR002.1 and SR003.1 eluates over the pH domain $5.4 \leq \text{pH} \leq 12.4$, own pH concentrations from SR002.1 at LS = 10mL/g, and reference data ranges derived from the EPRI database of field leachate and pore water concentrations (EPRI SI – surface impoundments; EPRI LF – landfills) and the EPA Risk Report (EPA, 2007b)..... 176

Figure 107. Minimum attenuation factor needed for the maximum eluate concentration ($5.4 \leq \text{pH} \leq 12.4$) to be reduced below the MCL or DWEL for all COPCs considered in this study. COPC requiring the greatest attenuation factor is indicated for each CCR..... 178

Figure 108. Minimum attenuation factor needed for the own pH eluate concentration to be reduced below the MCL or DWEL for all COPCs considered in this study. COPC requiring the greatest attenuation factor is indicated for each CCR..... 179

1. INTRODUCTION

More wide-spread implementation of multi-pollutant controls is occurring at U.S. coal-fired power plants. Although much research has occurred to characterize high-volume coal combustion residues [i.e., fly ash, bottom ash, boiler slag, and flue gas desulfurization (FGD) solids] extending back to the 1970s, previous research has not considered the wide range of field conditions that occur for coal combustion residues (CCRs) during land disposal and use in agricultural, commercial, and engineering applications. The objective of this research is to characterize the changes in total composition and constituent release potential occurring to CCRs resulting from wider use of multi-pollutant controls at U.S. coal-fired power plants. This characterization includes detailed analysis of the fly ash and other air pollution control residues in relationship to differences in air pollution control configurations and coal rank. The characterization also includes evaluating the leaching potential of constituents of potential concern (COPCs) across the range of plausible management conditions that CCRs are likely to encounter during land disposal or use in agricultural, commercial, and engineering applications. This research was cited as a priority in EPA's Mercury Roadmap (EPA, 2006b) to evaluate the potential for any cross-media transfers from the management of CCRs resulting from more stringent air pollution control at coal fired power plants. This report is part of a series of reports helping to document the findings of this research to provide more credible, up-to-date data on CCRs to identify any potential cross-media transfers.

The focus of this report is to present an evaluation of air pollution control residues that may result from the use of SO₂ scrubbers and other air pollution control technologies being used to control multiple pollutants at coal-fired power plants. The pathway of concern addressed in this report is the potential for transfer of pollutants to water resources or other environmental systems (e.g., soils, sediments). The residues studied for this report were fly ashes, unwashed and washed flue gas desulfurization (FGD) gypsum, scrubber sludge, blended CCR residues "as managed" (mixtures of fly ash and scrubber residues with and without added lime or mixture of fly ash and gypsum), and wastewater filter cake generated from power plants with a range of air pollution control configurations.

In particular, this report focuses on the potential for leaching of mercury and other COPCs during land disposal or beneficial use of the CCRs is the focus of this report. This research is part of an on-going effort by EPA to use an integrated, comprehensive approach to account for the fate of mercury and other metals in coal throughout the life-cycle stages of CCR management (Sanchez et al., 2006; Thorneloe et al., 2009; Thorneloe et al., 2008). Related research and assessment on environmental fate of constituents during CCR management includes conducting thermal stability studies, leach testing, and probabilistic assessment modeling to determine the fate of mercury and other metals that are in coal combustion residues resulting from implementation of multi-pollutant control technology (EPA, 2002; Kilgroe et al., 2001).

CCRs include bottom ash, boiler slag, fly ash, scrubber residues and other miscellaneous solids generated during the combustion of coal. Air pollution control can concentrate or partition metals to fly ash and scrubber residues. The boiler slag and bottom ash are not of interest in this study because air emission controls are not expected to change their composition. Use of multi-pollutant controls minimizes air emissions of mercury and other metals by the transfer of the metals to the fly ash and other CCRs. This research will help determine the fate of mercury and other COPCs from the management of CCRs through either disposal or reuse. Fly ash may

Characterization of Coal Combustion Residues III

include unburned carbonaceous materials and inorganic materials in coal that do not burn, such as oxides of silicon, aluminum, iron, and calcium. Fly ash is light enough to be entrained in the flue gas stream and captured in the air pollution control equipment.

The type and characteristics of FGD scrubber residue produced is primarily a function of (i) the scrubber sorbent used (i.e., limestone, lime, magnesium enriched lime referred to as Mg lime, or alkaline fly ash), (ii) the extent of oxidation during scrubbing (i.e., forced oxidation, natural oxidation, or inhibited oxidation), (iii) post-scrubber processing, including possibly dewatering or thickening, drying, water rinsing, or blending with other materials, and (iv) coal rank combusted. The presence and leaching characteristics of the COPCs in air pollution control residues is a consequence of the coal combusted, process sequence employed, process conditions, process additives and use or disposal scenario.

Figure 1 illustrates the processes used in the production of materials that were sampled for this study, sample nomenclature, and the typical management pathways for each material. FGD gypsum is defined here as the by-product of the SO₂ wet scrubbing process when the scrubber residue is subjected to forced oxidation. In forced oxidation systems, nearly all of the by-product is calcium sulfate dihydrate (CaSO₄•H₂O). The resulting wet gypsum is partially dewatered and then either disposed in a landfill (unwashed gypsum; Gyp-U) or water rinsed (in some cases) and dried to produce washed gypsum (washed gypsum; Gyp-W) that then potentially can be used in wallboard manufacturing or agricultural applications. Scrubber sludge (ScS) is the by-product of the SO₂ wet scrubbing process resulting from neutralization of acid gases at facilities that use either inhibited oxidation or natural oxidation of scrubber residue. In inhibited oxidation systems, nearly all of the by-product is calcium sulfite hemihydrates (CaSO₃•½H₂O). In natural oxidation systems, the by-product is a mixture of CaSO₃•½H₂O and CaSO₄•H₂O. Scrubber sludge typically will be either partially dewatered in a thickener and then disposed in a surface impoundment, or after thickening, further dewatered and mixed with fly ash to form blended CCRs “as managed¹⁴.” In most cases, additional lime is also blended with the scrubber sludge and fly ash. The blend of fly ash and scrubber sludge is typically between 0.5 to 1.5 parts fly ash to 1 part scrubber sludge on a dry weight basis, with 0 or 2-4% additional lime added. Blended CCRs typically are either disposed in a landfill or supplied to a beneficial use (e.g., fill in mining applications). Facilities that have spray dryer absorbers (SDA) collect fly ash and FGD residues simultaneously as a sample residue stream.

This report evaluates the characteristics of fly ash, FGD gypsum, SDA, scrubber sludge, and blended CCRs “as managed” from thirty one (31) coal combustion facilities. In addition filter cake from waste water treatment was evaluated from four facilities.

¹⁴ As managed is defined as how the material is managed by the coal-fired power plant either through disposal or reuse.

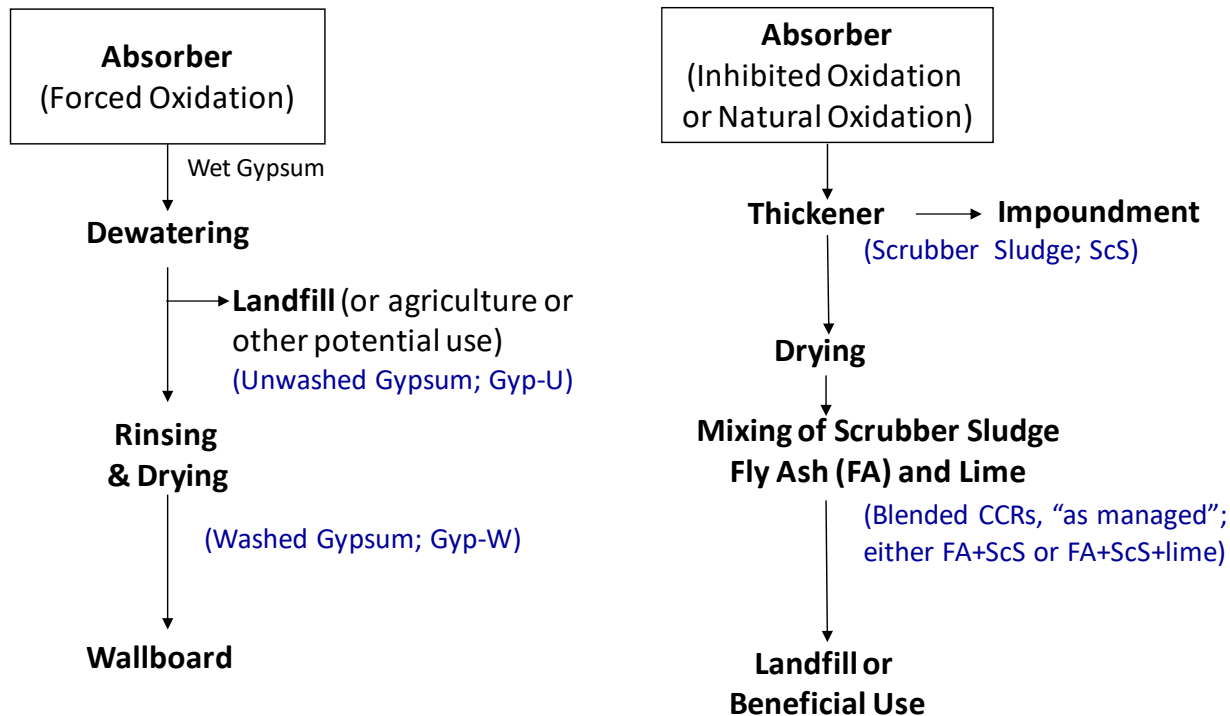


Figure 1. Flow diagram describing processing and nomenclature of FGD scrubber residues and samples included in this study.

When coal is burned in an electric utility boiler, the resulting high combustion temperatures vaporize the Hg in the coal to form gaseous elemental mercury (Hg^0). Subsequent cooling of the combustion gases and interaction of the gaseous Hg^0 with other combustion products may result in a portion of the Hg being converted to gaseous oxidized forms of mercury (Hg^{2+}) and particle-bound mercury (Hg_p). The specific chemical form—known as the speciation—has a strong impact on the capture of mercury and other metals by boiler air pollution control (APC) equipment (EPA, 2001).

Mercury and other elements partition between the combustion gas, fly ash and scrubber residues. Depending upon the gas conditioning, presence or absence of post-combustion NO_x control and other air pollution control technology in use, there may be changes occurring to the fly ash that can affect the stability and mobility of mercury and other metals in the CCRs. Similarly, NO_x control and SO_2 scrubber technology may affect the content, stability and mobility of mercury and other metals in scrubber residues.

The specific objectives of the research reported here are to:

1. Conduct analysis on range of air pollution control residues (i.e., fly ash, FGD residues and other CCRs) resulting from differences in coal rank and air pollution control configurations;
2. Evaluate the potential for leaching to groundwater of mercury and other COPCs (i.e., aluminum, antimony, arsenic, barium, boron, cadmium, chromium, cobalt, lead, molybdenum, selenium, and thallium) removed from the flue gas of coal-fired power plants using multi-pollutant controls to reduce air pollution; and

Characterization of Coal Combustion Residues III

3. Provide the foundation for assessing the impact of enhanced mercury and multi-pollutant control technology on leaching of mercury and other COPCs from CCR management including storage, beneficial use, and disposal.

This is the third of a series of reports that addresses the potential for cross-media transfer of COPCs from CCRs. The first report focused on the use of sorbent injection (activated carbon and brominated activated carbon) for enhanced mercury control (Sanchez et al., 2006). The second report focused on facilities that use wet scrubbers for multi-pollutant control and includes results for 23 CCRs (fly ash, gypsum, scrubber sludge, fixated scrubber sludge) sampled from eight facilities (Sanchez et al., 2008). This report focuses on CCRs from coal-fired power plants that use air pollution control technologies, other than those evaluated in the first two reports, necessary to span the range of anticipated coal-types and air pollution control technology configurations. A subsequent report will address:

- Assessment of leaching of COPCs under additional management scenarios, including impoundments and beneficial use on the land (report 4); and,
- Broader correlation of CCR leaching characteristics to coal rank, combustion facility characteristics and geochemical speciation within CCRs supported by information and analysis on additional trace elements and primary constituents (report 4).

Sampled CCRs were subjected to multiple leaching conditions according to the designated leaching assessment approach, which is designed to examine leaching potential over a range of pH and LS ratios. Leaching conditions included batch equilibrium¹⁵ extractions at acidic, neutral and alkaline conditions at an LS of 10 mL/g, and LS from 0.5 to 10 mL/g using distilled water as the leachant. In this report, the results of this testing are being used to evaluate the likely range of leaching characteristics during land disposal (i.e., landfill or surface impoundment) scenarios. Results of the laboratory leaching tests carried out in this study were compared to the range of observed constituent concentrations in field leachates reported in a U.S. EPA database (EPA, 2007b) and an Electric Power Research Institute (EPRI) database (EPRI, 2006). The testing results presented here will be used for evaluating disposal and beneficial use scenarios in a subsequent report.

The extensive nature of the results reported here necessitates detailed data presentation with only a broad assessment overview. Future reports will provide more detailed data evaluation and application of the data to evaluation of specific CCR management scenarios.

As part of this research program, a quality assurance/quality control (QA/QC) plan consistent with EPA requirements was developed for the leaching assessment approach (see Section 2.4). The QA/QC methodology included initial verification of acceptable mercury retention during laboratory testing through evaluation of a mass balance around testing procedures (Sanchez et al., 2006). Modifications to the QA/QC program to reduce the experimental and analytical burden while maintaining confidence in the resulting data, based on program results to date, are presented in Report 2 (Sanchez et al., 2008); further modifications are identified in this report.

¹⁵ In the context of leaching tests, the term “equilibrium” is used to indicate that the test method result is a reasonable approximation of chemical equilibrium conditions even though thermodynamic equilibrium may not be approached for all constituents.

Laboratory testing for leaching assessment was carried out at the EPA National Risk Management Research Laboratory (Research Triangle Park, North Carolina).

1.1. REGULATORY CONTEXT

1.1.1. Waste Management

The management of coal combustion residues is subject to the Resource Conservation and Recovery Act (RCRA) which is the federal law regulating both solid and hazardous wastes. Hazardous waste regulations are developed under Subtitle C of RCRA whereas other solid and non-hazardous wastes fall under RCRA Subtitle D. Subtitle C wastes are federally regulated while Subtitle D wastes are regulated primarily at the state level. The original version of RCRA did not specify whether CCRs were Subtitle C or D wastes. In 1980, the Solid Waste Disposal Act (SWDA) amendments to RCRA conditionally excluded CCRs from Subtitle C regulation pending completion of a study of CCR hazards. Since that time, CCRs have been regulated at the state level under Subtitle D.

The SWDA amendments to RCRA required EPA to prepare a Report to Congress identifying CCR hazards and recommending a regulatory approach for CCRs. In this report (EPA, 1988) and the subsequent regulatory determination, EPA recommended that CCRs generated by electric utilities continue to be regulated under RCRA Subtitle D (See 58 FR 42466, August 9, 1993).

Other residues generated at coal-fired electric utilities were not included in this 1993 decision. EPA conducted a follow-up study specifically aimed at low-volume, co-managed wastes¹⁶ and issued another Report to Congress (EPA, 1999) with a similar recommendation. In April 2000, EPA issued a regulatory determination retaining the existing exemption from hazardous waste regulation for these wastes, although national regulation under RCRA Subtitle D were considered to be warranted (see 65 FR 32214, May 22, 2000). Concern also was expressed over the use of CCRs as backfill for mine reclamation operations, and it was determined that this practice should also be regulated under a federal Subtitle D rule. No regulation of other beneficial uses of CCRs was considered necessary at that time. Currently, the agency is in the process of developing these regulations (<http://www.epa.gov/osw/nonhaz/industrial/special/index.htm>). The results presented in this report, and subsequent reports, will help provide the information needed to identify the release potential of mercury and other metals that have been removed from stack gases into air pollution control residues, over a range of plausible management options. These data will help identify those conditions that will either reduce or enhance releases to the land so that the effects of different management conditions can be factored into any controls developed under the regulations.

1.1.2. Air Pollution Control

Coal-fired power plants are the largest remaining source of anthropogenic mercury emissions in the country. Power plants are also a major source of nitrogen and sulfur oxides, particulate matter, and carbon dioxide. New environmental regulations in the U.S. will result in lower mercury air emissions, but potentially more mercury in CCRs. The Clean Air Mercury Rule (CAMR) would have required the electric utility sector to remove at least 70% of the mercury

¹⁶ Co-managed wastes are low-volume wastes that are co-managed with the high-volume CCRs.

Characterization of Coal Combustion Residues III

released from power plant stack emissions by 2018. However, CAMR was vacated by the United States Court of Appeals for the District of Columbia Circuit in 2008. EPA is currently developing regulations under Section 112 of the Clean Air Act to reduce hazardous air pollutants (including mercury) from coal-fired power plants. Twenty states have implemented their own mercury regulations already, according to the National Association of Clean Air Agencies (Senior et al., 2009). Other EPA regulations¹⁷ will necessitate the addition of new air pollution control devices for NO_x and SO₂ at some power plants. This can also affect the fate of mercury and other COPCs.

1.2. CONFIGURATIONS OF U.S. COAL FIRED POWER PLANTS AND MULTI-POLLUTANT CONTROL TECHNOLOGIES

In the U.S., there are approximately 1,100 units at approximately 500 coal-fired electricity generating facilities. These facilities represent a range of coal ranks, boiler types, and air pollution control technologies. The combined capacity of U.S. coal-fired power plants as of 2007 is 315 GW with a projection to 360 GW by 2030 (DOE-EIA, 2009). The coal rank burned and facility design characteristics affect the effectiveness of multi-pollutant control technologies that are or could be used at these plants. The U.S. coal-fired power plants typically burn one of three types of fuel: (1) bituminous coal (also referred to as “high rank” coal), (2) sub-bituminous coal, and (3) lignite (sub-bituminous coal and lignite are referred to as “low rank” coals). Some of the characteristics of interest related to the possible environmental impacts of burning these different coal ranks are given in Table 1 (EPA, 2005).

Table 1. General characteristics of coals burned in U. S. power plants (EPA, 2005).

Coal	Mercury		Chlorine		Sulfur		Ash		HHV ^a	
	ppm (dry)		ppm (dry)		% (dry)		% (dry)		BTU/lb (dry)	
	Range	Avg	Range	Avg	Range	Avg	Range	Avg	Range	Avg
Bituminous	0.036 - 0.279	0.113	48 - 2,730	1,033	0.55 - 4.10	1.69	5.4 - 27.3	11.1	8,650-14,000	13,200
Sub-bituminous	0.025 - 0.136	0.071	51 - 1,143	158	0.22 - 1.16	0.50	4.7 - 26.7	8.0	8,610-13,200	12,000
Lignite	0.080 - 0.127	0.107	133 - 233	188	0.8 - 1.42	1.30	12.2 - 24.6	19.4	9,490-10,700	10,000

^a Higher Heating Value.

¹⁷On March 10, 2005, EPA announced the Clean Air Interstate Rule (CAIR) (FR 25612, May 2005) which is expected to increase the use of wet scrubbers and selective catalytic reduction (SCR) units to help reduce sulfur dioxide and nitrogen oxides emissions from coal-fired power plants. On July 11, 2008, United States Court of Appeals for the District of Columbia Circuit remanded CAIR back to EPA for further review and clarification. Thus the rule remains in effect; however, EPA is in the process of developing a replacement rule that will address the Court’s concerns.

1.2.1. Current Air Pollution Control Technologies

A range of pollution control technologies is used to reduce particulate, SO₂, and NO_x and these technologies also impact the emission of mercury and other metals. The pollution control technology type and configurations vary across facilities.¹⁸

Table 2 shows the current and projected coal-fired capacity by air pollution control technology configuration using data published in a 2005 report (EPA, 2005). Although the projected capacity information is considered dated, the projections for air pollution control appear relevant. The major finding from this report is the projected usage for wet scrubbers which are expected to double or triple in response to implementation of CAIR. Post-combustion particulate matter controls used at coal-fired utility boilers in the United States can include electrostatic precipitators (ESPs), fabric filters (FFs), particulate scrubbers (PSs), or mechanical collectors (MCs). Post-combustion SO₂ controls can consist of a wet scrubber (WS), spray dryer adsorber (SDA), or duct injection. Post-combustion NO_x controls typically involve selective catalytic reduction (SCR) or selective non-catalytic reduction (SNCR).

In response to current and proposed NO_x and SO₂ control requirements, additional post-combustion NO_x control and flue gas desulfurization (FGD) systems for SO₂ control are expected to be installed and more widely used in the future. Some estimates project a doubling or tripling of the number of wet scrubbers as a result of CAIR implementation. Over half of the U.S. coal-fired capacity is projected to be equipped with SCR and, or, FGD technology by 2020. Currently, some power plants only use post-combustion NO_x controls during summer months or when tropospheric ozone is more of a concern. However, likely changes will involve using post-combustion NO_x control year-round.

The mercury capture efficiency of existing ESPs and FFs appears to be heavily dependent on the partitioning of mercury between the particulate and vapor phases and the distribution of mercury species (e.g., elemental or oxidized) in the vapor phase. In general, ESPs and FFs which are designed for particulate control are quite efficient at removing mercury in the particulate phase; however, the overall mercury removal efficiency in these devices may be low if most of the mercury entering the device is in the vapor phase (MTI, 2001). Many factors contribute to the observed differences in mercury removal efficiency, such as the mercury oxidation state. Differences in mercury contents of U.S. coals also result in a range of mercury concentrations in the flue gas from the boiler. In general, it is easier to achieve higher mercury percent removal with higher mercury inlet concentrations (MTI, 2001). Further, the chlorine content of the coal may have an impact on mercury removal because the oxidation state of mercury is strongly affected by the presence of halides in the flue gas. In general, the higher the chlorine content of the coal, the more likely the mercury will be present in its oxidized state, enhancing the likelihood of its removal from the gas stream. The addition of post-combustion NO_x controls may improve mercury capture efficiency of particulate collection devices for some cases as a result of the oxidation of elemental mercury (EPA, 2001).

¹⁸ Concerns regarding carbon dioxide emissions from coal fired power plants are beyond the scope of this report.

Characterization of Coal Combustion Residues III

Table 2. Projected coal-fired capacity by air pollution control configuration as per data collection in 1999 (EPA, 2005). CCR samples evaluated in this report are from configurations indicated by shaded (light gray) rows. 2005 capacity reflects date of data collection for EPA report (EPA, 2005).

Air Pollution Control Configuration	2005 Capacity, MW	2010 Capacity, MW (projected)	2020 Capacity, MW (projected)
Cold-side ESP	111,616	75,732	48,915
Cold-side ESP + Wet Scrubber	41,745	34,570	33,117
Cold-side ESP + Wet Scrubber + ACI	-	379	379
Cold-side ESP + Dry Scrubber	2,515	3,161	5,403
Cold-side ESP + SCR	45,984	35,312	22,528
Cold-side ESP + SCR + Wet Scrubber	27,775	62,663	98,138
Cold-side ESP + SCR + Dry Scrubber	-	11,979	13,153
Cold-side ESP + SNCR	7,019	4,576	2,534
Cold-side ESP + SNCR + Wet Scrubber	317	2,830	6,088
Fabric Filter	11,969	10,885	7,646
Fabric Filter + Dry Scrubber	8,832	8,037	9,163
Fabric Filter + Wet Scrubber	4,960	4,960	4,960
Fabric Filter + Dry Scrubber + ACI	-	195	195
Fabric Filter + SCR	2,210	2,950	1,330
Fabric Filter + SCR + Dry Scrubber	2,002	2,601	4,422
Fabric Filter + SCR + Wet Scrubber	805	805	2,363
Fabric Filter + SNCR	267	267	345
Fabric Filter + SNCR + Dry Scrubber	559	557	557
Fabric Filter + SNCR + Wet Scrubber	932	932	1,108
Hot-side ESP	18,929	11,763	10,160
Hot-side ESP + Wet Scrubber	8,724	10,509	10,398
Hot-side ESP + Dry Scrubber	-	538	538
Hot-side ESP + SCR	5,952	3,233	1,847
Hot-side ESP + SCR + Wet Scrubber	688	6,864	9,912
Hot-side ESP + SNCR	684	1,490	1,334
Hot-side ESP + SNCR + Wet Scrubber	474	474	627
Existing or Planned Retrofit Units	~305,000	~298,000	297,000
New Builds of Coal Steam Units	2005 Capacity, MW	2010 Capacity, MW	2020 Capacity, MW
Fabric Filter + SCR + Wet Scrubber	-	221	17,292
Total All Units	~305,000	~298,500	~314,400
<p>Note: IGCC units are not included as part of this list. Note: Current capacity includes some SCR and FGD projected to be built in 2005 and 2006. Note: 2010 and 2020 is capacity projected for final CAIR rule. Note: Integrated Planning Model (IPM) projects some coal retirements and new coal in 2010 and 2020. (http://www.epa.gov/airmarkt/progsregs/epa-ipm/index.html)</p>			

1.2.2. Wet Scrubbers, NO_x Controls and Multi-pollutant Controls

Wet FGD scrubbers are the most widely used technology for SO₂ control. Scrubbers are typically installed downstream of particulate control (i.e., ESP or FF). Removal of PM from the flue gas before it enters the wet scrubber reduces solids in the scrubbing solution and minimizes impacts to the fly ash that might affect its beneficial use.

FGD technology uses sorbents and chemical reactants such as limestone (calcium carbonate) or lime (hydrated to form calcium hydroxide) to remove sulfur dioxide from the flue gas created from coal combustion. Limestone is ground into a fine powder and then combined with water to spray the slurry into combustion gases as they pass through a scrubber vessel. The residues are collected primarily as calcium sulfite (a chemically reduced material produced in natural oxidation or inhibited oxidation scrubbers), or can be oxidized to form calcium sulfate or FGD gypsum (using forced oxidation). The most widely used FGD systems use either forced oxidation scrubbers with limestone addition, or natural/inhibited oxidation scrubbers with lime or Mg-lime addition¹⁹. Wet scrubbers that use forced oxidation produce calcium sulfate (gypsum) and are expected to be the most prevalent technology because of the potential beneficial use of gypsum and easier management and handling of the residues. There are also dry FGD systems that include spray dryer absorbers, usually in combination with a FF (EPA, 2001; Srivastava et al., 2001).

NO_x emissions are controlled through the use of low NO_x producing burners and use of a selective catalytic reduction (SCR) system in the flue gas that is capable of a 90% reduction of flue gas NO_x emissions. SCR is typically installed upstream of the PM control device. Sometimes selective non-catalytic reduction (SNCR) is used for NO_x control, although use of SNCR is less common.

Figure 2 illustrates options for multi-pollutant control at power plants.

¹⁹ As of 1999: Total FGD units–151; limestone forced oxidation (FO)-38 units (25%); limestone natural/inhibited oxidation - 65 (43%); lime FO (all forms other than Mg-lime) - 1 (<1%); lime natural/inhibited oxidation (all forms other than Mg-lime) - 23 (15%); Mg-lime FO - 0 (0%); Mg-lime natural/inhibited oxidation - 25 (17%). It is estimated that the numbers of natural/inhibited systems has remained nearly the same since 1999, and the limestone FO units have increased significantly. In the future, limestone FO units will increase significantly, and all types of natural/inhibited units will likely decrease (Ladwig, 2007).

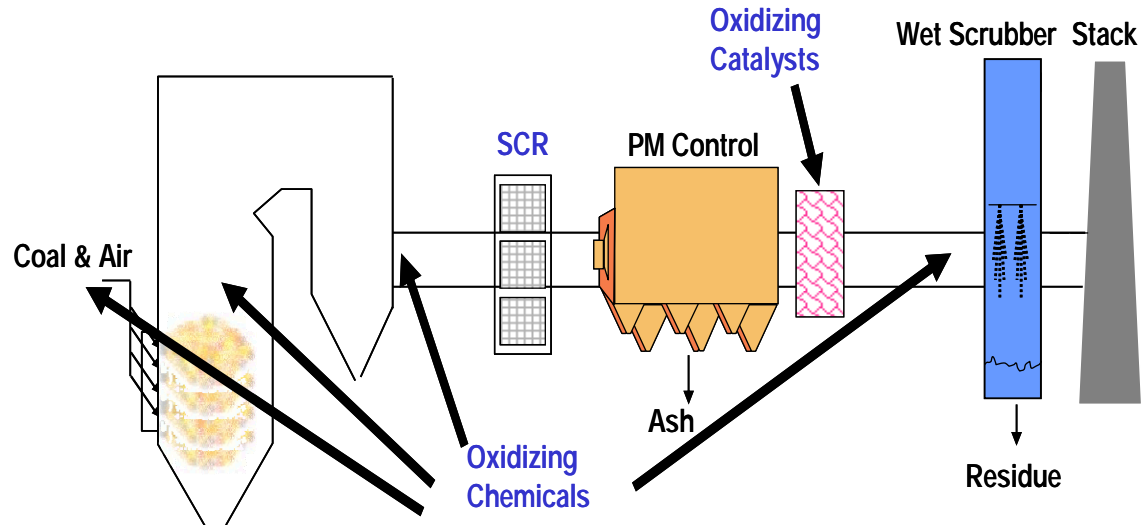


Figure 2. Illustration of available technology for multi-pollutant control at coal-fired power plants.

Improvements in wet scrubber performance to enhance mercury capture depend on oxidizing elemental mercury (Hg^0) to Hg^{2+} by using additives to the flue gas or scrubber. A DOE-funded study found that wet scrubbers can remove as much as 90% of the oxidized gaseous mercury (Hg^{2+}) in the flue gas but none of the elemental mercury (Pavlish et al., 2003). The percentage of total Hg removed by multi-pollutant controls (particulate and scrubber devices) is influenced by coal chlorine content, which determines the Hg oxidation status exiting the particulate control and entering the scrubber. Fuel blending, addition of oxidizing chemicals, controlling unburned carbon content in the fly ash, and addition of a mercury-specific oxidizing catalyst downstream of the particulate matter control can help improve mercury capture (EPA, 2005).

1.2.3. Mercury Control Using Sorbent Injection

Injection of dry sorbents, such as powdered activated carbon (PAC), has been used for control of mercury emissions from waste combustors and has been tested at numerous utility units in the United States. There are different approaches that can be used to increase mercury capture efficiency as illustrated in Figure 3 and Figure 4. Figure 3 presents a coal-fired boiler with sorbent injection and spray cooling. Figure 4 presents a power plant with a hot-side ESP (HS-ESP), carbon injection, and a compact hybrid particle collector (COHPAC™). Dry sorbent is typically injected into the ductwork upstream of a PM control device – normally either an ESP or FF. Usually the sorbent is pneumatically injected as a powder. The injection location is determined by the existing plant configuration. Another approach, designed to segregate collected fly ash from collected sorbent, would be to retrofit a pulse-jet FF (PJFF) downstream of an existing ESP and inject the sorbent between the ESP and the PJFF. This type includes of COHPAC™ and when combined with sorbent injection is referred to as Toxic Emission Control (TOXECON™). The TOXECON configuration can be useful because it avoids commingling the larger fly ash stream with mercury recovered on the injected sorbent. Implementation of sorbent injection for mercury control will likely entail either:

- Injection of powdered sorbent upstream of the existing PM control device (ESP or FF); or
- Injection of powdered sorbent downstream of the existing ESP and upstream of a retrofit fabric filter, the TOXECON™ option; or
- Injection of powdered sorbent between ESP fields (TOXECON-II™ approach).

In general, factors that affect the performance of sorbent technology for mercury methods include:

- Injection rate of the sorbent measured in lb/MMacf²⁰;
- Flue gas conditions, including temperature and concentrations of HCl and sulfur trioxide (SO₃), and oxidation state of the mercury present;
- The air pollution control configuration;
- The characteristics of the sorbent (e.g., conventional or halogenated); and
- The method of injecting the sorbent.

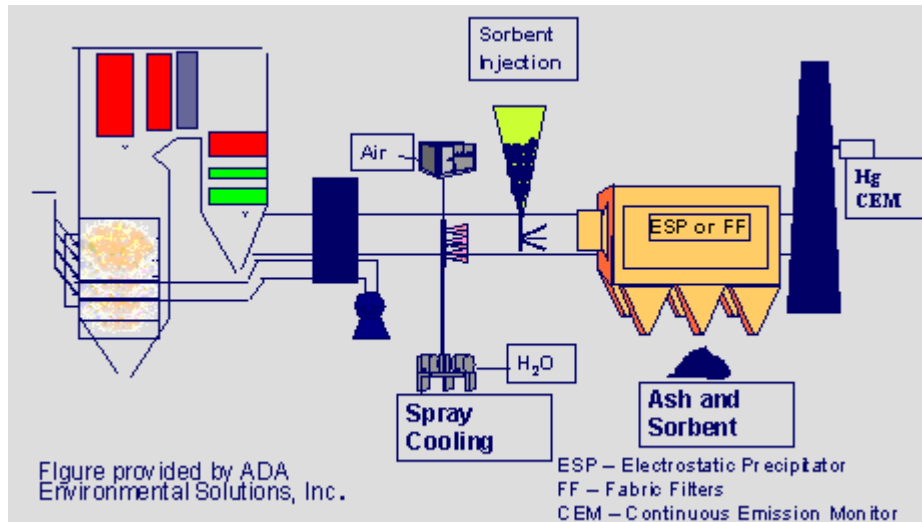


Figure 3. Coal-fired boiler with sorbent injection and spray cooling (Senior et al., 2003).

²⁰ Sorbent injection rate is expressed in lb/MMacf, i.e., pounds of sorbent injected for each million actual cubic feet of gas. For a 500 MW boiler, a sorbent rate of 1.0 lb/MMacf will correspond to approximately 120 lb/hour of sorbent.

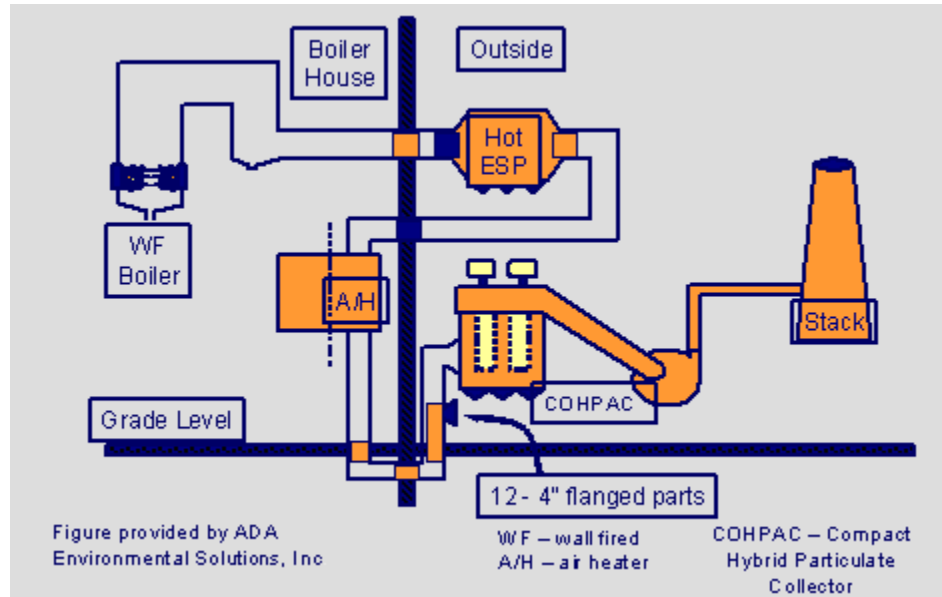


Figure 4. Flow diagram for power plant with a hot ESP, carbon injection, and a compact hybrid particulate collector (Senior et al., 2003).

1.2.4. Mercury Control by Conventional PAC Injection

The most widely tested sorbent for mercury control at utility boilers is PAC.

In general, the efficacy of mercury capture using standard PAC increases with the relative amount of Hg^{2+} (compared with Hg^0) in flue gas²¹, the number of active sites²² in the PAC, and lower temperature. The amount of Hg^{2+} in flue gas is usually directly influenced by the amount of chlorine present in the flue gas, with higher chlorine content enhancing Hg^{2+} formation. Based on these factors, standard PAC injection appears to be generally effective for mercury capture on low-sulfur bituminous coal applications, but less effective for the following applications:

- Low-rank coals with ESP (current capacity of greater than 150 GW; the capacity with this configuration is not expected to increase significantly in the future). Lower chlorine and higher calcium contents in coal lead to lower levels of chlorine in flue gas, which results in reduced oxidation of mercury and, therefore, lower Hg^{2+} in flue gas;
- Low-rank coals with SDA and FF (current capacity of greater than 10 GW; the number of facilities with this configuration is expected to increase significantly in the future). Similar effect as above, except lime reagent from the SDA scavenges even more chlorine from flue gas;

²¹ Standard PAC binds mercury via physical (i.e., weak) bonds, which are formed more easily with Hg^{2+} . There have been results that show a similar removal for both elemental and oxidized mercury. However, the results do not account for surface catalyzed oxidation of Hg^0 followed by sorption on the carbon (EPA, 2005).

²² These are collection of atoms/radicals such as oxygen, chlorine, hydroxyls, which provide binding sites.

- High-sulfur coal (current capacity with wet FGD of approximately 100 GW; the number of facilities with this configuration is likely to increase to more than 150 GW). Relatively high levels of SO₃ compete for active sites on PAC, which reduces the number of sites available for mercury. Generally, plants will use wet FGD and, in many cases, SCR; PAC injection may be needed to meet mercury reduction limits; and
- Hot-side ESPs (current capacity of approximately 30 GW; the number of facilities with this configuration is not likely to increase). Weak (physical) bonds get ruptured at higher temperatures resulting in lower sorption capacity.

1.2.5. Mercury Control by Halogenated PAC Injection

Some situations, as described above, may not have adequate chlorine present in the flue gas for good mercury capture by standard PAC. Pre-halogenated PAC sorbents have been developed to overcome some of the limitations associated with PAC injection for mercury control in power plant applications (Nelson, 2004; Nelson et al., 2004).

Halogenated PACs offer several potential benefits. Relative to standard PAC, halogenated PAC use:

- may expand the usefulness of sorbent injection to many situations where standard PAC may not be as effective;
- may avoid the need for installation of downstream FF, thereby improving cost-effectiveness of mercury capture;
- would, in general, be at lower injection rates, which potentially will lead to fewer plant impacts and a lower carbon content in the captured fly ash;
- may result in somewhat better performance with low-sulfur (including low-rank) coals because of less competition from SO₃; and,
- may be a relatively inexpensive and attractive control technology option for technology transfer to developing countries as it does not involve the capital intensive FF installation.

Performance of a halogenated sorbent such as brominated PAC appears to be relatively consistent regardless of coal type and appears to be mostly determined by whether or not the capture is in-flight (as in upstream of a CS-ESP) or on a fabric filter.

1.3. COAL COMBUSTION RESIDUES

In 2006, 125 million tons of coal combustion residues were produced with ~54 million tons being used in commercial, engineering, and agricultural applications (ACAA, 2007). CCRs result from unburned carbon and inorganic materials in coals that do not burn, such as oxides of silicon, aluminum, iron, and calcium. Fly ash is the unburned material from coal combustion that is light enough to be entrained in the flue gas stream, carried out of the process, and collected as a dry material in the APC equipment. Bottom ash and boiler slag are not affected by post-combustion APC technology and, therefore, these materials are not being evaluated as part of this study. Bottom ash is the unburned material that is too heavy to be entrained in the flue gas

Characterization of Coal Combustion Residues III

stream and drops out in the furnace. Boiler slag, unburned carbon or inorganic material in coal that does not burn, falls to the bottom of the furnace and melts.

The properties of fly ash and flue gas desulfurization residues are likely to change as a result of APC changes to reduce emissions of concern from coal-fired power plants. The chemical and physical properties may also change as a result of sorbents and other additives being used to improve air pollution control.

1.4. RESIDUE MANAGEMENT PRACTICES

CCRs can be disposed in landfills or surface impoundments or used in commercial applications to produce concrete and gypsum wallboard, among other products. Research on the impact of CCR disposal on the environment has been conducted by many researchers and has been summarized by the (EPA, 1988; EPA, 1999). However, most of the existing CCR data are for CCRs prior to implementation of mercury or multi-pollutant controls.

1.4.1. Beneficial Use

In the United States, approximately 43% percent (or 54 million tons out of total 125 million tons produced) of all CCRs produced are reused in commercial applications or other uses that are considered beneficial and avoid landfilling. Of the 125 million tons of CCRs produced as of 2006, about 60 percent (72.4 million tons of fly ash out of 125 million tons of CCRs) of CCRs is fly ash which is potential candidate for use in commercial applications such as making concrete/grout, cement, structural fill, and highway construction (ACAA, 2007; Thorneloe, 2003). Twelve million tons of the FGD gypsum was produced in 2006 with 7.6 million tons (i.e., 62% or 7.6 million out of 12 million) used in making wall board (ACAA, 2007). Table 3 and Figure 5 present the primary commercial uses of CCRs, and a breakdown of U.S. production and usage by CCR type.

Some beneficial uses may involve high temperature processing that may increase the potential for release of mercury and other metals. In cement manufacturing, for example, CCRs may be raw feed for producing clinker in cement kilns. Because of the high temperatures (~1450 °C), virtually all mercury will be volatilized from CCRs when they are used as feedstock to cement kilns. EPA has proposed (74 FR 21136m May 6, 2009) regulations to reduce mercury emissions from cement kilns, which may result in use of air pollution control technology similar to that used at coal-fired power plants (e.g, wet scrubbers and sorbents for enhanced Hg capture). The addition of air pollution control at cement kilns should not affect the ability to use fly ash or FGD gypsum in the production of clinker. However, to avoid installation of air pollution control, kiln inputs (such as fly ash) containing mercury may be avoided which could impact usage of some CCRs.

Through a separate study by EPA's Air Pollution Prevention and Control Division, three high-temperature processes using coal ash have been evaluated for stability of mercury and other COPCs found in coal ash. This research is documented in a separate EPA report (Thorneloe, 2009).

The fate of mercury and other metals is also a potential concern when CCRs are used on the land (mine reclamation, building highways, soil amendments, agriculture and in making concrete, cement) or to make products that are subsequently disposed (e.g., disposal of wallboard in

unlined landfill). The potential for leaching is a function of the characteristics of the material and the conditions under which it is managed.

For some commercial uses, it appears unlikely that mercury in CCRs will be reintroduced into the environment, at least during the lifetime of the product (e.g., encapsulated uses such as in the production of concrete). However, the impact of advanced mercury emissions control technology (e.g., activated carbon injection) on beneficial use applications is uncertain. There is concern that the presence of increased concentrations of mercury, certain other metals, or high carbon content may reduce the suitability of CCRs for use in some applications (e.g., carbon content can limit fly ash use in Portland cement concrete).

1.4.2. Land Disposal

There are approximately 600 land-based CCR waste disposal units (landfills or surface impoundments) being used by the approximately 500 coal-fired power plants in the United States (EPA, 1999). About 60% of the 125 million tons of CCRs generated annually are land disposed. Landfills may be located either on-site or off-site while surface impoundments are almost always located on-site with the combustion operations. Although the distribution of units is about equal between landfills and surface impoundments, there is a trend toward increased use of landfills as the primary disposal method.

Characterization of Coal Combustion Residues III

Table 3. Beneficial uses of CCRs (ACAA, 2007). Total production of CCRs during 2006 was 124,795,124 short tons (values indicated are as reported in the primary reference and precision should not be inferred from the number of significant figures reported).

CCR Categories (Short Tons)	Fly Ash	Bottom Ash	FGD Gypsum	FGD Wet Scrubbers	Boiler Slag ¹	FGD Dry Scrubbers ¹	FGD Other
CCR Production Category Totals ²	72,400,000	18,600,000	12,100,000	16,300,000	2,026,066	1,488,951	299,195
CCR Used Category Totals ³	32,423,569	8,378,494	9,561,489	904,348	1,690,999	136,639	29,341
CCR Use By Application ⁴	Fly Ash	Bottom Ash	FGD Gypsum	FGD Wet Scrubbers	Boiler Slag ¹	FGD Dry Scrubbers ¹	FGD Other
1. Concrete/Concrete Products/Grout	15,041,335	597,387	1,541,930	0	0	9,660	0
2. Cement/Raw Feed for Clinker	4,150,228	925,888	264,568	0	17,773	0	0
3. Flowable Fill	109,357	0	0	0	0	9,843	0
4. Structural Fills/Embankments	7,175,784	3,908,561	0	131,821	126,280	0	0
5. Road Base/Sub-base/Pavement	379,020	815,520	0	0	60	249	0
6. Soil Modification/Stabilization	648,551	189,587	0	0	0	299	1,503
7. Mineral Filler in Asphalt	26,720	19,250	0	0	45,000	0	0
8. Snow and Ice Control	0	331,107	0	0	41,549	0	0
9. Blasting Grit/Roofing Granules	0	81,242	0	232,765	1,445,933	0	0
10. Mining Applications	942,048	79,636	0	201,011	0	115,696	0
11. Wallboard	0	0	7,579,187	0	0	0	0
12. Waste Stabilization/Solidification	2,582,125	105,052	0	0	0	0	27,838
13. Agriculture	81,212	1,527	168,190	0	0	846	846
14. Aggregate	271,098	647,274	0	0	416	0	0
15. Miscellaneous/Other	1,016,091	676,463	7,614	338,751	13,988	46	46
CCR Category Use Totals	32,423,569	8,378,494	9,561,489	904,348	1,690,999	136,639	29,341
Application Use to Production Rate	44.8%	45.0%	79.0%	5.5%	83.5%	9.2%	9.8%

¹ As submitted based on 54 percent coal burn.

² CCR Production totals for Fly Ash, Bottom Ash, FGD Gypsum, and Wet FGD are extrapolated estimates rounded off to nearest 50,000 tons.

³ CCR Used totals for Fly Ash, Bottom Ash, FGD Gypsum, and Wet FGD are per extrapolation calculations (not rounded off).

⁴ CCR Uses by application for Fly Ash, Bottom Ash, FGD Gypsum, and Wet FGD are calculated by proportioning the CCR Used Category Totals by the same percentage as each of the individual application types' raw data contributions to the as-submitted raw data submittal total (not rounded off).

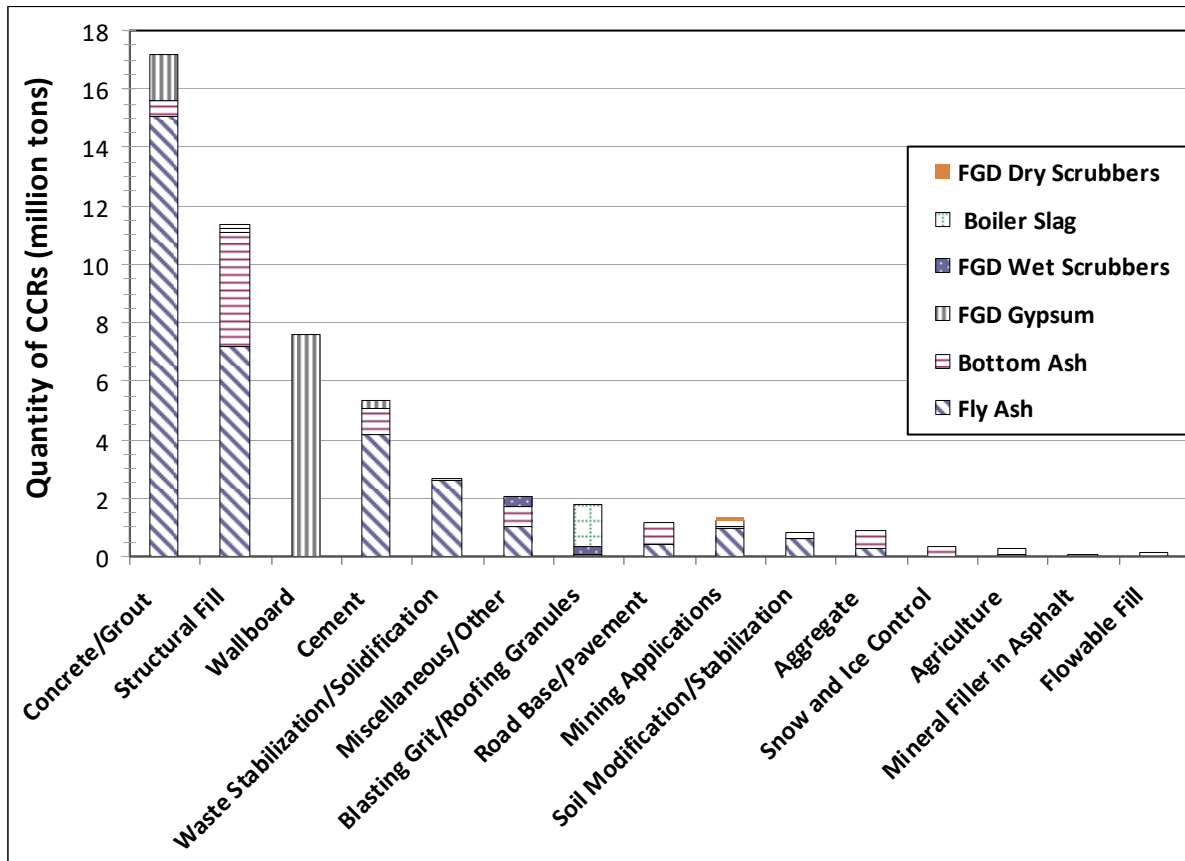


Figure 5. Uses of CCRs based on 2006 industry statistics (ACAA, 2007).

1.5. LEACHING PROTOCOL

One of the major challenges initially facing this research was identification of an appropriate test protocol for evaluating the leaching potential of CCRs that may have increased levels of several metals, particularly mercury. The goal of this research is to develop more accurate estimates of likely constituent leaching when CCRs are used or disposed on land. These estimates of leaching need to be appropriate for assessing at a national level the likely impacts through leaching of pollutants from CCRs that is a consequence of installation of enhanced mercury and, or, multi-pollutant controls. Because management conditions are known to affect the leaching of many metals, evaluation of leaching potential for CCRs over a range of test conditions is needed to consider a range of as managed scenarios (to the degree this is known), and provide leach testing results that can be appropriately extrapolated to a national assessment. A significant consideration in this research has been to identify and evaluate CCR samples collected from the most prevalent combinations of power plant design (with a focus on air pollution control technology configurations) and coal rank used. In addition, the resulting data set is expected to serve as foundation for evaluation of CCR management options for different types of CCRs at specific sites.

Characterization of Coal Combustion Residues III

As a key part of this assessment approach, data have been collected on the actual disposal conditions for CCRs. These conditions are determined by a number of factors, and conditions will vary over time, which also needs to be considered when evaluating leaching (EPA, 1999; EPA, 2002; EPA, 2007b). When disposed, CCRs are typically monofilled²³ or disposed with other CCRs, so initial conditions may be determined largely by the tested material, and any co-disposed CCRs. However, CCR composition can change over time, due to reactions with the atmosphere (e.g., carbonation and oxidation), leaching out of soluble species, creation of reducing conditions at lower landfill levels, changes in the source of coal or coal rank burned, or due to installation of additional pollution control equipment.

Many leaching tests have been developed by regulatory agencies, researchers, or third-party technical standards organizations, and are described in the published literature. States and others have expressed concern with the variety of leaching protocols in use, the lack of correlation of test results with field conditions and actual leaching, and lack of comparability of available data because of incomplete reporting of test conditions. There is also limited or no quality assurance (QA) information for many of these tests. Leaching tests such as the Toxicity Characterization Leaching Procedure (TCLP)²⁴ (which reflects municipal solid waste co-disposal conditions) or the synthetic precipitation leaching procedure (SPLP), or any number of deionized water based tests may be inappropriate, or are at least not optimal for evaluating the leaching potential of CCRs as they are actually managed (i.e., monofilled or co-disposed with other CCRs). These tests either presume a set of prevailing landfill conditions (which may or may not exist at CCR disposal sites; e.g., TCLP), try to account for an environmental factor considered to be important in leaching (e.g., SPLP), or presume that the waste as tested in the laboratory will define the disposal conditions [such as deionized (DI) water tests]. Most existing leaching tests are empirical, in that results are presented simply as the contaminant concentrations leached when using the test, and without measuring or reporting values for factors that may occur under actual management and affect waste leaching, or that provide insight into the chemistry that is

²³ The term “monofilled” refers to when a CCR is the only or dominant component in a landfill or disposal scenario.

²⁴ The Toxicity Characterization Leaching Procedure (TCLP) was not included as part of this study for several reasons. First, EPA previously made a waste status determination under RCRA that coal combustion residues are non-hazardous (65 FR 32214, May 22, 2000). Therefore, use of TCLP was not required as indicated under the RCRA toxicity characteristic regulation for determination of whether or not CCRs were hazardous. Second, TCLP was developed to simulate co-disposal of industrial waste with municipal solid waste as a mismanagement scenario, and to reflect conditions specific to this scenario. However, although MSW co-disposal of CCRs is plausible, the vast majority of CCRs are not being managed through co-disposal with municipal solid waste, and the test conditions for TCLP are different from the actual management practices for most CCRs. Third, SAB and NAS expressed concerns that a broader set of conditions and test methods other than TCLP are needed to evaluate leaching under conditions other than co-disposal with municipal solid waste. In seeking a tailored, “best-estimate” of CCR leaching, the leaching framework is responsive to SAB and NAS concerns and provides the flexibility to consider the effects of actual management conditions on these wastes, and so will be more accurate in this case.

occurring in leaching. Most tests are performed as a single batch test, and so do not consider the effect of variations in conditions on waste constituent leaching²⁵.

In searching for a reliable procedure to characterize the leaching potential of metals from the management of CCRs, EPA sought an approach that (i) considers key aspects of the range of known CCR chemistry and management conditions (including re-use); and (ii) permits development of data that are comparable across U.S. coal and CCR types. Because the data resulting from this research will be used to support regulations, scrutiny of the data is expected. Therefore, the use of a published, peer-reviewed (but not promulgated) protocol is also considered to be an essential element of this work.²⁶

EPA ORD has worked closely with EPA's Office of Solid Waste and Emergency Response (OSWER) to identify an appropriate leaching protocol for evaluating CCRs. The protocol that has been adopted is the "Integrated Framework for Evaluating Leaching in Waste Management and Utilization of Secondary Materials" (Kosson et al., 2002) and referred to here as the "leaching framework." The leaching framework consists of a tiered approach to leaching assessment. The general approach under the leaching framework is to use laboratory testing to measure intrinsic leaching characteristics of a material (i.e., liquid-solid equilibrium partitioning as a function of pH and LS ratio, mass transfer rates) and then use this information in conjunction with mass transfer models to estimate constituent release by leaching under specific management scenarios (e.g., landfilling). Unlike other laboratory leaching tests, under this approach, laboratory testing is not intended to directly simulate or mimic a particular set of field conditions. Development work to-date on the leaching framework has focused on assessing metals leaching, and this work includes equilibrium batch testing (over a range of pH and LS ratio values), diffusion-controlled mass transfer, and percolation-controlled (column) laboratory test methods in conjunction with mass transfer models, to estimate release for specific management scenarios based on testing results from a common set of leaching conditions. EPA OSWER and ORD believe that this approach successfully addresses the concerns identified above, in that it seeks to consider the effect of key disposal conditions on constituent leaching, and to understand the leaching chemistry of wastes tested.

The following attributes of the leaching framework were considered as part of the selection process:

- The leaching framework will permit development of data that are comparable across U.S. coal and CCR types;
- The leaching framework will permit comparison with existing laboratory and field leaching data on CCRs;

²⁵ Many factors are known or may reasonably be expected to affect waste constituent leaching. The solubility of many metal salts is well known to vary with pH; adsorption of metals to the waste matrix varies with pH; redox conditions may determine which metal salts are present in wastes; temperature may affect reaction rates; water infiltration can affect the leaching rate, and also affect leaching chemistry and equilibrium.

²⁶ EPA is working to include the leaching test methods used in this research as part of standard methods in SW-846.

Characterization of Coal Combustion Residues III

- The leaching framework was published in the peer-reviewed scientific literature (Kosson et al., 2002);
- On consultation with EPA's OSWER, it was recommended as the appropriate protocol based on review of the range of available test methods and assessment approaches; and
- On consultation with the Environmental Engineering Committee of the Science Advisory Board (SAB, 2003), the committee considered the leaching framework responsive to earlier SAB criticisms of EPA's approach to leaching evaluation, and also was considered broadly applicable and appropriate for this study

For this study, the primary leaching tests used from the leaching framework were Solubility and Release as a Function of pH (SR002.1) and Solubility and Release as a Function of the Liquid-Solid Ratio (LS) (SR003.1)²⁷. These tests represent equilibrium-based leaching characterization (Kosson et al., 2002). The range of pH and LS ratio used in the leaching tests is within the range of conditions observed for current CCR management practices. Results of these tests provide insights into the physical-chemical mechanisms controlling constituent leaching. When used in conjunction with mass transfer and geochemical speciation modeling, the results can provide conservative²⁸ but realistic estimates of constituent leaching under a variety of environmental conditions (pH, redox, salinity, carbonation) and management scenarios.

This test set is considered Tier 2 testing (equilibrium-based) for detailed characterization, which was selected to develop a comprehensive data set of CCR characteristics (Kosson et al., 2002). Mass transfer rate testing (Tier 3, detailed characterization) may be carried out in the future for specific cases where results from equilibrium-based characterization indicate a need for detailed assessment.

Eluates from leaching tests were analyzed for more than 35 constituents (e.g., elements, anions, DIC, DOC) and characteristics (e.g., pH and conductivity), however, 13 constituents were selected to be the focus of this report based on input from OSWER due to potential concern for human health and the environment.

Laboratory testing for leaching assessment was carried out at EPA's National Risk Management Research Laboratory (Research Triangle Park, NC) with technical assistance from Vanderbilt University.

²⁷ LS refers to liquid to solid ratio (mL water/g CCR or L water/kg CCR) occurring during laboratory leaching tests or under field conditions. SR002.1 is carried out at LS=10 with several parallel batch extractions over a range of pH, while SR003.1 is carried out using several parallel batch extractions with deionized water at LS= 0.5, 1, 2, 5 and 10. Under field conditions, LS refers to the cumulative amount of water passing through the total mass of CCR subject to leaching. SR002.1 and SR003.1 are Vanderbilt University test method designations. An appropriately defined and structured version of test method SR002.1 is being proposed as SW-846 Draft Method 1313 – Leaching Test (Liquid-Solid Partitioning as a Function of Extract pH) of Constituents in Solid Materials Using a Parallel Batch Extraction Test; similarly, test method SR003.1 is being proposed as SW-846 Draft Method 1316 – Leaching Test (Liquid-Solid Partitioning as a Function of Liquid-to-Solid Ratio) of Constituents in Solid Materials Using a Parallel Batch Extraction Test.

²⁸ In this report, “conservative” implies that the constituent release estimates are likely to be equal to or greater than actual expected release under field conditions.

2. MATERIALS AND METHODS

The following sections discuss the specific CCR materials evaluated in this report and the specific methods of characterization, including physical and chemical properties, elemental composition and leaching characteristics. The Quality Assurance Project Plan supporting this work is provided as Appendix B and assessment of quality assurance results is discussed in section 2.4.

2.1. CCR MATERIALS FOR EVALUATION

The 73 CCR samples tested in this study (inclusive of all three reports) include 27 fly ashes without Hg sorbent injection, 7 fly ashes with Hg sorbent injection, 2 spray dryers with fabric filter, 11 unwashed gypsum, 9 washed gypsum, 5 scrubber sludges, 8 blended CCRs (7 mixed fly ash and scrubber sludges; 1 mixed fly ash and gypsum) from 31 coal fired power plants (Table 4). Most coal fired power plants providing samples are identified by a single or two letter code (i.e., Facility T or Facility Ba) to allow specific facilities to remain anonymous. In addition, 4 filter cake samples from the waste water treatment process associated with the management of CCRs were evaluated. Table 5 summarizes the CCR samples evaluated, grouped by residue type, coal type and air pollution control (APC) configuration. Description of the facilities and CCR sampling points is provided in Appendix A.

The facilities and CCRs that were sampled were selected to allow comparisons:

1. Between fly ashes for different coal types (bituminous *vs.* sub-bituminous *vs.* lignite²⁹), particulate control devices (cold-side ESP *vs.* hot-side ESP *vs.* fabric filter), and NO_x control (none or by passed, SNCR or SCR);
2. Between fly ashes from the same facility without and with Hg sorbent injection (Brayton Point, Salem Harbor, Pleasant Prairie, and Facilities J, L, C, and Ba);
3. Between unwashed and washed gypsum from the same facility (Facilities N, O, S, T, W, X, and Aa); and,
4. On the impact of different FGD scrubber types on scrubber sludge (Facilities A, B, and K), blended fly ash and scrubber sludge (Facilities A, B, K and M), and blended fly ash and gypsum (Facility U).

²⁹ This project had a difficult time obtaining coal ash samples from lignite coal. Samples (fly ash and FGD gypsum) were obtained from one facility using Gulf Coast lignite. For facility Ba, the obtained fly ash was from a coal blend of PRB and North Dakota lignite.

Characterization of Coal Combustion Residues III

Table 4. Summary of facility configurations, CCR sample types and sample codes.

Facility Information						CCR Sample Types and Sample Codes								
Facility Code	Coal Type	NO _x Control	PM Control	FGD Scrubber		Fly Ash	Spray Dryer Ash	Gypsum		ScS	Blended CCRs			Filter Cake
				Limestone or Mg Lime	Oxidation			Gyp-U	Gyp-W		FA+Gyp	FA+ScS	FA+ScS+Lime	
¹ Brayton Point	East-Bit	None	CS-ESP	None	None	BPB								
¹ Brayton Point	East-Bit	None	ACI+ CS-ESP	None	None	BPT								
¹ Pleasant Prairie	PRB Sub-Bit	None	CS-ESP	None	None	PPB								
¹ Pleasant Prairie	PRB Sub-Bit	None	ACI+ CS-ESP	None	None	PPT								
¹ Salem Harbor	Low S East-Bit	SNCR	CS-ESP	None	None	SHB								
¹ Salem Harbor	Low S East-Bit	SNCR	ACI+ CS-ESP	None	None	SHT								
² A	East-Bit	SNCR-BP ³	Fabric Filter	Limestone	Natural	CFA						CCC		
² A	East-Bit	SNCR	Fabric Filter	Limestone	Natural	AFA						ACC		
² B	East-Bit	SCR-BP*	CS-ESP	Mg Lime	Natural	BFA			CGD	BGD			BCC	
² B	East-Bit	SCR	CS-ESP	Mg Lime	Natural	DFA			AGD				DCC	
¹ C	Low S Bit	None	HS-ESP with COHPAC	None	None	GAB								
¹ C	Low S Bit	None	HS-ESP + ACI + COHPAC	None	None	GAT			DGD					
E	Med S East-Bit	SCR (in use and BP)	CS-ESP	None	None	EFA, EFB								

Table 4. Summary of facility configurations, CCR sample types and sample codes.

Facility Information						CCR Sample Types and Sample Codes								
Facility Code	Coal Type	NO _x Control	PM Control	FGD Scrubber		Fly Ash	Spray Dryer Ash	Gypsum		ScS	Blended CCRs			Filter Cake
				Limestone or Mg Lime	Oxidation			Gyp-U	Gyp-W		FA+Gyp	FA+ScS	FA+ScS+Lime	
E	High S East-Bit	SCR (in use and BP)	CS-ESP	None	None	EFC								
F	Low S Bit	None	CS-ESP	None	None	FFA								
G	Low S Bit	SNCR	CS-ESP	None	None	GFA								
H	High S Bit	SCR	CS-ESP	Limestone	Forced	HFA								
¹ J	Sub-Bit	None	CS-ESP	None	None	JAB								
¹ J	Sub-Bit	None	Br-ACI + CS-ESP	None	None	JAT								
² K	Sub-Bit	SCR	CS-ESP	Mg Lime	Natural	KFA							KCC	
¹ L	Southern Appalachian	SOFA ⁴	HS-ESP	None	None	LAB								
¹ L	Southern Appalachian	SOFA	Br-ACI + HS-ESP	None	None	LAT			KGD					
² M	Bit	SCR-BP	CS-ESP	Limestone	Inhibited								MAD	
² M	Bit	SCR	CS-ESP	Limestone	Inhibited								MAS	
² N	Bit	None	CS-ESP	Limestone	Forced			NAU	NAW					
² O	Bit	SCR	CS-ESP	Limestone	Forced			OAU	OAW					
² P	Bit	SCR & SNCR ⁵	CS-ESP	Limestone	Forced			PAD						
² Q	Sub-Bit	None	HS-ESP	Limestone	Forced			QAU						
R	Sub-Bit PRB	None	CS-ESP	Wet Limestone	Forced			RAU						

Characterization of Coal Combustion Residues III

Table 4. Summary of facility configurations, CCR sample types and sample codes.

Facility Information						CCR Sample Types and Sample Codes								
Facility Code	Coal Type	NO _x Control	PM Control	FGD Scrubber		Fly Ash	Spray Dryer Ash	Gypsum		ScS	Blended CCRs			Filter Cake
				Limestone or Mg Lime	Oxidation			Gyp-U	Gyp-W		FA+Gyp	FA+ScS	FA+ScS+Lime	
S	High S Bit	SCR	CS-ESP	Limestone	Forced			SAU	SAW					
T	East-Bit	SCR	CS-ESP	Lime	Forced	TFA		TAU	TAW					TFC
U	Low S Bit	SCR	CS-ESP	Limestone	Forced	UFA		UAU			UGF			
V	Sub-Bit PRB	SCR	Spray Dryer / Baghouse	slaked lime	None		VSD							
W	East-Bit	SCR-BP	CS-ESP	Limestone Trona	Forced	WFA		WAU	WAW					WFC
X	Sub-Bit PRB	SCR	CS-ESP	Limestone	Forced	XFA		XAU	XAW					XFC
Y	Sub-Bit PRB	SCR before air preheater	Baghouse	Slaked Lime / Spray Dryer Adsorber	Natural		YSD							
Z	Sub-Bit PRB	None	CS-ESP	None	None	ZFA ZFB (totals only)								
Aa	East-Bit	SCR	CS-ESP	Limestone	Forced	AaFA AaFB AaFC		AaAU	AaAW					

Table 4. Summary of facility configurations, CCR sample types and sample codes.

Facility Information					CCR Sample Types and Sample Codes									
Facility Code	Coal Type	NO _x Control	PM Control	FGD Scrubber		Fly Ash	Spray Dryer Ash	Gypsum		ScS	Blended CCRs			Filter Cake
				Limestone or Mg Lime	Oxidation			Gyp-U	Gyp-W		FA+Gyp	FA+ScS	FA+ScS+Lime	
Ba	Sub-Bit PRB / Lignite (Gulf Coast)		CS-ESP w/ COHPAC NH ₃ inj. before ESP for flue gas conditioning	None	None	BaFA								
Ca	Gulf Coast Lignite	Low NO _x burner	CS-ESP	Wet Limestone	Forced	CaFA			CaAW					
Da	East-Bit	SCR	CS-ESP	Limestone	Forced	DaFA			DaAW					DaFC

¹(Sanchez et al., 2006)

²(Sanchez et al., 2008)

³BP – designates that the post-NO_x combustion control (either SCR or SNCR) was not in use or by-passed during sample collection. Clean Air Interstate Rule requires year-round use of post-NO_x combustion whereas previously if used, then it was seasonal during the summer months.

⁴SOFA - Separate overfire air, it is often added above the burner level to stage combustion.

⁵Facility P has one wet scrubber for two boilers. Both boilers have post-combustion NO_x control – one with SCR and the other with SNCR. The sample collected for this facility is from the wet scrubber.

Characterization of Coal Combustion Residues III

Table 5. CCR samples evaluated in this study, grouped by residue type, coal type and air pollution control configuration.

Facility	Sample ID	Coal Source (Region)	PM Capture	NO _x Control	Hg Sorbent Injection	SO ₃ Control
----------	-----------	----------------------	------------	-------------------------	----------------------	-------------------------

Fly Ash without Hg Sorbent Injection

Bituminous, Low S

Brayton Point	BPB	Eastern bituminous	CS ESP	None	None	None
Facility F	FFA	Eastern bituminous	CS ESP	None	None	None
Facility B	DFA	Eastern bituminous	CS ESP	SCR-BP	None	None
Facility A	CFA	Eastern bituminous	Fabric F.	SNCR-BP	None	None
Facility B	BFA	Eastern bituminous	CS ESP	SCR	None	None
Facility U	UFA	Southern Appalachian	CS ESP	SCR	None	None
Salem Harbor	SHB	Eastern bituminous	CS ESP	SNCR	None	None
Facility G	GFA	Eastern bituminous	CS ESP	SNCR	None	None
Facility A	AFA	Eastern bituminous	Fabric F.	SNCR	None	None
Facility L	LAB	Southern Appalachian	HS ESP	SOFA	None	None
Facility C	GAB	Eastern bituminous	HS ESP w/ COHPAC	None	None	None

Bituminous, Med S

Facility T	TFA	Eastern bituminous	CS ESP	None	None	None
Facility E	EFB	Eastern bituminous	CS ESP	SCR-BP	None	None
Facility W	WFA	Eastern bituminous	CS ESP	SCR-BP	None	Duct Sorbent injection - Trona
Facility E	EFA	Eastern bituminous	CS ESP	SCR	None	None
Facility K	KFA	Eastern bituminous	CS ESP	SCR	None	None
Facility Aa	AaFA	Eastern bituminous	CS ESP	SCR	None	None
Facility Aa	AaFB	Eastern bituminous	CS ESP	SCR	None	None
Facility Da	DaFA	Eastern bituminous	CS ESP	SCR	None	None
Facility Aa	AaFC	Eastern bituminous	HS ESP	SCR	None	None

Characterization of Coal Combustion Residues III

Table 5 (continued). CCR samples evaluated in this study, grouped by residue type, coal type and air pollution control configuration.

Facility	Sample ID	Coal Source (Region)	PM Capture	NO _x Control	Hg Sorbent Injection	SO ₃ Control
----------	-----------	----------------------	------------	-------------------------	----------------------	-------------------------

Fly Ash without Hg Sorbent Injection

Bituminous, High S

Facility E	EFC	Eastern bituminous	CS ESP	SCR	None	None
Facility H	HFA	Eastern bituminous	CS ESP	SCR	None	None

Sub-Bituminous & Sub-bit/bituminous mix

Pleasant Prairie	PPB	Powder River Basin	CS ESP	None	None	None
Facility J	JAB	PRB (85%)/Bit (15%)	CS ESP	None	None	None
Facility Z	ZFA	Powder River Basin	CS ESP	None	None	None
Facility X	XFA	Powder River Basin	CS ESP	SCR	None	None

Lignite

Facility Ca	CaFA	Gulf Coast	CS ESP	None	None	None
-------------	------	------------	--------	------	------	------

Characterization of Coal Combustion Residues III

Table 5 (continued). CCR samples evaluated in this study, grouped by residue type, coal type and air pollution control configuration.

Facility	Sample ID	Coal Source (Region)	PM Capture	NO _x Control	Hg Sorbent Injection	SO ₃ Control
----------	-----------	----------------------	------------	-------------------------	----------------------	-------------------------

Fly Ash without and with Hg Sorbent Injection Pairs

Bituminous, Low S

Brayton Point	BPB	Eastern bituminous	CS ESP	None	None	None
Brayton Point	BPT	Eastern bituminous	CS ESP	None	PAC	None
Salem Harbor	SHB	Eastern bituminous	CS ESP	SNCR	None	None
Salem Harbor	SHT	Eastern bituminous	CS ESP	SNCR	PAC	None
Facility L	LAB	Southern Appalachian	HS ESP	SOFA	None	None
Facility L	LAT	Southern Appalachian	HS ESP	SOFA	Br-PAC	None
Facility C	GAB	Eastern bituminous	HS ESP w/ COHPAC	None	None	None
Facility C	GAT	Eastern bituminous	HS ESP w/ COHPAC	None	PAC	None

Sub-bituminous

Pleasant Prairie	PPB	Powder River Basin	CS ESP	None	None	None
Pleasant Prairie	PPT	Powder River Basin	CS ESP	None	PAC	None
Facility J	JAB	Other	CS ESP	None	None	None
Facility J	JAT	Other	CS ESP	None	Br-PAC	None

Lignite

Facility Ba	BaFA	PRB/Lignite blend	CS ESP w/ COHPAC+ Ammonia Injection	None	PAC	None
-------------	------	-------------------	-------------------------------------	------	-----	------

Table 5 (continued). CCR samples evaluated in this study, grouped by residue type, coal type and air pollution control configuration.

Facility	Sample ID	Coal Source (Region)	PM Capture	NO _x Control	Hg Sorbent Injection	FGD Scrubber additive	SO ₃ Control
----------	-----------	----------------------	------------	-------------------------	----------------------	-----------------------	-------------------------

Spray dryer with Fabric Filter (fly ash and FGD collected together)

Sub-Bituminous

Facility V	VSD	Powder River Basin	Fabric F.	SCR	None	Slaked Lime	None
Facility Y	YSD	Powder River Basin	Fabric F.	SCR	None	Slaked Lime	None

Characterization of Coal Combustion Residues III

Table 5 (continued). CCR samples evaluated in this study, grouped by residue type, coal type and air pollution control configuration.

Facility	Sample ID	Region	Residue type	PM Capture	NO _x Control	Wet Scrubber type	FGD Scrubber additive	SO ₃ Control
----------	-----------	--------	--------------	------------	-------------------------	-------------------	-----------------------	-------------------------

Gypsum, unwashed and washed

Bituminous, Low S

Facility U	UAU	Southern Appalachian	Gyp-U	CS ESP	SCR	Forced Ox.	Limestone	None
------------	-----	----------------------	-------	--------	-----	------------	-----------	------

Bituminous, Med S

Facility T	TAU	Eastern bituminous	Gyp-U	CS ESP	None	Forced Ox.	Limestone	None
Facility T	TAW	Eastern bituminous	Gyp-W	CS ESP	None	Forced Ox.	Limestone	None
Facility W	WAU	Eastern bituminous	Gyp-U	CS ESP	SCR-BP	Forced Ox.	Limestone	Duct Sorbent inj. - Trona
Facility W	WAW	Eastern bituminous	Gyp-W	CS ESP	SCR-BP	Forced Ox.	Limestone	Duct Sorbent inj. - Trona
Facility Aa	AaAU	Eastern bituminous	Gyp-U	CS ESP	SCR	Forced Ox.	Limestone	None
Facility Aa	AaAW	Eastern bituminous	Gyp-W	CS ESP	SCR	Forced Ox.	Limestone	None
Facility Da	DaAW	Eastern bituminous	Gyp-W	CS ESP	SCR	Forced Ox.	Limestone	None
Facility P	PAD	Eastern bituminous	Gyp-U	CS ESP	SCR & SNCR	Forced Ox.	Limestone	None

Table 5 (continued). CCR samples evaluated in this study, grouped by residue type, coal type and air pollution control configuration.

Facility	Sample ID	Region	Residue type	PM Capture	NO _x Control	Wet Scrubber type	FGD Scrubber additive	SO ₃ Control
Gypsum, unwashed and washed								
Bituminous, High S								
Facility N	NAU	Eastern bituminous	Gyp-U	CS ESP	None	Forced Ox.	Limestone	None
Facility N	NAW	Eastern bituminous	Gyp-W	CS ESP	None	Forced Ox.	Limestone	None
Facility S	SAU	Illinois Basin	Gyp-U	CS ESP	SCR	Forced Ox.	Limestone	None
Facility S	SAW	Illinois Basin	Gyp-W	CS ESP	SCR	Forced Ox.	Limestone	None
Facility O	OAU	Other	Gyp-U	CS ESP	SCR	Forced Ox.	Limestone	None
Facility O	OAW	Other	Gyp-W	CS ESP	SCR	Forced Ox.	Limestone	None
Sub-bituminous								
Facility R	RAU	Powder River Basin	Gyp-U	CS ESP	None	Forced Ox.	Limestone	None
Facility Q	QAU	Powder River Basin	Gyp-U	HS ESP	None	Forced Ox.	Limestone	Other
Facility X	XAU	Powder River Basin	Gyp-U	CS ESP	SCR	Forced Ox.	Limestone	None
Facility X	XAW	Powder River Basin	Gyp-W	CS ESP	SCR	Forced Ox.	Limestone	None
Lignite								
Facility Ca	CaAW	Gulf Coast	Gyp-U	CS ESP	None	Forced Ox.	Limestone	None

Characterization of Coal Combustion Residues III

Table 5 (continued). CCR samples evaluated in this study, grouped by residue type, coal type and air pollution control configuration.

Facility	Sample ID	Region	Residue type	PM Capture	NO _x Control	Wet Scrubber type	FGD Scrubber additive	SO ₃ Control
----------	-----------	--------	--------------	------------	-------------------------	-------------------	-----------------------	-------------------------

Scrubber Sludge

Bituminous, Low S

Facility B	DGD	Eastern bituminous	Scrubber sludge	Cold-side ESP	SCR-BP	Natural Ox.	Mg lime	None
Facility A	CGD	Eastern bituminous	Scrubber sludge	Fabric Filter	SNCR-BP	Natural Ox.	Limestone	None
Facility B	BGD	Eastern bituminous	Scrubber sludge	Cold-side ESP	SCR	Natural Ox.	Mg lime	None
Facility A	AGD	Eastern bituminous	Scrubber sludge	Fabric Filter	SNCR	Natural Ox.	Limestone	None

Bituminous, Med S

Facility K	KGD	Eastern bituminous	Scrubber sludge	Cold-side ESP	SCR	Natural Ox.	Mg lime	None
------------	-----	--------------------	-----------------	---------------	-----	-------------	---------	------

Table 5 (continued). CCR samples evaluated in this study, grouped by residue type, coal type and air pollution control configuration.

Facility	Sample ID	Region	Residue type	PM Capture	NO _x Control	Wet Scrubber type	FGD Scrubber additive	SO ₃ Control
Mixed Fly Ash and Scrubber Sludge (as managed)								
Bituminous, Low S								
Facility B	DCC	Eastern bituminous	FA+ScS+ lime	CS ESP	SCR-BP	Natural Ox.	Mg lime	None
Facility A	CCC	Eastern bituminous	FA+ScS	Fabric Filter	SNCR-BP	Natural Ox.	Limestone	None
Facility B	BCC	Eastern bituminous	FA+ScS+ lime	CS ESP	SCR	Natural Ox.	Mg lime	None
Facility A	ACC	Eastern bituminous	FA+ScS	Fabric Filter	SNCR	Natural Ox.	Limestone	None
Bituminous Med S								
Facility K	KCC	Eastern bituminous	FA+ScS+ lime	CS ESP	SCR	Natural Ox.	Mg lime	None
Bituminous Med S								
Facility M	MAD	Illinois Basin	FA+ScS+ lime	CS ESP	SCR-BP	Inhibited Ox.	Limestone	None
Facility M	MAS	Illinois Basin	FA+ScS+ lime	CS ESP	SCR	Inhibited Ox.	Limestone	None

2.2. LEACHING ASSESSMENT PROTOCOLS

Laboratory testing for this study focused on leaching as a function of pH and LS ratio as defined by the leaching framework. This test set is considered Tier 2 testing (equilibrium-based) for detailed characterization, which was selected to develop a comprehensive data set of CCR characteristics. Mass transfer rate testing (Tier 3, detailed characterization) may be carried out in the future for specific cases where results from equilibrium-based characterization indicate a need for detailed assessment.

2.2.1. Alkalinity, Solubility and Release as a Function of pH (SR002.1)

Alkalinity, solubility and release as a function of pH were determined according to method SR002.1 (Kosson et al., 2002). This method is currently under review as a preliminary version of Method 1313³⁰ for publication in SW-846. This protocol consists of 11 parallel extractions of particle size reduced material, at different pH values ranging from pH 2-13, and at a LS ratio of 10 mL extractant/g dry sample. In this method, particle-size reduction is used when necessary to prepare large-grained samples for extraction so that the approach toward liquid-solid equilibrium concentrations of the COPCs is enhanced. For the samples evaluated in this study, particle size reduction was required infrequently. Each extraction condition was carried out with replication as appropriate³¹ using 40 g of material for each material evaluated. In addition, three method blanks were included, consisting of the DI water, nitric acid and potassium hydroxide used for extractions. Typical particle size of the tested materials was less than 300 μm using standard sieves according to ASTM E-11-70 (1995). An acid or base addition schedule is formulated based on initial screening for eleven eluates with final solution pH values between 3 and 12, through addition of aliquots of nitric acid or potassium hydroxide as needed. The exact schedule is adjusted based on the nature of the material; however, the range of pH values includes the natural pH of the matrix that may extend the pH domain (e.g., for very alkaline or acidic materials). The final LS ratio is 10 mL extractant/g dry sample which includes DI water, the added acid or base, and the amount of moisture that is inherent to the waste matrix as determined by moisture content analysis. The eleven extractions were tumbled in an end-over-end fashion at 28 ± 2 rpm for 24 hours followed by filtration separation of the solid phase from the eluate using a 0.45 μm polypropylene filter. Each eluate then was analyzed for constituents of interest. The acid and base neutralization behavior of the materials is evaluated by plotting the pH of each eluate as a function of equivalents of acid or base added per gram of dry solid. Concentration of constituents of interest for each eluate is plotted as a function of eluate final pH to provide liquid-solid partitioning equilibrium as a function of pH. Initially, the SR002.1 test was carried out in triplicate; however, replication was reduced to two replicates of the test method for later

³⁰Preliminary version denotes that this method has not been endorsed by EPA but is under consideration for inclusion into SW-846. This method has been derived from published procedures (Kosson et al, 2002) using reviewed and accepted methodologies (USEPA 2006, 2008, 2009). The method has been submitted to the USEPA Office of Resource Conservation and Recovery and is currently under review for development of interlaboratory validation studies to develop precision and bias information.

³¹ Initial replication was in triplicate (as indicated in Report 1 and for some of the samples in Report 2), which was reduced to duplicate based on quality assurance review of the triplicate analyses results.

samples based on good replication and consistency amongst the early results (Sanchez et al., 2006).

2.2.2. Solubility and Release as a Function of LS Ratio (SR003.1)

Solubility and release as a function of LS ratio was determined according to method SR003.1 (Kosson et al., 2002). This method is currently under review as a preliminary version of Method 1314³² for promulgation in SW-846. This protocol consists of five parallel batch extractions over a range of LS ratios (i.e., 10, 5, 2, 1, and 0.5 mL/g dry material), using DI water as the extractant with aliquots of material that has been particle size reduced. Typical particle size of the material tested was less than 300 μm . Between 40 and 200 g of material were used for each extraction, based on the desired LS ratio. All extractions are conducted at room temperature (20 ± 2 °C) in leak-proof vessels that are tumbled in an end-over-end fashion at 28 ± 2 rpm for 24 hours. Following gross separation of the solid and liquid phases by centrifuge or settling, leachate pH and conductivity measurements are taken and the phases are separated by pressure filtration using 0.45- μm polypropylene filter membrane. The five leachates are collected, and preserved as appropriate for chemical analysis. Initially, the SR003.1 test was carried out in triplicate; however, replication was reduced to two replicates of the test method for later samples based on good replication and consistency amongst the early results.

2.3. ANALYTICAL METHODS

2.3.1. Surface Area and Pore Size Distribution

A Quantachrome Autosorb-1 C-MS chemisorption mass spectrometer was used to perform 5-point Brunauer, Emmett, and Teller (BET) method surface area, pore volume, and pore size distribution analyses on each as-received and size-reduced CCR. A 200 mg sample was degassed under vacuum at 200 °C for at least one hour in the sample preparation manifold prior to analysis with N₂ as the analysis gas. Standard materials with known surface area were routinely run as a QC check. Tabular results for each CCR are provided in Appendix C.

2.3.2. pH and Conductivity

pH and conductivity were measured for all aqueous eluates using an Accumet 925 pH/ion meter. The pH of the leachates was measured using a combined pH electrode accurate to 0.1 pH units. A 3-point calibration was performed daily using pH buffer solutions at pH 4.0, 7.0 and 10.0. Conductivity of the leachates was measured using a standard conductivity probe. The conductivity probe was calibrated using appropriate standard conductivity solutions for the conductivity range of concern. Conductivity meters typically are accurate to $\pm 1\%$ and have a precision of $\pm 1\%$.

³² Method SR003.1 was developed into a preliminary version of Method 1314: Leaching Test (Liquid-Solid Partitioning as a Function of Liquid-to-Solid Ratio) for Constituents in Solid Materials using an Up-flow Percolation Column Test, 2009 (submitted to EPA Office of Solid Waste; under review for inclusion in SW-846).

Characterization of Coal Combustion Residues III

2.3.3. Moisture Content

Moisture content of the “as received” CCRs was determined using American Society for Testing and Materials (ASTM) D 2216-92. This procedure supersedes the method indicated in the version of the leaching procedure published by (Kosson et al., 2002). Tabular results are provided in Appendix C.

2.3.4. Carbon Content - Organic Carbon/Elemental Carbon Analyzer

Organic carbon (OC) and elemental carbon (EC) content of each CCR tested was measured using a Sunset Lab thermal-optical EC/OC analyzer using the thermal/optical method (NIOSH Method 5040). The sample collected on quartz fiber filters is heated under a completely oxygen-free helium atmosphere in a quartz oven in four increasing temperature steps (375 °C, 540 °C, 670 °C and 870 °C) at 60 second ramp times for the first three temperatures and a ramp time of 90 seconds for the final temperature. The heating process removes all organic carbon on the filter. As the organic compounds are vaporized, they are immediately oxidized to carbon dioxide in an oxidizer oven which follows the sample oven. The flow of helium containing the produced carbon dioxide then flows to a quartz methanator oven where the carbon dioxide is reduced to methane. The methane is then detected by a flame ionization detector (FID). After the sample oven is cooled to 525 °C, the pure helium eluent is switched to an oxygen/helium mixture in the sample oven. At that time, the sample oven temperature is stepped up to 850 °C. During this phase, both the original elemental carbon and the residual carbon produced by the pyrolysis of organic compounds during the first phase are oxidized to carbon dioxide due to the presence of oxygen in the eluent. The carbon dioxide is then converted to methane and detected by the FID. After all carbon has been oxidized from the sample, a known volume and concentration of methane is injected into the sample oven. Thus, each sample is calibrated to a known quantity of carbon as a means of checking the operation of the instrument. The calibration range for these analyses was from 10 to 200 $\mu\text{g}/\text{cm}^2$ of carbon using a sucrose solution as the standard. The detection limit of this instrument is approximately 100 ng/cm^2 with a linear dynamic range from 100 ng/cm^2 to 1 g/cm^2 . Tabular results of OC and EC content are presented in Appendix C.

2.3.5. Dissolved Inorganic Carbon (DIC) and Dissolved Organic Carbon (DOC)

Analyses of total organic carbon and inorganic carbon were performed on a Shimadzu model TOC-V CPH/CPN. Five-point calibration curves, for both dissolved inorganic carbon (DIC) and non-purgeable dissolved organic carbon (DOC) analyses, were generated for an analytical range between 5 ppm and 100 ppm and are accepted with a correlation coefficient of at least 0.995. An analytical blank and check standard at approximately 10 ppm were run every 10 samples. The standard was required to be within 15% of the specified value. A volume of approximately 16 mL of undiluted sample was loaded for analysis. DIC analysis was performed first for the analytical blank and standard and then the samples. DOC analysis was carried out separately after completion of DIC analysis. DOC analysis began using addition of 2 M (mole/L) of hydrochloric acid to achieve a pH of 2 along with a sparge gas flow rate of 50 mL/min to purge inorganic carbon prior to analysis. Method detection limit (MDL) and minimum level of quantification (ML) are shown in Table 6. All DIC and DOC results will be made available separately through an electronic format as part of the leaching assessment tool (LeachXS Lite®).

Table 6. MDL and ML of analysis of DIC and DOC.

	MDL ($\mu\text{g/L}$)	ML ($\mu\text{g/L}$)
DIC	130	410
DOC	170	550

2.3.6. Mercury (CVAA, Method 3052, and Method 7473)

Liquid samples were preserved for mercury analysis by additions of nitric acid and potassium permanganate and then prepared prior to analysis according to the following method. For each 87 mL of sample, 3 mL of concentrated nitric acid and 5 mL of 5 wt% aqueous potassium permanganate solution were added prior to storage. Immediately before cold vapor atomic absorption (CVAA) analysis, 5 mL of hydroxylamine were added to clear the sample and then the sample was digested according to ASTM Method D6784-02 (i.e., Ontario Hydro) as described for the permanganate fraction (ASTM, 2002). On completion of the digestion, the sample was analyzed for mercury by CVAA. Samples with known additions of mercury for matrix analytical spikes also were digested as described above prior to CVAA analysis.

Sample preparation of the solids and filters was carried out by HF/HNO₃ microwave digestion according to Method 3052 (EPA, 1996) followed by CVAA analysis as indicated above. No additional preservation or digestion was carried out prior to CVAA analysis.

Mercury analysis of each digest, eluate and leachate was carried out by CVAA according to EPA SW846 Method 7470A “Mercury in Liquid Waste (Manual Cold Vapor Technique)” (EPA, 1998a). A Perkin Elmer FIMS 100 Flow Injection Mercury System was used for this analysis. The instrument was calibrated with known standards ranging from 0.025 to 1 $\mu\text{g/L}$ mercury.

Solids also were analyzed by Method 7473 “Mercury in Solids and Solutions by Thermal Decomposition, Amalgamation, and Atomic Absorption Spectrophotometry” (EPA, 1998b). A Nippon MD-1 mercury system was used for this analysis. The instrument was calibrated with known standards ranging from 1 to 20 ng of mercury. The method detection limit for mercury in solids is 0.145 $\mu\text{g/kg}$.

2.3.7. Other Metals (ICP-MS, ICP-AES, Method 3052, Method 6020, and Method 6010)

Liquid samples for ICP-MS and ICP-AES analysis were preserved through addition of 3 mL of concentrated nitric acid (trace metal grade) per 97 mL of sample. Known quantities of each analyte were also added to sample aliquots for analytical matrix spikes. Solid samples were digested by EPA Method 3052 (EPA, 1996) prior to ICP-MS and ICP-AES analysis. Table 7 indicates the switch from ICP-MS to ICP-AES for specific elements and samples.

Characterization of Coal Combustion Residues III

Table 7. ICP instrument used for each element.* Elements indicated in bold are discussed in this report; results for all other indicated elements will be available through the leaching assessment tool.

Symbol	Instrument	Used	Switch Date
Al		ICP-OES	Report 3 Samples
Sb	ICP-MS	ICP-OES*	Only SR003.1 Report 1 Samples*
As	ICP-MS		
Ba	ICP-MS		
Be	ICP-MS		
B		ICP-OES	Report 1 and 3 Samples
Cd	ICP-MS		
Ca		ICP-OES	Report 3 Samples
Cr	ICP-MS		
Co	ICP-MS		
Cu	ICP-MS		
Fe		ICP-OES	Report 3 Samples
Pb	ICP-MS		
Mg		ICP-OES	Report 3 Samples
Mn	ICP-MS		
Mo	ICP-MS	ICP-OES*	*Only Report 1 Samples
Ni	ICP-MS		
K		ICP-OES	Report 3 Samples
Re	ICP-MS		
Se	ICP-MS		
Si		ICP-OES	Report 3 Samples
Na		ICP-OES	Report 3 Samples
Sr		ICP-OES	Report 3 Samples
Tl	ICP-MS	ICP-OES*	Only SR003.1 Report 1 Samples*
Sn	ICP-MS		
Ti		ICP-OES	Report 3 Samples
U	ICP-MS		
V	ICP-MS		
Zn	ICP-MS		

*Samples were analyzed on the ICP-OES for the indicated elements. Measurements for the same elements on Facility T samples (TFA, TFC, TAW, and TAU) were also completed on the ICP-MS for comparison. Precision of results was within 15% for concentrations above 100 µg/L and within 25% for concentrations below 100 µg/L.

2.3.7.1. ICP-MS Analysis (SW-846 Method 6020)

ICP-MS analyses of aqueous samples from laboratory leaching tests were carried out at Vanderbilt University (Department of Civil and Environmental Engineering) using a Perkin Elmer model ELAN DRC II in both standard and dynamic reaction chamber (DRC) modes. Standard analysis mode was used for all analytes except for As and Se, which were run in DRC mode with 0.5 mL/min of oxygen as the reaction gas. Seven-point standard curves were used for an analytical range between approximately 0.5 µg/L and 500 µg/L and completed before each analysis. Analytical blanks and analytical check standards at approximately 50 µg/L were run every 10 to 20 samples and required to be within 15% of the specified value. Samples for analysis were diluted gravimetrically to within the targeted analytical range using 1% v/v Optima grade nitric acid (Fisher Scientific). Initially, analyses for 10:1 dilutions were performed to minimize total dissolved loading to the instrument. Additional dilutions at 100:1 and 1000:1 were analyzed if the calibration range was exceeded with the 10:1 dilution. 50 µL of a 10 mg/L internal standard consisting of indium (In) (for mass range below 150) and bismuth (Bi) (for mass range over 150) was added to 10 mL of sample aliquot prior to analysis. Analytical matrix spikes were completed for one of each of the replicate eluates from SR002.1. For each analytical matrix spike, a volume between 10 µL and 100 µL of a 10 mg/L standard solution was added to 10 mL of sample aliquot. Table 8 provides the element analyzed, method detection limit (MDL) and minimum level of quantification (ML). Analyte concentrations measured that are less than the ML and greater than the MDL are reported as estimated value using the instrument response. The values reflect the initial 10:1 dilution used for samples from laboratory leaching tests.

Characterization of Coal Combustion Residues III

Table 8. Method detection limits (MDLs) and minimum level of quantification (ML) for ICP-MS analysis on liquid samples. Elements indicated in bold are discussed in this report; results for all other indicated elements will be available through the leaching assessment tool.

Symbol	Units	MDL	ML
Al	µg/L	0.96	3.06
Sb	µg/L	0.08	0.25
As	µg/L	0.64	2.04
Ba	µg/L	0.57	1.82
Be	µg/L	0.64	2.03
B	µg/L	0.65	2.06
Cd	µg/L	0.17	0.54
Ca	µg/L	1.02	3.24
Cr	µg/L	0.50	1.58
Co	µg/L	0.41	1.32
Cu	µg/L	0.70	2.23
Fe	µg/L	0.94	3.00
Pb	µg/L	0.23	0.73
Mg	µg/L	0.57	1.83
Mn	µg/L	0.34	1.09
Mo	µg/L	0.76	2.41
Ni	µg/L	0.73	2.31
K	µg/L	1.38	4.38
Re	µg/L	0.24	0.77
Se	µg/L	0.52	1.65
Si	µg/L	1.56	4.97
Na	µg/L	0.74	2.35
Sr	µg/L	0.52	1.66
Tl	µg/L	0.51	1.61
Sn	µg/L	0.70	2.22
Ti	µg/L	0.52	1.66
U	µg/L	0.30	0.95
V	µg/L	0.31	0.98
Zn	µg/L	0.92	2.94
Zr	µg/L	0.47	1.48

2.3.7.2. ICP-OES Analysis (SW-846 Method 6010)

ICP-OES analyses of aqueous samples from laboratory leaching tests were carried out at Vanderbilt University (Department of Civil and Environmental Engineering) using a Varian ICP Model 720-ES. Five-point standard curves were used for an analytical range between approximately 0.1 mg/L and 25 mg/L for trace metals. Seven-point standard curves were used for an analytical range between approximately 0.1 mg/L and 500 mg/L for minerals. Analytical blanks and analytical check standards at approximately 0.5 mg/L were run every 10 to 20 samples and required to be within 15% of the specified value. Initially, analyses were performed on undiluted samples to minimize total dissolved loading to the instrument. Samples for analysis

Characterization of Coal Combustion Residues III

were diluted gravimetrically to within the targeted analytical range using 1% v/v Optima grade nitric acid (Fisher Scientific) if the maximum calibration was exceeded. Yttrium at 10 mg/L was used as the internal standard. Analytical matrix spikes were completed for three test positions from one of the replicate eluates from SR002.1. For each analytical matrix spike, a volume of 500 μ L of a 10 mg/L standard solution was added to 5 mL of sample aliquot. Table 9 provides the element analyzed, method detection limit (MDL), and minimum level of quantification (ML). Analyte concentrations measured that are less than the ML and greater than the MDL are reported as estimated value using the instrument response.

Table 9. Method detection limits (MDLs) and minimum level of quantification (ML) for ICP-OES analysis on liquid samples.

Symbol	Units	MDL	ML
Al	μ g/L	1.00	3.18
Sb	μ g/L	8.00	25.4
As	μ g/L	15.0	47.7
Ba	μ g/L	1.00	3.18
Be	μ g/L	5.00	15.9
B	μ g/L	1.00	3.18
Cd	μ g/L	6.00	19.1
Ca	μ g/L	3.50	11.1
Cr	μ g/L	1.00	3.18
Co	μ g/L	1.00	3.18
Cu	μ g/L	4.1	13.0
Fe	μ g/L	2.90	9.22
Pb	μ g/L	7.00	22.3
Li	μ g/L	6.00	19.1
Mg	μ g/L	1.00	3.18
Mn	μ g/L	3.60	11.4
Mo	μ g/L	1.00	3.18
Ni	μ g/L	2.20	7.00
K	μ g/L	1.50	4.77
P	μ g/L	6.2	19.7
Se	μ g/L	17.0	54.1
Si	μ g/L	2.80	8.90
Ag	μ g/L	18.00	57.2
Na	μ g/L	3.50	11.1
Sr	μ g/L	1.00	3.18
S	μ g/L	8.30	26.4
Tl	μ g/L	5.00	15.9
Sn	μ g/L	17.0	54.1
Ti	μ g/L	6.40	20.3
V	μ g/L	1.30	4.13
Zn	μ g/L	2.50	7.95
Zr	μ g/L	2.70	8.59

Characterization of Coal Combustion Residues III

2.3.8. X-Ray Fluorescence (XRF)

XRF analysis was performed on each CCR to provide additional information on each CCR total elemental composition. For each CCR two pellets were prepared as follows. 3000 mg of material was weighed and mixed with 1.5 mL (100 mg dry solids) of liquid binder to give a 32 mm diameter pellet weighing 3150 mg with a material-to-diluent ratio of 0.05. For high carbon content samples 3.0 ml (100 mg dry solids) of liquid binder was used to give a 32 mm diameter pellet weighing 3300 mg with a material-to-diluent ratio of 0.1. XRF intensities were collected on each side of each pellet using Philips SuperQ data collection software and evaluated using Omega Data System's UniQuant 4 XRF "standardless" data analysis software. The UQ/fly ash calibration was used to analyze the samples. The pellets were evaluated as oxides. Known fly ash Standard Reference Materials (SRMs) were also run to assess the accuracy of the analysis. This information is useful in supplementing CVAA and ICP results.

X-Ray Fluorescence Spectrometry was used in the Research Triangle Park laboratories of EPA-NRMRL to analyze these samples. A Philips model PW 2404 wavelength dispersive instrument, equipped with a PW 2540 VRC sample changer, was used for these analyses. The manufacturer's software suite, "SuperQ", was used to operate the instrument, collect the data, and perform quantification.

The instrument was calibrated at the time of installation of the software plus a new X-ray tube using a manufacturer-supplied set of calibration standards. On a monthly basis, manufacturer-supplied drift correction standards were used to create an updated drift correction factor for each potential analytical line. On a monthly basis, a dedicated suite of QC samples were analyzed before and after the drift correction procedure. This data was used to update and maintain the instrument's QC charts.

The software suite's "Measure and Analyze" program was used to collect and manage the sample data. Quantification was performed post-data collection using the program "IQ+". IQ+ is a "first principles" quantification program that includes complex calculations to account for a wide variety of sample-specific parameters. For this reason, sample-specific calibrations were not necessary. This program calculates both peak heights and baseline values. The difference is then used, after adjustment by drift correction factors, for elemental quantification versus the calibration data. Inter-element effects are possible and the software includes a library of such parameters. Data from secondary lines may be used for quantification where inter-element effects are significant or the primary peak is overloading the data acquisition system. Where the difference between the calculated peak height and baseline is of low quality, the program will not identify a peak and will not report results. IQ⁺ permits the inclusion of data from other sources by manual entry. Carbon was an example of this for these samples. Entry of other source data for elements indeterminable by XRF improves the mass balance.

Table 10 presents detection limit data in two forms. The two forms are not mutually exclusive. The "reporting limit" is built into the software and reflects the manufacturer's willingness to report low-level data. Data listed in the "detection limit" column were based upon the short-term reproducibility of replicate analyses (two standard deviations, 2σ) and were sample matrix specific. These calculations are likely to report higher detection limits for elements present at high concentrations than what would be reported if the same element was present at trace levels. In this data set, calcium is a likely example of this behavior.

Characterization of Coal Combustion Residues III

Table 10. XRF detection limits.

Analyte	Reporting Limit mg/kg	Detection Limit, wt % 2 σ (wt. %)
Al	20	0.016
As	20	0.038
Ba	20	0.0084
Br	20	0.02
Ca	20	0.1
Cd	20	0.064
Ce	20	0.022
Cl	20	0.0046
Co	20	0.0024
Cr	20	0.0028
Cu	20	0.0014
F	20	0.082
Fe	20	0.034
Ga	20	0.0016
Ge	20	0.0014
K	20	0.0048
La	20	0.0054
Mg	20	0.01
Mn	20	0.0032
Mo	20	0.0026
Na	20	0.0076
Nb	20	0.0018
Ni	20	0.0048
Pb	20	0.0034
Px	20	0.004
Rb	20	0.0016
Sc	20	0.0016
Se	20	0.0018
Si	20	0.092
Sr	20	0.0016
Sx	20	0.05
Ti	20	0.003
V	20	0.0038
W	20	0.0036
Y	20	0.0018
Zn	20	0.0014
Zr	20	0.0024

Characterization of Coal Combustion Residues III

2.3.9. XAFS

XANES and EXAFS spectra were collected using the MR-CAT (Sector 10 ID) beamline at the Advanced Photon Source (APS) at Argonne National Laboratory (ANL, Argonne, IL) and beamline X18B at the National SynchrotronLight Source (NSLS) at Brookhaven National Laboratory (BNL, Upton, NY) and analyzed according to the methods previously described (Hutson et al., 2007).

2.3.10. Determination of Hexavalent Chromium (Cr^{6+}) and Total Chromium Species in CCR Eluates

Fly ash samples were leached at three different pH values in duplicate using the SR002.1.1 leaching procedure for the determination of hexavalent and total chromium concentrations. The pH target values for the leachates were defined as 7-7.5, 10.5-11, and the natural CCR pH. The eluates were split into three samples for analysis by Eastern Research Group (ERG) and Vanderbilt University. ERG received one unpreserved and one nitric acid preserved sample. Vanderbilt University received one nitric acid preserved sample. Samples were preserved by adding 97 mL of leachate with 3 mL concentrated nitric acid.

Hexavalent chromium concentrations of the un-preserved CCR leachate eluates were determined using ion-chromatography. This procedure was modified from the EPA Urban Air Toxics Monitoring Programs (UATMP) method developed by ERG for the determination of Cr^{6+} in air by analyzing the eluates from sodium-bicarbonate impregnated cellulose filters (EPA, 2007a). The ion chromatography system was comprised of a guard column, an analytical column, a post-column derivatization module, and a UV/VIS detector. In the analysis procedure, Cr^{6+} exists as chromate due to the near neutral pH of the eluent. After separation through the column, the Cr^{6+} forms a complex with 1,5-diphenylcarbohydrazide (DPC) and was detected at 530 nm (EPA, 2006c). This method had a reporting limit (RL) of 0.03 ng/mL.

The total chromium species for the nitric acid preserved samples were analyzed by ERG and Vanderbilt University using inductively-coupled plasma / mass spectroscopy (ICP/MS) found in SW-846 Method 6020.

2.3.11. MDL and ML for Analytical Results

The MDL is defined by 40 CFR Part 136, Appendix B, July 1, 1995, Revision 1.11 as “the minimum concentration of a substance that can be measured and reported with 99% confidence that the analyte concentration is greater than zero and is determined from analysis of a sample in a given matrix containing the analyte.”

The MDL was determined statistically from data generated by the analysis of seven or more aliquots of a spiked reagent matrix³³ and verified by the analysis of calibration standards near the calculated MDL according to (EPA, 2004). The MDL then was determined by multiplying the

³³ Establishing spikes in an actual leaching extract matrix is not possible because the sample being extracted dictates the matrix composition by virtue of the constituents that partition into the resulting aqueous extract, which varies by test position and material being tested. However, the extract aliquots are diluted at least 10:1 with 1% nitric acid (prepared from Optima grade nitric acid, Fisher Scientific), and the COPCs are dilute in the resulting analytical sample. Therefore, the 1% nitric acid solution was used as the matrix for MDL and ML determinations.

standard deviation of the replicate measurements by the appropriate Students t value for a 99% confidence level (two tailed) and n-1 (six) degrees of freedom and also multiplying by the minimum dilution factor required for matrix preservation and analysis.

The ML is defined by 40 CFR Part 136, 1994 as “the lowest level at which the entire analytical system must give a recognizable signal and acceptable calibration point for the analyte.” According to (EPA, 2004), the ML is intended to be the nearest integer value (i.e., 1, 2 or 5×10^n , where n is an integer) to 10 times the standard deviation observed for determination of the MDL. This value is also multiplied by the minimum dilution factor required for preservation and analysis of the sample matrix to obtain the ML reported here.

The above methodology for determination of MDL and ML values was used for all ICP-MS and ICP-OES measurements (Table 8 and Table 9).

Mercury, as measured by CVAA, required modification of the calculation of the MDL and ML because very consistent replication resulted in calculation of a MDL lower than the instrument detection limit. For this case, the standard deviation of seven replicate analyses of 0.025 $\mu\text{g/L}$ was 0.00069. Therefore, the MDL was set equal to the instrument detection limit of 0.001 $\mu\text{g/L}$ times the minimum dilution factor from sample preparation (3.59) to result in an MDL of 0.0036 $\mu\text{g/L}$. The ML was set to 10 times the instrument detection limit and rounded to the nearest integer value as above. The resulting ML was 0.01 $\mu\text{g/L}$.

2.4. QUALITY ASSURANCE ASSESSMENT

2.4.1. Homogenization of Individual CCR Samples and Aliquots for Analyses

To ensure sample homogeneity the fly ashes were mixed using a Morse single can tumbler model 1-305 as described in (Sanchez et al., 2006). Scrubber sludges that were flowable slurries were mixed using a paddle mixer. Gypsum and CCRs samples were mixed by repetitively coning and quartering while passing through a mesh screen.³⁴ After mixing, ten subsamples were taken from sample MAD (blended CCRs) and analyzed by XRF to evaluate the homogeneity of the resultant material; the total content variability for primary and most trace constituents was less than 20% for this set of samples [see Report 2 (Sanchez et al., 2008)].

2.4.2. Leaching Test Methods and Analytical QA/QC

One of the requirements of this project was to establish a QA/QC framework for the leaching assessment approach developed by (Kosson et al., 2002). The developed QA/QC framework incorporates the use of blanks, spiked samples, and replicates. Appendix B provides the complete Quality Assurance Project Plan, as updated for this phase of the study. For each designated leaching test condition (i.e., acid or base addition to establish end-point pH values and LS value), triplicate leaching test extractions were completed (i.e., three separate aliquots of CCR were each extracted at the designated test condition) for early samples, while duplicate extractions were

³⁴ "Coning and quartering" is a term used to describe how the material is mixed. The approach is to pass the material through a screen so that a "cone" forms in the collection container. Then the cone is bisected twice into quarters (quarter sections of the cone) and each section then is passed sequentially through the screen again to form a new cone. This sequence is repeated several times to achieve desired mixing.

Characterization of Coal Combustion Residues III

used after evaluation of initial results. The three types of method blanks were the deionized water case, the most concentrated nitric acid addition case, and the most concentrated potassium hydroxide addition case. Each method blank was carried through the entire protocol, including tumbling and filtration, except an aliquot of CCR was not added.

During analysis for mercury by CVAA and elemental species by ICP-MS and ICP-OES, multipoint calibration curves using at least seven standards and an initial calibration verification (ICV) using a standard obtained from a different source than the calibration standards were completed daily or after every 50 samples, whichever was more frequent. In addition, instrument blanks and continuing calibration verification (CCV) standards were analyzed after every 10 analytical samples and required to be within 10 percent of the expected value based on the standards used. Samples were rerun if they were not within 10 percent of the expected value. CCV standards and instrument blanks also were run at the end of each batch of samples.

For ICP-MS and CVAA analyses, analytical spikes (aliquot of the sample plus a known spike concentration of the element of interest) for the constituents of interest were carried out for one replicate of each test case to assess analytical recoveries over the complete range of pH and liquid matrix conditions. For ICP-OES analyses, analytical matrix spikes were completed for three test positions from one of the replicate eluates. The “spike recovery” was required to be within 80 – 120% of the expected value for an acceptable analytical result.

2.4.3. Improving QA/QC Efficiency

Throughout the study, the approach to QA/QC was regularly reviewed to seek out opportunities for increased evaluation efficiency without unacceptable degradation of precision or accuracy in results. Based on evaluation of results from the first several facilities [Report 1, (Sanchez et al., 2006)], the number of replicates for Method SR002.1 (solubility as a function of pH) and Method SR003.1 (solubility as a function of liquid/solid ratio) was reduced from three to two [Report 2, (Sanchez et al., 2008)]. Results from Report 1 (Sanchez et al., 2006) and Report 2 (Sanchez et al., 2008) show that the precision between duplicate analyses is acceptable and that the triplicate set does not significantly increase the quality of the data set. This finding follows from recognition that (i) the data sets generated by Method SR002.1 and SR003.1 must provide both consistency between replicate extractions and analyses, and internal consistency between results at different pH and LS ratio, and (ii) precision is controlled primarily by the degree of homogeneity of the CCR under evaluation and representative sub-sampling, rather than by the intrinsic variability of the leaching test methods.

Data were screened for outliers based on comparison of individual data points (i) relative to replicate extractions (i.e., parallel extractions of aliquots of the same material under the same extraction conditions), and (ii) relative to the other data points in the extraction series [i.e., parallel extractions of aliquots of the same material at different pH (SR002.1) and LS conditions (SR003.1)] because of the expected systematic response behavior. The pH was considered an outlier when the final pH of the eluate deviated from the other replicates by more than 0.5 pH units and the corresponding constituent analyses did not follow systematic behavior indicated by other eluates across multiple constituents. Individual constituent results were considered outliers when results of constituent analyses deviated from the systematic behavior indicated by results in the extraction series (as a function of pH or as a function of LS) by more than one-half to one order of magnitude. Results were screened through inspection of the appropriately plotted results.

There were more than 80,000 final data observations required to complete this study, not including additional observations required for quality control and quality assurance purposes. Leaching test results required 69,733 observations considering all leaching test eluate analytes. The 13 constituents analyzed in leaching test eluates evaluated in detail in this report required 27,849 final observations.

As part of the QA/QC review of the data, two authors independently reviewed the data. The observations were screened for outliers based on comparison of individual observations as noted above. Anomalous observations were flagged for further review by the other reviewing author before a determination of outlier status was made.

Of the final 27,849 observations, 28 eluate concentration observations were considered as outliers relative to the data set. Additionally, 20 pH observations out of a total of 2,042 pH observations were considered as outliers relative to the data set. A pH observation was considered to be an outlier when the reported pH value was clearly incorrect in the context of the test method and other results. When a pH observation was determined to be an outlier, then all eluate concentration observations associated with the particular eluate were also considered outliers because they would be evaluated as a function of pH at an incorrect pH value. This resulted in an additional 252 eluate concentrations being considered as outliers based on the pH observation. The 300 total outlier observations were excluded from the statistical, graphical, and tabular evaluations. The specific outliers are tabulated in Appendix K.

Overall, these results indicate an error rate of approximately 0.1 percent for determination of constituent concentrations in leaching test eluates and an error rate of less than 1.0 percent for pH measurements.

Data quality indicators (DQIs) were measured for all parameters continuously during the leaching experiments and during analytical tasks. Chemical (ICP, CVAA, XRF, IC, EC/OC) and physical (surface area, pore size distribution and density) characterization data were reduced and reports were generated automatically by the instrument software. The primary analyst reviewed 100% of the report data for completeness to ensure that quality control checks met established criteria. Sample analysis was repeated for any results not meeting acceptance criteria. A secondary review was performed by the Inorganic Laboratory Manager to validate the analytical report.

2.4.4. Data Management

Data quality indicator (DQI) goals for critical measurements in terms of accuracy, precision and completeness are shown in Table 11.

Table 11. Data quality indicator goals.

Measurement	Method	Accuracy	Precision	Completeness
Hg Concentration	CVAA/7470A	80 – 120 %	10%	>90%
Non-Hg Metals Concentration	ICP/6010	80 – 120 %	10%	>90%

Characterization of Coal Combustion Residues III

Accuracy was determined by calculating the percent bias from a known standard. Precision was calculated as relative percent difference (RPD) between duplicate values and relative standard deviation (RSD) for parameters that have more than two replicates. Completeness is defined as the percentage of measurements that meet DQI goals of the total number measurements taken. Types of QC samples used in this project included blanks, instrument calibration samples, replicates, and matrix spikes.

Accuracy and precision for the samples analyzed for mercury concentration leachate determinations were made using replicates and matrix spike analyses. Data validation for the mercury samples was performed after the analyses and outliers for accuracy were re-analyzed to improve results. Mercury samples not meeting the accuracy goals occurred most often in samples at the alkaline end of the pH testing and with the blank samples. The greatest mercury leaching occurred in the samples with the lower pH where there was greater availability. The samples not meeting the accuracy goals for matrix spiking did not affect the quality of the data. Limited volume of leachate collected for the SR003.1 samples resulted in only one spike being performed per replicate set.

QC samples required for CVAA analysis are detailed in Method 7470A. The mercury analyzer software was programmed with the acceptance criteria for Method 7470A with respect to independent calibration verifications, continuous calibration verifications, and blank solution concentrations. All calibrations and samples analysis parameters passed the QA/ QC criteria and may be considered valid samples.

The pH meter was calibrated daily before each batch of measurements. Standards purchased from Thomas scientific (Swedesboro, NJ) were used to calibrate the probe at pH values of 4, 7, and 10. Each solution was certified to a precision of ± 0.01 at 25 °C and was traceable to the National Institute of Standards Technology (NIST) standard reference material (SRM) SRM-186-I-c and 186-II-c.

2.5. INTERPRETATION AND PRESENTATION OF LABORATORY LEACHING DATA

Complete laboratory leaching test results for each facility are presented in Appendix F. For each facility, results are organized by constituent of interest in the alphabetic order of the symbol (aluminum [Al], arsenic [As], boron [B], barium [Ba], cadmium [Cd], cobalt [Co], chromium [Cr], mercury [Hg], molybdenum [Mo], lead [Pb], antimony [Sb], selenium [Se], and thallium [Tl]). For each constituent, results of Solubility and Release as a Function of pH (from test method SR002.1) and results of Solubility and Release as a Function of LS ratio (from test method SR003.1) are presented side by side. Results of pH as a function of acid or base addition (from test method SR002.1) are presented in Appendix G.

In addition, comparisons of results of Solubility and Release as a function of pH (SR002.1) are provided in Section 3.2.1. Comparisons are grouped by residue type (fly ash, gypsum, scrubber sludge, spray dryer absorber residues, and blended CCRs), followed by coal type and air pollution control configurations, and are organized by constituent of interest. For each grouping, selected results of Solubility and Release as a Function of pH (SR002.1) are also presented to illustrate characteristic leaching behaviors.

For Solubility and Release as a Function of pH (SR002.1), results are presented as eluate concentrations as a function of pH. The “own pH³⁵” of the system is indicated by a circle surrounding the corresponding data point. Included with each figure are horizontal lines at the drinking water maximum concentration level (MCL) or drinking water equivalent level (DWEL)³⁶, or action limit (AL, for lead) and analytical limits (ML and MDL) to provide a frame of reference for the results. Also included with each figure are vertical lines indicating the 5th and 95th percentiles of pH from field observations of leachates from landfills and surface impoundments containing combustion residues (see Section 2.5.2). An annotated example of the results is provided as Figure 6. Actual results are presented in the following sections.

For Solubility and Release as a Function of LS ratio (SR003.1), results are presented as eluate concentrations as a function of LS ratio. Also indicated are the relevant ML, MDL, MCL, DWEL, or AL. An annotated example of the results is provided as Figure 7.

2.5.1. Interpretation of Mechanisms Controlling Constituent Leaching

Constituent (e.g., mercury, arsenic, and selenium) concentrations observed in laboratory leach test eluates and in field leachate samples may be the result of several mechanisms and factors. The discussion presented here focuses on constituent leaching and source term modeling approaches. Source term is defined here as the flux or amount of constituent released from the waste or secondary material (e.g., CCRs). Factors controlling constituent release and transport in and within the near field of the CCRs are often distinctly different from the factors and

³⁵ The “own pH” of a material refers to the equilibrium pH when the material is placed in deionized water at a ratio of 10 g CCR per 100 mL of water.

³⁶ MCL, DWEL, and AL values used are as reported in (EPA, 2006a).

Characterization of Coal Combustion Residues III

mechanisms which are important for subsequent vadose zone or groundwater transport outside of the near field area.

In general, constituents are present in the waste or secondary material either as adsorbed species, co-precipitated as amorphous or crystalline solid phases, or incorporated as trace components in solid phases. These three different cases can often be distinguished from one another based on the results of these leaching tests, either through direct interpretation of leaching results or in conjunction with geochemical speciation modeling. If chemical equilibrium conditions are approached (as is the approximate case for the laboratory and field sample conditions discussed in this report), then the functional behavior of the aqueous solution concentrations reflects the nature of the constituent species in the waste or secondary material, the presence of any co-constituents in the aqueous phase influencing aqueous solution speciation (e.g., effects of high ionic strength, chelating or complexing constituents), and the presence of species in the solution that may compete for adsorption sites if adsorption is the controlling solid phase mechanism. If the constituent is present in the waste or secondary material as an adsorbed species, many different adsorption/desorption characteristic patterns are possible (Duong, 1998; Ruthven, 1984).

The simplest case is when the constituent of interest is present at very low concentration in the waste or secondary material, relatively weakly adsorbed, and the presence of complexing and/or, competing species in solution is at a constant concentration. For this case, leaching test results will indicate a constant concentration as a function of pH at a fixed LS ratio, and linearly increasing concentration as LS ratio decreases at constant pH. This case is represented mathematically as a linear equilibrium partitioning function, where the critical constant of proportionality is the partitioning coefficient, commonly known as K_d . Linear partitioning and use of K_d values is a common approach for mathematically modeling contaminant transport at low contaminant concentrations in soils. Assumption of linear partitioning is a valid and useful approach when the necessary conditions (discussed above) are fulfilled³⁷.

A different case is when mercury is adsorbed on activated carbon. For mercury adsorbed on activated carbon or char particles in fly ash, a complex combination of adsorption mechanisms is indicated. During laboratory leaching tests, mercury concentrations in the leaching test eluates are relatively constant over the pH range and LS ratio of interest, and independent of total mercury content in the CCR. In addition, the total mercury content in the CCR is very low. These results are indicative of adsorption phenomena where, in the adsorbed state, interactions between adsorbed mercury species are stronger (thermodynamically) than the interactions between the adsorbed mercury species and carbon surface³⁸. This observation has been supported by the observation of mercury dimer formation during sorption (Munro et al., 2001) and the occurrence

³⁷ Often specific K_d values are a function of pH because of competition for adsorption sites by hydrogen ions. Therefore, in cases where hydrogen ions do compete for binding sites, the varying of pH would violate the condition that competing species are at constant concentration, and the leaching curve would not be linear. However, often a single K_d or range of K_d values are used in contaminant fate and transport models, without accounting for any specific relationship between pH and K_d which can result in misrepresentation of actual contaminant behavior.

³⁸ For this case, the first mercury molecule is adsorbed more weakly than subsequent mercury molecules because the adsorbed mercury-mercury interaction is stronger than the adsorbed mercury-carbon surface interaction [see (Sanchez et al., 2006) for further discussion].

of chemisorption as the dominant adsorption mechanism at temperatures above 75 °C (consistent with conditions in air pollution control devices (Vidic, 2002)). In other studies, this phenomenon has been observed as the formation of molecular clusters on the adsorbent surface (Duong, 1998; Rudzinski et al., 1997; Ruthven, 1984). For this case, use of a K_d approach would underestimate release because desorption is best represented as a constant aqueous concentration until depletion occurs, rather than the linearly decreasing aqueous concentration indicated by a K_d approach.

A third case is encountered when the constituent of interest is present in the waste or secondary material (e.g., CCR) as a primary or trace constituent in either an amorphous or crystalline solid phase and there may be complexing or chelating co-constituents in the aqueous phase. Observed aqueous concentrations are a non-linear function of pH and LS ratio, and reflect aqueous saturation with respect to the species of interest under the given conditions (pH, co-constituents). For these cases, an approximation of field conditions can be made empirically based on laboratory testing and observed saturation over the relevant domain (as applied in this report), or geochemical speciation modeling coupled with mass transfer modeling can be used to assess release under specific field scenarios (the subject of a future report). Use of a K_d approach would not be appropriate for these cases because constituent concentrations will remain relatively constant at a given pH until the controlling solid phase is depleted and control is shifted to a new solid phase or mechanism.

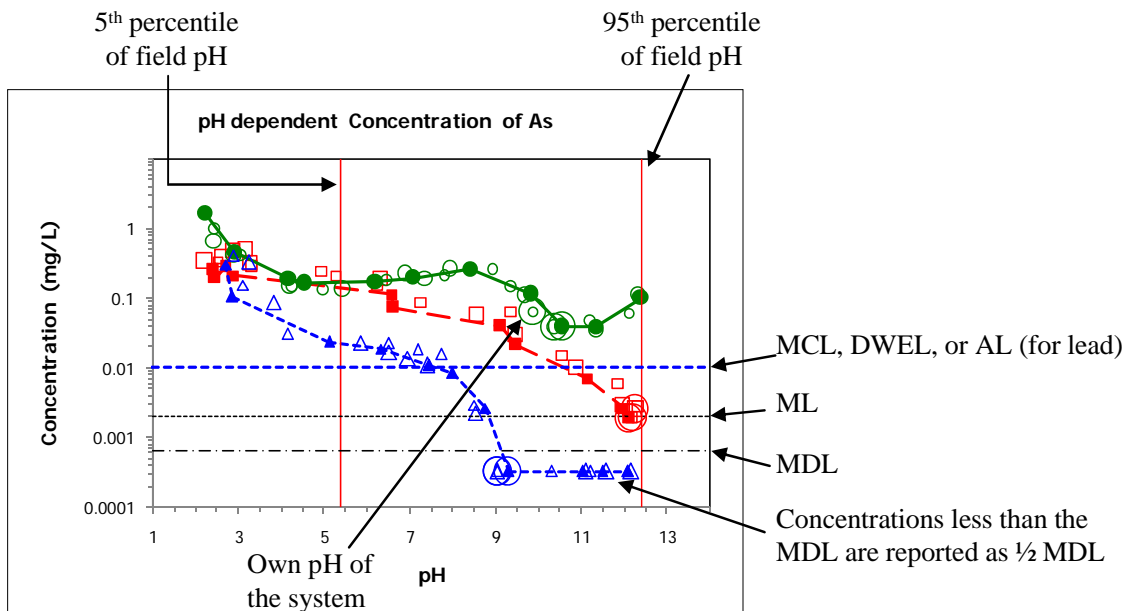


Figure 6. An example of eluate concentrations as a function of pH from SR002.1. Different colors, symbols and line types are used to represent different data sets. In this example figure, green, red, and blue indicate different CCR samples and open symbols are used to represent replicate data.

Characterization of Coal Combustion Residues III

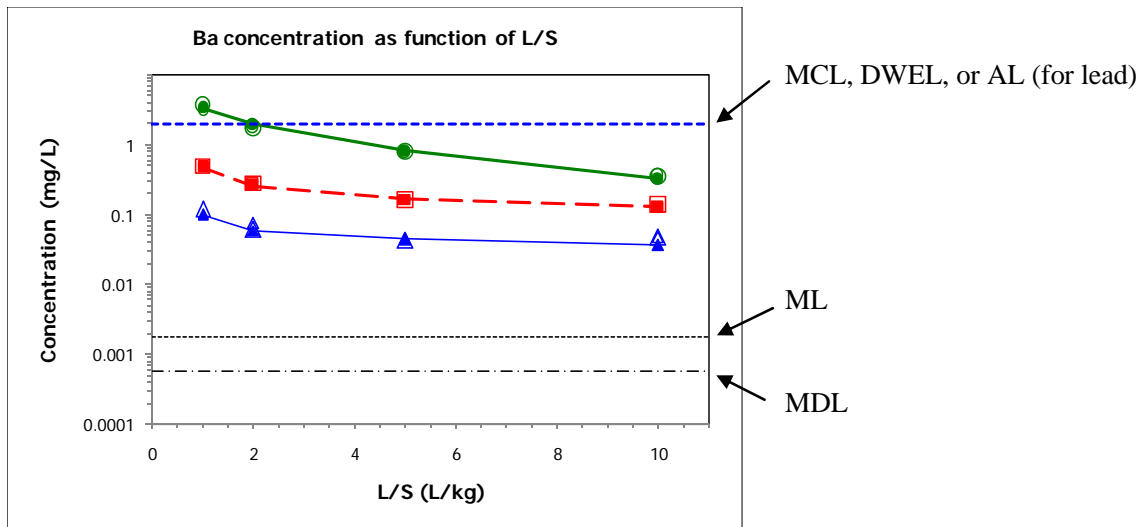


Figure 7. An example of eluate concentrations as a function of LS ratio from SR003.1.

2.5.2. Field pH Probability Distribution

A probability distribution of field leachate pH values from coal combustion waste landfills was derived, as described below, from the set of field pH observations included in the EPA Risk Report (EPA, 2007b). The data set developed for the EPA Risk Report included (i) observations from the comprehensive database of landfill leachate characteristics developed by the EPA's Office of Solid Waste (EPA, 2000), (ii) field observations from literature, primarily from EPRI reports, (iii) additional data reported to EPA, and (vi) pH observations from laboratory leaching tests.

Only pH measurements from field samples (i.e., leachate, pore water) were selected for use in development of the resulting pH probability distribution. The resulting data set included 580 observations from 42 CCR landfill disposal facilities and was highly unbalanced, with some sites having only a few (e.g., less than five) observations and some sites having many observations (e.g., greater than 20). To prevent the unbalanced data from skewing the resulting probability distribution, the minimum, 25th, 50th, 75th percentile, and maximum values of observations for each individual facility were compiled into a single data set. For facilities with fewer than five observations, all observations for that facility were included. This data set then served as the basis for determining a balanced statistical distribution function of field leachate pH values from the disposal sites with reported values. Different distribution functions were used to fit the data and the one providing the best data fit based on the chi-square test was selected. The resulting field pH probability distribution was truncated and normalized to the pH range of the field data (Figure 8) (EPA, 2000; EPA, 2007b; EPRI, 2006).

Field pH observations were also evaluated for surface impoundments that receive CCRs from coal combustion facilities with FGD scrubbers in use. Pore water pH values measured in samples obtained from within the settled CCRs were extracted from the EPRI database. These pH observations were across the same range as the landfill field pH observations, but were insufficient to develop an independent pH probability distribution for surface impoundments.

Therefore, the same pH probability distribution was used for both landfill and surface impoundment facilities.

The resulting 5th and 95th percentiles of observed field pH values, equal to pH 5.4 and 12.4, respectively, are indicated on the figures of eluate concentrations as a function of pH (Figure 6).

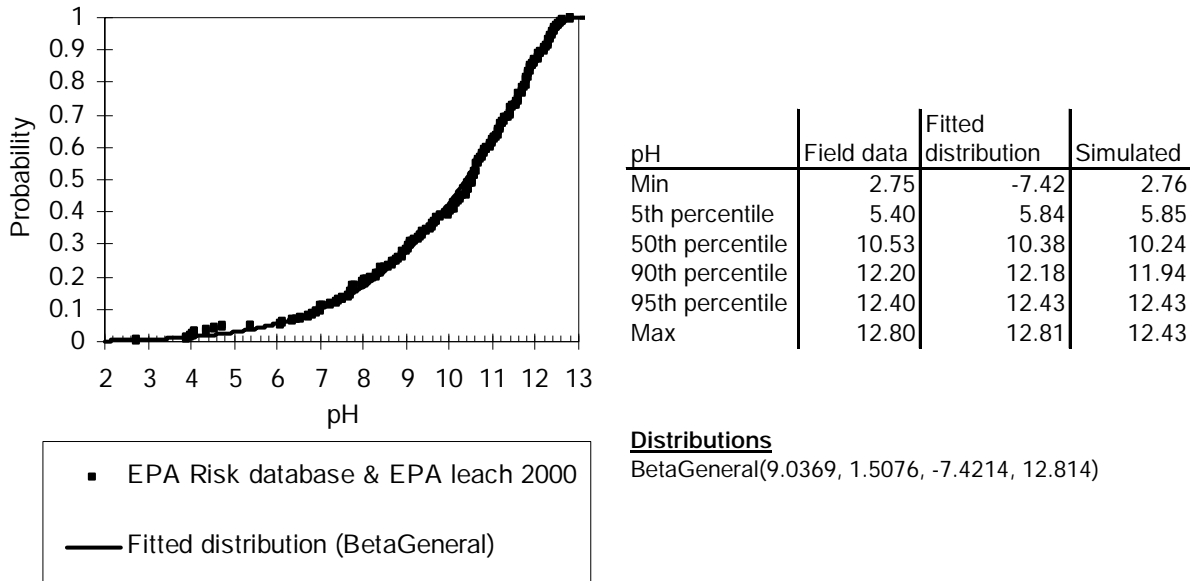


Figure 8. Probability distributions for field pH. Summary statistics for the field data and the probability distribution are provided to the right of the graph (EPA, 2000; EPA, 2007b; EPRI, 2006).

3. RESULTS AND DISCUSSION

The EPA Risk Report (EPA, 2007b) identified the following COPCs based on the potential for either human health or ecological impacts using a screening risk assessment: aluminum (Al), arsenic (As), antimony (Sb), barium (Ba), boron (B), cadmium (Cd), cobalt (Co), chromium (Cr), lead (Pb), mercury (Hg), molybdenum (Mo), selenium (Se), and thallium (Tl).³⁹ Thus, the evaluation provided here focuses on the same thirteen constituents and can be used in future risk and environmental assessments.

3.1. TOTAL ELEMENTAL CONTENT

Total elemental content of CCR samples was analyzed by acid digestion (digestion Method 3052 and ICP-MS analysis by Method 6020; see Section 2.3.7) for constituents of potential concern (Al, As, Ba, Cd, Co, Cr, Mo, Pb, Sb, Se, Tl)⁴⁰ and mercury was analyzed by Method 7470 with selected samples also analyzed by Method 7473; results of these analyses are provided in Figure 9 through Figure 21, with tabular results in Appendix D. Total elemental content for boron was not analyzed because of interferences by the sample digestion method. Total elemental content also was analyzed by XRF for major constituents and other detectable constituents (Al, Ba, Ca, Cl, F, Fe, K, Mg, Na, P, S, Si, Sr, Ti) and carbon was analyzed independently; results of these analyses are provided in Figure 22 through Figure 36, with tabular results provided in Appendices E and C. Several of the COPCs analyzed by ICP-MS were below the detection limits for XRF analysis (e.g., As, Sb, Se).

Two elements, Al and Ba, were analyzed by both acid digestion and XRF methods.

Measurement accuracy and precision is better by acid digestion for low concentrations (e.g., less than 10,000 µg/g) and better by XRF for higher concentrations (e.g., greater than 10,000 µg/g).

Results suggest higher content for some trace elements in CCRs when SCR is in use, however, these observations are based on single samples from a limited number of facilities and evaluation of additional samples from the same and additional facilities is warranted. Primary observations for the constituents of concern (Figure 9 through Figure 21 and Figure 22 through Figure 36) are as follows:

Aluminum (Al) (Figure 9 and Figure 22). Al content in fly ash was 6-15 percent, in gypsum between 0.3-1 percent, and in scrubber sludges 0.7-20 percent. There is no apparent systematic effect of coal type or air pollution control system on Al content in CCRs. One likely source of variability is the Al content of the additive used for flue gas desulfurization (e.g., limestone or magnesium lime).

Arsenic (As) (Figure 10). As content in fly ash was 10-200 µg/g, with a higher content (500 µg/g) observed in one sample from a COHPAC facility with ACI (Facility C, sample GAT). As content in gypsum was 1-10 µg/g, in scrubber sludge and blended CCRs 3-70 µg/g. There was

³⁹ The database used in the EPA Risk Report (EPA, 2007b) for the assessment was based on both measurements of field samples (e.g., leachate, pore water) and single point laboratory leaching tests (e.g., TCLP, SPLP).

⁴⁰ The total elemental content of boron in CCRs was not measured for samples reported here because of analytical interference (digestion Method 3052 uses boron as part of the method).

no clear effect of coal type at the high level categorization based on coal rank and region on As content in CCRs, although coal from within a region has been observed to have considerable variability with respect to trace element total content.

Barium (Ba) (Figure 11 and Figure 23). Ba content in fly ash from bituminous and lignite coals was 0.06-0.2 percent, and 0.6-1.5 percent in fly ash from sub-bituminous coals. Ba content in gypsum was 2-80 $\mu\text{g/g}$, and in scrubber sludges 80-3,000 $\mu\text{g/g}$. Likely sources of variability of Ba content in gypsum include the source of limestone used in flue gas desulfurization and the extent of carryover of fly ash into the gypsum.

Cadmium (Cd) (Figure 12). Cd content in all CCRs was less than 2 $\mu\text{g/g}$, with lower content typically in gypsum than fly ash samples. An exception was the fly ash sample from Facility U (UFA) which had Cd content of 15 $\mu\text{g/g}$.

Cobalt (Co) (Figure 13). Co content in fly ash was 20-70 $\mu\text{g/g}$, and 0.8-4 $\mu\text{g/g}$ in gypsum. Results for scrubber sludge suggest less Co content in samples from facilities without NO_x controls (1-2 $\mu\text{g/g}$) than for facilities with NO_x controls (SCR or SNCR) in operation (3-40 $\mu\text{g/g}$, including paired comparisons).

Chromium (Cr) (Figure 14). Cr content in fly ash was 70-200 $\mu\text{g/g}$, and 1-20 $\mu\text{g/g}$ in gypsum with no apparent relationship to coal type. Higher Cr content in scrubber sludges was associated with facilities using SCR (Facilities B and K, samples BGD and KGD; 50-300 $\mu\text{g/g}$ compared to 9-20 $\mu\text{g/g}$ for other samples).

Mercury (Hg) (Figure 15 and Figure 16). Hg content in all CCRs was from 0.01-20 $\mu\text{g/g}$ with highest Hg content associated with fly ash samples from facilities with ACI and gypsum from a facility burning lignite coal (Facility Ca, sample CaAW).

Molybdenum (Mo) (Figure 17). Mo content in fly ash and scrubber sludges was similar at 8-30 $\mu\text{g/g}$, with one exception in fly ash at 80 $\mu\text{g/g}$ (Facility U, sample UFA). Mo content in gypsum was 1-10 $\mu\text{g/g}$. No apparent relationship to coal type or air pollution control system was observed.

Lead (Pb) (Figure 18). Pb content in fly ash was 20-100 $\mu\text{g/g}$, 0.4-10 $\mu\text{g/g}$ in gypsum and 2-30 $\mu\text{g/g}$ in scrubber sludges. No apparent relationship to coal type or air pollution control system was observed.

Antimony (Sb) (Figure 19). Sb content in fly ash and scrubber sludge was 3-15 $\mu\text{g/g}$ and 0.15-8 $\mu\text{g/g}$ in gypsum. No apparent relationship to coal type or air pollution control system was observed.

Selenium (Se) (Figure 20). Se content in all CCRs was distributed over range with typical content of 2-50 $\mu\text{g/g}$ with two samples with approximately 200 $\mu\text{g/g}$ (Brayton Point, sample BPT; Facility C, sample GAT).

Thallium (Tl) (Figure 21). Tl content was 0.8-15 in fly ash and scrubber sludges, and 0.2-2 $\mu\text{g/g}$ in gypsum. No apparent relationship to coal type or air pollution control system was observed.

Major species analysis by XRF (Figure 22 to Figure 36) indicated that fly ash from facilities burning sub-bituminous coals had greater content of Ba, Ca, Mg, Na, P and Sr than fly ash from facilities burning bituminous or lignite coals. Total Ca content in fly ash can be divided into three groupings related to coal types: (i) sub-bituminous, 10-20%, (ii) high calcium bituminous and lignite, 1-6%, and (iii) low calcium bituminous, 0.3-0.7%. Fly ash samples with low total

Characterization of Coal Combustion Residues III

calcium had acidic own pH values (typically $4 < \text{pH} < 5$) compared to samples with medium and high calcium content that had alkali own pH values (typically $\text{pH} > 10$). The relationship between total calcium content (by XRF) and own pH for fly ash samples is illustrated in Figure 37. Higher calcium content results in greater fly ash alkalinity, as indicated by higher pH values.

Major species analysis also indicated that gypsum contained up to 5 wt% carbon and up to 7 wt% Si, both indicative of fly ash carry over into the FGD scrubber. Based on Si content in gypsum, this suggests up to 5% of the non-carbon content is comprised of fly ash.

In interpreting these results, please note that the CCRs analyzed in this report are not considered to be a representative sample of all CCRs produced in the U.S. For many of the observations, only a few data points were available. It is hoped that through broader use of the improved leach test methods (as used in this report), that additional data from CCR characterization will become available. That will help better define trends associated with changes in air pollution control at coal-fired power plants.

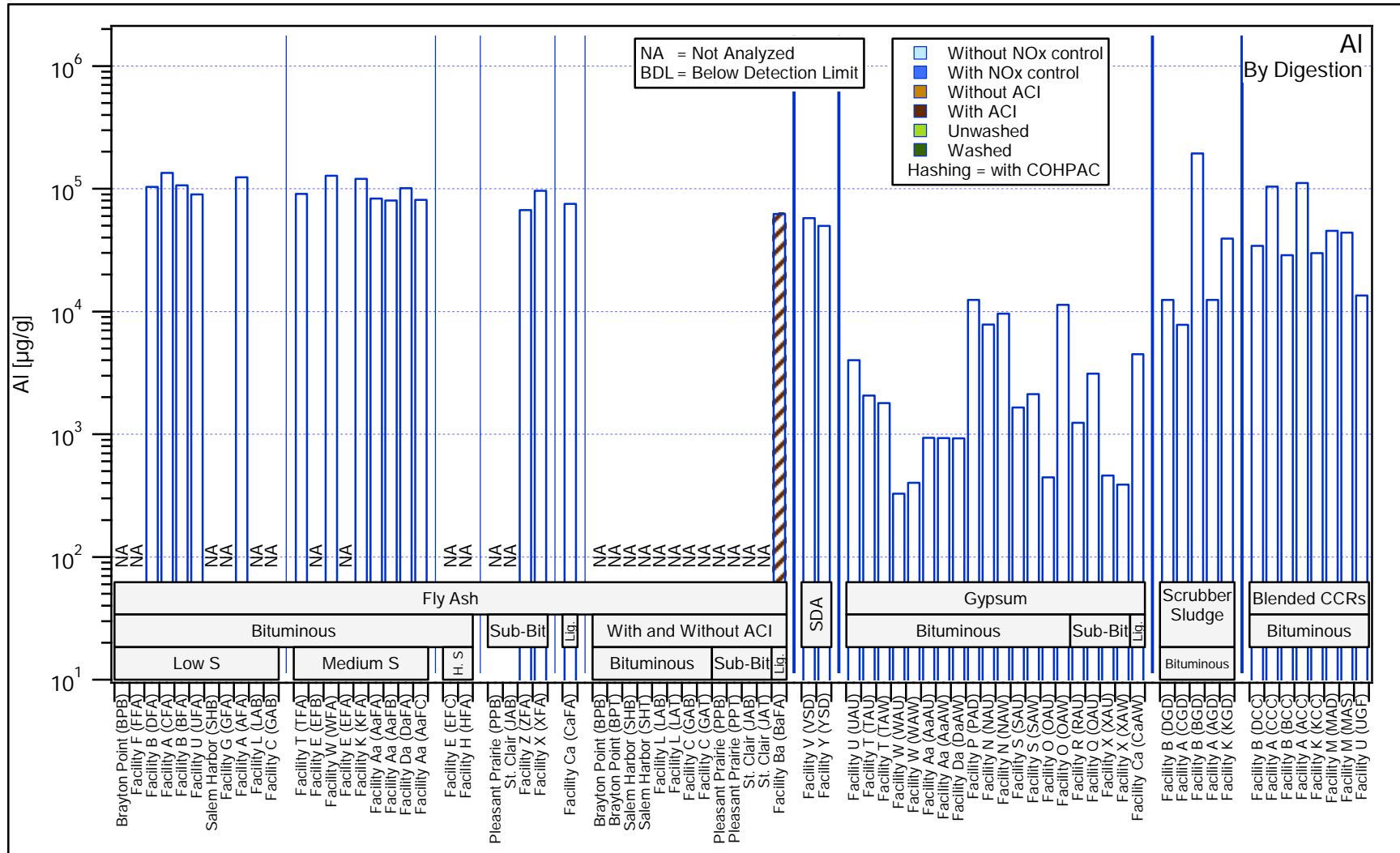


Figure 9. Aluminum. Comparison of total elemental content by digestion (Methods 3052 and 6020).

Characterization of Coal Combustion Residues III

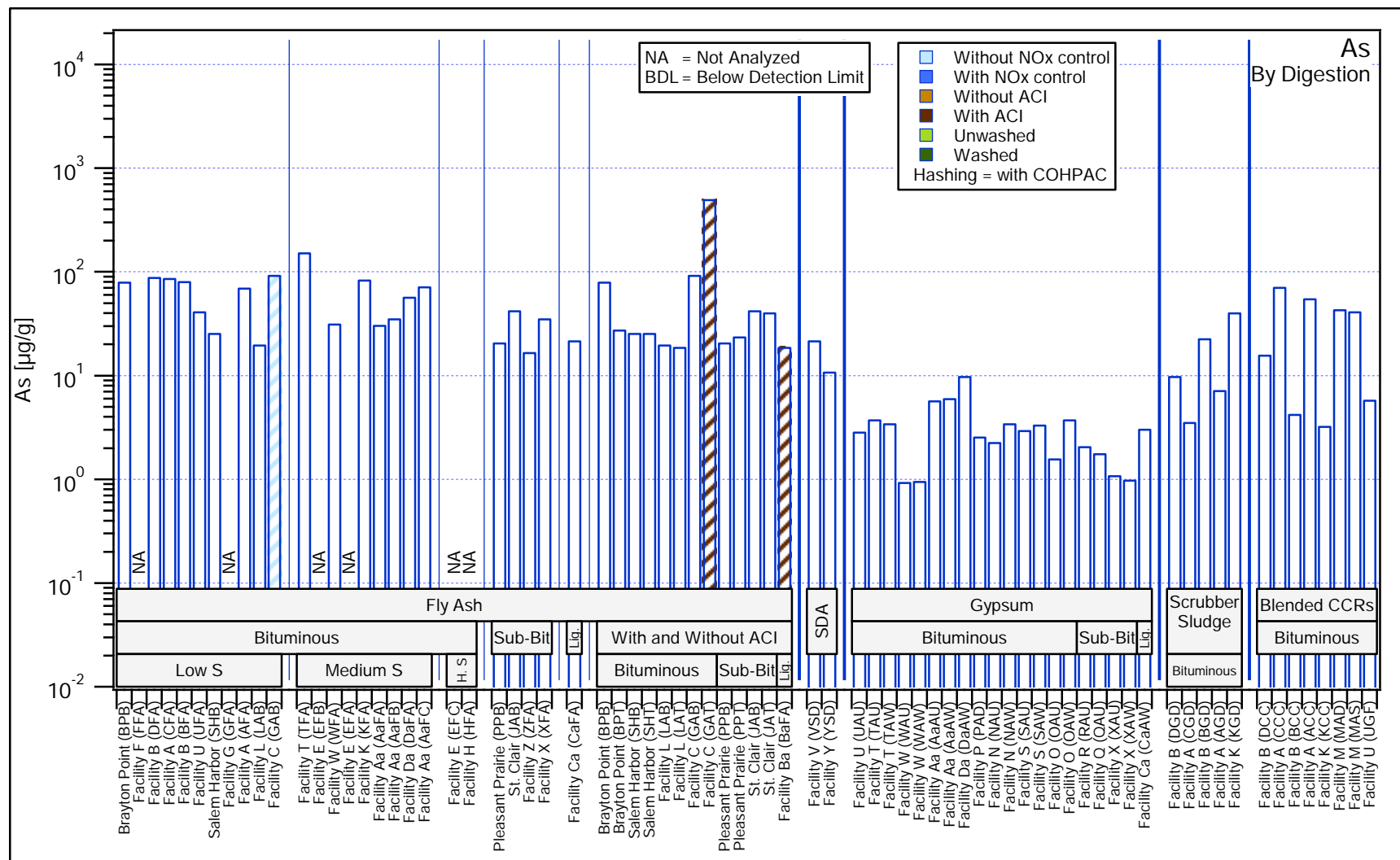


Figure 10. Arsenic. Comparison of total elemental content by digestion (Methods 3052 and 6020).

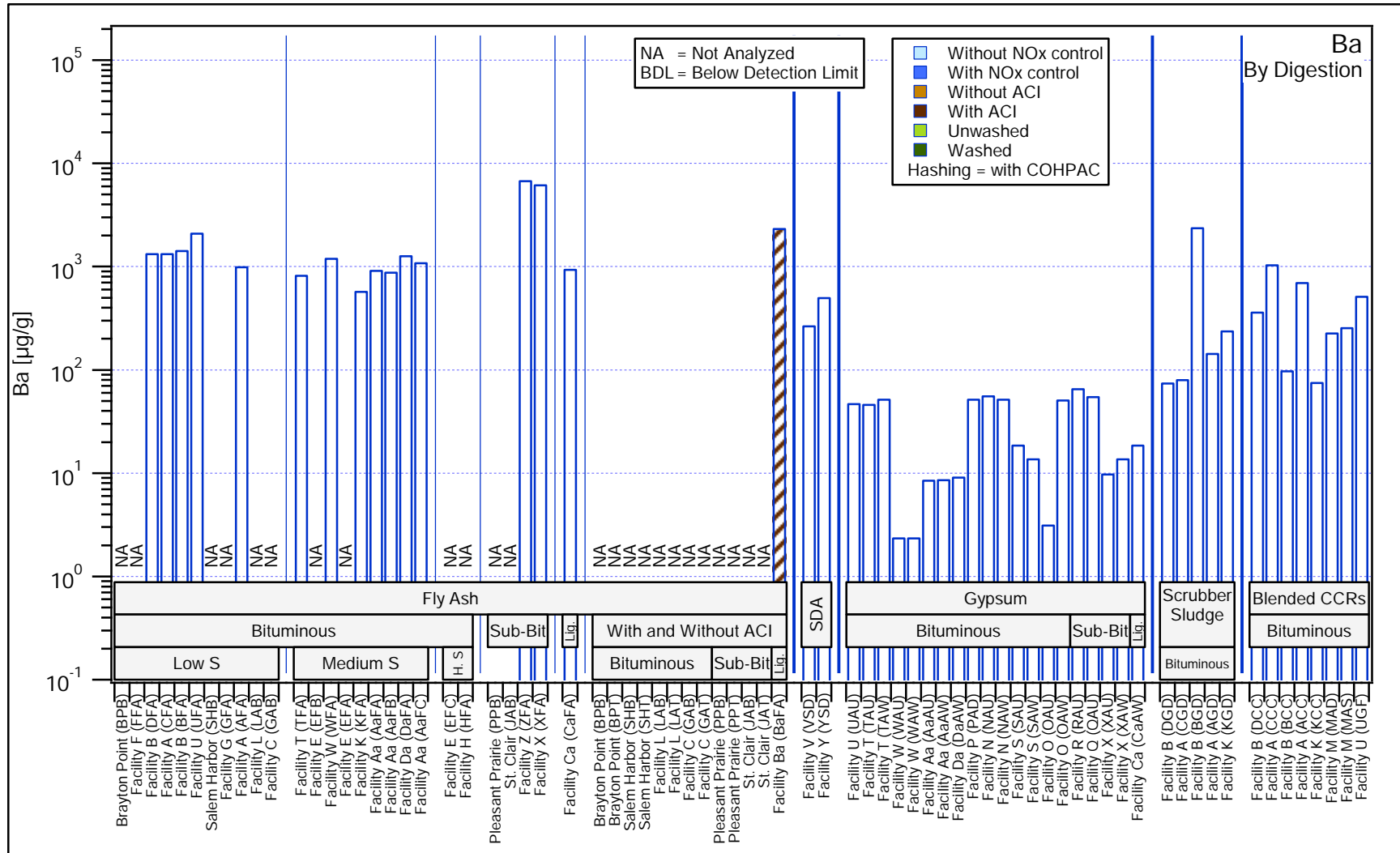


Figure 11. Barium. Comparison of total elemental content by digestion (Methods 3052 and 6020).

Characterization of Coal Combustion Residues III

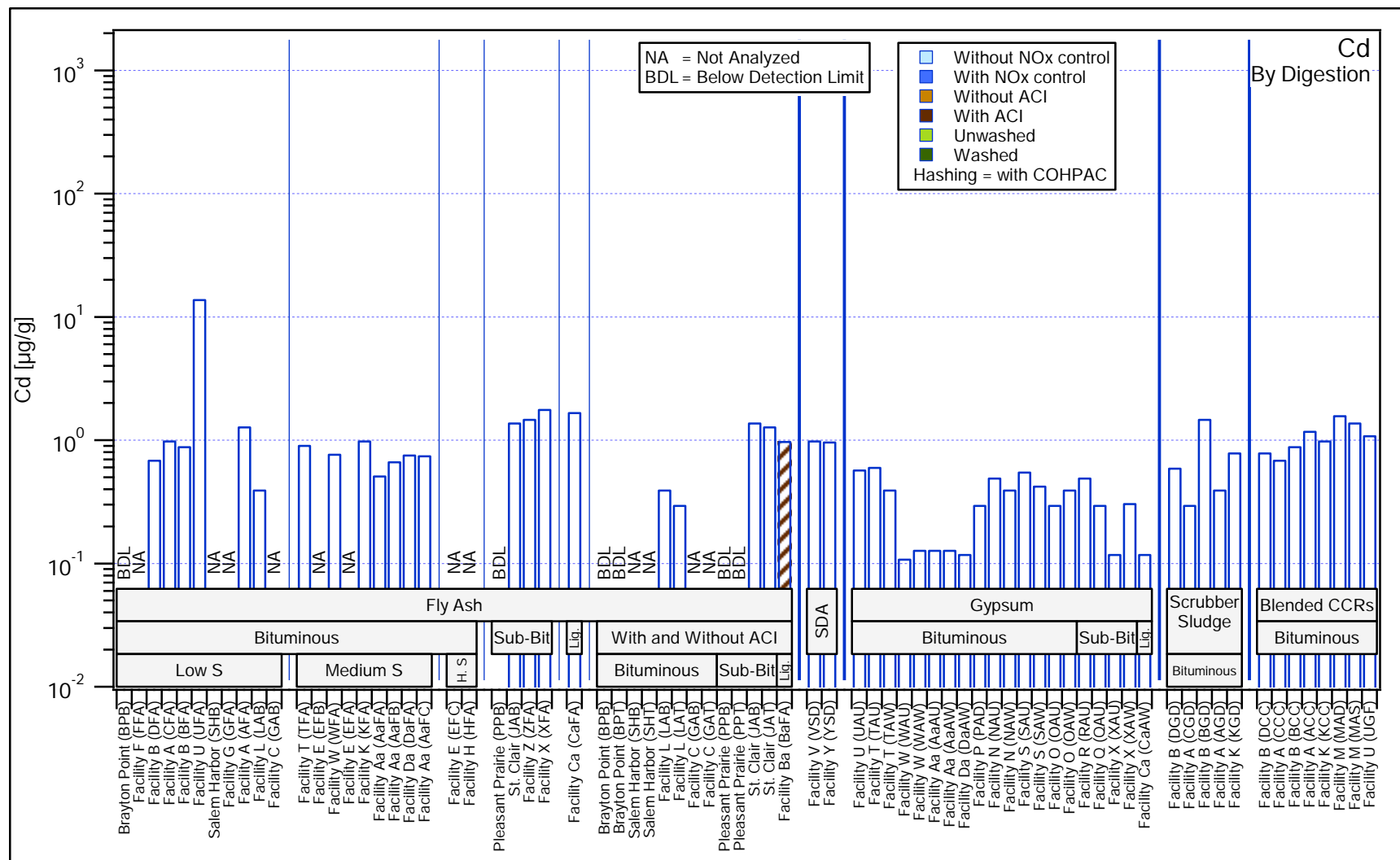


Figure 12. Cadmium. Comparison of total elemental content by digestion (Methods 3052 and 6020).

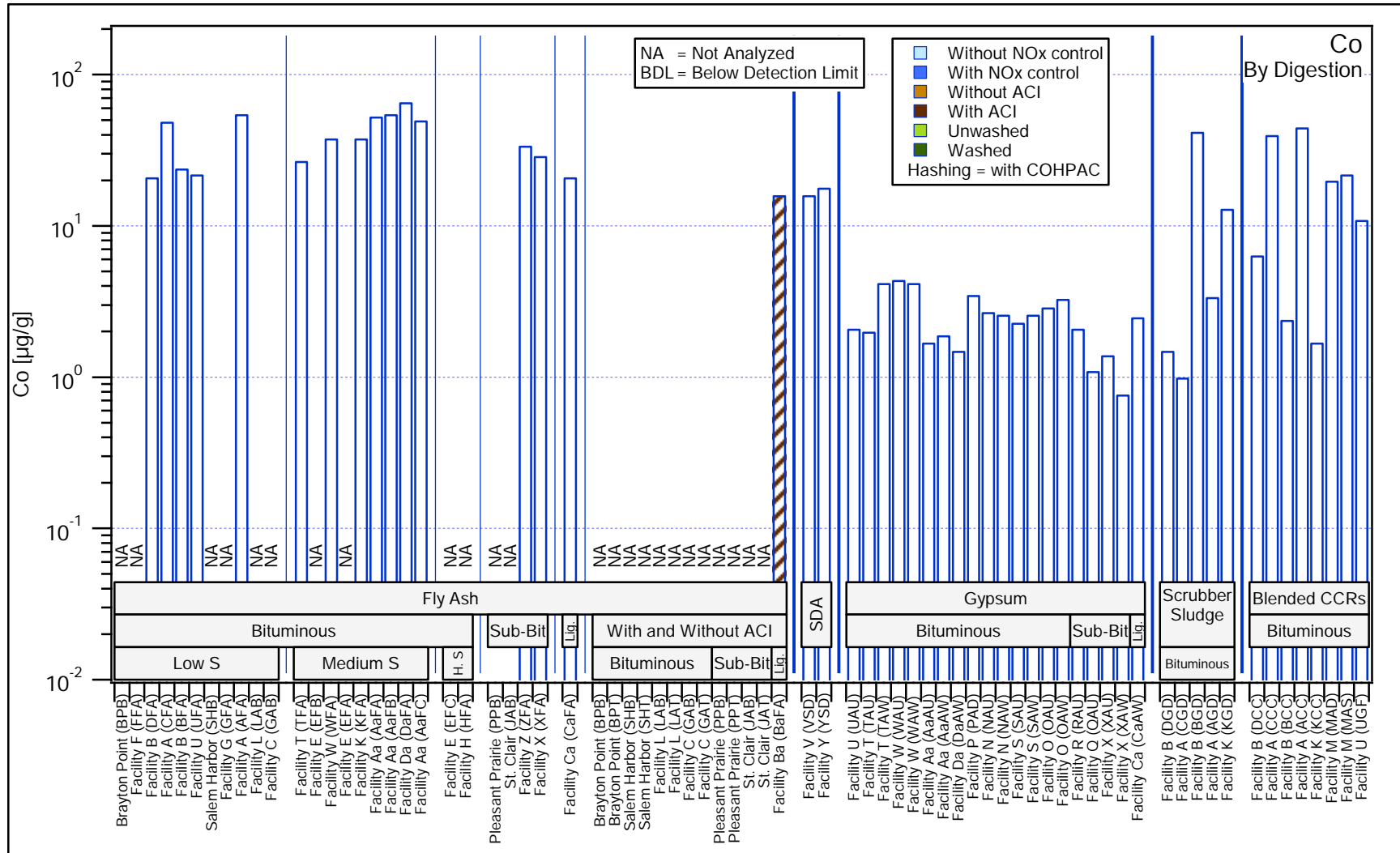


Figure 13. Cobalt. Comparison of total elemental content by digestion (Methods 3052 and 6020).

Characterization of Coal Combustion Residues III

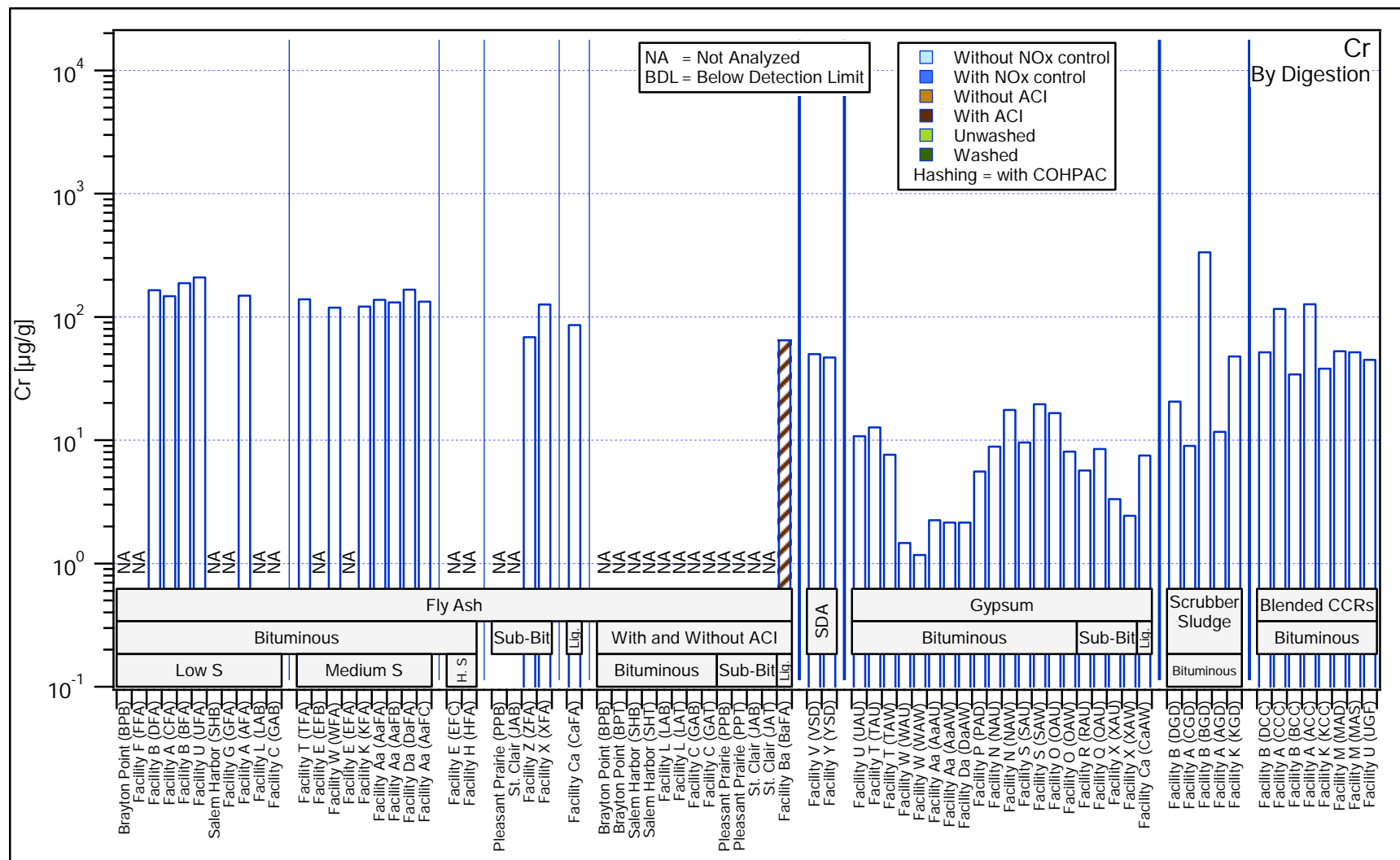


Figure 14. Chromium. Comparison of total elemental content by digestion (Methods 3052 and 6020).

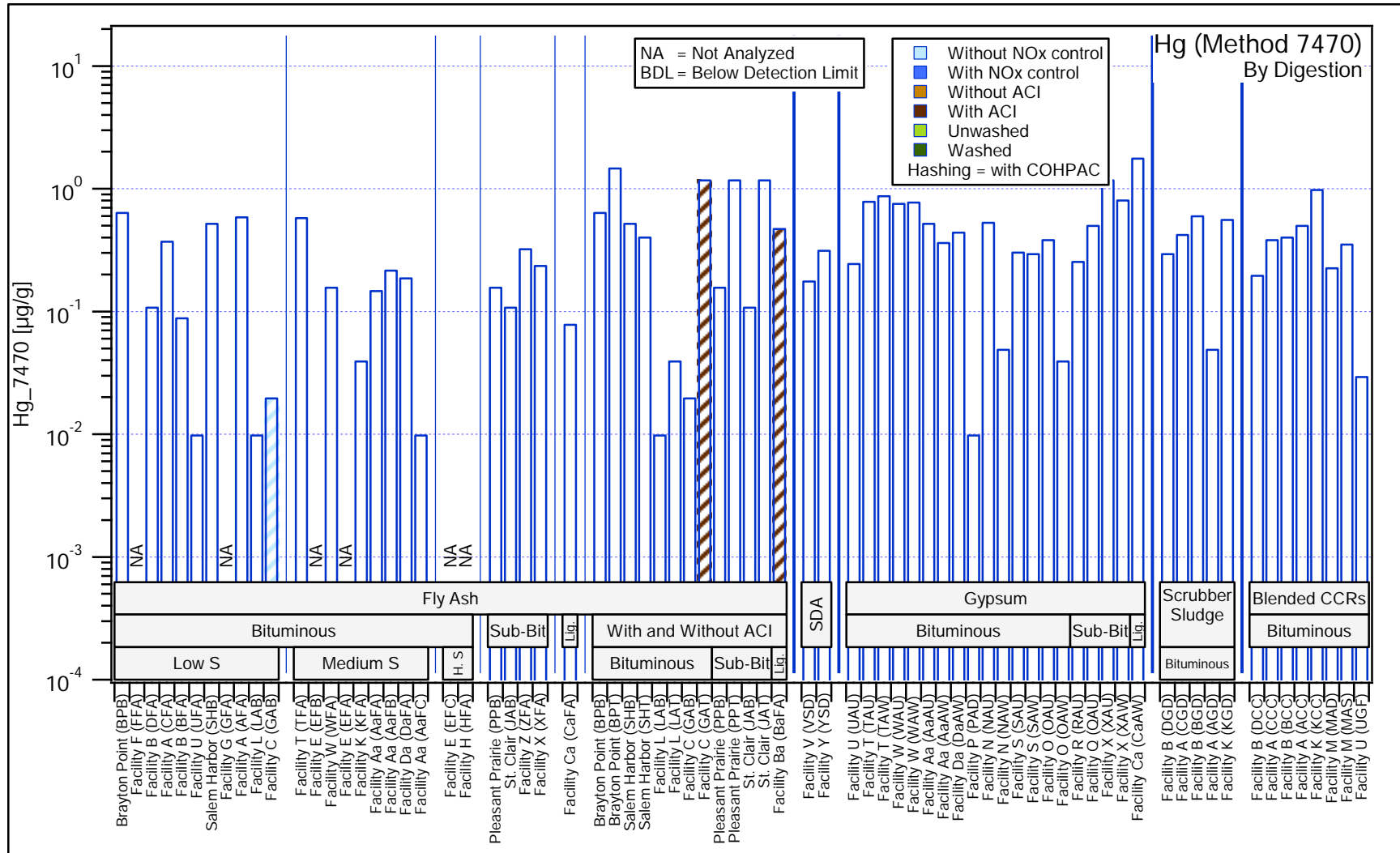


Figure 15. Mercury. Comparison of total elemental content by digestion (Method 7470).

Characterization of Coal Combustion Residues III

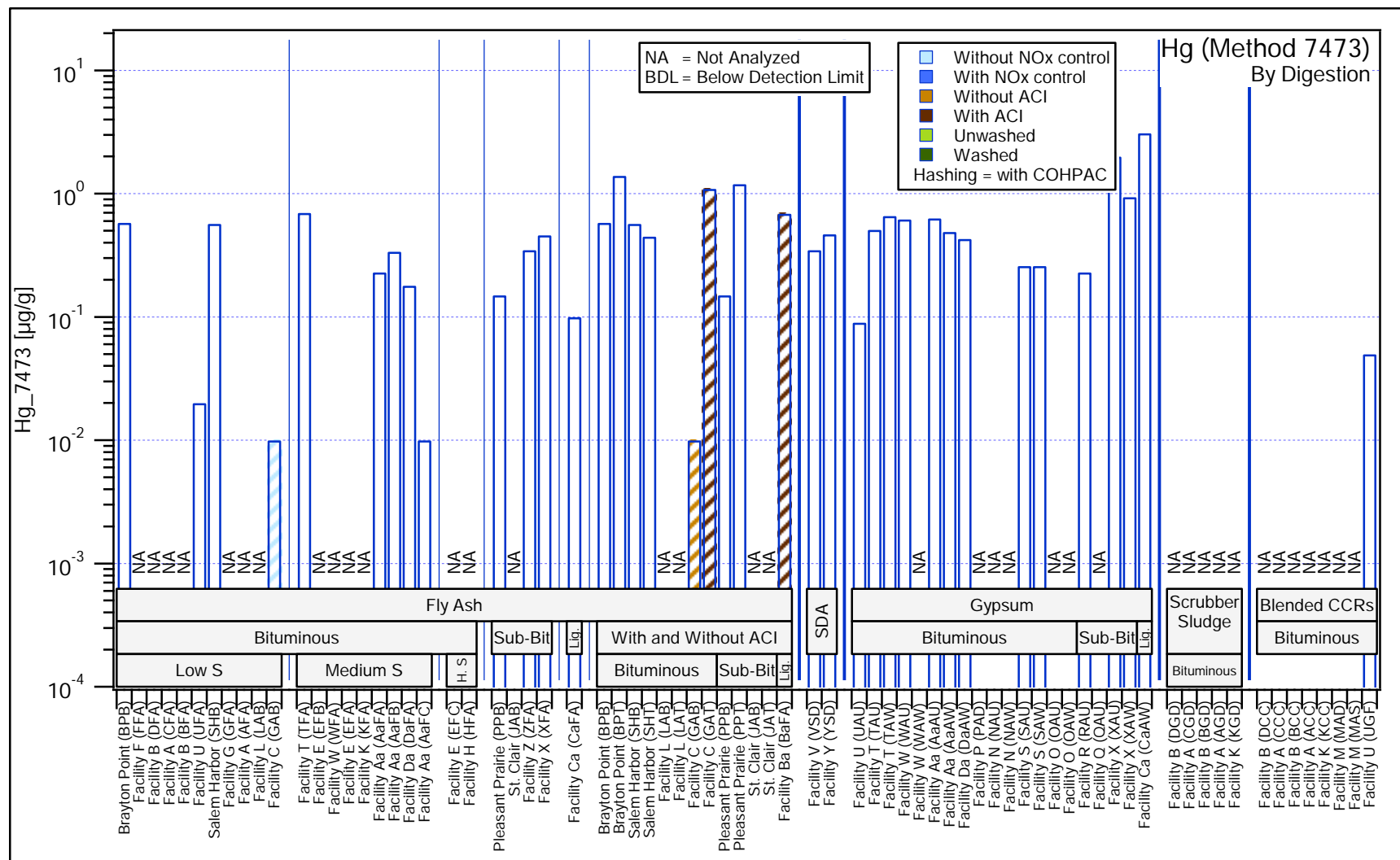


Figure 16. Mercury. Comparison of total elemental content by digestion (Method 7473).

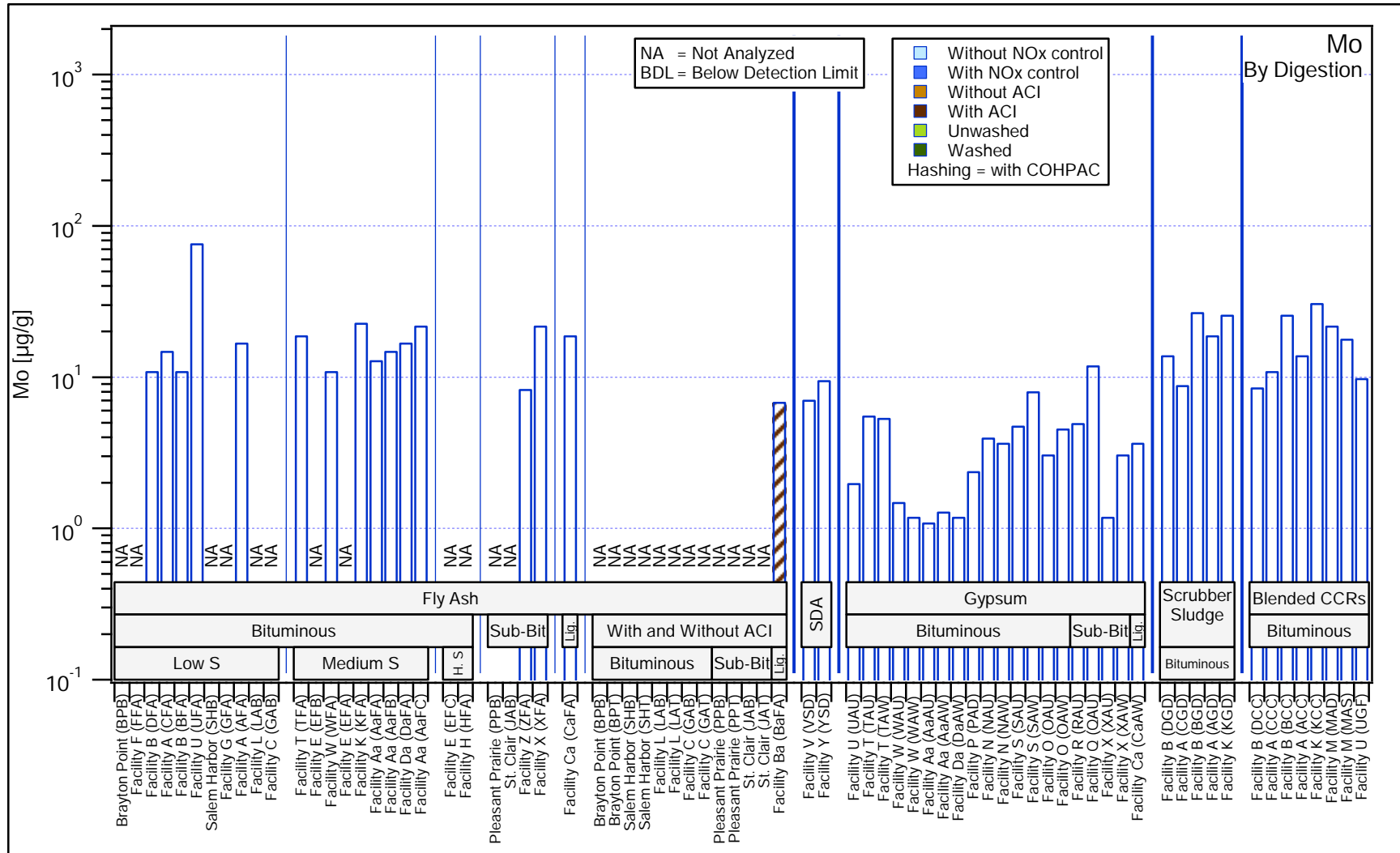


Figure 17. Molybdenum. Comparison of total elemental content by digestion (Methods 3052 and 6020).

Characterization of Coal Combustion Residues III

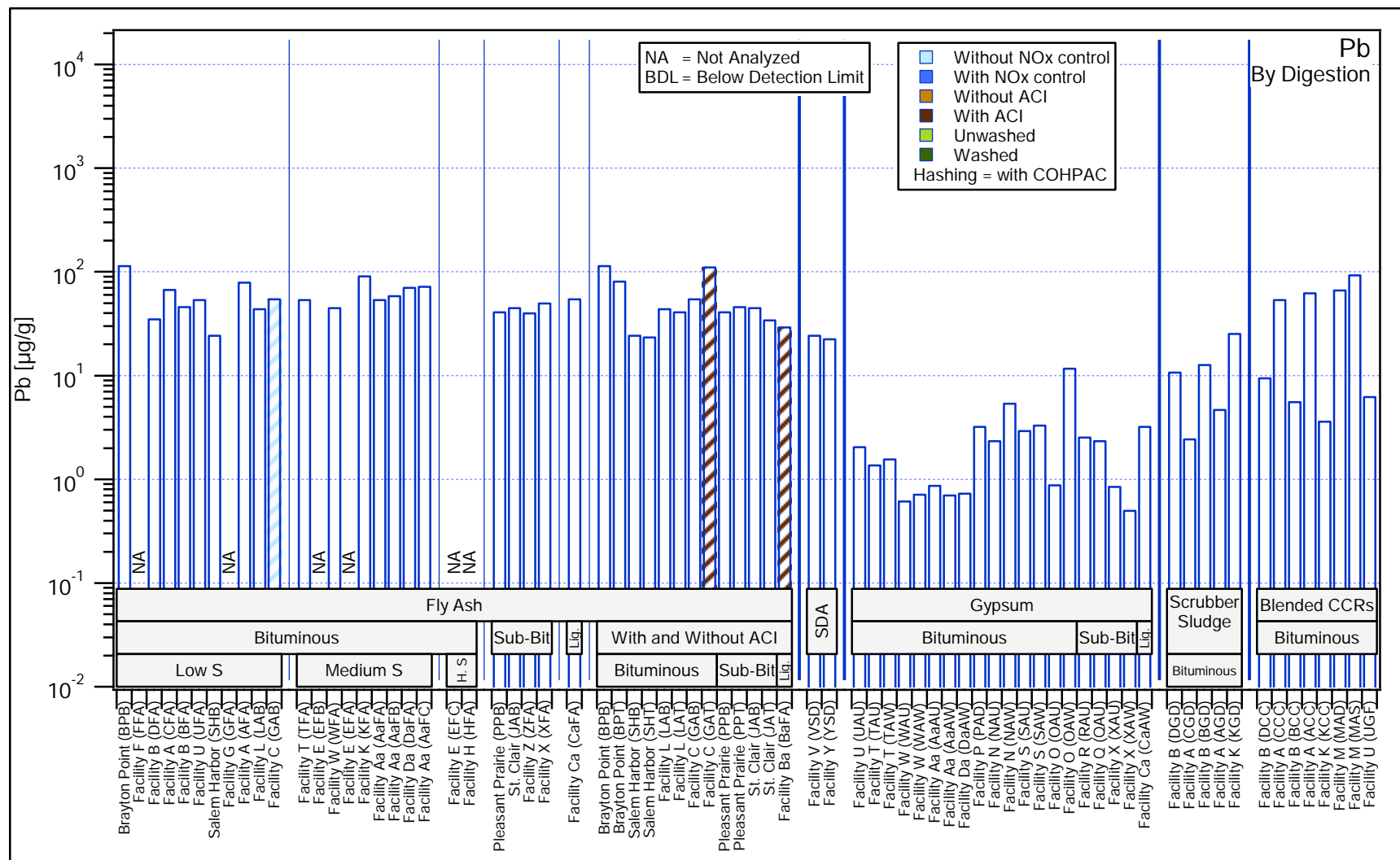


Figure 18. Lead. Comparison of total elemental content by digestion (Methods 3052 and 6020).

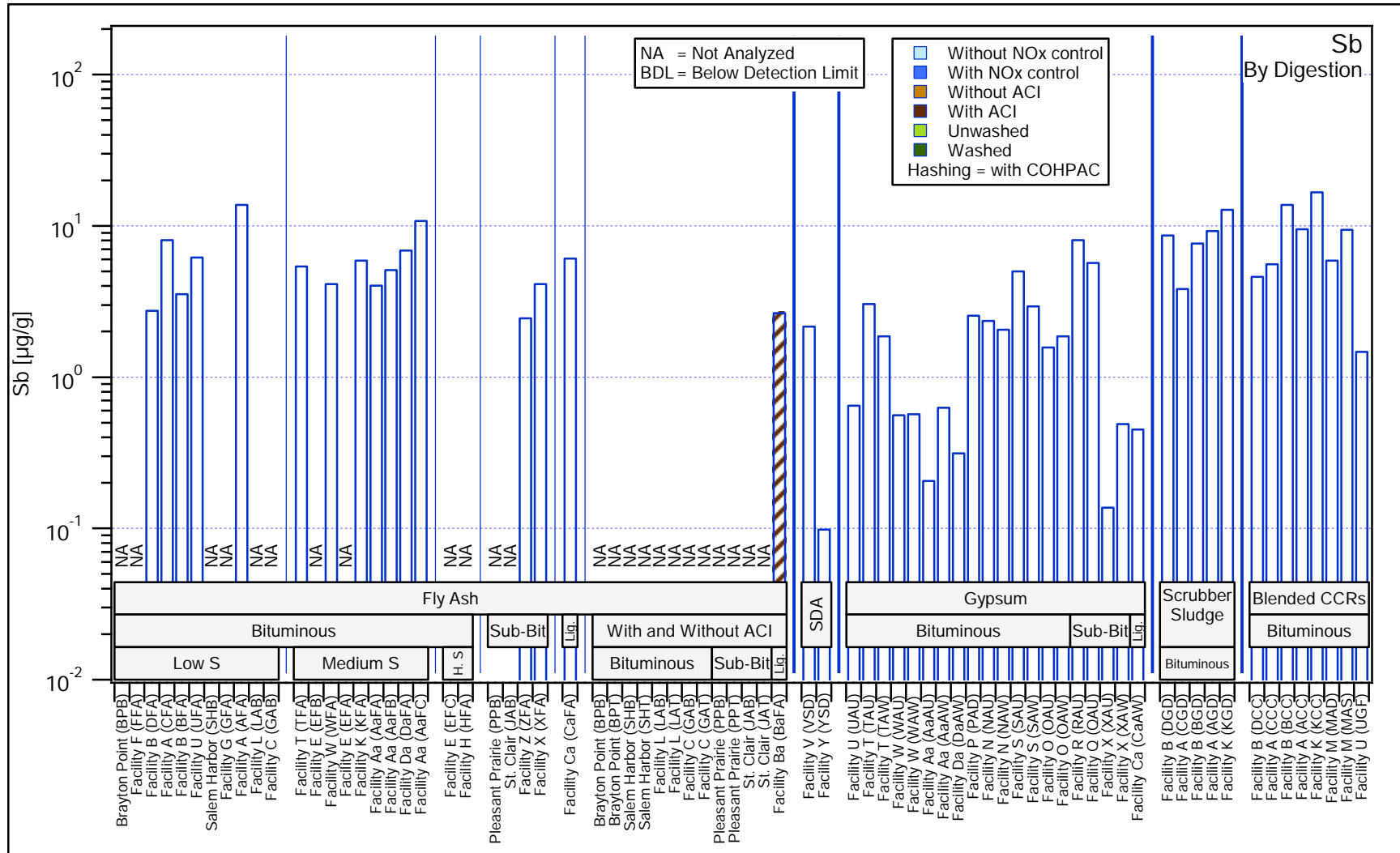


Figure 19. Antimony. Comparison of total elemental content by digestion (Methods 3052 and 6020).

Characterization of Coal Combustion Residues III

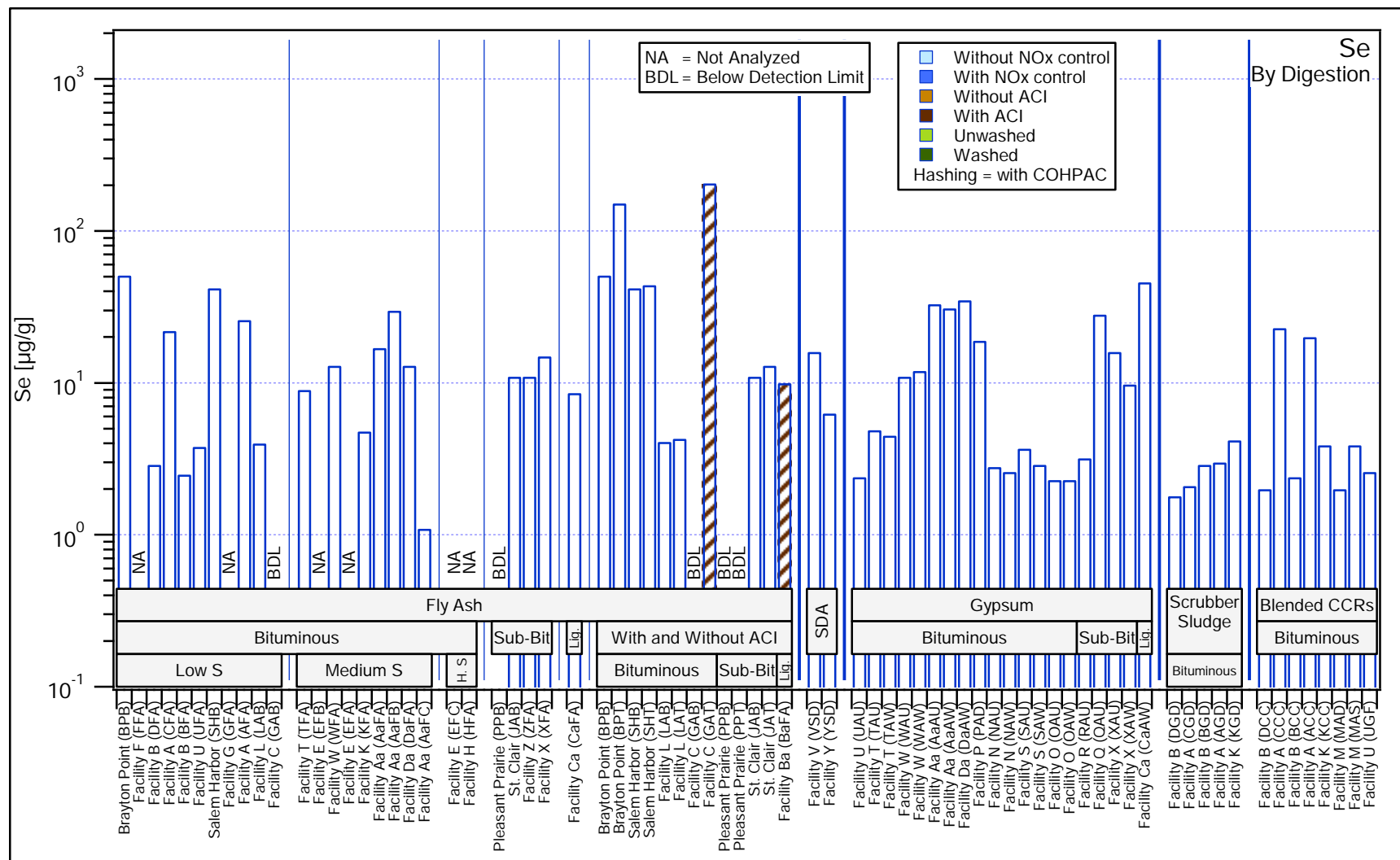


Figure 20. Selenium. Comparison of total elemental content by digestion (Methods 3052 and 6020).

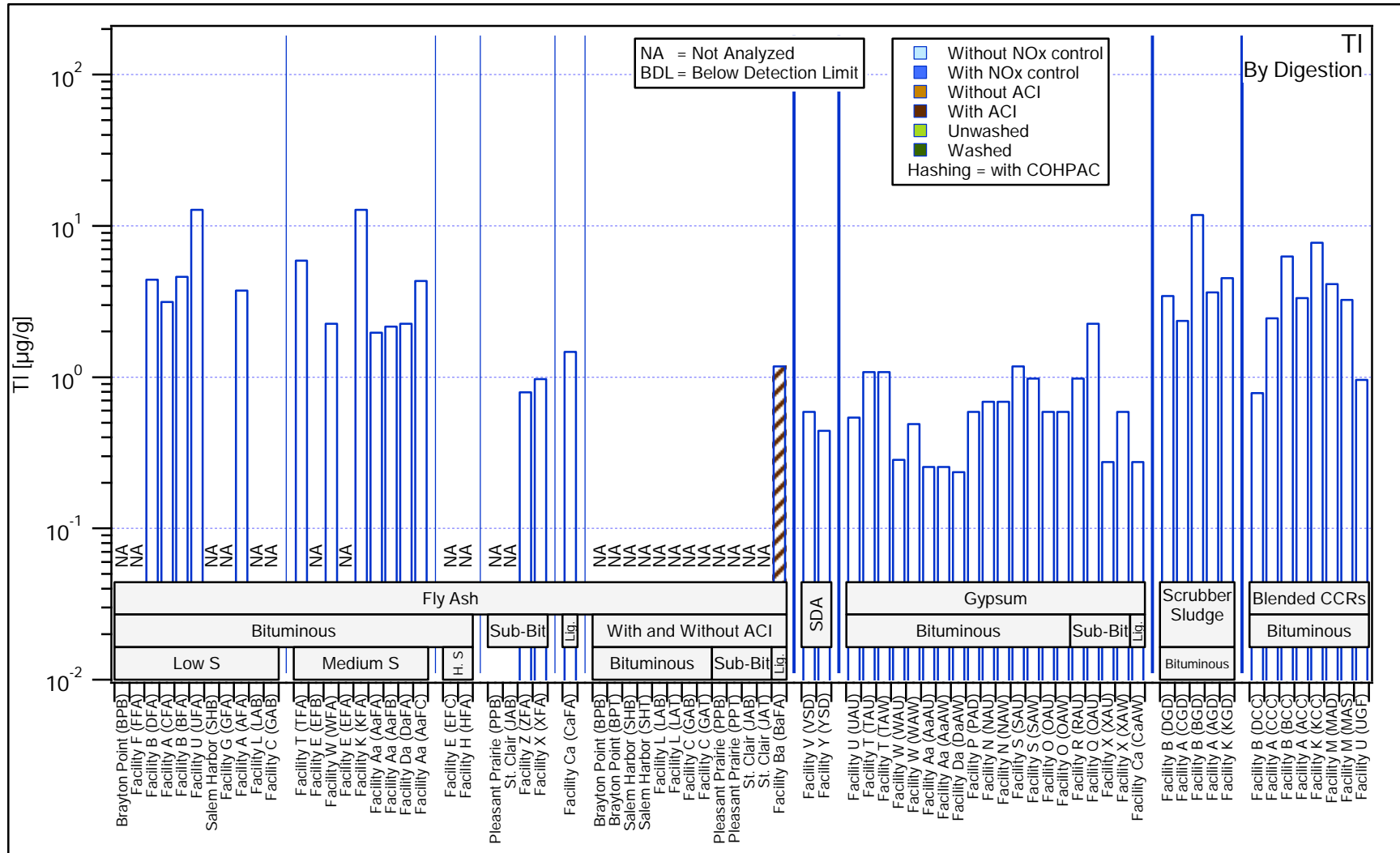


Figure 21. Thallium. Comparison of total elemental content by digestion (Methods 3052 and 6020).

Characterization of Coal Combustion Residues III

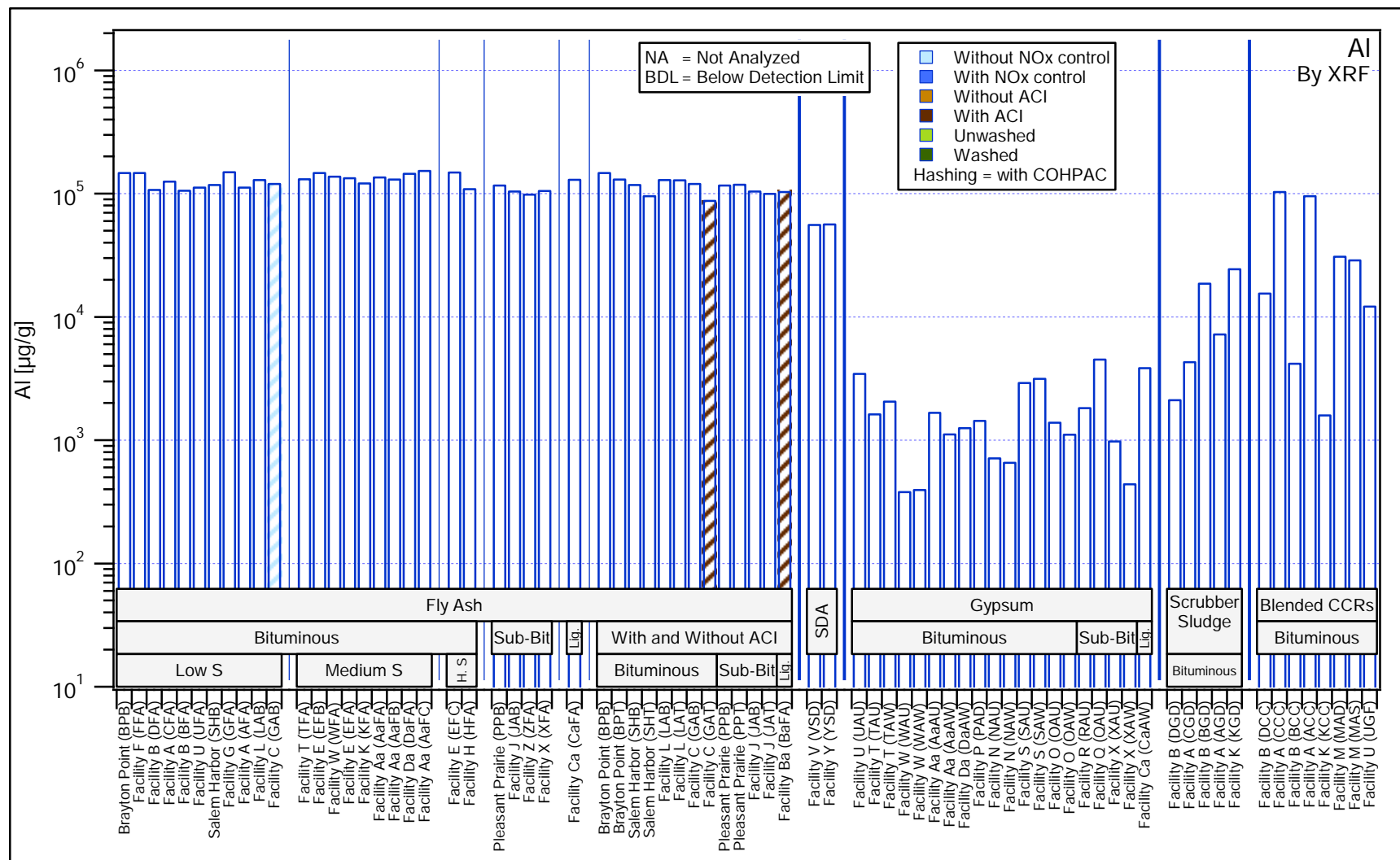


Figure 22. Aluminum. Comparison of total elemental content by XRF.

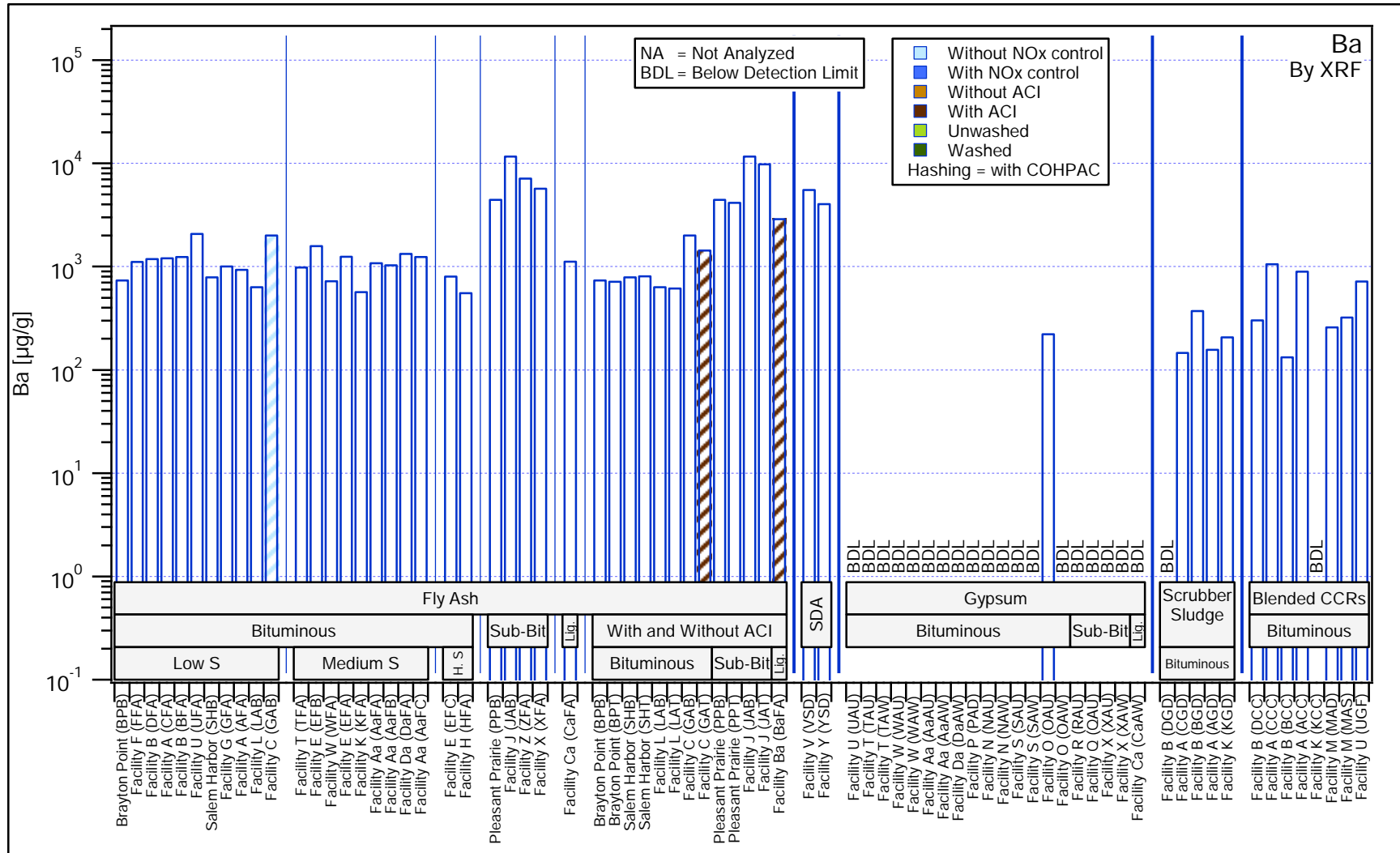


Figure 23. Barium. Comparison of total elemental content by XRF.

Characterization of Coal Combustion Residues III

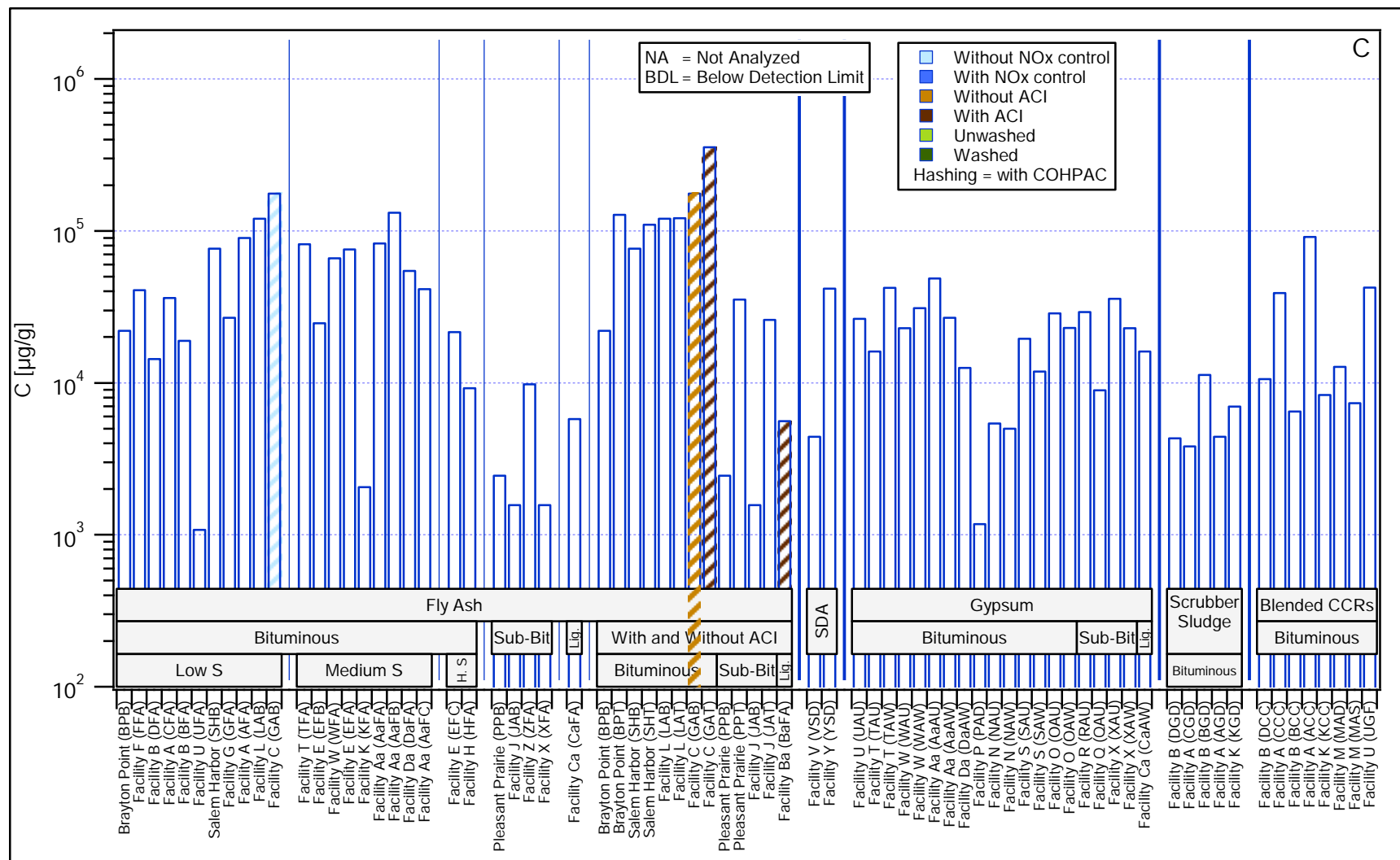


Figure 24. Carbon. Comparison of total elemental content.

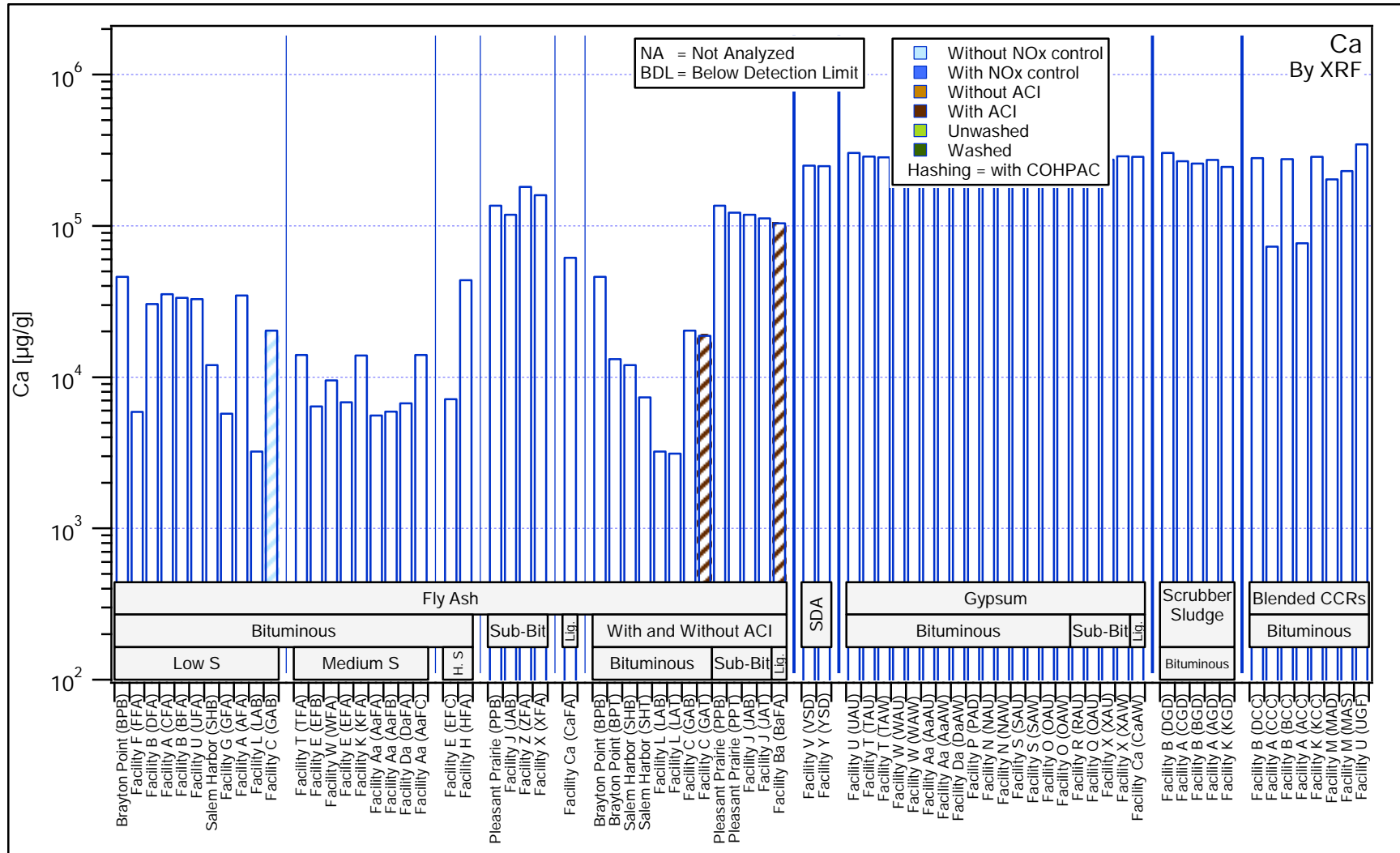


Figure 25. Calcium. Comparison of total elemental content by XRF.

Characterization of Coal Combustion Residues III

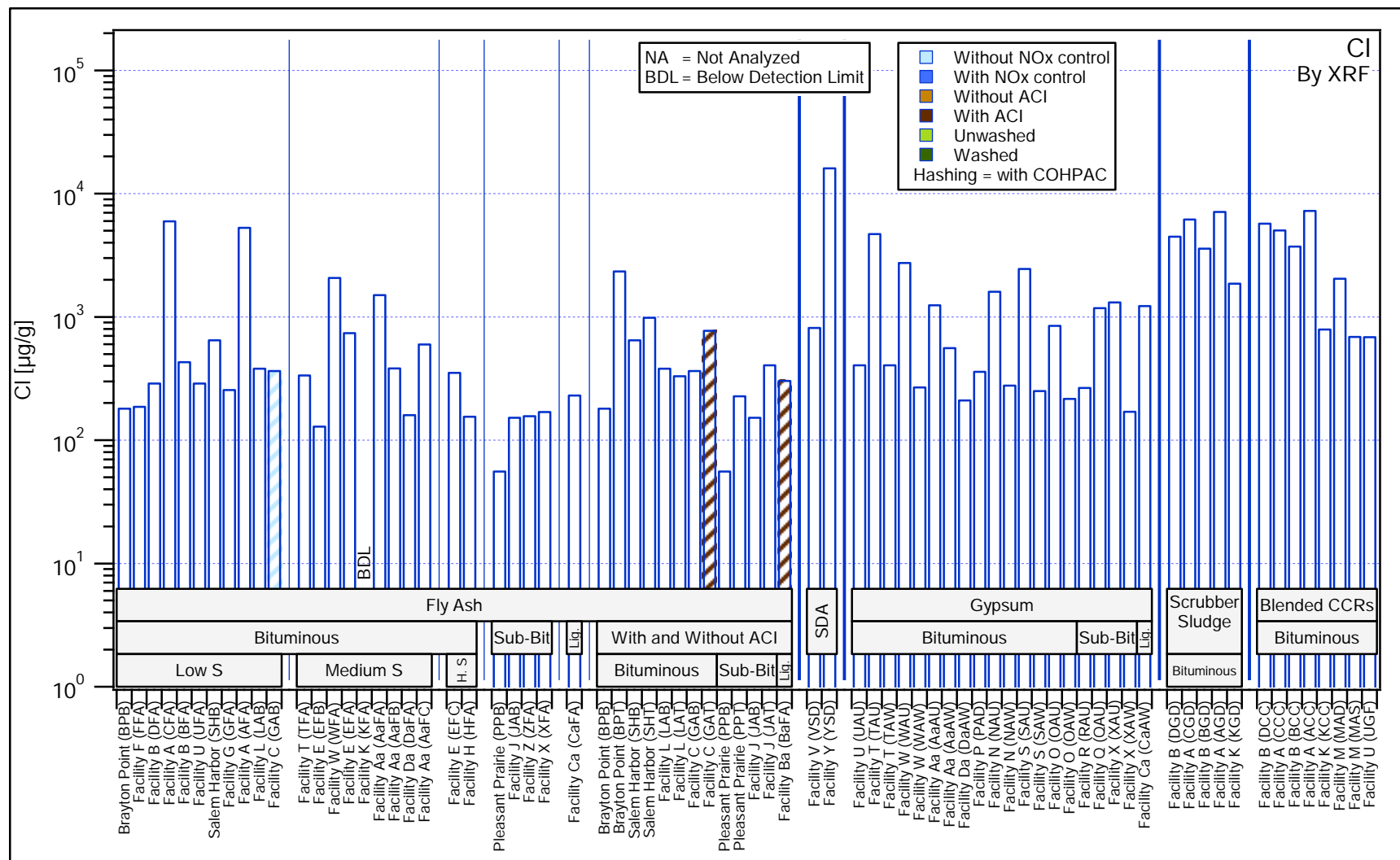


Figure 26. Chloride. Comparison of total elemental content by XRF.

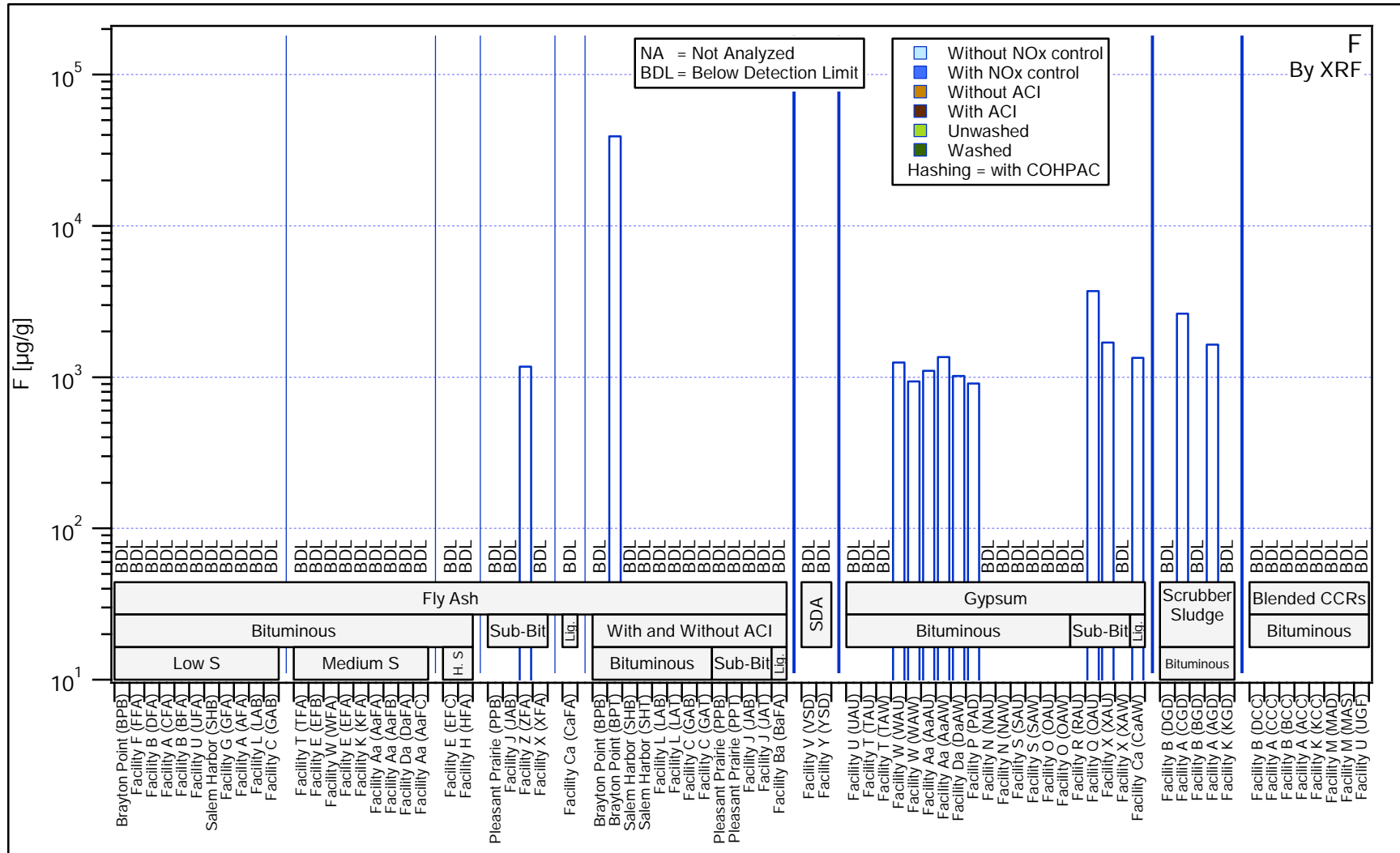


Figure 27. Fluoride. Comparison of total elemental content by XRF.

Characterization of Coal Combustion Residues III

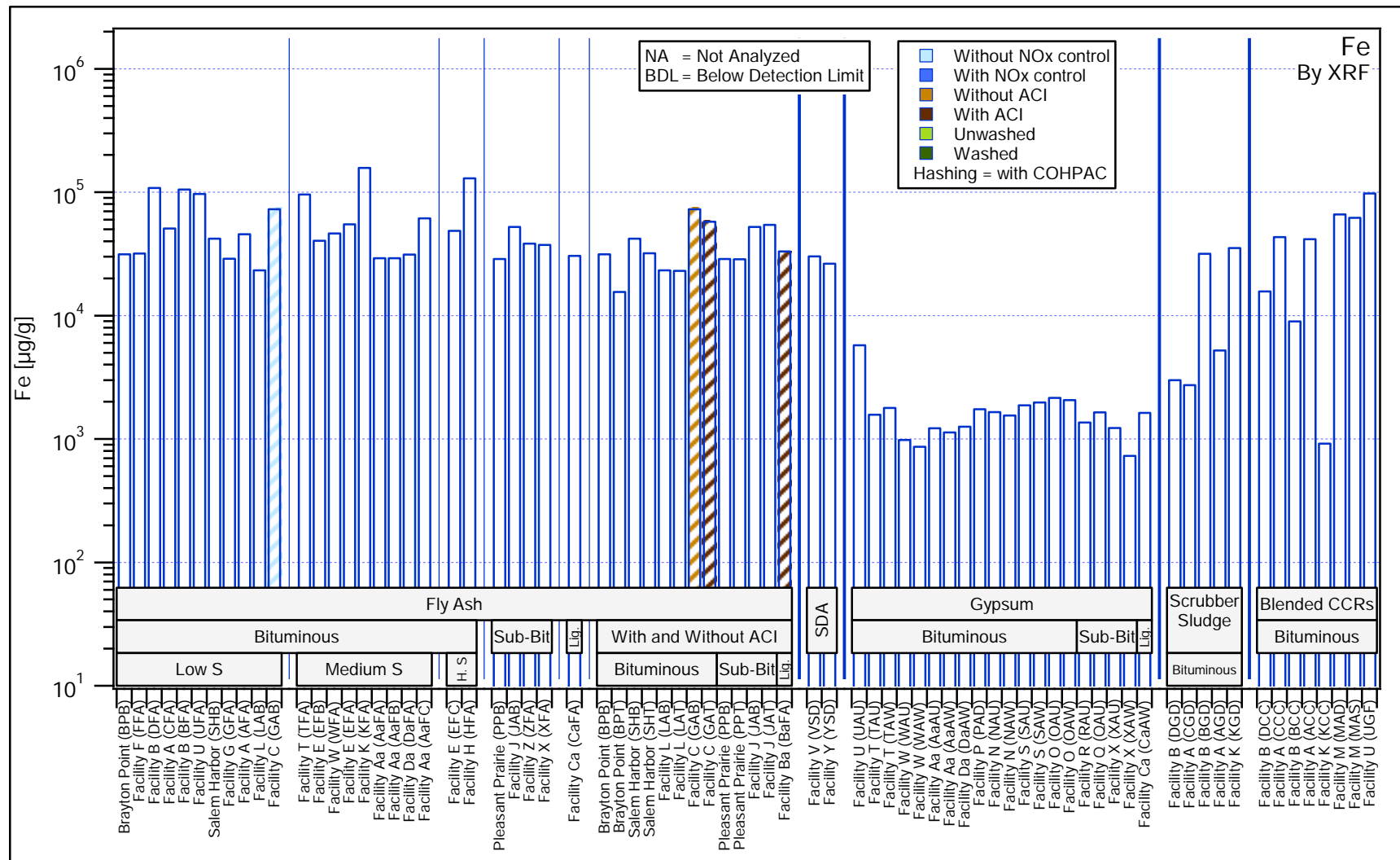


Figure 28. Iron. Comparison of total elemental content by XRF.

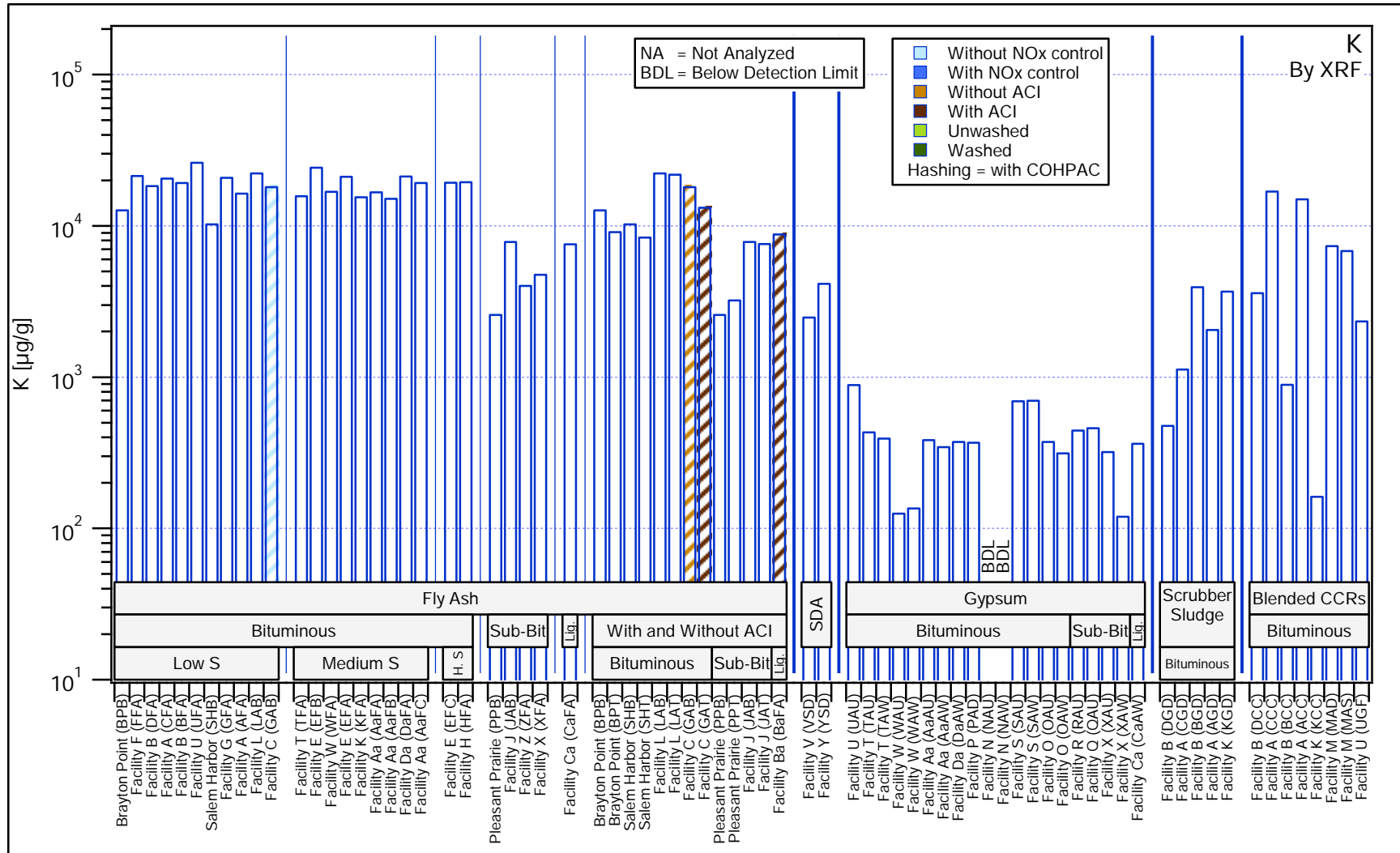


Figure 29. Potassium. Comparison of total elemental content by XRF.

Characterization of Coal Combustion Residues III

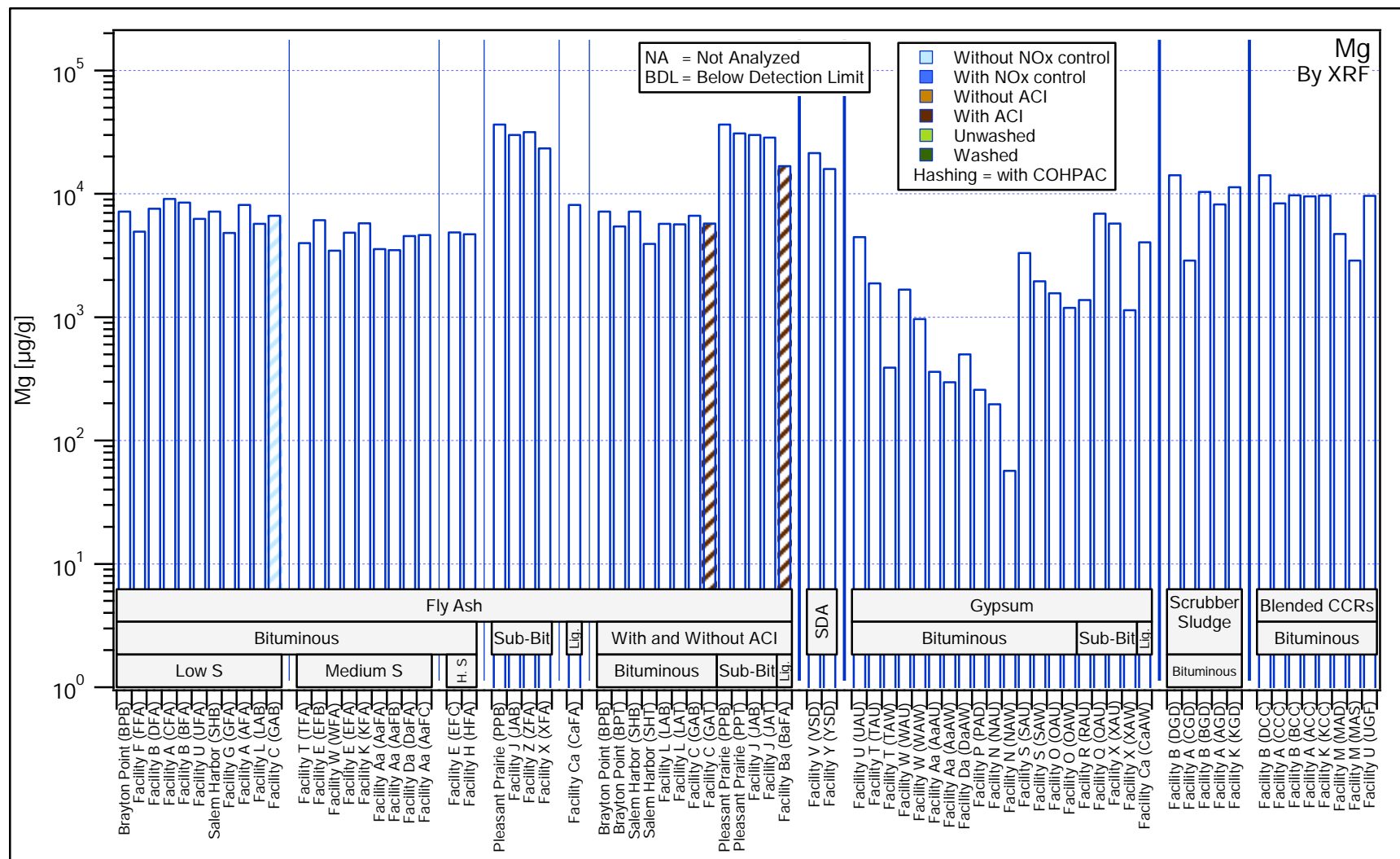


Figure 30. Magnesium. Comparison of total elemental content by XRF.

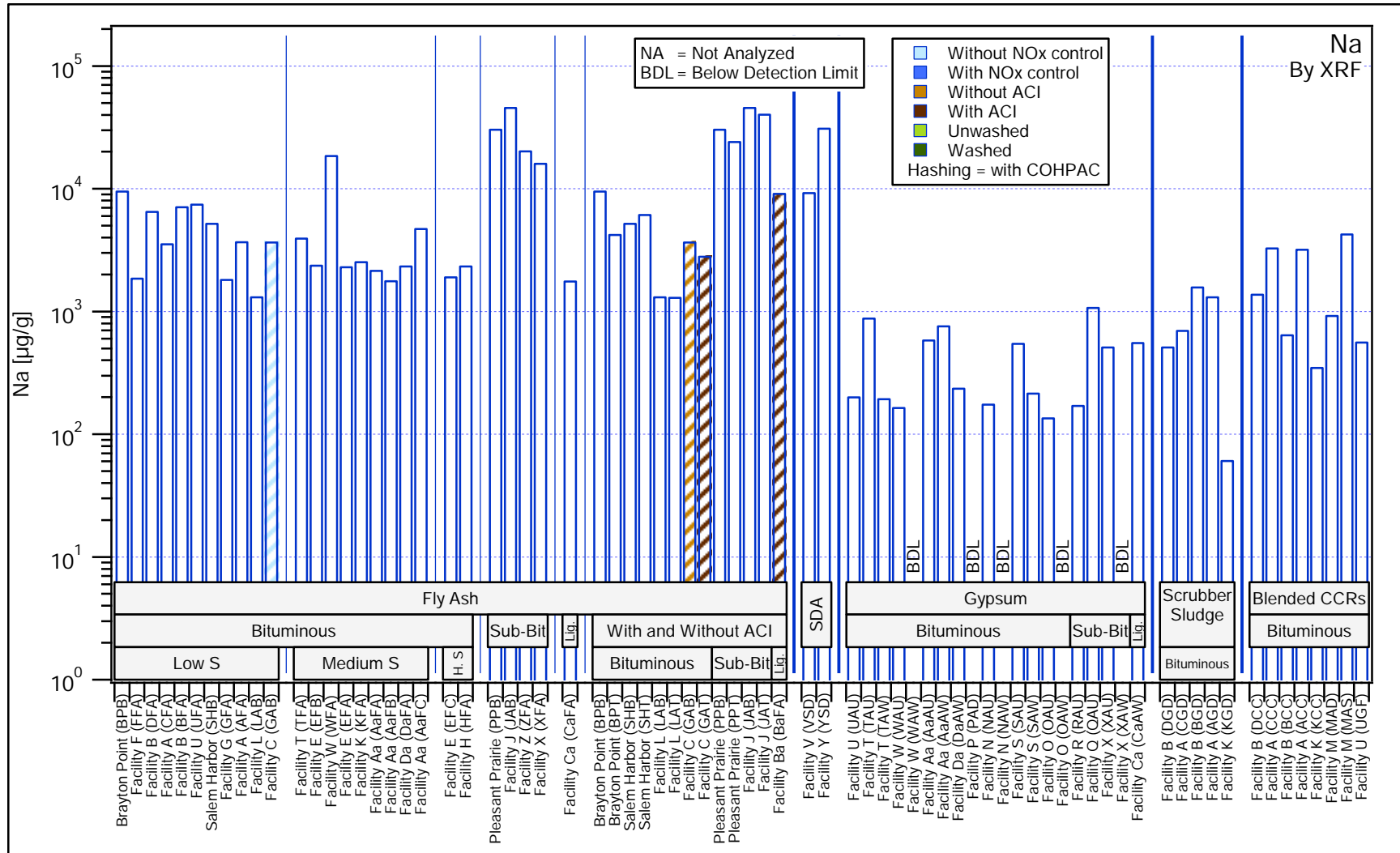


Figure 31. Sodium. Comparison of total elemental content by XRF.

Characterization of Coal Combustion Residues III

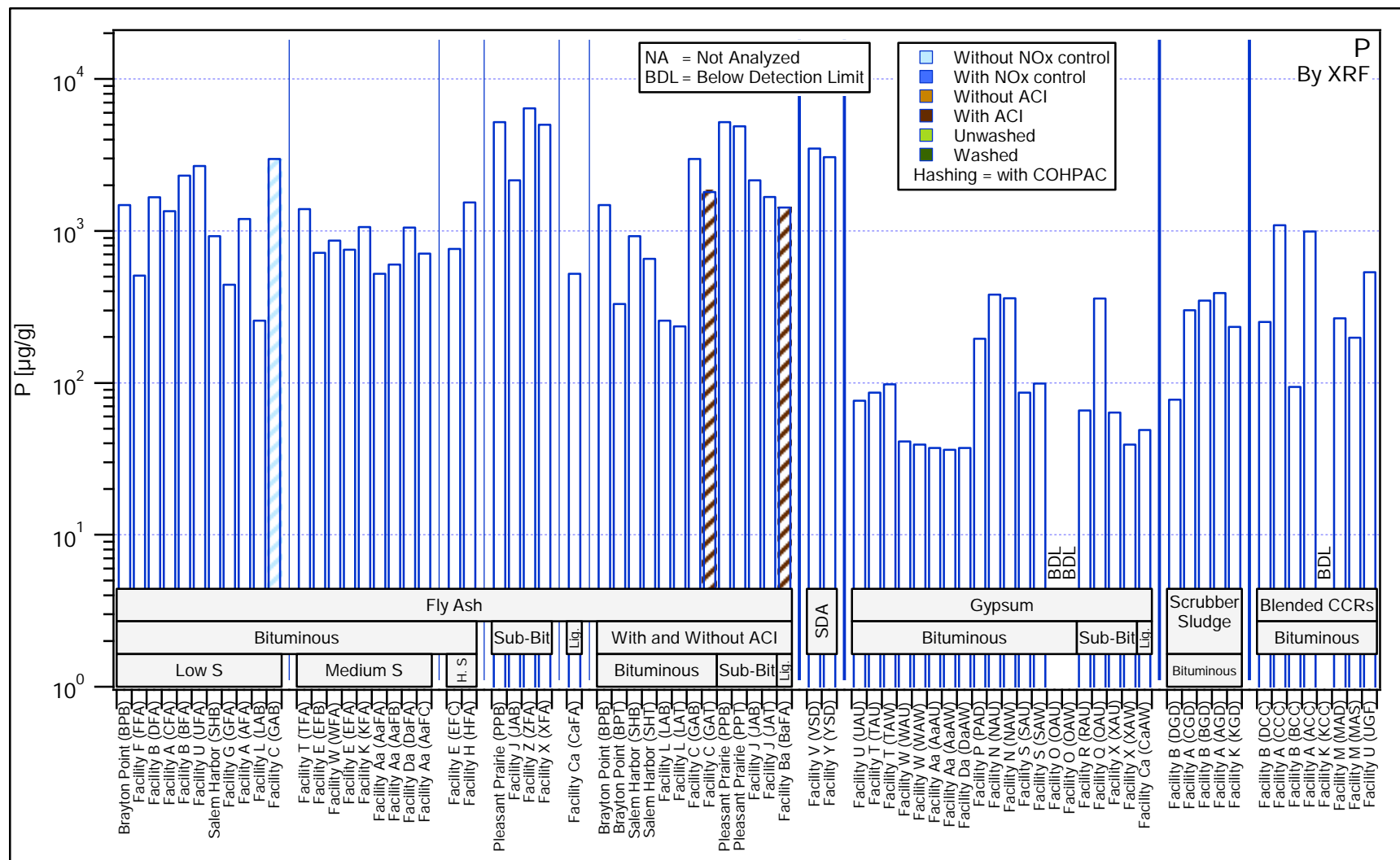


Figure 32. Phosphorous. Comparison of total elemental content by XRF.

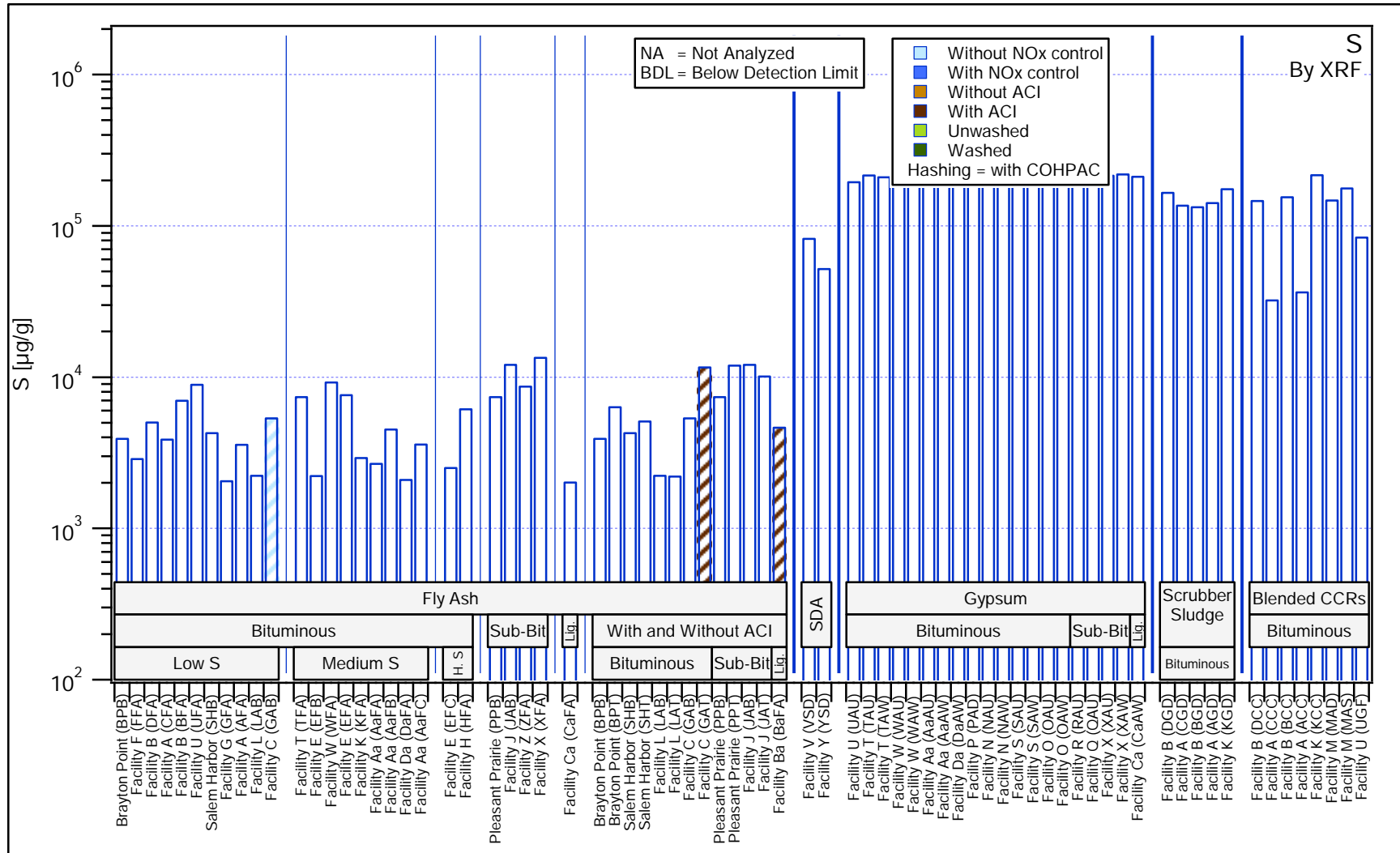


Figure 33. Sulfur. Comparison of total elemental content by XRF.

Characterization of Coal Combustion Residues III

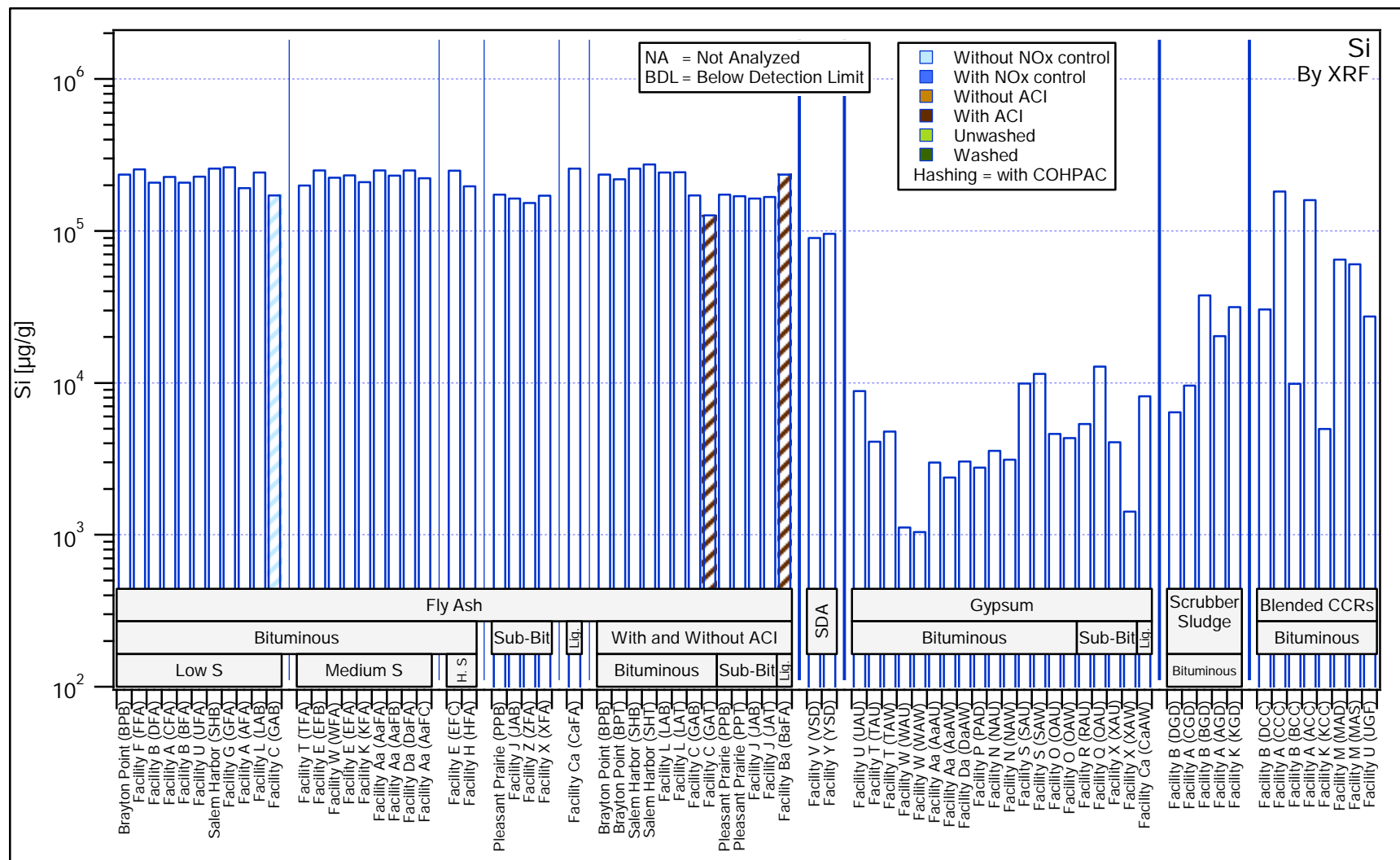


Figure 34. Silicon. Comparison of total elemental content by XRF.

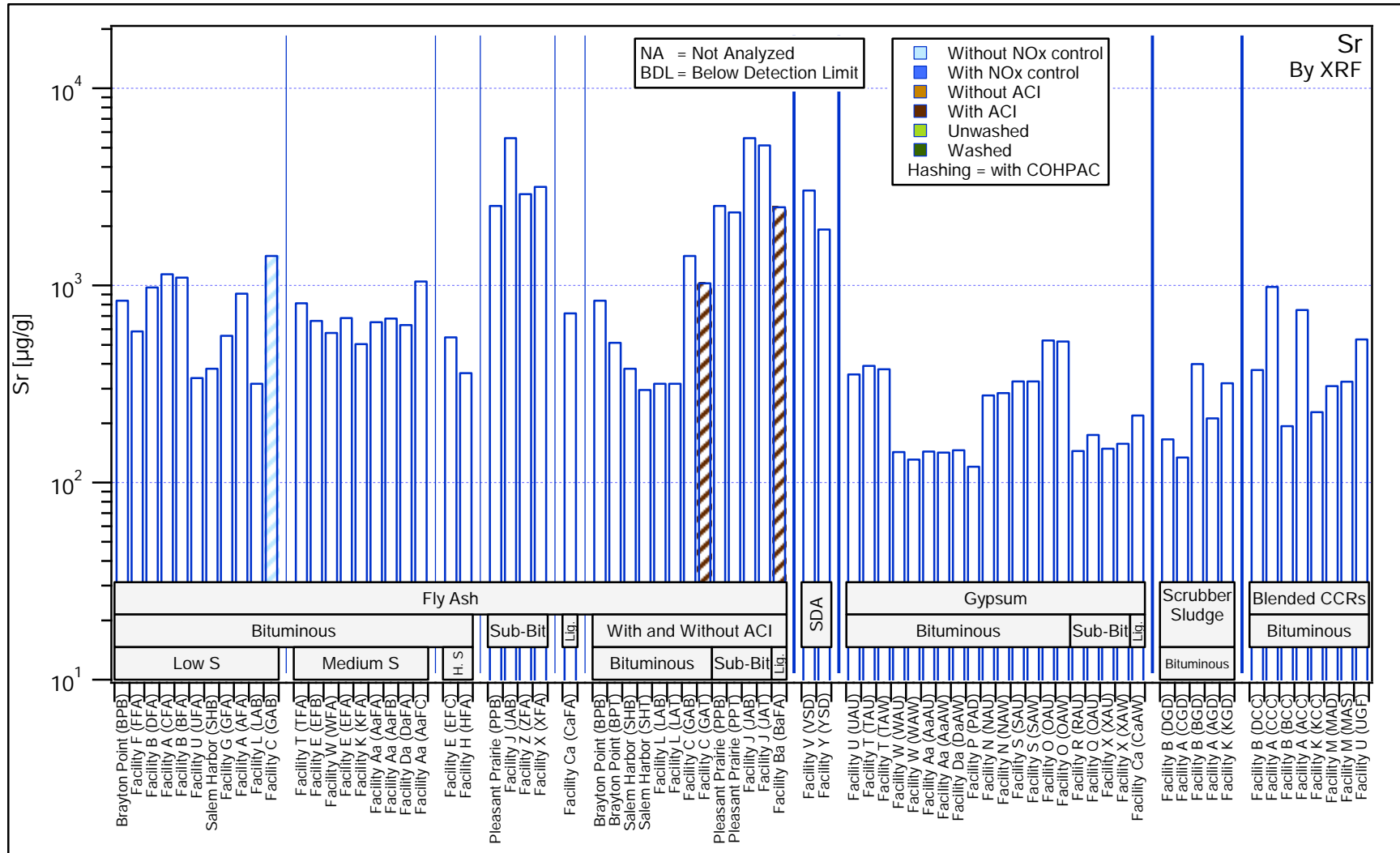


Figure 35. Strontium. Comparison of total elemental content by XRF.

Characterization of Coal Combustion Residues III

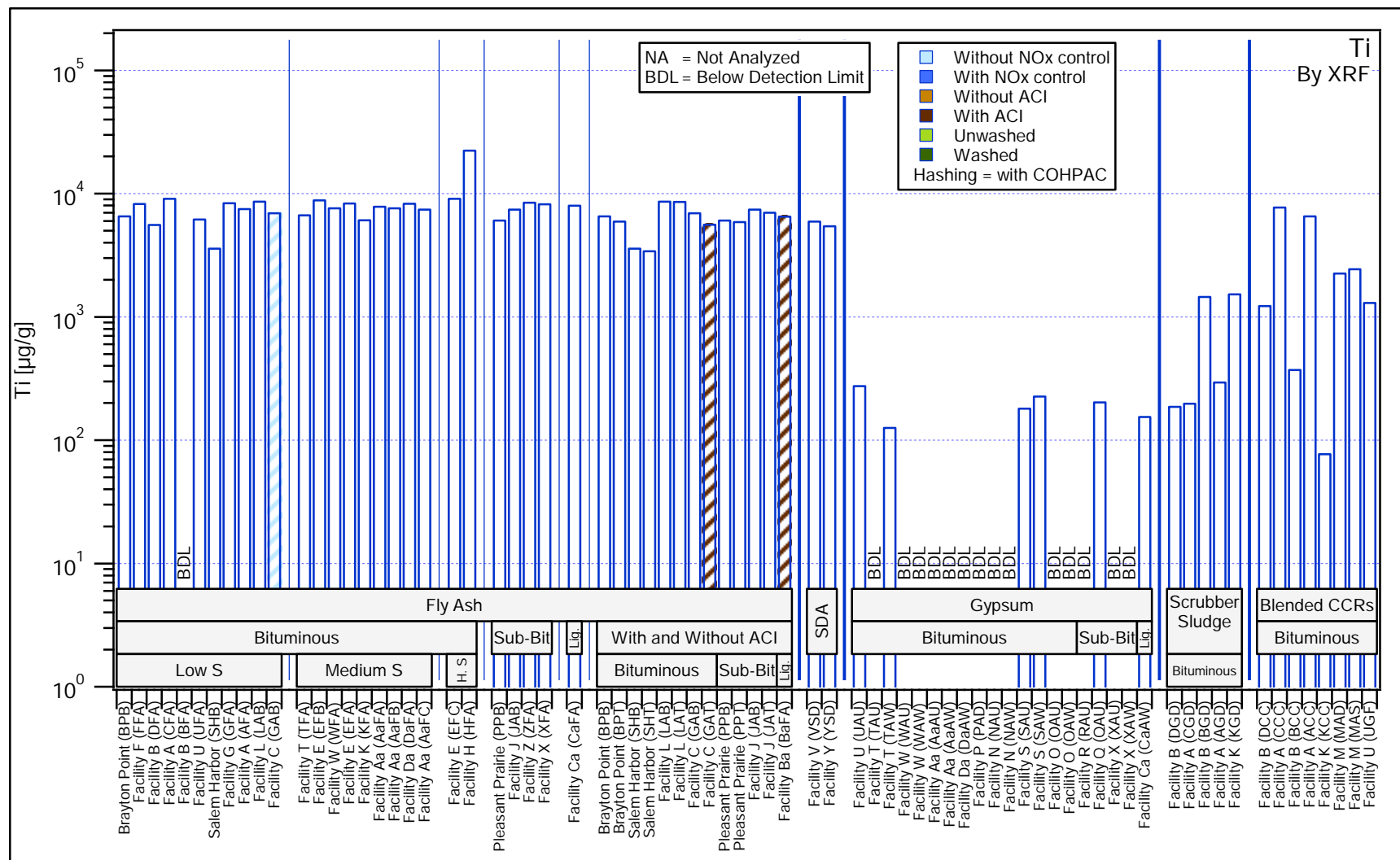


Figure 36. Thallium. Comparison of total elemental content by XRF.

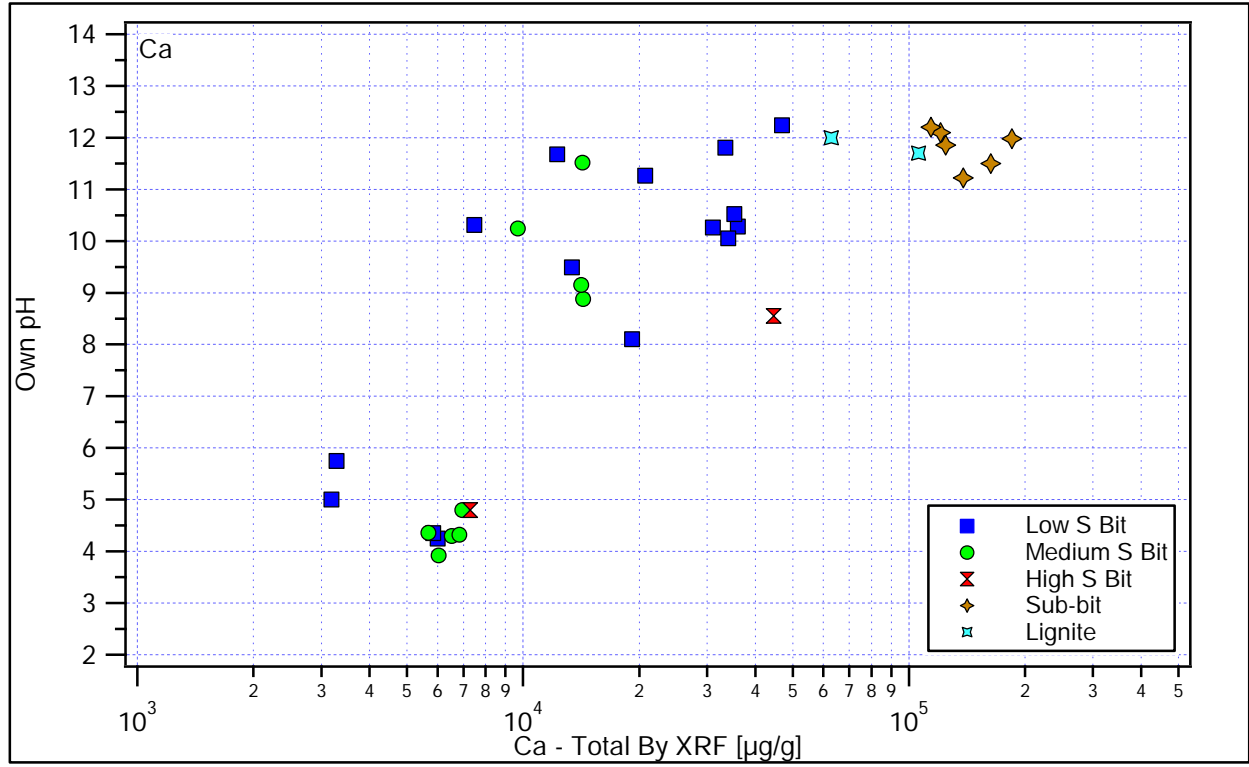


Figure 37. Total calcium content (by XRF) and own pH for fly ash samples.

3.2. LABORATORY LEACHING TEST RESULTS

Appendix F provides graphical presentation of the results of Solubility and Release as a Function of pH (SR002.1) and Solubility and Release as a Function of LS (SR003.1) for the 13 constituents of interest in this report. Results are grouped by facility type and within each facility comparisons are made by CCR type (fly ash without Hg sorbent injection, fly ash without and with Hg sorbent injection pairs, spray dryer, gypsum, scrubber sludge, blended CCRs, and filter cake) and constituent of interest. Appendix G provides graphical presentation of the pH titration curves from test method SR002.1.

Discussed below are:

1. Typical characteristic results for pH and each of the 13 constituents of interest (Section 3.2.1);
2. Comparison of the ranges of observed constituent leaching concentrations from laboratory testing (minimum concentrations, maximum concentrations, and concentrations at the materials' own pH – Section 3.2.2);
3. Comparison of the constituent maximum leaching concentrations and concentrations at the materials' own pH from laboratory testing grouped by material type with measurements reported elsewhere on field leachate and pore water samples for CCR disposal sites and the database used in the EPA Risk Report (EPA, 2007b) (Section 3.2.3); and,
4. pH at the maximum concentration value versus the materials' own pH (Section 3.2.4).

Complete data also have been developed for other constituents (e.g., other ions, DOC, etc.) to facilitate evaluation of geochemical speciation of constituents of concern and provide more thorough evaluation of leaching under alternative management scenarios in the future if warranted.

For each CCR evaluated, results of the leaching tests provide the following information:

- Leachate concentrations for the constituents of interest as a function of pH over the range of reported field management conditions (from test method SR002.1);
- pH titration curves (from test method SR002.1). This information is useful in characterizing the CCR and assessing how it will respond to environmental stresses and material aging (e.g., carbon dioxide uptake, acid precipitation, co-disposal, mixing with other materials); and,
- Leachate concentrations for the constituents of interest and pH as a function of LS ratio when contacted with distilled water (from test method SR003.1). This information provides insight into the initial leachate concentrations expected during land disposal and effects of pH and ionic strength at low LS ratio. Often these concentrations can be either greater than or less than concentrations observed at higher LS ratio (i.e., LS=10 mL/g as used in SR002.1) because of ionic strength and co-constituent concentration effects.

The MCL, DWEL, or AL (for lead) as available is used as a reference value for the constituent of interest. However, laboratory leaching test results presented here are estimates of concentrations

potentially leaching from landfills, not the concentrations at potential points of exposure. Any assessment of the environmental impact of these releases needs to consider the dilution and attenuation of these constituents in ground water, and the plausibility of drinking water well contamination resulting from the release. Dilution and attenuation factors for metals (DAFs) have been estimated to be potentially as low as 2 to 10 on a national basis or as high as 8,000 at a particular site with hydrogeology that indicated low transport potential⁴¹. Therefore, comparison of the laboratory leach test results with thresholds greater than the MCL and developed for specific scenarios may be appropriate.

3.2.1. Typical Characteristic Leaching Behavior as a Function of pH

Comparisons of the leaching behavior as a function of pH for each of the 13 elements of interest are presented in Section 3.2.1.1 for fly ashes without Hg sorbent injection (as a baseline measure), Section 3.2.1.2 for fly ashes without and with Hg sorbent injection pairs, Section 3.2.1.3 for unwashed and washed gypsum, Section 3.2.1.4 for scrubber sludges, Section 3.2.1.5 for spray dryer absorber residues, and Section 3.2.1.6 for blended CCRs (mixed fly ash and scrubber sludge/mixed fly ash and gypsum). These comparisons illustrate on an empirical basis some of the differences in leaching behavior for different CCRs that result from the combination of the coal type combusted and air pollution control configuration used, including particulate control devices (cold-side ESP, hot-side ESP, or fabric filter), NO_x control (none or by passed, SNCR or SCR), and without and with Hg sorbent injection.

These figures illustrate that for a particular constituent, the chemistry controlling release or aqueous-solid equilibrium may be similar within a material type (i.e., mercury behavior for fly ash or scrubber sludge) or across material types (i.e., the same behavior for aluminum in fly ash and blended CCRs) but that there are not necessarily generalized behaviors present for each constituent that are consistent across all samples within a material type or between material types. The most robust groupings of leaching behavior will result from the development of geochemical speciation models of the materials that account for the underlying solid phase speciation (e.g., solid phases, adsorption behavior) and modifying solution characteristics (e.g., dissolved organic matter, pH, ionic strength, co-dissolved constituents). Development of the needed geochemical speciation models, and associated leaching behavior groupings as a function of coal rank, combustion facility design, and CCR type, will be the subject of a subsequent report (Report 4). The resulting models and groupings, in turn, are expected to allow for more detailed constituent release predictions based on limited testing for a broader set of facilities.

⁴¹ See 60 FR 66372, Dec. 21, 1995, for a discussion of model parameters leading to low DAFs, particularly the assumption of a continuous source landfill. Implied DAFs for the metals of interest here can be found at 60 FR 66432-66438 in Table C-2. Site specific high-end DAFs are discussed in 65 FR 55703, September 14, 2000.

3.2.1.1. Fly Ash without Hg Sorbent Injection

Figure 38 through Figure 40 present comparisons of leaching behavior as a function of pH for fly ash without Hg sorbent injection for each of the 13 elements of interest. Results are organized by coal type: bituminous, low sulfur coal (Figure 38); bituminous, medium and high sulfur coal (Figure 39); and sub-bituminous, sub-bituminous/bituminous mix, and lignite coal (Figure 40).

Figure 41 shows the main characteristic leaching behaviors observed for each element of interest for the different coal types and air pollution control configurations. Figure 42 presents the leaching behavior of calcium, magnesium, iron, strontium, and sulfur, expected to control or have an effect on the chemistry of the materials. Figure 43 illustrates the effect of NO_x controls (none or by-passed, SNCR or SCR) for facilities burning Eastern Bituminous coal and using CS-ESP for particulate control. Figure 44 illustrates the effect of fabric filters versus CS-ESP with and without SNCR for facilities burning Eastern Bituminous coal. Chromium speciation in selected fly ash samples and eluates is shown in Figure 45.

Main characteristics leaching behavior (Figure 41 and Figure 42)

The discussion of the results provided below is solely empirical and intends to show the range of leaching characteristics as a function of pH that were encountered for the fly ash without Hg sorbent injection. Details of speciation are beyond the scope of this report and require development of geochemical speciation models of the materials, which will be part of a subsequent report.

Aluminum (Al). The behavior of Al was generally amphoteric with a broad minimum between $4 < \text{pH} < 8.5$ and minima observed at different levels depending upon the ash type. The concentration of the minimum is typically influenced by the amount of DOC complexing aluminum in solution (increased complexation increases dissolved aluminum). Several samples, e.g. UFA, exhibited dramatically decreased leaching at $\text{pH} > 11$.

Arsenic (As). Six different leaching behaviors were observed for As. Sample LAB provides an example of a typical amphoteric behavior with minimum leaching occurring at a $\text{pH} \sim 5.2$. Sample UFA is an example of typical oxyanionic behavior with increasing As concentration as pH decreased from *ca.* 10.5 to less than 3. Sample GAB shows an example where As concentration peaked at $\text{pH} \sim 8$, which was, in this case, most likely a consequence of the presence of the COHPAC. Sample ZFA shows an example where As release was below the MDL for all pHs and was representative of the sub-bituminous and sub-bit/bituminous mix coal, reflecting the relatively high total content of calcium and magnesium of this coal type compared to the other coal types. Sample AaFC also showed amphoteric behavior but was distinctly different from that of sample LAB. Sample AFA also showed oxyanionic behavior but at a lower concentration level than sample UAF. As concentrations were at or above the MCL value for most pHs, except for the sub-bituminous coal, e.g. ZFA, for which arsenic concentrations were below the MDL across the full pH range examined.

In general, As leaching behavior had been reported to be influenced by precipitation/co-precipitation with group II elements (Mg, Ca, Ba, and Sr) and precipitation/adsorption onto iron oxide (Drahota et al., 2009; Mohan et al., 2007). Figure 42 presents the characteristic leaching behavior of these constituents, which shows significant differences between ash types. Sample ZFA had overall the greatest concentrations of group II elements while sample LAB had the

lowest concentrations of group II elements. As a general observation, the bituminous coal fly ashes having a low own pH and corresponding to eluate calcium concentrations of less than 120 mg/L, tended to exhibit amphoteric behavior. Detailed mechanistic evaluation is, however, beyond the scope of this report and will be addressed in Report 4.

Boron (B). Most samples showed relatively constant boron concentrations for $\text{pH} < 10.5$ with a few samples, e.g. AFA, showing a decrease in B eluate concentration with increasing pH for $\text{pH} > 8$. In general, samples with decreasing concentration for $\text{pH} > 8$ were those with higher own pH and eluate calcium concentration greater than 120 mg/L. B is highly soluble at neutral to acidic pHs and as a result observed B concentrations were most likely controlled by the total B content of the material.

Barium (Ba). All samples showed a similar leaching behavior of Ba with the exceptions of samples ZFA and XFA for which a much greater release of barium was observed, in agreement with a much greater Ba content for these samples (as much as 12 times greater than for the other samples). All own pH results were less than the MCL except for the sub-bituminous and lignite coal samples.

Cadmium (Cd). Typical behavior of increasing eluate concentration with decreasing pH for $\text{pH} < 5$ was observed for Cd for most cases except for sample AFA that showed increasing eluate concentration with decreasing pH for $\text{pH} < 8$.

Cobalt (Co). Cobalt leaching behavior was similar for all samples tested with minimum values observed for $\text{pH} > 11$, an increase in eluate concentration with decreasing pH for $\text{pH} < 11$, and a maximum concentration reached for pH less than 5.

Chromium (Cr). Three different leaching behaviors were observed for Cr: (i) amphoteric behavior (e.g., UFA and AaFC), (ii) relatively constant concentration for $\text{pH} > 5$ with an increase in concentration for $\text{pH} < 5$ (e.g., AFA and GAB) [Both have fabric filter (one fabric filter and one COHPAC)], and (iii) concentration peaking at $8 < \text{pH} < 10$ with low concentrations at both low and high pH values (e.g., ZFA, typical for all sub-bituminous coal and sub-bit/bituminous mix samples). The amphoteric behavior was typical for all bituminous coal samples with the exceptions of the samples where SCR or SNCR resulted in elevated ammonia concentrations (e.g., BFA) and the samples where a fabric filter (e.g., CFA) or COHPAC (GAB) was used.

Mercury (Hg). Three different leaching behaviors were observed for Hg: (i) an increasing concentration peaking at $\text{pH} \sim 8$ (e.g., AFA), most likely indicative of ammonium complexation from the use of SNCR (Wang et al., 2007), (ii) an increasing concentration with decreasing pH for $\text{pH} < 5$ with a peak concentration at $\text{pH} \sim 3.8$ and a relatively constant concentration for $\text{pH} > 5.5$ (e.g., GAB, most likely, in this case, a consequence from the use of HS ESP with COHPAC), and (iii) concentrations below the MDL for most pHs (e.g., ZFA and UFA).

Molybdenum (Mo). All bituminous coal and lignite samples, except when SCR or SNCR resulted in elevated ammonia (e.g., AFA), showed relatively constant concentrations with a decrease at $\text{pH} < 7$ (e.g., GAB and LAB) or $\text{pH} < 4$ (UFA) followed by an increase. As with Hg, sample AFA exhibited a Mo concentration peaking at $\text{pH} \sim 8$, most likely indicative of ammonium complexation from the use of SNCR in conjunction with fabric filter. As with Cr, all sub-bit/bituminous mixes showed an increased Mo concentration peaking at $\text{pH} \sim 8$ (e.g., ZAF).

Characterization of Coal Combustion Residues III

Lead (Pb). Minimal lead leaching was observed. In all cases, lead leaching was below the MDL between pH 4 and 12. For some samples, e.g. AaFC, typical amphoteric behavior was observed with increased concentrations for pHs above 12 and below 4.

Antimony (Sb). Several leaching behaviors were observed for Sb: (i) a decreasing concentration with decreasing pH (e.g., LAB), (ii) an increasing concentration with decreasing pH (e.g., UAF), (iii) concentrations below the MDL over the entire pH range (e.g., ZFA), (iv) a concentration peaking at pH~8 (e.g., AFA), most likely indicative of ammonium complexation from the use of SNCR, and (v) concentrations peaking at $7 < \text{pH} < 10$ (e.g., GAB)

Selenium (Se). Four different leaching behaviors were observed for Se. Sample LAB provides an example of typical amphoteric behavior with minimum leaching occurring at $5 < \text{pH} < 6$. Sample GAB illustrates an example of decreasing leaching with decreasing pH while sample ZAF is an example of increasing leaching with decreasing pH. Sample AFA shows an example of increasing concentration peaking at pH~8, most likely indicative of ammonium complexation from the use of SNCR. In most cases, Se concentrations were above the MCL.

Thallium (Tl). Two different leaching behaviors were observed for Tl: (i) increasing concentration with decreasing pH at $\text{pH} < 12$ (e.g., UAF and AaFC), $\text{pH} < 9$ (e.g., AFA), or $\text{pH} < 7$ (e.g., LAB and ZFA) and (ii) relatively constant concentration with an increase at $\text{pH} < 7$ (e.g., GAB).

Effect of coal type (Figure 38, Figure 39, and Figure 40)

In general, the bituminous coal samples and the lignite sample (CaFA) behaved similarly with respect to leaching while the sub-bituminous coal and sub-bit/bituminous mix exhibited a significantly different behavior for most elements of interest. A greater release of group II elements (Mg, Ca, Ba, and Sr) was generally observed for the sub-bituminous coal and sub-bit/bituminous mix samples compared to the bituminous coal and lignite samples, in agreement with an overall greater total content of these elements for the sub-bituminous coal and sub-bit/bituminous mix.

Effect of NO_x control (SNCR vs. SCR, Figure 43)

The effect of NO_x control (none or by passed, SNCR or SCR) was examined for the facilities burning Eastern Bituminous coal and using CS-ESP for particulate control. No significant effect on the leaching behavior could be attributed to the presence of SCR or SNCR except one where a pairwise comparison (with and without NO_x control at the same facility) was possible. For Facility B, an increase in Cr and Co with SCR was observed (BFA vs. DFA), when NO_x control was in use. This observation and the Cr leaching observed across the set of facilities is likely the result of complex phenomena associated with gas conditioning (addition of ammonia or sulfuric acid) to improve particulate capture, such as for coals with low sulfur and high calcium, and ammonium residual from NO_x control.

Effect of fabric filter vs. CS-ESP (Figure 44)

The effect of fabric filter vs. CS-ESP with and without SNCR was examined for the facilities burning Eastern Bituminous coal. An effect was seen only on Cr, Hg, Co, and Mo concentrations with an increase in the release in some cases by a factor much greater than 10 (e.g., Cr from CFA vs. FFA, DFA, TFA, and EFB). The effect of ammonia complexation from the use of SNCR was seen with an increase in Hg and Mo concentrations peaking at pH~8 (AFA).

Chromium speciation in selected fly ash samples and eluates (Figure 45)

Chromium leaching as a function of pH (SR002.1) was analyzed for all samples. Leaching results for samples from selected facilities are provided in Figure 45 to illustrate (i) comparative results from the sample facility operated without and with NO_x controls and bituminous coal (Facility A, SCR-BP and SCR on [samples CFA and AFA, respectively] and Facility B, SNCR-BP and SNCR on [samples DFA and BFA, respectively]), and (ii) for a facility with relatively high chromium leaching but not having NO_x controls and burning sub-bituminous coal (Facility J, sample JAB). Initial review of these results suggested that fly ash samples obtained from facilities with NO_x controls (i.e., SNCR or SCR) resulted in higher chromium concentrations in the leachates as a consequence of the NO_x controls. Leaching results as a function of pH also indicated concentration profiles indicative of Cr(VI) leaching. Selected fly ash samples were leached using the SR002.1 procedure at subset of desired endpoint pH values, with the resulting eluates analyzed directly to differentiate between Cr(III) and Cr(VI) in solution. Results of solution phase chromium speciation are provided in a tabular format in Appendix H, and plotted along with the initial SR002.1 results in Figure 45. Chromium speciation in the solid phase of fly ash samples was also confirmed using X-ray absorption fine structure spectroscopy (XAFS; Appendix H). Results of these analyses indicate:

1. Comparison of leaching of the same samples from facilities without and with NO_x controls indicated higher chromium concentrations in eluates when NO_x controls were in use. However, direct comparisons are limited to two facilities and a similar range of leaching results was observed for other facilities that both did and did not have post-combustion NO_x controls.
2. For all of the cases except one examined, the chromium in eluates at pH > 7 was determined to nearly 100 percent Cr(VI), within the uncertainty of the analytical method.
3. The amount of chromium leached under the test conditions and pH > 5 is a small fraction (< 1% up to <10 %) of the total chromium present in the solid phase.
4. The amount of the chromium present in the solid phase as Cr(VI) is on the same order of magnitude as the amount of Cr(VI) leached at neutral to alkaline pH but precise quantification by XAFS is uncertain.

It is hypothesized that residual ammonia injected as part of NO_x controls or to facilitate particulate capture by ESPs may play a role in solubilizing Cr(VI) in the fly ash. If this is the case, it would explain why samples BFA and AFA had relatively less chromium leaching when analyzed after several months of storage in comparison to testing recently sampled fly ash. The expected cause would be loss of ammonia during sample storage. However, although this mechanism is consistent with operations of air pollution control devices (EPRI, 2008) and residual ammonia observed, ammonia content was not measured in CCR samples for this study.

Characterization of Coal Combustion Residues III

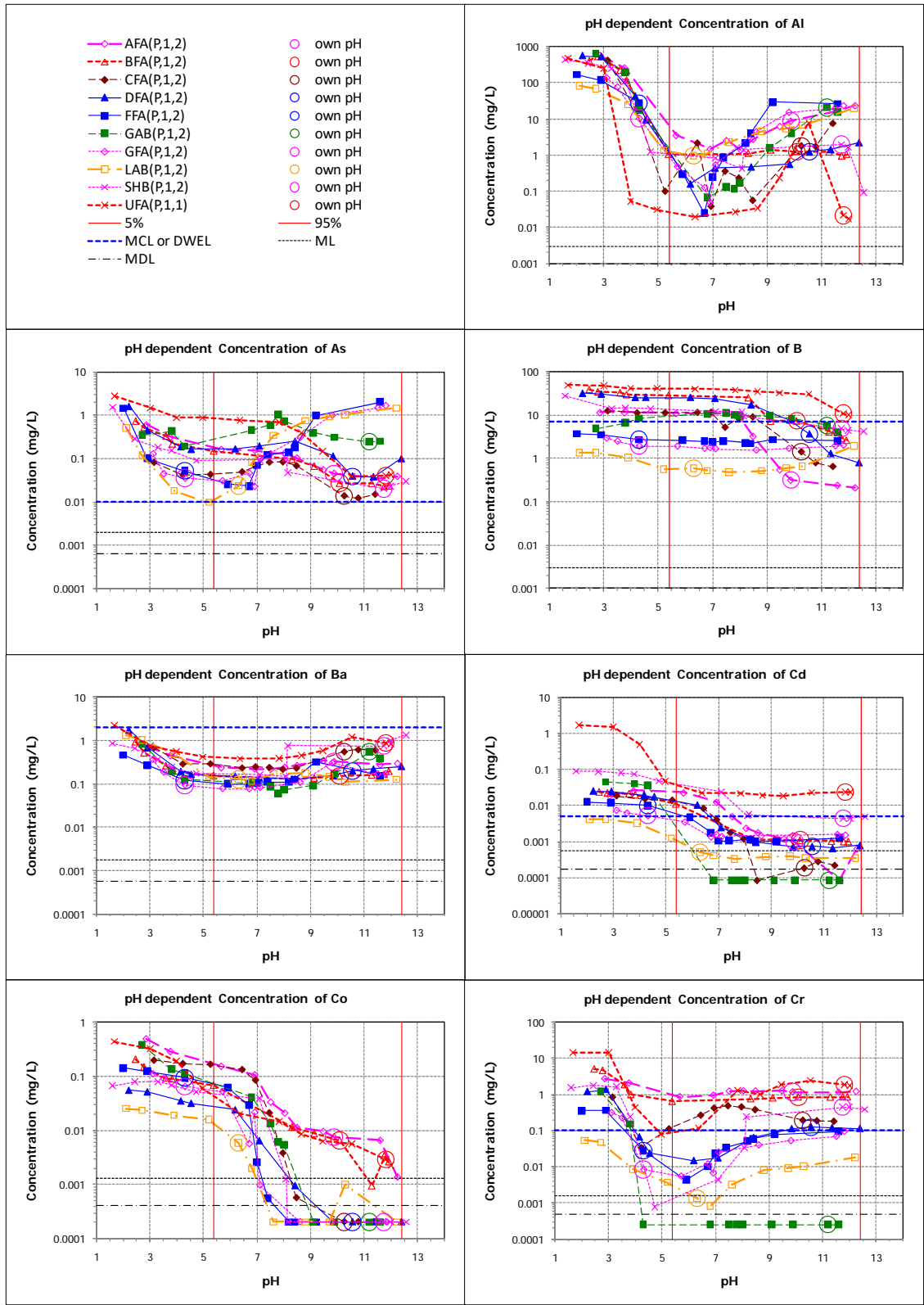


Figure 38. pH dependent leaching results. Fly ash samples from facilities without mercury sorbent injection [bituminous low sulfur coal]. Facility A (AFA, CFA), Facility B (BFA, DFA), Facility C (GAB), Facility G (GFA), Facility L (LAB), Salem Harbor (SHB).

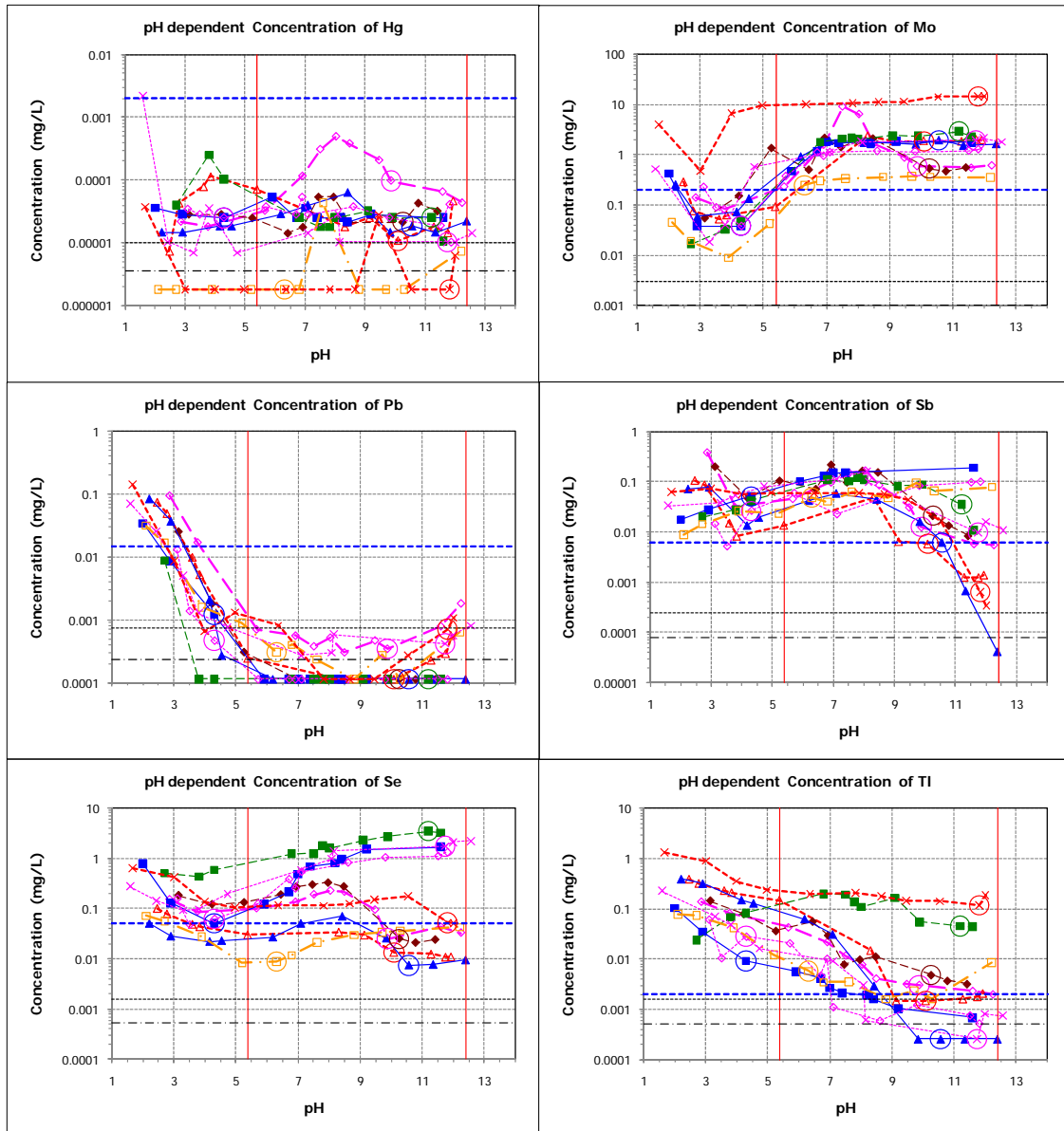


Figure 38 (continued). pH dependent leaching results. Fly ash samples from facilities without mercury sorbent injection [bituminous low sulfur coal]. Facility A (AFA, CFA), Facility B (BFA, DFA), Facility C (GAB), Facility G (GFA), Facility L (LAB), Salem Harbor (SHB).

Characterization of Coal Combustion Residues III

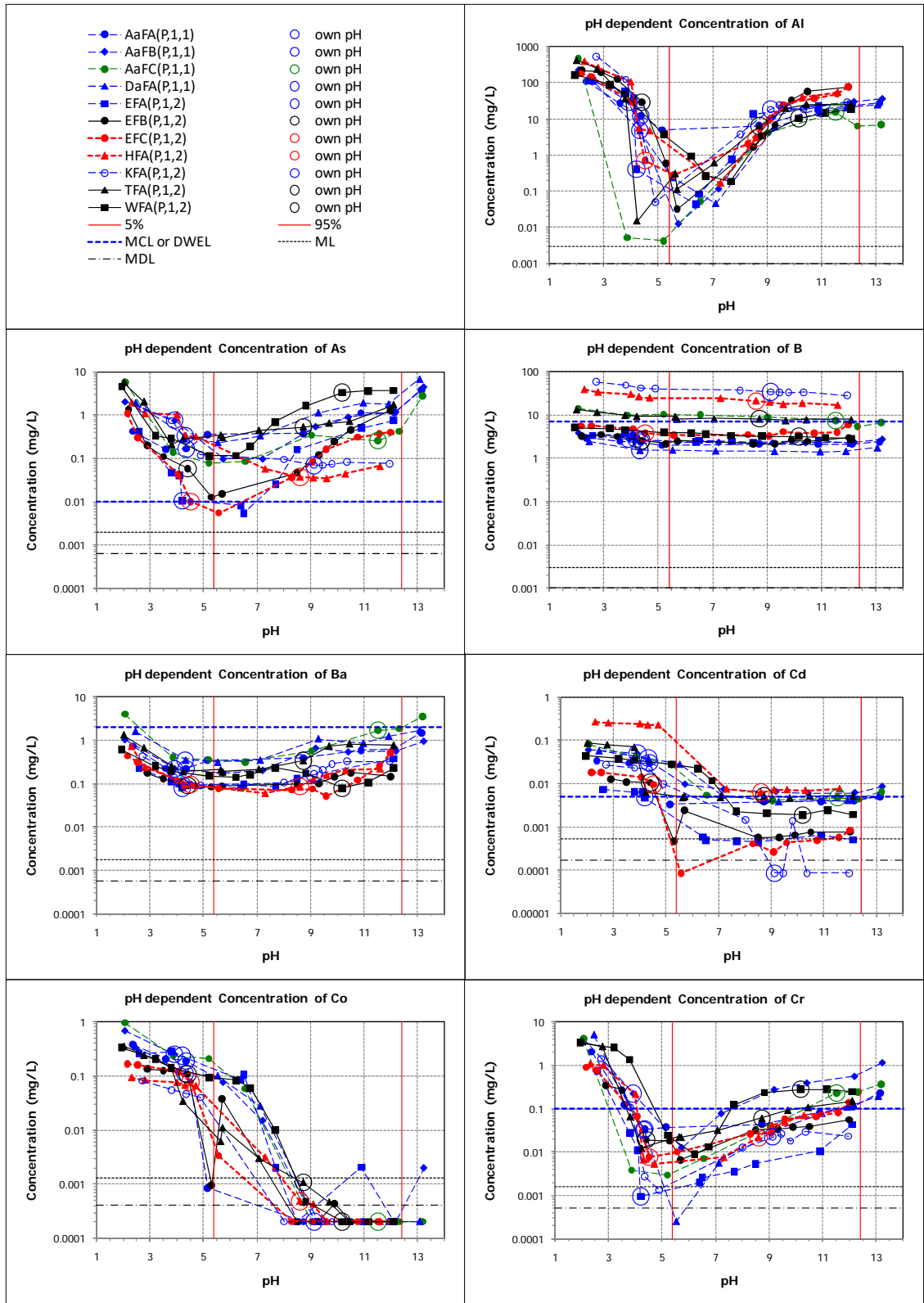


Figure 39. pH dependent leaching results. Fly ash samples from facilities without mercury sorbent injection [bituminous medium and high sulfur coal]. Facility E (EFA, EFB), Facility K (KFA), Facility T (TFA), Facility W (WFA), Facility Aa (AaFA, AaFB, AaFC), Facility Da (DaFA).

Characterization of Coal Combustion Residues III

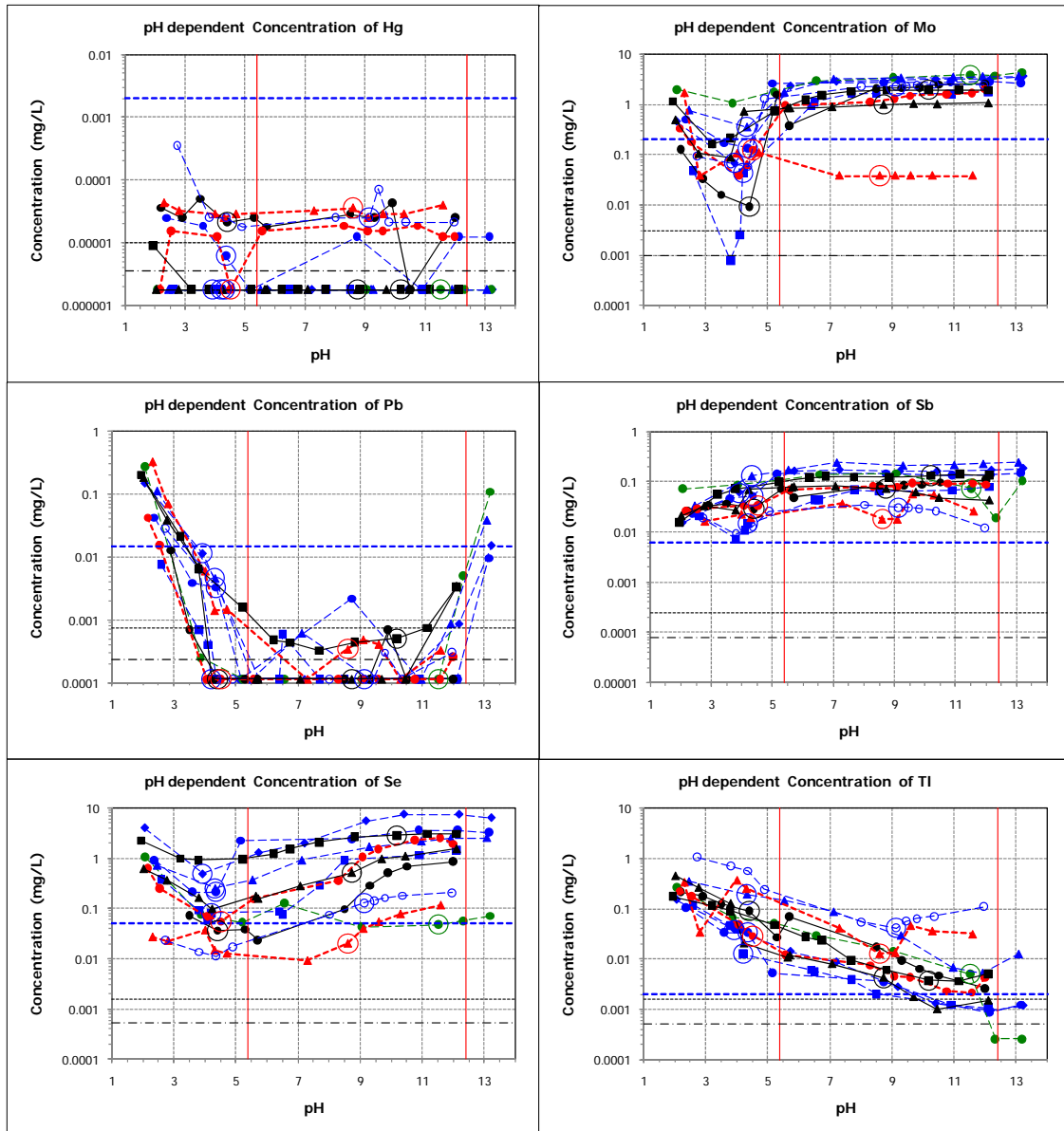


Figure 39 (continued). pH dependent leaching results. Fly ash samples from facilities without mercury sorbent injection [bituminous medium and high sulfur coal]. Facility E (EFA, EFB), Facility K (KFA), Facility T (TFA), Facility W (WFA), Facility Aa (AaFA, AaFB, AaFC), Facility Da (DaFA).

Characterization of Coal Combustion Residues III

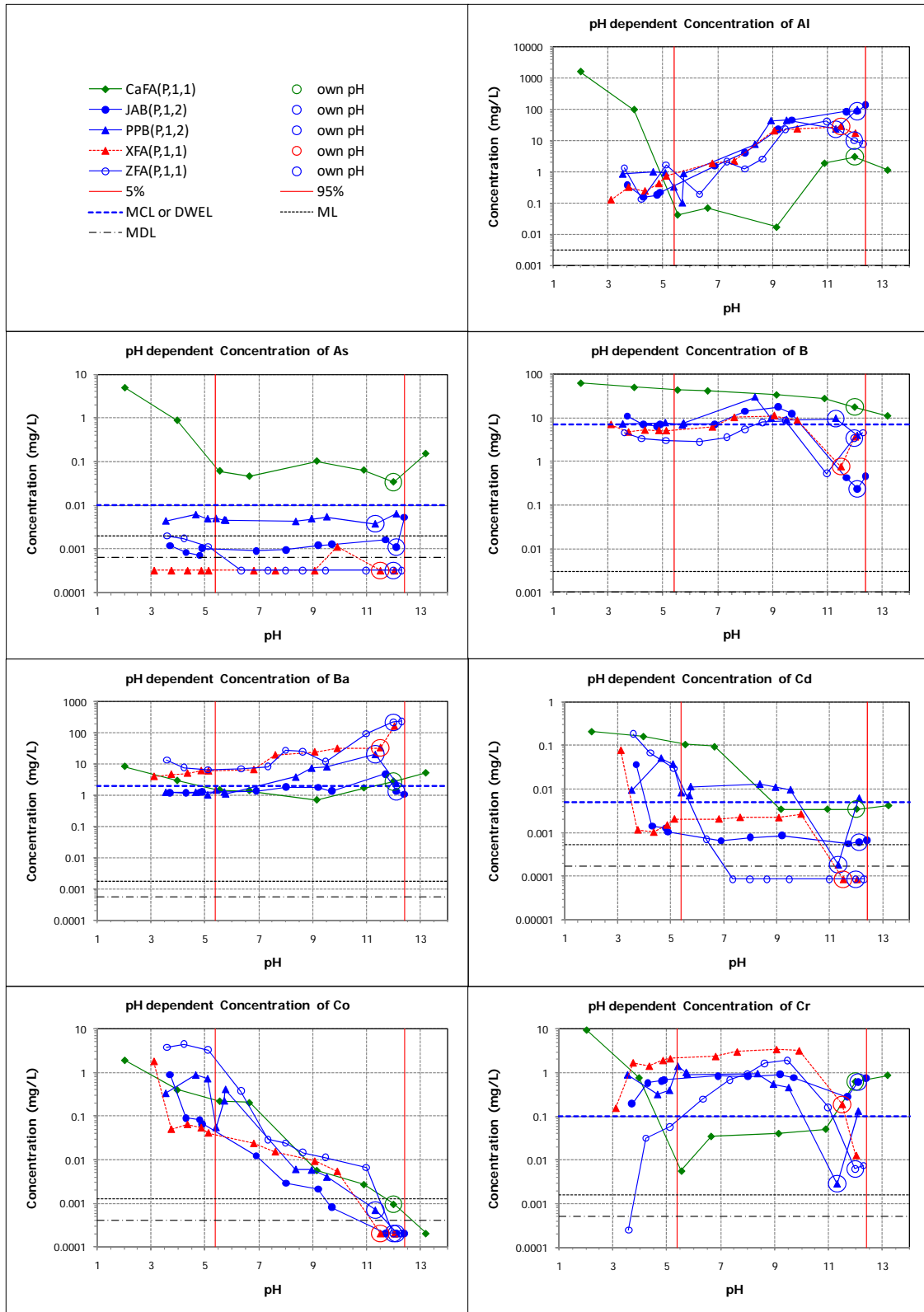


Figure 40. pH dependent leaching results. Fly ash samples from facilities without mercury sorbent injection [sub-bituminous and lignite coal]. Sub-bituminous: Facility J (JAB), Facility X (XFA), Facility Z (ZFA), Pleasant Prairie (PPB). Lignite: Facility Ca (CaFA).

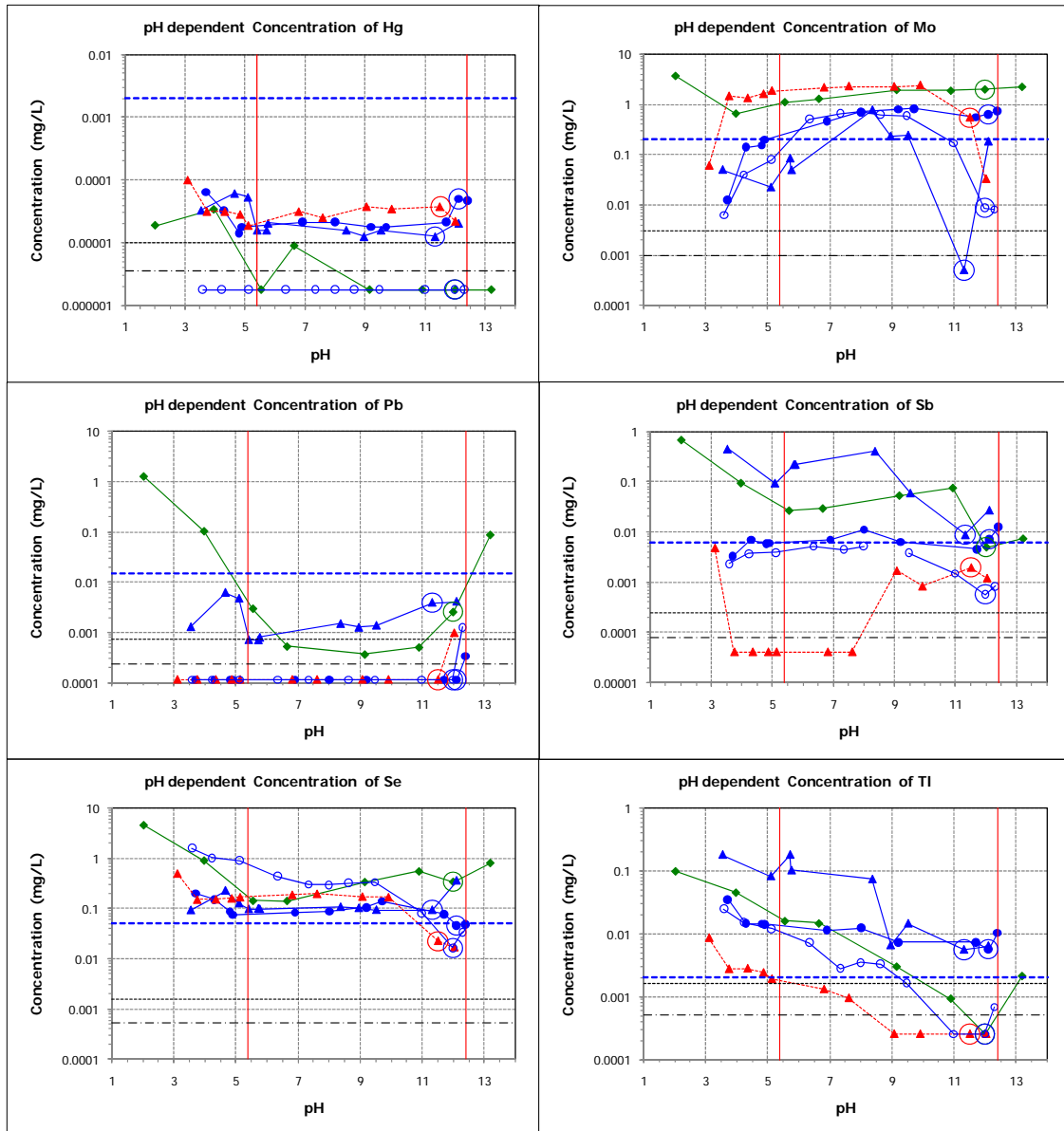


Figure 40 (continued). pH dependent leaching results. Fly ash samples from facilities without mercury sorbent injection [sub-bituminous and lignite coal]. Sub-bituminous: Facility J (JAB), Facility X (XFA), Facility Z (ZFA), Pleasant Prairie (PPB). Lignite: Facility Ca (CaFA).

Characterization of Coal Combustion Residues III

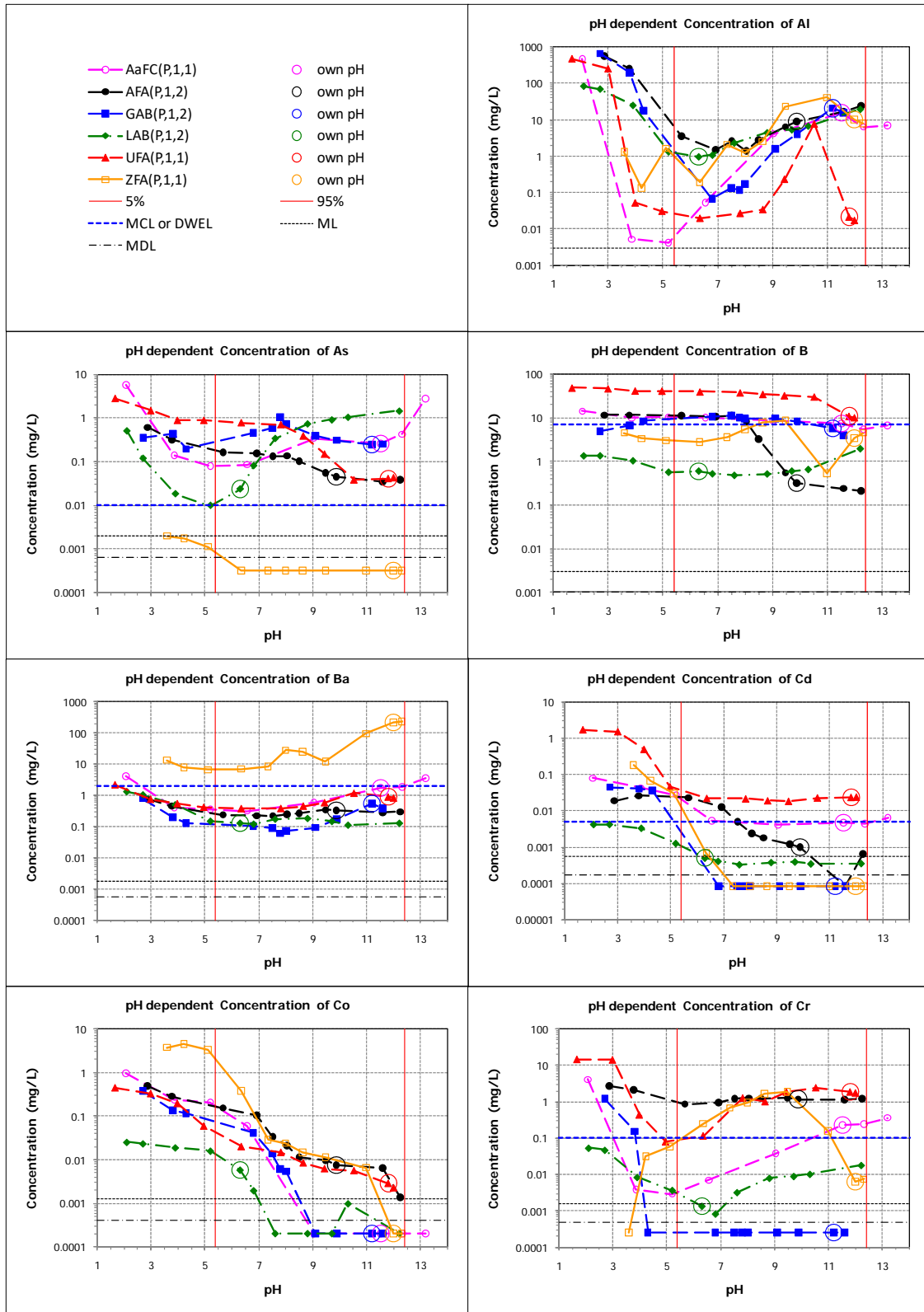


Figure 41. pH dependent leaching results. Selected results to illustrate characteristic leaching behavior.

Characterization of Coal Combustion Residues III

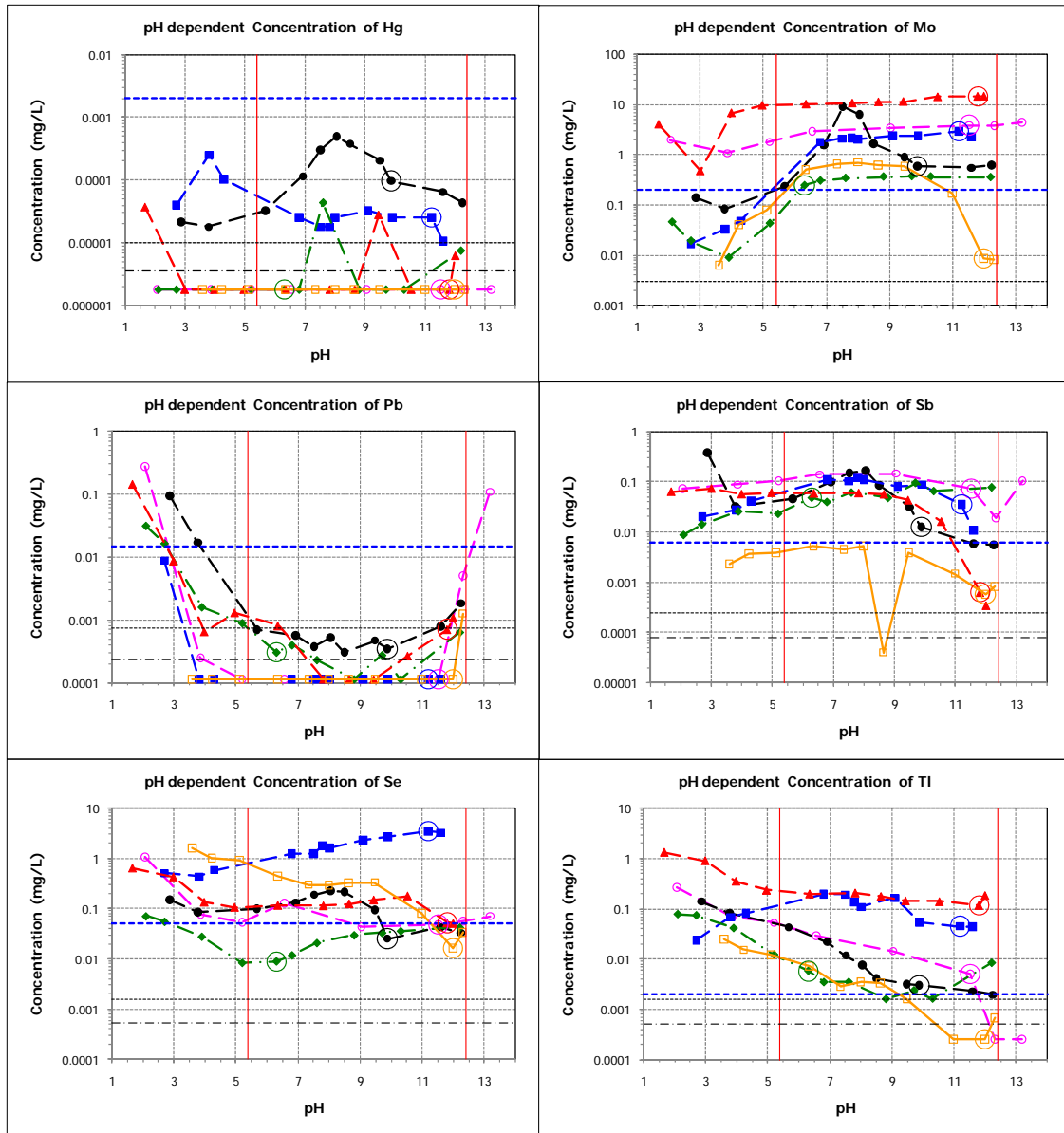


Figure 41 (continued). pH dependent leaching results. Selected results to illustrate characteristic leaching behavior.

Characterization of Coal Combustion Residues III

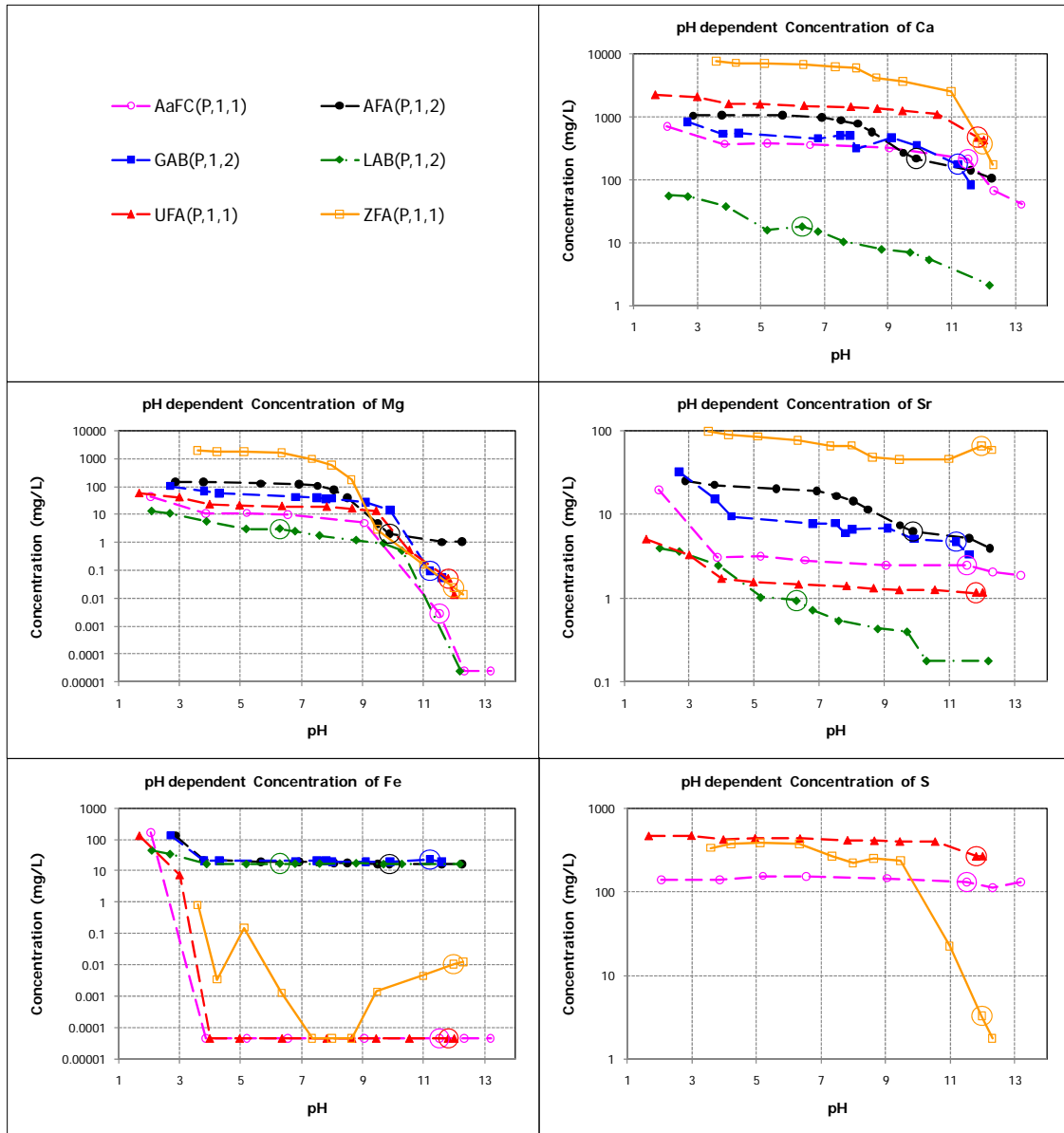


Figure 42. pH dependent leaching results. Selected results to illustrate characteristic leaching behavior of calcium, magnesium, strontium, iron, and sulfur.

Characterization of Coal Combustion Residues III

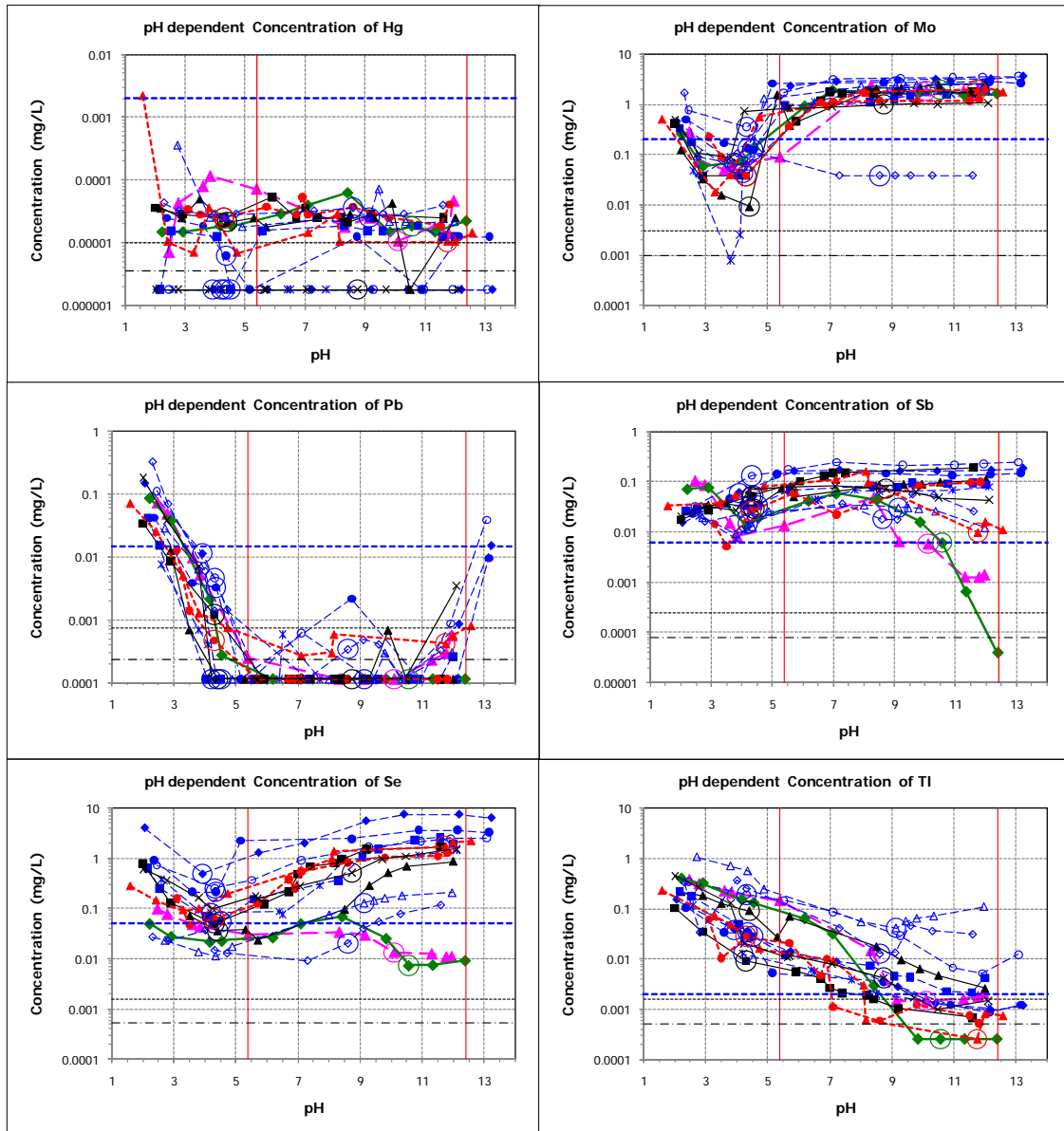


Figure 43 (continued). Effect of NO_x controls - none (or by-passed; samples DFA, EFB, FFA, TFA), SNCR (samples GFA, SHB) or SCR (all other samples) for facilities burning Eastern Bituminous coal and using CS-ESP for particulate control.

Characterization of Coal Combustion Residues III

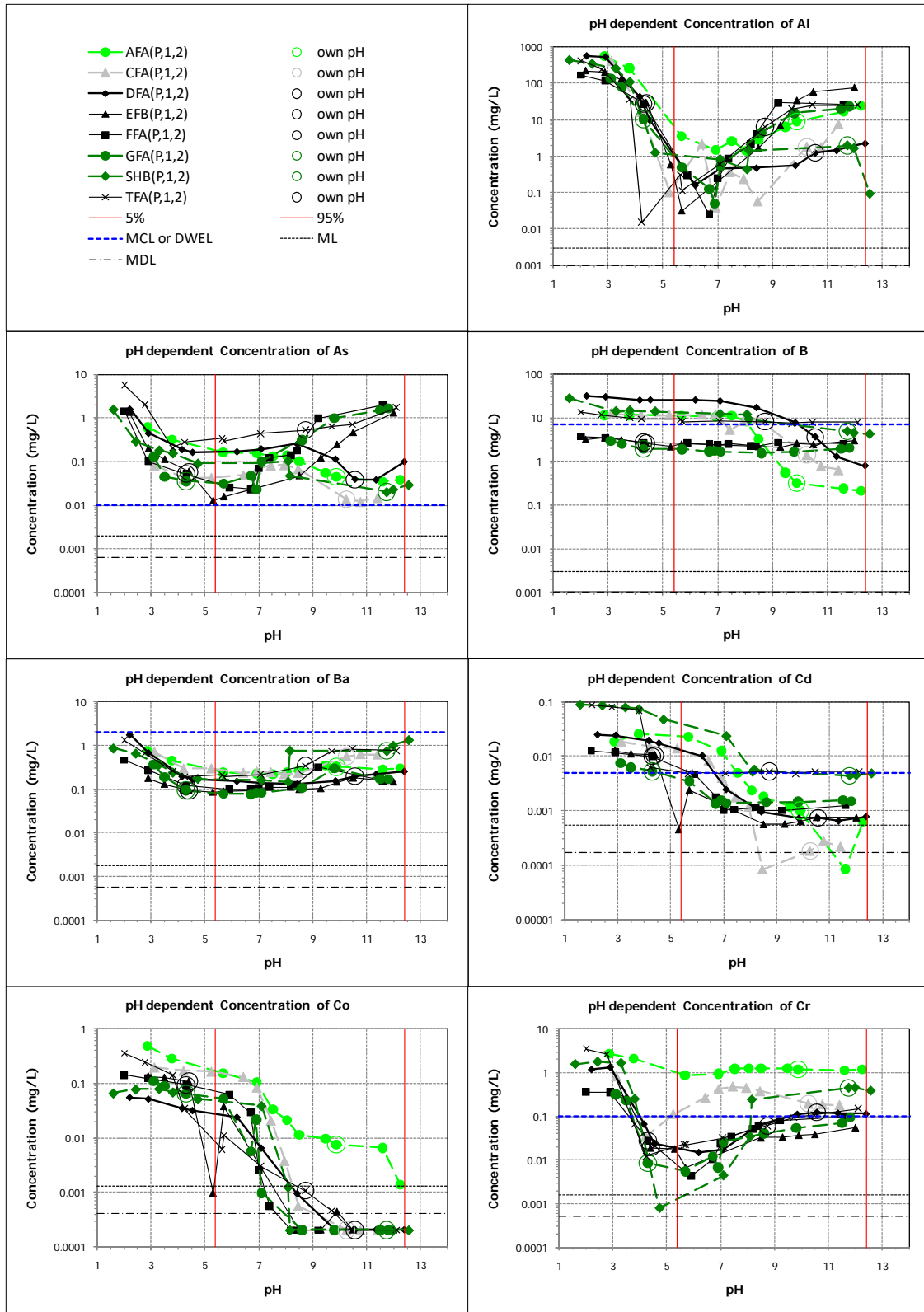


Figure 44. Effect of fabric filter vs. CS-ESP (fabric filter without NO_x control, sample CFA; with SNCR, sample AFA; CS-ESP without NO_x control, samples DFA, EFB, FFA, TFA; with SNCR, samples GFA, SHB) for facilities burning Eastern Bituminous coal.

Characterization of Coal Combustion Residues III

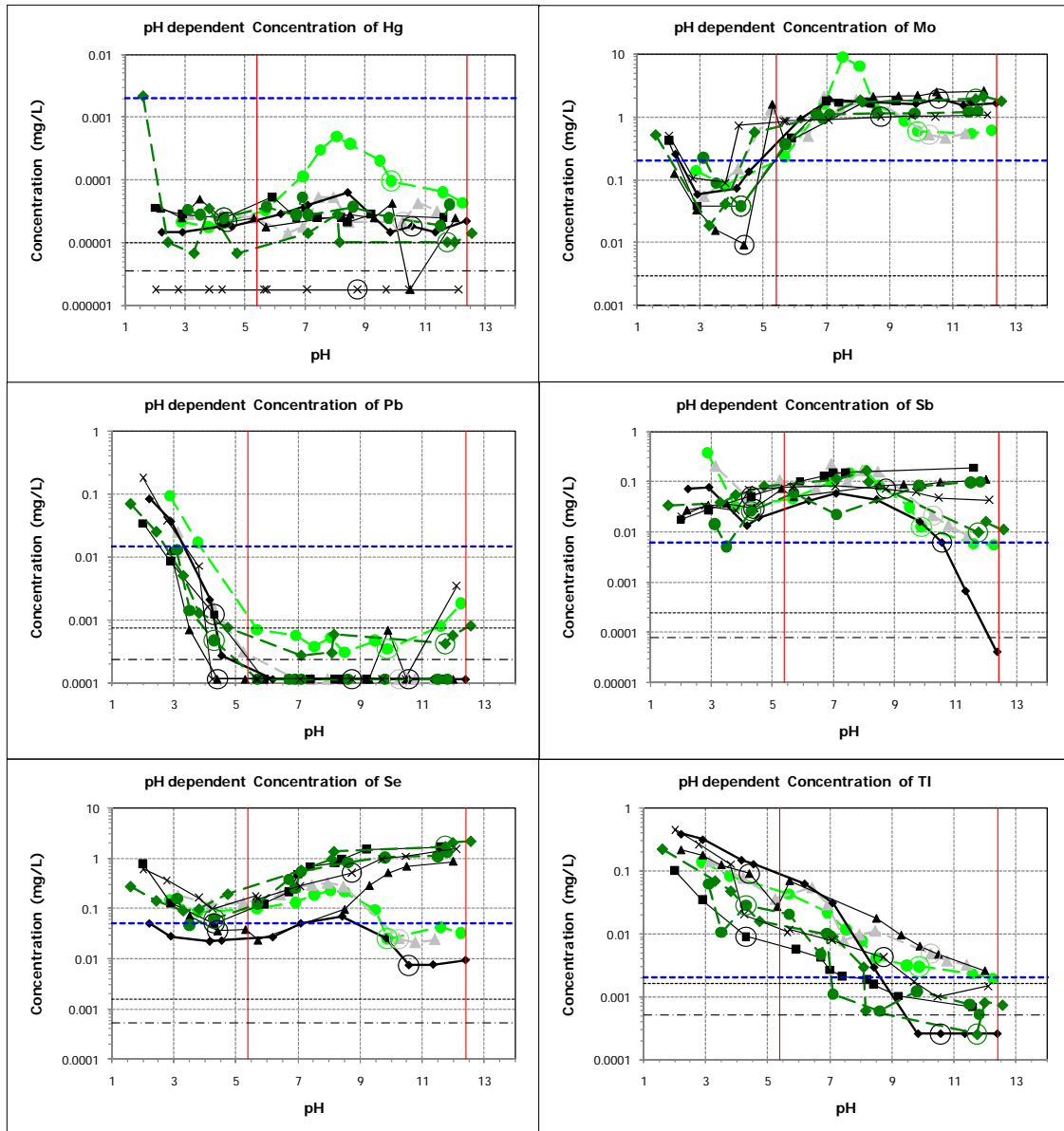


Figure 44 (continued). Effect of fabric filter vs. CS-ESP (fabric filter without NO_x control, sample CFA; with SNCR, sample AFA; CS-ESP without NO_x control, samples DFA, EFB, FFA, TFA; with SNCR, samples GFA, SHB) for facilities burning Eastern Bituminous coal.

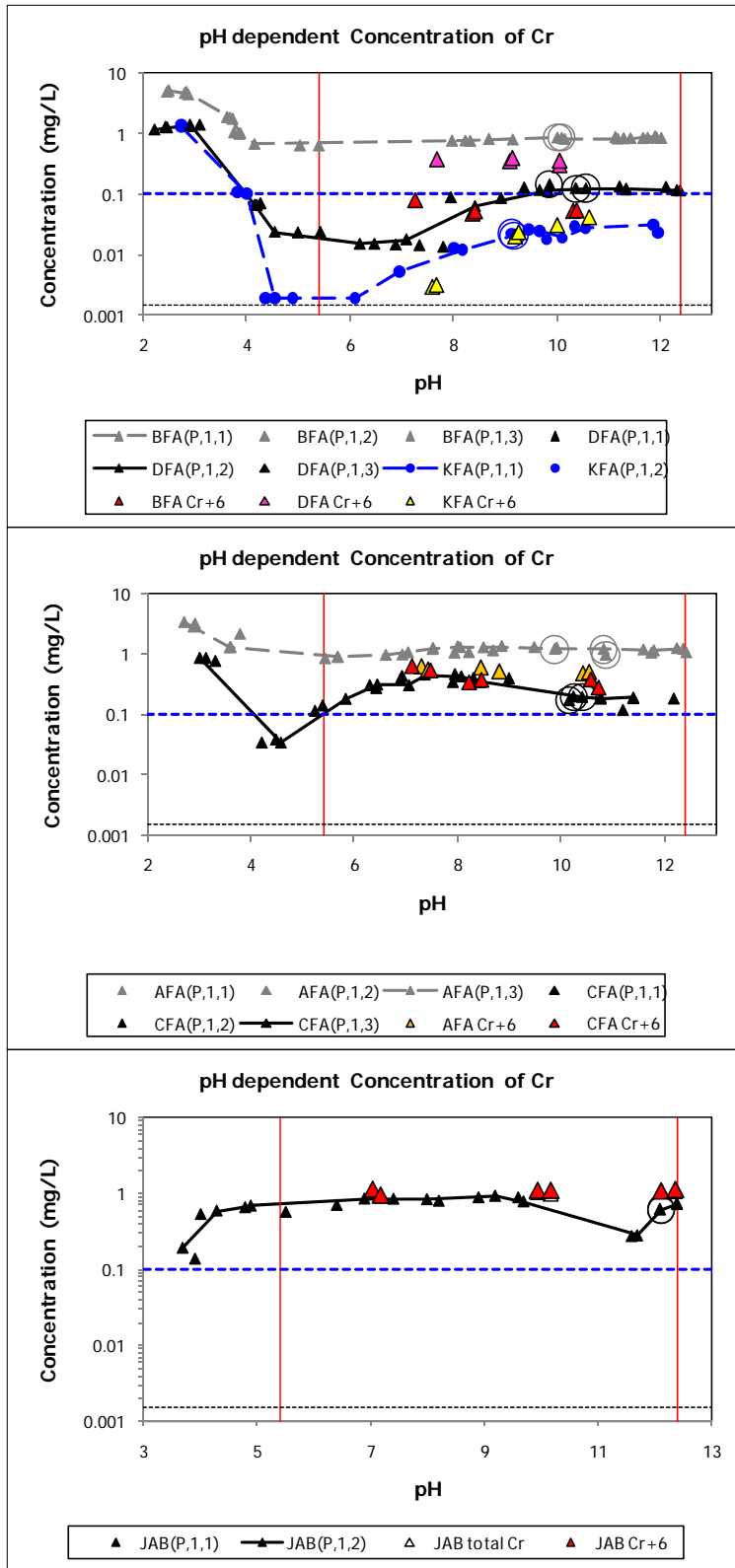


Figure 45. Chromium speciation results. Bituminous coal: Facility B with SCR (BFA), with SCR-BP (DFA); Facility K with SCR (KFA); Facility A with SNCR (AFA), with SNCR-BP (CFA). Sub-bituminous coal: Facility J with SCR (JAB).

3.2.1.2. Fly ash without and with Hg Sorbent Injection Pairs

Figure 46 presents comparisons of leaching behavior as a function of pH for fly ash without and with Hg sorbent injection pairs for each of the 13 elements of interest. For each facility, the baseline case and the treatment case (with Hg sorbent injection), either activated carbon injection or brominated activated carbon injection for facilities J and L, are compared. Also, note that Facilities C and Ba use COHPAC air pollution control configuration. Report 1 (Sanchez *et al.*, 2006) provided results for Hg, As, and Se. The discussion below expands the list to also include Al, B, Ba, Cd, Co, Cr, Mo, Pb, Sb, and Tl.

Considering the results provided in Appendix F and comparisons in Figure 46, the following observations were made.

Aluminum (Al). Al eluate concentrations as a function of pH showed typical amphoteric behavior. For Brayton Point and Facility C, the cases with ACI showed overall an increase in Al concentrations compared to the same facility without. For Facilities J and L, no significant change was observed, while a corresponding decrease was seen for Pleasant Prairie.

Arsenic (As). There was not a consistent pattern with respect to the effect of ACI on the range of laboratory eluate concentrations. For Salem Harbor and slightly for Pleasant Prairie facilities, the cases with ACI had an increase in the upper bound of eluate concentrations compared to the same facility without ACI. For Brayton Point and Facilities C and J, a corresponding decrease was observed.

Very low eluate concentrations were observed for the Facility J without and with brominated PAC, even though the total arsenic content was comparable to several of the other cases. Conversely, relatively high eluate concentrations were observed for Facility L without and with brominated PAC, even though the total arsenic concentration was low compared to the other cases. Thus, the presence of other constituents in the CCRs or the formation conditions appears to have a strong influence on the release of arsenic.

The range of arsenic concentrations observed in the laboratory eluates is consistent with the range of values reported for field leachates from landfills and impoundments. For some cases, both laboratory (Salem Harbor, Facility C, Facility L) and field concentrations exceeded the MCL by greater than a factor of 10. The expected range of arsenic concentrations under field conditions is less than 10 µg/L to approximately 1000 µg/L.

Arsenic leachate concentrations typically are strongly a function of pH over the entire pH range examined and within the pH range observed for field conditions. For some cases (for example, see Facility J, Appendix F), measured concentrations of arsenic are strongly a function of LS ratio at the material's natural pH, with much greater concentrations observed at low LS ratio. Therefore, testing at a single extraction final pH or LS ratio would not provide sufficient information to characterize the range of expected leachate concentrations under field conditions. Furthermore, for some of the CCRs a shift from the CCR's natural pH within the range of anticipated conditions (e.g., Facility L, Brayton Point with ACI, Salem Harbor baseline, Facility C baseline) can result substantial increases in leachate concentrations. Therefore, co-disposal of these CCRs with other materials should be carefully evaluated.

For several cases [Brayton Point, Salem Harbor, Facility C (without ACI), Facility L], arsenic concentrations in laboratory eluates appear to be controlled by solid phase solubility, while

adsorption processes appear to play a more important role for other cases [Pleasant Prairie, Facility C (with ACI), Facility J].

Boron (B). No significant effect of ACI on B eluate concentrations as a function of pH was observed, except for Brayton Point that showed an increase in B concentrations for $8 < \text{pH} < 12$ with ACI. Facility L showed the lowest B eluate concentrations with and without ACI (by a factor greater than 10). Most samples showed a relatively constant B concentrations over the entire pH range, except for the samples from Facility J showing an increase with decreasing pH for $9.5 < \text{pH} < 12$.

Barium (Ba). No significant effect of ACI on Ba eluate concentrations as a function of pH was seen, except for Pleasant Prairie for which a decrease in Ba concentrations was observed with ACI for $6 < \text{pH} < 11.5$ and Brayton Point for which a decrease was seen over the entire pH range examined. Sample BaFA (lignite, ACI + COHPAC) had the greatest Ba release for $\text{pH} < 7$ and $\text{pH} > 12$ (above the MCL).

Cadmium (Cd). For Salem Harbor, the case with ACI had an increase in Cd eluate concentrations for $\text{pH} > 4.5$ compared to the same facility without ACI. For Brayton Point a decrease in Cd concentrations was observed with ACI for $\text{pH} < 7$. No significant effect of ACI was seen for the other facilities tested.

Cobalt (Co). Sample BaFA (lignite, ACI + COHPAC) showed the greatest Co eluate concentrations for all pHs examined. No significant effect of ACI on Co eluate concentrations was observed, except for Brayton Point that showed a decrease in Co concentration with ACI.

Chromium (Cr). For most cases a decrease in Cr eluate concentrations was observed for the cases with ACI compared to the same facility without ACI. Facility C showed, however, an increase in Cr concentrations for $\text{pH} > 7$ for the case with ACI.

Mercury (Hg). Although the use of activated carbon injection substantially increases the total Hg content in the fly ashes, the range of laboratory leaching eluate concentrations in the baseline cases and cases with sorbent injection are either unchanged or the maximum leaching concentration is reduced as a consequence of activated carbon injection. The exceptions are Facility C and Facility L, which have an increased maximum eluate concentration for the case with sorbent injection.

The expected range of Hg leachate concentrations based on these results is from < 0.004 (below MDL) to $0.2 \mu\text{g/L}$ over the range of pH conditions expected in coal ash landfill leachate.

The range of Hg concentrations observed from laboratory eluates is consistent with the range reported for field leachates from landfills in the EPRI database.

All concentrations observed in laboratory leach test eluates from fly ash over $5.4 \leq \text{pH} \leq 12.4$ were at least an order of magnitude less than the MCL.

For all cases of laboratory eluates, Hg concentrations in eluates from fly ash were consistent without any significant effect of total mercury content, pH, or LS ratio observed. Mercury leaching appears to be controlled by adsorption from the aqueous phase with strong interaction between adsorbed mercury molecules, indicating that use of a linear partition coefficient (K_d) approach to model source term mercury leaching would not be appropriate. Variability observed in concentrations observed within individual cases is likely the result of sampling and CCR heterogeneity at the particle scale (i.e., resulting from mercury adsorption specifically onto

Characterization of Coal Combustion Residues III

carbon surfaces and relatively more or less carbon particles in a specific subsample used for extraction).

Molybdenum (Mo). For all cases, there was no significant effect of ACI on Mo eluate concentrations as a function of pH.

Lead (Pb). Minimal Pb leaching was overall observed. In most cases, Pb leaching was at or below the MDL for $4 < \text{pH} < 12$. For Facility J, the case with ACI showed an increase in Pb eluate concentrations for $4 < \text{pH} < 10$ compared to the same facility without.

Antimony (Sb). There was no significant effect of ACI on Sb eluate concentrations, except for Salem Harbor that showed an increase in Sb concentrations with ACI over the entire pH range and Brayton Point for which an increase in Sb concentrations for $\text{pH} > 8$ and a decrease for $\text{pH} < 7.5$ was observed with ACI.

Selenium (Se). The range of selenium concentration in laboratory leach test eluates is not correlated with total selenium content in the CCRs. For example, Brayton Point with ACI had much greater total selenium content than the other cases except Facility C with ACI, but had only the fifth highest selenium concentration under the laboratory leaching conditions. Conversely, Facility C baseline had one of the lowest selenium total content (less than MDL) but had second greatest selenium concentration under the laboratory leaching conditions.

The range of selenium concentrations observed in laboratory leach test eluates for Facility C are much greater than the concentrations observed for other cases and for field conditions. This is a COHPAC facility and field leachate composition data for CCRs from this type of facility were not available in the EPA or EPRI databases. For all other facilities, the range of concentrations observed from laboratory testing is consistent with the range reported in the EPRI database for landfills. The concentration range reported in the EPA database for CCR landfills has a much lower upper bound than reported in the EPRI database.

The concentration range for laboratory eluates and field observations exceeded the MCL for all cases except Facility L. For 5 out of 12 of the cases used for laboratory evaluation, and for some field observations, the MCL is exceeded by more than a factor of 10.

Selenium concentrations in laboratory leach test eluates typically are strongly a function of pH over the entire pH range examined and within the pH range observed for field conditions (for example, see leaching test results for Brayton Point, Salem Harbor, Facility C). For some cases (for example, see Brayton Point, Salem Harbor, and Facility J in Appendix F), measured concentrations of selenium are strongly a function of LS ratio at the material's natural pH, with much greater concentrations observed at low LS ratio. Therefore, testing at a single extraction final pH or LS ratio would not provide sufficient information to characterize the range of expected leachate concentrations under field conditions.

For several cases (Brayton Point, Salem Harbor, Facility C, Facility L) selenium concentrations in laboratory eluates appears to be controlled by solid phase solubility, while adsorption processes appear to play a more important role for other cases (Pleasant Prairie and Facility J).

Thallium (Tl). For Pleasant Prairie, the case with ACI resulted in an increase in Tl concentrations over the entire pH range compared to the same facility without ACI. For Facility J, a decrease in Tl eluate concentrations with ACI was observed for all pHs examined. For Brayton Point, the case with ACI showed an increase in Tl concentrations for $\text{pH} > 10$ and a decrease for $\text{pH} < 9$.

Characterization of Coal Combustion Residues III

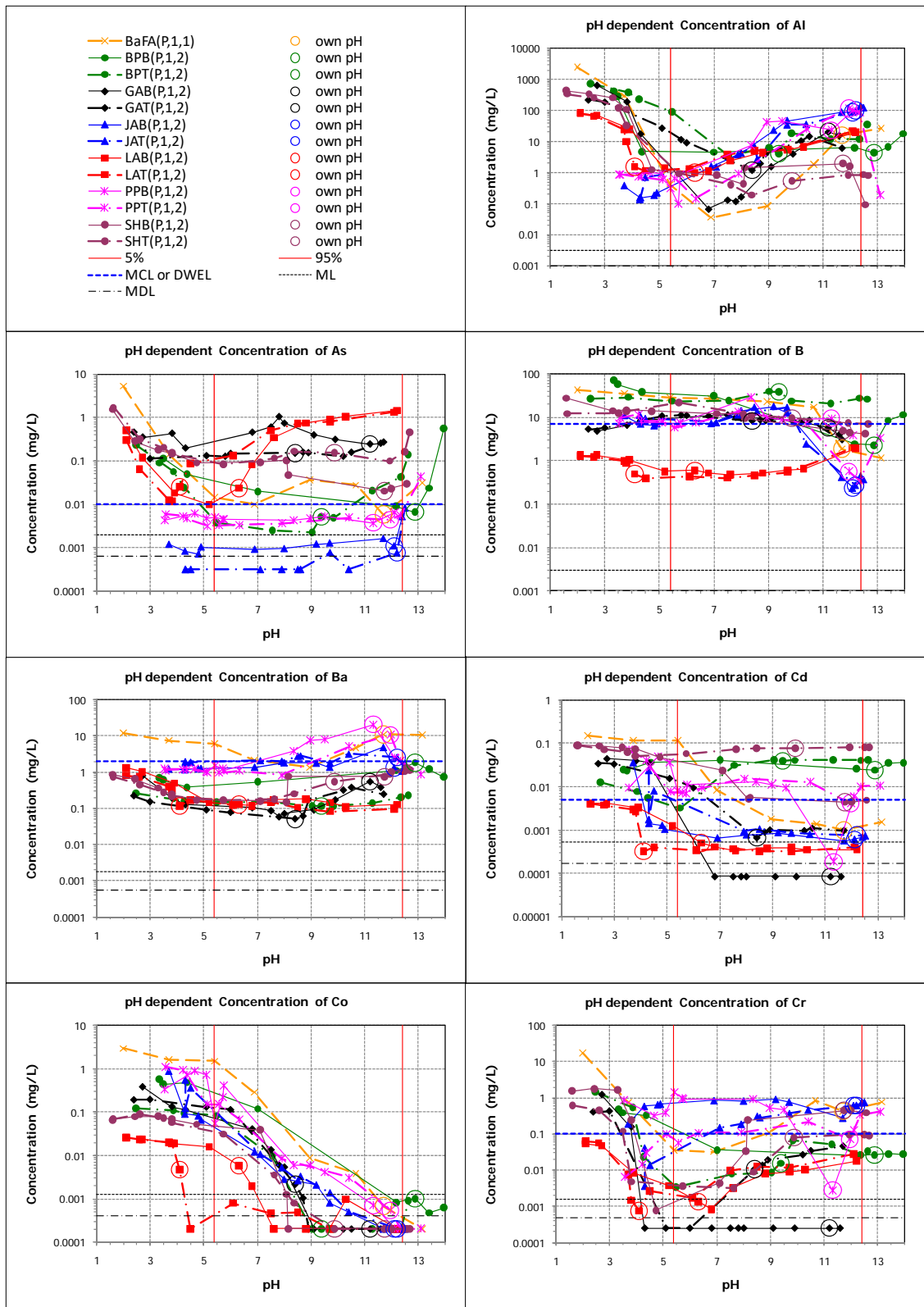


Figure 46. pH dependent leaching results. Fly ash samples from facility pairs with and without mercury sorbent injection. Sample codes ending __B (BPB) indicate without sorbent injection; Sample codes ending __T (BPT) indicate with sorbent injection for the corresponding facility.

Characterization of Coal Combustion Residues III

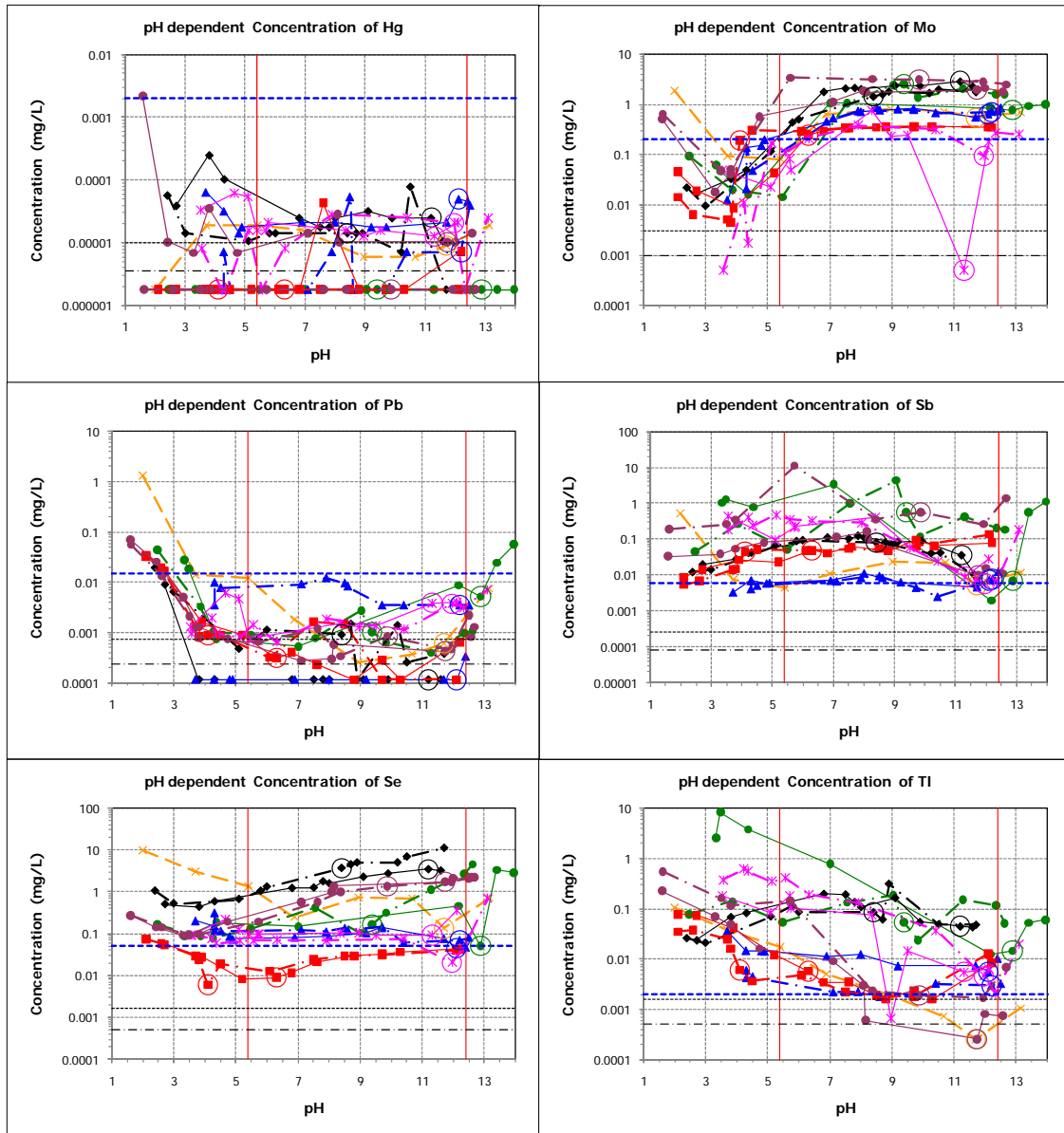


Figure 46 (continued). pH dependent leaching results. Fly ash samples from facility pairs with and without mercury sorbent injection. Fly ash samples from facility pairs with and without mercury sorbent injection. Sample codes ending __B (BPB) indicate without sorbent injection; Sample codes ending __T (BPT) indicate with sorbent injection for the corresponding facility.

3.2.1.3. Gypsum, Unwashed and Washed

The effect of the washing step on the leaching behavior of gypsum as a function of pH for each of the 13 elements of interest is illustrated in Figure 47, Figure 48, and Figure 49. Typically, washing resulted in at least an order of magnitude reduction in the observed leached concentrations for the soluble species (e.g., B, Tl) and the oxyanions (e.g., Se). B and Tl release from both unwashed and washed gypsum were generally relatively constant as a function of pH for most facilities. Se release was either relatively constant as a function of pH (Facilities O, P) or amphoteric (Facilities N, Q).

The washing step resulted, however, in greater leaching concentrations of Hg ($7 < \text{pH} < 10$) and Cr ($4 < \text{pH} < 12$) for Facility X. Also, the washed gypsum sample from lignite (CaAW) showed a greater release for Pb and Se compared to washed and unwashed gypsum samples from facilities using high sulfur bituminous or sub-bituminous coal.

The unwashed sample from Facility W (WAU) showed greater concentrations of As, Pb, and Tl, which was most likely a consequence of the Trona injection used for SO_3 control by this facility.

Characterization of Coal Combustion Residues III

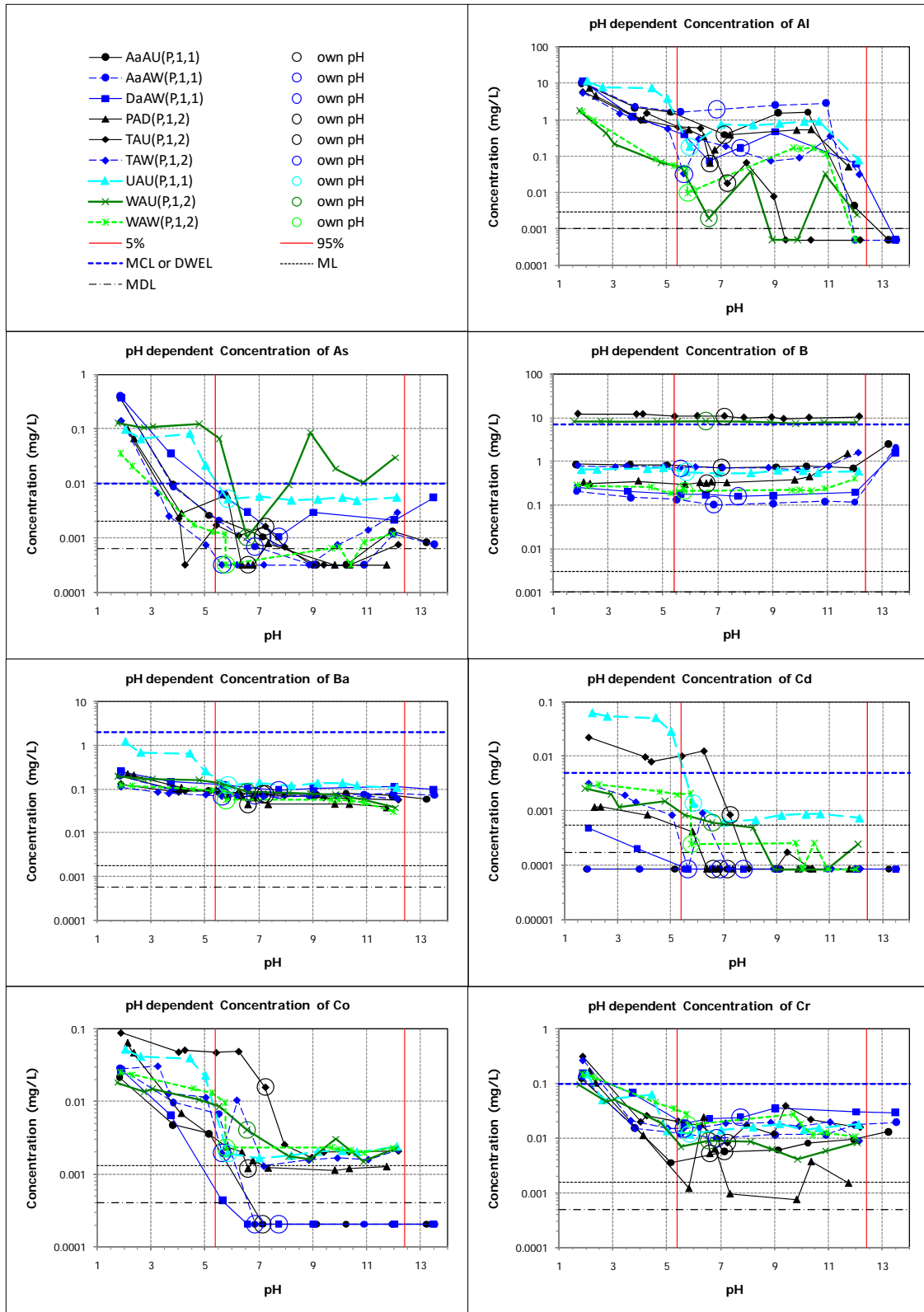


Figure 47. pH dependent leaching results. Gypsum samples unwashed (sample codes __U) and washed (sample codes __W) from facilities using low and medium sulfur bituminous coals.

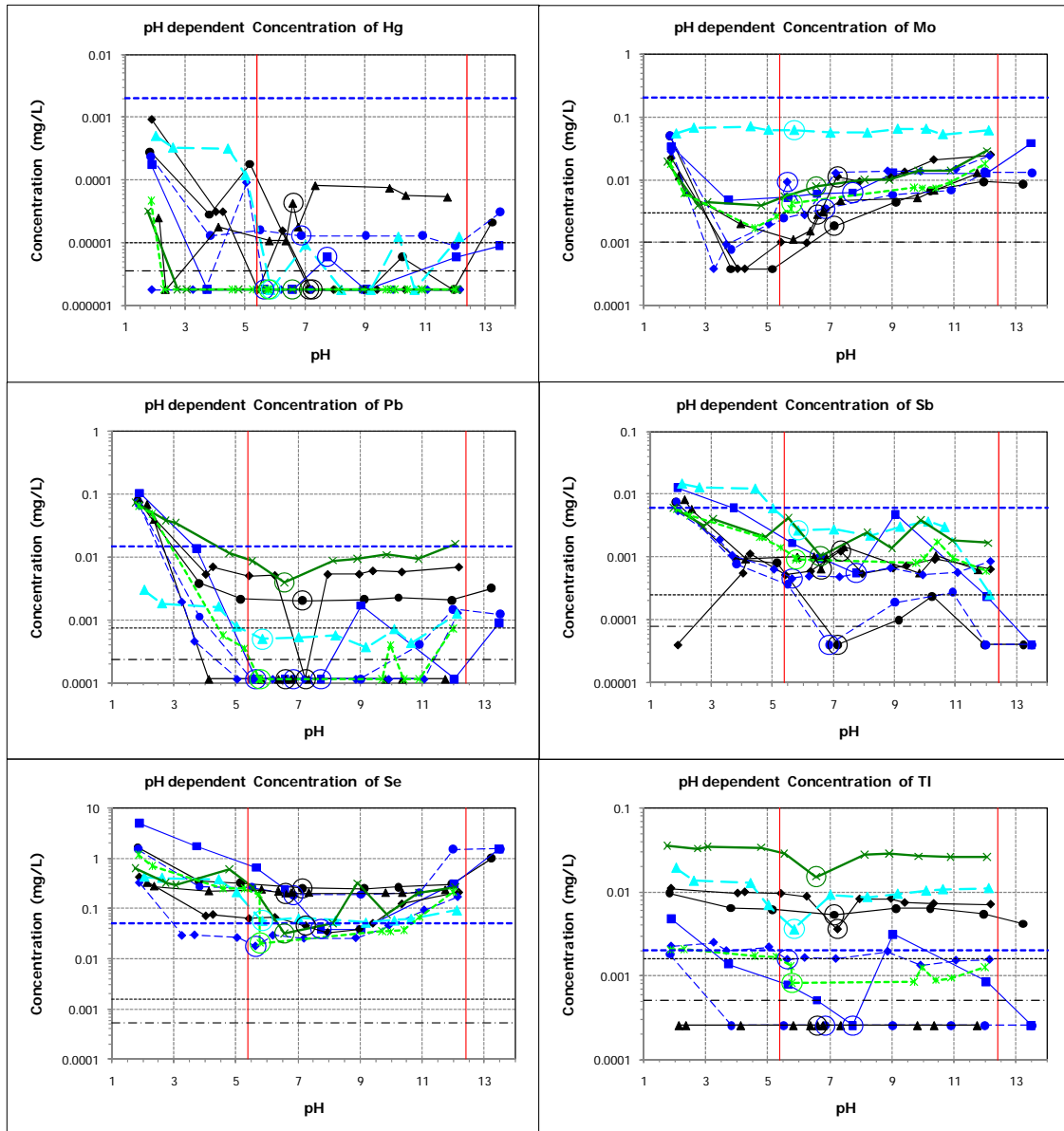


Figure 47 (continued). pH dependent leaching results. Gypsum samples unwashed (sample codes __U) and washed (sample codes __W) from facilities using low and medium sulfur bituminous coals.

Characterization of Coal Combustion Residues III

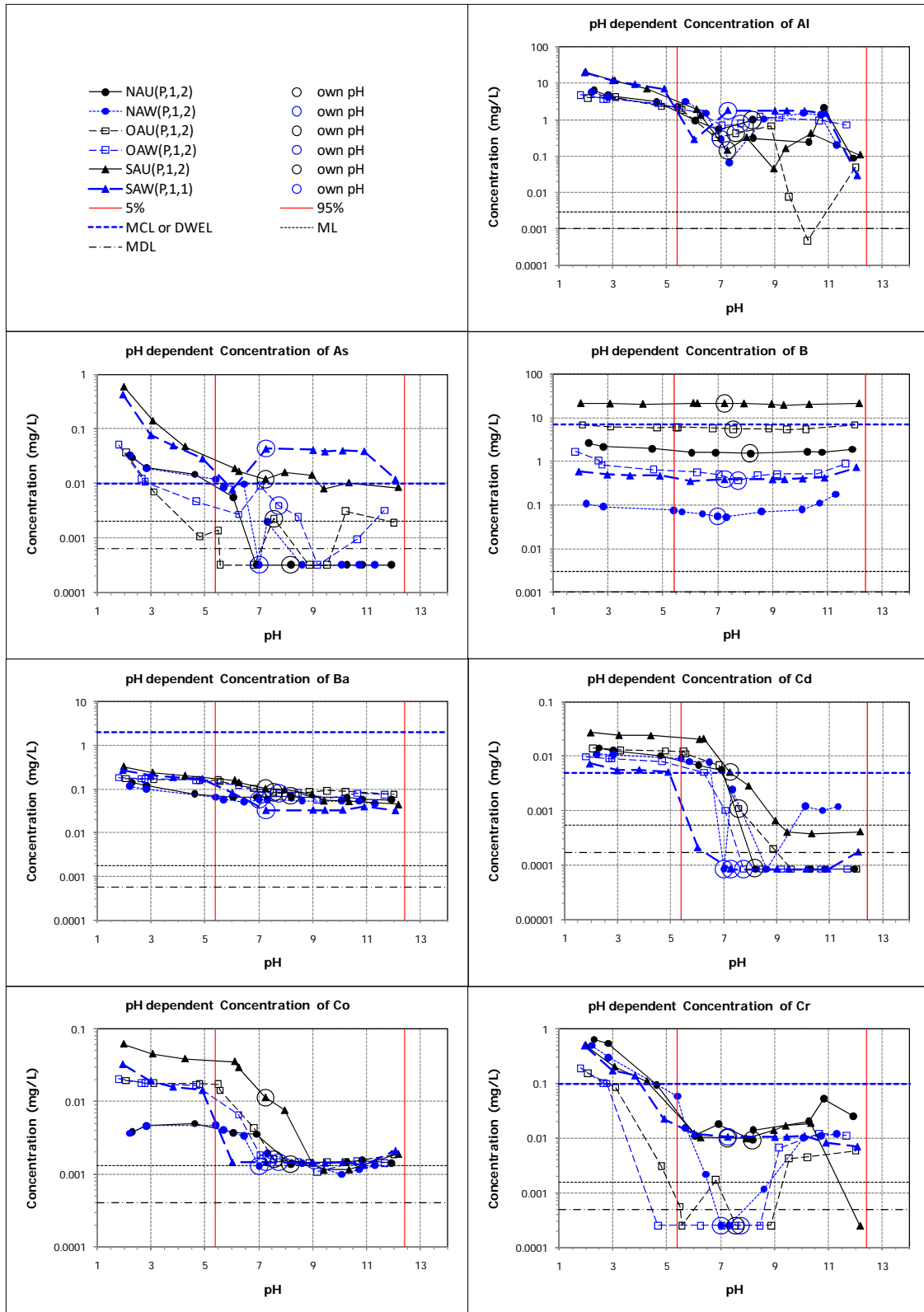


Figure 48. pH dependent leaching results. Gypsum samples unwashed (sample codes __U) and washed (sample codes __W) from facilities using high sulfur bituminous coal.

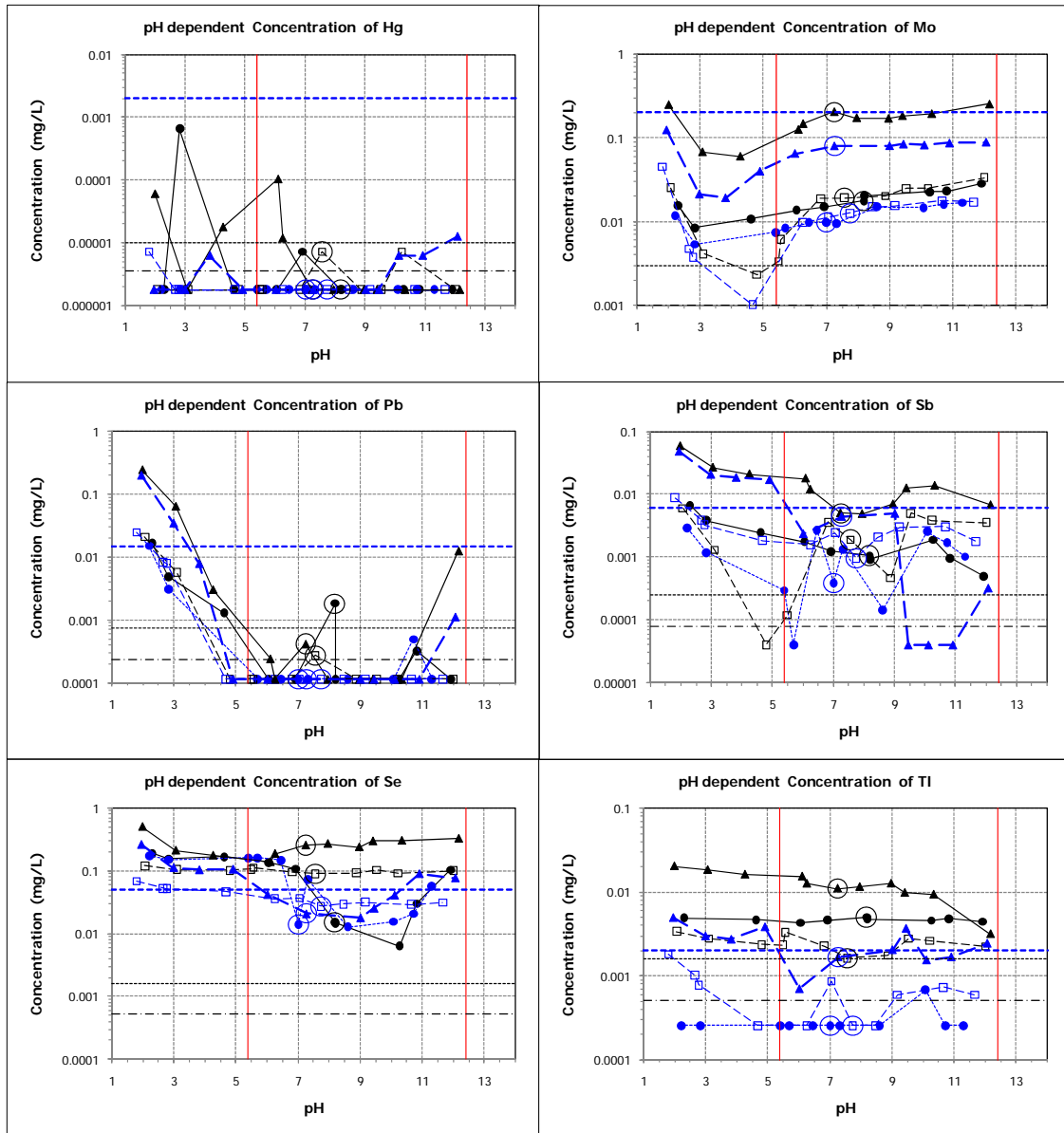


Figure 48 (continued). pH dependent leaching results. Gypsum samples unwashed (sample codes __U) and washed (sample codes __W) from facilities using high sulfur bituminous coal.

Characterization of Coal Combustion Residues III

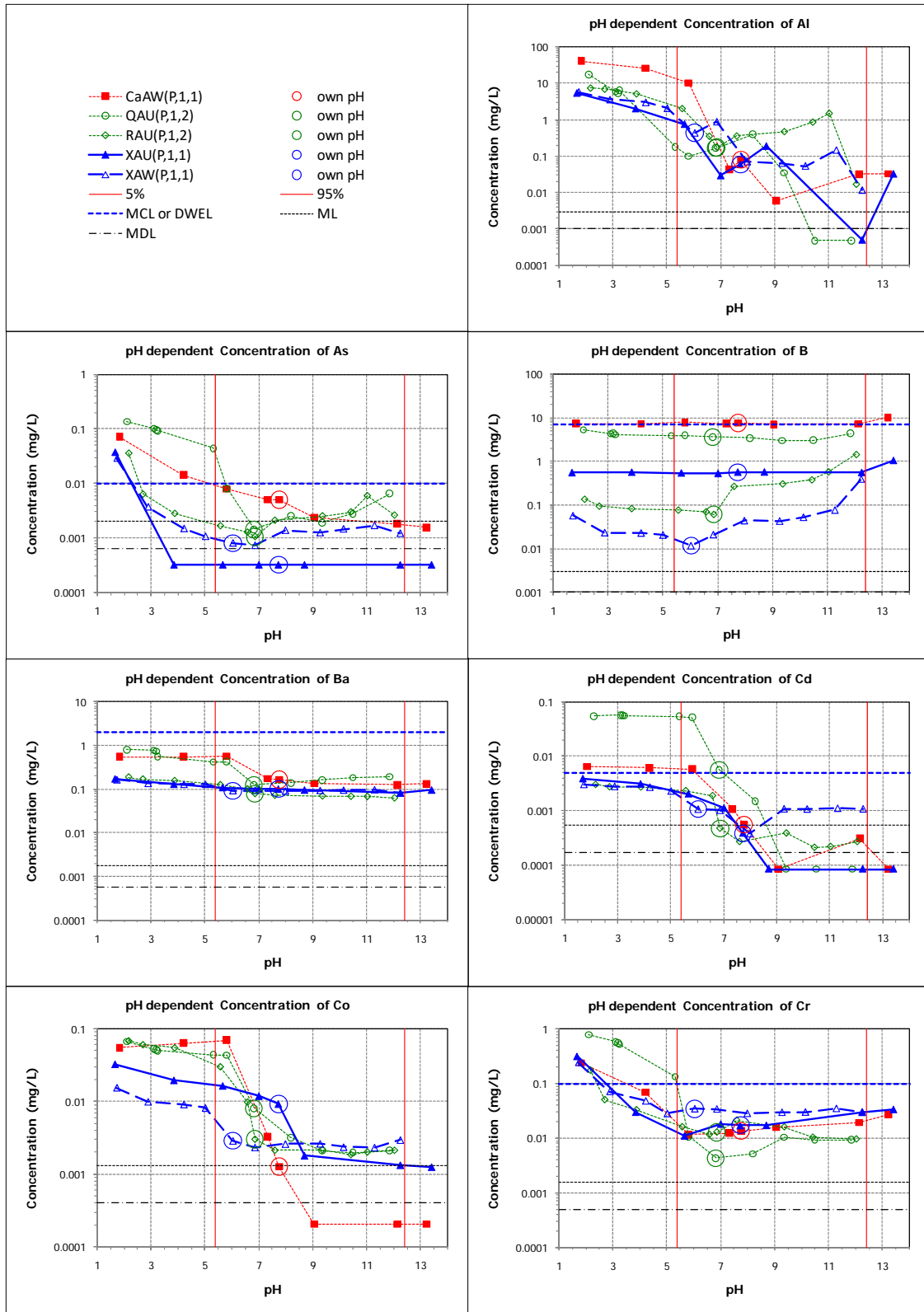


Figure 49. pH dependent leaching results. Gypsum samples unwashed (sample codes __U) and washed (sample codes __W) from facilities using sub-bituminous and lignite bituminous coals.

Characterization of Coal Combustion Residues III

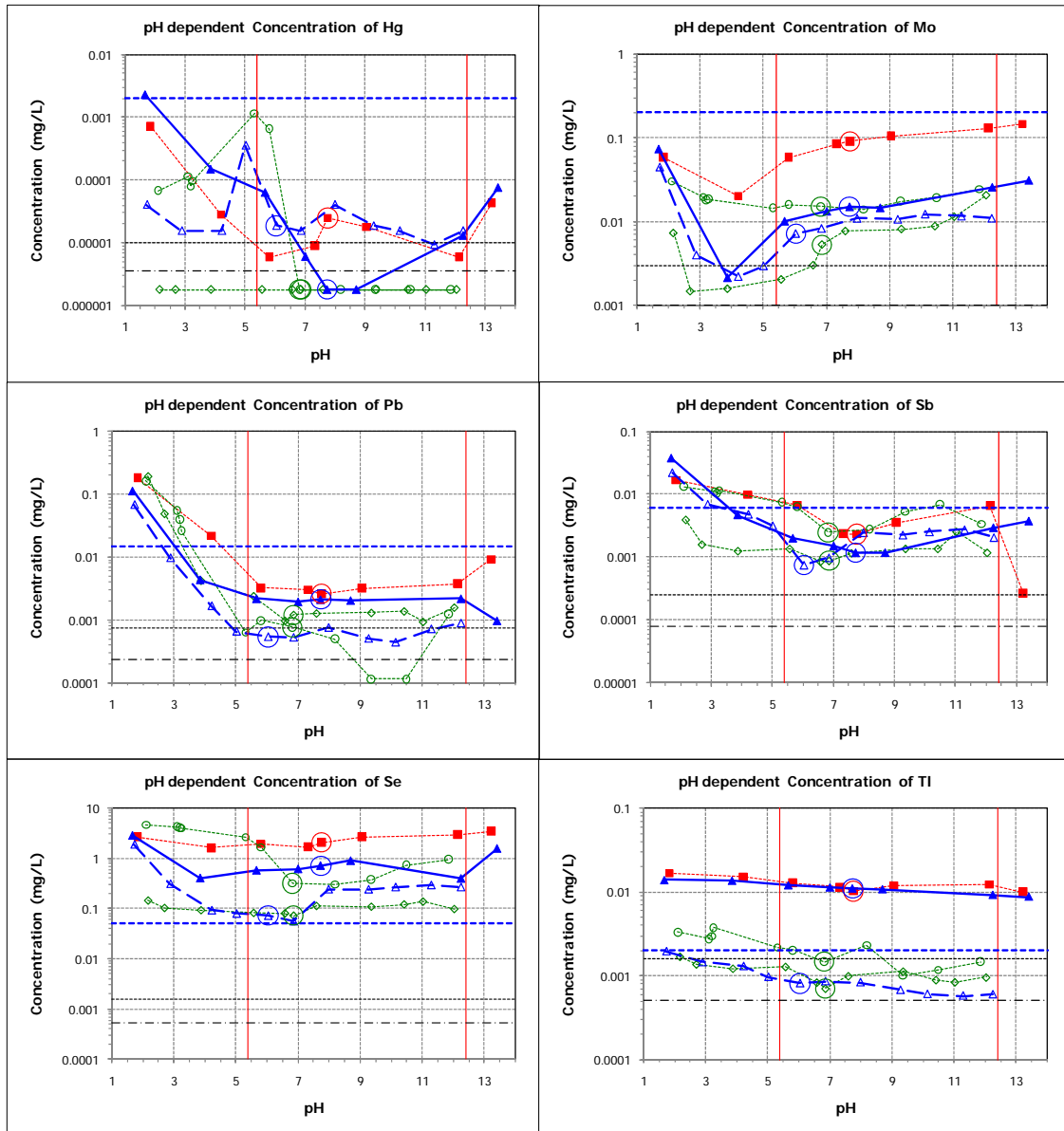


Figure 49 (continued). pH dependent leaching results. Gypsum samples unwashed (sample codes __U) and washed (sample codes __W) from facilities using sub-bituminous and lignite bituminous coals.

3.2.1.4. Scrubber Sludge

Figure 50 presents results of the leaching behavior as a function of pH for the scrubber sludge samples. The effect of SNCR in combination with a fabric filter (AGD *vs.* CGD) was manifested by (i) a significant increase in the leaching concentrations of Cr over the entire pH range examined, (ii) a slight reduction in Hg, and (iii) an increase in Tl. An effect of SCR (BGD *vs.* DGD) was seen for As (slight increase with SCR), Ba (increase with SCR), Co (increase with SCR), and Cr (significant increase with SCR). Sample KGD exhibited the highest leaching concentrations for Ba, Cd, Co, Mo, Se, and Tl.

Characterization of Coal Combustion Residues III

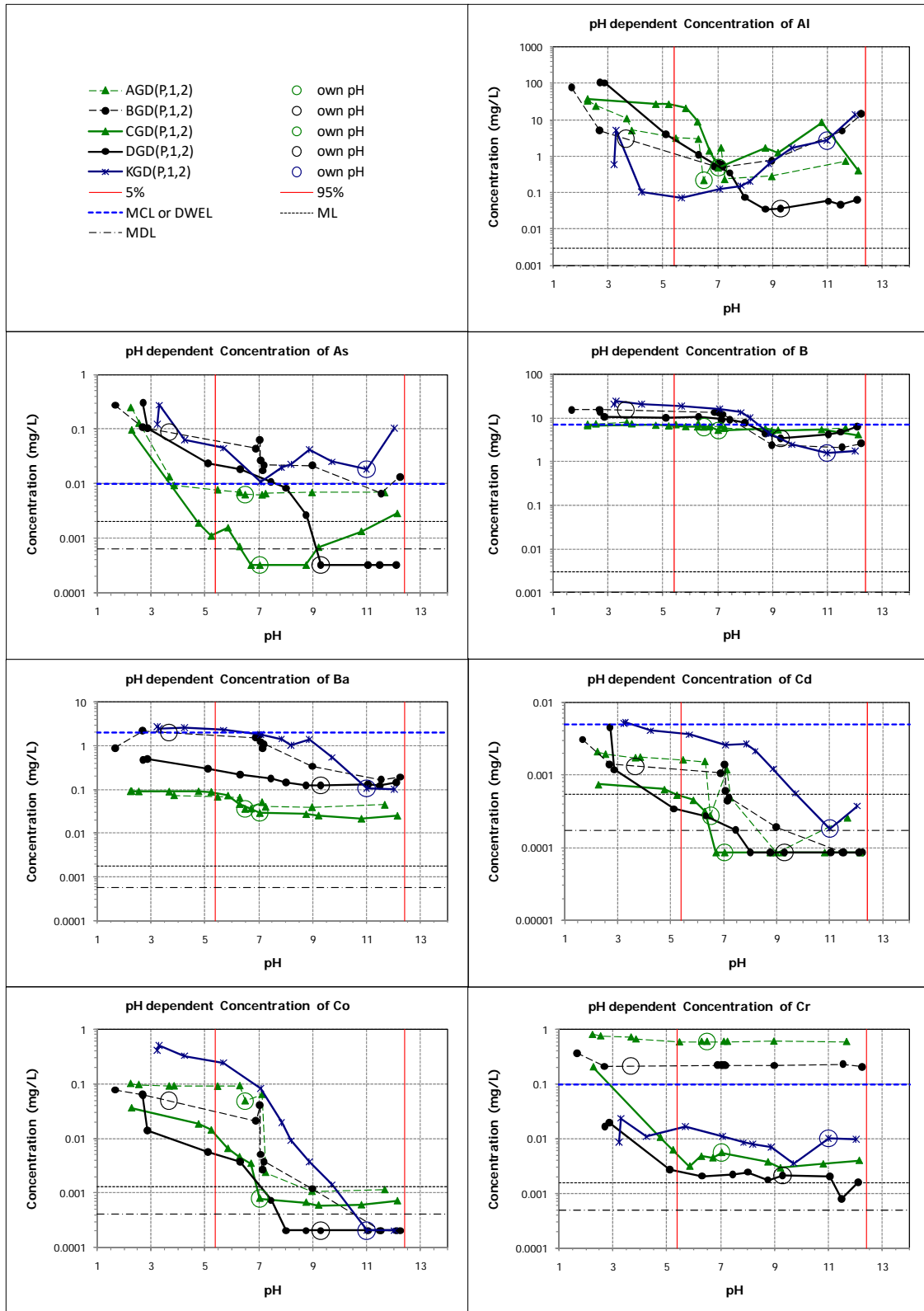


Figure 50. pH dependent leaching results. Scrubber sludges. Facility A (AGD, CGD), Facility B (BGD, DGD), Facility K (KGD). Samples DGD and KGD with SCR, Samples BGD with SNCR. Samples CGD and DGD without post-combustion NO_x controls.

Characterization of Coal Combustion Residues III

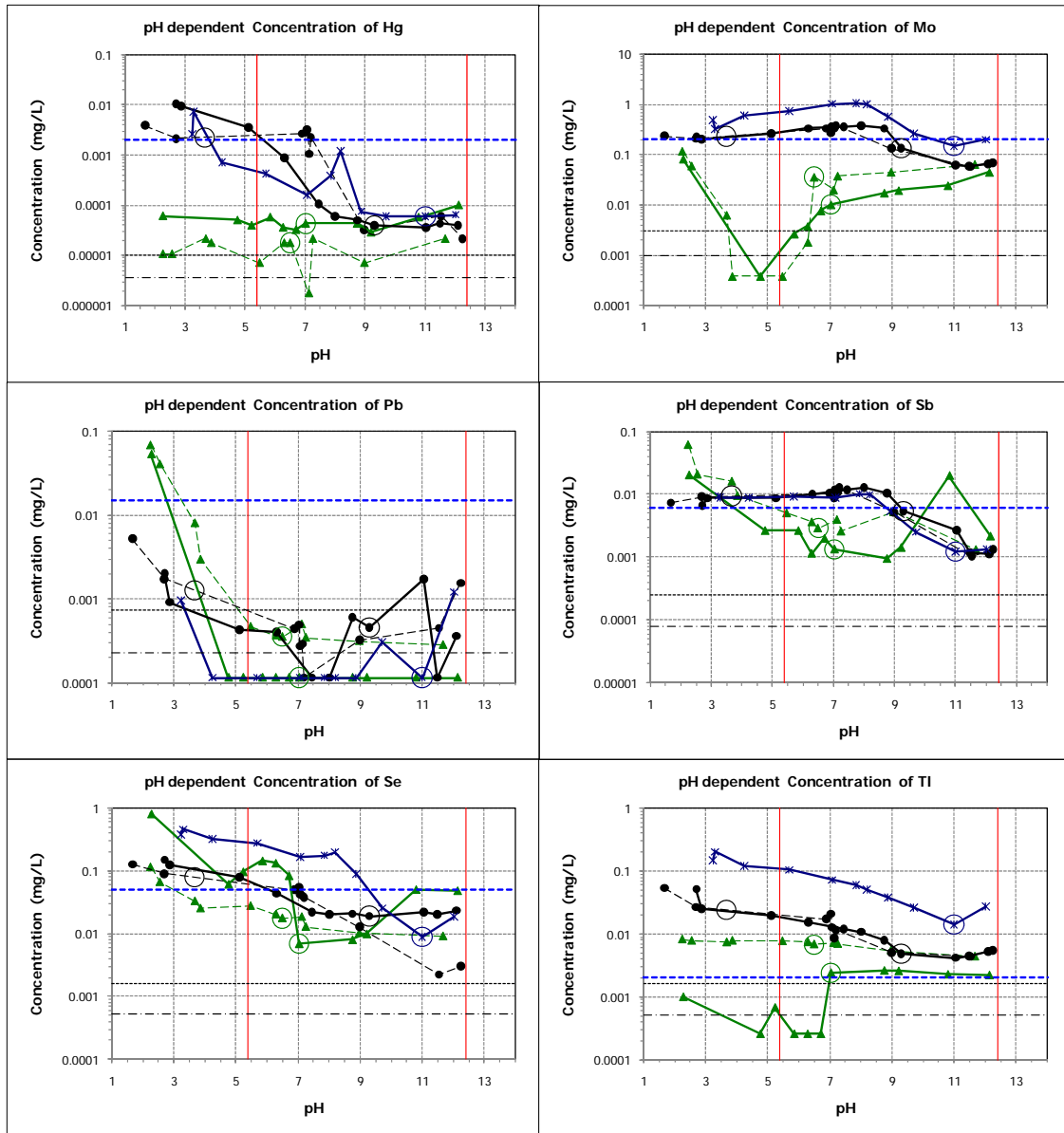


Figure 50 (continued). pH dependent leaching results. Scrubber sludges. Facility A (AGD, CGD), Facility B (BGD, DGD), Facility K (KGD). Samples DGD and KGD with SCR, Samples BGD with SNCR. Samples CGD and DGD without post-combustion NO_x controls.

3.2.1.5. Spray Dryer Absorber Residues

Figure 51 presents results of leaching behavior as a function of pH for spray dryer residue samples. Sample VSD showed a greater release of Al ($9 < \text{pH} < 12$), Ba ($8 < \text{pH} < 12$), Cr ($\text{pH} < 6$), and Tl ($\text{pH} < 6$) and a lower release of Co and Pb ($4 < \text{pH} < 12$) than sample YSD, though the two samples are from the same coal type and air pollution control configurations. The observed differences between the two samples could be due to differences in the lime used.

Characterization of Coal Combustion Residues III

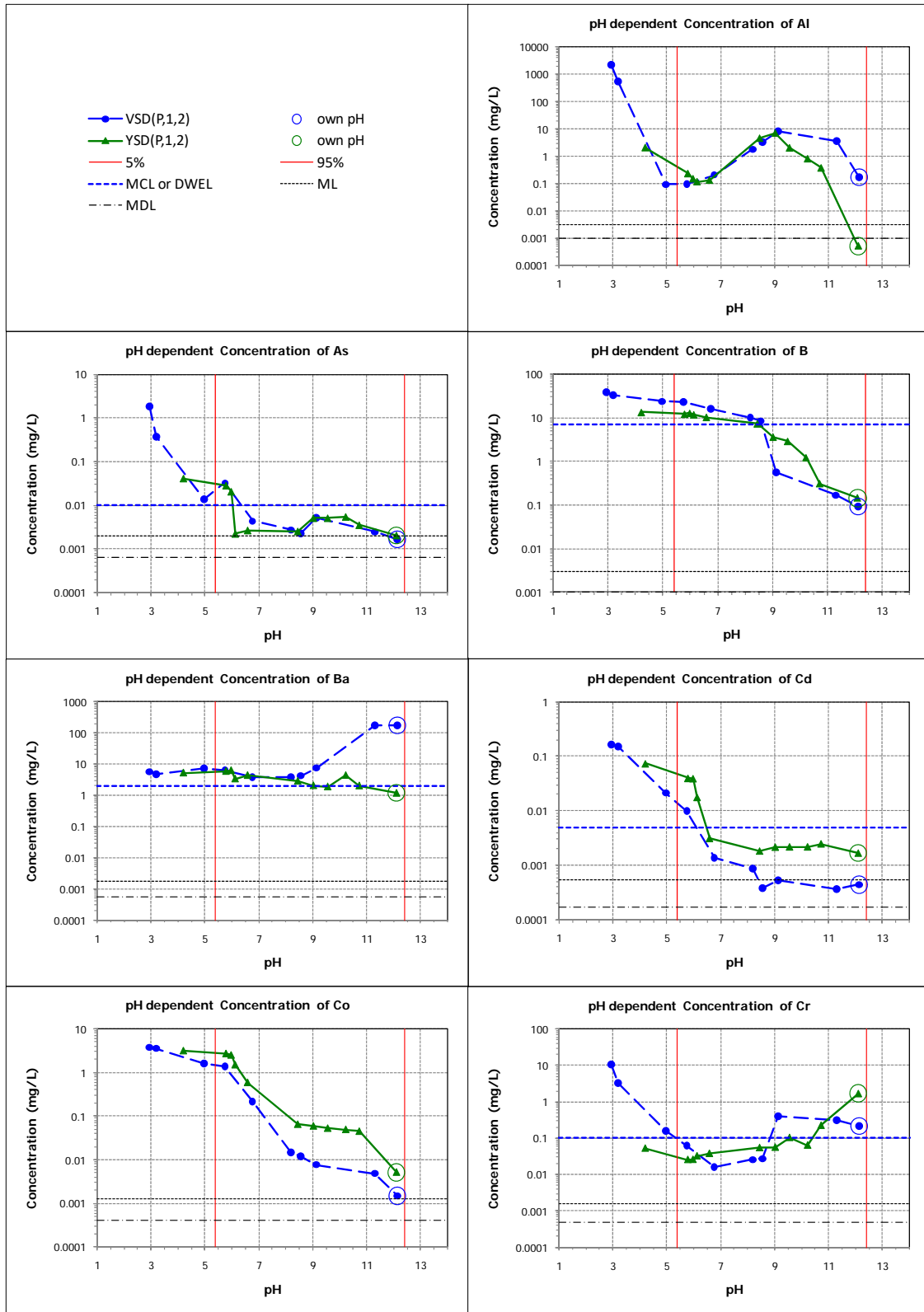


Figure 51. pH dependent leaching results. Spray dryer residue samples (sub-bituminous coal).

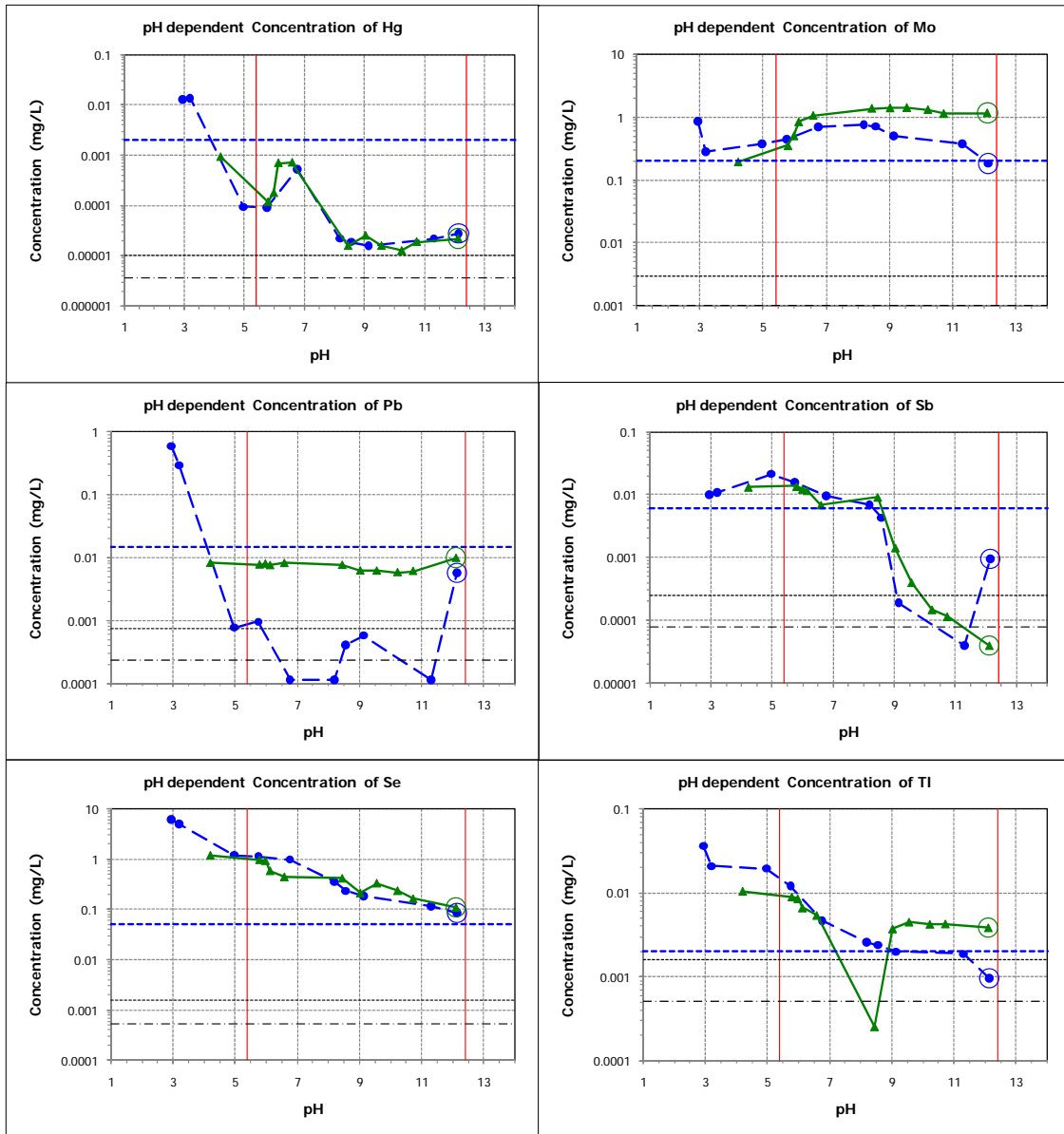


Figure 51 (continued). pH dependent leaching results. Spray dryer residue samples (sub-bituminous coal).

3.2.1.6. Blended CCRs (Mixed Fly Ash and Scrubber Sludge/Mixed Fly Ash and Gypsum)

The leaching behavior of the blended CCRs (mixed fly ash and scrubber sludge/mixed fly ash and gypsum) was mainly controlled by the behavior of the fly ash. This behavior is illustrated in Figure 52 (Facility A, SNCR-BP) that shows comparisons of pH dependent leaching results for fly ash (CFA), scrubber sludge (CGD), and blended fly ash and scrubber sludge (CCC). Results for the blended fly ash and gypsum can be found in Appendix F (UGF).

Characterization of Coal Combustion Residues III

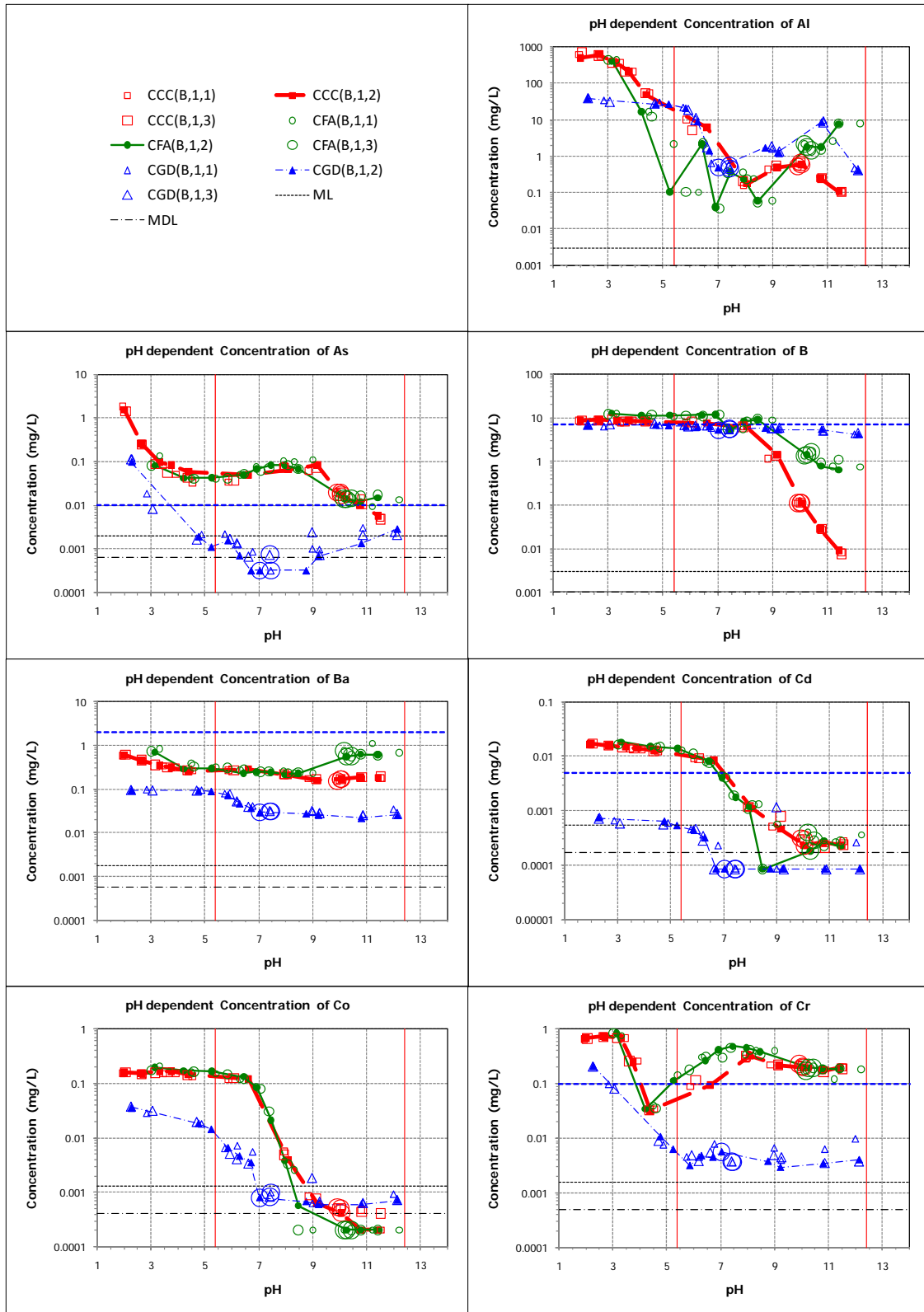


Figure 52. pH dependent leaching results. Facility A samples (low S east-bit., fabric filter, limestone, natural oxidation). SNCR-BP. Fly ash (CFA); scrubber sludge (CGD); blended fly ash and scrubber sludge (“as managed,” CCC).

Characterization of Coal Combustion Residues III

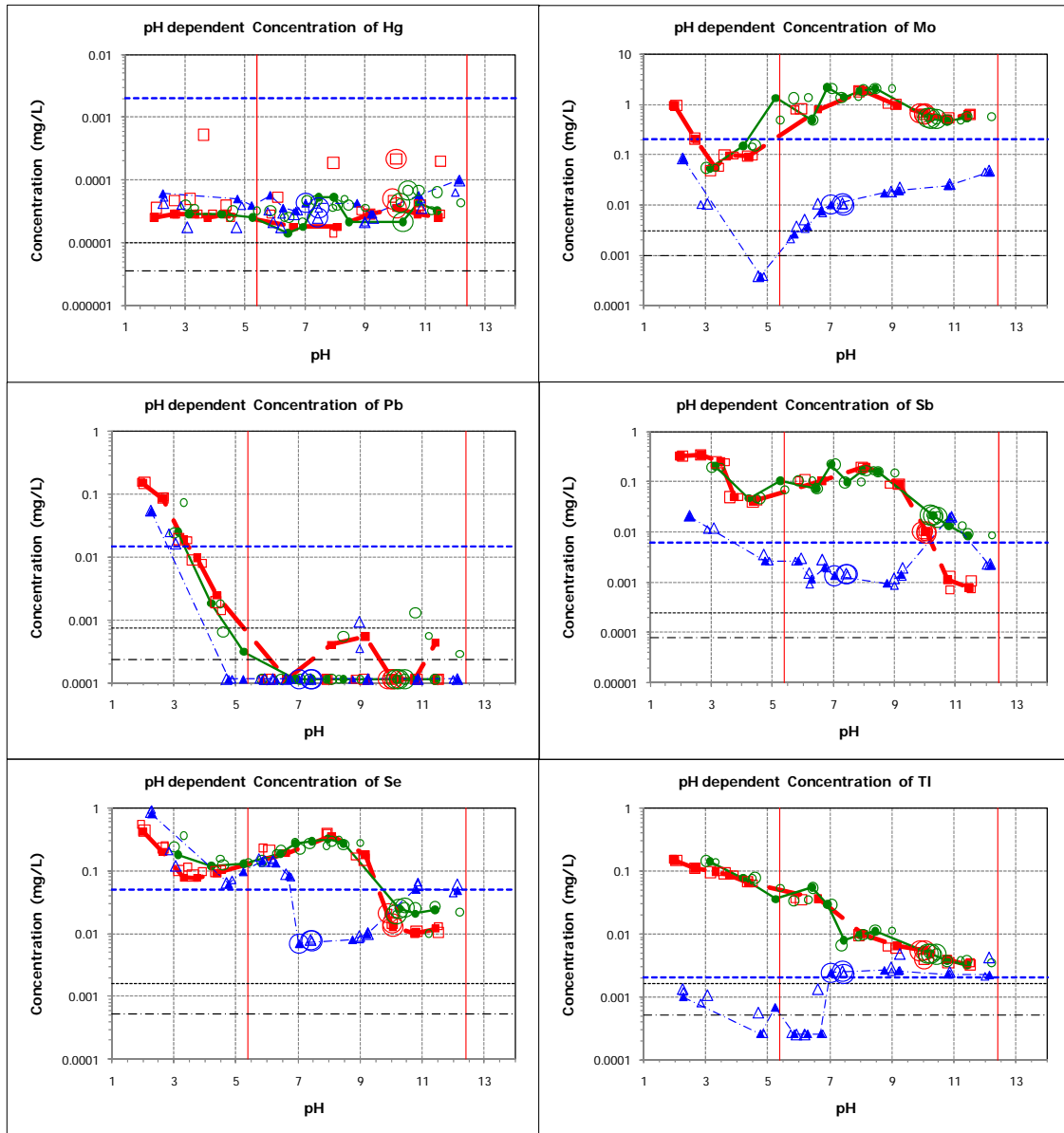


Figure 52 (continued). pH dependent leaching results. Facility A samples (Low S East-Bit., Fabric F., Limestone, Natural Oxidation). SNCR-BP. Fly ash (CFA); Scrubber sludge (CGD); Blended fly ash and scrubber sludge (“as managed,” CCC).

3.2.1.7. Waste Water Filter Cake

Figure 53 presents results of leaching behavior as a function of pH for waste water filter cake for each of the 13 elements of interest. These are samples with waste water treatment process associated with management of CCRs and are not a direct product of the air pollution control systems. Overall similar results were observed for all samples tested except for sample XFC that showed a greater release for Hg, Mo, Pb, and Se.

Characterization of Coal Combustion Residues III

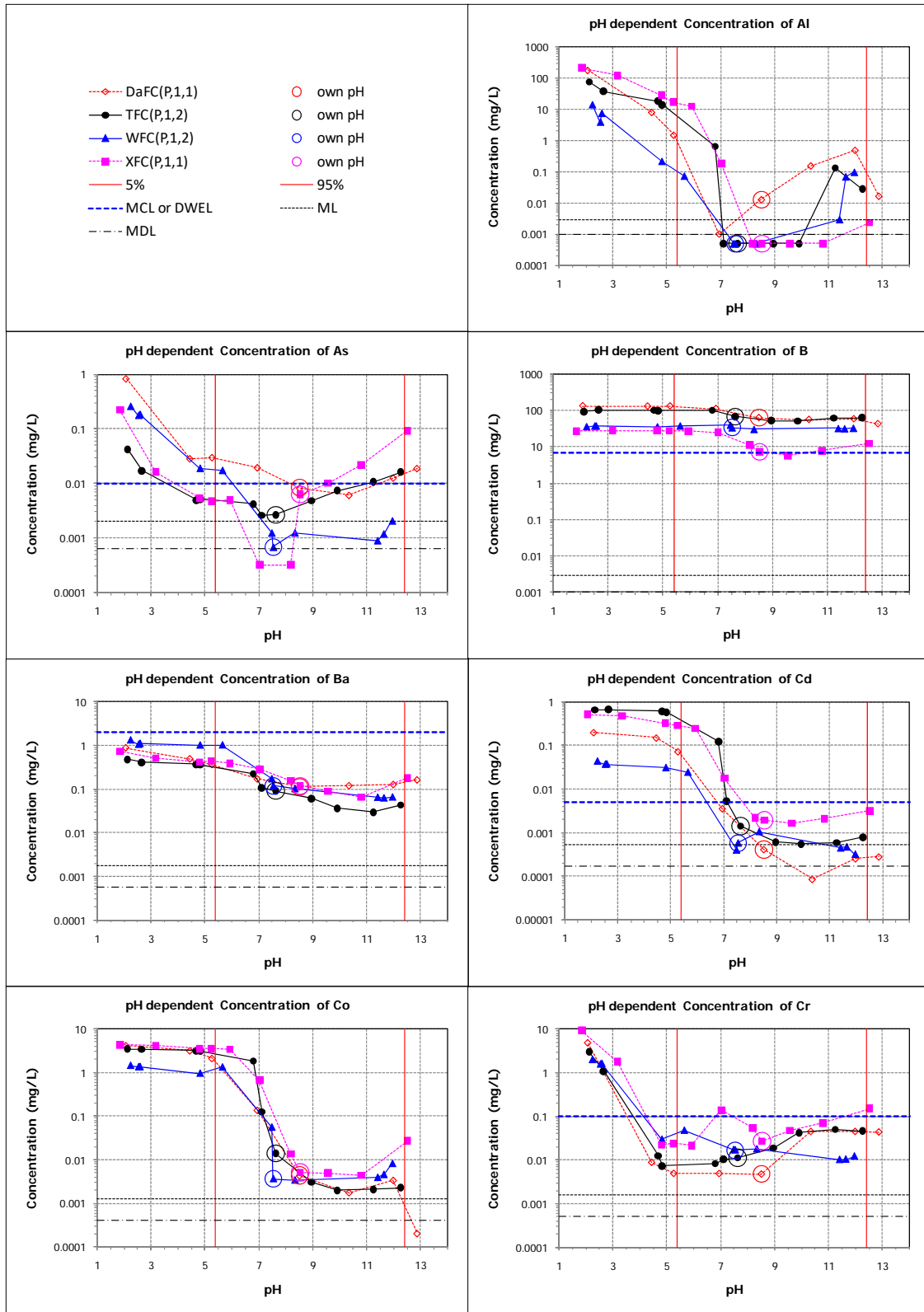


Figure 53. pH dependent leaching results. Filter cake samples.

Characterization of Coal Combustion Residues III

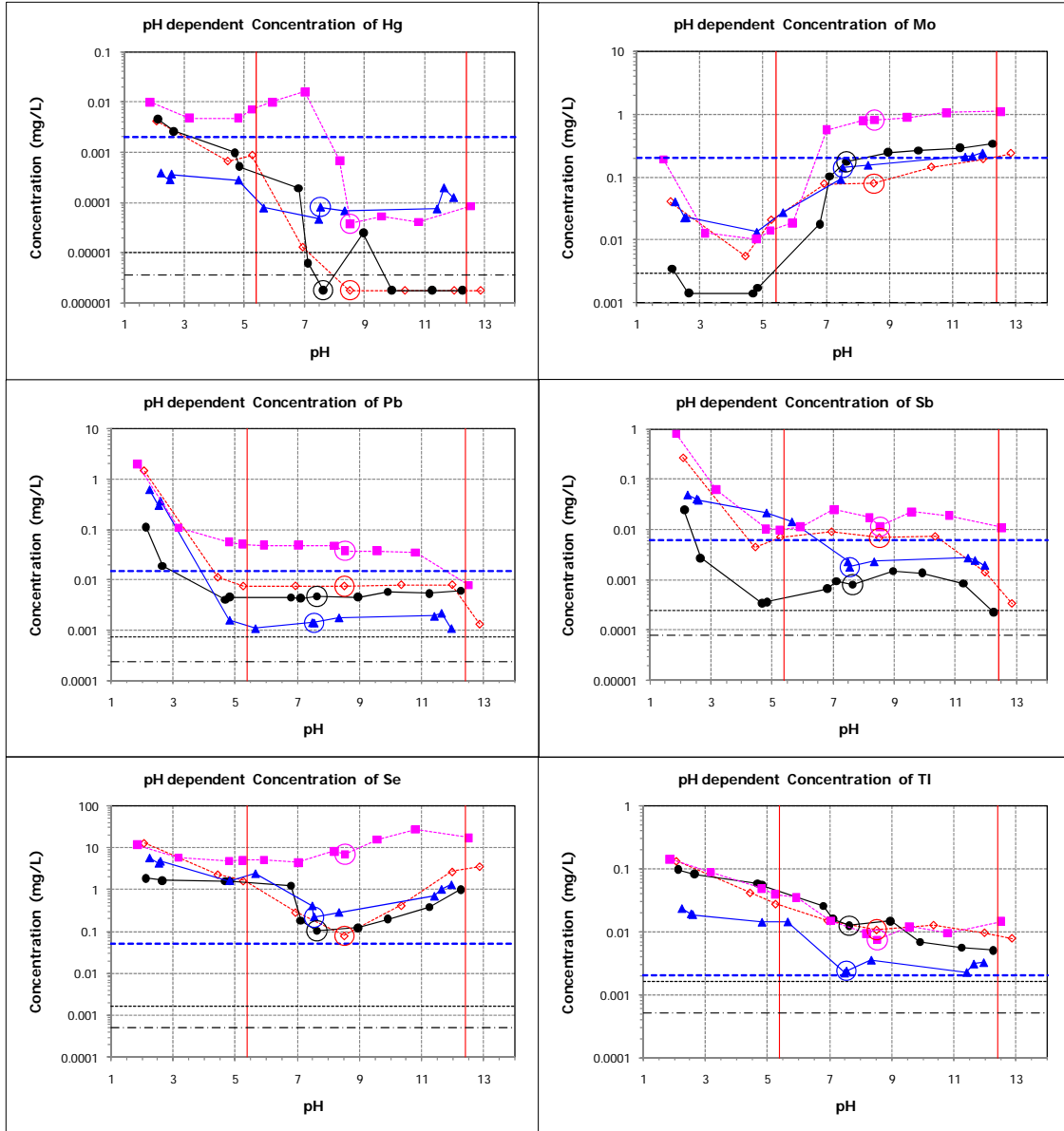


Figure 53 (continued). pH dependent leaching results. Filter cake samples.

3.2.2. Comparisons of the Ranges of Constituent Concentrations from Laboratory Testing (Minimum Concentrations, Maximum Concentrations, and Concentrations at the Materials' Own pH)

Figure 54 through Figure 66 present comparisons of the range of constituent concentrations observed in laboratory eluates from testing as a function of pH and LS (SR002.1 and SR003.1) over the pH range from 5.4 to 12.4 and LS ratios from 0.5 to 10. This pH range represents the 5th and 95th percentiles of pH observed in field samples from CCR landfills and surface impoundments, as discussed in Section 2.5.2. For laboratory leaching test eluates, the presented data represent the observed maximum and minimum concentrations within the pH range from 5.4 to 12.4 from both test methods (upper and lower whiskers) and the concentration at the materials' own pH (closed circles or asterisks), which may be outside the pH range criteria. Including results from testing as a function of LS allows consideration of potentially higher concentrations observed for initial releases that may occur at low LS ratios in the field. The TC and MCL, DWEL, or AL (as available) is included in each figure as a dashed horizontal line to provide a reference value. The concentration ranges indicated in the figures as results of this study are direct measurements of laboratory eluates of the CCRs and do not consider attenuation that may occur in the field. Tabular results are provided in Appendix I.

Important observations from these figures are summarized as follows.

Aluminum (Al). Gypsum generally had lower eluate concentration ranges than the other CCR types. No trend was readily discernable with respect to coal type or facility configuration.

Arsenic (As). Lower eluate concentration ranges were associated with fly ash produced from sub-bituminous coal than other coal types. Many of the values for eluates from fly ash exceeded the MCL but results only for one fly ash sample (WFA) exceeded the TC. Results for five of the gypsum samples exceeded the MCL. For scrubber sludges, results suggest that use of post-combustion NO_x controls may increase As leachability.

Boron (B). Washed gypsum samples all had lower eluate concentrations for B than unwashed gypsum samples, indicating the effectiveness of the washing process in reducing leachable B. All of the CCR types had a significant fraction of the samples that exceeded the DWEL.

Barium (Ba). The greatest Ba concentrations in eluates was from fly ash and SDA sample produced from sub-bituminous coal. All gypsum samples had barium eluate concentrations less than the MCL. Use of post-combustion NO_x controls appears to have reduced Ba leachability in blended CCRs.

Cadmium (Cd). All CCR types had a significant fraction of samples from which eluate concentrations exceeded the MCL. For many samples of all CCR types, the own pH concentration was less than the method detection limit.

Cobalt (Co). All CCR types had samples with cobalt eluate concentrations from less than the method detection limit up to three orders of magnitude greater. SDA residues had the greatest range in Co eluate concentrations.

Chromium (Cr). Use of post-combustion NO_x controls appeared to increase the eluate concentrations for fly ash, scrubber sludges, and blended CCRs when samples were collected from the same facility. All gypsum samples except one unwashed gypsum, had eluate

concentrations less than the MCL. All other CCR types had multiple samples with eluates that exceeded the MCL.

Mercury (Hg). The greatest Hg concentrations in eluates were from scrubber sludges and blended CCRs, including all of those that exceeded the MCL.

Molybdenum (Mo). Higher eluate concentration ranges were associated with fly ash, SDA residues and blended CCRs (which include fly ash) than associated with gypsum and scrubber sludge samples. All CCR types had multiple samples with eluates that exceeded the DWEL.

Lead (Pb). Eluate concentrations were below the AL for eluates from all samples except for 8 samples. There was no clear trend with respect to coal type, facility configuration or CCR type.

Antimony (Sb). Higher eluate concentration ranges were associated with fly ash samples than with gypsum samples although there were exceptions to this trend. All CCR types had samples for which eluate concentrations exceeded the MCL.

Selenium (Se). All CCR types had similar ranges in Se eluate concentrations with several fly ash and gypsum samples having notably higher Se eluate concentrations without any clear dependence on coal type or facility configuration.

Thallium (Tl). Most CCR samples had eluate concentrations that exceeded the MCL with no apparent trend with respect to coal type or facility configuration.

pH. Figure 67 presents the pH ranges (minimum and maximum) of actual samples observed in SR002.1 and SR003.1 over the pH domain $5.4 \leq \text{pH} \leq 12.4$. The closed circles represent the material's own pH. When the closed circle is outside the range $5.4 \leq \text{pH} \leq 12.4$, this means that the material's own pH was more acidic than pH 5.4. Fly ash samples exhibited own pH values ranging from acidic ($4 \leq \text{pH} \leq 6$) to moderately alkaline ($8 \leq \text{pH} \leq 11$) to highly alkaline ($11 < \text{pH}$) with a high degree of correlation with total calcium content. The own pH range for gypsum samples was between 5.5 and 8, while the range was much larger for scrubber sludges and blended CCRs.

Characterization of Coal Combustion Residues III

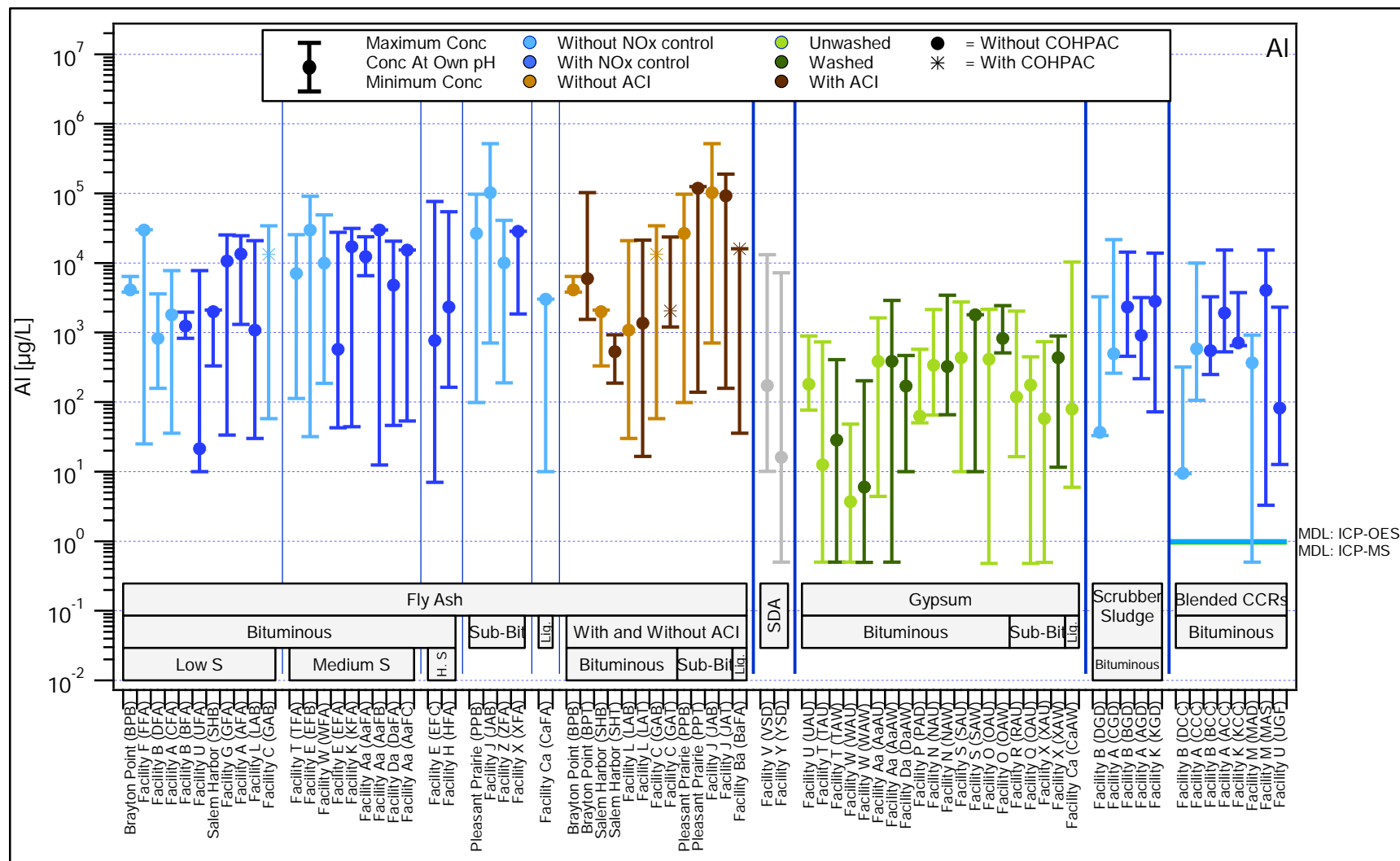


Figure 54. Aluminum. Comparison of maximum, minimum and own pH concentrations observed in SR002.1 and SR003.1 eluates over the pH domain $5.4 \leq \text{pH} \leq 12.4$. SDA samples were from facilities burning sub-bituminous coal.

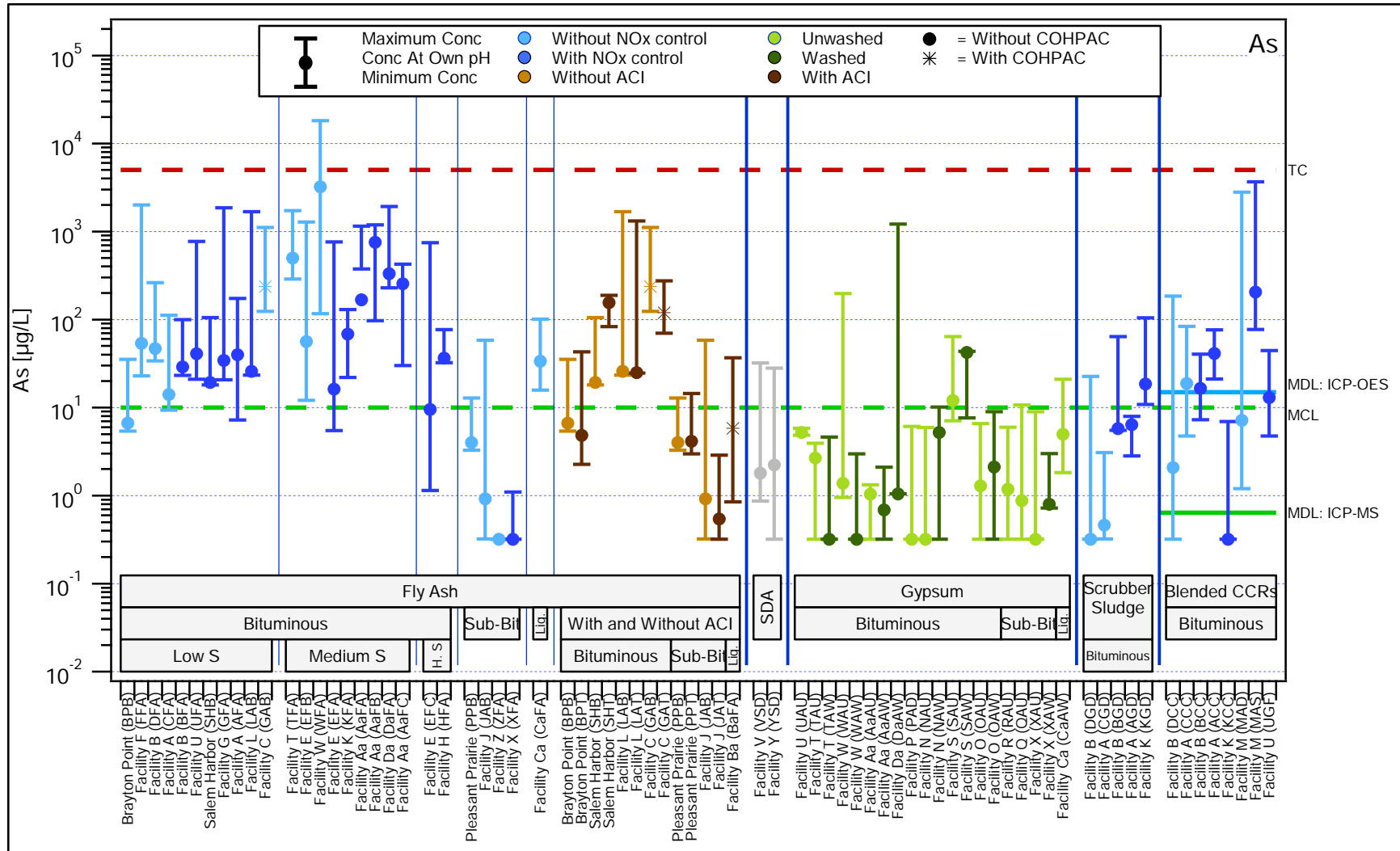


Figure 55. Arsenic. Comparison of maximum, minimum and own pH concentrations observed in SR002.1 and SR003.1 eluates over the pH domain $5.4 \leq \text{pH} \leq 12.4$. SDA samples were from facilities burning sub-bituminous coal.

Characterization of Coal Combustion Residues III

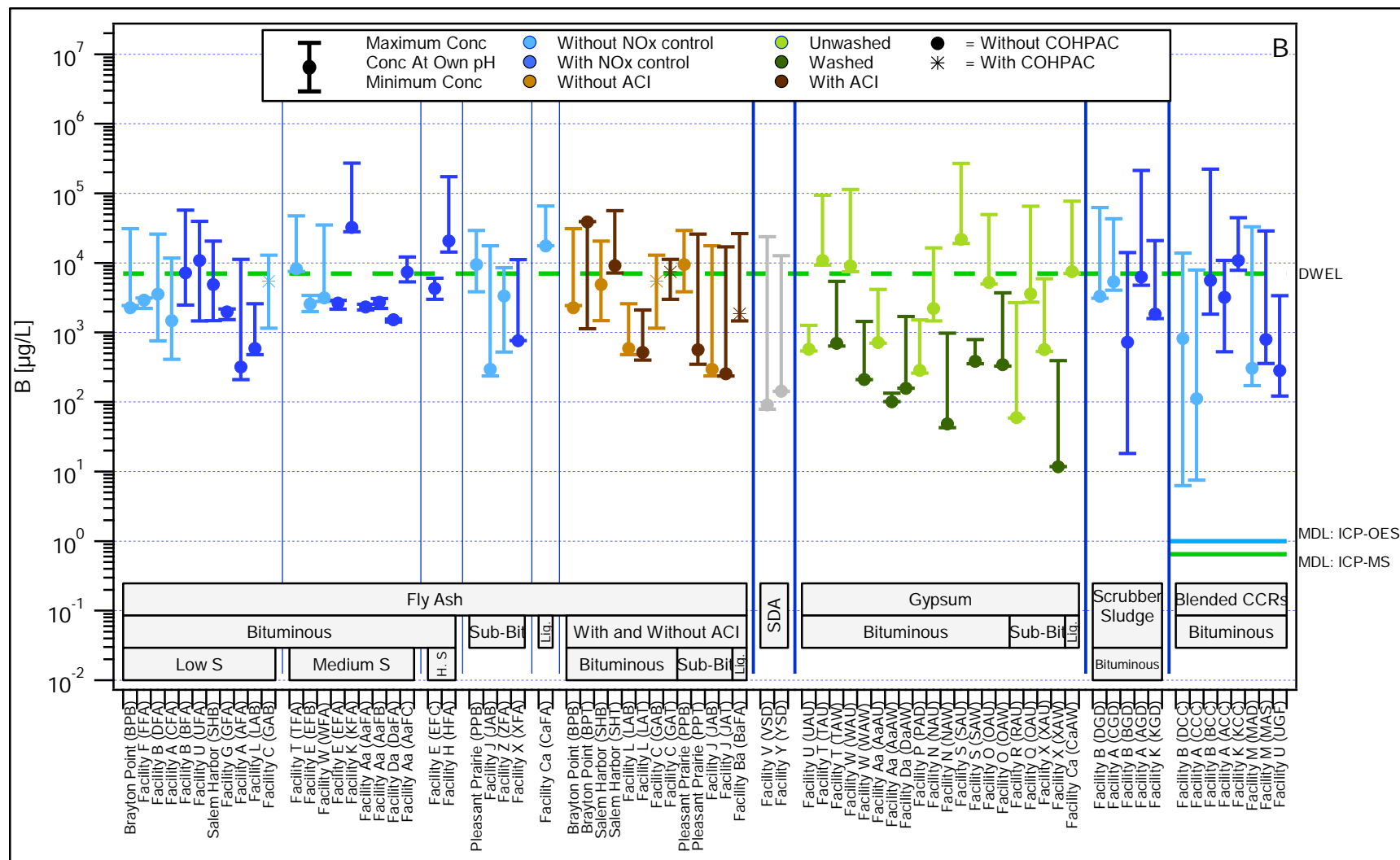


Figure 56. Boron. Comparison of maximum, minimum and own pH concentrations observed in SR002.1 and SR003.1 eluates over the pH domain 5.4 ≤pH≤ 12.4. SDA samples were from facilities burning sub-bituminous coal.

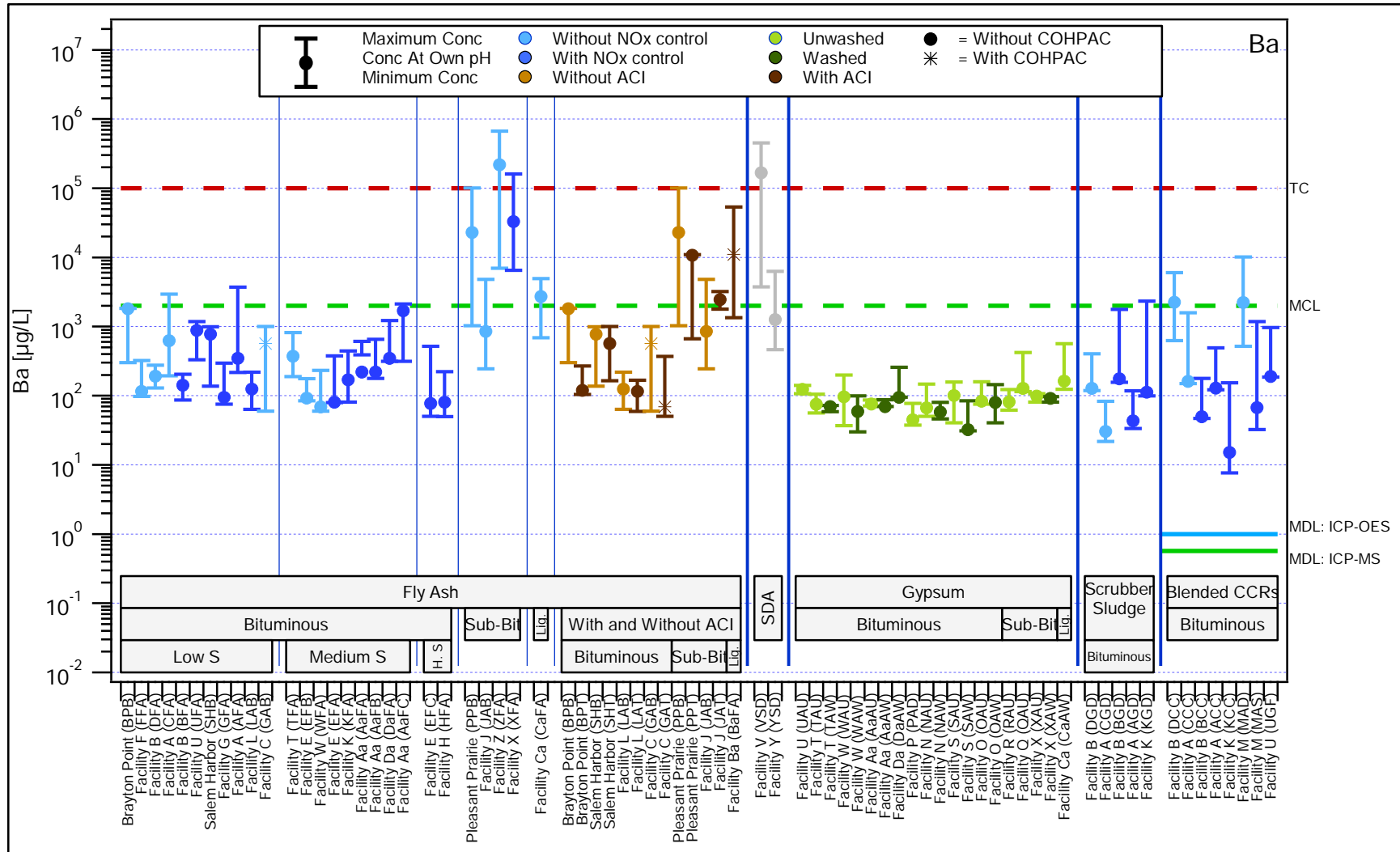


Figure 57. Barium. Comparison of maximum, minimum and own pH concentrations observed in SR002.1 and SR003.1 eluates over the pH domain 5.4 ≤ pH ≤ 12.4. SDA samples were from facilities burning sub-bituminous coal.

Characterization of Coal Combustion Residues III

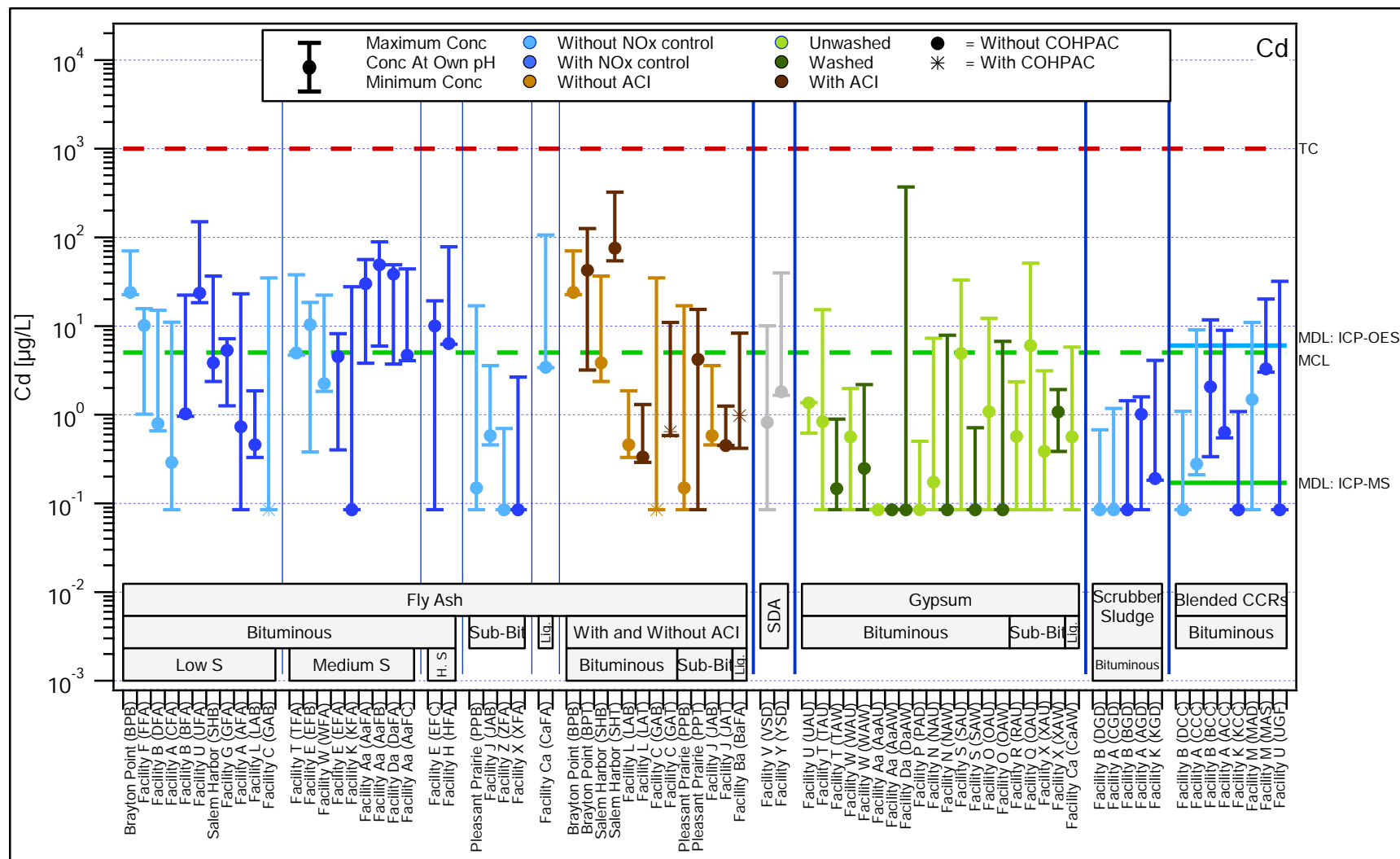


Figure 58. Cadmium. Comparison of maximum, minimum and own pH concentrations observed in SR002.1 and SR003.1 eluates over the pH domain $5.4 \leq \text{pH} \leq 12.4$. SDA samples were from facilities burning sub-bituminous coal.

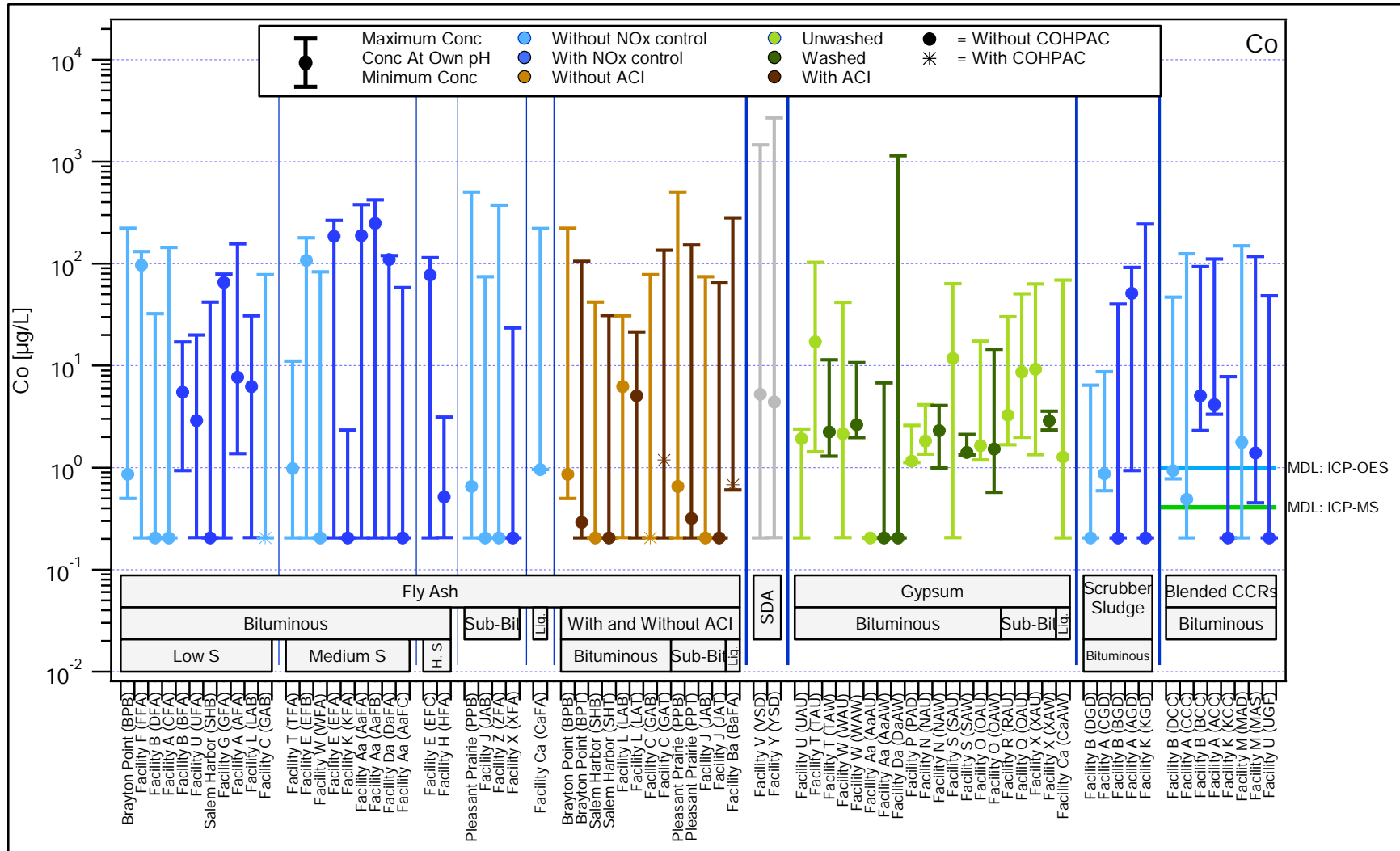


Figure 59. Cobalt. Comparison of maximum, minimum and own pH concentrations observed in SR002.1 and SR003.1 eluates over the pH domain $5.4 \leq \text{pH} \leq 12.4$. SDA samples were from facilities burning sub-bituminous coal.

Characterization of Coal Combustion Residues III

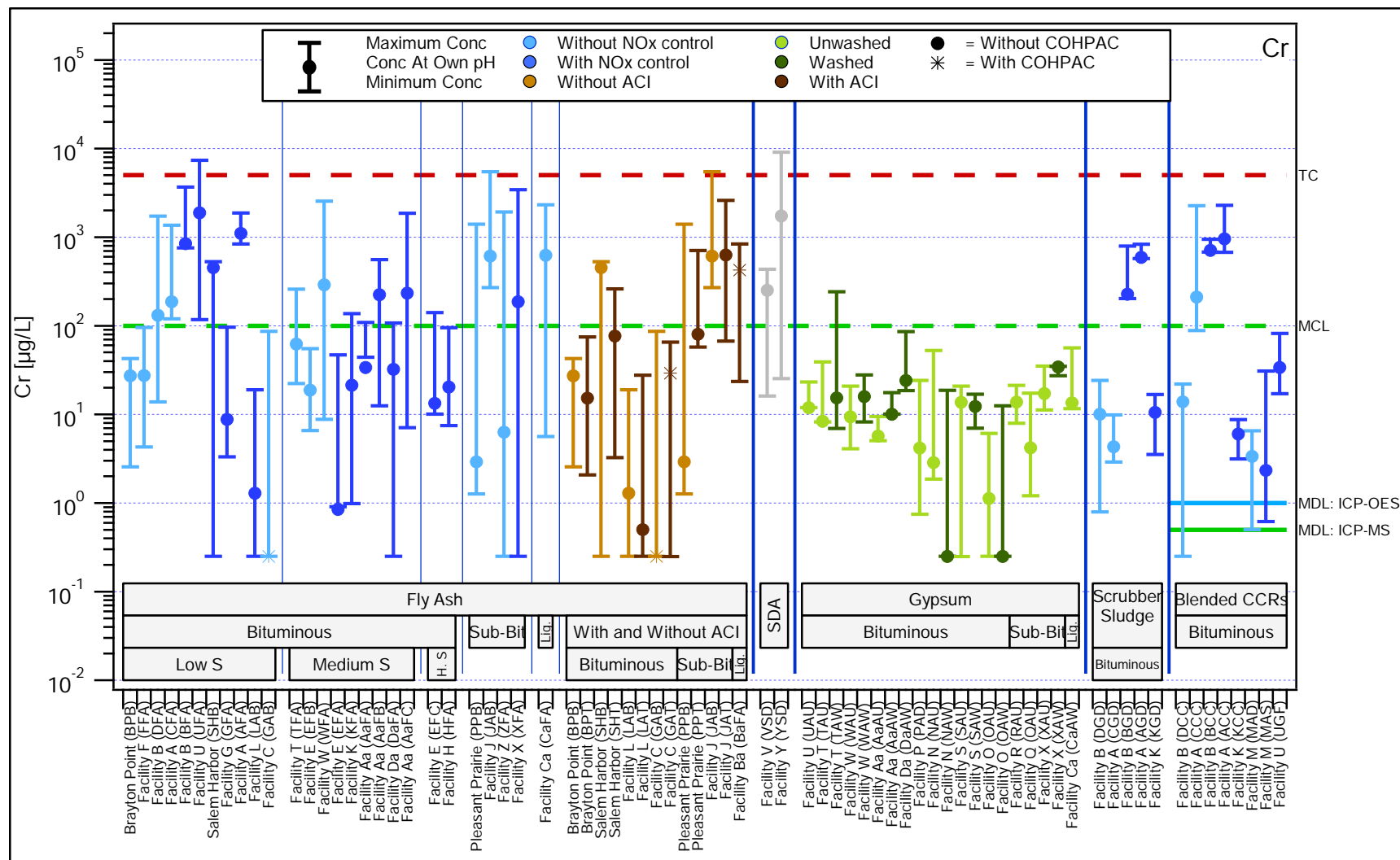


Figure 60. Chromium. Comparison of maximum, minimum and own pH concentrations observed in SR002.1 and SR003.1 eluates over the pH domain $5.4 \leq \text{pH} \leq 12.4$. SDA samples were from facilities burning sub-bituminous coal.

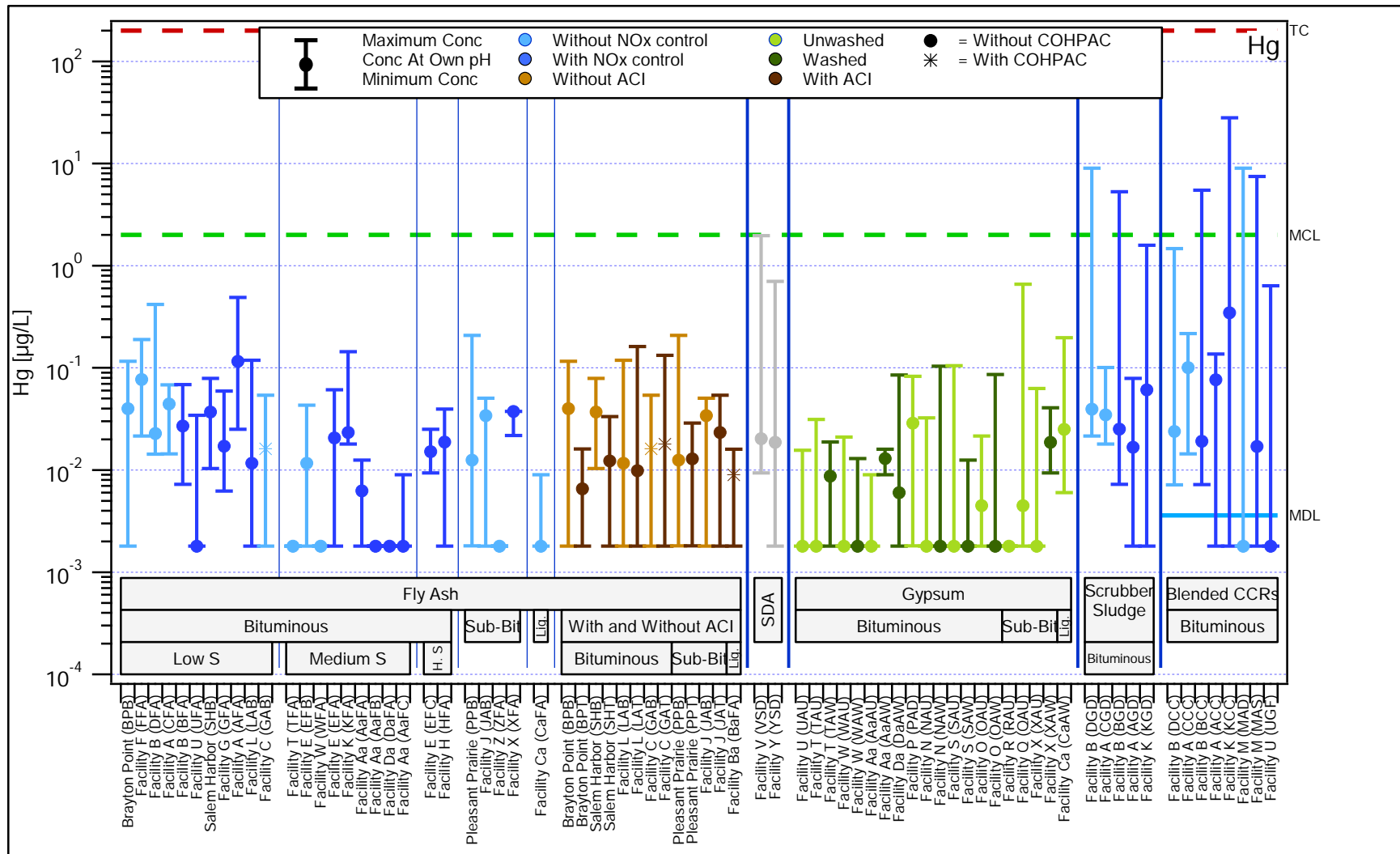


Figure 61. Mercury. Comparison of maximum, minimum and own pH concentrations observed in SR002.1 and SR003.1 eluates over the pH domain $5.4 \leq \text{pH} \leq 12.4$. SDA samples were from facilities burning sub-bituminous coal.

Characterization of Coal Combustion Residues III

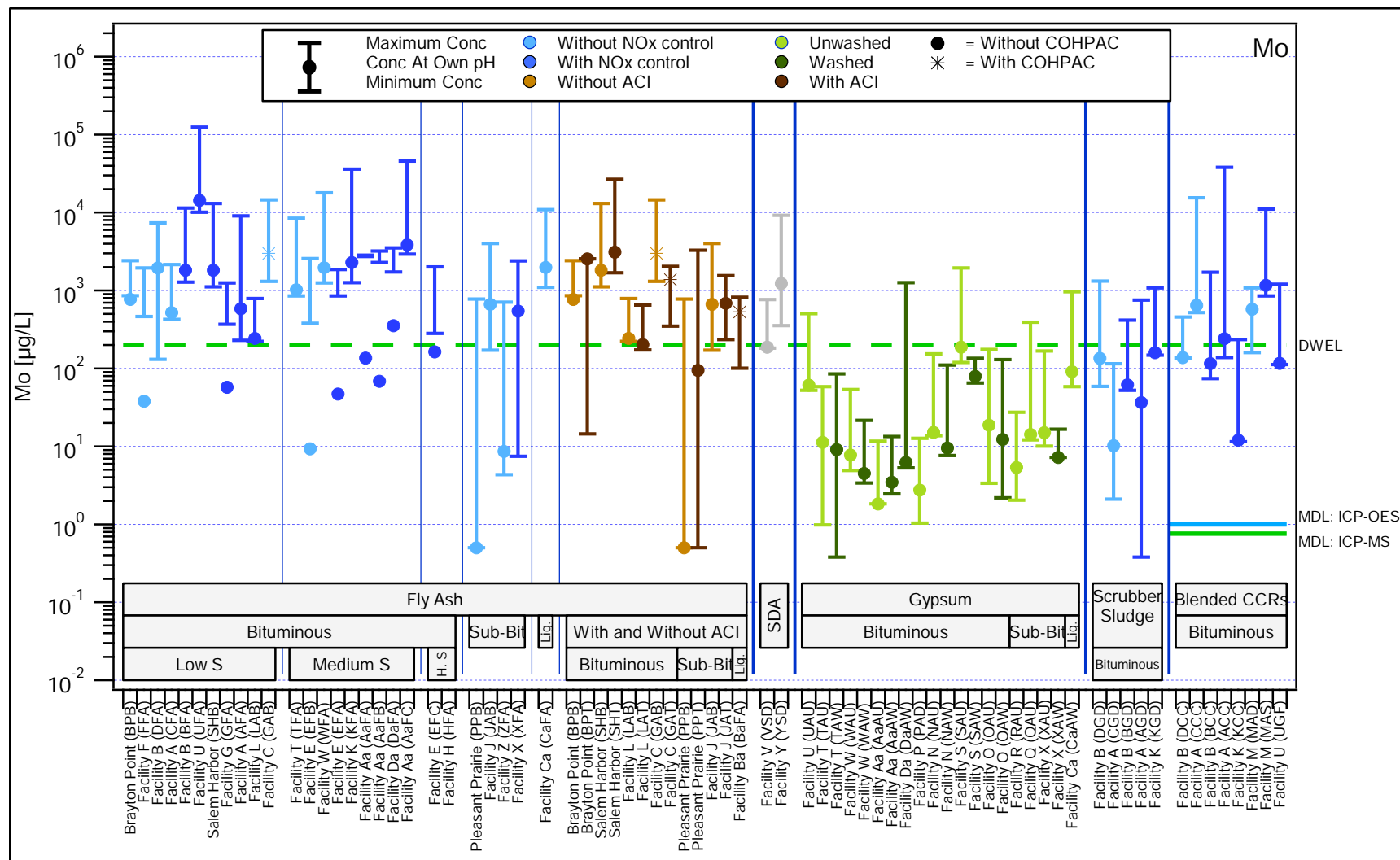


Figure 62. Molybdenum. Comparison of maximum, minimum and own pH concentrations observed in SR002.1 and SR003.1 eluates over the pH domain $5.4 \leq \text{pH} \leq 12.4$. SDA samples were from facilities burning sub-bituminous coal.

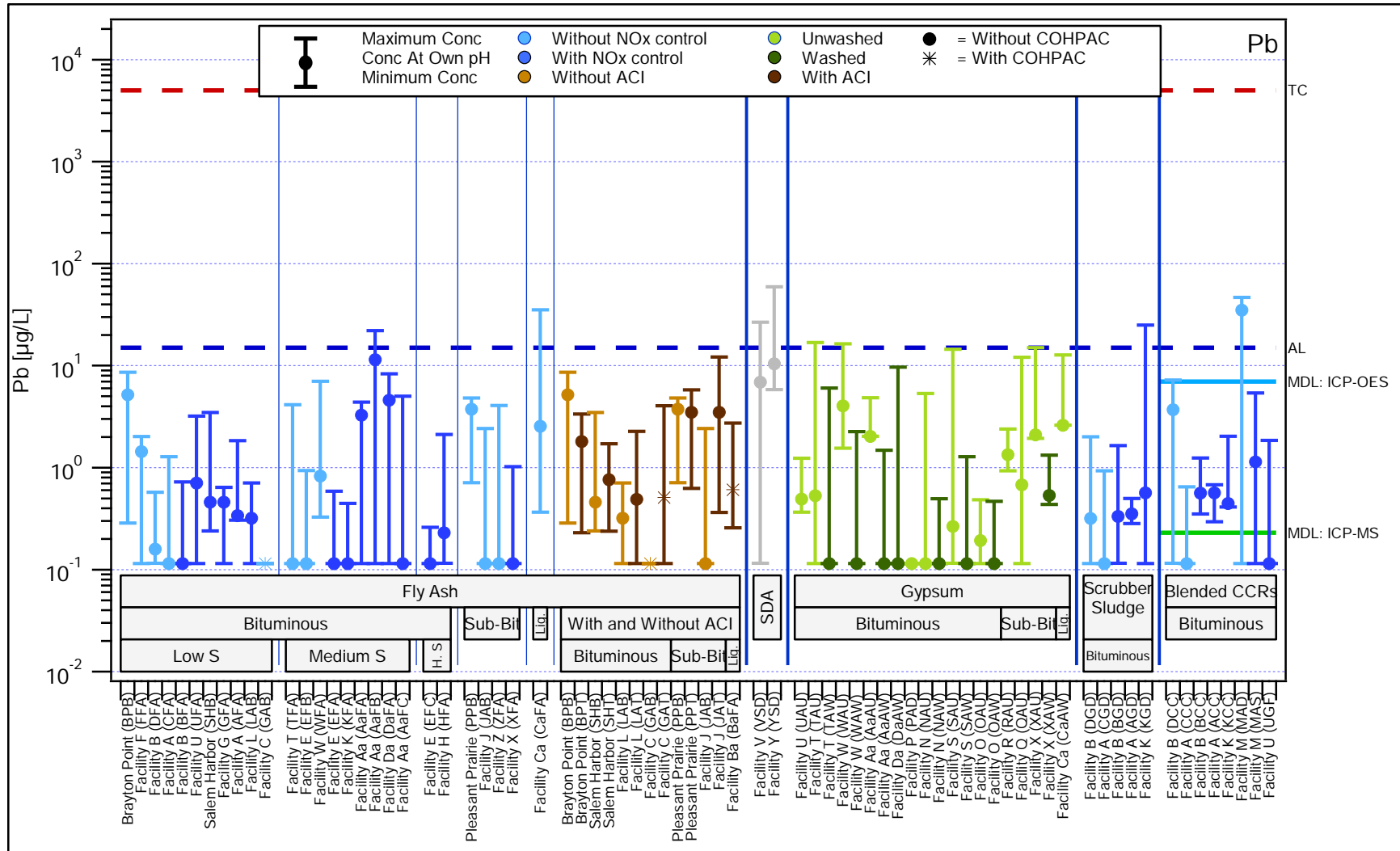


Figure 63. Lead. Comparison of maximum, minimum and own pH concentrations observed in SR002.1 and SR003.1 eluates over the pH domain $5.4 \leq \text{pH} \leq 12.4$. SDA samples were from facilities burning sub-bituminous coal.

Characterization of Coal Combustion Residues III

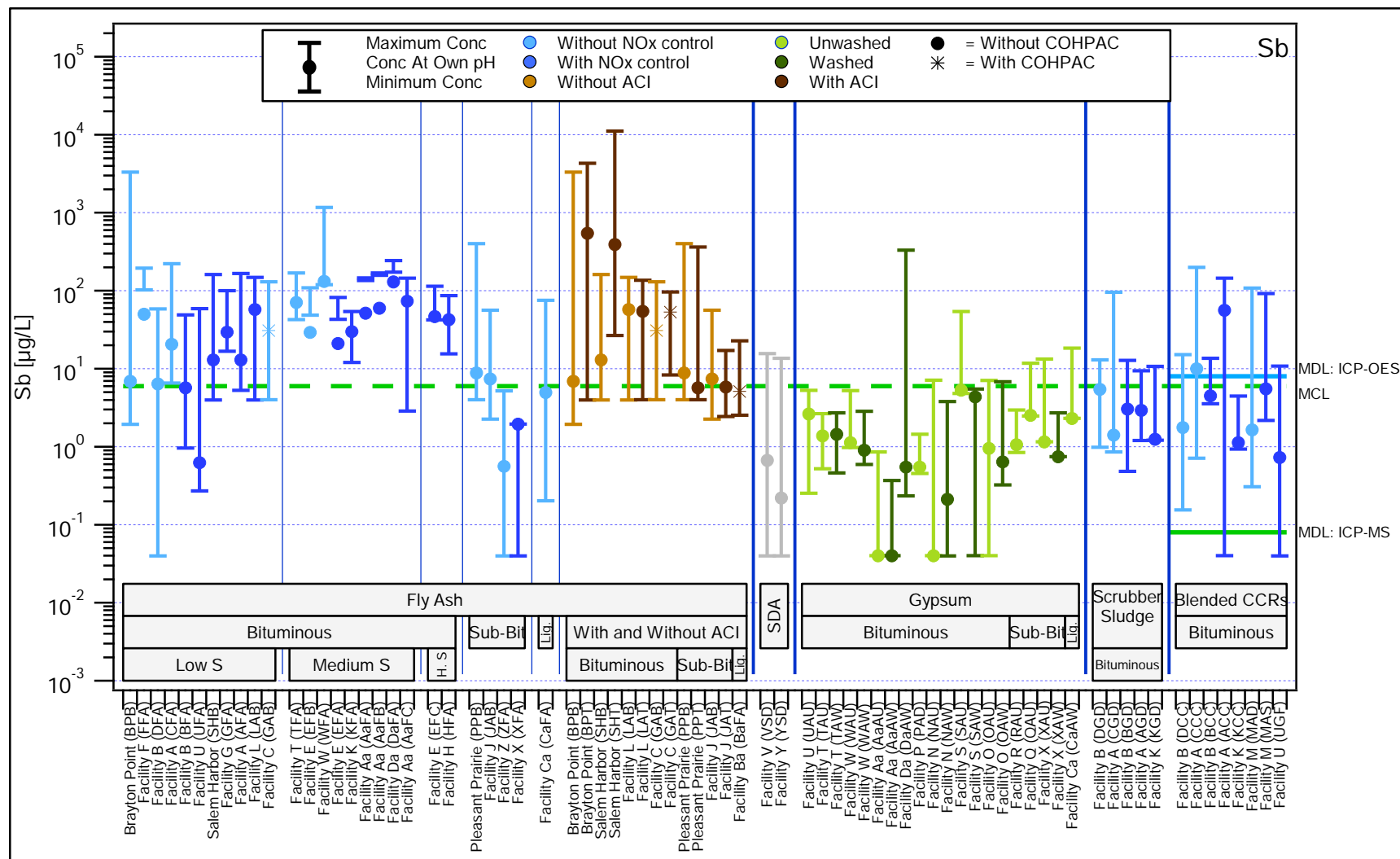


Figure 64. Antimony. Comparison of maximum, minimum and own pH concentrations observed in SR002.1 and SR003.1 eluates over the pH domain $5.4 \leq \text{pH} \leq 12.4$. SDA samples were from facilities burning sub-bituminous coal.

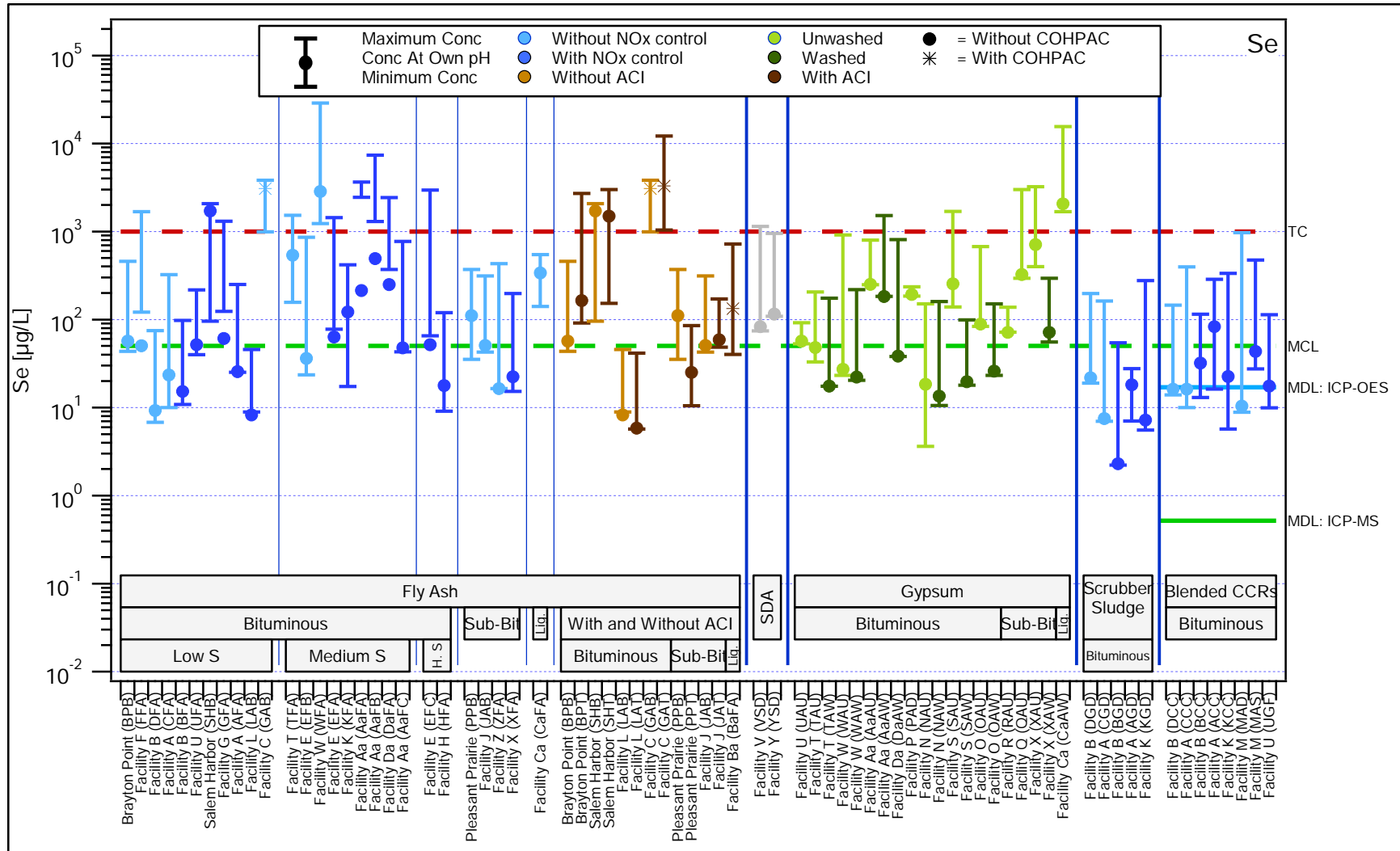


Figure 65. Selenium. Comparison of maximum, minimum and own pH concentrations observed in SR002.1 and SR003.1 eluates over the pH domain $5.4 \leq \text{pH} \leq 12.4$. SDA samples were from facilities burning sub-bituminous coal.

Characterization of Coal Combustion Residues III

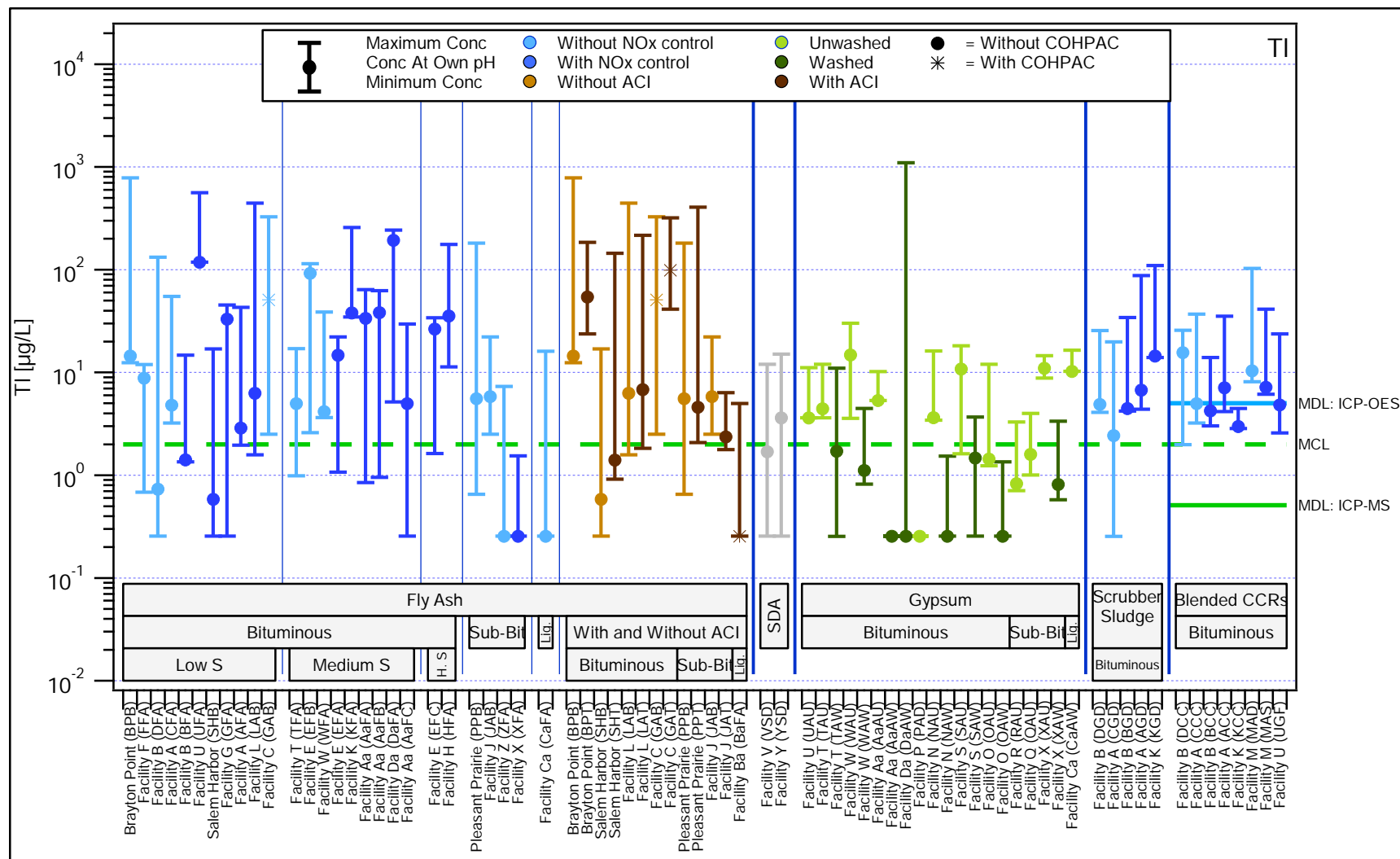


Figure 66. Thallium. Comparison of maximum, minimum and own pH concentrations observed in SR002.1 and SR003.1 eluates over the pH domain $5.4 \leq \text{pH} \leq 12.4$. SDA samples were from facilities burning sub-bituminous coal.

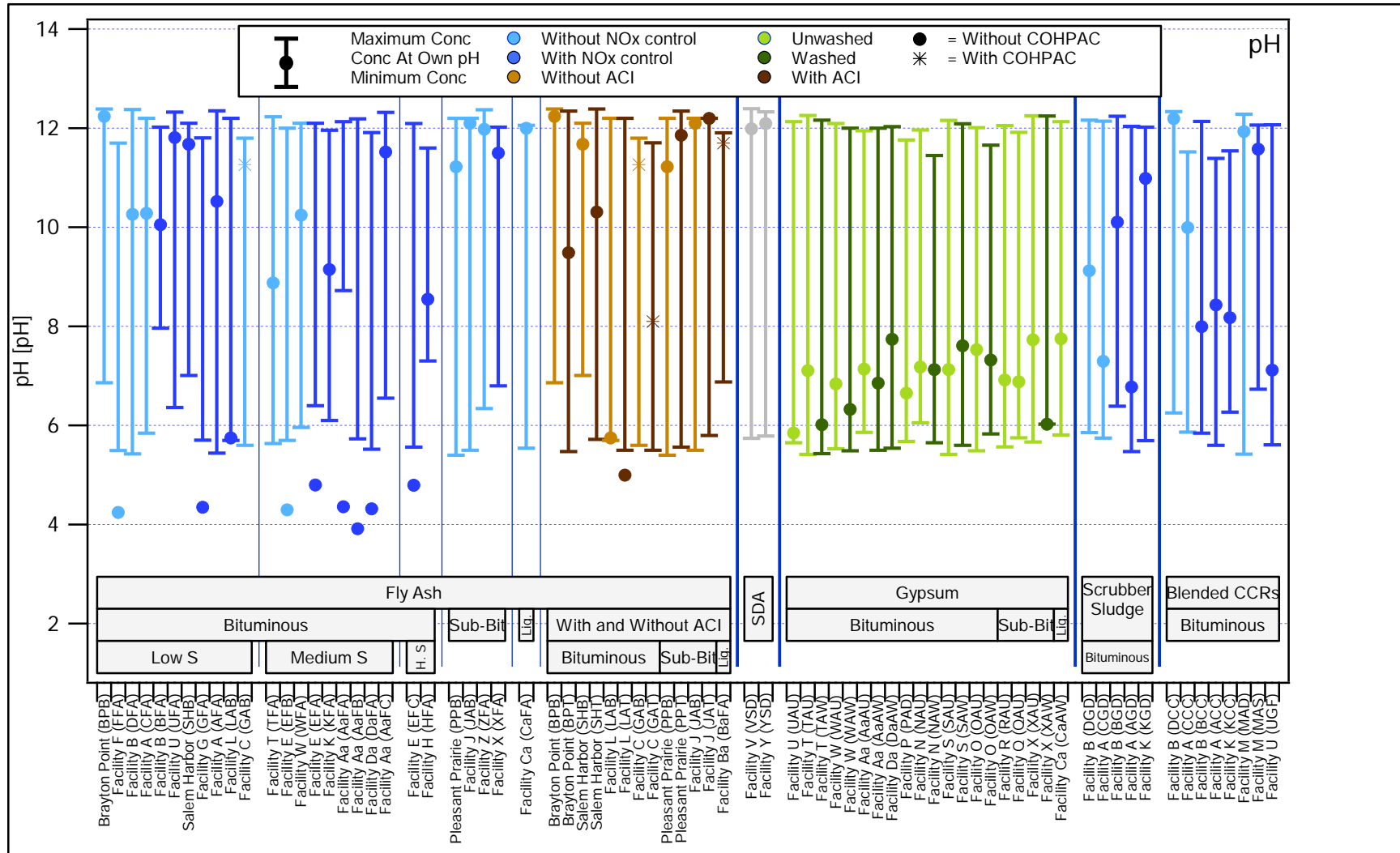


Figure 67. pH. Comparison of maximum, minimum and own pH observed in SR002.1 and SR003.1 eluates over the pH domain $5.4 \leq \text{pH} \leq 12.4$. SDA samples were from facilities burning sub-bituminous coal.

3.2.3. Leaching Dependency on Total Content

An on-going question has been whether or not total content of an element in a CCR sample is a useful indicator of potential environmental impact by leaching. This question was evaluated by comparing for the COPCs (i) the maximum eluate concentration over the pH domain $5.4 \leq \text{pH} \leq 12.4$ with the total content by digestion (Figure 68 to Figure 79), and (ii) the eluate concentration at own pH with the total content by digestion (results not shown). The maximum eluate concentration as a function of total content is presented in Figure 68 to Figure 79 because in understanding the meaning of research results, the focus is often on the potential for exceedance of a particular threshold value. However, results of own pH eluate concentration as a function of total content were similar. Results are annotated on Figure 69 (arsenic) for illustration purposes.

Each of these figures show (i) there is a poor correlation between leachate concentration and total content of any of the elements considered, (ii) a wide range of total content values (over more than one order of magnitude) can result in the same or very similar eluate concentrations, and (iii) a wide range of eluate concentrations (over more than one order of magnitude) can be observed for CCRs with similar total content values. If leaching correlated closely with total concentration, the data on these figures would be expected to show strong linearity, and relatively less scatter. Thus, it is clear that leaching phenomena is controlled by complex solid-liquid partitioning chemistry and that total content is not a good indicator of leaching. Furthermore, the absence of a linear or unique monotonic relationship between total content and eluate concentrations indicates that representation of leaching as a linear partitioning phenomenon (i.e., the linear distribution coefficient, K_d , approach) is not appropriate.

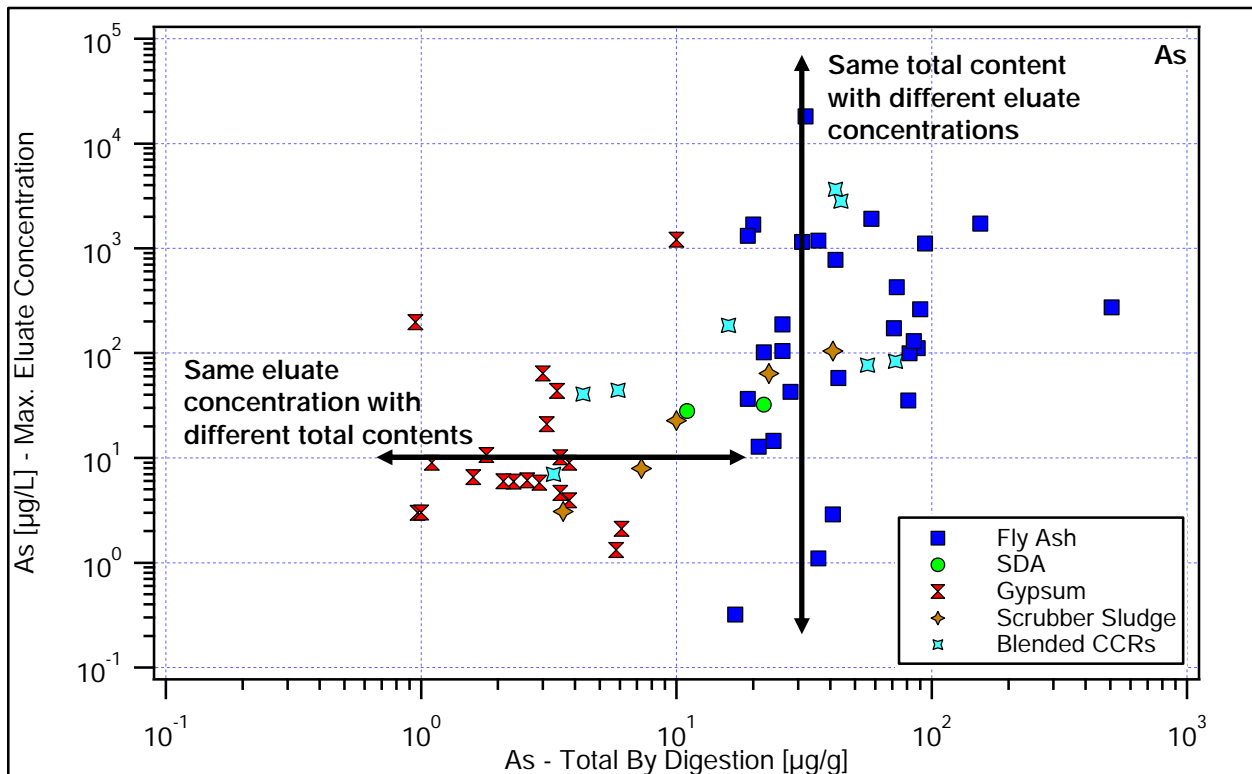
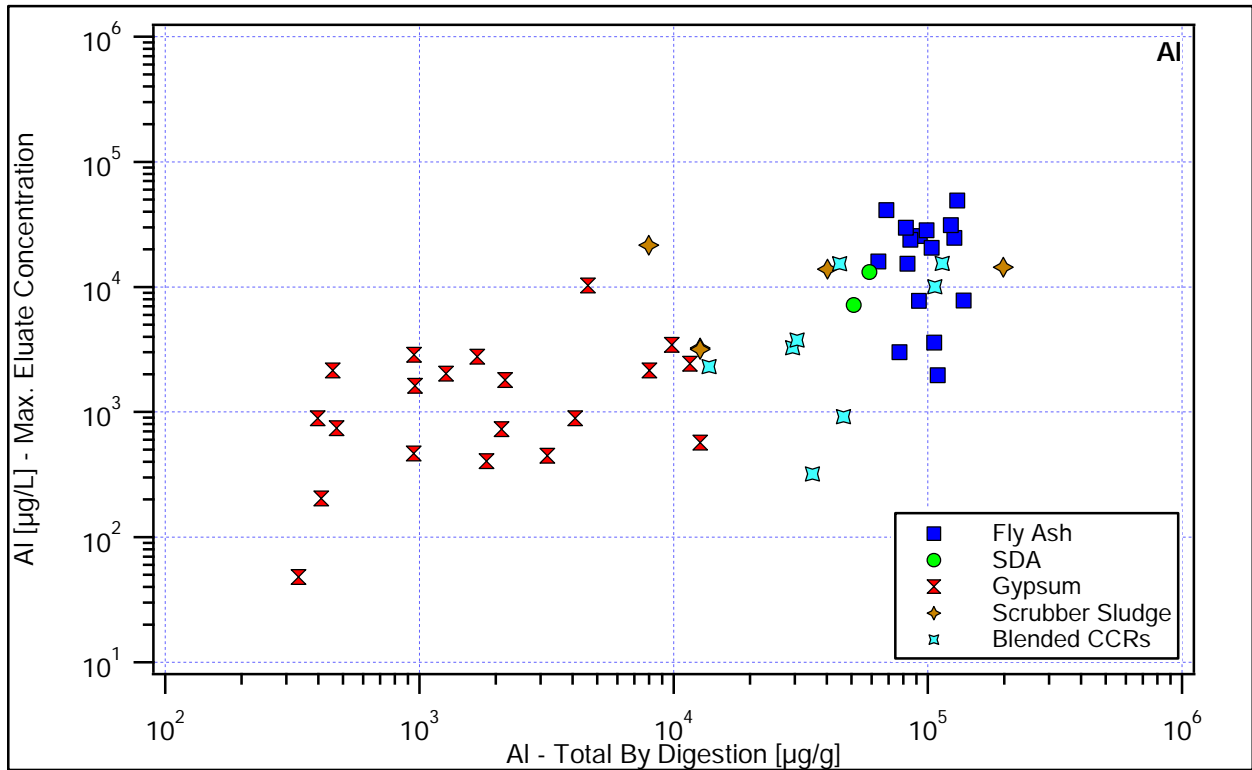


Figure 68 and Figure 69. Aluminum and Arsenic. Maximum eluate concentration ($5.4 \leq \text{pH} \leq 12.4$) as a function of total content by digestion.

Characterization of Coal Combustion Residues III

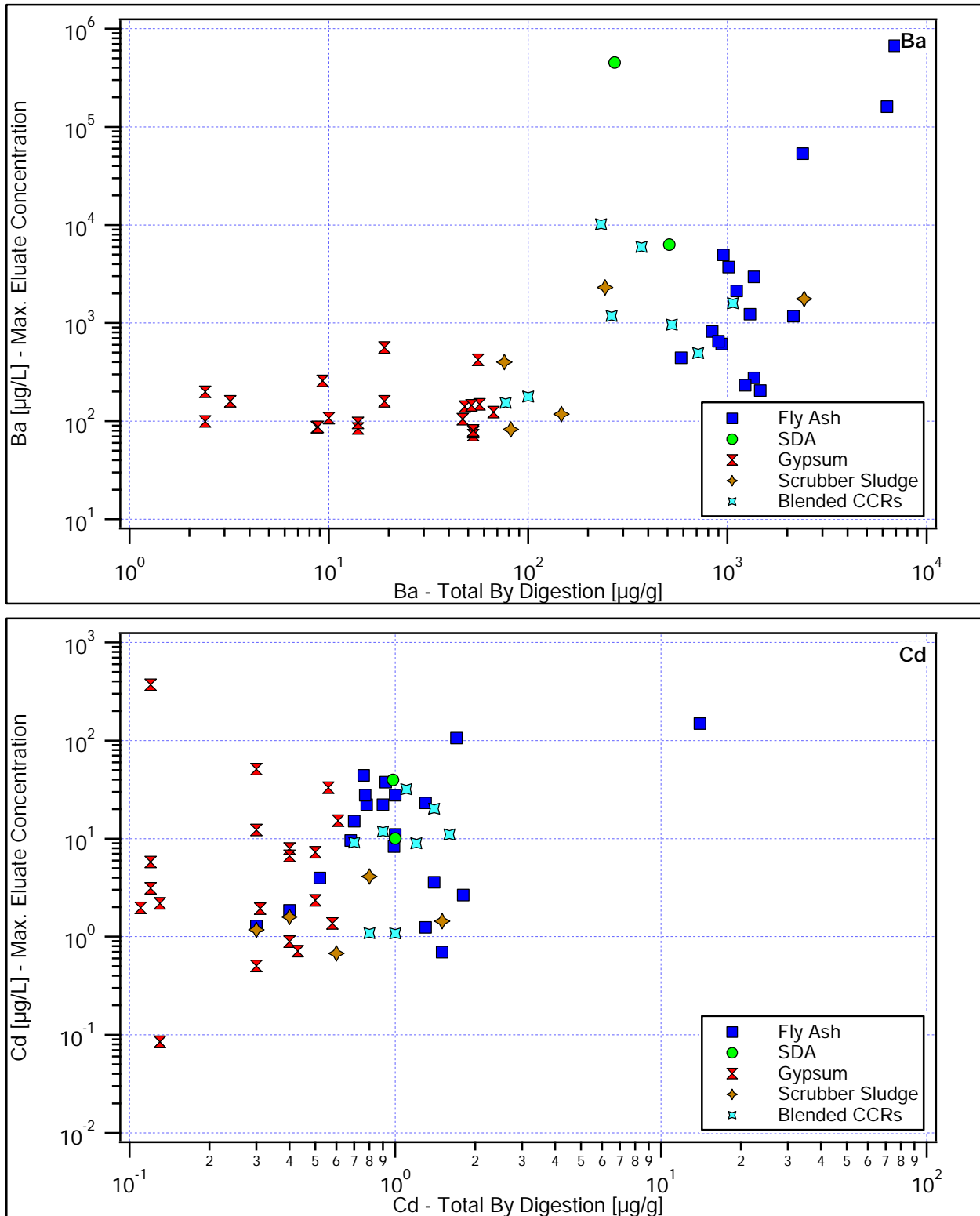


Figure 70 and Figure 71. Barium and Cadmium. Maximum eluate concentration ($5.4 \leq \text{pH} \leq 12.4$) as a function of total content by digestion.

Characterization of Coal Combustion Residues III

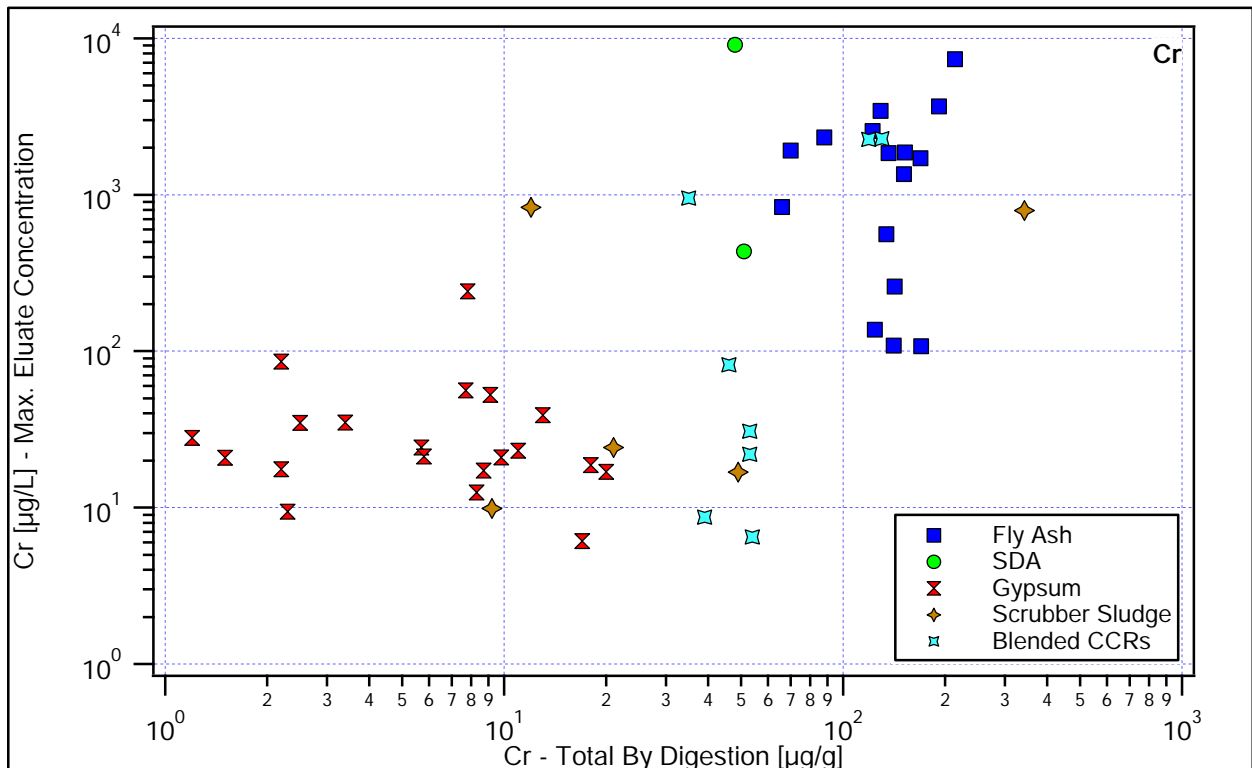
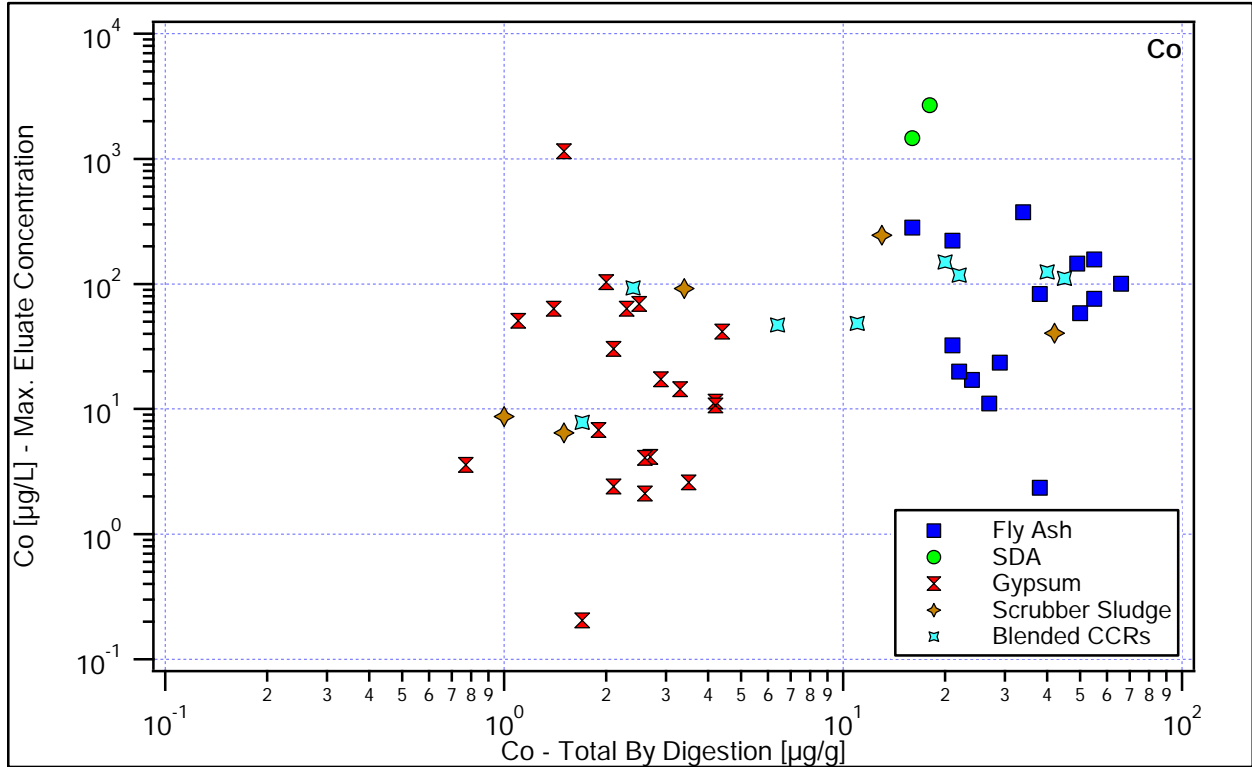


Figure 72 and Figure 73. Cobalt and Chromium. Maximum eluate concentration (5.4 ≤ pH ≤ 12.4) as a function of total content by digestion.

Characterization of Coal Combustion Residues III

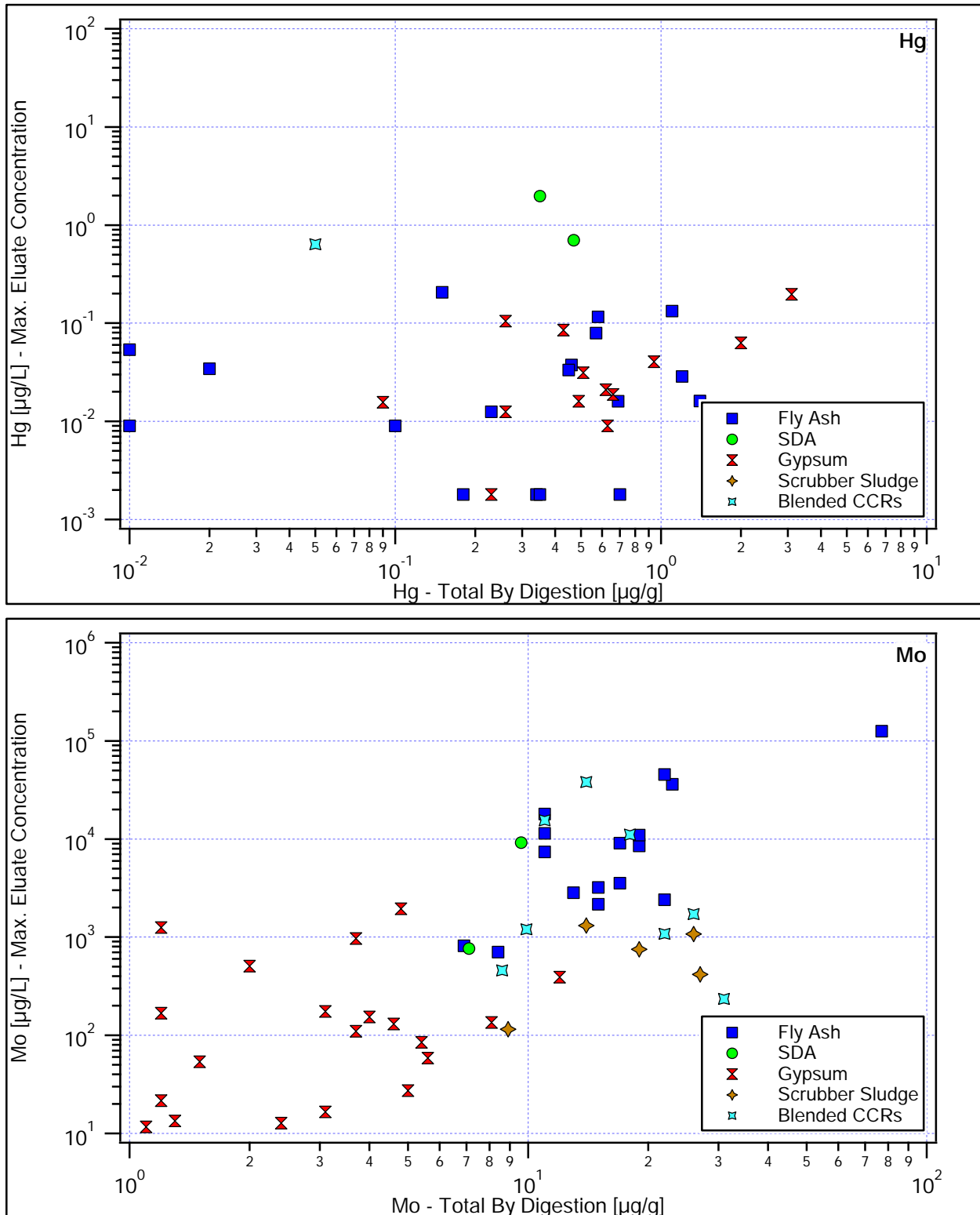


Figure 74 and Figure 75. Mercury and Molybdenum. Maximum eluate concentration ($5.4 \leq \text{pH} \leq 12.4$) as a function of total content by digestion.

Characterization of Coal Combustion Residues III

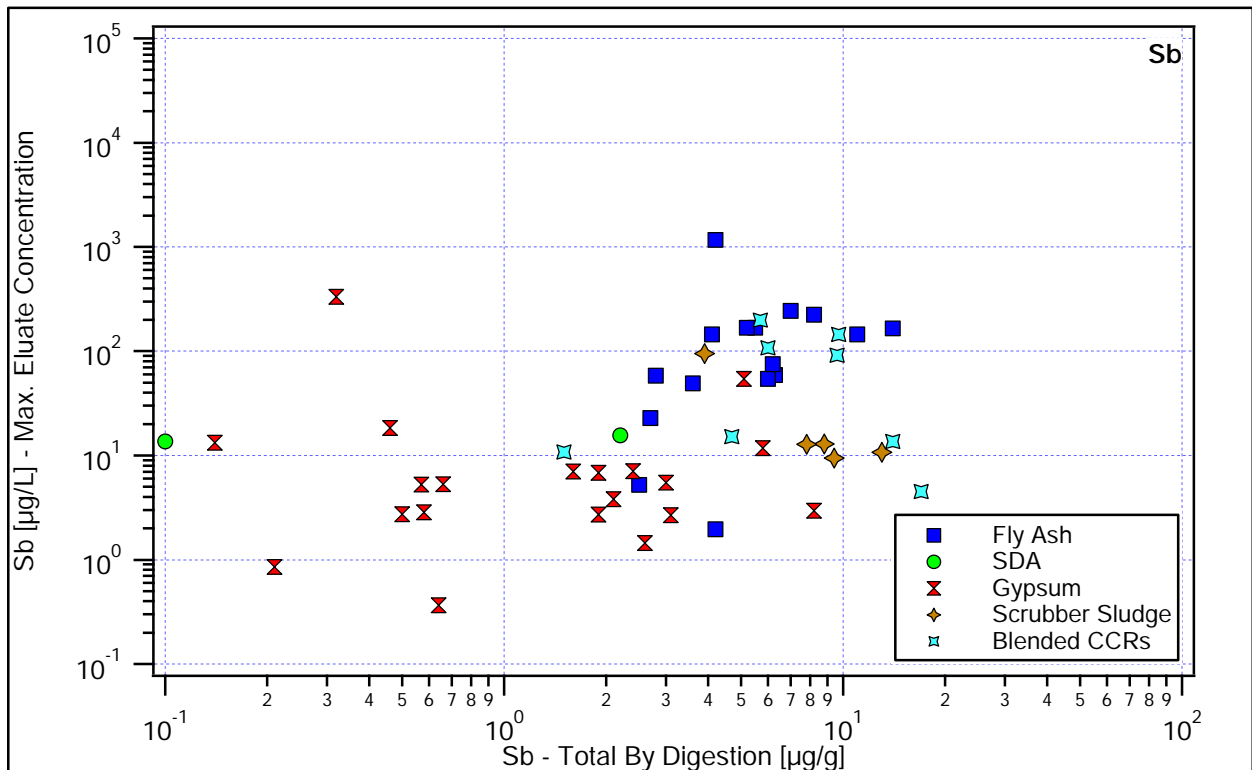
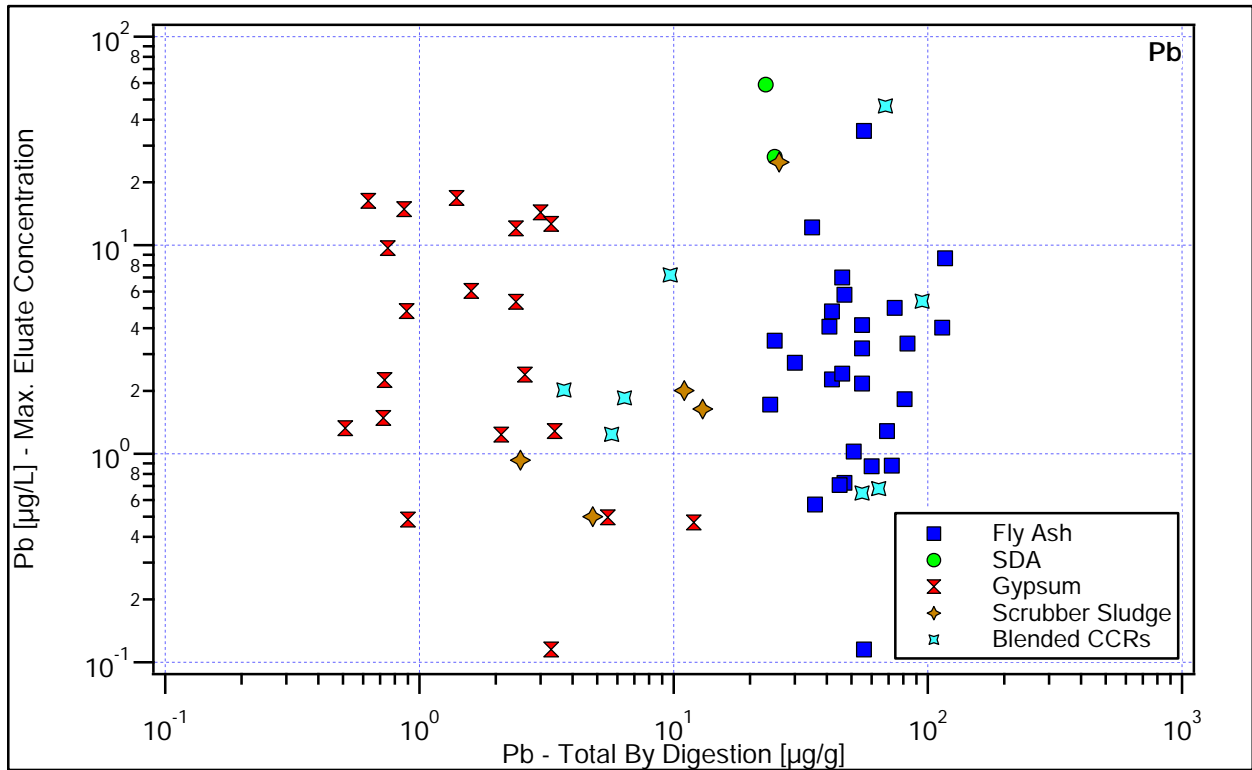


Figure 76 and Figure 77. Lead and Antimony. Maximum eluate concentration ($5.4 \leq \text{pH} \leq 12.4$) as a function of total content by digestion.

Characterization of Coal Combustion Residues III

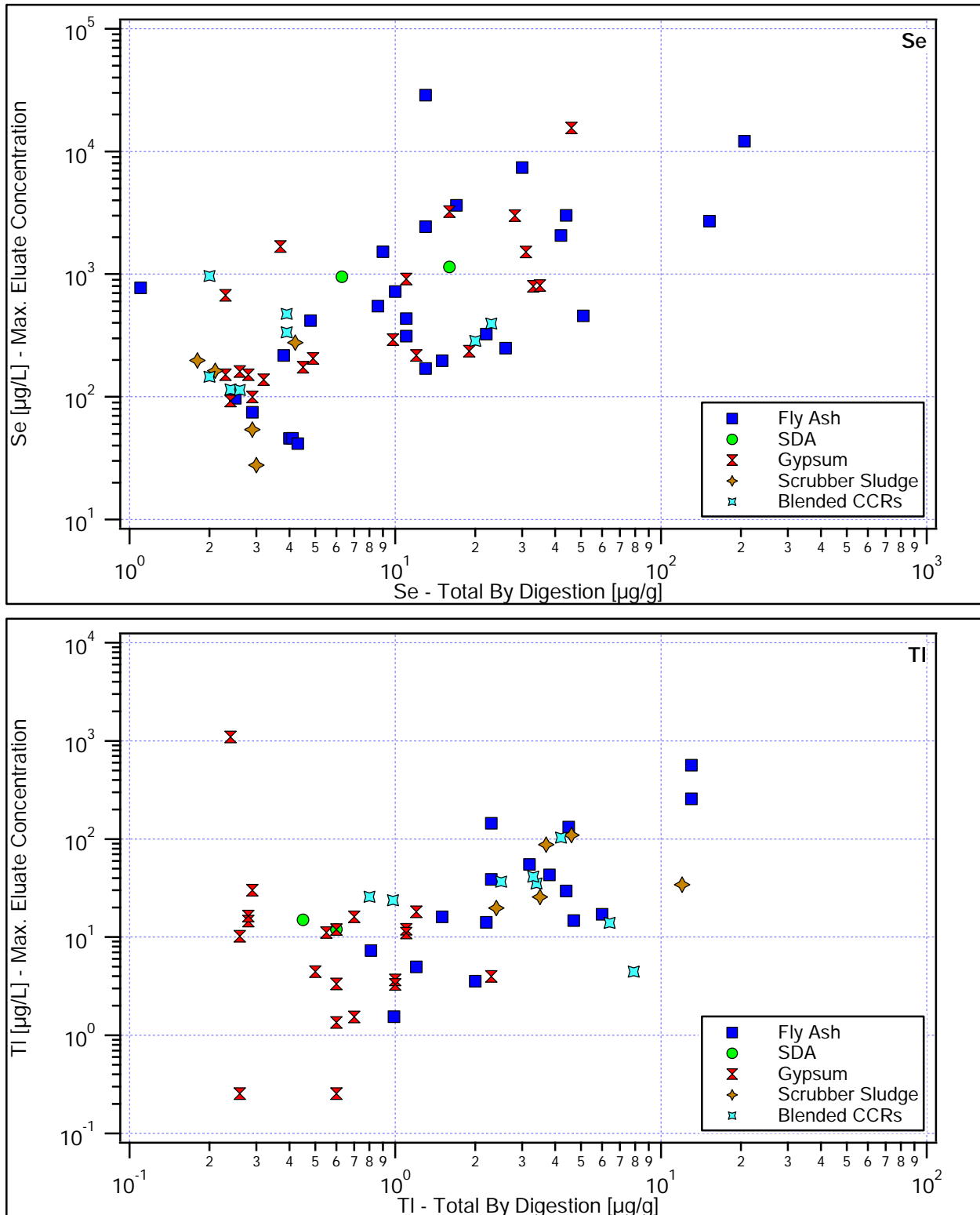


Figure 78 and Figure 79. Selenium and Thallium. Maximum eluate concentration ($5.4 \leq \text{pH} \leq 12.4$) as a function of total content by digestion.

3.2.4. pH at the Maximum Concentration Value versus the Materials' Own pH

Figure 81 through Figure 93 plot the pH at which the maximum eluate concentration for a CCR sample occurs over the domain $5.4 \leq \text{pH} \leq 12.4$ as a function of the own pH for the same sample. Results for arsenic are annotated as Figure 80. The diagonal gray line indicates a slope equal to one; when a data point falls on or near (within the light gray band) this line, the maximum eluate concentration occurs at or near the own pH for the specific CCR sample. Data points indicated with an open symbol have maximum eluate concentrations that are less than either the MCL or DWEL as indicated for the element of interest. Data points indicated with a filled symbol have maximum eluate concentrations that are greater than either the MCL or DWEL. When a sample falls above the gray diagonal line, processes that result in increased elution pH (e.g., mixing with other materials such as lime, other CCRs or other alkaline materials) are indicated to lead to increased leachate concentration for that element. When a sample falls below the gray diagonal line, processes that result in decreased elution pH (e.g., mixing with other more acidic materials or uptake of atmospheric carbon dioxide) are indicated to lead to increased leachate concentration for that element. For example, uptake of atmospheric carbon dioxide (carbonation) occurs when pore solution pH is greater than 8, with the most pronounced effect when pore solution pH is greater than 10. Carbonation results in decreases in pH typically to between 8 and 9. These potential changes must be qualified with the caveat that changes that result in increased or decreased elution pH may also result in significantly changed chemistry (e.g., redox changes) that may also influence leaching.

Important observations from these figures include:

1. Often the maximum eluate concentration occurs at a pH other than the material's own pH, regardless of the element or material being evaluated.
2. The maximum eluate concentration varies over a wide range in pH and is different for different CCR types and elements. This indicates that there is not a single pH for which testing is likely to provide confidence in release estimates over a wide range of disposal and beneficial use options, emphasizing the benefit of multi-pH testing.
3. Multi-pH testing provides useful insights into the CCR management scenarios that have the potential to increase release of specific constituents beyond that indicated by monofill management scenarios.

Characterization of Coal Combustion Residues III

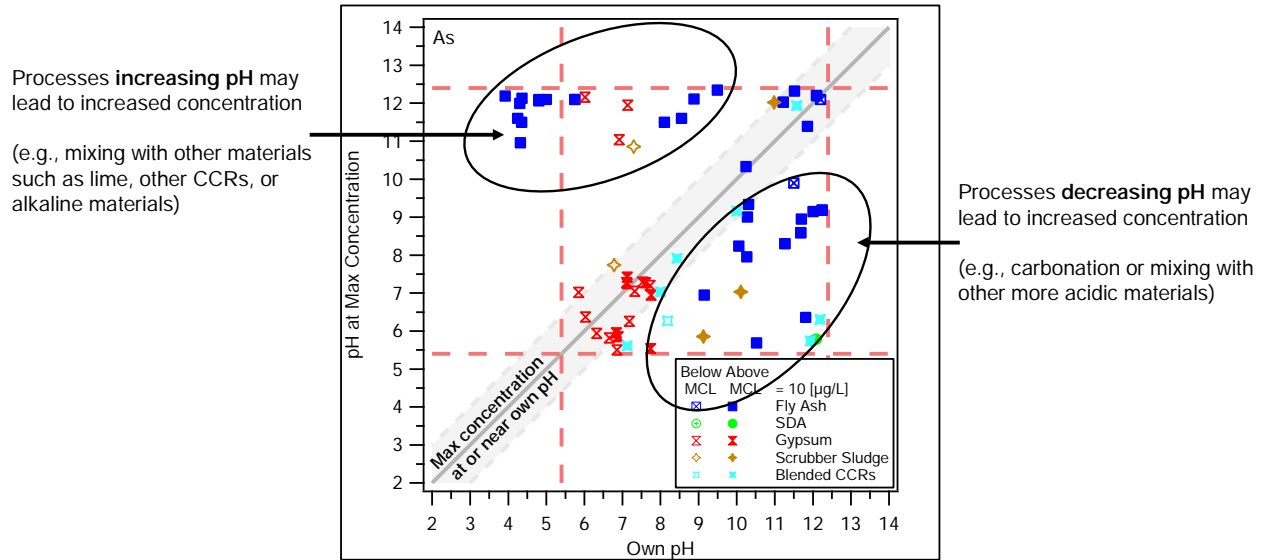


Figure 80. An example of pH identity plot. Dashed red lines are used to indicate the pH domain of 5.4 to 12.4.

Characterization of Coal Combustion Residues III

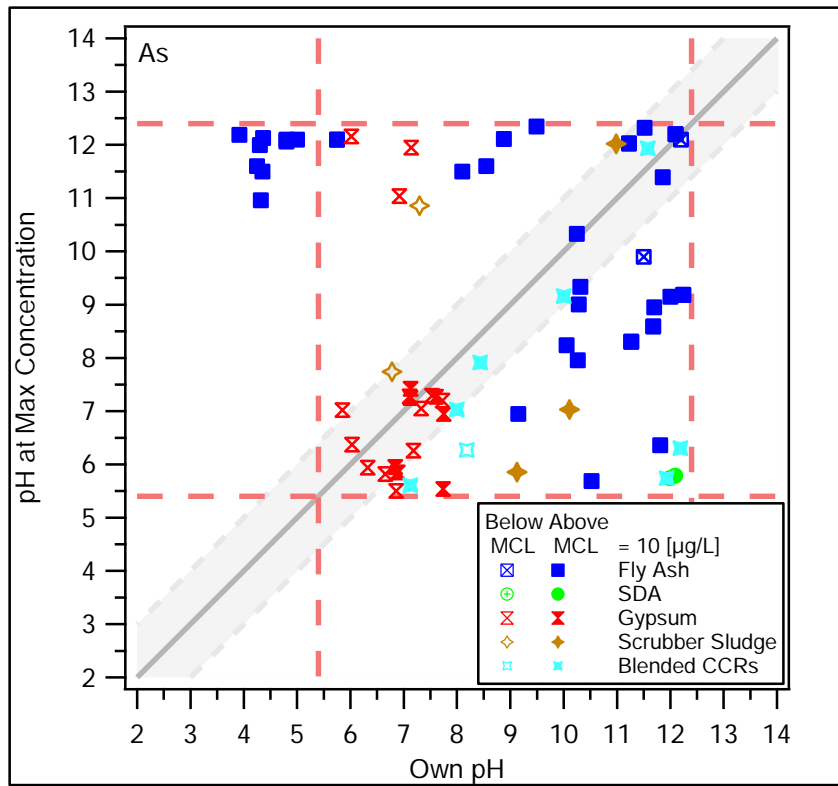
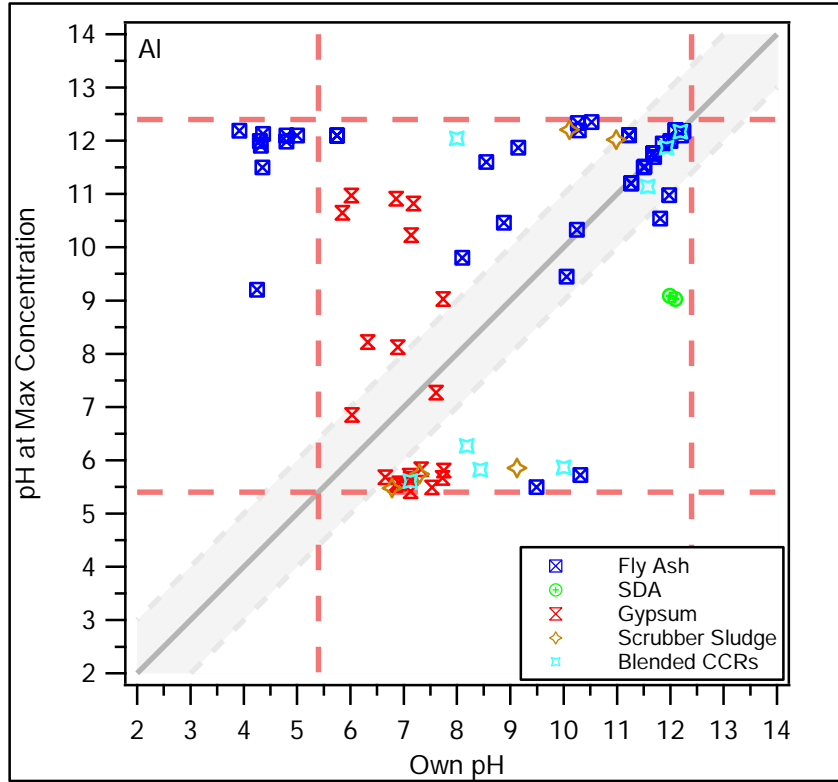


Figure 81 and Figure 82. Aluminum and Arsenic. pH identity plots.

Characterization of Coal Combustion Residues III

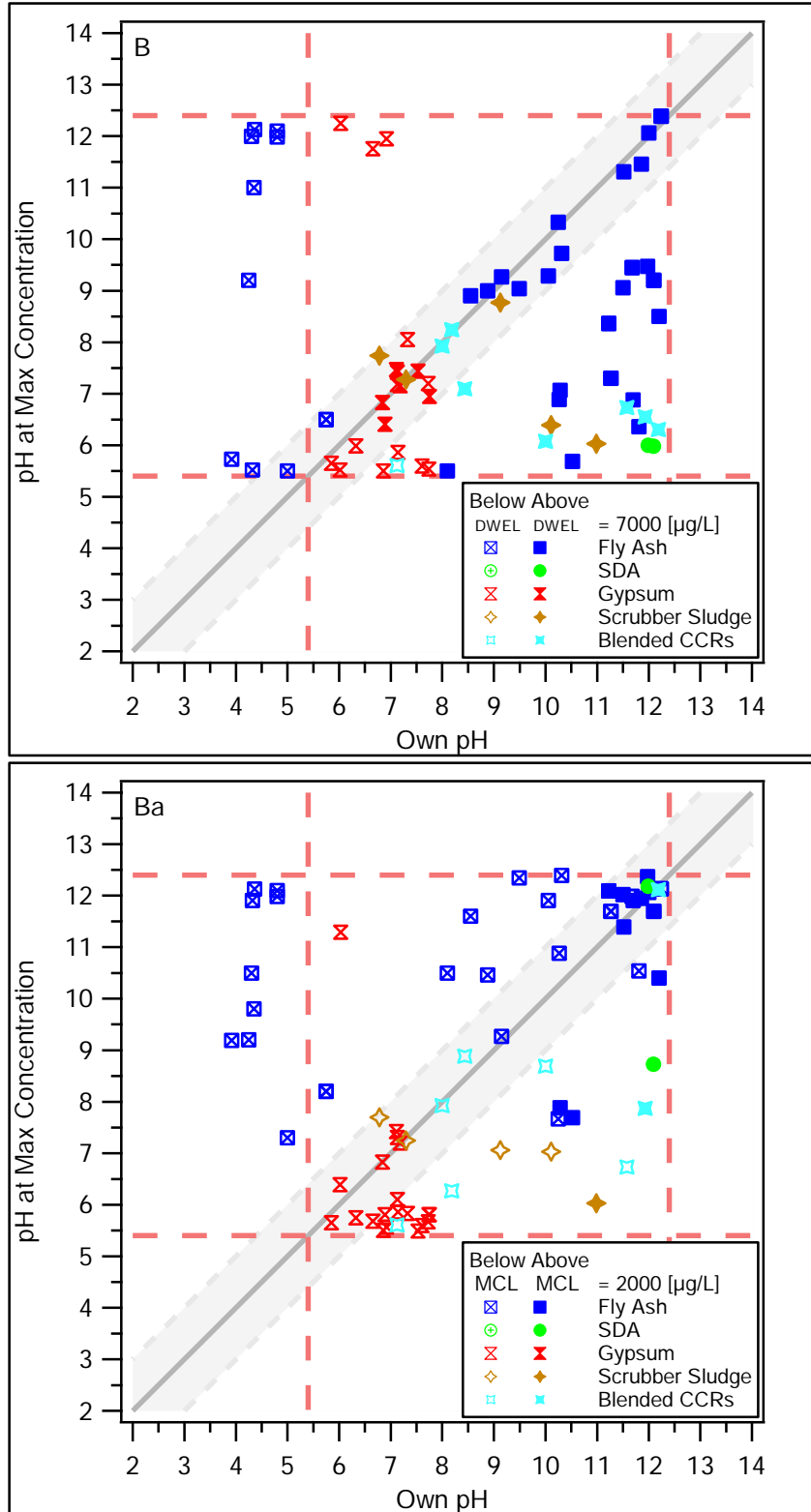


Figure 83 and Figure 84. Boron and Barium. pH identity plots.

Characterization of Coal Combustion Residues III

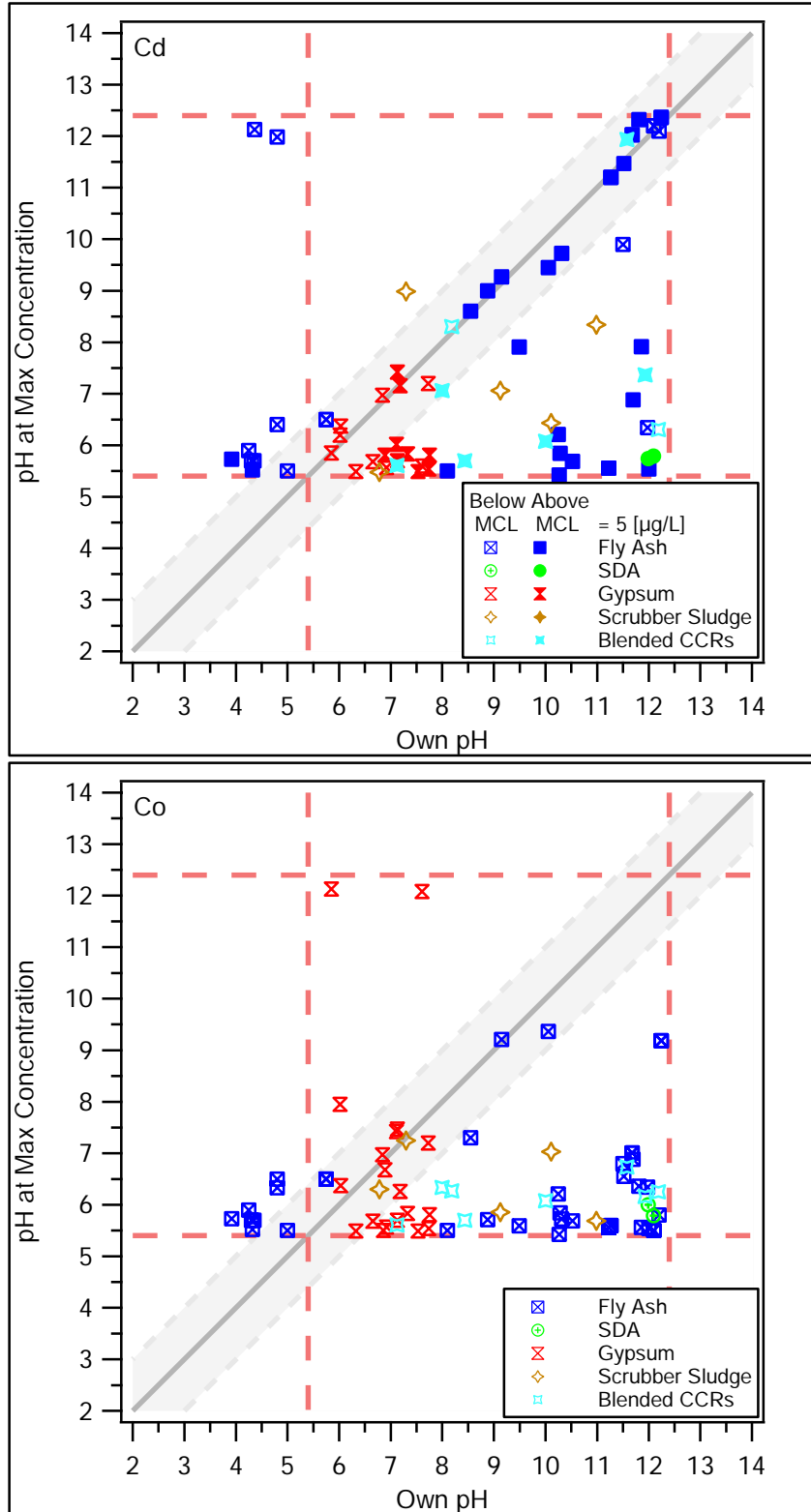


Figure 85 and Figure 86. Cadmium and Cobalt. pH identity plots.

Characterization of Coal Combustion Residues III

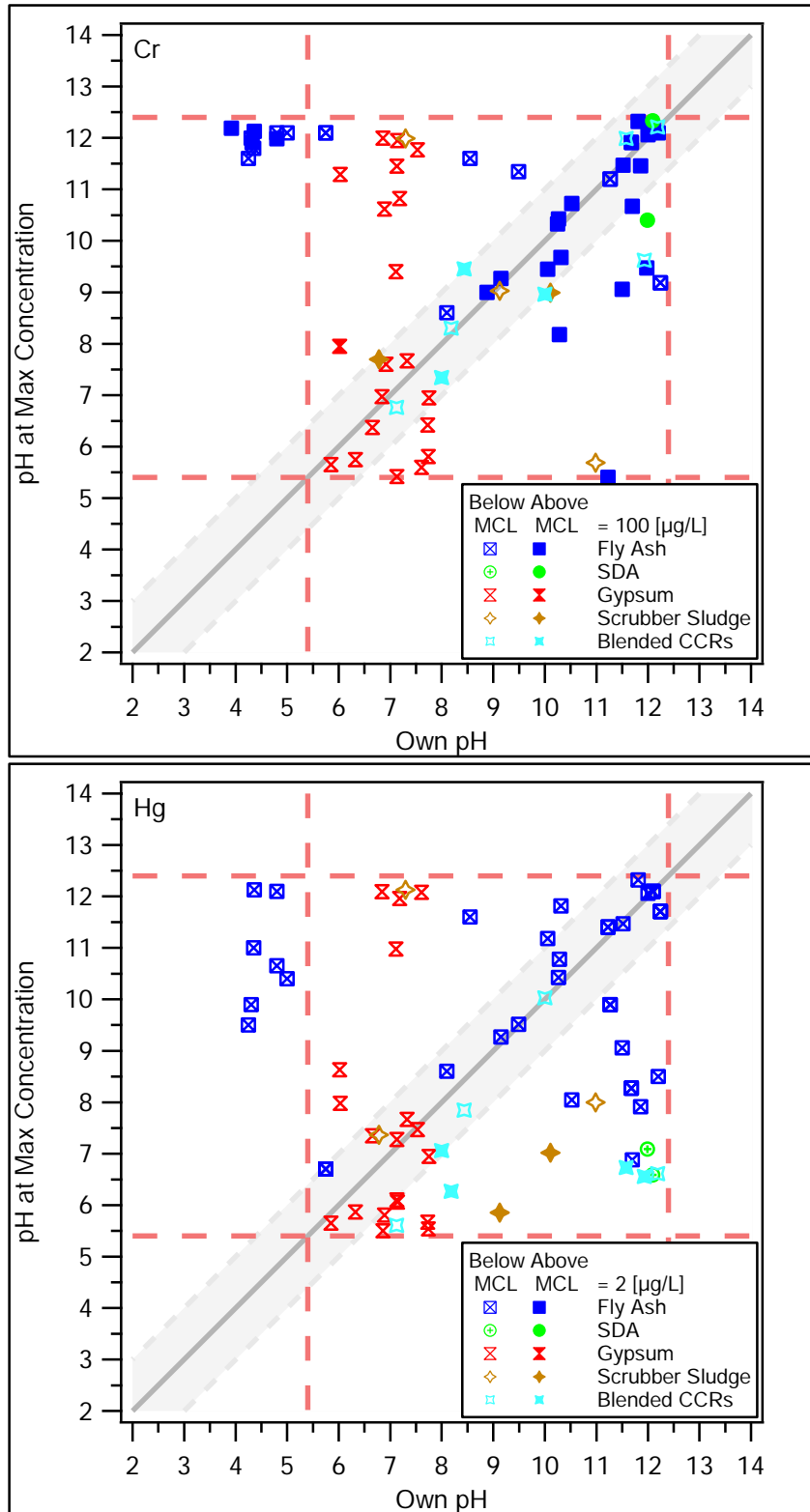


Figure 87 and Figure 88. Chromium and Mercury. pH identity plots.

Characterization of Coal Combustion Residues III

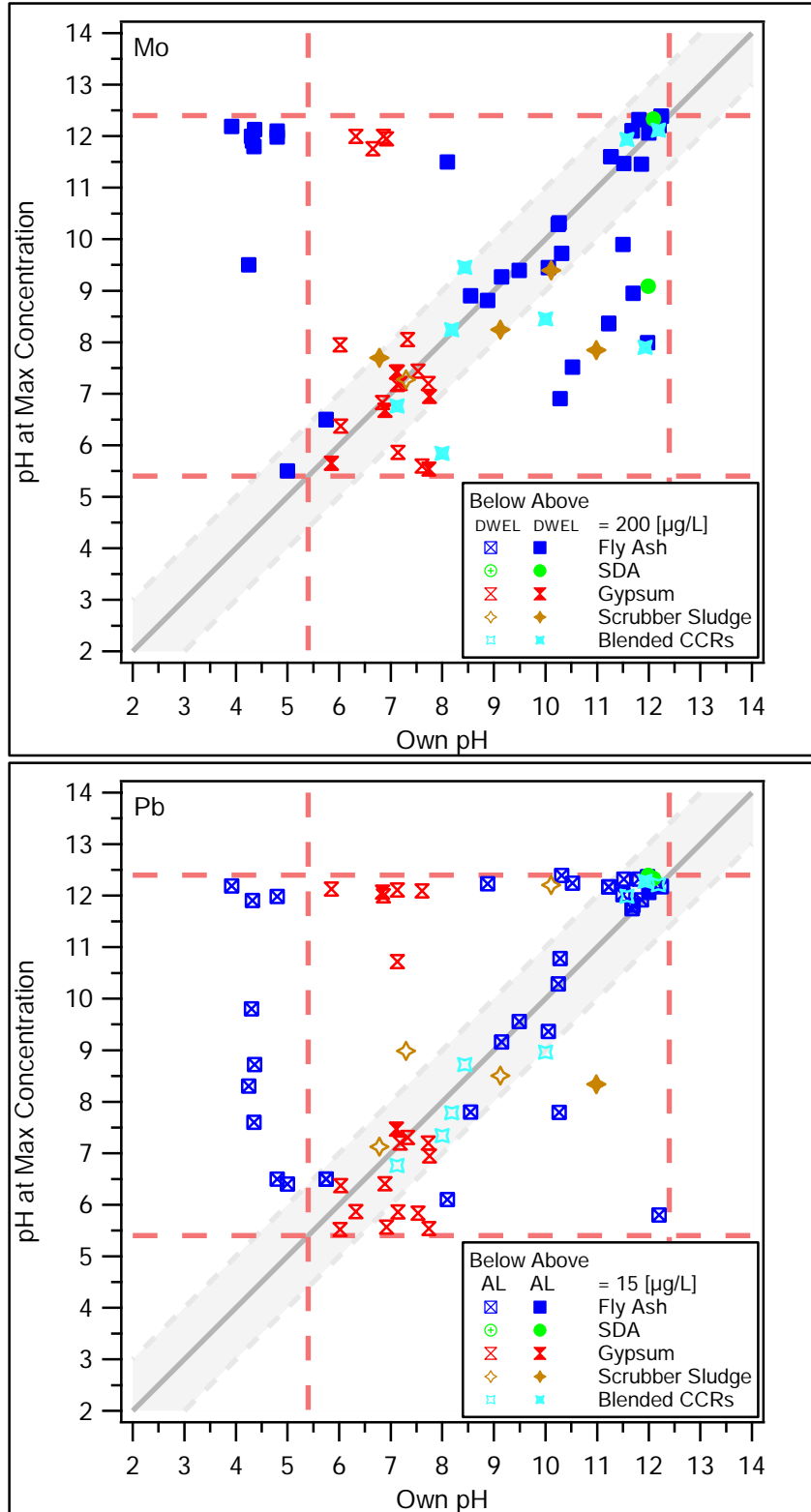


Figure 89 and Figure 90. Molybdenum and Lead. pH identity plots.

Characterization of Coal Combustion Residues III

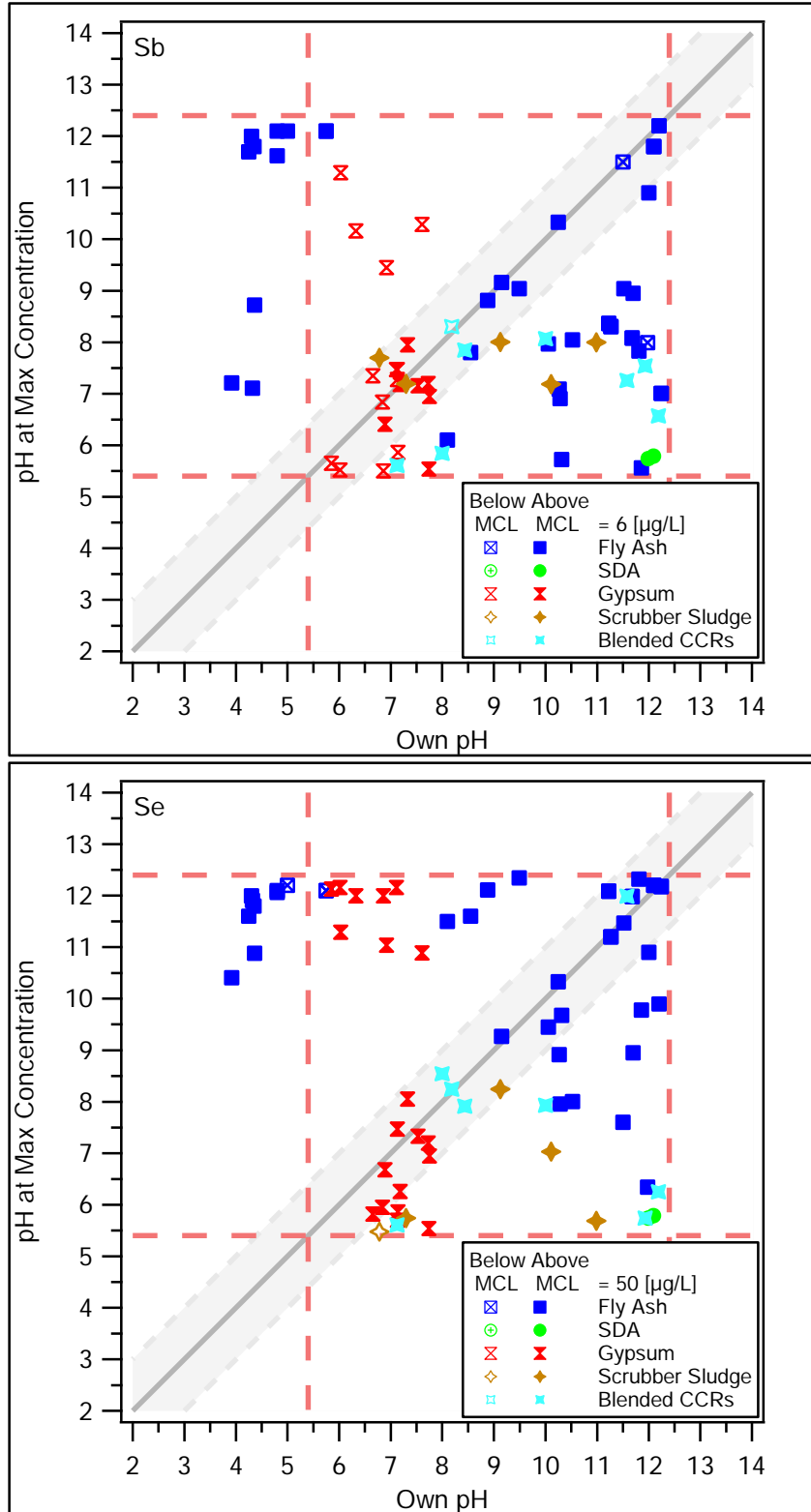


Figure 91 and Figure 92. Antimony and Selenium. pH identity plots.

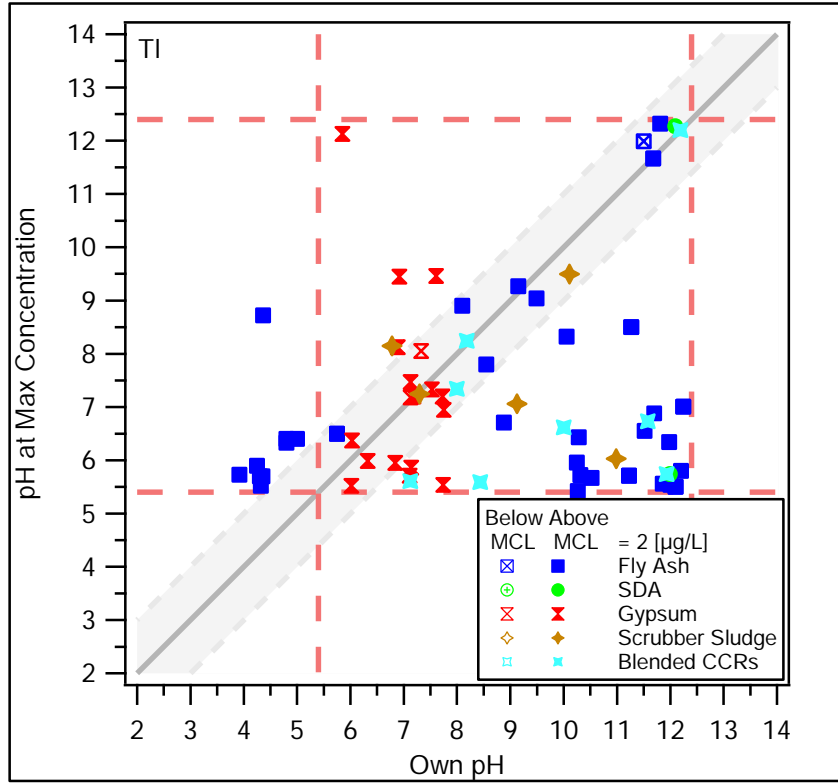


Figure 93. Thallium. pH identity plots.

3.2.5. Comparison of Constituent Maximum Concentrations and Concentrations at the Materials' Own pH from Laboratory Testing Grouped by Material Type with Measurements of Field Samples and the EPA Risk Report Database

Figure 94 through Figure 106 provide summary comparisons for each element by material type of (i) the maximum eluate concentration observed during leaching testing as a function of pH (SR002.1) and as a function of LS (SR003.1)⁴² over the domain $5.4 \leq \text{pH} \leq 12.4$, and (ii) the eluate concentration observed at “own pH” by leaching with deionized water at LS=10 mL/g (SR002.1), and (iii) reference data ranges derived from the EPRI database of field leachate and pore water concentrations (surface impoundments - “EPRI SI”; landfills – “EPRI LF”) and derived from the EPA Risk Report (EPA, 2007b). These are the same reference data ranges used previously as part of this study (Sanchez et al., 2008). Tabular results are provided in Appendix J.

The category “Fly Ash” includes data from all fly ash samples tested (n=34), including those from all coal types and all air pollution control configurations. The category “SDA” represents the results of the two samples of spray dryer residue tested. The category “Gypsum” represents the results from all FGD gypsum samples tested (n=20), including unwashed and washed gypsum samples from all coal types and air pollution control configurations. The category “FGD Residues” represents the results from all FGD scrubber residue samples (n=5) except gypsum. The category “Blended CCRs” represents mixed residues as managed (n=8), including mixtures of fly ash with scrubber residues and with or without added lime, and one as managed sample that was comprised of mixed fly ash with gypsum. The distinction between Blended CCRs and SDA categories was made because Blended CCRs are formed by blending materials captured as separate streams in the air pollution control system, while for SDA fly ash and scrubber residue are captured together.

When five or more data points were available in a given category of test data (“Maximum Values” and “Values at Own pH”), a “box plot” was used to represent the data set, with the following information indicated (from bottom to top of the box and whisker symbol): (i) minimum value (the lowermost whisker), (ii) 5th percentile (mark on lower whisker), (iii) 10th percentile (mark on lower whisker), (iv) 25th percentile (bottom of box), (v) 50th percentile or median value (middle line in box), (vi) 75th percentile (top of box), (vii) 90th percentile (mark on upper whisker), (viii) 95th percentile (mark on upper whisker), (ix) maximum value (the uppermost whisker). To the left of each box plot figure, open circles represent each individual value within the data set. This representation of individual values is used to provide an indication of the distribution of values within the data set because they typically are not normally distributed and in some cases the maximum or minimum values may be very different from the next value or majority of the data. For the SDA category, only each value is displayed because only two data values are contained in the set.

Representation of “Reference Data Ranges” indicates the 5th, median, and 95th percentile of field data for surface impoundments [“EPRI SI”] and landfills [“EPRI LF”]. Ranges of field observations are included for comparison as derived from the EPRI database, considering only observations from disposal sites associated with facilities that have wet FGD scrubbers. Surface

⁴² Including results from testing as a function of LS allows consideration of potentially higher concentrations observed for initial releases that may occur at low LS ratios in the field.

impoundment data are comparable with scrubber sludge results because scrubber sludges are most likely to be disposed in this manner. Landfill data are comparable to blended CCR data because these blended materials are likely to be disposed in landfills. Also included for comparison is the 5th percentile, median, and 95th percentile of the database used to carry out human and ecological health risk evaluations in the EPA Risk Report (EPA, 2007) (“CCW Ash,” “CCW FGD,” and “CCW Ash and Coal Waste” referring to monofilled fly ash, disposed FGD scrubber sludge, and combined CCR disposal, respectively).

The MCL or DWEL or AL (for lead) if available is included in each figure as a green dashed horizontal line to provide a reference value. The TC, if available, is included in each figure as a maroon dashed line as a second reference value. However, the concentration ranges indicated in the figures as results of this study are direct measurements of laboratory eluates and do not consider attenuation that may occur in the field.

For almost all constituents, a greater range of observed values was evident from laboratory testing compared to the reference data sets. The upper bound concentrations observed for laboratory testing over the domain of $5.4 \leq \text{pH} \leq 12.4$ exceeded the upper bound of reference data sets by one or more orders-of-magnitude for Ba, Cr, Hg, Mo, Sb, Se, and Tl. The upper bound concentrations observed for laboratory testing over the domain of $5.4 \leq \text{pH} \leq 12.4$ were less than the upper bound of reference data sets by one or more orders-of-magnitude for Co and Pb. The MCL or DWEL values were exceeded by the maximum laboratory eluate concentration by one or more samples for fly ash (As, B, Ba, Cd, Cr, Mo, Sb, Se, Tl), SDA residues (As, B, Ba, Cd, Cr, Mo, Sb, Se, Tl), gypsum (As, B, Cd, Cr, Mo, Sb, Se, Tl), FGD residues (As, B, Ba, Cr, Hg, Mo, Sb, Se, Tl), and blended CCRs (As, B, Ba, Cd, Cr, Hg, Mo, Sb, Se).

The observation that most constituent concentrations, both maximum values and own pH values in laboratory eluates, as well as field observations spanned several orders-of-magnitude indicates the very substantial roles that coal type, facility design and operating conditions, and field conditions have on expected concentrations of constituents of concern in leachates from beneficial use or disposal. For example, the observed laboratory eluate concentrations from fly ash samples spanned more than four orders of magnitude, both for maximum values and own pH values.

Characterization of Coal Combustion Residues III

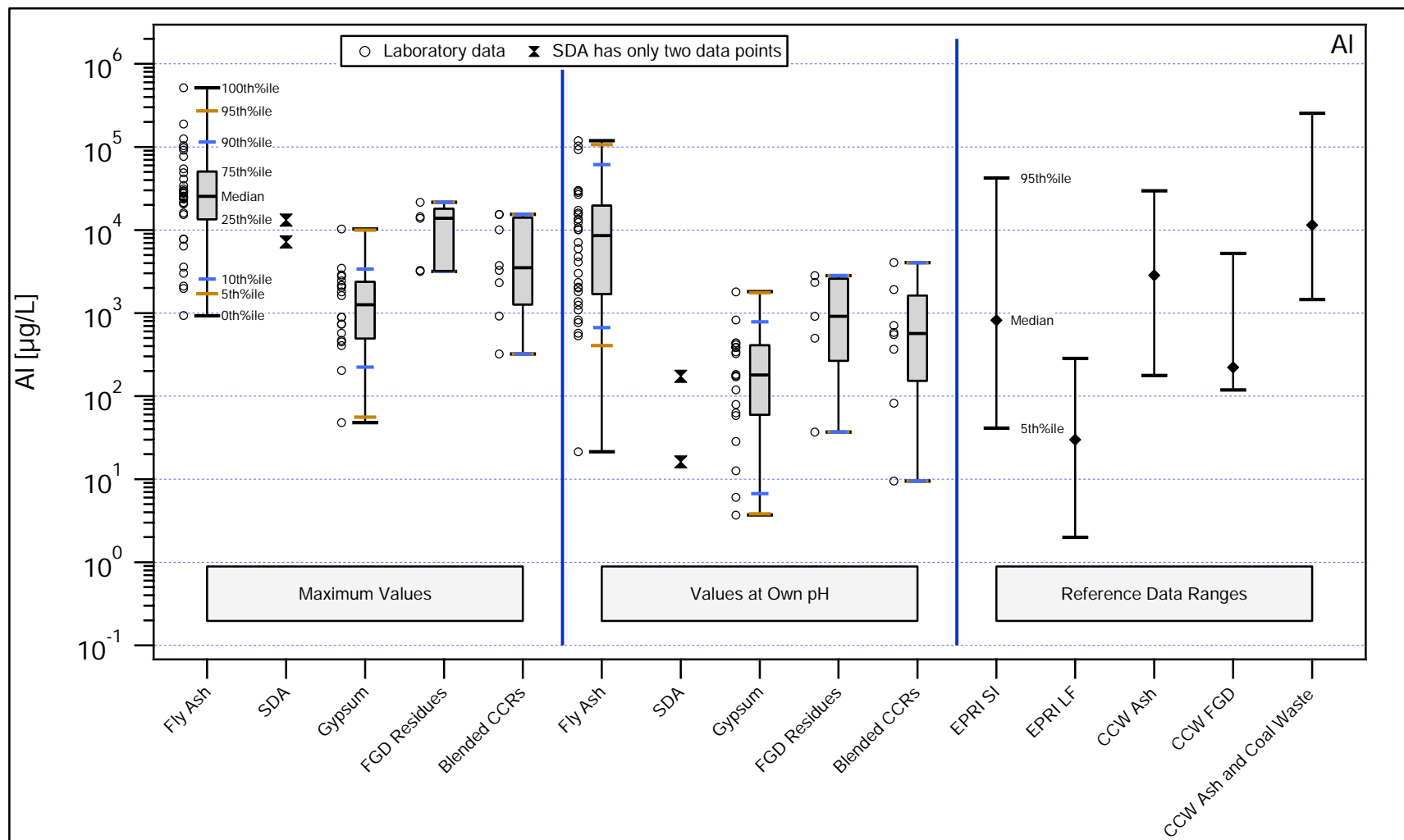


Figure 94. Aluminum. Comparison of maximum concentrations observed in SR002.1 and SR003.1 eluates over the pH domain $5.4 \leq \text{pH} \leq 12.4$, own pH concentrations from SR002.1 at LS = 10mL/g, and reference data ranges derived from the EPRI database of field leachate and pore water concentrations (EPRI SI – surface impoundments; EPRI LF – landfills) and the EPA Risk Report (EPA, 2007b).

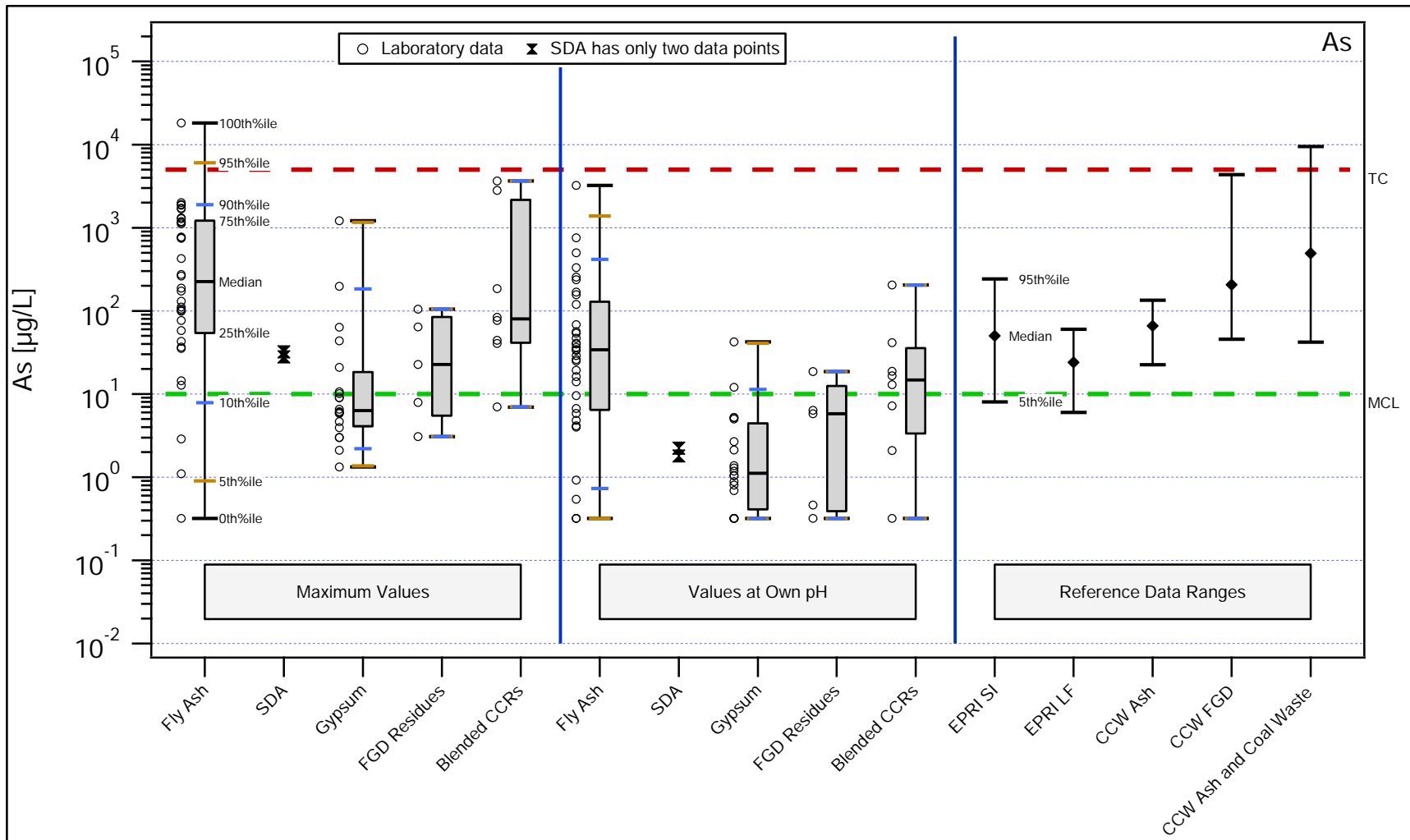


Figure 95. Arsenic. Comparison of maximum concentrations observed in SR002.1 and SR003.1 eluates over the pH domain $5.4 \leq \text{pH} \leq 12.4$, own pH concentrations from SR002.1 at LS = 10mL/g, and reference data ranges derived from the EPRI database of field leachate and pore water concentrations (EPRI SI – surface impoundments; EPRI LF – landfills) and the EPA Risk Report (EPA, 2007b).

Characterization of Coal Combustion Residues III

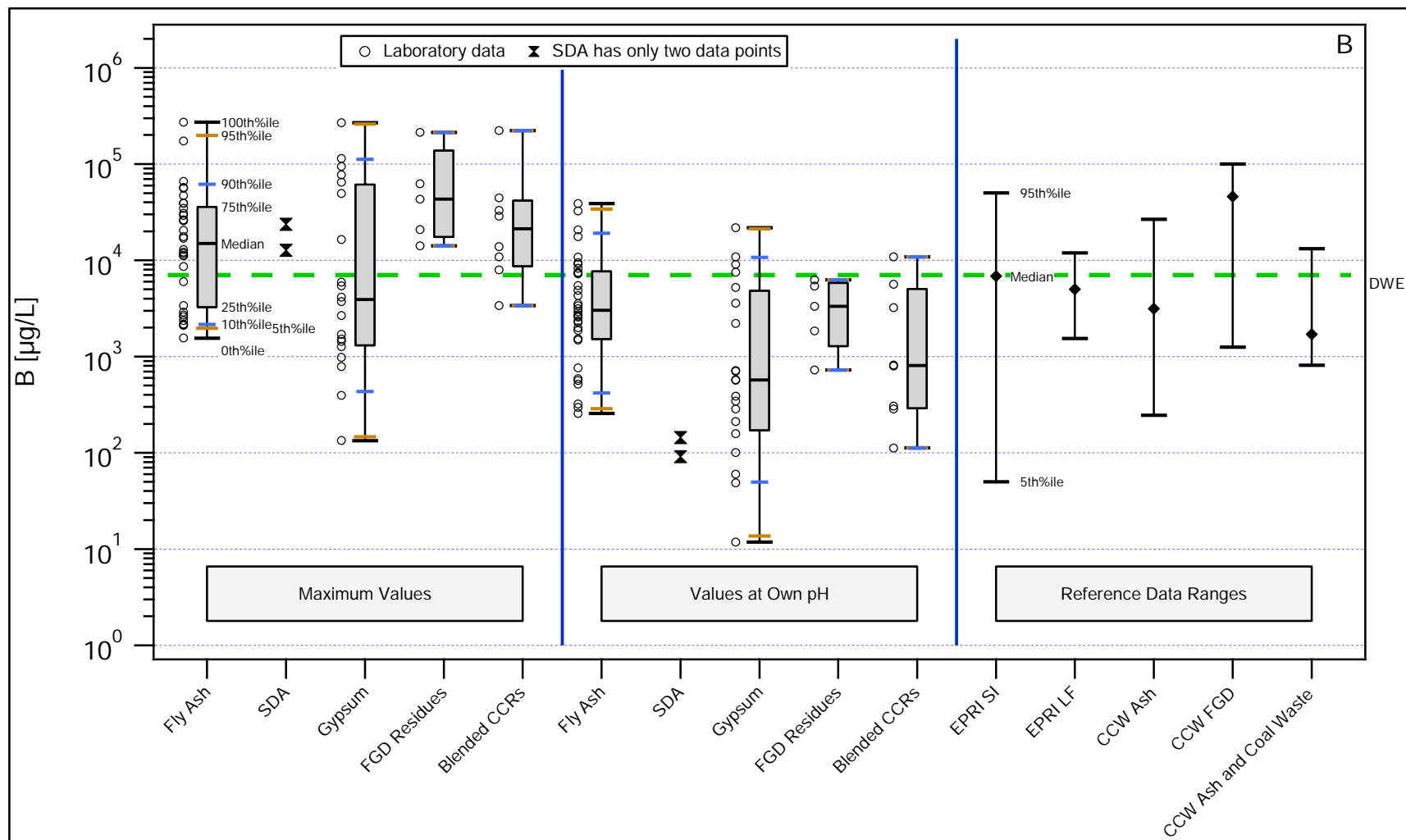


Figure 96. Boron. Comparison of maximum concentrations observed in SR002.1 and SR003.1 eluates over the pH domain $5.4 \leq \text{pH} \leq 12.4$, own pH concentrations from SR002.1 at LS = 10mL/g, and reference data ranges derived from the EPRI database of field leachate and pore water concentrations (EPRI SI – surface impoundments; EPRI LF – landfills) and the EPA Risk Report (EPA, 2007b).

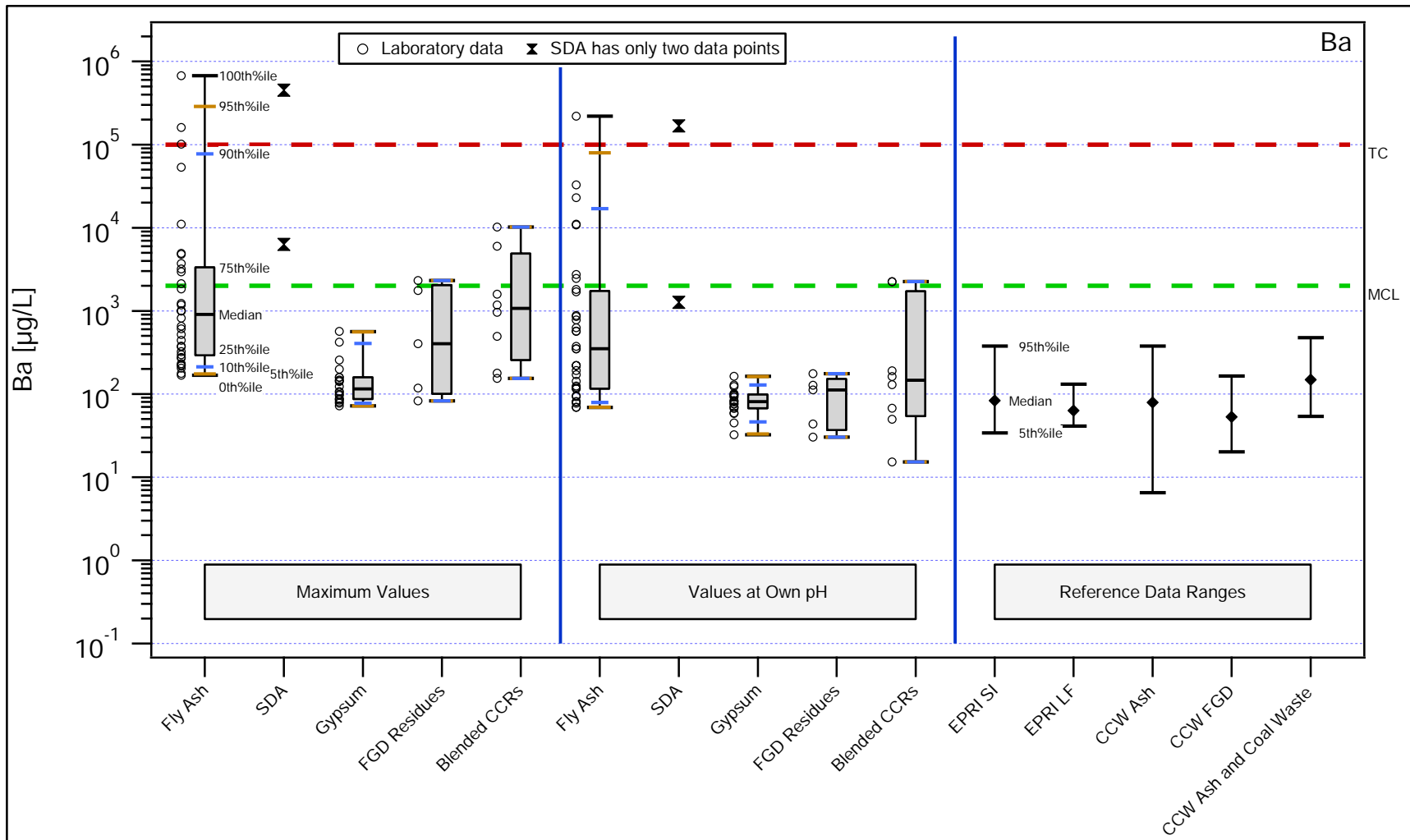


Figure 97. Barium. Comparison of maximum concentrations observed in SR002.1 and SR003.1 eluates over the pH domain $5.4 \leq \text{pH} \leq 12.4$, own pH concentrations from SR002.1 at $LS = 10\text{mL/g}$, and reference data ranges derived from the EPRI database of field leachate and pore water concentrations (EPRI SI – surface impoundments; EPRI LF – landfills) and the EPA Risk Report (EPA, 2007b).

Characterization of Coal Combustion Residues III

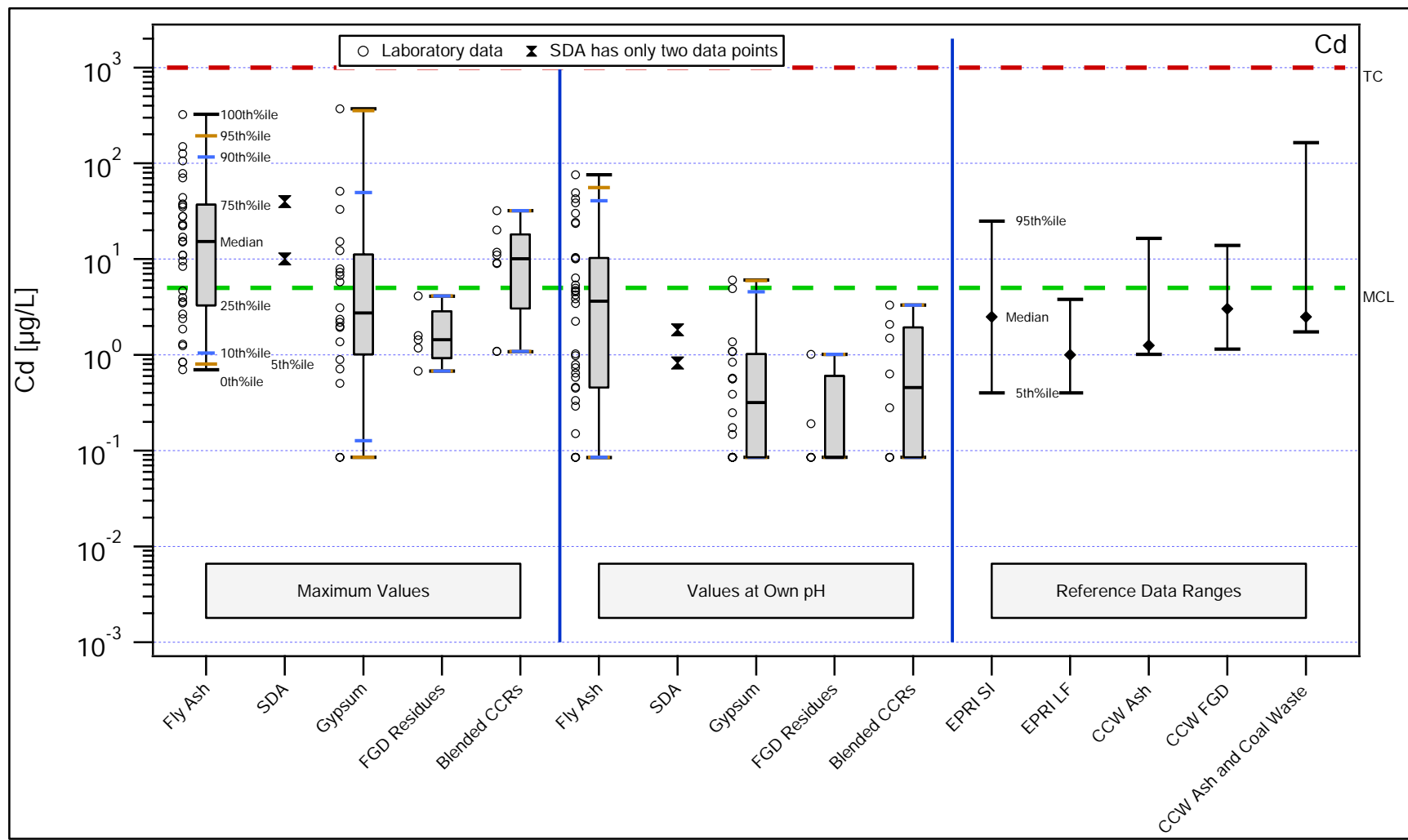


Figure 98. Cadmium. Comparison of maximum concentrations observed in SR002.1 and SR003.1 eluates over the pH domain $5.4 \leq \text{pH} \leq 12.4$, own pH concentrations from SR002.1 at LS = 10mL/g, and reference data ranges derived from the EPRI database of field leachate and pore water concentrations (EPRI SI – surface impoundments; EPRI LF – landfills) and the EPA Risk Report (EPA, 2007b).

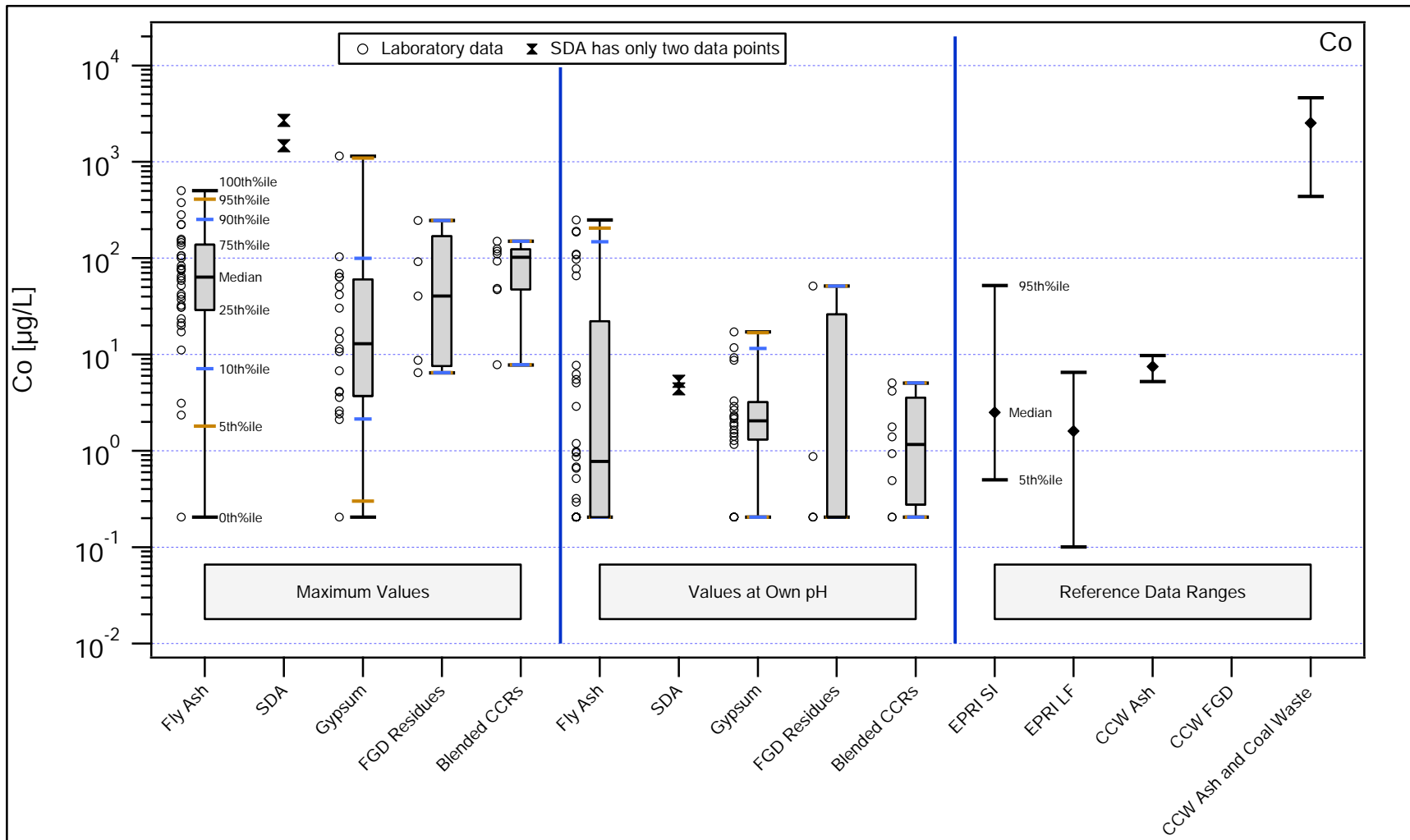


Figure 99. Cobalt. Comparison of maximum concentrations observed in SR002.1 and SR003.1 eluates over the pH domain $5.4 \leq \text{pH} \leq 12.4$, own pH concentrations from SR002.1 at LS = 10mL/g, and reference data ranges derived from the EPRI database of field leachate and pore water concentrations (EPRI SI – surface impoundments; EPRI LF – landfills) and the EPA Risk Report (EPA, 2007b).

Characterization of Coal Combustion Residues III

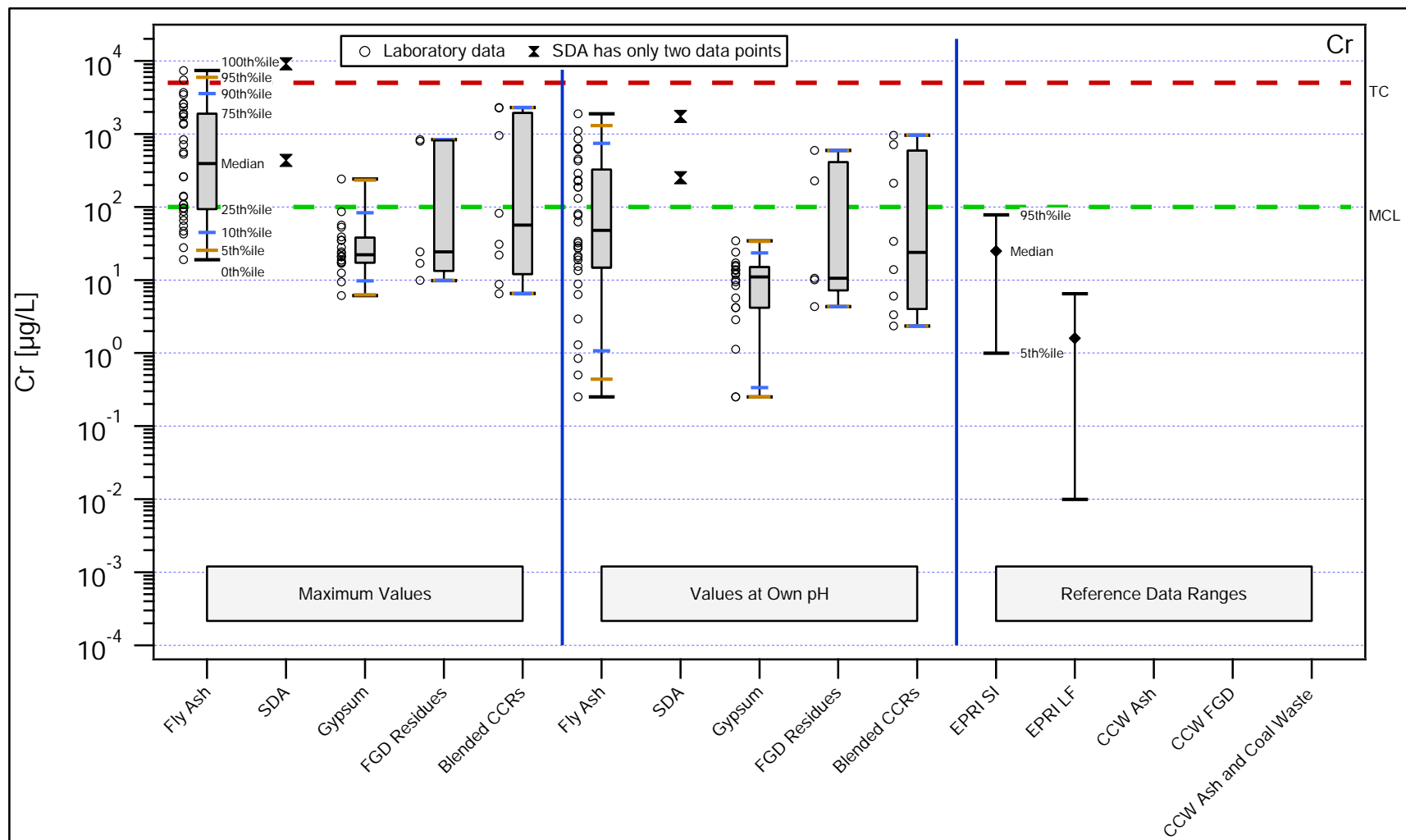


Figure 100. Chromium. Comparison of maximum concentrations observed in SR002.1 and SR003.1 eluates over the pH domain $5.4 \leq \text{pH} \leq 12.4$, own pH concentrations from SR002.1 at $\text{LS} = 10\text{mL/g}$, and reference data ranges derived from the EPRI database of field leachate and pore water concentrations (EPRI SI – surface impoundments; EPRI LF – landfills) and the EPA Risk Report (EPA, 2007b).

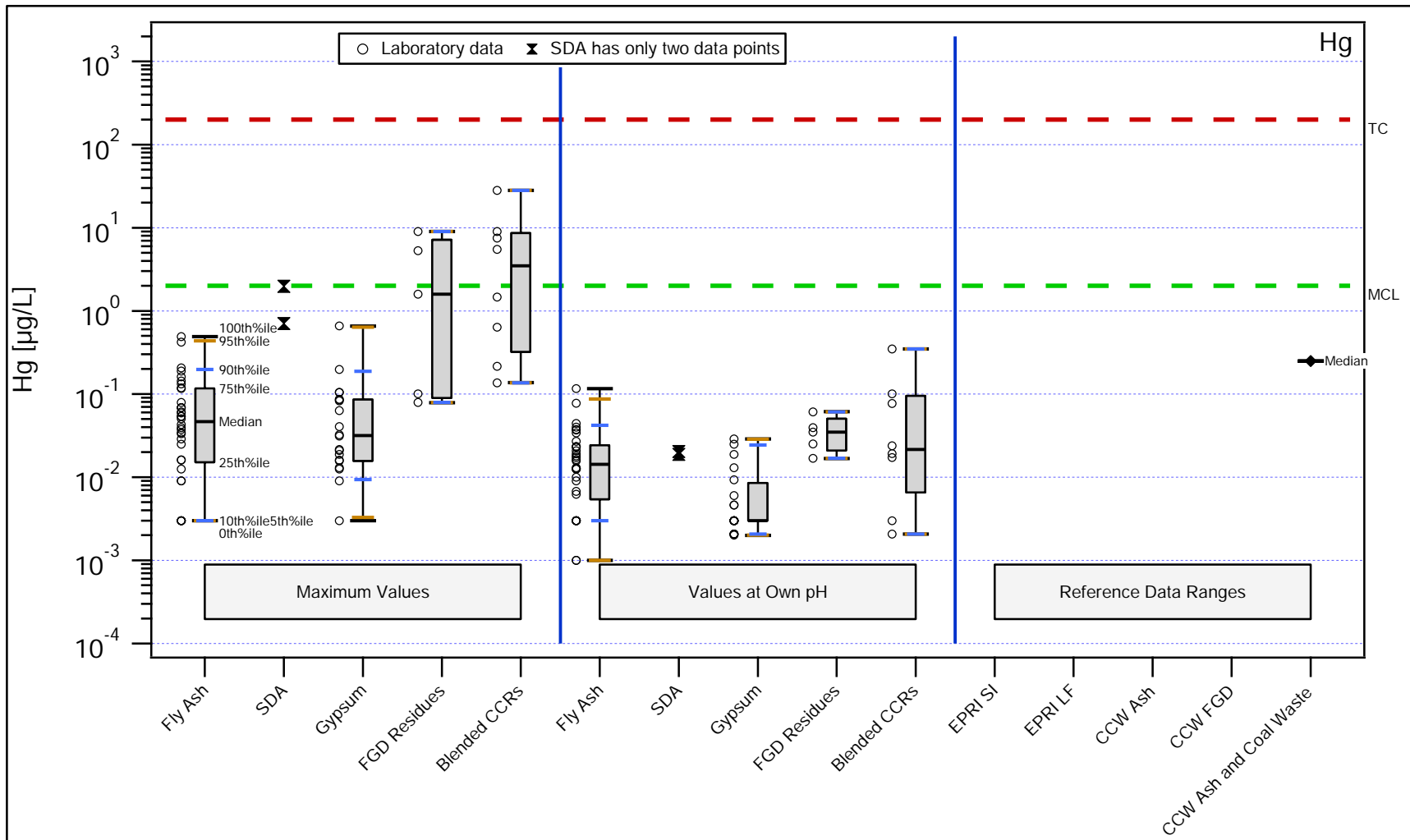


Figure 101. Mercury. Comparison of maximum concentrations observed in SR002.1 and SR003.1 eluates over the pH domain $5.4 \leq \text{pH} \leq 12.4$, own pH concentrations from SR002.1 at LS = 10mL/g, and reference data ranges derived from the EPRI database of field leachate and pore water concentrations (EPRI SI – surface impoundments; EPRI LF – landfills) and the EPA Risk Report (EPA, 2007b).

Characterization of Coal Combustion Residues III

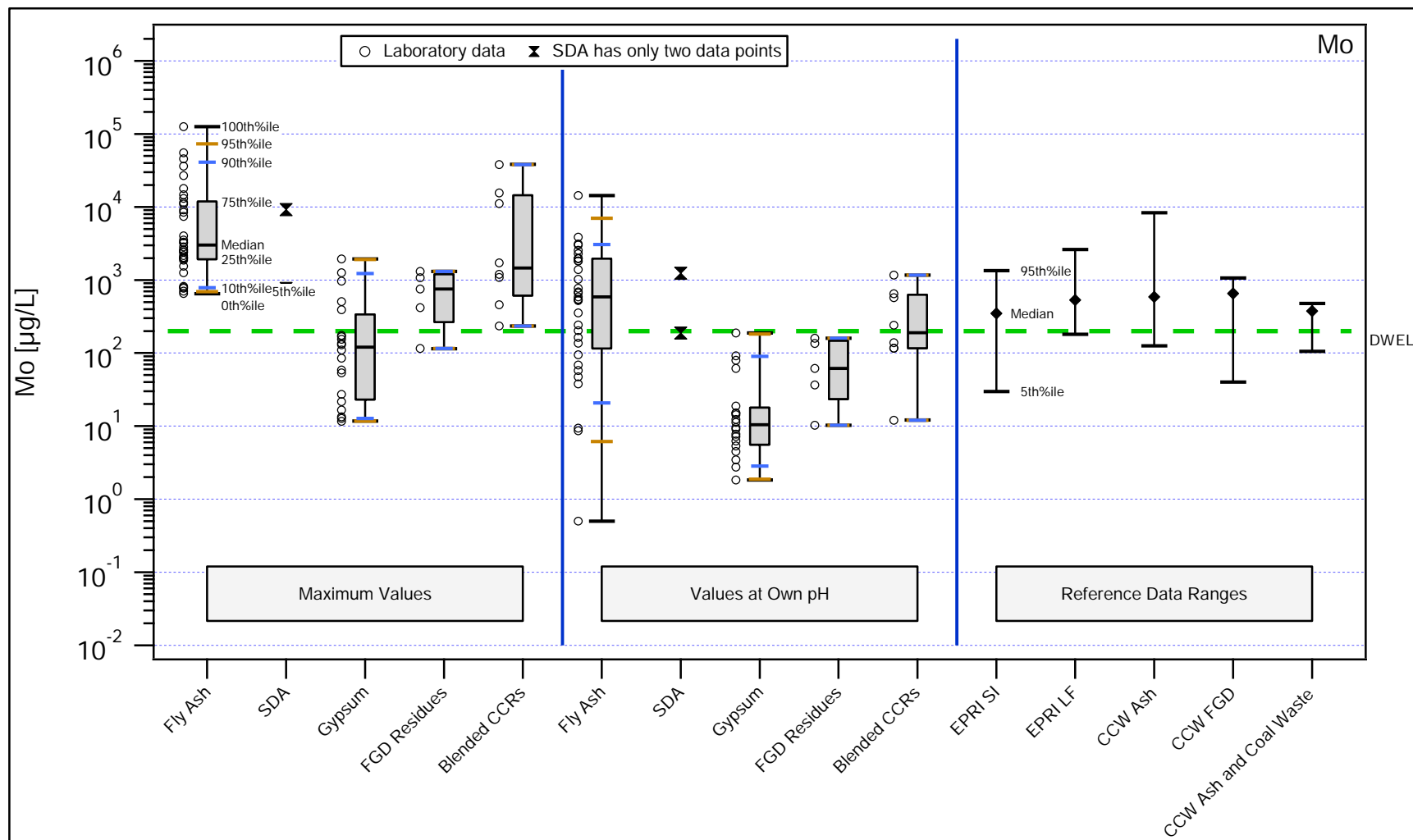


Figure 102. Molybdenum. Comparison of maximum concentrations observed in SR002.1 and SR003.1 eluates over the pH domain $5.4 \leq \text{pH} \leq 12.4$, own pH concentrations from SR002.1 at LS = 10mL/g, and reference data ranges derived from the EPRI database of field leachate and pore water concentrations (EPRI SI – surface impoundments; EPRI LF – landfills) and the EPA Risk Report (EPA, 2007b).

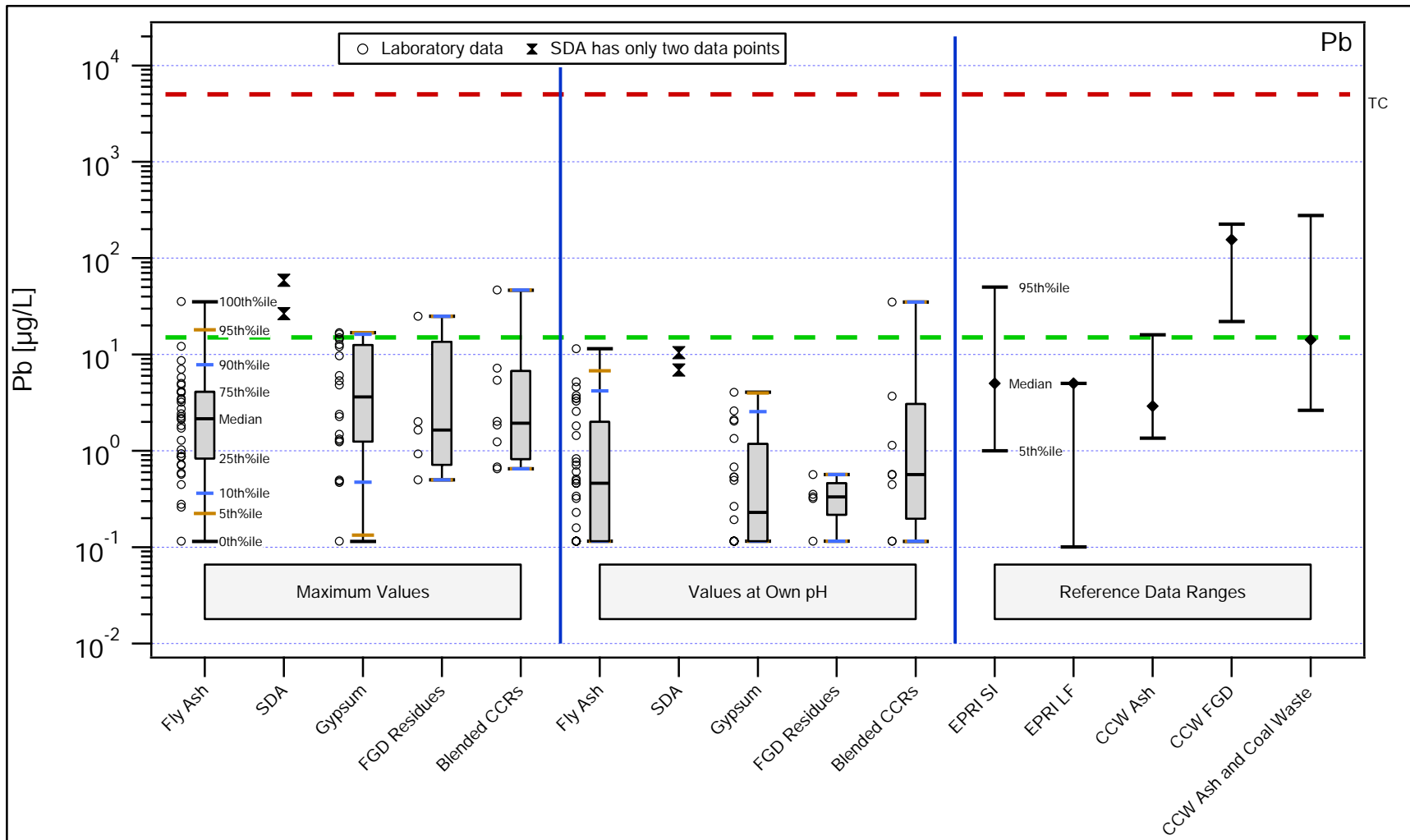


Figure 103. Lead. Comparison of maximum concentrations observed in SR002.1 and SR003.1 eluates over the pH domain $5.4 \leq \text{pH} \leq 12.4$, own pH concentrations from SR002.1 at $\text{LS} = 10\text{mL/g}$, and reference data ranges derived from the EPRI database of field leachate and pore water concentrations (EPRI SI – surface impoundments; EPRI LF – landfills) and the EPA Risk Report (EPA, 2007b).

Characterization of Coal Combustion Residues III

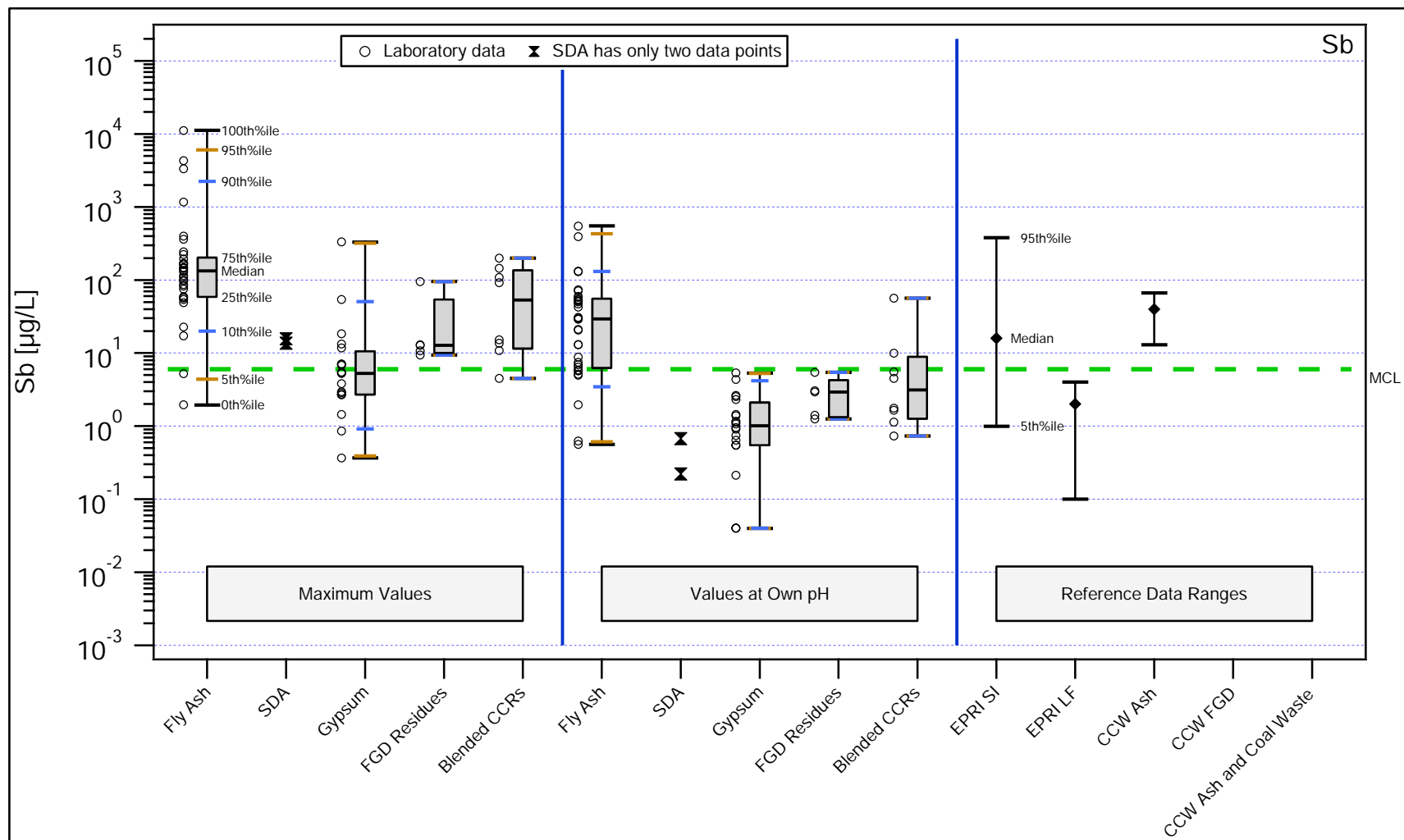


Figure 104. Antimony. Comparison of maximum concentrations observed in SR002.1 and SR003.1 eluates over the pH domain $5.4 \leq \text{pH} \leq 12.4$, own pH concentrations from SR002.1 at LS = 10mL/g, and reference data ranges derived from the EPRI database of field leachate and pore water concentrations (EPRI SI – surface impoundments; EPRI LF – landfills) and the EPA Risk Report (EPA, 2007b).

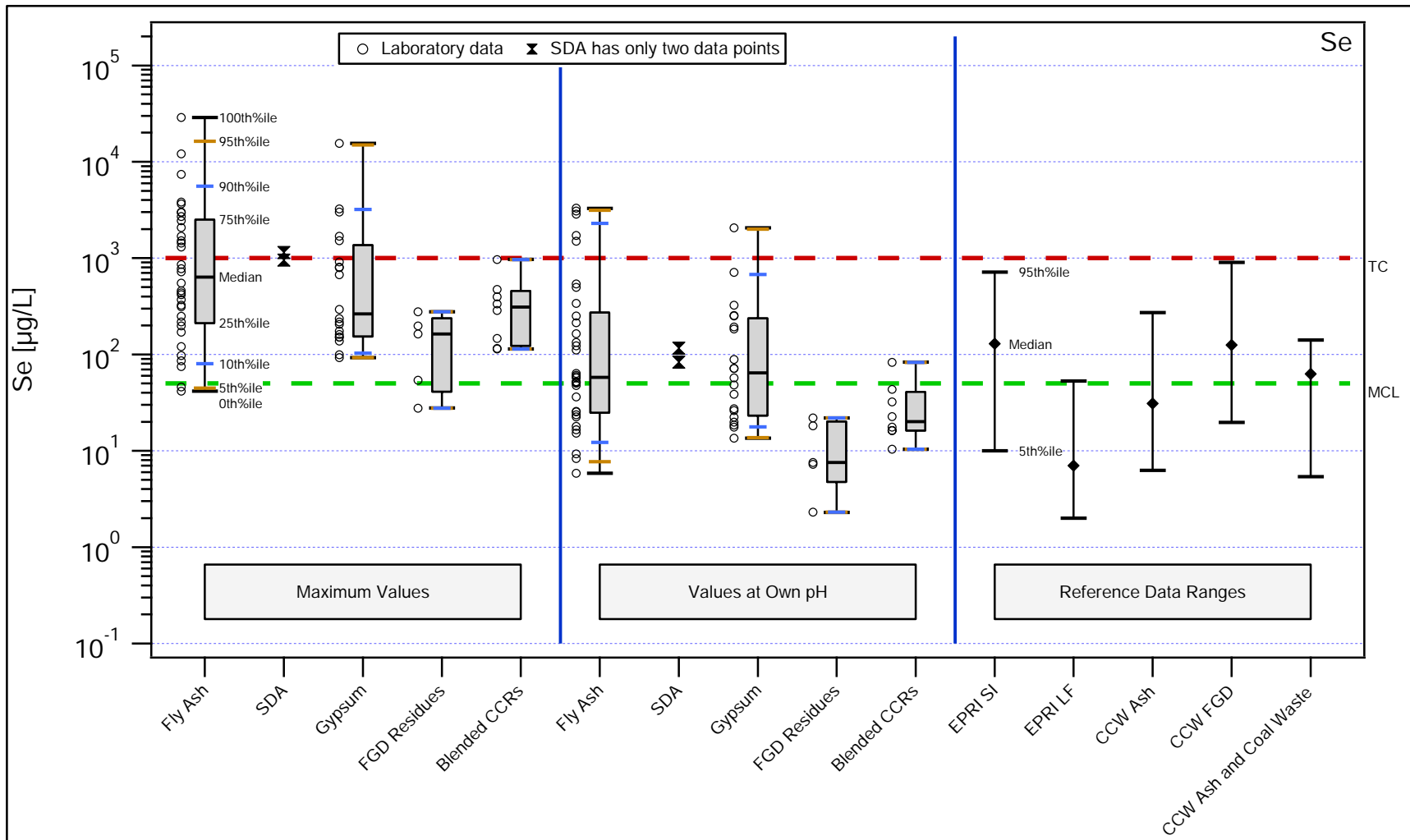


Figure 105. Selenium. Comparison of maximum concentrations observed in SR002.1 and SR003.1 eluates over the pH domain $5.4 \leq \text{pH} \leq 12.4$, own pH concentrations from SR002.1 at LS = 10mL/g, and reference data ranges derived from the EPRI database of field leachate and pore water concentrations (EPRI SI – surface impoundments; EPRI LF – landfills) and the EPA Risk Report (EPA, 2007b).

Characterization of Coal Combustion Residues III

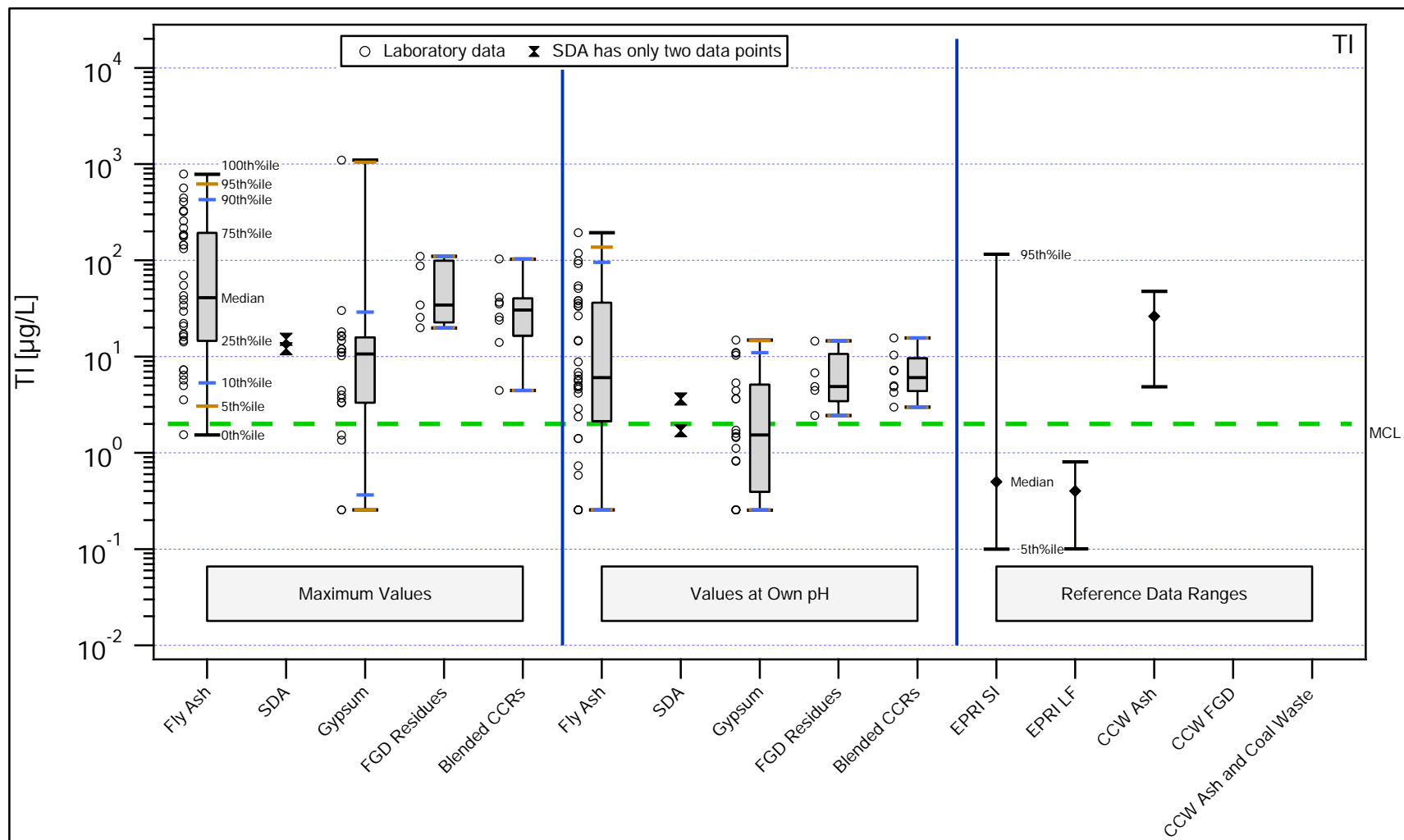


Figure 106. Thallium. Comparison of maximum concentrations observed in SR002.1 and SR003.1 eluates over the pH domain $5.4 \leq \text{pH} \leq 12.4$, own pH concentrations from SR002.1 at LS = 10mL/g, and reference data ranges derived from the EPRI database of field leachate and pore water concentrations (EPRI SI – surface impoundments; EPRI LF – landfills) and the EPA Risk Report (EPA, 2007b).

3.2.6. Attenuation Factors Needed to Reduce Estimated Leachate Concentrations to Less Than Reference Indicators

Comparison of leaching test results to reference indicators does not consider dilution and attenuation factors (collectively referred to here as attenuation factors) that arise as a consequence of disposal or beneficial use designs that limit release and attenuation that occurs during transport from the point of release to the potential receptor. Minimum attenuation factors needed to reduce maximum leach concentrations (based on laboratory test results for $5.4 \leq \text{pH} \leq 12.4$) to less than MCL or DWEL values were calculated for each COPC to illustrate the importance of consideration of attenuation factors during evaluation of management options. Minimum attenuation factors needed to reduce own pH leach concentrations (based on laboratory test results using DI water as the eluant) to less than MCL or DWEL values also were calculated. The resulting attenuation values were calculated by dividing the appropriate measured laboratory leaching test concentration by the respective MCL or DWEL for each COPC. Thus, values greater than one reflect concentrations greater than the MCL or DWEL. Appendix L provides figures comparing attenuation factors calculated for CCR for individual elements and also provides a summary table of all calculated values.

Based on evaluation of the results for each COPC, one consideration was to evaluate across the entire set of COPCs the minimum attenuation factor needed for each CCR sample to result in all COPCs being less than the MCL or DWEL. Furthermore, this evaluation was used to identify the specific COPC (e.g., As, Cd, etc.) that required the greatest attenuation factor for each CCR sample (i.e., the controlling COPC). Results of this analysis are provided in Figure 107 and Figure 108. For each CCR sample, the minimum attenuation factor needed for all COPCs to be less than the MCL or DWEL is graphed, along with identification of the specific COPC driving the result. Two important observations result from this data analysis:

1. Maximum leaching concentrations between pH 5.4 and 12.4 from all CCRs tested in this study require some attenuation to reduce concentrations to less than the MCL or DWEL across all COPCs evaluated; and,
2. For fly ash, the controlling constituent (i.e., the constituent within each sample that required the largest attenuation factor) and the number of samples (..) in which that constituent is controlling are As (11), Ba (3), Cr (4), Sb (5), Se (3), Tl (8); for gypsum the controlling constituents are As (2), Se (13), Tl (5); for scrubber sludge the controlling constituents are Sb (1), Tl (5); for blended, as managed CCRs the controlling constituents are As (3), Cr (1), Hg (1), Sb (2), Tl (1). Thus, it is important to consider these constituents when evaluating the potential impacts from CCR management on human health and the environment.

Characterization of Coal Combustion Residues III

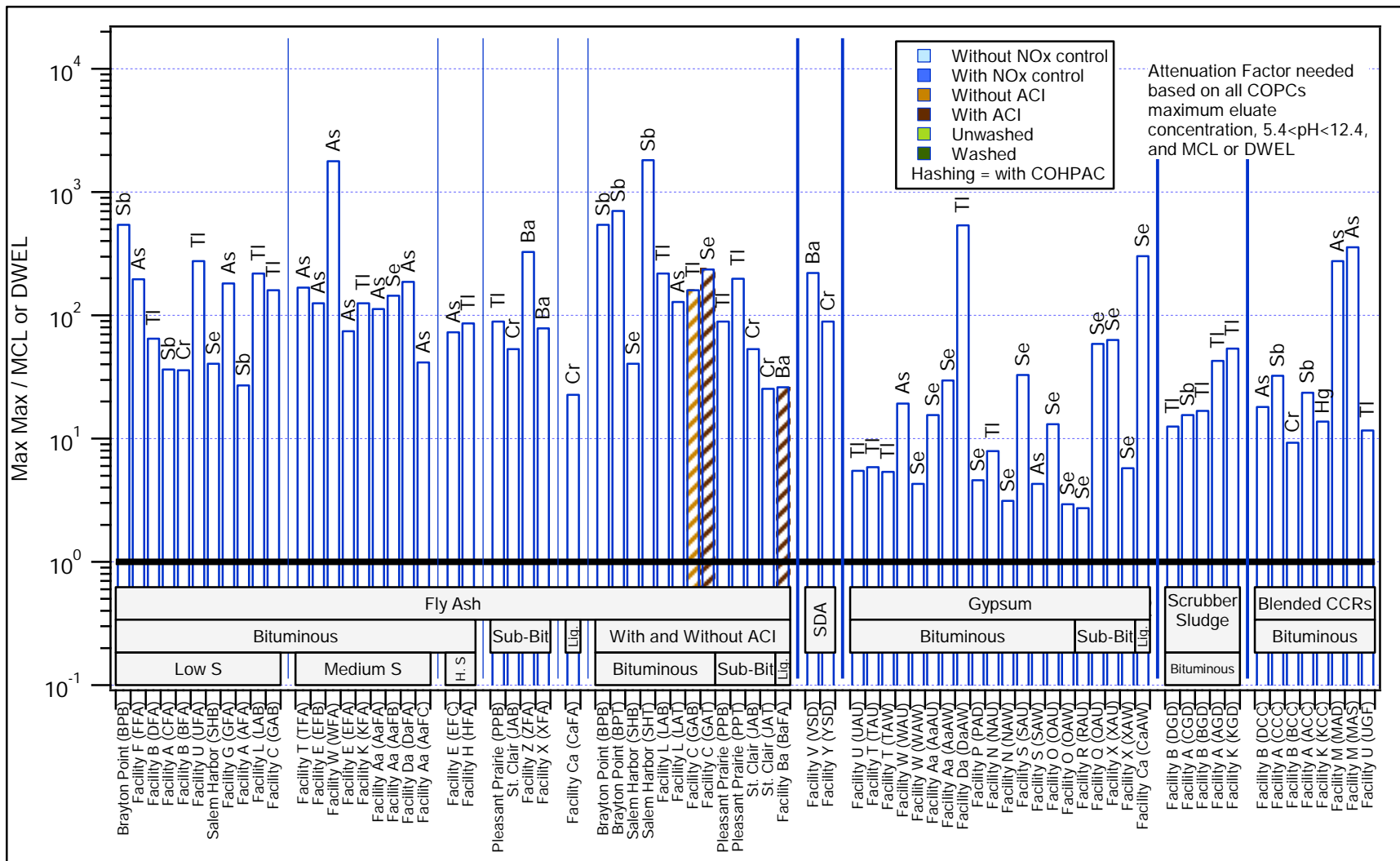


Figure 107. **Minimum attenuation factor** needed for the **maximum eluate concentration** ($5.4 \leq \text{pH} \leq 12.4$) to be reduced below the MCL or DWEL for all COPCs considered in this study. COPC requiring the greatest attenuation factor is indicated for each CCR.

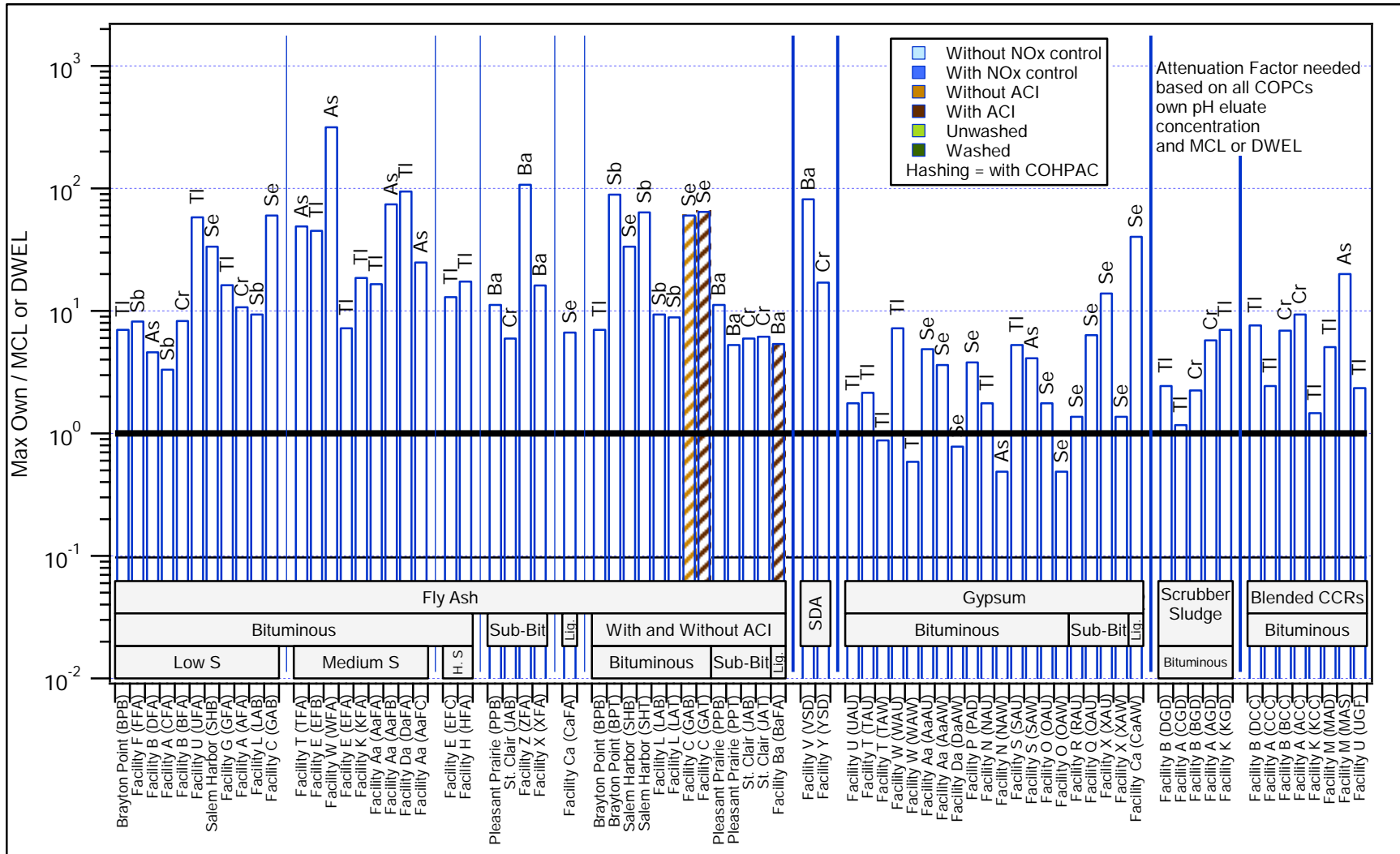


Figure 108. **Minimum attenuation factor** needed for **the own pH eluate concentration** to be reduced below the MCL or DWEL for all COPCs considered in this study. COPC requiring the greatest attenuation factor is indicated for each CCR.

4. SUMMARY OF RESULTS, CONCLUSIONS AND RECOMMENDATIONS

The following sections present conclusions from the results presented in this report.

Changes to fly ash and other coal combustion residues (CCRs) are expected to occur as a result of increased use and application of advanced air pollution control technologies in coal-fired power plants. These technologies include flue gas desulfurization (FGD) systems for SO₂ control, selective catalytic reduction (SCR) systems for NO_x control, and activated carbon injection systems for mercury control. These technologies are being or are expected to be installed in response to federal regulations [e.g., Clean Air Interstate Rule (CAIR), Utility MACT Rule], state regulations, legal consent decrees, and voluntary actions taken by industry to adopt more stringent air pollution control.

The Air Pollution Prevention and Control Division (APPCD) of EPA's Office of Research and Development (ORD) has been working since 2000, to evaluate the potential for leaching and cross media transfer of mercury and other constituents of potential concern (COPCs) from management of these modified CCRs (primarily disposal, but also reuse). This research was cited as a priority in EPA's Mercury Roadmap (<http://www.epa.gov/mercury/roadmap.htm>) to ensure that the solution to one environmental problem is not causing another.

CCR samples of each material type were collected in an attempt to span the range of likely coal types [i.e., low, medium and high sulfur bituminous, sub-bituminous and lignite] and air pollution control configurations reflecting use of more stringent air pollution control. This report presents results from the evaluation of 73 CCRs from 31 coal-fired power plants with various combinations of particulate matter, NO_x, Hg, and SO₂ control. For several of the 31 plants, samples were obtained before and after changes were made in air pollution control.

CCRs have been grouped into the five categories as shown in Table 12. Each of the CCR samples was analyzed for a range of physical properties, total metals content, and leaching characteristics. The testing methods used in this research assess CCR leaching potential over a range of values for two parameters that both vary in the environment and can affect the rate of constituent leaching from a material. These are: (1) the pH and (2) the amount of water contact [in the test, the ratio of liquid-to-solids (LS) being tested]. These are considered improved leaching test methods that address key concerns with single point testing that were raised by EPA's Science Advisory Board and the National Academy of Sciences. An advantage of using this testing approach is that analysis of the data can be tailored or targeted to particular waste management or use conditions. When key material management conditions are known, the data can be used to estimate leaching over the range of plausible management conditions for that particular material. This can be done for either a broad range of conditions (e.g., in assessing release potential on a national basis) or more narrowly (as in estimating release potential at a particular site or limited set of sites).

Characterization of Coal Combustion Residues III

Table 12. Identification of CCRs evaluated and included in this Report.

Samples Evaluated by CCR Category	Report 1*	Report 2**	Additional Samples Collected for this report	Total Samples Evaluated in this Report
1. Fly Ash	12	5	17	34
2. FGD Gypsum	-	6	14	20
3. "Other" FGD Residues (primarily calcium sulfite from scrubbers that do not use oxidation to generate gypsum)	-	5	2	7
4. Blended CCRs (typically a mixture of fly ash, calcium sulfite, and lime)	-	7	1	8
5. Wastewater Treatment Filter Cake	-		4	4

* (Sanchez et al., 2006).

** (Sanchez et al., 2008).

Provided below in a summary table for each CCR category are the range of leach results over the pH range of 5.4 and 12.4⁴³, along with comparison to available regulatory or reference indicators including TC, MCL, and DWEL. In making such comparisons, it is critical to bear in mind that these test results represent an estimate of constituent release from the material as disposed or used on the land. They do not include any attempt to estimate the amount of constituent that may reach an aquifer or drinking water well. Leachate leaving a landfill is invariably diluted in ground water or constituent concentration attenuated by sorption and other chemical reactions in groundwater and sediment. Also, groundwater pH may be different from the pH at the site of contaminant release, and so the solubility and mobility of leached contaminants may change when they reach groundwater. None of these dilution or attenuation processes is incorporated into the leaching values presented, and so comparison with regulatory reference values, particularly drinking water values, must be done with caution.

The principle conclusions are:

1. Review of the data presented in Table 13 and Table 14, for fly ash and FGD gypsum, show a range of total concentration of constituents, but a much broader range (by orders of magnitude) of leaching values, in nearly all cases. This much greater range of leaching values only partially illustrates what more detailed review of the data shows: that for CCRs, the rate of constituent release to the environment is affected by leaching conditions (in some cases dramatically so), and that leaching evaluation under a single set of conditions will, in many cases, lead to inaccurate conclusions about expected leaching in the field.

⁴³ This pH range could understate potential concerns when these materials are used in agricultural, commercial, and engineering applications if the field conditions are more variable than during disposal. For example, 9 of the 34 fly ash samples evaluated indicated the eluate pH in deionized water (i.e., the pH generated by the tested material itself) to be more acidic than pH 5.4.

Characterization of Coal Combustion Residues III

2. Comparison of the ranges of totals values and leachate data also supports earlier conclusions that the rate of constituent leaching cannot be reliably estimated based on total constituent concentration alone or with use of linear K_d partitioning values.
3. The maximum eluate concentration from leaching test results varies over a wide range in pH and is different for different CCR types and elements. This indicates that there is not a single pH for which testing is likely to provide confidence in release estimates over a wide range of disposal and beneficial use options, emphasizing the benefit of multi-pH testing.
4. Distinctive patterns are observed in leaching behavior over the range of pH values that would plausibly be encountered on CCR disposal, depending upon the type of material and element.
5. Summary data in Table 14 on the leach results from evaluation of 34 fly ash samples across the plausible management pH range of 5.4 to 12.4, indicates leaching concentration ranges over several orders of magnitude as a function of pH and ash source:
 - a. the leach results at the upper end of the concentration ranges exceeded the TC values for As, Ba, Cr, and Se.
 - b. the leach results at the upper end of the concentration ranges exceeded the MCL or DWEL for Sb, As, Ba, B, Cd, Cr, Pb, Mo, Se, and Tl.
6. Summary data in Table 15 on the leach results from evaluation of 20 FGD gypsum samples across the plausible management pH domain of 5.4 to 12.4, indicates leaching concentration ranges over several orders of magnitude as a function of pH and FGD gypsum source:
 - a. the leach results at the upper end of the concentration ranges exceeded the TC values for Se.
 - b. the leach results at the upper end of the concentration ranges exceeded the MCL or DWEL for Sb, As, B, Cd, Cr, Mo, Se, and Tl.
7. There is considerable variability in total content and the leaching of constituents of potential within a material type (e.g., fly ash, gypsum) such that while leaching of many samples, without adjustment for dilution and attenuation, exceeds one or more of the available reference indicators, many of the other samples within the material type may be less than the available regulatory or reference indicators. This suggests that materials from certain facilities may be acceptable for particular disposal and beneficial use scenarios while the same material type from a different facility or the same facility produced under different operating conditions (i.e., different air pollution controls) may not be acceptable for the same management scenario.

In interpreting these results, please note that the CCRs analyzed in this report are not considered to be a representative sample of all CCRs produced in the U.S. For many of the observations, only a few data points were available. It is hoped that through broader use of the improved leach test methods (as used in this report), that additional data from CCR characterization will become available. That will help better define trends associated with changes in air pollution control at coal-fired power plants.

Characterization of Coal Combustion Residues III

Table 13. **Fly Ash** - Laboratory leach test eluate concentrations for $5.4 \leq \text{pH} \leq 12.4$ and at “own pH” from evaluation of thirty-four fly ash samples.

	<u>Hg</u>	<u>Sb</u>	<u>As</u>	<u>Ba</u>	<u>B</u>	<u>Cd</u>	<u>Cr</u>	<u>Co</u>	<u>Pb</u>	<u>Mo</u>	<u>Se</u>	<u>TI</u>
Total in Material (mg/kg)	0.01 – 1.5	3 – 14	17 – 510	590 – 7,000	NA	0.3 – 1.8	66 – 210	16 – 66	24 – 120	6.9 – 77	1.1 – 210	0.72 – 13
Leach results (µg/L)	<0.01 – 0.50	<0.3 – 11,000	0.32 – 18,000	50 – 670,000	210 – 270,000	<0.1 – 320	<0.3 – 7,300	<0.3 – 500	<0.2 – 35	<0.5 – 130,000	5.7 – 29,000	<0.3 – 790
TC (µg/L)	200	-	5,000	100,000	-	1,000	5,000	-	5,000	-	1,000	-
MCL (µg/L)	2	6	10	2,000	7,000 DWEL	5	100	-	15	200 DWEL	50	2

Note: The shade is used to indicate where there could be a potential concern for a metal when comparing the leach results to the MCL, DWEL, or TC. Note that MCL and DWEL values represent well concentrations; leachate dilution and attenuation processes that would occur in groundwater before leachate reaches a well are not accounted for, and so MCL and DWEL values are compared to leaching concentrations here to provide context for the test results and initial screening.

Table 14. **FGD Gypsum** - Laboratory leach test eluate concentrations for $5.4 \leq \text{pH} \leq 12.4$ and at “own pH” from evaluation of twenty FGD gypsum samples.

	<u>Hg</u>	<u>Sb</u>	<u>As</u>	<u>Ba</u>	<u>B</u>	<u>Cd</u>	<u>Cr</u>	<u>Co</u>	<u>Pb</u>	<u>Mo</u>	<u>Se</u>	<u>TI</u>
Total in Material (mg/kg)	0.01 – 3.1	0.14 – 8.2	0.95 – 10	2.4 – 67	NA	0.11 – 0.61	1.2 – 20	0.77 – 4.4	0.51 – 12	1.1 – 12	2.3 – 46	0.24 – 2.3
Leach results (µg/L)	<0.01 – 0.66	<0.3 – 330	0.32 – 1,200	30 – 560	12 – 270,000	<0.2 – 370	<0.3 – 240	<0.2 – 1,100	<0.2 – 12	0.36 – 1,900	3.6 – 16,000	<0.3 – 1,100
TC (µg/L)	200	-	5,000	100,000	-	1,000	5,000	-	5,000	-	1,000	-
MCL (µg/L)	2	6	10	2,000	7,000 DWEL	5	100	-	15	200 DWEL	50	2

Note: The shade is used to indicate where there could be a potential concern for a metal when comparing the leach results to the MCL, DWEL, or TC. Note that MCL and DWEL values represent well concentrations; leachate dilution and attenuation processes that would occur in groundwater before leachate reaches a well are not accounted for, and so MCL and DWEL values are compared to leaching concentrations here to provide context for the test results and initial screening.

5. REFERENCES

- ACAA (American Coal Ash Association), (2007). "2006 Coal Combustion Product (CCP) Production and Use Survey." Retrieved August 6, 2009, from [http://www.acaa-usa.org/associations/8003/files/2006_CCP_Survey_\(Final-8-24-07\).pdf](http://www.acaa-usa.org/associations/8003/files/2006_CCP_Survey_(Final-8-24-07).pdf).
- ASTM (2002). Method D 6784-02: Standard Test Method for Elemental, Oxidized, Particle-Bound, and Total Mercury in Flue Gas Generated from Coal-Fired Stationary Sources (Ontario-Hydro Method), American Society for Testing and Materials.
- DOE-EIA (Official Energy Statistics from the US Government - Energy Information Administration), (2009). "Annual Energy Outlook 2009 with Projections to 2030." Retrieved November 24, 2009, from [http://www.eia.doe.gov/oiaf/aeo/pdf/0383\(2009\).pdf](http://www.eia.doe.gov/oiaf/aeo/pdf/0383(2009).pdf).
- Drahota, P., and M. Filippi (2009). "Secondary arsenic minerals in the environment: A review." Environment International 35(8): 1243-1255.
- Duong, D. D. (1998). Adsorption Analysis: Equilibria and Kinetics. London: Imperial College Press, 892 p.
- EPA (1988). Report to Congress - Wastes from the Combustion of Coal by Electric Utility Power Plants, EPA/530-SW-88-002. Washington, D.C.: U.S. Environmental Protection Agency, Office of Solid Waste and Emergency Response.
- EPA (1996). Method 3052, "Microwave Assisted Acid Digestion of Siliceous and Organically Based Matrices." Test Methods for Evaluating Solid Waste, Physical/Chemical Methods (SW-846), U.S. Environmental Protection Agency.
- EPA (1998a). Method 7470A, "Mercury in Liquid Waste (Manual Cold-Vapor Technique)." Test Methods for Evaluating Solid Waste, Physical/Chemical Methods (SW-846), U.S. Environmental Protection Agency.
- EPA (1998b). Method 7473, "Mercury in Solids and Solutions by Thermal Decomposition, Amalgamation, and Atomic Absorption Spectrophotometry." Test Methods for Evaluating Solid Waste, Physical/Chemical Methods (SW-846), U.S. Environmental Protection Agency.
- EPA (1999). Report to Congress - Wastes from the Combustion of Fossil Fuels: Volume 2 - Methods, Findings and Recommendations, EPA 530-R-99-010. Washington, D.C.: U.S. Environmental Protection Agency, Office of Solid Waste and Emergency Response.
- EPA (2000). Characterization and Evaluation of Landfill Leachate, Draft Report, 68-W6-0068. U.S. Environmental Protection Agency, September 2000.
- EPA (2001). Control of Mercury Emissions from Coal-Fired Electric Utility Boilers: Interim Report, EPA-600/R-01-109. December 2001.

- EPA (2002). Characterization and Management of Residues from Coal-Fired Power Plants, Interim Report, EPA-600/R-02-083. U.S. Environmental Protection Agency, December 2002.
- EPA (2004). Revised Assessment of Detection and Quantitation Approaches, EPA-821-B-04-005. U.S. Environmental Protection Agency, Office of Science and Technology Engineering and Analysis Division, Office of Water (4303T), October 2004.
<http://epa.gov/waterscience/methods/det/rad.pdf> (accessed August 21, 2009).
- EPA (2005). Control of Mercury Emissions from Coal Fired Electric Utility Boilers: An Update, U.S. Environmental Protection Agency, National Risk Management Research Laboratory Air Pollution Prevention and Control Division, Office of Research and Development,
http://www.epa.gov/ttn/atw/utility/ord_whtpaper_hgcontroltech_oar-2002-0056-6141.pdf (accessed August 4, 2009).
- EPA (2006a). 2006 Edition of the Drinking Water Standards and Health Advisories, EPA 822-R-06-013 (updated August, 2006). Washington, D.C.: U.S. Environmental Protection Agency, Office of Water.
- EPA (2006b). EPA's Roadmap for Mercury, EPA-HQ-OPPT-2005-0013. U.S. Environmental Protection Agency, <http://www.epa.gov/mercury/pdfs/FINAL-Mercury-Roadmap-6-29.pdf> (accessed August 21, 2009).
- EPA (2006c). Standard Operating Procedure for the Determination of Hexavalent Chromium in Ambient Air Analyzed by Ion Chromatography (IC), U.S. Environmental Protection Agency, December 2006. <http://www.epa.gov/ttn/amtic/airtox.html> (accessed September 17, 2009).
- EPA (2007a). 2005 Urban Air Toxics Monitoring Program (UATMP) - Hexavalent Chromium, EPA-454/R-07-005. U.S. Environmental Protection Agency, February 2007.
- EPA (2007b). Human and Ecological Risk Assessment of Coal Combustion Wastes, Docket # EPA-HQ-RCRA-2006-0796; Docket Item# EPA-HQ-RCRA-2006-0796-0009. Released as part of notice of data availability on August 29, 2007,
<http://www.epa.gov/epaoswer/other/fossil/noda07.htm> (accessed August 29, 2007).
- EPRI (2006). Characterization of Field Leachates at Coal Combustion Product Management Sites: Arsenic, Selenium, Chromium, and Mercury Speciation, EPRI Report Number 1012578. Electric Power Research Institute (EPRI), Palo Alto, CA and U.S. Department of Energy, Pittsburgh, PA.
- EPRI (2008). Impact of Air Emissions Controls on Coal Combustion Products, EPRI Report Number 1015544. Electric Power Research Institute (EPRI), Palo Alto, CA.
- Hutson, N. D., B. C. Attwood, and K. G. Scheckel (2007). "XAS and XPS Characterization of Mercury Binding on Brominated Activated Carbon." *Environmental Science and Technology* 41: 1747-1752.

Characterization of Coal Combustion Residues III

- Kilgroe, J., C. Sedman, R. Srivastava, J. Ryan, C. W. Lee, and S. Thorneloe (2001). Control of Mercury Emissions from Coal-Fired Electric Utility Boilers: Interim Report, EPA-600/R-01-109. U.S. Environmental Protection Agency, December 2001.
- Kosson, D. S., H. A. v. d. Sloot, F. Sanchez, and A. C. Garrabrants (2002). "An Integrated Framework for Evaluating Leaching in Waste management and Utilization of Secondary Materials." Environmental Engineering Science 19(3): 159-204.
- Ladwig, K., 2007. Personal Communication. November 15, 2007.
- Mohan, D., and J. C. U. Pittman (2007). "Arsenic removal from water/wastewater using adsorbents--A critical review." Journal of Hazardous Materials 142(1-2): 1-53.
- MTI (McDermott Technology, Inc.), (2001). "Mercury Emissions Predictions." Retrieved November 2002, from <http://www.mtiresearch.com/aecdp/mercury.html#Coal%20Analyses%20and%20Mercury%20Emissions%20Predictions>
- Munro, L. J., K. J. Johnson, and K. D. Jordan (2001). "An interatomic potential for mercury dimer." Journal of Chemical Physics 114(13): 5545-5551.
- Nelson, S. (2004). Advanced Utility Sorbent Field Testing Program. Mercury Control Technology R&D Review. DOE/NETL. Pittsburgh, PA. July 14-15, 2004.
- Nelson, S., R. Landreth, Q. Zhou, and J. Miller (2004). Accumulated Power-Plant Mercury-Removal Experience with Brominated PAC Injection. Joint EPRI DOE EPA Combined Utility Air Pollution Control Symposium, The Mega Symposium. Washington, D.C. August 30-September 2, 2004.
- Pavlish, J. H., E. A. Sondreal, M. D. Mann, E. S. Olson, K. C. Galbreath, D. L. Laudal, and S. A. Benson (2003). "Status Review of Mercury Control Options for Coal-Fired Power Plants." Fuel Processing Technology 82: 89-165.
- Rudzinski, W., W. A. Steele, and G. Zgrablich, Eds. (1997). Equilibria and dynamics of gas adsorption on heterogeneous solid surfaces. Studies in Surface Science and Catalysis. Amsterdam, Elsevier Science B.V.
- Ruthven, D. M. (1984). Principles of Adsorption and Adsorption Processes. New York: Wiley-Interscience, 464 p.
- SAB (Environmental Engineering Committee EPA Science Advisory Board) (2003). "TCLP Consultation Summary." Presented at the Science Advisory Board (SAB) Environmental Engineering Committee consultation with U.S. Environmental Protection Agency, Washington D.C. June 17-18, 2003.
- Sanchez, F., R. Keeney, D. S. Kosson, and R. Delapp (2006). Characterization of Mercury-Enriched Coal Combustion Residues from Electric Utilities Using Enhanced Sorbents for Mercury Control, EPA-600/R-06/008. Research Triangle Park, NC: U.S. Environmental

Characterization of Coal Combustion Residues III

Protection Agency, Air Pollution Prevention and Control Division, Contract No. EP-C-04-023, Work Assignment 1-31, February 2006.

www.epa.gov/nrmrl/pubs/600r06008/600r06008.pdf (accessed August 5, 2009).

Sanchez, F., D. S. Kosson, R. Keeney, R. Delapp, L. Turner, P. Kariher, and S. Thorneloe (2008). Characterization of Coal Combustion Residues from Electric Utilities Using Wet Scrubbers for Multi-Pollutant Control, EPA-600/R-08/077. Research Triangle Park, NC: U.S. Environmental Protection Agency, Air Pollution Prevention and Control Division, July 2008. www.epa.gov/nrmrl/pubs/600r08077/600r0877.pdf (accessed August 5, 2009).

Senior, C., C. J. Bustard, K. Baldrey, K. Starns, and M. Durham (2003). "Characterization of Fly Ash From Full-Scale Demonstration of Sorbent Injection For Mercury Control on Coal-Fired Power Plants." Presented at the Combined Power Plant Air Pollutant Control Mega Symposium, Washington D.C. May 19-22, 2003.

Senior, C., S. Thorneloe, B. Khan, and D. Goss (2009). "Fate of Mercury Collected from Air Pollution Control Devices." Environmental Management, Journal of the Air & Waste Management Association (A&WMA): 15-21.

Srivastava, R. K., and W. Jozewicz (2001). "Flue Gas Desulfurization: The State of the Art." Journal of Air and Waste Management 51: 1676-1688.

Thorneloe, S. (2003). "Application of Leaching Protocol to Mercury-Enriched Coal Combustion Residues." Presentation to the U.S. Environmental Protection Agency (EPA) Science Advisory Board (SAB), Washington D.C., Environmental Engineering Committee. June 17, 2003.

Thorneloe, S. (2009). Evaluating the Thermal Stability of Mercury and Other Metals in Coal Combustion Residues Used in the Production of Cement Clinker, Asphalt, and Wallboard, EPA-600/R-09/152, December 2009.

Thorneloe, S., D. S. Kosson, G. Helms, and A. Garrabrants (2009). "Improved Leaching Test Methods for Environmental Assessment of Coal Ash and Recycled Materials Used in Construction." Proceedings for the or the International Waste Management and Landfill Symposium, S. Margherita di Pula, Cagliari, Italy; 2009 by CISA, Environmental Sanitary Engineering Centre, Italy. 5-9 October 2009.

Thorneloe, S., D. S. Kosson, F. Sanchez, B. Khan, and P. Kariher (2008). "Improved Leach Testing for Evaluating the Fate of Mercury and Other Metals from Management of Coal Combustion Residues." Proceedings for the Global Waste Management Symposium, Copper Mountain Conference Center, Colorado, USA. Sept. 7-10, 2008.

Vidic, R. D. (2002). Combined Theoretical and Experimental Investigation of Mechanisms and Kinetics of Vapor-Phase Mercury Uptake by Carbonaceous Surfaces, National Energy Technology Laboratory, US Department of Energy (DOE), Final Report. Grant No. DE-FG26-98FT40119.

Characterization of Coal Combustion Residues III

Wang, J., T. Wang, H. Mallhi, Y. Liu, H. Ban, and K. Ladwig (2007). "The role of ammonia on mercury leaching from coal fly ash." Chemosphere 69(10): 1586-1592.

Appendix A

Facility Descriptions and CCR Sample Locations

Facility Descriptions

<u>Brayton Point</u>	<u>A-1</u>
<u>Pleasant Prairie</u>	<u>A-1</u>
<u>Salem Harbor</u>	<u>A-2</u>
<u>Facility A</u>	<u>A-3</u>
<u>Facility B</u>	<u>A-3</u>
<u>Facility C</u>	<u>A-4</u>
<u>Facility E</u>	<u>A-4</u>
<u>Facility F</u>	<u>A-4</u>
<u>Facility G</u>	<u>A-5</u>
<u>Facility H</u>	<u>A-5</u>
<u>Facility J</u>	<u>A-5</u>
<u>Facility K</u>	<u>A-5</u>
<u>Facility L</u>	<u>A-6</u>
<u>Facility M</u>	<u>A-6</u>
<u>Facility N</u>	<u>A-7</u>
<u>Facility O</u>	<u>A-7</u>
<u>Facility P</u>	<u>A-8</u>
<u>Facility Q</u>	<u>A-8</u>
<u>Facility R</u>	<u>A-8</u>
<u>Facility S</u>	<u>A-9</u>
<u>Facility T</u>	<u>A-9</u>
<u>Facility U</u>	<u>A-9</u>
<u>Facility V</u>	<u>A-9</u>
<u>Facility W</u>	<u>A-10</u>
<u>Facility X</u>	<u>A-10</u>
<u>Facility Y</u>	<u>A-11</u>
<u>Facility Z</u>	<u>A-11</u>
<u>Facility Aa</u>	<u>A-11</u>
<u>Facility Ba</u>	<u>A-12</u>
<u>Facility Ca</u>	<u>A-12</u>
<u>Facility Da</u>	<u>A-12</u>

Facility Flow Diagrams

<u>Brayton Point</u>	<u>A-13</u>
<u>Pleasant Prairie</u>	<u>A-15</u>
<u>Salem Harbor</u>	<u>A-17</u>
<u>Facility A</u>	<u>A-19</u>
<u>Facility B</u>	<u>A-21</u>
<u>Facility C</u>	<u>A-23</u>
<u>Facility E</u>	<u>A-25</u>
<u>Facility F</u>	<u>A-28</u>
<u>Facility G</u>	<u>A-29</u>
<u>Facility H</u>	<u>A-30</u>
<u>Facility J</u>	<u>A-31</u>
<u>Facility K</u>	<u>A-33</u>
<u>Facility L</u>	<u>A-34</u>
<u>Facility M</u>	<u>A-36</u>
<u>Facility N</u>	<u>A-38</u>
<u>Facility O</u>	<u>A-39</u>
<u>Facility P</u>	<u>A-40</u>
<u>Facility Q</u>	<u>A-41</u>
<u>Facility R</u>	<u>A-42</u>
<u>Facility S</u>	<u>A-43</u>
<u>Facility T</u>	<u>A-44</u>
<u>Facility U</u>	<u>A-45</u>
<u>Facility V</u>	<u>A-47</u>
<u>Facility W</u>	<u>A-48</u>
<u>Facility X</u>	<u>A-49</u>
<u>Facility Y</u>	<u>A-50</u>
<u>Facility Z</u>	<u>A-51</u>
<u>Facility Aa</u>	<u>A-52</u>
<u>Facility Ba</u>	<u>A-54</u>
<u>Facility Ca</u>	<u>A-55</u>
<u>Facility Da</u>	<u>A-56</u>

Appendix A

Facility and Sampling Descriptions

Brayton Point

Brayton Point Station (Somerset, MA) is operated by PG&E National Energy Group. This facility is composed of four fossil fuel fired units designated as Units 1, 2, 3, and 4. The test unit selected, unit 1, has a tangentially fired boiler rated at 245 MW. Brayton Point Unit 1 was chosen for this evaluation because of its combination of firing low-sulfur bituminous coal with a cold-side ESP. This configuration represents a wide range of coal-fired power plants located in the eastern U.S. (Senior et al., 2003a).

The primary particulate control equipment consists of two CS-ESPs in series, with an EPRICON flue gas conditioning system that provides SO_3 for fly ash resistivity control.

The EPRICON system is not used continuously, but on an as-needed basis. The first ESP (“Old ESP”) in this particular configuration was designed and manufactured by Koppers. The Koppers ESP has a weighted wire design and a specific collection area (SCA) of $156 \text{ ft}^2/1000 \text{ acfm}$. The second ESP (“New ESP”) in the series configuration was designed and manufactured by Research-Cottrell. The second ESP has a rigid electrode design and an SCA of $403 \text{ ft}^2/1000 \text{ acfm}$. Total SCA for the unit is $559 \text{ ft}^2/1000 \text{ acfm}$. The precipitator inlet gas temperature is nominally $280 \text{ }^\circ\text{F}$ at full load (Senior et al., 2003a).

Hopper ash is combined between both precipitators in the dry ash-pull system. The ash is processed by an on-site Separation Technology Inc. (STI) carbon separation system, to reduce the carbon content. This processed ash is sold as base for concrete and the remainder of the higher carbon ash is land disposed (Senior et al., 2003a).

The injection rate of the PAC was 20 lb of sorbent used for each million actual cubic feet of gas (lb/MMacf) at the time when the CCR with ACI in use was collected from this facility.

The baseline and post-control ashes used for this study were collected as composite samples from the C-row ash hoppers of the new ESP before processing for carbon separation. Ash for this study¹ was collected before processing for carbon separation because not all facilities do this processing. The baseline ash was collected on 6 June 2002. The post-control fly ash was collected on 21 July 2002. Both fly ashes were stored in covered five gallon buckets in the onsite trailer at ambient temperatures.

Pleasant Prairie

Wisconsin Electric Power Company, a subsidiary of Wisconsin Energy, owns and operates Pleasant Prairie Power Plant located near Kenosha, WI. The plant has two 600 MW balanced-draft coal-fired boilers designated Units 1 and 2. Unit 2 is the test unit. This site was of key interest because it was the only plant in the NETL program that burns a variety of Powder River

Basin (PRB) low sulfur, sub-bituminous coals. In addition, this facility has the ability to isolate one ESP chamber (1/4 of the unit) (Starns et al., 2002).

The primary particulate control equipment consists of CS-ESPs of weighted wire design with a Wahlco gas conditioning system that provides SO₃ for fly ash resistivity control. The precipitators were designed and built by Research-Cottrell. The design flue gas flow was 2,610,000 acfm. The precipitator inlet gas temperature is nominally 280 °F at full load (Starns et al., 2002).

Precipitator #2 is comprised of four electrostatic precipitators that are arranged piggyback style and designated 2-1, 2-2, 2-3, and 2-4. Each of the four precipitators is two chambers wide and four mechanical fields deep with eight electrical fields in the direction of gas flow. The SCA is 468 ft²/kacfm (Starns et al., 2002).

Hopper ash is combined from all four precipitators in the dry ash-pull system and sold as base for concrete (Starns et al., 2002). The PAC injection rate was 10 lb/MMacf at the time when the CCR with ACI in use was collected from this facility.

The baseline ash was collected as a composite sample from ash hoppers 7-1 and 7-2 of ESP 2-4. The post-control ash was collected as a grab sample from ash hopper 7-2 of ESP 2-4 (see Appendix B for flow diagram). The baseline ash was collected on 11 September 2001, and the post-control fly ash was collected on 13 November 2001. Both fly ashes were stored in covered five gallon buckets in the onsite trailer at ambient temperatures.

Salem Harbor

PG&E National Energy Group owns and operates Salem Harbor Station located in Salem, MA. There are four fossil fuel fired units at the facility designated as Units 1, 2, 3, and 4. Units 1–3 fire a low sulfur, bituminous coal and use oil for startup. Unit 4 fires #6 fuel oil. Unit 1, the test unit, is a B&W single-wall-fired unit with twelve DB Riley CCV90 burners. It is rated at 88 gross MW. Salem Harbor Unit 1 was chosen for this evaluation because of its combination of firing low-sulfur bituminous coal with urea-based SNCR, high LOI, and a CS-ESP. The opportunity to quantify the impact of SNCR on mercury removal and sorbent effectiveness is unique in this program. In addition, test results from prior mercury tests have indicated 87% to 94% mercury removal efficiency on this unit without sorbent injection (Senior et al., 2003a). However, fly ash from this facility has a relatively high percentage of total carbon without carbon injection (7.8%, see Table 6), which likely serves as a sorbent for mercury.

The particulate control equipment consists of a two-chamber CS-ESP (chambers designated 1-1 and 1-2), which provides two separate gas flow paths from the outlet of the tubular air heaters to the ID fan inlets. This Environmental Elements ESP has a rigid electrode design and a SCA of 474 ft²/1000 acfm. The precipitator inlet gas temperature is nominally 255 °F at full load. Typical LOI or carbon content of the Unit 1 ash is about 25%. This ash is landfilled. The PAC injection rate was 10 lb/MMacf at the time when the CCR with ACI in use was collected from this facility.

The baseline and post-control ashes used for this study were collected as grab samples from the first ash hopper (hopper A) of row 1-1 of the ESP. The baseline ash was collected on 6 June 2002, and the post-control fly ash was collected on 7 July 2002. Both fly ashes were stored in covered five gallon buckets in an onsite trailer at ambient temperatures.

Facility A

Facility A is a 440-MW coal-fired power plant with a reverse-air fabric filter followed by a wet FGD system. The unit burns ~1 percent sulfur eastern bituminous coal. The unit operated at nominally full load for the duration of the test program. The unit is equipped with a pulverized-coal boiler and in-furnace selective SNCR; urea was injected into the boiler during the course of operations within the duration of the initial part of this test program. However, urea was not injected into the boiler for the final comparison test (“SNCR off”). Gas exiting the furnace is split between two flues equipped with comparable control equipment. Particulate is removed with a reverse-air fabric filter. Flue gas is then scrubbed through a multiple tower wet FGD unit; FGD is a limestone natural-oxidation design. The two flues are joined prior to exhausting to a common stack. The annular stack rises 308 feet above the top of the incoming flue. The stack is operated in a saturated condition with no reheat. The fly ash and FGD waste are combined and then dewatered before landfill disposal.

Facility A was sampled in September 2003. During the period of time while the SCR was operating, two 5 gallon buckets of fly ash (AFA), two 5 gallon buckets of scrubber sludge (AGD), and two buckets of scrubber sludge fixated with lime (ACC) were collected. In February 2004, during the period of time while the SCR was bypassed and not operating, two 5 gallon buckets of fly ash (CFA), two 5 gallon buckets of scrubber sludge (CGD), and two buckets of scrubber sludge fixated with lime (CCC) were collected. All samples were collected by plant personnel.

Facility B

Facility B is a 640 MW coal-fired power plant with cold side ESP followed by a wet FGD system with Mg-lime. The unit burns medium to high sulfur eastern bituminous coals. The unit is equipped with a pulverized coal boiler and selective catalytic reduction composed of vanadium pentoxide (V_2O_5) and tungsten trioxide (WO_3), on titanium dioxide (TiO_2) supporting matrix. One set of samples was collected during the season of elevated ozone, when ammonia is injected into the ductwork in front of the SCR catalyst, resulting in a flue gas mixture with a concentration of 320 ppm ammonia as it enters the catalyst. Samples were also collected during the winter when ammonia was not being injected (“SCR off”). Particulate is removed with a cold-side ESP. Flue gas is then scrubbed through a wet FGD unit; FGD is an inhibited mag-lime design. The FGD sludge is thickened and then mixed with fly ash and magnesium-enhanced lime before landfill disposal in a clay-lined site.

Three samples were collected in September 2003 when the SCR was operating: one fresh fly ash sample collected from the ash hopper (sample BFA), one scrubber sludge filter cake sample collected after the centrifuge but before mixing with other materials in the pug mill (sample BGD), and one fixated scrubber sludge sample collected after mixing the scrubber sludge with fly ash and

magnesium-enhanced lime in the pug mill (sample BCC). Three additional samples were collected from the same locations in February 2004 when the SCR was not in use (samples DFA, DGD and DCC, respectively). Each sample consisted of one 5-gallon pails of the material, and all were collected by Natural Resource Technology (NRT) personnel contractors working for EPRI.

Facility C

This plant has four 270 MW balanced draft coal-fired boilers designated as Units 1–4. All of these units fire a variety of low-sulfur, washed, Eastern bituminous coals. Unit #3 was used for the ACI studies.

All of the units at this plant employ HS-ESP as the primary particulate control equipment. The HS-ESP of unit #3 is followed by COHPAC. The COHPAC system is a pulse-jet cleaned baghouse designed to treat flue gas volumes of 1,070,000 acfm at 290 °F. The COHPAC baghouse consist of two sides, with the A-side being the control and the B-side being the side where activated carbon was injected after the HS-ESP but before the COHPAC. An ESP followed by COHPAC and combined with sorbent injection is referred to as the TOXECON configuration.

The injection rate of the PAC was 1.5 lb/MMacf at the time when the CCR with ACI in use was collected from this facility.

One 5-gallon bucket of fly ash without the PAC injection (GAB) and one 5 gallon bucket of fly ash with PAC injection (GAT) were collected.

Facility E

This test site has four boilers producing 2,424 megawatt (MW) of power. The plant eastern-bituminous coal in a dry-bottom pulverizer boiler. Cold-side electrostatic precipitators (ESPs) are used on three units and hot-side ESP on one unit for particulate control. One five gallon bucket of fly ash was collected from each of the four boilers. Sample EFA was collected from a cold-side ESP from Boiler #1 burning medium sulfur eastern bituminous coal which when the SCR was operating. Sample EFB was collected from a cold-side ESP from Boiler #2 burning medium sulfur eastern bituminous coal which when the SCR was not operating. Sample EFC was collected from a cold-side ESP from Boiler #3 burning high sulfur eastern bituminous coal which when the SCR was operating.

Facility F

This test site unit has is a 165 megawatt (MW) per boiler power plant. The plant burns low sulfur eastern bituminous coal in a dry-bottom pulverizer boiler. Cold-side electrostatic precipitators (ESPs) are used for particulate control. One 5 gallon bucket of fly ash (FFA) was collected from the ESP hopper by NRT personnel in August 2004.

Facility G

This test site is a 165 megawatt (MW) power plant. The plant burns low sulfur eastern-bituminous coal in a dry-bottom pulverizer boiler. Cold-side electrostatic precipitators (ESPs) are used for particulate control. A SNCR system was operating to control NO_x. One 5 gallon bucket of fly ash (GFA) was collected from the ESP hopper by NRT personnel in August 2004.

Facility H

Facility H is a 500 MW power plant. The plant burns Illinois Basin coal in a dry-bottom pulverizer boiler. Cold-side ESPs are used on all units for particulate control, an SCR system was operating, and wet FGD systems were used to reduce SO₂ emissions. The wet FGD systems utilize limestone slurry sorbents and an inhibited oxidation process. The FGD sludge, consisting primarily of calcium sulfite, is pumped from the absorber to a thickener. Liquid overflow from the thickener is recycled back into the FGD system, and the thickened sludge is pumped to a series of drum vacuum filters for further dewatering. Water removed by the drum vacuum filters is recycled back into the FGD system, and the filter cake is taken by conveyor belt to a pug mill, where it is mixed with dry fly ash and dry quicklime for stabilization. The resulting scrubber FGD solids are taken by conveyor to a temporary outdoor stockpile, and then transported by truck either to a utilization site or to an on-site landfill. One 5 gallon bucket of fly ash (HFA) was collected from the ESP hopper by NRT personnel in August 2004.

Facility J

Facility J has a 160 MW boiler that typically burns a 85:15 blend of PRB and bituminous coals. The unit sometimes switches to 100% PRB on the weekends. However, during our flue gas/fly ash sampling, the unit was burning the PRB/bituminous blend. The flue gas from the boiler splits and is directed into two parallel CS-ESPs (designated the "South ESP" and the "North ESP", each treating half of the flue gas). The flue gas is then recombined before exiting the stack. During testing, B-PAC was injected upstream of the South ESP. The unit has no NO_x or SO₂ controls.

The injection rate of the B-PAC was 5 lb/MMacf at the time when the CCR with B-PAC in use was collected from this facility.

One 5-gallon bucket of fly ash without the B-PAC injection (JAB) and one 5 gallon bucket of fly ash with PAC injection (JAT) were collected.

Facility K

Facility K is two tangentially fired 400 MW coal-fired boilers with cold side ESP followed by a wet flue gas desulfurization system with wet Mg-lime natural oxidation. These units burn medium sulfur eastern bituminous coals from Ohio, Pennsylvania and West Virginia. Flue gas is scrubbed through a common wet FGD unit; FGD is a wet Mg-lime natural oxidation design. FGD sludge is mixed with fly ash and quicklime for stabilization prior to disposal.

Two samples were collected on November 29, 2004: one scrubber sludge filter cake before mixing in the pug mill (sample KGD), and one fixated scrubber sludge collected after mixing the scrubber sludge with fly ash and 2-3% lime in the pugmill (sample KCC). On January 12, 2005, one fly ash sample was collected directly from the ESP before the fly ash storage silo (sample KFA, collected in January 2005). Each sample consisted of four 5-gallon bucket of the material, and were collected by plant personnel.

Facility L

This facility is configured similarly to St. Clair except that it used one HS-ESP with two compartments rather than two CS-ESPs, and it uses separated overfired air (SO_fA) ports for NO_x control. As a result, the fly ash collection temperature is between 300 and 450 °F. Samples were collected from hoppers which were evacuated under negative pressure. The pneumatic hopper controls were turned off to allow enough samples to collect for the leaching evaluation. The controls were off for about 4 hr. There is concern that because of the high temperature within the fly ash collection hoppers, some mercury may have desorbed prior to sampling. Therefore, the samples obtained for evaluation may have a lower metal content. Because of the concern about mercury desorbing from the fly ash, additional fly ash was collected by turning off the pneumatic transfer for 30 min (2 weeks after the original samples were collected). Total metal content determinations were completed for all samples, which includes with and without brominated powdered activated carbon (BPAC) for fly ash collected after accumulation in the hopper for 4 hr (first sampling) and 30 min (second sampling). The leaching evaluation was conducted only on the samples collected over 4 hr intervals since this provided adequate sample size (5 gallons).

One 5 gallon bucket of fly ash without BPAC (LAB) and one 5 gallon bucket of fly ash with BPAC (LAT) was collected by ARCADIS personnel.

Facility M

Facility M is a 600 MW per unit power plant. The plant burns bituminous coal in a dry-bottom pulverizer boiler. Cold-side ESPs are used on all units for particulate control, and wet FGD systems are used to reduce SO₂ emissions on two units. The wet FGD systems utilize limestone slurry and an inhibited oxidation process. The FGD sludge, consisting primarily of calcium sulfite, is pumped from the absorber to a thickener. Liquid overflow from the thickener is recycled back into the FGD system, and the thickened sludge is pumped to a series of drum vacuum filters for further dewatering. Water removed by the drum vacuum filters is recycled back into the FGD system, and the filter cake is taken by conveyor belt to a pug mill, where it is mixed with dry fly ash and dry quicklime for stabilization. The resulting scrubber FGD solids are taken by conveyor to a temporary outdoor stockpile, and then transported by truck either to a utilization site or to an on-site landfill. The currently active portion of the landfill is lined and includes leachate collection. An older inactive portion of the landfill is clay-lined but does not have leachate collection.

Three samples were obtained from the Pug Mill Area by the EPRI contractor during the week of March 6, 2006 when the SCR was not operating: fly ash, vacuum drum filter cake, and fixated scrubber sludge with lime (only FSSL was used in this study, sample MAD). In each case, the

samples were collected daily during the four day sample collection (four daily samples of each), for compositing in the laboratory. All of the samples were collected into clean 5 gallon plastic pails. Excess sample was containerized and discharged back into the appropriate system. The drum filter cake was sampled daily from the conveyor belt leading into the pug mill. Two of the three drum filters were running simultaneously; both were feeding the conveyor belt. The same drums were running each day of sampling. Each 5 gallon bucket was sealed immediately after collection and the lid secured with duct tape. The dry fly ash sample was obtained directly from the day tank via a hose connected to a sampling port. Each 5 gallon bucket was sealed immediately after collection and the lid secured with duct tape. FSS was sampled from the conveyor belt on the outlet side of the pug mill on the first, third and fourth days. A clean, short handled spade was used to collect sample from the conveyor belt into a 2 gallon bucket. The sample in the bucket was placed on a clean piece of 3 mm plastic sheeting; then more sample was collected from the conveyor belt into the bucket and added to the sheet until at least 6 gallons of sample was collected. Each sample was homogenized on the sheet using the spade and placed into a 5 gallon bucket, sealed immediately, and the lid secured with duct tape. A similar process was used to collect three more samples the week of May 9, 2006 when the SCR was in use (FSSL sample MAS).

Facility N

Facility N is a wall fired 715 MW coal-fired power plant with cold side ESP followed by a wet FGD system using wet limestone in a forced oxidation process. The unit burns medium to high sulfur eastern bituminous coals with approximately 3% sulfur. The gypsum is washed, dried and then sold to the wallboard industry.

One 5 gallon bucket of un-washed gypsum (NAU) and one 5 gallon bucket of washed gypsum (NAW) were collected from this site. Facility N was sampled on June 1, 2006. Samples were provided by RMB Consulting & Research, Inc. (Raleigh, NC).

Facility O

Facility O is a tangentially fired 500 MW coal-fired plant with cold side ESP followed by a wet FGD system with wet limestone forced oxidation. The unit is equipped with a pulverized coal boiler and ammonia based SCR. This unit burns high sulfur eastern bituminous coals. Slurry from the absorber goes to a primary hydrocyclone for initial dewatering. The gypsum (hydrocyclone underflow) is dried on a vacuum belt and washed to remove chlorides, before use in wallboard.

Two samples were collected from the FGD gypsum drying facility by compositing samples collected on June 10, 11, and 12, 2006 when the SCR was operating. On each day, two gallon pails of unwashed gypsum and washed/dried gypsum were collected. The unwashed gypsum was collected from the vacuum belt prior to the chloride spray wash. The washed/dried gypsum was collected from the end of the vacuum belt. The three daily samples were sent to Arcadis for compositing to form sample OAU (unwashed gypsum) and sample OAW (washed gypsum). All samples were collected by plant personnel.

Facility P

Facility P is two wall fired 200 MW coal-fired boilers with cold side ESP followed by a wet FGD system with wet limestone forced oxidation. Unit 1 is equipped with SNCR and Unit 2 is equipped with SCR. These units burn medium sulfur eastern bituminous coals. Particulate is removed with a cold-side ESP. Flue gas is then scrubbed through a common wet FGD unit; FGD is a wet limestone forced oxidation design. The gypsum provided was not washed.

Facility P was sampled in October 2006 when both SCR and SNCR were operating and the residues from Unit 1 and Unit 2 were commingled during collection. One 5 gallon bucket of the un-washed gypsum (PAD) was collected by plant personnel.

Facility Q

Facility Q is a 1800 MW coal fired plant with hot side ESP followed by a wet flue gas desulfurization system with wet limestone forced oxidation. This plant burns sub-bituminous coal. FGD is a wet limestone forced oxidation design that includes the addition of dibasic acid to the absorber¹ for to buffer the scrubber liquor and control calcium scaling. Gypsum is not washed, but make up water is added continually rather than operating closed loop to maintain low chloride concentrations.

One 5 gallon bucket of un-washed gypsum (QAU) was collected on October 30, 2006. The sample was collected by NRT personnel. The sample was shipped to ARCADIS for analysis on Mary 4, 2007.

Facility R

This test site is a 175.5 megawatt (MW) power plant. The plant burns sub-bituminous PRB coal in a dry-bottom pulverizer boiler. Cold-side electrostatic precipitators (ESPs) are used on all units for particulate control, and wet FGD systems are used to reduce SO₂ emissions on two units. The wet FGD system utilizes a wet limestone slurry sorbent and a forced oxidation process. Gypsum from the FGD system uses a hydrocyclone and a vacuum drum filter to remove residual water from the product. Gypsum is not washed, but make up water is added continually rather than operating closed loop, so the chlorides stay low. The system was originally designed to wash filter cake. The gypsum material is recycles for use in wallboard.

One 5 gallon bucket of un-washed gypsum (RAU) was collected on May 3, 2007. The sample was collected by a contractor for EPRI.

¹ Dibasic acid (DBA) is a commercial mixture of glutaric, succinic, and adipic acids: HOOC(CH₂)₂₋₄COOH.

Facility S

This test site is a 600 megawatt (MW) per unit power plant. The plant burns eastern high sulfur bituminous coal in a dry-bottom pulverizer boiler. Cold-side electrostatic precipitators (ESPs) are used on all units for particulate control, and wet FGD systems are used to reduce SO₂ emissions on two units. The wet FGD systems utilize limestone slurry sorbents and an forced oxidation process

Samples of washed (SAW) and unwashed (SAU) gypsum were collected at this site in July, 2007. One five-gallon bucket of each was collected by plant personnel.

Facility T

This power plant test site has three boilers producing a total of a 2,000+ megawatts (MW). The plant burns medium sulfur eastern bituminous coal in a dry-bottom pulverizer boiler. Units 1 and 2 have coal cleaning equipment to reduce ash and SO_x emissions. All three of these units have low NO_x burners and selective catalytic reduction systems for NO_x control. Ammonia was injected upstream of the SCR catalysts. Cold-side electrostatic precipitators (ESPs) are used on all three units for particulate control. A wet FGD systems using limestone in a forced oxidation mode are used to reduce SO₂ emissions on Unit 3.

Four samples were collected by plant personnel on September 17, 2007: one 5 gallon bucket of fly ash from Unit 2 (TFA), one 5 gallon bucket of un-washed gypsum from Unit 3 (TAU), one 5 gallon bucket of washed gypsum from Unit 3 (TAW), and one 5 gallon bucket of FGD waste water treatment plant filter cake from Unit 3 (TFC).

Facility U

This test site has eight boilers producing a total of 1,629 megawatts (MW). The plant burns low sulfur eastern bituminous coal in a dry-bottom pulverizer boiler. Samples from this site were collected from units 7 and 8. Both of these units have low NO_x burners and selective catalytic reduction systems for NO_x control. A cold-side electrostatic precipitator (ESP) were used on unit 7 for particulate control, and a wet FGD system using limestone in a forced oxidation mode is used to reduce SO₂ emissions. Due to low capture efficiency of the ESP on unit 7, approximately 25% of the FGD gypsum is fly ash. Unit 8 has no ESP but has a FGD system that captures approximately 100% of the fly ash with the gypsum.

Four 5-gallon buckets of fly ash were collected from the hoppers of unit 7. The four fly ash samples were combined and homogenized to produce one fly ash sample for the leaching study (UFA). One five gallon bucket of the un-washed fly ash/FGD gypsum material from unit 7 was collected (UAU). One bucket of the fly ash/FGD gypsum material from unit 8 (UGF) was also collected. These samples were collected by plant personnel on March 12, 2008.

Facility V

This test site is a 450 megawatt (MW) power plant. The plant burns sub-bituminous PRB coal in a dry-bottom pulverizer boiler. A SCR system was operating during the collection of this sample. The unit uses a spray dryer with slaked lime for FGD control. A baghouse with a fabric filter is used to control the fly ash and spray dryer ash emissions. The ash is collected in hoppers before disposal in a landfill.

One five gallon bucket of the spray dryer adsorber material (VSD) was collected by NRT personnel in April, 2008. This sample was delivered to ARCADIS on 4/15/08.

Facility W

This site is operated by American Electric Power (AEP) and has two 800 MW coal-fired boilers for a plant total of 1,600 MW. The plant burns eastern bituminous coal in a dry-bottom pulverizer boiler. Cold-side electrostatic precipitators (ESPs) are used on both units for particulate control, and wet FGD systems are used to reduce SO₂ emissions on two units. The wet FGD systems utilize limestone slurry sorbents and a forced oxidation process. SO₂ concentrations of the inlet FGD are approximately 1990 ppm with removal efficiencies of 98%. The plant has a Trona injection system for SO₃ control, but this system was not operating at the time of sampling.

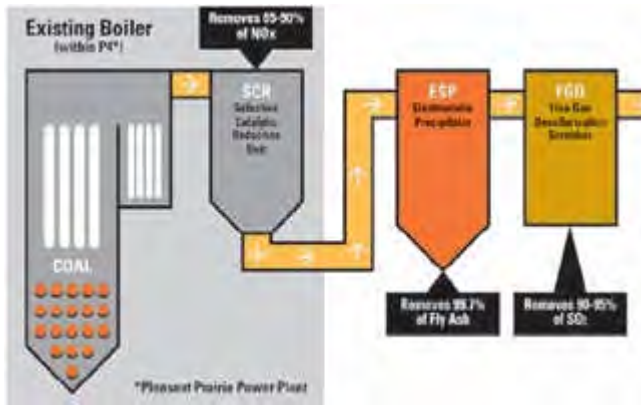
Samples were collected as follows: dry FGD gypsum after water wash (WAW), moist FGD gypsum before the water wash (WAU), wastewater treatment system filter cake (WFC), and dry fly ash (WFA). Five gallon buckets of each of the samples were collected by plant personnel on 11/20/08. Samples were delivered to ARCADIS on 11/28/07.

Facility X

Wisconsin Electric Power Company, a subsidiary of Wisconsin Energy, owns and operates Pleasant Prairie Power Plant located near Kenosha, Wisconsin. The plant has two 600 MW balanced-draft coal-fired boilers designated units 1 and 2. Unit 2 was selected for inclusion in the NETL program because it burns a variety of Powder River Basin low sulfur, sub-bituminous coals. In addition, this facility has the ability to isolate one ESP chamber (1/4 of the unit) (Starns et al., 2002).

The primary pollution control equipment consists of SCR, cold-side ESPs, and a wet-FGD system. NO_x is controlled in the SCR by injecting ammonia in the presence of a catalyst. The forced oxidation FGD system uses wet-limestone as a sorbent for SO₂ control. This site also contains an additional mercury oxidation catalyst.

Samples were collected as follows: dry FGD gypsum after water wash (XAW), moist FGD gypsum before the water wash (XAU), FGD wastewater treatment system filter cake (XFC), and dry fly ash (XFA). Five gallon buckets of each of the samples were collected by plant personnel and delivered to ARCADIS on 6/16/08.



Facility Y

This test site is a 450 megawatt (MW) power plant. The plant burns sub-bituminous PRB coal in a dry-bottom pulverizer boiler. An SCR before the air preheater was operating at the time of sampling. The unit uses a spray dryer with slaked lime for SO₂ control. A baghouse with a fabric filter is used to control the fly ash and spray dryer adsorber particulate emissions. The ash is collected in hoppers before disposal in a landfill or recycles as an additive for stucco.

One five-gallon bucket of the spray dryer absorber (SDA) material (YSD) sample was collected by plant personnel in December, 2007. This sample was delivered to ARCADIS on 12/18/07.

Facility Z

The samples from this power plant facility are generated from four boilers producing 1,135 megawatt (MW) of power. The plant burns sub-bituminous PRB coal in a dry-bottom pulverizer boiler. Cold-side electrostatic precipitators (ESPs) are used on all units for particulate control. This plant produces approximately 112,000 tons of fly ash and 23,000 tons of bottom ash yearly. The fly ash and bottom materials are stored separately.

Samples of the fly ash from Unit 6 and 7 were collected by plant personnel on 8/28/08. One five gallon bucket of fly ash was collected from Unit 6 (ZFB) and one from Unit 7 (ZFA). Samples were received by ARCADIS on 9/1/08.

Facility Aa

This test site has four boilers producing a total of 2,424 megawatt (MW) of power. The plant burns eastern-bituminous coal in a dry-bottom pulverizer boiler. Cold-side electrostatic precipitators (ESPs) are used on three units and hot-side ESP on one unit for particulate control. Unit 1 at this plant was burning medium sulfur coal and the SCR was operating. Unit 2 was burning medium sulfur coal and the SCR was not operating. Unit 3 was burning high sulfur coal and the SCR was operating. Unit 4 was burning low sulfur coal, the SCR was operating, and uses a hot-side ESP to control particulate. A dry handling system is used to collect the fly ash from the ESPs.

Units 3 and 4 were connected to a single FGD system. The wet FGD systems utilize limestone slurry sorbents and a forced oxidation process. Samples of the washed and un-washed FGD gypsum were collected. Fly ash was collected from units 1, 3, and 4. Unit 2 was not operating at the time of sampling.

Facility Ba

This test site has two boilers producing 1,150 megawatt (MW) of power. The plant burns a mixture of 54% Powder River Basin sub-bituminous and 46% Gulf Coast Lignite coal in a dry-bottom pulverizer boiler. Cold-side electrostatic precipitators (CS-ESPs) and a Compact Hybrid Particulate Collector (COPAC) baghouse system are used on both units. To increase the particulate collection efficiency, ammonia injection is used for particulate conditioning. A dry handling system was used to collect the fly ash from the fly ash hoppers.

A combined fly ash sample (BaFA) was collected from units 1 and 2. One five gallon bucket of the fly ash material was collected by plant personnel November 5, 2008.

Facility Ca

This site has one 454 megawatt (MW) boiler and another boiler currently under construction. The plant burns Gulf Coast Lignite coal in a dry-bottom pulverizer boiler. The plant uses low NO_x burners with cold-side electrostatic precipitators (CS-ESPs) for particulate control. A dry handling system was used to collect the fly ash from the ESPs. A wet FGD scrubber using limestone in a forced oxidation configuration is used to control SO_x emissions.

Fly ash from this plant is recycled for use in cinder block and cement. Gypsum is in wallboard.

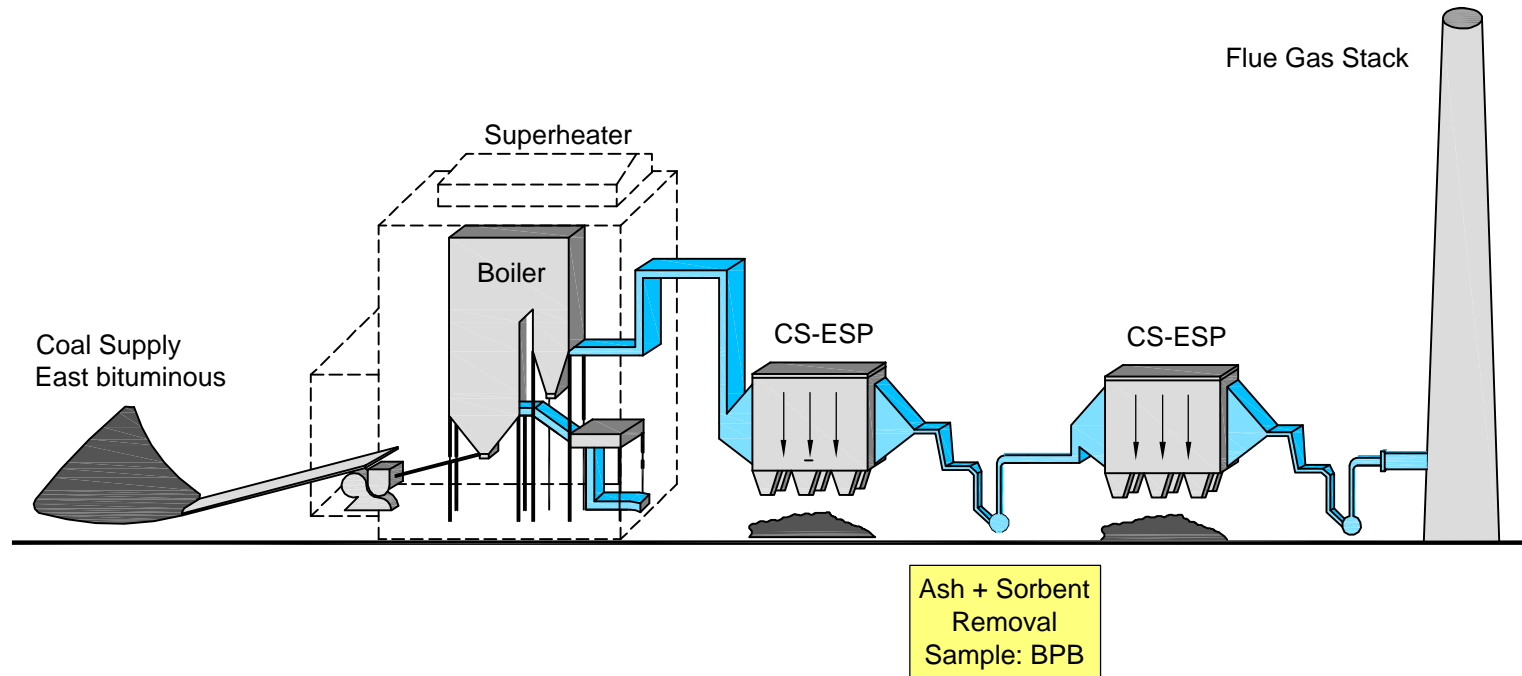
One five gallon bucket of the fly ash material (CaFA) and one five gallon bucket of washed FGD gypsum (CaAW) were collected by plant personnel November 6, 2008.

Facility Da

This test site has two supercritical boilers producing 2,240 megawatts (MW) of power. The plant burns eastern-bituminous coal in a dry-bottom pulverizer boiler. The primary pollution control equipment consists of low NO_x burners, SCR, cold-side ESPs, and a wet-FGD system. NO_x is controlled in the SCR by injecting ammonia in the presence of a catalyst. The forced oxidation FGD system uses wet-limestone as a sorbent for SO₂ control. A dry handling system is used to collect the fly ash from the ESPs.

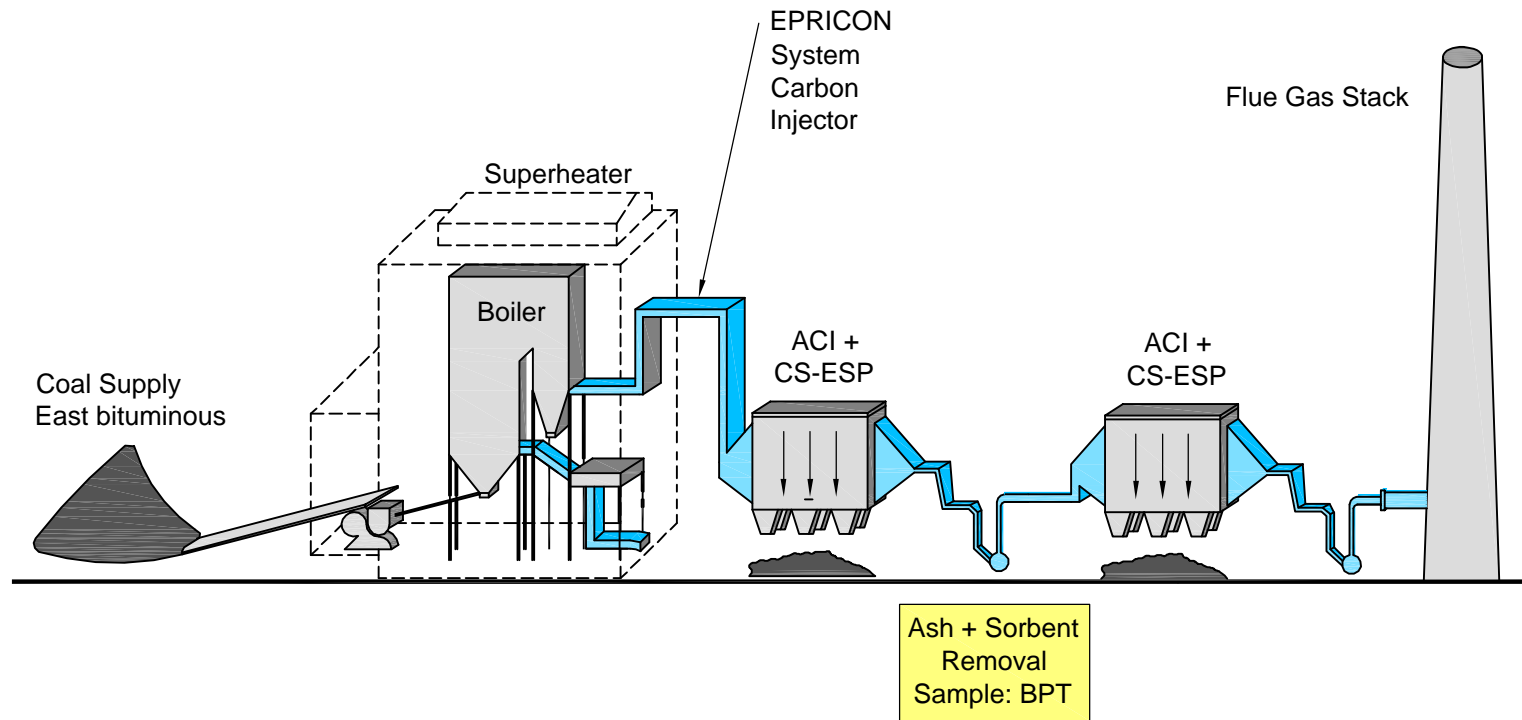
One five gallon bucket each of fly ash (DaFA), washed gypsum (DaAW), and FGD waste water treatment plant filter cake (DaFC) were collected by plant personnel. Samples were received by ARCADIS on 12/12/2008.

Facility: Brayton Point



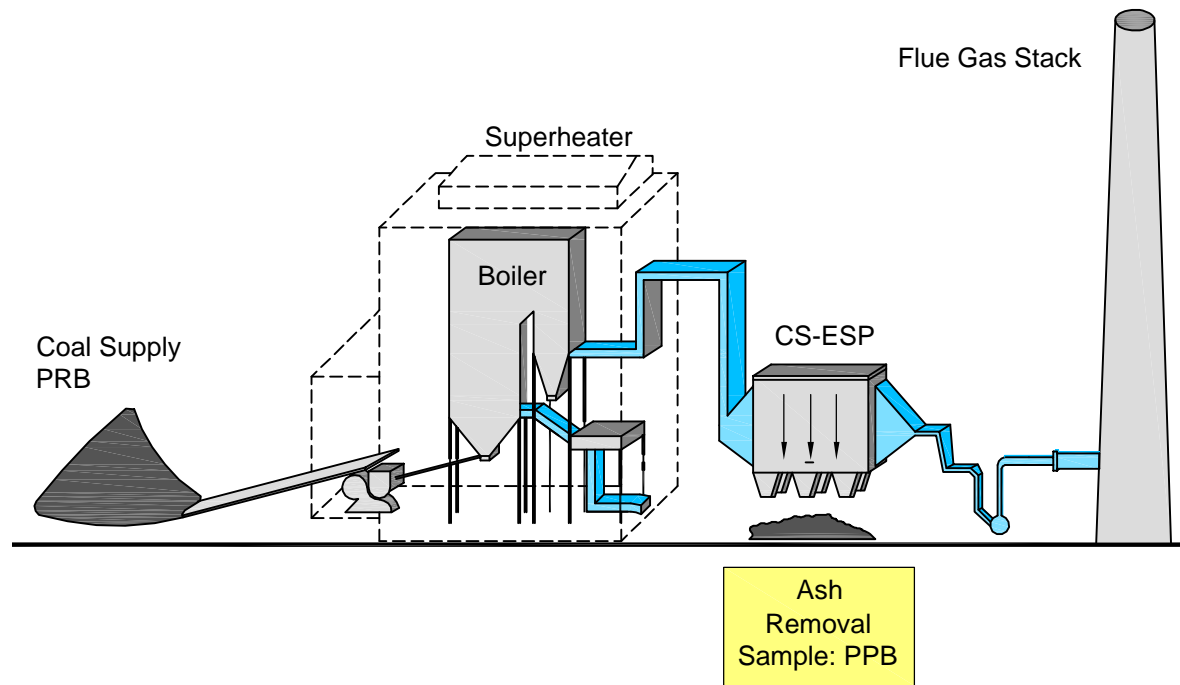
CS-ESP - Cold Side-Electrostatic Precipitator

Facility: Brayton Point with ACI



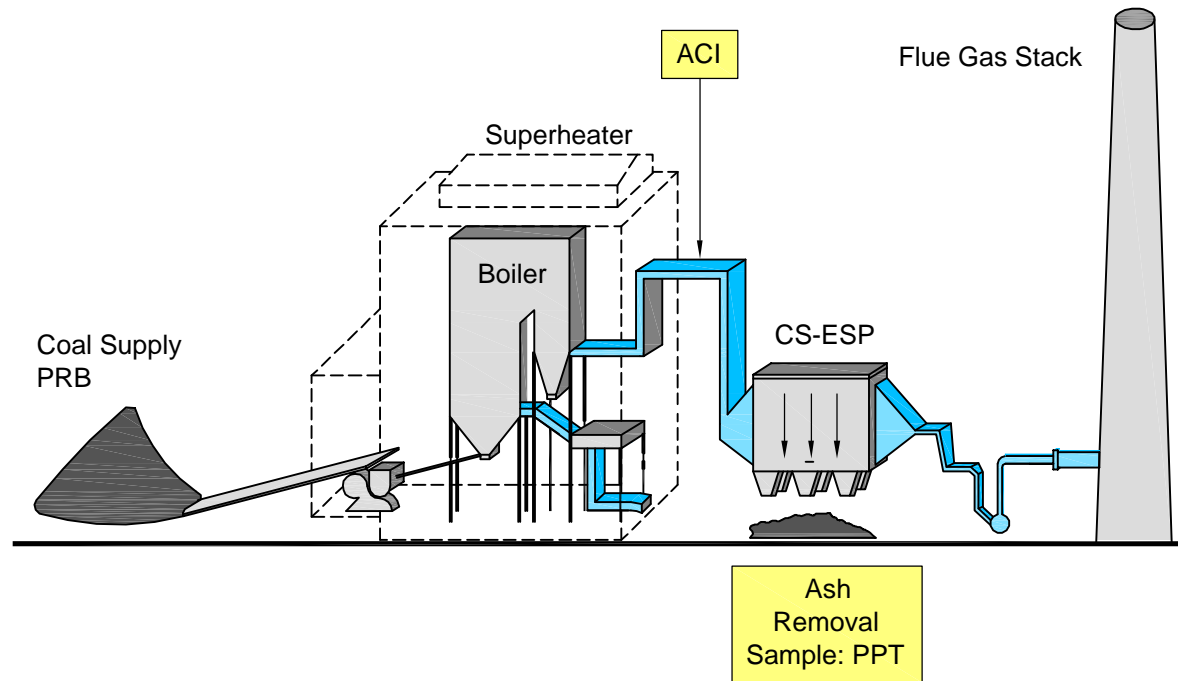
ACI - Activated Carbon Injector
CS-ESP - Cold Side-Electrostatic Precipitator

Facility: Pleasant Prairie



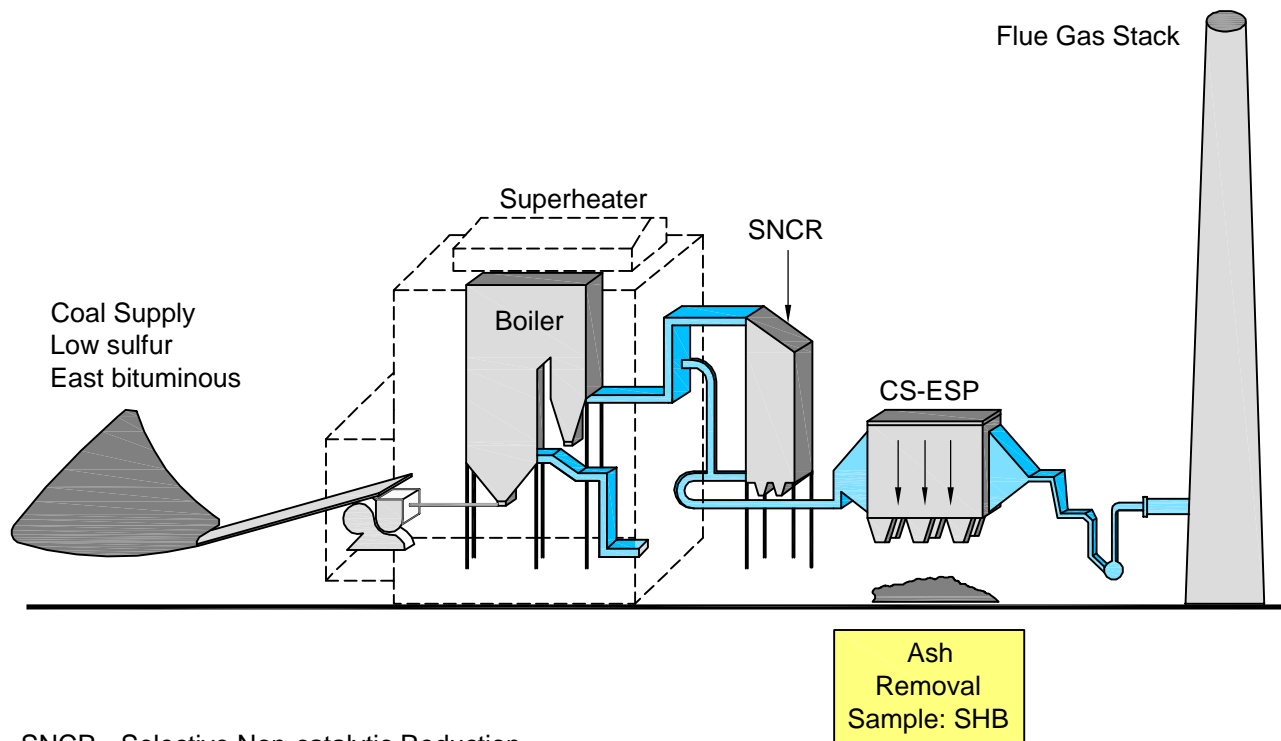
PRB - Powder River Basin
CS-ESP - Cold Side-Electrostatic Precipitator

Facility: Pleasant Prairie with ACI



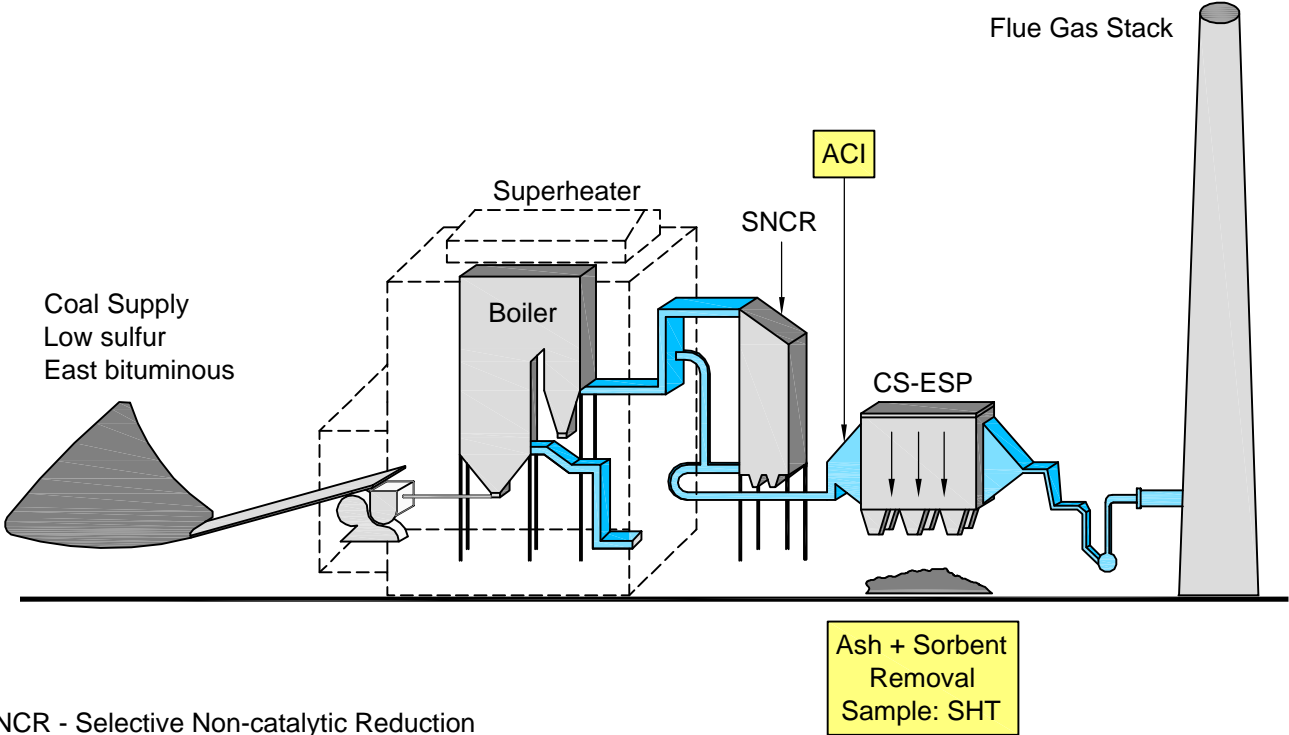
ACI - Activated Carbon Injector
CS-ESP - Cold Side-Electrostatic Precipitator

Facility: Salem Harbor



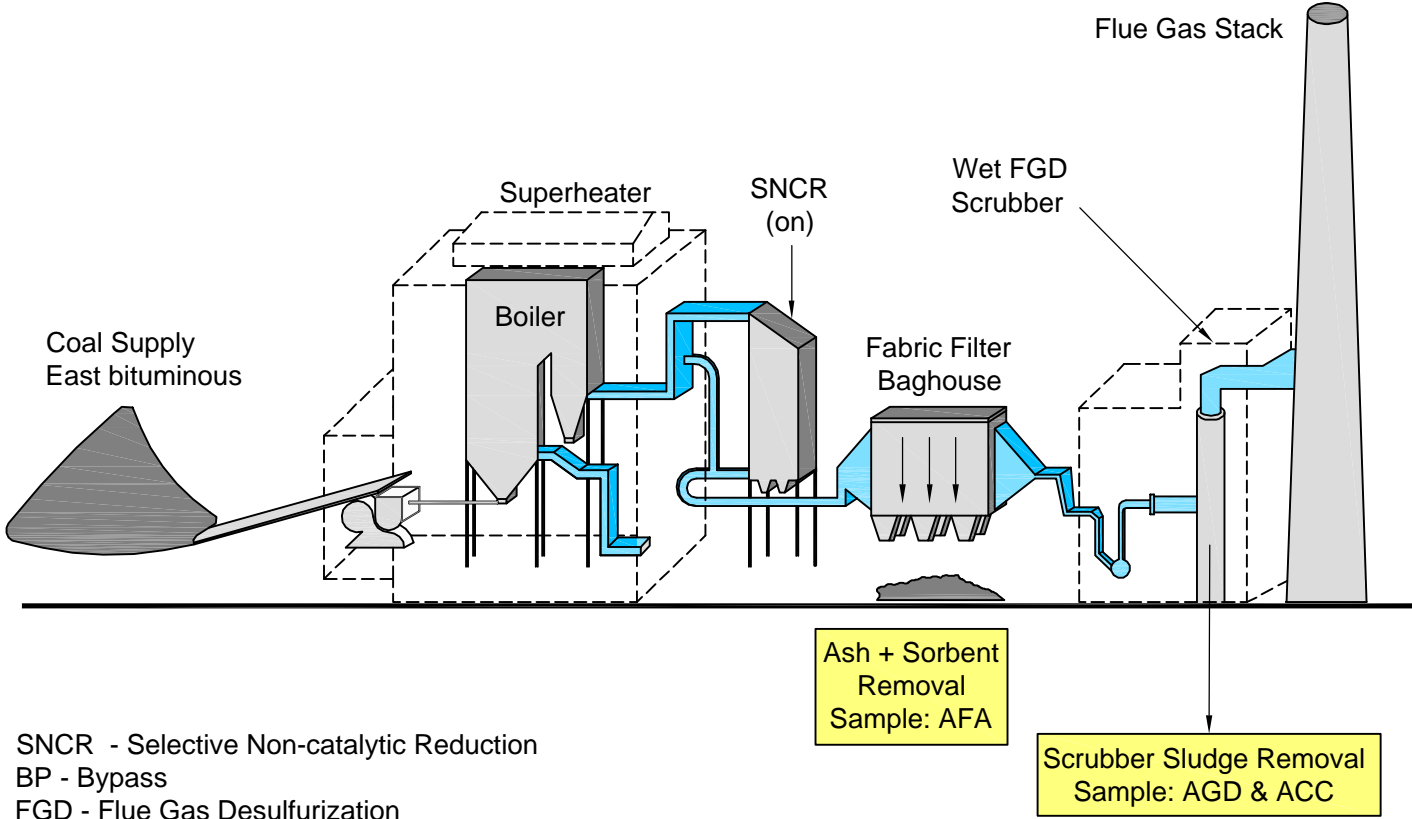
SNCR - Selective Non-catalytic Reduction
CS-ESP - Cold Side-Electrostatic Precipitator

Facility: Salem Harbor with ACI

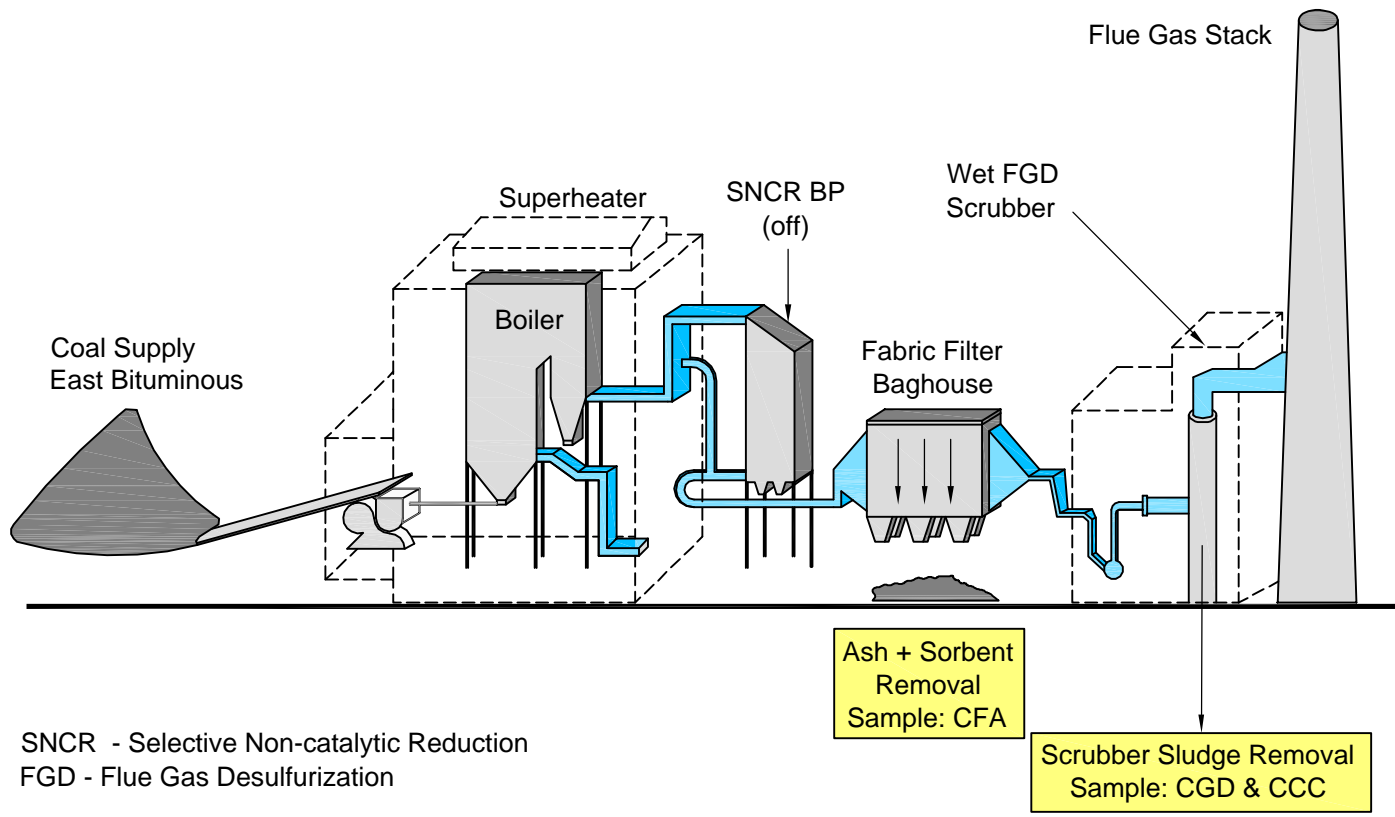


SNCR - Selective Non-catalytic Reduction
ACI - Activated Carbon Injector
CS-ESP - Cold Side-Electrostatic Precipitator

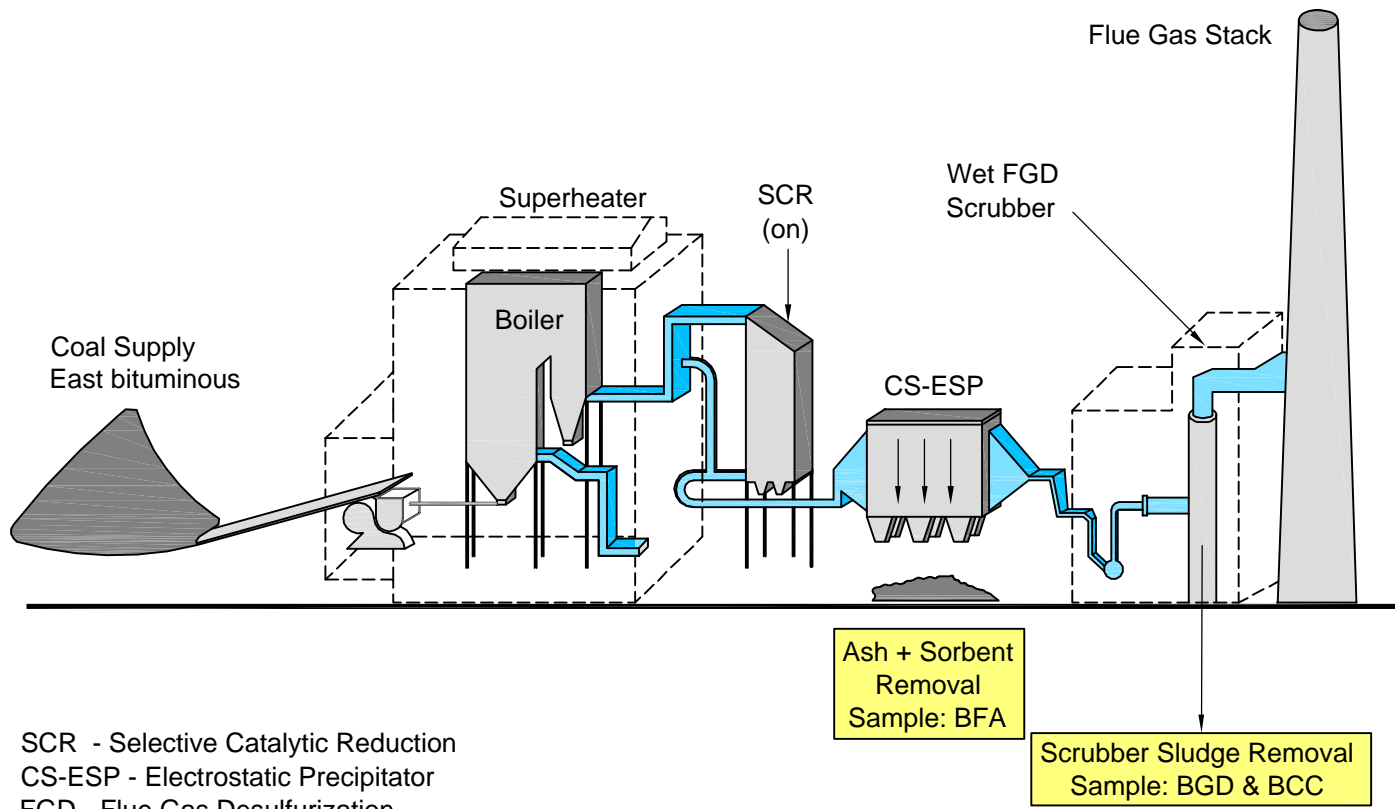
Facility: A



Facility: C

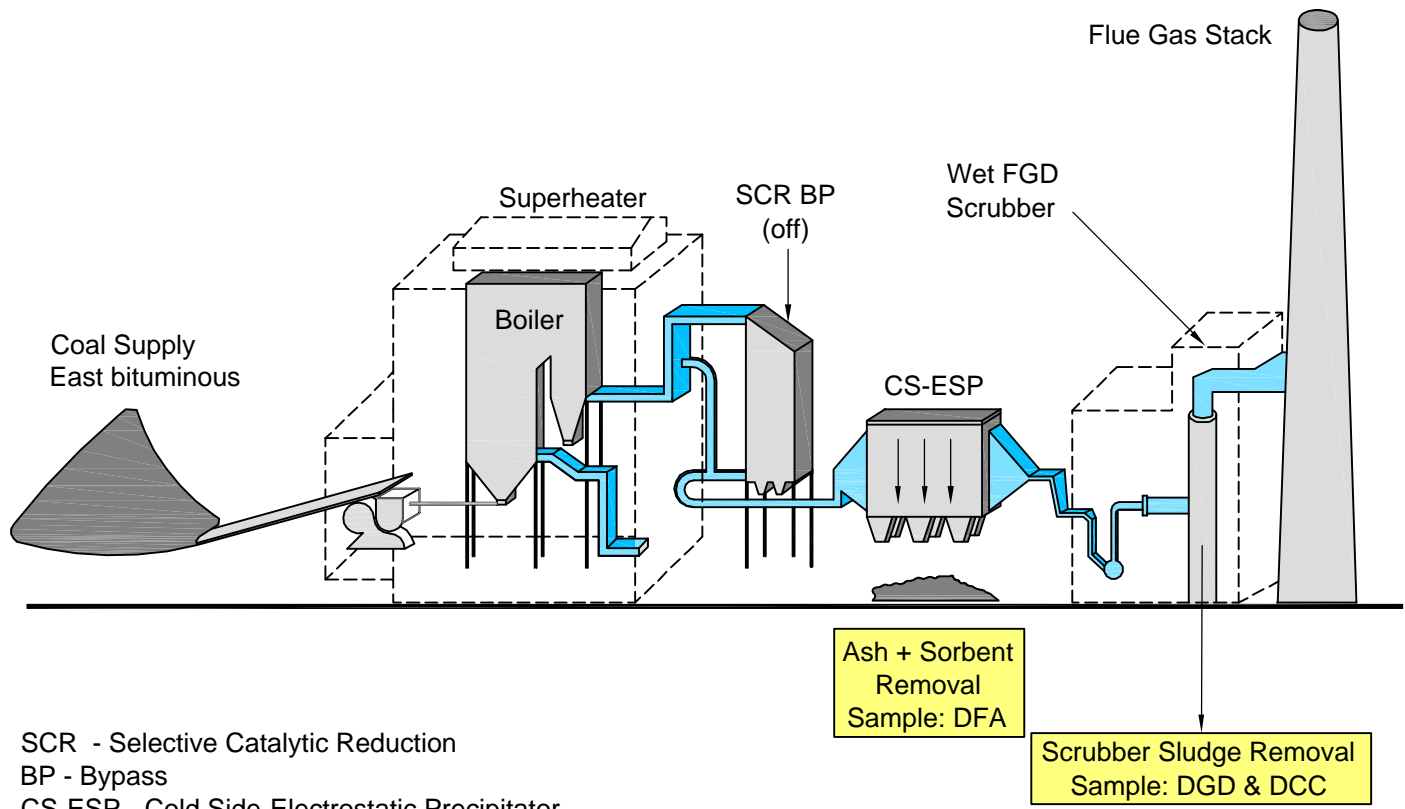


Facility: B SCR on



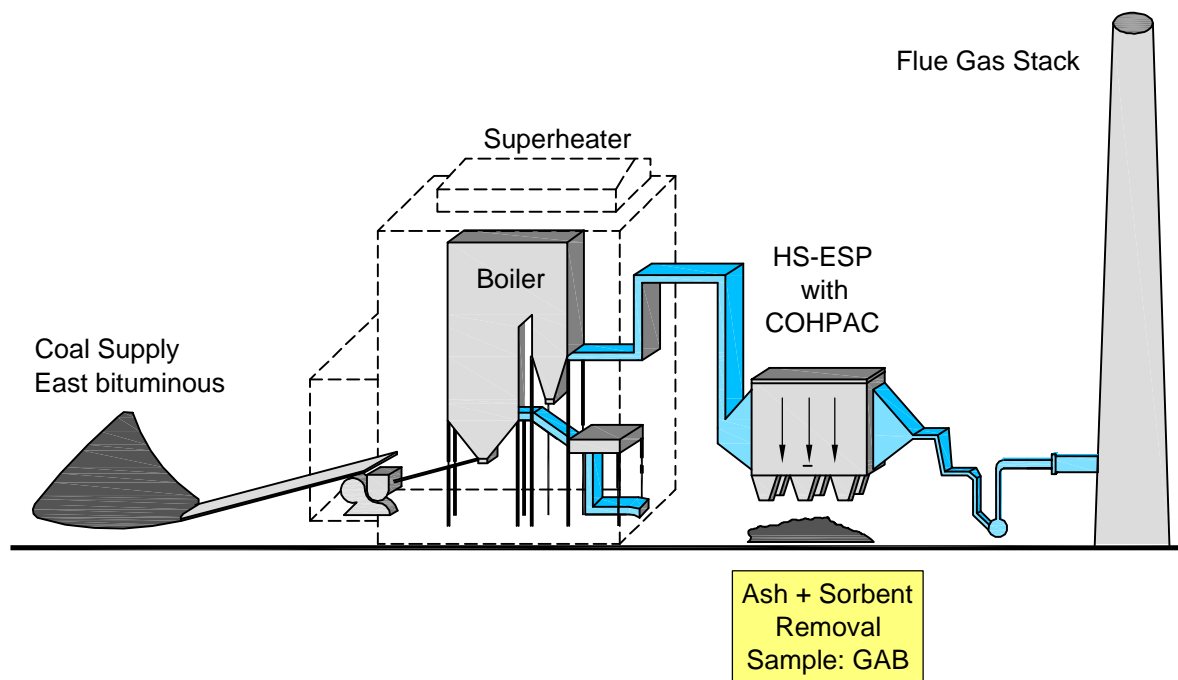
SCR - Selective Catalytic Reduction
CS-ESP - Electrostatic Precipitator
FGD - Flue Gas Desulfurization

Facility: B SCR off



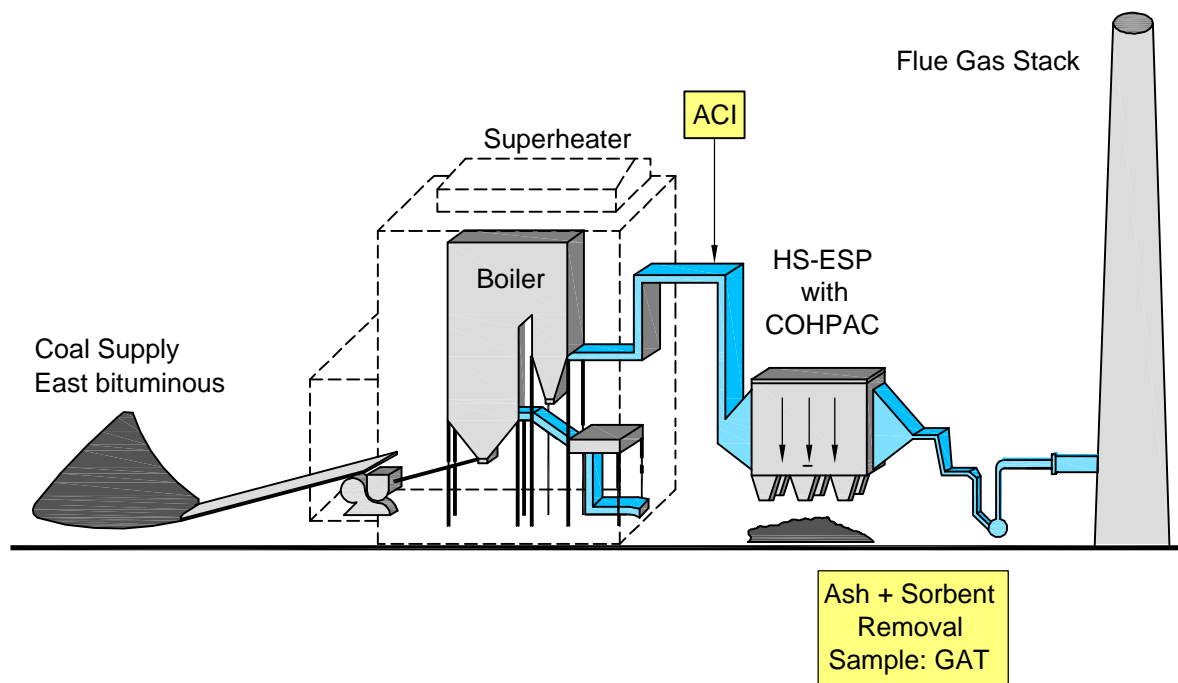
SCR - Selective Catalytic Reduction
BP - Bypass
CS-ESP - Cold Side-Electrostatic Precipitator
FGD - Flue Gas Desulfurization

Facility: C



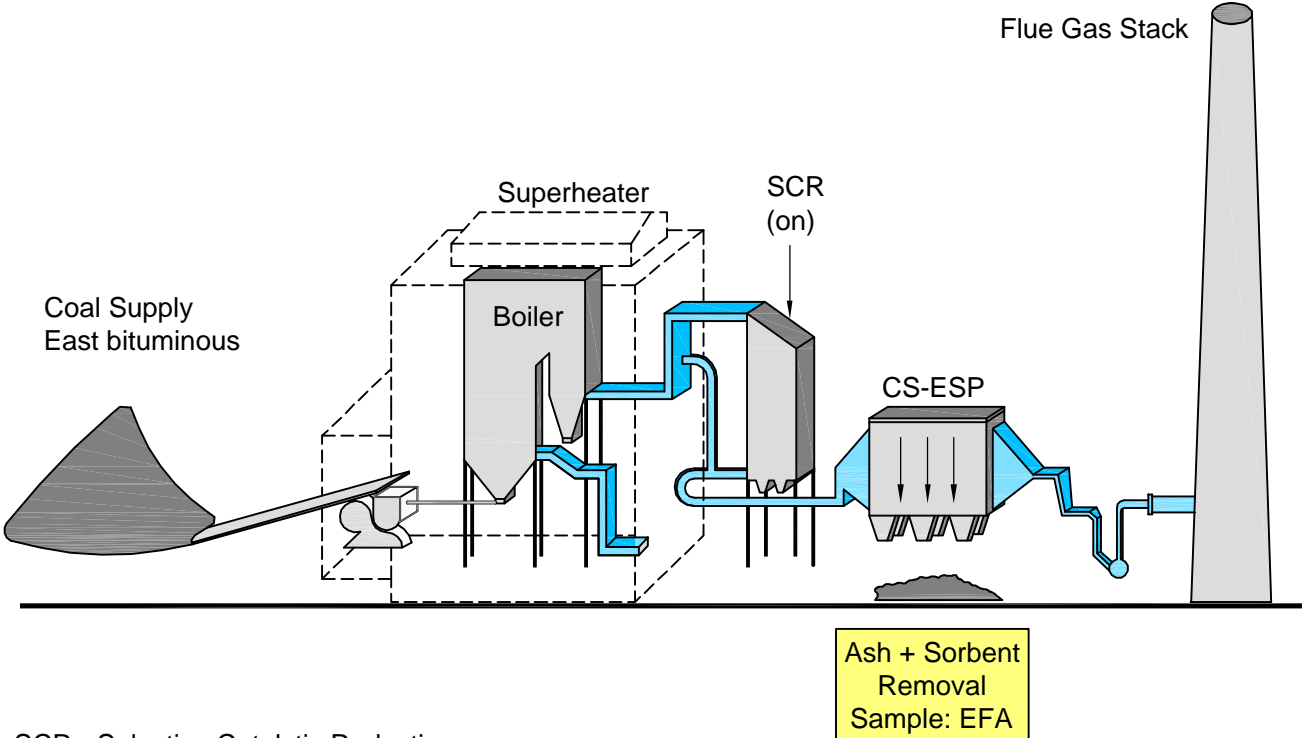
HC-ESP - Hot Side-Electrostatic Precipitator
COHPAC - Compact Hybrid Particulate Collector

Facility: C with ACI



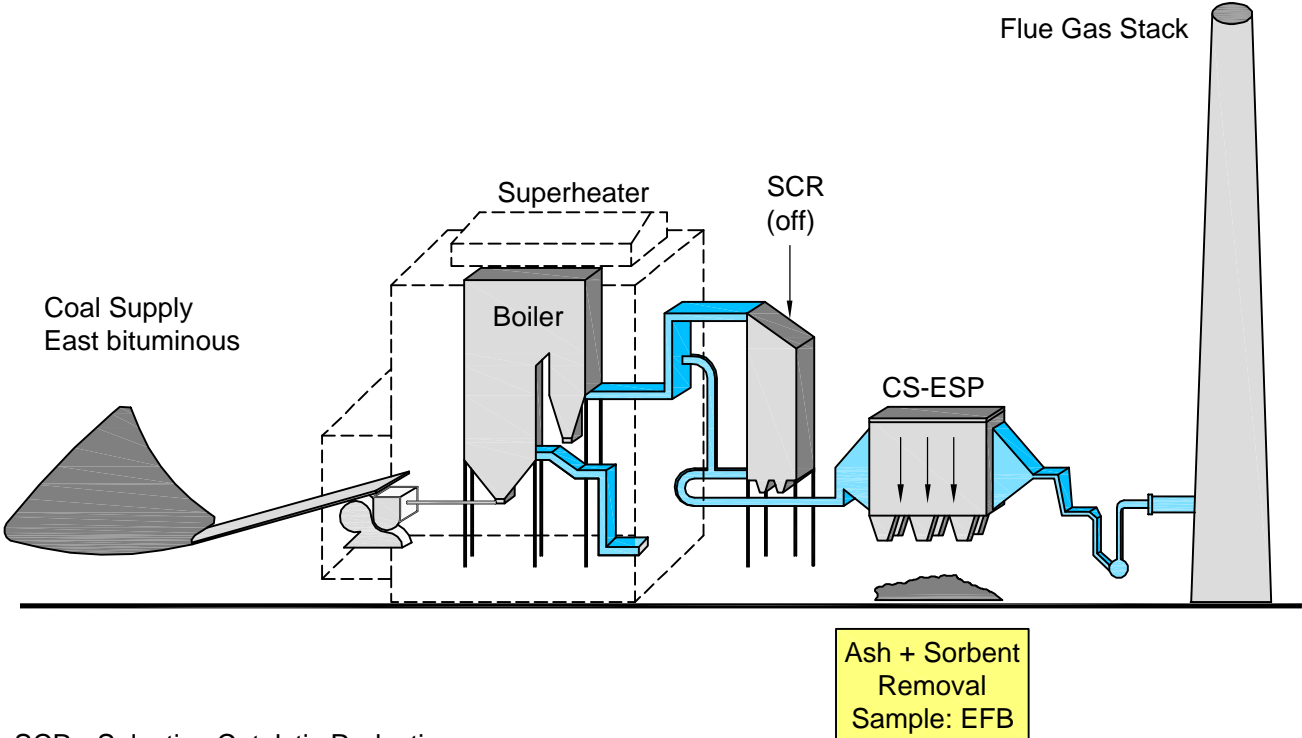
ACI - Activated carbon Injector
HS-ESP - Hot Side-Electrostatic Precipitator
COHPAC - Compact Hybrid Particulate Collector

Facility: E SCR on



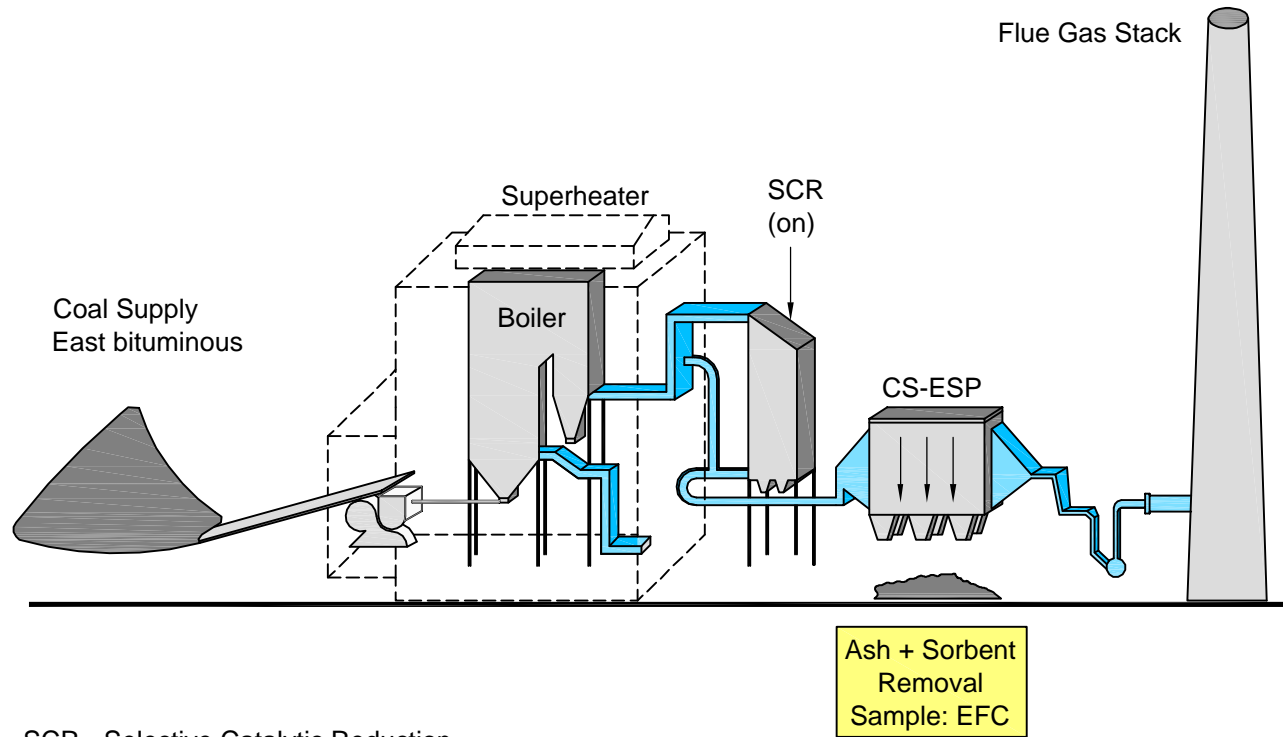
SCR - Selective Catalytic Reduction
CS-ESP - Electrostatic Precipitator

Facility: E SCR off



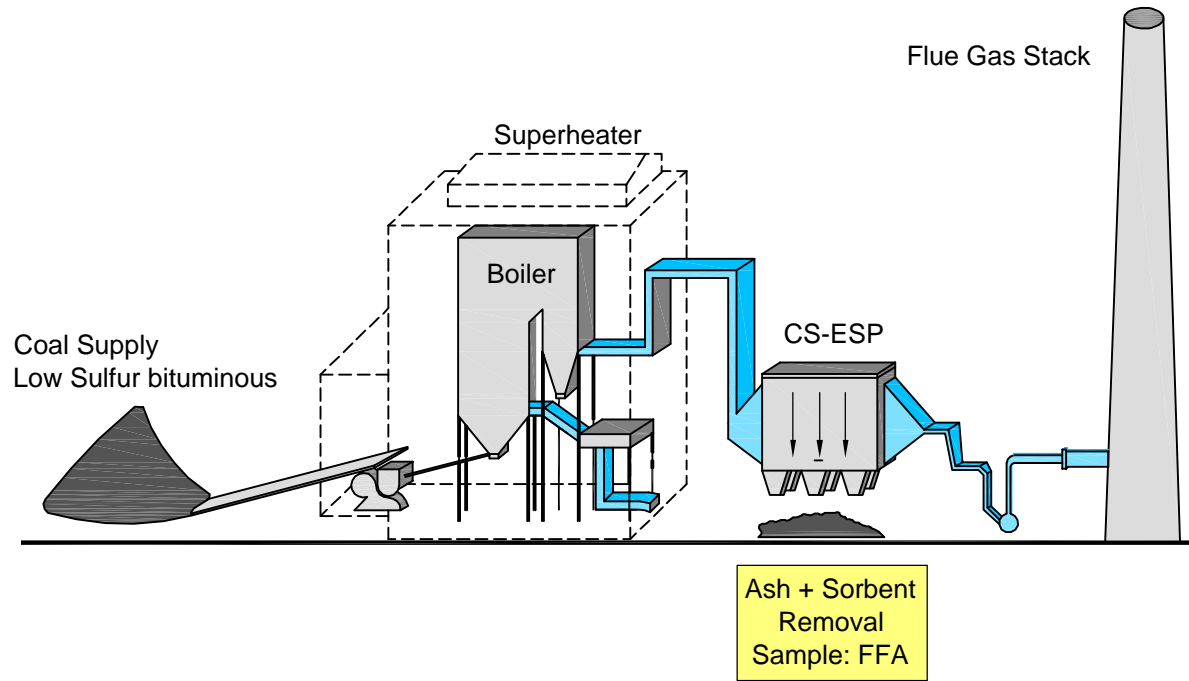
SCR - Selective Catalytic Reduction
CS-ESP - Electrostatic Precipitator

Facility: E SCR on



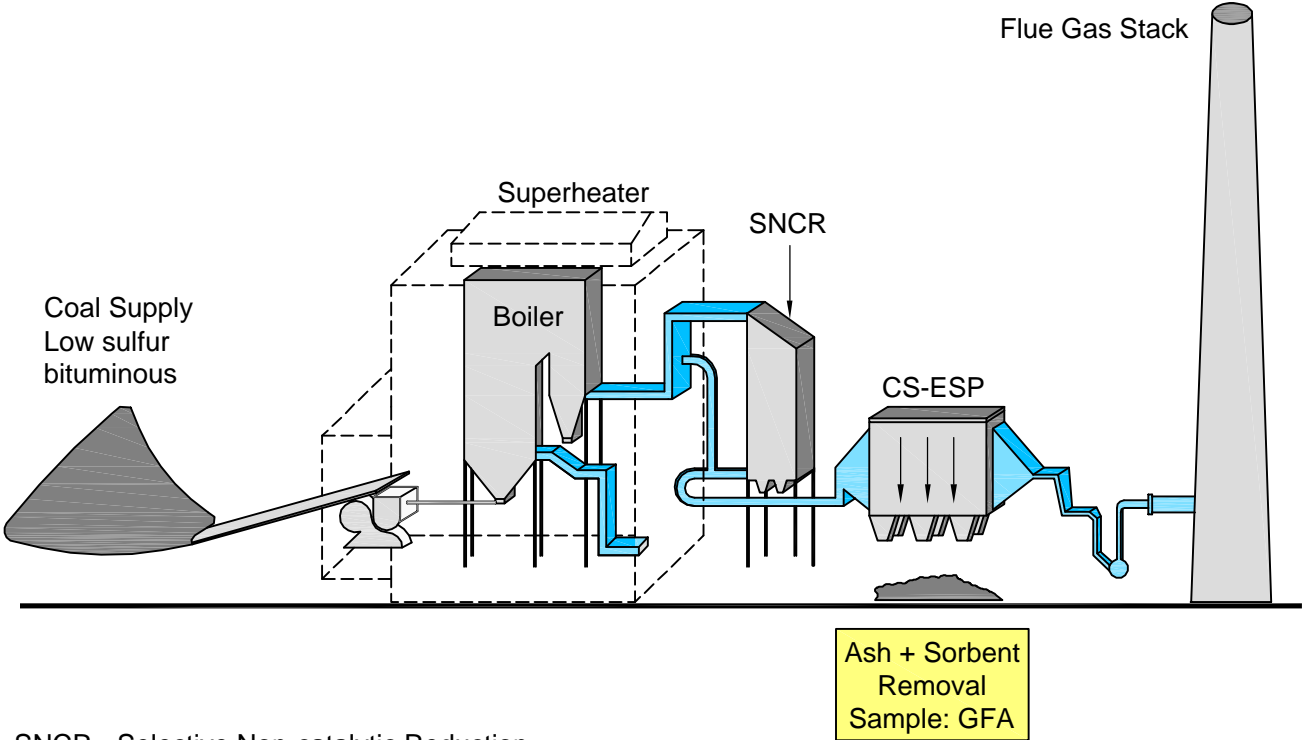
SCR - Selective Catalytic Reduction
CS-ESP - Electrostatic Precipitator

Facility: F



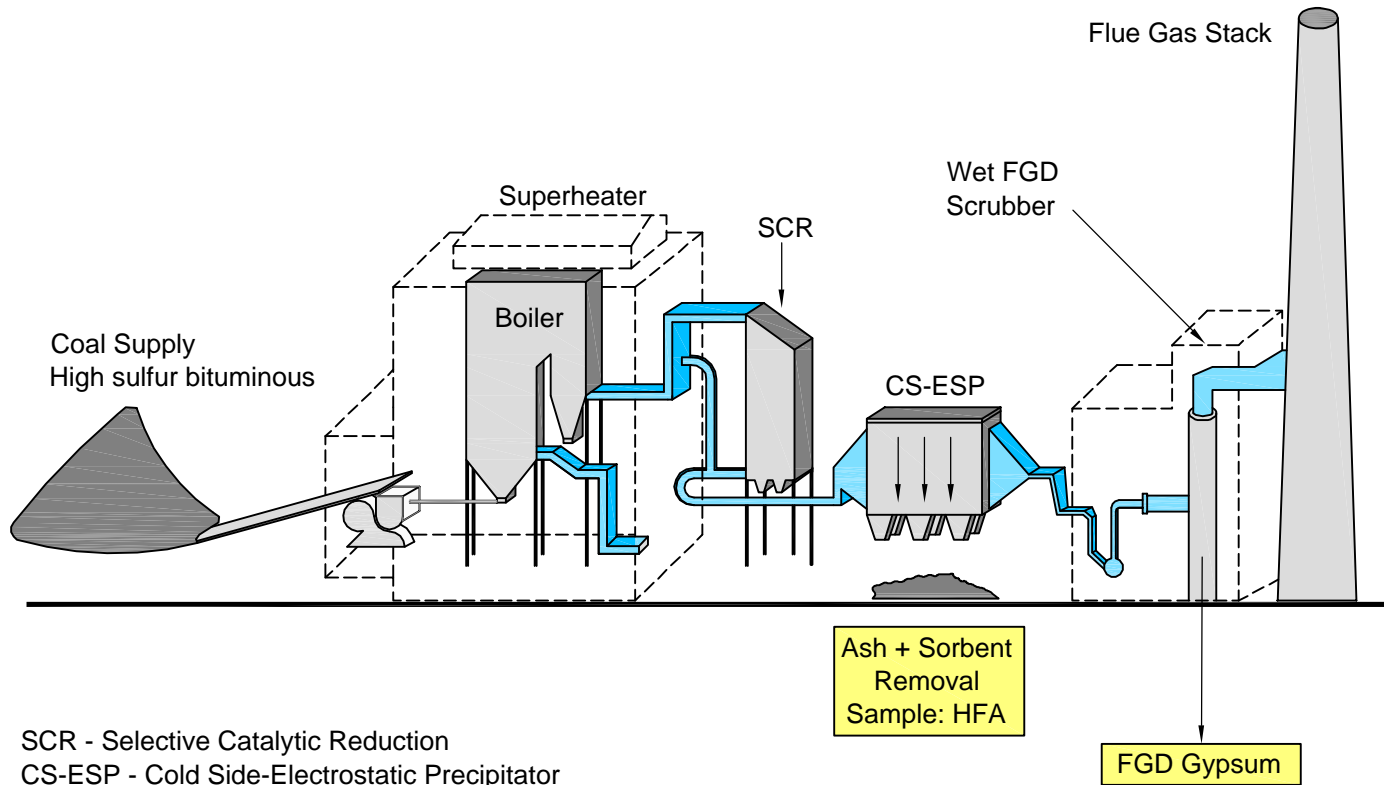
CS-ESP - Cold Side-Electrostatic Precipitator

Facility: G



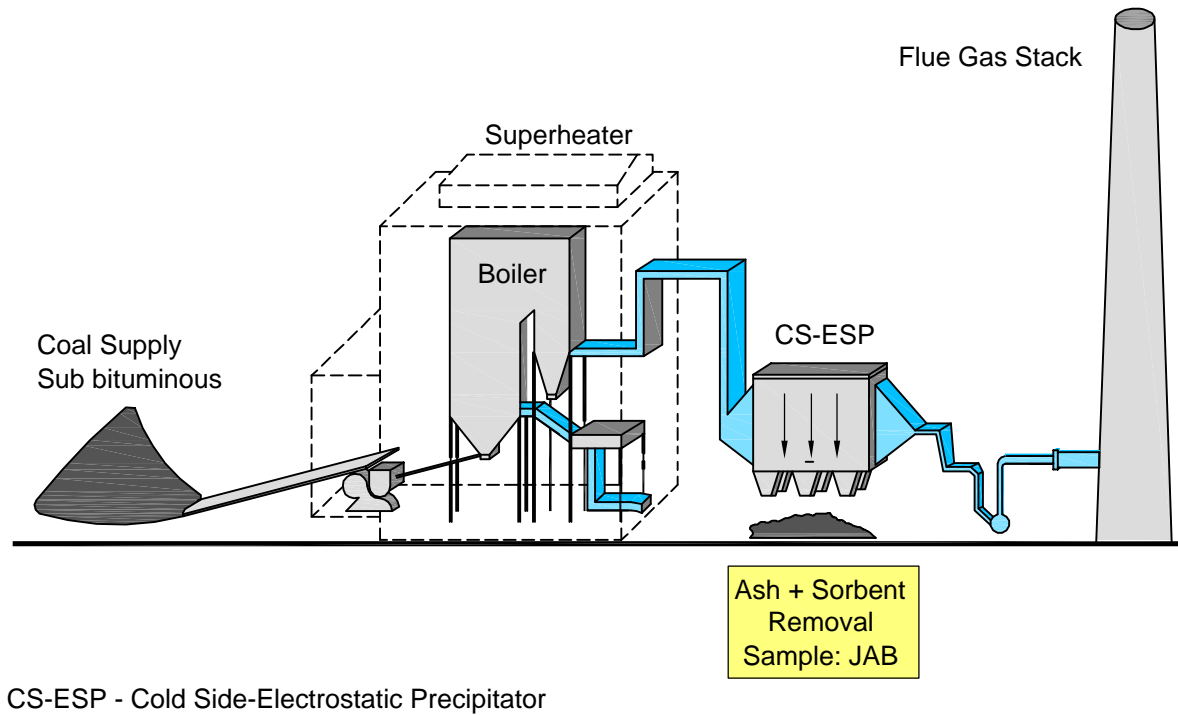
SNCR - Selective Non-catalytic Reduction
CS-ESP - Cold Side-Electrostatic Precipitator

Facility: H

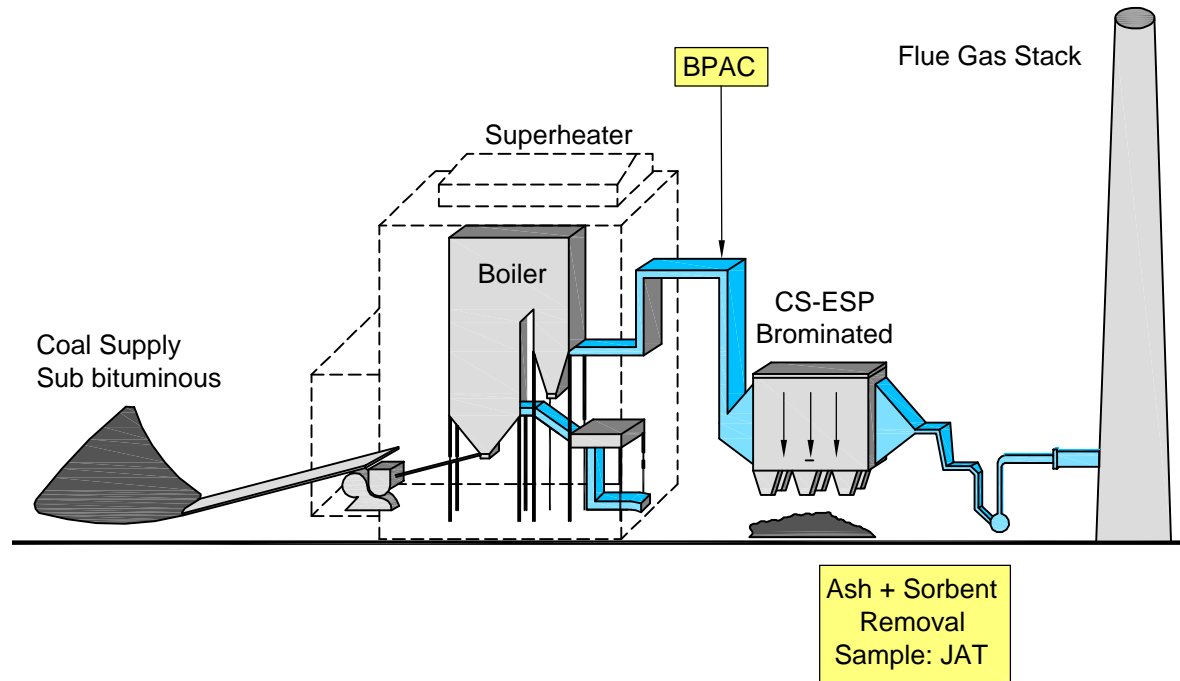


SCR - Selective Catalytic Reduction
CS-ESP - Cold Side-Electrostatic Precipitator
FGD - Flue Gas Desulfurization

Facility: J

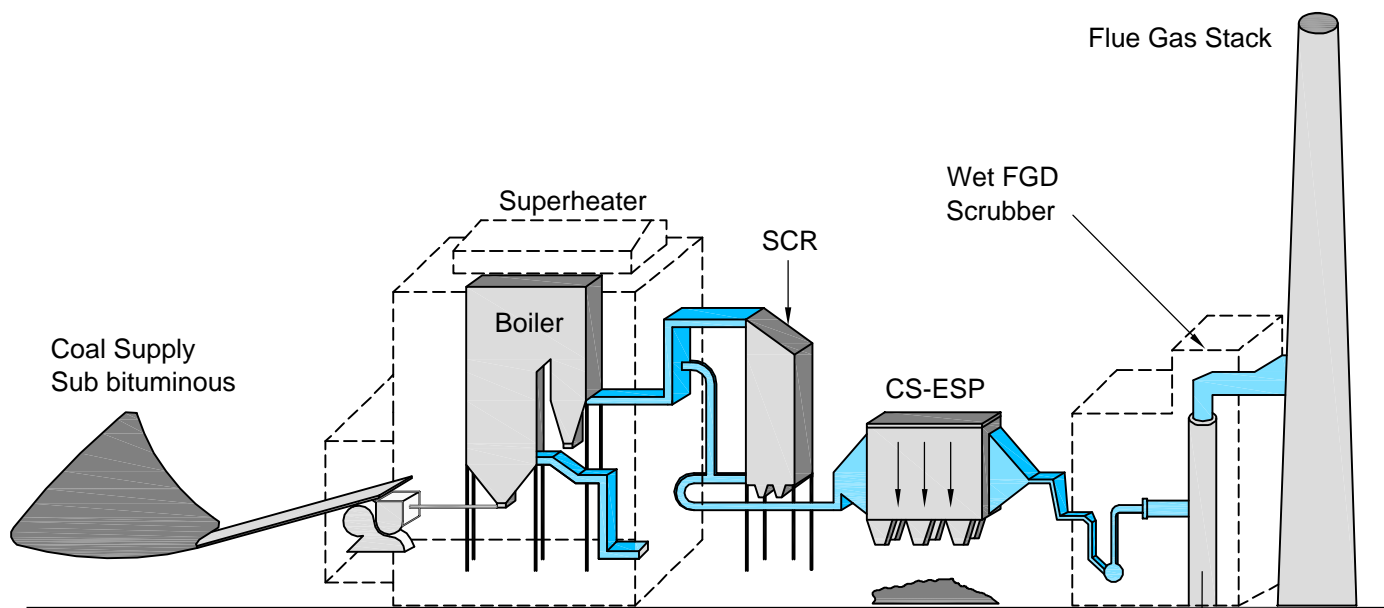


Facility: J with BPAC



BPAC - Biominated Powder Activated Carbon
CS-ESP - Cold Side-Electrostatic Precipitator
FGD - Flue Gas Desulfurization

Facility: K

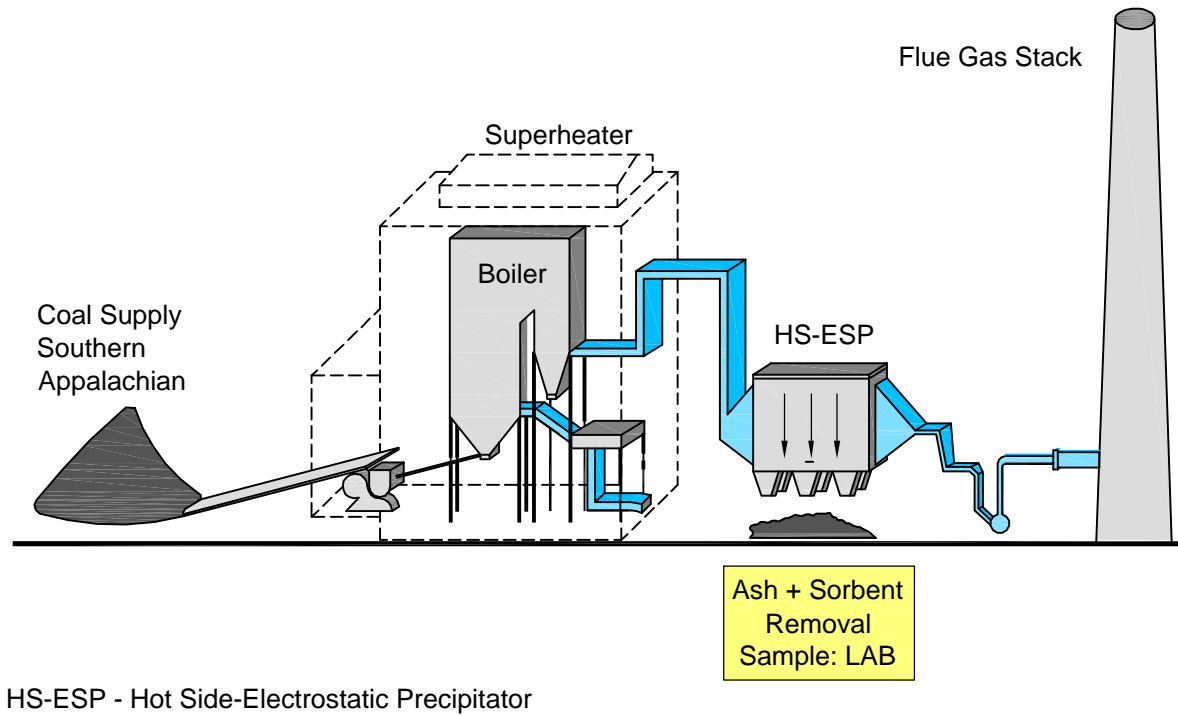


Ash + Sorbent
Removal
Sample: KFA

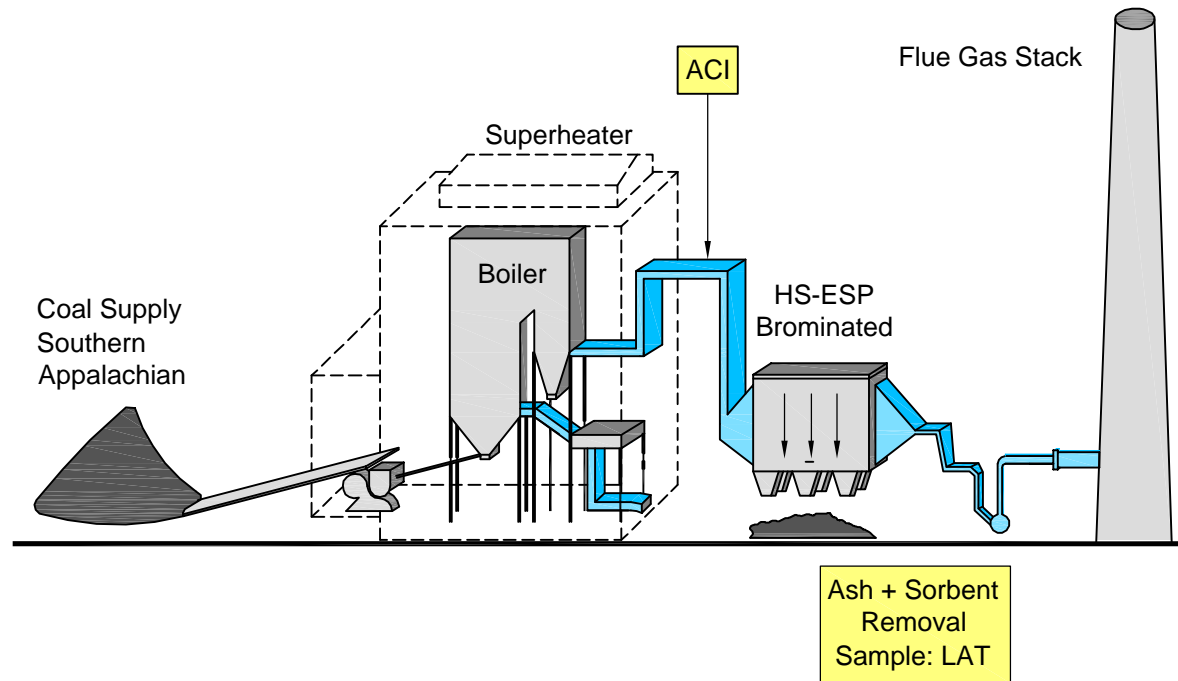
Scrubber Sludge Removal
Sample: KGD & KCC

SCR - Selective Catalytic Reduction
CS-ESP - Cold Side-Electrostatic Precipitator
FGD - Flue Gas Desulfurization

Facility: L

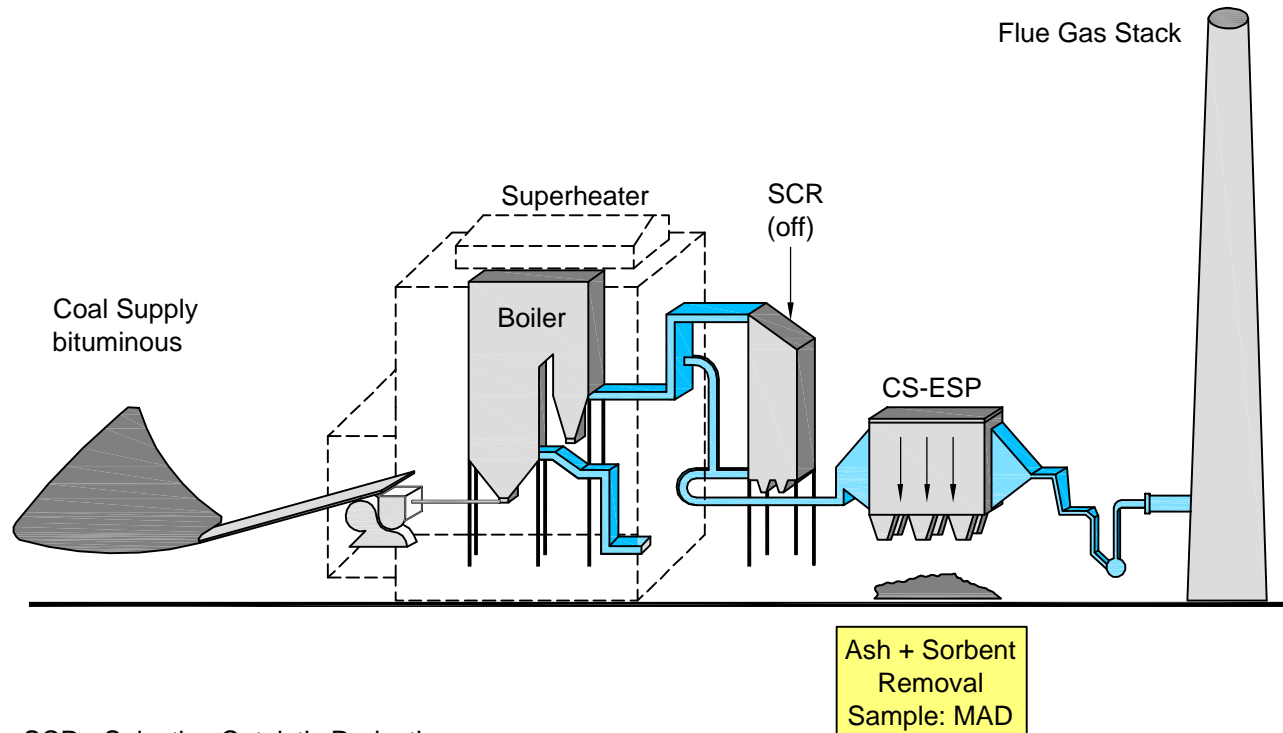


Facility: L with ACI



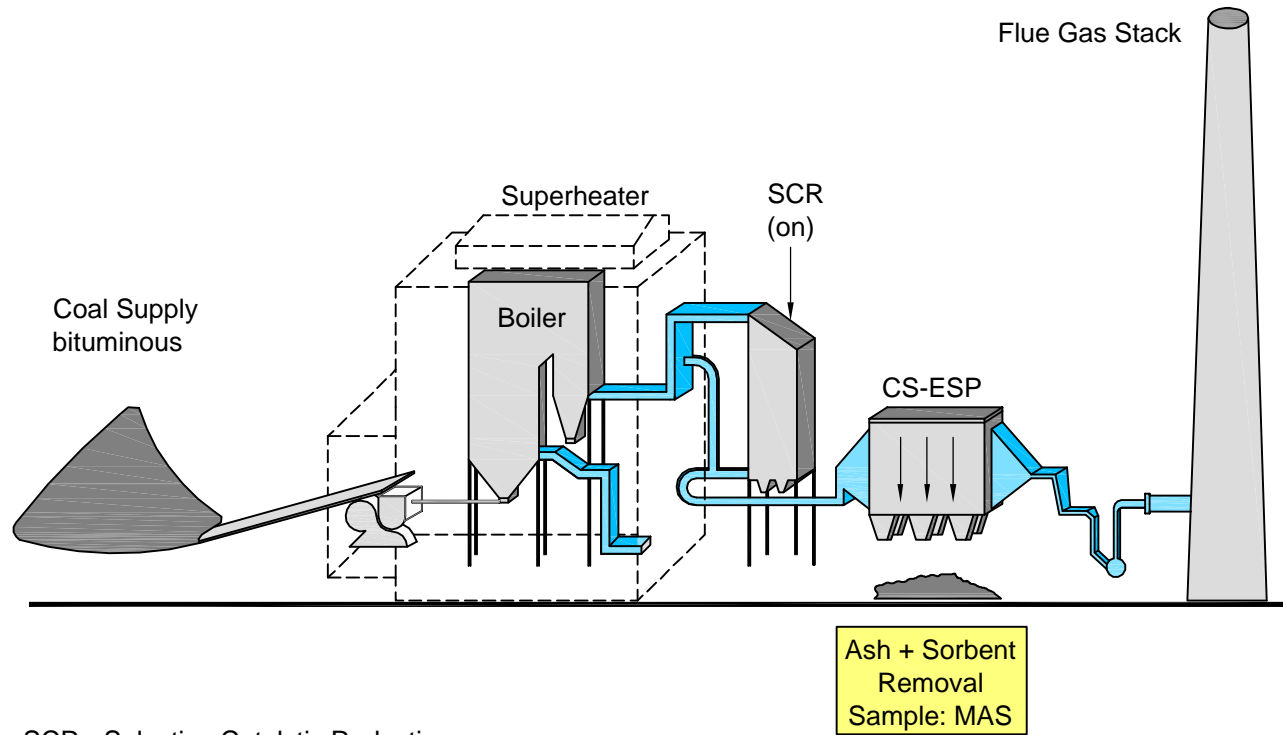
ACI - Activated Carbon Injector
HS-ESP - Hot Side-Electrostatic Precipitator

Facility: M SCR off



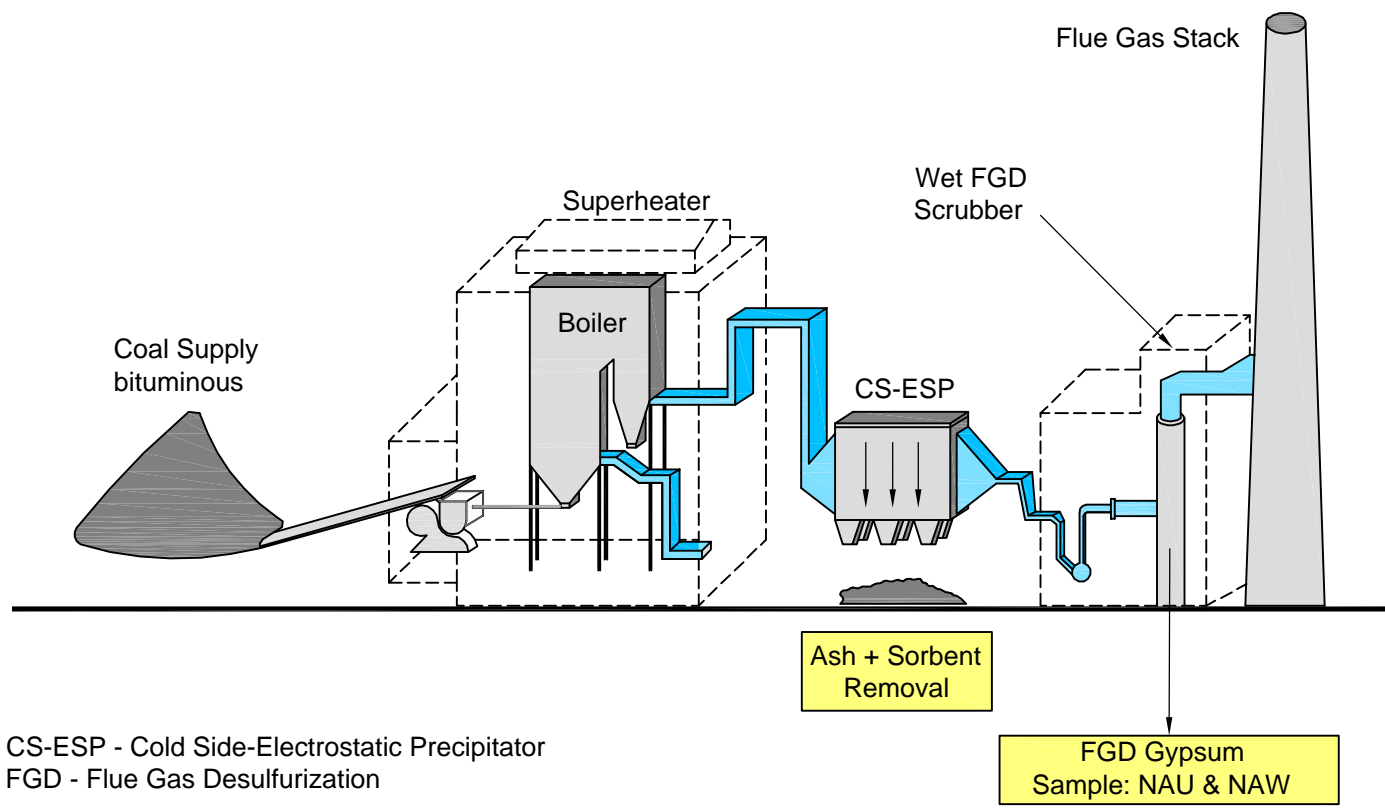
SCR - Selective Catalytic Reduction
BP - Bypass
CS-ESP - Cold Side-Electrostatic Precipitator

Facility: M SCR on

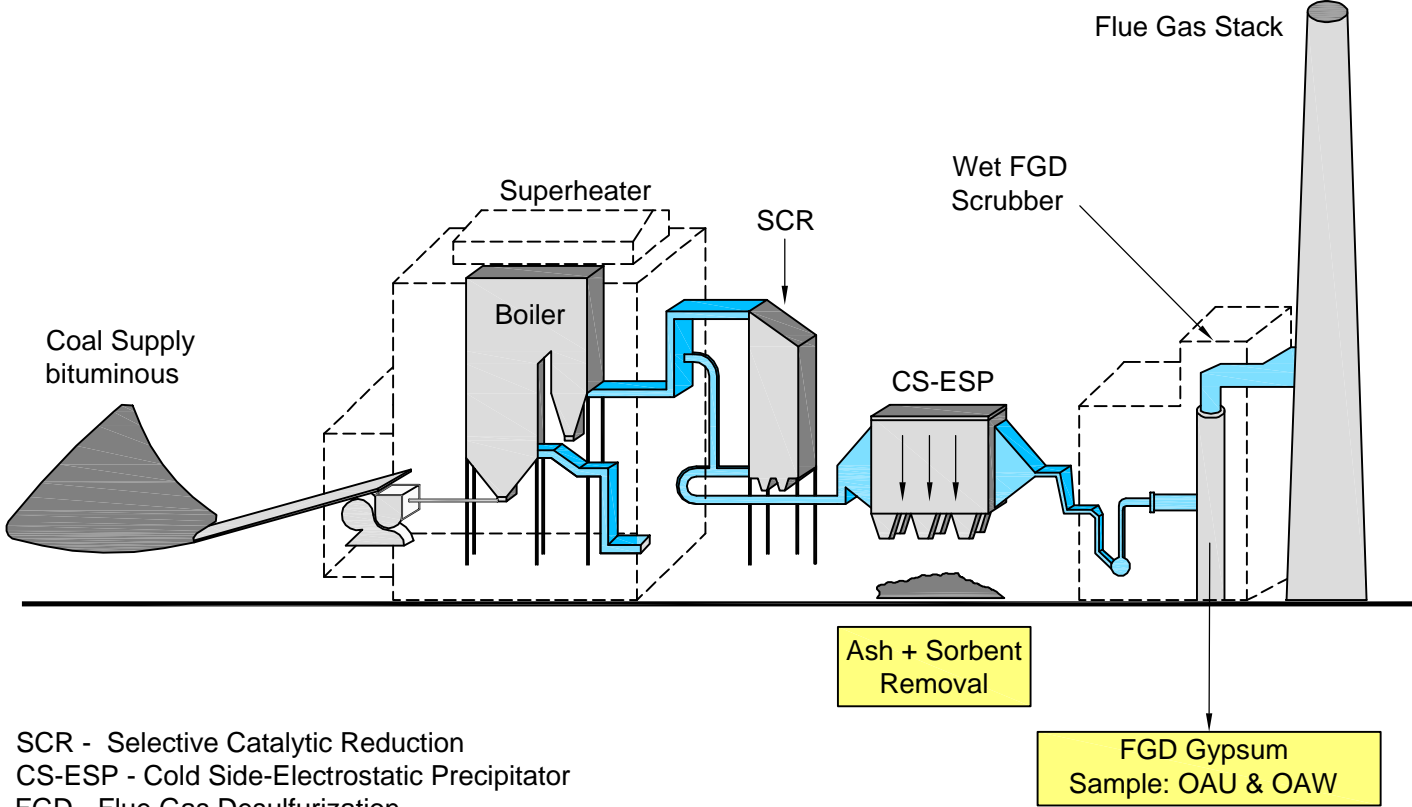


SCR - Selective Catalytic Reduction
BP - Bypass
CS-ESP - Cold Side-Electrostatic Precipitator

Facility: N

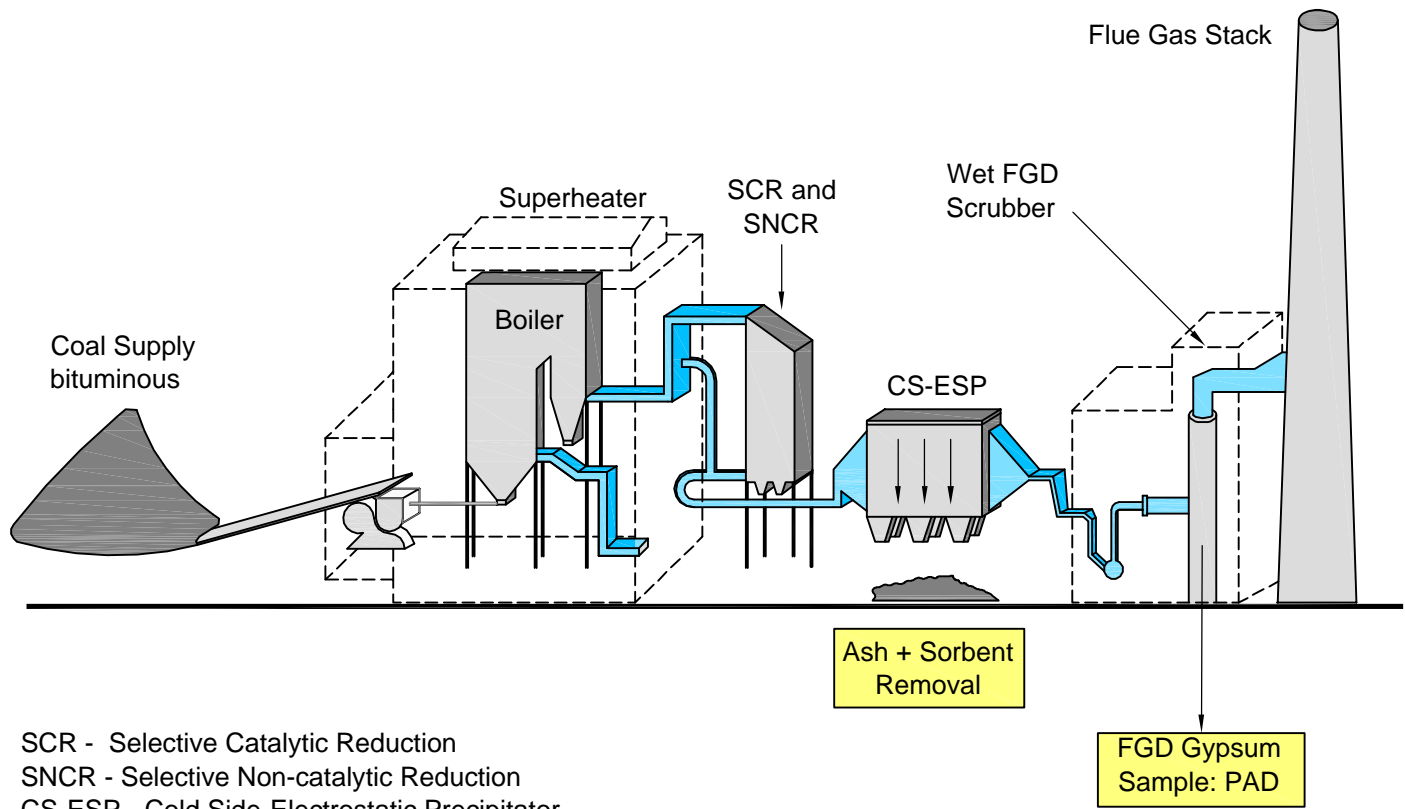


Facility: O



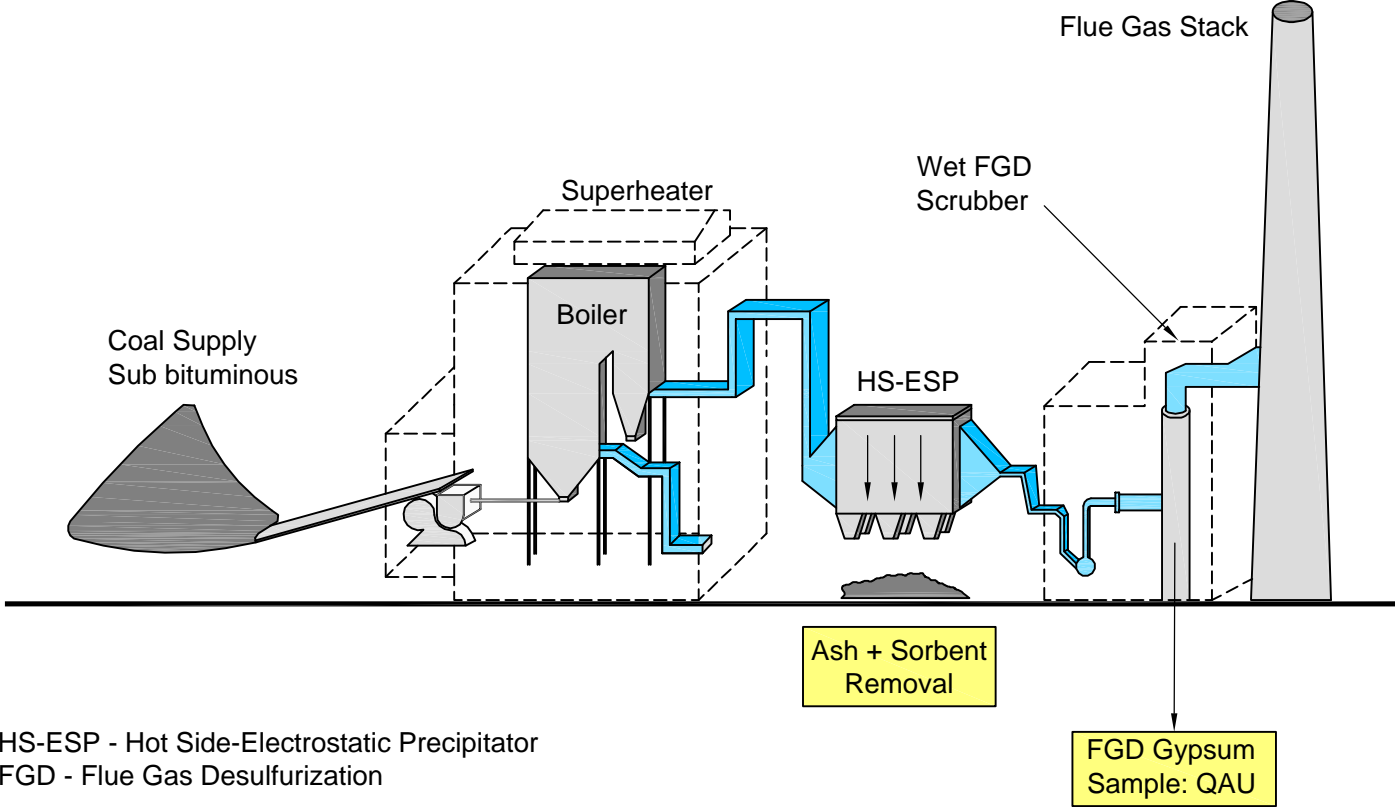
SCR - Selective Catalytic Reduction
CS-ESP - Cold Side-Electrostatic Precipitator
FGD - Flue Gas Desulfurization

Facility: P

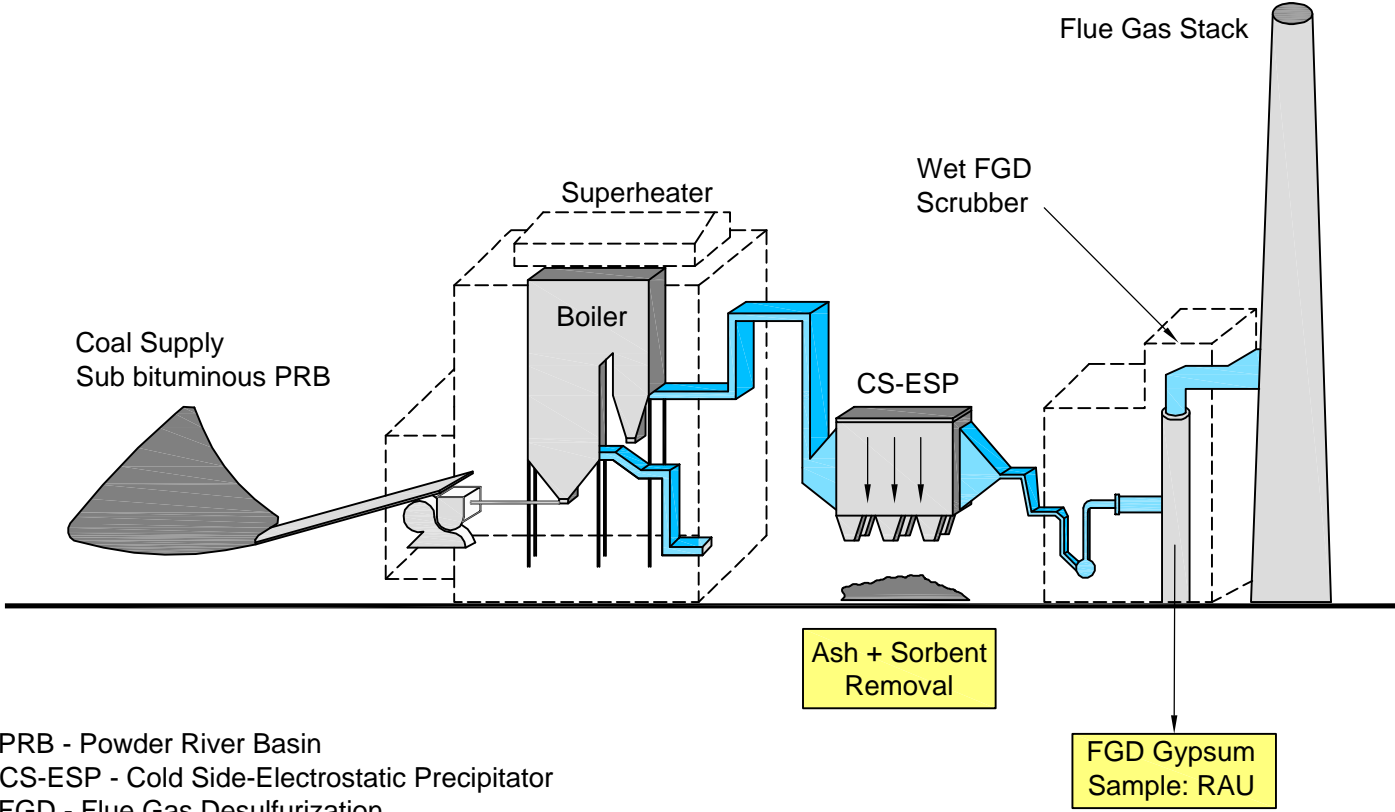


SCR - Selective Catalytic Reduction
SNCR - Selective Non-catalytic Reduction
CS-ESP - Cold Side-Electrostatic Precipitator
FGD - Flue Gas Desulfurization

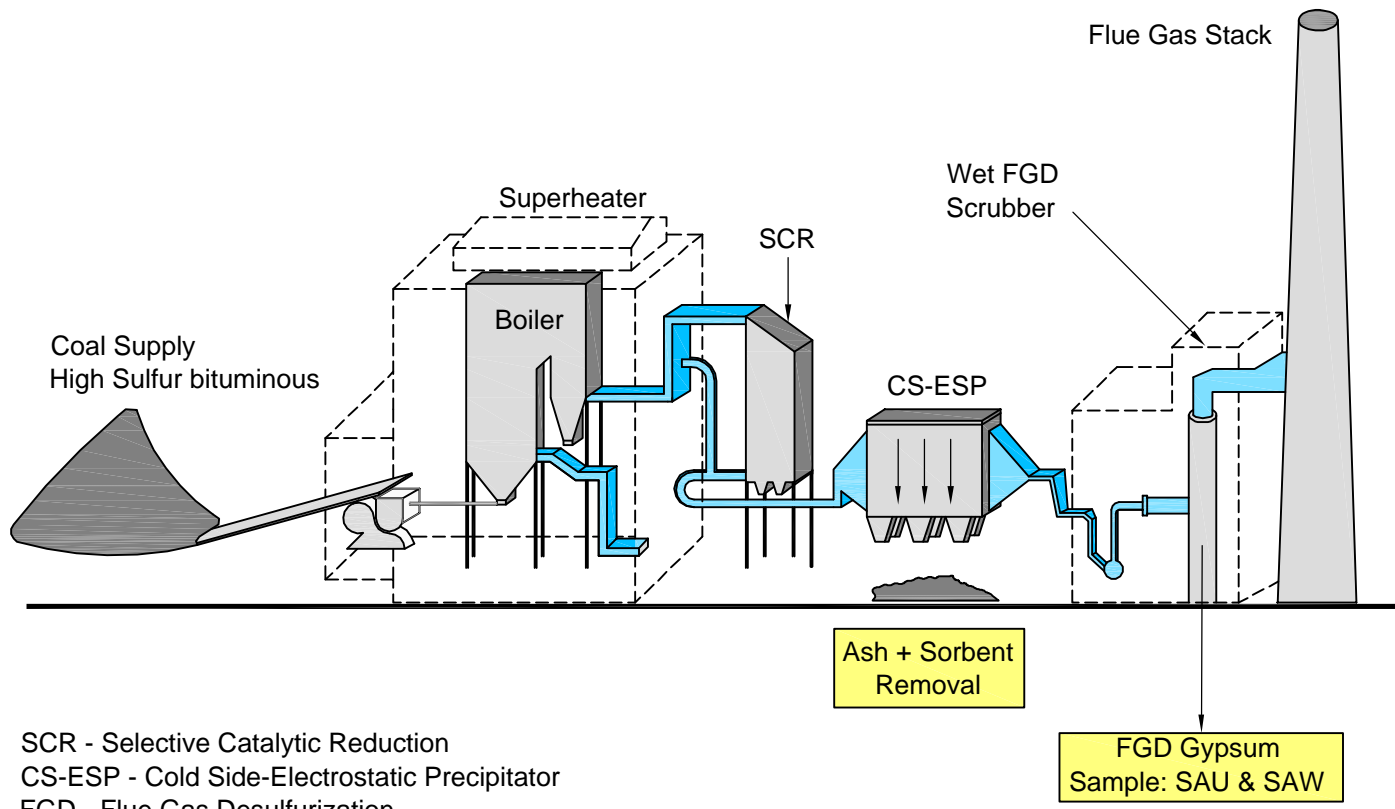
Facility: Q



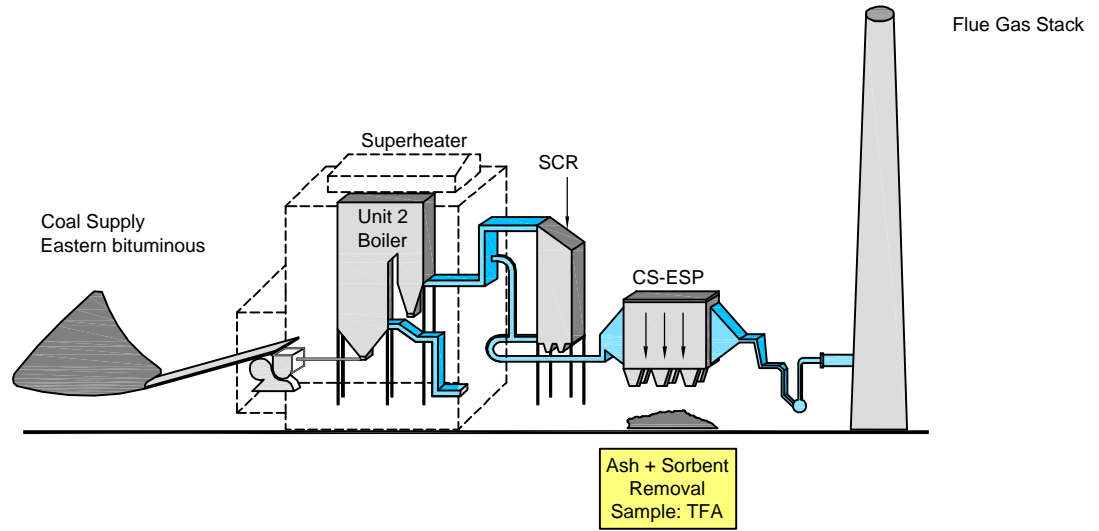
Facility: R



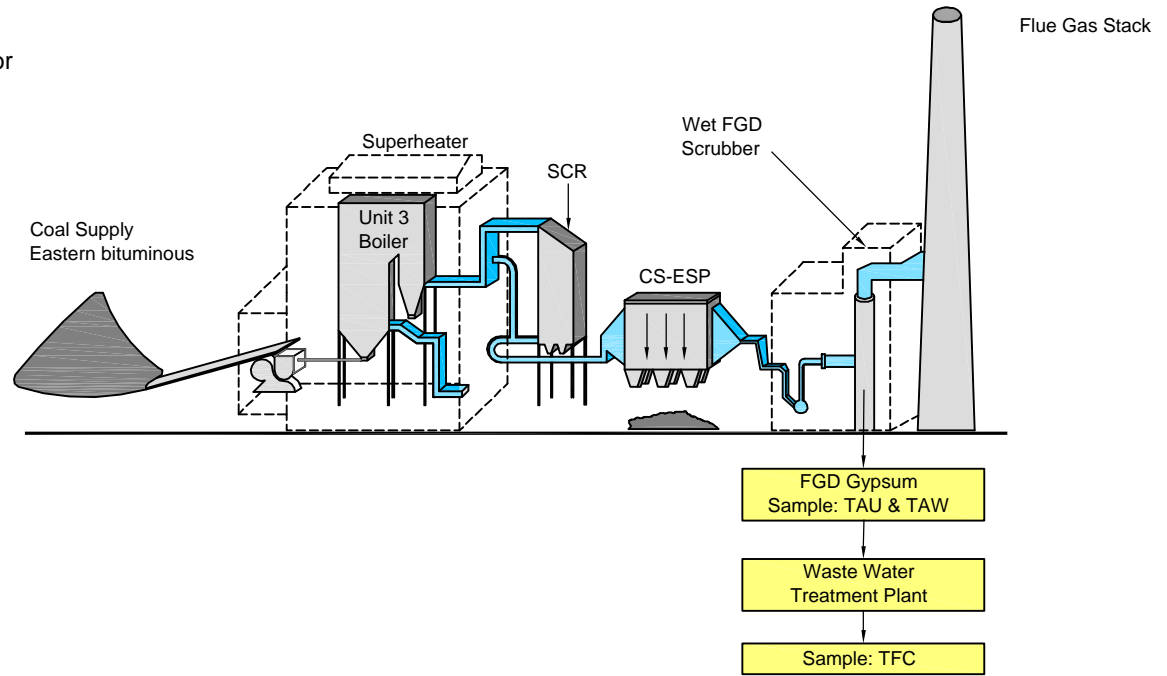
Facility: S



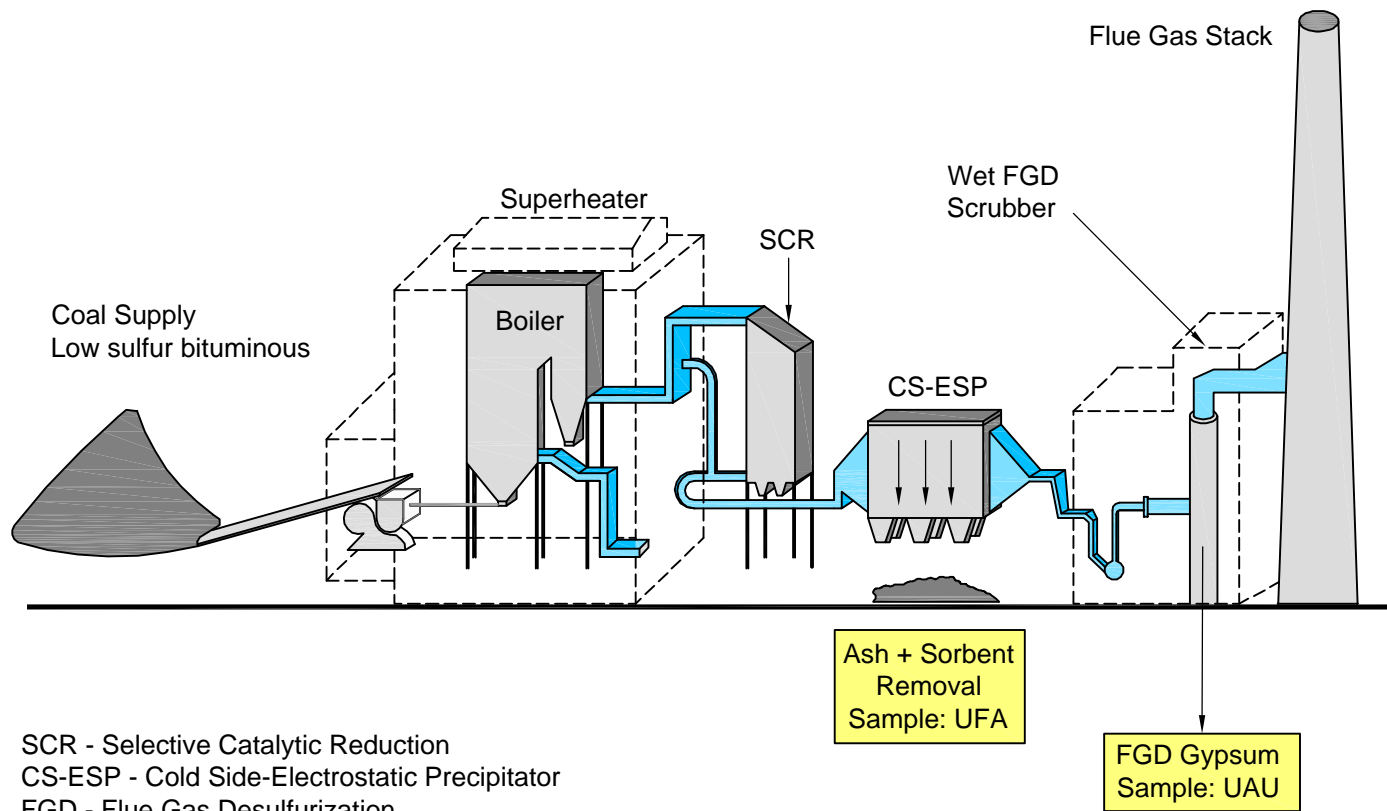
Facility: T



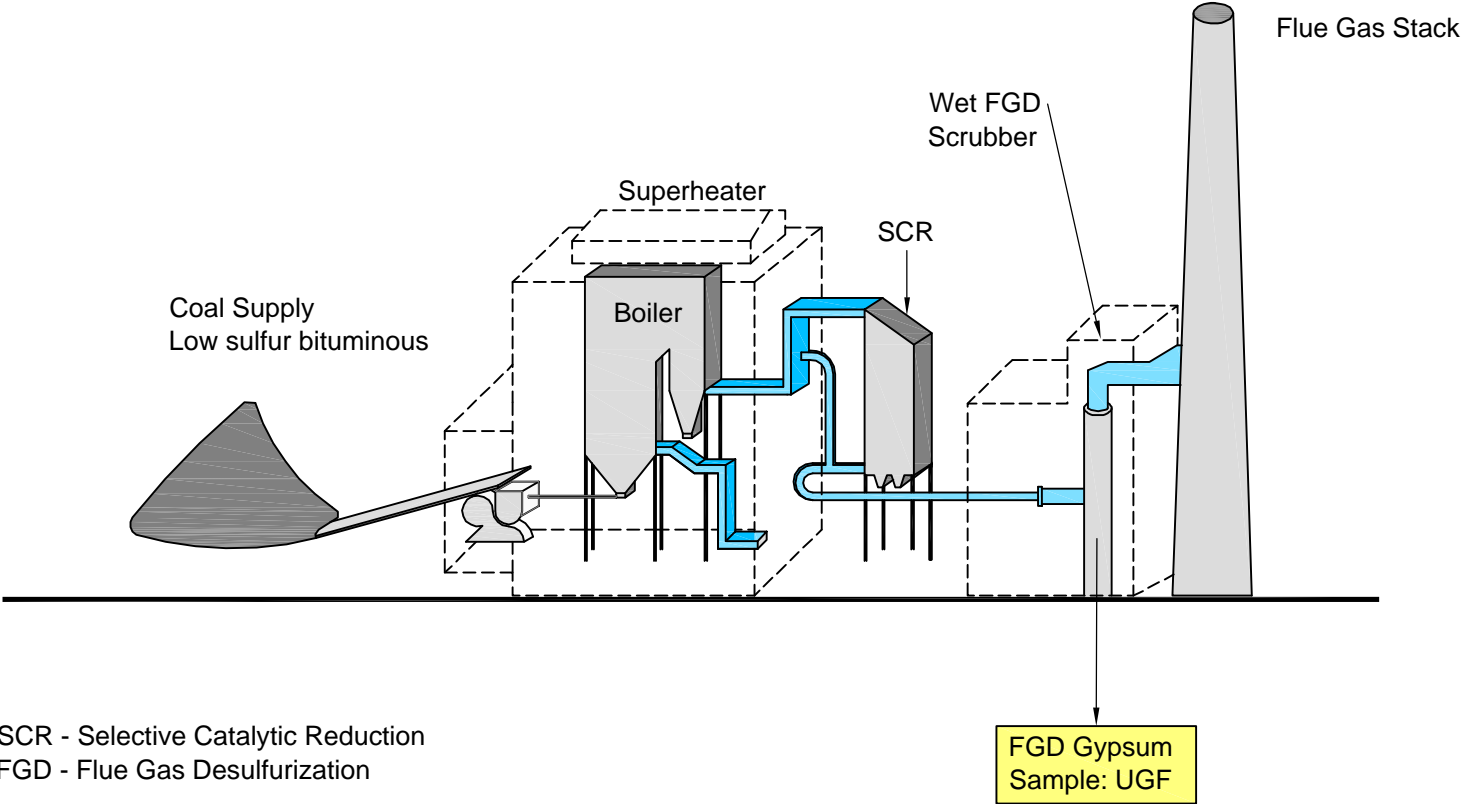
SCR - Selective Catalytic Reduction
CS-ESP - Cold Side-Electrostatic Precipitator
FGD - Flue Gas Desulfurization



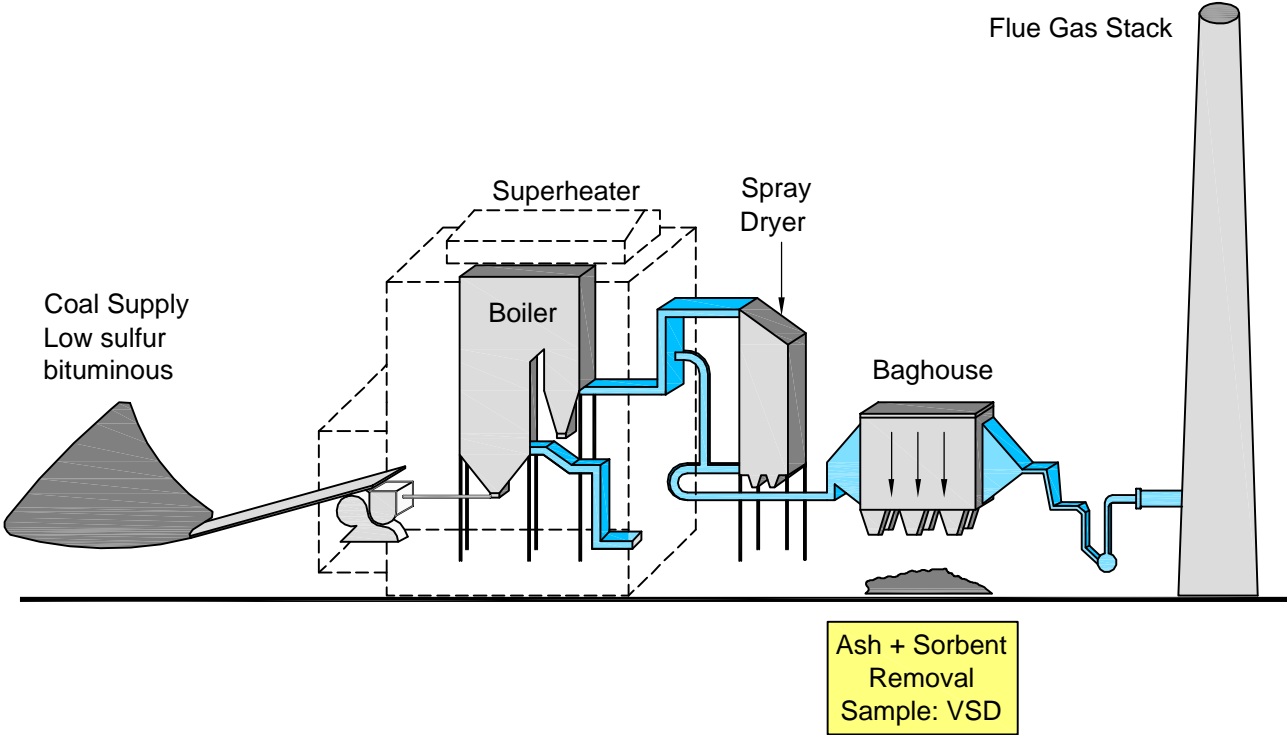
Facility: U Unit 7



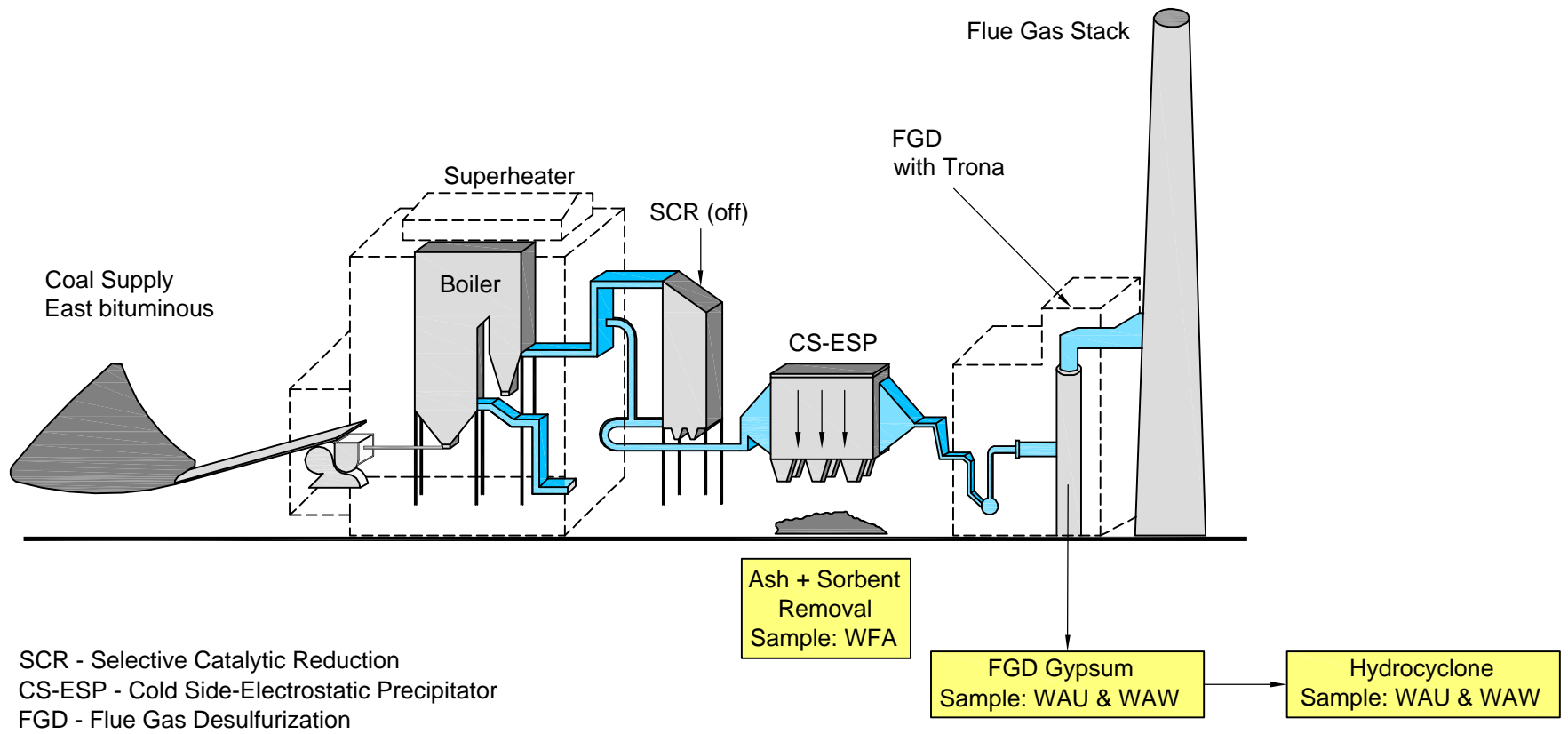
Facility: U Unit 8



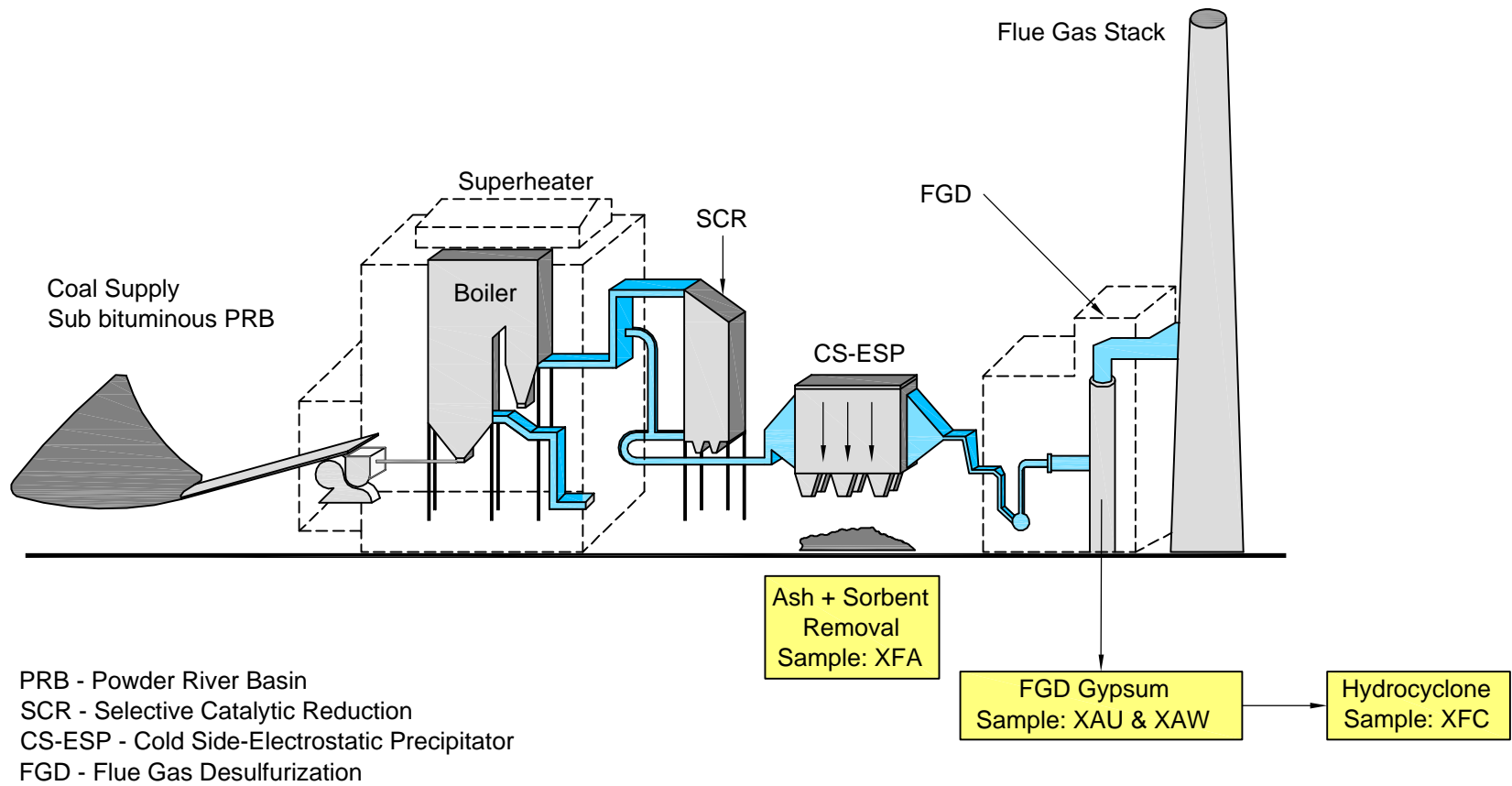
Facility: V



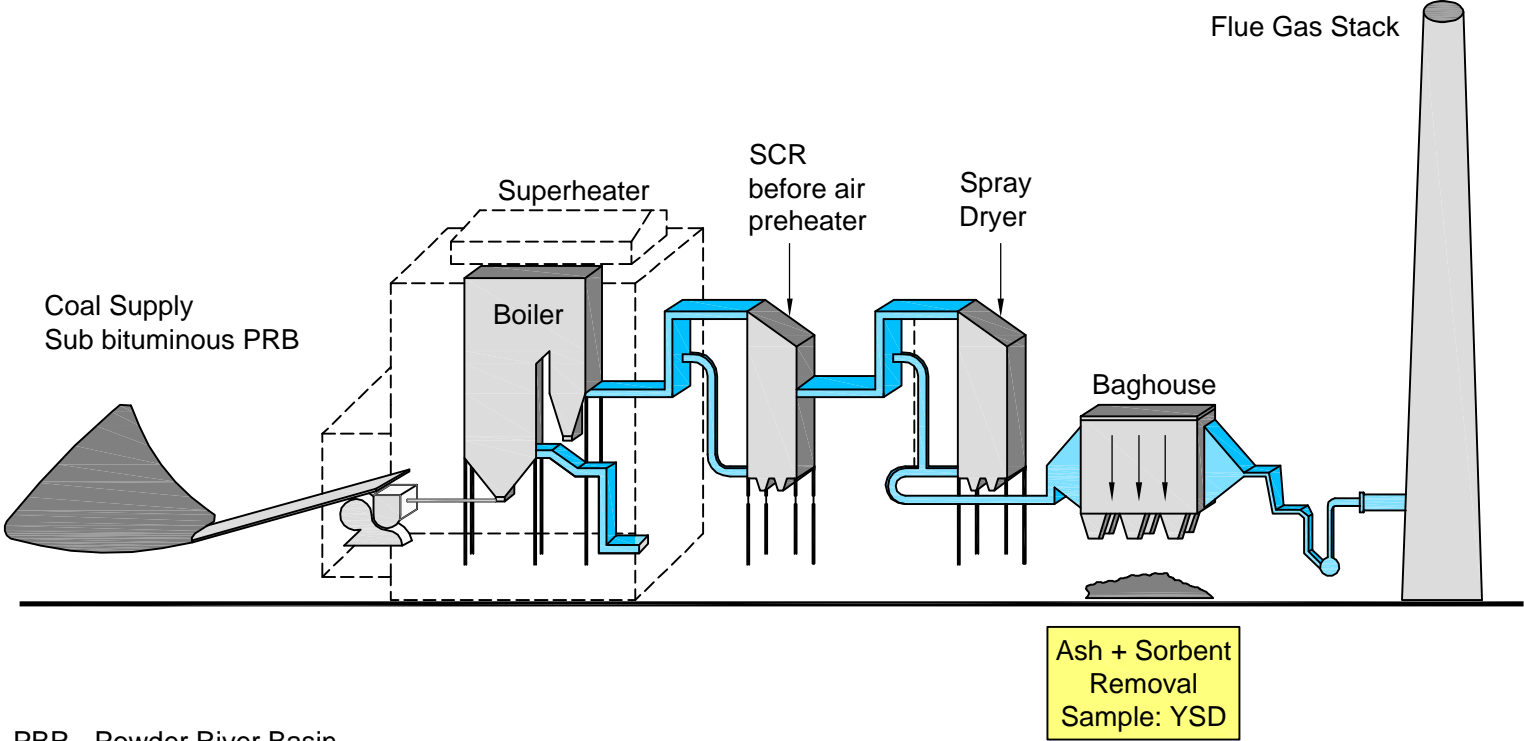
Facility: W



Facility: X

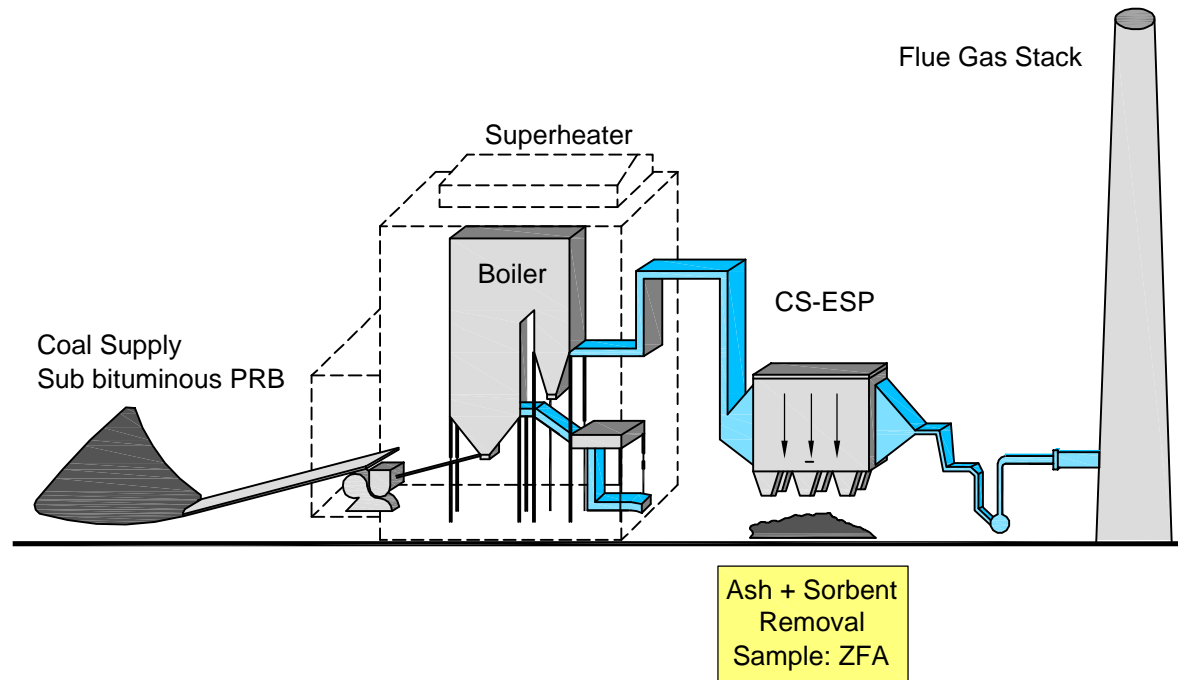


Facility: Y



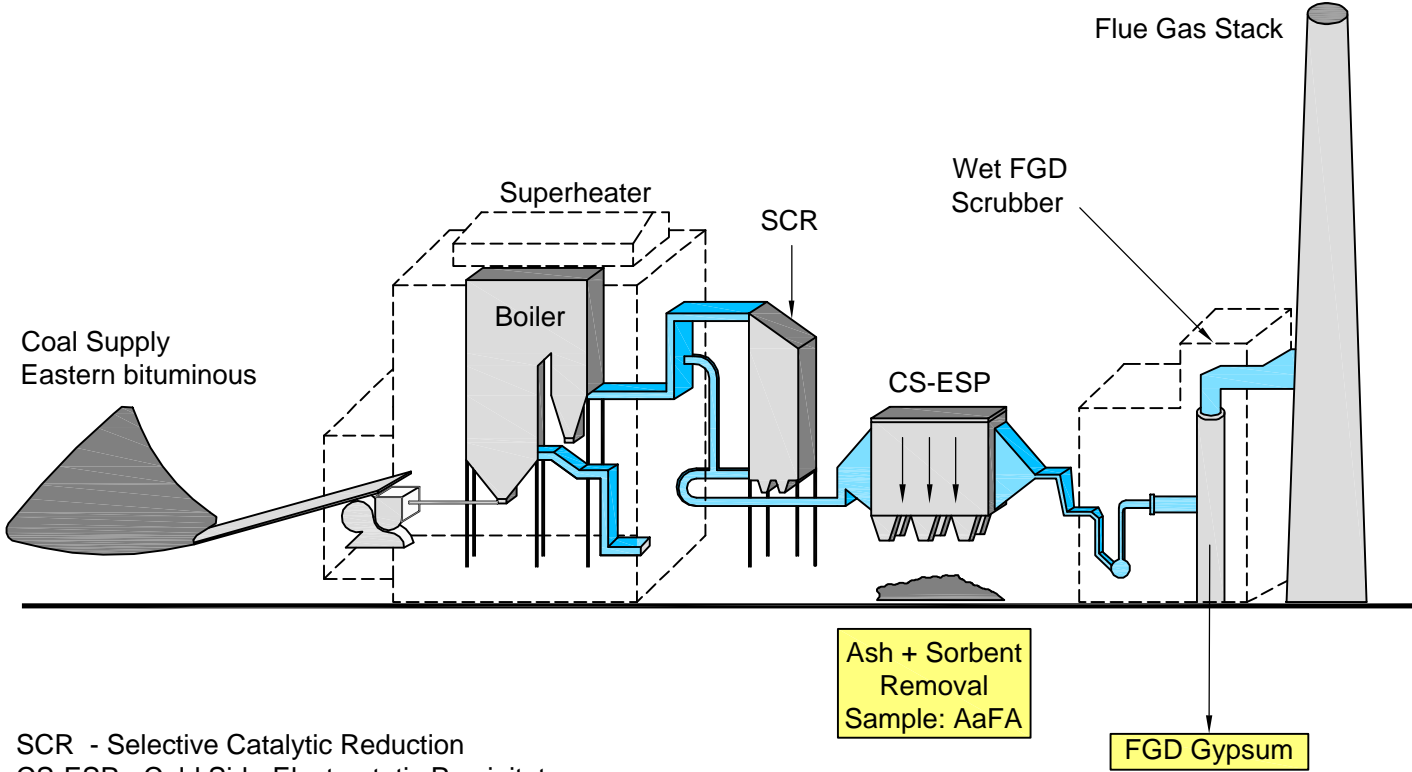
PBR - Powder River Basin
SCR - Selective Catalytic Reduction

Facility: Z



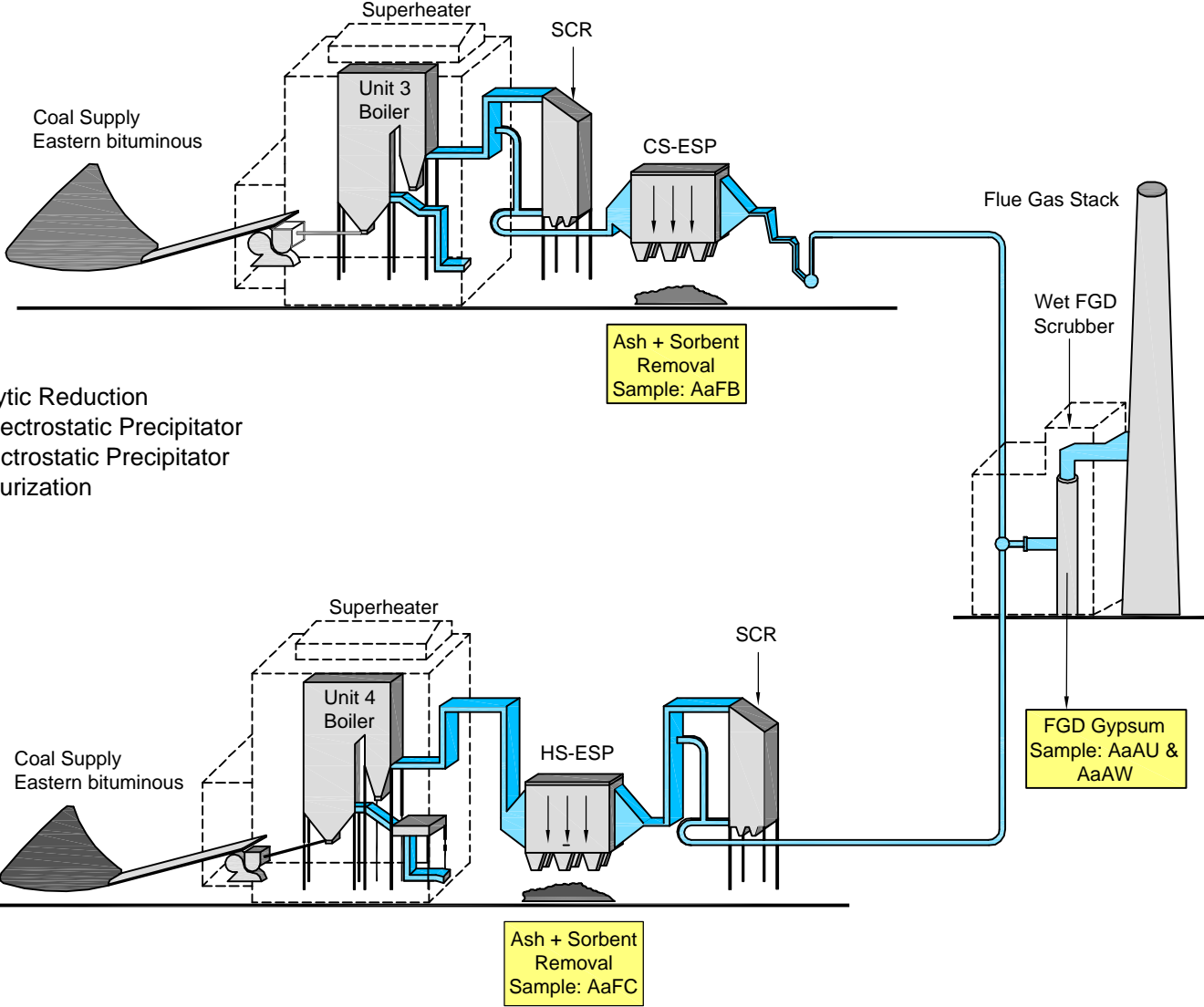
PRB - Powder River Basin
CS-ESP - Cold Side-Electrostatic Precipitator

Facility: Aa Unit 1



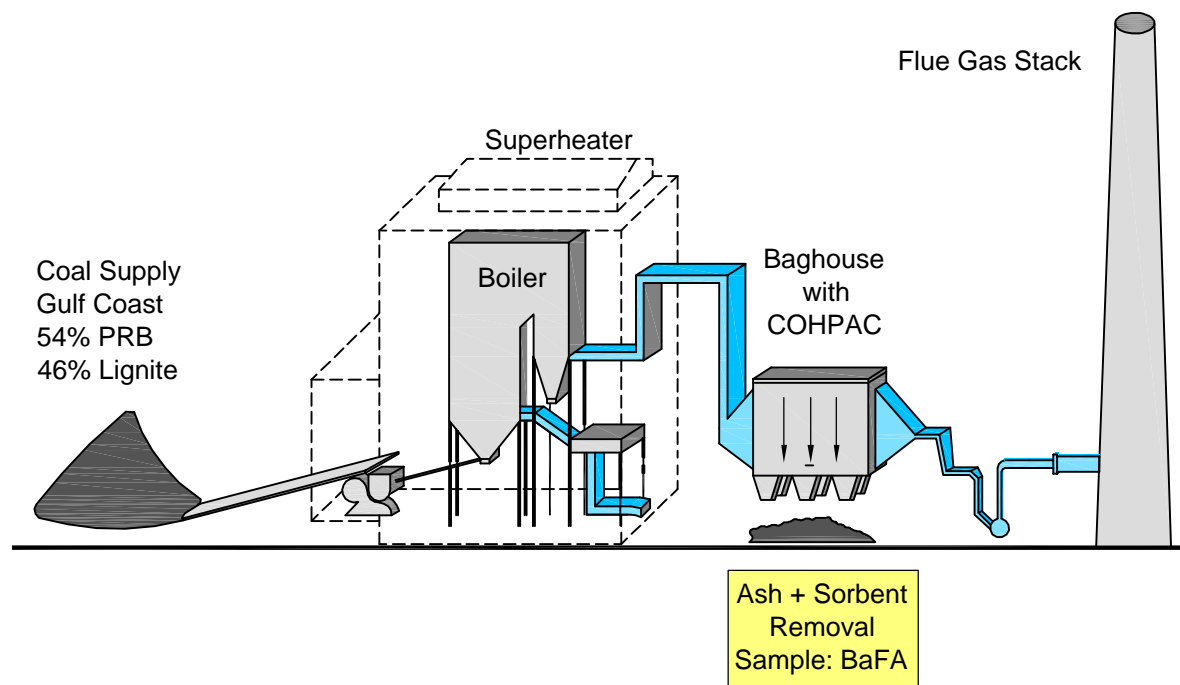
SCR - Selective Catalytic Reduction
CS-ESP - Cold Side-Electrostatic Precipitator
FGD - Flue Gas Desulfurization

Facility: Aa Unit 3 & 4



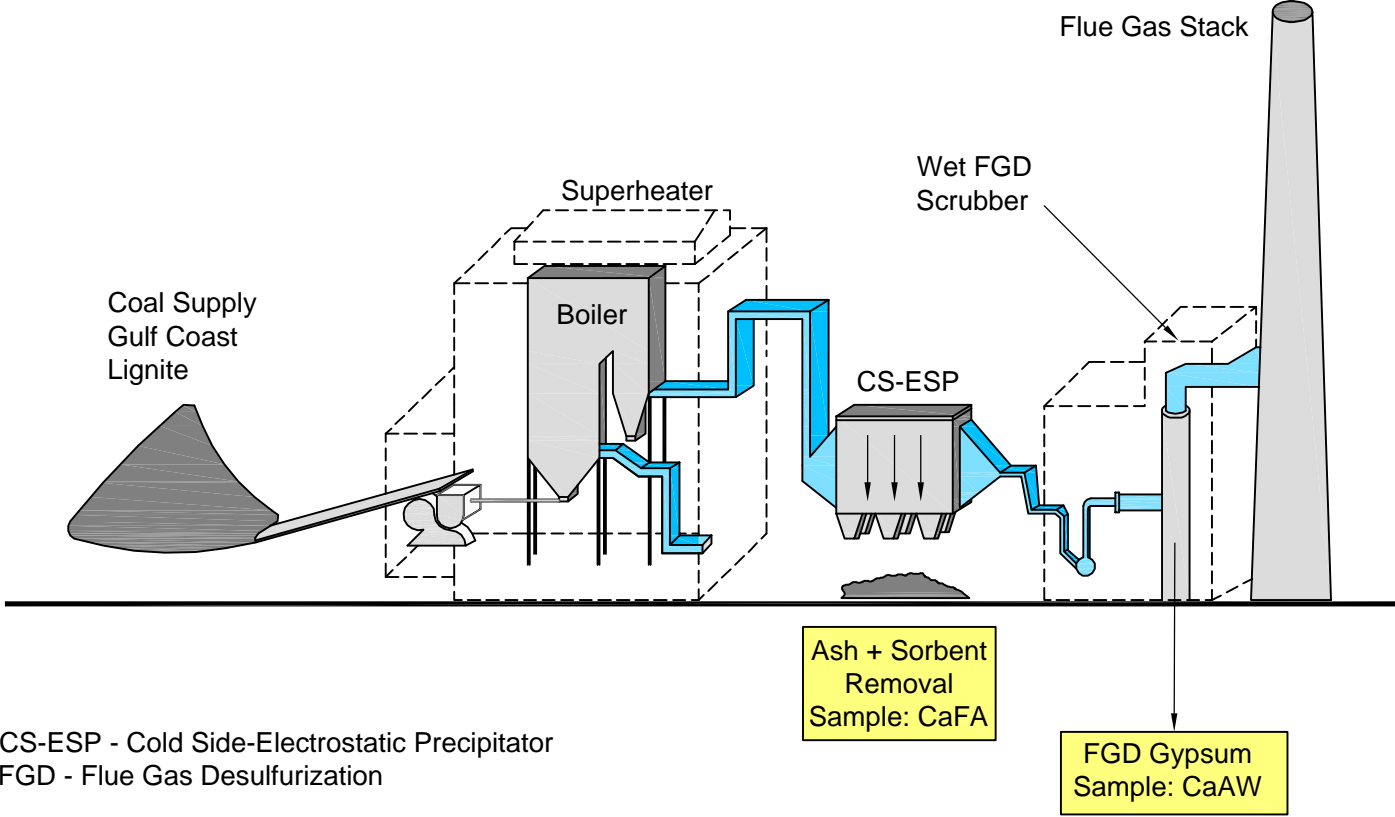
SCR - Selective Catalytic Reduction
 CS-ESP - Cold Side-Electrostatic Precipitator
 HS-ESP - Hot Side-Electrostatic Precipitator
 FGD - Flue Gas Desulfurization

Facility: Ba



PRB - Powder River Basin
COHPAC - Compact Hybrid Particulate Collector

Facility: Ca



Facility: Da

